Supplemental Environmental Impact Statement for the Designation of Dredged Material Disposal Site(s) in Eastern Long Island Sound, Connecticut and New York

APPENDIX C

Physical Oceanography of Eastern Long Island Sound Region

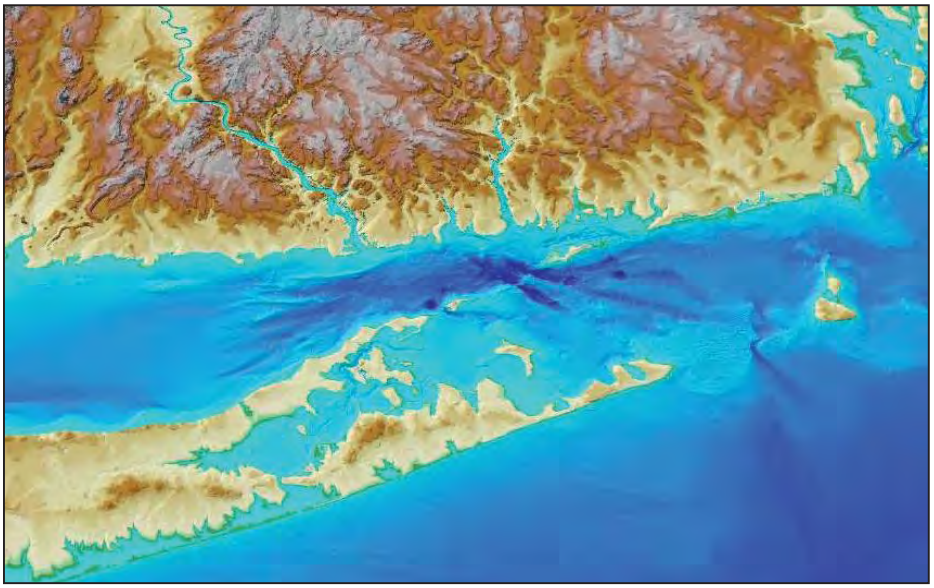

Prepared for: **United States Environmental Protection Agency**

Sponsored by: **Connecticut Department of Transportation**

Prepared by: **University of Connecticut**

with support from

Louis Berger

December 2015

[This page intentionally left blank.]

APPENDIX C

PHYSICAL OCEANOGRAPHY OF EASTERN LONG ISLAND SOUND REGION

Prepared for:

United States Environmental Protection Agency
5 Post Office Square, Suite 100
Boston, MA 02109

Sponsored by:

Connecticut Department of Transportation
Waterways Administration
2800 Berlin Turnpike
Newington, CT 06131-7546

Prepared by:

University of Connecticut
James O'Donnell (Project Manager)
Department of Marine Sciences
1080 Shennecossett Road
Groton, CT 06340

with support from

Louis Berger
117 Kendrick Street
Needham, MA 02494

December 2015

[This page intentionally left blank.]

PHYSICAL OCEANOGRAPHY OF EASTERN LONG ISLAND SOUND REGION

OVERVIEW

In 2005, the USEPA designated the Western and Central Long Island Sound dredged material disposal sites, following the preparation of an EIS. The two disposal sites in the eastern Long Island Sound, Cornfield Shoals and New London, are scheduled to close in December 2016. The USEPA is in the process of preparing a Supplemental EIS (SEIS) for the potential designation of one or more disposal sites needed to serve the eastern Long Island Sound region. The SEIS is being prepared in accordance with Section 102(c) of the Marine Protection Research and Sanctuaries Act (MPRSA; also referred to as Ocean Dumping Act [ODA]) of 1972.

The objective of the physical oceanography study was to collect data and information for candidate sites within a Zone of Siting Feasibility (ZSF) to support the SEIS. The ZSF is the area considered for the potential siting of open-water disposal sites; it consists of the eastern Long Island Sound and Block Island Sound. The stability of bottom sediments and the movement of suspended matter in estuaries is strongly influenced by the character of the circulation. Determining the magnitude and pattern of the water movement, its variability, the response to severe storms, and the potential impacts on bottom sediments are central elements of the discipline of physical oceanography. Therefore, collected physical oceanography data were used to determine bottom shear stresses and water circulation to characterize and rank potential disposal sites, since these factors determine the erosion potential and fate of the sediment (including disposed dredged material).

The physical oceanography data needs were addressed with a combination of continuous data collection at moorings and boat-based surveys and instrument casts at multiple locations in the ZSF, in addition to secondary data sources. The data analysis was conducted using several models. The study was performed following the preparation of a Quality Assurance Project Plan (QAPP), approved by USEPA in May 2013.

Study results were prepared as three stand-alone reports that are attached within this Appendix C:

- **Appendix C-1 (Field Data):** This report contains the results of the field data collection in the field. It includes a description of the methodology, sampling periods, data types, and appendices with data.

- **Appendix C-2 (Modeling):** The data collected in the field were used to characterize the physical oceanographic conditions in the ZSF, using the unstructured grid Finite Volume Coastal Ocean Model (FVCOM), nested within the University of Massachusetts-Dartmouth Regional Model. The development and the evaluation of the numerical model are described. Modeling determined bottom shear stresses and water circulation in the ZSF since these factors determine the erosion potential of the sediment, particularly during worst-case storm events such as in the late fall, winter, and spring months. Results were used primarily for the site screening of candidate sites in the ZSF.

- **Appendix C-3 (Sediment Transport):** This report describes the distribution and transport of sediment at three alternative sites in eastern Long Island Sound, identified during site screening as alternative sites for the potential designation of one or more open-water dredged material disposal site(s). These sites were New London, Niantic Bay and Cornfield Shoals. The analysis was conducted using the models STFATE, LTFATE, and FVCOM.

Supplemental Environmental Impact Statement for the Designation of Dredged Material Disposal Site(s) in Eastern Long Island Sound, Connecticut and New York

Appendix C-1

Physical Oceanography of Eastern Long Island Sound Region: Field Data

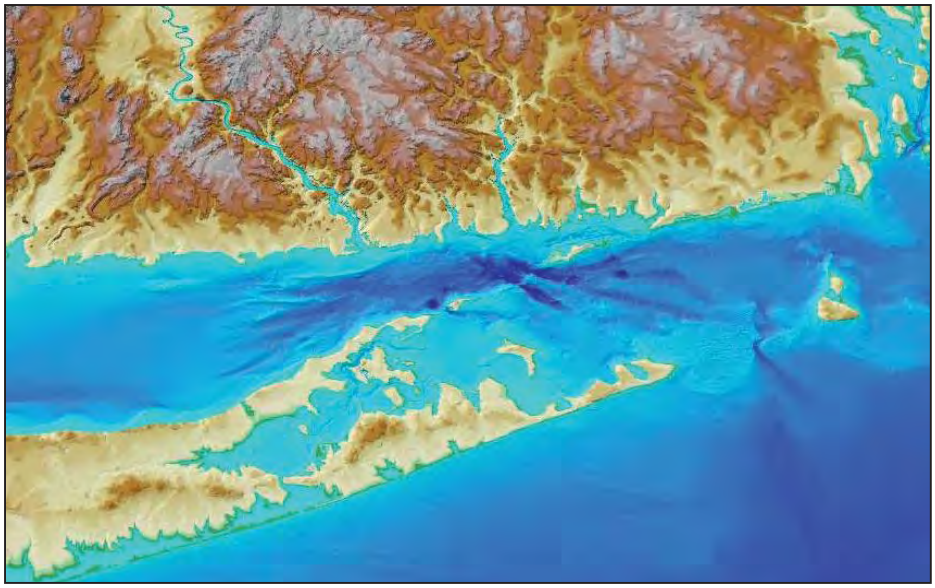

Prepared for: **United States Environmental Protection Agency**

Sponsored by: **Connecticut Department of Transportation**

Prepared by: **University of Connecticut**

with support from

Louis Berger

August 2014

Supplemental Environmental Impact Statement for the Designation of Dredged Material Disposal Site(s) in Eastern Long Island Sound, Connecticut and New York

---

PHYSICAL OCEANOGRAPHY OF EASTERN LONG ISLAND SOUND REGION: FIELD DATA

Prepared for:

United States Environmental Protection Agency
5 Post Office Square, Suite 100
Boston, MA 02109

Sponsored by:

Connecticut Department of Transportation
Waterways Administration
2800 Berlin Turnpike
Newington, CT 06131-7546

Prepared by:

James O'Donnell (Project Manager), Kay Howard-Strobel, David Cohen, Steven Ackleson, Alejandro Cifuentes-Lorenzen, Diane Fribance, Rachel Horwitz, Grant McCardell, Frank Bohhlen, and Todd Fake

University of Connecticut
Department of Marine Sciences
1080 Shennecossett Road
Groton, CT 06340

with support from

Louis Berger
117 Kendrick Street
Needham, MA 02494

August 2014

Table of Contents

Page

Executive Summary

1. Introduction 1
   1.1 Background 1
   1.2 Study Overview 2
   1.3 Use of Field Data for Modeling 4
   1.4 Report Organization 5

2. Methodology 6
   2.1 Field Program 6
      2.1.1 Overview 6
      2.1.2 Instrument Moorings 7
         2.1.2.1 Temperature and Salinity (SBE SMP37) 8
         2.1.2.2 Waves and Currents in the Water Column (RDI ADCP) 9
         2.1.2.3 Currents near the Seafloor (Nortek ADCP) 11
         2.1.2.4 Suspended Sediment Concentrations near the Seafloor (OBS3+ sensors) 11
      2.1.3 Ship Surveys 11
         2.1.3.1 Temperature and Salinity (Profiling CTD) 13
         2.1.3.2 Currents throughout the ZSF (RDI ADCP) 14
         2.1.3.3 Optical Suspended Sediment Measurements in the Water Column (WET Labs sensors) 15
         2.1.3.4 Water Sampling for Suspended Sediment and Particulate Organic Carbon Concentrations 15
         2.1.3.5 Grain Size of Seafloor Sediment 16
   2.2 Sample and Data Processing 16
      2.2.1 Moored Instruments 16
         2.2.1.1 Temperature and Salinity 16
         2.2.1.2 Waves and Currents in the Water Column 17
         2.2.1.3 Currents near the Seafloor 18
         2.2.1.4 Suspended Sediment Concentrations near the Seafloor 18
      2.2.2 Ship Surveys 20
         2.2.2.1 Temperature and Salinity (Profiling CTDs) 20
         2.2.2.2 Currents throughout the ZSF (Ship-board RDI ADCP) 22
         2.2.2.3 Optical Suspended Sediment Measurements in the Water Column22 (WET Labs sensors) 22
         2.2.2.4 Water Sample Analyses for Suspended Sediment and Particulate Organic Carbon Concentrations 22
         2.2.2.5 Grain Size of Seafloor Sediments 22
   2.3 Regional Wind and Wave Observations 23
   2.4 Summary 23
      2.4.1 Field Program 23
      2.4.2 Data Recovery 25

3. Temperature and Salinity (Ship Surveys) 28
3.1 Data 28
3.2 Summary 28

4. Currents throughout the ZSF (Ship Surveys) 40
4.1 Data 40
4.2 Summary 42

5. Temperature and Salinity (Moored Instruments) 43
5.1 Data 43
5.2 Summary 44

6. Currents in the Water Column (Moored Instruments) 63
6.1 Data 63
6.1.1 Tidal Velocities 63
6.1.2 Subtidal Velocities 64
6.1.3 Depth-averaged Velocities and Time-averaged Velocity Profiles 65
6.14 Near-bottom Velocities 66
6.2 Summary 69

7. Currents at the Seafloor (Moored Instruments) 70
7.1 Calculation of Bottom Stress 70
7.2 Data 72
7.3 Summary 78

8. Wave Observations 100
8.1 Data - Meteorological Conditions 100
8.2 Data - Wave Observations 102
8.3 Summary 104

9. Suspended Sediment in the Water Column (Ship Surveys) 129
9.1 Data - Water Samples 129
9.2 Data - Optical Sensors 132
9.2.1 Calibrations 132
9.2.1.1 Suspended Sediment Concentrations 132
9.2.1.2 Particle Size Distribution 133
9.2.1.3 Chlorophyll Absorption 135
9.2.2 Suspended Sediment Concentrations 135
9.3 Summary 135

10. Suspended Sediment near the Seafloor (Moored Instruments) 143
10.1 Data 143
10.1.1 Data Quality 143
10.1.2 Suspended Sediment Concentrations 144
10.2 Summary 144

11. Grain Size of Seafloor Sediments 162
11.1 Data 162
11.2 Summary 163

12. Summary 164
12.1 Study Design 164
12.2 Instrumentation 164
12.3 Data and Results 164
12.4 Conclusion 166

References 167

Appendices

Appendix 1: Cruise Summary Report, Cruise CTDOT1
Appendix 2: Cruise Summary Report, Cruise CTDOT2
Appendix 3: Cruise Summary Report, Cruise CTDOT3
Appendix 4: Cruise Summary Report, Cruise CTDOT4
Appendix 5: Cruise Summary Report, Cruise CTDOT5
Appendix 6: Cruise Summary Report, Cruise CTDOT6
Appendix 7: Cruise Summary Report, Cruise CTDOT7
Appendix 8: Cruise Summary Report, Cruise CTDOT8
Appendix 9: Currents near the Seafloor: Data from the Nortek ADCP
Appendix 10: Profiling CTD Casts – Ship Surveys
Appendix 11: Velocity Profiles at all Mooring Stations for all Campaigns (RDI ADCP Data)
Appendix 12: Suspended Sediment and Particulate Organic Carbon Concentrations from Water Samples
Appendix 13: Sediment Grain Size Analysis Data Sheets

List of Tables

Table 1-1 Seasonal field observation periods (referred to as 'campaigns')

Table 1-2 Key terms used for field activities

Table 2-1 Field activities of the PO study

Table 2-2 Locations and water depths of survey stations

Table 2-3 RDI ADCP sampling configuration

Table 2-4 Activities during each ship survey at each of the 11 stations

Table 2-5 Calibration fits of the OBS3+ sensor

Table 2-6 Size classification used in grain size analysis

Table 2-7 Sources for wind and wave data

Table 2-8 Number of days with data from all moored instruments available for modeling

Table 5-1 Mean salinity during each campaign

Table 6-1 Statistics of near-bottom current observations

Table 7-1 Characteristics of principal tidal constituent (M2) at each mooring station for each deployment

Table 8-1 Wind speed statistics during the three campaigns

Table 8-2 Summary of wave field characteristics

Table 8-3 Significant wave height statistics during the three campaigns

Table 8-4 Mean dominant wave periods

Table 11-1 Grain size distribution at mooring stations

List of Figures

Figure 1-1 Zone of Siting Feasibility (ZSF)

Figure 2-1 Survey stations in the ZSF

Figure 2-2 Location of instruments in moored tripod frame, and a close-up of the OBS3+ mounts

Figure 2-3 OBS3+ sensor and Nortek ADCP connected to an OBS3+ sensor after a recovery

Figure 2-4 Example of a cruise track for ship surveys

Figure 2-5 Rosette of the *R/V Connecticut,* equipped with a profiling CTD, Niskin bottles, and various optical sensors and particle analyzers

Figure 2-6 Bottom sediment grab samplers used during the study

Figure 2-7 Suspended sediment concentrations versus raw counts used in the calibration of OBS 3+ sensors on May 23 (Stations DOT1,2,3,4,6,7) and June 7, 2013 (Station DOT5)

Figure 2-8 Suspended sediment concentrations versus raw counts used in calibration of OBS 3+ sensors for all seven DOT mooring stations, November 18, 2013

Figures 3-1 to 3-11 Temperature, conductivity, and density in the water column at Station CTD9, measured with the Profiling CTD.

Figure 4-1 Time-series view of the current velocity components from ship-based ADCP measurements during Cruise CTDOT1

Figure 4-2 Map of eastern Long Island Sound and Block Island Sound with vectors representing the currents observed by the *R/V Connecticut* during Cruise CTDOT1

Figure 4-3 Smoothed fit for residual velocities at 5 m below MLLW (red) and 'de-tided' velocities at moorings (black)

Figures 5-1 to 5-7 Measurements of near-bottom temperature at Stations DOT1 to DOT 7 during the three campaigns

Figures 5-8 to 5-14 Measurements of near-bottom salinity at Stations DOT1 to DOT 7 during the three campaigns

Figure 5-15 Low-pass filtered records of near bottom temperature in eastern Long Island Sound at Stations DOT1, DOT2, DOT3, and DOT7 for Campaigns 1, 2 and 3

Figure 5-16 Low-pass filtered records of near bottom temperature in eastern Long Island Sound at Stations DOT4, DOT5, and DOT6 for Campaigns 1, 2 and 3

Figure 5-17 Low-pass filtered records of near bottom salinity in eastern Long Island Sound at Stations DOT1, DOT2, DOT3, and DOT7 for Campaigns 1, 2 and 3

Figure 5-18 Low-pass filtered records of near bottom salinity in eastern Long Island Sound at Stations DOT4, DOT5, and DOT6 for Campaigns 1, 2 and 3

Figure 6-1 M2 tidal ellipses for all station , plotted on top of local bathymetry

Figure 6-2 Full velocity profiles and surface elevation at Station DOT7 for four days

Figure 6-3 Low-pass filtered velocities for Station DOT5, Campaign 2

Figure 6-4 Time-series of (a) water depth, (b) depth-average velocity components, (c) bottom temperature, and (d, e) profiles of time-averaged velocities for all three field campaigns at Station DOT1

Figure 6-5 Eastward and northward components of the current observed at 3.54m above the bottom at Station DOT2 during Campaign 2

Figure 6-6 Mean currents at bin 3 of the RDI ADCP measurements during all campaigns

Figure 7-1 Significant wave height H_s at Station DOT5 during Campaign 3 measured by the RDI ADCP, and the bottom stress τ estimated from the log law

Figure 7-2 The variation of $u(z)$ with log(z) for ensembles 297 and 317 in Figure 7-1

Figure 7-3 Ensemble mean currents at bin 5, 0.565m above the bottom, at Station DOT4 in Campaign 1

Figure 7-4 Ensemble mean currents at bin 5, 0.565m above the bottom, at Station DOT4 in Campaign 2

Figure 7-5 Mean velocity vectors at each moored station from the Nortek ADCP immediatle near the bottom

Figure 7-6 M2 tidal ellipses for Campaign 1 at each moored station

Figure 7-7 Time-series of bottom pressure, temperature, battery voltage and the OBS sensor outputs (counts) from Station DOT4, Campaign 1

Figure 7-8 Time-series of bottom pressure, temperature, battery voltage and the OBS sensor outputs (counts) from Station DOT4, Campaign 2

Figures 7-9 to 7-29 Characteristics at all DOT stations during all campaigns

Figure 8-1 Time-series of the observed wind speed at meteorological stations CLIS, ELIS, LEDG, and 44017 during the three campaigns

Figures 8-2 to 8-20 Wave conditions at all DOT stations during all campaigns

Figure 8-21 Cumulative Probability Distribution Function (CPDF) of significant wave heights during Campaign 1 for each station

Figure 8-22 Cumulative Probability Distribution Function (CPDF) of significant wave heights during Campaign 2 for each station

Figure 8-23 Cumulative Probability Distribution Function (CPDF) of significant wave heights during Campaign 3 for each station

Figure 8-24 Time-series of the observed significant wave height at metocean Stations CLIS, CDIP, and 44017 during the three campaigns

Figure 8-25 Time-series of the observed dominant wave periods at metocean Stations CLIS, CDIP, and 44017 during the three campaigns

Figure 9-1 Suspended sediment concentration data determined from water samples collected during Campaign 1 at approximately one meter off the bottom (BTM)

Figure 9-2 Suspended sediment concentrations and particulate organic carbon concentrations determined from water samples collected during Campaign 2

Figure 9-3 Suspended sediment concentrations and particulate organic carbon concentrations determined from water samples collected during Campaign 3

Figure 9-4 Beam attenuation measured at 650 nm plotted against SSC for data collected during the Cruises CTDOT3 (June) and CTDOT5 (August)

Figure 9-5 The slope of total particle light scatter, measured between 532 nm and 650 nm

Figures 9-6 to 9-12 Suspended sediment concentrations, slope of particle size spectrum and chlorophyll-a concentration during Cruises CTDOT1, 2, and 3 all DOT stations

Figures 10-1 to 10-7 Digitized data from the OBS3+ sensors at all DOT stations for all campaigns

Figure 10-8 Response of the OBS3+ sensor (counts) at Station DOT1 from an hour on March 18, 2013

Figures 10-9 to 10-15 Suspended sediment concentrations (SSC) estimated by applying the coefficients in Table 2-5 to the OBS3+ observations at all DOT stations for all campaigns

Figure 10-16 Time-series of the screened, and bin-averaged OBS3+ observations at eastern Long Island Sound Stations DOT1, 2, 3, and 7

Figure 10-17 Time-series of the screened, and bin averaged OBS3 observations at Block Island Sound Stations DOT4, 5, and 6

Acronyms and Abbreviations

ADCP	Acoustic Doppler current profiler
BIS	Block Island Sound
CDIP	Coastal Data Information Program
C.F.R.	Code of Federal Regulations
CLDS	Central Long Island Sound Disposal Site (formerly abbreviated as CLIS in the literature)
CLIS	Central Long Island Sound
cm	centimeter
CSDS	Cornfield Shoals Disposal Site (formerly abbreviated as CFDS in the literature)
CTD	Conductivity/temperature/depth sensor
CTDEEP	Connecticut Department of Energy and Environmental Protection
CTDOT	Connecticut Department of Transportation
EIS	Environmental Impact Statement
ELIS	Eastern Long Island Sound
FVCOM	Finite Volume Coastal Ocean Model (The model, nested within the University of Massachusetts-Dartmouth Regional Model, was used as the primary model for assessing the bottom stress, salinity, temperature, currents, waves, and horizontal circulation based on the data collected during the Physical Oceanographic study. The model is not commercially available.)
GPS	Global Positioning System
LEDG	Ledge Light meteorological station
LIS	Long Island Sound
LTFATE	Long Term FATE (USACE model that simulates the evolution of dredged material mounds by erosion and bed load transport. This secondary model will not be used to in this modeling report.
m	meter
μm	micrometer
NEPA	National Environmental Policy Act
NLDS	New London Disposal Site
NOAA	National Oceanic and Atmospheric Administration

Nortek ADCP	Downward-looking Nortek Aquadopp HR 2-Hertz ADCP
OBS3+ sensor	Campbell Scientific OBS3+ optical backscatter sensor
PO	Physical oceanography
POC	Particulate Organic Carbon
Profiling CTD	Sea-Bird Electronics Model 9 CTD with a Model 11 deck unit
QAPP	Quality Assurance Project Plan
RDI	RD Instruments
RDI ADCP	Upward-looking Sentinel Workhorse ADCP from RD Instruments
RISDS	Rhode Island Sound Disposal Site
SBE 19+	Sea-Bird Electronics Model 19+ profiling CTD
SBE SMP37	Sea-Bird Electronics Model SMP37 instrument
SEIS	Supplemental Environmental Impact Statement
STFATE	Short-Term FATE (USACE model simulating water column concentration of dredged material and any associated chemical contaminants when the material is released from a barge. This secondary model will not be used to in this modeling report.
UCONN	University of Connecticut
USACE	U.S. Army Corps of Engineers
USEPA	U.S. Environmental Protection Agency
USGS	U.S. Geological Survey
WavesMon	RDI's proprietary wave modeling software
WLDS	Western Long Island Sound Disposal Site (formerly abbreviated as WLIS in the literature)
ZSF	Zone of Siting Feasibility

[This page intentionally left blank.]

EXECUTIVE SUMMARY

The purpose of the Physical Oceanography (PO) study was to assess the physical oceanographic characteristics in the eastern Long Island Sound (ELIS) and Block Island Sound (BIS) in support of the Eastern Long Island Sound Supplemental Environmental Impact Statement (SEIS)[1]. Specifically, the study assessed the circulations patterns, stress from the movement of water on the sediments at the seafloor, and sediment transport. It included collection of data in the field during different seasons as well as modeling of worst-case storm conditions. The area of the ELIS and BIS is referred to as the Zone of Siting Feasibility (ZSF). The SEIS is prepared by the U.S. Environmental Protection Agency (USEPA) for the potential designation of one or more dredged material disposal sites in the ZSF. The PO study was supported by the Connecticut Department of Transportation (CTDOT). This first report of the PO study is a summary of the field program and collected data.

Characterizing potential disposal sites in the ZSF requires an understanding of the relationships between tidal forcing, freshwater inflow, salinity patterns, and the range and nature of circulation. There are three important regimes of forcing of the circulation in the ZSF: spring with high river discharge and high winds, summer with low winds but with the freshest waters, and winter with low river flows and strong winds. Field data were collected during each of these seasons. Specifically, the field data collection consisted of a combination of continuous data recordings at seven stations with moored instrument arrays throughout the ZSF, as well as eight ship surveys and instrument casts at eleven stations. In addition, wind, wave, and river discharge data were obtained from secondary data sources and included in the data analysis.

Data collected and methods used consisted of the following:

- Temperature and salinity, measured with conductivity/temperature/density sensors (CTDs) both at the seven mooring stations and during the ship surveys.
- Currents in the water column and at the sea floor, measured with acoustic Doppler current profiler (ADCPs)[2] both at the seven mooring stations and during the ship surveys.
- Suspended sediment concentrations and characteristics in the water column and near the seafloor at eleven stations, measured through optical instruments and through water samples with subsequent laboratory analysis.
- Wind and wave conditions, determined from wave data by the seven moored ADCPs and from wind and wave data collected by several meteorological and ocean data buoys within and outside of the ZSF. The buoys are operated by the National Oceanographic and Atmospheric Administration (NOAA), the U.S. Army Corps of Engineers (USACE), and the University of Connecticut (UCONN).
- Sediment grain size of bottom sediments at the mooring stations, using a grab sampler for

[1] The SEIS supplements the EIS prepared in 2004 for the designation of the dredged material disposal sites in the Central and Western Long Island Sound (CLDS and WLDS) (USEPA and USACE, 2004a).

[2] An ADCP is a hydroacoustic current meter that measures water current velocities over a depth range using the Doppler effect of sound waves scattered back from particles within the water column.

the assessment of the potential for bed level changes and future evaluation of sediment resuspension models.

These collected PO data will be used to assess sediment transport and characterize the physical oceanographic conditions in the ZSF, using the unstructured grid Finite Volume Coastal Ocean Model (FVCOM), nested within the University of Massachusetts-Dartmouth Regional Model[3]. Modeling will determine bottom shear stresses and water circulation in the ZSF since these factors determine the erosion potential of the sediment, particularly during worst-case storm events such as in the late fall, winter, and spring months. The modeling approach and findings will be prepared as a separate second report as part of the PO study[4].

[3] FVCOM was developed jointly by the University of Massachusetts-Dartmouth and the Woods Hole Oceanographic Institution; see *http://fvcom.smast.umassd.edu/FVCOM/index.html* for additional information.

[4] *Physical Oceanography of Eastern Long Island Sound Region: Modeling Report* (in preparation)

1. Introduction

1.1 Background

The objective of the Physical Oceanography (PO) study was to assess the physical oceanographic characteristics (circulation patterns, stress from the movement of water on the sediments at the seafloor, and sediment transport) in the eastern Long Island Sound (ELIS) and Block Island Sound (BIS). The area of the ELIS and BIS is referred to as the Zone of Siting Feasibility (ZSF), which is evaluated in a Supplemental Environmental Impact Statement (SEIS) prepared by the U.S. Environmental Protection Agency (USEPA) for the potential designation of one or more dredged material disposal sites. The PO study was supported by the Connecticut Department of Transportation (CTDOT).

The ZSF, shown in Figure 1-1, contains the active New London and Cornfield Shoals Disposal Sites (NLDS and CSDS), as well as several historic disposal sites. The closest active dredged material disposal site outside of the ZSF is the Rhode Island Sound Disposal Site (RISDS). This site, as well as the Central and Western Long Island Sound Disposal Sites (CLDS and WLDS), have been designated by the USEPA.

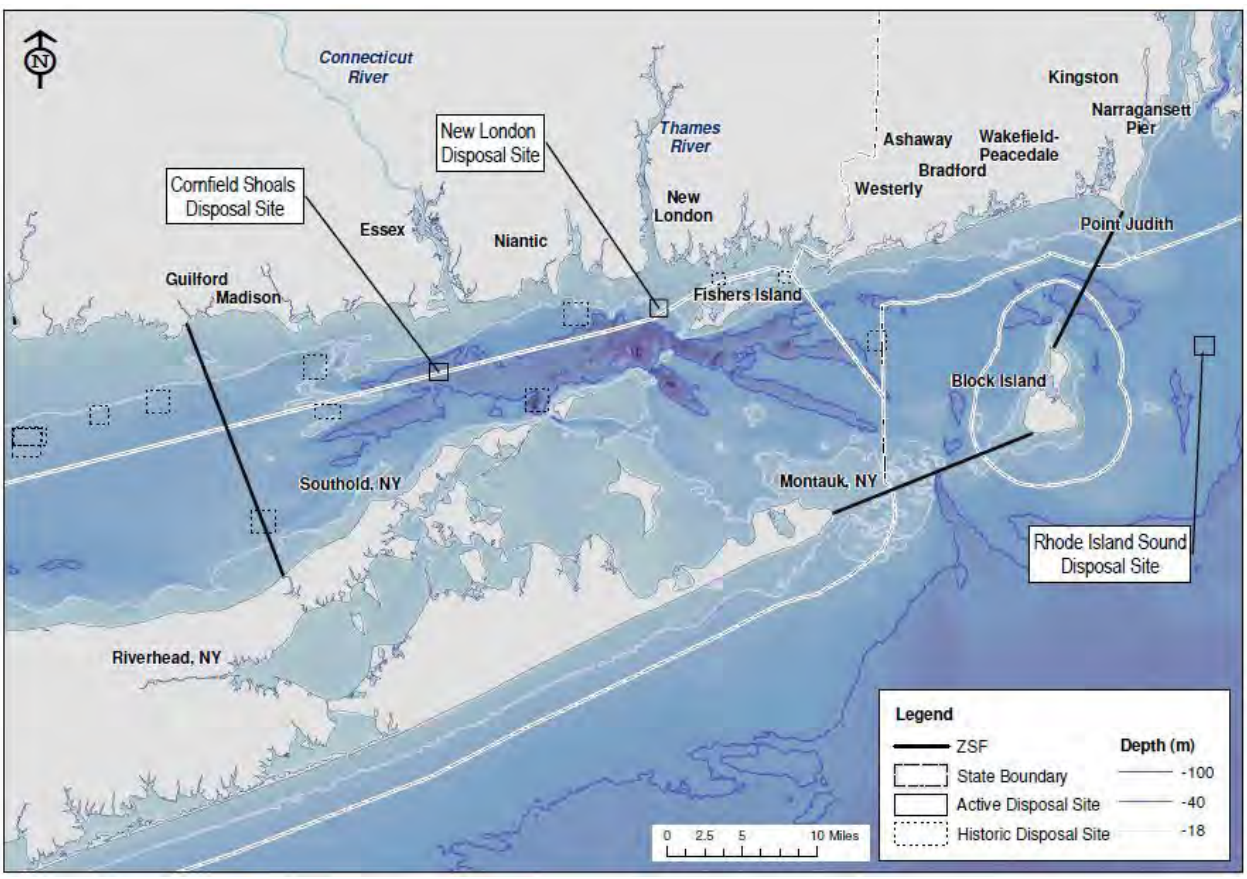

Figure 1-1. Zone of Siting Feasibility (ZSF). The background of the map represents bathymetry.

The SEIS is being prepared in accordance with Section 102(c) of the Marine Protection Research and Sanctuaries Act (MPRSA; also referred to as Ocean Dumping Act [ODA]) of 1972. The USEPA has the responsibility of designating sites under Section 102(c) of the Act and 40 C.F.R. Part 228.4 of its regulations. The PO study supplements work previously conducted in the region as part of the Long Island Sound and Rhode Island Sound Environmental Impact Statements (EIS) for the CLDS, WLDS, and RSDS (USEPA and USACE, 2004a, 2004b).

1.2 Study Overview

Waves and currents determine the bottom stress and the potential for sediment erosion, settling, and resuspension of the deposited materials, and thus also affect the fate and transport of disposed dredged material. Current magnitudes and wave parameters in the ELIS and the BIS vary seasonally and there are substantial interannual variations associated with meteorological conditions. The delivery of freshwater to the ELIS in the spring largely determines the salinity patterns and dominates the variability in the circulation. Large rain events in the watershed (e.g., from hurricanes) also change the circulation and the suspended sediment distribution in the ZSF. Therefore, the PO study included collection of data in the field during different seasons as well as modeling of storm conditions, particularly during worst-case storm events such as in the late fall, winter, and spring months.

To resolve the effect of the range of river discharge and wind patterns on the circulation and hydrography in the ZSF, six months of field observations over three approximately two-month long periods were conducted (Table 1-1). These periods are herein referred to as 'Campaigns'; a summary of all key terms used for field activities is provided in Table 1-2. Campaign 1 spanned the March to May (spring) high river discharge period. Campaign 2 spanned June to the beginning of August (summer) period with low discharge and low wind conditions. Campaign 3 spanned the November to January (winter) period with high winds.

Table 1-1. Seasonal Field Observation Periods (referred to as 'Campaigns')

Campaign	Period	Interval	Conditions
1	Spring	March 12 - May 17, 2013 (66 days)	High river discharge
2	Summer	June 11 - August 8, 2013 (58 days)	Low flow, Low wind
3	Winter	November 20, 2013 - January 16, 2014 (57 days)	Low flow, High wind

The field program of the PO study provided data to address the spatial (north-south and east-west) and temporal variability of hydrography, currents, bottom stress, and sediment characteristics through a combination of ship instrument surveys and long-term moored instrument deployments. Collected data needed to characterize the area included temperature, salinity, current parameters, wave parameters, the characteristics of sediment particles in the water column and on the seafloor, and wind patterns. The field program consisted of the following components:

- **Deployed Moorings:** Instrument moorings were deployed at the bottom of seven stations

during each campaign. Each mooring included an upward-looking acoustic Doppler current profiler (ADCP) and bottom pressure sensor to measure the current structure, sea level, and wave parameters; a downward-directed near-bottom acoustic current meter to measure the current near the seafloor; and two optical backscatter sensors to estimate suspended sediment concentrations near the bottom.

- **Ship Surveys:** Ship surveys were made in conjunction with recovery and deployment operations for the instrument moorings. The surveys consisted of water column measurements with profiling and undulating CTDs, optical sensors, and ship-mounted ADCPs to assess current velocity magnitudes and directions throughout the water column; water sampling to estimate bottom suspended sediment concentrations; and bottom sediment sampling to determine grain size as input to the modeling effort.

Table 1-2. Key Terms used for Field Activities

Term	Explanation
Campaign	Period of mooring deployments during three seasons: spring (Campaign 1), summer (Campaign 2), and winter (Campaign 3). Each campaign was approximately two months long.
Cruise	Each time the ship conducted field activities in the ZSF. A cruise consisted of two parts: (1) Deployment or recovery of 'Moorings', and (2) Measurements of water column parameters and sampling of sediment as part of 'Ship surveys'). There were a total of eight cruises (Cruises CTDOT1-8), each lasting 1 to 3 days.
Mooring	An instrument frame moored on the seafloor at seven stations. Each frame included several oceanographic instruments, including ADCPs. Mooring stations are labeled DOT1-7*.
Deployment	Period during which the seven instrument moorings were moored on the seafloor between each deployment and recovery during a cruise. There were five deployments during the PO study. Campaign 1 was a single continuous deployment (Deployment 1). There were two consecutive deployments during both Campaign 2 (i.e., Deployments 2 and 3) and Campaign 3 (i.e., Deployments 4 and 5), as the moorings were recovered halfway through these two campaigns and generally redeployed within an hour after instrument maintenance.
Ship survey	Data and samples collected from the ship using various instruments at eleven stations; these stations consisted of the seven mooring stations (DOT1-7) and 4 additional stations (CTD8-11*; added to broaden the range of current and hydrographic measurements). Instruments used at these 11 stations during ship surveys included profiling CTDs, optical sensors, and a ship-mounted ADCP.

* The station locations were approved by the Cooperating agency representatives prior to the study.

These data were augmented with observations of waves and meteorology acquired by data buoys within and outside of the ZSF, operated by the National Oceanographic and Atmospheric Administration (NOAA), the USACE, and the University of Connecticut (UCONN). In addition, NOAA-funded buoys , and river discharge rates determined by the U.S. Geological Survey (USGS) were used in the study.

The study approach and station locations were presented to federal and state agencies on May 20, 2013 for review and comment. Comments were integrated in the final study plan. Prior to the study, a Quality Assurance Project Plan (QAPP) was prepared. The QAPP was approved by the USEPA on May 21, 2013.

1.3 Use of Field Data for Modeling

The site designation process for dredged material disposal sites requires that all alternatives in the ZSF be considered. Of particular concern are the magnitude and pattern of the near-bottom currents and bottom shear stress since these factors determine the erosion and transport potential of the sediment, particularly during worst-case storm events. Since it is impossible to make observations everywhere, we will use a numerical model to assess and compare the suitability of potential sites. To verify the effectiveness of the model, predictions must be compared to data from areas of high stress and areas of low stress and the results must show that errors are smaller than the differences between sites. The PO data described in this Field Data Report will be used to characterize the physical oceanographic conditions in the ZSF and, in particular, evaluate the predictions of the bottom shear stresses and water circulation. Since the stations selected for the field observations were intended for model evaluation, rather than site evaluation, an extensive description of the results is unwarranted. Therefore, this report describes the methods and the data collected. Note that the suspended and bottom sediment sampling was conducted during the field program of the PO study so that the data would be available for later analysis of sediment transport model results that will be conducted when sites have been selected.

The PO modeling results will be prepared as a separate report[5]. Specifically, modeling will use the Unstructured Grid Finite Volume Coastal Ocean Model (FVCOM), nested within the University of Massachusetts-Dartmouth Regional Model[6], to simulate/interpolate bottom stress magnitudes, salinity, temperature, currents, waves and horizontal circulation between PO measurement stations and data collection timeframes. Thereafter, the stress and current distribution predictions from FVCOM will be used to drive the USACE models Short Term Fate (STFATE) and Long Term Fate (LTFATE)[7]. STFATE models sediment transport during disposal. LTFATE models long-term transport of resuspended sediment from disposal mounds. The collected field data and output from these two models will assist further in the consideration of potential sites for dredged material disposal.

---

[5] *Physical Oceanography of Eastern Long Island Sound Region: Modeling Report* (in preparation)

[6] FVCOM was developed jointly by the University of Massachusetts-Dartmouth and the Woods Hole Oceanographic Institution; see *http://fvcom.smast.umassd.edu/FVCOM/index.html* for additional information.

[7] STFATE and LTFATE were developed by the USACE's Dredging Operations and Environmental Research (DOER) Program.

1.4 Report Organization

This Field Data Report describes the details of the field program of the PO study and summarizes the data collected. The methodology used during the field program, sample analyses, and data processing are described in Chapter 2; this chapter also provides details about the instrumentation used. The collected data are presented in Chapters 3 to 11. Chapter 3 describes measurements of the spatial structure of water temperature and salinity made by ship surveys. These data will be used to assess whether the model represents the seasonal variation in the water density which is an important factor in the determination of the non-tidal circulation. The ship surveys also acquired current measurements from a hull-mounted ADCP to assess prediction of the spatial structure of the flow, a critical factor in the prediction of the dispersion of materials; these observations are described in Chapter 4. The instrument moorings included salinity and temperature sensors and the data are described in Chapter 5; these measurements are also used to assess the model predictions of water density and temperature.

The evolution of the vertical structure of the currents was measured by an moored ADCP (manufactured by RDI) at each station that were oriented upward, to measure the velocity from approximately 3 m above the seafloor to near the water surface, and another ADCP (manufactured by Nortek) that was oriented downward to measure velocities between 75 cm and the seafloor. The Nortek ADCP also allowed measurement of bottom stress. The RDI ADCP data are described in Chapter 6 and the Nortek ADCP measurements are described in Chapter 7.

The RDI ADCP also measured wave characteristics which are described in Chapter 8. This chapter also contains a summary of wind and wave observations acquired at buoys in or near the ZSF. The ship surveys included optical measurements and water sample collection to determine the suspended material concentrations and these data are described in Chapter 9. Optical measurements were acquired by the moored instruments and these data are reported in Chapter 10.

The character of bottom sediments at the stations where instruments were deployed is described in Chapter 11. This information is essential for three reasons: to assess whether the distance the current meter was located above the seafloor is likely to change as a consequence of sediment transport; to guide the interpretation of the stress measurements; and for later evaluation of sediment transport models.

The results of the study are summarized in Section 12. Field reports of the eight cruises are included in Appendices 1 to 8. Detailed data complementing the information in several of the chapters are presented in Appendices 9 to 13.

2. Methodology

2.1 Field Program

2.1.1 Overview

The three campaigns required eight ship cruises for the ship surveys and for the deployment and recovery of instrument moorings. Activities performed during the field program of the PO study are provided in Table 2-1 and are described further below (see Table 1-2 for definition of terms used during these field activities). Cruise reports for each of the eight cruises are provided in Appendices 1 to 8.

Ship surveys included 'full' and 'limited' ship surveys (Table 2-1). Full ship surveys consisted of several different types of sampling and measurements (see Table 2-4 for further detail) and were performed once or twice during each campaign. One bullet in Table 2-1 indicates that each of the 11 ship survey stations was occupied once; two bullets indicate that each station was occupied twice at different times during the respective cruise to obtain additional data. A 'limited" ship survey consisted of only CTD casts at the seven mooring stations.

Table 2-1. Field Activities of the PO Study

Campaign No.	Cruise No.	Vessel	Dates	Moorings				Ship Surveys	
				Deployment	Recovery	Redeployment	Deployment No. *(1)*	Full Surveys *(2)*	Limited Surveys
1	CTDOT1	*R/V Connecticut*	March 12-13, 2013	●			1	●●	
	CTDOT2	*R/V Connecticut*	May 17, 2013		●			●	
2	CTDOT3	*R/V Connecticut*	June 11-12, 2013	●			2	●●	
	CTDOT4	*R/V Weicker*	July 10, 11, 16, 2013		●	●	3		●
	CTDOT5	*R/V Connecticut*	August 7-8, & 13		●			●●	
3	CTDOT6	*R/V Connecticut*	November 20-21, 2013	●			4	●●	
	CTDOT7	*R/V Connecticut*	December 12, 17-18, 2013		●	●	5		●
	CTDOT8	*R/V Connecticut*	January 15-16, 2014		●			●●	

(1) Deployment numbers were used for the data recording and processing of the data from the Nortek ADCPs, deployed at the seven mooring stations.

(2) ●: Each of the 11 ship survey stations was occupied once.
●●: Each station was occupied twice at different times during the respective cruise.

2.1.2 Instrument Moorings

The moorings with mounted instruments consisted of specially constructed tripod frames. These tripods were deployed during each campaign at seven stations (Figure 2-1; Table 2-2).

During Campaigns 2 and 3, maintenance cruises were added halfway through the deployment to change the batteries in the moored instruments (i.e., Cruises CTDOT4 and CTDOT7, respectively). This step was needed after it became apparent that some instruments moored during Campaign 1 had inadequate battery life, shortening the possible data collection duration. The manufacturer's model for the battery power drain had not adequately accounted for the processing required for logging the optical backscatter sensors. In subsequent campaigns we replaced the batteries by recovering the instruments after approximately 4 weeks (see Section 2.4.2 for further details). Moorings redeployed during Campaigns 2 and 3 were both located within about 100 m of the location occupied during Campaign 1, using dynamic positioning with the ship's GPS. This separation in locations did not affect the model evaluation since it was smaller than the model grid cells (i.e., the data were in essence acquired at the same model location).

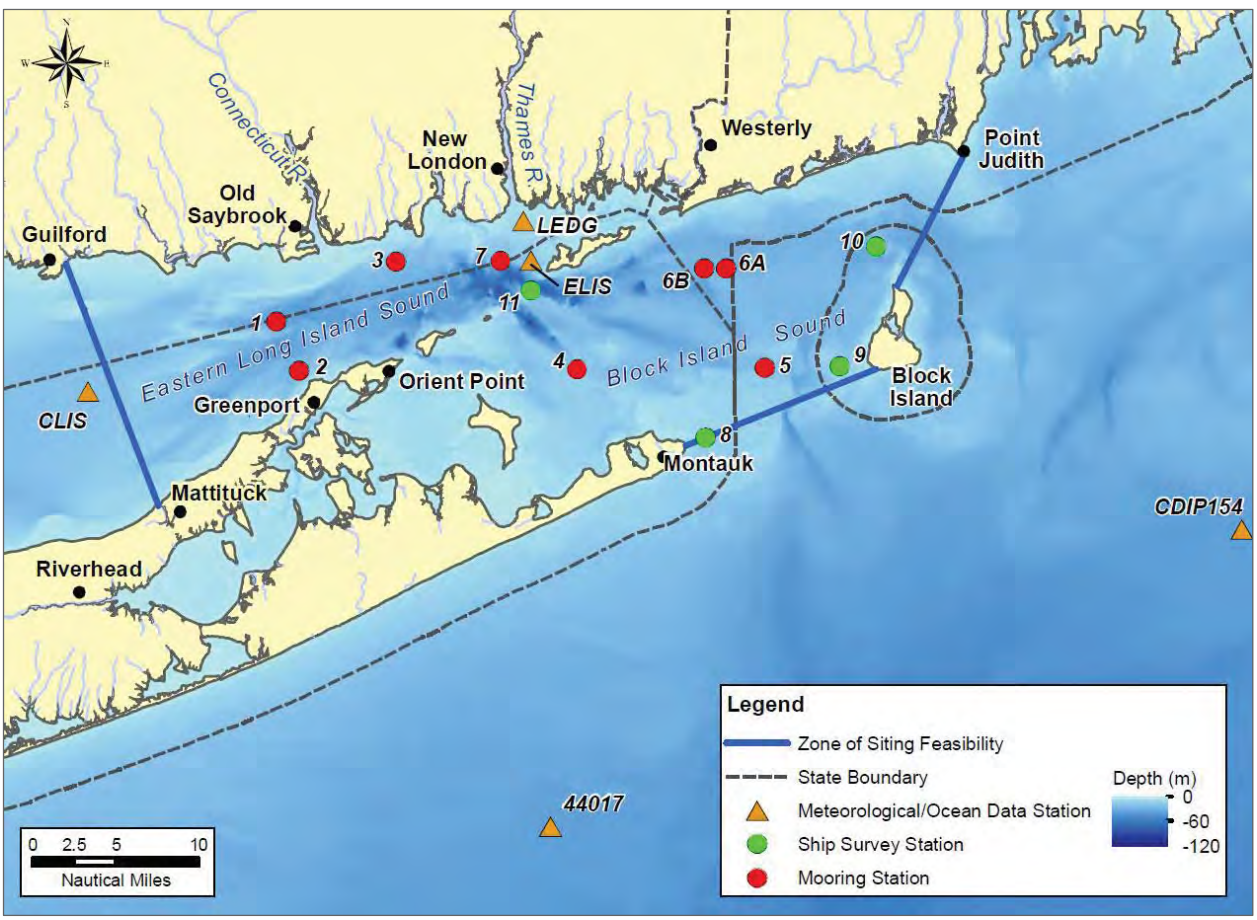

Figure 2-1. Survey stations in the ZSF, superimposed on bathymetry.

Table 2-2. Locations and Water Depths of Survey Stations *(1)*

Station	Moorings	Ship Surveys	Latitude *(2)*		Longitude *(2)*		Water Depth *(Mean low low water)*	
			deg.	deg. min.	deg.	deg. min.	m	ft
DOT1	●	●	41.20	41 12.0	72.40	72 24.0	36.6	120
DOT2	●	●	41.15	41 09.0	72.37	72 22.2	30.5	100
DOT3	●	●	41.26	41 15.5	72.24	72 14.5	27.1	89
DOT4	●	●	41.15	41 09.0	72.00	72 00.0	22.9	75
DOT5	●	●	41.15	41 09.0	71.75	71 45.0	30.5	100
DOT6A *(3)*	●	●	41.25	41 15.0	71.80	71 48.0	33.5	110
DOT6B *(3)*	●	●	41.25	41 14.9	71.83	71 49.9	34.0	112
DOT7	●	●	41.26	41 15.6	72.10	72 06.0	45.7	150
CTD8		●	41.08	41 04.9	71.83	71 49.6	13.0	43
CTD9		●	41.15	41 08.8	71.65	71 38.9	22.0	72
CTD10		●	41.27	41 16.2	71.60	71 36.0	36.0	118
CTD11		●	41.23	41 13.8	72.06	72 03.6	31.0	102

(1) Locations (lat./long.) of meteorological and ocean data buoys are included in Table 2-7.

(2) Latitude/longitude are from the first cruise (except for Station DOT6B). Lat/long for each mooring deployment and ship survey are included in the cruise reports (Appendices 1-8).

(3) Station DOT6 was relocated after Campaign 2 to avoid fish trawlers. The station is referred to as Station DOT6A for Campaigns 1 and 2, and as Station DOT6B for Campaign 3.

Four mooring stations were located to the west of The Race in eastern Long Island Sound; three stations were located to the east of The Race in Block Island Sound. During Campaigns 1 and 2, it appeared that the tripod at Station DOT6 (renamed to Station DOT6A) was struck by a fishing vessel, overturned and damaged. Data acquisition from both the RDI and Nortek ADCPs was terminated (see Section 2.4.2 for details). Therefore, the station was moved approximately 2 km to the west where fishing activity was expected to be less frequent. This modified station is herein referred to as Station DOT6B (Campaign 3).

Instruments on each mooring tripod frame (Figure 2-2) are described in more detail below for specific water column properties.

2.1.2.1 Temperature and Salinity (SBE SMP37)

A Sea-Bird Electronics (SBE) Model SMP37 instruments (herein referred to as SBE SMP37) was used at each mooring station to measure the temperature and salinity at 0.75 m above the seafloor (Figure 2-2). These data are used to assess near-bottom effects of storm and wind events and to quantify variability in the seasonal flow patterns. Data were recorded at 15-minutes intervals.

2.1.2.2 Waves and Currents in the Water Column (RDI ADCP)

An upward-looking Sentinel Workhorse ADCP from RD Instruments (herein referred to as RDI ADCP) with wave array sampling enabled was used at each mooring station for the simultaneous measurement of currents and waves in the water column. The RDI ADCP was positioned at 1.5 m above the seafloor. The RDI ADCP measures current magnitude and direction as well as the wave field above the Nortek ADCP (see Section 2.1.2.3). This yields a complete current profile of the water column and enables the determination of the amount of wave energy that contributes to the critical shear stress.

Current measurements by the RDI ADCP consisted of 180 pings sampled at 1 Hz. The number of bins and depth cell size varied slightly from station to station depending on the instrument frequency and water depth (Table 2-3). For the measurement of waves, the burst duration was set for 20 minutes.

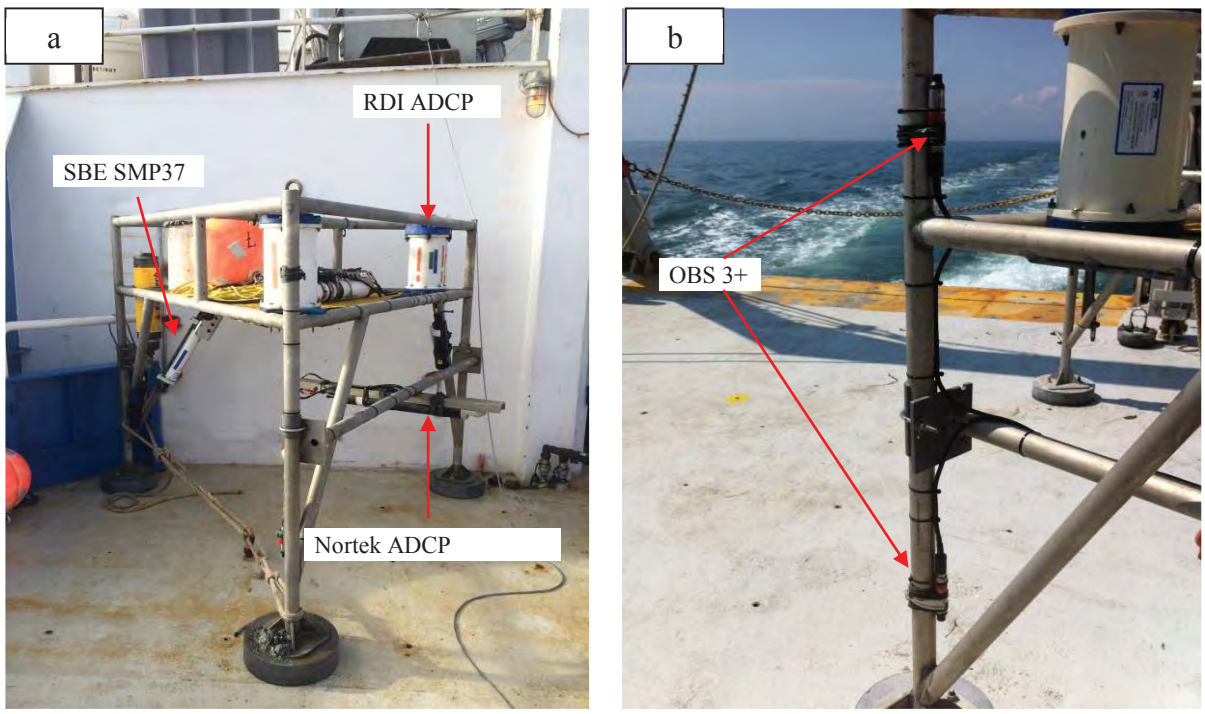

Figure 2-2. (a) Location of instruments in moored tripod frame, and (b) a close-up of the OBS3+ mounts.

2.1.2.3 Currents near the Seafloor (Nortek ADCP)

A downward-looking Nortek Aquadopp HR 2-Hertz ADCP (herein referred to as Nortek ADCP) was used at each mooring station to measure the currents near the seafloor. The instrument was positioned at 0.75 m above the seafloor, with the transducer directed downward toward the sediment. The Nortek ADCP measures current velocity at a high resolution in both space (cm scale) and time, which in combination with the optical backscatter sensors measuring suspended sediment concentration (see Section 2.1.2.4), enables the determination of the critical shear stress for initiation of erosion and transport of the bottom sediments.

Table 2-3. RDI ADCP Sampling Configuration

Station	Campaign 1			Campaign 2			Campaign 3		
	ADCP Freq. (kHz)	Current Bin Size (m)	Current n Bins	ADCP Freq. (kHz)	Current Bin Size (m)	Current n Bins	ADCP Freq. (kHz)	Current Bin Size (m)	Current n Bins
DOT1	300	1	40	300	1	40	300	1	40
DOT2	600	0.5	71	600	0.5	71	600	0.5	71
DOT3	300	1	32	300	1	32	600	0.5	66
DOT4	600	0.5	59	1200	1	26	1200	1	26
DOT5	600	0.5	71	300	0.5	71	600	0.5	71
DOT6A	600	1	40	600	1	40	–	–	–
DOT6B	–	–	–	–	–	–	600	1	40
DOT7	*	–	–	300	1	52	300	1	52

*The RDI ADCP for Station DOT7 was sent back to the manufacturer for repair and not deployed.

Specifically, the Nortek ADCP uses pulse-coherent signal processing (Rusello, 2009; Lacy and Sherwood, 2004) to estimate the mean current components in the direction of three beams emanating from the transducer head. The components are averaged in along-beam range bins and at sample rates specified in a configuration file. The uncertainty in the estimates and the velocity range of the instrument are determined by the bin size and sample rate (Nortek, 2008). Measurements are made at a high sampling frequency in order to resolve the wave and turbulence induced fluctuations. To allow long deployments, the Nortek ADCP can be configured in burst sampling mode in which intervals of high frequency sampling occur at selected times rather than continuously. The samples in each burst can be averaged to describe the slowly varying flow due to tides and winds while the high frequency data can be used to describe waves and turbulence.

The instrument produces measurements of the velocity component in the direction of each of the three beams in range cells (bins), together with the correlation level (a data quality index), and the acoustic backscatter intensity. These measurements, together with the water temperature and pressure at the instrument depth, are recorded and referred to as ‘raw data’.

As stated, the Nortek ADCP uses "pulse coherent mode processing" to obtain high accuracy estimates in small vertical averaging bins. This approach limits the maximum velocities that can be observed. Potentially, values outside the range can be reported as values inside the range. Nortek has developed an approach to limit the effect of this error, which they term Enhanced Velocity Range processing or EVR (Rusello, 2010). The approach intersperses the coherent mode acoustic pulses with ones of longer duration (the EVR pulse), which allow higher velocities to be estimated at 1/3 of the profile range. This preliminary velocity estimate is then used to resolve ambiguities in the measurements obtained from the shorter pulses.

An error in the manufacturer's power model for the instruments and the sampling parameters selected for the first deployment of the Nortek ADCPs led to an unexpectedly high power drain

and the batteries did not power the instruments for the whole duration. Approximately half of the data that were expected were recovered during Campaign 1; affected instruments consisted of the Nortek ADCP and the OBS3+ sensors (see additional discussion in Section 2.4.2 below). This issue was avoided during Campaigns 2 and 3 by changing batteries during maintenance cruises. The instrument configuration details are provided in the Cruise Reports (Appendices 1-8).

2.1.2.4 Suspended Sediment Concentrations near the Seafloor (OBS3+ sensors)

Connected to each Nortek ADCP were two Campbell Scientific OBS3+ optical backscatter sensors (herein referred to as OBS3+ sensors) to measure the suspended sediment concentration near the seafloor (Figures 2-2 and 2-3a). The two OBS3+ sensors were positioned at 0.30 m and 0.80 m above the seafloor during Campaign 1. Data review after Campaign 1 showed that there was little difference between the measurements (i.e., the suspended sediment concentrations) at elevations 0.30 and 0.80 m; therefore the upper sensor was moved to 1.37 m above the seafloor for Campaigns 2 and 3. The OBS3+ sensor measurements were logged by the Nortek ADCP that was connected to the sensors.

The OBS3+ sensor measures optical backscatter of near infra-red light which is proportional to the concentration of suspended sediment in close proximity to the sensor (Downing et al., 1981). The response of the instrument is sensitive to the size of the particles in suspension; therefore the calibration must be performed based on sediment characteristics of the deployment site. Sediment used in the calibrations of the OBS3+ sensors was collected from deposits trapped in the tripod frames at each station (Figure 2-3b); the sediment samples were bagged, labeled and stored at 4ºC until use. Sensor calibration is discussed in Section 2.2.1.4.

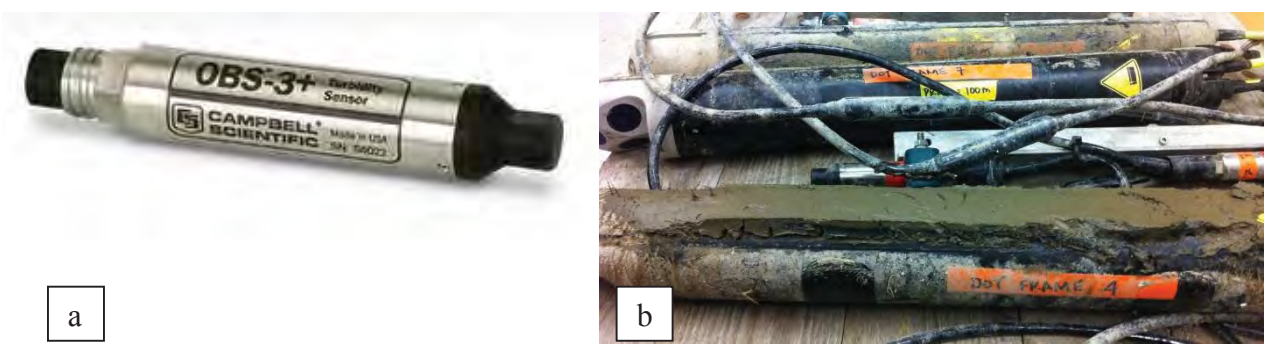

Figure 2-3. (a) OBS3+ sensor. (b) Nortek ADCP connected to an OBS3+ sensor after a recovery, showing sediment deposits used for calibration of the OBS3+ sensor.

2.1.3 Ship Surveys

The ship surveys were conducted at 11 stations (Figure 2-1), which consisted of the seven mooring stations and four additional stations to broaden the range of the current and hydrographic measurements. Cruise tracks varied during the eight cruises due to factors such as weather conditions and sea state. An example of a cruise track is shown in Figure 2-4.

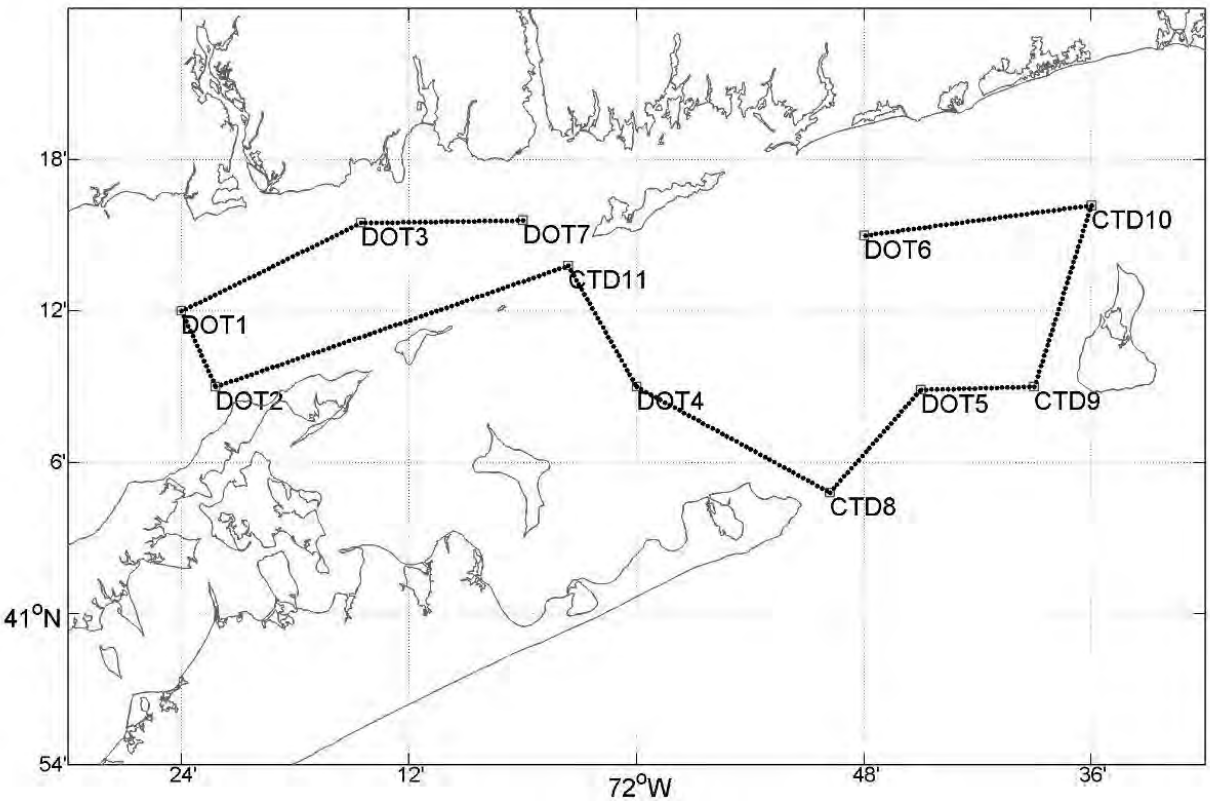

Figure 2-4. Example of a cruise track for ship surveys. The track varied for each cruise due to weather conditions and sea state.

Ship survey activities consisted of the following (Table 2-4):

- CTD measurements to determine temperature and salinity in the water column
- Continuous operation of a downward looking ADCP to measure currents
- Measurements and sampling of suspended sediment in the water column and near the seafloor
- Bottom sediment sampling for grain size

Sampling stations were visited twice during each cruise to provide additional data, except for Cruises CTDOT2, CTDOT4, and CTDOT7. Hydrographic profiles were obtained at all stations and at least one water sample was obtained at every station on each survey. Sediment grab samples were taken during three of the cruises (i.e., once for each campaign, encompassing the three different conditions: high river discharge (CTDOT1), low flow-low wind (CTDOT5), and low flow-high wind (CTDOT6). The activities during the ship surveys are described in more detail below. Additional information is available in the Standard Operating Procedures (SOPs), appended to the QAPP, as well as in the cruise reports attached herein (Appendices 1 to 8).

2.1.3.1 Temperature and Salinity (Profiling CTD)

A Sea-Bird Electronics Model 9 CTD with a Model 11 deck unit (SBE 9/11) was used for the collection of the salinity and temperature profiles at each of the eleven survey stations. The CTD was mounted on a SBE9 Rosette (Figure 2-5). The Rosette was lowered over the side of the ship by a winch with a conducting cable and the data logged on a computer. At a few stations, identified in Table 2-4, weather conditions prohibited using the SBE 9/11 rosette CTD and a smaller Sea-Bird Electronics Model 19+ (SBE19+) profiling CTD was hand-lowered instead. CTD casts from both instruments were combined during data processing and are therefore referred to herein as 'profiling–CTD'. The profiling CTD casts provided a means by which to quantify seasonal variability in the water column throughout the ZSF.

Table 2-4. Activities during each Ship Survey at each of the 11 Stations

Cruise No.	Campaign	Profiling CTD		Downward-looking ADCP	Water Sampling	Sediment Sampling *(7)*
		with Optical Instruments	without Optical instruments			
CTDOT1	1		●●*(1)*	●●	●●	●
CTDOT2			●	●	●	
CTDOT3	2	●●*(2)*		●●	●●	
CTDOT4			●*(3)*			
CTDOT5		●●		●●	●●	●*(8)*
CTDOT6	3	●●		●●	●●	●
CTDOT7			●*(4)*	●	●	
CTDOT8		●●*(5,6)*		●●	●●	

● Activity was performed once, as stations were visited only once during each cruise.
●● Activity was performed twice as stations visited twice during each cruise, using a SBE9/11 CTD.
(1) SBE 19+ CTD hand-lowered at Stations CTD8, CTD11 and DOT7, during first visit, due to poor weather.
(2) SBE 19+ CTD hand-lowered at Stations CTD8, CTD9 and DOT5, during first visit due to poor weather.
(3) SBE 19+ CTD used at the seven moored stations only, battery replacement cruise off *R/V Weicker*.
(4) SBE 19+ CTD at the seven moored stations only, battery replacement cruise.
(5) SBE 19+ CTD hand-lowered at Station CTD8, first visit, due to poor weather.
(6) No CTD data at Station DOT4 during second visit due to instrument problem.
(7) Sediment was collected once during each campaign which was considered representative for modeling sediment transport.
(8) No bottom grab samples at Stations CTD 9 (bottom substrate too hard) or CTD 11 (current too strong).

2.1.3.2 Currents throughout the ZSF (RDI ADCP)

A RDI ADCP (600 kHz Broadband), mounted on the ship's hull, was used to measure current magnitudes and directions over the entire water column, providing a means to assess seasonal variability in the flow field. The RDI ADCP was started once the *R/V Connecticut* was underway from Avery Point in Groton. The instrument was run continuously throughout each survey cruise. Data were logged by the software VmDas (RDI, Vessel Mounted Data Acquisition System). The RDI ADCP was configured to ping as fast as possible (0.3 sec/ping), with 50 1-m bins. The transducer depth was at 1.5 m and the blanking distance was 0.88 m. The top bin was centered at 3.42 m.

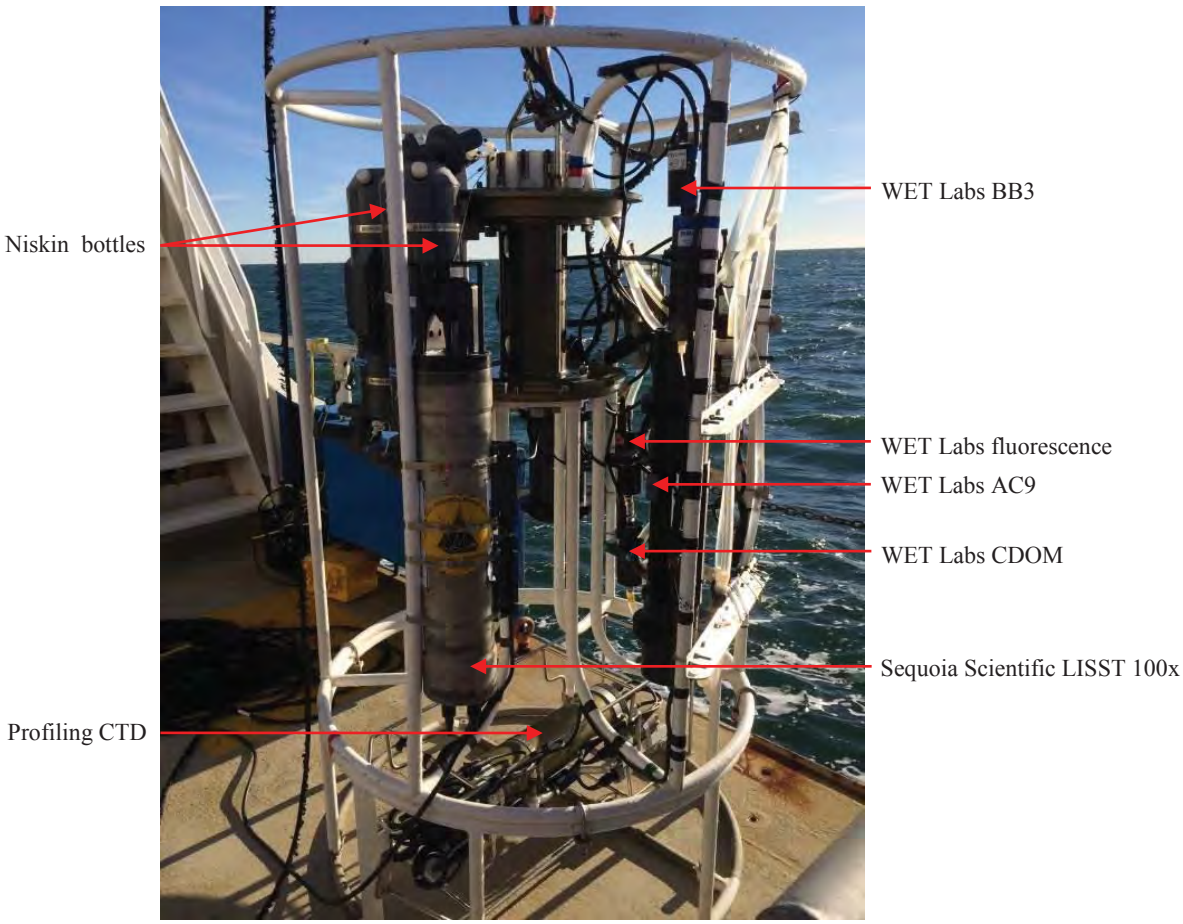

Figure 2-5. Rosette of the *R/V Connecticut,* equipped with a profiling CTD, Niskin bottles, and various optical sensors and particle analyzers. An additional CTD (not visible in the figure) was attached to the Rosette (SBE Model 25) specifically for use during the particulate organic carbon (POC) data analysis.

2.1.3.3 Optical Suspended Sediment Measurements in the Water Column (WET Labs sensors)

Attached to the Rosette were optical sensors to measure several characteristics of the suspended particulate matter in the water column at the 11 survey stations. Specifically, the optical sensors included a WET Labs BB3 (Model ECO Triplet - wavelengths of 450, 520 and 650 nm), a WET Labs AC9 absorption and attenuation meter, a WET Labs Fluorescence meter (Model ECO FL - chlorophyll-a concentrations), a WET Labs CDOM sensor (Model WETStar – colored dissolved organic matter concentrations), and a Sequoia Scientific Type C LISST100x particle size analyzer (Figure 2-5). The data from the optical sensors were logged by a custom data system manufactured by WET Labs.

The WET Labs AC9 were calibrated prior to each cruise. The instrument measures in-situ optical absorption and beam attenuation of water impurities; signals are referenced to clean water. Clean water calibrations were performed according to WET Lab prescriptions (WET Labs, 2011) prior to and after each survey using clean water from a milliQ water filtration system. The resulting clean water signals were subtracted from the in-situ signals in order to derive referenced impurity signals**.** The WET Labs BB3 sensors were calibrated after each cruise using the sediment from the bottom grabs collected at each station. The sensors were immersed in water of different suspended sediment concentrations; readings were then compared with the raw counts. A least squares fit was applied to allow for the conversion from counts to suspended sediment concentrations (SSC). The WET Labs fluorometer and CDOM sensor were factory-calibrated prior to the surveys. The Sequoia LISST 100x required initialization in clear water for 24 hours, similar to the AC9, prior to each cruise.

In addition, temperature and salinity data specifically for the POC data analyses were collected with a Sea-Bird Electronics Model 25 CTD (herein referred to as SBE Model 25) during Campaigns 2 and 3; the instrument was mounted on the Rosette.

2.1.3.4 Water Sampling for Suspended Sediment and Particulate Organic Carbon Concentrations

Water samples from the sea floor and the water column were collected at all 11 stations to be analyzed for suspended sediment concentrations (SSC) and particulate organic carbon concentrations (POC). During Campaign 1, water samples were collected at the bottom (1 m above seafloor), using a single 5-liter Niskin bottle lowered by winch. Approximately one minute was allowed to pass so that any sediment suspended by the Rosette was carried away by currents before closing the Niskin bottle.

In Campaigns 2 and 3, four additional samples were collected from various water depths (surface, mid-depth, and 4 m and 2 m from the seafloor) for calibration of the optical methods for suspended sediment distributions in anticipation of future modeling studies. These additional samples were collected using a 5-liter Niskin bottle that was attached to the Rosette used also for the CTD casts (Figure 2-5).

On deck, one liter of water each was withdrawn from each Niskin bottle for SSC and POC analyses. SSC samples were stored in rinsed one liter, clear polystyrene bottles. POC samples were stored in one liter, amber polystyrene, acid-washed bottles. All samples were labeled and

refrigerated at 4˚C immediately upon collection. Samples were collected at all stations on both survey loops when possible.

2.1.3.5 Grain Size of Seafloor Sediment

Bottom sediment samples were collected during all three campaigns using a galvanized modified Van Veen type grab (Campaigns 1 and 2), or a stainless modified Smith-Macintyre style grab sampler (Campaign 3) (Figure 2-6). Samples were collected for analysis of sand to mud (silt+clay) ratios. The grab samplers were deployed using the *R/V Connecticut's* A-frame. After retrieval of the bottom sediment sample, a scoop was used to transfer approximately 2000 grams to a one-gallon Ziploc bag, which was then labeled and refrigerated at 4˚C. Bottom grab samples were collected at all stations once on each campaign.

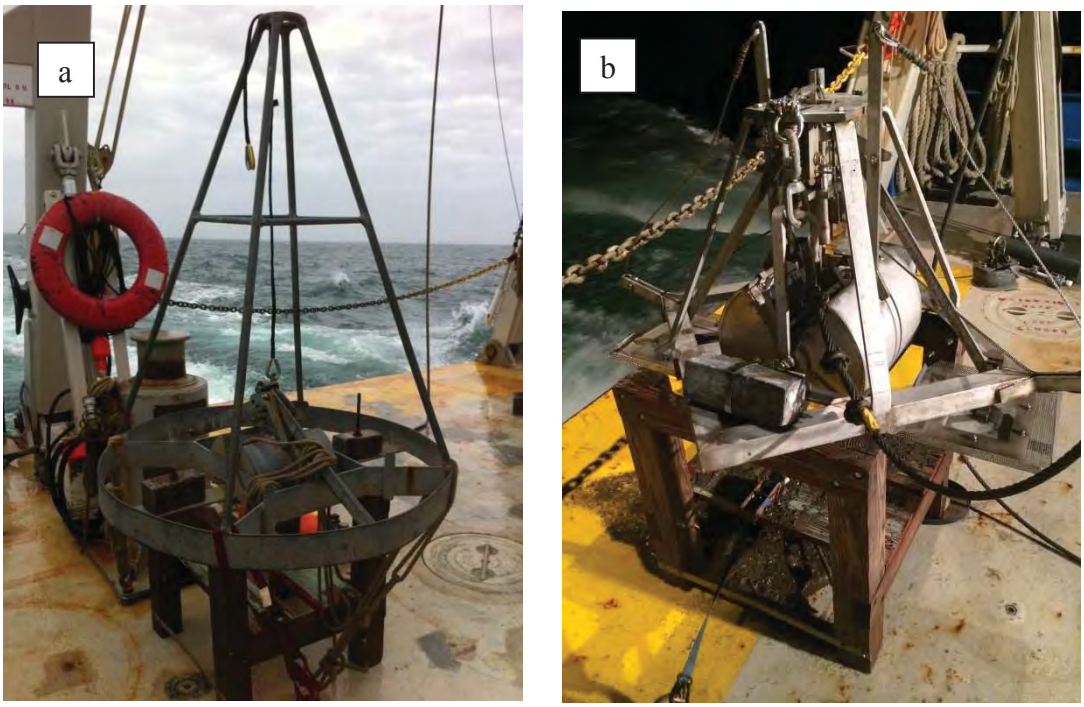

Figure 2-6. Bottom sediment grab samplers used during the study: (a) modified Van Veen sampler, (b) modified Smith-McIntyre sampler.

2.2 Sample and Data Processing

2.2.1 Moored Instruments

2.2.1.1 Temperature and Salinity

The measurements of temperature, conductivity and pressure, recorded at 15-minute intervals, were used to compute salinity and density. Data were logged by the SBE SMP37 instruments in a binary format. After mooring recovery, the data were converted to engineering units using the

manufacturer's software. A low-pass filter was used to highlight the longer trends in salinity and temperature by removing the effect of tides.

2.2.1.2 Waves and Currents in the Water Column

The raw RDI ADCP data were first processed by RDI's proprietary WavesMon software to separate the current and wave data that were recorded alternately in the raw binary file created by the instrument during data collection (RDI, 2008). This process created separate current and wave binary files for further processing.

Currents

For the processing of currents, data were then extracted from the current binary file and written to MATLAB[8] files. Thereafter, basic quality control was done in MATLAB, and NetCDF[9] data files were created.

- ***MATLAB processing:*** The MATLAB function *rdradcp.m*[10] was used to read data from the current binaries into MATLAB. The velocities were rotated to account for the local magnetic variation (-14°) into true east and north components. The pressure measurement on the ADCP was used to identify and eliminate data acquired during times that the instrument was out of the water. Finally, the vertical range of the velocity profiles was limited to 90% of the distance to the surface to eliminate the near surface values which are biased by surface reflections. The sea level was determined from the pressure measurements and confirmed by comparison to the acoustic backscatter signal strength, which has the strongest return from the sea surface. Data values above this height, which rises and falls with the tidal elevation, were set to NaN. As stated, during two deployments, the moored tripod frame at Station DOT6 was tipped over or dragged, presumably by fishing gear. Data from times when the heading, pitch, and roll sensors indicated the ADCP was tipped sideways were also masked with NaNs.

- ***NetCDF file creation:*** After processing, relevant ADCP variables were written to NetCDF files. Metadata collected at the time of deployment (including latitude, longitude, time zone, transducer height) were added to the files. Each file name included the station number, tripod frame number, deployment number, and instrument serial number.

Waves

The wave data files created by RDI's proprietary WavesMon software were converted to MATLAB format with variables containing fundamental wave statistics (e.g., significant wave height, peak period).

[8] MATLAB is a numerical computing environment and programming language, developed by MathWorks.

[9] NetCDF (Network Common Data Form) is a set of software libraries and self-describing, machine-independent data formats that support the creation, access, and sharing of array-oriented scientific data.

[10] The Code (authored by R. Pawlowicz) is available at: *http://www.eos.ubc.ca/$\sim$rich/\#RDADCP*

2.2.1.3 Currents near the Seafloor

Data from the Nortek ADCP were translated to ASCII files using Nortek's proprietary software package. Standard output includes the along beam velocities, acoustic backscatter, correlation data. Additional parameters, output to separate files and useful for screening the data, included the instrument's heading, pitch and roll, battery voltage, sound speed (derived using the measured temperature and a prescribed salinity), and the extended velocity range (EVR) estimates. Temperature, pressure, and the input from the external optical OBS3+ sensors were output as well.

The raw velocity estimates were subjected to data quality checks. Acoustic current meter measurements are susceptible to errors when scattering occurs from marine organisms, or high suspended concentrations, or when particle concentrations are too low. High frequency sampling of turbulent fluctuations are also prone to large outliers which can bias turbulence statistics. Turbulence calculations will be discussed at length in a subsequent report[11].

Data quality screening identified all samples in each beam and each level of a data ensemble[12] as follow:

- The mean of the ensemble was subtracted and low-pass filtered with a 10s cutoff and this was subtracted from the raw data to form the "residual".
- The standard deviation of the residual was then computed and values that were greater than three standard deviations from the mean and with low correlation (<0.4) were identified.
- These points were replaced by values that were equal to the mean plus a random number selected from a normal distribution of standard deviation equal to that computed.

The number of points adjusted and the effect of the mean and the standard deviation of the record were logged. Typically in an ensemble of 2048 samples, 20 samples would be 'screened' in this manner and the impact on the variance in an ensemble was less than 20% Results for all observations of Campaign 1 (Deployment 1), Campaign 2 (Deployments 2 and 3), and Campaign 3 (Deployments 4 and 5) are presented in Appendix 9 (a to c).

2.2.1.4 Suspended Sediment Concentrations near the Seafloor

Conversion of OBS3+ sensor data into suspended sediment concentrations required wet-sediment calibrations. These calibrations were performed on the OBS3+ sensors between Campaigns 1 and 2 deployments, and before the Campaign 3 deployment, except for those on frame of Station DOT5. These sensors of Station DOT5 were not calibrated until June 7, 2013 due to a delay in the recovery of the tripod frame at this station, later attributed to a malfunction of the acoustic release.

To calibrate the OBS3+ sensors in the laboratory, a large tub was fitted with a mount for the OBS 3+ sensors. After filling the tub with filtered seawater, sediment from the appropriate tripod frame

[11] *Physical Oceanography of Eastern Long Island Sound Region: Modeling Report* (in preparation)

[12] A 'ensemble' is defined as 2048 or 4096 velocity measurements obtained at 2 or 4 Hz (see Table 2-3).

was added to the water and circulated with two 360 gallon per hour bilge pumps. Once the readings on the OBS3+ sensors stabilized, measurements were recorded at 4 Hz for approximately 60 seconds. After each set of readings, a water sample was obtained for determination of suspended sediment concentration (SSC) by filtration and gravimetric methods. The amount of sediment in the tanks was increased and procedure repeated until we obtained at least 6 sets of OBS3+ reading. Figure 2-7 shows the results of the calibration for each OBS 3+ sensor for the May 23rd and June 7th calibrations. Figure 2-8 shows the results for the November 18th calibration. A linear regression was applied to estimate the coefficients for determination of SSC from the response for each OBS3+ sensor. The coefficients and goodness of fit parameters from these calibrations are presented in Table 2-5.

The calibration curves in Figures 2-7 and 2-8 are close to linear over a wide range of concentrations. The different instruments also appear to have very similar responses. Use of a mean of the calibration coefficients for either set of calibrations would lead to a difference in the prediction of the concentration of approximately 5%. The calibrations are also stable. The mean gain ('p1' in Table 2-5) is approximately 5% lower in the second set of calibrations.

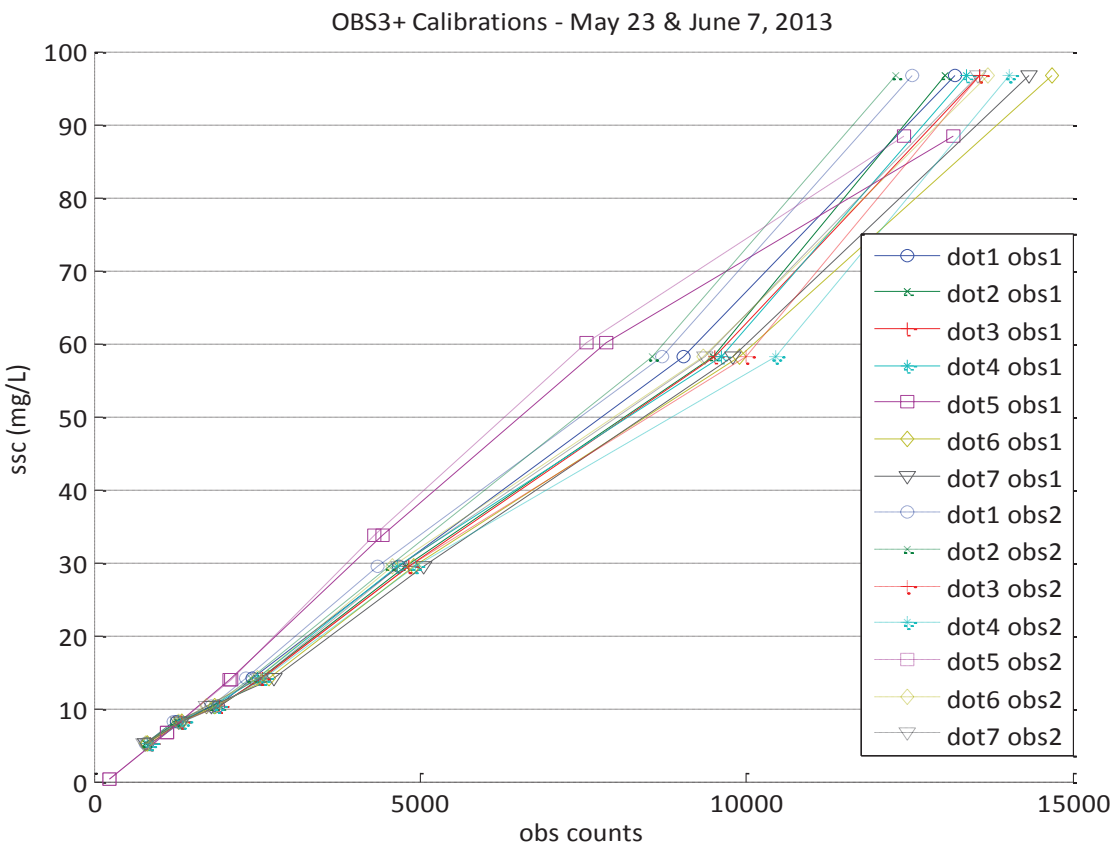

Figure 2-7. Suspended sediment concentrations versus raw counts used in the calibration of OBS 3+ sensors on May 23 (Stations DOT1,2,3,4,6,7) and June 7, 2013 (Station DOT5).

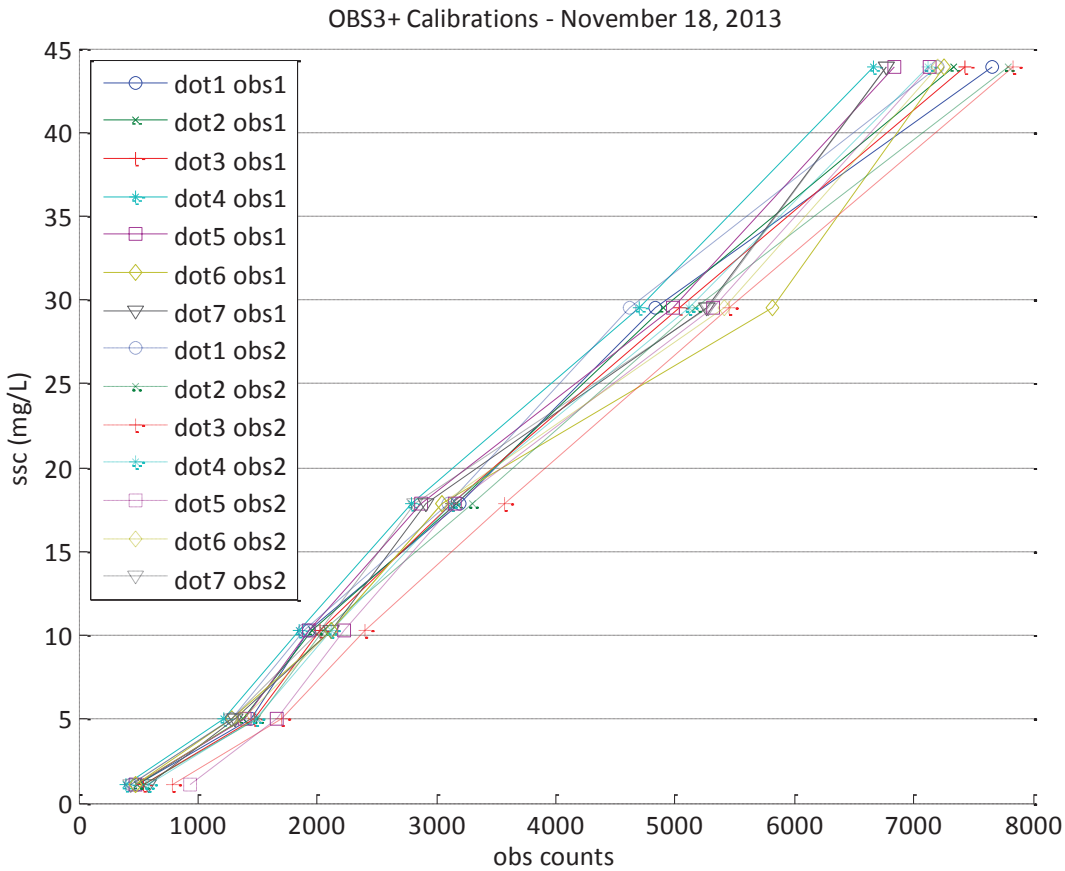

Figure 2-8. Suspended sediment concentrations versus raw counts used in calibration of OBS 3+ sensors for all seven DOT mooring stations, November 18, 2013.

2.2.2 Ship Surveys

2.2.2.1 Temperature and Salinity (Profiling CTDs)

Data from the profiling CTDs (SBE 9/11 and SBE 19+) were offloaded and converted to engineering units using Sea-Bird Electronics' proprietary software. The software included several modules which were used to correct and adjust the data due to the effects of the ship's roll, lag between the pump intake and actual sample, and speed of descent. Specifically, the modules used to process the data included *Filter* (low-pass filters the data), *Loop Edit* (eliminates reversals in the descent rate), *Derive* (derives salinity, density, and depth after the previous modules are run), and *Split* (splits the cast into a downcast and upcast). Since the sensors were on the bottom of the lowered instrument package, in keeping with industry practice, only the data from the downcast was used since it observed undisturbed fluid.

Table 2-5. Calibration Fits of the OBS3+ Sensor

Station ID/Analog Channel	Regression Coefficient		Goodness of Fit Parameters		
	Slope (p1) (95% Confidence Interval)	**Intercept (p2)** (95% Confidence Interval)	**Sum of the Squares of the Error (SSE)**	**Coefficient of Regression (R^2)**	**Root Square Mean Error (RMSE)**
Campaigns 1 and 2					
DOT1 OB1	0.007267 (0.006578, 0.007957)	-2.89 (-7.326, 1.547)	47.05	0.9932	3.068
DOT1 OB2	0.007628 (0.00685, 0.008406)	-2.827 (-7.594, 1.939)	54.38	0.9922	3.298
DOT2 OB1	0.007215 (0.006203, 0.008226)	-3.127 (-9.696, 3.442)	101.90	0.9854	4.515
DOT2 OB2	0.007807 (0.006946, 0.008668)	-3.532 (-8.741, 1.677)	63.47	0.9909	3.563
DOT3 OB1	0.007027 (0.00626, 0.007795)	-3.011 (-8.126, 2.105)	62.24	0.9911	3.528
DOT3 OB2	0.006891 (0.0059, 0.007883)	-2.833 (-9.545, 3.878)	107.40	0.9846	4.634
DOT4 OB1	0.007037 (0.006143, 0.00793)	-2.483 (-8.376, 3.41)	83.85	0.9880	4.095
DOT4 OB2	0.006611 (0.005604, 0.007618)	-2.414 (-9.467, 4.639)	120.0	0.9828	4.900
DOT5 OB1	0.007256 (0.00697, 0.007541)	-0.8515 (-5.006, 3.303)	70.89	0.9985	3.437
DOT5 OB2	0.007928 (0.007567, 0.00829)	-2.522 (-7.387, 2.343)	95.06	0.9979	3.980
DOT6 OB1	0.006503 (0.005958, 0.007048)	-1.868 (-5.728, 1.991)	36.81	0.9947	2.713
DOT6 OB2	0.00695 (0.006325, 0.007576)	-1.95 (-6.096, 2.196)	42.35	0.9939	2.910
DOT7 OB1	0.006647 (0.005993, 0.007302)	-2.358 (-6.926, 2.211)	50.73	0.9927	3.185
DOT7 OB2	0.007012 (0.006295, 0.00773)	-2.231 (-6.965, 2.504)	54.68	0.9921	3.307
Campaign 3					
DOT1 OB1	0.006155 (0.005479, 0.006832)	-2.104 (-4.84, 0.6321)	8.195	0.9938	1.431
DOT1 OB2	0.006508 (0.005965, 0.00705)	-2.138 (-4.217, -0.05867)	4.731	0.9964	1.088
DOT2 OB1	0.006386 (0.005979, 0.006793)	-2.519 (-4.128, -0.9106)	2.766	0.9979	0.832
DOT2 OB2	0.006037 (0.005579, 0.006495)	-2.552 (-4.469, -0.6349)	3.919	0.9970	0.990
DOT3 OB1	0.006336 (0.00588, 0.006792)	-2.794 (-4.629, -0.9595)	3.534	0.9973	0.940
DOT3 OB2	0.00619 (0.00587, 0.006511)	-4.487 (-5.877, -3.096)	1.826	0.9986	0.676
DOT4 OB1	0.006901 (0.006445, 0.007357)	-2.295 (-3.953, -0.6371)	2.981	0.9977	0.863
DOT4 OB2	0.006626 (0.006143, 0.007109)	-3.629 (-5.537, -1.72)	3.626	0.9972	0.952
DOT5 OB1	0.006755 (0.006079, 0.007431)	-2.862 (-5.416, -0.3066)	6.812	0.9948	1.305
DOT5 OB2	0.006827 (0.006165, 0.007489)	-5.296 (-7.966, -2.626)	6.388	0.9951	1.264
DOT6 OB1	0.00605 (0.005001, 0.0071)	-2.199 (-6.525, 2.128)	20.25	0.9846	2.250
DOT6 OB2	0.006311 (0.00559, 0.007031)	-2.701 (-5.598, 0.1965)	8.842	0.9933	1.487
DOT7 OB1	0.006742 (0.005804, 0.007681)	-3.349 (-6.954, 0.256)	13.1	0.9901	1.810
DOT7 OB2	0.006608 (0.005597, 0.007619)	-2.548 (-6.409, 1.313)	15.8	0.9880	1.987

* Linear model: f(x) = p1*x + p2

2.2.2.2 Currents throughout the ZSF (Ship-board RDI ADCP)

The ship-acquired ADCP data were processed using the University of Hawaii's CODAS system. The raw (binary) data from the ship's data acquisition system were saved in the CODAS LTA and STA format (long-term and short-term averages) and in the RDI binary format.

To avoid timing inconsistencies between the ADCP velocity measurements and the *R/V Connecticut's* navigation system, the binary ENR files were reprocessed after the cruise as single ping data, allowing checks and time averaging. For Cruise CTDOT1, the transducer angle (i.e., the orientation of the ADCP's beam three relative to the bow) was set at 45 degrees, and the ship data were processed using this angle and an averaging interval of 60 seconds.

A comparison of the velocity derived from the ship's navigation system to the velocity estimated by the bottom track mode of the ADCP showed that the ADCP was mis-aligned by 13.8 degrees. The water velocities estimates were then rotated by this amount (final angle 58.8 degrees). When this correction was applied to the bottom track velocity estimates, the residual offset was less than 0.1 degrees, well below the 0.5 degree tolerance suggested by the CODAS manual.

2.2.2.3 Optical Suspended Sediment Measurements in the Water Column (WET Labs sensors)

Raw WET Labs AC9 data referenced to clean water were transformed to calibrated scientific units (m^{-1}) using prescribed WET Labs methods. Data were then depth-averaged in 1-meter bins and the minimum and maximum values recorded for each bin identified. For each water sample, values were averaged across the time span required to collect each sample.

2.2.2.4 Water Sample Analyses for Suspended Sediment and Particulate Organic Carbon Concentrations

Suspended sediment concentrations were determined using filtration methods as described in the QAPP, Standard Operating Procedure (SOP) 06, *Procedures for Determining Suspended Sediment Concentration*. Protocols established in EPA Method 440 (Zimmerman et al., 1997) were followed for the analysis of particulate organic carbon concentrations.

2.2.2.5 Grain Size of Seafloor Sediments

In the laboratory, samples were transferred to an environmental chamber and maintained at a temperature of 4˚C. Fine fraction particle size analysis (<63 microns) was performed using timed pipette extractions as described by Plumb (1981). Percentages of sand and gravel (>63 microns) were determined by separation from fines through a 63 micron sieve (US Standard Sieve #230) and 2 mm sieve (US Standard Sieve #10) respectively. Sands were fractionated further using sieves at one phi intervals (Table 2-6). Gradistat (Blott and Pye, 2001) particle analysis software was used to calculate particle size statistics from the resulting weight data obtained for each size class.

Table 2-6. Size classification used in Grain Size Analysis*

phi scale	Grain Size Diameter (microns)	Size Boundary	Size Term for Sand
-1	2000	gravel	
0	1000	sand	very coarse
+1	500		coarse
+2	250		medium
+3	125		fine
+4	63		very fine
+9	2	silt	
	>2	clay	

* Modified from Wentworth (1922).

2.3 Regional Wind and Wave Observations

The evaluation of the circulation patterns in the ZSF required the characterization of winds and river flow and their vary seasonal variability. Therefore, wind and wave fields observed by instruments from five 'metocean stations' were analyzed; these buoys are located within the ZSF, in central LIS, and in the Atlantic Ocean (Figure 2-1). Specifically, there are four over-water sources of meteorological observation and three sources of wave measurements within or nearby the ZSF (Table 2-7). Metocean stations labeled CLIS and ELIS are UCONN-operated buoys. Both buoys are equipped with meteorological sensors. Station CLIS also has instruments to measure wave statistics. Station LEDG is 'Ledge Light', a lighthouse with meteorological sensors. Station 44017 is a NOAA buoy with both meteorological and wave sensors. Station CDIP154 is a USACE buoy that collects wave data. All these stations also have NOAA Data Buoy Center (NDBC) identification numbers; data are available from NDBC.

2.4 Summary

2.4.1 Field Program

The purpose of the PO Study and field program was to assess sediment stability or sediment transport at discrete locations in the ZSF in ELIS and BIS. In addition, the data were collected to assess worst case storm events. As specified in the QAPP, PO data were planned to be collected from approximately mid-March through December, 2013. Specifically, per QAPP, the following periods were selected to represent a range of conditions:

- windy, low and high-flow conditions (April – May)
- relatively calm, below average flow conditions (June – July)
- windy, low-flow conditions (November – December)

Table 2-7. Sources for Wind and Wave Data

Metocean Station*	**Measurements**	**Lati-tude** (deg)	**Longi-tude** (deg)	**Elevation above Water Surface** (m)	**Data Source** *http://www.ndbc.noaa.gov/*
ELIS (44060)	Meteorology	41.26	72.06	2.4	station_page.php?station=44060
CLIS (44039)	Meteorology, Waves	41.13	72.65	2.4	station_page.php?station=44039
LEDG (LDLC3)	Meteorology	41.30	72.07	20	station_page.php?station=LDLC3
44017	Meteorology, Waves	40.69	72.04	5	station_page.php?station=44017
CDIP154 (44097)	Waves	40.98	71.12	-	station_page.php?station=44097

* Numbers in brackets represent NDBC identification numbers.

The field program of the PO study met these objectives with Campaign 1 taking place March 12 to May 17, 2013; Campaign 2 from June 11 to August 8, 2013; and Campaign 3 from November 20, 2013 to January 16, 2014.

Data collection during each of these seasons was designed to include the deployment of seven moored, upward-looking ADCPs and bottom pressure sensors, together with seven downward-directed, high-resolution pulse-coherent near-bottom acoustic current meters with two backscatter sensors each to estimate suspended sediment. Although the instrument tripod frame at Station DOT6 was knocked over by fishing gear during Campaign 2 and the batteries in the Nortek ADCPs failed prematurely during Campaign 1 (see Section 2.4.2), sufficient data were recovered to adequately test and verify model predictions through a broad range of conditions.

Ship surveys were to be conducted in the ZSF during three seasons (spring, summer, winter) to complement the moored instrument deployments. Profiling CTDs, optical sensors, and ship-mounted ADCPs, as well as collection of water samples for suspended sediment concentration and particulate organic carbon content were also specified. Although the optical instrumentation was not in place until Campaign 2, CTD casts, water samples, and continuous current profiles were obtained for analysis during all three campaigns over two tidal cycles at all but two stations (due to weather conditions).

Collection of sediment grab samples for calibration of the sediment transport modeling (with STFATE and LTFATE) was also part of the field program of the PO study. Grab samples were collected at all mooring stations during each campaign and processed for grain size composition. These data were used for assessing the potential for sediment motion around the instruments and for future sediment transport modeling.

2.4.2 Data Recovery

To evaluate the effectiveness of the model's (FVCOM) ability to predict the circulation patterns and the magnitude of bottom stress at all sites in the ZSF in a typical year, a minimum of four working instrument moorings were needed for the modelling component. We selected seven stations, three in Block Island Sound and four in Long Island Sound, and three two-month time intervals for intensive measurements of both water column currents and bottom stress (and ancillary variables) on the basis of a review of existing data and preliminary model calculations that would exhibit differing conditions.

The challenges associated with using complex moored instrument systems in the coastal ocean resulted in fewer days for which data are available from the various instruments deployed at the seven mooring stations than anticipated. The data recovery is summarized in Table 2-8. Reduced data availability were largely a result of events in the field, although quality control steps during the data processing further reduced the available data by a very small amount.

The Nortek ADCPs (and the OBS3+ sensors that were connected to them) had the most data loss. The battery lifetime was projected to be 60 days using the manufacturer's software. However, the effects of the OBS3+ had not been included and the battery drain was approximately twice the rate anticipated and the data return in Campaign 1 was approximately 50% of that expected. Since the spring-neap tidal cycle is only 14 days, and 25-27 days of data were obtained, a wide range of conditions was sampled. In Campaign 2, we replaced the batteries after 30 days. However, the battery capacity was reduced by higher water temperatures and only 28-34 days of data were obtained. Prior to the start of Campaign 3, we examined the available data and designed a sampling scheme that would preserve data quality to allow sampling for the whole deployment. An impact with fishing gear curtailed sampling at 16 days at Station DOT6 in Campaign 2 and an electronic failure occurred at Station DOT7 in Campaign 3 resulting in only 27 days of data. Repairs of instruments and the tripod frame damaged at Station DOT6 delayed the redeployment for Campaign 3 by 10 days. Overall, we recovered 730 days of Nortek ADCP data of an expected 1,260 days (i.e., 7 stations times 60 days), a return of 58%.

Though the RDI ADCPs were refurbished and tested prior to deployment, the memory cards in the instruments at Stations DOT3 and DOT7 during Campaign 1 failed and the data files were irretrievably corrupted. Some additional data was lost at Station DOT6 due to fishing activities which turned the instruments upside down. However, 1,041 days of data were acquired, a success rate of 83%.

The SBE SMP37 sensors for pressure, salinity and temperature were the most resilient. They continued to work even after the tripods were overturned. The only data loss was a consequence of a deployment delay for repair of ADCPs. The data return was 98% of the return planned.

Though there were some data losses at Station DOT6 due to fishing activities and instrument failures at DOT3 and DOT7, and unanticipated instrument problems with the Nortek ADCPs during Campaigns 1 and 2, the field program successfully recovered data showing a wide range of current and stress conditions at all sites. Even the shortest Nortek ADCP deployments spanned several spring-neap cycles and allowed a wide range of stress values to be observed at all stations.

The minimum number of simultaneously operating Nortek ADCPs at any time was six since the instruments shared the same failure mode. This means that the representation of the spatial structure of the bottom stress was almost optimal; it was just a shorter duration than planned.

In summary, the field program has provided sufficient data with which to characterize the physical oceanography and suspended sediment distribution in the ZSF and to critically evaluate the model's ability to discriminate times and locations of high and low bottom shear stress. The number of instruments employed, and the duration of the measurements obtained in this program exceed those of all prior projects of this type and form a comprehensive data set with which to evaluate model predictions. The modeling approach and findings will be prepared as a separate second report as part of the PO study.

Table 2-8. Number of Days with Data from all Moored Instruments available for Modeling

Station	Instrument	Campaign 1 *(66 days)*		Campaign 3 *(58 days)*		Campaign 3 *(57 days)*		Total Data Days *(max: 181)*
		days	*Notes*	days	*Notes*	days	*Notes*	
DOT1	SBE SMP37 CTD	66		58		57		181
	Nortek ADCP & OBS3+	25	*(1)*	29	*(4)*	54		108
	RDI ADCP	66		58		57		181
DOT2	SBE SMP37 CTD	66		58		57		181
	Nortek ADCP & OBS3+	25	*(1)*	27	*(4)*	54		106
	RDI ADCP	66		58		57		181
DOT3	SBE SMP37 CTD	66		58		57		181
	Nortek ADCP & OBS3+	24	*(1)*	32	*(4)*	53		110
	RDI ADCP	0	*(2)*	58		57		115
DOT4	SBE SMP37 CTD	66		58		57		181
	Nortek ADCP & OBS3+	27	*(1)*	34	*(4)*	56		117
	RDI ADCP	66		58		57		181
DOT5	SBE SMP37 CTD	66		58		57		181
	Nortek ADCP & OBS3+	27	*(1)*	30	*(4)*	57		114
	RDI ADCP	66		58		57		181
DOT6 (A/B)	SBE SMP37 CTD	66		58		43	*(5)*	167
	Nortek ADCP & OBS3+	25	*(1)*	16	*(3)*	44	*(5)*	86
	RDI ADCP	28	*(3)*	16	*(3)*	43	*(5)*	87
DOT7	SBE SMP37 CTD	49		58		57		164
	Nortek ADCP & OBS3+	28	*(1)*	34	*(3)*	27	*(6)*	89
	RDI ADCP	0	*(2)*	58		57		115

Explanations for reduced data availability:

(1) Limitation due to power loss (battery drain was higher than predicted by manufacturer due to OBS3 operation).

(2) Memory card corrupted.

(3) Data loss because mooring was struck by fishing vessel. During Campaign 1, mooring was struck *after* battery had failed for Nortek and OBS sensor.

(4) Limitation due to power loss (battery drain was higher than predicted by manufacturer due to warmer temperatures).

(5) Deployment delayed for repair of instruments.

(6) Instrument failure (total memory card failure in second half of the deployment).

3. Temperature and Salinity (Ship Surveys)

To measure the structure of the temperature and salinity distribution in the ZSF during the three campaigns, the profiling CTD was deployed at each station during each of the eight cruises, as described in Section 2.1.3.1. During each survey, typically one or two casts were made; occasionally a third or fourth cast was made to provide additional data.

3.1 Data

Temperature, salinity and density measurements of each cast are summarized and graphically presented in Appendix 10. These data were subsequently used to assess the model performance[13]. Figures 3-1 to 3-11 represent summaries of the data at each station to facilitate the evaluation of the seasonal variation of the temperature, salinity and density. The seasons during which casts were made are marked by different colors in these figures.

All stations show a very large seasonal cycle in temperature and a weak vertical structure. Minimum water temperatures were 3ºC to 5ºC, rising to 23ºC at the surface in the summer. Vertical gradients in temperature and density were largest at Stations DOT5 and DOT6 in the summer.

Stations DOT1, 2, 3 and 7 were all located to the west of The Race and inside Long Island Sound. Although the temperatures at these stations were similar, the salinity varied along with the degree of vertical stratification. The minimum salinity at Stations DOT1, 2, and 3 occurred in the spring during Cruises CTDOT2 and 3. At Stations DOT4, DOT5, and CTD8 the minimum salinity occurred in the summer.

3.2 Summary

The data display the expected seasonal cycles and spatial structure and the observations of currents and stress will be representative of the range of conditions expected in the area. The data will be integrated in the analysis of the spatial and seasonal variations in the salinity, temperature and density fields in the ZSF, for the understanding of the regional circulation and transport patterns.

[13] Presented in a separate report: *Physical Oceanography of Eastern Long Island Sound Region: Modeling Report.* (in preparation)

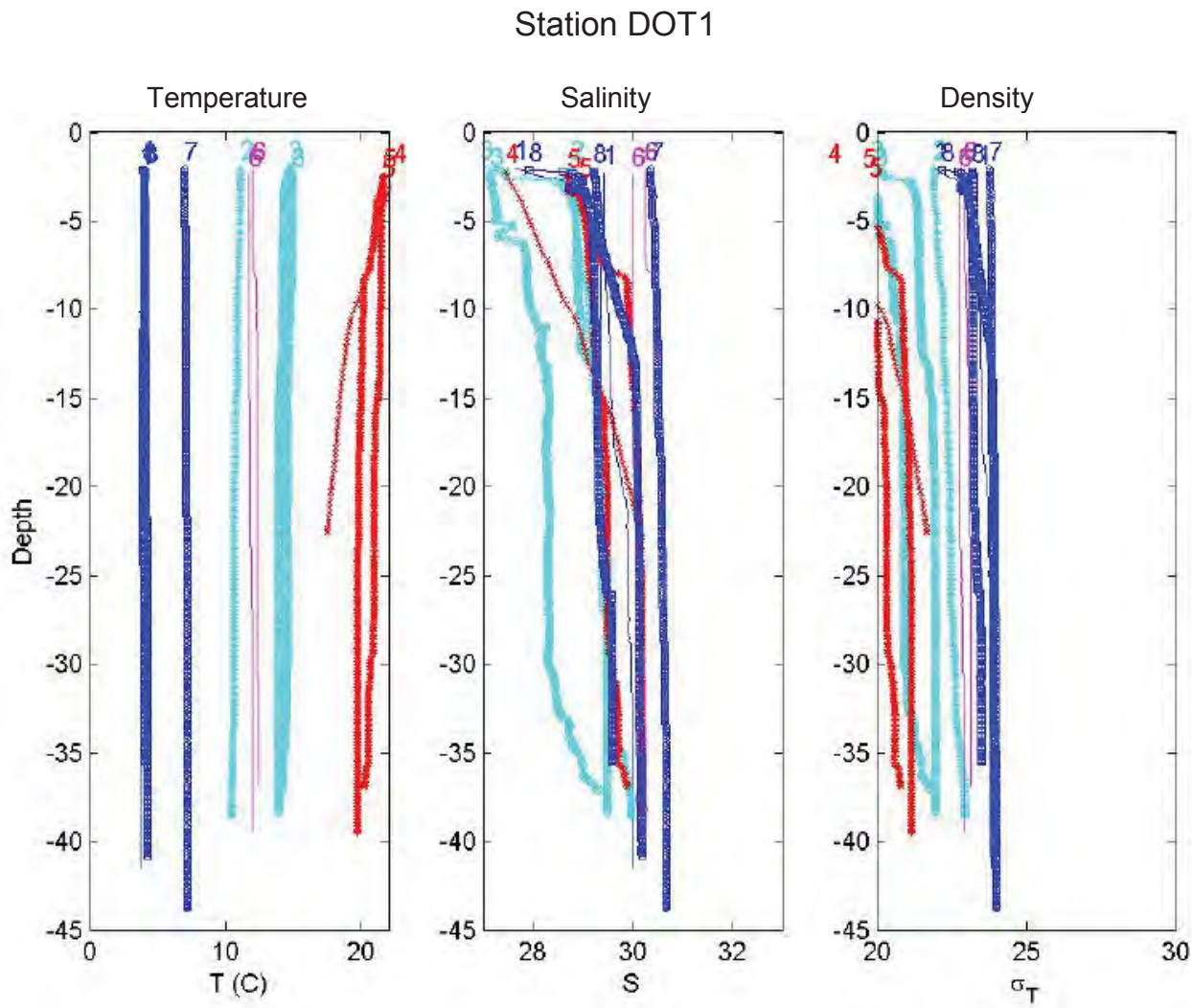

Figure 3-1. Temperature, conductivity, and density in the water column at Station DOT1, measured with the Profiling CTD. Each profile is labeled at the top with the cruise number. Colors reflect approximate seasons: Winter (Cruises CTDOT1,7,8; blue); spring (Cruises CTDOT2,3; turquoise); summer (Cruises CTDOT4,5; red), and late fall (Cruises CTDOT6; magenta).

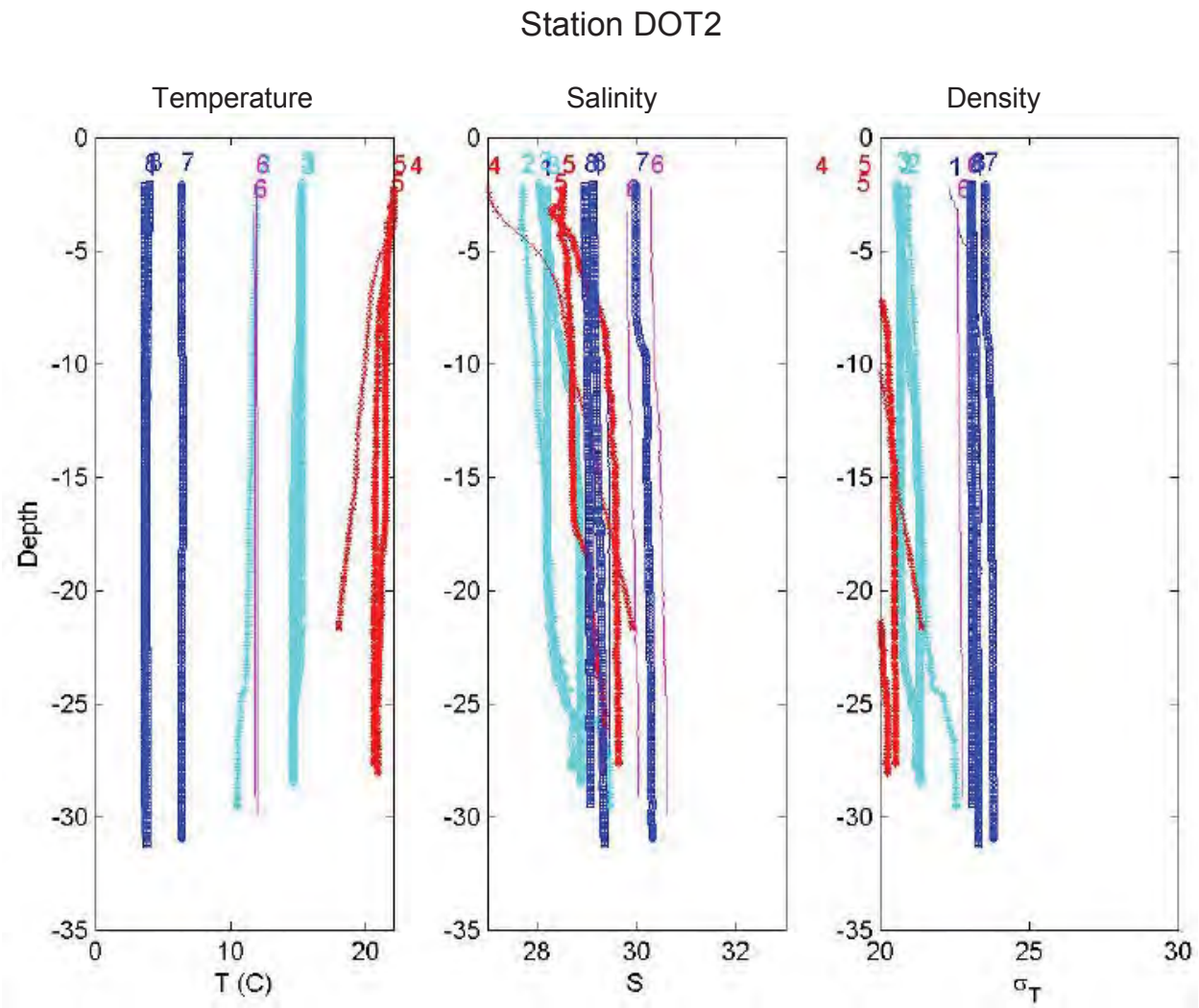

Figure 3-2. Temperature, conductivity, and density in the water column at Station DOT2, measured with the Profiling CTD. Each profile is labeled at the top with the cruise number. Colors reflect approximate seasons: Winter (Cruises CTDOT1,7,8; blue); spring (Cruises CTDOT2,3; turquoise); summer (Cruises CTDOT4,5; red), and late fall (Cruises CTDOT6; magenta).

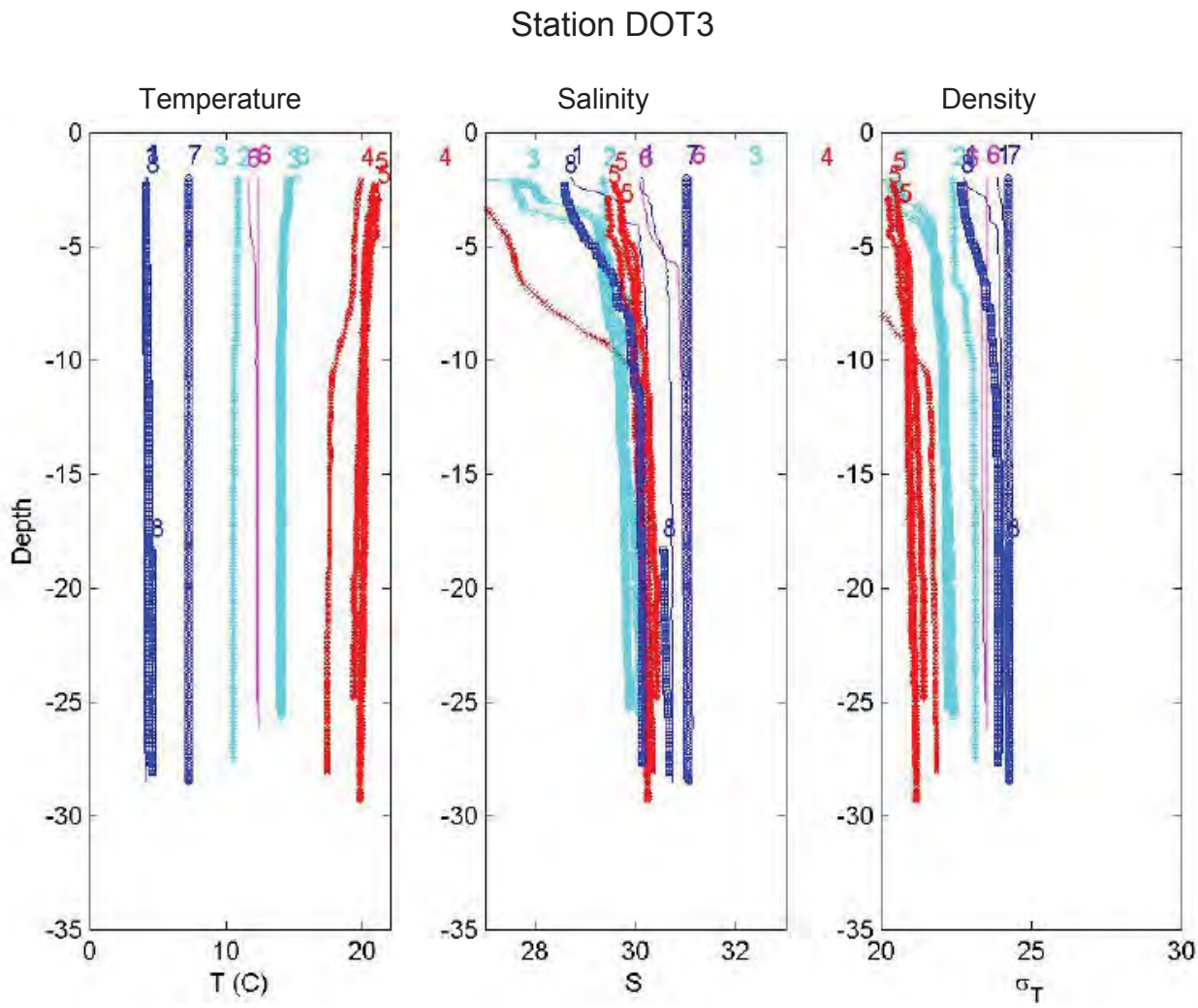

Figure 3-3. Temperature, conductivity, and density in the water column at Station DOT3, measured with the Profiling CTD. Each profile is labeled at the top with the cruise number. Colors reflect approximate seasons: Winter (Cruises CTDOT1,7,8; blue); spring (Cruises CTDOT2,3; turquoise); summer (Cruises CTDOT4,5; red), and late fall (Cruises CTDOT6; magenta).

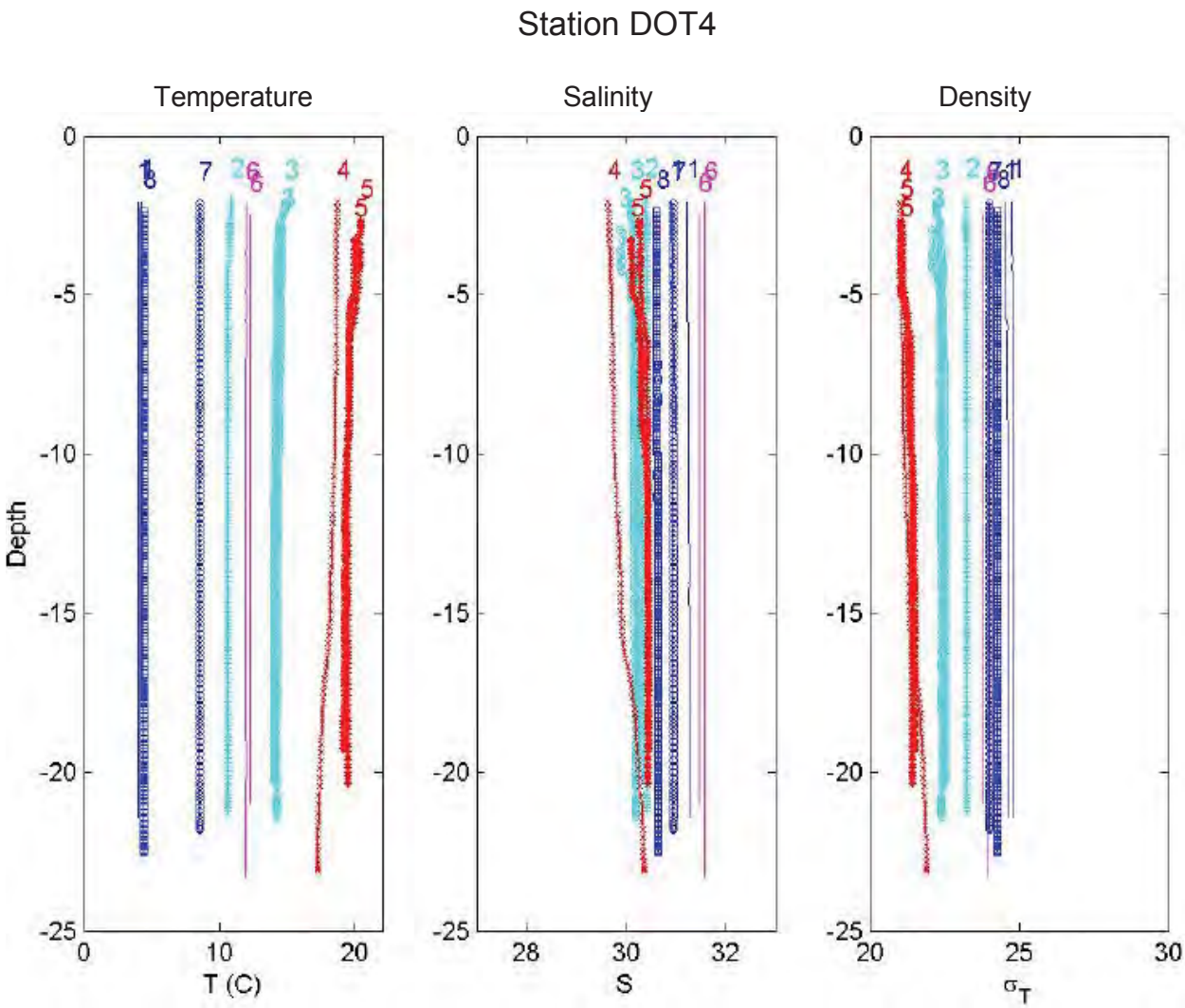

Figure 3-4. Temperature, conductivity, and density in the water column at Station DOT4, measured with the Profiling CTD. Each profile is labeled at the top with the cruise number. Colors reflect approximate seasons: Winter (Cruises CTDOT1,7,8; blue); spring (Cruises CTDOT2,3; turquoise); summer (Cruises CTDOT4,5; red), and late fall (Cruises CTDOT6; magenta).

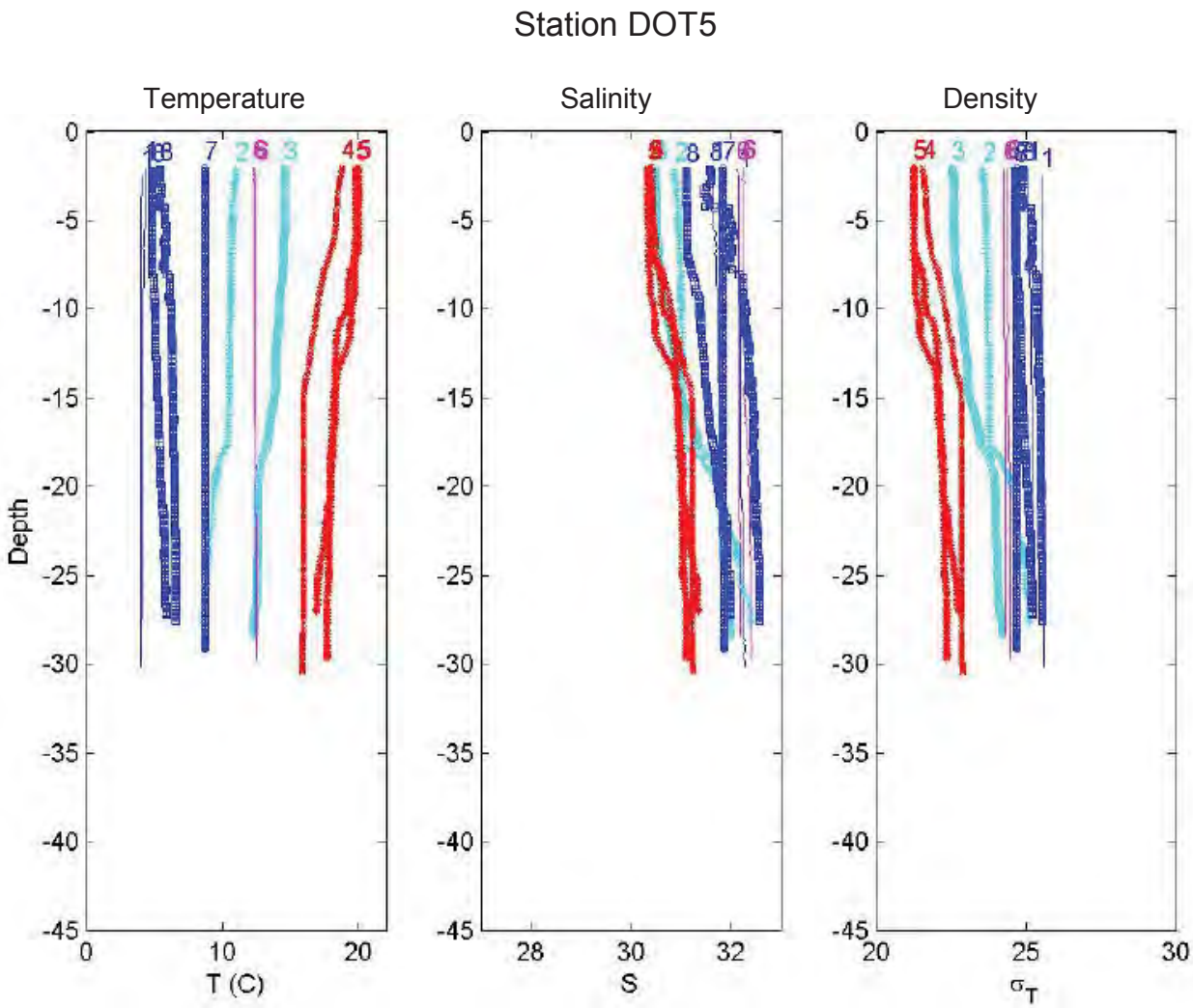

Figure 3-5. Temperature, conductivity, and density in the water column at Station DOT5, measured with the Profiling CTD. Each profile is labeled at the top with the cruise number. Colors reflect approximate seasons: Winter (Cruises CTDOT1,7,8; blue); spring (Cruises CTDOT2,3; turquoise); summer (Cruises CTDOT4,5; red), and late fall (Cruises CTDOT6; magenta).

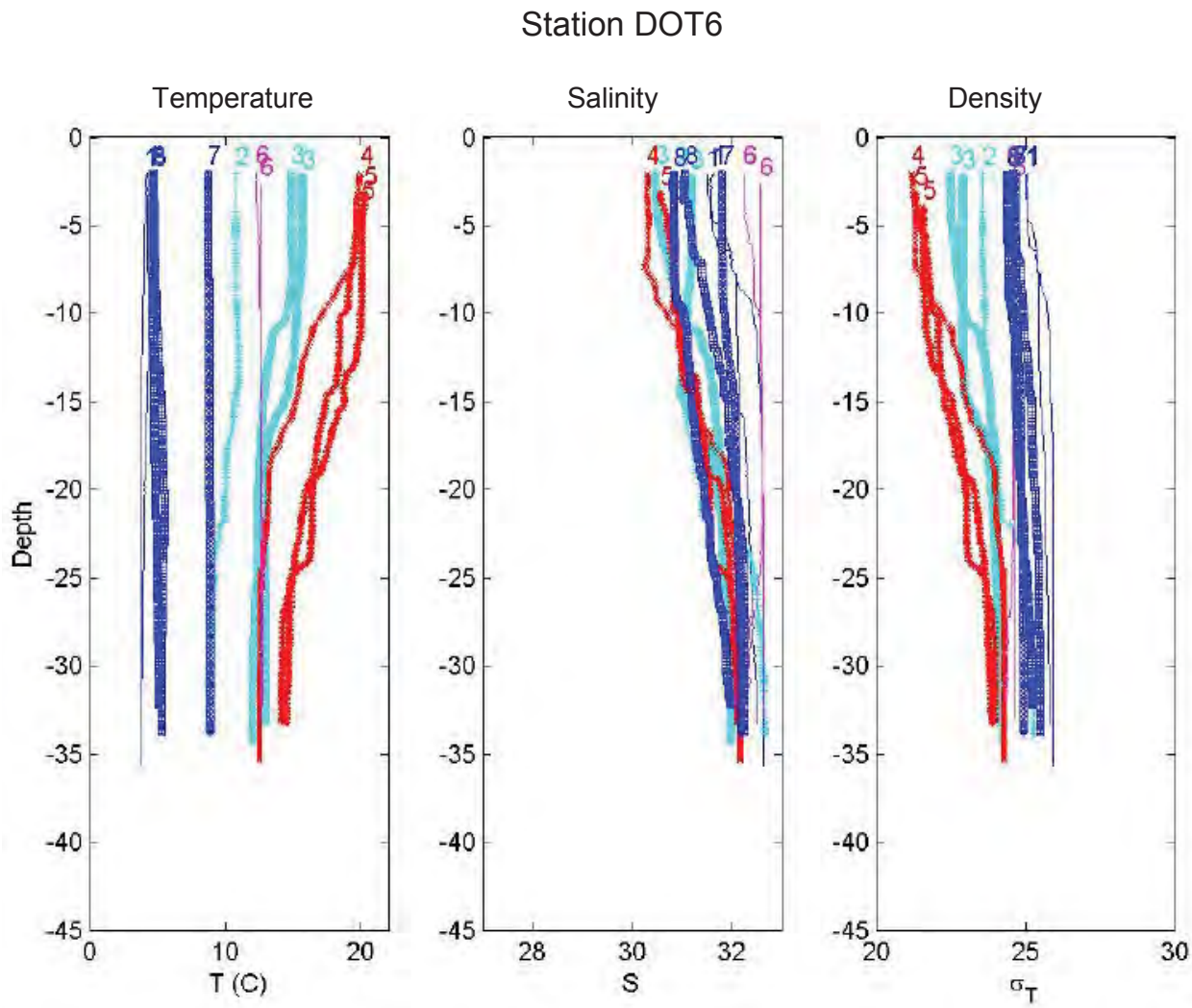

Figure 3-6. Temperature, conductivity, and density in the water column at Station DOT6, measured with the Profiling CTD. Each profile is labeled at the top with the cruise number. Colors reflect approximate seasons: Winter (Cruises CTDOT1,7,8; blue); spring (Cruises CTDOT2,3; turquoise); summer (Cruises CTDOT4,5; red), and late fall (Cruises CTDOT6; magenta).

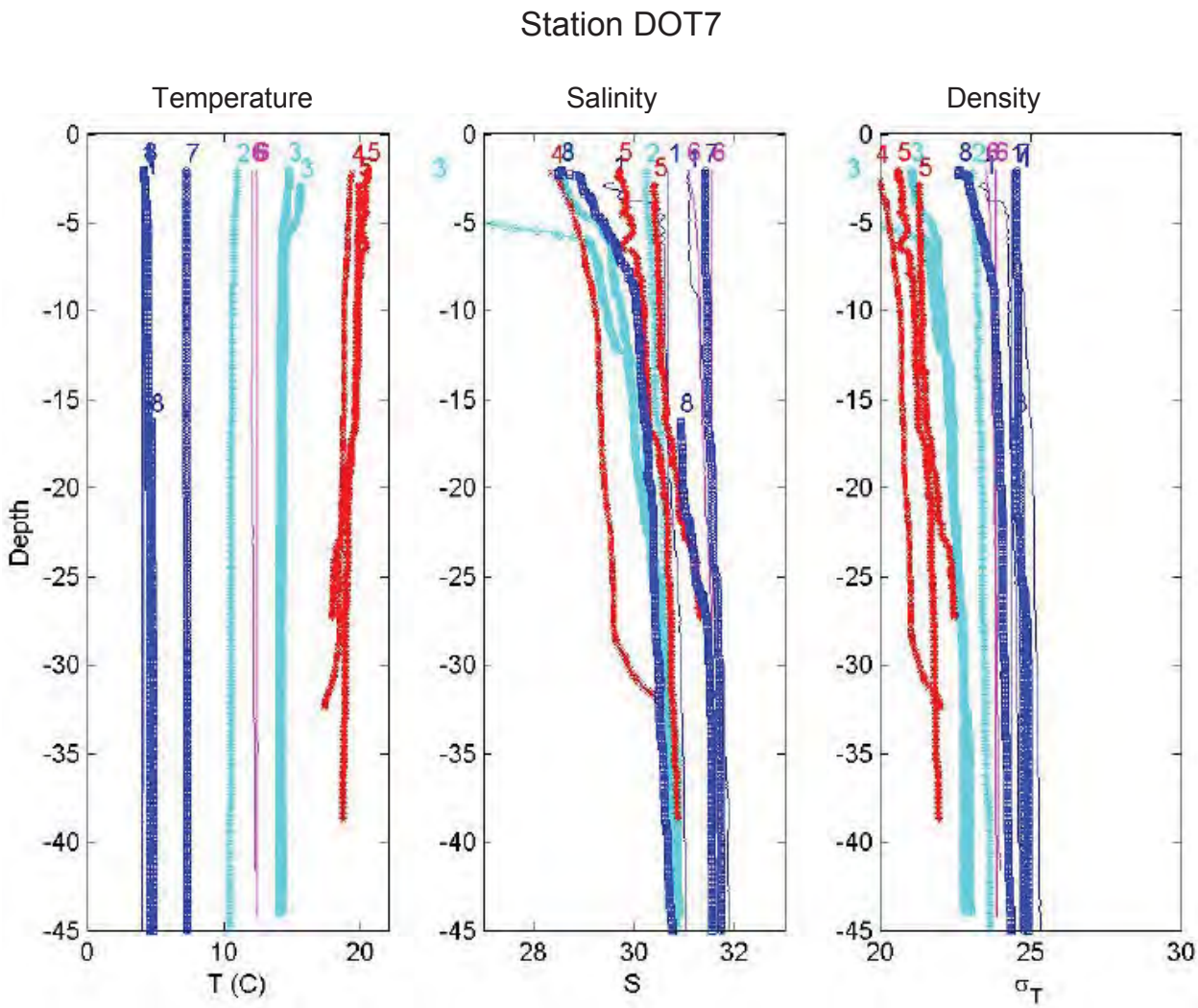

Figure 3-7. Temperature, conductivity, and density in the water column at Station DOT7, measured with the Profiling CTD. Each profile is labeled at the top with the cruise number. Colors reflect approximate seasons: Winter (Cruises CTDOT1,7,8; blue); spring (Cruises CTDOT2,3; turquoise); summer (Cruises CTDOT4,5; red), and late fall (Cruises CTDOT6; magenta).

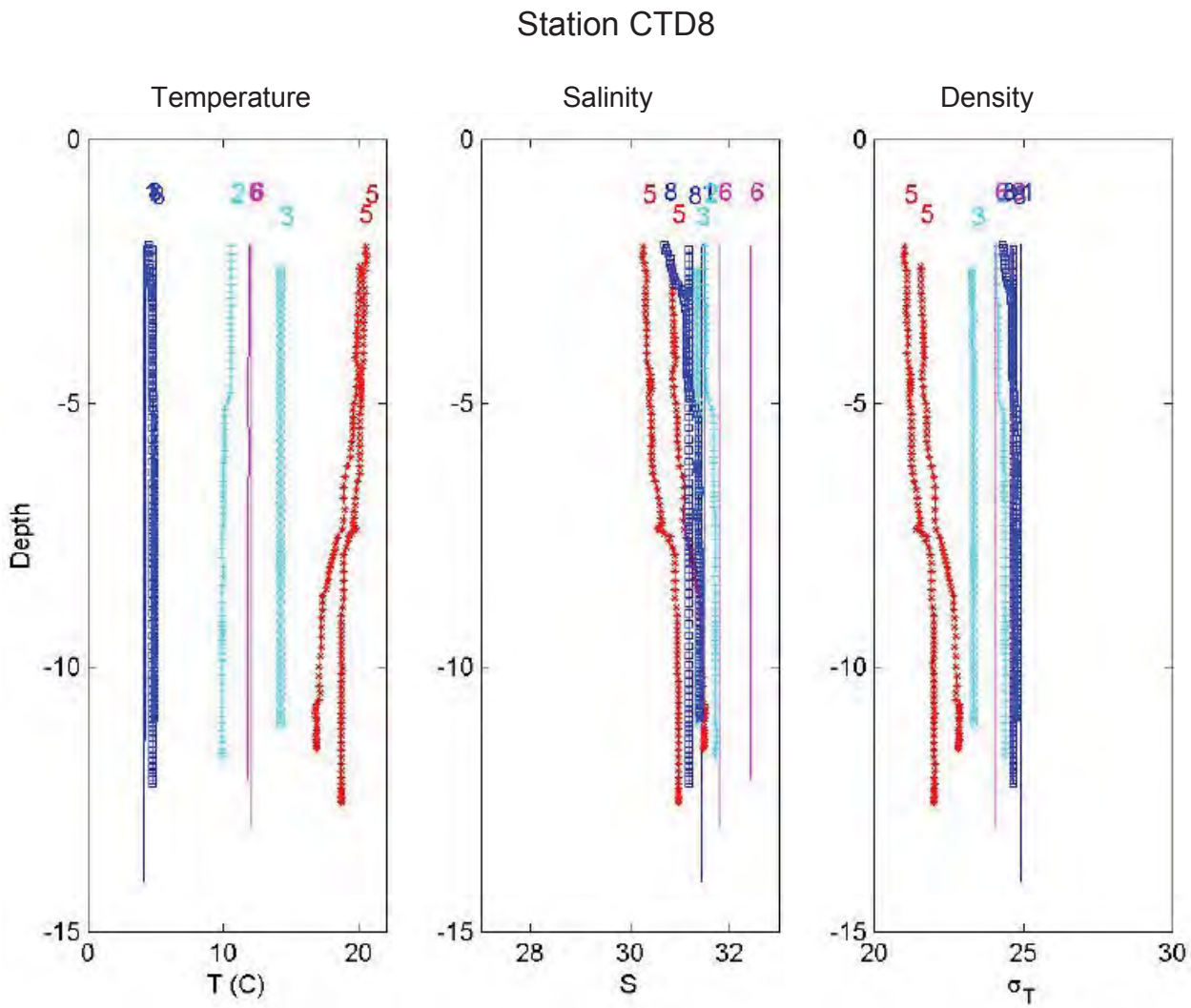

Figure 3-8. Temperature, conductivity, and density in the water column at Station CTD8, measured with the Profiling CTD. Each profile is labeled at the top with the cruise number. Colors reflect approximate seasons: Winter (Cruises CTDOT1,7,8; blue); spring (Cruises CTDOT2,3; turquoise); summer (Cruises CTDOT4,5; red), and late fall (Cruises CTDOT6; magenta).

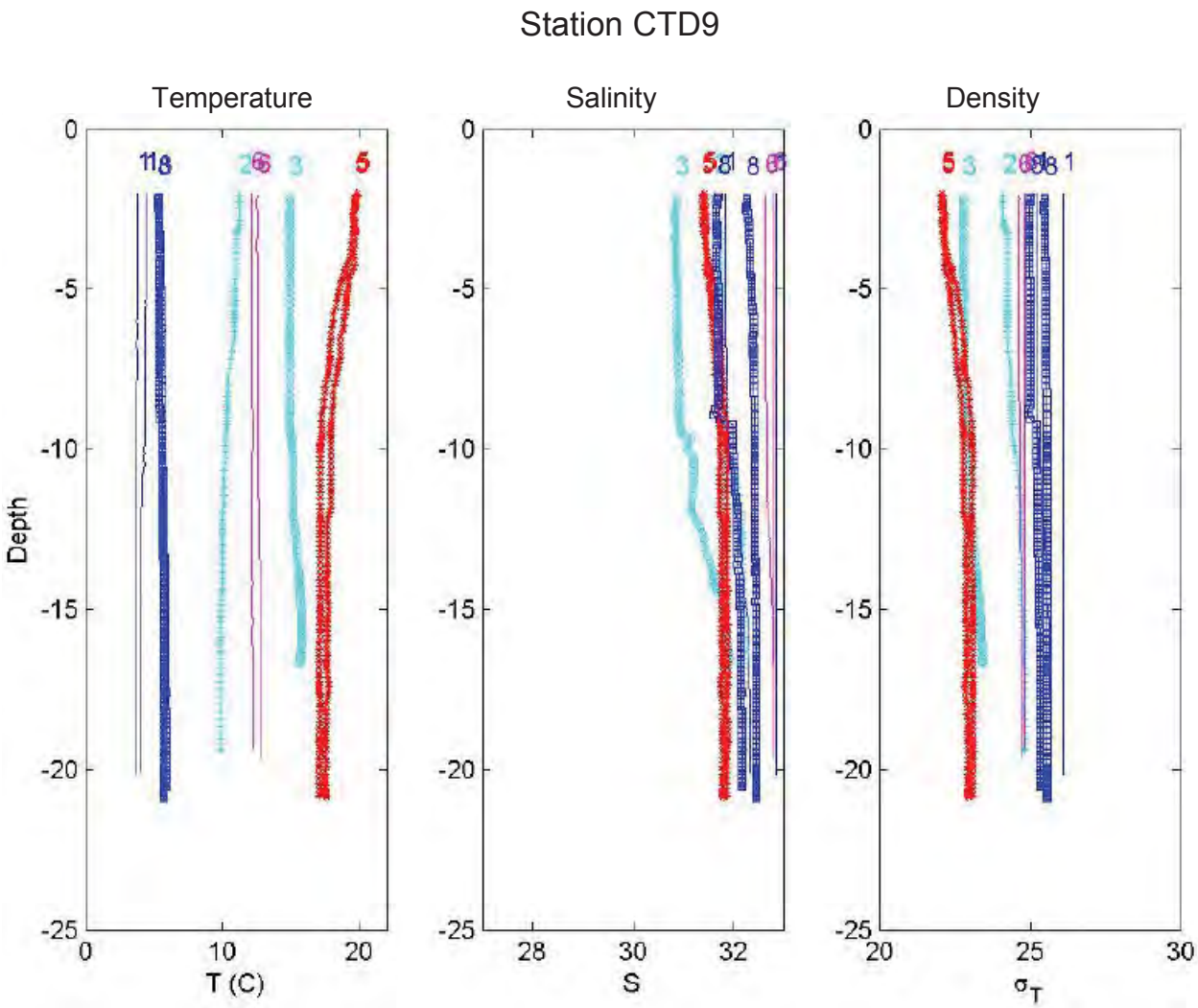

Figure 3-9. Temperature, conductivity, and density in the water column at Station CTD9, measured with the Profiling CTD. Each profile is labeled at the top with the cruise number. Colors reflect approximate seasons: Winter (Cruises CTDOT1,7,8; blue); spring (Cruises CTDOT2,3; turquoise); summer (Cruises CTDOT4,5; red), and late fall (Cruises CTDOT6; magenta).

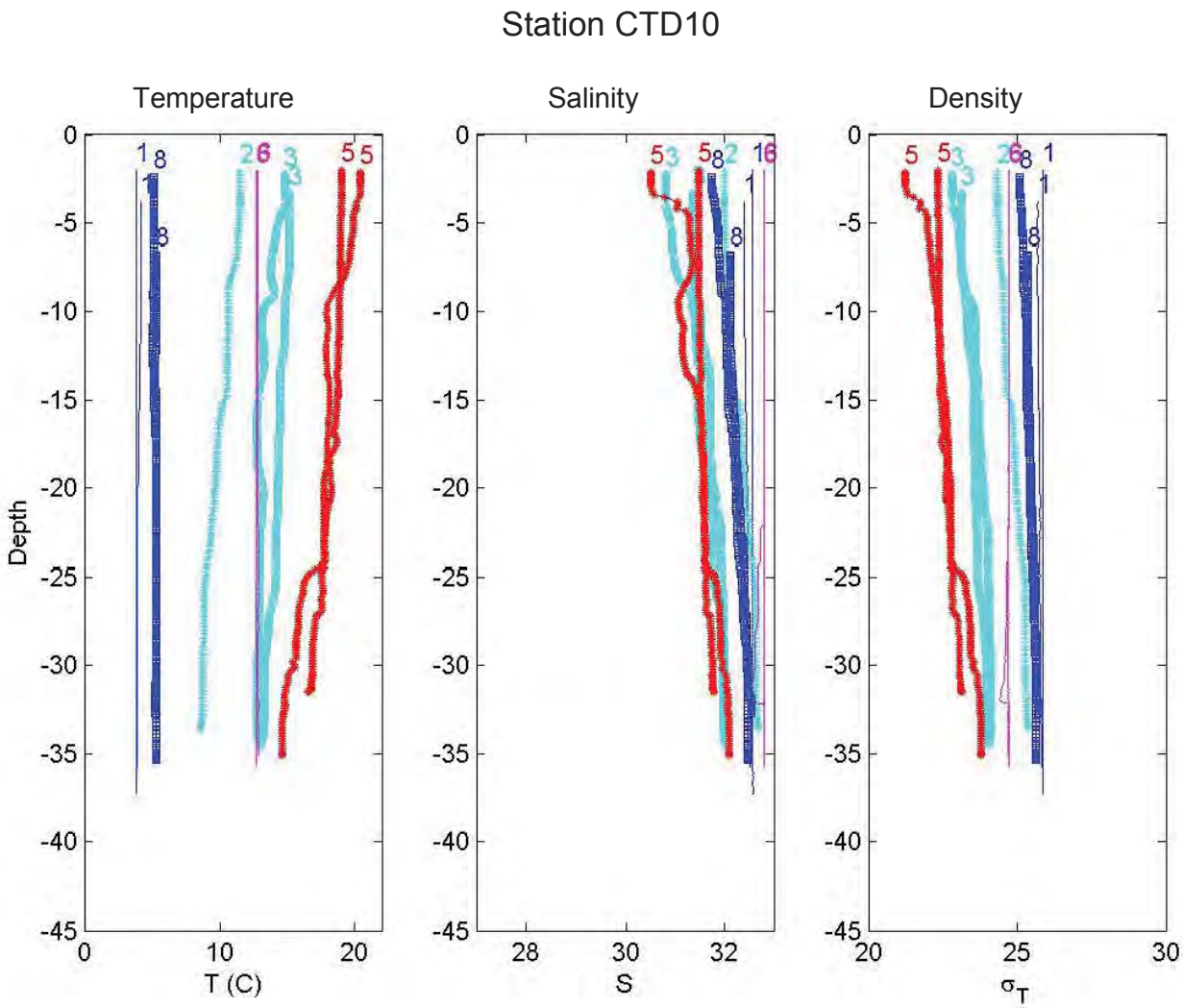

Figure 3-10. Temperature, conductivity, and density in the water column at Station CTD10, measured with the Profiling CTD. Each profile is labeled at the top with the cruise number. Colors reflect approximate seasons: Winter (Cruises CTDOT1,7,8; blue); spring (Cruises CTDOT2,3; turquoise); summer (Cruises CTDOT4,5; red), and late fall (Cruises CTDOT6; magenta).

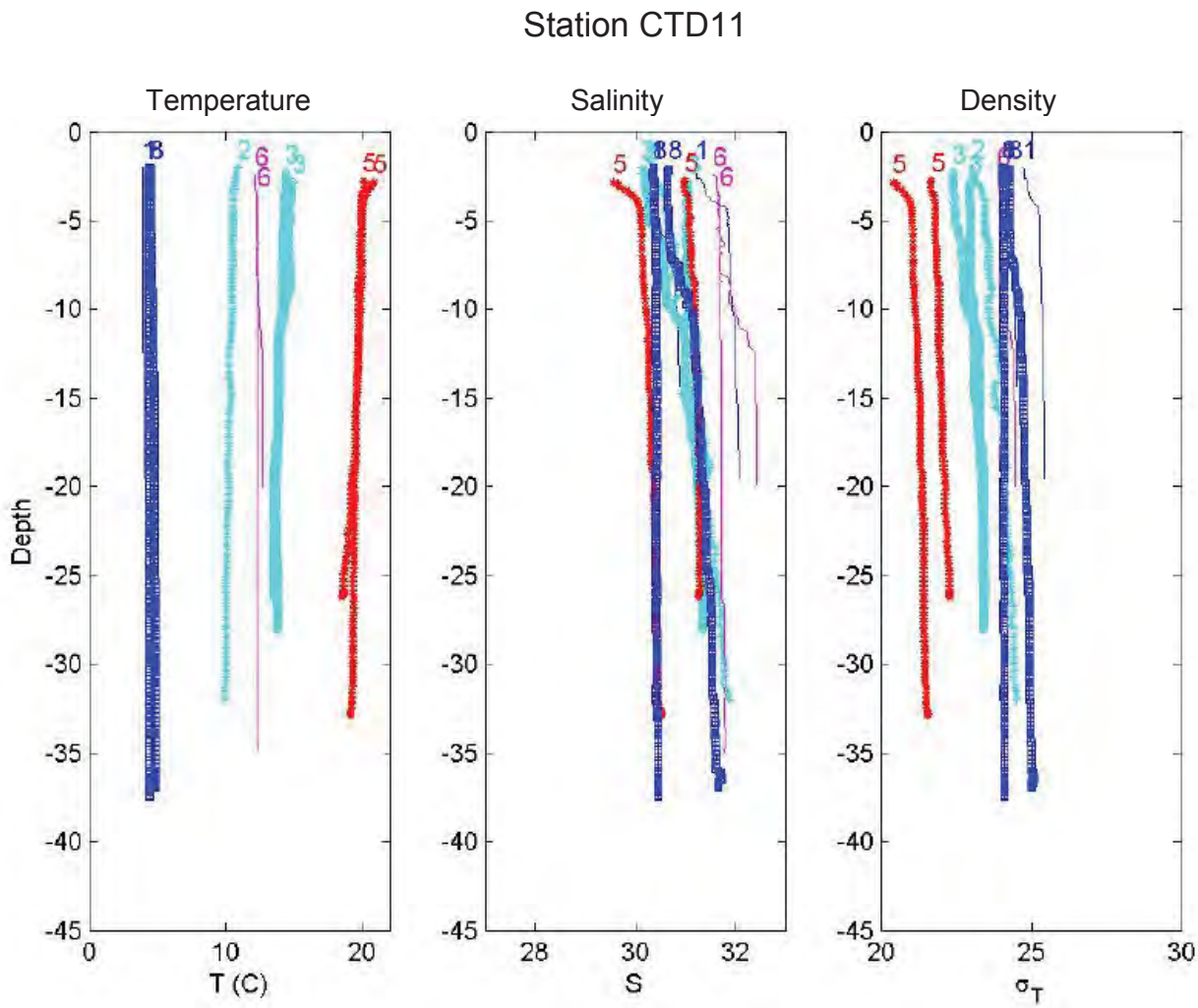

Figure 3-11. Temperature, conductivity, and density in the water column at Station CTD11, measured with the Profiling CTD. Each profile is labeled at the top with the cruise number. Colors reflect approximate seasons: Winter (Cruises CTDOT1,7,8; blue); spring (Cruises CTDOT2,3; turquoise); summer (Cruises CTDOT4,5; red), and late fall (Cruises CTDOT6; magenta).

4. Currents throughout the ZSF (Ship Surveys)

The spatial structure of the circulation was surveyed at all 11 stations (as described in Section 2.1.3.2) to complement the existing long-term time-series measurements of currents in the ZSF. This newly acquired information was used in the assessment of model predictions of current patterns as there is an expected difference between the currents measured by moored ADCPs at spatial scales of tens of meters and the predictions of the model for an average current over several hundreds of meters.

4.1 Data

The processed data consist of a set of vertical profiles of the east and north current components at the location of the ship. This data set, continuous in space and time, can be further processed and analyzed at varying spatial and temporal scales, facilitating the verification of model predictions. The data from Cruise CTDOT1 are shown as a time-series in Figure 4-1. The inherent complexity of the flow structure is further enhanced by the mixing-up of space and time. At the beginning of Day 71 in Figure 4-1 the ship was in the Race and the current was near maximum flood. An alternative view of this field is shown in Figure 4-2 which displays the current vectors at the single level (5.43 m) throughout the cruise.

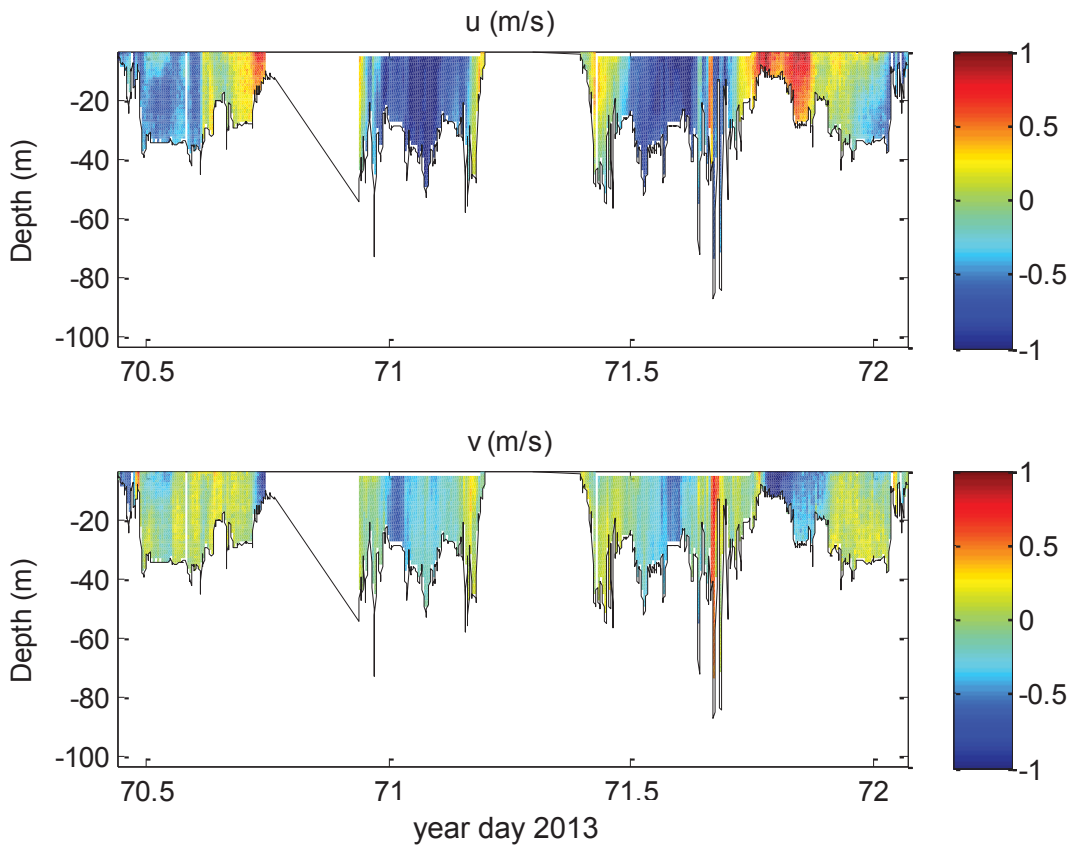

Figure 4-1. Time-series view of the current velocity components from ship-based ADCP measurements during Cruise CTDOT1. The upper graph shows the east component (u); the lower graph shows the north component (v). The bathymetry is shown by the black line in each graph.

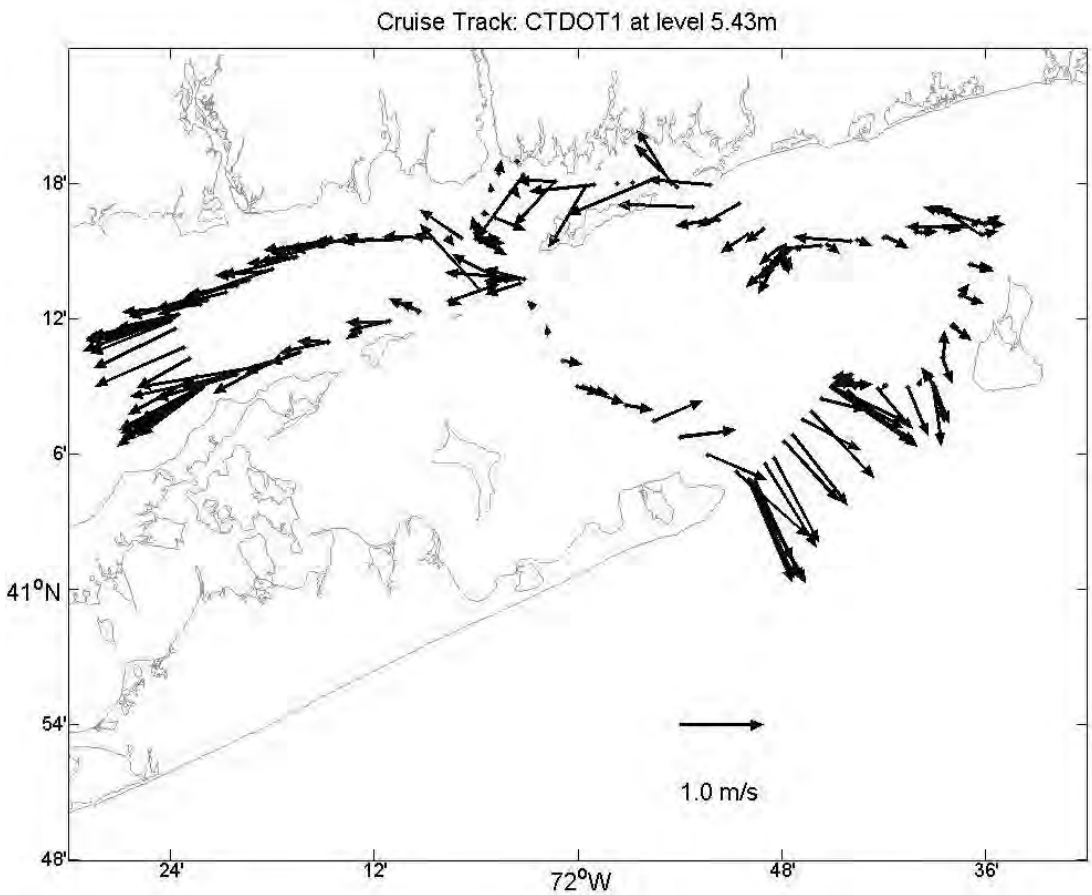

Figure 4-2. Map of eastern Long Island Sound and Block Island Sound with vectors representing the currents observed by the *R/V Connecticut* during Cruise CTDOT1. The velocity scale is shown in the lower right of the figure. The data were sub-sampled by a factor of 10 for clarity

The time-space distribution of data can be used directly to evaluate the model and to guide the assessment of the effects of spatial gradients on the evaluation of the model performance. However, the periodicity of the tides and the large-scale coherence of the velocity structure can be exploited to estimate the spatial structure of the mean flows.

The data files from all cruises were then combined into one data set and averaged to a spatial grid of 400m by 400m and a vertical extent of 2 m. This essentially creates a sparse time-series at grid points. If the ship was within 600 m of the closest bin center, the point is added to the closest depth bin. Once all velocities have been sorted into the appropriate bins, velocities are averaged so that each pass of the ship through a bin contributes one averaged velocity point at each depth.

The flow is then assumed to be composed of tidal frequency harmonics (M_2, N_2, and S_2) with amplitudes that vary spatially in a manner that can be approximated by bi-harmonic splines centered at 4 nodes. Results of this analysis are sensitive to the choice of these locations (Candela et al., 1992). Figure 4-3 shows a result of the procedure for the non-tidal flow at 5m below the surface with the node location shown in green. The black vectors show the means from the moored ADCPs at the same level for comparison. The error in the estimates increases rapidly away from

the ship tracks but the general eastward flow in Block Island Sound is consistent with the mooring results.

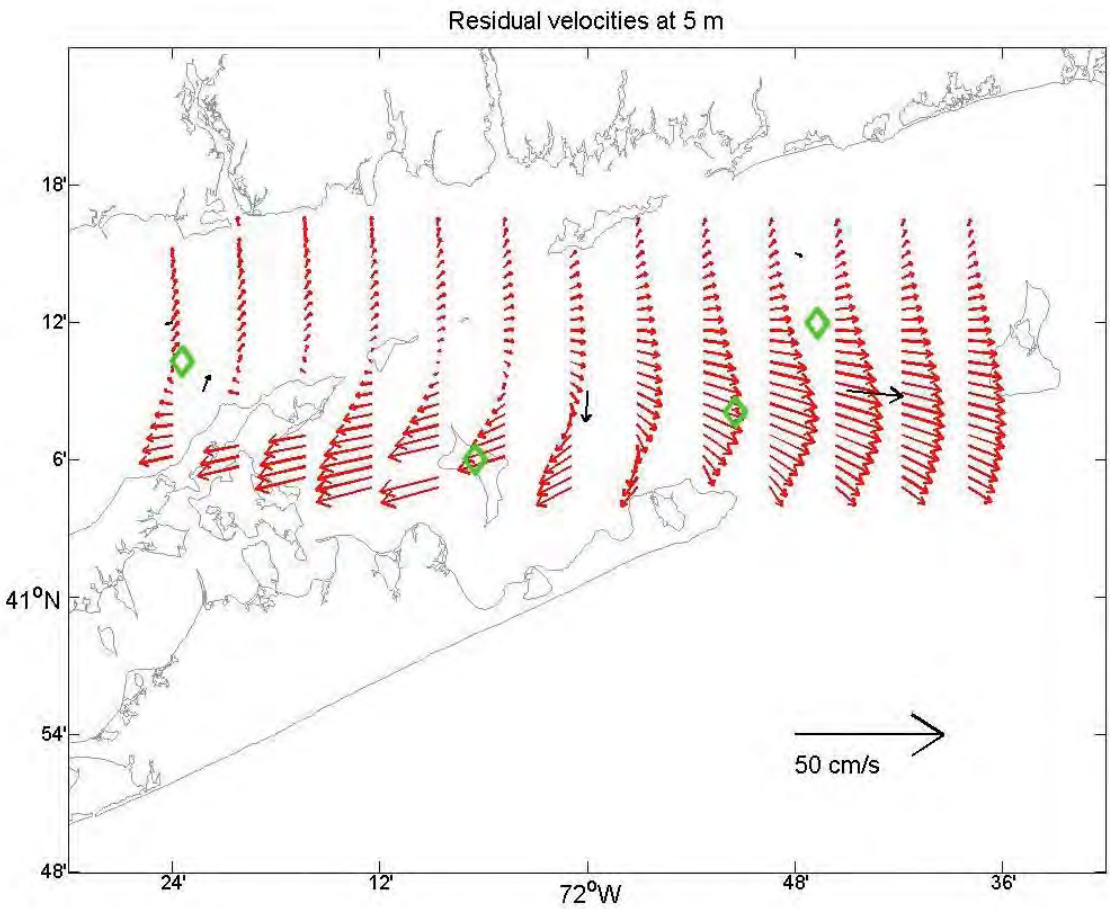

Figure 4-3. Smoothed fit for residual velocities at 5 m below MLLW (red) and 'de-tided'[14] velocities at moorings (black). Node locations are shown as green diamonds.

4.2 Summary

The spatial and time variations of currents in the ZSF were surveyed while the ship was transiting between the sampling stations and moored instrument locations. Though the data is noisy, it provides the only estimate of the magnitudes of the spatial gradients in current and therefore complements the time series acquired by the moored instruments. Since the model will only resolve gradients on a scale that is several times the grid spacing (i.e., approximately 250m), the spatial gradient estimates will allow an assessment of the difference between the model and the observations that can be attributed the scale disparity. The empirical analysis of the ship survey data is presented as a broad guide to the structure of the flow prior to the model evaluation.

[14] De-tided means that the signal of the tides was removed from the record.

5. Temperature and Salinity (Moored Instruments)

To observe the temporal variability of the water temperature and salinity near the sea bed in the ZSF, SBE SMP37 conductivity/temperature sensors were deployed at seven locations, as described in Section 2.1.2.1. The conductivity and temperature measurements were used to compute salinity and density.

5.1 Data

The variations in near-bottom temperature during the three campaigns are shown in Figures 5-1 to 5-7. Each station displays a similar warming trend throughout Campaigns 1 and 2 and a cooling trend during Campaign 3. Superimposed on the trends are tidal frequency variations that change in amplitude and are largest during Campaign 2 (summer) at Stations DOT2, 5, and 7. These variations are likely a consequence of the development of spatial gradients that are advected past the instruments by tidal currents.

Salinity[15] variations are shown in Figures 5-8 to 5-14. Seasonal trends in salinity during the three campaigns are weak and tidal frequency variations are much more substantial. Spatial variations are also large; Table 5-1 lists the mean salinity for each station and each campaign. The salinity at all stations is highest during Campaign 3 (winter) and lowest during Campaign 2 (summer). The lowest mean salinity during all campaigns was observed at Station DOT2 (located near Mattituck, NY); the second lowest mean salinity was observed at Station DOT1 (located near the Cornfield Shoals Disposal Site). Although Station DOT4 was located in Block Island Sound it had a lower mean salinity during all campaigns than Station DOT7 which was located in ELIS near the mouth of the Thames River and the New London Disposal Site (NLDS).

Table 5-1. Mean Salinity during each Campaign

Station	Salinity		
	Campaign 1	Campaign 2	Campaign 3
DOT1	29.76	29.50	30.30
DOT2	29.14	28.92	29.79
DOT3	30.21	29.84	30.82
DOT4	30.49	30.06	31.13
DOT5	31.92	31.42	32.14
DOT6	32.18	31.74	32.25
DOT7	30.91	30.73	31.46

[15] Salinity, often reported in practical salinity units (psu), is shown dimensionless in graphs and tables of this report.

A low-pass filter was used to highlight the longer trends in salinity and temperature by removing the effect of tides. Figure 5-15 shows the temperature series at the ELIS stations (DOT1, DOT2, DOT3 and DOT7) after a 5th order Butterworth filter with a cutoff frequency 0.66 cycles/day was applied. During Campaign 1 (spring) the temperature in the ELIS was remarkably uniform and warming occurred uniformly. By June the water temperature at all four stations was almost 15ºC. During Campaign 2 (summer) temperatures began to diverge, with temperatures at Station DOT2 warming fastest. Differences in water depths do not explain this divergence since Stations DOT1 and DOT3 remained in close agreement although Station DOT1 was deeper and Station DOT3 was shallower than Station DOT2. Station DOT2 remained coolest since it was influenced by the cool inflow from The Race and the BIS. In late November (Campaign 3) the bottom temperatures in the ELIS were uniform and cooling ensued at a remarkably uniform rate.

Figure 5-16 shows the low-pass filtered temperatures from the BIS stations. Similar to the ELIS, bottom temperatures and warming rates during the spring were uniform. In the summer, temperatures at Station DOT4 were the warmest, reaching 20ºC in August. Stations DOT5 and DOT6 remained cooler, reaching a maximum temperature of 18ºC in early August. Cooling in the winter was uniform and rapid with the temperature returning to 5ºC in early January.

The low-pass filtered salinity records from the ELIS stations are shown in Figure 5-17. During Campaign 1 there was a reduction in salinity by approximately 1 between mid-March and early May at each station. These reduced values persisted throughout Campaign 2 but by the start of Campaign 3 in mid-November salinities increased by 1 at all stations. The salinities subsequently decreased through December and January.

The low-pass filtered salinity records from the BIS stations are shown in Figure 5-18. At stations DOT5 and DOT6 the near bottom salinity varied around 32 throughout the three campaigns. The water was freshest in the summer. Station DOT4 had much lower salinity since it is influenced by the mean eastward flow from Long Island Sound (see Figure 4-3). The seasonal cycle was similar to that at Station DOT3 with maximum salinity in the winter, lowest in the summer, and intermediate salinity in the spring.

5.2 Summary

Temperature and salinity data were collected near the seafloor in the ZSF. Winter and spring water temperatures are uniform spatially but horizontal gradients develop in the summer. Tidal currents then create oscillations in water temperatures. Waters with the lowest salinity at the seafloor were observed on the south side of ELIS at Station DOT2 near Mattituck, New York.

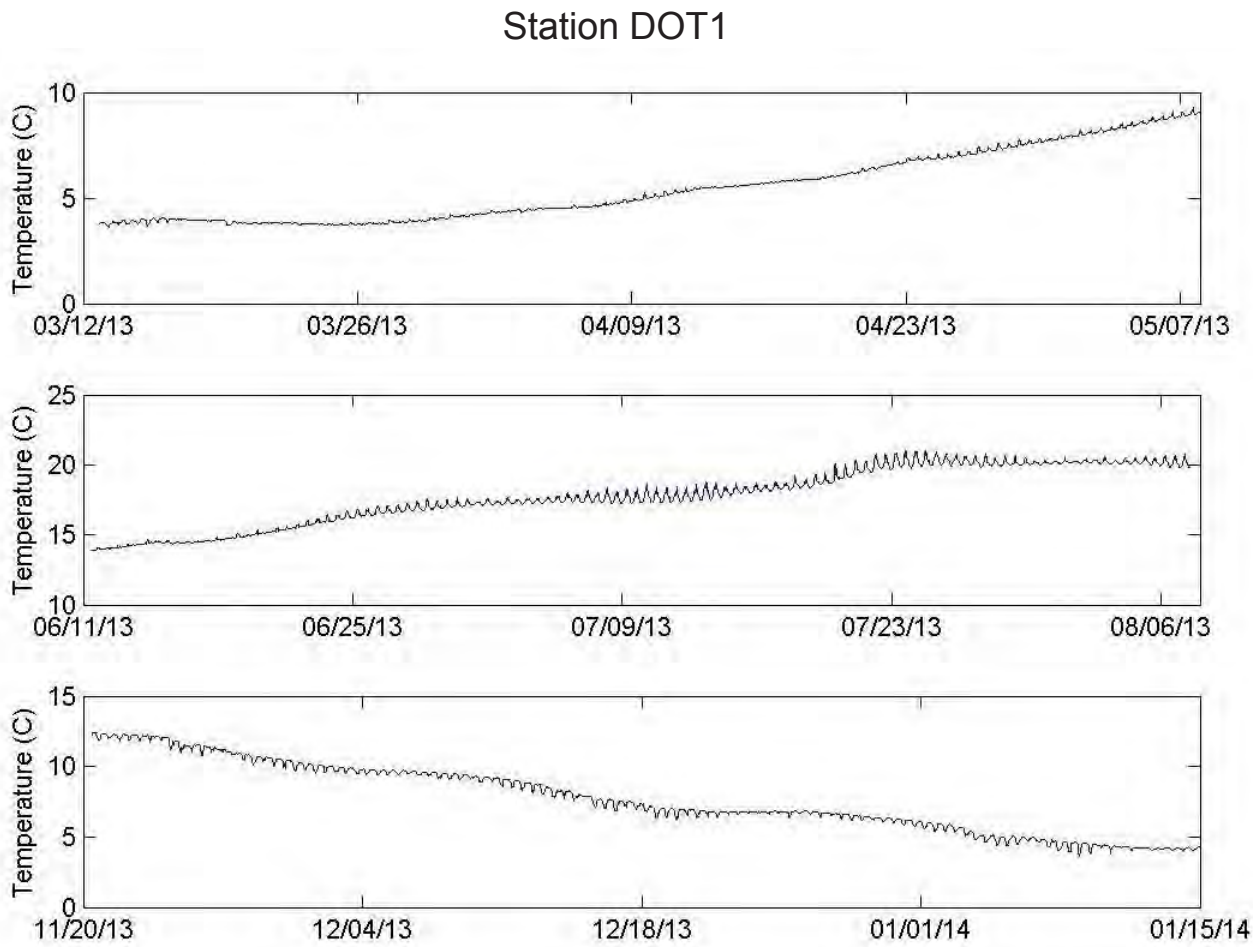

Figure 5-1. Measurements of near-bottom temperature at Station DOT1 during the three campaigns.

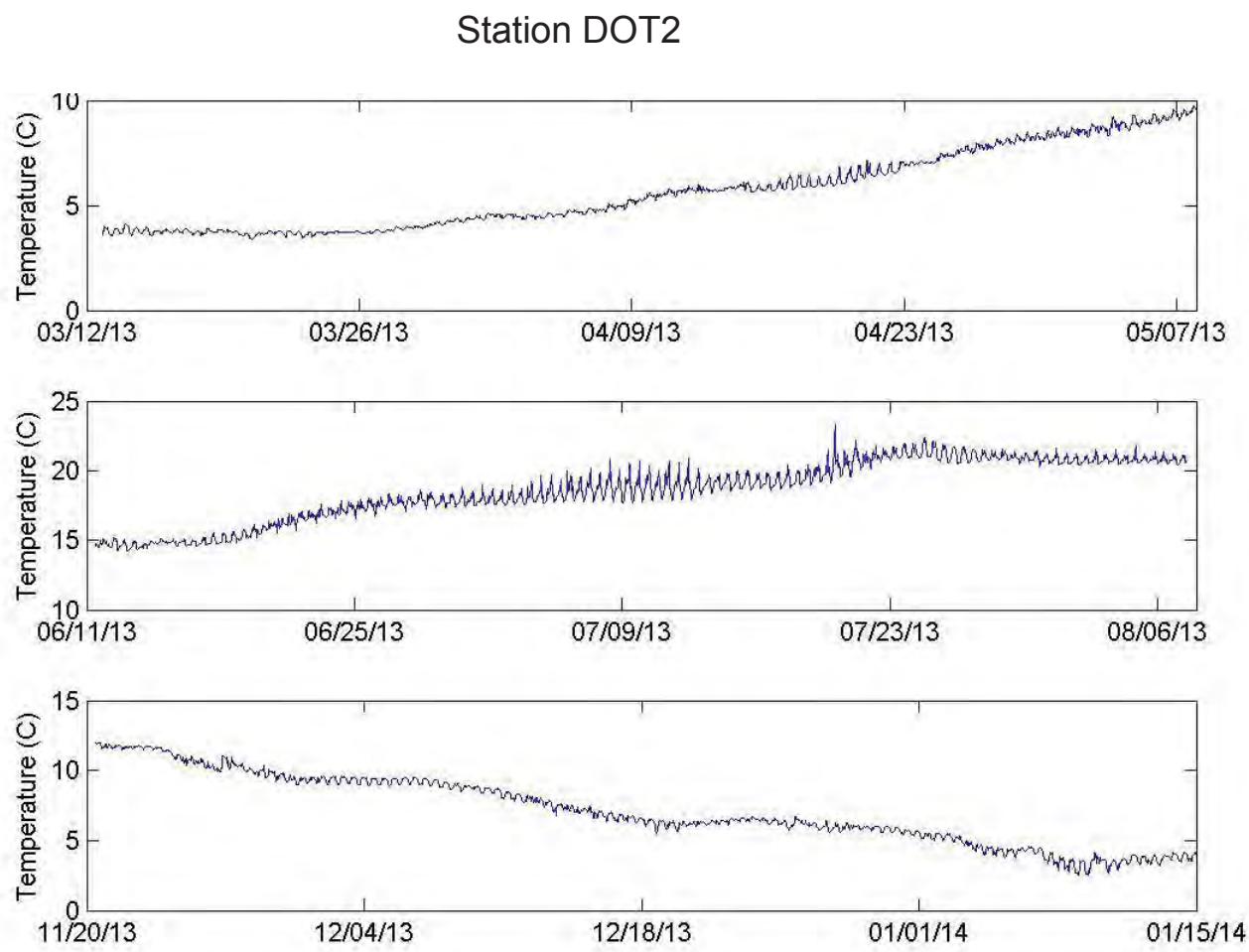

Figure 5-2. Measurements of near-bottom temperature at Station DOT2 during the three campaigns.

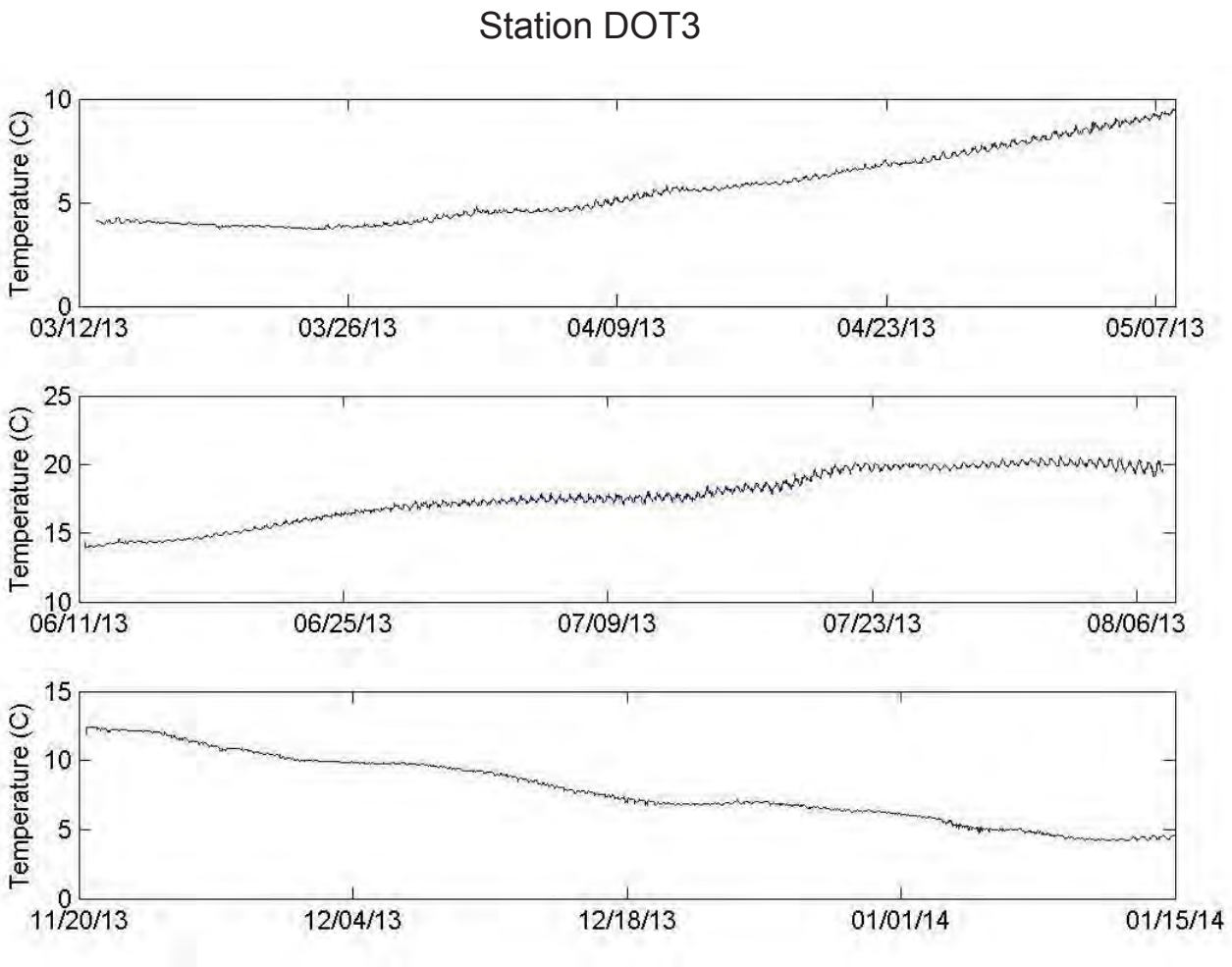

Figure 5-3. Measurements of near-bottom temperature at Station DOT3 during the three campaigns.

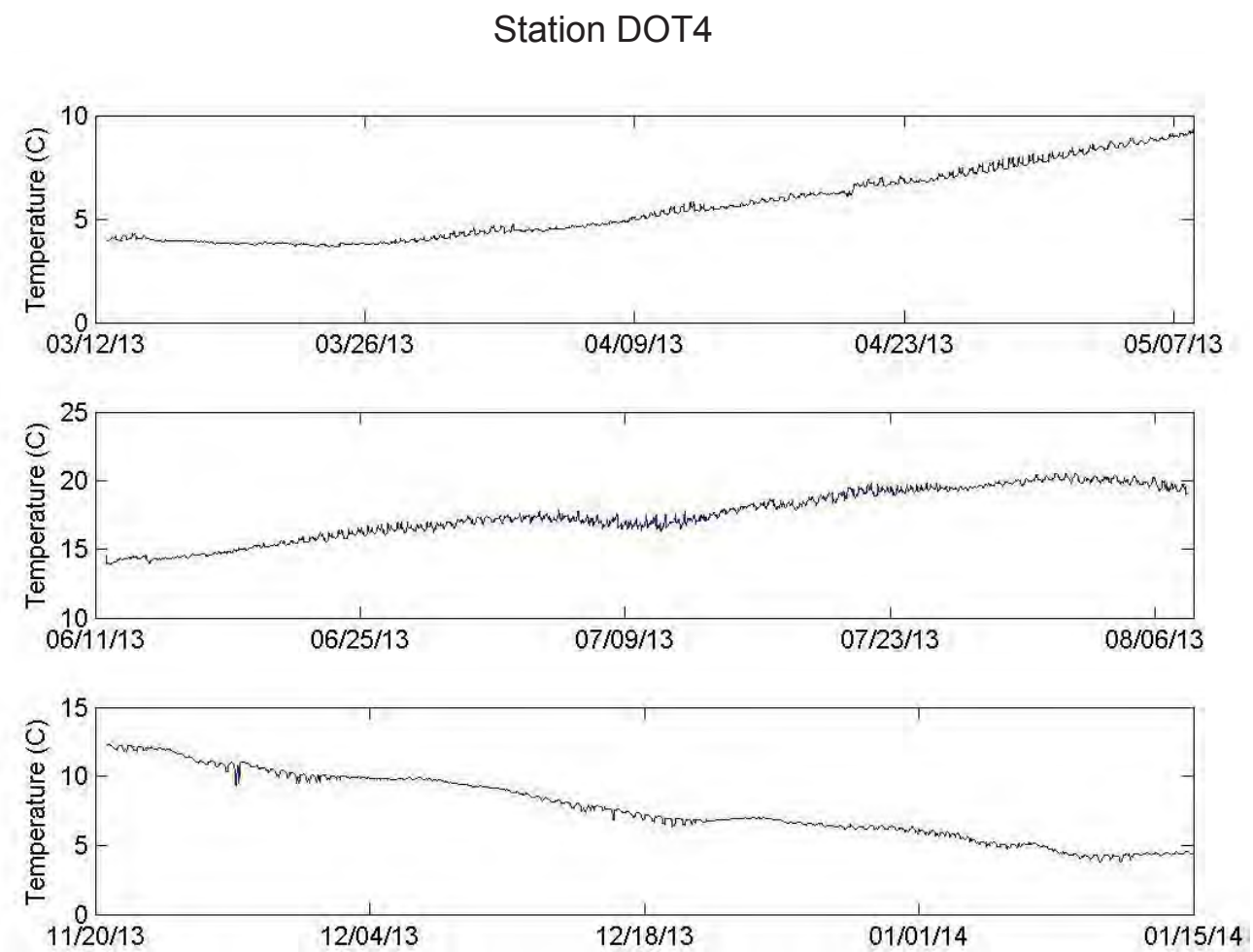

Figure 5-4. Measurements of near-bottom temperature at Station DOT4 during the three campaigns.

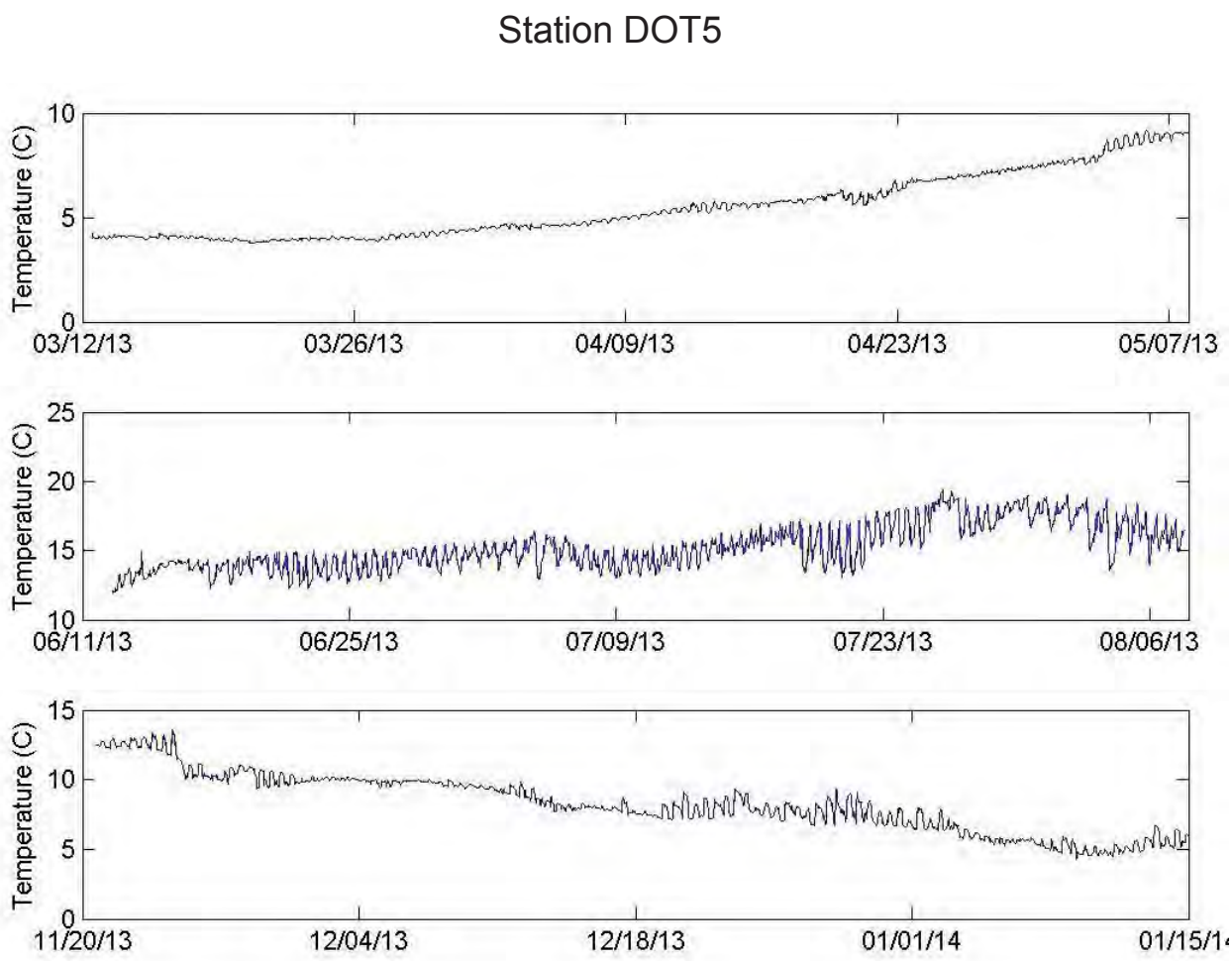

Figure 5-5. Measurements of near-bottom temperature at Station DOT5 during the three campaigns.

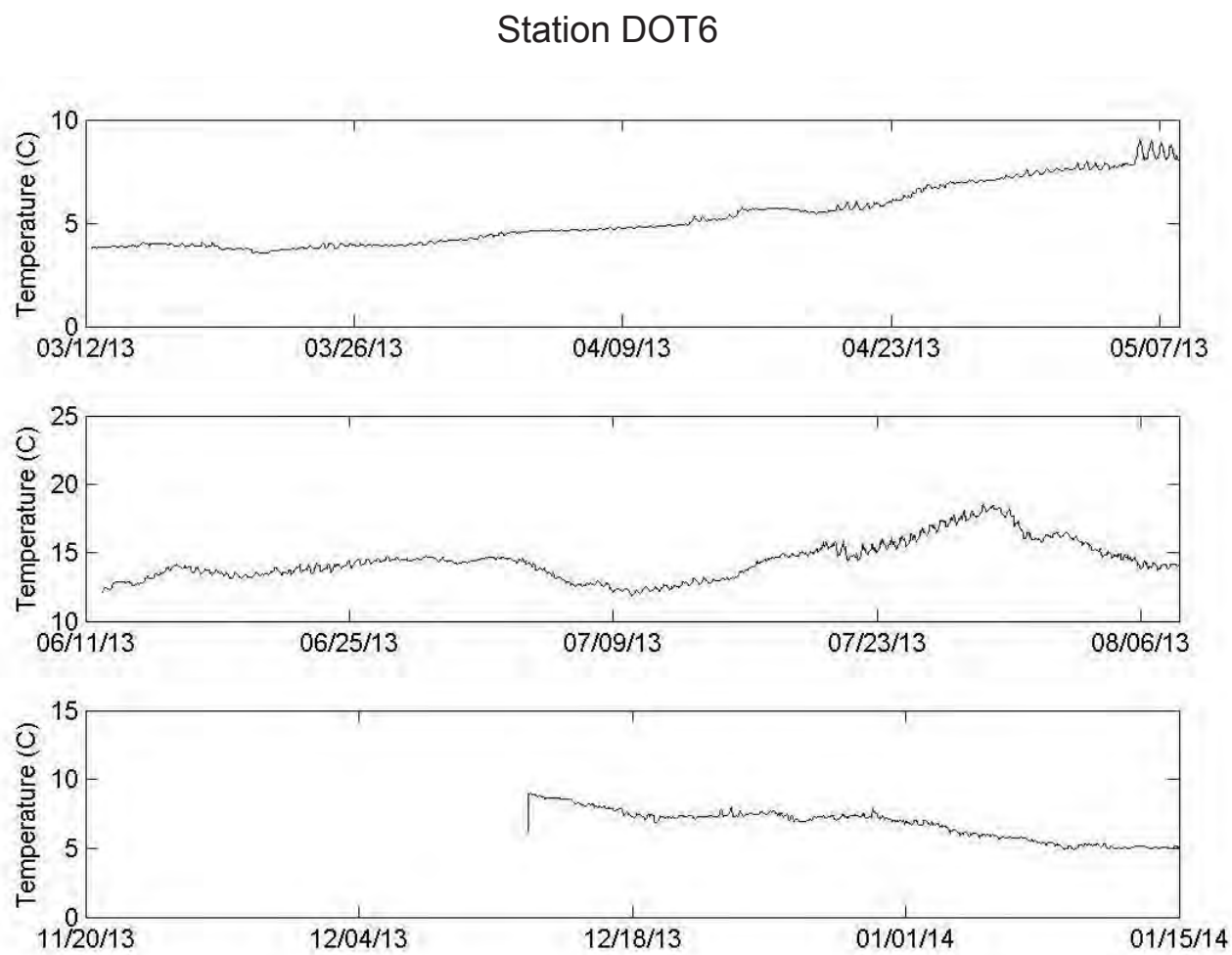

Figure 5-6. Measurements of near-bottom temperature at Station DOT6 during the three campaigns.

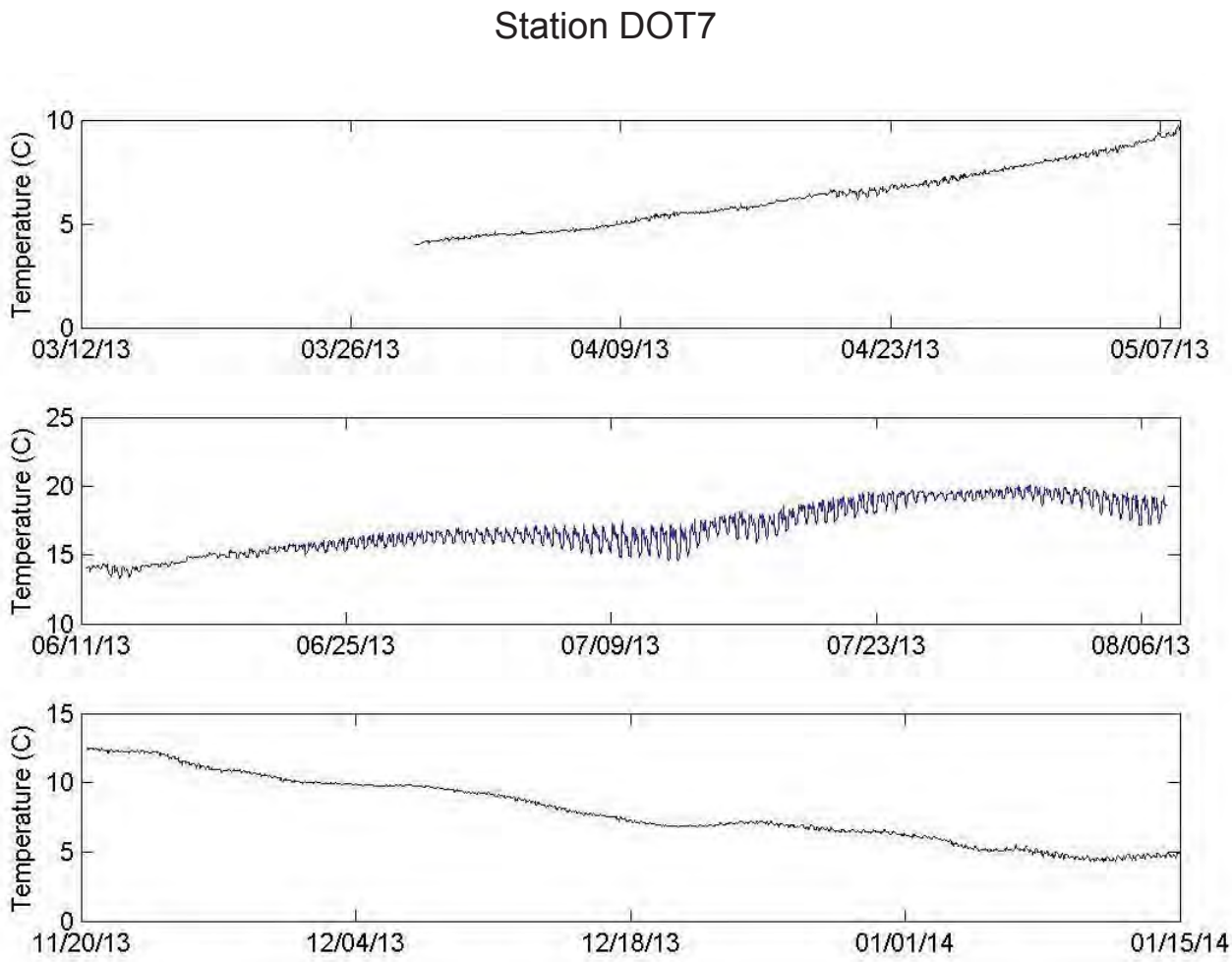

Figure 5-7. Measurements of near-bottom temperature at Station DOT7 during the three campaigns.

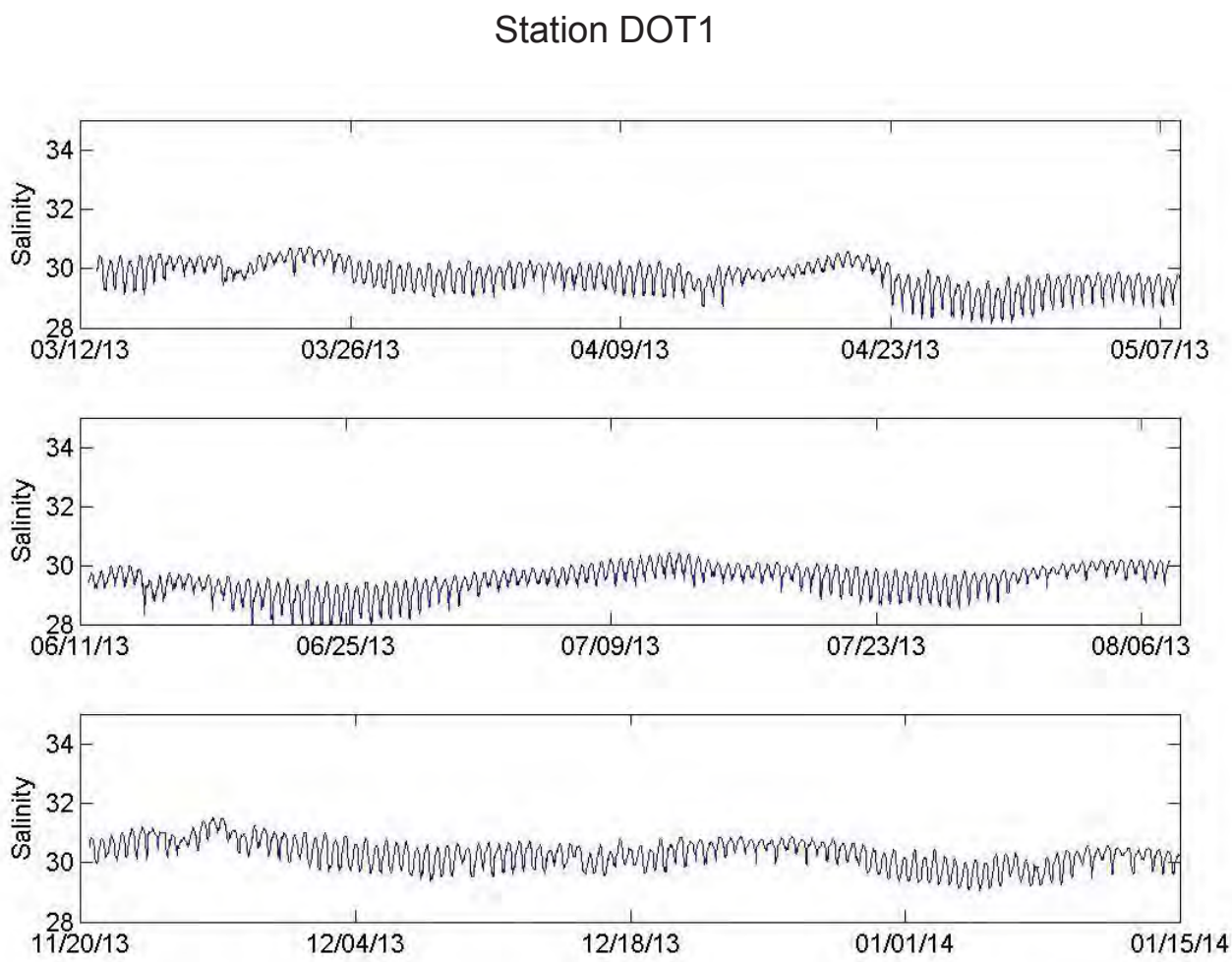

Figure 5-8. Measurements of near-bottom salinity at Station DOT1 during the three campaigns.

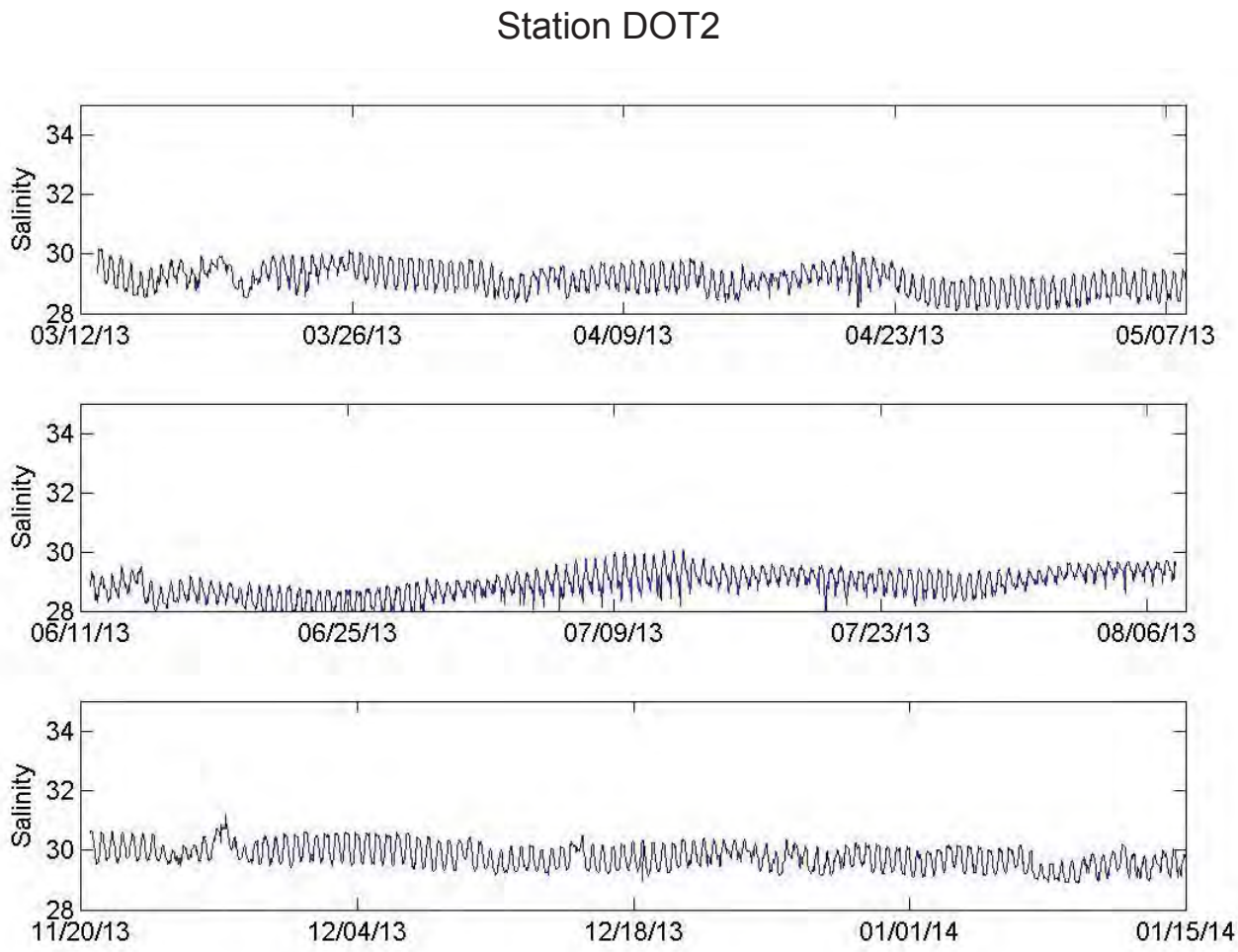

Figure 5-9. Measurements of near-bottom salinity at Station DOT2 during the three campaigns.

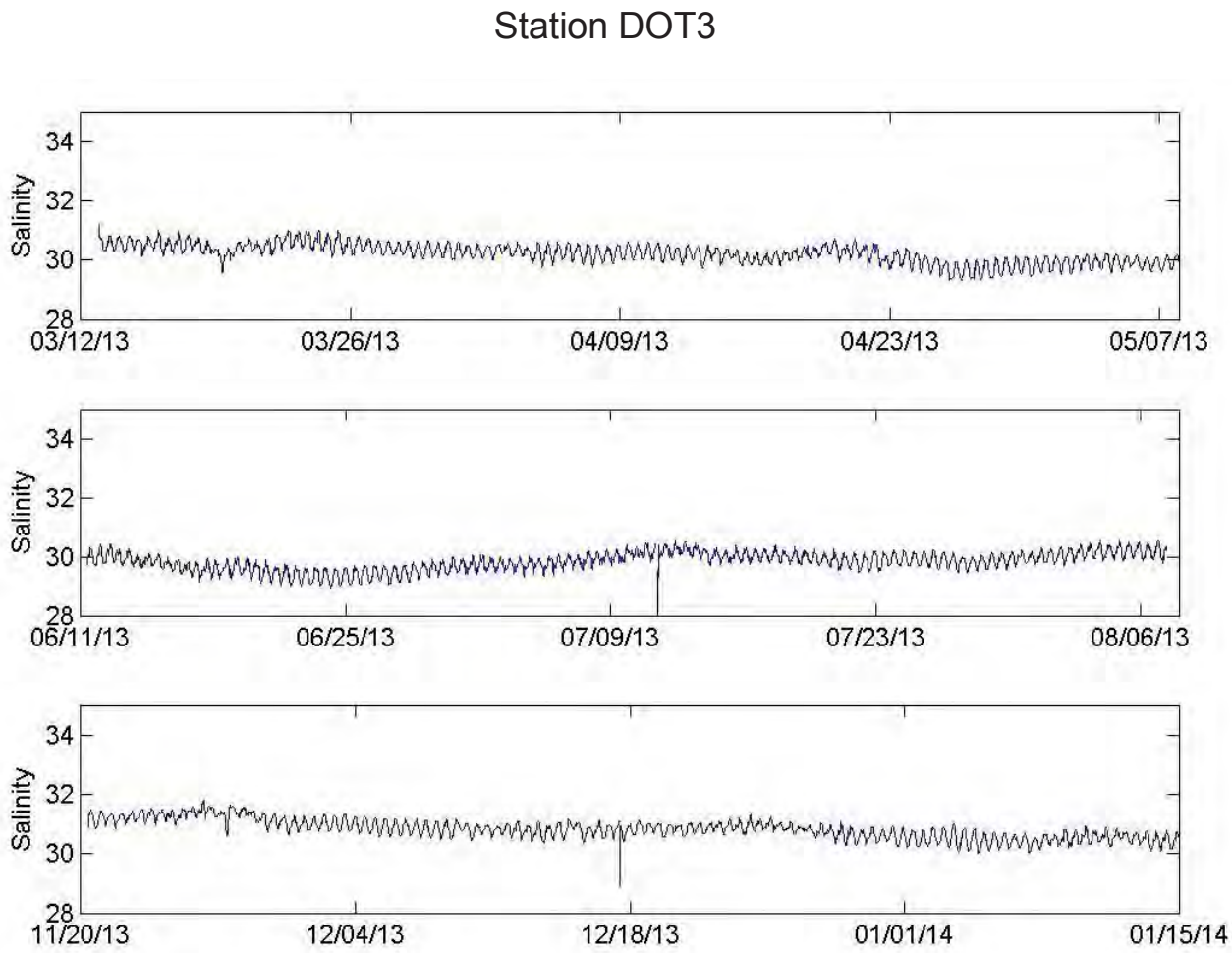

Figure 5-10. Measurements of near-bottom salinity at Station DOT3 during the three campaigns.

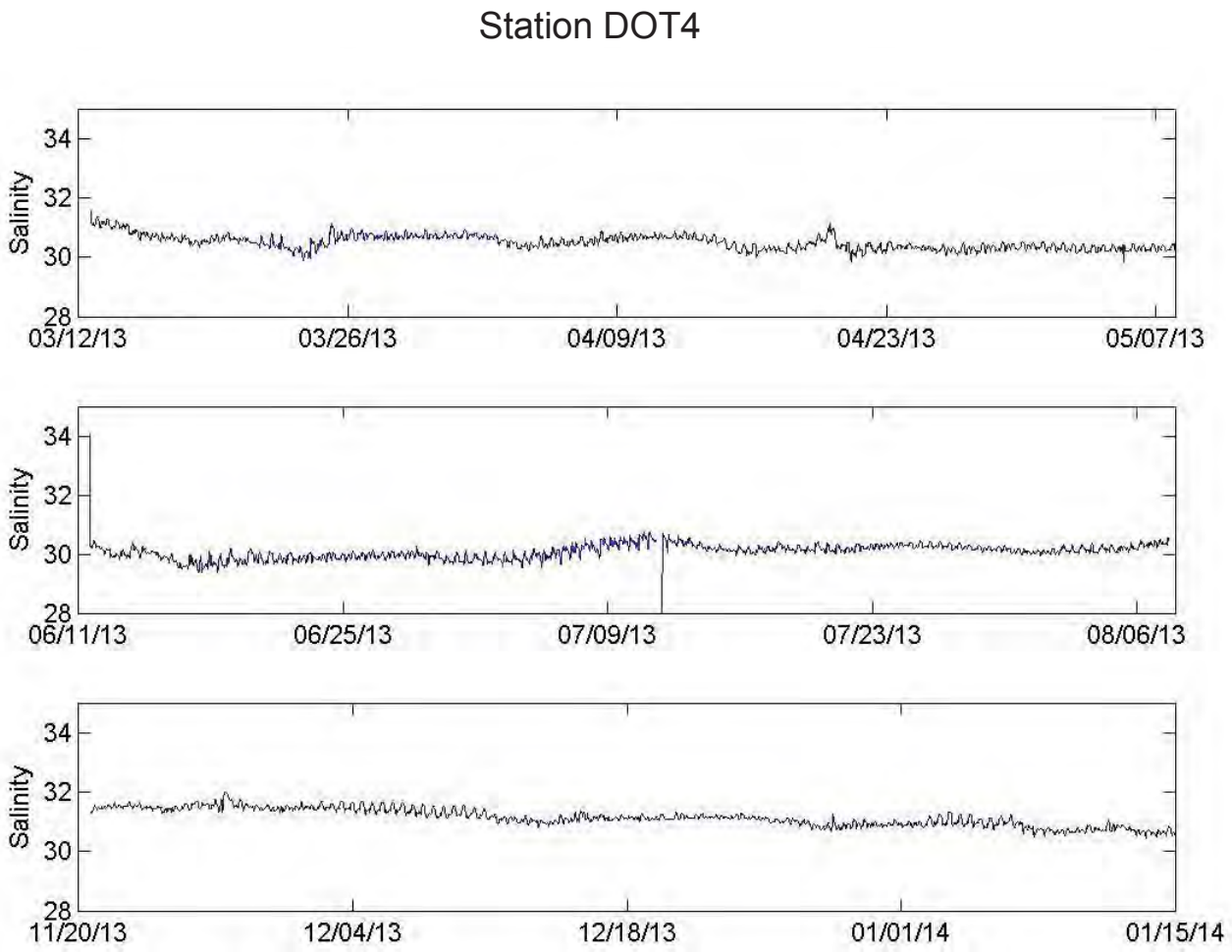

Figure 5-11. Measurements of near-bottom salinity at Station DOT4 during the three campaigns.

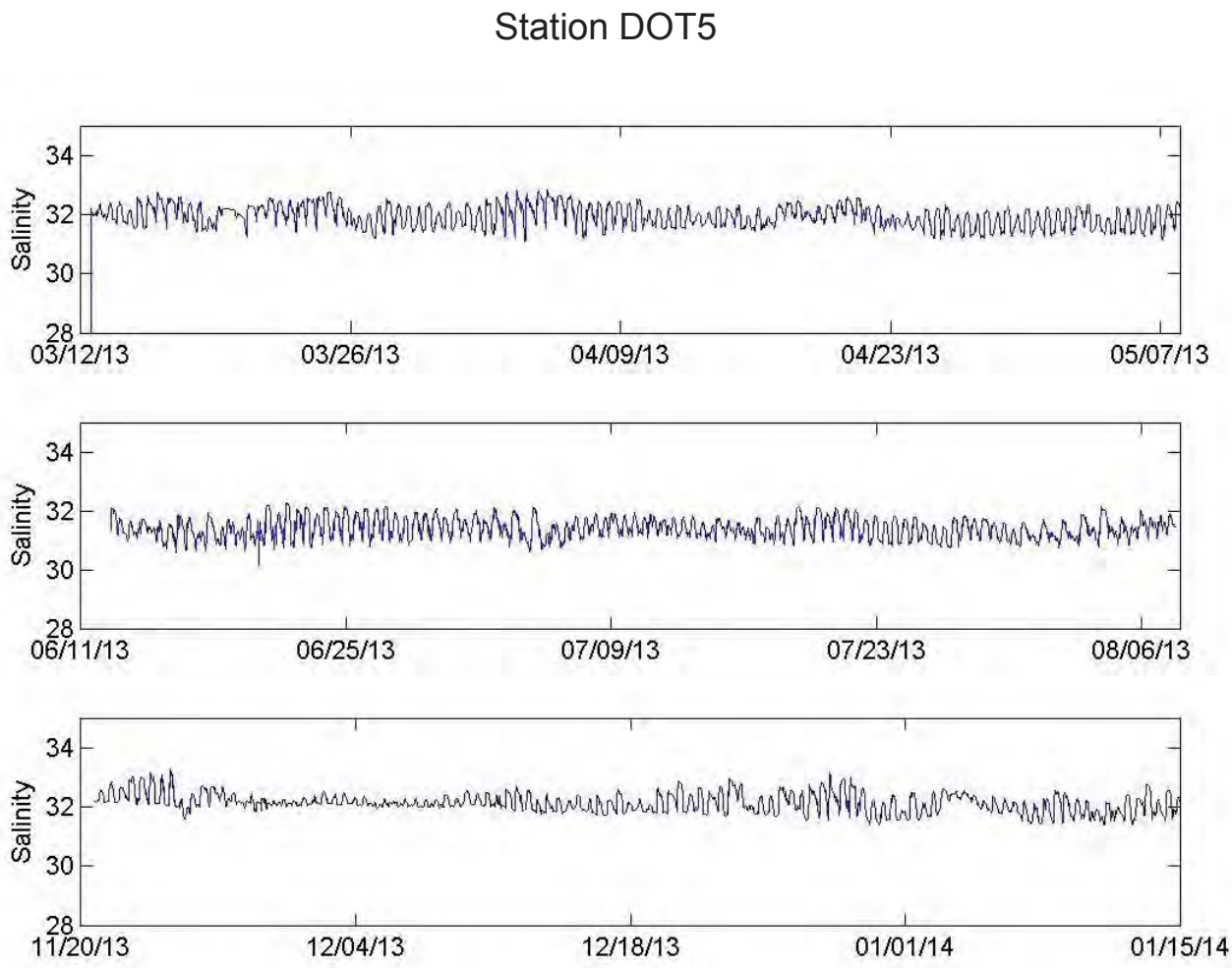

Figure 5-12. Measurements of near-bottom salinity at Station DOT5 during the three campaigns.

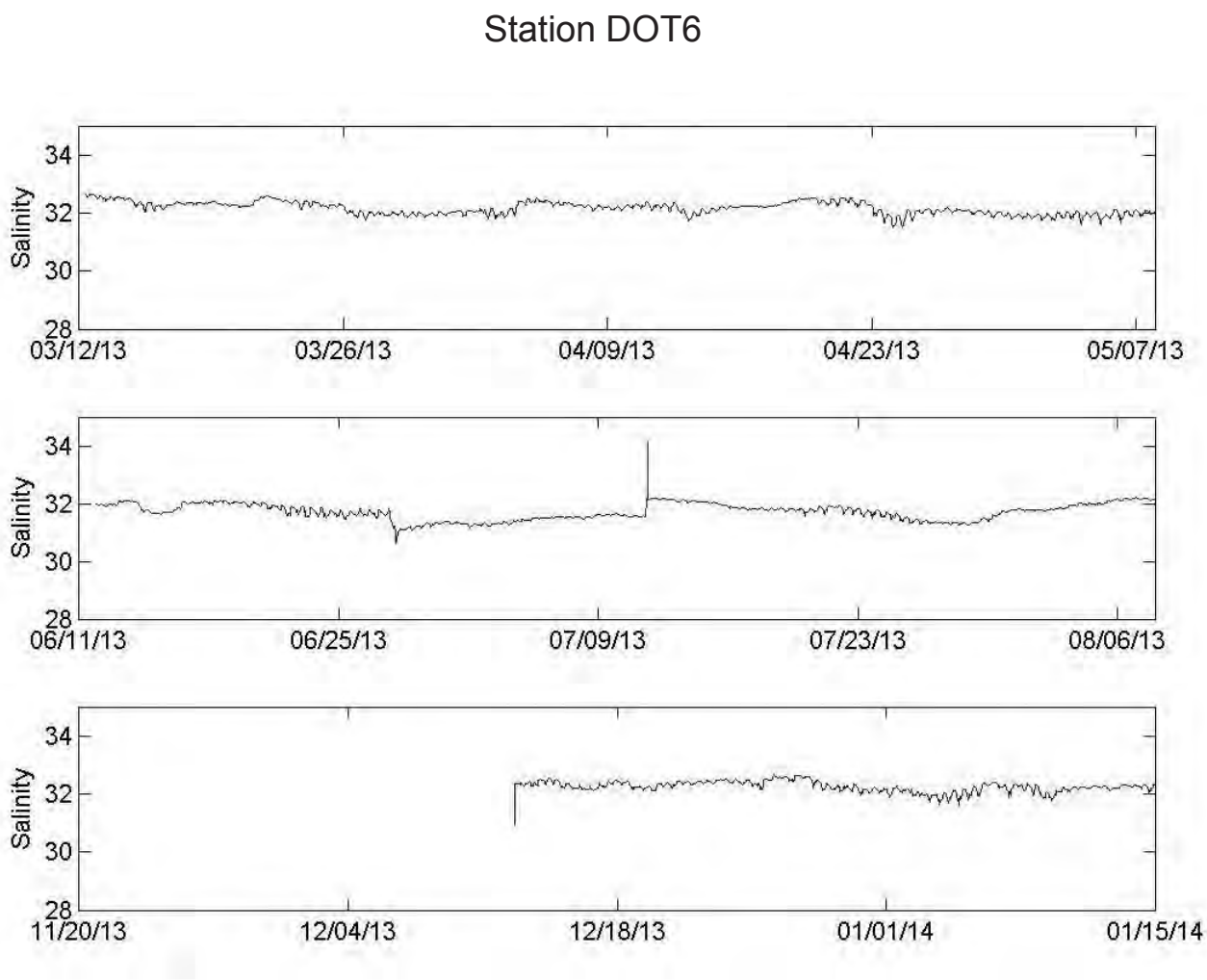

Figure 5-13. Measurements of near-bottom salinity at Station DOT6 during the three campaigns.

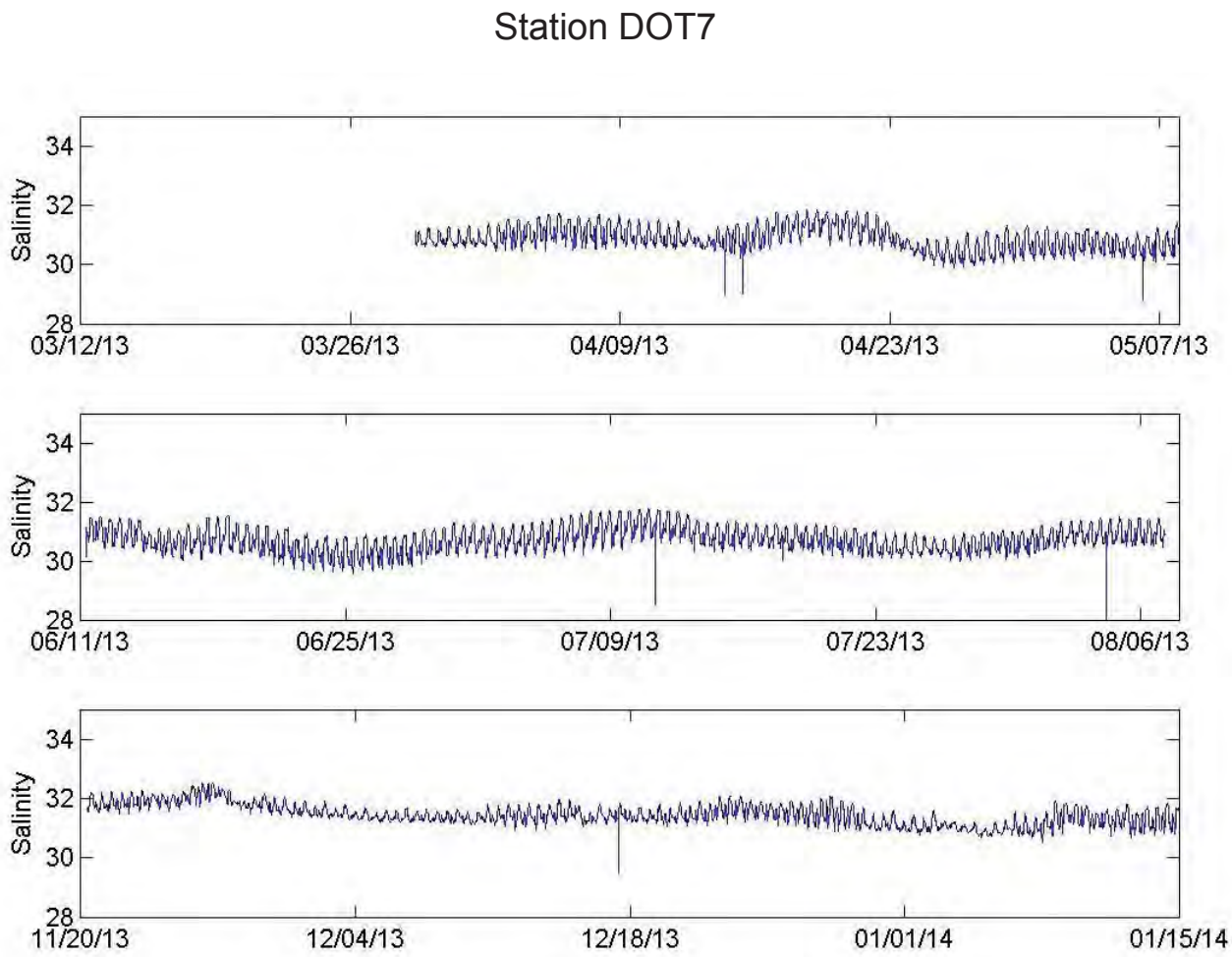

Figure 5-14. Measurements of near-bottom salinity at Station DOT7 during the three campaigns.

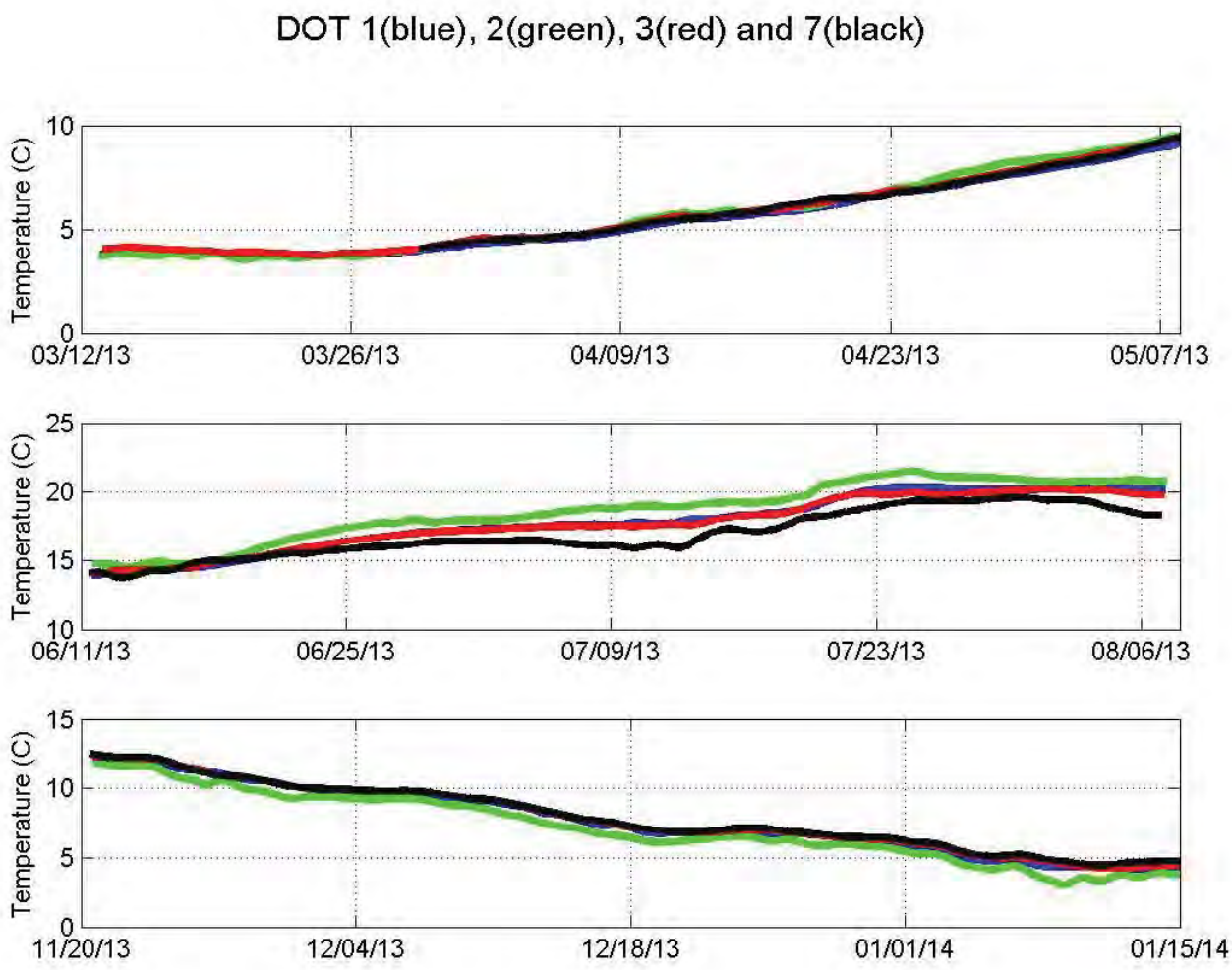

Figure 5-15. Low-pass filtered records of near bottom temperature in eastern Long Island Sound at Stations DOT1 (blue), DOT2 (green), DOT3 (red), and DOT7 (black) for Campaigns 1, 2 and 3.

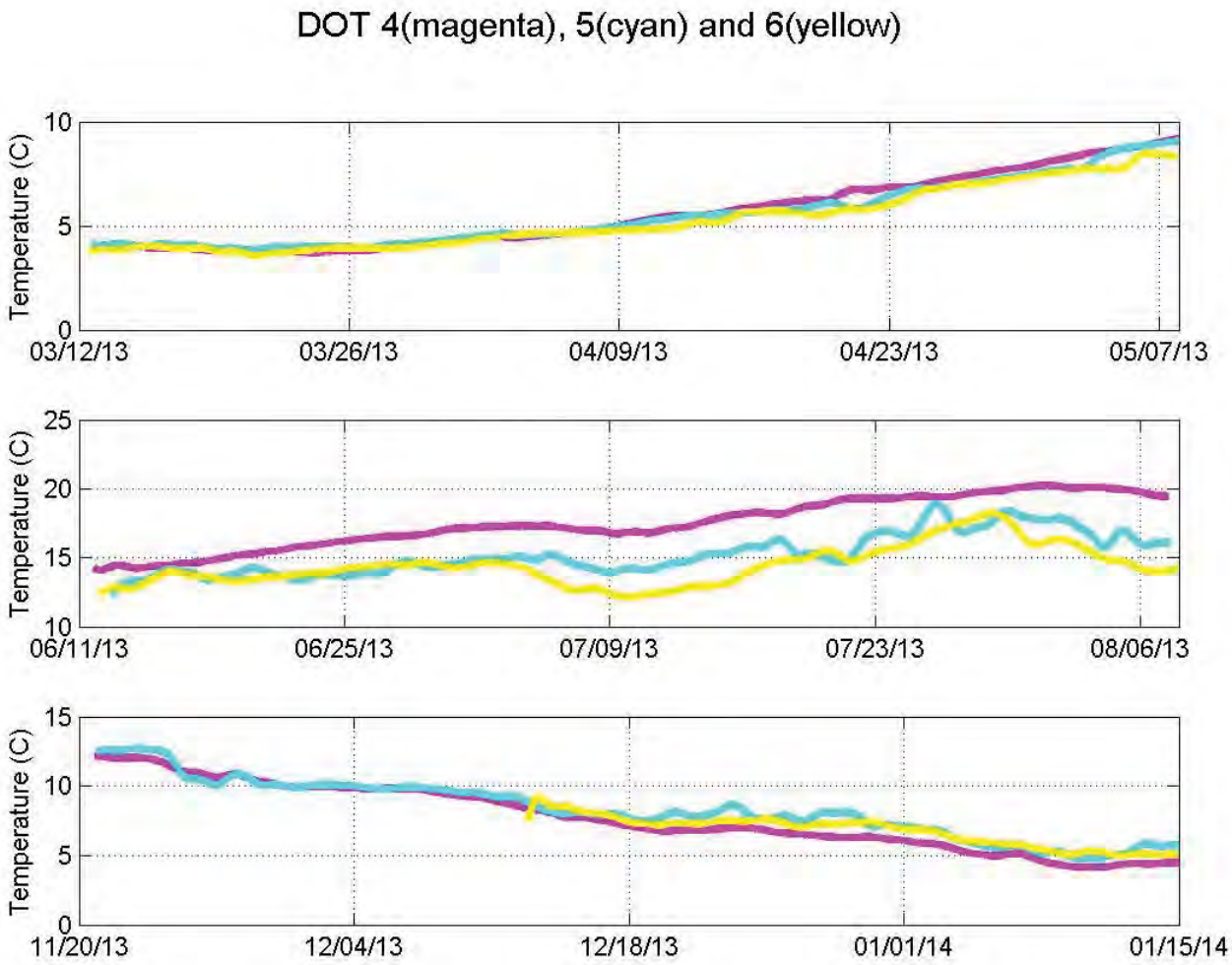

Figure 5-16. Low-pass filtered records of near bottom temperature in eastern Long Island Sound at Stations DOT4 (magenta), DOT5 (cyan), and DOT6 (yellow) for Campaigns 1, 2 and 3.

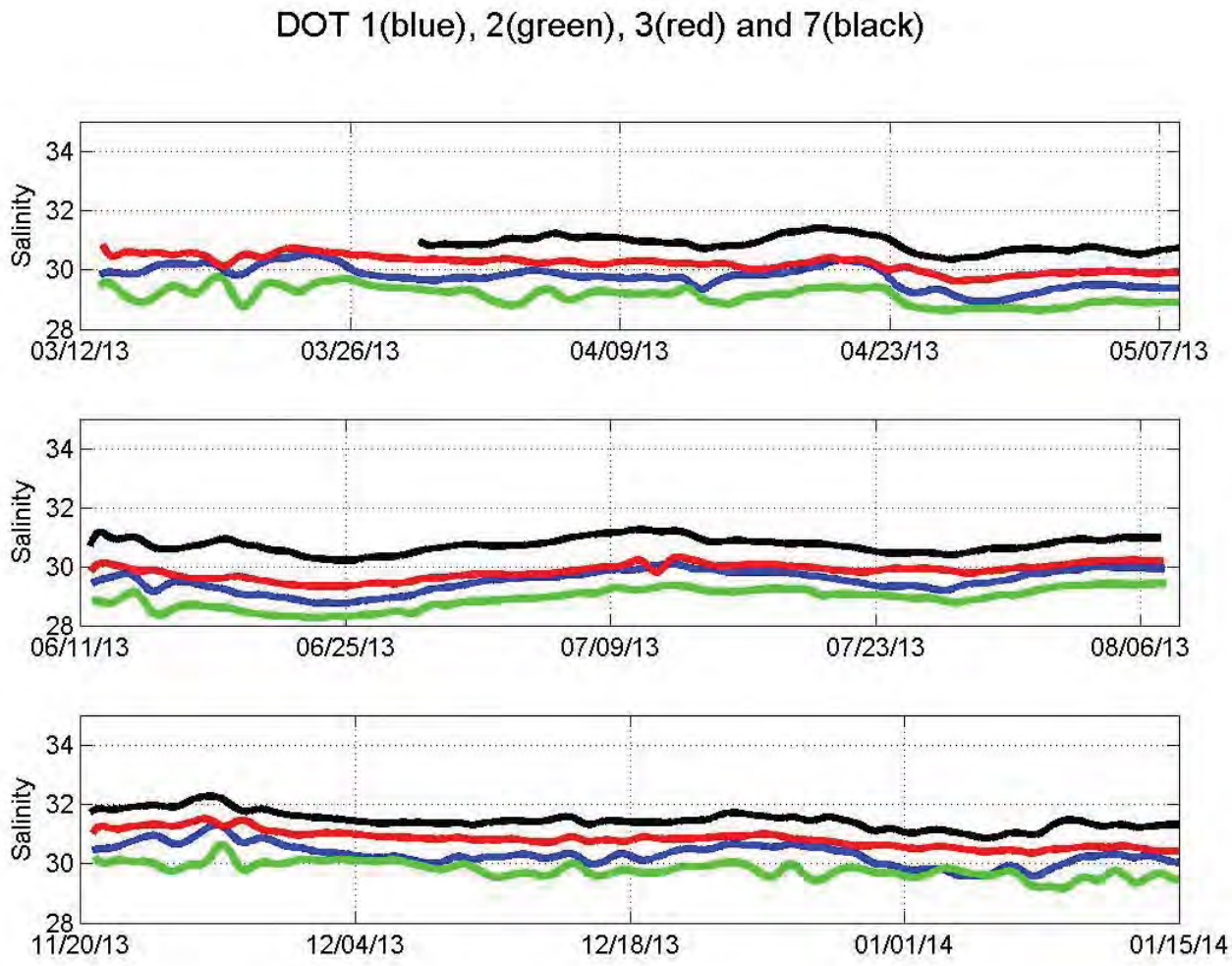

Figure 5-17. Low-pass filtered records of near bottom salinity in eastern Long Island Sound at Stations DOT1 (blue), DOT2 (green), DOT3 (red), and DOT7 (black) for Campaigns 1, 2 and 3.

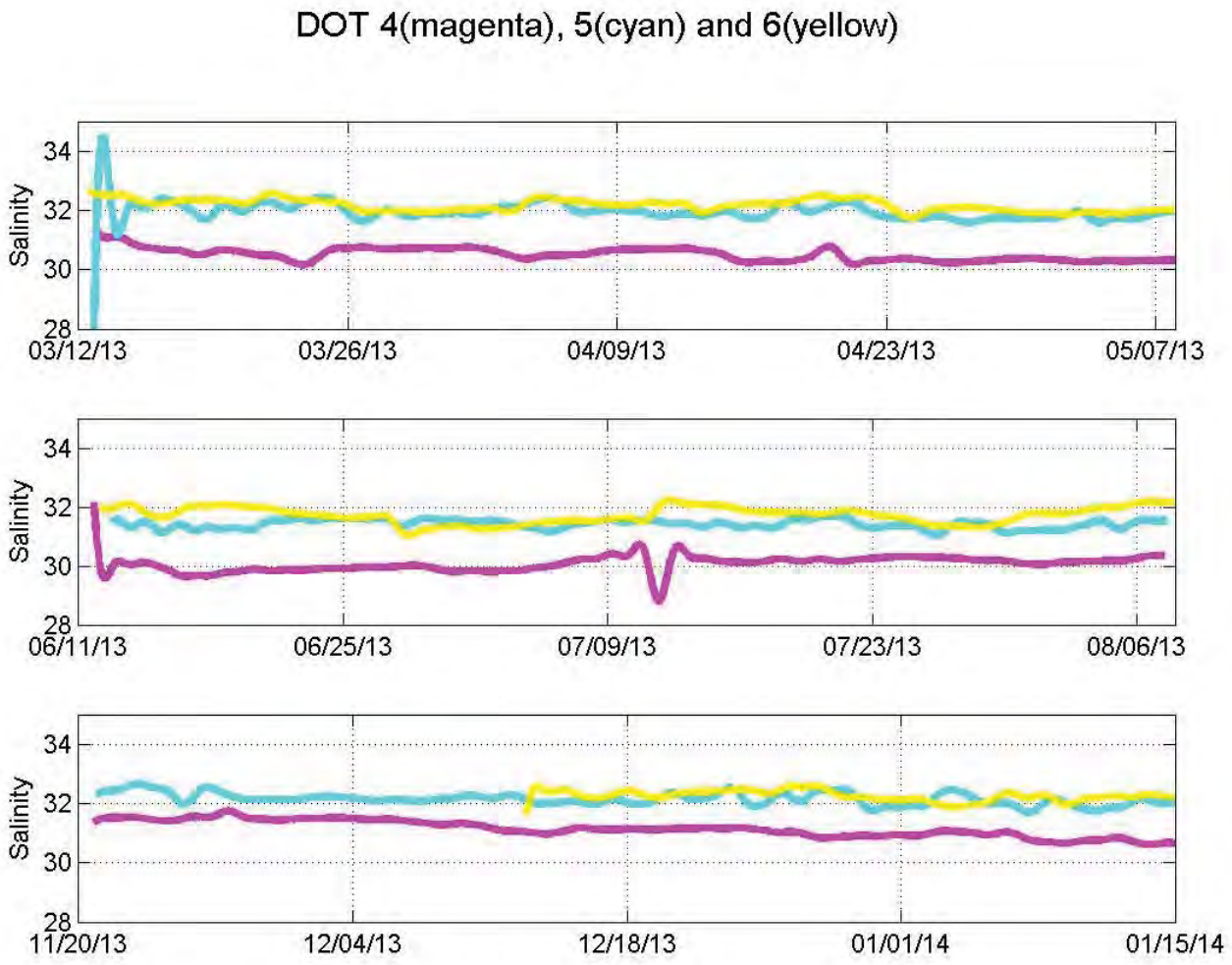

Figure 5-18. Low-pass filtered records of near bottom salinity in eastern Long Island Sound at Stations DOT4 (magenta), DOT5 (cyan), and DOT6 (yellow) for Campaigns 1, 2 and 3.

6. Currents in the Water Column (Moored Instruments)

Water column current measurements were made at the seven mooring stations by upward-looking RDI ADCPs (with waves array sampling enabled) positioned at 1.5 m above the seafloor, as described in Section 2.1.2.2. Most of the variability in the observations is due to periodic fluctuations at tidal frequencies and since they are of large amplitude, more subtle features of the data are obscured. To reveal more of the character of the data the tidal flow is described first. The tidal variations are then removed and the vertical structure of the low frequency variations is displayed. Thereafter, the vertical structure of the mean flow and the variation between the three campaigns is discussed.

6.1 Data

6.1.1 Tidal Velocities

The M2 tidal ellipses were calculated from the depth-averaged velocities at the seven mooring stations for the three campaigns (Figure 6-1). The M2 tidal constituent is the largest in Long Island Sound and tidal ellipses are oriented primarily east-west, following bathymetric contours. In BIS the orientation of the tidal ellipses varies at different stations.

The tides dominate daily velocity and sea surface elevation fluctuations. Figure 6-2 shows an example of four days of velocity measurements at Station DOT7 to demonstrate that tidal velocities dominate the velocity components on short (daily) time scales.

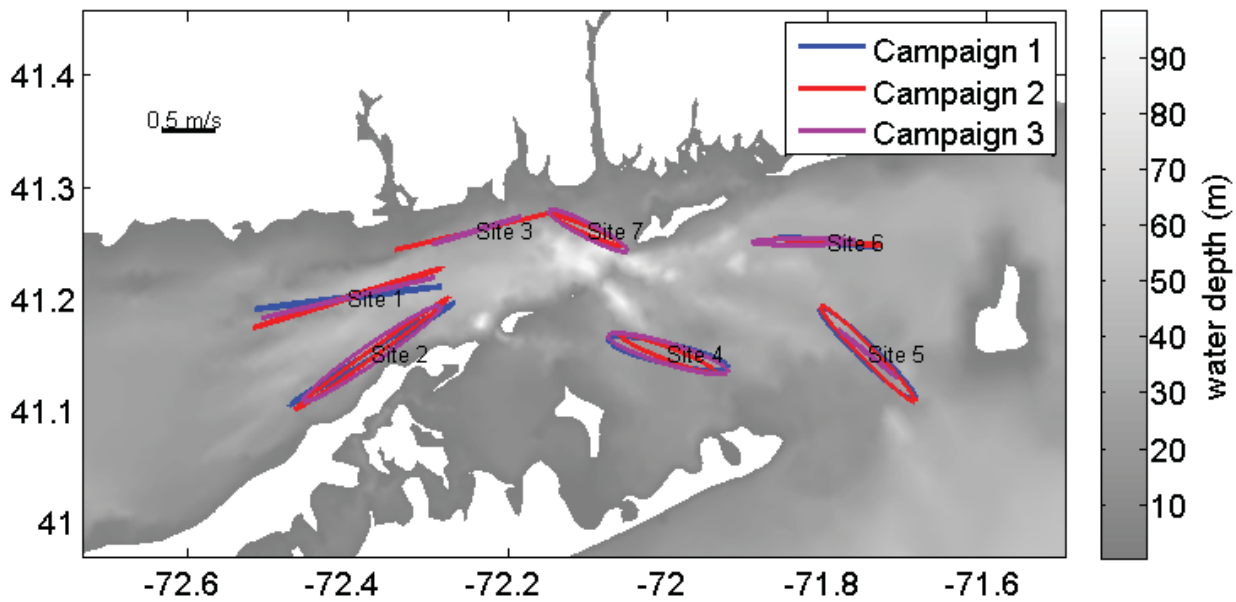

Figure 6-1. M2 tidal ellipses for all station (colors), plotted on top of local bathymetry.

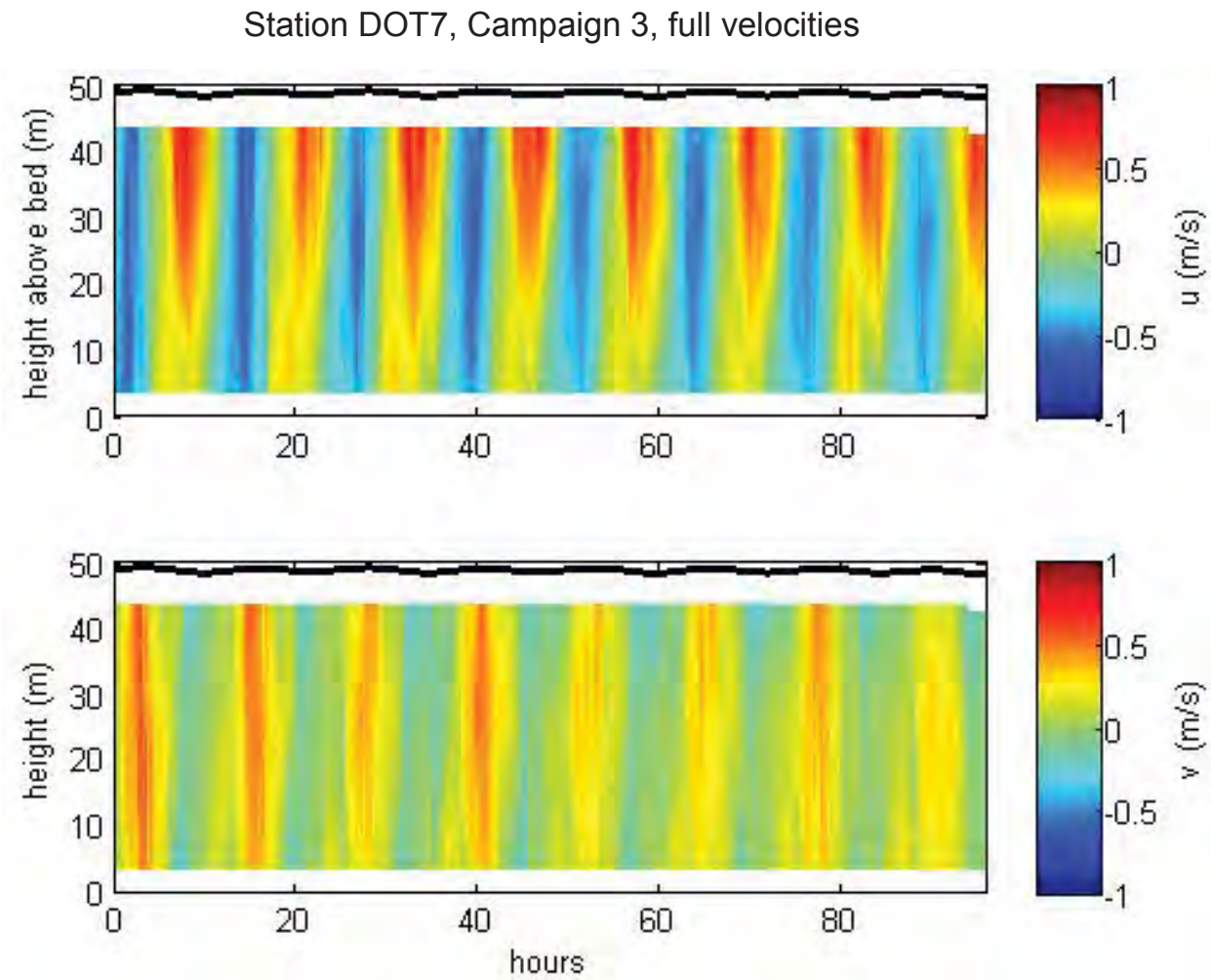

Figure 6-2. Full velocity profiles and surface elevation at Station DOT7 for four days. Tidal velocities dominate both the eastward (upper graph) and northward (lower graph) velocity components.

6.1.2 Subtidal Velocities

A low-pass filter was used on the velocities to analyze the slowly varying part of the velocity field. The M2 tide and any other fluctuations with periods shorter than 33 hours were removed. The remaining signal included the mean circulation, spring-neap cycle, and weather events. Figure 6-3 shows an example of the subtidal circulation at Station DOT5 during Campaign 2. The circulation at this site was typically eastward and southward near the surface, and westward and northward near the bottom. Graphs of the velocity profiles at all stations for all campaigns are presented in Appendix 11.

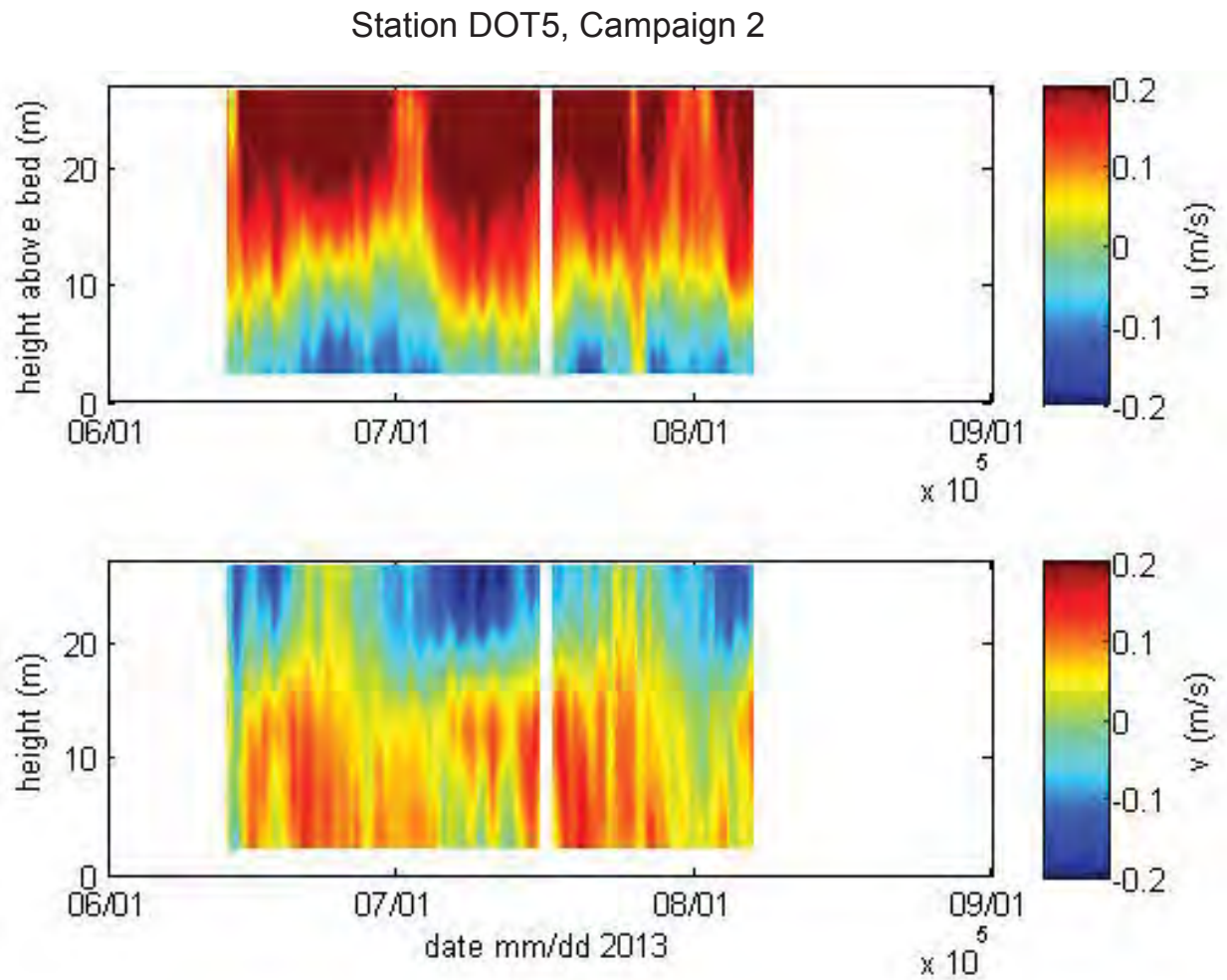

Figure 6-3. Low-pass filtered velocities for Station DOT5, Campaign 2. Eastward (upper graph) and northward (lower graph) components.

6.1.3 Depth-averaged Velocities and Time-averaged Velocity Profiles

There can be subtle differences between the mean flows observed during the three campaigns. As an example, the time-series at Station DOT1 (Figure 6-4) shows a water depth at about 37 m and a typical tidal range of 1 to 2 m. The water depth time-series also shows the slight change in water depth upon instrument recovery and redeployment of the tripod frame, both between campaigns and during mid-campaign service. The depth average velocities indicate a tidal range of +/- 1 m/s for the eastward velocity component and 0.2 m/s for the northward velocity component. The temperature time-series reflects the seasonal cycle of near-bottom temperature variation as well as some shorter event-scale variation.

Time-averaged velocity profiles of the eastward and northward velocity components show the vertical structure of the circulation at Station DOT1. All three campaigns show a similar vertical structure at Station DOT1, with mean flow toward the west and south and the strongest velocities

near the bottom of the water column (Figure 6-5). The large values at the top of each profile are from data bins at elevations that are only submerged during high tide, and therefore only record half of each tidal cycle. These values indicate the direction of the tidal Stokes transport, which is predominantly westward at this station. Because, near the mouth of Long Island Sound, the tide is a progressive wave rather than a standing wave, the tides transport water into the Long Island Sound. Graphs of all stations and campaigns are shown in Appendix 11b.

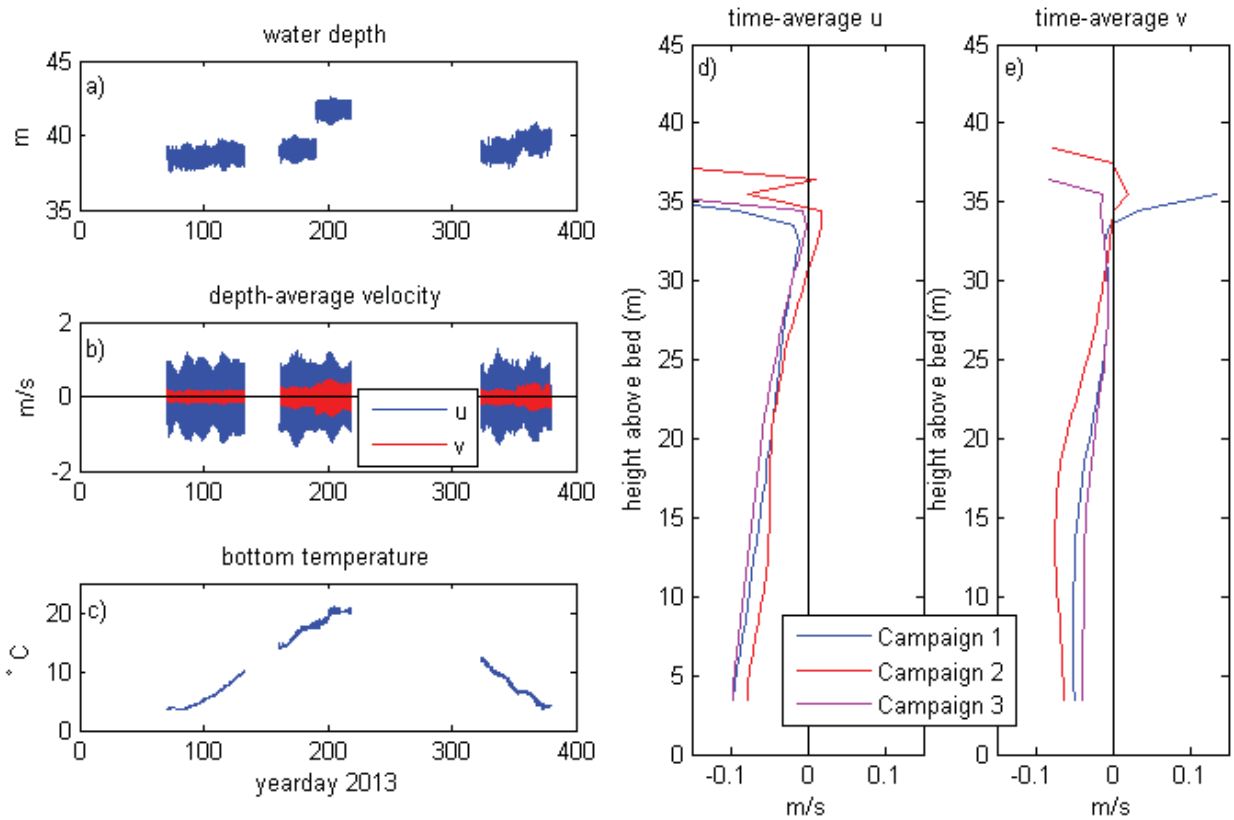

Figure 6-4. Time-series of (a) water depth, (b) depth-average velocity components, (c) bottom temperature, and (d, e) profiles of time-averaged velocities for all three field campaigns at Station DOT1.

6.1.4 Near-Bottom Velocities

The near-bottom velocity measurements are central to this physical oceanography study. Currents at all stations were dominated by the semidiurnal tidal constituents and modulated by wind and density driven flows. This condition is reflected in Figure 6-5 which shows the east and north component of the velocity at an elevation of 3.54 m above the seafloor, at Station DOT2 during Campaign 2. This record contains the maximum near-bottom velocity observed by the RDI ADCPs during this study. The spring-neap variation of the semi-diurnal amplitude is evident in the record, as are a significant southwest directed mean flow. Records for all deployments are provided in Appendix 11c.

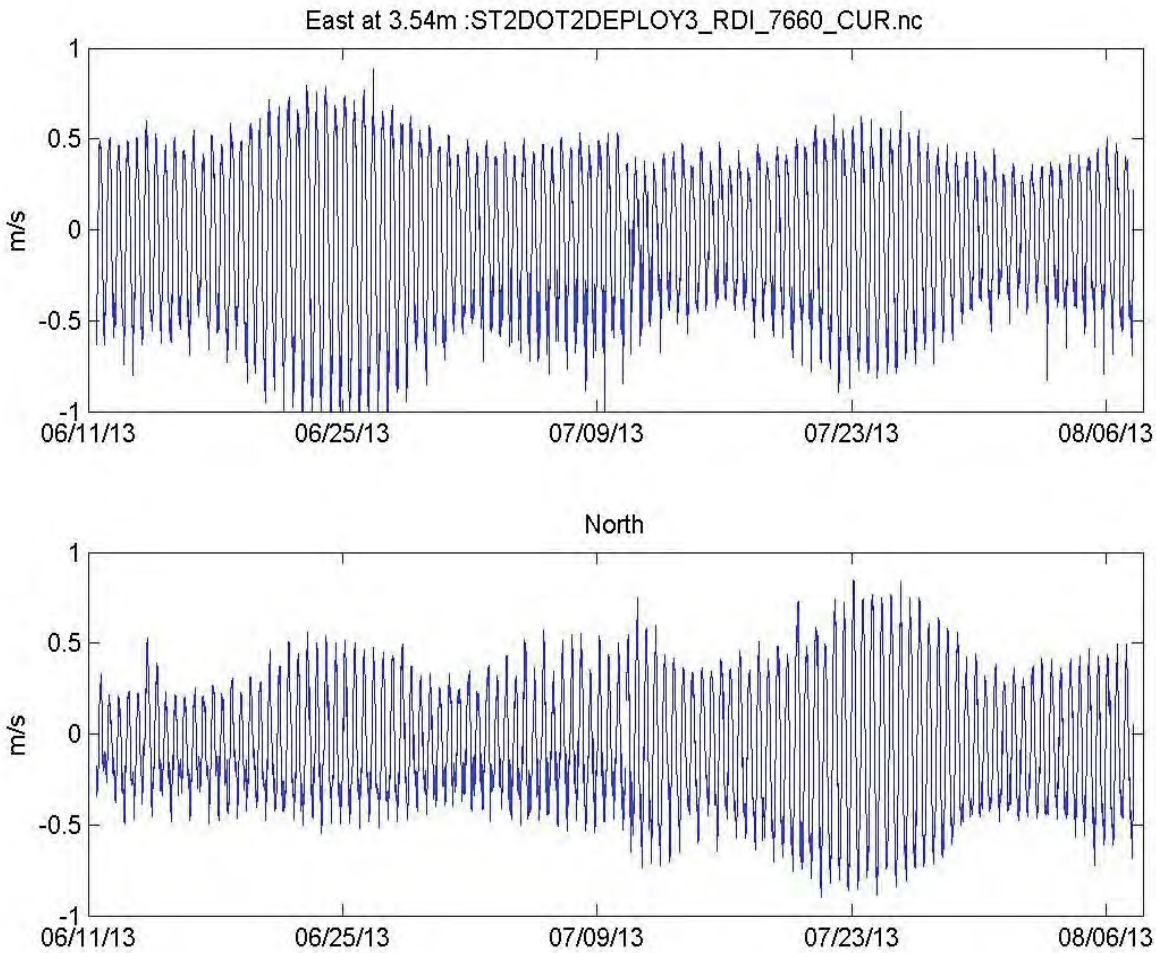

Figure 6-5. Eastward (top) and northward (bottom) components of the current observed at 3.54m above the bottom at Station DOT2 during Campaign 2.

The statistics of the near-bottom current records for all campaigns are summarized in Table 6-1. The mean east and north velocity components (first two columns) are also mapped in Figure 6-6. The currents are largely directed toward Long Island Sound and have velocities between 1 and 10 cm/s. The direction of the major axis of the variance in degrees counter-clockwise from the east is shown in column 5. The magnitude of the standard deviation of the current components in this direction is largely controlled by the pattern of the tidal currents (Figure 6-1). Consequently, the minor axis is typically only 10 to 30% of the major axis amplitude. The amplitudes of the major and minor axes do not vary substantially between deployments and the largest values were found at Stations DOT 1 and DOT2.

The maximum velocities observed by each RDI ADCP and campaign (Column 6 in Table 6-1) were typically twice the major axis standard deviation suggesting that infrequent events determine the magnitude of the maximum current. Again, highest maximum velocities were recorded at Stations DOT1 and DOT2. A dependence of the maximum velocity on season was not apparent.

Table 6-1. Statistics of Near-bottom Current Observations

Station	Velocity Components		Standard Deviation		Orientation of Major Axis of the Variance (*)	Max Velocity (m/s)
	Mean East (m/s)	Mean North (m/s)	Major Axis (m/s)	Minor Axis (m/s)		
Campaign 1						
DOT1	-0.09	-0.05	0.53	0.10	8.41	1.13
DOT2	-0.06	-0.03	0.53	0.10	33.99	1.12
DOT3						
DOT4	-0.03	-0.04	0.36	0.07	-12.10	0.74
DOT5	-0.07	0.06	0.30	0.07	-40.53	0.82
DOT6	-0.10	0.00	0.27	0.08	-15.74	0.60
DOT7						
Campaign 2						
DOT1	-0.07	-0.06	0.54	0.13	18.42	1.18
DOT2	-0.05	-0.07	0.51	0.15	37.82	1.26
DOT3	-0.06	0.03	0.46	0.08	15.30	1.01
DOT4	-0.03	-0.04	0.39	0.07	-24.04	0.81
DOT5	-0.06	0.07	0.32	0.08	-44.30	0.95
DOT6	-0.08	-0.01	0.27	0.13	-10.38	0.65
DOT7	-0.02	0.06	0.31	0.11	-36.04	0.90
Campaign 3						
DOT1	-0.09	-0.04	0.50	0.09	14.24	1.13
DOT2	-0.06	-0.01	0.54	0.11	36.62	1.25
DOT3	-0.05	0.03	0.44	0.05	18.98	0.97
DOT4	-0.01	-0.05	0.39	0.07	-14.79	0.87
DOT5	-0.01	0.05	0.35	0.07	-36.70	0.86
DOT6	-0.08	0.01	0.29	0.10	-2.96	0.70
DOT7	-0.05	0.11	0.30	0.11	-30.01	0.95

* Units are in degrees counterclockwise from the east.

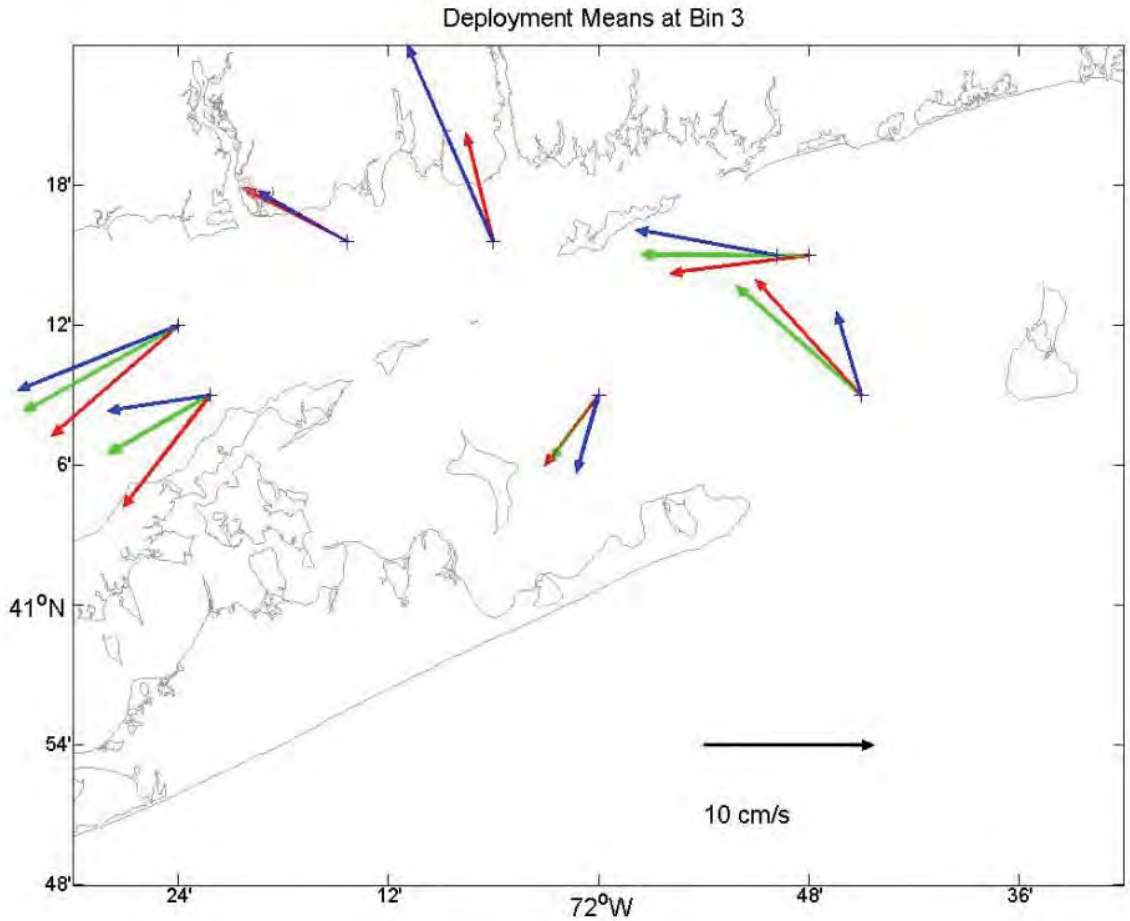

Figure 6-6. Mean currents at bin 3 of the RDI ADCP measurements during Campaigns 1 (green), 2 (red), and 3 (blue).

6.2 Summary

The pattern of mean tidal currents and mean flow in spring, summer and fall-winter in Long Island Sound are summarized in the water column and near the bottom of the seafloor. At all stations, except for Station DOT4, the near-bottom flow was toward Long Island Sound. At Station DOT4 the mean flow was directed to the southwest toward Napeague Bay. Maximum current velocities near the seafloor were not very sensitive to season. Maximum velocities reached 1.13 m/s at Station DOT2.

7. Currents at the Seafloor (Moored Instruments)

Currents near the seafloor were measured at the seven mooring stations by Nortek ADCPs positioned at 0.75 m above the seafloor, as described in Section 2.2.1.3. This chapter summarizes the processing of data to yield east, north and vertical velocity components, and then describes and evaluates the characteristics of the data.

7.1 Calculation of Bottom Stress

The velocity variation with distance from the boundary in an unstratified, uniform and unaccelerated turbulent boundary layer has been shown to be logarithmic and is often written as $u(z) = \frac{u_*}{\kappa}\ln(z/z_0)$ where u_* is called the stress velocity, $\kappa = 0.4$ is the Von Karman constant, and z_0 is the roughness length. In such flows the stress on the boundary is then $\tau = \rho u_*^2$ where ρ is the density of water. When the International System of Units (SI units) are used, τ has units of $Newtons/m^2$ or $Pascals$. This approach has been used extensively in estuaries (e.g., Cheng et al., 1999), and even though the flows don't always fully satisfy the assumptions underlying the argument for the log law structure, measurements generally show that the model structure is consistent with observations and linear regression of measurements of u on $log(z)$ are used to provide estimates of u_*. The uncertainty in the approach is determined by how well the observations conform to the log law structure and sometimes only a subset of the vertical structure is selected.

We implemented this approach to estimating the bed stress using data from the Nortek ADCP. For each ensemble the mean direction of the currents in bins 8-13 (distances above bottom of 0.36, 0.32, 0.28, 0.24, 0.20, 0.16 and 0.12 m) was calculated and the velocity components in that direction computed. If the maximum velocity component was less than 0.04 m/s then the stress was not computed. If the regression coefficient (r^2) for u on $log(z)$ was less than 90%, then the estimate of u_* was rejected. These quality control conditions were seldom violated.

Figure 7-1b shows an example of the calculation of $\tau = \rho u_*^2$ from Nortek data at Station DOT5 during Campaign 3. Values range between 0 and 2 Pa with a period of 6 hours. The significant wave heights observed by the co-located RDI ADCP during this period are shown in Figure 7-1a. There are several periods when the significant wave height was greater than 2 m; however, there is little evidence of their effect on the stress.

The two vertical lines indicate the times of ensembles 297 and 317. The structure of the near-bottom flow from the Nortek ADCP current measurements at these times is shown in Figure 7-2. The data are shown by the circles and the samples included in the log law fit have a red + symbol in the circle. The red line with the black + symbols are the least-squares fit to the data. It is clear that both sets of data show a distinct log law behavior near the bed but deviate from it near the current meter.

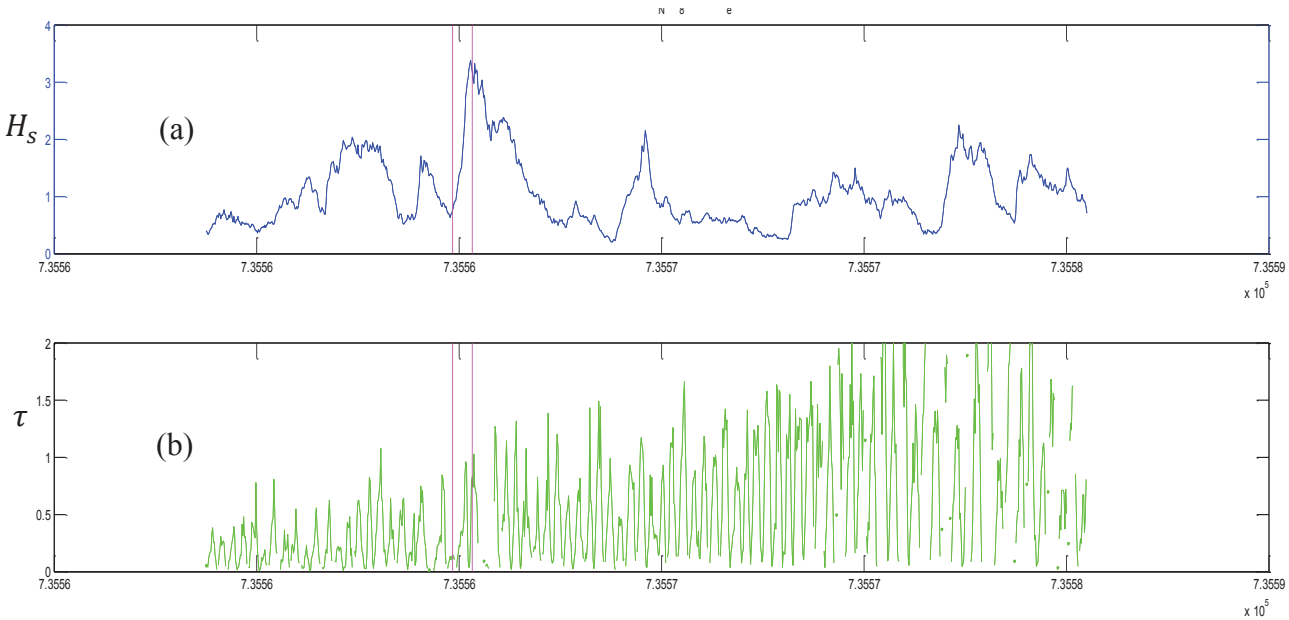

Figure 7-1. (a) Significant wave height H_s at Station DOT5 during Campaign 3 measured by the RDI ADCP, and (b) the bottom stress τ estimated from the log law.

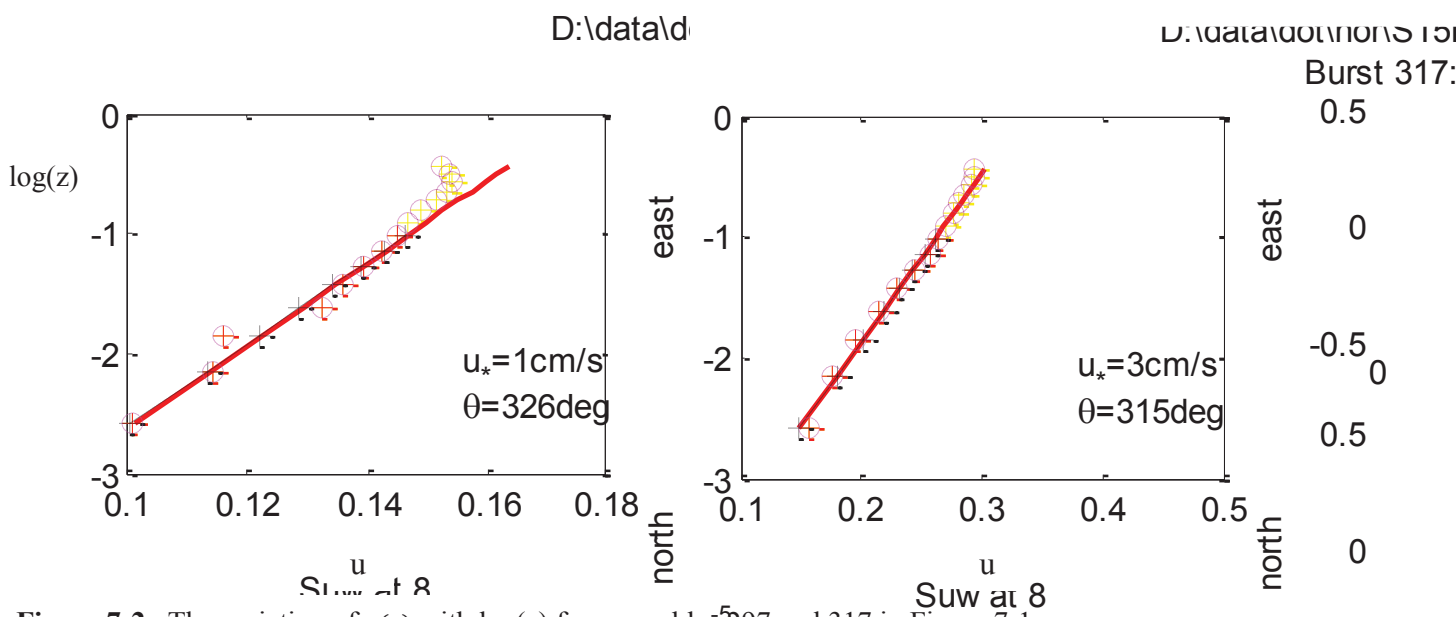

Figure 7-2. The variation of $u(z)$ with log(z) for ensembles 297 and 317 in Figure 7-1.

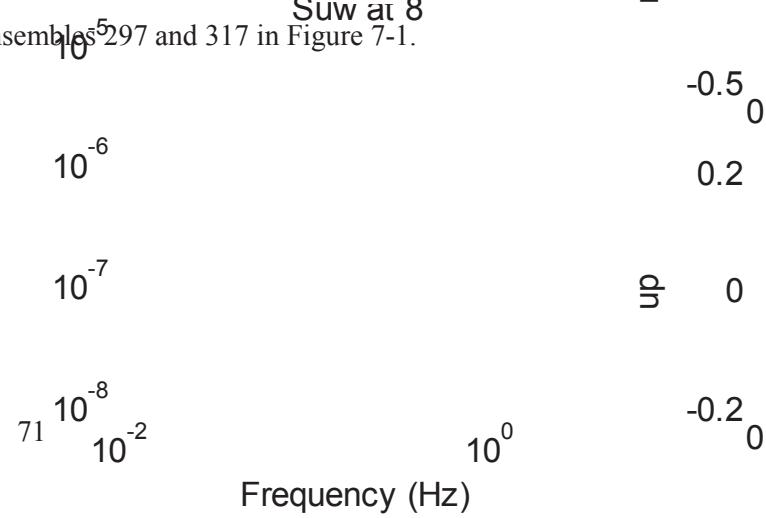

7.2 Data

The screened velocity data is extensive and comprised of two components (east and north) at 20 depth bins within 0.75 meters of the bed, sampled at relatively high frequency (2 or 4 Hz). An example data set from Station DOT4 during Campaigns 1 and 2 are shown in Figures 7-3 and 7-4, respectively. For simplicity, the data are plotted as ensemble means of the east-west and north-south components of current velocity at 0.565 m above the bottom. The currents are predominantly tidal as expected, with major axis amplitudes ranging from 0.20 m/s to 7.2 m/s. Table 7-1 presents the means and characteristics of the principal tidal constituent (M2) at each station for each deployment. The vector means are also shown in Figure 7-5 and the M2 tidal ellipses for the first campaign are shown in Figure 7-6. All stations are shown in Appendices 9d to 9f.

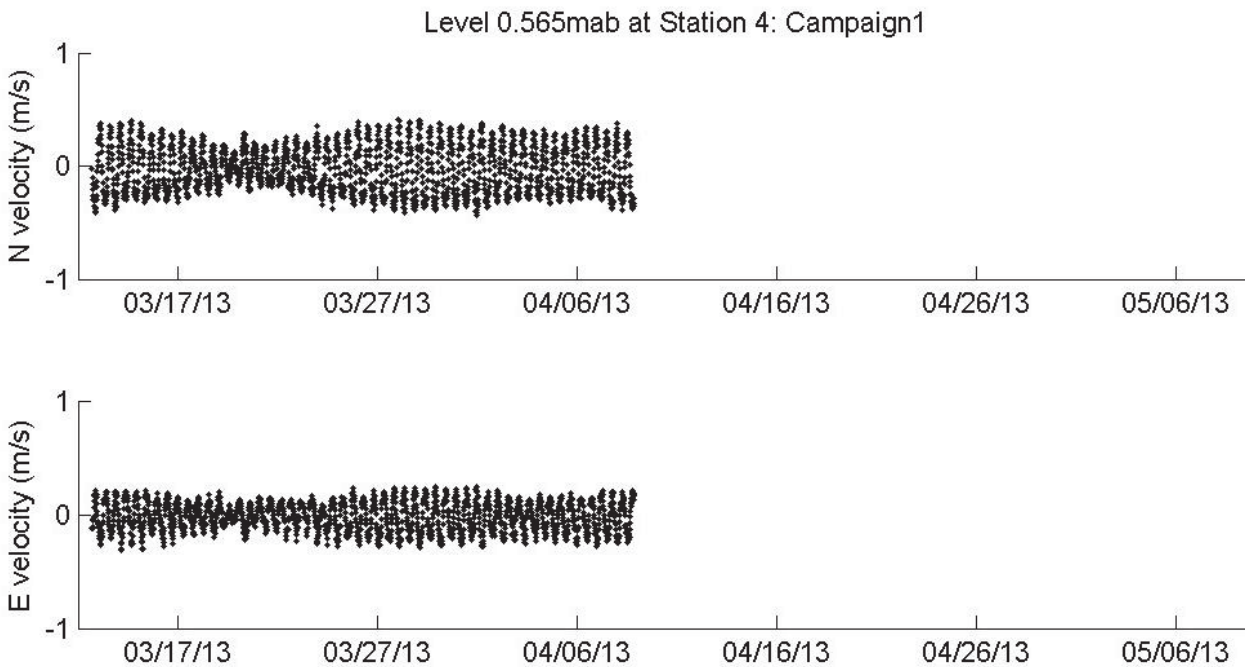

Figure 7-3. Ensemble mean currents at bin 5, 0.565m above the bottom, at Station DOT4 in Campaign 1.

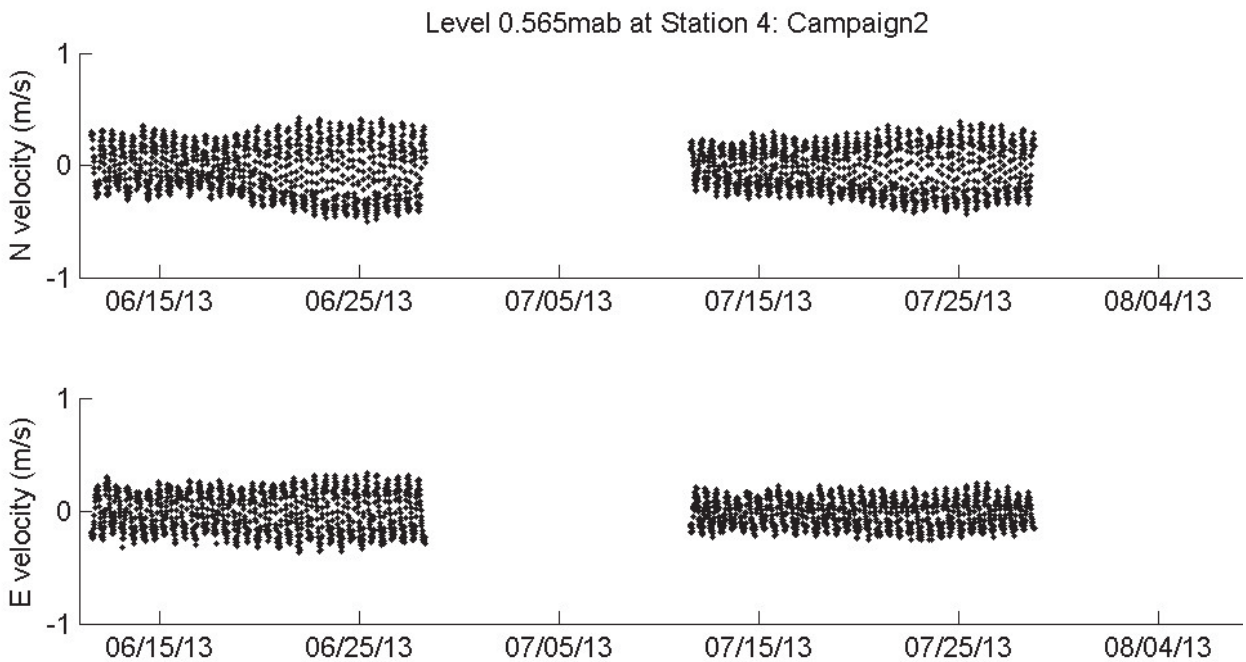

Figure 7-4. Ensemble mean currents at bin 5, 0.565m above the bottom, at Station DOT4 in Campaign 2.

Table 7-1. Characteristics of Principal Tidal Constituent (M2) at each Mooring Station for each Deployment

Station	Deploy-ment	File Number	East mean (m/s)	North mean (m/s)	Major Axis (m/s)	Minor Axis (m/s)	Orientation (deg)
DOT1	1	1	-0.0613	-0.0198	0.4861	0.0363	178.9848
DOT1	1	2	-0.0257	-0.0228	0.533	0.029	176.7234
DOT1	2	3	-0.0598	-0.0446	0.4567	0.0819	6.8213
DOT1	2	4	-0.068	-0.0234	0.5461	0.0197	3.2483
DOT1	3	5	-0.0391	-0.0229	0.4549	0.0854	12.6784
DOT1	3	6	-0.0632	-0.0112	0.5657	0.0078	11.3811
DOT1	4	7	-0.0741	-0.0025	0.4428	0.0189	177.9927
DOT1	5	8	-0.0859	-0.0052	0.4668	0.0745	175.1996
DOT2	1	1	-0.0392	-0.0178	0.5167	0.0583	23.8984
DOT2	1	2	-0.0147	-0.0448	0.5307	0.0223	21.8198
DOT2	2	3	-0.0646	-0.0623	0.4144	0.0588	28.2140
DOT2	3	4	-0.0425	-0.0428	0.4765	0.0755	22.6775
DOT2	3	5	-0.0247	0.0076	0.7186	0.0067	22.0401
DOT2	4	6	-0.0606	0.0117	0.5056	0.023	17.3895
DOT2	5	7	-0.0296	0.0003	0.5239	0.0756	24.9741

Station	Deploy-ment	File Number	East mean (m/s)	North mean (m/s)	Major Axis (m/s)	Minor Axis (m/s)	Orientation (deg)
DOT3	1	1	-0.05	0.0163	0.3756	0.0481	5.4994
DOT3	1	2	-0.0547	0.0264	0.3774	0.012	3.8086
DOT3	2	3	-0.0506	0.0288	0.3796	0.0587	8.6818
DOT3	2	4	-0.1136	0.0024	0.5347	0.0056	3.3880
DOT3	3	5	-0.0303	0.0354	0.4254	0.0815	5.8696
DOT3	3	6	-0.0406	0.0141	0.5499	0.0379	2.9607
DOT3	4	7	-0.0383	0.0426	0.4296	0.0773	5.1498
DOT3	5	8	-0.0512	0.0219	0.4575	0.073	9.4552
DOT4	1	1	-0.0272	-0.0167	0.3237	0.0387	149.9898
DOT4	1	2	-0.0427	-0.0238	0.3505	0.0092	149.2136
DOT4	2	3	-0.021	-0.0087	0.366	0.0555	140.4869
DOT4	2	4	-0.0671	-0.0136	0.4734	0.0239	144.8226
DOT4	3	5	-0.0394	-0.0195	0.3056	0.0374	148.1384
DOT4	3	6	-0.0397	-0.0239	0.3691	0.0217	152.6448
DOT4	4	7	-0.0203	-0.0247	0.342	0.0339	153.1025
DOT4	5	8	-0.0138	-0.0196	0.3372	0.0087	144.9742
DOT5	1	1	-0.0412	0.0662	0.2466	0.049	125.6754
DOT5	1	2	-0.0643	0.0964	0.262	0.0082	125.5203
DOT5	2	3	-0.0602	0.0494	0.2752	0.0358	138.7478
DOT5	2	4	-0.0994	0.0714	0.3972	0.0119	143.0324
DOT5	3	5	-0.0472	0.0792	0.3565	0.0711	127.6388
DOT5	3	6	-0.06	0.0515	0.2038	0.0149	131.8126
DOT5	4	7	0.0024	0.0378	0.3666	0.04	128.7326
DOT5	5	8	-0.0082	0.0282	0.3015	0.011	125.4626
DOT6	1	1	-0.0718	0.0047	0.2416	0.0234	157.3299
DOT6	1	2	-0.0912	0.0071	0.2433	0.007	160.3349
DOT6	3	3	-0.0742	0.0106	0.2535	0.0344	155.4660
DOT6	3	4	-0.0585	-0.0026	0.2722	0.0085	156.3309
DOT6	4	5	-0.0493	0.0397	0.3072	0.0354	162.8894
DOT6	5	6	-0.0608	0.0217	0.2583	0.0108	160.0011
DOT7	1	1	-0.023	0.0614	0.2366	0.0273	135.0569
DOT7	1	2	-0.0143	0.0841	0.2771	0.0337	137.7591
DOT7	2	3	-0.0227	0.0493	0.2803	0.0244	119.6345
DOT7	2	4	-0.0119	0.0554	0.3487	0.0147	133.6232
DOT7	3	5	-0.0085	0.0273	0.2814	0.0318	118.9636
DOT7	3	6	-0.0071	0.081	0.3335	0.0287	135.9460
DOT7	4	7	-0.0299	0.0859	0.2714	0.0343	144.3027

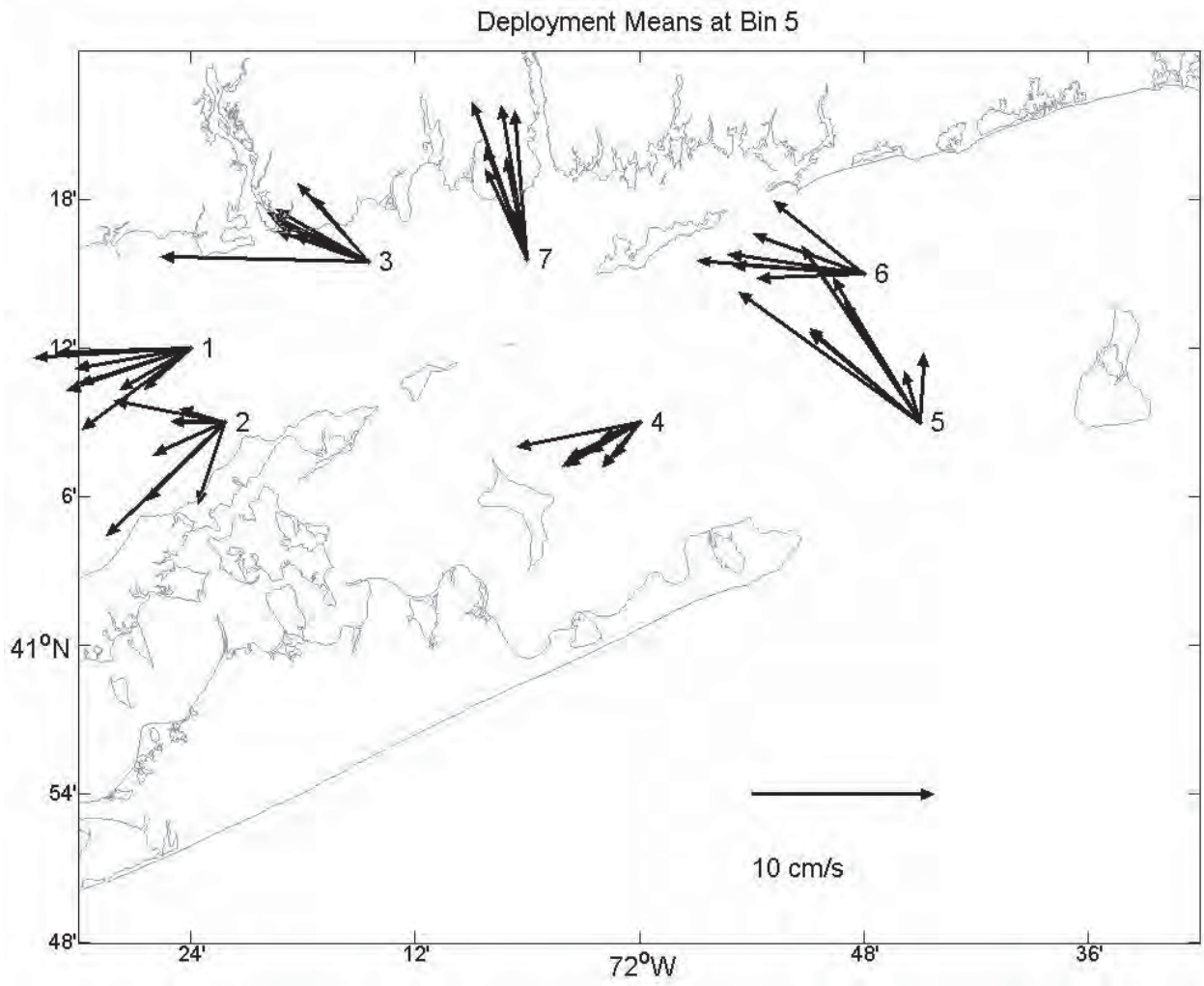

Figure 7-5. Mean velocity vectors at each moored station from the Nortek ADCP immediatle near the bottom. The velocity scale is shown in the lower right corner of the graphic.

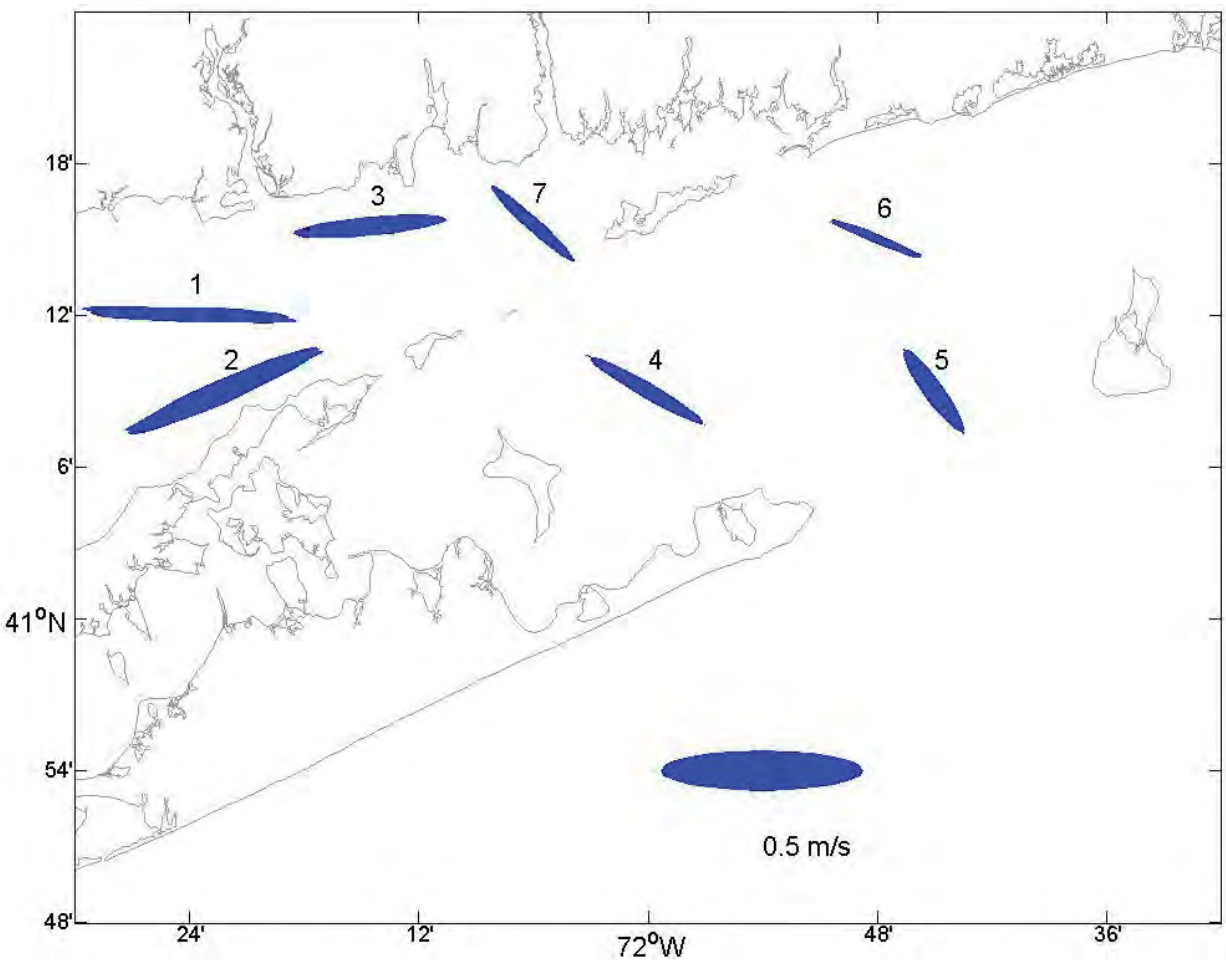

Figure 7-6. M2 tidal ellipses for Campaign 1 at each moored station.

The pressure, temperature, system battery voltage and OBS measurements[16] for Station DOT1 in Campaigns 1 and 2 are shown in Figures 7-7 and 7-8, respectively; results for all stations are included in Appendix 9g. As stated above, during Campaign 1 the system batteries on the Nortek ADCP were expended more quickly than anticipated and only 30 days of observations with complete ensembles were obtained. When the battery began to fail some samples were lost from each ensemble resulting in corrupted data formats. Only the complete data set was processed. The tripod frames with were recovered mid-way during Campaigns 2 and 3.

[16] Data from the OBS3+ sensors for suspended sediment concentration are included in Figures 7.7 and 7.8 as well as in Appendix 9g for comparison; these data are discussed in more detail in Chapter 10. Note that during the latter part of the record of the two OBS3+ sensors in Figure 7-8, there is an increase in the backscatter characteristic of bio-fouling.

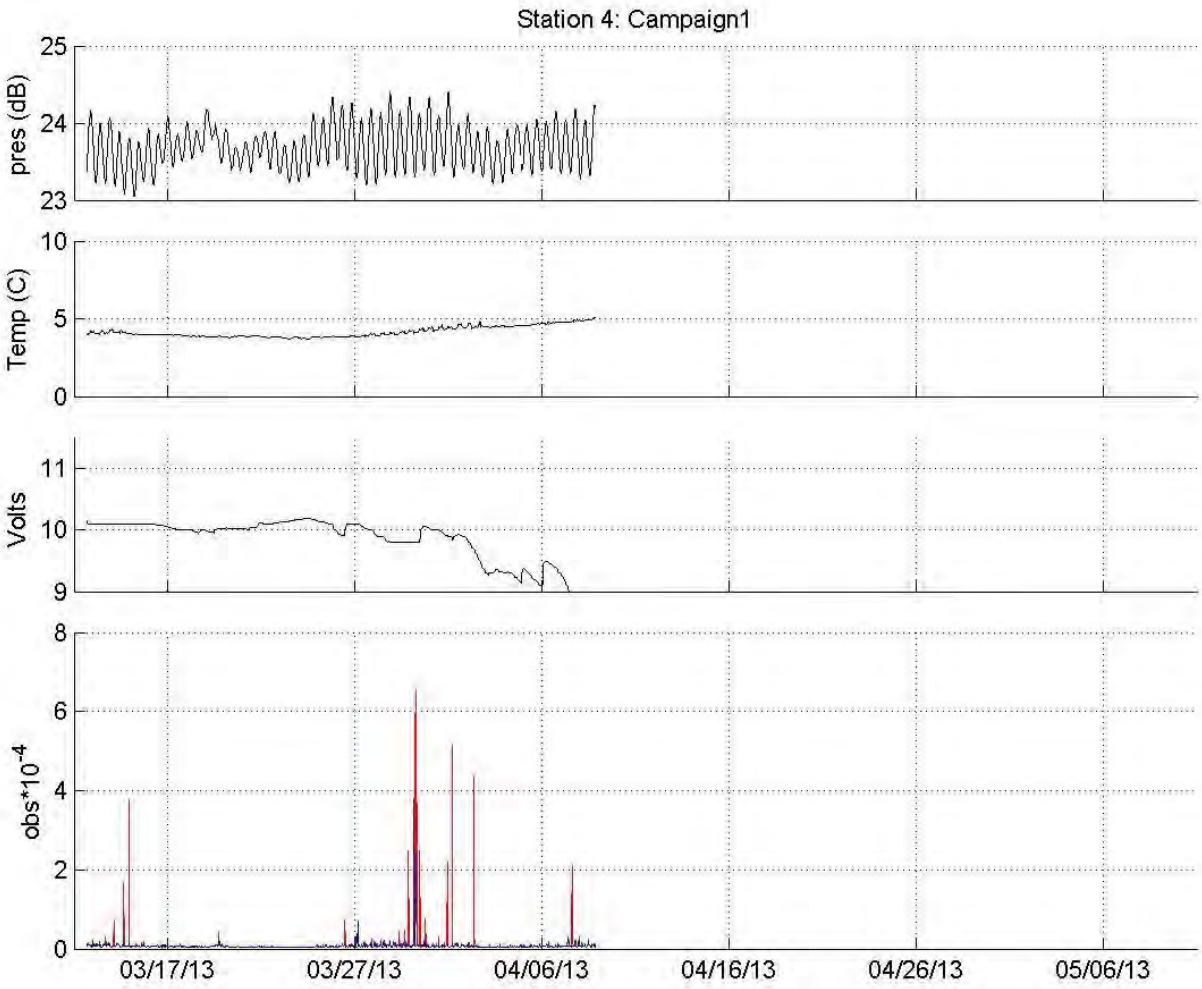

Figure 7-7. Time-series of bottom pressure, temperature, battery voltage and the OBS sensor outputs (counts) from Station DOT4, Campaign 1.

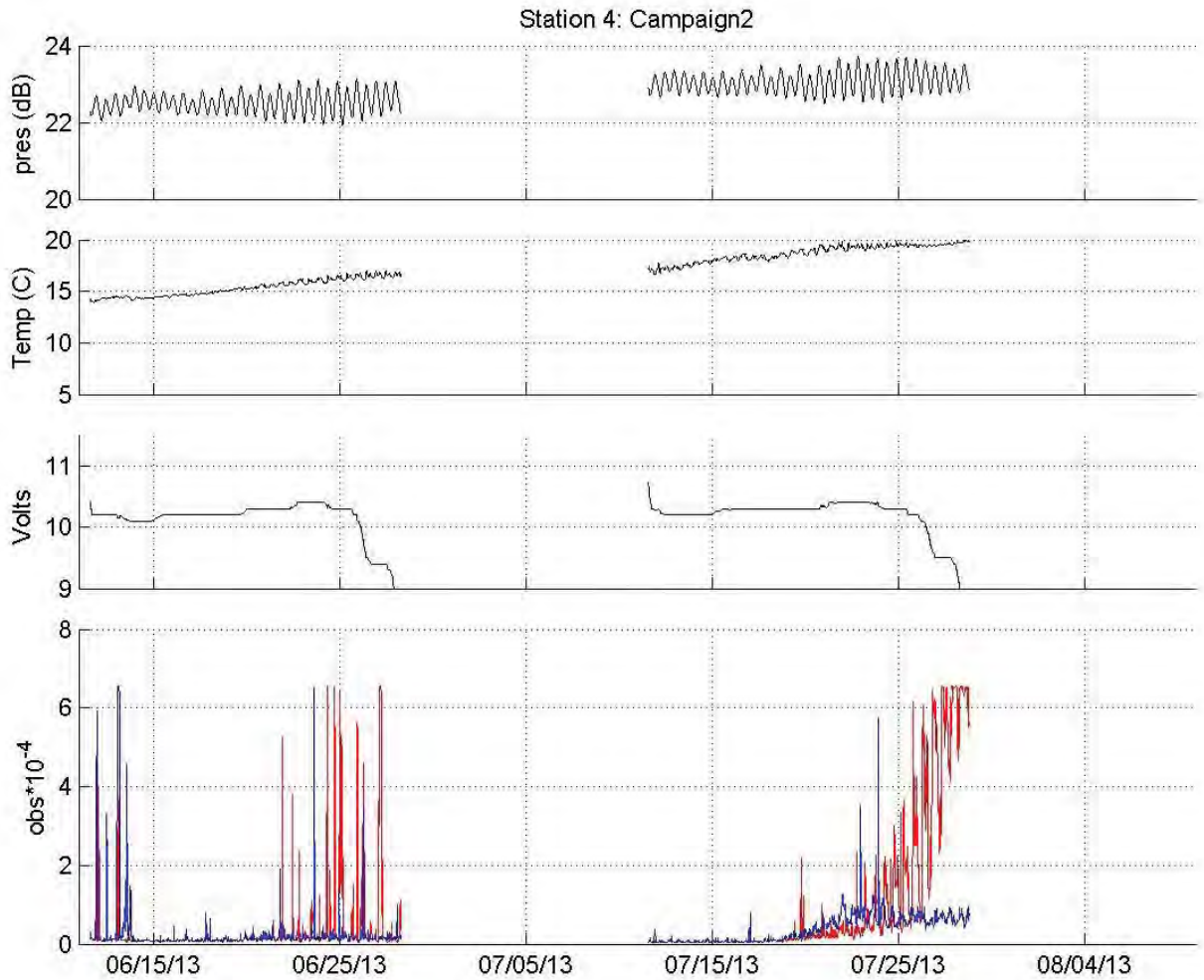

Figure 7-8. Time-series of bottom pressure, temperature, battery voltage and the OBS sensor outputs (counts) from Station DOT4, Campaign 2.

Figures 7-9 to 7-29 present the results for the measurement of bottom stress at all stations and all campaigns together with significant wave height and the mean and standard deviation of the high frequency velocity samples.

7.3 Summary

This chapter describes the data collected by the Nortek ADCP and methods necessary to turn the measurements into useful observations of velocity magnitude and direction, bottom shear stress, and variability in the bottom suspended sediment. The near bottom flow regime in eastern Long Island Sound and Block Island Sound is also summarized. Preliminary analyses indicate that the current patterns are dominantly tidal, with the M2 constituent the largest at all sites, though a significant mean flow was observed. Derived bottom shear stresses correlated well with the current flow.

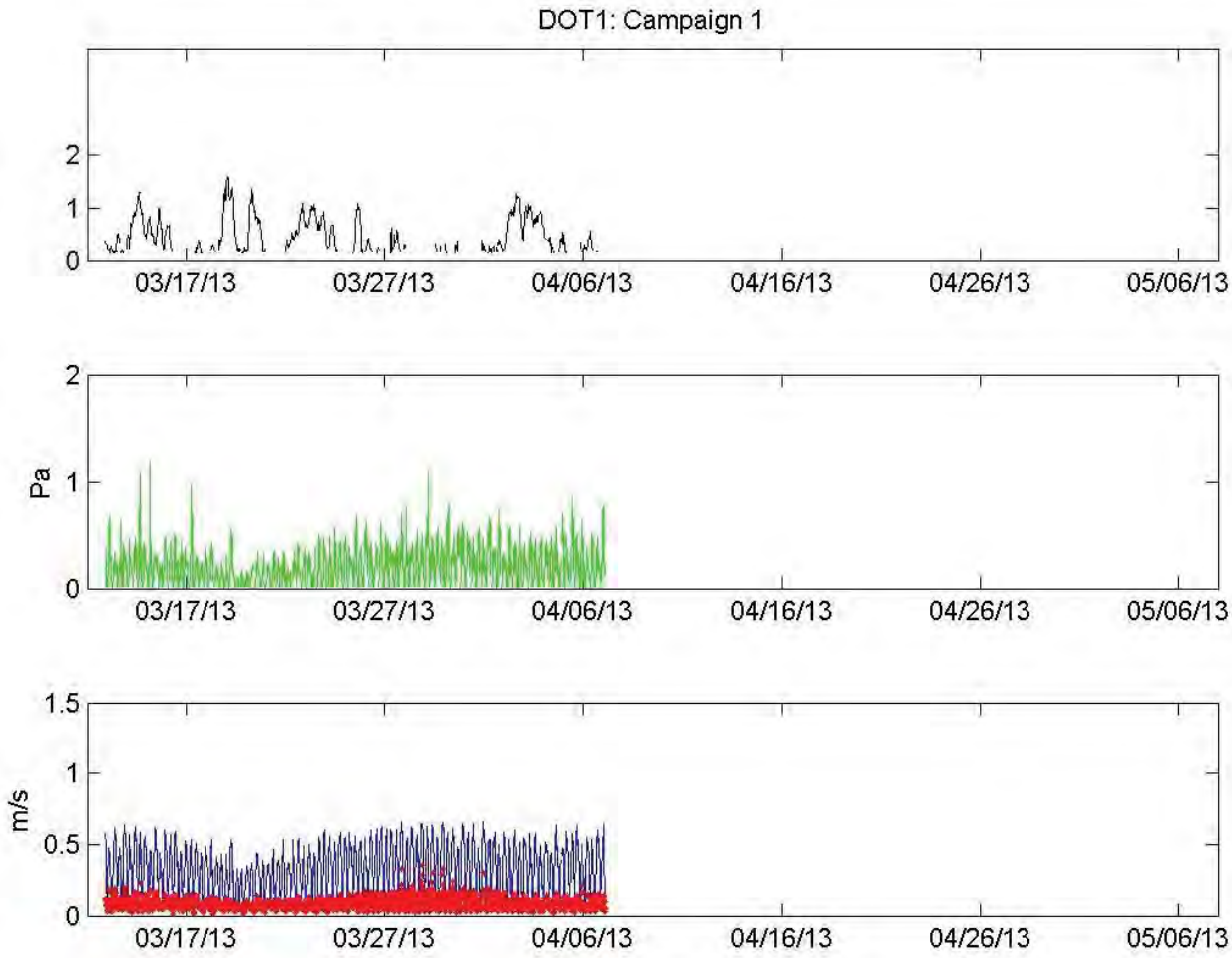

Figure 7-9. Characteristics at Station DOT1 during Campaign 1. (top) Significant wave height (in m); (middle) Stress; and (bottom) Standard deviation of the velocity estimates within the ensemble (red line) and the ensemble means (blue line).

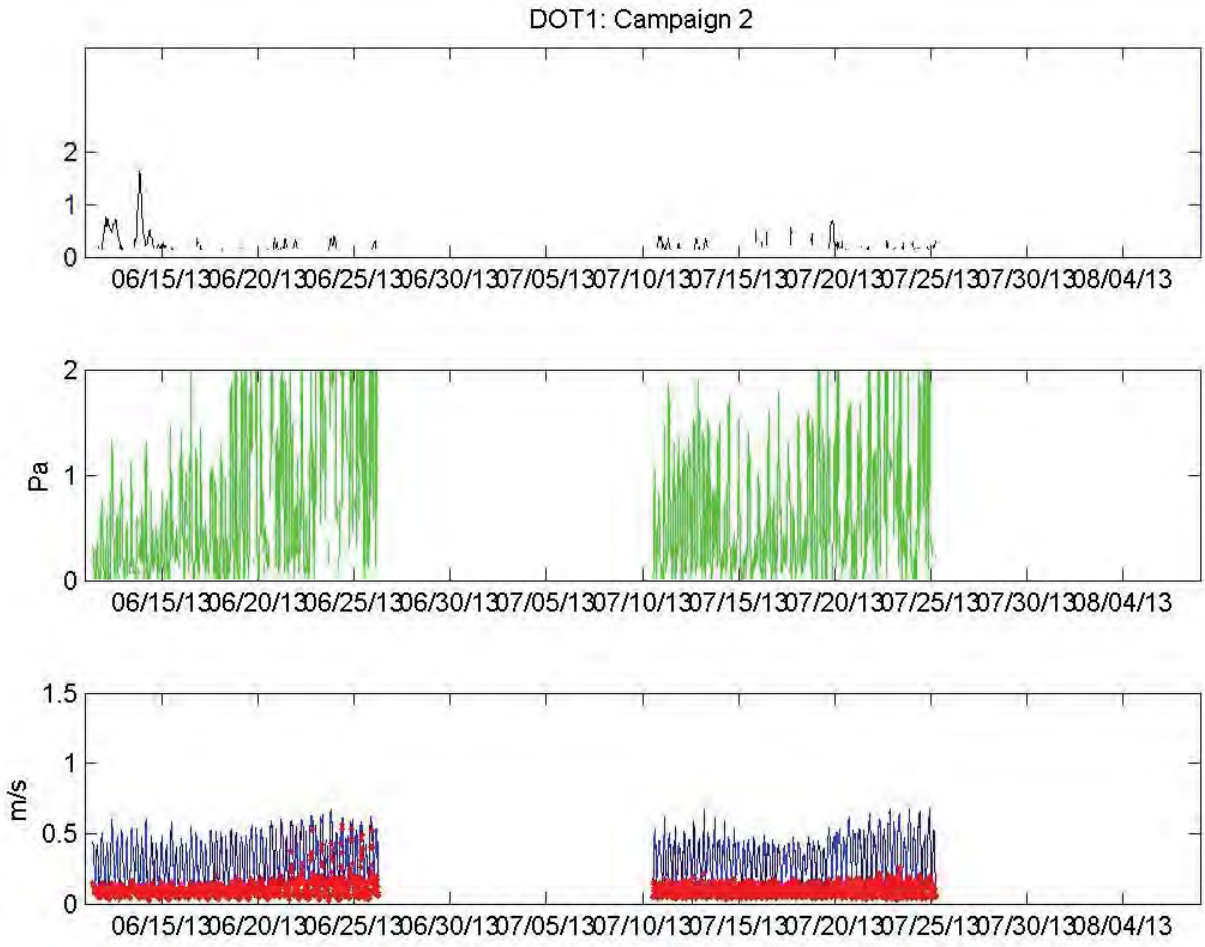

Figure 7-10. Characteristics at Station DOT1 during Campaign 2. (top) Significant wave height (in m); (middle) Stress; and (bottom) Standard deviation of the velocity estimates within the ensemble (red line) and the ensemble means (blue line).

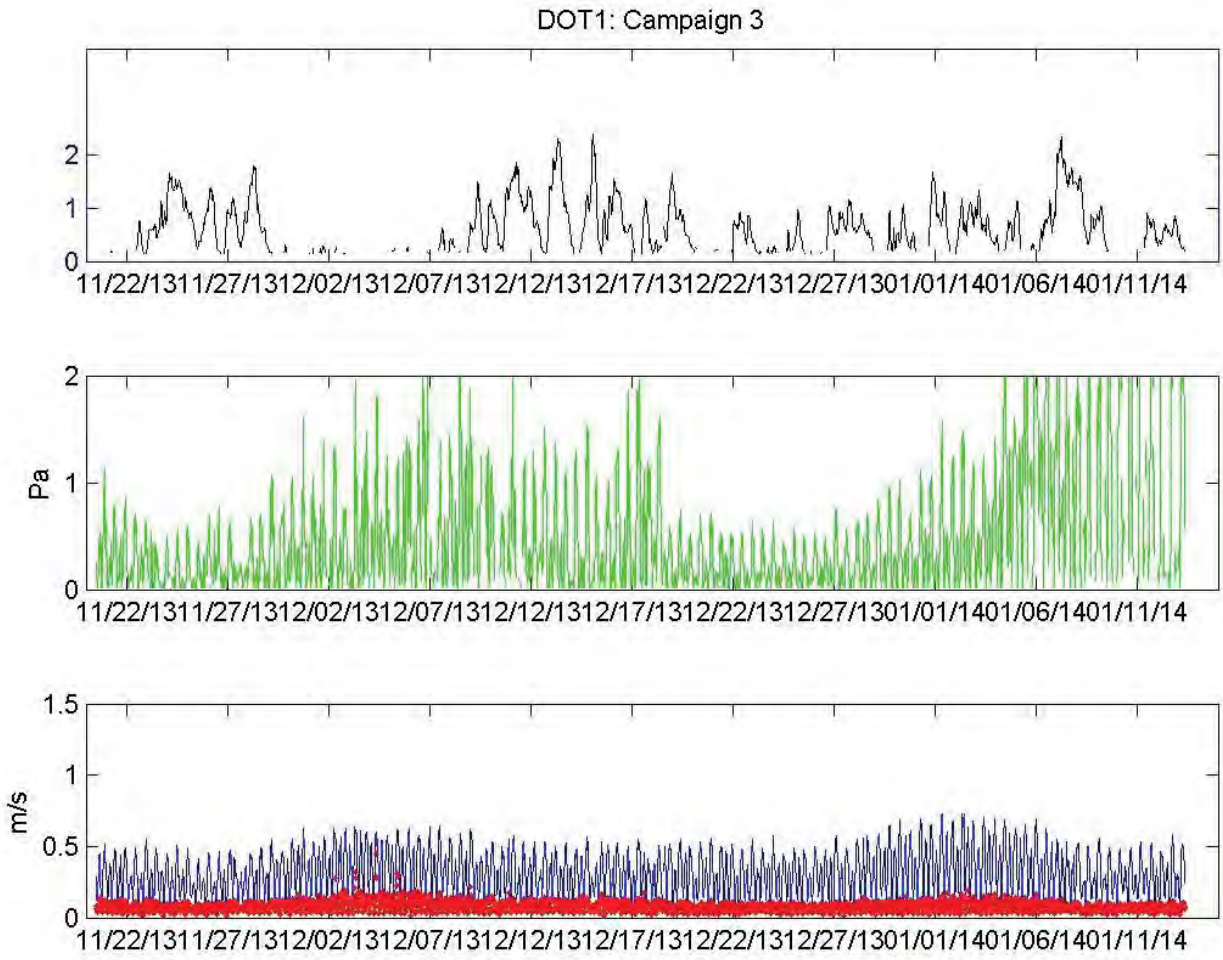

Figure 7-11. Characteristics at Station DOT1 during Campaign 3. (top) Significant wave height (in m); (middle) Stress; and (bottom) Standard deviation of the velocity estimates within the ensemble (red line) and the ensemble means (blue line).

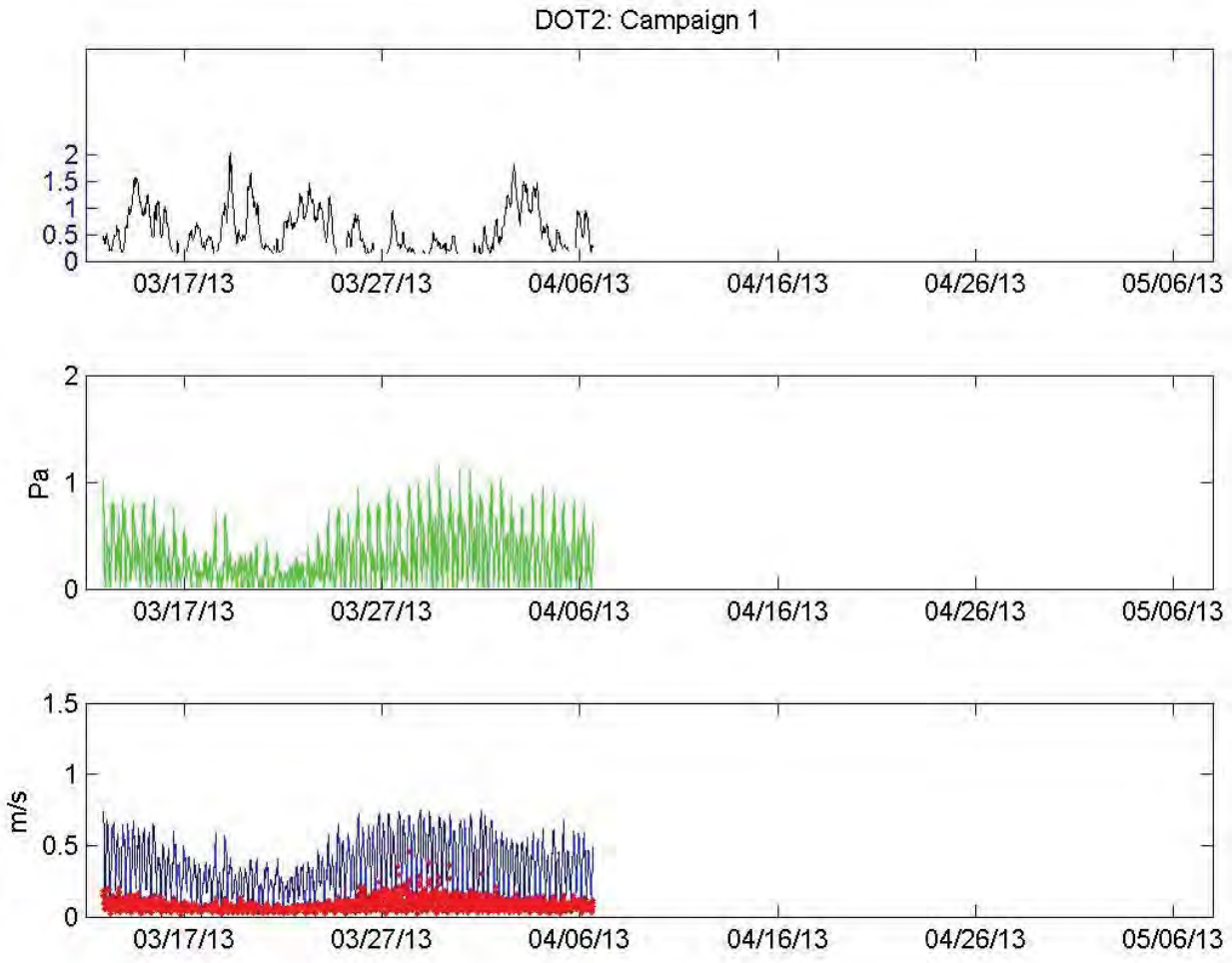

Figure 7-12. Characteristics at Station DOT2 during Campaign 1. (top) Significant wave height (in m); (middle) Stress; and (bottom) Standard deviation of the velocity estimates within the ensemble (red line) and the ensemble means (blue line).

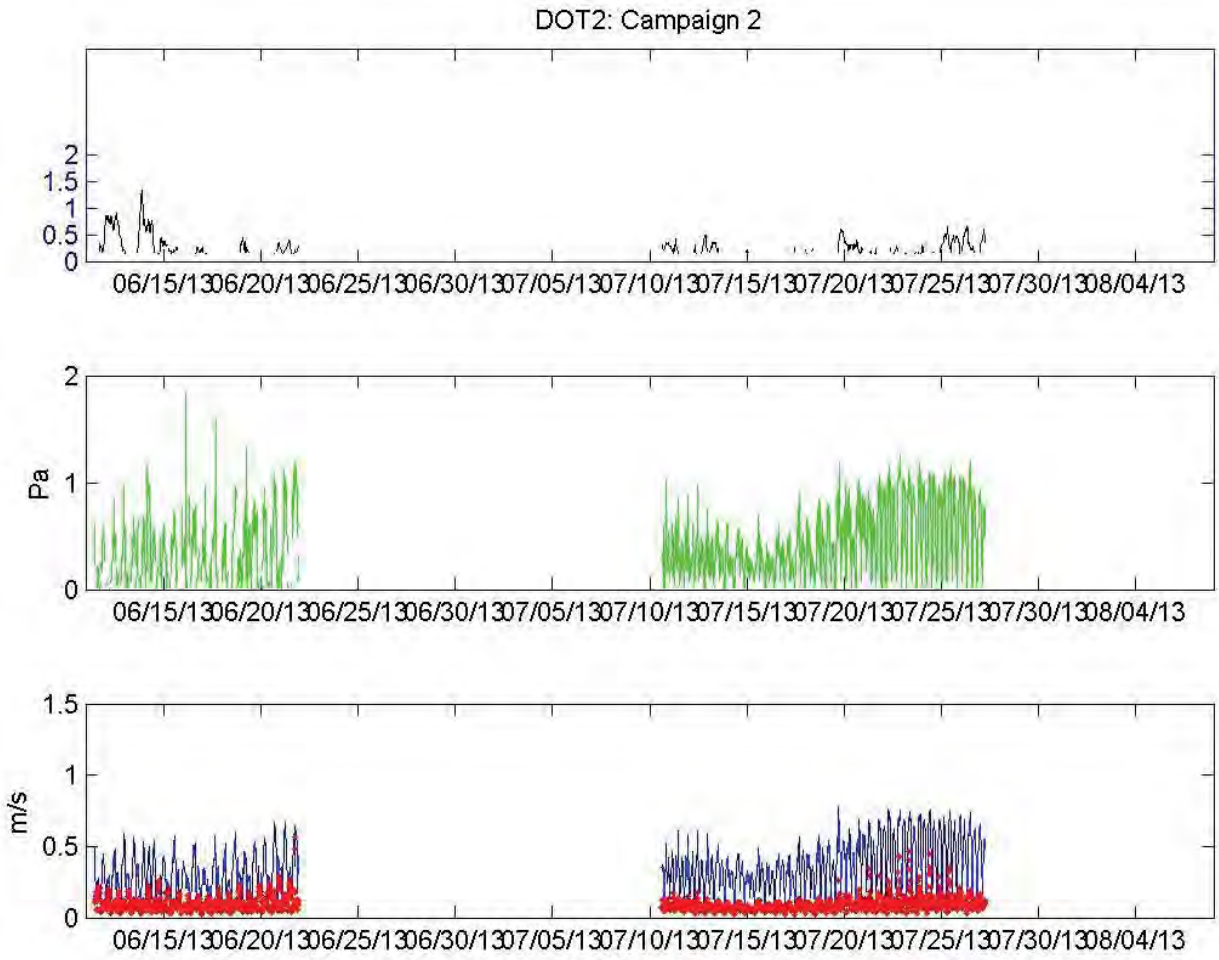

Figure 7-13. Characteristics at Station DOT2 during Campaign 2. (top) Significant wave height (in m); (middle) Stress; and (bottom) Standard deviation of the velocity estimates within the ensemble (red line) and the ensemble means (blue line).

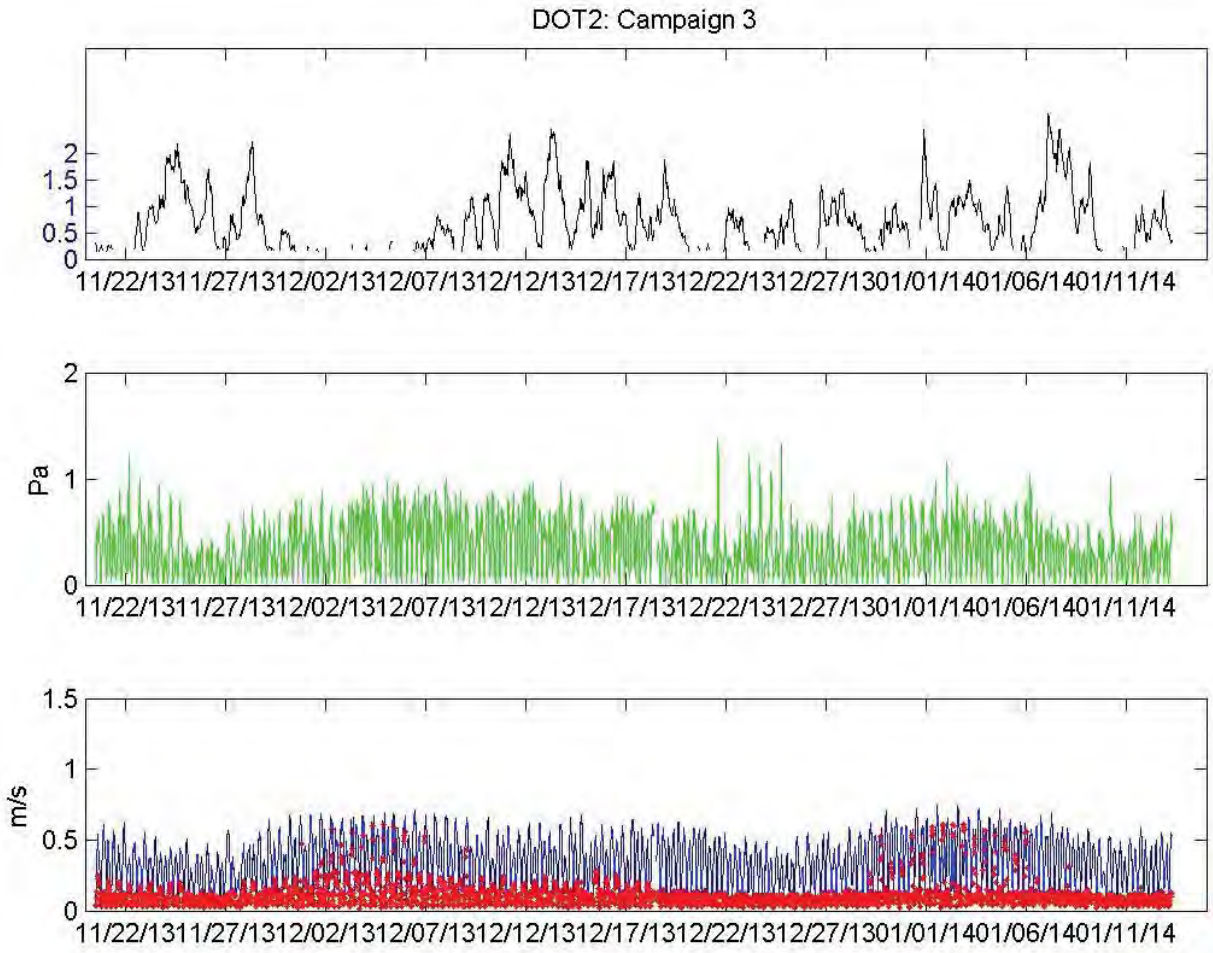

Figure 7-14. Characteristics at Station DOT2 during Campaign 3. (top) Significant wave height (in m); (middle) Stress; and (bottom) Standard deviation of the velocity estimates within the ensemble (red line) and the ensemble means (blue line).

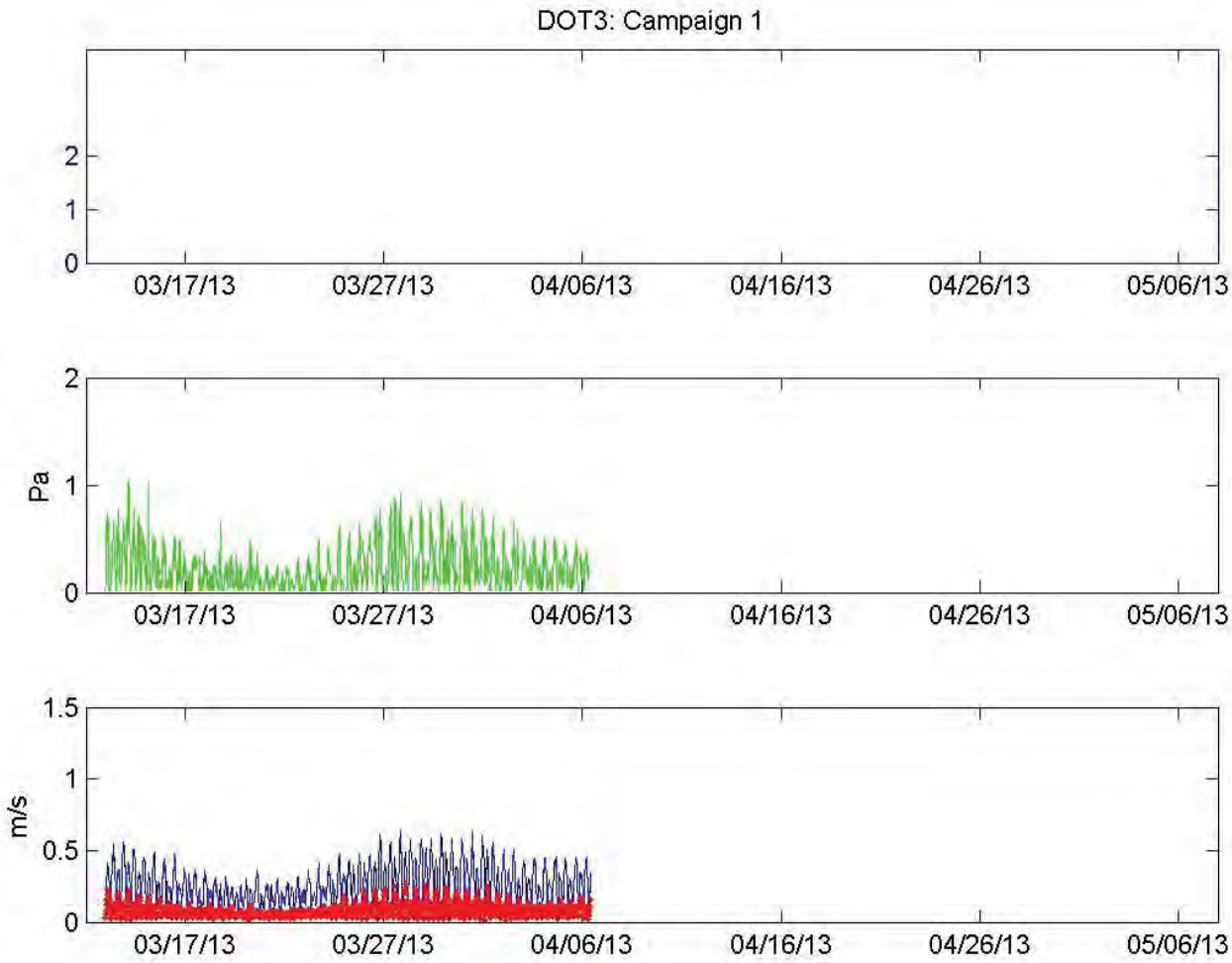

Figure 7-15. Characteristics at Station DOT3 during Campaign 1. (top) Significant wave height (in m); (middle) Stress; and (bottom) Standard deviation of the velocity estimates within the ensemble (red line) and the ensemble means (blue line).

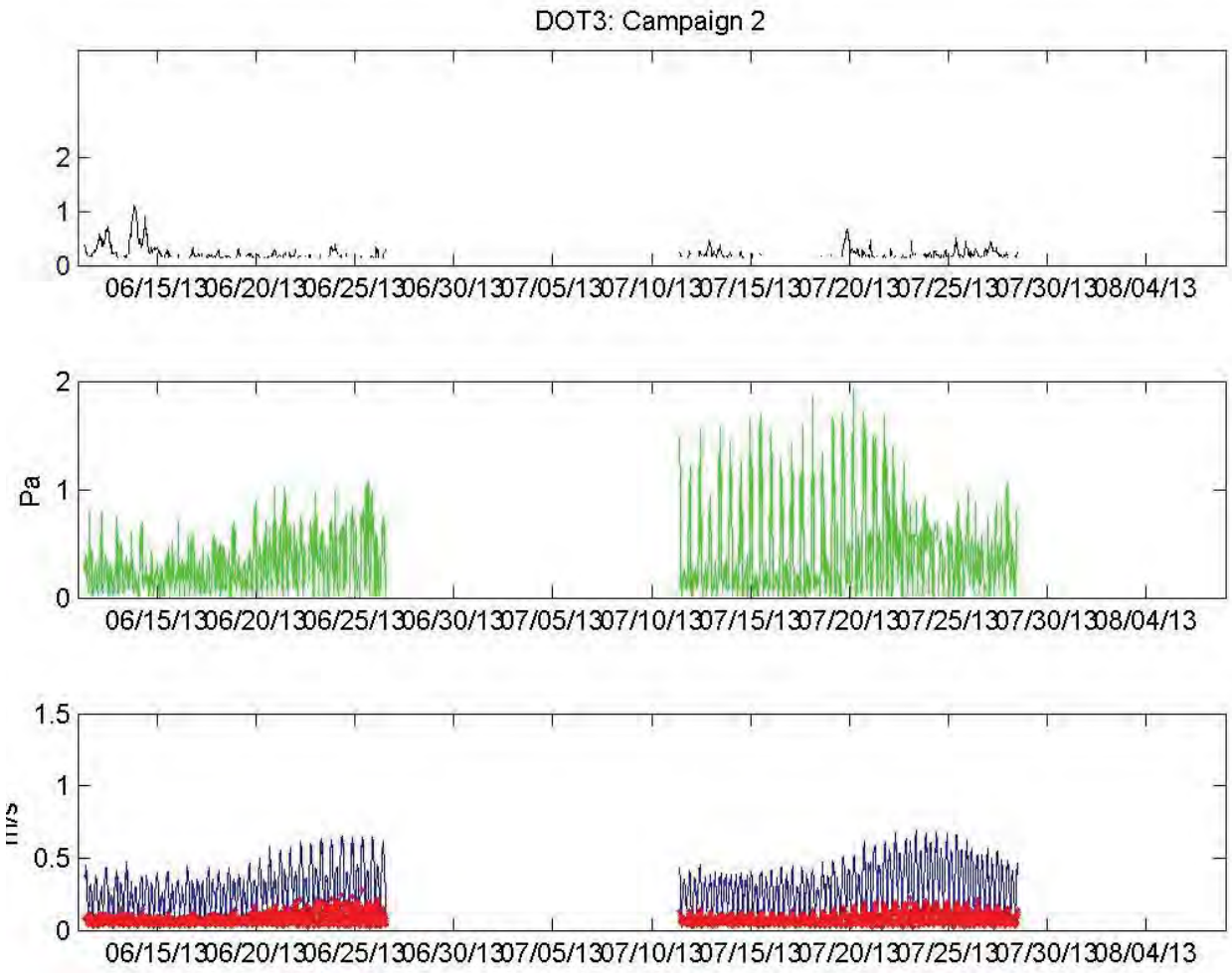

Figure 7-16. Characteristics at Station DOT3 during Campaign 2. (top) Significant wave height (in m); (middle) Stress; and (bottom) Standard deviation of the velocity estimates within the ensemble (red line) and the ensemble means (blue line).

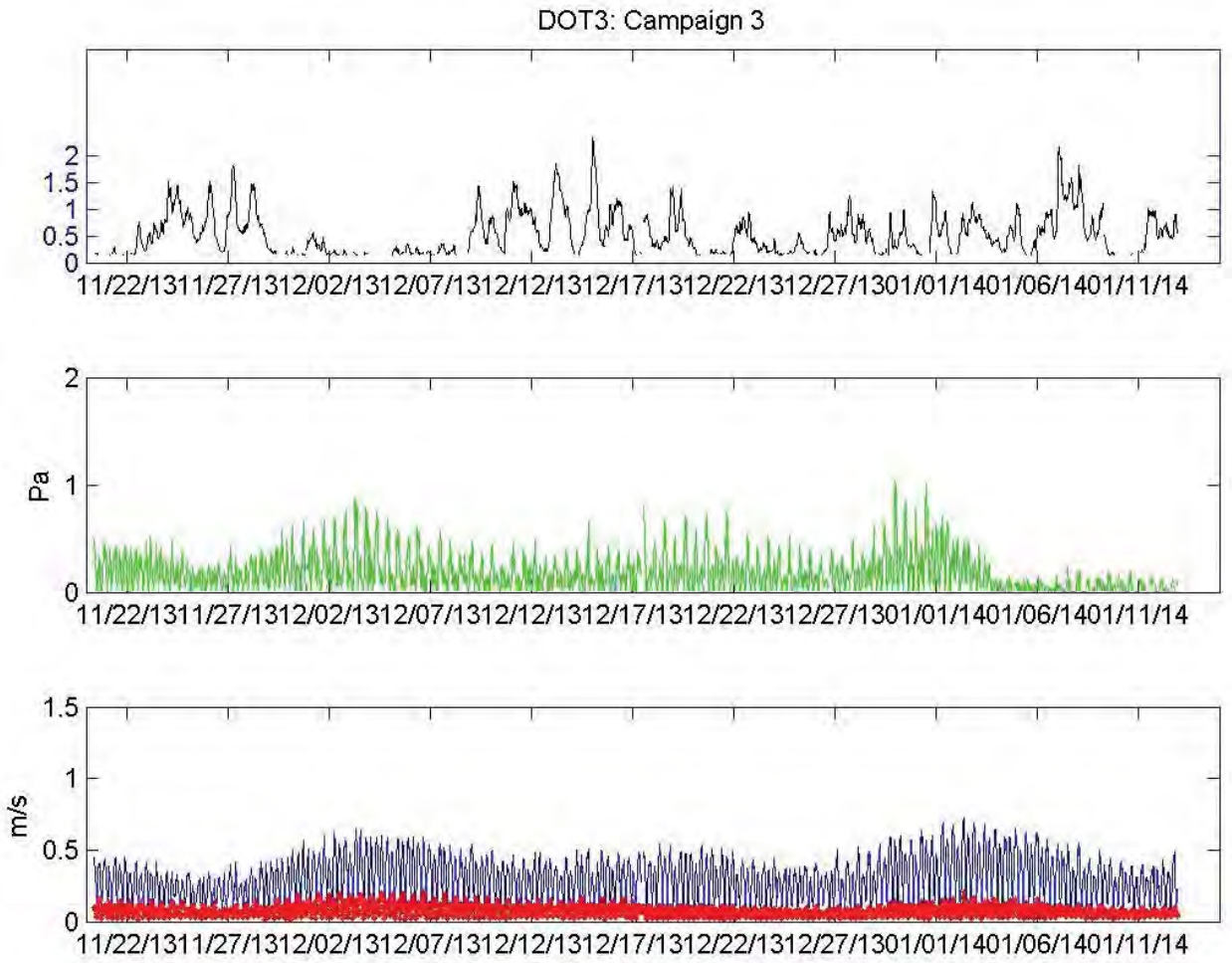

Figure 7-17. Characteristics at Station DOT3 during Campaign 3. (top) Significant wave height (in m); (middle) Stress; and (bottom) Standard deviation of the velocity estimates within the ensemble (red line) and the ensemble means (blue line).

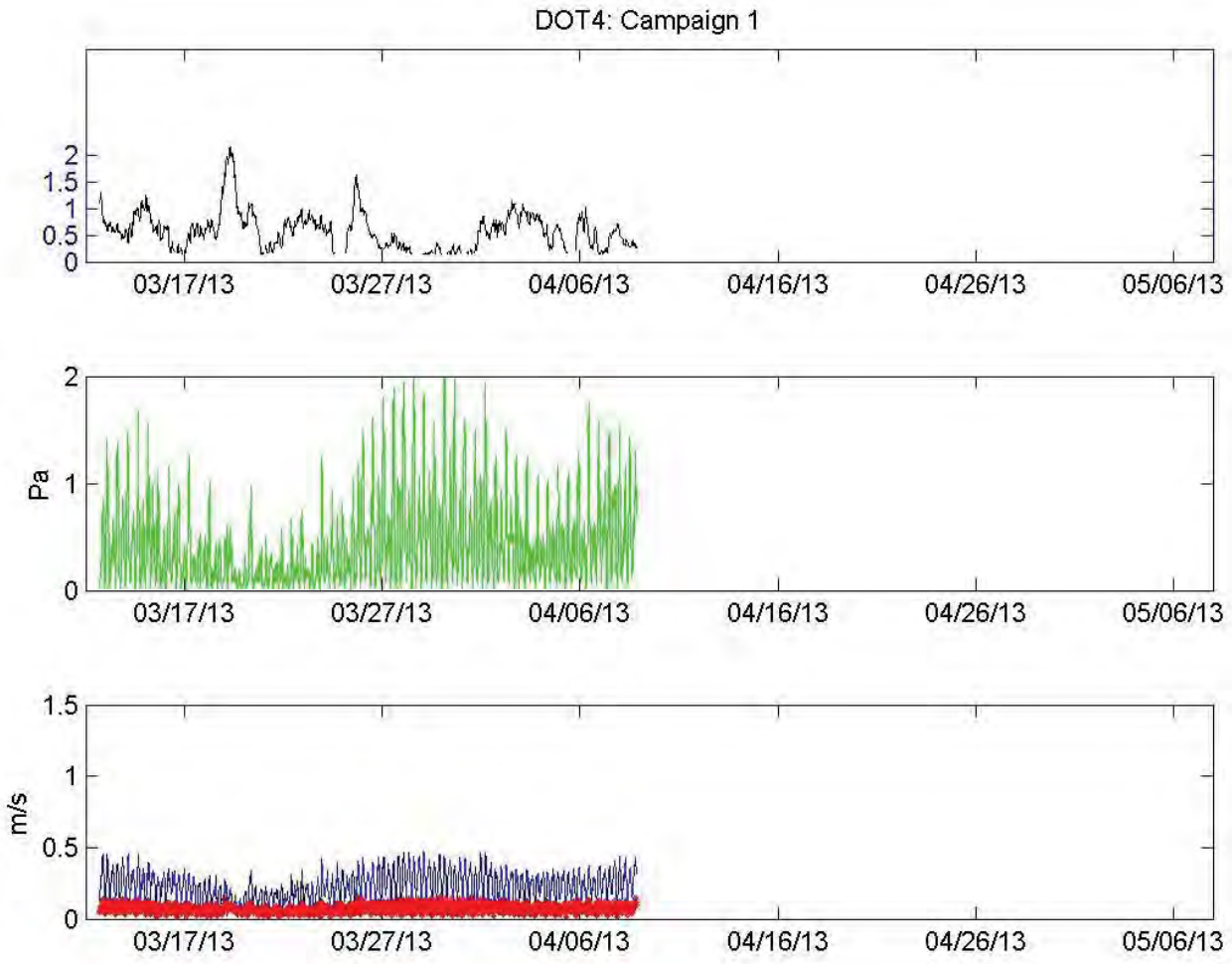

Figure 7-18. Characteristics at Station DOT4 during Campaign 1. (top) Significant wave height (in m); (middle) Stress; and (bottom) Standard deviation of the velocity estimates within the ensemble (red line) and the ensemble means (blue line).

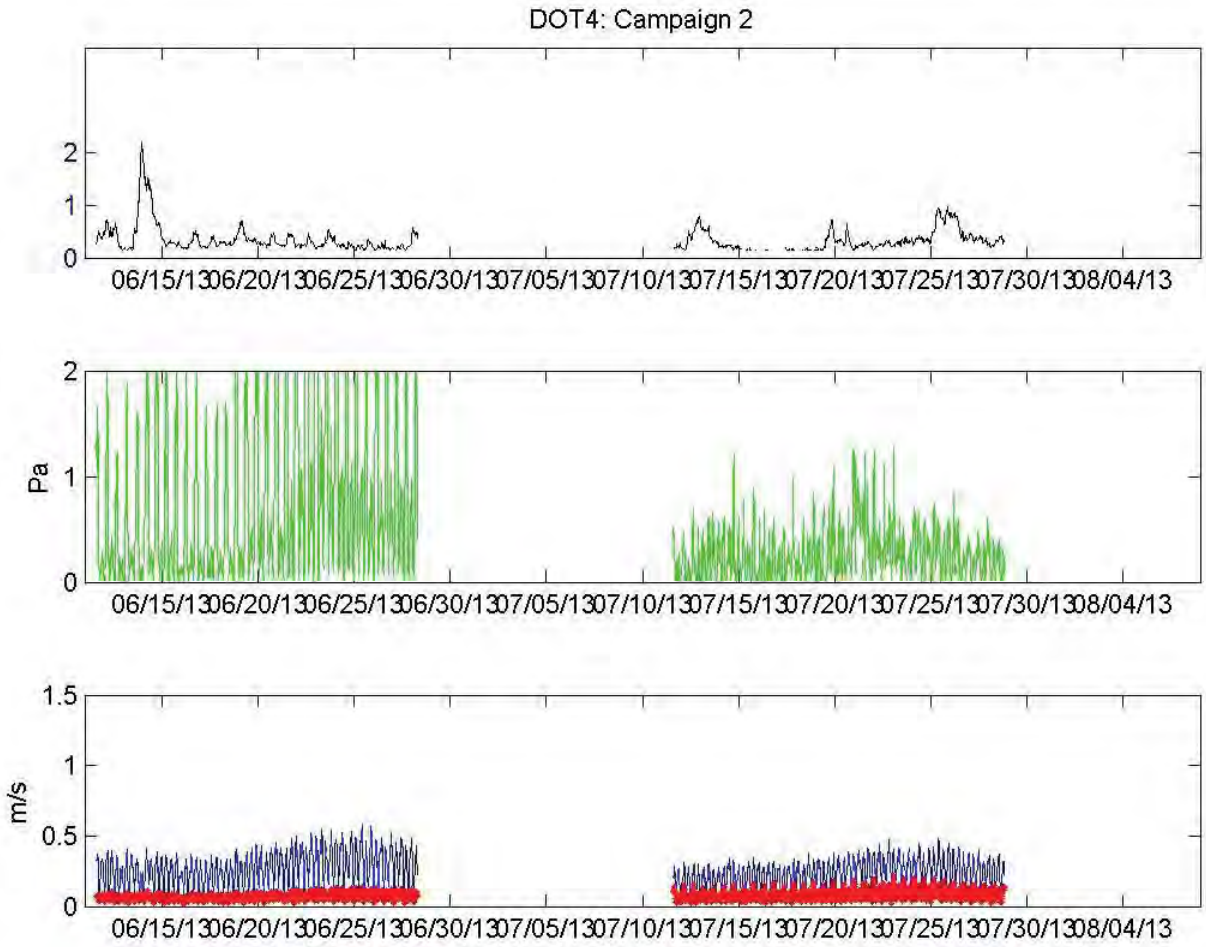

Figure 7-19. Characteristics at Station DOT4 during Campaign 2. (top) Significant wave height (in m); (middle) Stress; and (bottom) Standard deviation of the velocity estimates within the ensemble (red line) and the ensemble means (blue line).

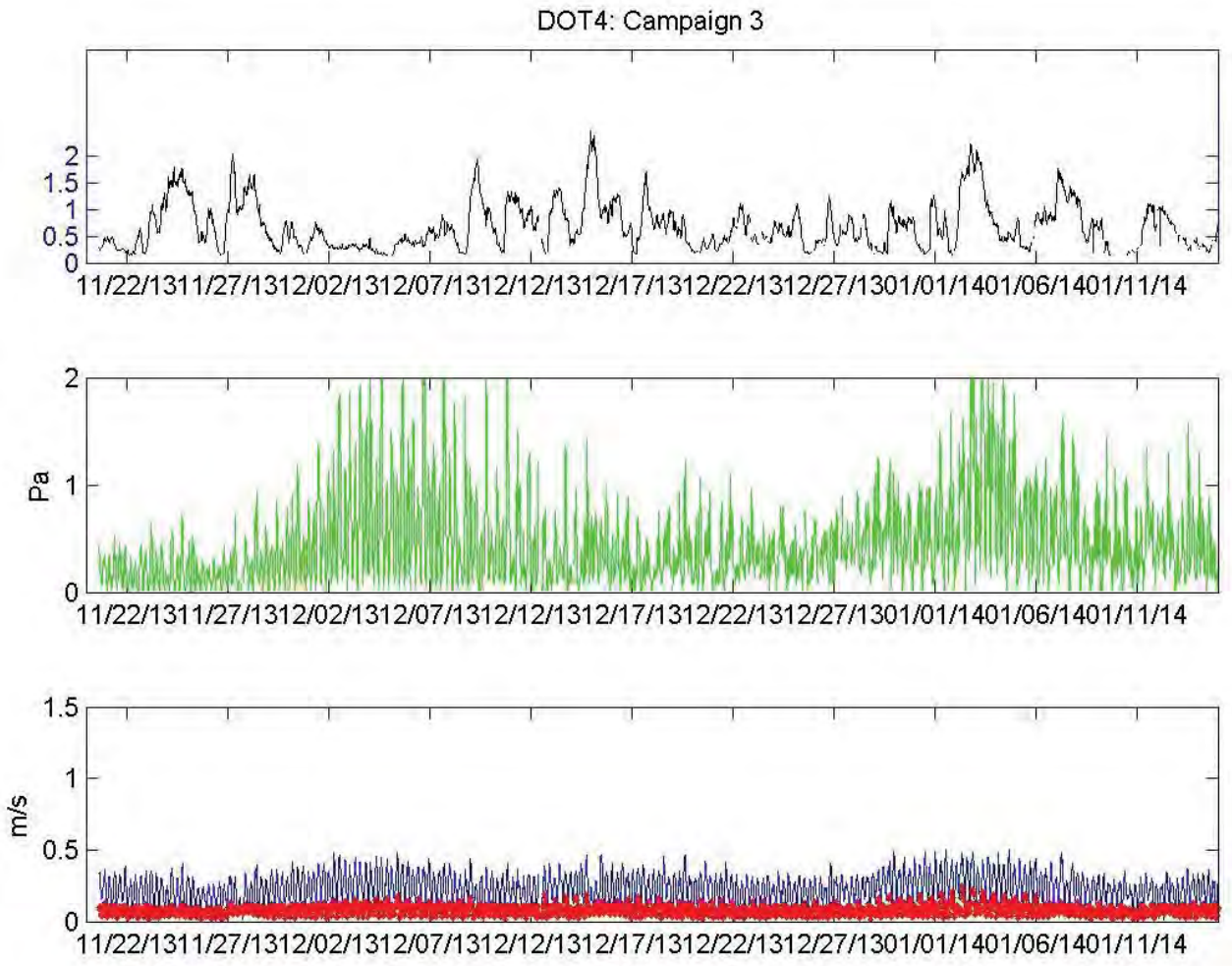

Figure 7-20. Characteristics at Station DOT4 during Campaign 3. (top) Significant wave height (in m); (middle) Stress; and (bottom) Standard deviation of the velocity estimates within the ensemble (red line) and the ensemble means (blue line).

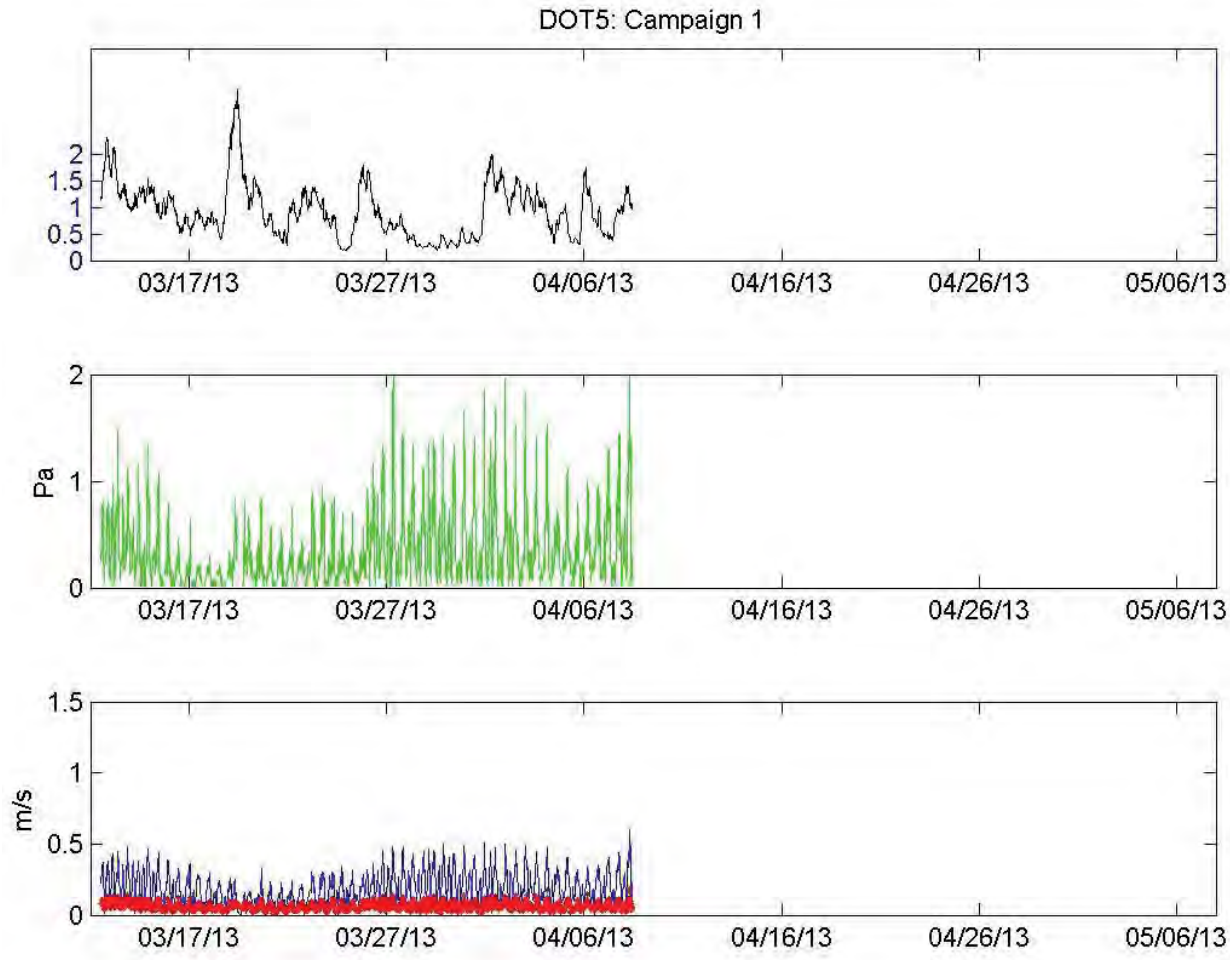

Figure 7-21. Characteristics at Station DOT5 during Campaign 1. (top) Significant wave height (in m); (middle) Stress; and (bottom) Standard deviation of the velocity estimates within the ensemble (red line) and the ensemble means (blue line).

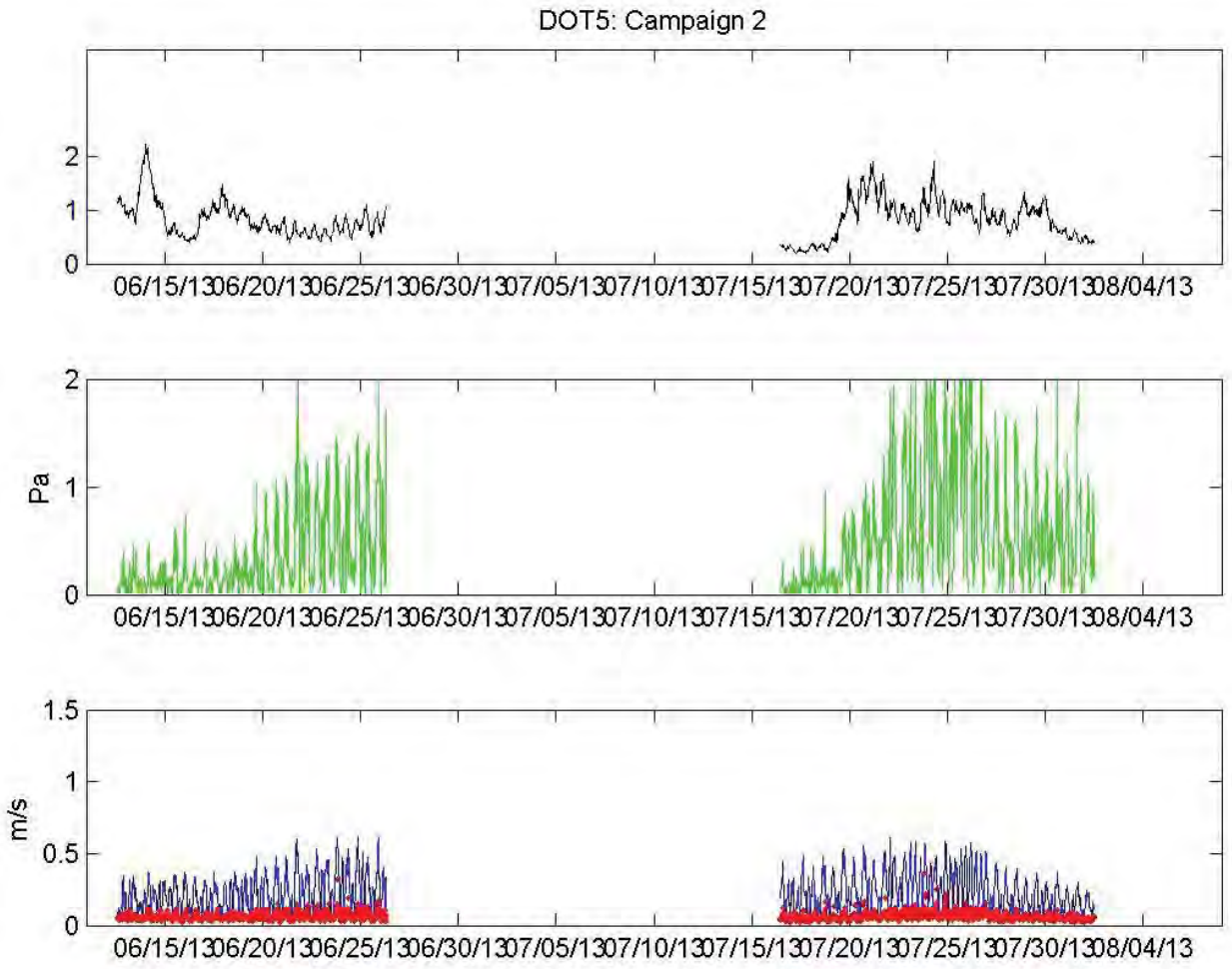

Figure 7-22. Characteristics at Station DOT5 during Campaign 2. (top) Significant wave height (in m); (middle) Stress; and (bottom) Standard deviation of the velocity estimates within the ensemble (red line) and the ensemble means (blue line).

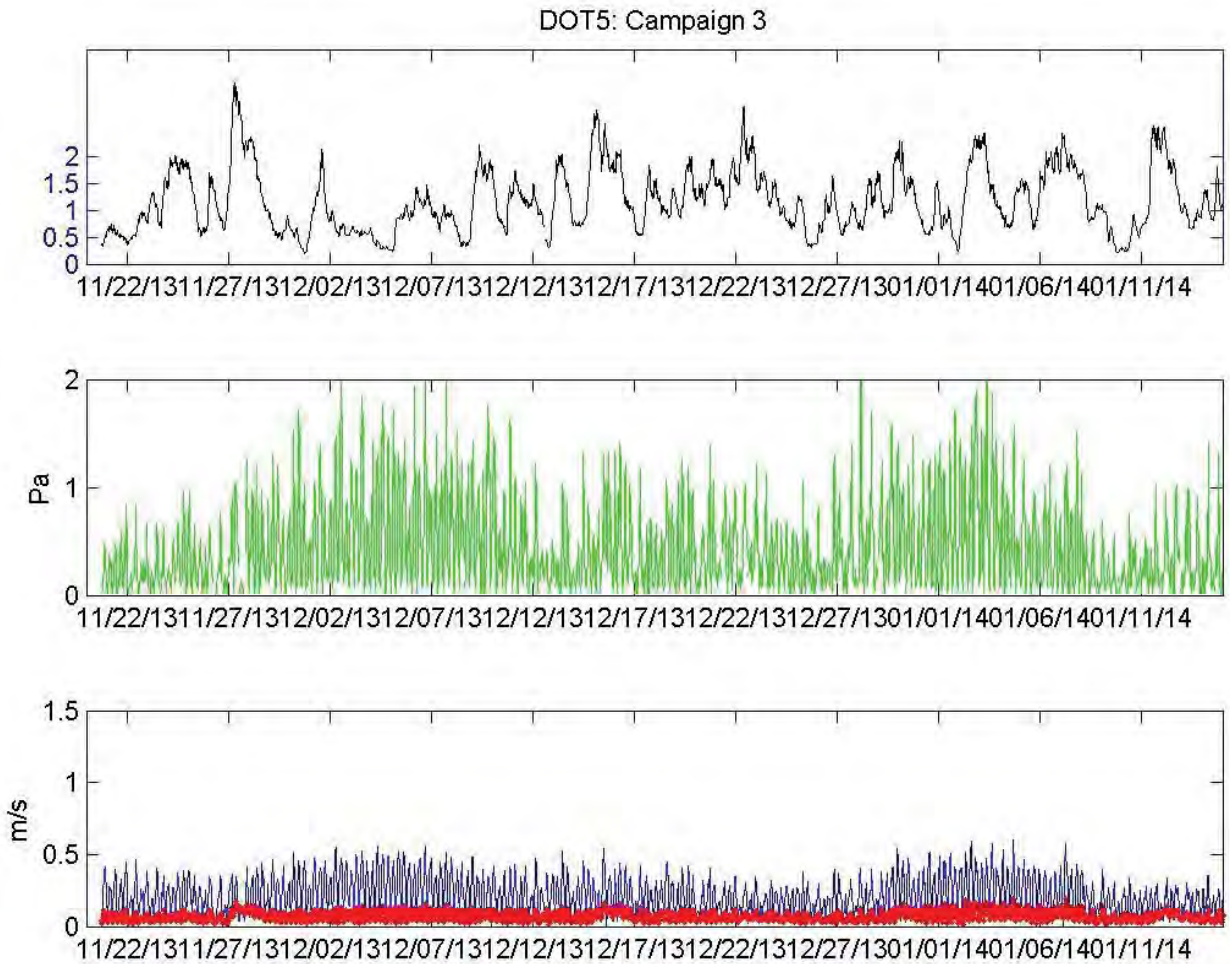

Figure 7-23. Characteristics at Station DOT5 during Campaign 3. (top) Significant wave height (in m); (middle) Stress; and (bottom) Standard deviation of the velocity estimates within the ensemble (red line) and the ensemble means (blue line).

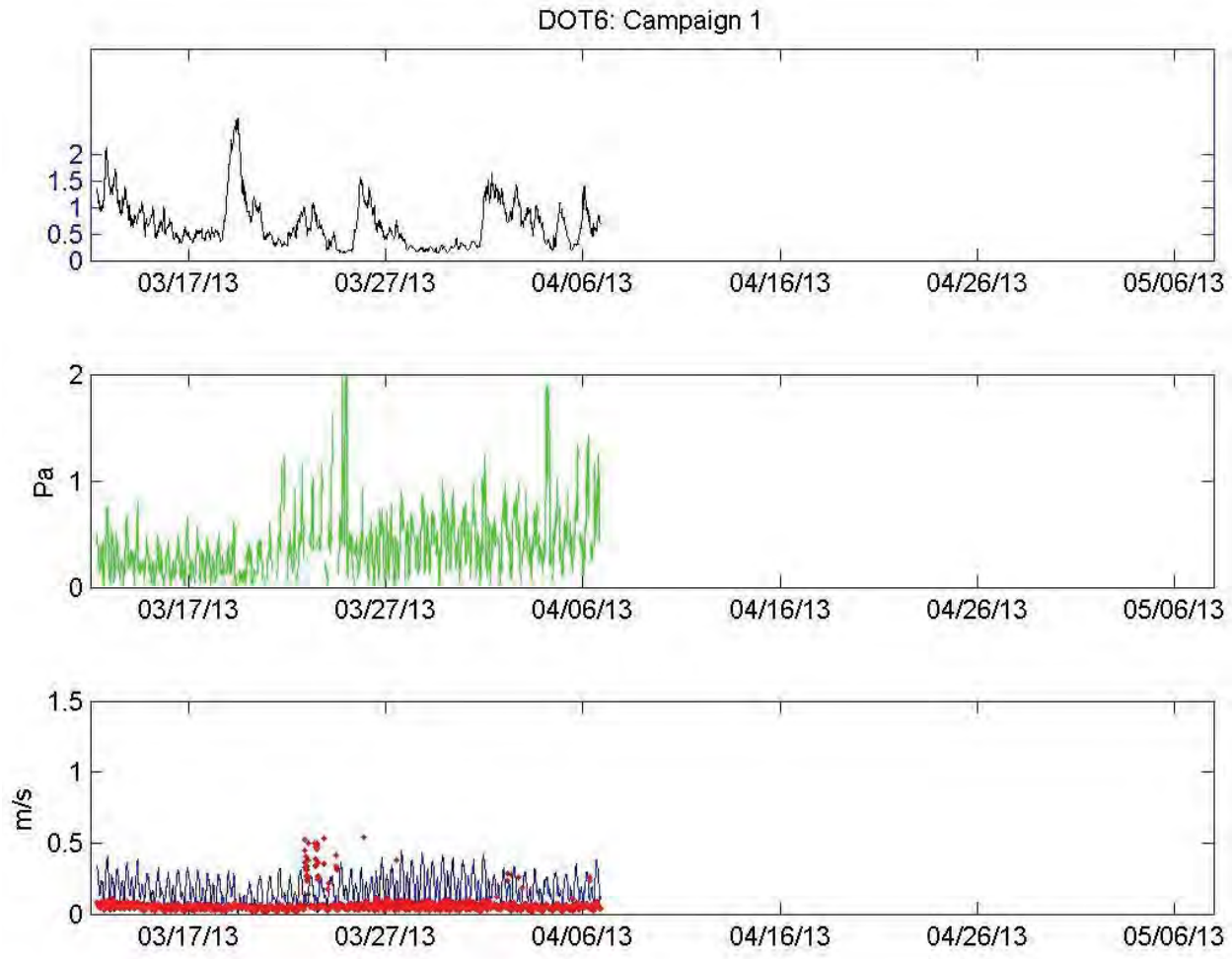

Figure 7-24. Characteristics at Station DOT6 during Campaign 1. (top) Significant wave height (in m); (middle) Stress; and (bottom) Standard deviation of the velocity estimates within the ensemble (red line) and the ensemble means (blue line).

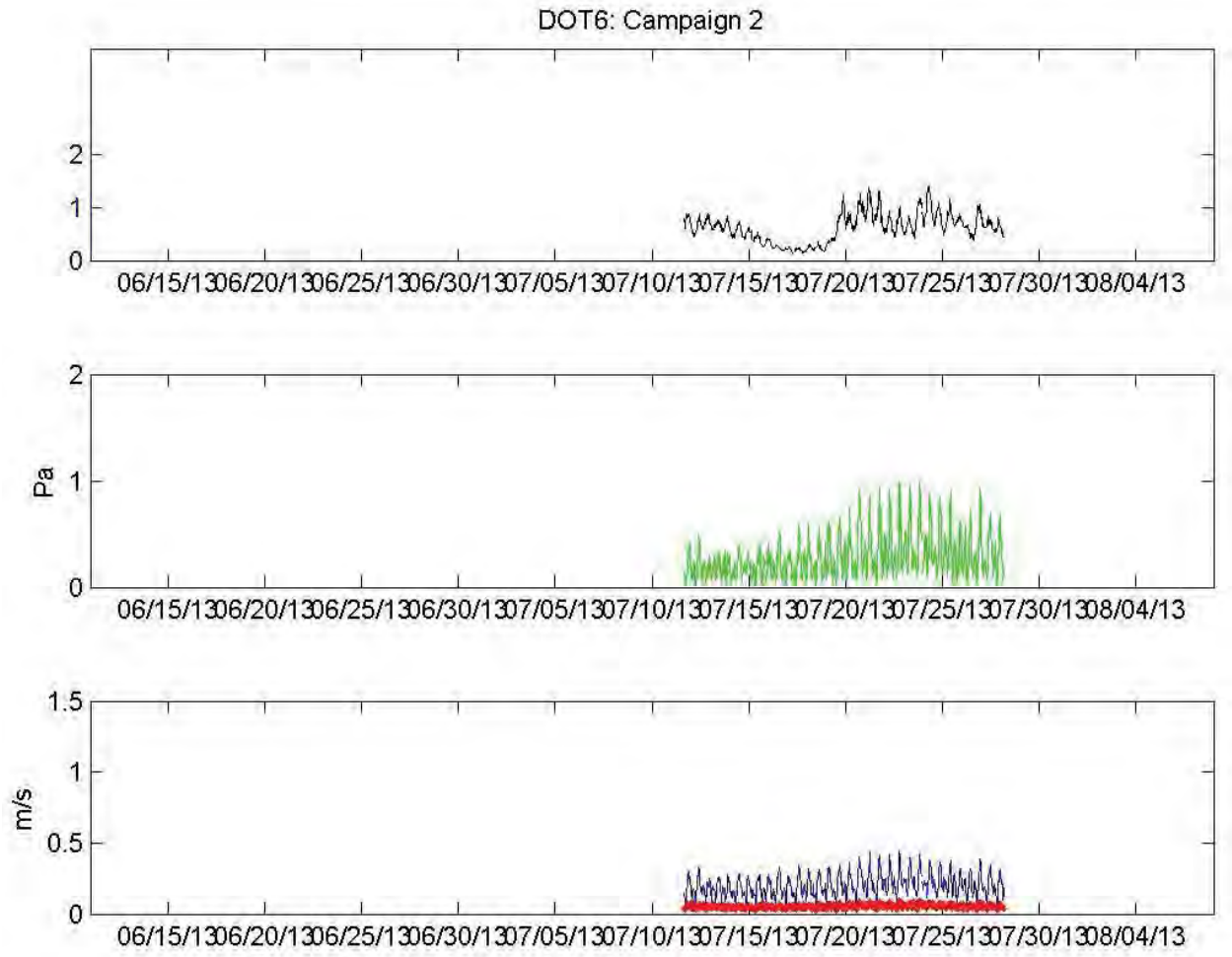

Figure 7-25. Characteristics at Station DOT6 during Campaign 2. (top) Significant wave height (in m); (middle) Stress; and (bottom) Standard deviation of the velocity estimates within the ensemble (red line) and the ensemble means (blue line).

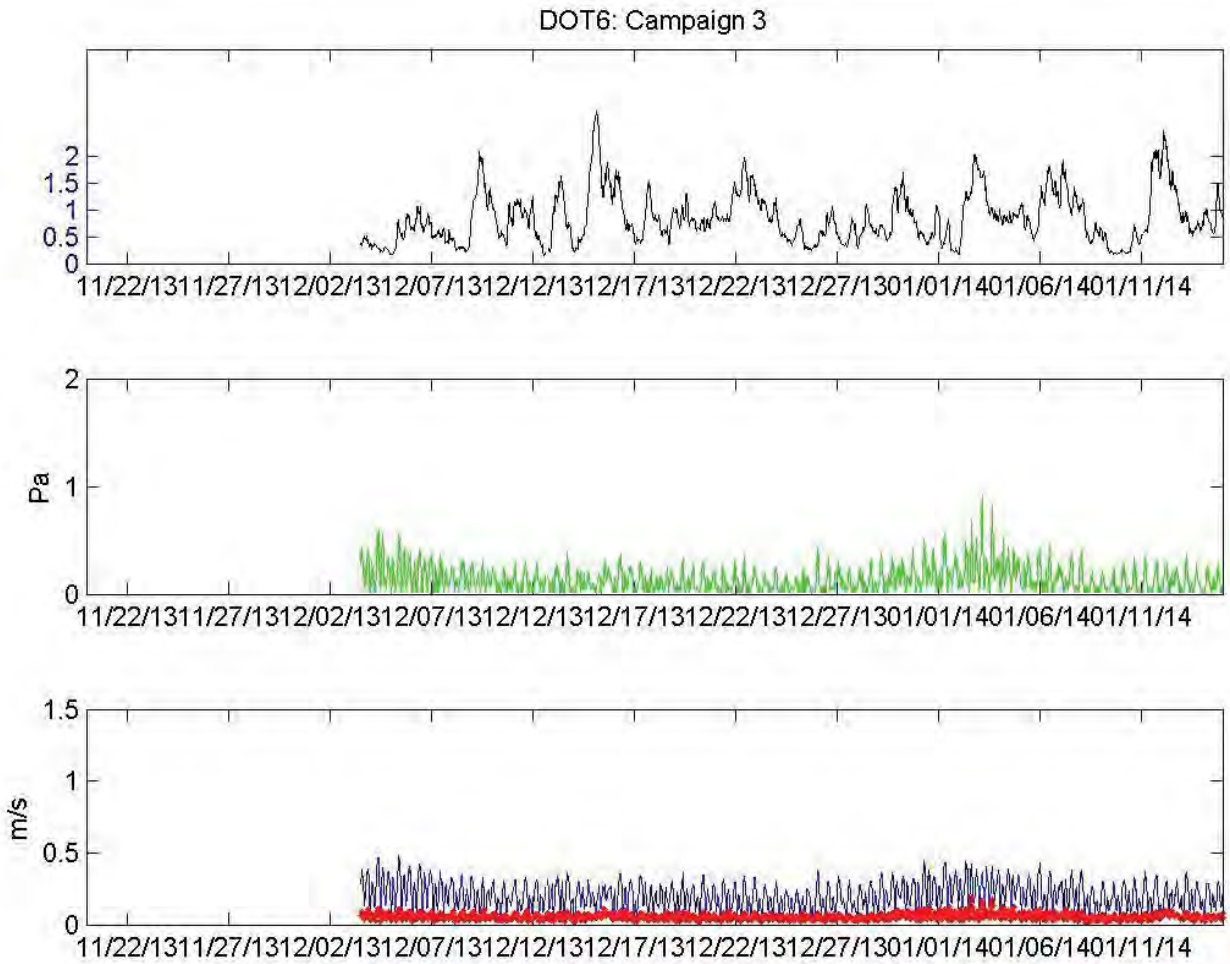

Figure 7-26. Characteristics at Station DOT6 during Campaign 3. (top) Significant wave height (in m); (middle) Stress; and (bottom) Standard deviation of the velocity estimates within the ensemble (red line) and the ensemble means (blue line).

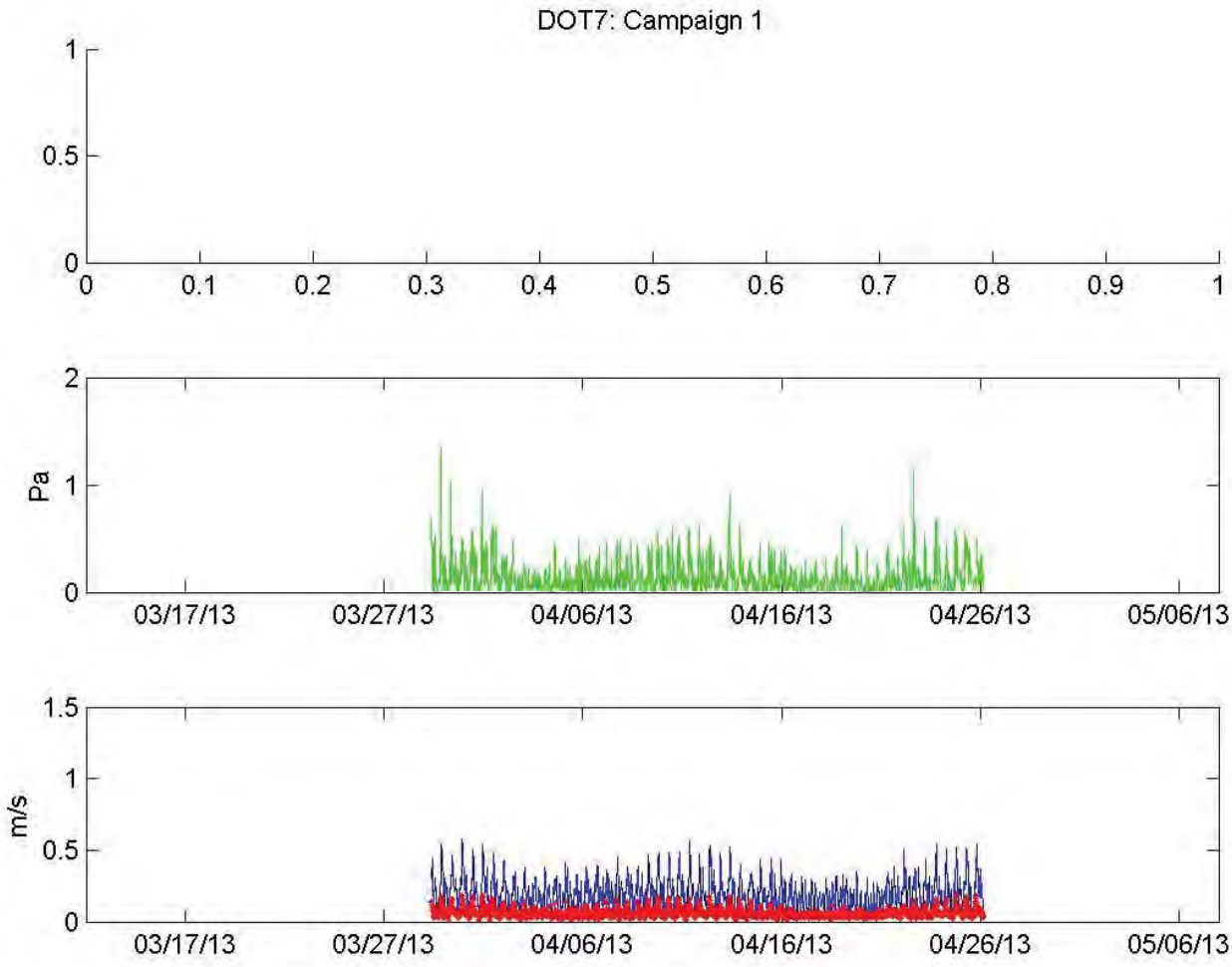

Figure 7-27. Characteristics at Station DOT7 during Campaign 1. (top) Significant wave height (in m); (middle) Stress; and (bottom) Standard deviation of the velocity estimates within the ensemble (red line) and the ensemble means (blue line).

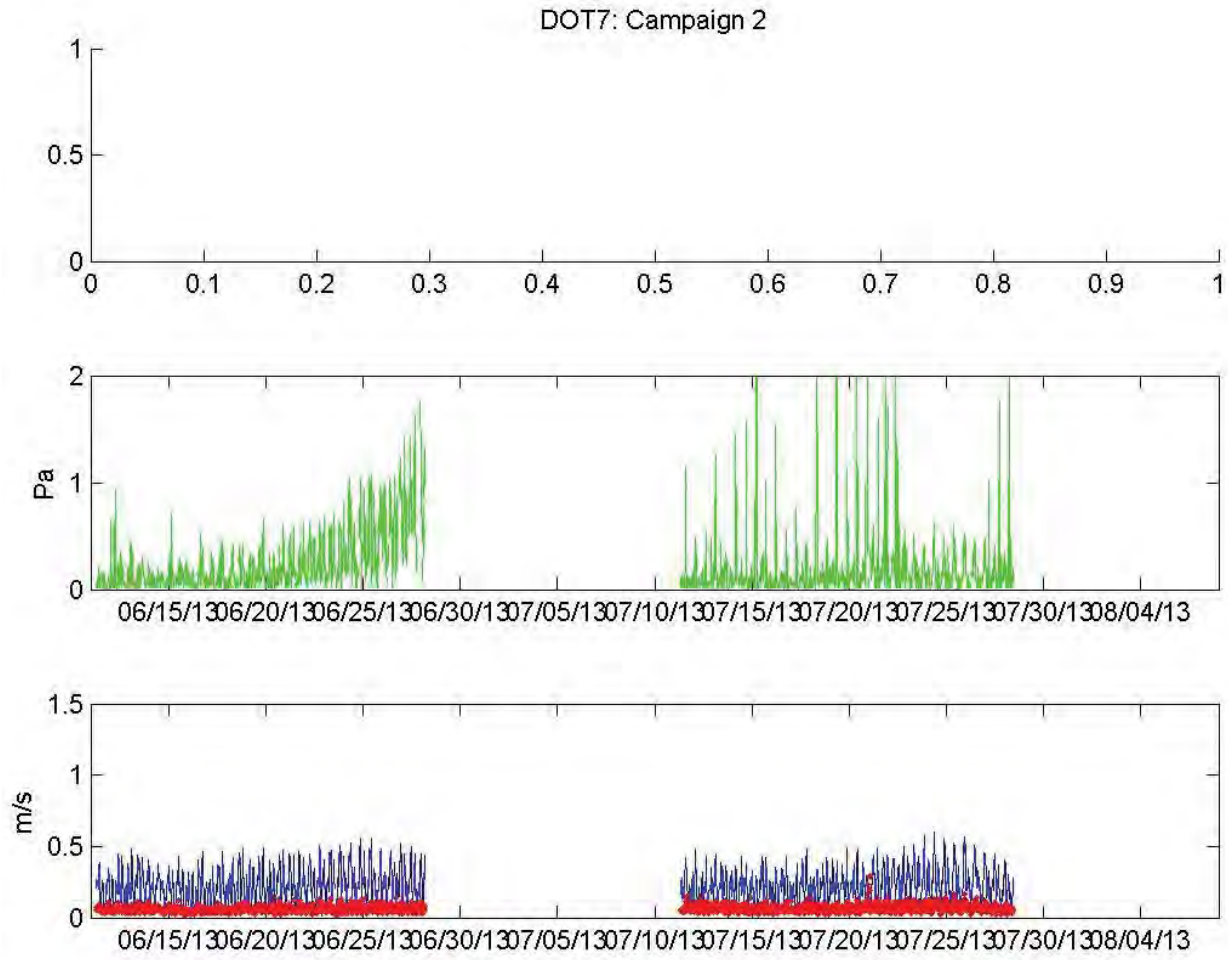

Figure 7-28. Characteristics at Station DOT7 during Campaign 2. (top) Significant wave height (in m); (middle) Stress; and (bottom) Standard deviation of the velocity estimates within the ensemble (red line) and the ensemble means (blue line).

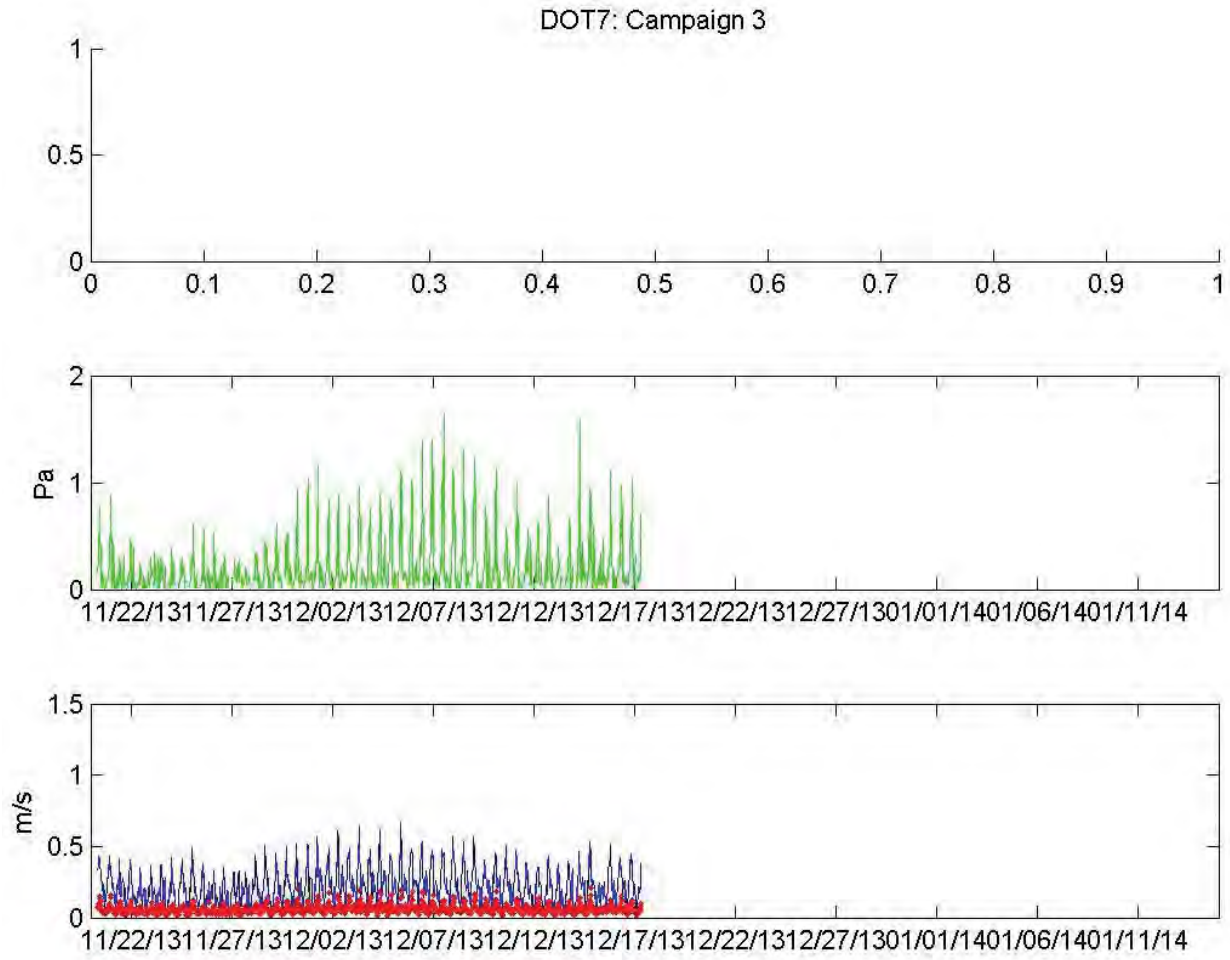

Figure 7-29. Characteristics at Station DOT7 during Campaign 3. (top) Significant wave height (in m); (middle) Stress; and (bottom) Standard deviation of the velocity estimates within the ensemble (red line) and the ensemble means (blue line).

8. Wave Observations

Wave conditions at each mooring station in the ZSF were characterized using the upward-looking RDI ADCP with wave array sampling enabled. The instrument measured the component of the wave velocity in the direction of the four beams, from which the directional frequency spectrum of waves was estimated. This chapter presents the significant wave height, dominant wave frequency, and wave direction at each mooring station. It incorporates wind and wave data from the five metocean stations in the eastern Long Island Sound (CLIS, ELIS, LEDG) and Atlantic Ocean (44017, CDIP154). LEDG is a lighthouse; the other four stations are buoys.

8.1 Data - Meteorological Conditions

Figure 8-1 shows the wind speed during Campaign 1 at the four metocean stations where measurements were available. The winds in the eastern Long Island Sound are represented best by the Station ELIS. Winds reported at Station 44017 are likely more representative of the Block Island Sound. The wind data from all four metocean stations are highly correlated. Figures 8-1b and 8-1c show the wind speeds from the same metocean stations during Campaigns 2 and 3. Note that the scale in Figure 8-1c differs from the scale in Figures 8-1a and 8-1b, and that the data from Station CLIS end on December 24 due to a failure of the power system.

The mean and maximum wind speeds during the three campaigns are presented in Table 8-1. The highest mean wind speeds occurred always at the offshore buoy (Station 44017) and during Campaign 3. Mean wind speeds were lowest in the summer (Campaign 2). The maximum wind speeds display the same general pattern.

Table 8-1. Wind Speed Statistics during the three Campaigns

	Mean Wind Speed (m/s)				**Maximum Wind Speed** (m/s)			
	Metocean Station				**Metocean Station**			
Campaign	**ELIS**	**CLIS**	**LEDG**	**44017**	**ELIS**	**CLIS**	**LEDG**	**44017**
1	5.34	5.27	5.61	6.58	13.9	15.4	16.5	16.6
2	3.61	4.60	5.07	5.46	12.4	16.5	15.4	16.2
3	6.51	7.08*	6.84	8.50	14.9	16.5*	18.5	18.4

* Records from Site CLIS ended 22 days early.

(a)

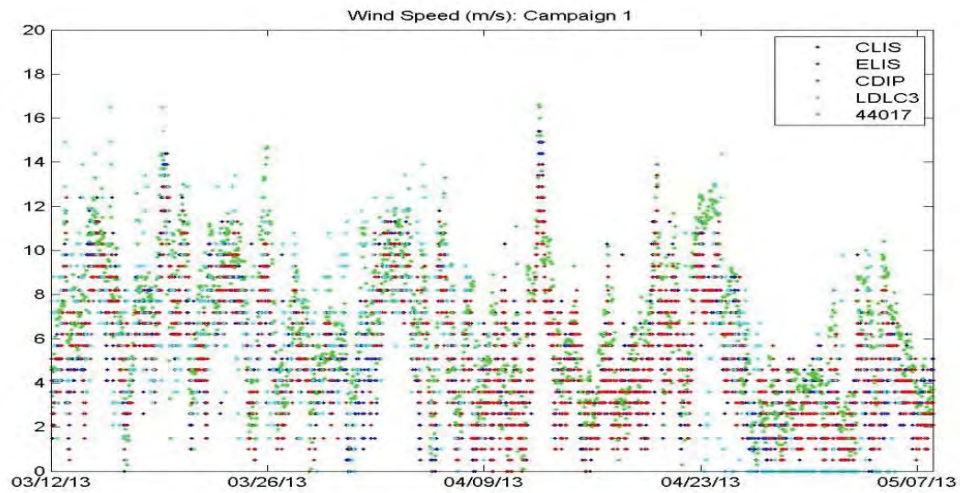

(b)

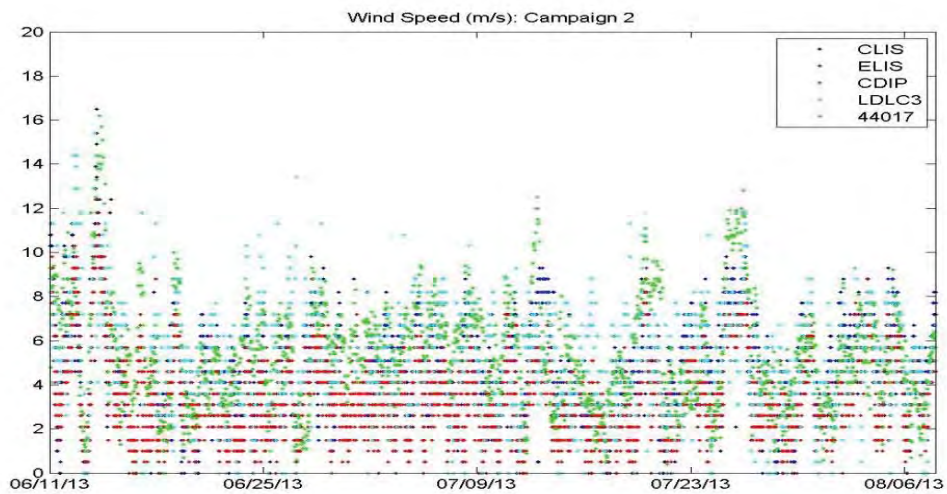

(c)

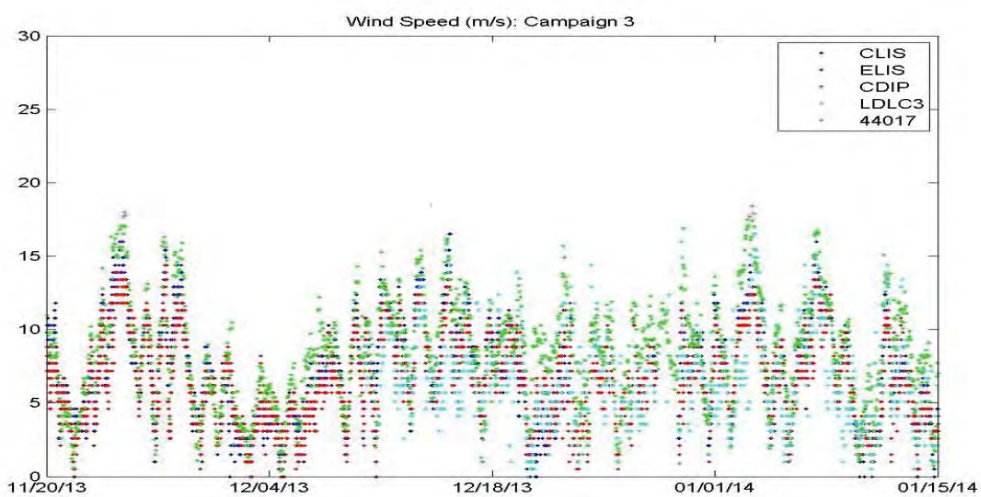

Figure 8-1. Time-series of the observed wind speed at meteorological stations CLIS (blue), ELIS (red), LEDG (cyan), and 44017 (green) during the three campaigns.

8.2 Data - Wave Observations

The time-series of significant wave height, dominant wave direction, and dominant period for each campaign and each of the seven mooring stations in the ZSF are presented in Figures 8-2 to 8-20. The period and direction are noisy and not meaningful when the significant wave height is low. To emphasize the variability over a longer time-scale a 5-day running average was computed and superimposed on each graph.

The time-series of significant wave height (H_s) and dominant period (T_p) in Figures 8-2 to 8-20 can be contrasted simply by comparing the record means for each campaign. Table 8-2 lists the means for each station and each campaign. It is clear that the longest periods and largest waves occur during the winter (Campaign 3) and in the Block Island Sound.

Table 8-2. Summary of Wave Field Characteristics

Station	**Wave Height** (H_s) (m)	**Dominant Period** (T_p) **(s)**
Campaign 1		
DOT1	0.56	3.3
DOT2	0.49	3.3
DOT3		
DOT4	0.61	5.2
DOT5	1.03	7.7
DOT6	0.93	7.7
DOT7		
Campaign 2		
DOT1	0.59	2.94
DOT2	0.45	2.94
DOT3	0.46	3.43
DOT4	0.76	3.5
DOT5	1.00	6.7
DOT6	1.32	7.7
DOT7	0.97	6.7
Campaign 3		
DOT1	0.73	3.84
DOT2	0.67	3.84
DOT3	0.53	4.37
DOT4	0.63	4.1
DOT5	1.11	6.67
DOT6	0.94	7.45
DOT7	0.74	4.20

Since waves are not normally distributed, the results can be more usefully summarized by a cumulative probability distribution functions (CPDF). Figures 8-21 to 8-23 show the CPDF of the data (blue line), contrasted with the Rayleigh distribution and the Normal (Gaussian) distributions (red and black dashed lines, respectively). The Rayleigh distribution has been found to be useful representation of significant wave height (H_S) variability. The figures reveal that the ELIS stations had lower H_s more frequently that predicted by the Rayleigh distribution; at the BIS stations, larger waves were more common. This spatial variability is a consequence of the coastal geometry.

Comparing the wave data from the moored stations with wave data obtained from several metocean buoy stations located within and near the ZSF shows good agreement between the two data sets. Figure 8-24 is the significant wave height at metocean Stations CLIS, 44017, and CDIP154 for each of the three campaigns. Wave heights at Stations 44017 and CDIP154 in Figure 8-24a are in close alignment indicating that the field is coherent in the alongshore direction on the shelf. The significant wave height at these metocean stations seldom dropped below 1 m during any of the three campaigns, which is consistent with the observations from the Block Island Sound mooring stations. At the CLIS buoy the significant wave height was much lower but many of the larger events are correlated with the offshore records. During Campaign 2, the CLIS buoy did not record significant wave heights intervals with waves over 0.5 m. In the winter, however, there were two periods with larger waves.

A summary of the mean and maximum wave heights from the metocean stations are presented in Table 8-3. The mean wave heights were much lower at Station CLIS during all three campaigns, ranging from 0.32 m in the summer to 6.7 m in the winter. The maximum significant wave heights ranged from 1.8 m to 2.3 m at Station CLIS but waves were much larger offshore with a winter maximum of 5.4 m at Station 44017.

Table 8-3. Significant Wave Height Statistics during the three Campaigns

	Mean Significant Wave Height (m)			**Maximum Significant Wave Height (**m)		
	Metocean Station			**Metocean Station**		
Campaign	**CLIS**	**CDIP**	**44017**	**CLIS**	**CDIP**	**44017**
1	0.42	1.44	1.35	2.0	4.5	4.3
2	0.32	1.14	1.05	1.8	3.0	3.3
3	0.67	1.82	1.63	2.3	6.5	5.4

The dominant wave period records are shown in Figure 8-25; averages for each campaign are presented in Table 8-4. The mean dominant wave period in the eastern Long Island Sound was seldom in excess of 5s and even in the winter the mean was 3.79s. The maximum values observed in the winter were 7s. Since Stations 44017 and CDIP are exposed to deep water, the waves at these locations have much longer periods; mean values were greater than 7s during all three campaigns.

Table 8-4. Mean Dominant Wave Periods (s)

Campaign	Sites		
	CLIS	CDIP	44017
1	3.45	8.27	8.05
2	2.95	7.00	7.01
3	3.79	7.52	7.47

8.3 Summary

Results show that sufficient wave data were collected for a spatial and temporal study of the wave field. Generally, mooring stations DOT4, 5 and 6 located in Block Island Sound are influenced by waves from the Atlantic Ocean. Stations DOT1, 2, 3 and 7 located in the eastern Long Island Sound are dominated more by the regional wind field. The available observations of wind and waves within and bounding the ZSF also exhibit a wide range of conditions during the three campaigns; the observations will be used for the purposes of forcing in the circulation model as part of this physical oceanography study.

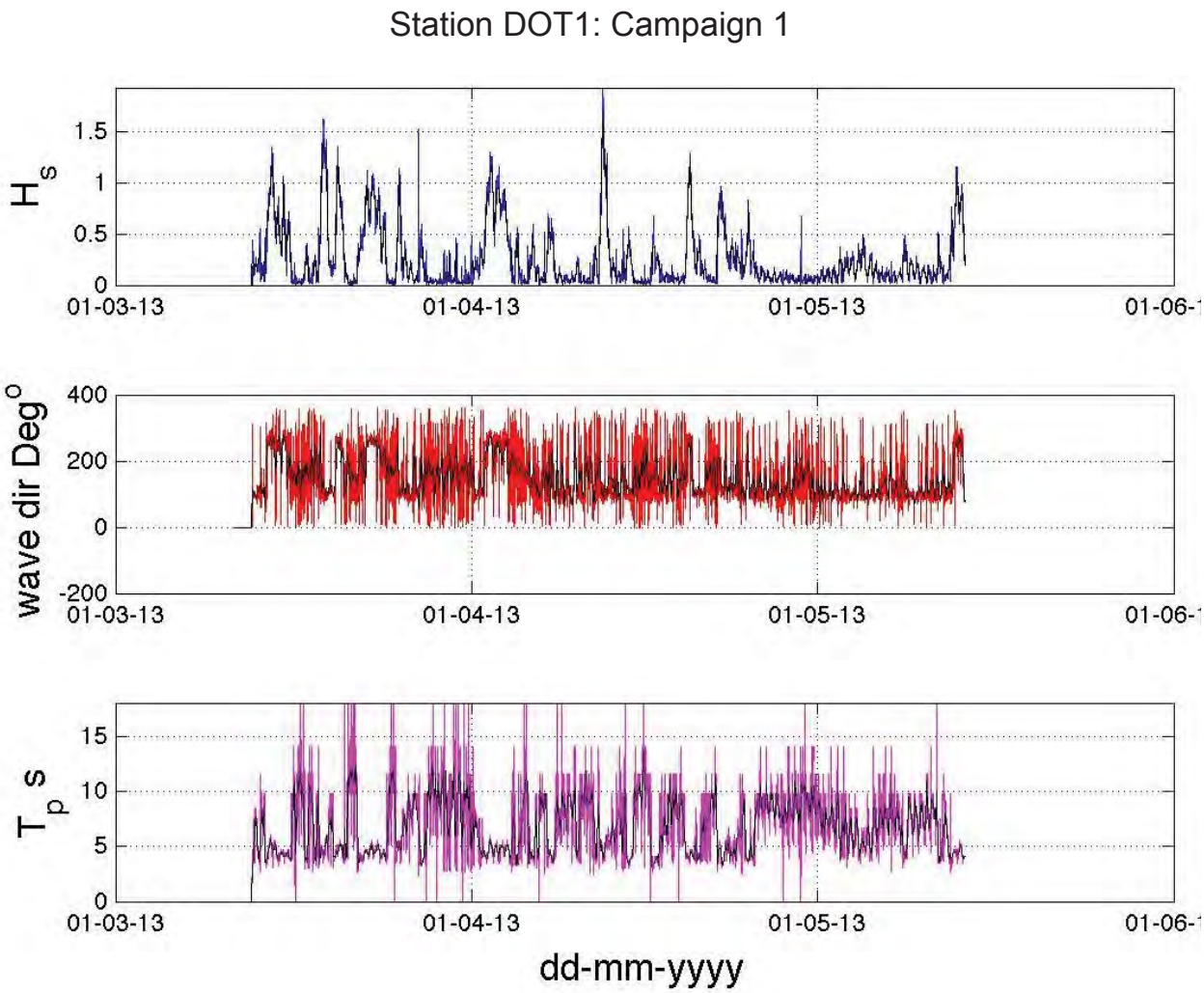

Figure 8-2. Wave conditions at Station DOT1 during Campaign 1: Significant wave height (top), wave direction (oceanographic convention; middle), dominant wave period obtained from the spectral peak frequency (bottom). All graphs contain a 5-day moving average (black lines).

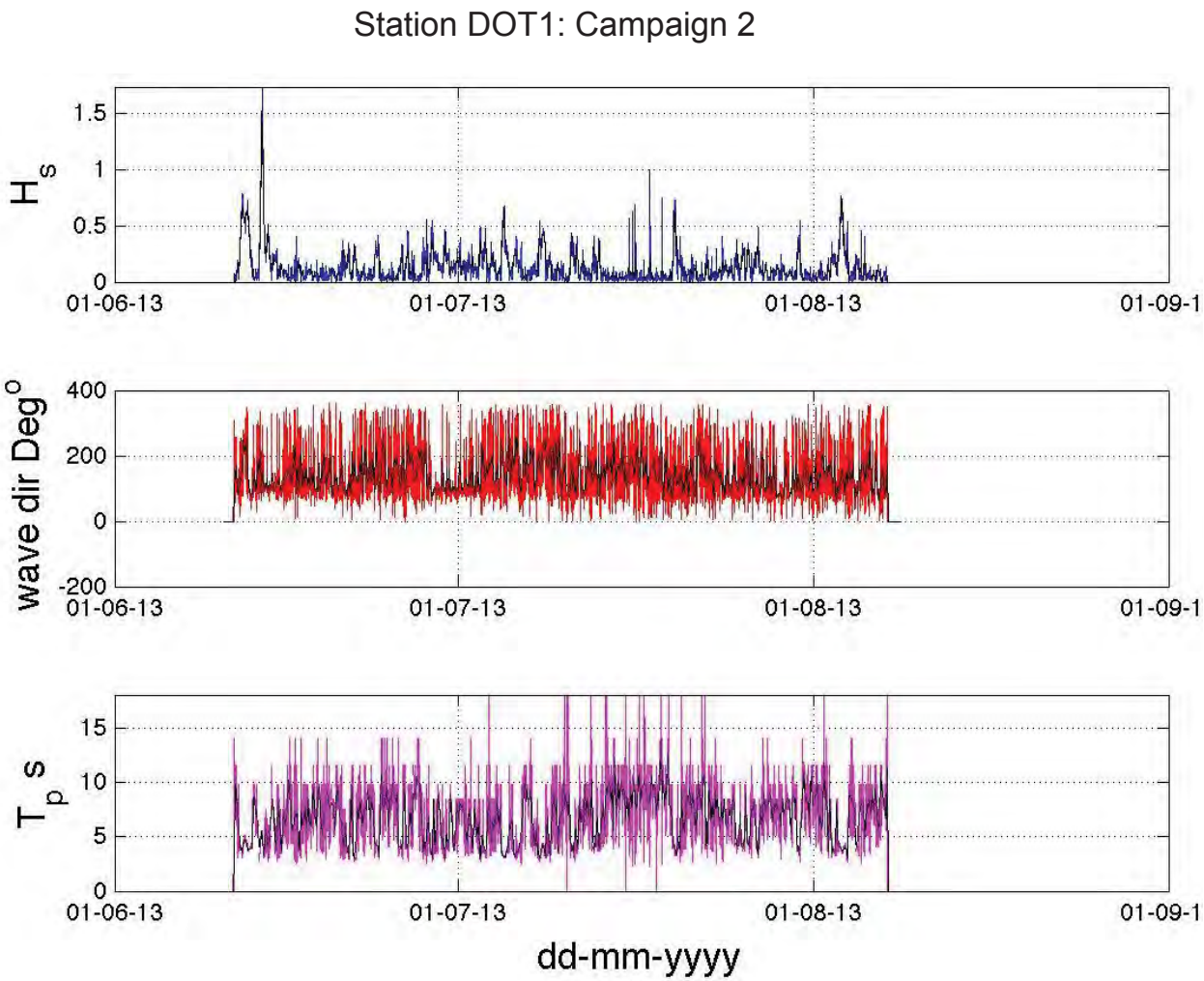

Figure 8-3. Wave conditions at Station DOT1 during Campaign 2: Significant wave height (top), wave direction (oceanographic convention; middle), dominant wave period obtained from the spectral peak frequency (bottom). All graphs contain a 5-day moving average (black lines).

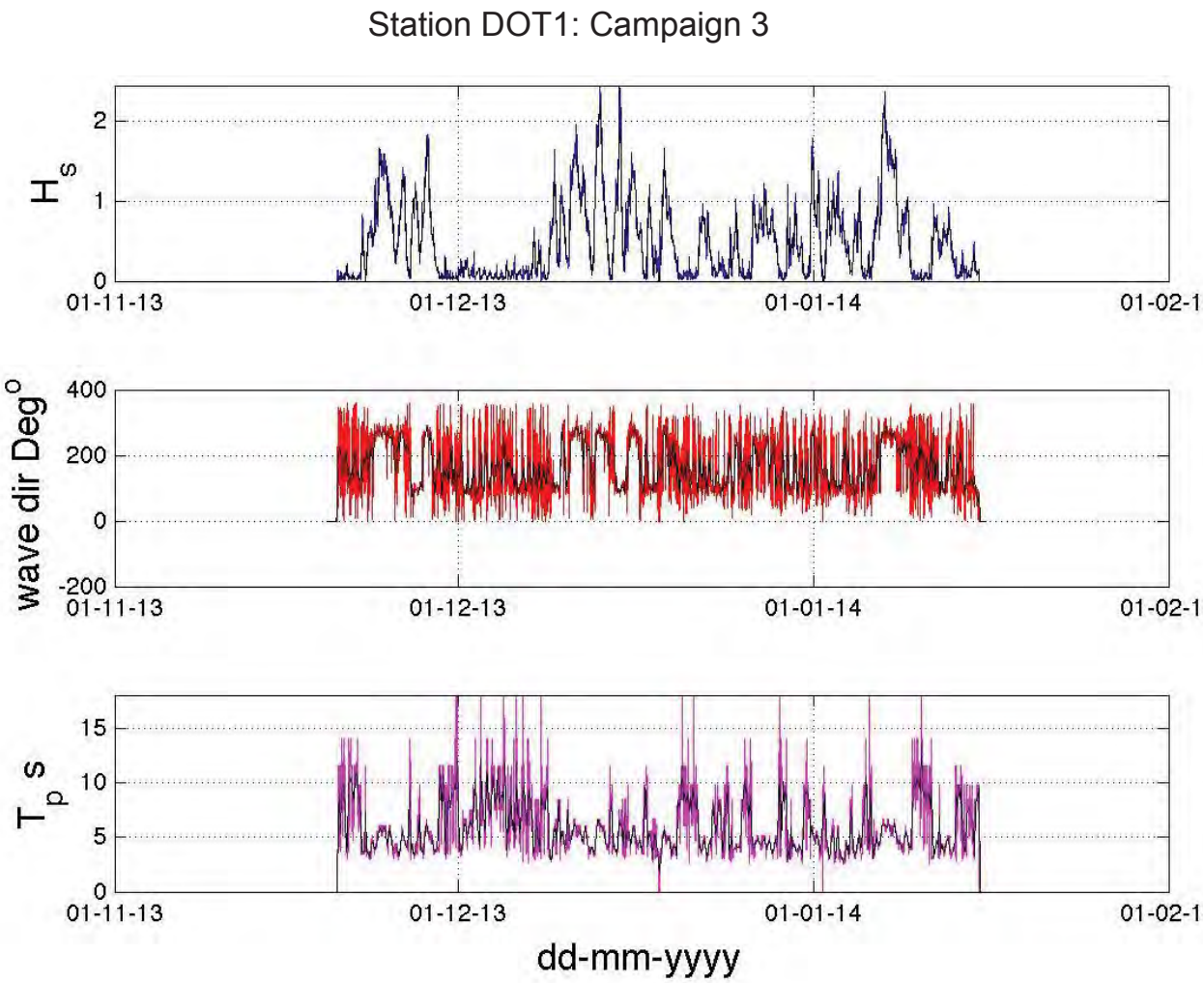

Figure 8-4. Wave conditions at Station DOT1 during Campaign 3: Significant wave height (top), wave direction (oceanographic convention; middle), dominant wave period obtained from the spectral peak frequency (bottom). All graphs contain a 5-day moving average (black lines).

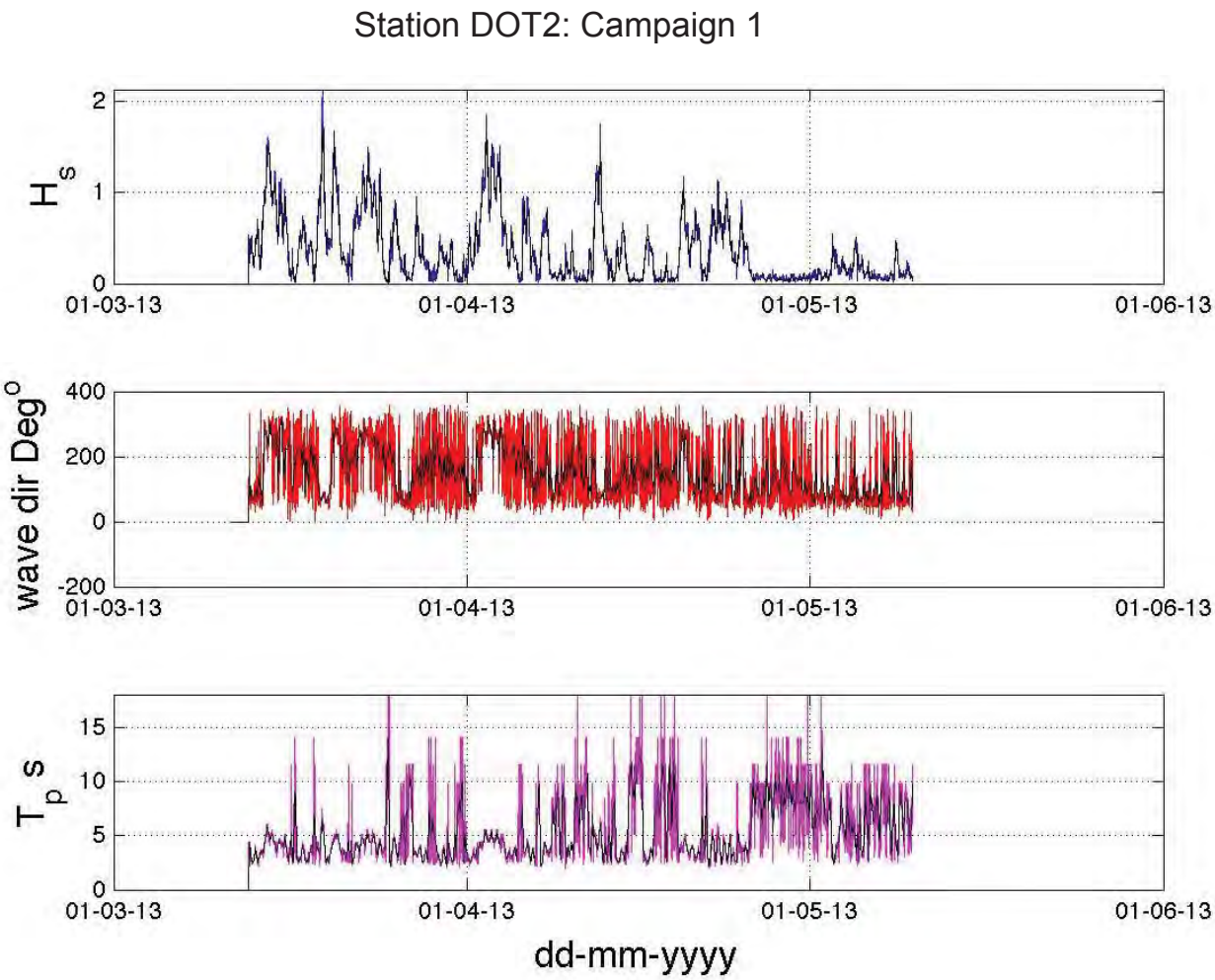

Figure 8-5. Wave conditions at Station DOT2 during Campaign 1: Significant wave height (top), wave direction (oceanographic convention; middle), dominant wave period obtained from the spectral peak frequency (bottom). All graphs contain a 5-day moving average (black lines).

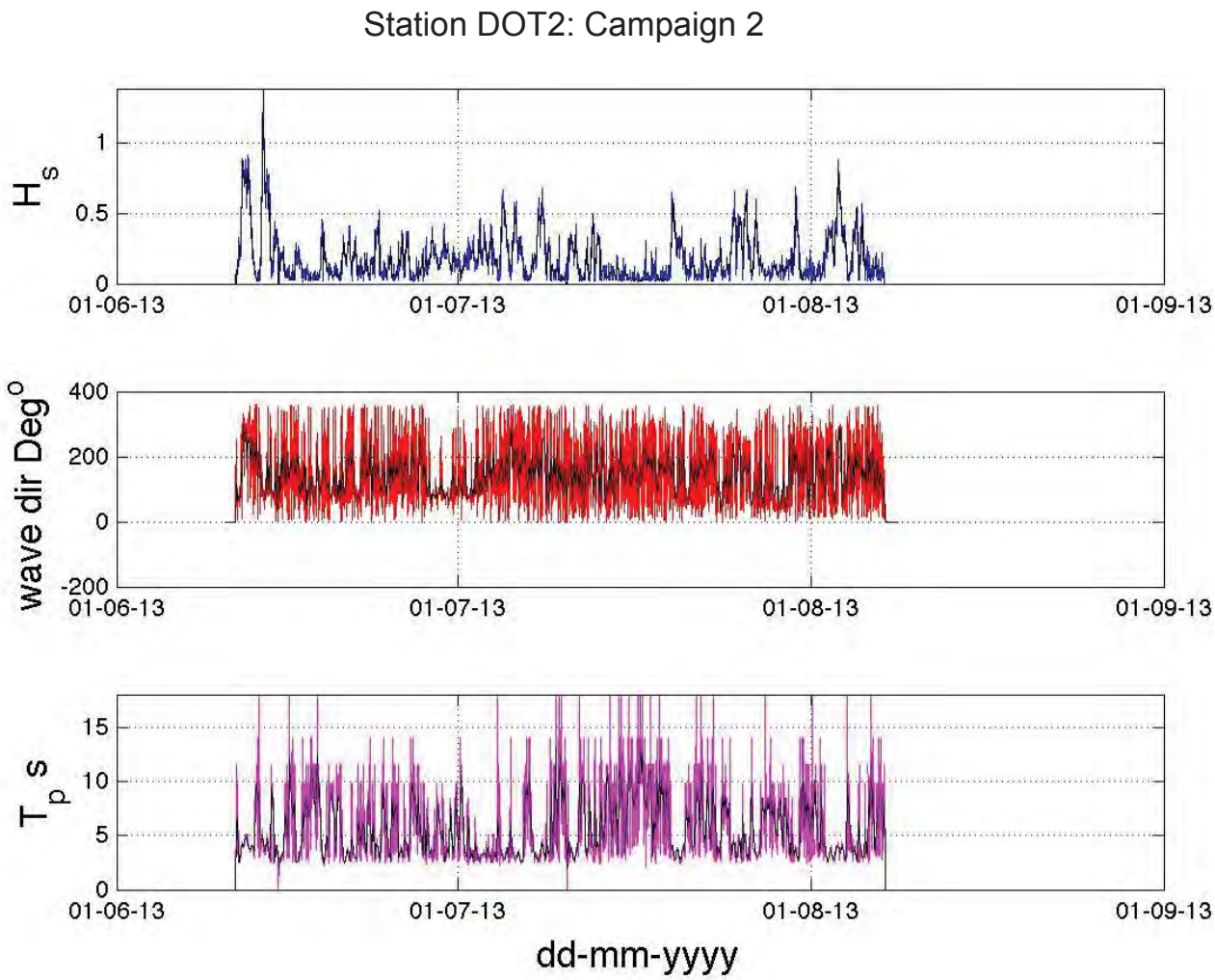

Figure 8-6. Wave conditions at Station DOT2 during Campaign 2: Significant wave height (top), wave direction (oceanographic convention; middle), dominant wave period obtained from the spectral peak frequency (bottom). All graphs contain a 5-day moving average (black lines).

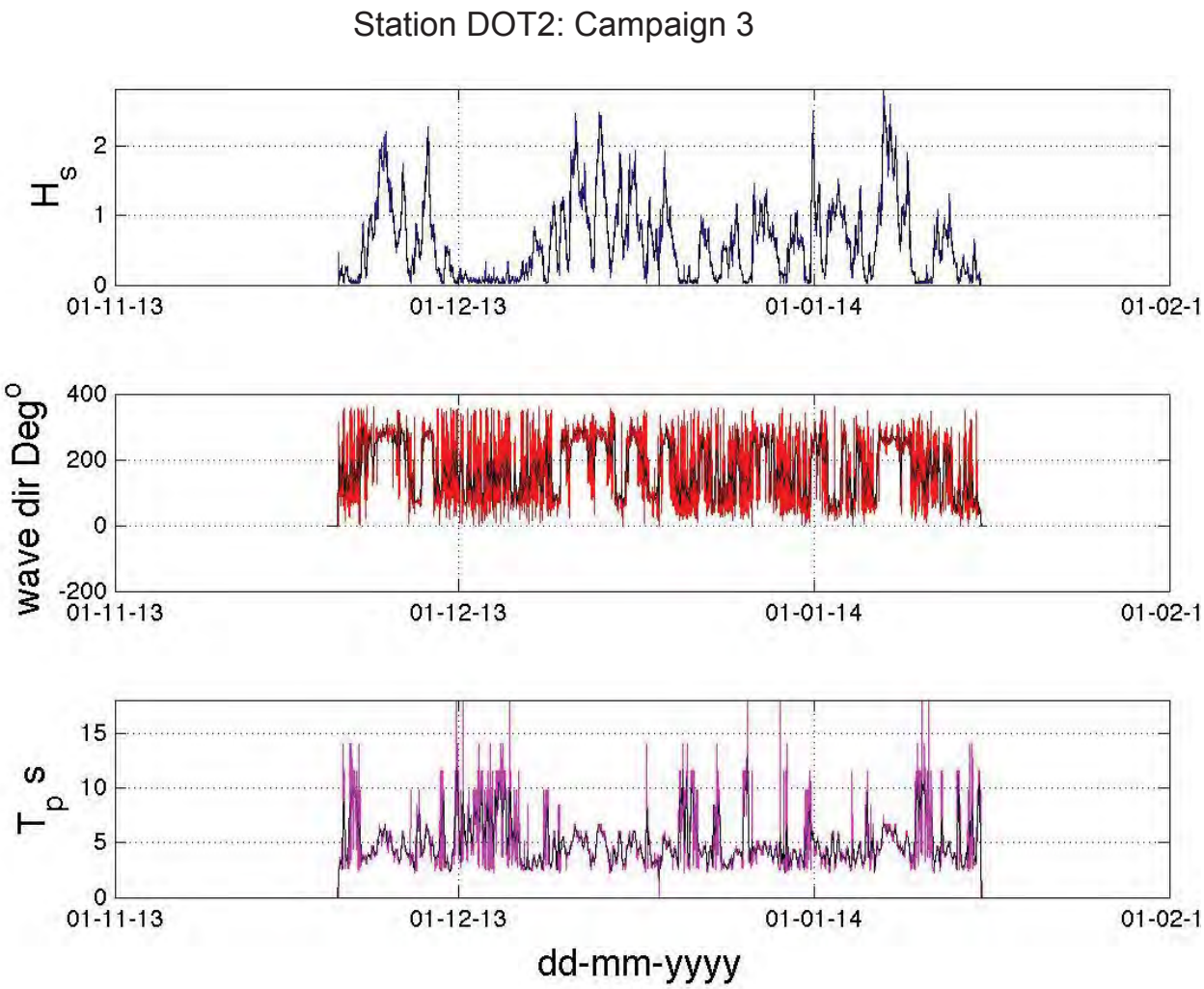

Figure 8-7. Wave conditions at Station DOT2 during Campaign 3: Significant wave height (top), wave direction (oceanographic convention; middle), dominant wave period obtained from the spectral peak frequency (bottom). All graphs contain a 5-day moving average (black lines).

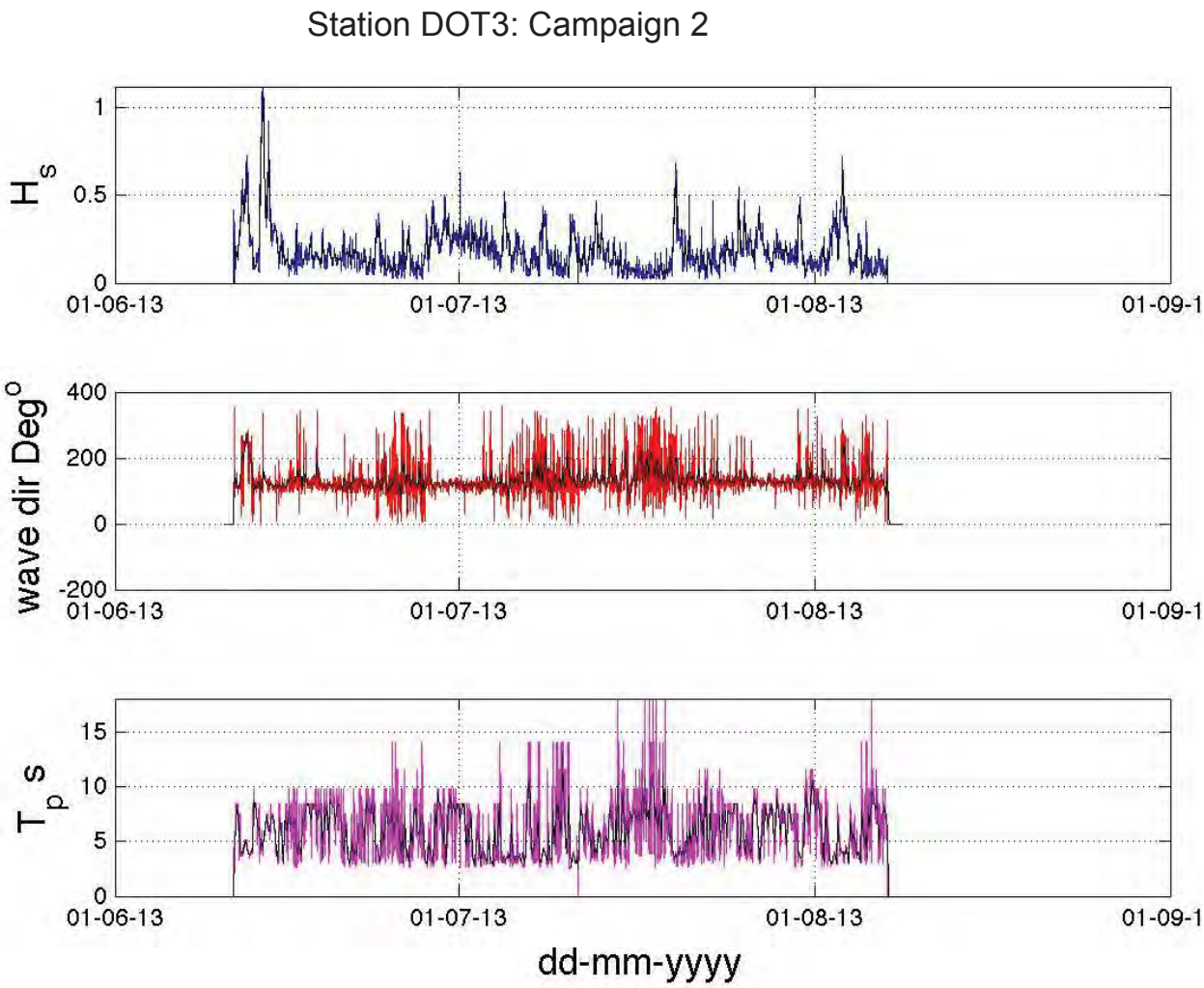

Figure 8-8. Wave conditions at Station DOT3 during Campaign 2: Significant wave height (top), wave direction (oceanographic convention; middle), dominant wave period obtained from the spectral peak frequency (bottom). All graphs contain a 5-day moving average (black lines).

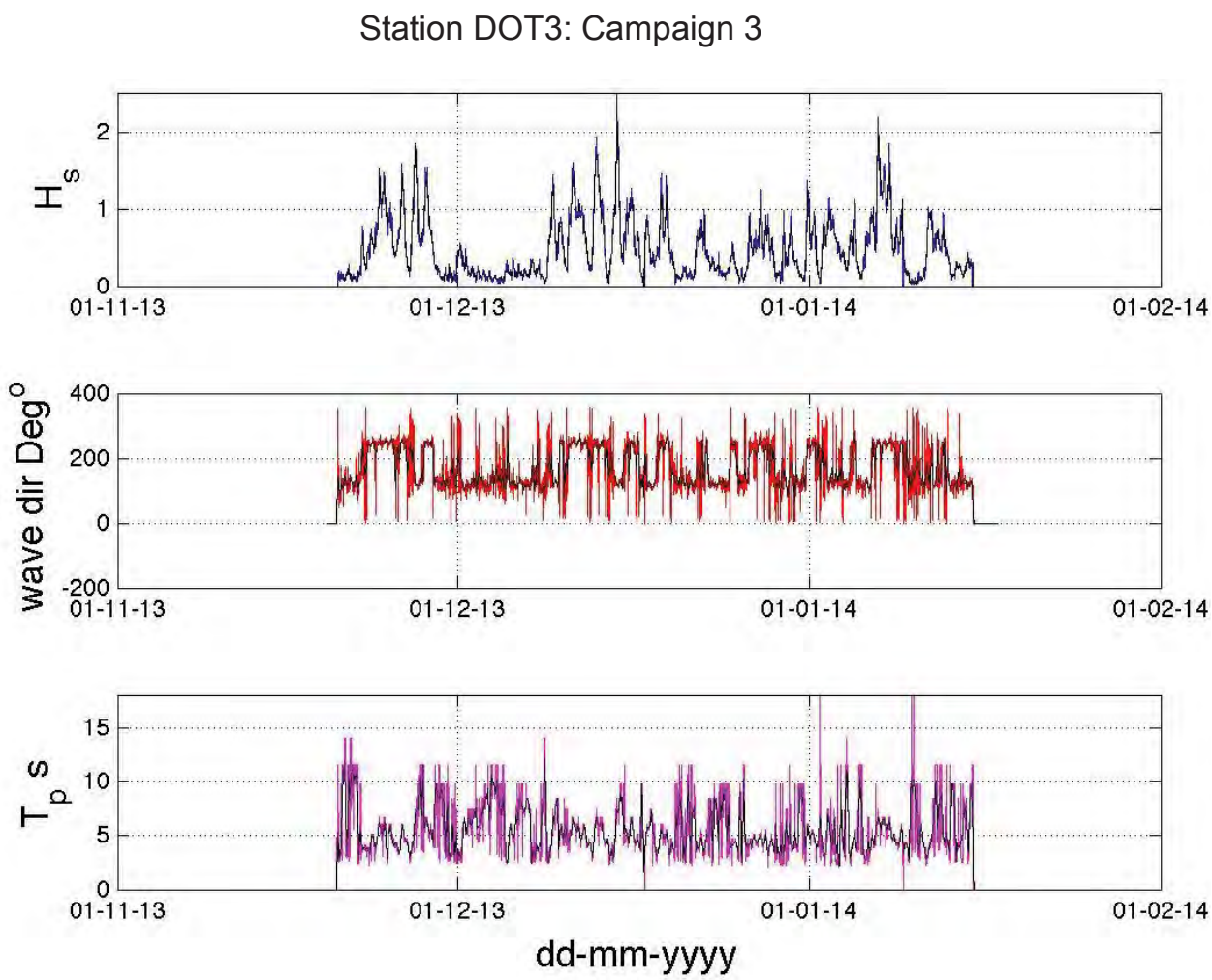

Figure 8-9. Wave conditions at Station DOT3 during Campaign 3: Significant wave height (top), wave direction (oceanographic convention; middle), dominant wave period obtained from the spectral peak frequency (bottom). All graphs contain a 5-day moving average (black lines).

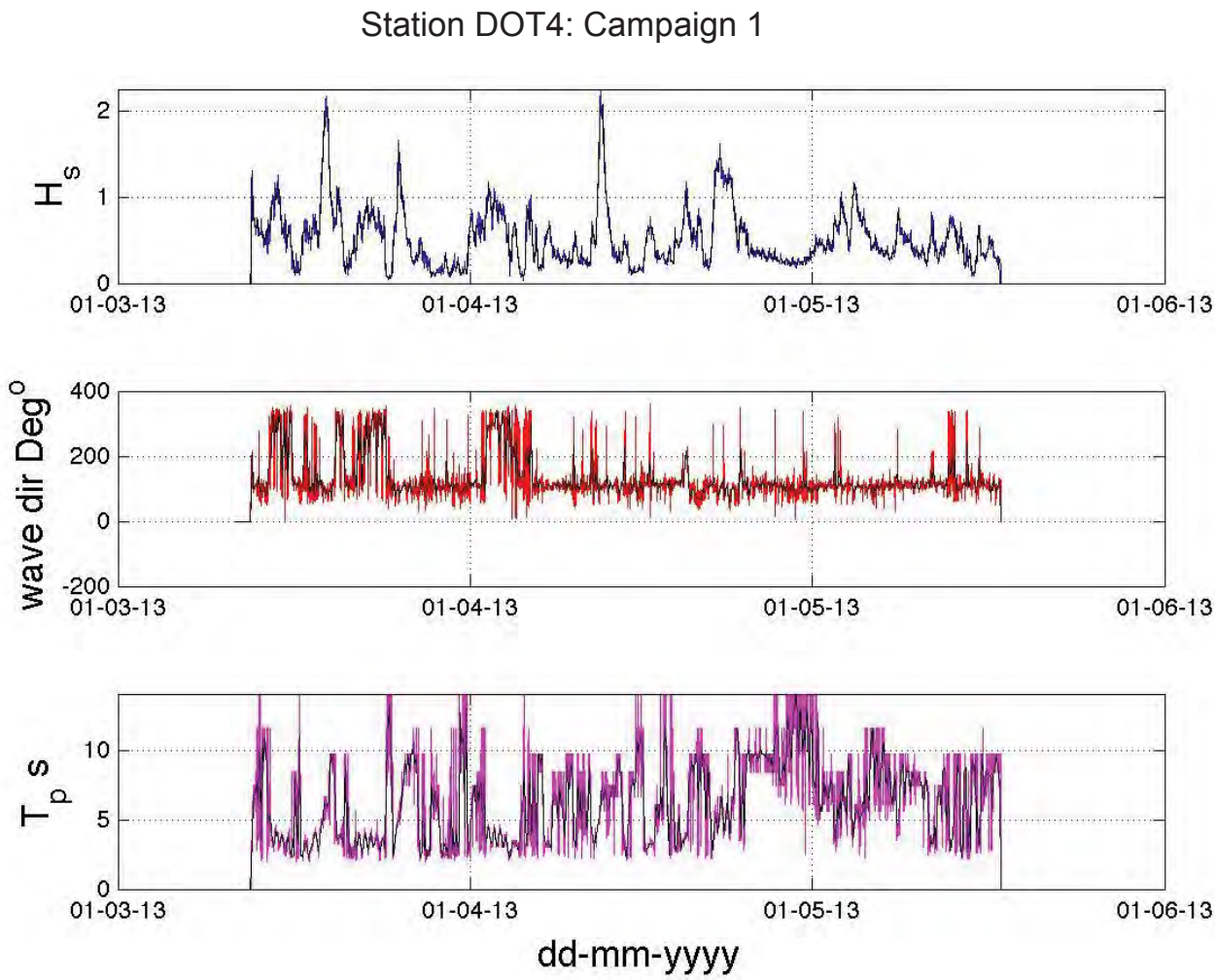

Figure 8-10. Wave conditions at Station DOT4 during Campaign 1: Significant wave height (top), wave direction (oceanographic convention; middle), dominant wave period obtained from the spectral peak frequency (bottom). All graphs contain a 5-day moving average (black lines).

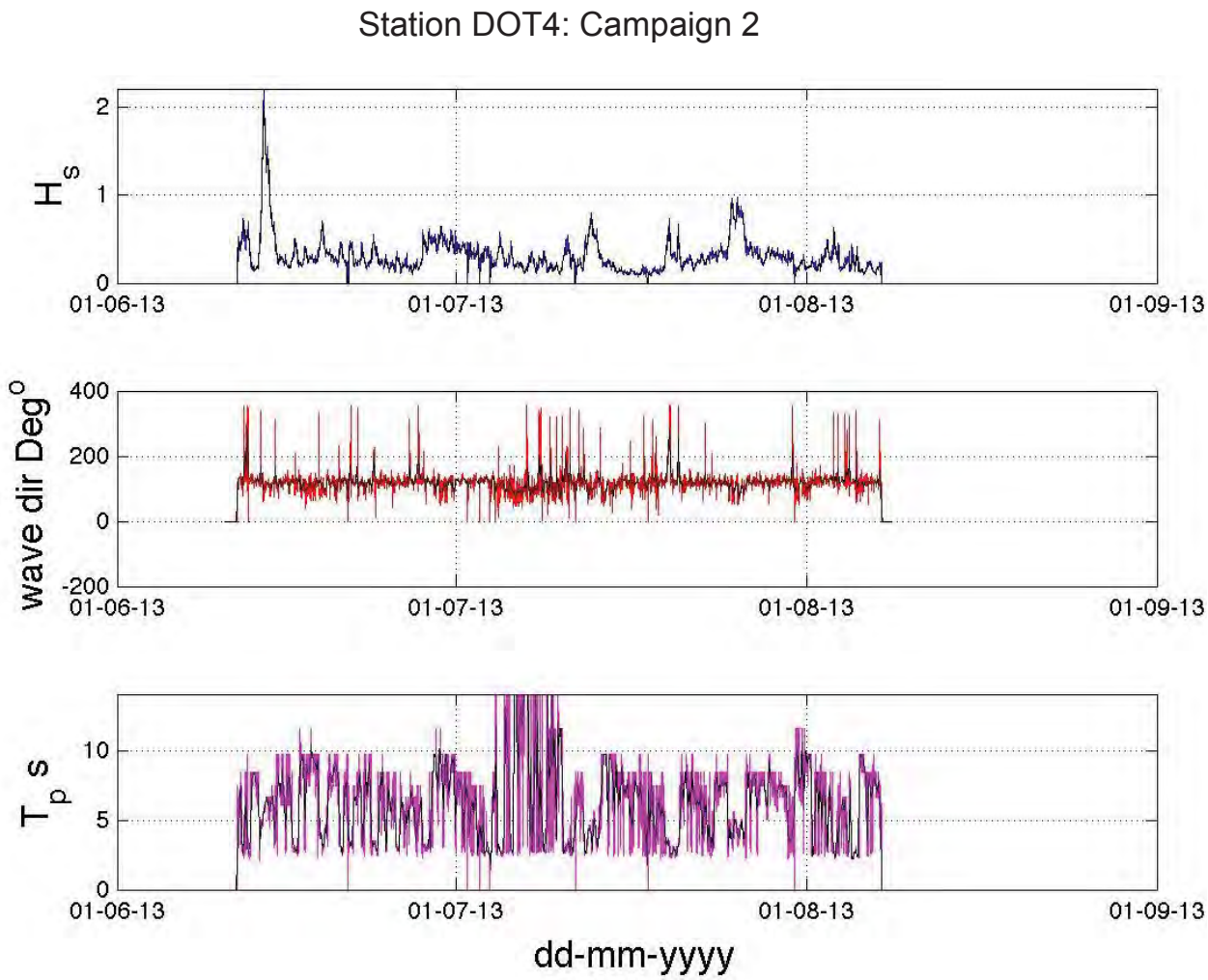

Figure 8-11. Wave conditions at Station DOT4 during Campaign 2: Significant wave height (top), wave direction (oceanographic convention; middle), dominant wave period obtained from the spectral peak frequency (bottom). All graphs contain a 5-day moving average (black lines).

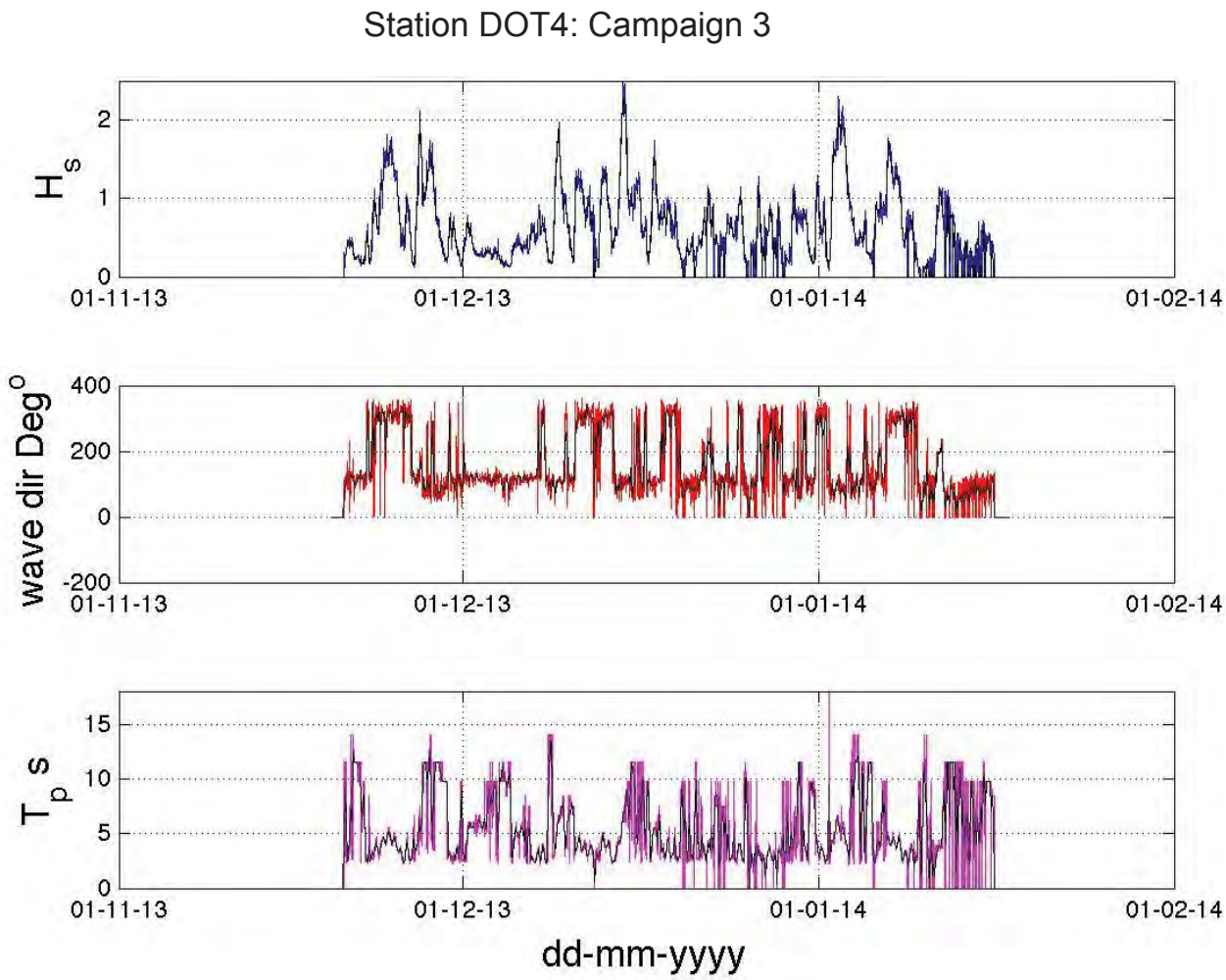

Figure 8-12. Wave conditions at Station DOT4 during Campaign 3: Significant wave height (top), wave direction (oceanographic convention; middle), dominant wave period obtained from the spectral peak frequency (bottom). All graphs contain a 5-day moving average (black lines).

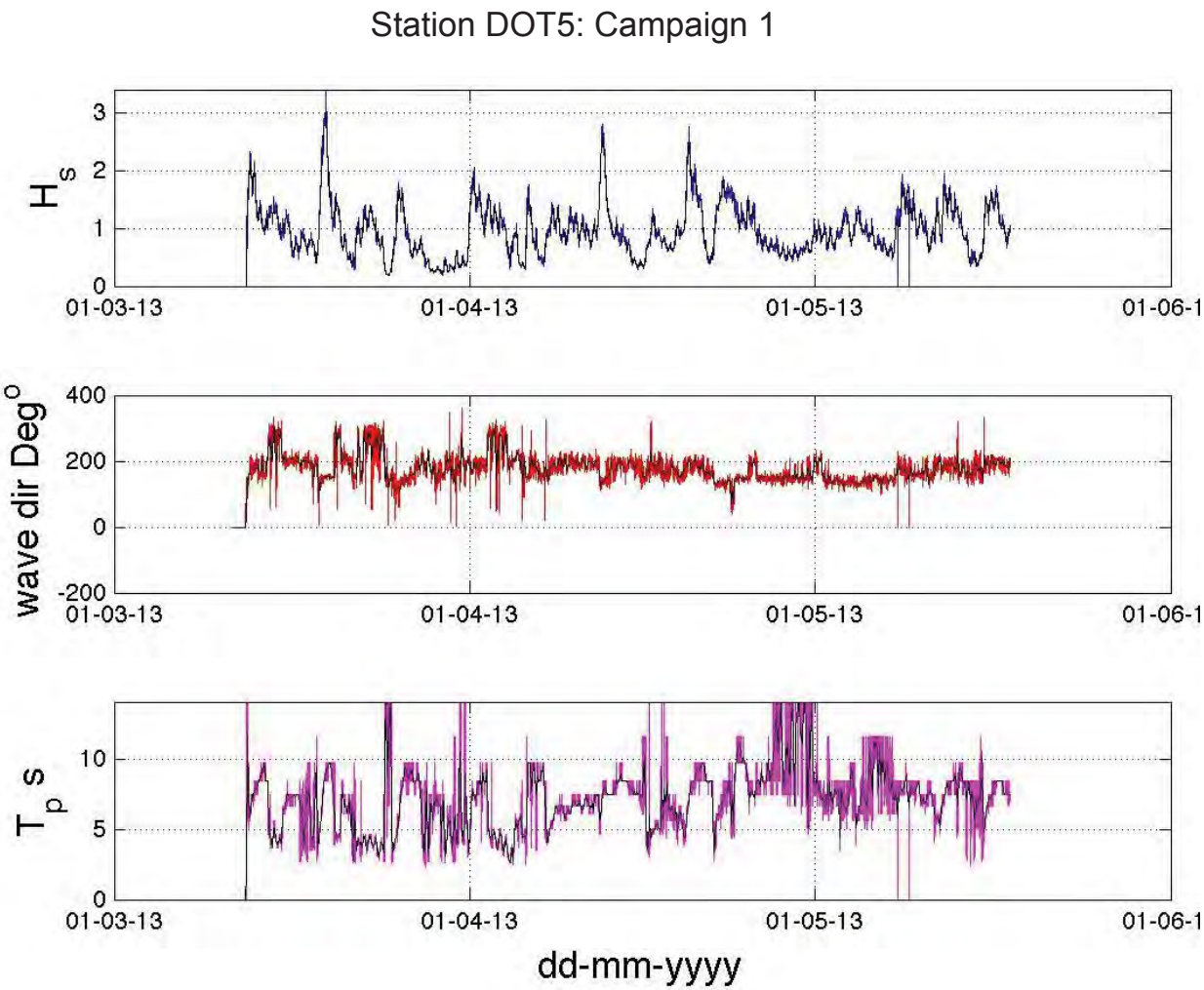

Figure 8-13. Wave conditions at Station DOT5 during Campaign 1: Significant wave height (top), wave direction (oceanographic convention; middle), dominant wave period obtained from the spectral peak frequency (bottom). All graphs contain a 5-day moving average (black lines).

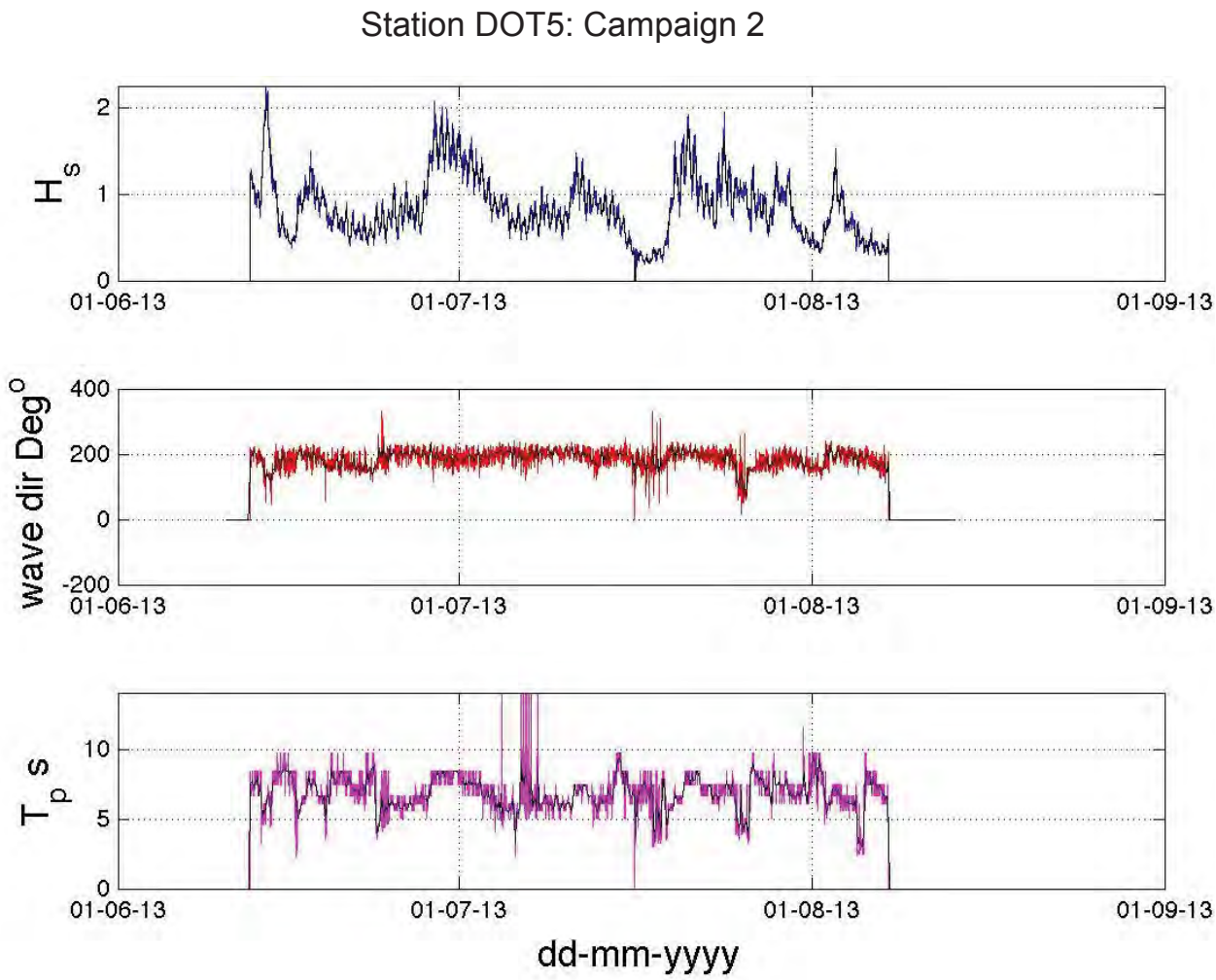

Figure 8-14. Wave conditions at Station DOT5 during Campaign 2: Significant wave height (top), wave direction (oceanographic convention; middle), dominant wave period obtained from the spectral peak frequency (bottom). All graphs contain a 5-day moving average (black lines).

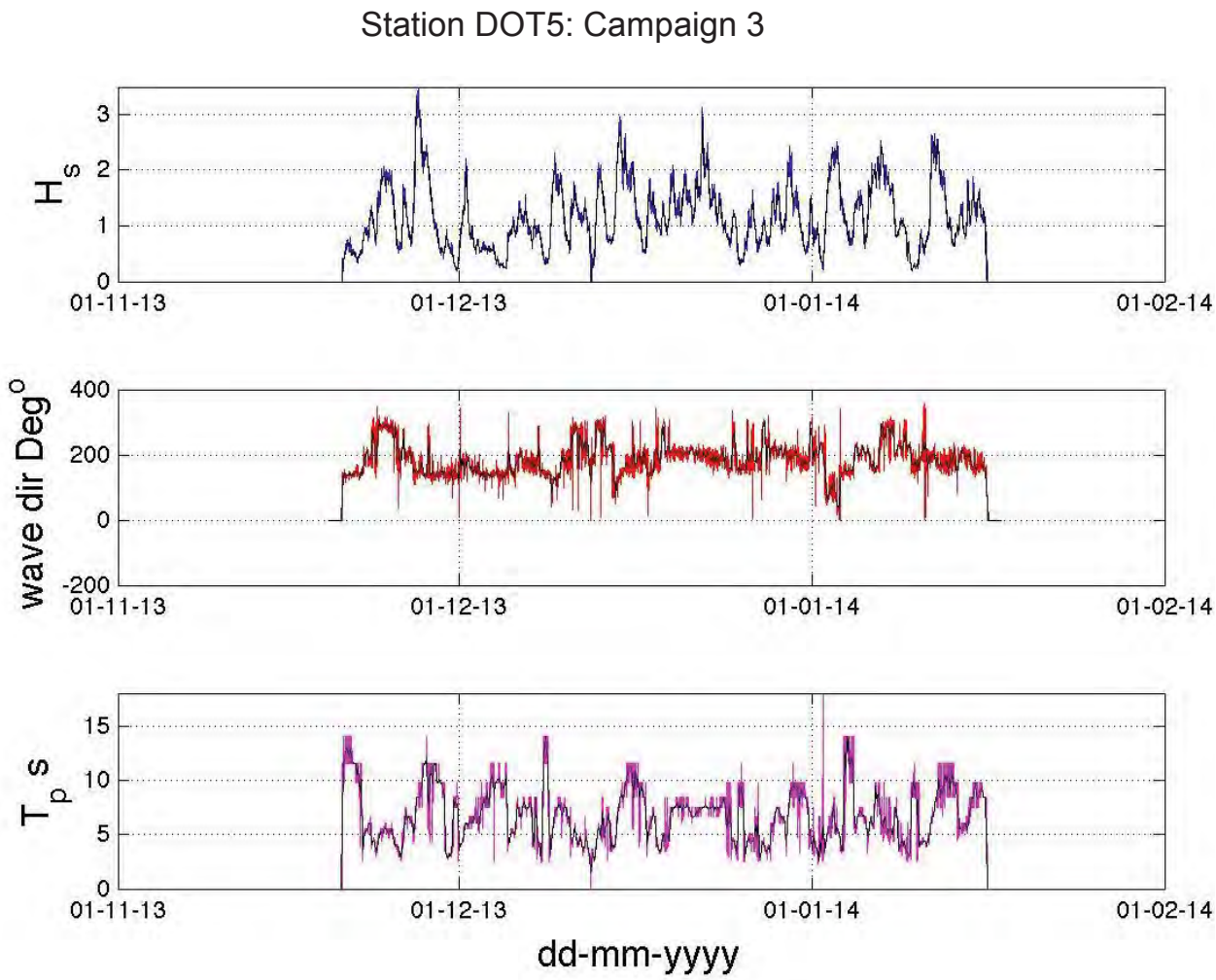

Figure 8-15. Wave conditions at Station DOT5 during Campaign 3: Significant wave height (top), wave direction (oceanographic convention; middle), dominant wave period obtained from the spectral peak frequency (bottom). All graphs contain a 5-day moving average (black lines).

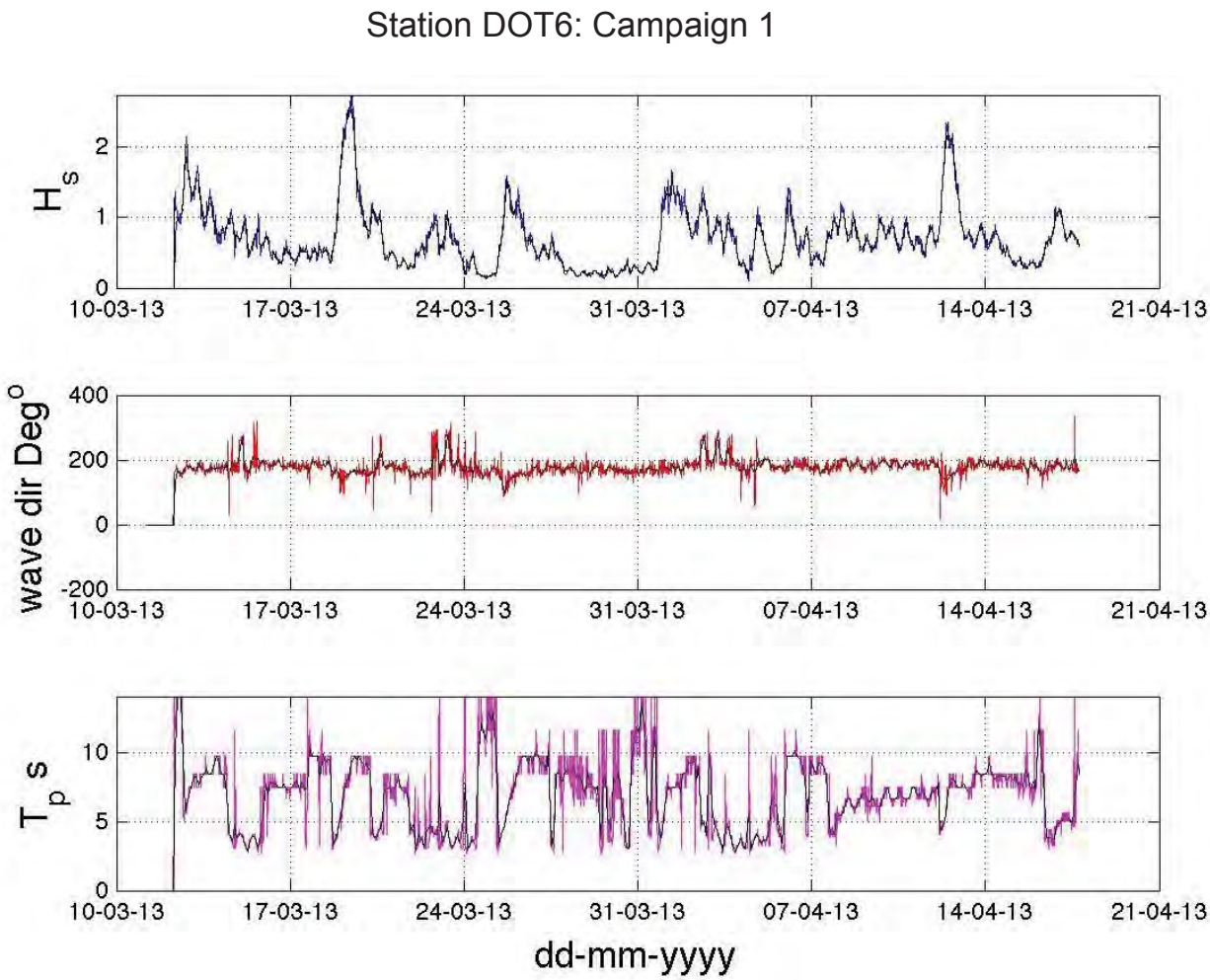

Figure 8-16. Wave conditions at Station DOT6 during Campaign 1: Significant wave height (top), wave direction (oceanographic convention; middle), dominant wave period obtained from the spectral peak frequency (bottom). All graphs contain a 5-day moving average (black lines).

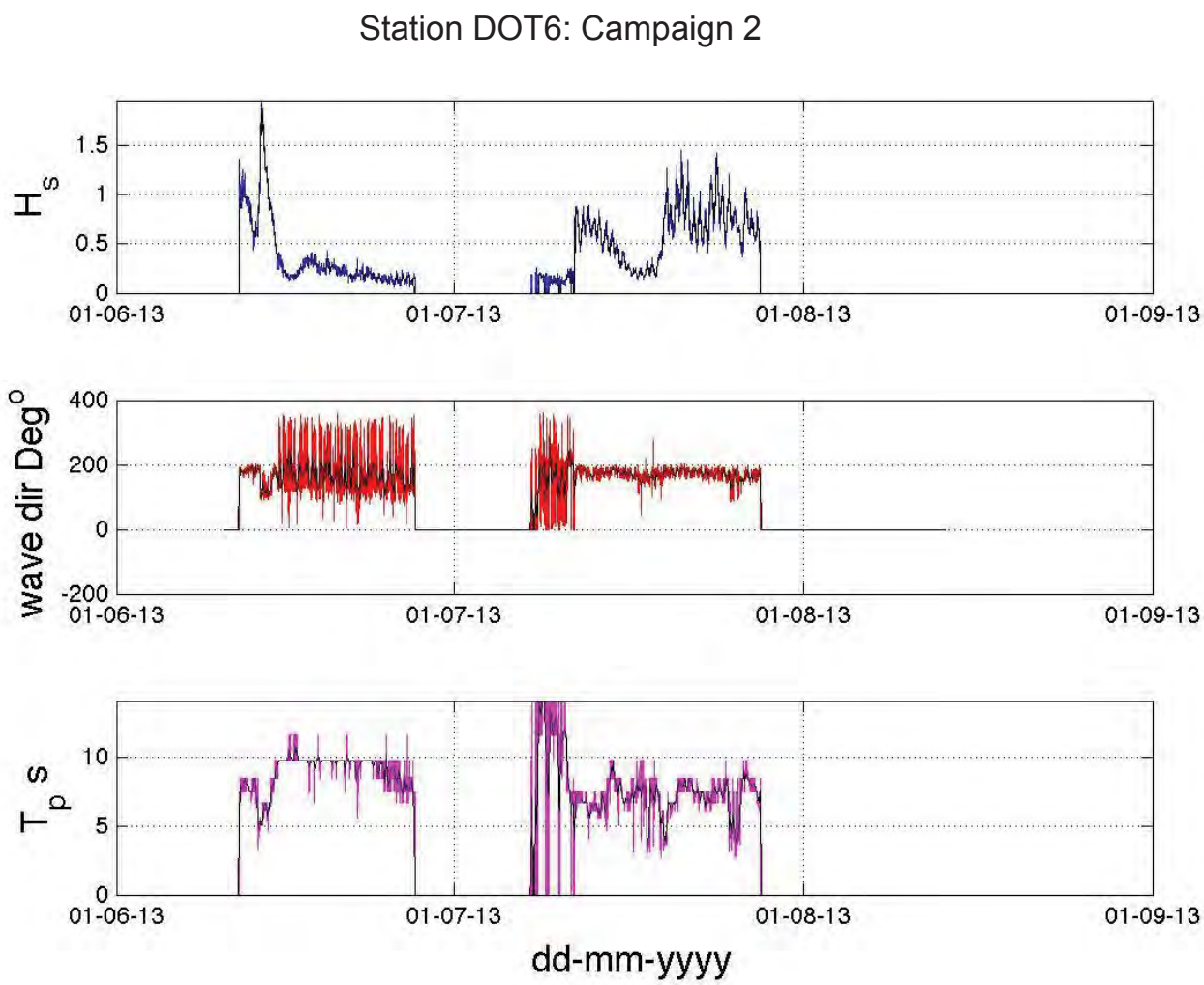

Figure 8-17. Wave conditions at Station DOT6 during Campaign 2: Significant wave height (top), wave direction (oceanographic convention; middle), dominant wave period obtained from the spectral peak frequency (bottom). All graphs contain a 5-day moving average (black lines).

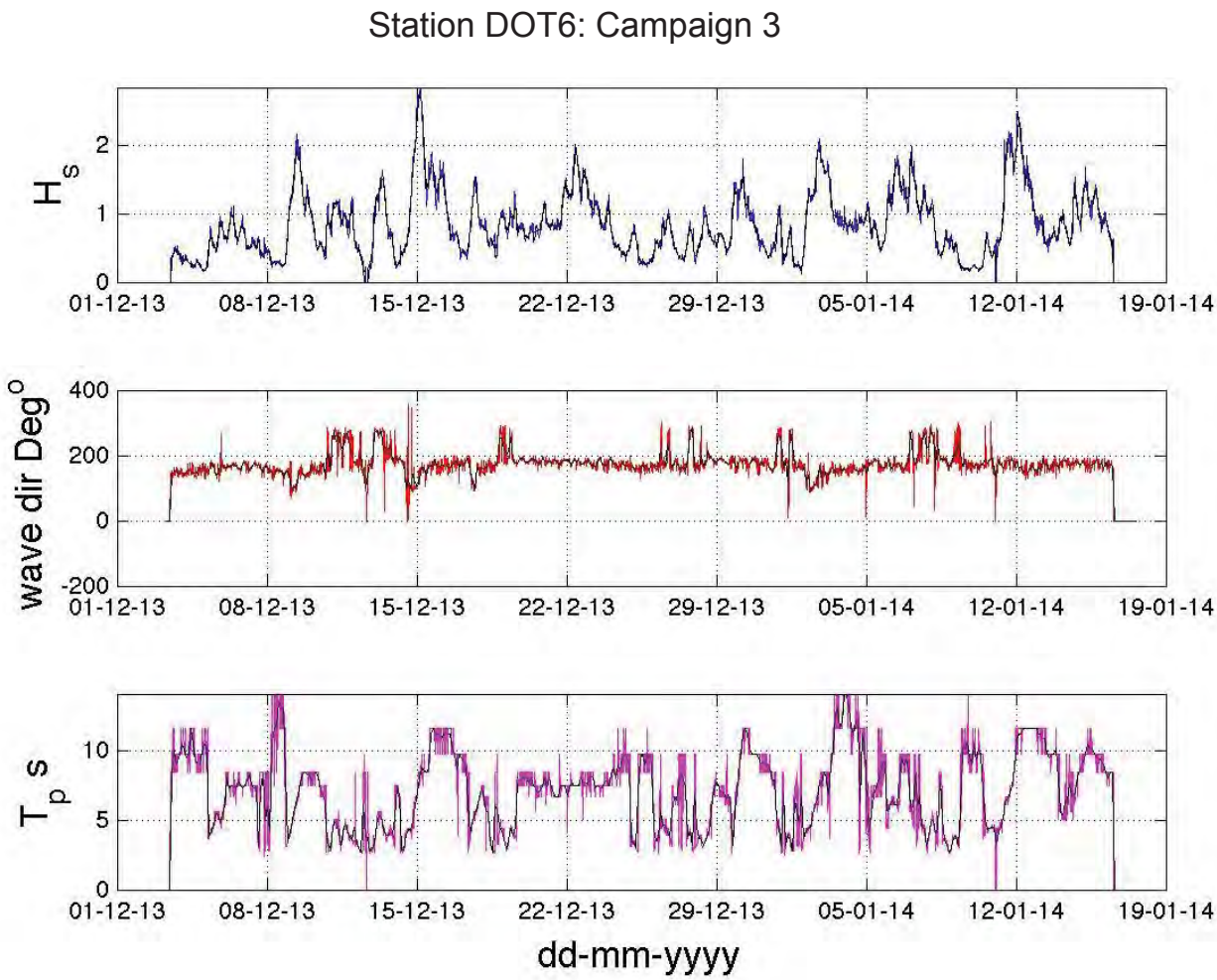

Figure 8-18. Wave conditions at Station DOT6 during Campaign 3: Significant wave height (top), wave direction (oceanographic convention; middle), dominant wave period obtained from the spectral peak frequency (bottom). All graphs contain a 5-day moving average (black lines).

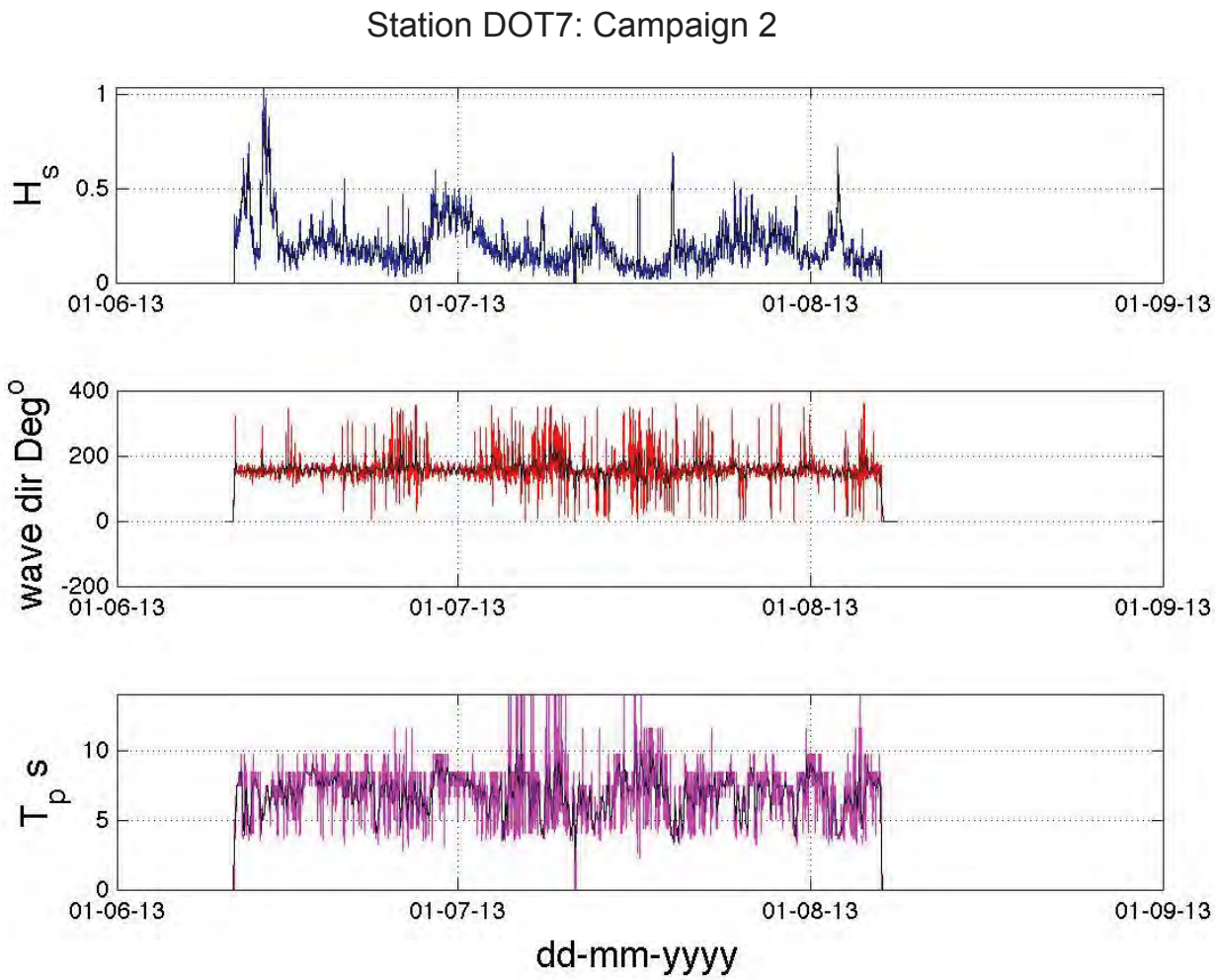

Figure 8-19. Wave conditions at Station DOT7 during Campaign 2: Significant wave height (top), wave direction (oceanographic convention; middle), dominant wave period obtained from the spectral peak frequency (bottom). All graphs contain a 5-day moving average (black lines).

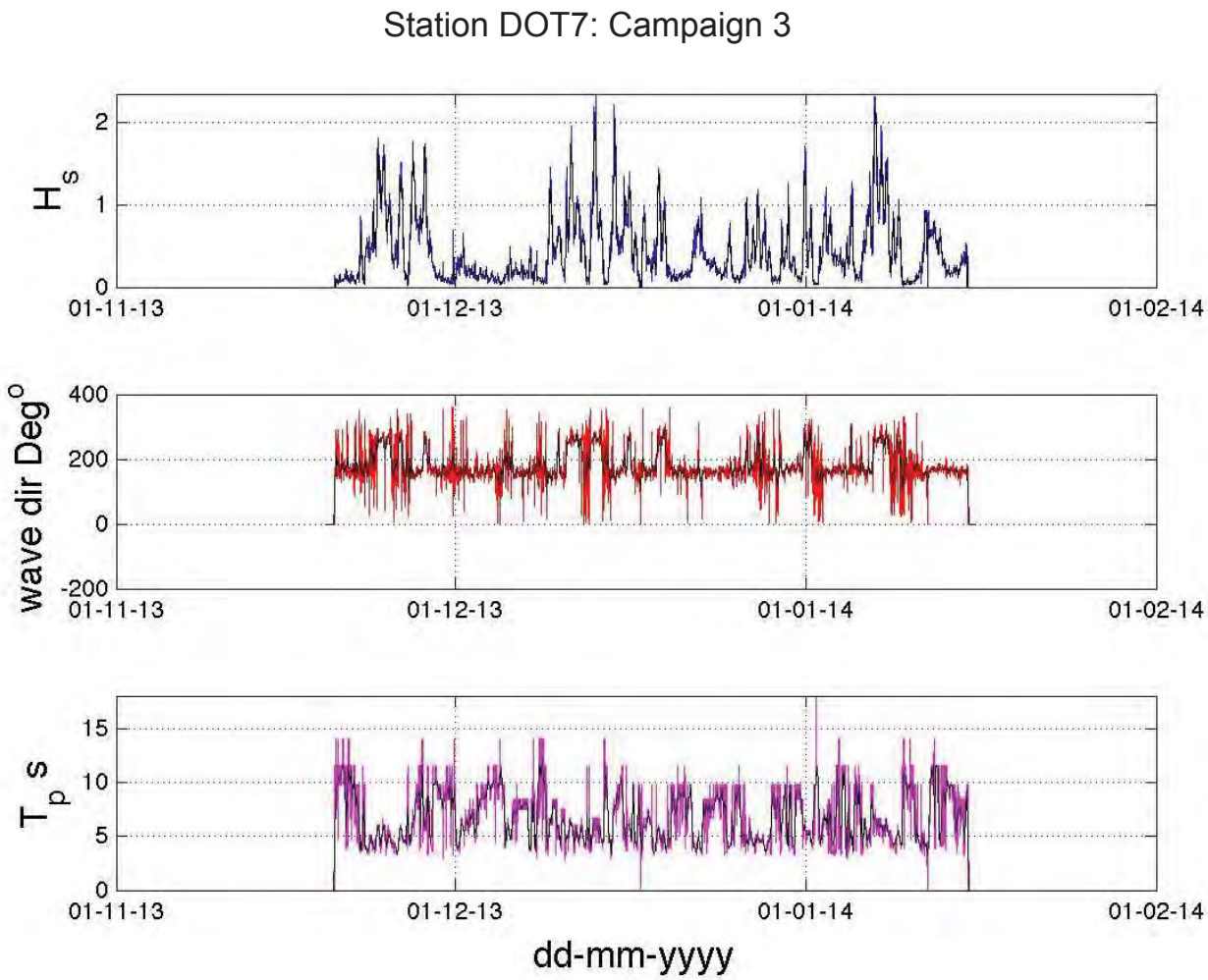

Figure 8-20. Wave conditions at Station DOT7 during Campaign 3: Significant wave height (top), wave direction (oceanographic convention; middle), dominant wave period obtained from the spectral peak frequency (bottom). All graphs contain a 5-day moving average (black lines).

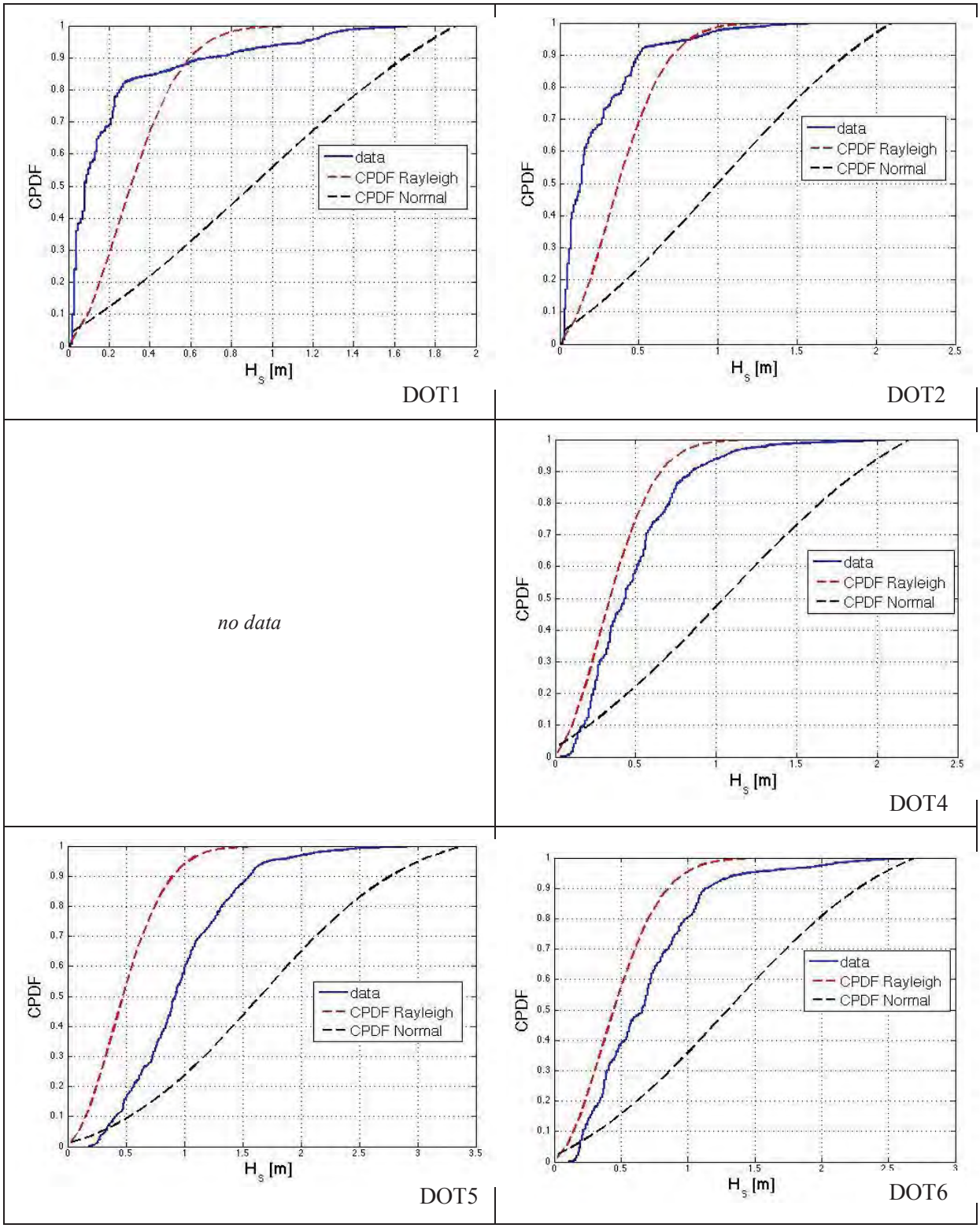

Figure 8-21. Cumulative Probability Distribution Function (CPDF) of significant wave heights during Campaign 1 for each station (blue line). The data are compared to two other CPDF: The Rayleigh probability distribution (red line) and the Normal probability distribution (black line).

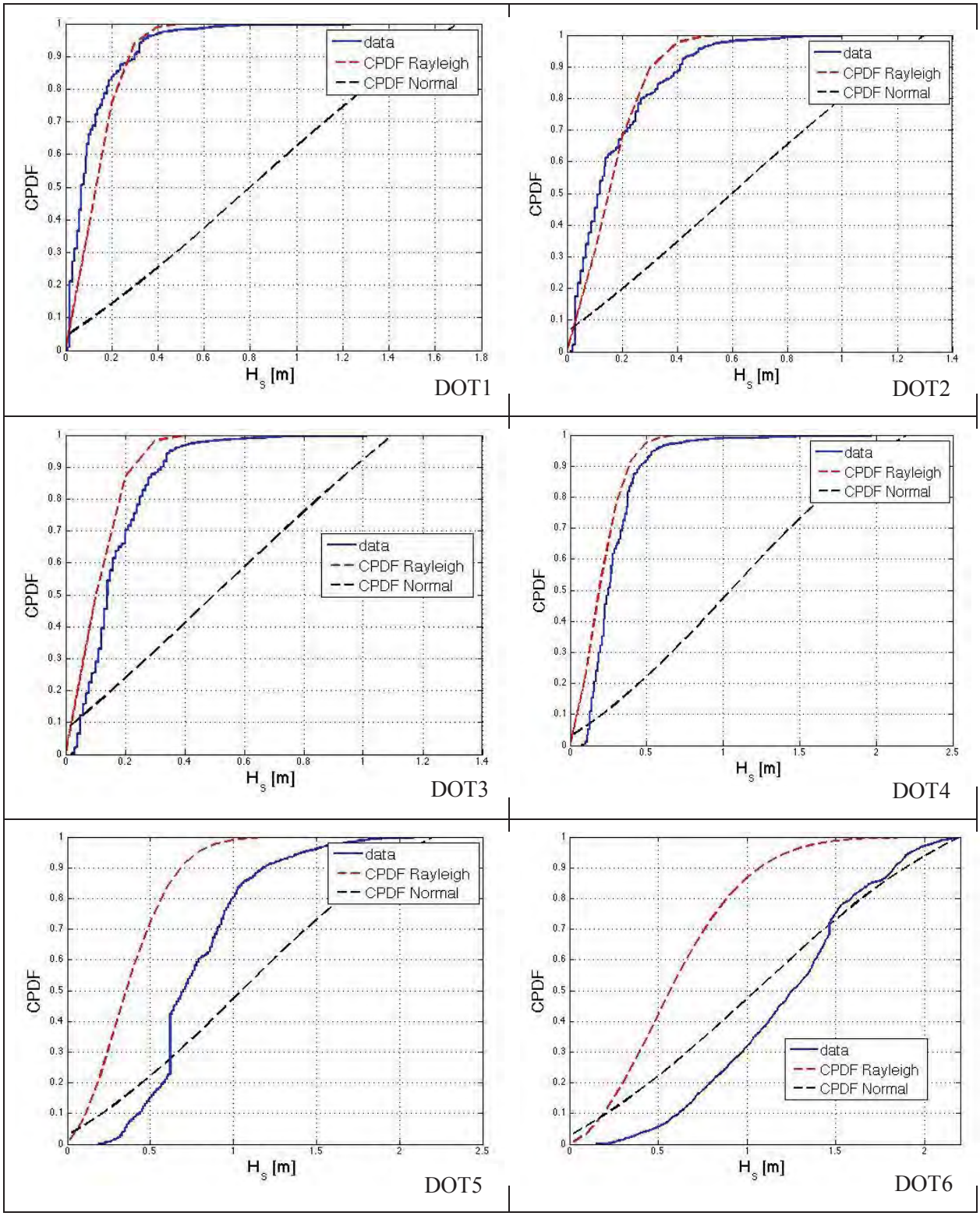

Figure 8-22. Cumulative Probability Distribution Function (CPDF) of significant wave heights during Campaign 2 for each station (blue line). The data are compared to two other CPDF: The Rayleigh probability distribution (red line) and the Normal probability distribution (black line).

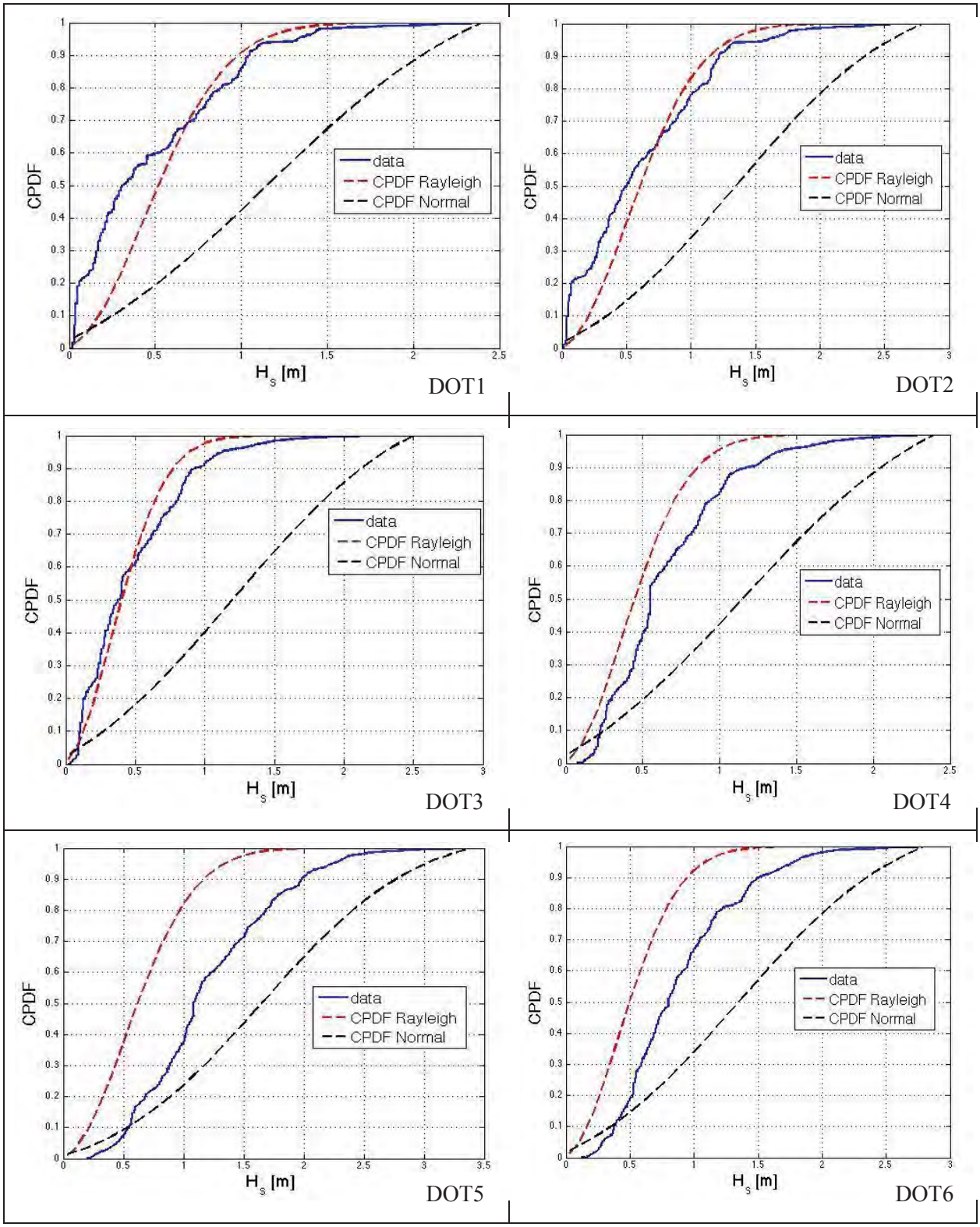

Figure 8-23. Cumulative Probability Distribution Function (CPDF) of significant wave heights during Campaign 3 for each station (blue line). The data are compared to two other CPDF: The Rayleigh probability distribution (red line) and the Normal probability distribution (black line).

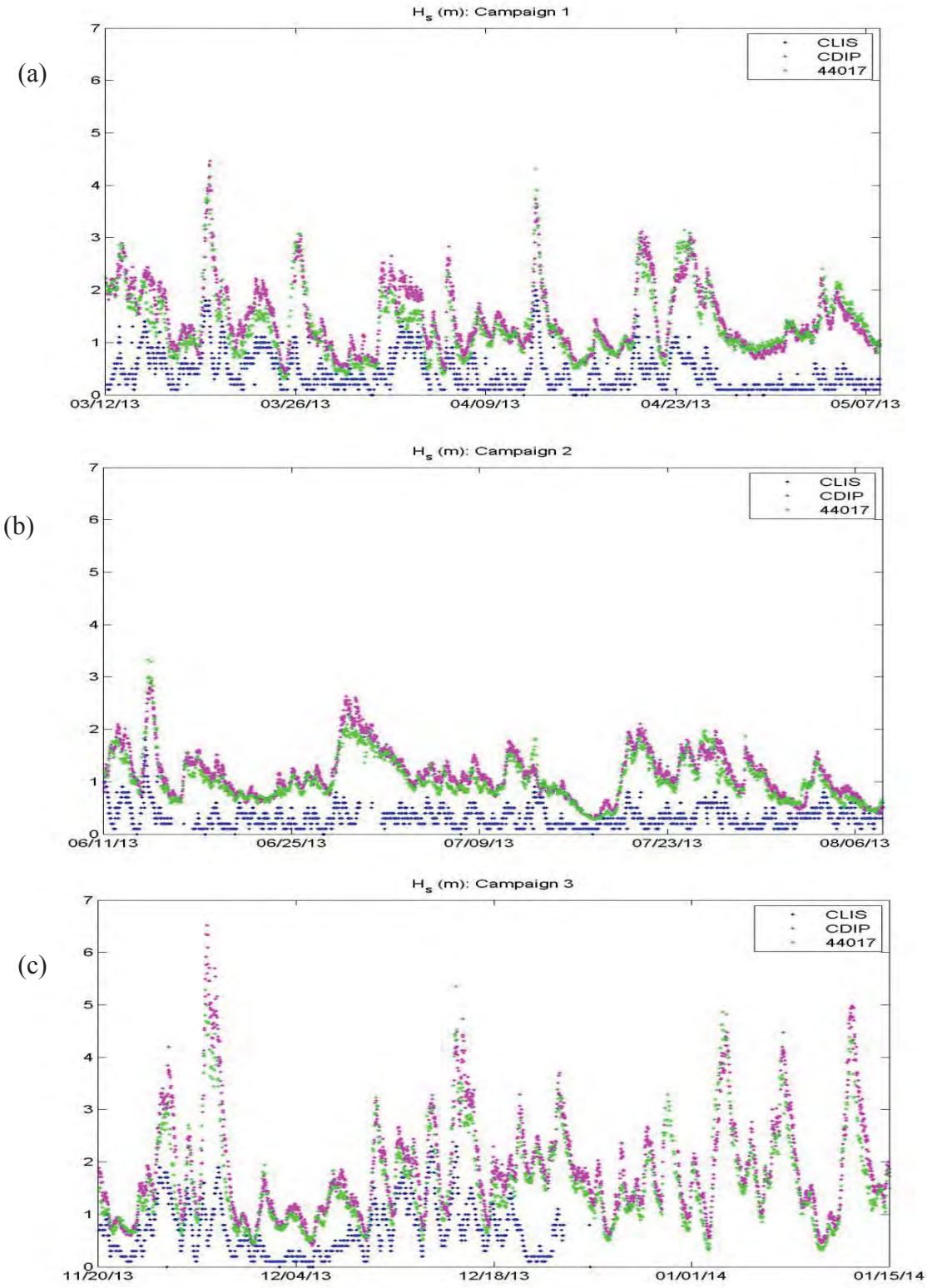

Figure 8-24. Time-series of the observed significant wave height at metocean Stations CLIS (blue), CDIP (magenta), and 44017 (green) during the three campaigns.

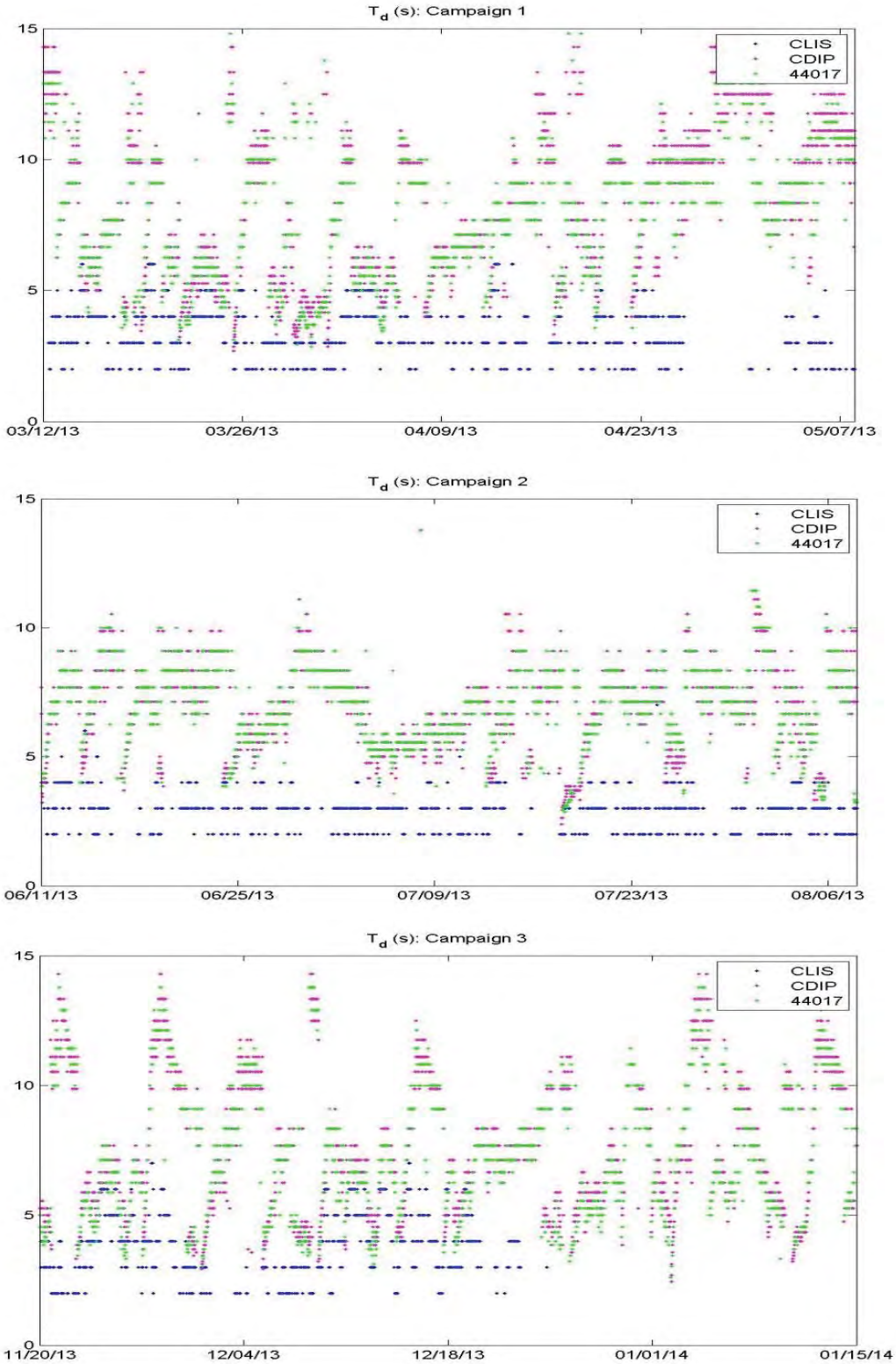

Figure 8-25. Time-series of the observed dominant wave periods at metocean Stations CLIS (blue), CDIP (magenta), and 44017 (green) during the three campaigns.

9. Suspended Sediment in the Water Column (Ship Surveys)

This chapter describes both the suspended sediment and particulate organic carbon concentrations from water samples. Results are to be used for verifying the moored instrument observations as well as the modeled sediment concentrations. Initial analyses of the profiles obtained from the WET Labs optical absorption and backscatter sensors are also compared with the water sample data and presented in this chapter. The profile analyses examined data obtained during Cruises CTDOT3 (June 11-12, 2013), CTDOT5 (August 7-8, 2013), and CTDOT6 (November 20-21, 2013) at the locations of the seven moored stations. Final analyses with all survey data will be presented in a future report.

9.1 Data - Water Samples

Suspended sediment and particulate carbon concentrations (SSC and POC, respectively) from all water samples are presented in Figures 9-1 to 9-3; raw data are presented in Appendix 12. Water samples collected during Campaign 1 (Figure 9-1) were only processed for SSC as the POC analyses instrumentation and protocols were not yet in place. POC are also not available for Cruises CTDOT4 and CTDOT7 as the optical profiling equipment was unavailable.

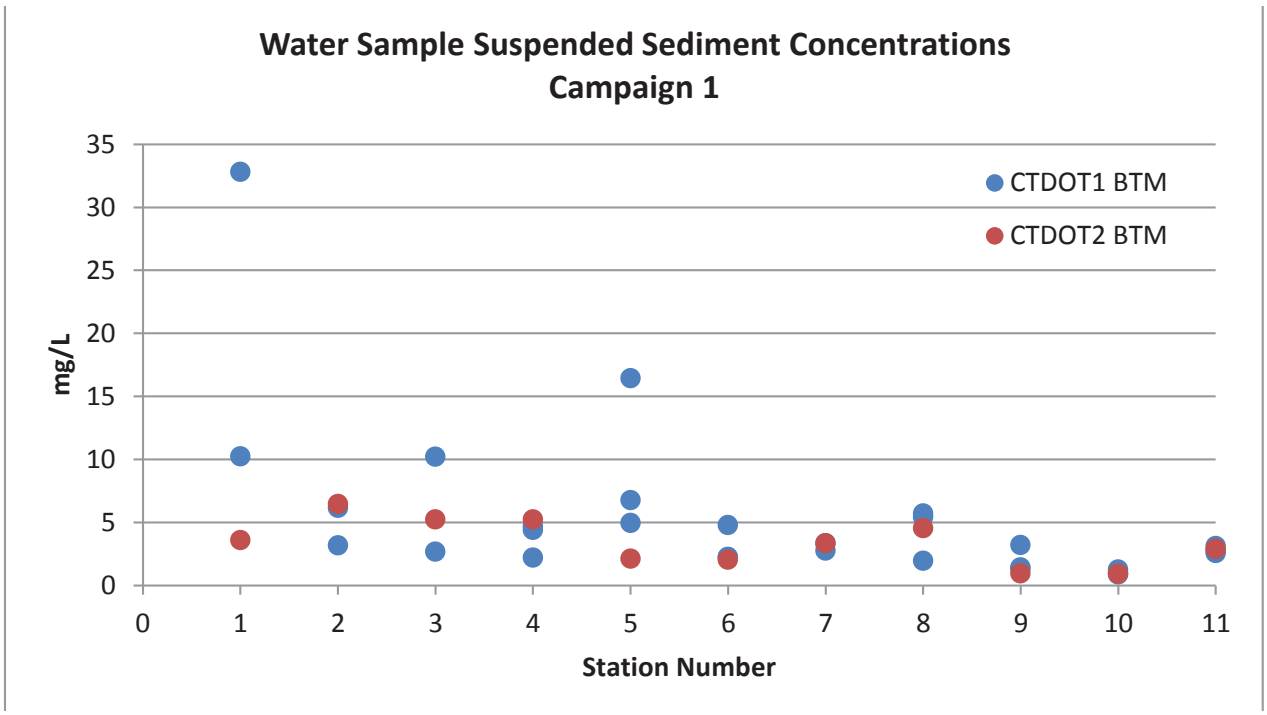

Figure 9-1. Suspended sediment concentration data determined from water samples collected during Campaign 1 at approximately one meter off the bottom (BTM). CTDOT# identifies the cruise number during which samples were collected.

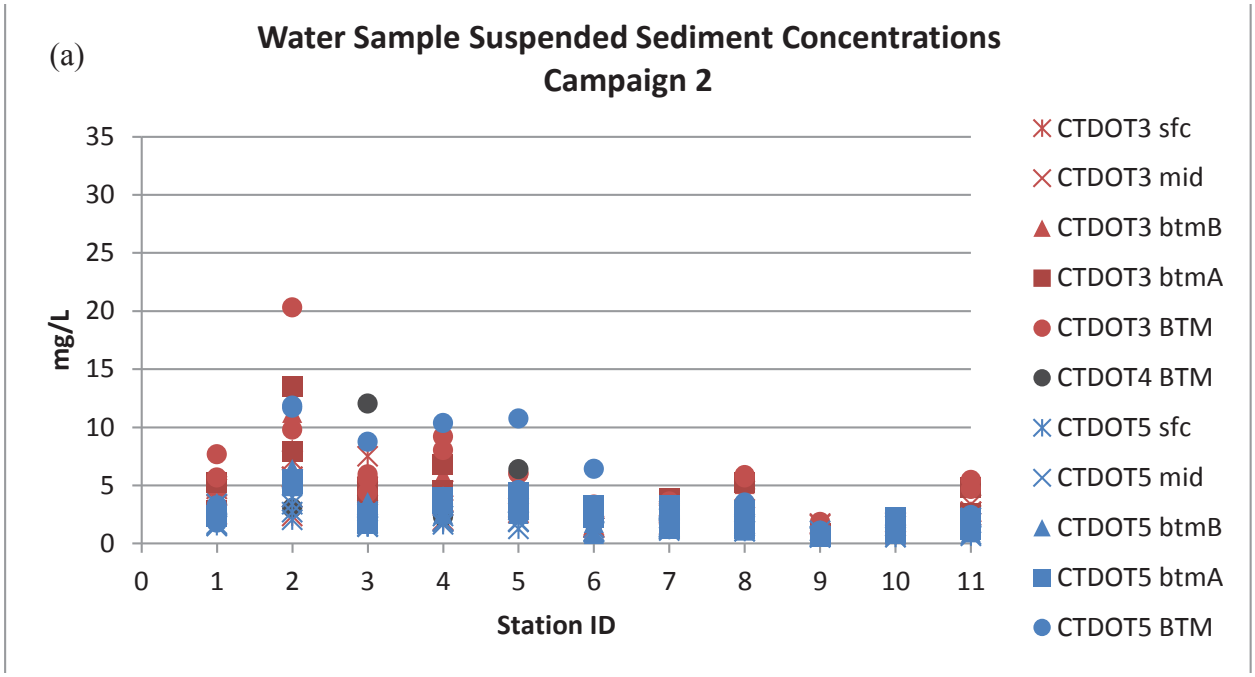

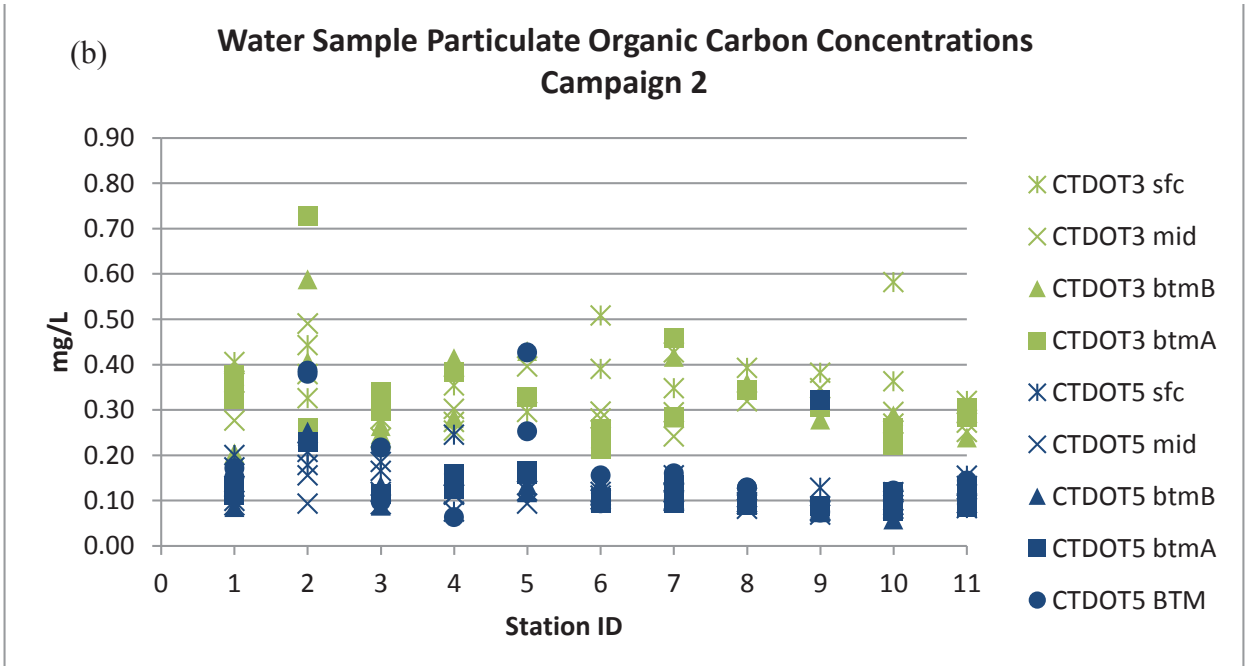

Figure 9-2. (a) Suspended sediment concentrations and (b) particulate organic carbon concentrations determined from water samples collected during Campaign 2. Depths are approximately 1 m off the bottom (BTM), 2 m off the bottom (btmA), 4 m off the bottom (btmB), mid-depth in the water column (mid), and approximately 1.5 m below the water surface (sfc). CTDOT# identifies the cruise number during which samples were collected.

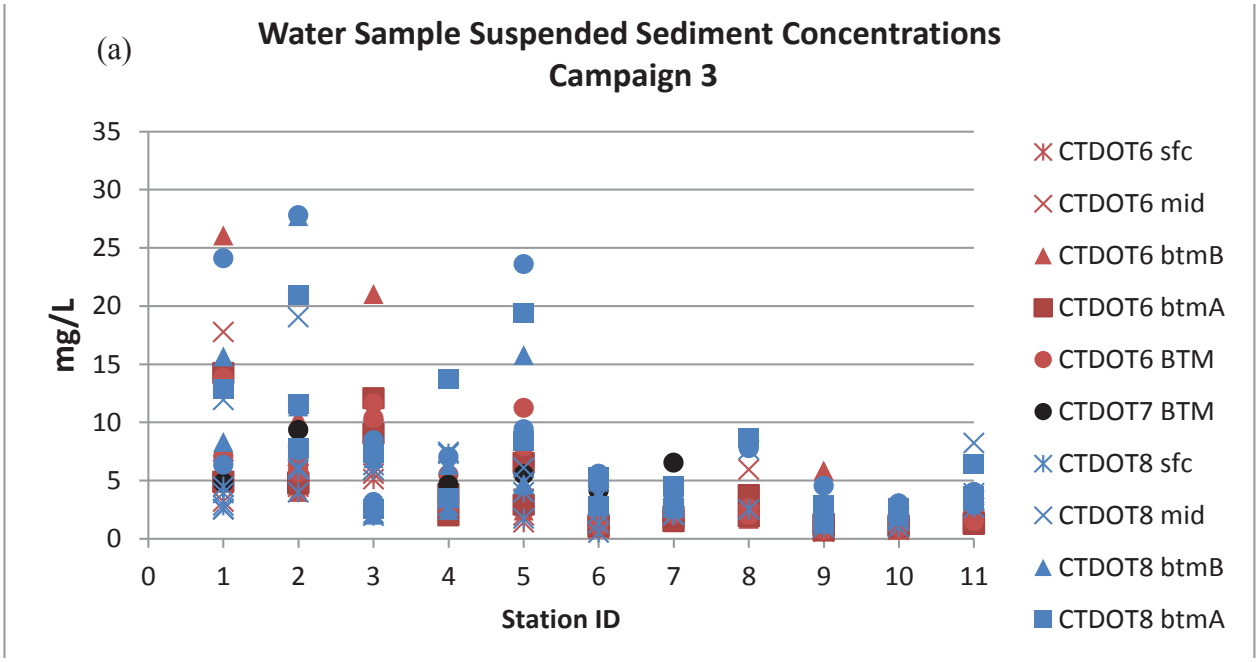

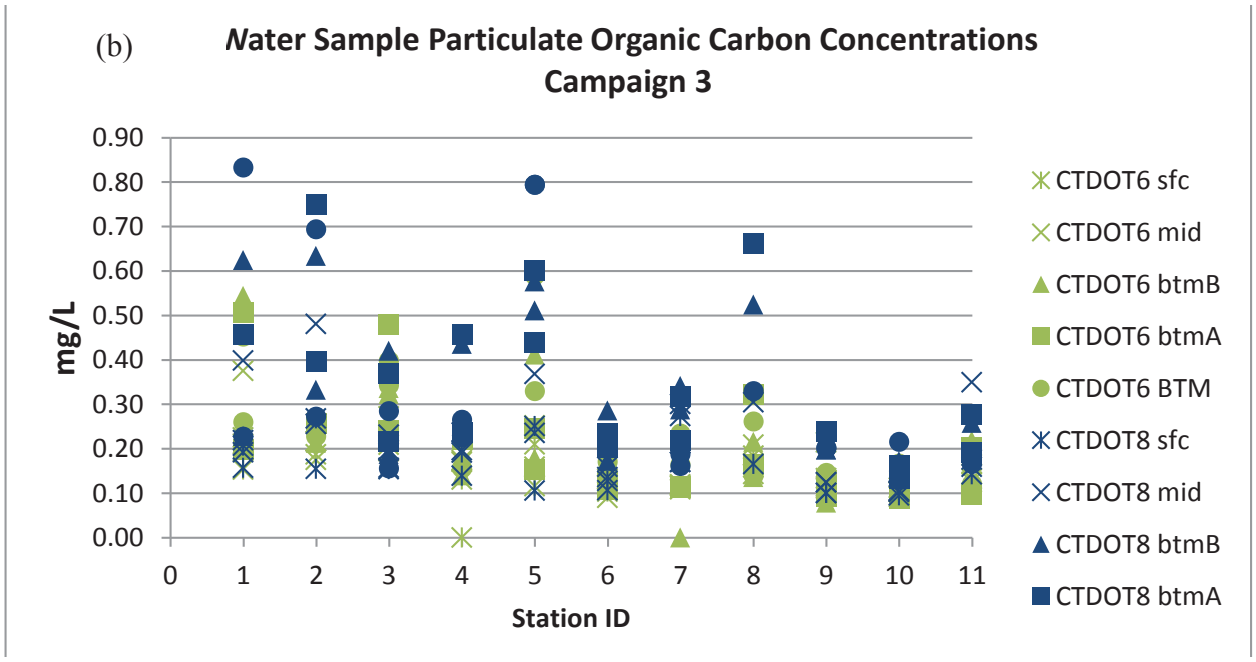

Figure 9-3. (a) Suspended sediment concentrations and (b) particulate organic carbon concentrations determined from water samples collected during Campaign 3. Depths are approximately 1 m off the bottom (BTM), 2 m off the bottom (btmA), 4 m off the bottom (btmB), mid-depth in the water column (mid), and approximately 1.5 m below the water surface (sfc). CTDOT# identifies the cruise number during which samples were collected.

SSC were generally lower than 30 mg/l from all three campaigns for eastern Long Island Sound. The highest concentrations were observed at the westernmost stations (DOT1 and DOT2); the lowest concentrations were observed at the easternmost stations (DOT9 and DOT10).

POC concentrations tended to be higher in June than in August during Campaign 2, and of the same order of magnitude, but more variable during the winter months (Campaign 3).

9.2 Data - Optical Sensors

9.2.1 Calibrations

9.2.1.1 Suspended Sediment Concentrations

Variability in beam attenuation from the optical sensors is primarily the result of changes in SSC and the transformations of the size spectra. While potentially specific to location and time of year, the relationship between the beam attenuation (c) and concentration have been reported many times to be linear (Boss et al., 2009 and citations within). Transformations for the eastern Long Island Sound and Block Island Sound were investigated by comparing the results of the water sample analyses for each cruise with the associated c observations, averaged across each sampling interval.

SSC was found to be highly correlated with c for each cruise, although there were differences in the regression coefficients between cruises. While all wavelengths measured produced similar levels of correlation, we chose 650 nm as the reference wavelength as it is likely to be the least impacted by absorption due to dissolved matter. Results of a least-squared linear regression analysis are:

CTDOT3 (June): $SSC = 3.74 * c_{650} - 2.42, \quad r^2 = 0.85, N = 63$ (1)

CTDOT5 (August): $SSC = 2.91 * c_{650} - 0.90, \quad r^2 = 0.61, N = 75$ (2)

CTDOT6 (November): $SSC = 3.70 * c_{650} - 0.54, \quad r^2 = 0.40, N = 76$ (3)

Cruise CTDOT6 (November) resulted in a large amount of scatter and, thus, lower correlation. However, the pooled data from the first two cruises resulted in the fit shown in Figure 9-4 and the regression relationship

$$SSC = 3.24 * c_{650} - 1.39, r^2 = 0.82, N = 138 \quad (4)$$

The correlation relationship between the SSC and the beam attenuation at 650 nm is excellent and the predictions have a root mean square error of approximately 1 mg/l.

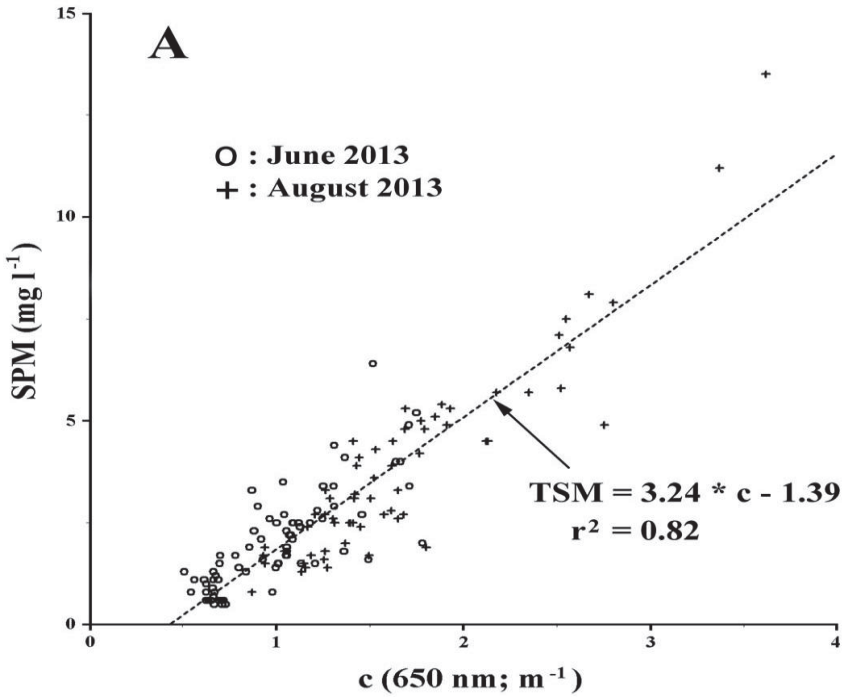

Figure 9-4. Beam attenuation measured at 650 nm plotted against SSC for data collected during the Cruises CTDOT3 (June) and CTDOT5 (August).

9.2.1.2 Particle Size Distribution

Attenuation due to suspended particulate matter tends to decrease toward the red portion of the spectrum and the spectral dependence can be represented as $c_p = A_c\,\lambda^{-\gamma}$, where the constant A_c is related to concentration and the shape of the spectrum is controlled by the exponent γ. Diehl and Haardt (1980) reported that for Mie-like biological particles (i.e., spherical, homogeneous, and having a refractive index close to unity) and a power law particle size distribution (*PSD*), $N(D) = N_0\left(\frac{D}{D_0}\right)^{-\xi}$, where D is the particle diameter and D_0 and N_0 are reference diameter and concentration, $\xi = \gamma + 3$. Changes in the *PSD* resulting from an increase in the proportion of larger (smaller) particles will result in a reduction (increase) in γ. Field observations of $c_p(\lambda)$ and numerical simulations using Mie theory indicate that even for natural populations of particles where the refractive index is significantly greater than that expected for purely biological particles, γ is sensitive to changes in the *PSD* in the way that the simple model predicts (Kitchen et al., 1982; Boss et al., 2001). Thus, changes in γ obtained from in-situ measurements provide at least a qualitative indication of shifts in the size distribution of suspended particle populations (Ackleson, 2006; Ackleson and O'Donnell, 2011).

The computation of γ depends on the measurement of attenuation for suspended particles,

independent from associated optical effects of dissolved matter. This is typically achieved with two WET Labs AC9 instruments performing simultaneous observations; one recording signals from unaltered water (c_{pd}) and the other where all particulate matter has been filtered out (c_d). Thus, differencing the two measurements results in signals specific to only particulate matter; $c_p = c_{pd} - c_d$. However, our observations only included a single instrument observing unfiltered water and the resulting signals are expected to include both particles and dissolved matter.

To adjust for this, we first computed total light scatter ($b = c - a$). Since the absorbing fraction is only weekly scattering, the resulting signal primarily represents particles. Furthermore, since the underlying theory of how γ relates to *PSD* only applies to non-absorbing or, at most, weakly absorbing particles, applying this adjustment to wavelengths outside of primary absorption bands to avoid anomalous light scatter should result in $b \cong c_p$. With these assumptions, we computed an adjusted spectral slope, γ_b, as:

$$\gamma_b = -\log[\frac{b_{532}}{b_{650}}]/\log[\frac{532}{650}] \qquad (5)$$

As with γ, γ_b is expected to be proportional to ξ (Figure 9-5) and inversely proportional to average particle size.

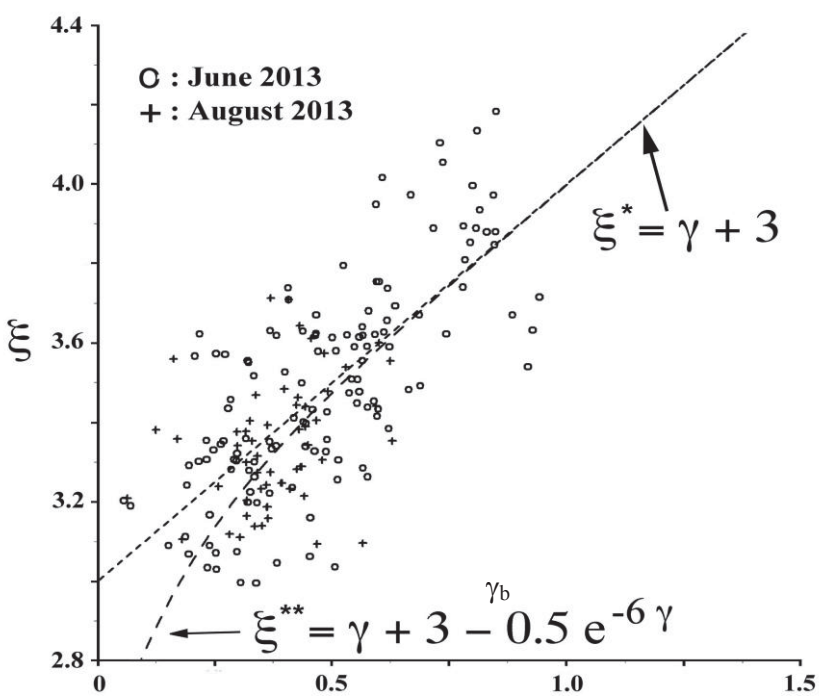

Figure 9-5. The slope of total particle light scatter, ξ_b, measured between 532 nm and 650 nm, is linearly correlated with the slope of the particle size distribution, γ (symbols) and comports well with theory reported for weakly absorbing particles by Diehl and Haardt (1980; dotted line) for spherical particles and Boss et al. (2001; dashed curve) for oblate spheroids.

9.2.1.3 Chlorophyll Absorption

Chlorophyll absorption[17] at 676 nm was estimated using the absorption line height method (Roesler and Barnard, 2013). This method assumes a non-pigment linear change across the narrow chlorophyll absorption region centered at 676 nm. Thus, absorption measured on either side of the chlorophyll absorption region, e.g., 650 nm and 715 nm, can be used to compute the non-pigment absorption baseline at 676 nm, a_{BL}. The difference between the measured absorption and the computed baseline absorption is an estimate of the chlorophyll absorption, a_{CHL}:

$$a_{CHL}(676) = a_m - \frac{a(715)-a(650)}{715-650} * (676-650) + a(650) \quad (6)$$

9.2.2 Suspended Sediment Concentrations

The correlation between the beam attenuation at 650 nm and the SSC measured in water samples allows the SSC profile to the estimated by the optical instruments at much higher resolution than can be accomplished otherwise. Figures 9-6 to 9-12 show the distribution of the SSC estimated in this way for all stations for all surveys. When two profiles are available both are shown. The concentrations are highly variable. At Station DOT1, for example, two profiles obtained within 24 hours differed by 3 to 5 mg/l at all depths. Largest values of 10 mg/l were observed near the bottom at ELIS Stations DOT1 and DOT2. The lowest values (1 mg/l) were observed at Station DOT6 in the summer.

The variability in particle size distributions can partially be explained by the organic content and chlorophyll-a measurements. These are also provided in Figures 9-6 to 9-12. The larger particles are more prevalent in near-bottom samples and in the summer there are high concentrations of organic-rich particles near the surface of the water column.

9.3 Summary

Sufficient water sample data are available for model verification. The suspended sediment data used with optical attenuation, backscatter, and chlorophyll profiles, will aid in the differentiation of the water column particle size classes. Preliminary analyses demonstrate that the larger particles are more prevalent in near-bottom samples and in the summer there are high concentrations of organic-rich particles near the surface of the water column.

[17] The units for chlorophyll absorption, which scales with chlorophyll, are m^{-1}.

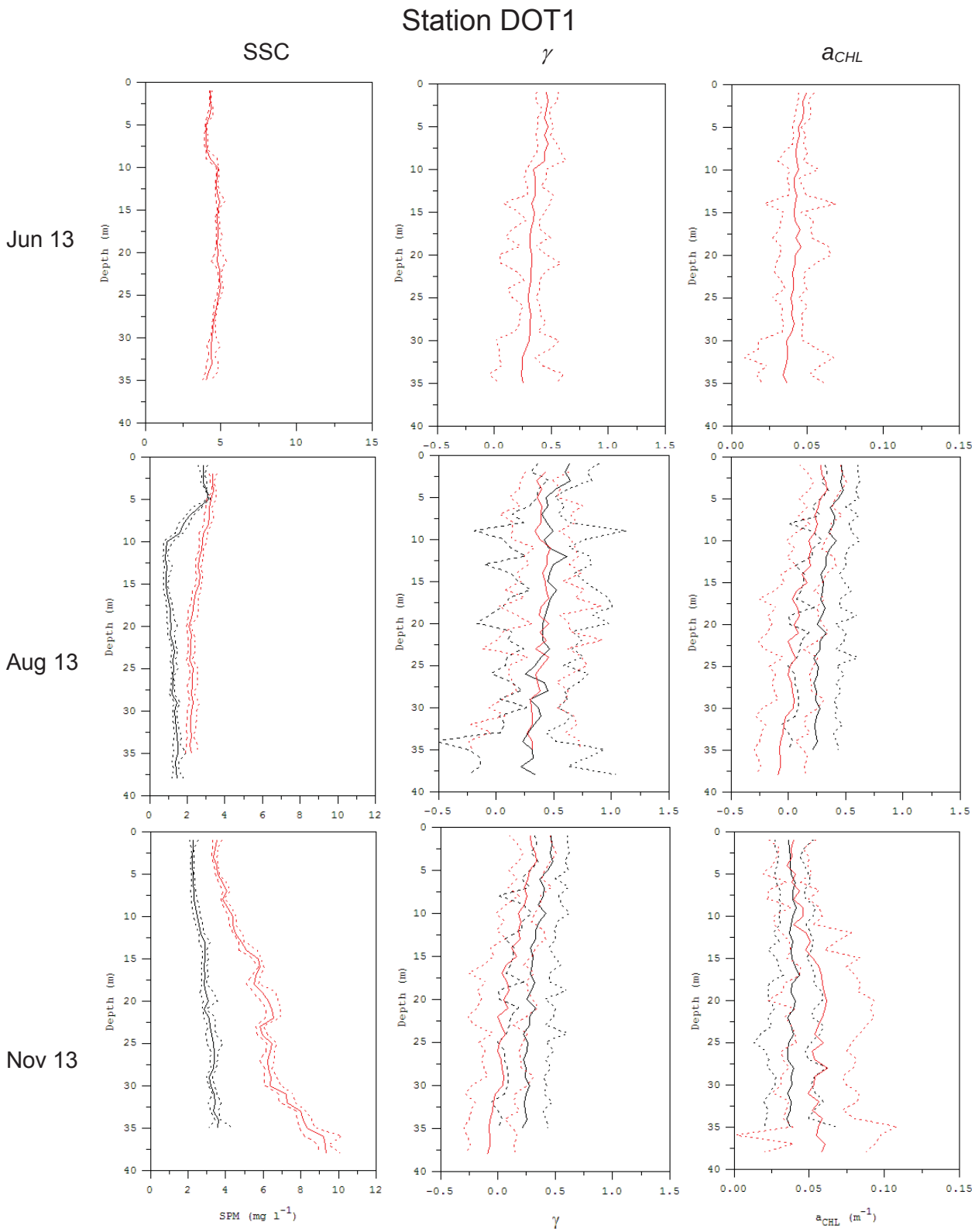

Figure 9-6. Suspended sediment concentrations (SSC) (left), slope of particle size spectrum (center) and chlorophyll-a concentration (right) during Cruises CTDOT1 (top), 2 (middle) and 3 (bottom) at Station DOT1.

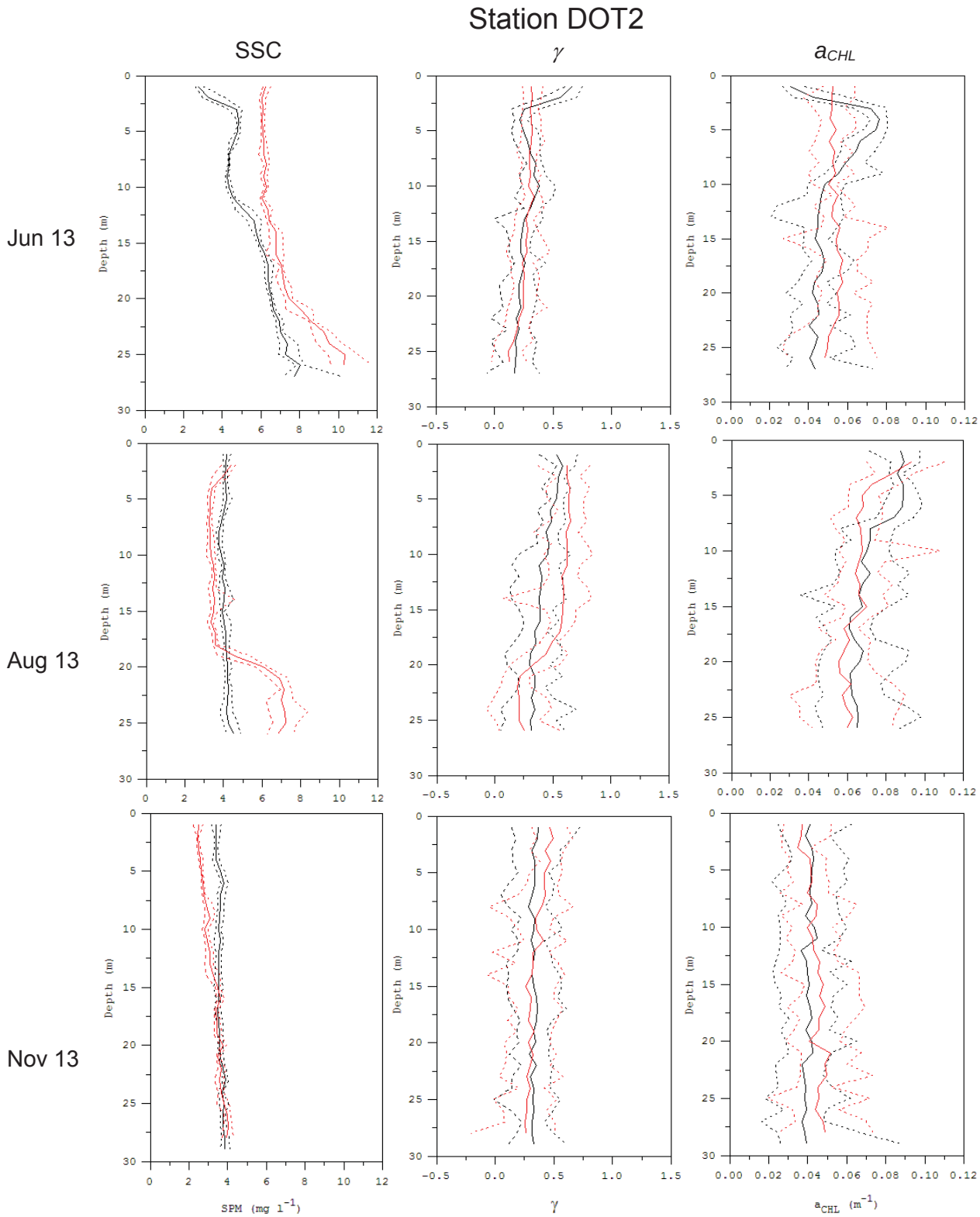

Figure 9-7. Suspended sediment concentrations (SSC) (left), slope of particle size spectrum (center) and chlorophyll-a concentration (right) during Cruises CTDOT1 (top), 2 (middle) and 3 (bottom) at Station DOT2.

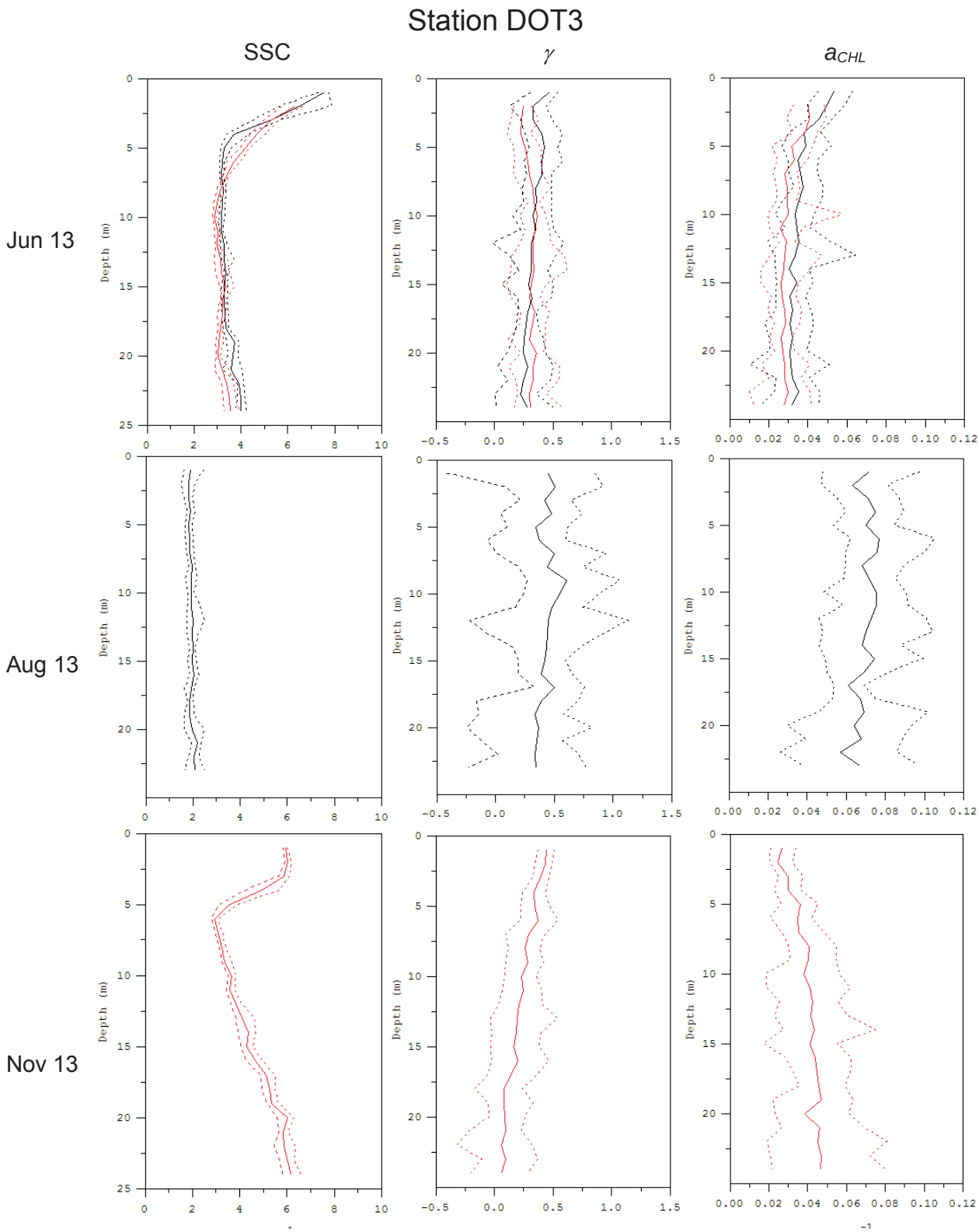

Figure 9-8. Suspended sediment concentrations (SSC) concentration (left), slope of particle size spectrum (center) and chlorophyll-a concentration (right) during Cruises CTDOT1 (top), 2 (middle) and 3 (bottom) at Station DOT3.

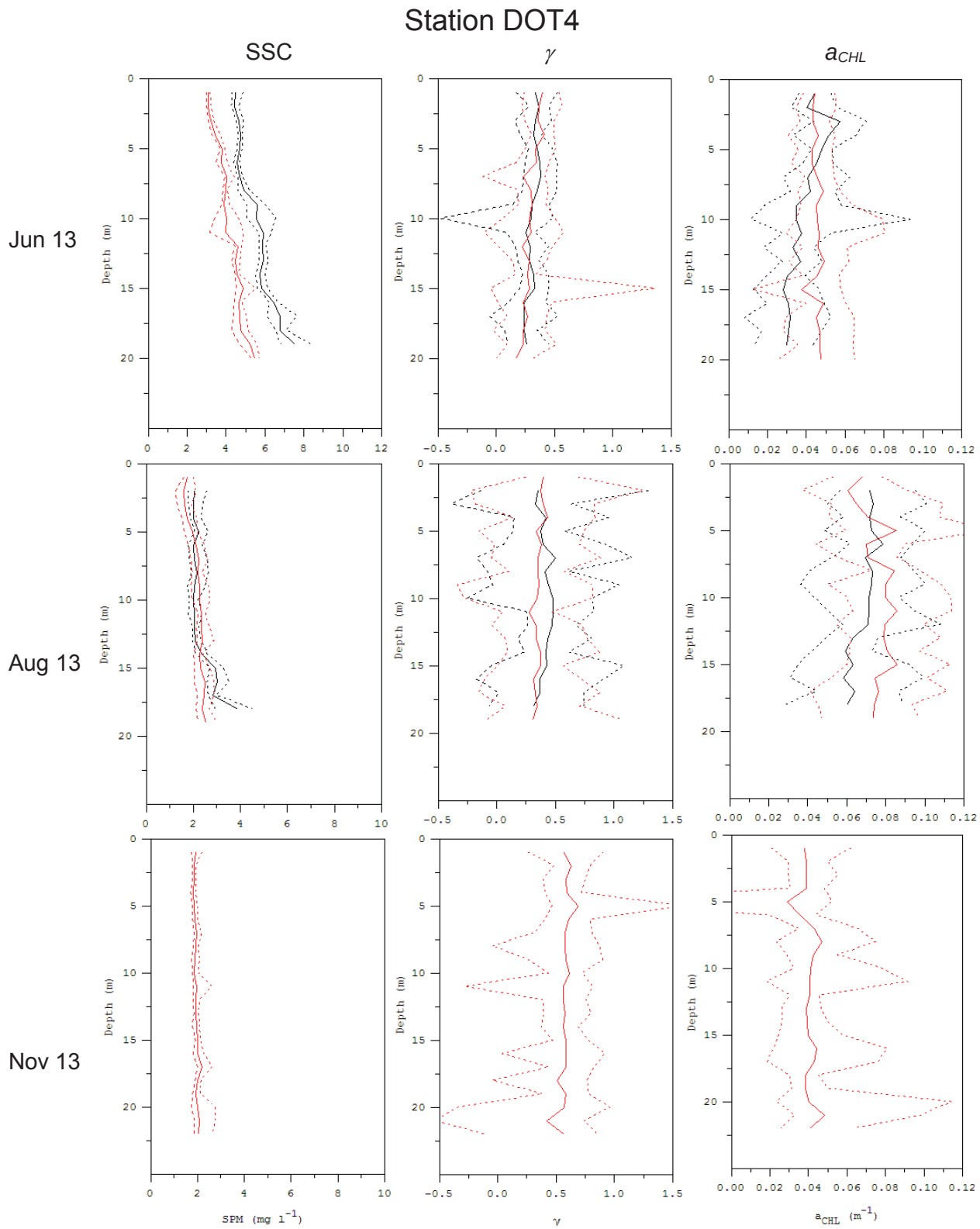

Figure 9-9. Suspended sediment concentrations (SSC) concentration (left), slope of particle size spectrum (center) and chlorophyll-a concentration (right) during Cruises CTDOT1 (top), 2 (middle) and 3 (bottom) at Station DOT4.

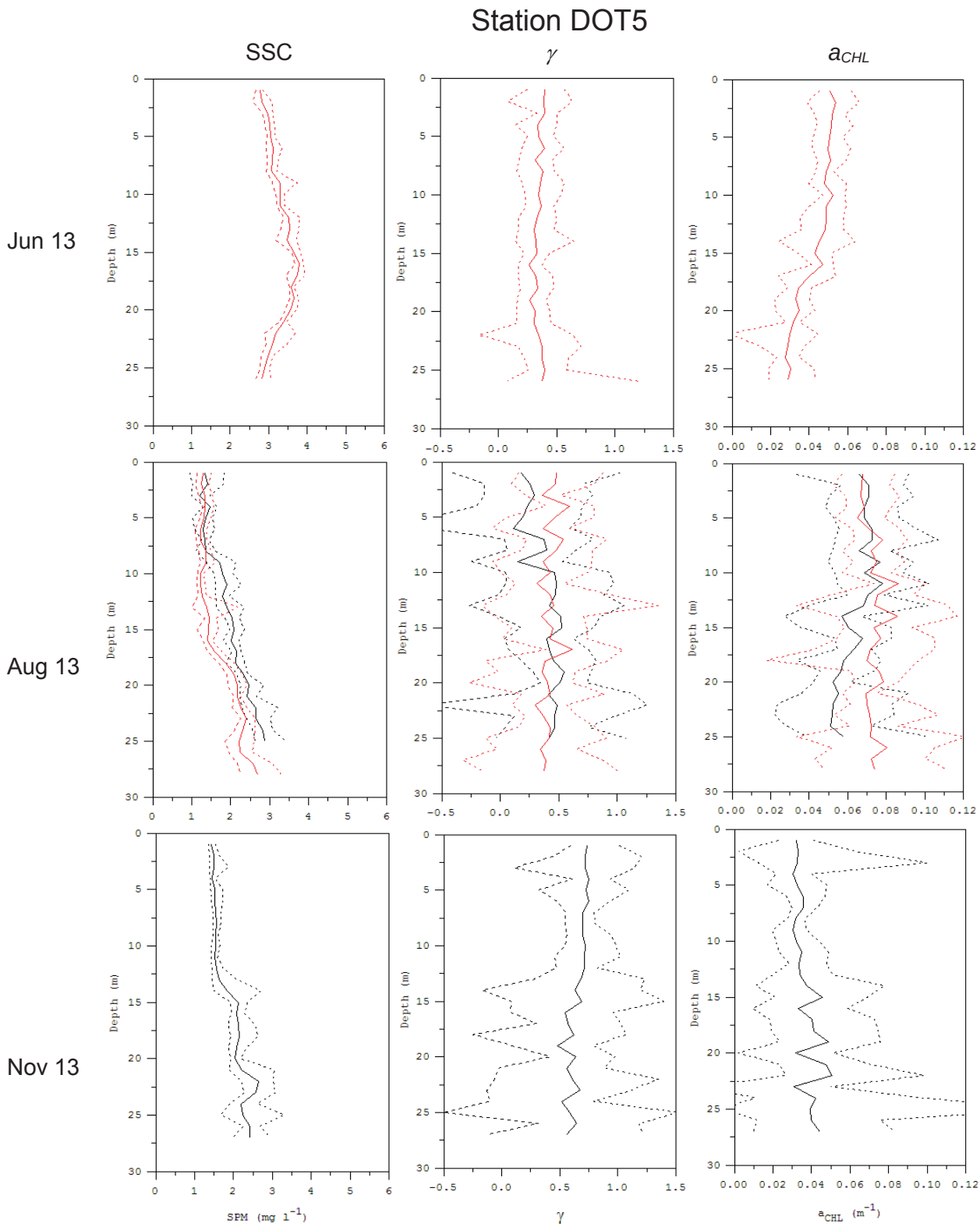

Figure 9-10. Suspended sediment concentrations (SSC) (left), slope of particle size spectrum (center) and chlorophyll-a concentration (right) during Cruises CTDOT1 (top), 2 (middle) and 3 (bottom) at Station DOT5.

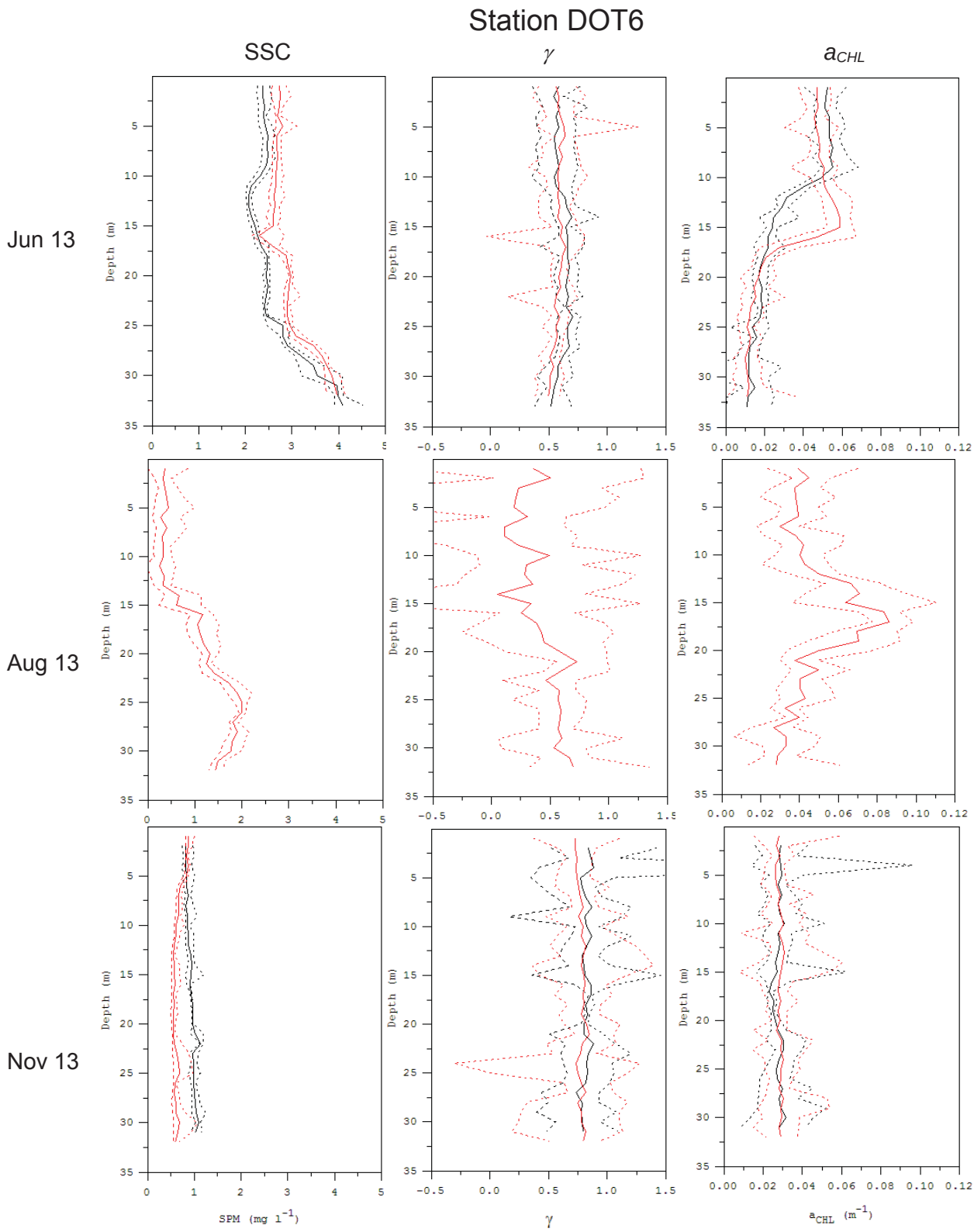

Figure 9-11. Suspended sediment concentrations (SSC) (left), slope of particle size spectrum (center) and chlorophyll-a concentration (right) during Cruises CTDOT1 (top), 2 (middle) and 3 (bottom) at Station DOT6.

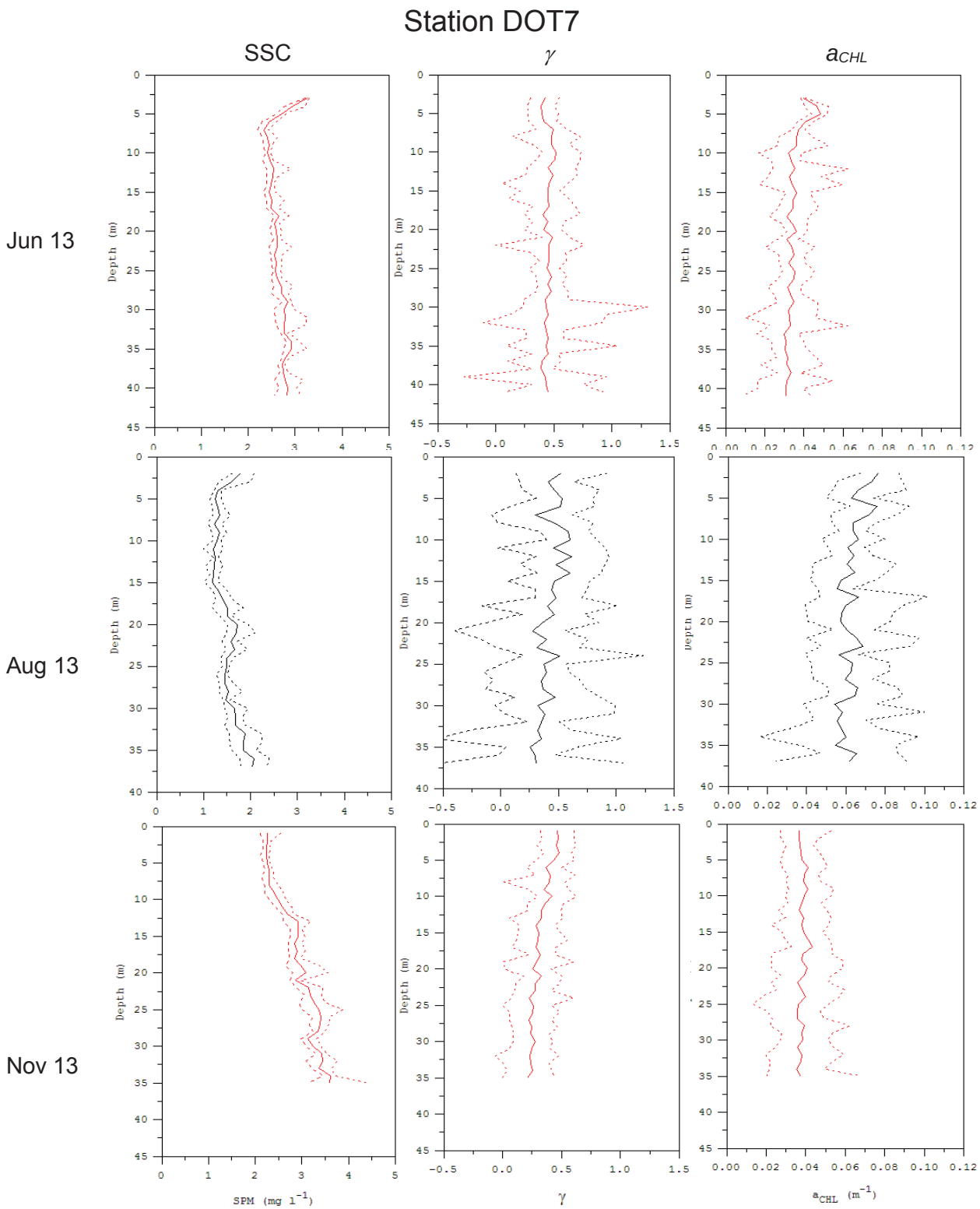

Figure 9-12. Suspended sediment concentrations (SSC) (left), slope of particle size spectrum (center) and chlorophyll-a concentration (right) during Cruises CTDOT1 (top), 2 (middle) and 3 (bottom) at Station DOT7.

10. Suspended Sediment near the Seafloor (Moored Instruments)

The suspended sediment concentration near the seafloor were measured OBS3+ sensors mounted at two elevations on the tripods frames, as described in Section 2.1.2.4.

10.1 Data

Figures 10-1 to 10-7 show the raw ensemble-averaged measurements from the OBS3+ sensors for both elevation above the seafloor for all deployments. The scale is counts on the digitizer and is logarithmic. The data reflect variations with a 6-hour period, longer time scale trends, and many isolated high values.

10.1.1 Data Quality

It is important to assess whether the high values of backscatter are a consequence of high concentrations of sediment or artifacts. When the tripod frames were recovered there was generally evidence of bio-fouling and it was particularly severe during the second (summer) campaign. The consequences of this bio-fouling on the OBS3+ measurements are clear in the records for Stations DOT1 to DOT4 after approximately July 20th, and for Station DOT5 at the beginning of August. These problems are characterized by a persistent increase in the minimum backscatter observed in a tidal cycle to levels that is very high.

Close examination of the high frequency observations which were acquired at 2 or 4 Hz provide guidance on what may be more transient biological effects. The data in Figure 10-1 contain a large peak in the upper level concentration on March 18. This peak is expanded in Figure 10-8 to reveal the high-frequency fluctuations. It is clear that the high backscatter started suddenly, persisted for more than 2000 seconds, and then disappeared. It seems likely that such events could be due to debris or aquatic plants. However, since it is impossible to be sure, we have not screened data from these intervals..

Figures 10-9 to 10-15 show the data contained in Figures 10-1 to 10-7 after the calibration coefficients listed in Table 2-5 were applied to convert counts to concentration in the units mg/l. Superimposed on the time-series of OBS3+ derived suspended sediment concentrations are green squares which show the results of the water sample analyses (Chapter 9). Considering the difficulty of obtaining water samples near the instruments and at the same distance above bottom, the agreement between the near OBS3+ derived estimates and the water samples is very good.

An important characteristic of all of the observations is that the concentrations at the two levels are highly correlated and the difference between them is seldom significant. The spatial and temporal variability is much larger than the instantaneous difference in the vertical. To suppress the noise in the data in order to reveal the longer-term variations, we exploited this correlation and performed time-averaging. To isolate spikes we computed the correlation between the concentrations at the two levels and then identified times when discrepancies between the regression prediction and data exceeded a threshold. We chose 40 mg/l because such differences were very infrequent. Other thresholds in this range did not influence the results significantly.

These points were eliminated from the data set. The remaining data were then bin-averaged in 6-hour intervals (Figures 10-16 and 10-17).

10.1.2 Suspended Sediment Concentrations

The variations in suspended sediment concentrations at the eastern Long Island Sound stations (DOT1,2,3,7) are compared in Figure 10-16. The record at Station DOT3 (near Niantic Bay) shows the highest concentrations (approximately 30 mg/l) during Campaign 1. The values at Station DOT2 were approximately 50% lower. Concentrations at Station DOT1 varied between 1 and 10 mg/l. During the Campaign 2 (summer) concentrations at all the stations were between 1 and 10 mg/l. The high concentrations in late August were likely due to bio-fouling. In the winter the suspended sediment concentrations varied with a 14-day periodicity, with the exception of Station DOT2 which showed a more persistent concentration of approximately 10 mg/l. Concentrations at Stations DOT1, 3 and 7 varied in phase with each other by at least by a factor of 10. Of the ELIS stations, Station DOT1 had the highest concentrations (up to 30-40 mg/l) and Station DOT7 had the lowest concentrations.

The variations in suspended sediment concentrations for the Block Island Sound stations (DOT4,5,6) are compared in Figure 10-17. The concentrations at the northern-most station (DOT6) are persistently the lowest, just above 1 mg/l in the spring and summer. The late August concentrations show an increase but this is likely due to bio-fouling. Concentrations in the winter (Campaign 3) were between 2 and 3 mg/l. Station DOT5 had the highest concentrations (about 5 mg/l) in the spring and winter (Campaigns 1 and 3), varying between 3 and 10 mg/l. Concentrations at Station DOT4 were approximately half of that.

10.2 Summary

The study developed a data set of bottom suspended sediment concentrations and variability estimates at the seven mooring stations that span a wide range of conditions. The data show good agreement between the calibrated OBS3+ concentrations and the concentrations based on water sample analyses. The screened and averaged data show consistent patterns across the eastern Long Island Sound and Block Island Sound.

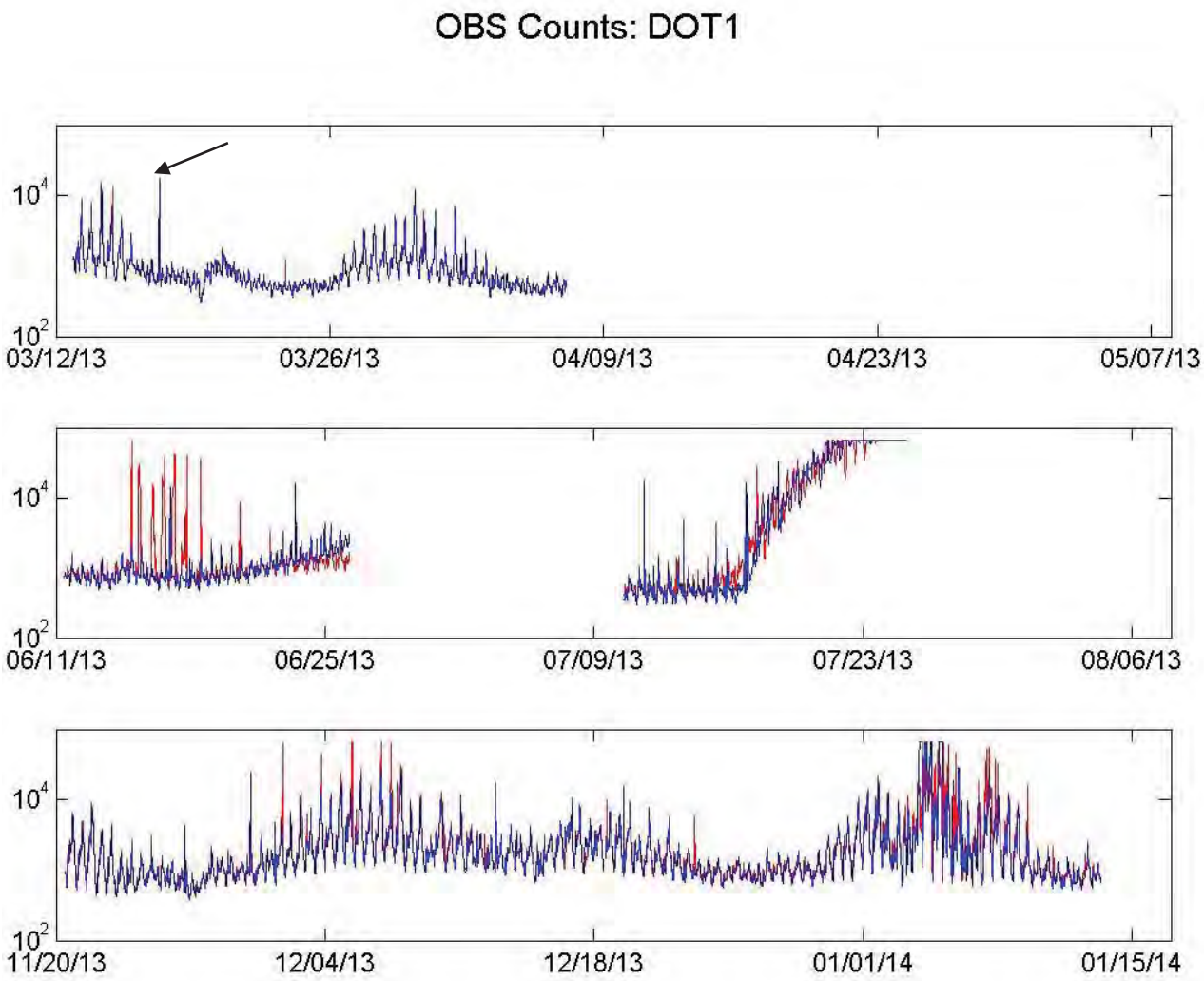

Figure 10-1. Digitized data from the OBS3+ sensors at Station DOT1 for the lower elevation 30 cm; red line) and higher elevation (80 cm in Campaign 1, 137 cm in Campaigns 2 and 3; blue line). The arrow points to a peak on March 18th that is expanded in Figure 10-8. The vertical scale is counts on the digitizer.

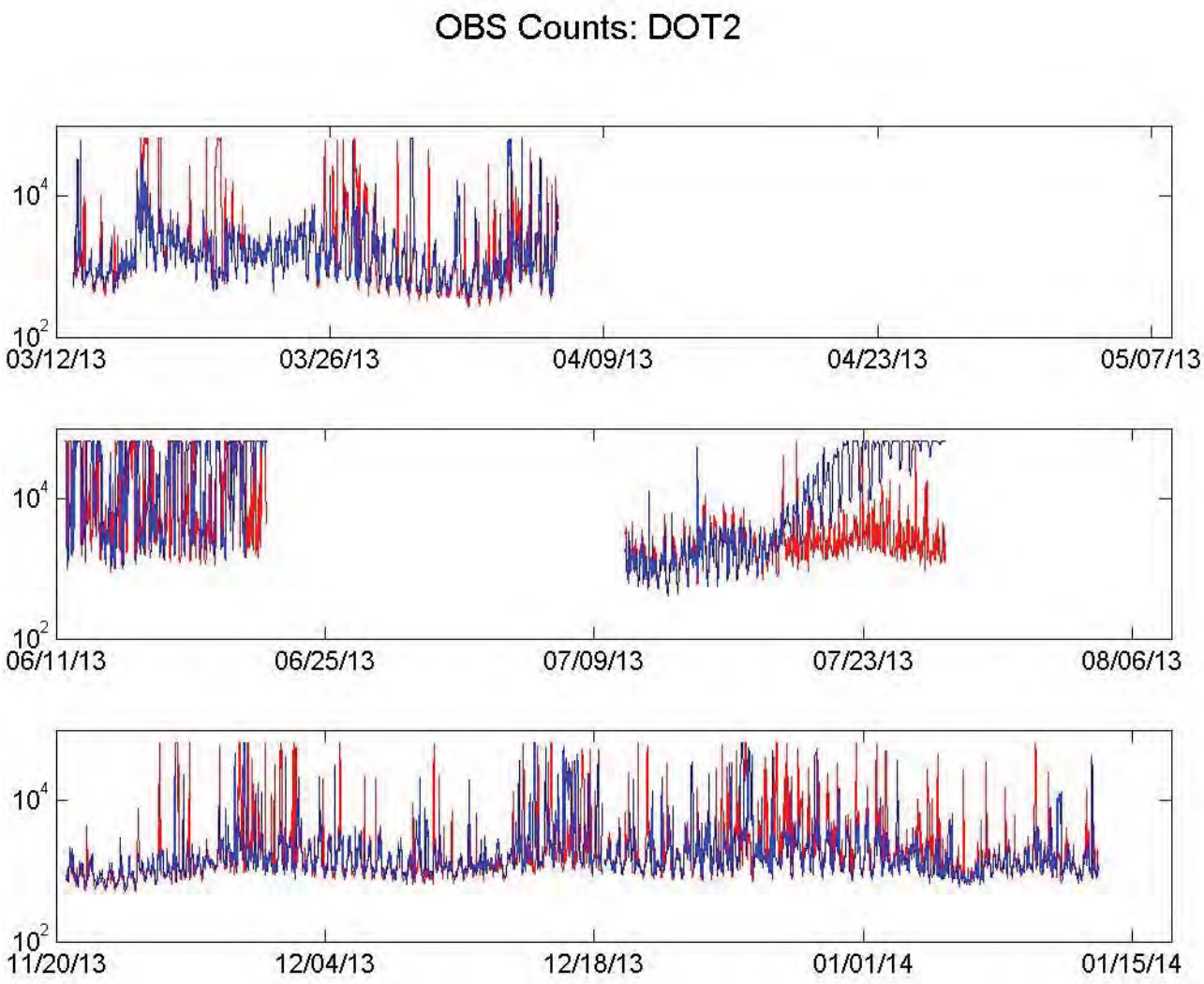

Figure 10-2. Digitized data from the OBS3+ sensors at Station DOT2 for the lower elevation 30 cm; red line) and higher elevation (80 cm in Campaign 1, 137 cm in Campaigns 2 and 3; blue line). The vertical scale is counts on the digitizer.

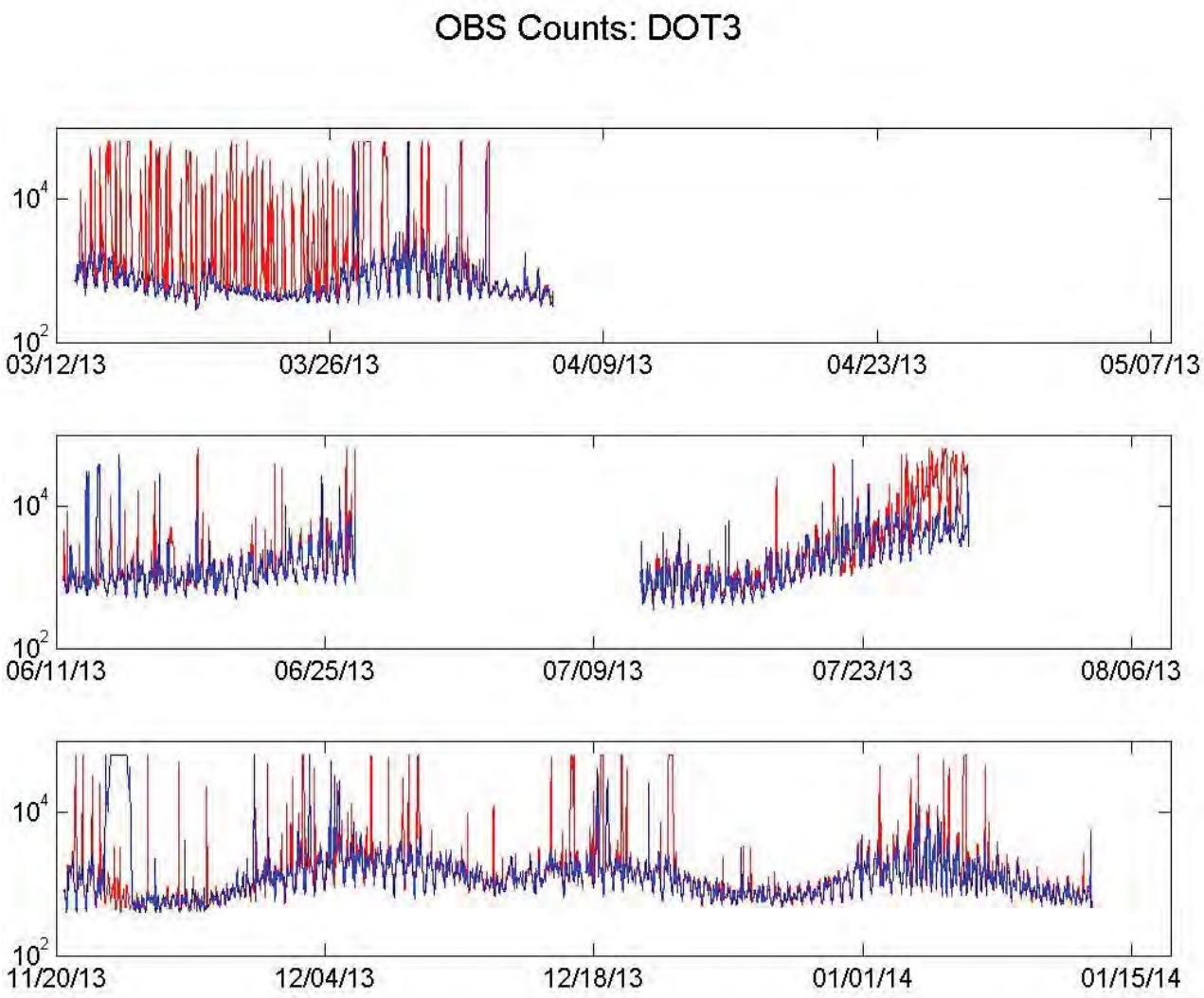

Figure 10-3. Digitized data from the OBS3+ sensors at Station DOT3 for the lower elevation 30 cm; red line) and higher elevation (80 cm in Campaign 1, 137 cm in Campaigns 2 and 3; blue line). The vertical scale is counts on the digitizer.

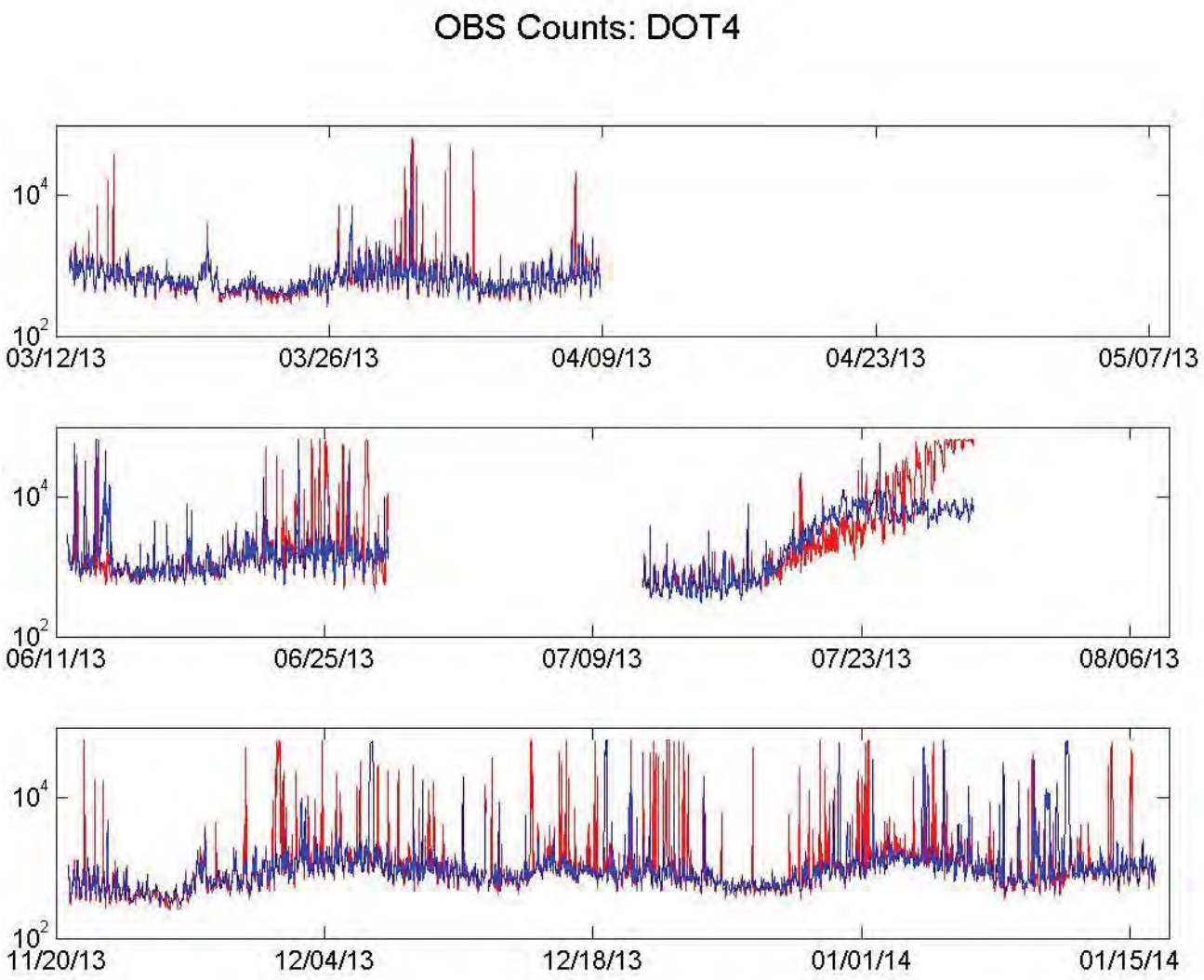

Figure 10-4. Digitized data from the OBS3+ sensors at Station DOT4 for the lower elevation 30 cm; red line) and higher elevation (80 cm in Campaign 1, 137 cm in Campaigns 2 and 3; blue line). The vertical scale is counts on the digitizer.

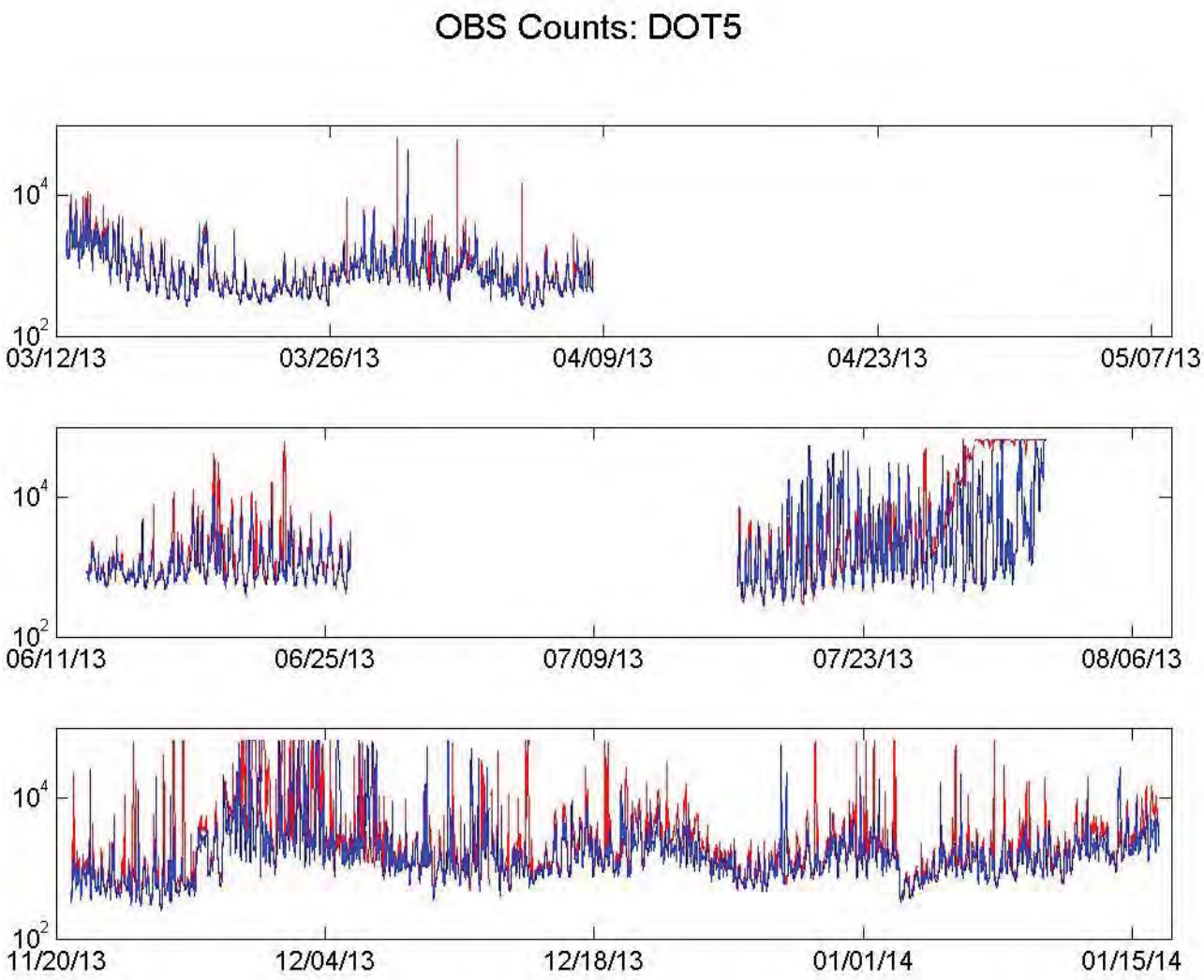

Figure 10-5. Digitized data from the OBS3+ sensors at Station DOT5 for the lower elevation 30 cm; red line) and higher elevation (80 cm in Campaign 1, 137 cm in Campaigns 2 and 3; blue line). The vertical scale is counts on the digitizer.

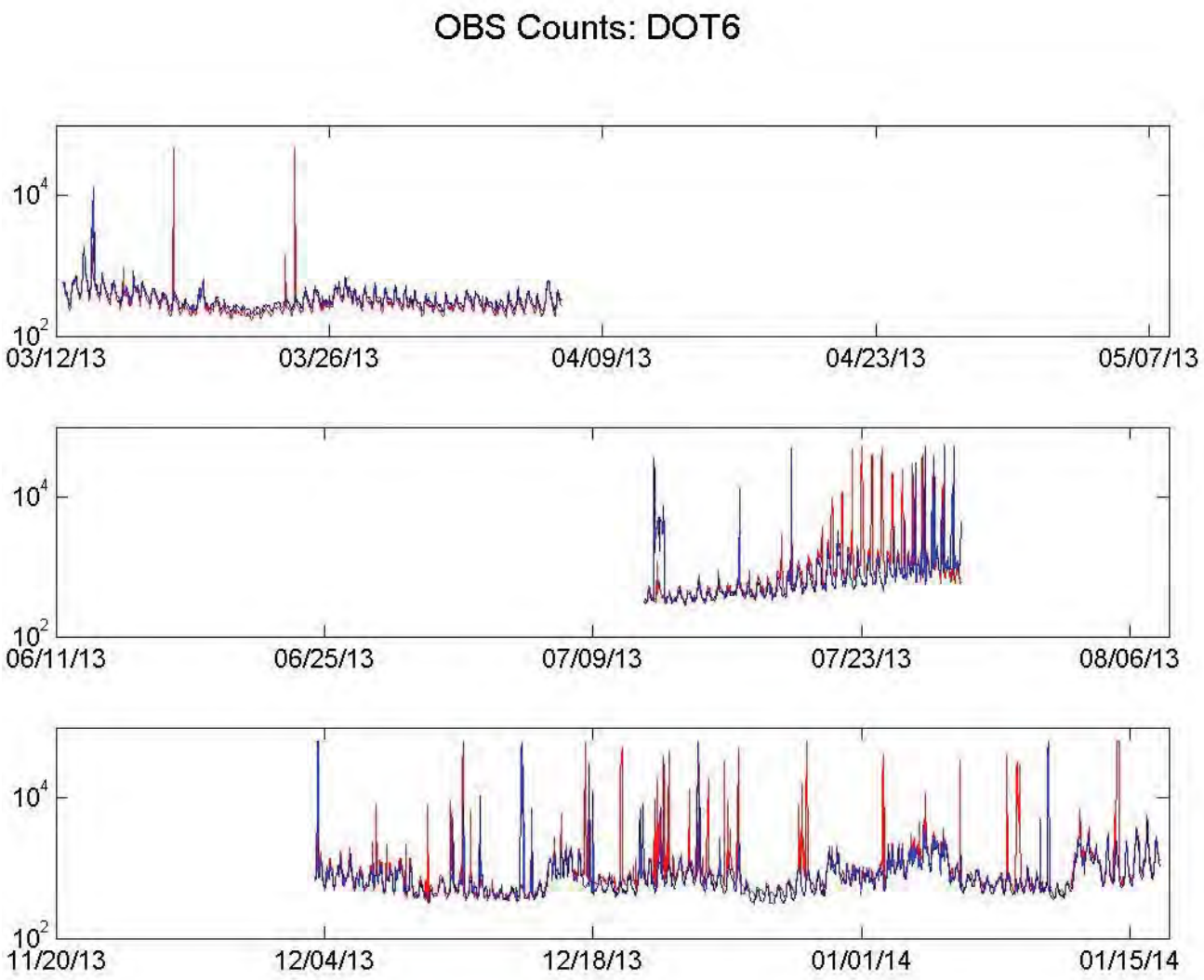

Figure 10-6. Digitized data from the OBS3+ sensors at Station DOT6 for the lower elevation 30 cm; red line) and higher elevation (80 cm in Campaign 1, 137 cm in Campaigns 2 and 3; blue line). The vertical scale is counts on the digitizer.

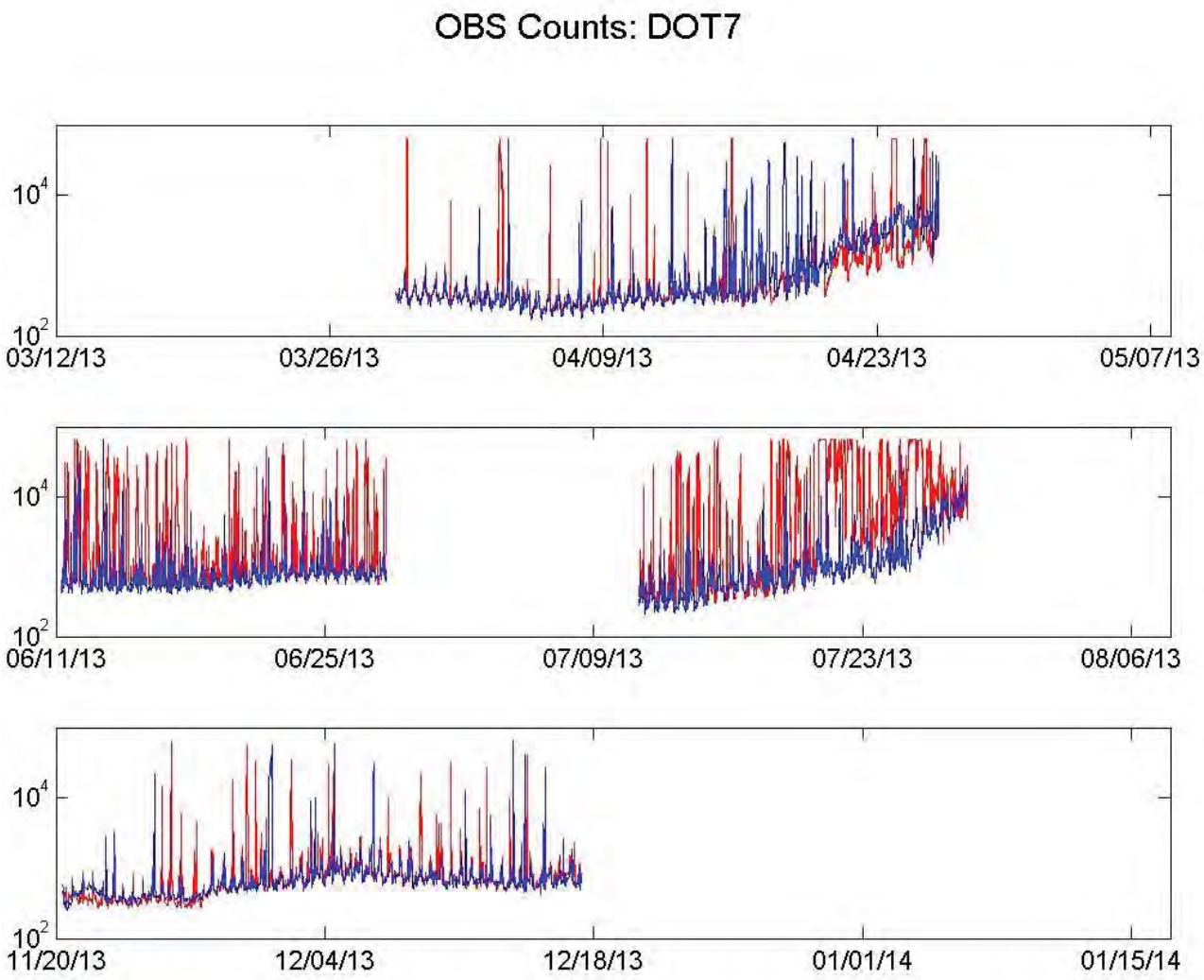

Figure 10-7. Digitized data from the OBS3+ sensors data at Station DOT7 for the lower elevation 30 cm; red line) and higher elevation (80 cm in Campaign 1, 137 cm in Campaigns 2 and 3; blue line). The vertical scale is counts on the digitizer.

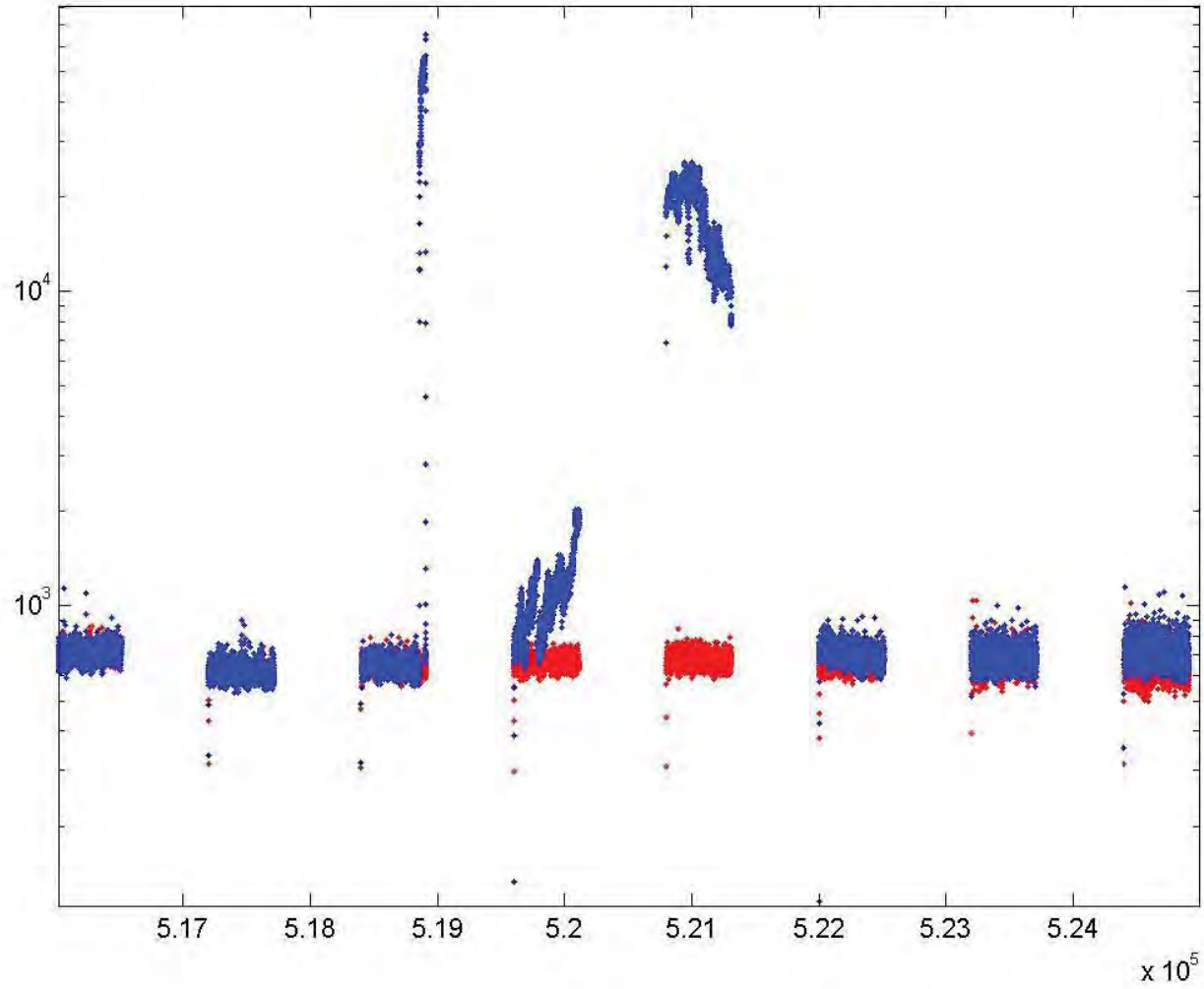

Figure 10-8. Response of the OBS3+ sensor (counts) at Station DOT1 from an hour on March 18, 2013. The values in excess of $\mathbf{10^3}$ are data anomalies, attributed to marine organisms; such values were eliminated from the data record prior to the estimation of suspended material concentration.

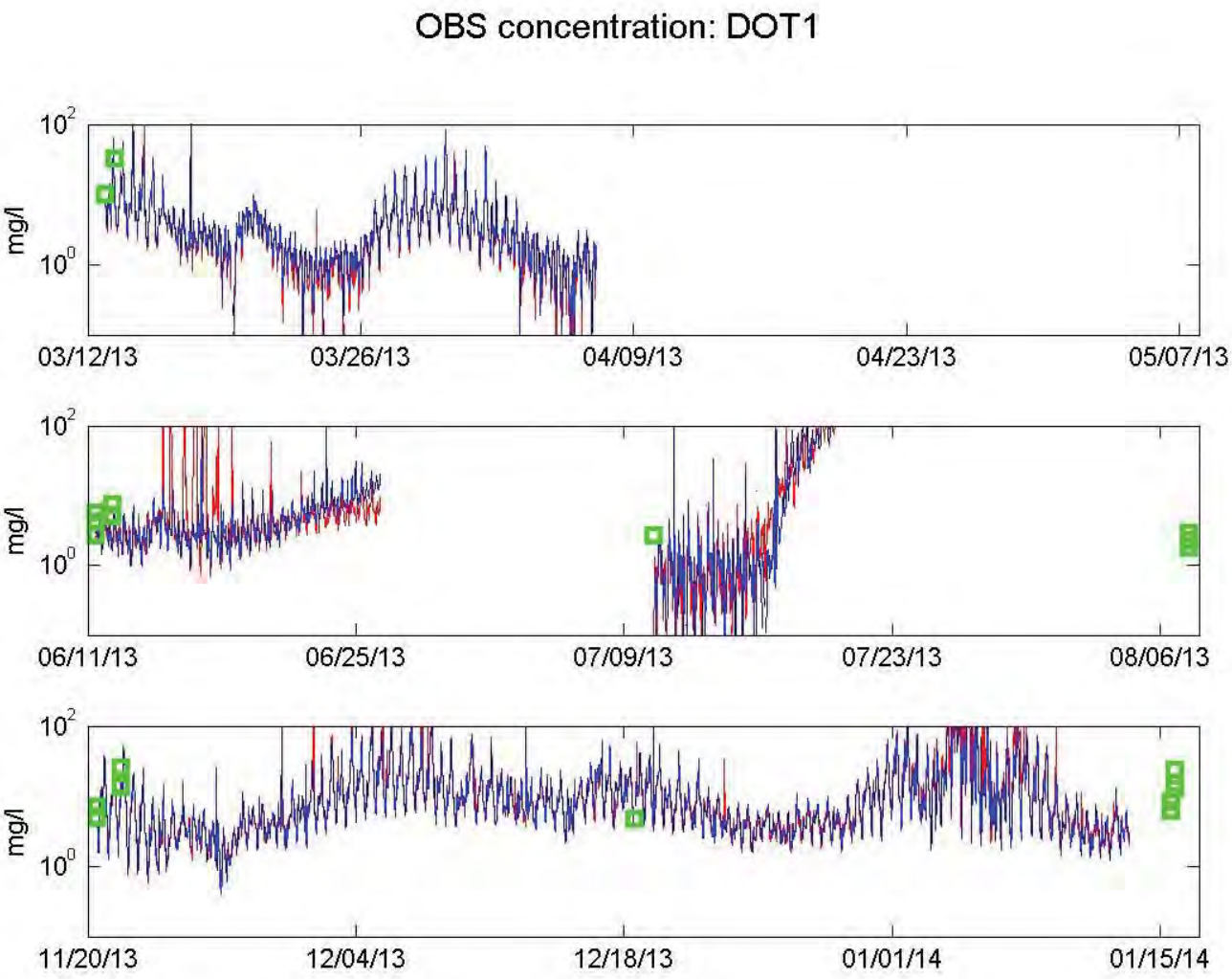

Figure 10-9. Suspended sediment concentrations (SSC) estimated by applying the coefficients in Table 2-5 to the OBS3+ observations at Station DOT1 for the lower elevation 30 cm; red line) and higher elevation (80 cm in Campaign 1, 137 cm in Campaigns 2 and 3; blue line). The green symbols are the water concentrations (SSC) from water samples (see Chapter 9).

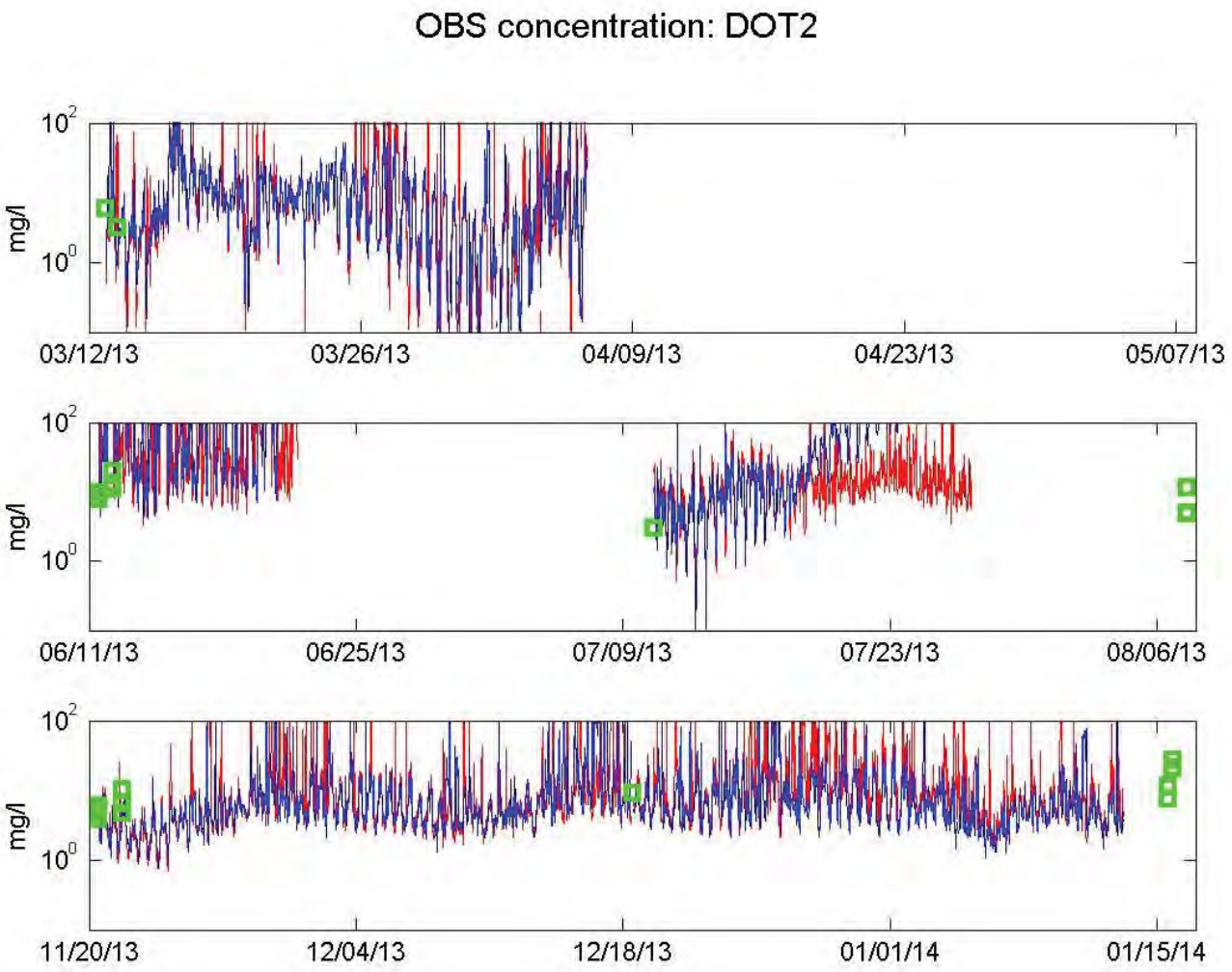

Figure 10-10. Suspended sediment concentrations (SSC) estimated by applying the coefficients in Table 2-5 to the OBS3+ observations at Station DOT2 for the lower elevation 30 cm; red line) and higher elevation (80 cm in Campaign 1, 137 cm in Campaigns 2 and 3; blue line). The green symbols are the water concentrations (SSC) from water samples (see Chapter 9).

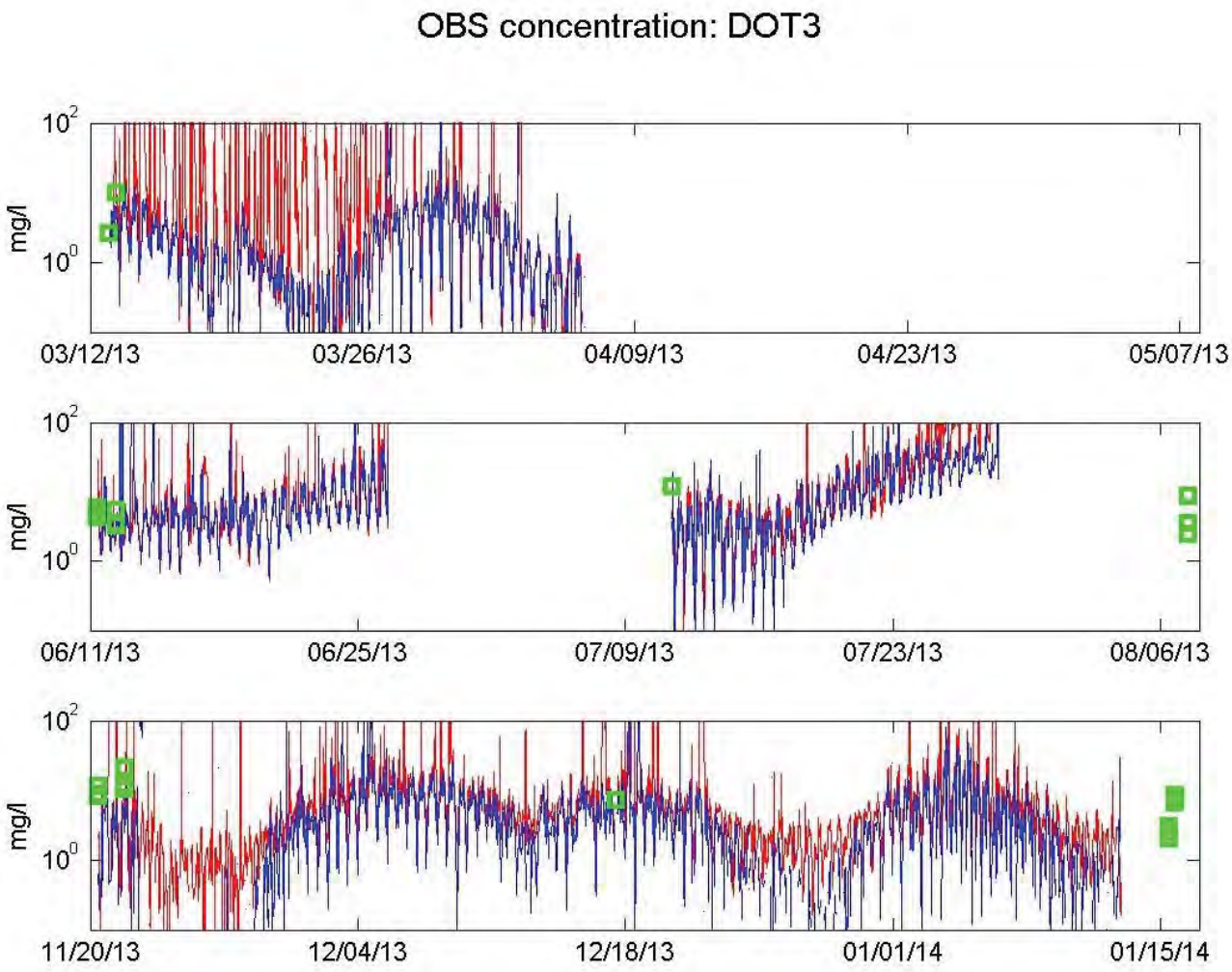

Figure 10-11. Suspended sediment concentrations (SSC) estimated by applying the coefficients in Table 2-5 to the OBS3+ observations at Station DOT3 for the lower elevation 30 cm; red line) and higher elevation (80 cm in Campaign 1, 137 cm in Campaigns 2 and 3; blue line). The green symbols are the water concentrations (SSC) from water samples (see Chapter 9).

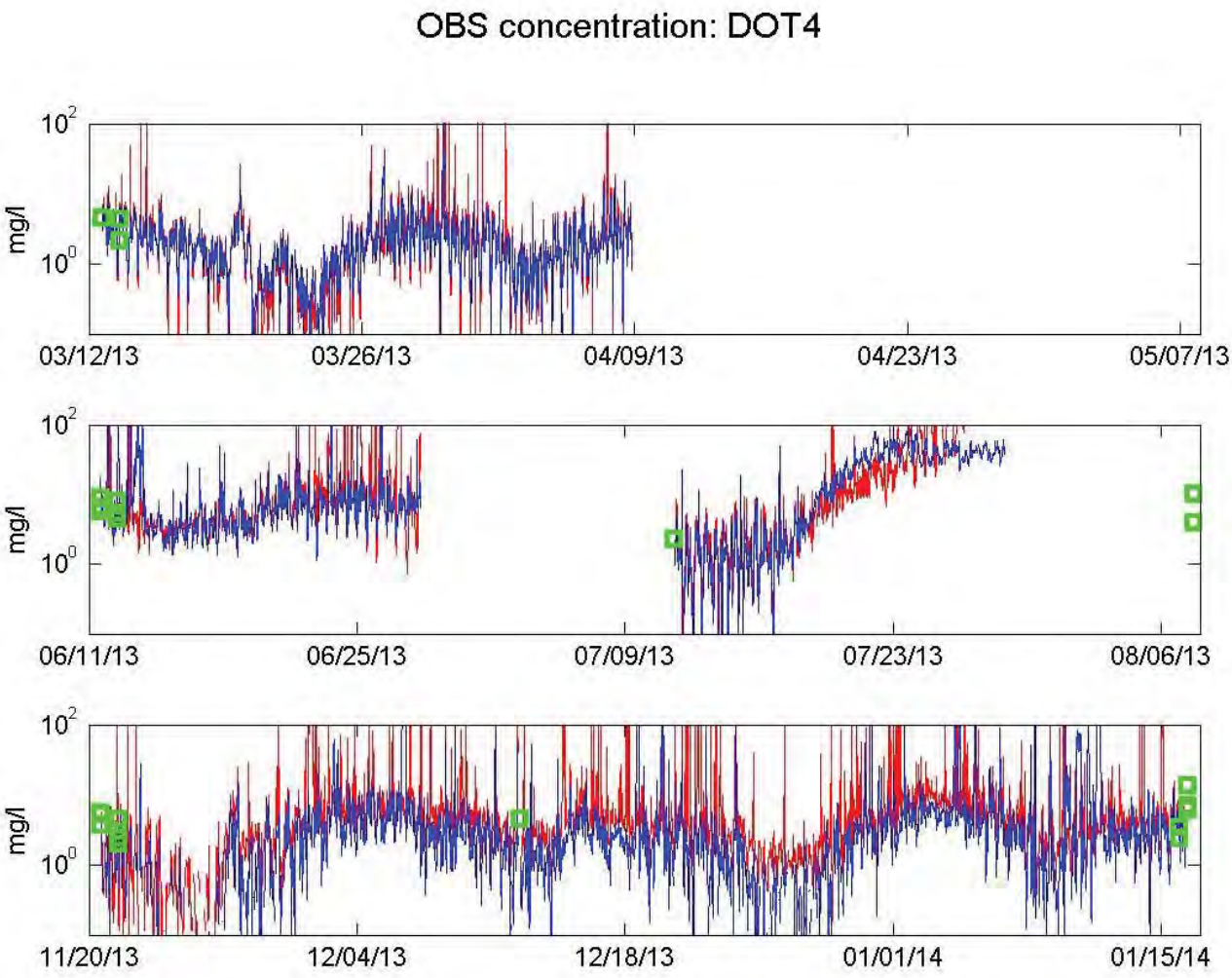

Figure 10-12. Suspended sediment concentrations (SSC) estimated by applying the coefficients in Table 2-5 to the OBS3+ observations at Station DOT4 for the lower elevation 30 cm; red line) and higher elevation (80 cm in Campaign 1, 137 cm in Campaigns 2 and 3; blue line). The green symbols are the water concentrations (SSC) from water samples (see Chapter 9).

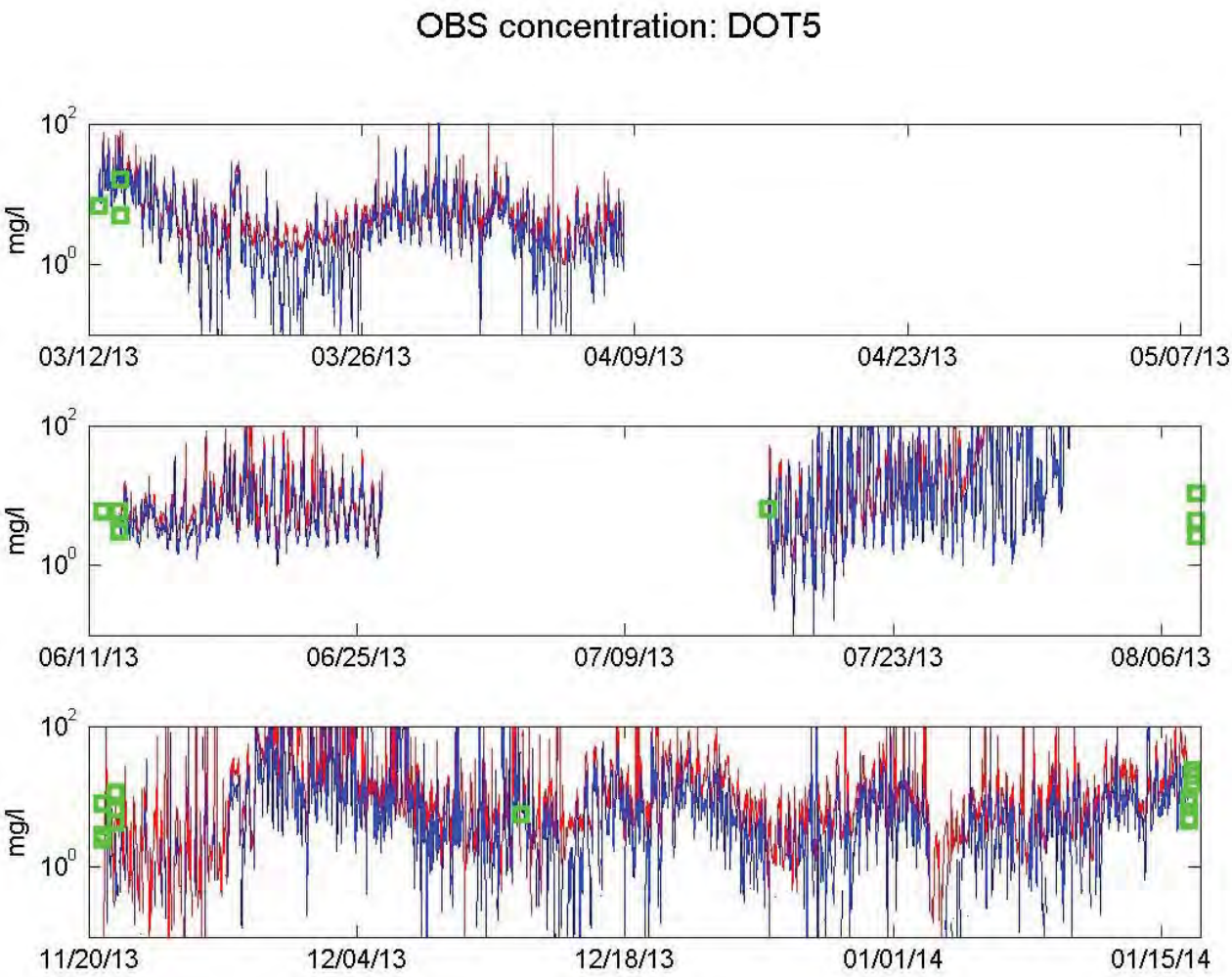

Figure 10-13. Suspended sediment concentrations (SSC) estimated by applying the coefficients in Table 2-5 to the OBS3+ observations at Station DOT5 for the lower elevation 30 cm; red line) and higher elevation (80 cm in Campaign 1, 137 cm in Campaigns 2 and 3; blue line). The green symbols are the water concentrations (SSC) from water samples (see Chapter 9).

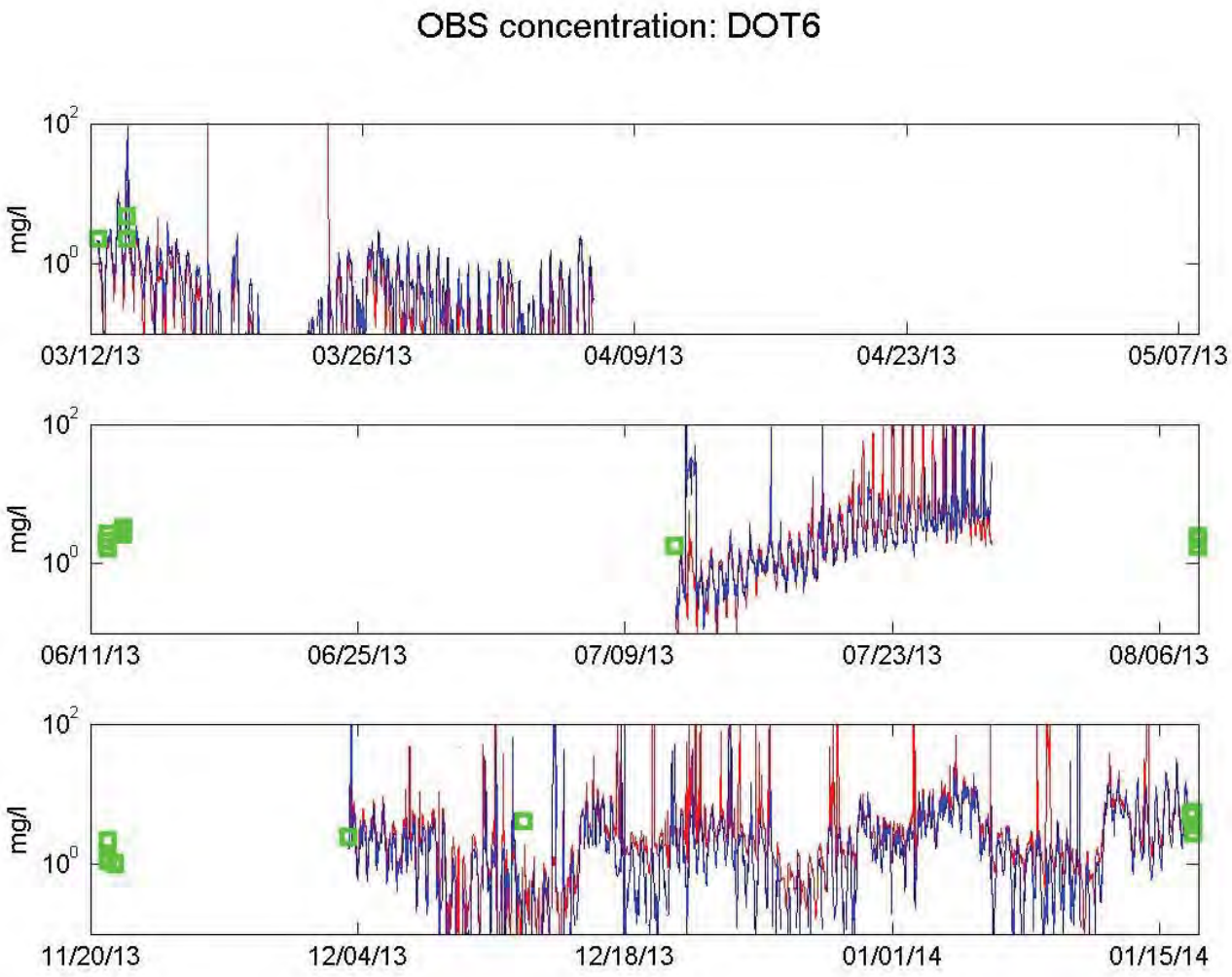

Figure 10-14. Suspended sediment concentrations (SSC) estimated by applying the coefficients in Table 2-5 to the OBS3+ observations at Station DOT6 for the lower elevation 30 cm; red line) and higher elevation (80 cm in Campaign 1, 137 cm in Campaigns 2 and 3; blue line). The green symbols are the water concentrations (SSC) from water samples (see Chapter 9).

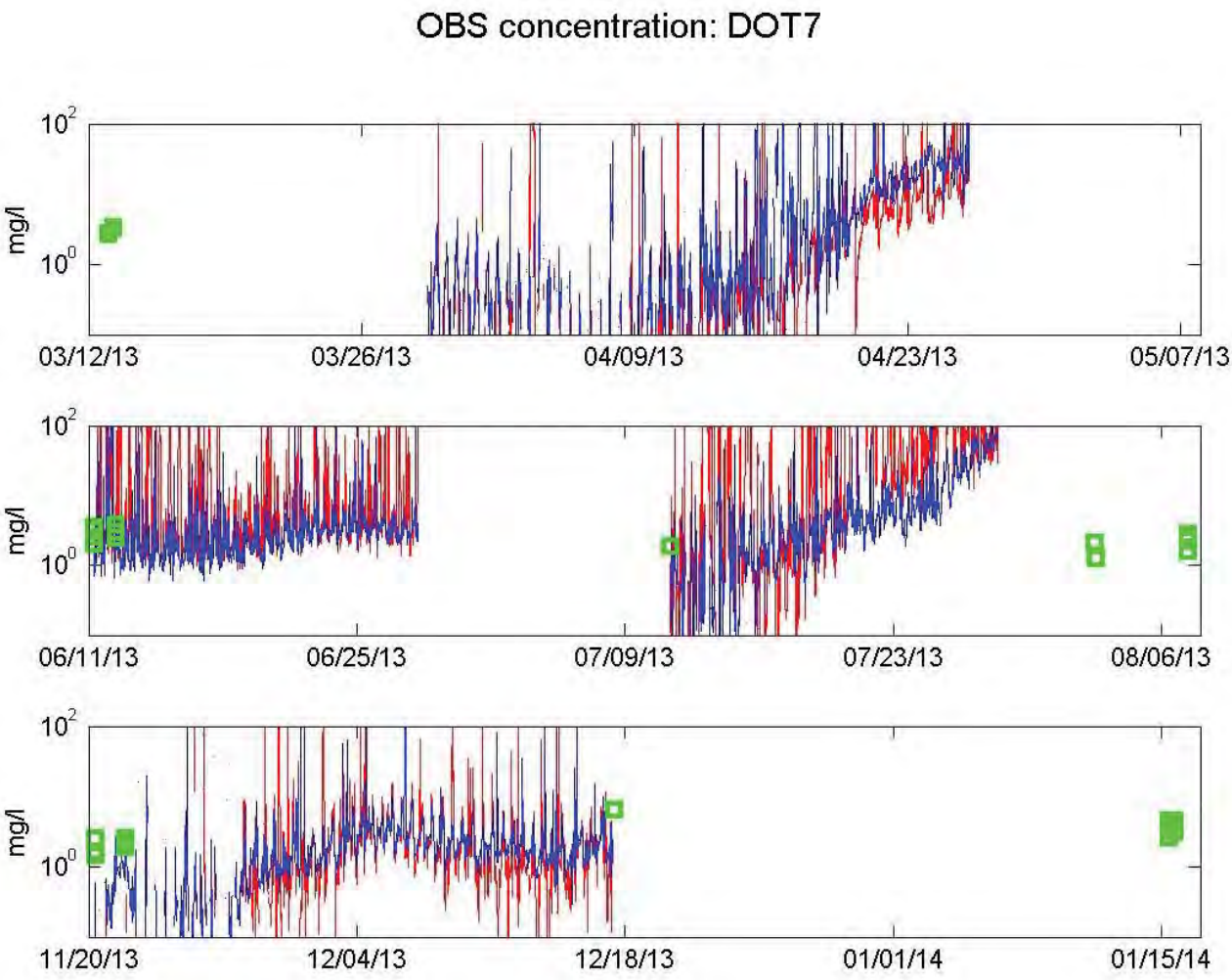

Figure 10-15. Suspended sediment concentrations (SSC) estimated by applying the coefficients in Table 2-5 to the OBS3+ observations at Station DOT7 for the lower elevation 30 cm; red line) and higher elevation (80 cm in Campaign 1, 137 cm in Campaigns 2 and 3; blue line). The green symbols are the water concentrations (SSC) from water samples (see Chapter 9).

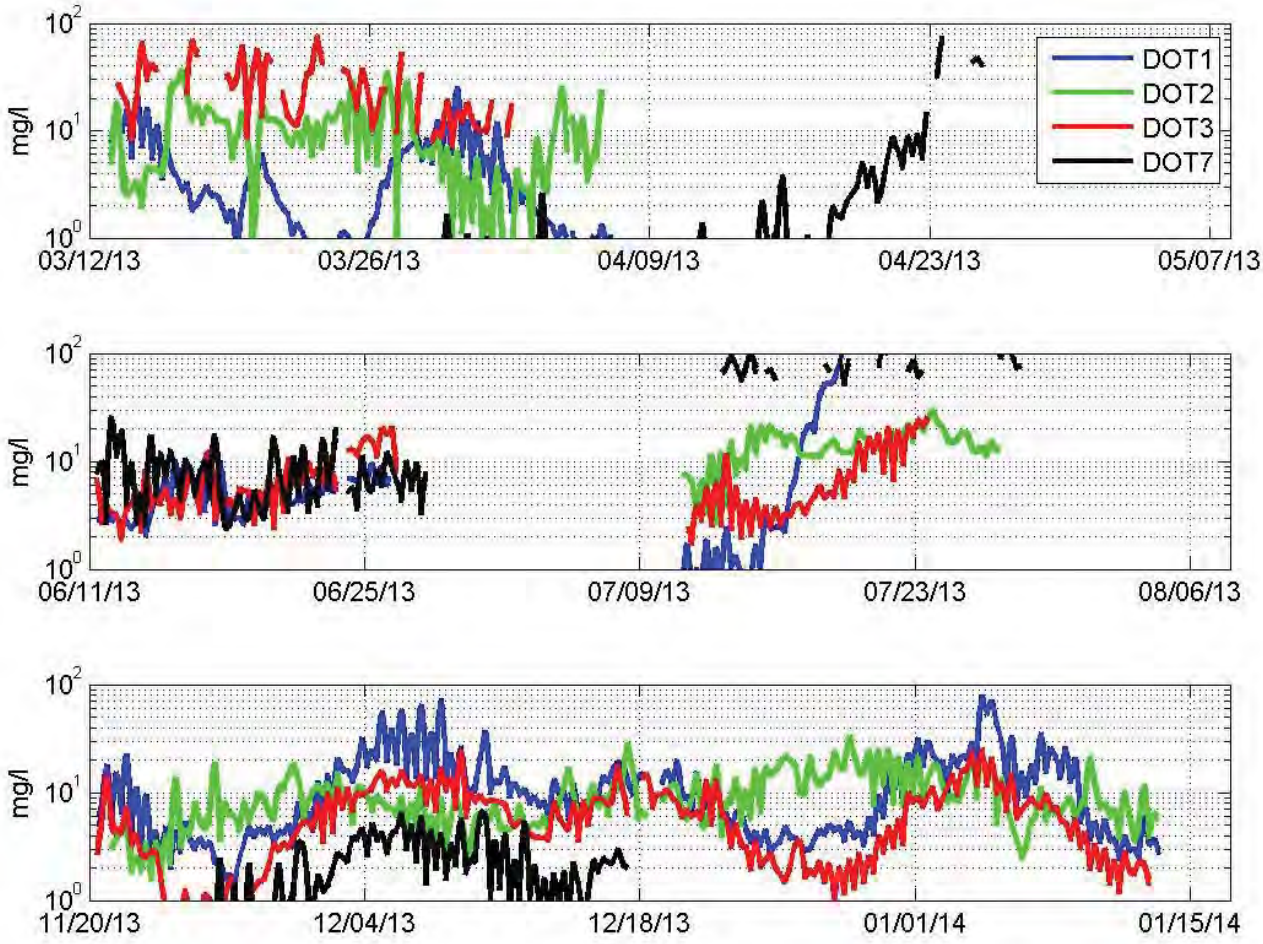

Figure 10-16. Time-series of the screened, and bin-averaged OBS3+ observations at eastern Long Island Sound Stations DOT1, 2, 3, and 7.

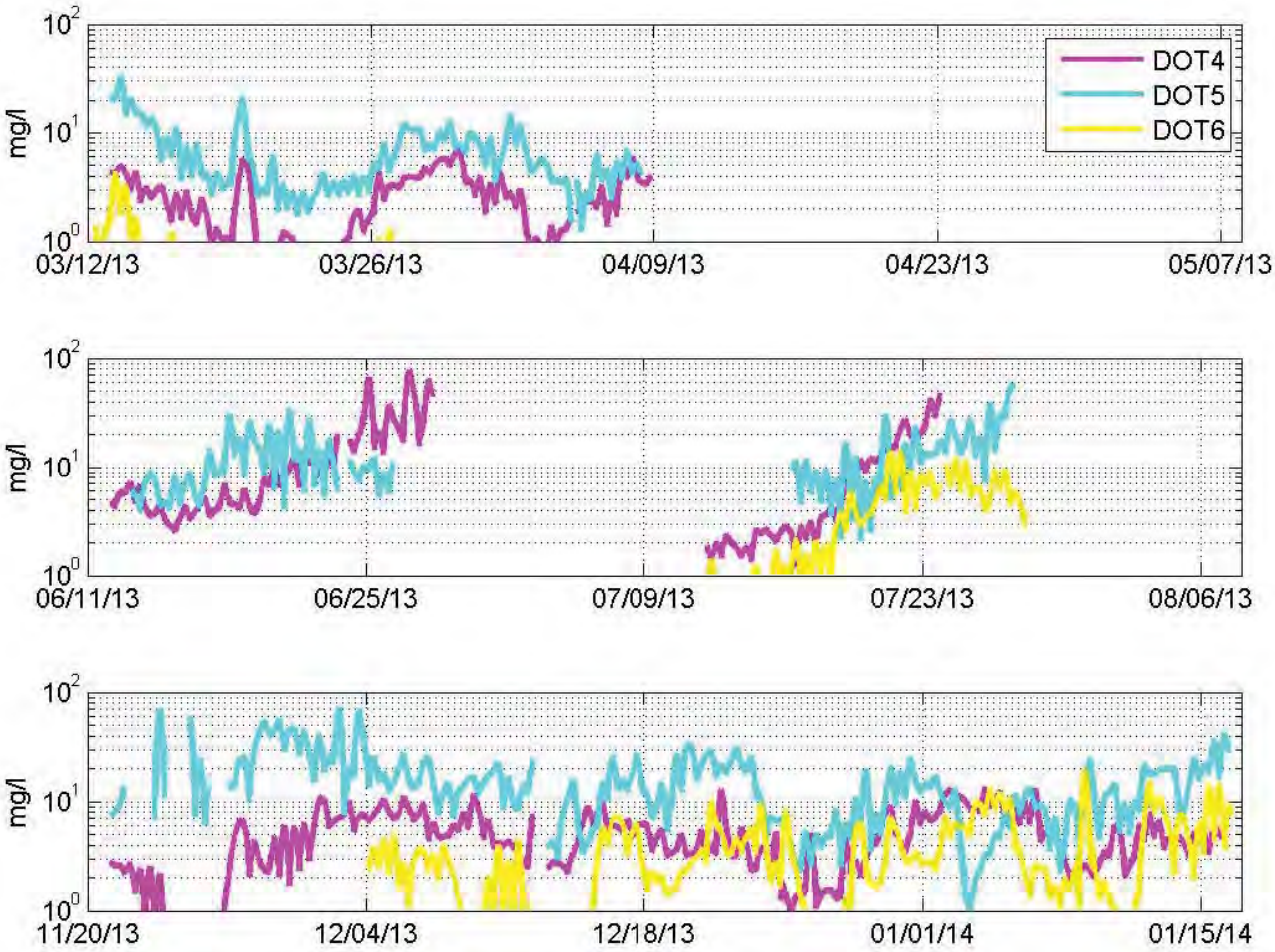

Figure 10-17. Time-series of the screened, and bin averaged OBS3 observations at Block Island Sound Stations DOT4, 5, and 6.

11. Grain Size of Seafloor Sediments

Bottom sediment samples were collected by grab sampler at the seven mooring stations, as described in Section 2.1.3.5. The data were used primarily as input to the physical oceanography model to calculate bottom stress.

11.1 Data

The grain size distribution for each sample is presented in Table 11-1. Table 11-2 presents the median grain size statistic, or D50, for each sample. Sediments at all stations consisted predominantly of sand. The highest concentration of fines (silt and clay) was observed at Station DOT6; the average of the three samples was 17%. Complete sample statistics are included in Appendix 13.

Table 11-1. Grain Size Distribution at Mooring Stations

Station	Main Size Fractions (%)			Breakdown of Sand Sizes (%)				
	Gravel	Sand	Silt+Clay	Very Coarse Sand	Coarse Sand	Medium Sand	Fine Sand	Very Fine Sand
Campaign 1 (March 13, 2013)								
DOT 1	2.6	95.8	1.6	9.5	44.5	35.6	6.0	0.1
DOT 2	32.4	62.4	5.2	9.3	10.2	24.4	14.8	0.7
DOT 3	12.0	77.5	10.5	10.0	15.7	22.0	20.5	9.4
DOT 4	0.1	97.8	2.1	0.1	0.4	27.1	69.0	1.2
DOT 5	0.1	98.0	1.9	8.0	49.5	28.9	11.2	0.4
DOT 6A	2.1	79.3	18.7	3.4	7.5	14.8	45.0	8.5
DOT 7	3.1	93.3	3.6	10.3	38.9	36.7	6.9	0.5
Campaign 2 (August 7, 2013)								
DOT 1	6.3	92.7	1.0	11.5	44.4	34.5	2.3	0.0
DOT 2	25.8	69.9	4.3	10.4	13.2	28.5	17.0	0.9
DOT 3	11.6	81.8	6.6	10.8	21.3	23.7	20.4	5.6
DOT 4	0.1	97.7	2.2	0.1	0.3	5.6	87.2	4.5
DOT 5	0.1	97.3	2.6	1.8	33.6	44.1	17.7	0.1
DOT 6B	4.5	74.3	21.2	4.8	8.2	14.3	38.2	8.9
DOT 7	0.8	93.6	5.6	2.6	16.2	57.3	15.6	2.0
Campaign 3 (November 20-21, 2013)								
DOT 1	0.6	97.9	1.5	5.4	47.0	43.7	1.7	0.1
DOT 2	3.0	94.7	2.3	3.8	13.1	57.1	20.2	0.5
DOT 3	15.6	79.8	4.6	11.5	18.1	21.5	21.7	7.0
DOT 4	0.0	98.2	1.8	0.0	0.4	7.7	89.0	1.1
DOT 5	0.0	97.5	2.5	2.0	27.7	46.8	20.5	0.5
DOT 6B	0.3	87.6	12.0	3.4	14.3	25.4	38.4	6.1
DOT 7	7.2	82.7	10.1	3.4	6.3	29.3	38.2	5.5

Table 11-2. Median Grain Size, or D50, at the Mooring Stations

Station	Campaign 1 Sampling Date: March 13, 2013	Campaign 2 Sampling Date: August 7, 2013	Campaign 3 Sampling Date: Nov 20-21, 2013
	D50 (µm)		
DOT 1	554.6	604.8	523.2
DOT 2	567.4	492.0	346.7
DOT 3	338.5	415.4	427.6
DOT 4	199.7	176.3	180.4
DOT 5	556.4	397.7	370.3
DOT 6A	177.6	179.5	–
DOT 6B	–	–	222.3
DOT 7	521.1	345.8	233.1

11.2 Summary

Grab samples were collected at all mooring stations during each campaign and processed for grain size composition for characterizing the bottom roughness and future sediment transport modeling.

12. Summary

The field program of the PO study was designed to acquire data that could evaluate a high-resolution circulation model. The data alone are insufficient of providing a comprehensive description of conditions or guidance on disposal site selection, which instead is the goal of the modeling component of the PO study. Therefore, the Field Data Report summarizes the field program design and the general character of the data acquired.

12.1 Study Design

The sampling plan for the data set described in this report was based on the need to assess the effectiveness of a three-dimensional circulation model to predict the spatial structure of the circulation and bottom stress during fair weather and storm conditions. Since the program was extensive and additional model development was anticipated to predict the transport of suspended sediment, supplementary data was acquired to support that future work.

To assess the model performance effectively it is critical that the density field, waves and wind are predicted well so that the bottom stress in as accurate as possible. The density field varies with season as a consequence of the seasonal cycles of hearing and runoff so the field program was divided into three, approximately 2-month long, observation campaigns in the spring and summer of 2013 and the winter of 2013-14. Seven sites were selected that were expected to exhibit a range of current bottom stress conditions and an extensive set of instruments was deployed at each station. The measurements made by this instruments were complemented by ship surveys that collected data of the current and density field and the suspended sediment distribution.

12.2 Instrumentation

A comprehensive description of the observation systems is provided in Chapter 2. The instruments that were central to the measurement of waves, currents and bottom stress were bottom-mounted ADCPs. RDI ADCPs were oriented upwards to (a) record the motion of water from 3 m above bottom to the water surface and (b) the statistics of surface gravity waves. Nortek ADCPs were oriented downwards to measure the structure of the flow near the seafloor and to estimate bottom stress magnitudes. These instruments were complemented by salinity-temperature sensors and optical instruments to estimate the suspended sediment concentrations. The ship surveys used a profiling instrument suite to measure salinity, temperature and density, and the optical properties of seawater required to estimate suspended sediment concentration. Water samples and bottom sediment grabs were also collected.

12.3 Data and Results

Chapter 3 displays the vertical structure of the salinity, temperature, and density acquired during the ship surveys. There is a very large seasonal cycle in temperature and a clear salinity cycle correlated with the river discharge. Minimum water temperatures were 3ºC to 5ºC, rising to 23ºC at the surface in the summer. Vertical gradients in temperature and density were largest at Stations

DOT5 and DOT6 in the summer. Winter and spring water temperatures are fairly uniform spatially, but horizontal gradients develop in the summer. Waters with the lowest salinity at the seafloor were observed on the south side of ELIS at Station DOT2 near Mattituck, New York. The data display the expected seasonal cycles and spatial structure and the observations of currents and stress are considered representative of the range of conditions expected in the area.

The measurements from the moored temperature and salinity sensors at the bottom (summarized in Chapter 5) complement the ship surveys and reveal the magnitude of the variation at higher frequency. Tidal currents then create oscillations in water temperatures due to horizontal advection and vertical mixing. These data will provide a critical assessment of the model performance.

The spatial and time variations of currents in the ZSF were surveyed while the ship was transiting between the stations where CTD profiles were required. These data are summarized in Chapter 4. Though these types of data are inherently noisy, they provide the only estimate of the magnitudes of the spatial gradients in current and, therefore, complement the time-series acquired by the moored instruments. A simple empirical analysis shows that the data are consistent with those of the moored instruments. Using the results of the moored current observations, it is shown in Chapter 6 that at all stations, except for Station DOT4, the flow at approximately 3 m above bottom was toward Long Island Sound. At Station DOT4 the mean flow was directed to the southwest toward Napeague Bay. Maximum current velocities near the seafloor were not very sensitive to season at the locations of the instruments. Maximum velocities reached 1.13 m/s at Station DOT2.

Close to the seabed (within 75 cm) current measurements were collected by the Nortek ADCPs (described in Chapter 7). Preliminary analyses indicate that the current patterns are dominantly tidal, with the M2 tidal constituent the largest at all sites, though a significant mean flow was observed. Derived bottom shear stresses were highly variable but correlated with the current magnitude. A wide range of conditions was observed as anticipated.

Surface wave observation were obtained from the bottom-mounted ADCPs (summarized in Chapter 8). These observations showed that Stations DOT4, 5 and 6, in Block Island Sound, are influenced by long-period waves from the Atlantic Ocean. Stations DOT1, 2, 3 and 7, in eastern Long Island Sound, are dominated more by the regional wind field. The wave data reveal that the observation campaigns captured a wide range of conditions with which to assess the model predictions.

The suspended sediment samples and optical attenuation, backscatter, and chlorophyll profiles from ship measurements allow for calculations of the distribution of particle concentrations by size classes. Preliminary analyses presented in Chapter 9 demonstrate that the larger particles are more prevalent in near-bottom samples, and in the summer there are high concentrations of organic-rich particles near the surface of the water column. Chapter 10 describes the bottom suspended sediment concentrations and variability at the seven mooring stations. The data show good agreement between the calibrated OBS3+ sensor concentrations and the concentrations based on water sample analyses. The screened and averaged data show consistent patterns across the eastern Long Island Sound and Block Island Sound and will be available for future modeling. The

characteristics of the bottom sediments at the mooring sites are summarized in Chapter 11.

12.4 Conclusion

The field program of the PO study provided a diverse data set for a wide range of conditions with which to evaluate the circulation model and support the designation of dredged material disposal sites.

References

Ackleson, S.G. 2006. Optical determinations of suspended sediment dynamics in western Long Island Sound and the Connecticut River plume. *J. Geophys. Res.* 111: C07009, doi:10.1029/2005JC003214.

Ackleson, S.G. and J. O'Donnell. 2011. Small-scale variability in suspended matter associated with the Connecticut River plume front. *J. Geophys. Res.* 116: C10013, doi:10.1029/2011JC007053.

Blott, S.J. and K. Pye. 2001. GRADISTAT: a grain size distribution and statistics package for the analysis of unconsolidated sediments. *Earth Surface Processes and Landforms* 26: 1237-1248.

Boss, E., W.S. Pegau, W.D. Gardner, J.R.V. Zaneveld, A.H. Barnard, M.S. Twardowski, G.C. Chang, and T.D. Dickey. 2001. Spectral particulate attenuation and particle size distribution in the bottom boundary layer of a continental shelf. *J. Geophys. Res.* 106: 9509-9516.

Boss, E., L. Taylor, S. Gilbert, K. Gundersen, N. Hawley, C. Janzen, T. Johengen, H. Purcell, C. Robertson, D.W. Schar, G.J. Smith, and M.N. Tamburri. 2009. Comparison of inherent optical properties as a surrogate for particulate matter concentration in coastal waters. *Limnol. Oceanogr.: Methods.* 7: 803-810.

Candela, J., R.C. Beardsley, and R. Limeburner. 1992. Separation of tidal and subtidal currents in ship-mounted acoustic Doppler current profiler observations. *J. Geophys. Res*. 97: 769–788.

Cheng, R.T., C-H Ling and J.W. Gartner. 1999. Estimates of bottom roughness length and bottom shear stress in South San Francisco Bay, California. *J. Geophys. Res.* 104: 7715-7728.

Diehl, P. and H. Haardt. 1980. Measurement of the spectral attenuation to support biological research in a “phytoplankton tube” experiment. *Oceanol. Acta* 3: 89-96.

Downing, J.P., Sternberg, R.W. and Lister, C.R.B., 1981. New Instrument for the Investigation of Sediment Suspension Processes in the Shallow Marine Environment. *Marine Geology*, 42, p. 19-34.

Kitchen, J.C., J.R.V. Zaneveld, and H. Pak. 1982. Effect of particle size distribution and chlorophyll content on beam attenuation spectra. *Appl. Opt.* 21: 3913-3918.

Lacy, J.R. and C.R. Sherwood. 2004. Accuracy of Pulse-Coherent Acoustic Doppler Profiler in a wave-dominated Flow. *J. Atmos. and Ocean Tech.* 21: 1448-1461.

Nortek. 2008. Aquadopp current profiler, User Guide. NortekAS. Vangkroken 2NO-1351 RUD, Norway. 86p.

Plumb, R.H., Jr. 1981. Procedure for Handling and Chemical Analysis of Sediment and Water Samples. Tech. Rep. EPA/CE-81-1. Prepared by Great Lakes Laboratory, State University College at Buffalo, Buffalo, NY, for the Environmental Protection Agency/U.S. Army Corps of Engineers Technical Committee on Criteria for Dredged and Fill Material. U.S. Army Engineer Waterways Experiment Station, Vicksburg, MS.

RDI (RD Instruments). 2008. WavesMon v3.04 User's Guide. Teledyne RD Instruments, Poway, California 92064, 62p.

Roesler, C.S. and A.H. Barnard. 2013. Optical proxy for phytoplankton biomass in the absence of phytophysiology: rethinking the absorption line height. *Methods in Oceanography. http://dx.doi.org/10.1016/j.mio.2013.12.003.*

Rusello, P.J. 2009. A practical primer for pulse coherent Instruments. Nortek Technical Note No.: TN-027. *http://www.nortek-as.com/lib/technical-notes/tn-027-pulse-coherent-primer*

Rusello, P.J. 2010. Aquadopp HR Profiler: Extended Velocity Range Mode, Nortek Technical Note No.: TN-028. *http://www.nortek-as.com/lib/technical-notes/tn-028-extended-velocity-range*

USEPA and USACE. 2004a. Final Environmental Impact Statement for the Designation of Dredged Material Disposal Sites in Central and Western Long Island Sound, Connecticut and New York. Prepared by the USEPA New England Region, in cooperation with the USACE New England District (April 2004).

USEPA and USACE. 2004b. Rhode Island Region Long-term Dredged Material Disposal Site Evaluation Project. Prepared by the USEPA New England Region, in cooperation with the USACE New England District (October 2004).

Wentworth, C.K. 1922. A scale of grade and class terms for clastic sediments. *Journal of Geology* 30: 377-392.

WETLabs, Inc. 2011. Ac Meter Protocol Document. Revision Q, 51p.

Zimmerman, C., Keefe, C.W., and Bashe, J., 1997. Method 440.0, Determination of Carbon and Nitrogen and Particulates of Estuarine/Coastal Waters Using Elemental Analysis. September 1997, National Exposure Research Laboratory, ORD, EPA, Cincinnati, Ohio.

Appendix 1

CRUISE SUMMARY REPORT

CRUISE CTDOT1: March 12-13, 2013

Appendix 1: Cruise 1

CT DOT - ELIS SEIS

Physical Data Collection in Eastern Long Island Sound
Deployment Cruise Summary: March 12-13, 2013
R/V Connecticut

Area of Operations

Eastern Long Island Sound, extending east from the Connecticut River to Block Island, within the area designated as the Zone of Siting Feasibility (ZSF).

Objectives

The objectives of the cruise were to deploy seven instrument frames, collect water samples, obtain bottom sediment grabs, and take CTD casts for the purpose of characterizing the spatial and temporal variations in hydrography, currents, and bottom stress.

Scientific Party

The scientific party included Kay Howard-Strobel, David Cohen, and Christian Fox, all from the University of Connecticut.

General Operations

Operations consisted of running two circuits of the seven designated moored instrument array locations and four additional CTD stations. Deployment of six instrument arrays with CTD casts and water samples, as well as the four additional sites was completed on the first circuit. The seventh frame was not deployed due to ADCP failure prior to the cruise, this frame will be deployed as soon as the ADCP is repaired. Water samples, CTD casts, and bottom grabs were obtained at the seventh site. The second circuit revisited all eleven stations with a CTD cast, water sample, and bottom sediment grab collected at each location.

Frame Deployments

Six frames were deployed this cruise at the locations listed in Table 1 and plotted in Figure 1. The seventh frame was held for deployment until an RDI ADCP that failed testing was to be returned. However, the repair was expected to take up to 6 weeks, so the seventh frame was deployed on March 29th, without the RDI ADCP, from the RV Weicker. Instrumentation on each frame included a downward looking Nortek Aquadopp 2Hz high resolution pulse coherent current profiler (Figure 2a) with two Campbell Scientific OBS3+ optical backscatter units (Figure 2b), an upward-looking RDI acoustic Doppler current profiler (ADCP) with waves array sampling enabled (Figure 2a), and a Sea-Bird Electronics Model SMP37 conductivity/temperature

sensor(Figure 2c). The height of the base of the RDI ADCP above bottom is 1.5 meters and the height of the Nortek Aquadopp above the bottom is 0.75 meters. The OBS3+ backscatter units are mounted at 30 and 80 cm above the bottom. The seventh frame (DOT7) also carried two WET Labs EcoTriplet backscatter units (Figure 2c) sampling at 470, 532 and 660 nm. Table 1 documents the specifics for each instrument on each frame. The deployment configuration files (*.whp) file for each RDI ADCP are located in Appendix A. Appendix B and Appendix C contain the log files for each Nortek Aquadopp HR and Sea-Bird SMP37 configuration, respectively.

ADCP Operations

The ship-board ADCP (RD Instruments, 600 kHz) was started once the RV Connecticut was underway from Avery Point. VmDas (RD Instruments, Vessel Mounted Data Acquisition System) software was used to setup and run the ADCP. The ADCP was run continuously throughout the survey cruise. Figure 1 shows the survey track with the seven moored station locations and four additional CTD stations superimposed. Ten files are generated each time an ADCP VmDas session is started, and within that session there are multiple file segments created depending on the data size limit that was set in the VmDas options. This ensures that a significant amount of data is not lost if there is a catastrophic failure of the instrument. The default file size 1.38 MB. The naming convention of the ADCP data files is as follows:

ADCP001_000000.ENR, .ENS, .ENX, .LOG, .LTA, .N1R, .N2R, .NMS, .STA, .VMO
ADCP001_000001.ENR, …
ADCP001_000002.ENR, …
.
.
.
ADCP017_000006.ENR, …

Example: ADCP017_000006.ENR; 17 is the session number incremented when the instrument is stopped and started, 6 is the file segment number incremented every 1.38 MB.

The file types and extensions generated by VmDas are as follows:

*.ENR - Raw binary ADCP data file which contains every ping
*.ENS - Binary ADCP data after the data has been screening for backscatter and correlation
*.ENX - Binary ADCP data after screening and rotation to earth coordinates
*.STA - Binary ADCP ensemble data that has been averaged into short term averages
*.LTA - Binary ADCP ensemble data that has been averaged into long term averages
*.N1R - Raw NMEA ASCII data from the primary navigation source
*.N2R - Raw NMEA ASCII data from the secondary navigation source, if available

*.NMS - Binary screened and averaged navigation data
.VMO - ASCII file copy of the.ini options file that was used during the data collection
*.LOG - ASCII file containing a log of any errors the ADCP detected during the session

The ADCP was set to ping as fast as possible (0.3 secs/ping), with 50 bins, 1 ping/ensemble and 1 meter bins. The transducer depth was at 1.5 meters and the blanking distance was 0.88 meters. There are 54 raw ensemble ADCP data files (*.ENR) encompassing approximately 40 hours.

Files are currently located on UConn's FTP server:
/d2/dot/vmdasSurveys/vmdas ELIS CTDOT March2013

CTD Operations

A SeaBird Electronics Model 9 CTD with a Model 11 deck unit (Figure 3a) was used for the collection of the salinity and temperature profiles at each of the seven moored instrument stations and at four additional stations designated for CTD casts (Figure 1). On Day 1 of the survey cruise a SBE 19+ was used to acquire the CTD data at two of the stations (see Table 2) as the sea state was deemed too rough to safely use the SBE911. The SBE19+ was hand lowered off the stern. Latitude and longitude for each station profiled are presented in Table 1. The naming convention utilized for the CTD data files is as follows:

Example: dotXcastY.hex or ctdXcastY.hex

dot prefix indicates a moored instrument array station
ctd prefix indicates a CTD only station, no moored instruments
X is the station ID
Y is the cast number; 2 casts were taken each station
.hex is the native SBE CTD raw file format

When the file has been processed using the proprietary data processing program provided by SeaBird, the file extension becomes *.cnv. A "d" will be prepended if the cast is a downcast only, a "u" will be prepended if the cast is an upcast only. The data processing program also appends to the original file name, in order, the type of post-processing performed.

Example: ddot7cast1filtloopderivesplited.cnv

ddot is the downcast only
7 is the station ID
1 is the cast number
filt – the raw data was filtered using the SBE Data Processing filter module
loop – cast reversals were eliminated using the SBE Data Processing loop module

derive – salinity, density, depth were derived from the post-processed data
split – the cast was split into downcast and upcast
ed – the post-processed cast was edited manually if needed to remove any other errors or outliers

Files are currently located on UConn's FTP server:
/d2/dot/ctdSurveys/March2013

Water Sample Collection

A 5 liter Niskin bottle (Figure 3b) was used to collect 1000 mL of sample water to be filtered for suspended sediment concentration. The Niskin bottle was deployed using the RV Connecticut's A-frame. The Niskin was lowered to the bottom and then raised one meter. Approximately one minute was allowed to pass so that any sediment suspended by the bottle weight was carried away by currents before sending the messenger down the line to trigger the Niskin. The samples were labeled and refrigerated at 4°C immediately upon collection. Samples were collected at all stations on both survey loops.

Bottom Sediment Grabs

A modified Van-Veen type surface sediment grab (Figure 3c) was used to collect bottom sediment samples for analysis of sand to mud ratios. The grab was deployed using the RV Connecticut's A-frame. After retrieval of a bottom sediment sample, a scoop was used to transfer approximately 2000 grams to a one gallon Ziploc bag, which was then labeled and refrigerated at 4°C. Bottom grabs were collected at all stations on the second survey loop only.

Table 1. Mooring Instrumentation.

Station	Lat	Lon	Depth (m)	SBE37 SN	ADCP SN	ADCP kHz	AQD SN	AQD Press	OBS3+ SN
DOT1	41 12.00	72 24.01	36.6	9693	195	300	8456	100	T8838,T8834
DOT2	41 08.96	72 22.20	30.5	9694	7660	600	8428	50	T8727,T8835
DOT3	41 15.49	72 14.53	27.1	9695	1349	300	8445	100	T8863, T8861
DOT4	41 08.99	72 00.01	22.9	9696	13197	600	8438	50	T8862,T8872
DOT5	41 09.01	71 45.01	30.5	9673	6615	600	8453	50	T8782,T8837
DOT6	41 15.00	71 48.02	33.5	9674	1094	600	8455	50	T8874,T8871
DOT7*	41 15.65	72 06.02	45.7	10237	1113	300	8432	100	T8786,T8783

*DOT7 also equipped with two ECO Triplets: SN191 and SN321

Figure 1. Locations of moored instrument arrays (DOT1-DOT7) and CTD profiles (CTD8-CTD11). LEDG is UConn's New London Ledge Light meteorological station and ELIS is UConn's metocean observation buoy. White line delineates the survey tracks for both days.

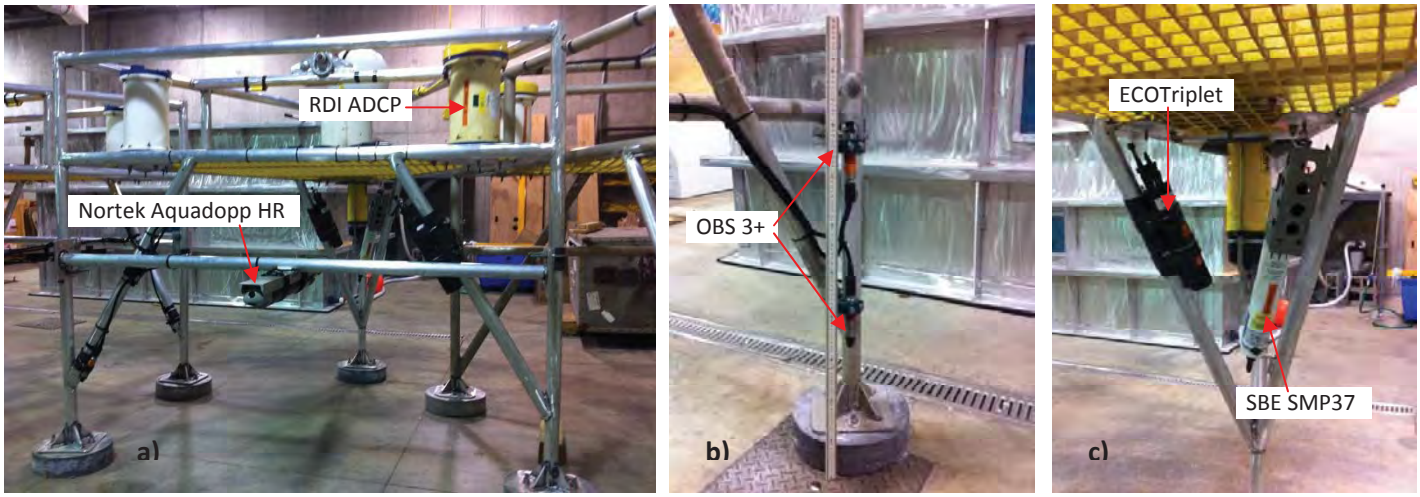

Figure 2. a) instrument mooring, b) OBS3+ mounts, c) WETLabs ECOTriplet mount and SBE SMP37 CT sensor.

Table 2. CTD Station Locations.

Date/Time (EST)	CTD Filename	Latitude (DDM)	Longitude (DDM)	Depth (m)	Notes
12-Mar-13 08:00	dot6cast1	41 15.000	71 48.020	35.0	
12-Mar-13 09:21	ctd10cast1	41 16.201	71 36.003	39.0	
12-Mar-13 10:35	ctd9cast1	41 08.992	71 39.005	18.4	
12-Mar-13 11:21	dot5cast1	41 09.090	71 45.056	30.0	
12-Mar-13 13:24	ctd8cast1	41 04.802	71 49.859	15.0	19+
12-Mar-13 14:53	dot4cast1	41 09.014	72 00.006	23.0	
12-Mar-13 16:57	ctd11cast2	41 13.761	72 03.710	14.5	19+
12-Mar-13 19:13	dot2cast1	41 08.941	72 22.140	32.0	
12-Mar-13 20:27	dot1cast1	41 12.083	72 24.131	43.0	
12-Mar-13 21:48	dot3cast1	41 15.477	72 14.556	30.0	
12-Mar-13 23:10	dot7cast1	41 75.616	72 05.946	48.0	
13-Mar-13 05:22	dot7cast2	41 15.570	72 06.066	46.0	
13-Mar-13 06:39	dot3cast2	41 15.462	72 14.521	29.0	
13-Mar-13 07:57	dot1cast2	41 12.014	72 24.042	42.0	
13-Mar-13 08:57	dot2cast2	41 08.950	72 22.177	30.0	
13-Mar-13 11:36	ctd11cast3	41 13.791	72 03.645	18.5	
13-Mar-13 12:39	dot4cast2	41 09.003	72 59.916	22.5	
13-Mar-13 13:59	ctd8cast2	41 04.785	71 49.820	13.5	
13-Mar-13 15:15	dot5cast2	41 08.890	71 44.928	29.0	
13-Mar-13 16:18	ctd9cast2	41 08.916	71 39.978	22.0	
13-Mar-13 17:35	ctd10cast2	41 16.211	71 35.968	38.0	
13-Mar-13 19:08	dot6cast2	41 14.970	71 47.963	37.2	
29-Mar-13 09:22	dot7cast3	41 15.643	72 05.983	45.7	19+

Notes: 19+, seas too rough to deploy SBE911, a SBE19+ hand lowered.

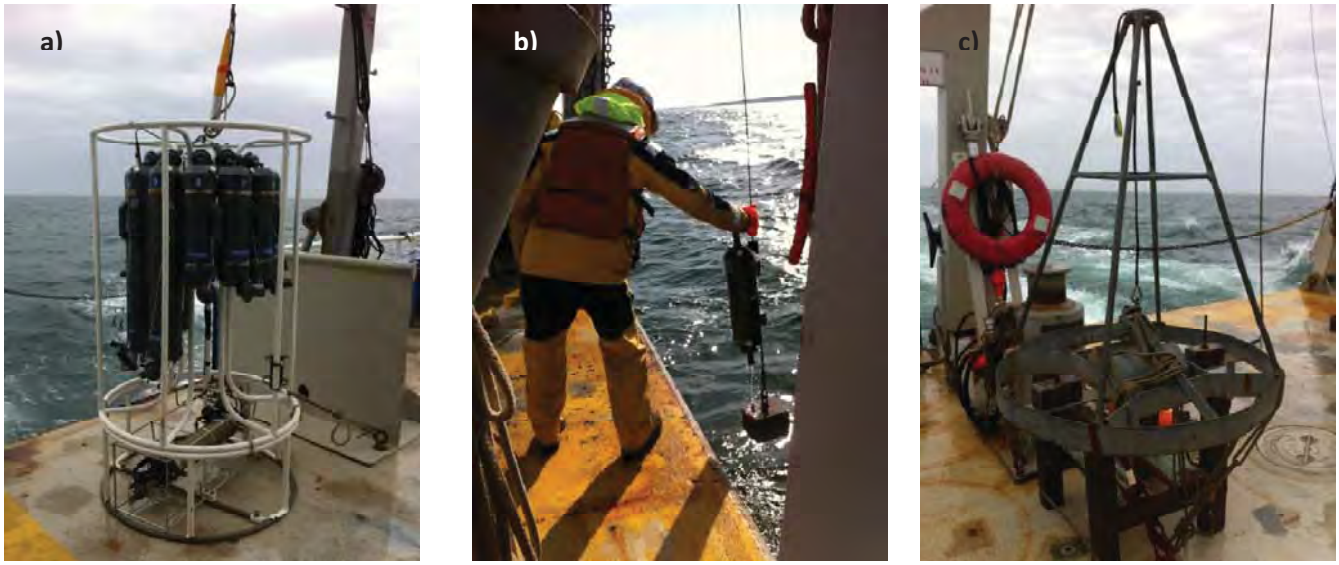

Figure 3. a) SBE 911 CTD, b) Niskin 5L water sampler, c) modified Van-Veen type bottom grab sampler.

Appendices

Appendix A contains RDI ADCP configuration files.

Appendix B includes the Nortek Aquadopp HR configuration files.

Appendix C includes the SBE SMP37 setup files.

Appendix D is a scanned copy of the field notebook.

Appendix A

RDI ADCP Configuration Files

DOT Frame 1

```
CR1
CF11101
EA0
EB0
ED370
ES30
EX11111
EZ1111101
WA255
WB0
WD111100000
WF50
WN40
WP180
WS100
WV175
HD111000000
HB5
HP2400
HR00:30:00.00
HT00:00:00.50
TE00:15:00.00
TP00:01.00
TF13/03/11 06:00:00
RNDOT1_
CK
CS
;
;Instrument         = Workhorse Sentinel
;Frequency          = 307200
;Water Profile      = YES
;Bottom Track       = NO
;High Res. Modes    = NO
;High Rate Pinging  = NO
;Shallow Bottom Mode= NO
;Wave Gauge         = YES
;Lowered ADCP       = NO
;Ice Track          = NO
;Surface Track      = NO
;Beam angle         = 20
;Temperature        = 5.00
;Deployment hours   = 720.00
;Battery packs      = 3
;Automatic TP       = NO
;Memory size [MB]   = 2048
;Saved Screen       = 1
;
;Consequences generated by PlanADCP version 2.06:
;First cell range   = 1.95 m
;Last cell range    = 40.95 m
;Max range          = 86.38 m
;Standard deviation = 1.01 cm/s
;Ensemble size      = 954 bytes
;Storage required   = 259.81 MB (272430720 bytes)
;Power usage        = 1051.06 Wh
;Battery usage      = 2.3
;Samples / Wv Burst = 2400
;Min NonDir Wave Per= 2.84 s
;Min Dir Wave Period= 4.79 s
;Bytes / Wave Burst = 187280
;
; WARNINGS AND CAUTIONS:
; Waves Gauge feature has to be installed in Workhorse to use selected option.
; Advanced settings have been changed.
; Expert settings have been changed.
```

DOT Frame 2

```
CR1
CF11101
EA0
EB0
ED330
ES30
EX11111
EZ1111101
WA255
WB0
WD111100000
WF30
WN71
WP180
WS50
WV175
HD111000000
HB5
HP2400
HR00:30:00.00
HT00:00:00.50
TE00:15:00.00
TP00:01.00
TF13/03/11 06:00:00
RNDOT2_
CK
CS
;
;Instrument         = Workhorse Sentinel
;Frequency          = 614400
;Water Profile      = YES
;Bottom Track       = NO
;High Res. Modes    = NO
;High Rate Pinging  = NO
;Shallow Bottom Mode= NO
;Wave Gauge         = YES
;Lowered ADCP       = NO
;Ice Track          = NO
;Surface Track      = NO
;Beam angle         = 20
;Temperature        = 5.00
;Deployment hours   = 720.00
;Battery packs      = 3
;Automatic TP       = NO
;Memory size [MB]   = 304
;Saved Screen       = 2
;
;Consequences generated by PlanADCP version 2.06:
;First cell range   = 1.02 m
;Last cell range    = 36.02 m
;Max range          = 38.74 m
;Standard deviation = 1.02 cm/s
;Ensemble size      = 1574 bytes
;Storage required   = 261.51 MB (274216320 bytes)
;Power usage        = 965.68 Wh
;Battery usage      = 2.1
;Samples / Wv Burst = 2400
;Min NonDir Wave Per= 2.69 s
;Min Dir Wave Period= 4.52 s
;Bytes / Wave Burst = 187280
;
; WARNINGS AND CAUTIONS:
; Waves Gauge feature has to be installed in Workhorse to use selected option.
; Advanced settings have been changed.
; Expert settings have been changed.
```

DOT Frame 3

```
CR1
CF11101
EA0
EB0
ED270
ES30
EX11111
EZ1111101
WA255
WB0
WD111100000
WF50
WN32
WP180
WS100
WV175
HD111000000
HB5
HP2400
HR00:30:00.00
HT00:00:00.50
TE00:15:00.00
TP00:01.00
TF13/03/11 06:00:00
RNDOT3_
CK
CS
;
;Instrument         = Workhorse Sentinel
;Frequency          = 307200
;Water Profile      = YES
;Bottom Track       = NO
;High Res. Modes    = NO
;High Rate Pinging  = NO
;Shallow Bottom Mode= NO
;Wave Gauge         = YES
;Lowered ADCP       = NO
;Ice Track          = NO
;Surface Track      = NO
;Beam angle         = 20
;Temperature        = 5.00
;Deployment hours   = 720.00
;Battery packs      = 3
;Automatic TP       = NO
;Memory size [MB]   = 4000
;Saved Screen       = 1
;
;Consequences generated by PlanADCP version 2.06:
;First cell range   = 1.95 m
;Last cell range    = 32.95 m
;Max range          = 86.34 m
;Standard deviation = 1.01 cm/s
;Ensemble size      = 794 bytes
;Storage required   = 259.37 MB (271969920 bytes)
;Power usage        = 989.88 Wh
;Battery usage      = 2.2
;Samples / Wv Burst = 2400
;Min NonDir Wave Per= 2.48 s
;Min Dir Wave Period= 4.09 s
;Bytes / Wave Burst = 187280
;
; WARNINGS AND CAUTIONS:
; Waves Gauge feature has to be installed in Workhorse to use selected option.
; Advanced settings have been changed.
; Expert settings have been changed.
```

DOT Frame 4

```
CR1
CF11101
EA0
EB0
ED260
ES30
EX11111
EZ1111101
WA255
WB0
WD111100000
WF30
WN59
WP180
WS50
WV175
HD111000000
HB5
HP2400
HR00:30:00.00
HT00:00:00.50
TE00:15:00.00
TP00:01.00
TF13/03/11 06:00:00
RNDOT4_
CK
CS
;
;Instrument         = Workhorse Sentinel
;Frequency          = 614400
;Water Profile      = YES
;Bottom Track       = NO
;High Res. Modes    = NO
;High Rate Pinging  = NO
;Shallow Bottom Mode= NO
;Wave Gauge         = YES
;Lowered ADCP       = NO
;Ice Track          = NO
;Surface Track      = NO
;Beam angle         = 20
;Temperature        = 5.00
;Deployment hours   = 720.00
;Battery packs      = 3
;Automatic TP       = NO
;Memory size [MB]   = 1221
;Saved Screen       = 3
;
;Consequences generated by PlanADCP version 2.06:
;First cell range   = 1.02 m
;Last cell range    = 30.02 m
;Max range          = 38.73 m
;Standard deviation = 1.02 cm/s
;Ensemble size      = 1334 bytes
;Storage required   = 260.85 MB (273525120 bytes)
;Power usage        = 893.16 Wh
;Battery usage      = 2.0
;Samples / Wv Burst = 2400
;Min NonDir Wave Per= 2.44 s
;Min Dir Wave Period= 4.01 s
;Bytes / Wave Burst = 187280
;
; WARNINGS AND CAUTIONS:
; Waves Gauge feature has to be installed in Workhorse to use selected option.
; Advanced settings have been changed.
; Expert settings have been changed.
```

DOT Frame 5

```
CR1
CF11101
EA0
EB0
ED330
ES30
EX11111
EZ1111101
WA255
WB0
WD111100000
WF30
WN71
WP180
WS50
WV175
HD111000000
HB5
HP2400
HR00:30:00.00
HT00:00:00.50
TE00:15:00.00
TP00:01.00
TF13/03/11 06:00:00
RNDOT5_
CK
CS
;
;Instrument         = Workhorse Sentinel
;Frequency          = 614400
;Water Profile      = YES
;Bottom Track       = NO
;High Res. Modes    = NO
;High Rate Pinging  = NO
;Shallow Bottom Mode= NO
;Wave Gauge         = YES
;Lowered ADCP       = NO
;Ice Track          = NO
;Surface Track      = NO
;Beam angle         = 20
;Temperature        = 5.00
;Deployment hours   = 720.00
;Battery packs      = 3
;Automatic TP       = NO
;Memory size [MB]   = 975
;Saved Screen       = 2
;
;Consequences generated by PlanADCP version 2.06:
;First cell range   = 1.02 m
;Last cell range    = 36.02 m
;Max range          = 38.74 m
;Standard deviation = 1.02 cm/s
;Ensemble size      = 1574 bytes
;Storage required   = 261.51 MB (274216320 bytes)
;Power usage        = 965.68 Wh
;Battery usage      = 2.1
;Samples / Wv Burst = 2400
;Min NonDir Wave Per= 2.69 s
;Min Dir Wave Period= 4.52 s
;Bytes / Wave Burst = 187280
;
; WARNINGS AND CAUTIONS:
; Waves Gauge feature has to be installed in Workhorse to use selected option.
; Advanced settings have been changed.
; Expert settings have been changed.
```

DOT Frame 6

```
CR1
CF11101
EA0
EB0
ED360
ES30
EX11111
EZ1111101
WA255
WB0
WD111100000
WF30
WN40
WP180
WS100
WV175
HD111000000
HB5
HP2400
HR00:30:00.00
HT00:00:00.50
TE00:15:00.00
TP00:01.00
TF13/03/11 06:00:00
RNDOT6_
CK
CS
;
;Instrument         = Workhorse Sentinel
;Frequency          = 614400
;Water Profile      = YES
;Bottom Track       = NO
;High Res. Modes    = NO
;High Rate Pinging  = NO
;Shallow Bottom Mode= NO
;Wave Gauge         = YES
;Lowered ADCP       = NO
;Ice Track          = NO
;Surface Track      = NO
;Beam angle         = 20
;Temperature        = 5.00
;Deployment hours   = 792.00
;Battery packs      = 3
;Automatic TP       = NO
;Memory size [MB]   = 2048
;Saved Screen       = 1
;
;Consequences generated by PlanADCP version 2.06:
;First cell range   = 1.52 m
;Last cell range    = 40.52 m
;Max range          = 42.66 m
;Standard deviation = 0.52 cm/s
;Ensemble size      = 954 bytes
;Storage required   = 285.79 MB (299673792 bytes)
;Power usage        = 958.35 Wh
;Battery usage      = 2.1
;Samples / Wv Burst = 2400
;Min NonDir Wave Per= 2.80 s
;Min Dir Wave Period= 4.72 s
;Bytes / Wave Burst = 187280
;
; WARNINGS AND CAUTIONS:
; Waves Gauge feature has to be installed in Workhorse to use selected option.
; Advanced settings have been changed.
; Expert settings have been changed.
```

DOT Frame 7

```
CR1
CF11101
EA0
EB0
ED460
ES30
EX11111
EZ1111101
WA255
WB0
WD111100000
WF50
WN49
WP180
WS100
WV175
HD111000000
HB5
HP2400
HR00:40:00.00
HT00:00:00.50
TE00:15:00.00
TP00:01.00
TF13/03/11 06:00:00
RNDOT7_
CK
CS
;
;Instrument         = Workhorse Sentinel
;Frequency          = 307200
;Water Profile      = YES
;Bottom Track       = NO
;High Res. Modes    = NO
;High Rate Pinging  = NO
;Shallow Bottom Mode= NO
;Wave Gauge         = YES
;Lowered ADCP       = NO
;Ice Track          = NO
;Surface Track      = NO
;Beam angle         = 20
;Temperature        = 5.00
;Deployment hours   = 720.00
;Battery packs      = 3
;Automatic TP       = NO
;Memory size [MB]   = 2048
;Saved Screen       = 2
;
;Consequences generated by PlanADCP version 2.06:
;First cell range   = 1.95 m
;Last cell range    = 49.95 m
;Max range          = 86.41 m
;Standard deviation = 1.01 cm/s
;Ensemble size      = 1134 bytes
;Storage required   = 196.01 MB (205528320 bytes)
;Power usage        = 879.34 Wh
;Battery usage      = 2.0
;Samples / Wv Burst = 2400
;Min NonDir Wave Per= 3.17 s
;Min Dir Wave Period= 5.34 s
;Bytes / Wave Burst = 187280
;
; WARNINGS AND CAUTIONS:
; Waves Gauge feature has to be installed in Workhorse to use selected option.
; Advanced settings have been changed.
; Expert settings have been changed.
```

Appendix B

Nortek Aquadopp HR Configuration Files

```
============================================================
Deployment   : dot1
Current time : 3/7/2013 8:10:33 PM
Start at     : 3/11/2013 6:00:00 AM
Comment:
DOT1 - March 11 2011 deployment
------------------------------------------------------------
Measurement interval  (s) : 1200
Cell size            (mm) : 37
Orientation               : DOWNLOOKING
Distance to bottom    (m) : 0.75
Pulse distance        (m) : 0.84
Profile range         (m) : 0.74
Horiz. vel. range   (m/s) : 1.10
Vert. vel. range    (m/s) : 0.46
Number of cells           : 20
Average interval      (s) : 1
Blanking distance     (m) : 0.050
Measurement load      (%) : 20
Samples per burst         : 2048
Sampling rate        (Hz) : 4
Compass upd. rate     (s) : 1
Coordinate System         : Beam
Speed of sound      (m/s) : MEASURED
Salinity            (ppt) : 30
Analog input 1            : PROFILE
Analog input 2            : PROFILE
Analog input power out    : ENABLED
File wrapping             : OFF
TellTale                  : OFF
Acoustic modem            : OFF
Serial output             : OFF
Baud rate                 : 115200
------------------------------------------------------------
Assumed duration   (days) : 30.0
Battery utilization   (%) : 52.0
Battery level         (V) : 11.1
Recorder size        (MB) : 3886
Recorder free space  (MB) : 3885.972
Memory required      (MB) : 1248.8
------------------------------------------------------------
Instrument ID             : AQD 8456
Head ID                   : ASP 5868
Firmware version          : 3.14 HR
ProLog ID                 : 786
ProLog firmware version   : 4.14
------------------------------------------------------------
SD Card Inserted          : YES
SD Card Ready             : YES
SD Card Write protected   : NO
SD Card Type              : SDHC
SD Card Supported         : YES
------------------------------------------------------------
AquaProHR Version 1.10.08
Copyright (C) Nortek AS
============================================================
```

```
============================================================
Deployment   : dot2
Current time : 3/7/2013 8:26:14 PM
Start at     : 3/11/2013 6:00:00 AM
Comment:
DOT 2 - March 11 2011 deployment
------------------------------------------------------------
Measurement interval  (s) : 1200
Cell size            (mm) : 37
Orientation               : DOWNLOOKING
Distance to bottom    (m) : 0.75
Pulse distance        (m) : 0.84
Profile range         (m) : 0.74
Horiz. vel. range   (m/s) : 1.10
Vert. vel. range    (m/s) : 0.46
Number of cells           : 20
Average interval      (s) : 1
Blanking distance     (m) : 0.050
Measurement load      (%) : 20
Samples per burst         : 2048
Sampling rate        (Hz) : 4
Compass upd. rate     (s) : 1
Coordinate System         : Beam
Speed of sound      (m/s) : MEASURED
Salinity            (ppt) : 30
Analog input 1            : PROFILE
Analog input 2            : PROFILE
Analog input power out    : ENABLED
File wrapping             : OFF
TellTale                  : OFF
Acoustic modem            : OFF
Serial output             : OFF
Baud rate                 : 115200
------------------------------------------------------------
Assumed duration   (days) : 30.0
Battery utilization   (%) : 52.0
Battery level         (V) : 11.1
Recorder size        (MB) : 3886
Recorder free space  (MB) : 3885.972
Memory required      (MB) : 1248.8
------------------------------------------------------------
Instrument ID             : AQD 8428
Head ID                   : ASP 5866
Firmware version          : 3.14 HR
ProLog ID                 : 763
ProLog firmware version   : 4.14
------------------------------------------------------------
SD Card Inserted          : YES
SD Card Ready             : YES
SD Card Write protected   : NO
SD Card Type              : SDHC
SD Card Supported         : YES
------------------------------------------------------------
AquaProHR Version 1.10.08
Copyright (C) Nortek AS
============================================================
```

```
============================================================
Deployment   : dot3
Current time : 3/7/2013 8:17:23 PM
Start at     : 3/11/2013 6:00:00 AM
Comment:
DOT3 - March 11 2011 deployment
------------------------------------------------------------
Measurement interval  (s) : 1200
Cell size            (mm) : 37
Orientation               : DOWNLOOKING
Distance to bottom    (m) : 0.75
Pulse distance        (m) : 0.84
Profile range         (m) : 0.74
Horiz. vel. range   (m/s) : 1.10
Vert. vel. range    (m/s) : 0.46
Number of cells           : 20
Average interval      (s) : 1
Blanking distance     (m) : 0.050
Measurement load      (%) : 20
Samples per burst         : 2048
Sampling rate        (Hz) : 4
Compass upd. rate     (s) : 1
Coordinate System         : Beam
Speed of sound      (m/s) : MEASURED
Salinity            (ppt) : 30
Analog input 1            : PROFILE
Analog input 2            : PROFILE
Analog input power out    : ENABLED
File wrapping             : OFF
TellTale                  : OFF
Acoustic modem            : OFF
Serial output             : OFF
Baud rate                 : 115200
------------------------------------------------------------
Assumed duration   (days) : 30.0
Battery utilization   (%) : 52.0
Battery level         (V) : 11.0
Recorder size        (MB) : 3886
Recorder free space  (MB) : 3885.972
Memory required      (MB) : 1248.8
------------------------------------------------------------
Instrument ID             : AQD 8445
Head ID                   : ASP 5867
Firmware version          : 3.14 HR
ProLog ID                 : 766
ProLog firmware version   : 4.14
------------------------------------------------------------
SD Card Inserted          : YES
SD Card Ready             : YES
SD Card Write protected   : NO
SD Card Type              : SDHC
SD Card Supported         : YES
------------------------------------------------------------
AquaProHR Version 1.10.08
Copyright (C) Nortek AS
============================================================
```

```
============================================================
Deployment   : dot4
Current time : 3/7/2013 8:03:32 PM
Start at     : 3/11/2013 6:00:00 AM
Comment:
DOT4 - March 11 2011 deployment
------------------------------------------------------------
Measurement interval  (s) : 1200
Cell size            (mm) : 37
Orientation               : DOWNLOOKING
Distance to bottom    (m) : 0.75
Pulse distance        (m) : 0.84
Profile range         (m) : 0.74
Horiz. vel. range   (m/s) : 1.10
Vert. vel. range    (m/s) : 0.46
Number of cells           : 20
Average interval      (s) : 1
Blanking distance     (m) : 0.050
Measurement load      (%) : 20
Samples per burst         : 2048
Sampling rate        (Hz) : 4
Compass upd. rate     (s) : 1
Coordinate System         : Beam
Speed of sound      (m/s) : MEASURED
Salinity            (ppt) : 30
Analog input 1            : PROFILE
Analog input 2            : PROFILE
Analog input power out    : ENABLED
File wrapping             : OFF
TellTale                  : OFF
Acoustic modem            : OFF
Serial output             : OFF
Baud rate                 : 115200
------------------------------------------------------------
Assumed duration   (days) : 30.0
Battery utilization   (%) : 52.0
Battery level         (V) : 11.1
Recorder size        (MB) : 3886
Recorder free space  (MB) : 3885.972
Memory required      (MB) : 1248.8
------------------------------------------------------------
Instrument ID             : AQD 8438
Head ID                   : ASP 5865
Firmware version          : 3.14 HR
ProLog ID                 : 791
ProLog firmware version   : 4.14
------------------------------------------------------------
SD Card Inserted          : YES
SD Card Ready             : YES
SD Card Write protected   : NO
SD Card Type              : SDHC
SD Card Supported         : YES
------------------------------------------------------------
AquaProHR Version 1.10.08
Copyright (C) Nortek AS
============================================================
```

```
============================================================
Deployment   : dot5
Current time : 3/7/2013 7:59:44 PM
Start at     : 3/11/2013 6:00:00 AM
Comment:
DOT5 - March 11 2011 deployment
------------------------------------------------------------
Measurement interval  (s) : 1200
Cell size            (mm) : 37
Orientation               : DOWNLOOKING
Distance to bottom    (m) : 0.75
Pulse distance        (m) : 0.84
Profile range         (m) : 0.74
Horiz. vel. range   (m/s) : 1.10
Vert. vel. range    (m/s) : 0.46
Number of cells           : 20
Average interval      (s) : 1
Blanking distance     (m) : 0.050
Measurement load      (%) : 20
Samples per burst         : 2048
Sampling rate        (Hz) : 4
Compass upd. rate     (s) : 1
Coordinate System         : Beam
Speed of sound      (m/s) : MEASURED
Salinity            (ppt) : 30
Analog input 1            : PROFILE
Analog input 2            : PROFILE
Analog input power out    : ENABLED
File wrapping             : OFF
TellTale                  : OFF
Acoustic modem            : OFF
Serial output             : OFF
Baud rate                 : 115200
------------------------------------------------------------
Assumed duration   (days) : 30.0
Battery utilization   (%) : 52.0
Battery level         (V) : 11.0
Recorder size        (MB) : 3886
Recorder free space  (MB) : 3885.972
Memory required      (MB) : 1248.8
------------------------------------------------------------
Instrument ID             : AQD 8453
Head ID                   : ASP 5684
Firmware version          : 3.14 HR
ProLog ID                 : 762
ProLog firmware version   : 4.14
------------------------------------------------------------
SD Card Inserted          : YES
SD Card Ready             : YES
SD Card Write protected   : NO
SD Card Type              : SDHC
SD Card Supported         : YES
------------------------------------------------------------
AquaProHR Version 1.10.08
Copyright (C) Nortek AS
============================================================
```

```
============================================================
Deployment   : dot6
Current time : 3/7/2013 8:06:55 PM
Start at     : 3/11/2013 6:00:00 AM
Comment:
DOT6 - March 11 2011 deployment
------------------------------------------------------------
Measurement interval  (s) : 1200
Cell size            (mm) : 37
Orientation               : DOWNLOOKING
Distance to bottom    (m) : 0.75
Pulse distance        (m) : 0.84
Profile range         (m) : 0.74
Horiz. vel. range   (m/s) : 1.10
Vert. vel. range    (m/s) : 0.46
Number of cells           : 20
Average interval      (s) : 1
Blanking distance     (m) : 0.050
Measurement load      (%) : 20
Samples per burst         : 2048
Sampling rate        (Hz) : 4
Compass upd. rate     (s) : 1
Coordinate System         : Beam
Speed of sound      (m/s) : MEASURED
Salinity            (ppt) : 30
Analog input 1            : PROFILE
Analog input 2            : PROFILE
Analog input power out    : ENABLED
File wrapping             : OFF
TellTale                  : OFF
Acoustic modem            : OFF
Serial output             : OFF
Baud rate                 : 115200
------------------------------------------------------------
Assumed duration   (days) : 30.0
Battery utilization   (%) : 52.0
Battery level         (V) : 11.0
Recorder size        (MB) : 3886
Recorder free space  (MB) : 3885.972
Memory required      (MB) : 1248.8
------------------------------------------------------------
Instrument ID             : AQD 8455
Head ID                   : ASP 5864
Firmware version          : 3.14 HR
ProLog ID                 : 730
ProLog firmware version   : 4.14
------------------------------------------------------------
SD Card Inserted          : YES
SD Card Ready             : YES
SD Card Write protected   : NO
SD Card Type              : SDHC
SD Card Supported         : YES
------------------------------------------------------------
AquaProHR Version 1.10.08
Copyright (C) Nortek AS
============================================================
```

```
==============================================================
Deployment   : dot7
Current time : 3/28/2013 6:30:48 PM
Start at     : 3/29/2013 6:00:00 AM
Comment:
DOT7 - March 29 2013 deployment
--------------------------------------------------------------
Measurement interval  (s) : 1200
Cell size            (mm) : 37
Orientation               : DOWNLOOKING
Distance to bottom    (m) : 0.75
Pulse distance        (m) : 0.84
Profile range         (m) : 0.74
Horiz. vel. range   (m/s) : 1.10
Vert. vel. range    (m/s) : 0.46
Number of cells           : 20
Average interval      (s) : 1
Blanking distance     (m) : 0.050
Measurement load      (%) : 20
Samples per burst         : 2048
Sampling rate        (Hz) : 4
Compass upd. rate     (s) : 1
Coordinate System         : Beam
Speed of sound      (m/s) : MEASURED
Salinity            (ppt) : 30
Analog input 1            : PROFILE
Analog input 2            : PROFILE
Analog input power out    : ENABLED
File wrapping             : OFF
TellTale                  : OFF
Acoustic modem            : OFF
Serial output             : OFF
Baud rate                 : 115200
--------------------------------------------------------------
Assumed duration   (days) : 30.0
Battery utilization   (%) : 52.0
Battery level         (V) : 11.1
Recorder size        (MB) : 3886
Recorder free space  (MB) : 3885.972
Memory required      (MB) : 1248.8
--------------------------------------------------------------
Instrument ID             : AQD 8432
Head ID                   : ASP 5869
Firmware version          : 3.14 HR
ProLog ID                 : 754
ProLog firmware version   : 4.14
--------------------------------------------------------------
SD Card Inserted          : YES
SD Card Ready             : YES
SD Card Write protected   : NO
SD Card Type              : SDHC
SD Card Supported         : YES
--------------------------------------------------------------
AquaProHR Version 1.10.08
Copyright (C) Nortek AS
==============================================================
```

Appendix C

Sea-Bird Electronics SMP37 Configuration Files

```
DOT1
<Executed/>
ds
SBE37SM-RS232 v4.1  SERIAL NO. 9693  07 Mar 2013 18:41:44
vMain = 13.43, vLith =  3.10
samplenumber = 0, free = 559240
not logging, stop command
sample interval = 900 seconds
data format = converted engineering
output salinity
transmit real-time = yes
sync mode = no
pump installed = yes, minimum conductivity frequency = 3148.2
<Executed/>
StartDateTime=03112013060000
<start dateTime = 11 Mar 2013 06:00:00/>
<Executed/>
StartLater
<!--start logging at = 11 Mar 2013 06:00:00, sample interval = 900
seconds-->
<Executed/>
ds
SBE37SM-RS232 v4.1  SERIAL NO. 9693  07 Mar 2013 18:42:13
vMain = 13.41, vLith =  3.10
samplenumber = 0, free = 559240
not logging, waiting to start at 11 Mar 2013 06:00:00
sample interval = 900 seconds
data format = converted engineering
output salinity
transmit real-time = yes
sync mode = no
pump installed = yes, minimum conductivity frequency = 3148.2
<Executed/>
```

```
DOT2
<Executed/>
ds
SBE37SM-RS232 v4.1  SERIAL NO. 9694  07 Mar 2013 18:44:59
vMain = 13.40, vLith =  3.09
samplenumber = 0, free = 559240
not logging, stop command
sample interval = 900 seconds
data format = converted engineering
output salinity
transmit real-time = yes
sync mode = no
pump installed = yes, minimum conductivity frequency = 3182.2
<Executed/>
StartDateTime=03112013060000
<start dateTime = 11 Mar 2013 06:00:00/>
<Executed/>
StartLater
<!--start logging at = 11 Mar 2013 06:00:00, sample interval = 900
seconds-->
<Executed/>
ds
SBE37SM-RS232 v4.1  SERIAL NO. 9694  07 Mar 2013 18:45:31
vMain = 13.37, vLith =  3.09
samplenumber = 0, free = 559240
not logging, waiting to start at 11 Mar 2013 06:00:00
sample interval = 900 seconds
data format = converted engineering
output salinity
transmit real-time = yes
sync mode = no
pump installed = yes, minimum conductivity frequency = 3182.2
<Executed/>
```

```
DOT3
<Executed/>
ds
SBE37SM-RS232 v4.1  SERIAL NO. 9695  07 Mar 2013 18:49:42
vMain = 13.42, vLith =  3.16
samplenumber = 0, free = 559240
not logging, stop command
sample interval = 900 seconds
data format = converted engineering
output salinity
transmit real-time = yes
sync mode = no
pump installed = yes, minimum conductivity frequency = 3101.8
<Executed/>
StartDateTime=03112013060000
<start dateTime = 11 Mar 2013 06:00:00/>
<Executed/>
StartLater
<!--start logging at = 11 Mar 2013 06:00:00, sample interval = 900
seconds-->
<Executed/>
ds
SBE37SM-RS232 v4.1  SERIAL NO. 9695  07 Mar 2013 18:50:11
vMain = 13.40, vLith =  3.16
samplenumber = 0, free = 559240
not logging, waiting to start at 11 Mar 2013 06:00:00
sample interval = 900 seconds
data format = converted engineering
output salinity
transmit real-time = yes
sync mode = no
pump installed = yes, minimum conductivity frequency = 3101.8
<Executed/>
```

```
DOT4
<Executed/>
ds
SBE37SM-RS232 v4.1  SERIAL NO. 9696  07 Mar 2013 18:34:16
vMain = 13.35, vLith =  3.15
samplenumber = 0, free = 559240
not logging, stop command
sample interval = 900 seconds
data format = converted engineering
output salinity
transmit real-time = yes
sync mode = no
pump installed = yes, minimum conductivity frequency = 3160.9
<Executed/>
StartDateTime=03112013060000
<start dateTime = 11 Mar 2013 06:00:00/>
<Executed/>
StartLater
<!--start logging at = 11 Mar 2013 06:00:00, sample interval = 900
seconds-->
<Executed/>
ds
SBE37SM-RS232 v4.1  SERIAL NO. 9696  07 Mar 2013 18:34:53
vMain = 13.33, vLith =  3.15
samplenumber = 0, free = 559240
not logging, waiting to start at 11 Mar 2013 06:00:00
sample interval = 900 seconds
data format = converted engineering
output salinity
transmit real-time = yes
sync mode = no
pump installed = yes, minimum conductivity frequency = 3160.9
<Executed/>
```

```
DOT 5
<Executed/>
ds
SBE37SM-RS232 v4.1  SERIAL NO. 9673  07 Mar 2013 18:28:37
vMain = 13.31, vLith =  3.09
samplenumber = 0, free = 559240
not logging, stop command
sample interval = 900 seconds
data format = converted engineering
output salinity
transmit real-time = yes
sync mode = no
pump installed = yes, minimum conductivity frequency = 3144.2
<Executed/>
StartDateTime=03112013060000
<start dateTime = 11 Mar 2013 06:00:00/>
<Executed/>
StartLater
<!--start logging at = 11 Mar 2013 06:00:00, sample interval = 900
seconds-->
<Executed/>
ds
SBE37SM-RS232 v4.1  SERIAL NO. 9673  07 Mar 2013 18:29:20
vMain = 13.29, vLith =  3.09
samplenumber = 0, free = 559240
not logging, waiting to start at 11 Mar 2013 06:00:00
sample interval = 900 seconds
data format = converted engineering
output salinity
transmit real-time = yes
sync mode = no
pump installed = yes, minimum conductivity frequency = 3144.2
<Executed/>
```

```
DOT6
<Executed/>
ds
SBE37SM-RS232 v4.1  SERIAL NO. 9674  07 Mar 2013 18:38:31
vMain = 13.40, vLith =  3.10
samplenumber = 0, free = 559240
not logging, stop command
sample interval = 900 seconds
data format = converted engineering
output salinity
transmit real-time = yes
sync mode = no
pump installed = yes, minimum conductivity frequency = 3152.1
<Executed/>
StartDateTime=03112013060000
<start dateTime = 11 Mar 2013 06:00:00/>
<Executed/>
StartLater
<!--start logging at = 11 Mar 2013 06:00:00, sample interval = 900
seconds-->
<Executed/>
ds
SBE37SM-RS232 v4.1  SERIAL NO. 9674  07 Mar 2013 18:39:02
vMain = 13.38, vLith =  3.10
samplenumber = 0, free = 559240
not logging, waiting to start at 11 Mar 2013 06:00:00
sample interval = 900 seconds
data format = converted engineering
output salinity
transmit real-time = yes
sync mode = no
pump installed = yes, minimum conductivity frequency = 3152.1
<Executed/>
```

```
DOT7
<Executed/>
ds
SBE37SMP-ODO-RS232 v1.1.0  SERIAL NO. 10237  28 Mar 2013 18:13:51
vMain = 13.24, vLith =  2.82
samplenumber = 0, free = 399457
not logging, stop command
sample interval = 900 seconds
data format = converted engineering
output salinity
transmit real time data = yes
sync mode = no
minimum conductivity frequency = 3167.0
adaptive pump control enabled
<Executed/>
StartDateTime=03292013060000
<start dateTime = 29 Mar 2013 06:00:00/>
<Executed/>
StartLater
<!--start logging at = 29 Mar 2013 06:00:00, sample interval = 900
seconds-->
<Executed/>
ds
SBE37SMP-ODO-RS232 v1.1.0  SERIAL NO. 10237  28 Mar 2013 18:14:30
vMain = 13.24, vLith =  2.82
samplenumber = 0, free = 399457
not logging, waiting to start at 29 Mar 2013 06:00:00
sample interval = 900 seconds
data format = converted engineering
output salinity
transmit real time data = yes
sync mode = no
minimum conductivity frequency = 3167.0
adaptive pump control enabled
<Executed/>
```

Appendix D

Physical Data Collection in Eastern Long Island Sound
Field Logs

7 MARCH 2013

DOT 1	✓ CT SN 9693	✓ AQHD	✓ ADCP SN 1113
DOT 2	✓ CT SN 9694	✓ AQHD	✓ ADCP SN 7660
DOT 3	✓ CT SN 9695	✓ AQHD SN [illegible]	✓ ADCP SN 1349
DOT 4	✓ CT SN 9696	✓ AQHD	✓ ADCP SN 13197
DOT 5	✓ CT SN 9673	✓ AQHD	✓ ADCP SN 6645
DOT 6	✓ CT SN 9674	✓ AQHD	✓ ADCP SN 1094
⊛ DOT 7	✓ CT SN 10237 000	✓ AQHD	✗ ADCP NO

⊛ not deploying on the 11th. ADCP failed H/W tests, going back to RDI. We'll deploy ASA returned.

deployed frame 7 on March 29 w/out ADCP.

· DOT 7 BB3 191
BB3 321

AVG = 20
SAMPLE RATE = 0.96 HZ
30 samples
65535 cycles
30 min interval

12 March 2013

RV CT

Christian, David, Kay, Aaron, Marco, Dan, Miles
re: CT DOT Frame Deployment & Survey

EDT

0600 u/w for DOT6.

~0615 start VMDAS & ADCP
ADCP028.00000.ENR, etc.

0825 @ DOT6

0839 deploy DOT6 FRAME 37 m (121')
4115.0 7148.02

0849 (water) 4115.0 7148.01 DOTCAST1

0900 DOT6 CAST 1 35 m (CTD)

we think that ADCP direction off turned around in well on setup hdg needs to change from -45 to +135

0941 restart ADCP w/ new heading
ADCP029.0000

"Rite in the Rain"

EDT 12 March 2013

ADCP030

ADCP31

dev of beam 3 from N

1000 have set new ADCP file
ADCP032.00000
using RVCT default.ini

WX notes: 25 Kts east wind, 4-7' seas

1018 @ CTD10

1021 CTD CAST 39 m (CTD10CAST1)
41 16.201 71 36.003

1030 WATER SAMPLE CTD10CAST1

1129 @ CTD09 22 m

1135 CTD CAST 18.4 (CTD09CAST1)
41 08.992 71 39.005

WATER SAMPLE
41 09.008 71 38.997

EDT 12 March 2013

1217 @ DOT5 32.5m

1221 CTD CAST 30 m (DOT5CAST1)
41 09.09 71 45.056

1232 WATER SAMPLE
41 09 71 45 010

1259 FRAME DEPLOYMENT
41 09.008 71 38.997

1416 @ CTD8 15 m (CTD8CAST1)
4-7' SEAS NO SPREG, SBE 19+

WATER SAMPLE 15 m
41 04.750
71 49.719

1424 SBE 19+ 15 m
41 04.802
71 49.859

1544 @ DOT4 23 m

1553 CTD CAST 23 m (DOT4CAST1)
41 09.014 72 00.006

"Rite in the Rain"

EDT 12 MARCH 2013

1559 WATER SAMPLE 23 m
41 08,997 72 00,015

1640 FRAME DEPLOYMENT 22.5

wx- nasty, 6'-7' seas, rain, wind

1736 @ CTD11 17m 2kts current
(CTD11CAST1)
CTDCAST 38 m
↳ aborted, taken w/ SBE19+

1757 CTD Cast w/ SBE19+ 14.5m
41 13.761 N 72 03,710 W
(CTD11CAST2)

1800 WATER SAMPLE
41 13.875 72 03.469
to 120'

1810 u/w for DOT2

1832 Water deep > lost bottom tracking while running along north shore of LI from CTD11 to DOT2. stopped ADCP - switched to 2m bins: ADCP033.000000

EDT 12 March 2013

2002 @ DOT2 105' 32m

2013 CTD CAST (DOT2CAST1) 105'
41 08.941 72 22.140

2019 WATER SAMPLE 103'
41 08.967 72 22.17

2036 FRAME DEPLOYMENT 103'
41 08.967 72 22.2041

2kts current

2105 @ DOT 1 43 m
(DOT1CAST1)

2127 CTD CAST 43m
41 12.083 72 24.131

2118 WATER SAMPLE
41 12.00 72 24.004

2113 FRAME DEPLOYMENT 131'
41 12.00 72 24.0079

2244 @ DOT3 30 m

2248 CTD CAST 30m
41 15.477 72 14.556
(DOT3CAST1)

"Rite in the Rain"

EDT 12 MARCH 2013

2256 WATER SAMPLE
41 15.530 72 14.464

2302 FRAME DEPLOYMENT
41 15.4963 30m
72 14.5347

EDT 13 MARCH 2013

0004 @ DOT 7 48 m
161 ft

(CTD7CAST1)
0010 CTD CAST 48 m
41 15.616 72 05.946

0015 WATER SAMPLE
41 15.606 72 05.939

0030 u/w for AP. Switched VMDAS
back to 1m bins - ADCP034.00000

13 MARCH 2013

EDT

0515 u/w DOT7 for start of second
circuit

0528 start VMDAS - file ADCP035.0000
0615 switch to 2m bins - file ADCP036.0000

0620 @ DOT7 46 m

0622 CTD CAST - (DOT7CAST2)
41 15.5701 72 06.066

0629 WATER SAMPLE
41 15.677 72 05.984

0645 BOTTOM GRAB
41 15.523 72 05.943
shelly sand - coarse

0735 @ DOT3 29m

0739 CTD CAST - (DOT3CAST2) 29m
41 15.462 72 14.521

0743 WATER SAMPLE
41 15.449 72 14.549

0750 BOTTOM GRAB 96'
Sandy w/ whole clam shells

Rite in the Rain

EDT 13 MAR 2013

DOT 3 BOTTOM GRAB LOCATION
41 15.519 72 14.511

0852 @ DOT 1 42 m

0857 CTD CAST (short) (DOT1CAST2)
41 12.014 72 24.042

0903 WATER SAMPLE
41 12.013 72 23.952

0910 BOTTOM GRAB
Coarse Sand
41 12.011 72 24.015

0919 CTD CAST (long) 36m
41 12.007 72 24.079
(DOT1CAST3)

0922 @ DOT 2 31 m

0957 CTD CAST (DOT2CAST2) 105'
41 08.950 72 22.177

1004 WATER SAMPLE 103'
41 09.011 72 22.252

13 MAR 2013

EDT

1011 BOTTOM GRAB
NG

wx note -
15-20 Kts
West wind,
3-4' seas

1018 BOTTOM GRAB
41 08.988 72 22.175
oyster shells, sand, sand dollar

1225 @ CTD 11

1236 CTD CAST (CTD11 CAST3) 18.5 m
41 13.791 72 03.645

1240 WATER SAMPLE 18.5m
41 13.799 72 03.652

1248 BOTTOM GRAB 48m
160 yds SE
41 13.778 shell hash, coral
72 03.506 rocks, pebble

1336 @ DOT 4 22.5m

1339 CTD CAST (DOT4CAST2) 22.5m
41 09.003 71 59.916

"Rite in the Rain"

EDT 13 MARCH 2013

1343 WATER SAMPLE 23m
41 08.99 71 59.827

1348 BOTTOM GRAB 23m
41 08.967 71 59.673
fine sand

1359 changed VMDAS back to 1m
being ADCP files = ADCP037.0000

1456 @ CTD 8 14m

1459 CTD CAST (CTD8CAST2) 13.5m
41 04.785 71 49.820

1506 WATER SAMPLE 13.0
41 04.840 71 49.920

1512 BOTTOM GRAB 15m
NG.

1521 BOTTOM GRAB 14.5
2 ROCKS -
41 04.802 71 49.844

EDT 13 March 2013

1612 @ DOT 5 31m

1615 CTD CAST (DOT5CAST2) 29m
41 08.89 71 44.928

1622 WATER SAMPLE 31.5m
41 08.949 71 44.859

1630 BOTTOM GRAB 29.0m
NG

1638 BOTTOM GRAB
sand w/ quahog 31m
41 08.894 71 44.832

1715 @ CTD9 22m

1718 CTD CAST (CTD9CAST2) 22m
41 08.916 71 39.978

1726 WATER SAMPLE 22m
41 09.022 71 39.008

1731 BOTTOM GRAB 21.5m
gravelly sand
41 08.981 71 39.009

"Rite in the Rain"

EDT

13 MAR 2013

@ CTD10

38 m

1835 CTD CAST (CTD10CAST2)
41 16.211 71 35.968

1841 WATER SAMPLE 125'
41 16.159 71 36.022

1847 BOTTOM GRAB 125'
41 16.216 71 36.007
sandy mud

2000 @ DOT6 36 m

2008 CTD CAST (DOT6CAST2) 122'
41 14.970 71 47.963

2013 WATER SAMPLE
41 14.944 71 47.985

2020 BOTTOM GRAB 121'
41 15.033 71 47.996
dense tube worms in sandy mud

2016 u/w AP 2145 Stop ADCP
(off Bluff Pt.)

29 March 2013

RV Weacker
Turner, Christian, David, Kay

to deploy DOT 7 frame w/out ADCP which is in repair @ RDI. Frame has AQUADOPP HR, (2) RBR's, SBE 37 CT (ODO).

EDT

0940 u/w DOT 7 location

1000 @ site

1007 deployed DOT 7
41 15.650 150'
072 06.020

1022 CTD CAST 150'
41 15.643
072 05.983

1024 u/w ELIS, 1033 u/w AP.
1048 @ AP.

"Rite in the Rain"

This page intentionally left blank.

Appendix 2

CRUISE SUMMARY REPORT

CRUISE CTDOT2: May 17, 2013

Appendix 2: Cruise 2

CT DOT - ELIS SEIS

Physical Data Collection in Eastern Long Island Sound

Recovery Cruise Summary: May 17, 2013

R/V Connecticut

Area of Operations

Eastern Long Island Sound, extending east from the Connecticut River to Block Island, within the area designated as the Zone of Siting Feasibility (ZSF).

Objectives

The objective of the cruise was to recover seven instrument frames, collect water samples, and take CTD casts for the purpose of characterizing the spatial and temporal variations in hydrography, currents, and bottom stress.

Scientific Party

The scientific party included Kay Howard-Strobel, David Cohen, and Christian Fox, from the University of Connecticut.

General Operations

Operations consisted of running one circuit of the seven designated moored instrument array locations and four CTD stations. At each station a CTD cast was taken with the SBE9 and a bottom water sample collected. If the site was designated for a bottom mooring, a frame was recovered.

Frame Recoveries

Six frames were recovered this cruise from the locations listed in Table 1 and shown in Figure 1. Frame 5 was not recovered during this cruise due to an errant release which did not fire. The frame was recovered on June 18th, divers reported that it was upright and in good condition.

ADCP Operations

The ship-board ADCP (RD Instruments, 600 kHz) was started once the RV Connecticut was underway from Avery Point. VmDas (RD Instruments, Vessel Mounted Data Acquisition System) software was used to setup and run the ADCP. The ADCP was run continuously throughout the survey cruise. Figure 1 shows the survey track with the seven moored station locations and four additional CTD stations superimposed. Ten files are generated each time an ADCP VmDas session is started, and within that session there are multiple file segments created depending on the data size limit that was set in the VmDas options. This ensures that a significant amount

of data is not lost if there is a catastrophic failure of the instrument. The default file size 1.38 MB. The naming convention of the ADCP data files is as follows:

ADCP001_000000.ENR, .ENS, .ENX, .LOG, .LTA, .N1R, .N2R, .NMS, .STA, .VMO
ADCP001_000001.ENR, …
ADCP001_000002.ENR, …
.
.
.
ADCP017_000006.ENR, …

Example: ADCP017_000006.ENR; 17 is the session number incremented when the instrument is stopped and started, 6 is the file segment number incremented every 1.38 MB.

The file types and extensions generated by VmDas are as follows:

*.ENR - Raw binary ADCP data file which contains every ping
*.ENS - Binary ADCP data after the data has been screening for backscatter and correlation
*.ENX - Binary ADCP data after screening and rotation to earth coordinates
*.STA - Binary ADCP ensemble data that has been averaged into short term averages
*.LTA - Binary ADCP ensemble data that has been averaged into long term averages
*.N1R - Raw NMEA ASCII data from the primary navigation source
*.N2R - Raw NMEA ASCII data from the secondary navigation source, if available
*.NMS - Binary screened and averaged navigation data
.VMO - ASCII file copy of the.ini options file that was used during the data collection
*.LOG - ASCII file containing a log of any errors the ADCP detected during the session

The ADCP was set to ping as fast as possible (0.3 secs/ping), with 50 bins, 1 ping/ensemble and 1 meter bins. The transducer depth was at 1.5 meters and the blanking distance was 0.88 meters. There are 54 raw ensemble ADCP data files (*.ENR) encompassing approximately 40 hours.

Files are currently located on UConn's NOPP server:
/d2/dot/vmdasSurveys/vmdas ELIS CTDOT May2013

CTD Operations

A SeaBird Electronics Model 9 CTD with a Model 11 deck unit was used for the collection of the salinity and temperature profiles at each of the seven moored instrument stations and at four additional stations designated for CTD casts (Figure 1). Latitude and longitude for each station profiled are presented in Table 2. The naming convention utilized for the CTD data files is as follows:

Example: dotX.hex or ctdX.hex

dot prefix indicates a moored instrument array station
ctd prefix indicates a CTD only station, no moored instruments
X is the station ID
.hex is the native SBE CTD raw file format

When the file has been processed using the proprietary data processing program provided by SeaBird, the file extension becomes *.cnv. A "d" will be prepended if the cast is a downcast only, a "u" will be prepended if the cast is an upcast only. The data processing program also appends to the original file name, in order, the type of post-processing performed.

Example: ddot7cast1filtloopderivesplited.cnv

ddot is the downcast only
7 is the station ID
filt – the raw data was filtered using the SBE Data Processing filter module
loop – cast reversals were eliminated using the SBE Data Processing loop module
derive – salinity, density, depth were derived from the post-processed data
split – the cast was split into downcast and upcast
ed – the post-processed cast was edited manually if needed to remove any other errors or outliers

Files are currently located on UConn's NOPP FTP server in:
/d2/dot/ctdSurveys/May2013

Water Sample Collection

A 5 liter Niskin bottle was used to collect 1000 mL of sample water to be filtered for suspended sediment concentration. The Niskin bottle was deployed using the RV Connecticut's A-frame. The Niskin was lowered to the bottom and then raised one meter. Approximately one minute was allowed to pass so that any sediment suspended by the bottle weight was carried away by currents before sending the messenger down the line to trigger the Niskin. All samples were labeled and refrigerated at 4°C immediately upon collection. Samples were collected at all stations.

Appendices

Appendix A includes a copy of the field logbook.

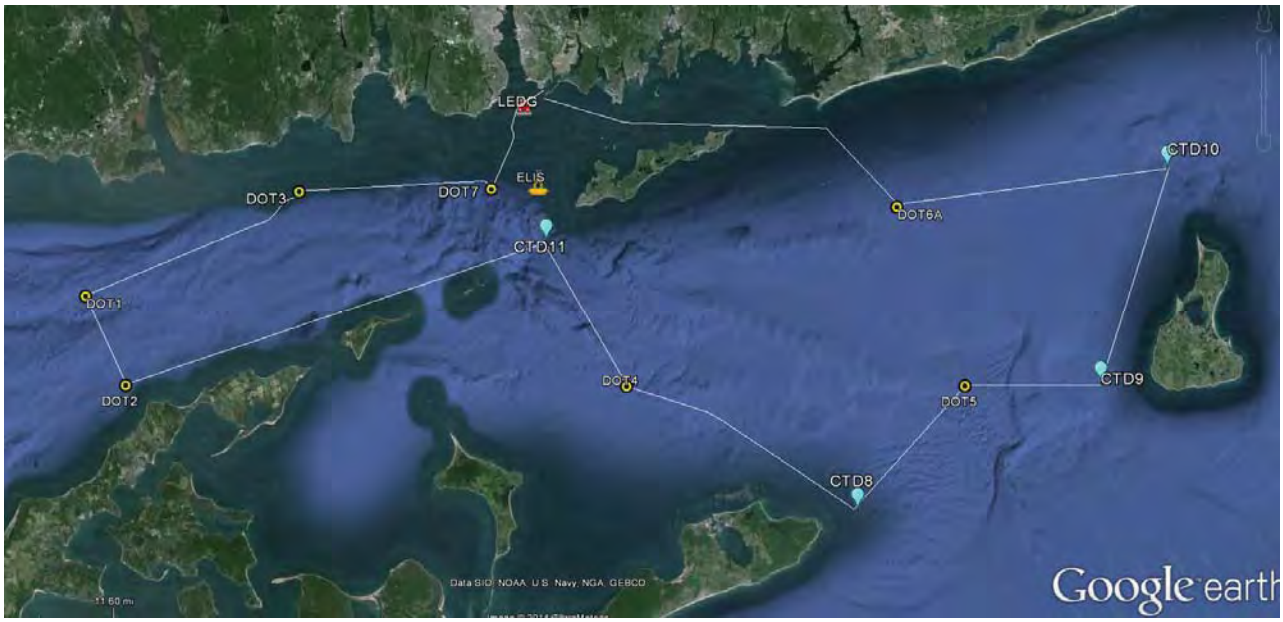

Figure 1. Locations of moored instrument arrays (DOT1-DOT7) and CTD profiles (CTD8-CTD11). LEDG is UConn's New London Ledge Light meteorological station and ELIS is UConn's metocean observation buoy. White line delineates the survey track.

Table 1. Mooring Locations and Instrumentation.

Station	Lat	Lon	Depth (m)	SBE37 SN	ADCP SN	ADCP kHz	AQD SN	AQD Pressure	OBS3+ SN
DOT1	41 12.00	72 24.01	36.6	9693	195	300	8456	100	T8838,T8834
DOT2	41 08.96	72 22.20	30.5	9694	7660	600	8428	50	T8727,T8835
DOT3	41 15.49	72 14.53	27.1	9695	1349	300	8445	100	T8863, T8861
DOT4	41 08.99	72 00.01	22.9	9696	13197	600	8438	50	T8862,T8872
DOT5	41 09.01	71 45.01	30.5	9673	6615	600	8453	50	T8782,T8837
DOT6	41 15.00	71 48.02	33.5	9674	1094	600	8455	50	T8874,T8871
DOT7*	41 15.65	72 06.02	45.7	10237	1113	300	8432	100	T8786,T8783

*DOT7 also equipped with two ECO Triplets: SN191 and SN321

Table 2. CTD Station Locations.

Date/Time (EST)	CTD Filename	Latitude (DDM)	Longitude (DDM)	Depth (m)	Notes
17-May-13 06:15	dot7	41 15.55	072 05.90	50.0	
17-May-13 08:11	dot3	41 15.48	072 14.48	29.6	
17-May-13 09:52	dot1	41 11.97	072 23.97	41.2	
17-May-13 10:50	dot2	41 08.96	072 22.17	30.0	
17-May-13 13:02	ctd11	41 13.62	072 03.45	35.0	
17-May-13 14:05	dot4	41 09.00	072 00.04	23.1	
17-May-13 15:25	ctd8	41 04.82	071 49.84	13.5	
17-May-13 17:30	dot5	41 09.00	071 44.98	28.5	
17-May-13 20:10	ctd9	41 08.97	071 38.99	21.0	
17-May-13 21:08	ctd10	41 16.20	071 35.95	36.0	
17-May-13 22:47	dot6	41 15.03	071 47.98	35.0	

Appendix A

Physical Data Collection in Eastern Long Island Sound
Field Logs

③ 5 min CTD
② 15 min NISKIN DOT only
① 15 min frame recover

90 min
11 hrs transit
5 hrs of station
2 hrs

17 May 2013

RV CT
Dan, Aaron, Marco, Franco
David, Christian, Kay

EDT recovery of CT DOT frames

0615 u/w for DOT 7

0655 on DOT-7, floats up

0710 frame on deck

0715 CTD cast 50 m ✓

0734 water sample
20 L carboy
1 L bottle

0742 u/w DOT 3

0835 @ DOT 3

Rite in the Rain

EDT 17 May 2013

0837 DOT3 floats up

0907 frame on deck

0911 CTD Cast ✓ 29.6m
41 15.460
72 14.460

0925 water sample
20 L carboy
1 L sample

0935 u/w for DOT 1

1030 @ DOT 1

1035 floats up

1048 frame on deck

1052 CTD Cast ✓ 41.2m
41 11.930
72 23.940

1108 water sample

EDT 17 May 2013

1117 u/w DOT 2

1139 @ DOT 2

1140 floats up

1148 frame on deck

1150 CTD Cast ✓ 30m
41 8.960
72 22.160

1205 water samples 41 09.048
20 L carboy 72 22.247
1 L sample 30 m

1213 u/w for CTD 11

1402 @ CTD 11 ✓ 35 meters
41 13.618
72 3.470

1410 water sample: 1L

EDT 17 May 2013

1412 u/w DOT4

1428 @ DOT4

1451 floats up

1500 frame on deck

1505 CTD cast ✓ 23.1 m
41 9.01
72 0.070

1518 water sample
20 L carboy
1 L sample

1524 u/w CTD8

1625 @ CTD8 ✓ 13.5 m
41 4.835
71 49.775

1630 water sample
1 L bottle

EDT 17 May 2013

1633 u/w DOT5

1707 @ DOT5

1726 no floats going to take CTD & water
41 09.0
71 45.0] where should be

1730 CTD cast ✓ 28.5 m
41 9.010
71 44.960

DOT5 Location from Fathom/Anton
41 09.003
71 45.004

1735 water samples
20 L carboy
1 L bottle

1740 troubleshooting & ranging
no floats
grapple - no luck ⊛ see note next page

2045 u/w CTD9

2110 @ CTD9 ✓ 21 m
41 8.980
71 39.020

Rite in the Rain

EDT 17 May 2013

2118 Water sample
1 liter

2221 w/w CTD 10

2208 @ CTD 10 ✓ 36m
41 16.232
71 35.939

2220 water sample
1 liter

2225 w/w for DOT6

2326 @ DOT6 note: this
ADCP poss
bad connector

2338 floats up

2345 frame on deck

35m

2347 CTD CAST ✓
41 15.060
71 47.990

0000 water sample
20L carboy
1 liter bottle

0016 w/w for AP.

~0120 @ AP.

DOTS frame:
(R) divers dove June 19th
and found frame upright;
release did not release!

Rite in the Rain

Appendix 3

CRUISE SUMMARY REPORT

CRUISE CTDOT3: June 11-12, 2013

Appendix 3: Cruise 3

CT DOT - ELIS SEIS

Physical Data Collection in Eastern Long Island Sound
Deployment Cruise Summary: June 11-12, 2013
R/V Connecticut

Area of Operations

Eastern Long Island Sound, extending east from the Connecticut River to Block Island, within the area designated as the Zone of Siting Feasibility (ZSF).

Objectives

The objectives of the cruise were to deploy seven instrument frames, collect water samples, and take CTD casts for the purpose of characterizing the spatial and temporal variations in hydrography, currents, and bottom stress.

Scientific Party

The scientific party included Kay Howard-Strobel, David Cohen, and Christian Fox, from the University of Connecticut, Tim O'Brien, a student, and Steve Ackleson of SA Oceans, LLC.

General Operations

Operations consisted of running two circuits of the seven designated moored instrument array locations and four additional CTD stations. At each station a CTD cast was taken with an optically enhanced SBE9 and a bottom water sample collected. If the site was designated for a bottom mooring, a frame was deployed. The second circuit revisited all eleven stations with a CTD cast, and bottom water sample at each location.

Frame Deployments

Seven frames were deployed this cruise at the locations listed in Table 1 and plotted in Figure 1. Instrumentation on each frame, also summarized in Table 1, included a downward looking Nortek Aquadopp 2Hz high resolution pulse coherent current profiler (Figure 2a) with two Campbell Scientific OBS3+ optical backscatter units (Figure 2b), an upward-looking RDI acoustic Doppler current profiler (ADCP) with waves array sampling enabled (Figure 2a), and a Sea-Bird Electronics Model SMP37 conductivity/temperature sensor(Figure 2a). The height of the base of the RDI ADCP above bottom is 1.5 meters and the height of the Nortek Aquadopp above the bottom is 0.75 meters. The OBS3+ backscatter units are mounted at 30 and 137 cm above the bottom. The top OBS is 57 cm higher than in the previous campaign. The frame at DOT7 also

had two WET Labs EcoTriplet backscatter units (Figure 2a) sampling at 470, 532 and 660 nm and a WET Labs Cstar 650 nm transmissometer (Figure 4). The deployment configuration files (*.whp) file for each RDI ADCP are located in Appendix A. Appendix B and Appendix C contain the log files for each Nortek Aquadopp HR and Sea-Bird SMP37 configuration, respectively.

ADCP Operations

The ship-board ADCP (RD Instruments, 600 kHz) was started once the RV Connecticut was underway from Avery Point. VmDas (RD Instruments, Vessel Mounted Data Acquisition System) software was used to setup and run the ADCP. The ADCP was run continuously throughout the survey cruise. Figure 1 shows the survey track with the seven moored station locations and four additional CTD stations superimposed. Ten files are generated each time an ADCP VmDas session is started, and within that session there are multiple file segments created depending on the data size limit that was set in the VmDas options. This ensures that a significant amount of data is not lost if there is a catastrophic failure of the instrument. The default file size 1.38 MB. The naming convention of the ADCP data files is as follows:

ADCP001_000000.ENR, .ENS, .ENX, .LOG, .LTA, .N1R, .N2R, .NMS, .STA, .VMO
ADCP001_000001.ENR, …
ADCP001_000002.ENR, …
.
.
.
ADCP017_000006.ENR, …

Example: ADCP017_000006.ENR; 17 is the session number incremented when the instrument is stopped and started, 6 is the file segment number incremented every 1.38 MB.
The file types and extensions generated by VmDas are as follows:

*.ENR - Raw binary ADCP data file which contains every ping
*.ENS - Binary ADCP data after the data has been screening for backscatter and correlation
*.ENX - Binary ADCP data after screening and rotation to earth coordinates
*.STA - Binary ADCP ensemble data that has been averaged into short term averages
*.LTA - Binary ADCP ensemble data that has been averaged into long term averages
*.N1R - Raw NMEA ASCII data from the primary navigation source
*.N2R - Raw NMEA ASCII data from the secondary navigation source, if available
*.NMS - Binary screened and averaged navigation data
.VMO - ASCII file copy of the.ini options file that was used during the data collection
*.LOG - ASCII file containing a log of any errors the ADCP detected during the session

The ADCP was set to ping as fast as possible (0.3 secs/ping), with 50 bins, 1 ping/ensemble and 1 meter bins. The transducer depth was at 1.5 meters and the blanking distance was 0.88 meters. There are 54 raw ensemble ADCP data files (*.ENR) encompassing approximately 40 hours.
Files are currently located on UConn's FTP server:
/d2/dot/vmdasSurveys/vmdas ELIS CTDOT June2013

CTD Operations

A SeaBird Electronics Model 9 CTD with a Model 11 deck unit (Figure 3) was used for the collection of the salinity and temperature profiles at each of the seven moored instrument stations and at four additional stations designated for CTD casts (Figure 1). Additional instruments were mounted on the SBE9 rosette to collect optical data for use in characterizing the suspended sediment within the ZSF. The optical sensors included a WET Labs EcoTriplet with wavelengths of 450, 520 and 650 nm, a WET Labs AC9 absorption and attenuation meter, a Sequoia Scientific Type C LISST100x particle size analyzer, and a Sea-Bird Electronics Model 25 CTD.

On Day 1 of the survey cruise a SBE 19+ was used to acquire the CTD data at three of the stations (see Table 2) as the sea state was deemed too rough to safely use the SBE9. A SBE19+ was hand lowered off the stern. Latitude and longitude for each station profiled are presented in Table 1. The naming convention utilized for the CTD data files is as follows:

Example: dotXcastY.hex or ctdXcastY.hex

dot prefix indicates a moored instrument array station
ctd prefix indicates a CTD only station, no moored instruments
X is the station ID
Y is the cast number; at least two casts were taken each station
.hex is the native SBE CTD raw file format

When the file has been processed using the proprietary data processing program provided by SeaBird, the file extension becomes *.cnv. A "d" will be prepended if the cast is a downcast only, a "u" will be prepended if the cast is an upcast only. The data processing program also appends to the original file name, in order, the type of post-processing performed.

Example: ddot7cast1filtloopderivesplited.cnv

ddot is the downcast only
7 is the station ID
1 is the cast number
filt – the raw data was filtered using the SBE Data Processing filter module

loop – cast reversals were eliminated using the SBE Data Processing loop module
derive – salinity, density, depth were derived from the post-processed data
split – the cast was split into downcast and upcast
ed – the post-processed cast was edited manually if needed to remove any other errors or outliers

Files are currently located on UConn's FTP server:
/d2/dot/ctdSurveys/June2013

Water Sample Collection

A 5 liter Niskin bottle was used to collect 2000 mL of sample water to be filtered for suspended sediment concentration and particulate organic carbon (POC) analysis. The Niskin bottle was deployed using the RV Connecticut's A-frame, lowered to the bottom and then raised one meter. Approximately one minute was allowed to pass so that any sediment suspended by the bottle weight was carried away by currents before sending the messenger down the line to trigger the Niskin. POC samples were collected and stored in one liter, amber polystyrene, acid washed bottles. SSC samples were stored in one liter, clear polystyrene bottles. All bottles were labeled and refrigerated at 4°C immediately upon collection. All samples were labeled and refrigerated at 4°C immediately upon collection. Samples were collected at all stations on both survey loops.

Table 1. Mooring Instrumentation.

Station	Lat	Lon	Depth (m)	SBE37 SN	ADCP SN	ADCP kHz	AQD SN	AQD Press	OBS3+ SN
DOT1	41 11.9999	72 24.0042	38.0	9693	1113	300	8456	100	T8838,T8834
DOT2	41 08.9977	72 22.2017	30.0	9694	7660	600	8428	50	T8727,T8835
DOT3	41 15.4973	72 14.5334	28.0	9695	1349	300	8445	100	T8863, T8861
DOT4	41 09.0035	71 59.9999	22.0	9696	10462	1200	8554	20	T8837,T8782
DOT5	41 09.0225	71 45.2258	30.0	10238	13197	600	8438	50	T8782,T8837
DOT6	41 15.0000	71 48.0000	36.0	9674	1094	600	8455	50	T8874,T8871
DOT7*	41 15.6001	72 05.9985	48.2	10237	195	300	8432	100	T8786,T8783

*DOT7 also equipped with two ECO Triplets: SN191 and SN321, and a Wetlabs CStar SN 1601PG transmissometer with SBE19 SN 6255.

Figure 1. Locations of moored instrument arrays (DOT1-DOT7) and CTD profiles (CTD8-CTD11). LEDG is UConn's New London Ledge Light meteorological station and ELIS is UConn's metocean observation buoy. White line delineates the survey tracks for both days.

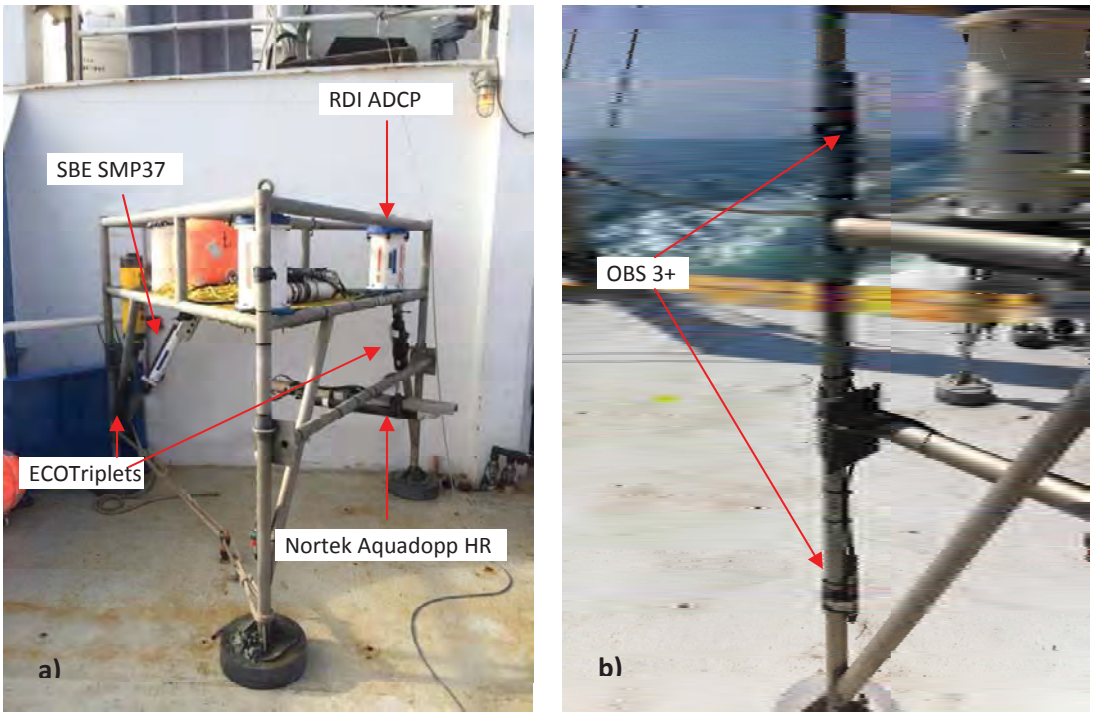

Figure 2. a) location of instruments on DOT7 bottom frame, b) OBS3+ mounts..

Table 2. CTD Station Locations.

Date/Time (EST)	CTD Filename	Latitude (DDM)	Longitude (DDM)	Depth (m)	Notes
11-Jun-13 07:11	dot7cast1	41 15.60	072 05.99	45.0	
11-Jun-13 08:30	dot3cast1	41 15.49	072 14.53	28.0	
11-Jun-13 08:30	dot1cast1	41 11.99	072 24.00	38.0	
11-Jun-13 09:53	dot2cast1	41 08.99	072 22.20	30.0	
11-Jun-13 13:07	ctd11cast1	41 13.80	072 03.59	31.0	
11-Jun-13 14:20	dot4cast1	41 09.00	072 59.99	22.0	
11-Jun-13 15:36	ctd8cast1	41 04.85	071 49.63	13.0	19+
11-Jun-13 17:05	dot5cast1	41 09.02	071 45.28	30.0	19+
11-Jun-13 17:58	ctd9cast1	41 08.84	071 38.92	22.0	19+
11-Jun-13 19:14	ctd10cast3	41 16.22	071 36.04	36.0	
11-Jun-13 21:09	dot6cast2	41 15.00	071 48.01	36.0	
12-Jun-13 05:25	dot2cast3	41 09.07	072 21.95	30.0	
12-Jun-13 06:58	dot1cast4	41 11.95	072 23.88	40.0	
12-Jun-13 08:18	dot3cast3	41 15.40	072 14.53	28.0	
12-Jun-13 09:27	dot7cast2	41 15.54	072 06.09	46.0	
12-Jun-13 10:19	ctd11cast2	41 13.62	072 03.64	27.0	
12-Jun-13 11:19	dot4cast2	41 08.96	072 00.03	22.5	
12-Jun-13 12:42	ctd8cast2	41 04.85	071 49.63	12.0	
12-Jun-13 14:03	dot5cast2	41 08.92	071 44.95	30.0	
12-Jun-13 15:05	ctd9cast2	41 08.84	071 38.92	18.5	
12-Jun-13 16:10	ctd10cast4	41 16.15	071 35.94	36.5	
12-Jun-13 17:34	dot6cast3	41 15.00	071 47.87	35.0	

Notes: 19+, seas too rough to deploy SBE911, a SBE19+ hand lowered.

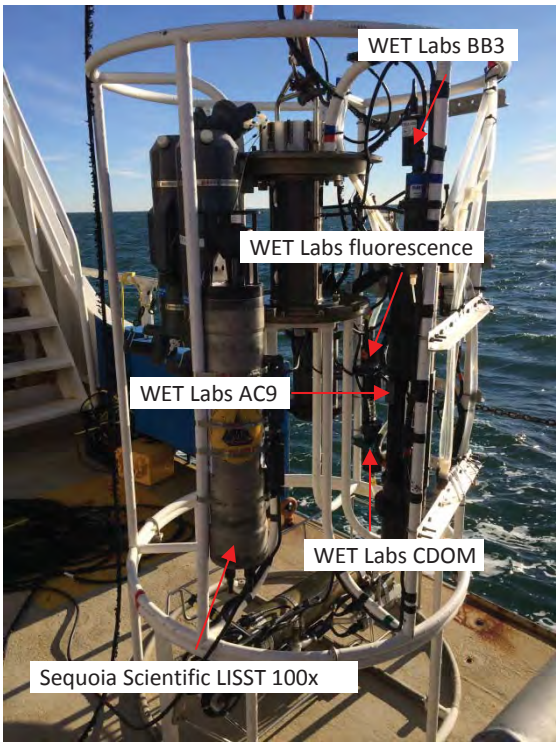

Figure 3. SBE 911 CTD with optical instruments.

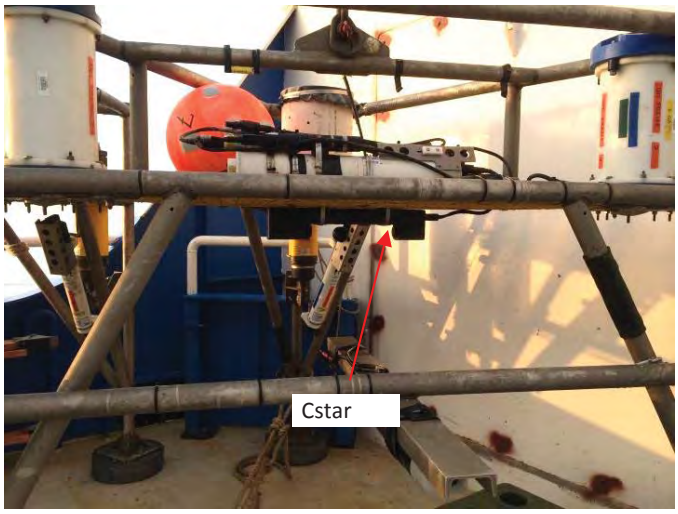

Figure 4. Frame 7 (DOT 7) with WETlabs 650 nm CStar transmissometer.

Appendices

Appendix A contains RDI ADCP configuration files.

Appendix B includes the Nortek Aquadopp HR configuration files.

Appendix C includes the SBE SMP37 setup files.

Appendix D is a scanned copy of the field notebook.

Appendix A
RDI ADCP Configuration Files

DOT Frame 1

```
CR1
CF11101
EA0
EB0
ED370
ES30
EX11111
EZ1111101
WA255
WB0
WD111100000
WF50
WN40
WP180
WS100
WV175
HD111000000
HB5
HP2400
HR00:30:00.00
HT00:00:00.50
TE00:15:00.00
TP00:01.00
TF13/06/10 12:00:00
RNDOT1_
CK
CS
;
;Instrument         = Workhorse Sentinel
;Frequency          = 307200
;Water Profile      = YES
;Bottom Track       = NO
;High Res. Modes    = NO
;High Rate Pinging  = NO
;Shallow Bottom Mode= NO
;Wave Gauge         = YES
;Lowered ADCP       = NO
;Ice Track          = NO
;Surface Track      = NO
;Beam angle         = 20
;Temperature        = 10.00
;Deployment hours   = 912.00
;Battery packs      = 3
;Automatic TP       = NO
;Memory size [MB]   = 2048
;Saved Screen       = 2
;
;Consequences generated by PlanADCP version 2.06:
;First cell range   = 1.95 m
;Last cell range    = 40.95 m
;Max range          = 82.81 m
;Standard deviation = 1.01 cm/s
;Ensemble size      = 954 bytes
;Storage required   = 329.09 MB (345078912 bytes)
;Power usage        = 1327.20 Wh
;Battery usage      = 2.9
;Samples / Wv Burst = 2400
;Min NonDir Wave Per= 2.84 s
;Min Dir Wave Period= 4.79 s
;Bytes / Wave Burst = 187280
;
; WARNINGS AND CAUTIONS:
; Waves Gauge feature has to be installed in Workhorse to use selected option.
; Advanced settings have been changed.
; Expert settings have been changed.
```

DOT Frame 2

```
CR1
CF11101
EA0
EB0
ED330
ES30
EX11111
EZ1111101
WA255
WB0
WD111100000
WF30
WN71
WP180
WS50
WV175
HD111000000
HB5
HP2400
HR00:30:00.00
HT00:00:00.50
TE00:15:00.00
TP00:01.00
TF13/06/10 12:00:00
RNDOT2_
CK
CS
;
;Instrument         = Workhorse Sentinel
;Frequency          = 614400
;Water Profile      = YES
;Bottom Track       = NO
;High Res. Modes    = NO
;High Rate Pinging  = NO
;Shallow Bottom Mode= NO
;Wave Gauge         = YES
;Lowered ADCP       = NO
;Ice Track          = NO
;Surface Track      = NO
;Beam angle         = 20
;Temperature        = 5.00
;Deployment hours   = 720.00
;Battery packs      = 3
;Automatic TP       = NO
;Memory size [MB]   = 304
;Saved Screen       = 2
;
;Consequences generated by PlanADCP version 2.06:
;First cell range   = 1.02 m
;Last cell range    = 36.02 m
;Max range          = 38.74 m
;Standard deviation = 1.02 cm/s
;Ensemble size      = 1574 bytes
;Storage required   = 261.51 MB (274216320 bytes)
;Power usage        = 965.68 Wh
;Battery usage      = 2.1
;Samples / Wv Burst = 2400
;Min NonDir Wave Per= 2.69 s
;Min Dir Wave Period= 4.52 s
;Bytes / Wave Burst = 187280
;
; WARNINGS AND CAUTIONS:
; Waves Gauge feature has to be installed in Workhorse to use selected option.
; Advanced settings have been changed.
; Expert settings have been changed.
```

DOT Frame 3

```
CR1
CF11101
EA0
EB0
ED270
ES30
EX11111
EZ1111101
WA255
WB0
WD111100000
WF50
WN32
WP180
WS100
WV175
HD111000000
HB5
HP2400
HR00:30:00.00
HT00:00:00.50
TE00:15:00.00
TP00:01.00
TF13/06/10 12:00:00
RNDOT3_
CK
CS
;
;Instrument         = Workhorse Sentinel
;Frequency          = 307200
;Water Profile      = YES
;Bottom Track       = NO
;High Res. Modes    = NO
;High Rate Pinging  = NO
;Shallow Bottom Mode= NO
;Wave Gauge         = YES
;Lowered ADCP       = NO
;Ice Track          = NO
;Surface Track      = NO
;Beam angle         = 20
;Temperature        = 5.00
;Deployment hours   = 960.00
;Battery packs      = 3
;Automatic TP       = NO
;Memory size [MB]   = 2048
;Saved Screen       = 2
;
;Consequences generated by PlanADCP version 2.06:
;First cell range   = 1.95 m
;Last cell range    = 32.95 m
;Max range          = 86.34 m
;Standard deviation = 1.01 cm/s
;Ensemble size      = 794 bytes
;Storage required   = 345.83 MB (362626561 bytes)
;Power usage        = 1319.84 Wh
;Battery usage      = 2.9
;Samples / Wv Burst = 2400
;Min NonDir Wave Per= 2.48 s
;Min Dir Wave Period= 4.09 s
;Bytes / Wave Burst = 187280
;
; WARNINGS AND CAUTIONS:
; Waves Gauge feature has to be installed in Workhorse to use selected option.
; Advanced settings have been changed.
; Expert settings have been changed.
```

DOT Frame 4

```
CR1
CF11101
EA0
EB0
ED230
ES30
EX11111
EZ1111101
WA255
WB0
WD111100000
WF44
WN26
WP180
WS100
WV175
HD111000000
HB5
HP2400
HR00:30:00.00
HT00:00:00.50
TE00:15:00.00
TP00:01.00
TF13/06/10 12:00:00
RNDOT4_
CK
CS
;
;Instrument         = Workhorse Sentinel
;Frequency          = 1228800
;Water Profile      = YES
;Bottom Track       = NO
;High Res. Modes    = NO
;High Rate Pinging  = NO
;Shallow Bottom Mode= NO
;Wave Gauge         = YES
;Lowered ADCP       = NO
;Ice Track          = NO
;Surface Track      = NO
;Beam angle         = 20
;Temperature        = 10.00
;Deployment hours   = 1080.00
;Battery packs      = 3
;Automatic TP       = NO
;Memory size [MB]   = 2048
;Saved Screen       = 2
;
;Consequences generated by PlanADCP version 2.06:
;First cell range   = 1.54 m
;Last cell range    = 26.54 m
;Max range          = 15.33 m
;Standard deviation = 0.26 cm/s
;Ensemble size      = 674 bytes
;Storage required   = 388.56 MB (407436480 bytes)
;Power usage        = 1080.33 Wh
;Battery usage      = 2.4
;Samples / Wv Burst = 2400
;Min NonDir Wave Per= 2.33 s
;Min Dir Wave Period= 3.78 s
;Bytes / Wave Burst = 187280
;
; WARNINGS AND CAUTIONS:
; Waves Gauge feature has to be installed in Workhorse to use selected option.
; Advanced settings have been changed.
```

DOT Frame 5

```
CR1
CF11101
EA0
EB0
ED330
ES30
EX11111
EZ1111101
WA255
WB0
WD111100000
WF30
WN71
WP180
WS50
WV175
HD111000000
HB5
HP2400
HR00:30:00.00
HT00:00:00.50
TE00:15:00.00
TP00:01.00
TF13/06/10 12:00:00
RNDOT5_
CK
CS
;
;Instrument         = Workhorse Sentinel
;Frequency          = 614400
;Water Profile      = YES
;Bottom Track       = NO
;High Res. Modes    = NO
;High Rate Pinging  = NO
;Shallow Bottom Mode= NO
;Wave Gauge         = YES
;Lowered ADCP       = NO
;Ice Track          = NO
;Surface Track      = NO
;Beam angle         = 20
;Temperature        = 10.00
;Deployment hours   = 960.00
;Battery packs      = 3
;Automatic TP       = NO
;Memory size [MB]   = 975
;Saved Screen       = 2
;
;Consequences generated by PlanADCP version 2.06:
;First cell range   = 1.02 m
;Last cell range    = 36.02 m
;Max range          = 40.70 m
;Standard deviation = 1.02 cm/s
;Ensemble size      = 1574 bytes
;Storage required   = 348.68 MB (365621761 bytes)
;Power usage        = 1286.83 Wh
;Battery usage      = 2.9
;Samples / Wv Burst = 2400
;Min NonDir Wave Per= 2.69 s
;Min Dir Wave Period= 4.52 s
;Bytes / Wave Burst = 187280
;
; WARNINGS AND CAUTIONS:
; Waves Gauge feature has to be installed in Workhorse to use selected option.
; Advanced settings have been changed.
; Expert settings have been changed.
```

DOT Frame 6

```
CR1
CF11101
EA0
EB0
ED360
ES30
EX11111
EZ1111101
WA255
WB0
WD111100000
WF30
WN40
WP180
WS100
WV175
HD111000000
HB5
HP2400
HR00:30:00.00
HT00:00:00.50
TE00:15:00.00
TP00:01.00
TF13/06/10 12:00:00
RNDOT6_
CK
CS
;
;Instrument         = Workhorse Sentinel
;Frequency          = 614400
;Water Profile      = YES
;Bottom Track       = NO
;High Res. Modes    = NO
;High Rate Pinging  = NO
;Shallow Bottom Mode= NO
;Wave Gauge         = YES
;Lowered ADCP       = NO
;Ice Track          = NO
;Surface Track      = NO
;Beam angle         = 20
;Temperature        = 5.00
;Deployment hours   = 1080.00
;Battery packs      = 3
;Automatic TP       = NO
;Memory size [MB]   = 2048
;Saved Screen       = 2
;
;Consequences generated by PlanADCP version 2.06:
;First cell range   = 1.52 m
;Last cell range    = 40.52 m
;Max range          = 42.66 m
;Standard deviation = 0.52 cm/s
;Ensemble size      = 954 bytes
;Storage required   = 389.72 MB (408646080 bytes)
;Power usage        = 1306.83 Wh
;Battery usage      = 2.9
;Samples / Wv Burst = 2400
;Min NonDir Wave Per= 2.80 s
;Min Dir Wave Period= 4.72 s
;Bytes / Wave Burst = 187280
;
; WARNINGS AND CAUTIONS:
; Waves Gauge feature has to be installed in Workhorse to use selected option.
; Advanced settings have been changed.
; Expert settings have been changed.
```

DOT Frame 7

```
CR1
CF11101
EA0
EB0
ED470
ES30
EX11111
EZ1111101
WA255
WB0
WD111100000
WF50
WN52
WP180
WS100
WV175
HD111000000
HB5
HP2400
HR00:30:00.00
HT00:00:00.50
TE00:15:00.00
TP00:01.00
TF13/06/10 12:00:00
RNDOT7_
CK
CS
;
;Instrument         = Workhorse Sentinel
;Frequency          = 307200
;Water Profile      = YES
;Bottom Track       = NO
;High Res. Modes    = NO
;High Rate Pinging  = NO
;Shallow Bottom Mode= NO
;Wave Gauge         = YES
;Lowered ADCP       = NO
;Ice Track          = NO
;Surface Track      = NO
;Beam angle         = 20
;Temperature        = 10.00
;Deployment hours   = 816.00
;Battery packs      = 3
;Automatic TP       = NO
;Memory size [MB]   = 2048
;Saved Screen       = 2
;
;Consequences generated by PlanADCP version 2.06:
;First cell range   = 1.95 m
;Last cell range    = 52.95 m
;Max range          = 82.86 m
;Standard deviation = 1.01 cm/s
;Ensemble size      = 1194 bytes
;Storage required   = 295.20 MB (309538177 bytes)
;Power usage        = 1291.52 Wh
;Battery usage      = 2.9
;Samples / Wv Burst = 2400
;Min NonDir Wave Per= 3.21 s
;Min Dir Wave Period= 5.40 s
;Bytes / Wave Burst = 187280
;
; WARNINGS AND CAUTIONS:
; Waves Gauge feature has to be installed in Workhorse to use selected option.
; Advanced settings have been changed.
; Expert settings have been changed.
```

Appendix B
Nortek Aquadopp HR Configuration Files

```
==============================================================
Deployment   : dot1
Current time : 6/10/2013 10:36:01 AM
Start at     : 6/11/2013 6:00:00 AM
Comment:
DOT1 - June 2013 deployment
--------------------------------------------------------------
Measurement interval  (s) : 1200
Cell size            (mm) : 37
Orientation               : DOWNLOOKING
Distance to bottom    (m) : 0.75
Pulse distance        (m) : 0.84
Profile range         (m) : 0.74
Horiz. vel. range   (m/s) : 1.10
Vert. vel. range    (m/s) : 0.46
Number of cells           : 20
Average interval      (s) : 1
Blanking distance     (m) : 0.048
Measurement load      (%) : 20
Samples per burst         : 4096
Sampling rate        (Hz) : 2
Compass upd. rate     (s) : 1
Coordinate System         : Beam
Speed of sound      (m/s) : MEASURED
Salinity            (ppt) : 30
Analog input 1            : PROFILE
Analog input 2            : PROFILE
Analog input power out    : ENABLED
File wrapping             : OFF
TellTale                  : OFF
Acoustic modem            : OFF
Serial output             : OFF
Baud rate                 : 115200
--------------------------------------------------------------
Assumed duration   (days) : 30.0
Battery utilization   (%) : 103.0
Battery level         (V) : 11.2
Recorder size        (MB) : 3886
Recorder free space  (MB) : 3885.972
Memory required      (MB) : 2497.5
--------------------------------------------------------------
Instrument ID             : AQD 8456
Head ID                   : ASP 5868
Firmware version          : 3.14 HR
ProLog ID                 : 786
ProLog firmware version   : 4.14
--------------------------------------------------------------
SD Card Inserted          : YES
SD Card Ready             : YES
SD Card Write protected   : NO
SD Card Type              : SDHC
SD Card Supported         : YES
--------------------------------------------------------------
AquaProHR Version 1.10.08
Copyright (C) Nortek AS
```

```
============================================================
Deployment   : dot2
Current time : 6/10/2013 10:39:24 AM
Start at     : 6/11/2013 6:00:00 AM
Comment:
DOT2 - June 2013 deployment
------------------------------------------------------------
Measurement interval  (s) : 1200
Cell size            (mm) : 37
Orientation               : DOWNLOOKING
Distance to bottom    (m) : 0.75
Pulse distance        (m) : 0.84
Profile range         (m) : 0.74
Horiz. vel. range   (m/s) : 1.10
Vert. vel. range    (m/s) : 0.46
Number of cells           : 20
Average interval      (s) : 1
Blanking distance     (m) : 0.048
Measurement load      (%) : 20
Samples per burst         : 4096
Sampling rate        (Hz) : 2
Compass upd. rate     (s) : 1
Coordinate System         : Beam
Speed of sound      (m/s) : MEASURED
Salinity            (ppt) : 30
Analog input 1            : PROFILE
Analog input 2            : PROFILE
Analog input power out    : ENABLED
File wrapping             : OFF
TellTale                  : OFF
Acoustic modem            : OFF
Serial output             : OFF
Baud rate                 : 115200
------------------------------------------------------------
Assumed duration   (days) : 30.0
Battery utilization   (%) : 103.0
Battery level         (V) : 11.2
Recorder size        (MB) : 3886
Recorder free space  (MB) : 3885.972
Memory required      (MB) : 2497.5
------------------------------------------------------------
Instrument ID             : AQD 8428
Head ID                   : ASP 5866
Firmware version          : 3.14 HR
ProLog ID                 : 763
ProLog firmware version   : 4.14
------------------------------------------------------------
SD Card Inserted          : YES
SD Card Ready             : YES
SD Card Write protected   : NO
SD Card Type              : SDHC
SD Card Supported         : YES
------------------------------------------------------------
AquaProHR Version 1.10.08
Copyright (C) Nortek AS
============================================================
```

```
============================================================
Deployment   : dot3
Current time : 6/10/2013 10:41:56 AM
Start at     : 6/11/2013 6:00:00 AM
Comment:
DOT3 - June 2013 deployment
------------------------------------------------------------
Measurement interval  (s) : 1200
Cell size            (mm) : 37
Orientation               : DOWNLOOKING
Distance to bottom    (m) : 0.75
Pulse distance        (m) : 0.84
Profile range         (m) : 0.74
Horiz. vel. range   (m/s) : 1.10
Vert. vel. range    (m/s) : 0.46
Number of cells           : 20
Average interval      (s) : 1
Blanking distance     (m) : 0.048
Measurement load      (%) : 20
Samples per burst         : 4096
Sampling rate        (Hz) : 2
Compass upd. rate     (s) : 1
Coordinate System         : Beam
Speed of sound      (m/s) : MEASURED
Salinity            (ppt) : 30
Analog input 1            : PROFILE
Analog input 2            : PROFILE
Analog input power out    : ENABLED
File wrapping             : OFF
TellTale                  : OFF
Acoustic modem            : OFF
Serial output             : OFF
Baud rate                 : 115200
------------------------------------------------------------
Assumed duration   (days) : 30.0
Battery utilization   (%) : 103.0
Battery level         (V) : 11.1
Recorder size        (MB) : 3926
Recorder free space  (MB) : 3925.972
Memory required      (MB) : 2497.5
------------------------------------------------------------
Instrument ID             : AQD 8445
Head ID                   : ASP 5867
Firmware version          : 3.14 HR
ProLog ID                 : 766
ProLog firmware version   : 4.14
------------------------------------------------------------
SD Card Inserted          : YES
SD Card Ready             : YES
SD Card Write protected   : NO
SD Card Type              : SDHC
SD Card Supported         : YES
------------------------------------------------------------
AquaProHR Version 1.10.08
Copyright (C) Nortek AS
============================================================
```

```
============================================================
Deployment   : dot4
Current time : 6/10/2013 10:44:44 AM
Start at     : 6/11/2013 6:00:00 AM
Comment:
DOT4 - June 2013 deployment
------------------------------------------------------------
Measurement interval  (s) : 1200
Cell size            (mm) : 37
Orientation               : DOWNLOOKING
Distance to bottom    (m) : 0.75
Pulse distance        (m) : 0.84
Profile range         (m) : 0.74
Horiz. vel. range   (m/s) : 1.10
Vert. vel. range    (m/s) : 0.46
Number of cells           : 20
Average interval      (s) : 1
Blanking distance     (m) : 0.048
Measurement load      (%) : 20
Samples per burst         : 4096
Sampling rate        (Hz) : 2
Compass upd. rate     (s) : 1
Coordinate System         : Beam
Speed of sound      (m/s) : MEASURED
Salinity            (ppt) : 30
Analog input 1            : PROFILE
Analog input 2            : PROFILE
Analog input power out    : ENABLED
File wrapping             : OFF
TellTale                  : OFF
Acoustic modem            : OFF
Serial output             : OFF
Baud rate                 : 115200
------------------------------------------------------------
Assumed duration   (days) : 30.0
Battery utilization   (%) : 103.0
Battery level         (V) : 11.2
Recorder size        (MB) : 3926
Recorder free space  (MB) : 3925.972
Memory required      (MB) : 2497.5
------------------------------------------------------------
Instrument ID             : AQD 8554
Head ID                   : ASP 5590
Firmware version          : 3.14 HR
ProLog ID                 : 648
ProLog firmware version   : 4.14
------------------------------------------------------------
SD Card Inserted          : YES
SD Card Ready             : YES
SD Card Write protected   : NO
SD Card Type              : SDHC
SD Card Supported         : YES
------------------------------------------------------------
AquaProHR Version 1.10.08
Copyright (C) Nortek AS
============================================================
```

```
============================================================
Deployment   : dot5
Current time : 6/10/2013 10:47:11 AM
Start at     : 6/11/2013 6:00:00 AM
Comment:
DOT5 - June 2013 deployment
------------------------------------------------------------
Measurement interval  (s) : 1200
Cell size            (mm) : 37
Orientation               : DOWNLOOKING
Distance to bottom    (m) : 0.75
Pulse distance        (m) : 0.84
Profile range         (m) : 0.74
Horiz. vel. range   (m/s) : 1.10
Vert. vel. range    (m/s) : 0.46
Number of cells           : 20
Average interval      (s) : 1
Blanking distance     (m) : 0.048
Measurement load      (%) : 20
Samples per burst         : 4096
Sampling rate        (Hz) : 2
Compass upd. rate     (s) : 1
Coordinate System         : Beam
Speed of sound      (m/s) : MEASURED
Salinity            (ppt) : 30
Analog input 1            : PROFILE
Analog input 2            : PROFILE
Analog input power out    : ENABLED
File wrapping             : OFF
TellTale                  : OFF
Acoustic modem            : OFF
Serial output             : OFF
Baud rate                 : 115200
------------------------------------------------------------
Assumed duration   (days) : 30.0
Battery utilization   (%) : 103.0
Battery level         (V) : 11.2
Recorder size        (MB) : 3886
Recorder free space  (MB) : 3885.972
Memory required      (MB) : 2497.5
------------------------------------------------------------
Instrument ID             : AQD 8438
Head ID                   : ASP 5865
Firmware version          : 3.14 HR
ProLog ID                 : 791
ProLog firmware version   : 4.14
------------------------------------------------------------
SD Card Inserted          : YES
SD Card Ready             : YES
SD Card Write protected   : NO
SD Card Type              : SDHC
SD Card Supported         : YES
------------------------------------------------------------
AquaProHR Version 1.10.08
Copyright (C) Nortek AS
============================================================
```

```
============================================================
Deployment   : dot6
Current time : 6/10/2013 10:49:33 AM
Start at     : 6/11/2013 6:00:00 AM
Comment:
DOT6 - June 2013 deployment
------------------------------------------------------------
Measurement interval  (s) : 1200
Cell size            (mm) : 37
Orientation               : DOWNLOOKING
Distance to bottom    (m) : 0.75
Pulse distance        (m) : 0.84
Profile range         (m) : 0.74
Horiz. vel. range   (m/s) : 1.10
Vert. vel. range    (m/s) : 0.46
Number of cells           : 20
Average interval      (s) : 1
Blanking distance     (m) : 0.048
Measurement load      (%) : 20
Samples per burst         : 4096
Sampling rate        (Hz) : 2
Compass upd. rate     (s) : 1
Coordinate System         : Beam
Speed of sound      (m/s) : MEASURED
Salinity            (ppt) : 30
Analog input 1            : PROFILE
Analog input 2            : PROFILE
Analog input power out    : ENABLED
File wrapping             : OFF
TellTale                  : OFF
Acoustic modem            : OFF
Serial output             : OFF
Baud rate                 : 115200
------------------------------------------------------------
Assumed duration   (days) : 30.0
Battery utilization   (%) : 103.0
Battery level         (V) : 11.2
Recorder size        (MB) : 3886
Recorder free space  (MB) : 3885.972
Memory required      (MB) : 2497.5
------------------------------------------------------------
Instrument ID             : AQD 8455
Head ID                   : ASP 5864
Firmware version          : 3.14 HR
ProLog ID                 : 730
ProLog firmware version   : 4.14
------------------------------------------------------------
SD Card Inserted          : YES
SD Card Ready             : YES
SD Card Write protected   : NO
SD Card Type              : SDHC
SD Card Supported         : YES
------------------------------------------------------------
AquaProHR Version 1.10.08
Copyright (C) Nortek AS
============================================================
```

```
============================================================
Deployment   : dot7
Current time : 6/10/2013 10:52:38 AM
Start at     : 6/11/2013 6:00:00 AM
Comment:
DOT7 - June 2013 deployment
------------------------------------------------------------
Measurement interval  (s) : 1200
Cell size            (mm) : 37
Orientation               : DOWNLOOKING
Distance to bottom    (m) : 0.75
Pulse distance        (m) : 0.84
Profile range         (m) : 0.74
Horiz. vel. range   (m/s) : 1.10
Vert. vel. range    (m/s) : 0.46
Number of cells           : 20
Average interval      (s) : 1
Blanking distance     (m) : 0.048
Measurement load      (%) : 20
Samples per burst         : 4096
Sampling rate        (Hz) : 2
Compass upd. rate     (s) : 1
Coordinate System         : Beam
Speed of sound      (m/s) : MEASURED
Salinity            (ppt) : 30
Analog input 1            : PROFILE
Analog input 2            : PROFILE
Analog input power out    : ENABLED
File wrapping             : OFF
TellTale                  : OFF
Acoustic modem            : OFF
Serial output             : OFF
Baud rate                 : 115200
------------------------------------------------------------
Assumed duration   (days) : 30.0
Battery utilization   (%) : 103.0
Battery level         (V) : 11.2
Recorder size        (MB) : 3926
Recorder free space  (MB) : 3925.972
Memory required      (MB) : 2497.5
------------------------------------------------------------
Instrument ID             : AQD 8432
Head ID                   : ASP 5869
Firmware version          : 3.14 HR
ProLog ID                 : 754
ProLog firmware version   : 4.14
------------------------------------------------------------
SD Card Inserted          : YES
SD Card Ready             : YES
SD Card Write protected   : NO
SD Card Type              : SDHC
SD Card Supported         : YES
------------------------------------------------------------
AquaProHR Version 1.10.08
Copyright (C) Nortek AS
============================================================
```

Appendix C
Sea-Bird Electronics SMP37 Configuration Files

DOT1

```
<Executed/>
InitLogging
<Executed/>
ds
SBE37SM-RS232 v4.1  SERIAL NO. 9693  10 Jun 2013 09:45:53
vMain = 13.30, vLith =  3.14
samplenumber = 0, free = 559240
not logging, stop command
sample interval = 900 seconds
data format = converted engineering
output salinity
transmit real-time = yes
sync mode = no
pump installed = yes, minimum conductivity frequency = 3148.2
<Executed/>
StartDateTime=06112013060000
<start dateTime = 11 Jun 2013 06:00:00/>
<Executed/>
StartLater
<!--start logging at = 11 Jun 2013 06:00:00, sample interval = 900 seconds-->
<Executed/>
ds
SBE37SM-RS232 v4.1  SERIAL NO. 9693  10 Jun 2013 09:46:26
vMain = 13.30, vLith =  3.14
samplenumber = 0, free = 559240
not logging, waiting to start at 11 Jun 2013 06:00:00
sample interval = 900 seconds
data format = converted engineering
output salinity
transmit real-time = yes
sync mode = no
pump installed = yes, minimum conductivity frequency = 3148.2
<Executed/>
```

DOT2

```
<Executed/>
InitLogging
<Executed/>
ds
SBE37SM-RS232 v4.1  SERIAL NO. 9694  10 Jun 2013 09:51:36
vMain = 13.33, vLith =  3.14
samplenumber = 0, free = 559240
not logging, stop command
sample interval = 900 seconds
data format = converted engineering
output salinity
transmit real-time = yes
sync mode = no
pump installed = yes, minimum conductivity frequency = 3182.2
<Executed/>
StartDateTime=06112013060000
<start dateTime = 11 Jun 2013 06:00:00/>
<Executed/>
StartLater
<!--start logging at = 11 Jun 2013 06:00:00, sample interval = 900 seconds-->
<Executed/>
ds
SBE37SM-RS232 v4.1  SERIAL NO. 9694  10 Jun 2013 09:52:01
vMain = 13.32, vLith =  3.14
samplenumber = 0, free = 559240
not logging, waiting to start at 11 Jun 2013 06:00:00
sample interval = 900 seconds
data format = converted engineering
output salinity
transmit real-time = yes
sync mode = no
pump installed = yes, minimum conductivity frequency = 3182.2
<Executed/>
```

DOT3

```
<Executed/>
InitLogging
this command will initialize memory
repeat the command to confirm
<Executed/>
InitLogging
<Executed/>
ds
SBE37SM-RS232 v4.1  SERIAL NO. 9695  10 Jun 2013 09:57:08
vMain = 13.35, vLith =  3.18
samplenumber = 0, free = 559240
not logging, stop command
sample interval = 900 seconds
data format = converted engineering
output salinity
transmit real-time = yes
sync mode = no
pump installed = yes, minimum conductivity frequency = 3101.8
<Executed/>
StartDateTime=06112013060000
<start dateTime = 11 Jun 2013 06:00:00/>
<Executed/>
StartLater
<!--start logging at = 11 Jun 2013 06:00:00, sample interval = 900 seconds-->
<Executed/>
ds
SBE37SM-RS232 v4.1  SERIAL NO. 9695  10 Jun 2013 09:57:40
vMain = 13.34, vLith =  3.18
samplenumber = 0, free = 559240
not logging, waiting to start at 11 Jun 2013 06:00:00
sample interval = 900 seconds
data format = converted engineering
output salinity
transmit real-time = yes
sync mode = no
pump installed = yes, minimum conductivity frequency = 3101.8
<Executed/>
```

DOT4

```
<Executed/>
InitLogging
<Executed/>
ds
SBE37SM-RS232 v4.1  SERIAL NO. 9696  10 Jun 2013 10:02:31
vMain = 13.33, vLith =  3.17
samplenumber = 0, free = 559240
not logging, stop command
sample interval = 900 seconds
data format = converted engineering
output salinity
transmit real-time = yes
sync mode = no
pump installed = yes, minimum conductivity frequency = 3160.9
<Executed/>
StartDateTime=06112013060000
<start dateTime = 11 Jun 2013 06:00:00/>
<Executed/>
StartLater
<!--start logging at = 11 Jun 2013 06:00:00, sample interval = 900 seconds-->
<Executed/>
ds
SBE37SM-RS232 v4.1  SERIAL NO. 9696  10 Jun 2013 10:02:56
vMain = 13.32, vLith =  3.17
samplenumber = 0, free = 559240
not logging, waiting to start at 11 Jun 2013 06:00:00
sample interval = 900 seconds
data format = converted engineering
output salinity
transmit real-time = yes
sync mode = no
pump installed = yes, minimum conductivity frequency = 3160.9
<Executed/>
```

DOT 5

```
<Executed/>
initlogging
this command will initialize memory
repeat the command to confirm
initlogging
<Executed/>
ds
SBE37SMP-ODO-RS232 v1.1.0  SERIAL NO. 10238  10 Jun 2013 10:08:10
vMain = 13.30, vLith =  3.20
samplenumber = 0, free = 399457
not logging, stop command
sample interval = 900 seconds
data format = converted engineering
output salinity
transmit real time data = yes
sync mode = no
minimum conductivity frequency = 3184.6
adaptive pump control enabled
<Executed/>
StartDateTime=06112013060000
<start dateTime = 11 Jun 2013 06:00:00/>
<Executed/>
StartLater
<!--start logging at = 11 Jun 2013 06:00:00, sample interval = 900 seconds-->
<Executed/>
ds
SBE37SMP-ODO-RS232 v1.1.0  SERIAL NO. 10238  10 Jun 2013 10:08:39
vMain = 13.30, vLith =  3.20
samplenumber = 0, free = 399457
not logging, waiting to start at 11 Jun 2013 06:00:00
sample interval = 900 seconds
data format = converted engineering
output salinity
transmit real time data = yes
sync mode = no
minimum conductivity frequency = 3184.6
adaptive pump control enabled
<Executed/>
```

```
DOT6

<Executed/>
initlogging
this command will initialize memory
repeat the command to confirm
<Executed/>
initlogging
<Executed/>
StartDateTime=06112013060000
<start dateTime = 11 Jun 2013 06:00:00/>
<Executed/>
StartLater
<!--start logging at = 11 Jun 2013 06:00:00, sample interval = 900
seconds-->
<Executed/>
ds
SBE37SM-RS232 v4.1  SERIAL NO. 9674  10 Jun 2013 10:14:32
vMain = 13.33, vLith =  3.14
samplenumber = 0, free = 559240
not logging, waiting to start at 11 Jun 2013 06:00:00
sample interval = 900 seconds
data format = converted engineering
output salinity
transmit real-time = yes
sync mode = no
pump installed = yes, minimum conductivity frequency = 3152.1
<Executed/>
```

DOT7

```
<Executed/>
initlogging
this command will initialize memory
repeat the command to confirm
initlogging
<Executed/>
StartDateTime=06112013060000
<start dateTime = 11 Jun 2013 06:00:00/>
<Executed/>
StartLater
<!--start logging at = 11 Jun 2013 06:00:00, sample interval = 900 seconds-->
<Executed/>
ds
SBE37SMP-ODO-RS232 v1.1.0  SERIAL NO. 10237  10 Jun 2013 10:22:05
vMain = 13.32, vLith =  3.11
samplenumber = 0, free = 399457
not logging, waiting to start at 11 Jun 2013 06:00:00
sample interval = 900 seconds
data format = converted engineering
output salinity
transmit real time data = yes
sync mode = no
minimum conductivity frequency = 3167.0
adaptive pump control enabled
<Executed/>
```

DOT7 SBE 19V2 WITH WET Labs CSTAR

```
<Executed/>ds
SBE 19plus V 2.5  SERIAL NO. 6255    10 Jun 2013 10:28:53
vbatt = 13.4, vlith =  8.5, ioper =  61.8 ma, ipump = 173.7 ma,
iext01 =   4.8 ma, iext2345 =  20.2 ma
status = not logging
sample interval = 900 seconds, number of measurements per sample = 20
samples = 0, free = 3463060
mode = moored, run pump for 0.5 sec, delay before sampling = 20.0 seconds,
delay after sampling = 0.0 seconds
transmit real-time = yes
battery type = alkaline, battery cutoff =  7.5 volts
pressure sensor = strain gauge, range = 508.0
SBE 38 = no, WETLABS = no, OPTODE = no, SBE63 = no, Gas Tension Device = no
Ext Volt 0 = yes, Ext Volt 1 = no
Ext Volt 2 = yes, Ext Volt 3 = no
Ext Volt 4 = no, Ext Volt 5 = no
echo characters = yes
output format = converted decimal
output salinity = yes, output sound velocity = no
append UCSD sigma-t, V, I
<Executed/>StartDateTime=06112013060000
<Executed/>StartLater
start logging at = 11 Jun 2013 06:00:00, sample interval = 900 seconds
```

Appendix D
Physical Data Collection in Eastern Long Island Sound
Field Logs

✓ program SBE19
✓ program BB3
✓ program SBE 37's
✓ program AQD's
⊛ new scheme [A076 samples @ 2 Hz

RV CT 10 June 2013

opt rosette - bottles 3, 4, 5, 6
check out cruise

1430 OPTI - Rosette in water
Several up & down
casts in test I. hex

1530 u/w AP.

notes for June 11

Frame 7 (DOT 7)
BB3 321 @ 35", BB3 191 @ 14"
all frames (optic end)
OBS's 1 @ 30 cm, OBS's 2 @ 137 cm

11 June 2013

RV CT
Dan, Marco, Frank, Aaron, Kay, David, Christian, Steve, Tim O'Brien
⇒ DOT survey cruise and frame deployments.

✓ Frame 1: 446065
4-4-4-4 37 kHz
✓ Frame 2: 446137
4-4-4-4 "
✓ Frame 3: 446152
4-4-4-4 "
✓ Frame 4: 127102
4-4-4-4 "
✓ Frame 5: 446000
4-4-4-4 "
✓ Frame 6: 446046
4-4-4-4 "
✓ Frame 7: 446023
4-4-4-4 "

EDT
0630 u/w DOT 7 station

"Rite in the Rain"

EDT 11 June 2013

0725 @ DOT 7 158'

0735 DOT frame 7 on btm

41 15.6001 72 05.9985

0750 btm water sample

0801 on station 44m

<DOT7CAST1>

0811 profile start 45m

(0711 EST) L1620659.DAT = LISST file

bottle 3 @ 43.9 BTM A

bottle 4 @ 41.2 BTM B

bottle 5 @ 23.01 MID

bottle 6 @ 1.5 SFC

0819 u/w DOT3

0906 @ DOT3 28 m

93'

0914 deploying frame

0915 deployed 41 15.4973 72 14.5334

0925 water sample-bottom

0930 profile start

(0830 EST) L1620828.dat - LISST file

<DOT3CAST1>

EDT 11 June 2013

bottle 3 @ 24.8 m BTM A

bottle 4 @ 21.9 m BTM B

bottle 5 @ 13.8 m MID

bottle 6 @ 2.0 m SFC

0939 u/w for DOT 1

1035 @ DOT 1 38 m

1040 frame deployed

41 11.9999 72 24.0042

1046 water sample

<DOT1CAST1>

1055 start cast - cast 40 m

(955 EST) L1620950 = LISST file

bottle 3 @ 37.9 m BTM A

bottle 4 @ 36.0 m BTM B

bottle 5 @ 20.2 m MID

bottle 6 @ 1.4 m SFC

1104 u/w for DOT 2

"Rite in the Rain"

EDT 11 June 2013

1139 deploying frame 2 @ DOT2

1141 frame deployed 30m
[41 08.9977 72 22.2017]

1147 btm water sample

1153 profile start 30m
1053 (EST) L1621048 = LISST file

<DOT2CAST1> bottle 3 @ 28.4 BTM A
bottle 4 @ 25.8 BTM B
bottle 5 @ 14.5 MID
bottle 6 @ 1.5 m SFC

1202 u/w for CTD11

1400 on station @ CTD11 32 m

1407 starting opticast 31m
1307 (EST) L1621305 = LISST file

<CTD11CAST1> bottle 3 @ 27.8 m BTM A
bottle 4 @ 26.0 m BTM B
bottle 5 @ 15.1 m MID
bottle 6 @ 1.7 m SFC

EDT 11 June 2013

1415 u/w for DOT4

1500 near station DOT4
1512 on station @ DOT4

1515 frame 4 deployed 22m
[41 09.0035 71 59.9999]

1520 btm water sample
<DOT4CAST1>

1523 start opticast 23.2m
(1423 EST) L1621422.dat = LISST file

bottle 3 @ 20.02 BTM A
bottle 4 @ 18.1 BTM B
bottle 5 @ 11.1 MID
bottle 6 @ 1.8 m SFC

1530 u/w for CTD08

1630 on Station CTD08 4-6' seas 10-20 kt wind
1636 too rough for big CTD 13m
<CTD8CAST1> CAST69 * use SBE19+ off stern
150' north for SBE19+
1642 290' south for water sample

"Rite in the Rain"

EDT 11 June 2013

1647 U/W for DOT5 - new location
4-6' seas 15-20kts wind
DP not holding
⊛ frame not deployed (deployed on June 12)

1755 Water sample @ 30m
<DOT5CAST1> (CAST70)

1805 * SBE19 + cast 29.1 m

1808 U/W CTD09
@ CTD09 22m

1852 Water Sample @ 74'
SWELL negates opti cast

1858 * SBE19 + Cast <CTD9CAST1> (CAST71)
4108.9658 7139.0567

1900 U/W for CTD10

Hi there
@ CTD10

1953 water sample 124'
37.7m

2000 Start opticast 36m

EDT 11 June 2013

bottle 3 @ 34.3
bottle 4 @ 32.3] cast aborted

2013 bubble check cast 2 3 full casts in LISST file

2014 opti-cast cast 3
(1914 EST) L1621857.dat = LISST file

<CTD10CAST3> bottle 3 @ 33.7 BTMA
bottle 4 @ 31.3 BTMB
bottle 5 @ 17.1 m MID
bottle 6 @ 2.1 m SFC

2021 opti rosette on deck
L1621857.dat = LISST file

2025 U/W DOT6

2131 on station 36m
DOT6

2134 water sample

2150 frame deployed
target location:
4115.0 7148.0

"Rite in the Rain"

EDT 11-12 June 2013

2159 opticast started 36m
bubble: cast = cast 1
check

2209 good: cast 2 <DOT6 CAST2>
(2109 EST) L1622052.dat = LISST file

BTM A	bottle 3	@	33.5m
BTM B	bottle 4	@	30.5m
MID	bottle 5	@	17.8m
SFC	bottle 6	@	1.6m

2215 u/w for DOT 2

note - changed ADCP
setup: not ready
KHDEF600.TXT
starts with files ADCP005 *

0607 on Station @ DOT2
31m

0609 water sample bottom

0617 opticast started 30m

0625 bubble: cast 2
check

EDT 12 June 2013

0625 good: cast 3
(0525 EST) L1630512.dat = LISST file

<DOT2CAST3>

bottle 3	@	27.2m	BTM A
bottle 4	@	25.0	BTM B
bottle 5	@	15.8m	MID
bottle 6	@	2.2m	SFC

0631 u/w for DOT 1

0700 @ Start on DOT1 40m

0705 water sample bottom

0712 opticast started 35m
bubble check cast #2 40m

~0735 SBE 25 failure - power cables loose?
restart → aborted @ sfc cast #3
aborted LISST file = L1630612.dat
cable jumped shive
redo cast #3 42m
↳ bubble check 36m

0758 good: cast #4 40m
(0658 EST) L1630643.dat = LISST file

<DOT1CAST4>

bottle 3	@	34.1	BTM A
bottle 4	@	32.5	BTM B
bottle 5	@	21.0	MID
bottle 6	@	1.9m	SFC

"Rite in the Rain"

EDT 12 June 2013

0806 u/w DOT3

LISST @ 8.68 volts

0905 water sample btm 28 m
93'

getting on deck pressure
w/ SBE9 this cast
~ -0.2 m

bubble check cast #2
<DOT3CAST3>

0918 (0818 EST) Good cast #3 27 m
L1630808.dat = LISST file

bottle 3@	25.2	BTM A
bottle 4@	22.7	BTM B
bottle 5@	14.5	MID
bottle 6@	2.2 m	SFC

0925 u/w for DOT7

0957 Switched ADCP to 2m bins
files start w/ ADCP006.*

EDT 12 June 2013

1014 on Station DOT 7

1016 water sample btm

1022 Starting opticast 46m

debubbler - cast #2
flooding only to 20 m
50 m/s overwrite cast 2

1027 (0927 EST) Good cast # 2 <DOT7CAST2>
L1630919.dat = LISST file

btm A	bottle 3 @	43.1 m
btm B	bottle 4 @	41.1 m
MID	bottle 5 @	23.2 m
SFC	bottle 6 @	2.6 m

1035 u/w CTD11
had to move 500' S - fishing boat recreational

1107 water sample btm 22m

1115 start opticast 27 m
41 13.709 72 03.573

"Rite in the Rain"

EDT 12 June 2013

debubbling cast #2
overwrite cast #2
<CTD11CAST2>

1119 (1019 EST) good cast #2 27 m
L1631009.dat = LISST file

flooding 2kts top → btm

bottle 3 @ BTMA 25.7
bottle 4 @ BTMB 23.2
bottle 5 @ MID 13.0
bottle 6 @ SFC 2.2 m

1125 u/w DOT 4

switched ADCP back to 1m. bins files ADCP007.*

1207 on station DOT 4 22.5 m

1200 water sample btm

1213 Start optcast 22.5 m
debubbling cast to 20 m
overwrite 2

1219 Good; cast 2 <DOT4CAST2>
L1631109.dat = LISST file

12 June 2013 EDT

(1119 EST) bottle 3 @ btmA 21.0 m
flooding bottle 4 @ MID 11.5 m
50 cm/s bottle 5 @ SFC 2.1 m
2-3' SFC waves bottle 6 @ btmB 18.7 m

~~retowered to grab sample~~

1229 SFC water sample taken off stern - bottle 5 did not fire

1233 u/w for CTD 8

1335 on station CTD 8 <CTD8CAST2>

1336 water sample btm @ 13.5 m
L1631238.dat = LISST file

1342 starting optcast 12 m
(1242 EST) debubbled to 10 m

EBBING 50 cm/s

bottle 3 @ 10.38 btmA
bottle 4 @ 7.46 btmB
bottle 5 @ 5.9 MID
bottle 6 @ 2.1 m SFC

1352 u/w DOT5

"Rite in the Rain"

12 June 2013

EDT

1428 on Station DOT5
1429 water sample btm 30m

1450 DOT frame 5 deployed

<DOT5CAST2> 41 09.0225
71 45.2258

1455 starting opti cast 29.5m
redo - SBE25 fail

1503 31.5
starting good cast 2
(1403 EST) L1631354.dat = LISST file 30m

closing ~30 cm/s
bottle 3@ 27.1 btmA
bottle 4@ 23.8 btmB
bottle 5@ 15.3 MID
bottle 6@ 2.4 SFC

1517 u/w for CTD9

12 June 2013

EDT

1548 on station CTD9 21m
1550 water sample btm
<CTDCAST2>

1556 starting opti cast 21m
L1631449.dat = LISST file

1605 cast 2 CTD9 18.5m
(1505 EST) bottle 3@ 16.0 btmA
SE currents bottle 4@ 13.6m btmB
~30-40 cm/s bottle 5@ 8.6m MID
bottle 6@ 2.6m SFC

1608 u/w CTD10

1703 on station CTD10
1705 water sample btm 36.5m
L1631608.dat = LISST file

1710 opti ctd10 cast 4 started
(1610 EST)
<CTD10CAST4> bottle 3@ 34.3
bottle 4@ 31.9
bottle 5@ 17.6m
bottle 6@ 3.2m

"Rite in the Rain"

12 June 2013

EDT

1719 u/w DOT6

1826 on station DOT6
water sample btm.
L1631729.dat = LISST file

1834 opticast started 35m
dot6 cast 3
(1734 EST) good cast 3 <DOT6CAST3>

ebbing bottle 3@ 32.5 btmA
30-40 cm/s bottle 4@ 30.7 btmB
bottle 5@ 17.1 MID
bottle 6@ 2.2 SFC

1850 u/w AP.

final voltage on the LISST = 8.58

2130 @ AP.

16 June 2013

✓ order flow sensor
✓ TOC samples process
✓ SMC calibrations
✓ SMC cruise
✓ cruise summary June 11-12
✓ process CTD
✓ process LISST
— conc v count ACD
— conc v count BB3 1062
— conc v count OBS's
✓ AQD batts for August changeout
✓ ADCP batts
✓ calib DOT5 obs's
✓ calib ADCP compass - DOT5
WFS-008 flow sensor power

DOT2CAST2 ⇒ 3

"Rite in the Rain"

Appendix 4

CRUISE SUMMARY REPORT

CRUISE CTDOT4: July 10, 11, 16, 2013

Appendix 4: Cruise 4

CT DOT - ELIS SEIS

Physical Data Collection in Eastern Long Island Sound
Battery Replacement Cruise Summary: July 10-11 & 16, 2013
R/V Weicker

Area of Operations

Eastern Long Island Sound, extending east from the Connecticut River to Block Island, within the area designated as the Zone of Siting Feasibility (ZSF).

Objectives

The objective of the cruise was to recover seven instrument frames and replace batteries in the Nortek Aquadopp High Resolution (HR) current profilers. Water samples and CTD profiles were also collected for the purpose of characterizing the spatial and temporal variations in hydrography, currents, and bottom stress.

Scientific Party

The scientific party included Kay Howard-Strobel, David Cohen, and Christian Fox, from the University of Connecticut.

General Operations

Operations consisted of visiting each of the seven designated moored instrument array locations, recovering the bottom frame, removing the Aquadopp HR from the frame and replacing batteries, reinstalling the Aquadopp HR, and redeploying the frame. At each station a CTD cast was taken with a SBE19plus profiler and a bottom water sample collected.

Frame Recoveries

Six frames were recovered this cruise from the locations listed in Table 1 and shown in Figure 1. Frame 5 was not recovered during this cruise due to an errant release which did not fire, but was recovered on June 18th. Divers reported that the frame was upright and in good condition.

ADCP Operations

The ADCP on the RV Weicker was not available this trip.

CTD Operations

A Sea-Bird Electronics Model 19plus was used for the collection of salinity and temperature profiles at each of the seven moored instrument stations. Latitude and longitude for each

station profiled is presented in Table 1. The naming convention utilized for the CTD data files is as follows:

Example: dotX.hex or ctdX.hex

dot prefix indicates a moored instrument array station
ctd prefix indicates a CTD only station, no moored instruments
X is the station ID
.hex is the native SBE CTD raw file format

When the file has been processed using the proprietary data processing program provided by SeaBird, the file extension becomes *.cnv. A "d" will be prepended if the cast is a downcast only, a "u" will be prepended if the cast is an upcast only. The data processing program also appends to the original file name, in order, the type of post-processing performed.

Example: ddot7cast1filtloopderivesplited.cnv

ddot is the downcast only
7 is the station ID
filt – the raw data was filtered using the SBE Data Processing filter module
loop – cast reversals were eliminated using the SBE Data Processing loop module
derive – salinity, density, depth were derived from the post-processed data
split – the cast was split into downcast and upcast
ed – the post-processed cast was edited manually if needed to remove any other errors or outliers

Files are currently located on UConn's NOPP FTP server in:
/d2/dot/ctdSurveys/May2013

Water Sample Collection

A 5 liter Niskin bottle was used to collect 1000 mL of sample water to be filtered for suspended sediment concentration. The Niskin bottle was deployed using the RV Weicker's A-frame. The Niskin was lowered to the bottom and then raised one meter. Approximately one minute was allowed to pass so that any sediment suspended by the bottle weight was carried away by currents before sending the messenger down the line to trigger the Niskin. All samples were labeled and refrigerated at 4°C immediately upon collection. Samples were collected at all seven stations.

Appendices

Appendix A includes a copy of the field logbook.

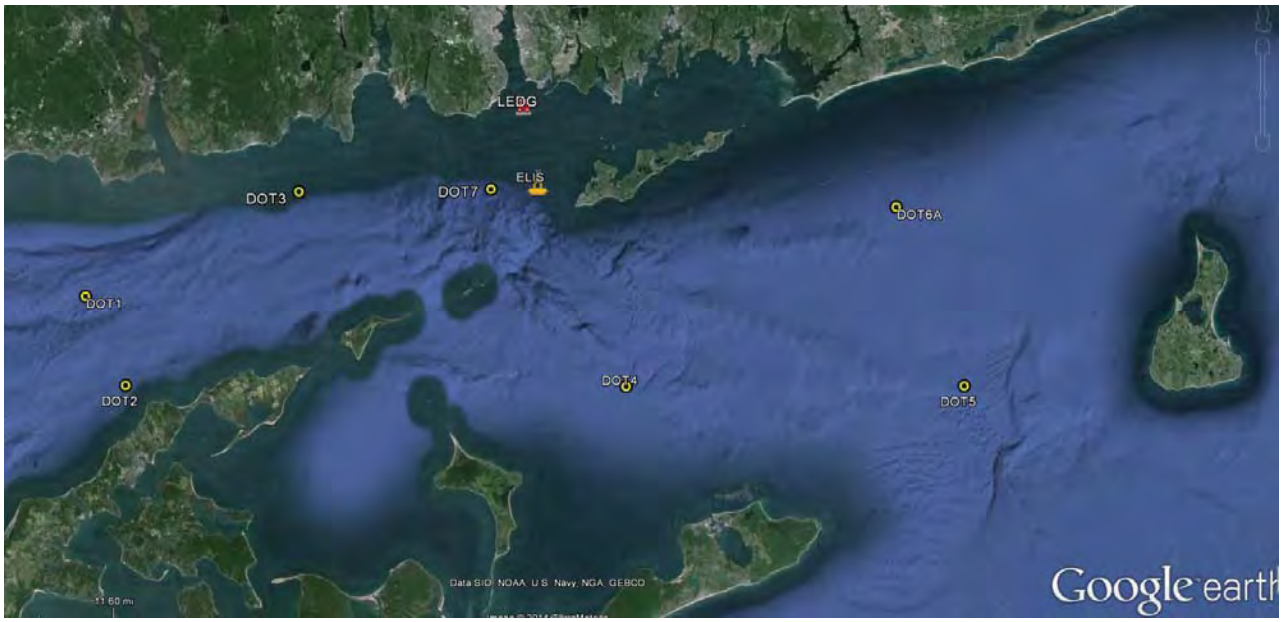

Figure 1. Locations of moored instrument arrays (DOT1-DOT7). LEDG is UConn's New London Ledge Light meteorological station and ELIS is UConn's metocean observation buoy.

Table 1. Location of Redeployed Frames and CTD Profiles.

Date/Time (EST)	CTD Filename	Latitude (DDM)	Longitude (DDM)	Depth (m)	Notes
10-July-13 12:25	dot1	41 12.039	072 23.957	45.0	
10-July-13 13:40	dot2	41 08.877	072 22.332	30.5	
11-July-13 07:45	dot7	41 15.660	072 05.961	40.8	
11-July-13 09:30	dot3	41 15.506	072 14.556	28.0	
11-July-13 13:05	dot4	41 09.005	071 59.974	22.8	
11-July-13 15:25	dot6	41 14.996	071 47.945	35.3	
16-July-13 10:50	dot5	41 08.999	071 41.984	30.5	

Appendix A

Physical Data Collection in Eastern Long Island Sound
Field Logs

10 July 2013

RV Weicker
Turner, Kay, David, Christian

EDT going to recover & replace batteries in Norteks

0752 v/w DOT1
0818 back @ Dock
too foggy, waiting for it to lift.

1109 trying again. v/w for DOT1

1210 on station DOT1

1225 frame on deck

1315 frame on bottom 41 12 039 / 72 23.957
1325 CTD cast (cast 74)
1330 water sample 148'
1334 v/w DOT 2 (45m)
1405 frame on deck

~1440 CTD cast (cast 75)
1453 frame deployed 41 08.877 / 72 22.332
(30.5m) ~100'

~1500 v/w for DOT3
~1530 abandon effort due to threat of thunderstorms w/ 30 knot winds

1615 back @ AP.

11 July 2013

RV Weicker
Turner, Kay, Christian, David

recover & replace Nortek batts

EDT
0730 v/w for DOT7
0746 @ DOT7

0800 frame on deck (40.8 m)
0841 frame deployed 134'
41 15 6601 72 05.961
0845 CTD cast (cast 76)
0852 water sample

"Rite in the Rain"

EDT

0855 u/w for DOT3

0950 frame on deck

1027 frame deployed 92.2'
41 15.506
72 14.556
(28m)

1030 CTD cast (cast 77)
1035 water sample
1040 u/w NLDS buoy
to swap sfc YSI

1118 @ NLDS buoy
1125 sfc YSI swapped

1127 u/w for AP to refuel

1242 after brief break -
headed out to DOT4

1325 @ DOT4
1340 frame on deck

EDT

1400 water sample
1405 CTD cast (cast 78)

1416 deploy frame 75'
41 09.005
71 59.974
(22.8m)

1420 u/w DOT6

1505 @ DOT6 bent CT connector
this frame has issues
bent jbolt, mud on AQD mount
1556 water sample
1615 frame deployed 116'
41 14.996 71 47.945
1625 CTD cast (cast 79)
(35.3m)

1630 u/w AP

Rite in the Rain

16 July 2013

RV Weicker
Turner, David, Kay, Christian

to replace batteries in AQD
& DOTS

EDT
0925 u/w DOTS

1045 @ DOTS
1055 frame on deck

1144 frame on bottom 100-
[41 08.999 71 44.984]
1150 CTD CAST (CTD cast 80) (30.5m)
1155 WATER SAMPLE
1200 u/w AP
1330 @ AP.

for Aug 7-8

(11 stations * 4 depths) * 2 carouls =
88 amber bottles
88 clear bottles

(11 stations * 1 depth) * 2 carouls =
22 clear bottles
~~22~~ amber bottles

have 150 clear
have 144 amber

110 clear bottles
110 amber bottles

— ACS CW CAL MILLQ
— MISLINS, funnel
— PUTZER'S
— labeling tape & markers
— Comm cables
— ADCP box
— NORTEK box
— SBE box

for frame recovery

SBE 25 ver 4.0A SN225
>CC J5 fluorometers
enable 4:5
stored as voltage #0 = EXT 4 - CDOM
stored as voltage #1 = EXT 5 - CHLOR

This page intentionally left blank.

Appendix 5

CRUISE SUMMARY REPORT

CRUISE CTDOT5: August 7, 8, 13, 2013

Appendix 5: Cruise 5

CT DOT - ELIS SEIS

Physical Data Collection in Eastern Long Island Sound

Recovery Cruise Summary: August 7-8, 2013

R/V Connecticut

Area of Operations

Eastern Long Island Sound, extending east from the Connecticut River to Block Island, within the area designated as the Zone of Siting Feasibility (ZSF).

Objectives

The objective of the cruise was to recover seven instrument frames, collect water samples, and take CTD casts for the purpose of characterizing the spatial and temporal variations in hydrography, currents, and bottom stress.

Scientific Party

The scientific party included Jim O'Donnell, Kay Howard-Strobel, David Cohen, and Christian Fox, and Alejandro Cifuentes from the University of Connecticut; Donna Aqueous, a volunteer and soon to be UConn student.

General Operations

Operations consisted of running two circuits of the seven designated moored instrument array locations and four additional CTD stations. Recovery of the seven bottom mounted instrument arrays, with CTD casts and water samples, was completed on the first circuit. The second circuit revisited all eleven stations with a CTD cast, and water sample collected at each location.

Frame Recoveries

Six frames were recovered this cruise at the locations listed in Table 1 and plotted in Figure 1. Frame 6 at station DOT6 never released floats, and appeared to be upside down on fathometer tracings at the location coordinates. The R/V Connecticut returned on August 13th with divers, located the frame at coordinates 41 14.9988 N and 71 47.9457 W and proceeded with recovery. After the frame was recovered, it was speculated that it had most likely been hit and pulled over by a dragger (see Figure 2).

ADCP Operations

The ship-board ADCP (RD Instruments, 600 kHz) was started once the RV Connecticut was underway from Avery Point. VmDas (RD Instruments, Vessel Mounted Data Acquisition System) software was used to setup and run the ADCP. The ADCP was run continuously throughout the

survey cruise. Figure 1 shows the survey track with the seven moored station locations and four additional CTD stations superimposed. Ten files are generated each time an ADCP VmDas session is started, and within that session there are multiple file segments created depending on the data size limit that was set in the VmDas options. This ensures that a significant amount of data is not lost if there is a catastrophic failure of the instrument. The default file size 1.38 MB. The naming convention of the ADCP data files is as follows:

ADCP001_000000.ENR, .ENS, .ENX, .LOG, .LTA, .N1R, .N2R, .NMS, .STA, .VMO
ADCP001_000001.ENR, …
ADCP001_000002.ENR, …
.
.
.
ADCP017_000006.ENR, …

Example: ADCP017_000006.ENR; 17 is the session number incremented when the instrument is stopped and started, 6 is the file segment number incremented every 1.38 MB.

The file types and extensions generated by VmDas are as follows:

*.ENR - Raw binary ADCP data file which contains every ping
*.ENS - Binary ADCP data after the data has been screening for backscatter and correlation
*.ENX - Binary ADCP data after screening and rotation to earth coordinates
*.STA - Binary ADCP ensemble data that has been averaged into short term averages
*.LTA - Binary ADCP ensemble data that has been averaged into long term averages
*.N1R - Raw NMEA ASCII data from the primary navigation source
*.N2R - Raw NMEA ASCII data from the secondary navigation source, if available
*.NMS - Binary screened and averaged navigation data
.VMO - ASCII file copy of the.ini options file that was used during the data collection
*.LOG - ASCII file containing a log of any errors the ADCP detected during the session

The ADCP was set to ping as fast as possible (0.3 secs/ping), with 50 bins, 1 ping/ensemble and 1 meter bins. The transducer depth was at 1.5 meters and the blanking distance was 0.88 meters. There are 54 raw ensemble ADCP data files (*.ENR) encompassing approximately 40 hours.

Files are currently located on UConn's FTP server:
/d2/dot/vmdasSurveys/vmdas ELIS CTDOT August2013

CTD Operations

A SeaBird Electronics Model 9 CTD with a Model 11 deck unit was used for the collection of the salinity and temperature profiles at each of the seven moored instrument stations and at four additional stations designated for CTD casts (Figure 1). Additional instruments were mounted

on the SBE9 rosette to collect optical data for use in characterizing the suspended sediment within the ZSF. The optical sensors included a Wetlabs EcoTriplet with wavelengths of 450, 520 and 650 nM, a Wetlabs AC9 (absortion and attenuation meter), a Sequoia Scientific Type C LISST100x particle size analyzer, and a SeaBird Electronics Model 25 CTD.

Latitude and longitude for each station profiled are presented in Table 2. The naming convention utilized for the CTD data files is as follows:

Example: dotXcastY.hex or ctdXcastY.hex

dot prefix indicates a moored instrument array station
ctd prefix indicates a CTD only station, no moored instruments
X is the station ID
Y is the cast number; 2 casts were taken each station
.hex is the native SBE CTD raw file format

When the file has been processed using the proprietary data processing program provided by SeaBird, the file extension becomes *.cnv. A “d” will be prepended if the cast is a downcast only, a “u” will be prepended if the cast is an upcast only. The data processing program also appends to the original file name, in order, the type of post-processing performed.

Example: ddot7cast1filtloopderivesplited.cnv

ddot is the downcast only
7 is the station ID
1 is the cast number
filt – the raw data was filtered using the SBE Data Processing filter module
loop – cast reversals were eliminated using the SBE Data Processing loop module
derive – salinity, density, depth were derived from the post-processed data
split – the cast was split into downcast and upcast
ed – the post-processed cast was edited manually if needed to remove any other errors or outliers

Files are currently located on UConn’s FTP server in:
/d2/dot/ctdSurveys/August2013

Water Sample Collection

A 5 liter Niskin bottle was used to collect 1000 mL of sample water to be filtered for suspended sediment concentration. The Niskin bottle was deployed using the RV Connecticut's A-frame, lowered to the bottom and then raised one meter. Approximately one minute was allowed to pass so that any sediment suspended by the bottle weight was carried away by currents before sending the messenger down the line to trigger the Niskin. POC samples were collected and stored in one liter, amber polystyrene, acid washed bottles. SSC samples were stored in one liter, clear polystyrene bottles. All bottles were labeled and refrigerated at 4°C immediately upon collection. The samples were labeled and refrigerated at 4°C immediately upon collection. Samples were collected at all stations on both survey loops.

Bottom Sediment Grabs

A modified Smith-MacIntyre type surface sediment grab was used to collect bottom sediment samples for analysis of sand to mud ratios. The grab was deployed using the RV Connecticut's A-frame. After retrieval of a bottom sediment sample, a scoop was used to transfer approximately 1000 grams to a one quart Ziploc bag which was then labeled and refrigerated at 4°C. Bottom grabs were collected at all stations on the first survey loop.

Table 1. Mooring Locations and Instrumentation.

Station	Lat	Lon	Depth (m)	SBE37 SN	ADCP SN	ADCP kHz	AQD SN	AQD Press	OBS3+ SN
DOT1	41 11.9999	72 24.0042	38.0	9693	1113	300	8456	100	T8838,T8834
DOT2	41 08.9977	72 22.2017	30.0	9694	7660	600	8428	50	T8727,T8835
DOT3	41 15.4973	72 14.5334	28.0	9695	1349	300	8445	100	T8863, T8861
DOT4	41 09.0035	71 59.9999	22.0	9696	10462	1200	8554	20	T8837,T8782
DOT5	41 09.0225	71 45.2258	30.0	10238	13197	600	8438	50	T8782,T8837
DOT6	41 15.0000	71 48.0000	36.0	9674	1094	600	8455	50	T8874,T8871
DOT7*	41 15.6001	72 05.9985	48.2	10237	195	300	8432	100	T8786,T8783

*DOT7 also equipped with two ECO Triplets: SN191 and SN321, and a Wetlabs CStar SN 1601PG transmissometer with SBE19 SN 6255.

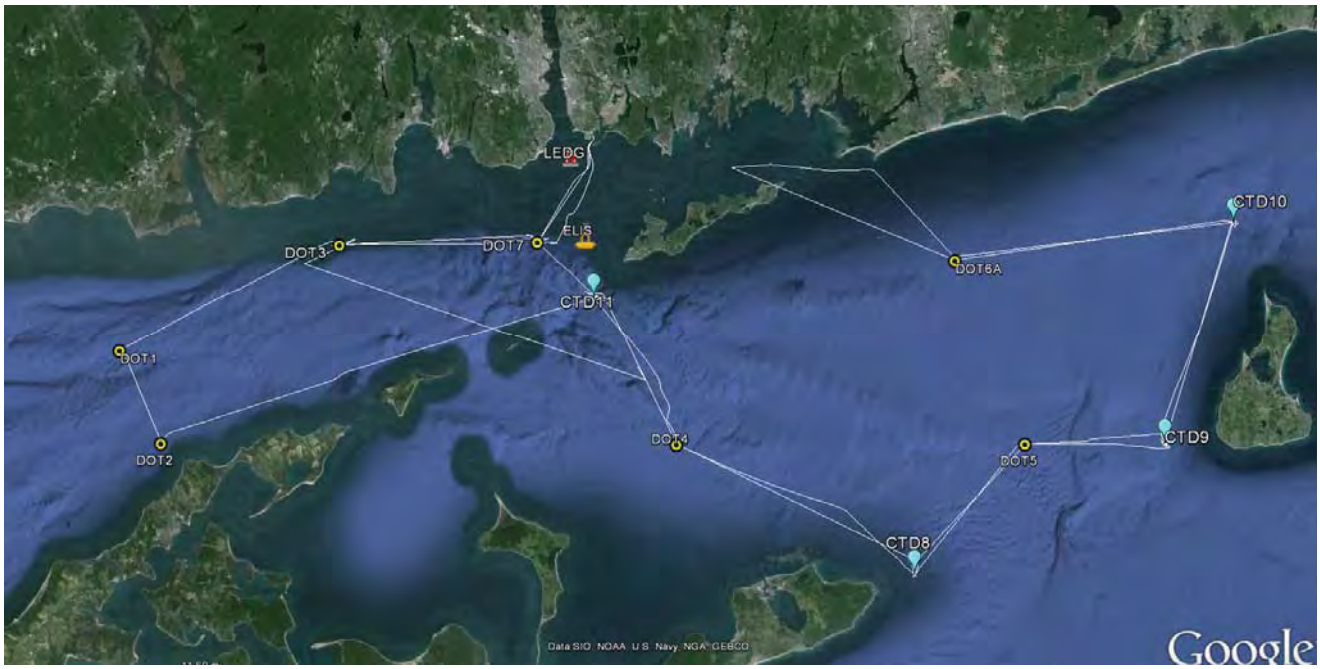

Figure 1. Locations of moored instrument arrays (DOT1-DOT7) and CTD profiles (CTD8-CTD11). LEDG is UConn's New London Ledge Light meteorological station and ELIS is UConn's metocean observation buoy. White line delineates the survey tracks for both days.

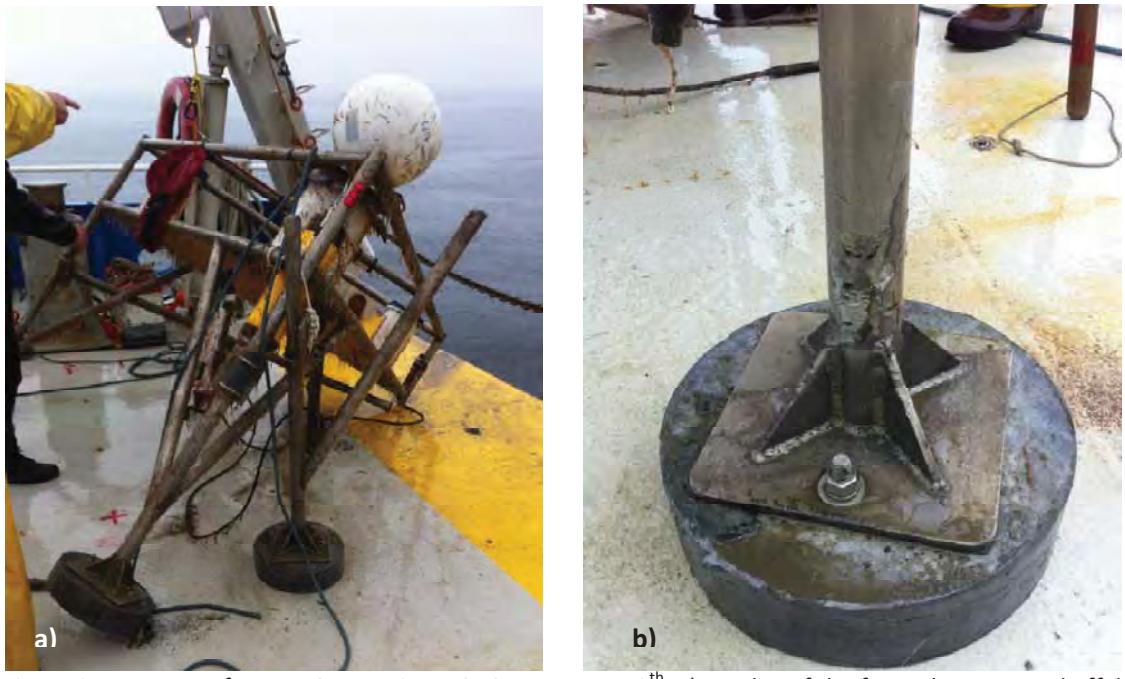

Figure 2. Recovery of Frame 6 at station DOT6 on August 13th, a) one leg of the frame has snapped off, b) abrasion on another leg.

Table 2. CTD Station Locations.

Date/Time (EST)	CTD Filename	Latitude (DDM)	Longitude (DDM)	Depth (m)	Notes
02-Aug-2013 12:30	dot7 (test)	41 15.57	072 05.68	35.0	
07-Aug-2013 08:06	dot7cast3	41 15.68	072 06.01	40.0	
07-Aug-2013 09:48	dot3cast1	41 15.56	072 14.70	27.0	
07-Aug-2013 11:20	dot1cast1	41 12.04	072 23.95	41.5	
07-Aug-2013 13:31	dot2cast1	41 09.00	072 22.26	30.0	
07-Aug-2013 14:42	ctd11cast1	41 13.95	072 03.75	43.0	
07-Aug-2013 16:00	dot4cast1	41 08.98	071 59.97	21.0	
07-Aug-2013 17:30	ctd8cast1	41 04.83	071 49.81	14.0	
07-Aug-2013 18:51	dot5cast1	41 09.00	071 44.99	28.5	
07-Aug-2013 20:05	ctd9cast1	41 09.20	071 39.03	22.5	
07-Aug-2013 21:44	ctd10cast1	41 16.12	071 36.04	36.0	
07-Aug-2013 23:54	dot6cast1	41 14.99	071 47.94	35.4	
08-Aug-2013 05:40	dot6cast2	41 15.03	071 47.97	35.0	
08-Aug-2013 07:00	ctd10cast2	41 16.32	071 36.01	33.0	
08-Aug-2013 08:16	ctd9cast2	41 09.09	071 39.01	22.0	
08-Aug-2013 10:05	ctd8cast2	41 04.86	071 49.75	30.0	
08-Aug-2013 11:23	dot4cast2	41 08.99	071 59.96	22.3	
08-Aug-2013 12:19	ctd11cast2	41 13.76	072 03.54	31.1	
08-Aug-2013 12:58	dot7cast4	41 15.66	072 05.75	29.0	
08-Aug-2013 14:09	dot3cast2	41 15.55	072 14.34	29.6	
08-Aug-2013 14:13	dot3cast3	41 15.62	072 14.12	30.2	
08-Aug-2013 15:47	dot1cast2	41 12.00	072 23.91	38.6	
08-Aug-2013 16:28	dot2cast2	41 09.22	072 21.99	31.0	

Appendices

Appendix A includes a copy of the field logbook.

Appendix A

Physical Data Collection in Eastern Long Island Sound
Field Logs

7 Aug 2013

RV CT

to recover frames
Kay, David, Jim, Christian,
Meg, Donna, Marco, Aaron
Dan, Bob

at each station frame,
grab, sample, opticast.

EDT

0708 on station DOT 7
41 15.6001, 72 05.9985

0722 frame flights
0738 frame on deck (43.8m)
0800 bottom grab 144
0810 bottom sample

0816 opticast 45 m
issues w/ power, ACS, flow sensor
done

0816 opticast start 43 m

EDT 7 Aug 2013

0851 veal cast 40 m

redo 37.8 m
35.46 m
19.1 m
2.2 m

0906 veal veal cast 44 m
< dot7cast3.hex > 40 m

btm A bottle 3 @ 38.2
btm B bottle 4 @ 35.4
mid bottle 5 @ 19.4
sfc bottle 6 @ 2.6 m

list file = no list file
did not start software

0910 u/w for DOT 3
41 15.4973, 72 14.5334

0953 frame flights
1008 frame on deck
1018 water sample 28 m
1040 bottom sample @ 28 m

Rite in the Rain.

EDT 7 August 2013

1048 start opticast 28 m
<dot3cast1.hex> 27 m

btm A bottle 3 @ 24.3 m
btm B bottle 4 @ 21.6 m
mid bottle 5 @ 14.1 m
sfc bottle 6 @ 2.3 m

did not start software ← LISST file = no LISST file

~1100 w/w for DOT 1
41 11.9999, 72 24.0042

1145 float frames
1155 frame on deck

1205 water sample 135° 41 m

1215 bottom sample (grab) 41.5 m
debubbling
1220 start opticast 41.5 m

<dot1cast1.hex>

7 Aug 2013

EDT

bottle 3 @ 39 m btm A
bottle 4 @ 36.4 m btm B
bottle 5 @ 21 m mid
bottle 6 @ 7.2 m sfc

1229 LISST file = no LISST file

1229 w/w DOT 2
41 08.9977, 72 22.2017

1300 floats
1312 frame on deck

→ water 30 m
→ bottom sed 30 m
debubbling
1331 start opticast 30 m
<DOT2CAST1.hex>

bottle 3 @ 26.4 btm A
bottle 4 @ 24.6 btm B
bottle 5 @ 14.9 mid
bottle 6 @ 1.5 sfc

DOT2 LISST file = L2191229.DAT

Rite in the Rain

EDT 7 Aug 2013

1348 u/w CTD11

1502 @ CTD11
1505 wire in 86 m
1520 abandon bottom grab
current too strong

stopped & started ADCP
for 2m bins
ADCP003_0000.*

1539 opticast started 43m
debubbling
1542 real cast 43m
<CTD11CAST2.hex>

btm A	bottle 3	32.4 m
btm B	bottle 4	320.5 m
mid	bottle 5	15.1 m
sfc	bottle 6	2.7 m

CTD11 LISST file = L2191437.DAT

1549 u/w DOT4
A1 09.0035, 71 59.9999

EDT 7 Aug 2013

1615 - switched ADCP back to
1m bins
ADCP004_0000.*

1622 on station DOT4

1625 floats
1641 frame on deck
1645 with sample 21.8m

1650 bottom grab 26m

1656 start opticast 22m
debubbling
1700 real cast 21m
<DOT4CAST1.hex>

btm A	bottle 3 e	19.1 m
btm B	bottle 4 e	16.8 m
mid	bottle 5 e	9.9
sfc	bottle 6 e	2.7 m

DOT4 LISST file = L2191556.dat

1707 u/w CTD8

Rite in the Rain

EDT 7 Aug 2013

1808 @ CTD8

1815 bottom grab 44' 13.4m
1820 water sample 45' 13.7m

48'
1827 start opticast 14m
debubbling
1830 start real cast
<CTD8 CAST1.hex>

btmA bottle 3 @ 12.1 m
btmB bottle 4 @ 10.1 m
went back down (had to refire ← bottle 5 @ 6.2 m
sfc bottle 6 @ 2.1 m

CTD8 LISST file = L2191718.dat
on/off/on? L2191722.dat
1835 u/w for DOT5
4109.0225
7145.2258

1916 floats
1930 frame on deck

1940 water sample
1945 bottom grab

EDT 7 Aug 2013

1947 opticast start 28.5m
debubbling
1951 real cast 28.5
<dot5cast1.hex>

btmA bottle 3 @ 26.5
btmB bottle 4 @ 23.7
mid bottle 5 @ 14.4
sfc bottle 6 @ 1.9

DOT5 LISST file = L2191845.dat

1956 u/w CTD9

2034 @ CTD9 currents ~3kts
tried: failed to get bottom grab
2100 water sample 21m
68'

2105 start opticast 22m
debubbling
2107 start real cast
<CTD9CAST1.hex>

Rite in the Rain

7 Aug 2013

EDT

22.5M

bottle 3 @ 20.5 btm A
bottle 4 @ 17.8 btm B
bottle 5 @ 10.9 Mid
bottle 6 @ 2.9 sfc

CTD9 USST file = no USST file

2112 going to try bottom grab
got a rock

2130 u/w CTD10

2227 bottom grab 120' 36.6m
muddy sand

2230 water sample 112' 34.1m

2241 start optic cast 36m
debubbling

2244 start real cast 36m
<CTD10CAST1.hex>

EDT

bottle 3 @ 34.4 btm A
bottle 4 @ 32.2 btm B
bottle 5 @ 18.2 Mid
bottle 6 @ 1.8 sfc

CTD10 USST file = L2192137.dat

2250 u/w DOT6 41 15.0, 71 48.0
cannot see floats

0040 on station for
water sample
no bottom grab

0045 water sample 35m

0049 start optic cast 35.4m
debubbling

0054 start real cast
<DOT6CAST1.hex>

bottle 3 @ 32.8 btm A
bottle 4 @ 30.3 btm B
bottle 5 @ 16.9 Mid
bottle 6 @ 2.9 m sfc

Rite in the Rain

8 Aug 2013

EDT

LISST file = L21923 48.dat

0117 headed to AP to drag off Alex.

looking for floats - not found 8 Aug 2013
frame trace on fathometer looks like it is upside down

0624 @ DOT 6

0639 bottom grab 115' 35m
0634 water sample 115'

tube worms, muddy sand

0640 start optical cast 35m
debubbling
start real cast
<dot6cast2.hex>

btm A bottle 3 @ 32.9 m
btm B bottle 4 @ 29.9 m
mid bottle 5 @ 16.0 m
sfc bottle 6 @ 1.8 m

8 Aug 2013

EDT DOT6
LISST file = L22 00539.dat

0649 u/w for CTD10

0745 @ CTD 10

0755 water 121'
sample 36 m

0756 start opt. cast 35m
debubbling

0800 start real cast 33m

btm A bottle 3 @ 31.3
btm B bottle 4 @ 29.2
mid bottle 5 @ 15.5
sfc bottle 6 @ 2.4
CTD10 LISST file = L22 00654.dat

0807 U/W CTD9

0858 on station CTD9

0905 water sample 73'
22.2 m

Rite in the Rain

EDT 8 Aug 2013

0911 Start optical cast 21m
debubbled

0916 start real cast 22m
<ctd9cast2.hex>

btmA bottle 3 @ 19.1
btmB bottle 4 @ 17.0
mid bottle 5 @ 10.6
sfc bottle 6 @ 2.2

CTD9 LISST filename = L2200810.dat

0919 u/w DOT5

0950 @ DOT5 102°
water sample 31m

0958 Start optical cast 30m
debubbling
start real cast
<dot5cast2.hex>

btmA bottle 3 @ 28.6
btmB bottle 4 @ 26.0
mid bottle 5 @ 14.1
sfc bottle 6 @ 2.3

EDT 8 Aug 2013

DOT5 LISST file = L2200857.dat

~1010 u/w for CTD8

Hi Kay!

1052 @ CTD8

47°
1055 water sample 14m

1105 starting optical cast 15m
debubbling
start real cast
<CTD8CAST2.HEX>

bottle 3 @ 10.4m btmA
bottle 4 @ 8.3m btmB
bottle 5 @ 5.4m mid
bottle 6 @ 2.0m sfc

CTD8 LISST file = L2201000.dat

~1115 u/w for DOT4

Rite in the Rain

EDT 8 Aug 2013

1208 @ DOT4
1212 water sample 22.9 m

1219 start opticast 22.3 m
debubbling

1223 Start real cast
<dot4cast2.hex>

btmA bottle 3 @ 20.1
btmB bottle 4 @ 18.1
mid bottle 5 @ 10.87
sfc bottle 6 @ 2.7 m

DOT4 LISST filename = L2201113.dat

~1230 u/w for CTD11

1302 @ CTD11 34.3 m

1307 water sample

EDT 8 Aug 2013

1312 Start opticast 25.1 m
debubbling 23.8 m
24.1 m

1319 Start real cast 31.1 m
<CTD11CAST2.hex>

btmA bottle 3 @ 25.81
btmB bottle 4 @ 23.5
mid bottle 5 @ 13.6
sfc bottle 6 @ 2.8

LISST filename = L2201211.dat

1325 u/w for DOT7 → ADCP005.0000
→ switch to 2m bins adcp 49 m
1346 @ DOT7
1348 water sample 47 m

1354 starting opticast 46 m
debubbling

1358 Start real cast 29 m
<dot7cast4.hex>

Rite in the Rain

8 Aug 2013

EDT

bottle 3@ 26.3 m btmA
bottle 4@ 24.1 m btmB
bottle 5@ 14.3 m mid
bottle 6@ 2.8 m sfc

LISST file = L2201251.dat
LISST @ 8.35v

1405 u/w for DOT3

1457 @ DOT3

1501 water sample 28 m

1507 start opti cast 28.4 m
debubbling
1509 real cast 29.6 m
<dot3cast2.hex>

btmA bottle 3@ 26.9 m
btmB bottle 4@ 24.4 m
mid bottle 5@ 15.6 m
sfc bottle 6@ 2.8 m

doing a second cast
Jim thinks went two jellyfish

8 Aug 2013

EDT

1513 dot3 cast3 30.2 m

LISST file = L2201401.dat

1518 u/w for DOT2

1520 reset ADCP back to 1m bins
ADCP006.000.*

1634 @ DOT2

1635 water sample 38.1 m

1644 start opticast 37.7 m
debubbling
1647 start real cast
<dot2cast2.hex> 38.6 m

bottle 3@ 36.5 m btmA
bottle 4@ 33.8 m btmB
bottle 5@ 19.37 m mid
bottle 6@ 3.04 m sfc

1650 LISST file = L2201543.dat

1652 u/w for DOT2

Rite in the Rain

1716 @ DOT2

1718 water sample 30 m

1725 start opticast 29.3 m
debubbling

1728 start real cast 31 m
<dot2cast2.hex>

btmA bottle 3 @ 26.8 m
btmB bottle 4 @ 25.4 m
mid bottle 5 @ 14.8 m
sfc bottle 6 @ 2.8 m

lisst file = L2201621.dat
8.34 volts

19:16 back @ AP.

13 Aug 2013

RN CT
Kay, David, Jeff, Joe
Christian, Marco, Frank
to retrieve frame 6

EDT

0800 u/w for station 6 location
~1020 found frame trace on fathometer
1030 shot line dropped
1100 divers in
1125 divers up
1128 divers on ~120'
~1200 frame on deck
1210 u/w for AP.
1335 back @ AP.

frame on sounder:
41 14.9988 N
71 49.9457 W

for TD conv
41° 14' 59.928"
71 49' 56.742"
7 transposed to 9 ⊛

note: frame was upside down, one leg broken

actual location was 71 47.9457

this sent to draggers and where we will deploy

Rite in the Rain

Appendix 6

CRUISE SUMMARY REPORT

CRUISE CTDOT6: November 20-21, 2013

Appendix 6: Cruise 6

CT DOT - ELIS SEIS

Physical Data Collection in Eastern Long Island Sound
Deployment Cruise Summary: November 20-21, 2013
R/V Connecticut

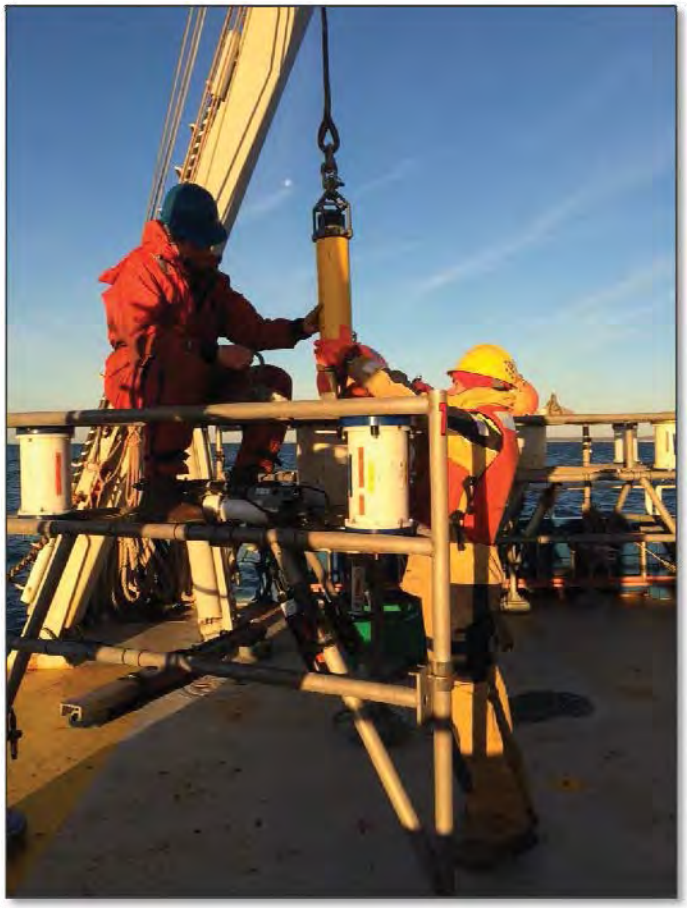

Area of Operations

Eastern Long Island Sound, extending east from the Connecticut River to Block Island, within the area designated as the Zone of Siting Feasibility (ZSF).

Objectives

The objectives of the cruise were to deploy six instrument frames, collect water samples, obtain bottom sediment grabs, and take CTD casts for the purpose of characterizing the spatial and temporal variations in hydrography, currents, and bottom stress. A seventh frame (DOT6) was to be deployed at a later date in a new location.

Scientific Party

The scientific party included, Kay Howard-Strobel, David Cohen, Christian Fox, and Alejandro Cifuentes, from the University of Connecticut, and Steve Ackleson of SA Oceans, LLC.

General Operations

Operations consisted of running two circuits of the seven designated moored instrument array locations (despite missing DOT6) and four additional CTD stations. Deployment of six instrument arrays with CTD casts and water samples, as well as the four additional sites was completed on the first circuit. The second circuit revisited all eleven stations with a CTD cast, bottom grab, and water sample collected at each location.

Frame Deployments

Six frames (DOT 1-5, and DOT 7) were deployed this cruise. Frame 6 for station DOT6 was not deployed until December 3, 2013 due to unavailability of several instruments. Frame 6 was deployed approximately 1.5 nautical miles to the east of the original location, as it had been hit by draggers twice previously. Locations for all the frames are listed in Table 1 and plotted in Figure 1. Instrumentation on each frame included a downward looking Nortek Aquadopp 2Hz high resolution pulse coherent current profiler with two Campbell Scientific OBS3+ optical backscatter units, an upward-looking RDI acoustic Doppler current profiler (ADCP) with waves array sampling enabled, and a Sea-Bird Electronics Model SMP37 conductivity/temperature sensor(Figure 2c). The height of the base of the RDI ADCP above bottom is 1.5 meters and the

height of the Nortek Aquadopp above the bottom is 0.75 meters. The OBS3+ backscatter units are mounted at 30 and 137 cm above the bottom. The frame at DOT7 also has WET Labs EcoTriplet backscatter units (Figure 2c) sampling at 470, 532 and 660 nm nm and a WET Labs Cstar 650 nm transmissometer. Table 1 documents the specifics for each instrument on each frame. The deployment configuration files (*.whp) file for each RDI ADCP are located in Appendix A. Appendix B and Appendix C contain the log files for each Nortek Aquadopp HR and Sea-Bird SMP37 configuration, respectively.

ADCP Operations

The ship-board ADCP (RD Instruments, 600 kHz) was started once the RV Connecticut was underway from Avery Point. VmDas (RD Instruments, Vessel Mounted Data Acquisition System) software was used to setup and run the ADCP. The ADCP was run continuously throughout the survey cruise. Figure 1 shows the survey track with the seven moored station locations and four additional CTD stations superimposed. Ten files are generated each time an ADCP VmDas session is started, and within that session there are multiple file segments created depending on the data size limit that was set in the VmDas options. This ensures that a significant amount of data is not lost if there is a catastrophic failure of the instrument. The default file size 1.38 MB. The naming convention of the ADCP data files is as follows:

ADCP001_000000.ENR, .ENS, .ENX, .LOG, .LTA, .N1R, .N2R, .NMS, .STA, .VMO
ADCP001_000001.ENR, …
ADCP001_000002.ENR, …
.
..
ADCP017_000006.ENR, …

Example: ADCP017_000006.ENR; 17 is the session number incremented when the instrument is stopped and started, 6 is the file segment number incremented every 1.38 MB.

The file types and extensions generated by VmDas are as follows:

*.ENR - Raw binary ADCP data file which contains every ping
*.ENS - Binary ADCP data after the data has been screening for backscatter and correlation
*.ENX - Binary ADCP data after screening and rotation to earth coordinates
*.STA - Binary ADCP ensemble data that has been averaged into short term averages
*.LTA - Binary ADCP ensemble data that has been averaged into long term averages
*.N1R - Raw NMEA ASCII data from the primary navigation source
*.N2R - Raw NMEA ASCII data from the secondary navigation source, if available
*.NMS - Binary screened and averaged navigation data
.VMO - ASCII file copy of the.ini options file that was used during the data collection

*.LOG - ASCII file containing a log of any errors the ADCP detected during the session

The ADCP was set to ping as fast as possible (0.3 secs/ping), with 50 bins, 1 ping/ensemble and 1 meter bins. The transducer depth was at 1.5 meters and the blanking distance was 0.88 meters. There are 54 raw ensemble ADCP data files (*.ENR) encompassing approximately 40 hours.

Files are currently located on UConn's NOPP FTP server in:
/d2/dot/vmdasSurveys/vmdas ELIS CTDOT Nov2013

CTD Operations

A SeaBird Electronics Model 9 CTD with a Model 11 deck unit (Figure 3) was used for the collection of the salinity and temperature profiles at each of the seven moored instrument stations and at four additional stations designated for CTD casts (Figure 1). Additional instruments were mounted on the SBE9 rosette to collect optical data for use in characterizing the suspended sediment within the ZSF. The optical sensors included a Wetlabs EcoTriplet with wavelengths of 450, 520 and 650 nM, a WET Labs AC9 (absorption and attenuation meter), a Sequoia Type C LISST100x (particle size analyzer), and a second SeaBird Electronics Model 25 CTD.

Latitude and longitude for each station profiled are presented in Table 1. The naming convention utilized for the CTD data files is as follows:

Example: dotXcastY.hex or ctdXcastY.hex

dot prefix indicates a moored instrument array station
ctd prefix indicates a CTD only station, no moored instruments
X is the station ID
Y is the cast number; 2 casts were taken each station
.hex is the native SBE CTD raw file format

When the file has been processed using the proprietary data processing program provided by SeaBird, the file extension becomes *.cnv. A "d" will be prepended if the cast is a downcast only, a "u" will be prepended if the cast is an upcast only. The data processing program also appends to the original file name, in order, the type of post-processing performed.

Example: ddot7cast1filtloopderivesplited.cnv

ddot is the downcast only
7 is the station ID
1 is the cast number

filt – the raw data was filtered using the SBE Data Processing filter module
loop – cast reversals were eliminated using the SBE Data Processing loop module
derive – salinity, density, depth were derived from the post-processed data
split – the cast was split into downcast and upcast
ed – the post-processed cast was edited manually if needed to remove any other errors or outliers

Files are currently located on UConn's NOPP FTP server in:
/d2/dot/ctdSurveys/November2013

Water Sample Collection

A 5 liter Niskin bottle was used to collect 1000 mL of sample water to be filtered for suspended sediment concentration. The Niskin bottle was deployed using the RV Connecticut's A-frame, lowered to the bottom and then raised one meter. Approximately one minute was allowed to pass so that any sediment suspended by the bottle weight was carried away by currents before sending the messenger down the line to trigger the Niskin. POC samples were collected and stored in one liter, amber polystyrene, acid washed bottles. SSC samples were stored in one liter, clear polystyrene bottles. All bottles were labeled and refrigerated at 4°C immediately upon collection. The samples were labeled and refrigerated at 4°C immediately upon collection. Samples were collected at all stations on both survey loops.

Bottom Sediment Grabs

A modified Smith-MacIntyre type surface sediment grab (Figure 4) was used to collect bottom sediment samples for analysis of sand to mud ratios. The grab was deployed using the RV Connecticut's A-frame. After retrieval of a bottom sediment sample, a scoop was used to transfer approximately 1000 grams to a one quart Ziploc bag which was then labeled and refrigerated at 4°C. Bottom grabs were collected at all stations on the second survey loop.

Table 1. Mooring Instrumentation.

Station	Lat	Lon	Depth (m)	SBE37 SN	ADCP SN	ADCP kHz	AQD SN	AQD Press	OBS3+ SN
DOT1	41 11.996	72 24.011	38.0	9693	1113	300	8456	100	T8838,T8834
DOT2	41 08.999	72 22.202	31.0	11315	7660	600	8428	50	T8862,T8872
DOT3	41 15.498	72 14.326	27.5	10237	6615	600	8445	100	T8863, T8861
DOT4	41 09.000	71 59.599	22.3	9696	10462	1200	8554	20	T8833,T8836
DOT5	41 08.996	71 45.001	29.0	11316	13197	600	8453	50	T8782,T8837
DOT6	41 14.999	71 49.939	34.0	11317	1094	600	8432	100	T8874,T8871
DOT7*	41 15.599	72 06.000	46.0	11318	195	300	8455	50	T8786,T8783

* DOT7 also equipped with two ECO Triplets: SN191 and SN321, and a Wetlabs CStar SN 1601PG transmissometer with SBE19 SN 6255

Figure 1. Locations of moored instrument arrays (DOT1-DOT7) and CTD profiles (CTD8-CTD11). LEDG is UConn's New London Ledge Light meteorological station and ELIS is UConn's metocean observation buoy. White line delineates the survey tracks for both days.

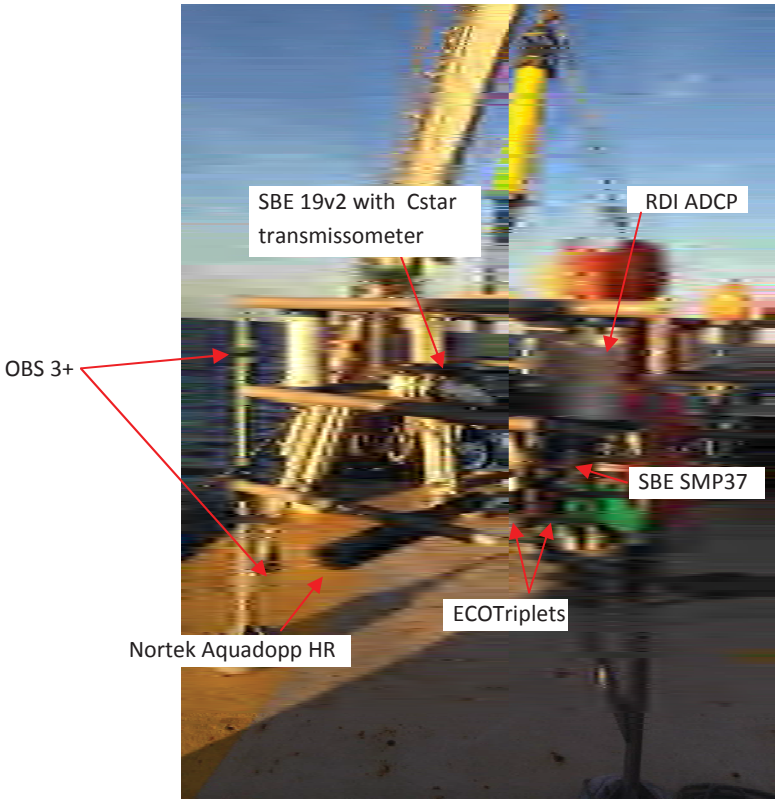

Figure 2. DOT7 bottom mooring prior to deployment.

Table 2. CTD Station Locations.

Date/Time (EST)	CTD Filename	Latitude (DDM)	Longitude (DDM)	Depth (m)	Notes
20-Nov-13 07:35	dot7cast1	41 15.63	072 06.00	46.0	
20-Nov-13 09:07	dot3cast1	41 15.47	072 14.59	28.0	drift
20-Nov-13 10:29	dot1cast1	41 11.96	072 24.15	38.0	drift
20-Nov-13 11:21	dot2cast1	41 09.00	072 22.21	31.0	
20-Nov-13 13:19	ctd11cast1	41 13.79	072 03.58	22.0	
20-Nov-13 14:30	dot4cast1	41 09.00	071 59.99	22.1	
20-Nov-13 15:47	ctd8cast1	41 04.73	071 49.83	14.0	
20-Nov-13 17:17	dot5cast1	41 09.01	071 45.00	29.6	
20-Nov-13 18:33	ctd9cast1	41 09.01	071 38.99	21.5	
20-Nov-13 20:00	ctd10cast1	41 16.21	071 35.99	36.0	
20-Nov-13 21:45	dot6cast1	41 15.00	071 49.93	34.0	
21-Nov-13 06:20	dot6cast2	41 15.01	071 49.97	33.9	
21-Nov-13 08:00	ctd10cast2	41 16.18	071 36.08	37.0	
21-Nov-13 09:12	ctd9cast2	41 09.02	071 39.02	21.0	
21-Nov-13 10:15	dot5cast2	41 09.03	071 45.03	31.5	
21-Nov-13 11:33	ctd8cast2	41 04.78	071 49.83	14.0	
21-Nov-13 12:58	dot4cast2	41 09.14	071 59.89	24.7	
21-Nov-13 13:55	ctd11cast2	41 13.72	072 03.48	37.0	
21-Nov-13 16:48	dot2cast2	41 09.09	072 22.14	30.5	
21-Nov-13 17:36	dot1cast2	41 12.05	072 23.94	41.1	
21-Nov-13 18:49	dot3cast2	41 15.56	072 14.59	27.4	
21-Nov-13 19:45	dot7cast2	41 15.66	072 06.06	43.0	

Notes: drift = currents too strong for DP, drifting with current.

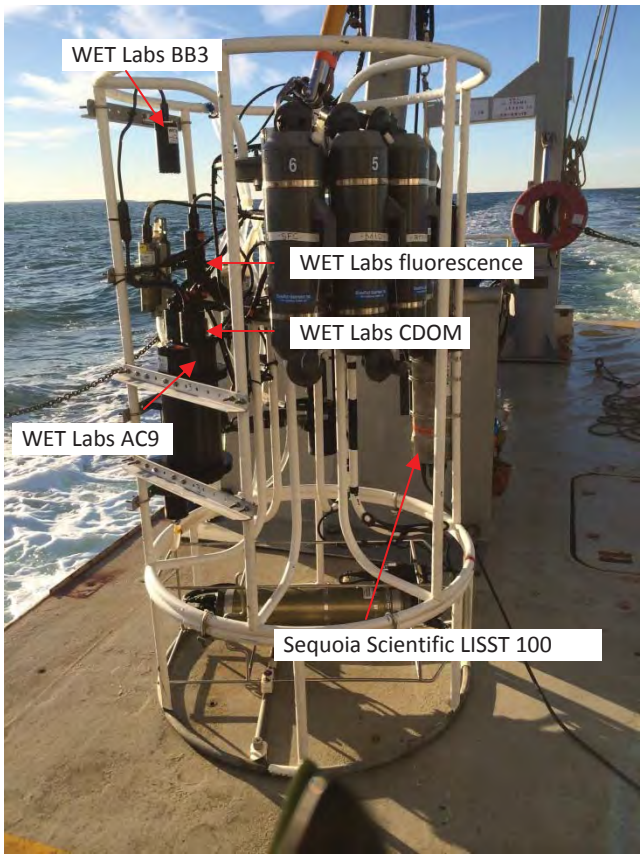

Figure 3. SBE 911 CTD with additional optical sensors.

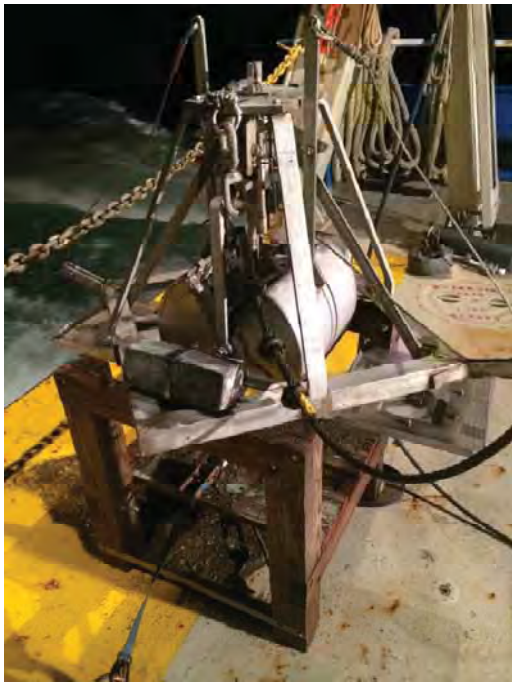

Figure 4. Modified Smith-Mac type bottom grab sampler.

Appendices

Appendix A contains RDI ADCP configuration files.

Appendix B includes the Nortek Aquadopp HR configuration files.

Appendix C includes the SBE SMP37 setup files.

Appendix D is a scanned copy of the field notebook.

Appendix A
RDI ADCP Configuration Files

DOT Frame 1

```
CR1
CF11101
EA0
EB0
ED370
ES30
EX11111
EZ1111101
WA255
WB0
WD111100000
WF50
WN40
WP180
WS100
WV175
HD111000000
HB5
HP2400
HR00:30:00.00
HT00:00:00.50
TE00:15:00.00
TP00:01.00
TF13/11/19 12:00:00
RNDOT1_
CK
CS
;
;Instrument         = Workhorse Sentinel
;Frequency          = 307200
;Water Profile      = YES
;Bottom Track       = NO
;High Res. Modes    = NO
;High Rate Pinging  = NO
;Shallow Bottom Mode= NO
;Wave Gauge         = YES
;Lowered ADCP       = NO
;Ice Track          = NO
;Surface Track      = NO
;Beam angle         = 20
;Temperature        = 10.00
;Deployment hours   = 912.00
;Battery packs      = 3
;Automatic TP       = NO
;Memory size [MB]   = 2048
;Saved Screen       = 2
;
;Consequences generated by PlanADCP version 2.06:
;First cell range   = 1.95 m
;Last cell range    = 40.95 m
;Max range          = 82.81 m
;Standard deviation = 1.01 cm/s
;Ensemble size      = 954 bytes
;Storage required   = 329.09 MB (345078912 bytes)
;Power usage        = 1327.20 Wh
;Battery usage      = 2.9
;Samples / Wv Burst = 2400
;Min NonDir Wave Per= 2.84 s
;Min Dir Wave Period= 4.79 s
;Bytes / Wave Burst = 187280
;
; WARNINGS AND CAUTIONS:
; Waves Gauge feature has to be installed in Workhorse to use selected option.
; Advanced settings have been changed.
; Expert settings have been changed.
```

DOT Frame 2

```
R1
CF11101
EA0
EB0
ED330
ES30
EX11111
EZ1111101
WA255
WB0
WD111100000
WF30
WN71
WP180
WS50
WV175
HD111000000
HB5
HP2400
HR00:30:00.00
HT00:00:00.50
TE00:15:00.00
TP00:01.00
TF13/11/19 12:00:00
RNDOT2_
CK
CS
;
;Instrument         = Workhorse Sentinel
;Frequency          = 614400
;Water Profile      = YES
;Bottom Track       = NO
;High Res. Modes    = NO
;High Rate Pinging  = NO
;Shallow Bottom Mode= NO
;Wave Gauge         = YES
;Lowered ADCP       = NO
;Ice Track          = NO
;Surface Track      = NO
;Beam angle         = 20
;Temperature        = 5.00
;Deployment hours   = 960.00
;Battery packs      = 3
;Automatic TP       = NO
;Memory size [MB]   = 304
;Saved Screen       = 2
;
;Consequences generated by PlanADCP version 2.06:
;First cell range   = 1.02 m
;Last cell range    = 36.02 m
;Max range          = 38.74 m
;Standard deviation = 1.02 cm/s
;Ensemble size      = 1574 bytes
;Storage required   = 348.68 MB (365621761 bytes)
;Power usage        = 1287.57 Wh
;Battery usage      = 2.9
;Samples / Wv Burst = 2400
;Min NonDir Wave Per= 2.69 s
;Min Dir Wave Period= 4.52 s
;Bytes / Wave Burst = 187280
;
; WARNINGS AND CAUTIONS:
; There is not enough memory for the deployment. (Memory of 304 MB will last 34 days).
; Waves Gauge feature has to be installed in Workhorse to use selected option.
; Advanced settings have been changed.
; Expert settings have been changed.
```

DOT Frame 3

```
CR1
CF11101
EA0
EB0
ED270
ES30
EX11111
EZ1111101
WA255
WB0
WD111100000
WF30
WN66
WP180
WS50
WV175
HD111000000
HB5
HP2400
HR00:30:00.00
HT00:00:00.50
TE00:15:00.00
TP00:01.00
TF13/11/19 12:00:00
RNDOT3_
CK
CS
;
;Instrument         = Workhorse Sentinel
;Frequency          = 614400
;Water Profile      = YES
;Bottom Track       = NO
;High Res. Modes    = NO
;High Rate Pinging  = NO
;Shallow Bottom Mode= NO
;Wave Gauge         = YES
;Lowered ADCP       = YES
;Ice Track          = NO
;Surface Track      = NO
;Beam angle         = 20
;Temperature        = 10.00
;Deployment hours   = 960.00
;Battery packs      = 3
;Automatic TP       = NO
;Memory size [MB]   = 1024
;Saved Screen       = 1
;
;Consequences generated by PlanADCP version 2.06:
;First cell range   = 1.02 m
;Last cell range    = 33.52 m
;Max range          = 40.69 m
;Standard deviation = 1.02 cm/s
;Ensemble size      = 1474 bytes
;Storage required   = 348.32 MB (365237761 bytes)
;Power usage        = 1246.54 Wh
;Battery usage      = 2.8
;Samples / Wv Burst = 2400
;Min NonDir Wave Per= 2.48 s
;Min Dir Wave Period= 4.09 s
;Bytes / Wave Burst = 187280
;
; WARNINGS AND CAUTIONS:
; Waves Gauge feature has to be installed in Workhorse to use selected option.
; Advanced settings have been changed.
; Expert settings have been changed.
```

DOT Frame 4

```
CR1
CF11101
EA0
EB0
ED230
ES30
EX11111
EZ1111101
WA255
WB0
WD111100000
WF44
WN26
WP180
WS100
WV175
HD111000000
HB5
HP2400
HR00:30:00.00
HT00:00:00.50
TE00:15:00.00
TP00:01.00
TF13/11/19 12:00:00
RNDOT4_
CK
CS
;
;Instrument         = Workhorse Sentinel
;Frequency          = 1228800
;Water Profile      = YES
;Bottom Track       = NO
;High Res. Modes    = NO
;High Rate Pinging  = NO
;Shallow Bottom Mode= NO
;Wave Gauge         = YES
;Lowered ADCP       = NO
;Ice Track          = NO
;Surface Track      = NO
;Beam angle         = 20
;Temperature        = 10.00
;Deployment hours   = 1080.00
;Battery packs      = 3
;Automatic TP       = NO
;Memory size [MB]   = 2048
;Saved Screen       = 2
;
;Consequences generated by PlanADCP version 2.06:
;First cell range   = 1.54 m
;Last cell range    = 26.54 m
;Max range          = 15.33 m
;Standard deviation = 0.26 cm/s
;Ensemble size      = 674 bytes
;Storage required   = 388.56 MB (407436480 bytes)
;Power usage        = 1080.33 Wh
;Battery usage      = 2.4
;Samples / Wv Burst = 2400
;Min NonDir Wave Per= 2.33 s
;Min Dir Wave Period= 3.78 s
;Bytes / Wave Burst = 187280
;
; WARNINGS AND CAUTIONS:
; Waves Gauge feature has to be installed in Workhorse to use selected option.
; Advanced settings have been changed.
```

DOT Frame 5

```
CR1
CF11101
EA0
EB0
ED330
ES30
EX11111
EZ1111101
WA255
WB0
WD111100000
WF30
WN71
WP180
WS50
WV175
HD111000000
HB5
HP2400
HR00:30:00.00
HT00:00:00.50
TE00:15:00.00
TP00:01.00
TF13/11/19 12:00:00
RNDOT5_
CK
CS
;
;Instrument         = Workhorse Sentinel
;Frequency          = 614400
;Water Profile      = YES
;Bottom Track       = NO
;High Res. Modes    = NO
;High Rate Pinging  = NO
;Shallow Bottom Mode= NO
;Wave Gauge         = YES
;Lowered ADCP       = NO
;Ice Track          = NO
;Surface Track      = NO
;Beam angle         = 20
;Temperature        = 10.00
;Deployment hours   = 960.00
;Battery packs      = 3
;Automatic TP       = NO
;Memory size [MB]   = 975
;Saved Screen       = 2
;
;Consequences generated by PlanADCP version 2.06:
;First cell range   = 1.02 m
;Last cell range    = 36.02 m
;Max range          = 40.70 m
;Standard deviation = 1.02 cm/s
;Ensemble size      = 1574 bytes
;Storage required   = 348.68 MB (365621761 bytes)
;Power usage        = 1286.83 Wh
;Battery usage      = 2.9
;Samples / Wv Burst = 2400
;Min NonDir Wave Per= 2.69 s
;Min Dir Wave Period= 4.52 s
;Bytes / Wave Burst = 187280
;
; WARNINGS AND CAUTIONS:
; Waves Gauge feature has to be installed in Workhorse to use selected option.
; Advanced settings have been changed.
; Expert settings have been changed.
```

DOT Frame 6

```
CR1
CF11101
EA0
EB0
ED360
ES30
EX11111
EZ1111101
WA255
WB0
WD111100000
WF30
WN40
WP180
WS100
WV175
HD111000000
HB5
HP2400
HR00:30:00.00
HT00:00:00.50
TE00:15:00.00
TP00:01.00
TF13/11/19 12:00:00
RNDOT6_
CK
CS
;
;Instrument         = Workhorse Sentinel
;Frequency          = 614400
;Water Profile      = YES
;Bottom Track       = NO
;High Res. Modes    = NO
;High Rate Pinging  = NO
;Shallow Bottom Mode= NO
;Wave Gauge         = YES
;Lowered ADCP       = NO
;Ice Track          = NO
;Surface Track      = NO
;Beam angle         = 20
;Temperature        = 5.00
;Deployment hours   = 1080.00
;Battery packs      = 3
;Automatic TP       = NO
;Memory size [MB]   = 2048
;Saved Screen       = 3
;
;Consequences generated by PlanADCP version 2.06:
;First cell range   = 1.52 m
;Last cell range    = 40.52 m
;Max range          = 42.66 m
;Standard deviation = 0.52 cm/s
;Ensemble size      = 954 bytes
;Storage required   = 389.72 MB (408646080 bytes)
;Power usage        = 1306.83 Wh
;Battery usage      = 2.9
;Samples / Wv Burst = 2400
;Min NonDir Wave Per= 2.80 s
;Min Dir Wave Period= 4.72 s
;Bytes / Wave Burst = 187280
;
; WARNINGS AND CAUTIONS:
; Waves Gauge feature has to be installed in Workhorse to use selected option.
; Advanced settings have been changed.
; Expert settings have been changed.
```

DOT Frame 7

```
CR1
CF11101
EA0
EB0
ED470
ES30
EX11111
EZ1111101
WA255
WB0
WD111100000
WF50
WN52
WP180
WS100
WV175
HD111000000
HB5
HP2400
HR00:30:00.00
HT00:00:00.50
TE00:15:00.00
TP00:01.00
TF13/11/19 12:00:00
RNDOT7_
CK
CS
;
;Instrument         = Workhorse Sentinel
;Frequency          = 307200
;Water Profile      = YES
;Bottom Track       = NO
;High Res. Modes    = NO
;High Rate Pinging  = NO
;Shallow Bottom Mode= NO
;Wave Gauge         = YES
;Lowered ADCP       = NO
;Ice Track          = NO
;Surface Track      = NO
;Beam angle         = 20
;Temperature        = 10.00
;Deployment hours   = 816.00
;Battery packs      = 3
;Automatic TP       = NO
;Memory size [MB]   = 2048
;Saved Screen       = 2
;
;Consequences generated by PlanADCP version 2.06:
;First cell range   = 1.95 m
;Last cell range    = 52.95 m
;Max range          = 82.86 m
;Standard deviation = 1.01 cm/s
;Ensemble size      = 1194 bytes
;Storage required   = 295.20 MB (309538177 bytes)
;Power usage        = 1291.52 Wh
;Battery usage      = 2.9
;Samples / Wv Burst = 2400
;Min NonDir Wave Per= 3.21 s
;Min Dir Wave Period= 5.40 s
;Bytes / Wave Burst = 187280
;
; WARNINGS AND CAUTIONS:
; Waves Gauge feature has to be installed in Workhorse to use selected option.
; Advanced settings have been changed.
; Expert settings have been changed.
```

Appendix B
Nortek Aquadopp HR Configuration Files

```
============================================================
Deployment   : dot1
Current time : 11/19/2013 10:05:24 AM
Start at     : 11/20/2013 6:00:00 AM
Comment:
DOT1 - November 2013 deployment
------------------------------------------------------------
Measurement interval  (s) : 1800
Cell size            (mm) : 37
Orientation               : DOWNLOOKING
Distance to bottom    (m) : 0.75
Pulse distance        (m) : 0.84
Profile range         (m) : 0.74
Horiz. vel. range   (m/s) : 1.10
Vert. vel. range    (m/s) : 0.46
Number of cells           : 20
Average interval      (s) : 1
Blanking distance     (m) : 0.048
Measurement load      (%) : 20
Samples per burst         : 2048
Sampling rate        (Hz) : 2
Compass upd. rate     (s) : 1
Coordinate System         : Beam
Speed of sound      (m/s) : MEASURED
Salinity            (ppt) : 30
Analog input 1            : PROFILE
Analog input 2            : PROFILE
Analog input power out    : ENABLED
File wrapping             : OFF
TellTale                  : OFF
Acoustic modem            : OFF
Serial output             : OFF
Baud rate                 : 115200
------------------------------------------------------------
Assumed duration   (days) : 30.0
Battery utilization   (%) : 34.0
Battery level         (V) : 11.2
Recorder size        (MB) : 3886
Recorder free space  (MB) : 3885.972
Memory required      (MB) : 832.5
------------------------------------------------------------
Instrument ID             : AQD 8456
Head ID                   : ASP 5868
Firmware version          : 3.14 HR
ProLog ID                 : 786
ProLog firmware version   : 4.14
------------------------------------------------------------
SD Card Inserted          : YES
SD Card Ready             : YES
SD Card Write protected   : NO
SD Card Type              : SDHC
SD Card Supported         : YES
------------------------------------------------------------
AquaProHR Version 1.10.08
Copyright (C) Nortek AS
============================================================
```

```
============================================================
Deployment   : dot2
Current time : 11/19/2013 9:52:58 AM
Start at     : 11/20/2013 6:00:00 AM
Comment:
DOT2 - November 2013 deployment
------------------------------------------------------------
Measurement interval  (s) : 1800
Cell size            (mm) : 37
Orientation               : DOWNLOOKING
Distance to bottom    (m) : 0.75
Pulse distance        (m) : 0.84
Profile range         (m) : 0.74
Horiz. vel. range   (m/s) : 1.10
Vert. vel. range    (m/s) : 0.46
Number of cells           : 20
Average interval      (s) : 1
Blanking distance     (m) : 0.048
Measurement load      (%) : 20
Samples per burst         : 2048
Sampling rate        (Hz) : 2
Compass upd. rate     (s) : 1
Coordinate System         : Beam
Speed of sound      (m/s) : MEASURED
Salinity            (ppt) : 30
Analog input 1            : PROFILE
Analog input 2            : PROFILE
Analog input power out    : ENABLED
File wrapping             : OFF
TellTale                  : OFF
Acoustic modem            : OFF
Serial output             : OFF
Baud rate                 : 115200
------------------------------------------------------------
Assumed duration   (days) : 30.0
Battery utilization   (%) : 34.0
Battery level         (V) : 11.2
Recorder size        (MB) : 3886
Recorder free space  (MB) : 3885.972
Memory required      (MB) : 832.5
------------------------------------------------------------
Instrument ID             : AQD 8428
Head ID                   : ASP 5866
Firmware version          : 3.14 HR
ProLog ID                 : 763
ProLog firmware version   : 4.14
------------------------------------------------------------
SD Card Inserted          : YES
SD Card Ready             : YES
SD Card Write protected   : NO
SD Card Type              : SDHC
SD Card Supported         : YES
------------------------------------------------------------
AquaProHR Version 1.10.08
Copyright (C) Nortek AS
============================================================
```

```
============================================================
Deployment   : dot3
Current time : 11/19/2013 10:08:37 AM
Start at     : 11/20/2013 6:00:00 AM
Comment:
DOT3 - November 2013 deployment
------------------------------------------------------------
Measurement interval  (s) : 1800
Cell size            (mm) : 37
Orientation               : DOWNLOOKING
Distance to bottom    (m) : 0.75
Pulse distance        (m) : 0.84
Profile range         (m) : 0.74
Horiz. vel. range   (m/s) : 1.10
Vert. vel. range    (m/s) : 0.46
Number of cells           : 20
Average interval      (s) : 1
Blanking distance     (m) : 0.048
Measurement load      (%) : 20
Samples per burst         : 2048
Sampling rate        (Hz) : 2
Compass upd. rate     (s) : 1
Coordinate System         : Beam
Speed of sound      (m/s) : MEASURED
Salinity            (ppt) : 30
Analog input 1            : PROFILE
Analog input 2            : PROFILE
Analog input power out    : ENABLED
File wrapping             : OFF
TellTale                  : OFF
Acoustic modem            : OFF
Serial output             : OFF
Baud rate                 : 115200
------------------------------------------------------------
Assumed duration   (days) : 30.0
Battery utilization   (%) : 34.0
Battery level         (V) : 11.1
Recorder size        (MB) : 3886
Recorder free space  (MB) : 3885.972
Memory required      (MB) : 832.5
------------------------------------------------------------
Instrument ID             : AQD 8445
Head ID                   : ASP 5867
Firmware version          : 3.14 HR
ProLog ID                 : 766
ProLog firmware version   : 4.14
------------------------------------------------------------
SD Card Inserted          : YES
SD Card Ready             : YES
SD Card Write protected   : NO
SD Card Type              : SDHC
SD Card Supported         : YES
------------------------------------------------------------
AquaProHR Version 1.10.08
Copyright (C) Nortek AS
============================================================
```

```
============================================================
Deployment   : dot4
Current time : 11/19/2013 10:01:39 AM
Start at     : 11/20/2013 6:00:00 AM
Comment:
DOT4 - November 2013 deployment
------------------------------------------------------------
Measurement interval  (s) : 1800
Cell size            (mm) : 37
Orientation               : DOWNLOOKING
Distance to bottom    (m) : 0.75
Pulse distance        (m) : 0.84
Profile range         (m) : 0.74
Horiz. vel. range   (m/s) : 1.10
Vert. vel. range    (m/s) : 0.46
Number of cells           : 20
Average interval      (s) : 1
Blanking distance     (m) : 0.048
Measurement load      (%) : 20
Samples per burst         : 2048
Sampling rate        (Hz) : 2
Compass upd. rate     (s) : 1
Coordinate System         : Beam
Speed of sound      (m/s) : MEASURED
Salinity            (ppt) : 30
Analog input 1            : PROFILE
Analog input 2            : PROFILE
Analog input power out    : ENABLED
File wrapping             : OFF
TellTale                  : OFF
Acoustic modem            : OFF
Serial output             : OFF
Baud rate                 : 115200
------------------------------------------------------------
Assumed duration   (days) : 30.0
Battery utilization   (%) : 34.0
Battery level         (V) : 11.1
Recorder size        (MB) : 3886
Recorder free space  (MB) : 3885.972
Memory required      (MB) : 832.5
------------------------------------------------------------
Instrument ID             : AQD 8554
Head ID                   : ASP 5590
Firmware version          : 3.14 HR
ProLog ID                 : 648
ProLog firmware version   : 4.14
------------------------------------------------------------
SD Card Inserted          : YES
SD Card Ready             : YES
SD Card Write protected   : NO
SD Card Type              : SDHC
SD Card Supported         : YES
------------------------------------------------------------
AquaProHR Version 1.10.08
Copyright (C) Nortek AS
============================================================
```

```
============================================================
Deployment   : dot5
Current time : 11/19/2013 9:57:33 AM
Start at     : 11/20/2013 6:00:00 AM
Comment:
DOT5 - November 2013 deployment
------------------------------------------------------------
Measurement interval  (s) : 1800
Cell size            (mm) : 37
Orientation               : DOWNLOOKING
Distance to bottom    (m) : 0.75
Pulse distance        (m) : 0.84
Profile range         (m) : 0.74
Horiz. vel. range   (m/s) : 1.10
Vert. vel. range    (m/s) : 0.46
Number of cells           : 20
Average interval      (s) : 1
Blanking distance     (m) : 0.048
Measurement load      (%) : 20
Samples per burst         : 2048
Sampling rate        (Hz) : 2
Compass upd. rate     (s) : 1
Coordinate System         : Beam
Speed of sound      (m/s) : MEASURED
Salinity            (ppt) : 30
Analog input 1            : PROFILE
Analog input 2            : PROFILE
Analog input power out    : ENABLED
File wrapping             : OFF
TellTale                  : OFF
Acoustic modem            : OFF
Serial output             : OFF
Baud rate                 : 115200
------------------------------------------------------------
Assumed duration   (days) : 30.0
Battery utilization   (%) : 34.0
Battery level         (V) : 11.1
Recorder size        (MB) : 3886
Recorder free space  (MB) : 3885.972
Memory required      (MB) : 832.5
------------------------------------------------------------
Instrument ID             : AQD 8453
Head ID                   : ASP 5684
Firmware version          : 3.14 HR
ProLog ID                 : 762
ProLog firmware version   : 4.14
------------------------------------------------------------
SD Card Inserted          : YES
SD Card Ready             : YES
SD Card Write protected   : NO
SD Card Type              : SDHC
SD Card Supported         : YES
------------------------------------------------------------
AquaProHR Version 1.10.08
Copyright (C) Nortek AS
============================================================
```

```
============================================================
Deployment   : dot6
Current time : 12/3/2013 10:18:05 AM
Start at     : 12/3/2013 10:30:00 AM
Comment:
DOT6 - November 2013 deployment
------------------------------------------------------------
Measurement interval  (s) : 1800
Cell size            (mm) : 37
Orientation               : DOWNLOOKING
Distance to bottom    (m) : 0.75
Pulse distance        (m) : 0.84
Profile range         (m) : 0.74
Horiz. vel. range   (m/s) : 1.10
Vert. vel. range    (m/s) : 0.46
Number of cells           : 20
Average interval      (s) : 1
Blanking distance     (m) : 0.048
Measurement load      (%) : 20
Samples per burst         : 2048
Sampling rate        (Hz) : 2
Compass upd. rate     (s) : 1
Coordinate System         : Beam
Speed of sound      (m/s) : MEASURED
Salinity            (ppt) : 30
Analog input 1            : PROFILE
Analog input 2            : PROFILE
Analog input power out    : ENABLED
File wrapping             : OFF
TellTale                  : OFF
Acoustic modem            : OFF
Serial output             : OFF
Baud rate                 : 115200
------------------------------------------------------------
Assumed duration   (days) : 30.0
Battery utilization   (%) : 34.0
Battery level         (V) : 10.5
Recorder size        (MB) : 3886
Recorder free space  (MB) : 3885.972
Memory required      (MB) : 832.5
------------------------------------------------------------
Instrument ID             : AQD 8432
Head ID                   : ASP 5869
Firmware version          : 3.14 HR
ProLog ID                 : 754
ProLog firmware version   : 4.14
------------------------------------------------------------
SD Card Inserted          : YES
SD Card Ready             : YES
SD Card Write protected   : NO
SD Card Type              : SDHC
SD Card Supported         : YES
------------------------------------------------------------
AquaProHR Version 1.10.08
Copyright (C) Nortek AS
============================================================
```

```
============================================================
Deployment   : dot7
Current time : 11/19/2013 10:11:38 AM
Start at     : 11/20/2013 6:00:00 AM
Comment:
DOT7 - November 2013 deployment
------------------------------------------------------------
Measurement interval  (s) : 1800
Cell size            (mm) : 37
Orientation               : DOWNLOOKING
Distance to bottom    (m) : 0.75
Pulse distance        (m) : 0.84
Profile range         (m) : 0.74
Horiz. vel. range   (m/s) : 1.10
Vert. vel. range    (m/s) : 0.46
Number of cells           : 20
Average interval      (s) : 1
Blanking distance     (m) : 0.048
Measurement load      (%) : 20
Samples per burst         : 2048
Sampling rate        (Hz) : 2
Compass upd. rate     (s) : 1
Coordinate System         : Beam
Speed of sound      (m/s) : MEASURED
Salinity            (ppt) : 30
Analog input 1            : PROFILE
Analog input 2            : PROFILE
Analog input power out    : ENABLED
File wrapping             : OFF
TellTale                  : OFF
Acoustic modem            : OFF
Serial output             : OFF
Baud rate                 : 115200
------------------------------------------------------------
Assumed duration   (days) : 30.0
Battery utilization   (%) : 34.0
Battery level         (V) : 11.1
Recorder size        (MB) : 3886
Recorder free space  (MB) : 3885.972
Memory required      (MB) : 832.5
------------------------------------------------------------
Instrument ID             : AQD 8455
Head ID                   : ASP 5864
Firmware version          : 3.14 HR
ProLog ID                 : 730
ProLog firmware version   : 4.14
------------------------------------------------------------
SD Card Inserted          : YES
SD Card Ready             : YES
SD Card Write protected   : NO
SD Card Type              : SDHC
SD Card Supported         : YES
------------------------------------------------------------
AquaProHR Version 1.10.08
Copyright (C) Nortek AS
============================================================
```

Appendix C
Sea-Bird Electronics SMP37 Configuration Files

DOT1

```
<Executed/>
InitLogging
this command will initialize memory
repeat the command to confirm
<Executed/>
InitLogging
<Executed/>
ds
SBE37SM-RS232 v4.1  SERIAL NO. 9693  15 Nov 2013 16:00:55
vMain = 13.43, vLith =  3.17
samplenumber = 0, free = 559240
not logging, stop command
sample interval = 900 seconds
data format = converted engineering
output salinity
transmit real-time = yes
sync mode = no
pump installed = yes, minimum conductivity frequency = 3148.2
<Executed/>
StartDateTime=11202013060000
<start dateTime = 20 Nov 2013 06:00:00/>
<Executed/>
StartLater
<!--start logging at = 20 Nov 2013 06:00:00, sample interval = 900
seconds-->
<Executed/>
ds
SBE37SM-RS232 v4.1  SERIAL NO. 9693  15 Nov 2013 16:01:46
vMain = 13.41, vLith =  3.17
samplenumber = 0, free = 559240
not logging, waiting to start at 20 Nov 2013 06:00:00
sample interval = 900 seconds
data format = converted engineering
output salinity
transmit real-time = yes
sync mode = no
pump installed = yes, minimum conductivity frequency = 3148.2
<Executed/>
```

DOT2

```
<Executed/>
InitLogging
this command will initialize memory
repeat command to confirm:
InitLogging
<Executed/>
ds
SBE37SMP-ODO-RS232 v2.3.1  SERIAL NO. 11315  15 Nov 2013 15:39:14
vMain = 13.32, vLith =  2.80
samplenumber = 0, free = 399457
not logging, stop command
sample interval = 900 seconds
data format = converted engineering
transmit real time data = yes
sync mode = no
minimum conductivity frequency = 3186.0
adaptive pump control enabled
<Executed/>
StartDateTime=11202013060000
<start dateTime = 20 Nov 2013 06:00:00/>
<Executed/>
StartLater
<!--start logging at = 20 Nov 2013 06:00:00, sample interval = 900
seconds-->
<Executed/>
ds
SBE37SMP-ODO-RS232 v2.3.1  SERIAL NO. 11315  15 Nov 2013 15:39:48
vMain = 13.31, vLith =  2.80
samplenumber = 0, free = 399457
not logging, start at 20 Nov 2013 06:00:00
sample interval = 900 seconds
data format = converted engineering
transmit real time data = yes
sync mode = no
minimum conductivity frequency = 3186.0
adaptive pump control enabled
<Executed/>
```

```
DOT3

<Executed/>
InitLogging
this command will initialize memory
repeat the command to confirm
InitLogging
<Executed/>
ds
SBE37SMP-ODO-RS232 v1.1.0  SERIAL NO. 10237  15 Nov 2013 15:53:49
vMain = 13.40, vLith =  3.19
samplenumber = 0, free = 399457
not logging, stop command
sample interval = 900 seconds
data format = converted engineering
output salinity
transmit real time data = yes
sync mode = no
minimum conductivity frequency = 3167.0
adaptive pump control enabled
<Executed/>
ds
SBE37SMP-ODO-RS232 v1.1.0  SERIAL NO. 10237  15 Nov 2013 15:54:10
vMain = 13.40, vLith =  3.19
samplenumber = 0, free = 399457
not logging, stop command
sample interval = 900 seconds
data format = converted engineering
output salinity
transmit real time data = yes
sync mode = no
minimum conductivity frequency = 3167.0
adaptive pump control enabled
<Executed/>
StartDateTime=11202013060000
<start dateTime = 20 Nov 2013 06:00:00/>
<Executed/>
StartLater
<!--start logging at = 20 Nov 2013 06:00:00, sample interval = 900
seconds-->
<Executed/>
ds
SBE37SMP-ODO-RS232 v1.1.0  SERIAL NO. 10237  15 Nov 2013 15:54:43
vMain = 13.38, vLith =  3.19
samplenumber = 0, free = 399457
not logging, waiting to start at 20 Nov 2013 06:00:00
sample interval = 900 seconds
data format = converted engineering
output salinity
transmit real time data = yes
sync mode = no
minimum conductivity frequency = 3167.0
adaptive pump control enabled
<Executed/>
```

DOT4

```
<Executed/>
InitLogging
this command will initialize memory
repeat the command to confirm
<Executed/>
InitLogging
<Executed/>
ds
SBE37SM-RS232 v4.1  SERIAL NO. 9696  15 Nov 2013 15:46:38
vMain = 13.42, vLith =  3.20
samplenumber = 0, free = 559240
not logging, stop command
sample interval = 900 seconds
data format = converted engineering
output salinity
transmit real-time = yes
sync mode = no
pump installed = yes, minimum conductivity frequency = 3160.9
<Executed/>
StartDateTime=11202013060000
<start dateTime = 20 Nov 2013 06:00:00/>
<Executed/>
StartLater
<!--start logging at = 20 Nov 2013 06:00:00, sample interval = 900
seconds-->
<Executed/>
ds
SBE37SM-RS232 v4.1  SERIAL NO. 9696  15 Nov 2013 15:47:13
vMain = 13.40, vLith =  3.20
samplenumber = 0, free = 559240
not logging, waiting to start at 20 Nov 2013 06:00:00
sample interval = 900 seconds
data format = converted engineering
output salinity
transmit real-time = yes
sync mode = no
pump installed = yes, minimum conductivity frequency = 3160.9
<Executed/>
```

DOT 5

```
<Executed/>
InitLogging
this command will initialize memory
repeat command to confirm:
InitLogging
<Executed/>
ds
SBE37SMP-ODO-RS232 v2.3.1  SERIAL NO. 11316  15 Nov 2013 15:29:12
vMain = 13.32, vLith =  2.86
samplenumber = 0, free = 399457
not logging, stop command
sample interval = 900 seconds
data format = converted engineering
output salinity
transmit real time data = yes
sync mode = no
minimum conductivity frequency = 3169.0
adaptive pump control enabled
<Executed/>
StartDateTime=11201013060000
<Error type='INVALID ARGUMENT' msg='invalid year'/>
<Executed/>
StartDateTime=11202013060000
<start dateTime = 20 Nov 2013 06:00:00/>
<Executed/>
StartLater
<!--start logging at = 20 Nov 2013 06:00:00, sample interval = 900
seconds-->
<Executed/>
ds
SBE37SMP-ODO-RS232 v2.3.1  SERIAL NO. 11316  15 Nov 2013 15:30:07
vMain = 13.32, vLith =  2.86
samplenumber = 0, free = 399457
not logging, start at 20 Nov 2013 06:00:00
sample interval = 900 seconds
data format = converted engineering
output salinity
transmit real time data = yes
sync mode = no
minimum conductivity frequency = 3169.0
adaptive pump control enabled
<Executed/>
```

```
DOT6

<Executed/>
InitLogging
this command will initialize memory
repeat command to confirm:
InitLogging
<Executed/>
ds
SBE37SMP-ODO-RS232 v2.3.1  SERIAL NO. 11317  15 Nov 2013 15:15:55
vMain = 13.30, vLith =  2.84
samplenumber = 0, free = 399457
not logging, stop command
sample interval = 900 seconds
data format = converted engineering
output salinity
transmit real time data = yes
sync mode = no
minimum conductivity frequency = 3135.8
adaptive pump control enabled
<Executed/>
StartDateTime=11202013060000
<start dateTime = 20 Nov 2013 06:00:00/>
<Executed/>
StartLater
<!--start logging at = 20 Nov 2013 06:00:00, sample interval = 900
seconds-->
<Executed/>
ds
SBE37SMP-ODO-RS232 v2.3.1  SERIAL NO. 11317  15 Nov 2013 15:16:41
vMain = 13.30, vLith =  2.84
samplenumber = 0, free = 399457
not logging, start at 20 Nov 2013 06:00:00
sample interval = 900 seconds
data format = converted engineering
output salinity
transmit real time data = yes
sync mode = no
minimum conductivity frequency = 3135.8
adaptive pump control enabled
<Executed/>
```

DOT7

```
<Executed/>
ds
SBE37SMP-ODO-RS232 v2.3.1  SERIAL NO. 11318  15 Nov 2013 15:04:13
vMain = 13.29, vLith =  2.82
samplenumber = 0, free = 399457
not logging, stop command
sample interval = 900 seconds
data format = converted engineering
output salinity
transmit real time data = yes
sync mode = no
minimum conductivity frequency = 3207.0
adaptive pump control enabled
<Executed/>
StartDateTime=11202013060000
<start dateTime = 20 Nov 2013 06:00:00/>
<Executed/>
StartLater
<!--start logging at = 20 Nov 2013 06:00:00, sample interval = 900
seconds-->
<Executed/>
ds
SBE37SMP-ODO-RS232 v2.3.1  SERIAL NO. 11318  15 Nov 2013 15:05:04
vMain = 13.28, vLith =  2.82
samplenumber = 0, free = 399457
not logging, start at 20 Nov 2013 06:00:00
sample interval = 900 seconds
data format = converted engineering
output salinity
transmit real time data = yes
sync mode = no
minimum conductivity frequency = 3207.0
adaptive pump control enabled
<Executed/>
```

DOT7 SBE 19V2 WITH WET Labs CSTAR

```
S>ds
SBE 19plus V 2.5  SERIAL NO. 6255    18 Nov 2013 21:10:42
vbatt = 12.2, vlith =  8.4, ioper =  61.7 ma, ipump = 169.7 ma,
iext01 =   3.6 ma, iext2345 =  22.9 ma
status = not logging
sample interval = 900 seconds, number of measurements per sample = 20
samples = 0, free = 3463060
mode = moored, run pump for 0.5 sec, delay before sampling = 20.0 seconds,
delay after sampling = 0.0 seconds
transmit real-time = yes
battery type = alkaline, battery cutoff =  7.5 volts
pressure sensor = strain gauge, range = 508.0
SBE 38 = no, WETLABS = no, OPTODE = no, SBE63 = no, Gas Tension Device = no
Ext Volt 0 = yes, Ext Volt 1 = no
Ext Volt 2 = yes, Ext Volt 3 = no
Ext Volt 4 = no, Ext Volt 5 = no
echo characters = yes
output format = converted decimal
output salinity = yes, output sound velocity = no
append UCSD sigma-t, V, I<Executed/>StartDateTime=11202013060000
<Executed/>StartLater
start logging at = 20 Nov 2013 06:00:00, sample interval = 900 seconds
```

Appendix D
Physical Data Collection in Eastern Long Island Sound
Field Logs

CONTENTS

PAGE	REFERENCE	FW	HC	KEY	DATE
1	AQD 8554	20m	5KJUN37RTDLX		
2	AQD 8456	100m	ZUJF29LPØKXX		
3	AQD 8428	50m	RUJG5MS6GXXX		
4	AQD 8445	100m	6MJYCERRSAXX		
5	AQD 8438	50m	XJJLØBKPP5XX		
6	AQD 8453	50m	FMJY5M6581XX		
7	AQD 8455	50m	SØJCJDG78KXX		
8	AQD 8432	100m	LEJFKJ8NPLXX		

NOVEMBER 2013 DEPLOYMENT:

FRAME1	446065	4-4-4-4	
FRAME2	446137	"	37 kHz
FRAME3	446152	"	
FRAME4	127144	"	
FRAME5	446046	"	
FRAME6	446000	"	
FRAME7	446023	"	39 kHz

QUICKWAVE HC: CX1DLEFIA5
STORM HC: KCNØ5CU3UK

implicit sample rate of 23 Hz
23 Hz × mount load = ping freq
52% → 23 × 0.52 = 11.9 Hz

tweak mount load for batt vs noise

20 Nov 2013

RV GT
Aaron, Dan, Frank, Marco
Kay, Dave, Steve, Alex,
Christian, Bob.

to deploy 6 frames for DOT project at two survey loops.

EST

0624 U/W for DOT 7
STARTED VMDAS

0720 DOT 7 frame deployed
41 15.5993 72 06.0001

0731 Niskin 41 15.6208 72 06.0042

0735 DOT 7 CTD cast 46m
debubbling

45.5 m

LISST file - did not record

Rite in the Rain

20 NOV 2013

0735 real cast 45.5 m
< dot7cast1 >

btm A	bottle 3	43.8
btm B	bottle 4	41.2
mid	bottle 5	22.5
sfc	bottle 6	2.1

0750 u/w DOT 3

0832 @ DOT 3

0853 DOT 3 deployed 41 15.4978 72 14.326

0856 Niskin 27.5 m

0903 DOT 3 debubbling cast
strong current - drifting
41 15.5113 28.5 m
72 14.5190

0907 real cast 28 m
< dot3cast1 >

20 NOV 2013

btm A	25.7 m	bottle 3
btm B	23.2 m	bottle 4
mid	14.1 m	bottle 5
sfc	2.0 m	bottle 6

LISST file = dot3_1.lsst.dat

0915 u/w DOT 1

0958 @ DOT 1

1011 DOT 1 deployed 38 m
41 11.9959
72 24.0119

1015 NISKIN 38 m
41 11.9890 72.24.215

1023 DOT 1 debubbling cast
strong current - drifting

1029 real cast 38 m
< dot1cast1 >

btm A	36.5	bottle 3
btm B	34.8	bottle 4
mid	19.9	bottle 5
sfc	1.0	bottle 6

LISST file = dot1_1.lsst.dat

Rite in the Rain

20 NOV 2013

1035 u/w DOT 2 31m

DOT 2 frame deployed
41 08.9999 72 22.2018

Niskin
41 08.9892 72 22.2179

1120 CTD debubbling cast

real cast 31 m
1124 dot2 cast 1

bottle 3 @ 29.7 m btm A
bottle 4 @ 26.2 m btm B
bottle 5 @ 15.9 m mid
bottle 6 @ 1.9 m sfc
LISST file = dot2_lisst.dat

1130 u/w CTD11

1305 @ CTD11

1308 NISKIN 18.3m

1317 CTD debubbling cast
no debubbling
straight cast

1319 real cast 22 m
< CTD11 CAST 2 >

bottle 3 @ 19.8m BTM A
bottle 4 @ 17.2m BTM B
bottle 5 @ 11.9 MID
bottle 6 @ 2.4 SFC

LISST file = CTD11_lisst.dat
this has DOT2 data mem not cleared

1323 u/w DOT 4

1400 @ DOT 4

1420 DOT4 frame deployed 22.3 m
41 09.0001 71 59.5994

1425 Niskin

1430 CTD debubbling cast 22.1m

bottle 3 @ 20.7 m BTM A
bottle 4 @ 18.1 m BTM B
bottle 5 @ 10.36 m MID
bottle 6 @ 1.8 m SFC

LISST file = dot4_lisst.dat

Rite in the Rain.

20 NOV 2013

EST

1440 u/w CTD8

1530 @ CTD8

1534 NISKIN 13m

CTD cast 12.8m
debubbling 13.7

1547 real cast 14
< ctd8 cast2 >
bottle 3 @ 12.7m btmA
bottle 4 @ 10.6 m btmB
bottle 5 @ 6.7 m mid
bottle 6 @ 1.6 m sfc

LISST file = CTD8_lisst.dat

1555 u/w DOT5

1635 @ DOT5

29 M

1640 Frame deployed
41 08.9996 71 45.0010

20 Nov 2013

EST

1652 NISKIN 29.2m

1717 CTD CAST 29.2m
debubbling

trouble w/ SBE25
& MODAPS

1720 real cast 29.6m
<dots cast2>
bottle 3 @ 28.3 m btmA
bottle 4 @ 25.6 m btmB
bottle 5 @ 14.8 m mid
bottle 6 @ 2.0 m sfc

LISST file = dots_lisst.dat

1736 u/w CTD9

1820 @ CTD9

21.5m

1824 bottom grab
41 08.9997 71.39.0002

1829 NISKIN

Rite in the Rain

20 Nov 2013

EST

1833 CTD cast 21.5m
<CTD9 cast 1>
bottle 3@ 19.4m btmA
bottle 4@ 17.0m btmB
bottle 5@ 11.0m mid
bottle 6@ 2.3m sfc

LISST file = ctd9_lisst.dat

1847 u/w CTD10

1938 @ CTD10

1948 grab 41 16.1990 36m
71 36.0007

1950 NISKIN
debubbled

2000 CTD CAST 36m
<CTD10CAST1>
btmA bottle 3@ 34.8m
btmB bottle 4@ 32.6m
mid bottle 5@ 18.1m
sfc bottle 6@ 2.5m

20 Nov 2013

EST LISST file = CTD10_1.lsst.dat

2010 u/w DOT6
actually deployed on Dec 3

2117 @ DOT6 (NEW LOCATION)
No frame deployment - short instruments

2124 grab 34m
41 14.9999
71 49.9412

2134 NISKIN

debubbled

2145 CTD CAST 34m
<dot6cast1>
bottle 3@ 32.1 btmA
bottle 4@ 30.0 btmB
bottle 5@ 16.0 mid
bottle 6@ 2.6 sfc

LISST filename = dot6_lisst.dat

completed first loop of survey. going to sit @ DOT6 till morning; work with tides.

Rite in the Rain.

21 Nov 2013

EST

0610 @ DOT6 41 15.013 / 71 49.945

NISKIN 41 15.006 / 71 49.965

0620 CTD CAST 33.9 m
< dot6cast2 >

bottle 3@ 32.5 btmA
bottle 4@ 30.1 btmB
bottle 5@ 15.9 mid
bottle 6@ 2.0 sfc

interesting fluor cast

LISST file = dot6_lisst2.dat

0632 u/w for CTD10

0745 @ CTD10 41 16.258 / 71 35.850

0748 NISKIN 31.5m
debubbled

0800 CTDCAST 37 m
<CTD10 CAST2>

way cool fluor signal here Sal 9
ctenophores, moon jellies sucked in?

21 Nov 2013

EST

bottle 3 @ 35.2m btmA
bottle 4 @ 33.0m btmB
bottle 5@ 16.9m mid
bottle 6@ 2.1m sfc

LISST file = ctd10_lisst2.dat

0812 u/w CTD9

0900 @ CTD9 41 08.925 / 71 38.919

0905 NISKIN 20.5m
debubbled

0912 CTDCAST 21 m
<CTD9CAST2>

bottle 3@ 19.1m
bottle 4@ 17.0m
bottle 5@ 10.2m
bottle 6@ 1.9m

LISST file = ctd9_lisst2.dat

0919 u/w DOT5

Rite in the Rain.

21 Nov 2013

EST

0950 on Station DOT5

0954 grab 31.5m
41 09.0393
71 45.0324

1000 NISKIN

1015 CTD CAST 31.5m
< dot5 cast2 >
bottle 3 @ 29.2m
bottle 4 @ 27.1m
bottle 5 @ 15.8m
bottle 6 @ 2.0m

LISST file = dot5_lisst2.dat

1020 u/w CTD8
1102 @ CTD 8

1107 Grab 14 m
41 04.676 71 49.71

21 Nov 2013

EST

1112 NISKIN 41 04.726
71 49.702

1133 CTD CAST 14.5m
< CTD8 CAST2 > 14.0m
bottle 3 @ 12m
bottle 4 @ 9.8m
bottle 5 @ 7.2m
bottle 6 @ 1.9m

LISST file = ctd8_lisst2.dat

1142 u/w DOT4

@ DOT4

1250 grab 41 09.005 23.2
72 00.029

1253 NISKIN

1258 CTD CAST 24.7m
41 09.103
71 59.962

Rite in the Rain

EST 21 Nov 2013

1258 <DOT4CAST2> 24.1 m
bottle 3 @ 23m 24.2 m
bottle 4 @ 20.7
bottle 5 @ 11.8m
bottle 6 @ 1.6m

~~LISST~~ file = dot4_lisst.dat

1311 U/W CTD11

1347 @ CTD11

1350 grab 19.1 m
41 13.816 72 03.633

1355 NISKIN
41 13.779 72 03.619

~ 1400 CTD CAST 37 m
41 13.722 72 03.613
bottle 3 @ 34.5m
bottle 4 @ 31.0m
bottle 5 @ 16.5m
bottle 6 @ 2.1m

LISST file = CTD11_LISST2.dat

21 Nov 2013

EST

1418 U/W DOT2

1626 @ DOT2

1630 Grab 41 09.003 72 22.154
30m

1636 NISKIN 41 09.048 72 22.203

1648 CTD CAST 30.6m
<DOT2CAST2> 30.5 m
bottle 3 @ 28.7
bottle 4 @ 26.0
bottle 5 @ 14.6
bottle 6 @ 2.1

LISST file = dot2_lisst2.dat

1657 U/W DOT1

1720 Grab 41 12.081 38.7m
72 23.993

1726 Niskin 40m

Rite in the Rain

21 Nov 2013

EST

1736 CTD Cast 39.3m
<DOT1CAST2> 41.1m

bottle 3@ 39.2
bottle 4@ 37.0
bottle 5@ 20.5
bottle 6@ 2.0

LIST file = dot1_lisst2.dat

1744 u/w DOT3

1830 @ DOT3

1833 grab 41 15.485 28m
72 14.453

1836 NISKIN 41 15.495
72 14.419

1849 CTD CAST 27.4m
<DOT3CAST2>

21 Nov 2013

EST

bottle 3@ 24.7
bottle 4@ 22.6
bottle 5@ 13.3
bottle 6@ 1.9

LISST file = dot3_lisst2.dat

1856 u/w DOT7

1938 @ DOT7

grab 41 15.627 43.7m
72 05.2416

NISKIN 41 15.646
72 05.784

CTD CAST 44m
<DOT7CAST2> 43m

41 15.666 bottle 3@ 41.2m
72.06.057 bottle 4@ 38.9m
bottle 5@ 21.0m
bottle 6@ 1.8m

16.2 volts LISST file = dot7_lisst2.dat

2008 u/w for AP

Rite in the Rain

3 Dec 2013

RV CT

Dan, Marco, Frank, Kay, David
Gary Grenier, Brennan Phillips,
Dennis Arbige, Yale: URI
guys for ROV

to deploy DOT6 @ 'new' location
URI ROV crew piggy-backing
to test out new ROV.

target location DOT6:
41 14.9988 N ≤ 41 15.00
71 49.9457 W not 71 47.9457
=71 50.00 which was orig location

EST
0945 u/w location for DOT6

1105 on station w/ DP
1112 DOT6 deployed 34 m
41 14.9996
71 49.9398

1122 CTD cast taken
30 m 313° T

1127 water sample
41 15.014
71 49.956

1130 preparing for ROV ops

ROV not doing well in
1-1.5 kts of current,
tide ebbing.

~1315 off to Brushy Pt area -
shallow water, less currents
ROV may work better.
it does.

~1445 near Brushy Pt buoy -
~1500 ROV ops, @ buoy. - dive class buoy
Found anchor.

1532 back @ AP.

Rite in the Rain

This page intentionally left blank.

Appendix 7

CRUISE SUMMARY REPORT

CRUISE CTDOT7: December 12, 17, 18, 2013

Appendix 7: Cruise 7

CT DOT - ELIS SEIS

Physical Data Collection in Eastern Long Island Sound

Battery Replacement Cruise: December 12 & 17-18, 2013

R/V Connecticut

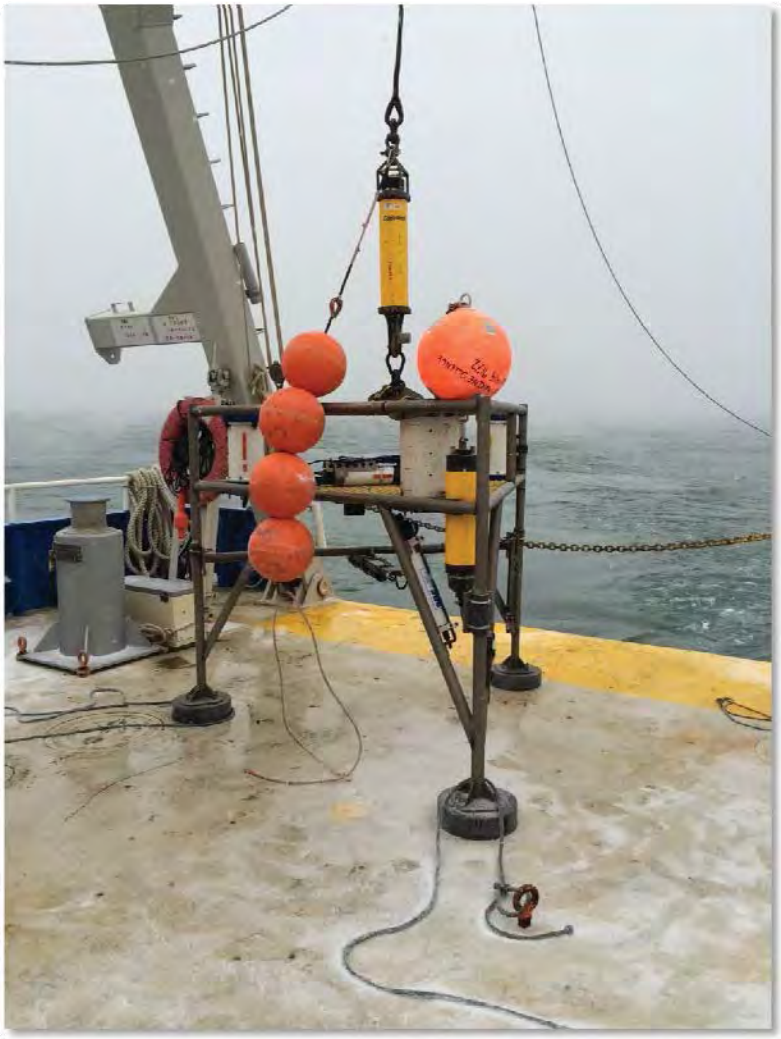

Area of Operations

Eastern Long Island Sound, extending east from the Connecticut River to Block Island, within the area designated as the Zone of Siting Feasibility (ZSF).

Objectives

The objective of the cruise was to recover seven instrument frames and replace batteries in the Nortek Aquadopp High Resolution (HR) current profilers. Water samples and CTD profiles were also collected for the purpose of characterizing the spatial and temporal variations in hydrography, currents, and bottom stress.

Scientific Party

The scientific party included Kay Howard-Strobel, David Cohen, and Christian Fox, from the University of Connecticut.

General Operations

Operations consisted of visiting each of the seven designated moored instrument array locations, recovering the bottom frame, removing the Aquadopp HR from the frame and replacing batteries, reinstalling the Aquadopp HR, and redeploying the frame. At each station a CTD cast was taken with a SBE911 profiler and a bottom water sample collected.

Frame Recoveries

All seven frames were recovered this cruise and redeployed at the locations listed in Table 1 and shown in Figure 1.

ADCP Operations

The ship-board ADCP (RD Instruments, 600 kHz) was started once the RV Connecticut was underway from Avery Point. VmDas (RD Instruments, Vessel Mounted Data Acquisition System) software was used to setup and run the ADCP. The ADCP was run continuously throughout the battery swap cruises. Figure 1 shows the December 12th survey track and the seven instrumented bottom moored stations. Figure 2 is the track from the second survey which spanned December 17 and 18th. Ten files are generated each time an ADCP VmDas session is started, and within that session there are multiple file segments created depending on the data size limit that was set in the VmDas options. This ensures that a significant amount of data is

not lost if there is a catastrophic failure of the instrument. The default file size 1.38 MB. The naming convention of the ADCP data files is as follows:

ADCP001_000000.ENR, .ENS, .ENX, .LOG, .LTA, .N1R, .N2R, .NMS, .STA, .VMO
ADCP001_000001.ENR, …
ADCP001_000002.ENR, …
.
.
ADCP017_000006.ENR, …

Example: ADCP017_000006.ENR; 17 is the session number incremented when the instrument is stopped and started, 6 is the file segment number incremented every 1.38 MB.

The file types and extensions generated by VmDas are as follows:

*.ENR - Raw binary ADCP data file which contains every ping
*.ENS - Binary ADCP data after the data has been screening for backscatter and correlation
*.ENX - Binary ADCP data after screening and rotation to earth coordinates
*.STA - Binary ADCP ensemble data that has been averaged into short term averages
*.LTA - Binary ADCP ensemble data that has been averaged into long term averages
*.N1R - Raw NMEA ASCII data from the primary navigation source
*.N2R - Raw NMEA ASCII data from the secondary navigation source, if available
*.NMS - Binary screened and averaged navigation data
.VMO - ASCII file copy of the.ini options file that was used during the data collection
*.LOG - ASCII file containing a log of any errors the ADCP detected during the session

The ADCP was set to ping as fast as possible (0.3 secs/ping), with 50 bins, 1 ping/ensemble and 1 meter bins. The transducer depth was at 1.5 meters and the blanking distance was 0.88 meters. There are 54 raw ensemble ADCP data files (*.ENR) encompassing approximately 40 hours.

Files are currently located on UConn's FTP server:
/d2/dot/vmdasSurveys/vmdas ELIS CTDOT 12Dec2013 and
/d2/dot/vmdasSurveys/vmdas ELIS CTDOT 17-18Dec2013

CTD Operations

A Sea-Bird Electronics Model 19plus was used for the collection of salinity and temperature profiles at each of the seven moored instrument stations. Latitude and longitude for each station profiled is presented in Table 2. The naming convention utilized for the CTD data files is as follows:

Example: dotX.hex or ctdX.hex

dot prefix indicates a moored instrument array station
ctd prefix indicates a CTD only station, no moored instruments
X is the station ID
.hex is the native SBE CTD raw file format

When the file has been processed using the proprietary data processing program provided by SeaBird, the file extension becomes *.cnv. A "d" will be prepended if the cast is a downcast only, a "u" will be prepended if the cast is an upcast only. The data processing program also appends to the original file name, in order, the type of post-processing performed.

Example: ddot7cast1filtloopderivesplited.cnv

ddot is the downcast only
7 is the station ID
filt – the raw data was filtered using the SBE Data Processing filter module
loop – cast reversals were eliminated using the SBE Data Processing loop module
derive – salinity, density, depth were derived from the post-processed data
split – the cast was split into downcast and upcast
ed – the post-processed cast was edited manually if needed to remove any other errors or outliers

Files are currently located on UConn's NOPP FTP server in:
/d2/dot/ctdSurveys/May2013

Water Sample Collection

A 5 liter Niskin bottle was used to collect 1000 mL of sample water to be filtered for suspended sediment concentration. The Niskin bottle was deployed using the RV Weicker's A-frame. The Niskin was lowered to the bottom and then raised one meter. Approximately one minute was allowed to pass so that any sediment suspended by the bottle weight was carried away by currents before sending the messenger down the line to trigger the Niskin. All samples were labeled and refrigerated at 4°C immediately upon collection. Samples were collected at all seven stations.

Appendices

Appendix A includes a copy of the field logbook.

Figure 1. ADCP survey track from Decmber 12th.. LEDG is UConn's New London Ledge Light meteorological station and ELIS is UConn's metocean observation buoy.

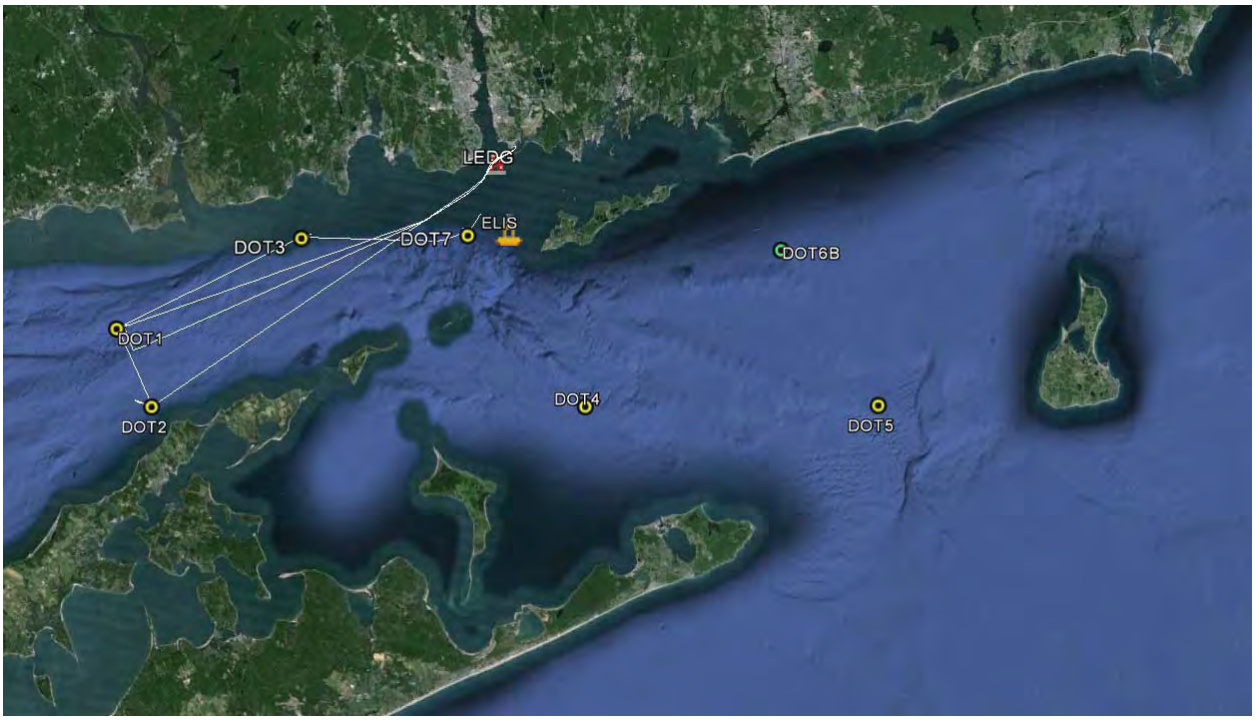

Figure 2. ADCP survey tracks from Dec 17th & 18th. LEDG is UConn's New London Ledge Light meteorological station and ELIS is UConn's metocean observation buoy.

Table 1. Location of Redeployed Frames.

Station	Lat	Lon	Depth (m)	SBE37 SN	ADCP SN	ADCP kHz	AQD SN	AQD Press	OBS3+ SN
DOT1	41 12.0016	72 23.9960	38.0	9693	1113	300	8456	100	T8838,T8834
DOT2	41 08.9996	72 22.1987	31.0	11315	7660	600	8428	50	T8862,T8872
DOT3	41 14.498	72 14.532	2.0	10237	6615	600	8445	100	T8863, T8861
DOT4	41 08.9997	71 59.9979	22.1	9696	10462	1200	8554	20	T8833,T8836
DOT5	41 09.012	71 45.003	31.2	11316	13197	600	8453	50	T8782,T8837
DOT6	41 14.999	71 49.949	35.2	11317	1094	600	8432	100	T8874,T8871
DOT7	41 15.6208	72 05.9858	48.5	11318	195	300	8455	50	T8786,T8783

Table 2. CTD Station Locations.

Date/Time (EST)	CTD Filename	Latitude (DDM)	Longitude (DDM)	Depth (m)	Notes
12-Dec-13 11:30	dot4	41 12.039	072 23.957	21.7	
12-Dec-13 15:00	dot5	41 09.024	071 45.000	30.1	
12-Dec-13 16:12	dot6	41 15.046	071 49.940	35.2	
17-Dec-13 09:59	dot7	41 15.620	072 06.115	48.5	
17-Dec-13 11:50	dot3	41 15.492	072 14.520	29.0	
18-Dec-13 11:30	dot2	41 08.999	071 22.199	31.0	
18-Dec-13 12:39	dot1	41 12.095	072 23.997	44.0	

Appendix A

Physical Data Collection in Eastern Long Island Sound
Field Logs

battery swap cruise:

- batteries! (14) for Nortek
- bottles 7 SSC (12) for BB3's
  7 POC
- niskin, messenger, funnel
- CTD
- deployment release
- deck boxes
- deployment floats
- Nortek box
- Wetlab optical box
- SBE box
- ADCP box
- manuals, contact cleaner
- tape, markers
- torgersen line box
- toughbooks & cables
- Spare AQDHR, CT, ADCP
- Voltmeter
- Passport drive

12 Dec 2013

RNCT
Dan, Marco, Frank, Aaron
Kay, Dave, Christian

battery swap on Norteks

EST
0830 u/w for DOT4.
See what we see

ADCP12 is while
we're on DOT4

0940 on station DOT4

~1010 DOT4 on deck

1100 water sample 41 08.901
22.2m 71 59.872

1110 CTD 21.7m

1130 frame on bottom
22.1m

DOT4
41 08.9997
71 59.9979

Rite in the Rain.

12 Dec 2013

EST

1140 u/w DOT5

~ 1200 DOT5 on deck

1320 water sample 30.1m
40 08.996 71 45.00

1340 CTD cast 41 09.024 30.1m
71 45.00

1400 frame deployed
DOT5 → 4109.012 71 45.003 31.2m

1405 u/w DOT6

~1500 @ DOT6
1515 frame on deck

1535 water sample 41 15.075 35m
71 49.942

1545 CTD cast 41 15.046 35.2m
71 49.940

12 Dec 2013

1612 frame deployed
41 14.999 71 49.949 DOT6

1618 u/w AP.

1740 @ AP.

Rite in the Rain

17 Dec 2013

RV-CT

Aaron, Dan, Marco,
Kay, David, Christian

to finish up batt swap in
ELIS snowing
east winds picking up

EST

0710 u/w DOT7

0758 on station - two grabs @ floats
0830 DOT7 on deck

0918 water sample 41 15.588
51 m 72 06.001

0925 CTD cast 41 15.620
48.5 m 72 06.115

move frame ~100' to north
b/c of lobster gear

17 Dec 2013

EST

0959 DOT7 deployed
41 15.6208
72 05.9858 DOT7

mem = 2028, receive file = 1802k
BB3-321 batts changed ~532k
BB3-191 batts changed ~532k in mem
mem = 2031
receive file = 1805k took about 20 min to offload

⇒ erased mems

1004 u/w for DOT3

1048 on Station DOT3
1102 DOT3 frame on deck

1136 water sample 41 15.487
29 m 72 14.486

1141 CTD cast 41 15.492
29 m 72 14.520

1150 DOT3 deployed 41 14.498
29 m 72 14.532

Rite in the Rain

17 Dec 2013

EST

1202 v/w DOT2

~1310 @ DOT2
winds east gusting to 30 kts
waves 4-6 ft.

~1325 we abort for the day
v/w for AP.

1520 back @ AP.

18 Dec 2013

EST

RV CT
Marco, Frank, Dan, Kay,
Christian, David

to finish battery swap on
frames 1 & 2

0830 v/w DOT2

1019 on station DOT2

1040 frame 2 on deck
1101 water sample
1109 CTD cast 31m

1130 frame deployed 31m

DOT2 → 41 08.9996
72 22.1987

1132 v/w DOT2

Rite in the Rain

1155 @ DOT 1

1210 frame on deck

1231 btm water sample
41 12.095
72 23.997

1239 CTD cast 44m

1303 frame on bottom

DOT 1 → 41 12.0016 / 72 23.9960 39m

1307 u/w AP

1500 back @ AP

RECOVERY → JANUARY 2014

- ✓ OPTI-ROSETTE GEAR
- X ACS ON CAL MILLQ CARBOY, PUMP
- ✓ WISKINS, FUNNEL, MESSENGER
- ✓ TOUGHBOOKS (2) & PASSPORT drive O
- ✓ LABELING TAPE & MARKERS
- X COM CABLE BOX
- ✓ ADCP BOX
- ✓ NORTEK BOX
- ✓ SPOE BOX
- ✓ OPTICALS BOX
- ✓ MANGANS CRATE
- ✓ KIMWIPES, DI BOTTLE, IPA BOTTLE
- ✓ 115 min clear bottls (+ >= 5 (dups))
- ✓ 115 min amber bottls (+ >= 5 (dups))

  11 stns * 4 depths * 2 circuits = 88
  11 stns * btm * 2 circuits = 22
  110 total

- X line bucklets ?
- ✓ coolers
- ✓ toolboxes - drill & VOLTMETER
- ✓ RELEASE CODES
- ✓ release boxes (2) ↗ & floats
- X release for deployment. first in case
- ✓ spare LISST 100 batt
- ✓ LISST BOX
- ✓ SPOE 19+
- X spare AQD

Rite in the Rain

This page intentionally left blank.

Appendix 8

CRUISE SUMMARY REPORT

CRUISE CTDOT8: January 15-16, 2014

Appendix 8: Cruise 8

CT DOT - ELIS SEIS
Physical Data Collection in Eastern Long Island Sound
Recovery Cruise Summary: January 15-16, 2014
R/V Connecticut

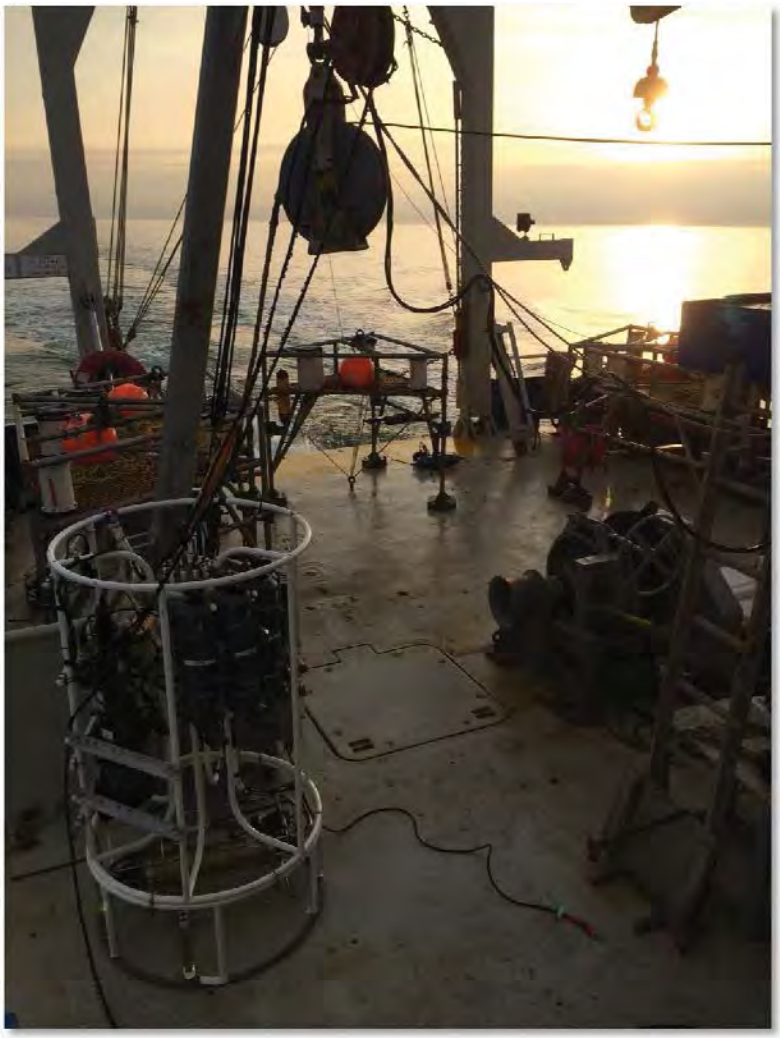

Area of Operations
Eastern Long Island Sound, extending east from the Connecticut River to Block Island, within the area designated as the Zone of Siting Feasibility (ZSF).

Objectives
The objectives of the cruise were to recover seven instrument frames, collect water samples, and take CTD casts for the purpose of characterizing the spatial and temporal variations in hydrography, currents and bottom stress.

Scientific Party
The scientific party included, Kay Howard-Strobel, David Cohen, Christian Fox, and Alejandro Cifuentes, from the University of Connecticut.

General Operations
At each station a CTD profile was taken with an optically enhanced rosette and a bottom water sample obtained using a Niskin bottle. If the station was a moored array station, the frame was recovered. After frames were recovered and all stations sampled once, a second set of CTD casts and bottom water samples were collected.

Frame Recoveries
All seven frames were recovered this cruise from the locations listed in Table 1 and shown in Figure 1.

ADCP Operations
The ship-board ADCP (RD Instruments, 600 kHz) was started once the RV Connecticut was underway from Avery Point. VmDas (RD Instruments, Vessel Mounted Data Acquisition System) software was used to setup and run the ADCP. The ADCP was run continuously throughout the survey cruise. Figure 1 shows the survey track with the seven moored station locations and four additional CTD stations superimposed. Ten files are generated each time an ADCP VmDas session is started, and within that session there are multiple file segments created depending on the data size limit that was set in the VmDas options. This ensures that a significant amount of data is not lost if there is a catastrophic failure of the instrument. The default file size 1.38 MB. The naming convention of the ADCP data files is as follows:
ADCP001_000000.ENR, .ENS, .ENX, .LOG, .LTA, .N1R, .N2R, .NMS, .STA, .VMO
ADCP001_000001.ENR, …
ADCP001_000002.ENR, …
.
.
.
ADCP017_000006.ENR, …
Example: ADCP017_000006.ENR; 17 is the session number incremented when the instrument is stopped and started, 6 is the file segment number incremented every 1.38 MB.
The file types and extensions generated by VmDas are as follows:

*.ENR - Raw binary ADCP data file which contains every ping
*.ENS - Binary ADCP data after the data has been screening for backscatter and correlation
*.ENX - Binary ADCP data after screening and rotation to earth coordinates
*.STA - Binary ADCP ensemble data that has been averaged into short term averages
*.LTA - Binary ADCP ensemble data that has been averaged into long term averages
*.N1R - Raw NMEA ASCII data from the primary navigation source
*.N2R - Raw NMEA ASCII data from the secondary navigation source, if available
*.NMS - Binary screened and averaged navigation data
.VMO - ASCII file copy of the.ini options file that was used during the data collection
*.LOG - ASCII file containing a log of any errors the ADCP detected during the session

The ADCP was set to ping as fast as possible (0.3 secs/ping), with 50 bins, 1 ping/ensemble and 1 meter bins. The transducer depth was at 1.5 meters and the blanking distance was 0.88 meters. There are 54 raw ensemble ADCP data files (*.ENR) encompassing approximately 40 hours.
Files are currently located on UConn's FTP server:
/d2/dot/vmdasSurveys/vmdas ELISCTDOT Jan2014

CTD Operations
A SeaBird Electronics Model 9 CTD with a Model 11 deck unit was used for the collection of the salinity and temperature profiles at each of the seven moored instrument stations and at four additional stations designated for CTD casts (Figure 1). Additional instruments were mounted on the SBE9 rosette to collect optical data for use in characterizing the suspended sediment within the ZSF (Figure 2). The optical sensors included a Wetlabs EcoTriplet with wavelengths of 450, 520 and 650 nM, a Wetlabs AC9 (absortion and attenuation meter), a Sequoia Type C LISST100x (particle size analyzer), and a second SeaBird Electronics Model 25 CTD.
On Day 1 of the survey cruise a SBE 19+ was used to acquire the CTD data at station CTD8 (see Table 2) as the sea state was deemed too rough to safely use the SBE911. The SBE19+ was hand lowered off the stern. Latitude, longitude, and depth for each station profiled are presented in Table 2. The naming convention utilized for the CTD data files is as follows:

Example: dotXcastY.hex or ctdXcastY.hex
dot prefix indicates a moored instrument array station
ctd prefix indicates a CTD only station, no moored instruments
X is the station ID
Y is the cast number; 2 casts were taken each station
.hex is the native SBE CTD raw file format

When the file has been processed using the proprietary data processing program provided by SeaBird, the file extension becomes *.cnv. A "d" will be prepended if the cast is a downcast

only, a "u" will be prepended if the cast is an upcast only. The data processing program also appends to the original file name, in order, the type of post-processing performed.

Example: ddot7cast1filtloopderivesplited.cnv

ddot is the downcast only
7 is the station ID
1 is the cast number
filt – the raw data was filtered using the SBE Data Processing filter module
loop – cast reversals were eliminated using the SBE Data Processing loop module
derive – salinity, density, depth were derived from the post-processed data
split – the cast was split into downcast and upcast
ed – the post-processed cast was edited manually if needed to remove any other errors or outliers

Files are currently located on UConn's NOPP FTP server in:
/d2/dot/ctdSurveys/January2014

Water Sample Collection

A 5 liter Niskin bottle was used to collect water for suspended sediment concentration and particulate organic carbon analysis. The Niskin bottle was deployed using the RV Connecticut's A-frame and lowered to the bottom then raised one meter. Approximately 30 seconds was allowed to pass so that any sediment suspended by the bottle weight was carried away by currents before sending the messenger down the line to trigger the Niskin. POC samples were collected and stored in one liter, amber polystyrene, acid washed bottles. SSC samples were stored in one liter, clear polystyrene bottles. All bottles were labeled and refrigerated at 4°C immediately upon collection. Bottom water samples were collected at all stations on both survey loops.

Table 1. Mooring Locations and Instrumentation.

Station	Lat	Lon	Depth (m)	SBE37 SN	ADCP SN	ADCP kHz	AQD SN	AQD Press	OBS3+ SN
DOT1	41 12.0016	72 23.9960	38.0	9693	1113	300	8456	100	T8838,T8834
DOT2	41 08.9996	72 22.1987	31.0	11315	7660	600	8428	50	T8862,T8872
DOT3	41 14.498	72 14.532	2.0	10237	6615	600	8445	100	T8863, T8861
DOT4	41 08.9997	71 59.9979	22.1	9696	10462	1200	8554	20	T8833,T8836
DOT5	41 09.012	71 45.003	31.2	11316	13197	600	8453	50	T8782,T8837
DOT6	41 14.999	71 49.949	35.2	11317	1094	600	8432	100	T8874,T8871
DOT7	41 15.6208	72 05.9858	48.5	11318	195	300	8455	50	T8786,T8783

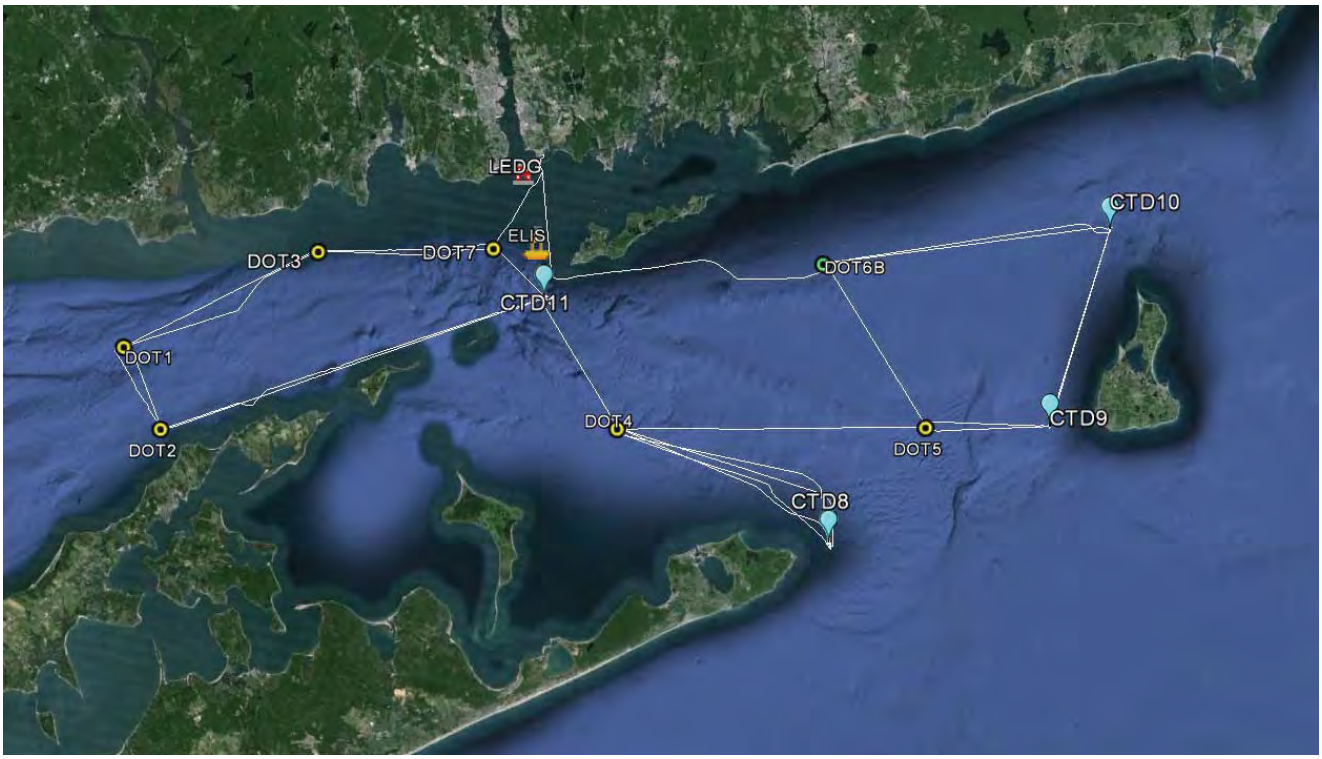

Figure 1. Locations of moored instrument arrays (DOT1-DOT7) and CTD (CTD8-CTD11) profiles. LEDG is UConn's New London Ledge Light meteorological station and ELIS is UConn's metocean observation buoy. White line delineates the survey tracks for both days.

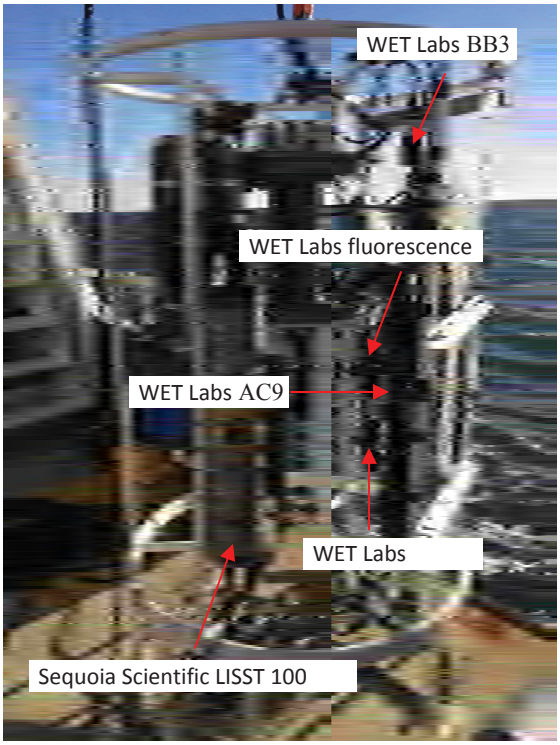

Figure 2. Optically modified SBE 911 rosette.

Figure 3. Frame 6 after recovery.

Table 2. CTD Station Locations.

Date/Time (EST)	CTD Filename	Latitude (DDM)	Longitude (DDM)	Depth (m)	Notes
15-Jan-2014 09:00	dot7cast1	41 15.582	072 06.007	46.0	drift
15-Jan-2014 10:43	dot3cast1	41 15.479	072 14.5572	29.5	drift
15-Jan-2014 12:26	dot1cast1	41 12.002	072 23.996	41.8	
15-Jan-2014 13:37	dot2cast1	41 08.950	072 22.159	32.0	
15-Jan-2014 15:14	ctd11cast1	41 13.599	072 03.357	44.0	drift
15-Jan-2014 15:52	dot7cast2	41 15.617	072 06.025	50.2	
15-Jan-2014 16:59	dot3cast2	41 15.510	072 14.560	28.3	
15-Jan-2014 18:05	dot1cast2	41 12.013	072 24.177	36.0	
15-Jan-2014 19:00	dot2cast2	41 08.967	072 22.243	30.5	
15-Jan-2014 21:33	ctd11cast2	41 13.791	072 03.211	87.5	drift
15-Jan-2014 22:36	dot4cast1	41 08.959	071 59.907	23.0	
15-Jan-2014 23:58	ctd8cast1	41 04.752	071 49.904	14.0	19+
16-Jan-2014 06:36	ctd8cast2	41 04.601	071 49.681	15.0	
16-Jan-2014 08:09	dot4cast2	41 08.973	072 00.099	23.0	
16-Jan-2014 10:00	dot5cast1	41 09.059	071 44.954	29.0	
16-Jan-2014 10:52	ctd9cast1	41 08.999	071 39.022	22.0	
16-Jan-2014 11:55	ctd10cast1	41 16.244	071 35.949	34.5	
16-Jan-2014 13:45	dot6cast1	41 15.999	071 41.883	35.3	
16-Jan-2014 14:50	dot5cast2	41 09.018	071 44.973	29.4	
16-Jan-2014 15:27	ctd9cast2	41 09.031	071 38.989	22.2	
16-Jan-2014 16:35	ctd10cast2	41 16.169	071 36.004	37.6	
16-Jan-2014 18:02	dot6cast2	41 14.934	071 49.959	33.0	

Notes: 19+, seas too rough to deploy SBE911, a SBE19+ hand lowered; drift – currents too strong for DP to hold, drifting with flow

Appendices

Appendix A includes a copy of the field logbook.

Appendix A
Physical Data Collection in Eastern Long Island Sound
Field Logs

Appendix 9

CURRENTS NEAR THE SEAFLOOR: DATA FROM THE NORTEK ADCP

a. Screening data from Campaign 1

b. Screening data from Campaign 2

c. Screening data from Campaign 3

d. Time-series of the velocity components during Campaign 1

e. Time-series of the velocity components during Campaign 2

f. Time-series of the velocity components during Campaign 3

g. Time-series of bottom pressure, temperature, battery voltage and OBS3+ sensor outputs for Campaigns 1 to 3

Appendix 9a: Nortek ADCP Data - Screening data from Campaign 1

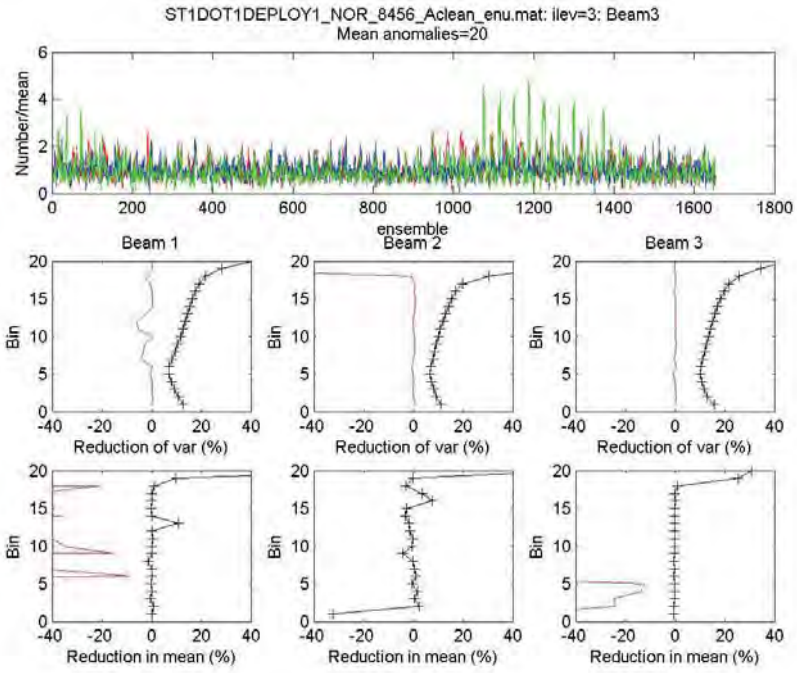

Figure 1: Screening results from Station1 on Deployment 1.: The top panel shows the time series of the number of anomalous samples in each ensemble divided by mean over all ensembels at level 3 in beams 1 (red), 2 (green) and (3) blue. The middle panels show the percentage reduction in the variance at each level and the lower panels show the change in ensemble means.

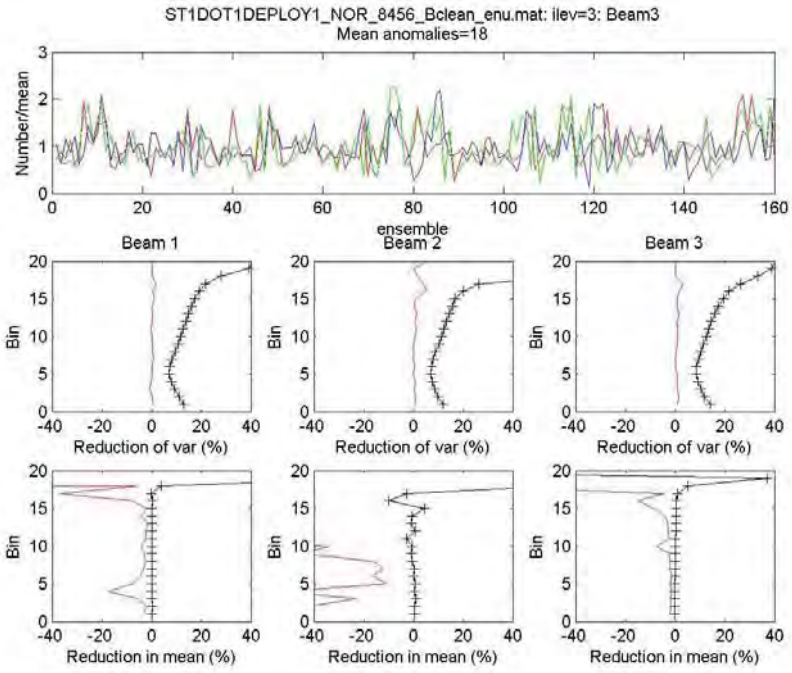

Figure 2: Screening results from Station1 on Deployment 1.: The top panel shows the time series of the number of anomalous samples in each ensembels divided by mean over all ensembels at level 3 in beams 1 (red), 2 (green) and (3) blue. The middle panels show the percentage reduction in the variance at each level and the lower panels show the change in ensemble means.

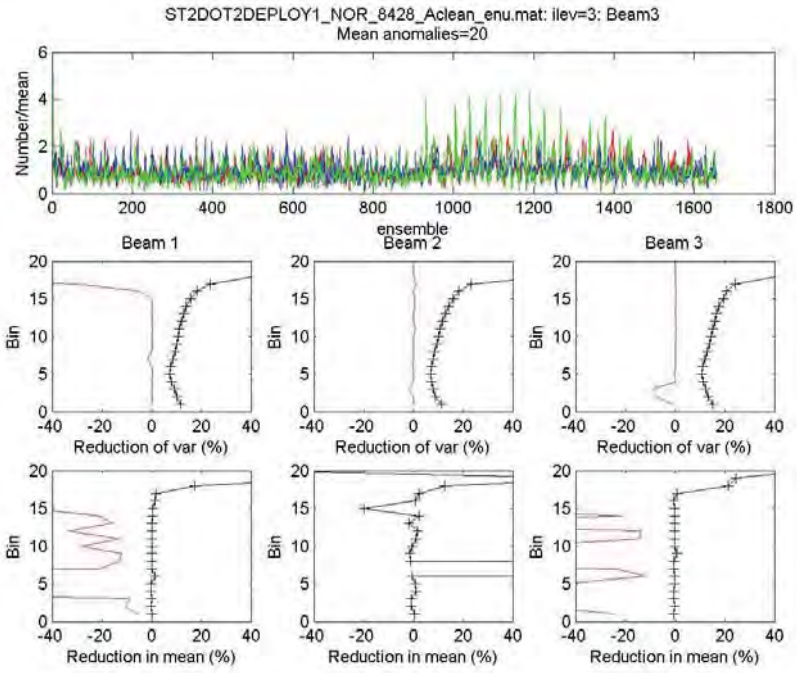

Figure 3: Screening results from Station2 on Deployment 1.: The top panel shows the time series of the number of anomalous samples in each ensembels at level 3 in beams 1 (red), 2 (green) and (3) blue. The middle panels show the percentage reduction in the variance at each level and the lower panels show the change in ensemble means.

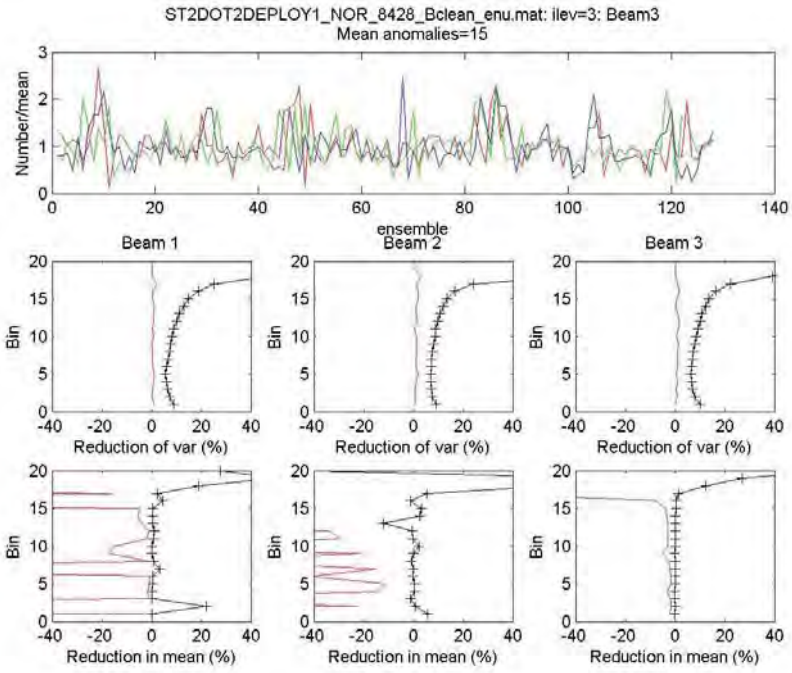

Figure 4: Screening results from Station2 on Deployment 1.: The top panel shows the time series of the number of anomalous samples in each ensembels divided by mean over all ensembels at level 3 in beams 1 (red), 2 (green) and (3) blue. The middle panels show the percentage reduction in the variance at each level and the lower panels show the change in ensemble means.

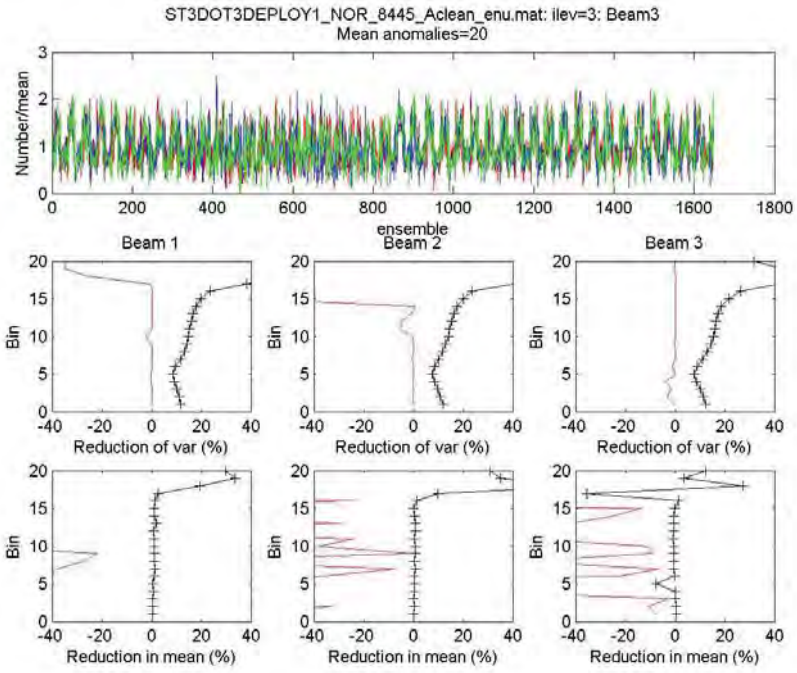

Figure 5: Screening results from Station3 on Deployment 1.: The top panel shows the time series of the number of anomalous samples in each ensembels at level 3 in beams 1 (red), 2 (green) and (3) blue. The middle panels show the percentage reduction in the variance at each level and the lower panels show the change in ensemble means.

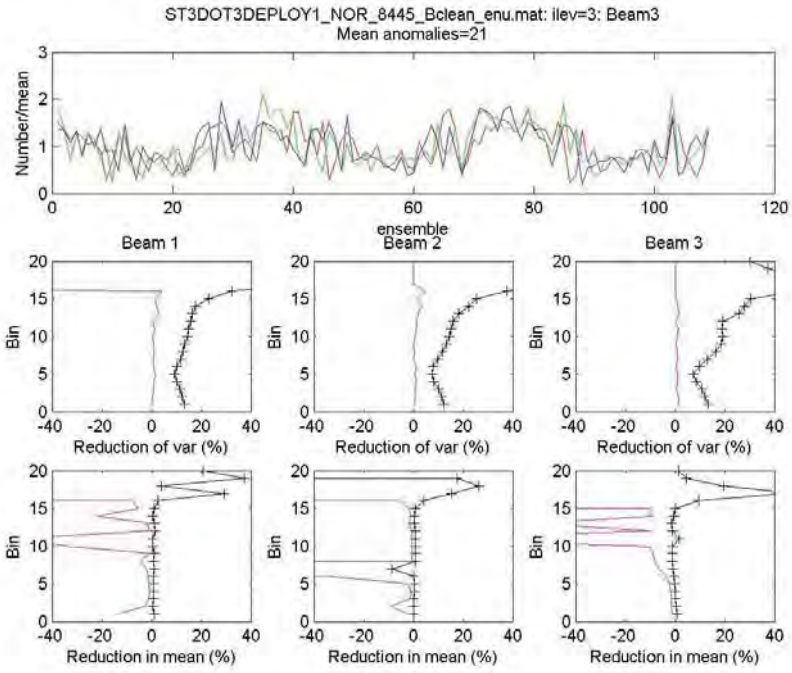

Figure 6: Screening results from Station3 on Deployment 1.: The top panel shows the time series of the number of anomalous samples in each ensembel divided by mean over all ensembels at level 3 in beams 1 (red), 2 (green) and (3) blue. The middle panels show the percentage reduction in the variance at each level and the lower panels show the change in ensemble means.

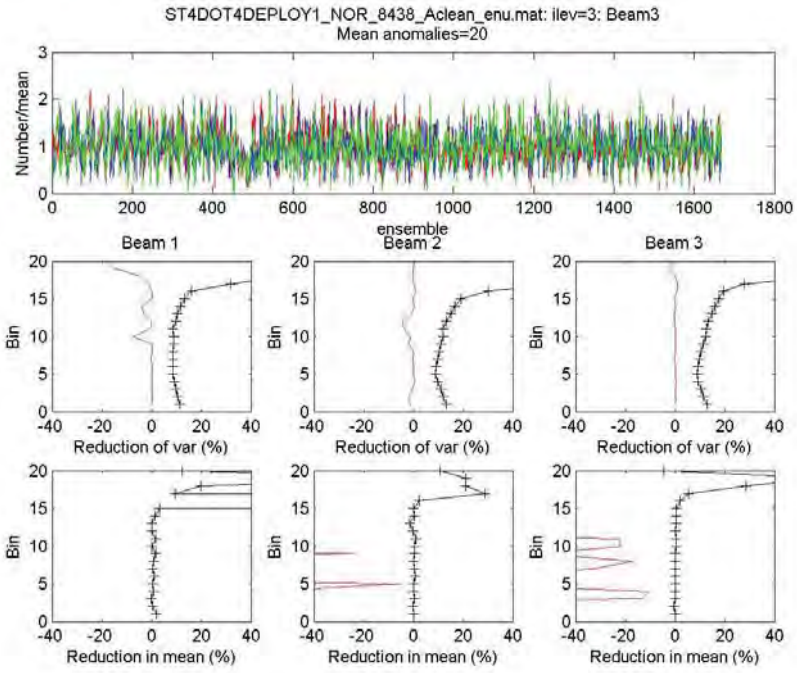

Figure 7: Screening results from Station4 on Deployment 1.: The top panel shows the time series of the number of anomalous samples in each ensembles divided by mean over all ensembels at level 3 in beams 1 (red), 2 (green) and (3) blue. The middle panels show the percentage reduction in the variance at each level and the lower panels show the change in ensemble means.

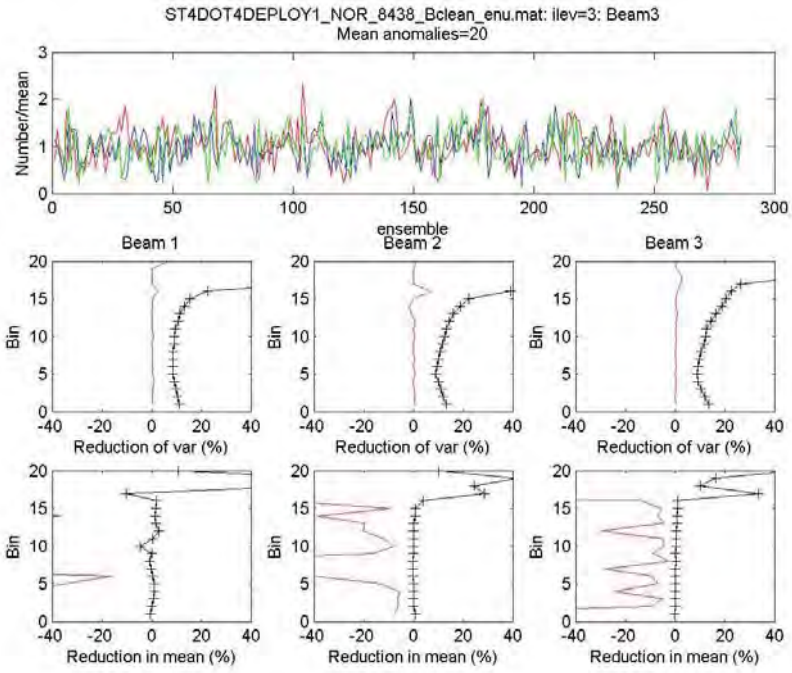

Figure 8: Screening results from Station4 on Deployment 1.: The top panel shows the time series of the number of anomalous samples in each ensemble divided by mean over all ensembels at level 3 in beams 1 (red), 2 (green) and (3) blue. The middle panels show the percentage reduction in the variance at each level and the lower panels show the change in ensemble means.

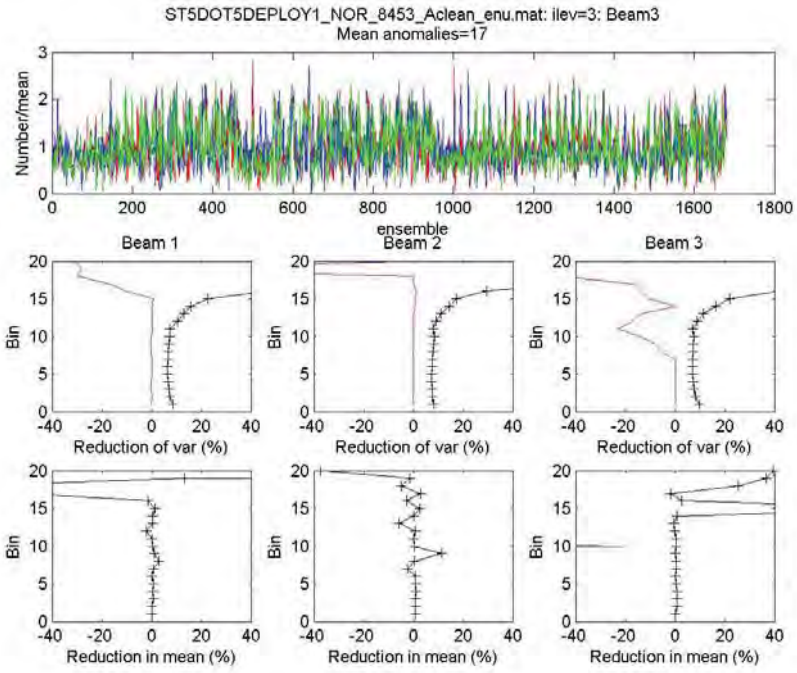

Figure 9: Screening results from Station5 on Deployment 1.: The top panel shows the time series of the number of anomalous samples in each ensemble divided by mean over all ensembels at level 3 in beams 1 (red), 2 (green) and (3) blue. The middle panels show the percentage reduction in the variance at each level and the lower panels show the change in ensemble means.

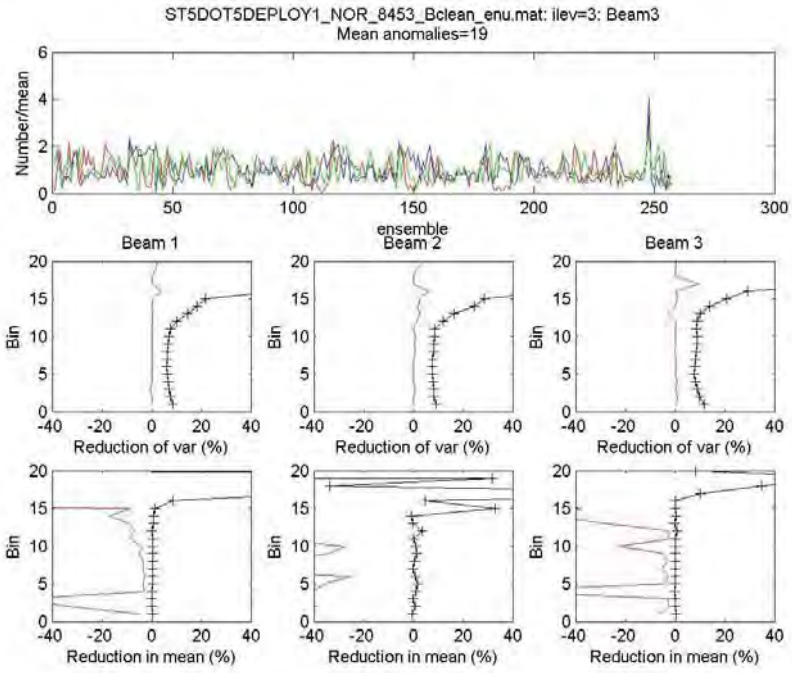

Figure 10: Screening results from Station5 on Deployment 1.: The top panel shows the time series of the number of anomalous samples in each ensembel divided by mean over all ensembels at level 3 in beams 1 (red), 2 (green) and (3) blue. The middle panels show the percentage reduction in the variance at each level and the lower panels show the change in ensemble means.

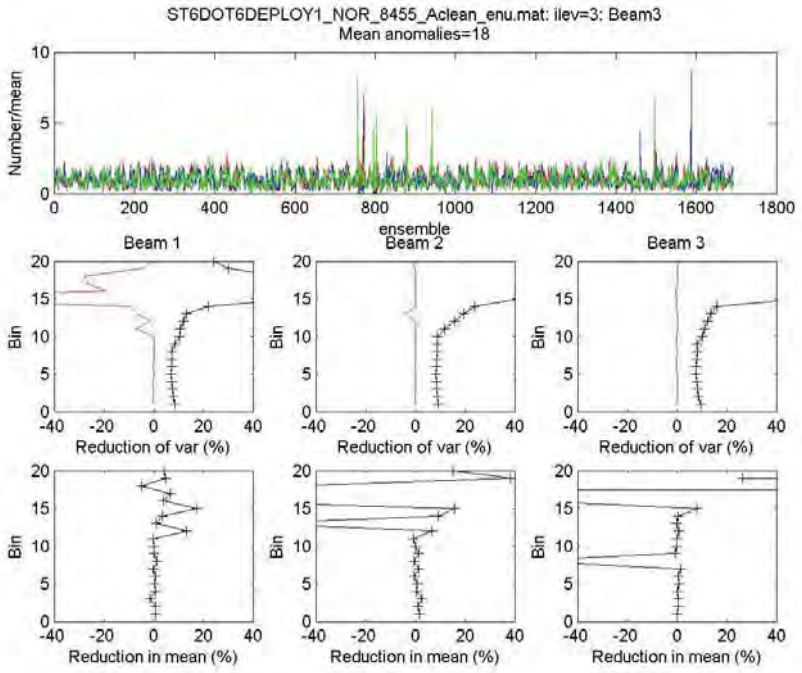

Figure 11: Screening results from Station6 on Deployment 1.: The top panel shows the time series of the number of anomalous samples in each ensembel divided by mean over all ensembels at level 3 in beams 1 (red), 2 (green) and (3) blue. The middle panels show the percentage reduction in the variance at each level and the lower panels show the change in ensemble means.

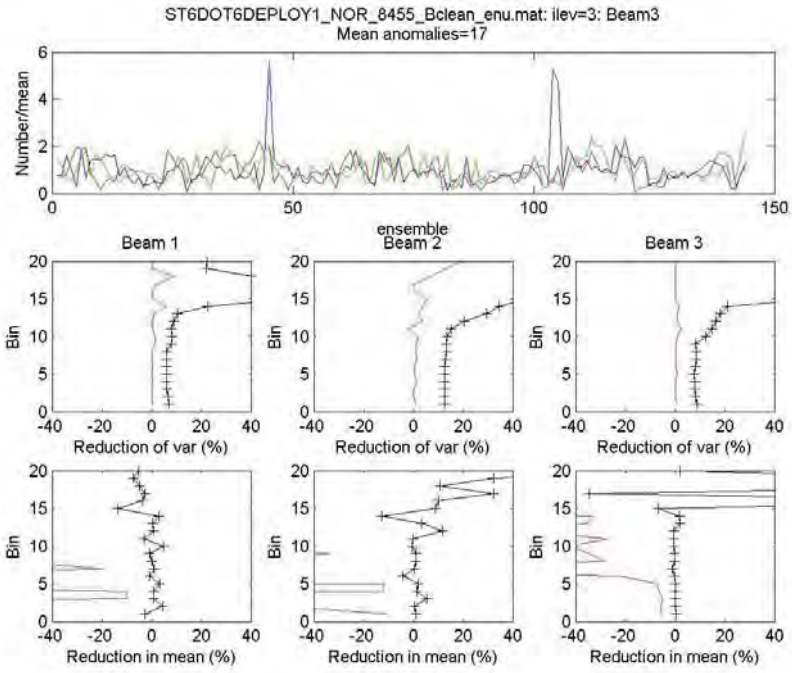

Figure 12: Screening results from Station6 on Deployment 1.: The top panel shows the time series of the number of anomalous samples in each ensemble divided by mean over all ensembels at level 3 in beams 1 (red), 2 (green) and (3) blue. The middle panels show the percentage reduction in the variance at each level and the lower panels show the change in ensemble means.

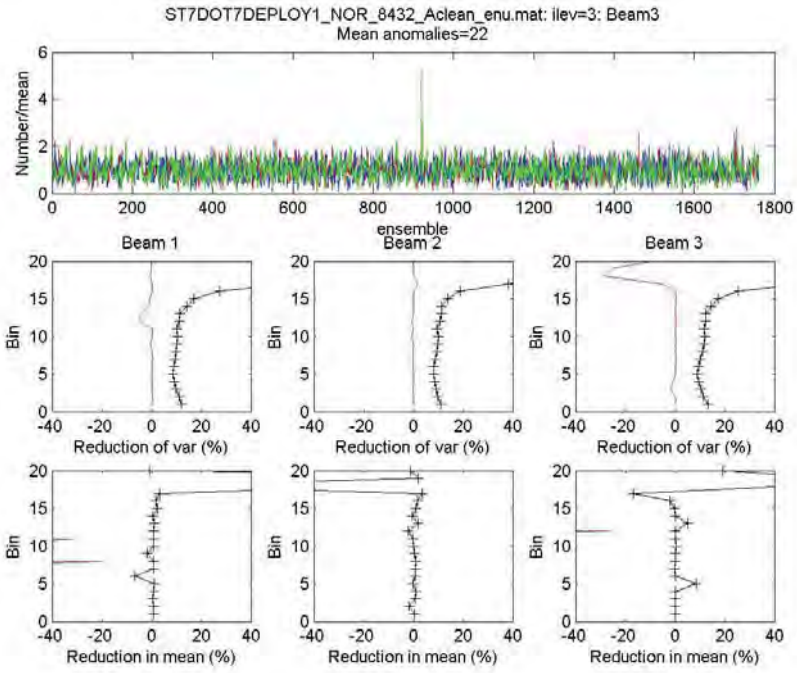

Figure 13: Screening results from Station7 on Deployment 1.: The top panel shows the time series of the number of anomalous samples in each ensembels at level 3 in beams 1 (red), 2 (green) and (3) blue. The middle panels show the percentage reduction in the variance at each level and the lower panels show the change in ensemble means.

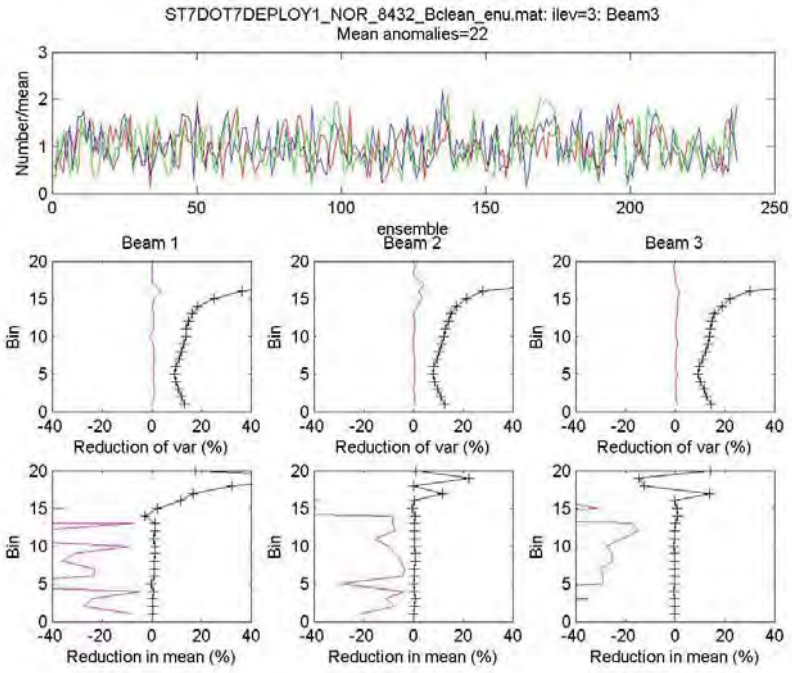

Figure 14: Screening results from Station7 on Deployment 1.: The top panel shows the time series of the number of anomalous samples in each ensembels divided by mean over all ensembels at level 3 in beams 1 (red), 2 (green) and (3) blue. The middle panels show the percentage reduction in the variance at each level and the lower panels show the change in ensemble means.

Appendix 9b: Nortek ADCP Data - Screening data from Campaign 2

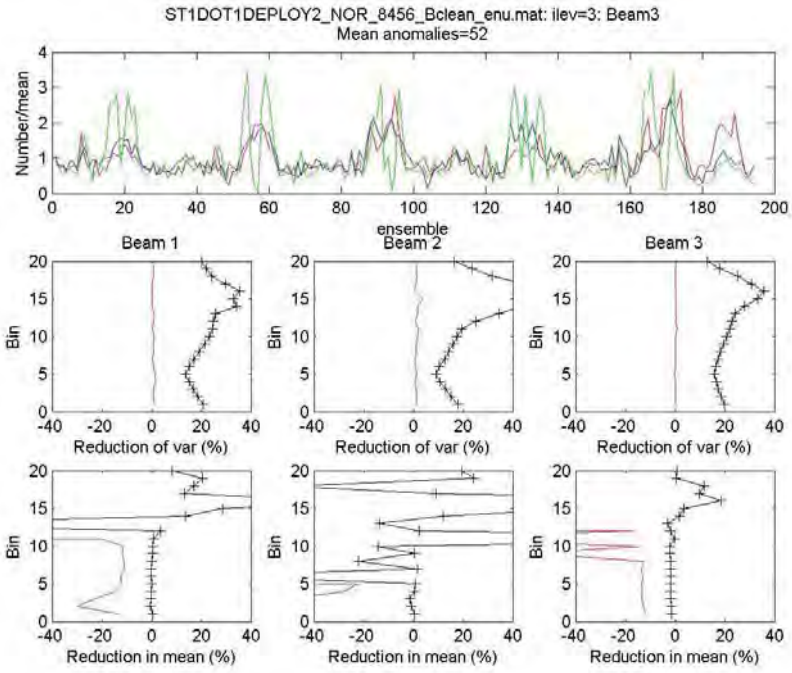

Figure 1: Screening results from Station1 on Deployment 2.: The top panel shows the time series of the number of anomalous samples in each ensemble divided by mean over all ensembels at level 3 in beams 1 (red), 2 (green) and (3) blue. The middle panels show the percentage reduction in the variance at each level and the lower panels show the change in ensemble means.

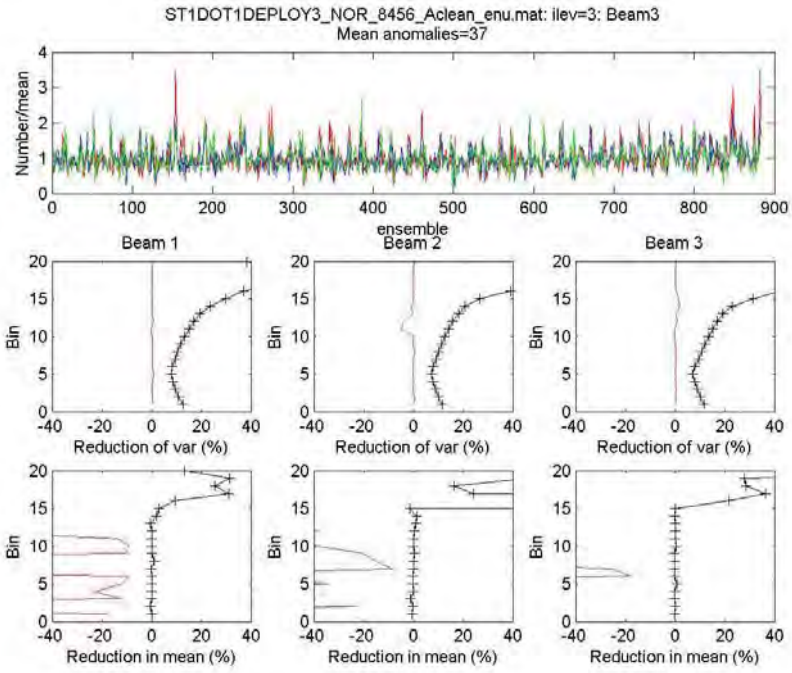

Figure 2: Screening results from Station1 on Deployment 3.: The top panel shows the time series of the number of anomalous samples in each ensemble divided by mean over all ensembels at level 3 in beams 1 (red), 2 (green) and (3) blue. The middle panels show the percentage reduction in the variance at each level and the lower panels show the change in ensemble means.

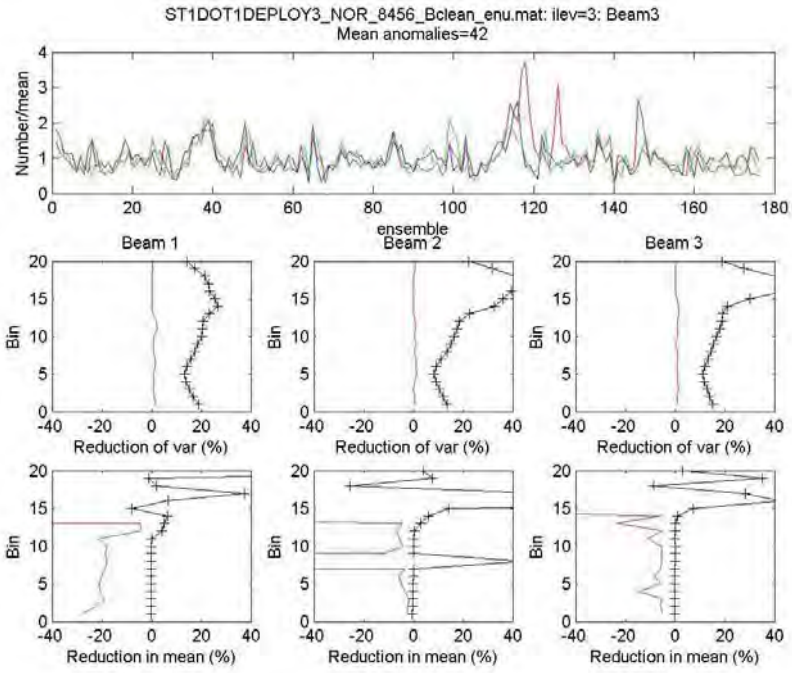

Figure 3: Screening results from Station1 on Deployment 3.: The top panel shows the time series of the number of anomalous samples in each ensemble divided by mean over all ensembels at level 3 in beams 1 (red), 2 (green) and (3) blue. The middle panels show the percentage reduction in the variance at each level and the lower panels show the change in ensemble means.

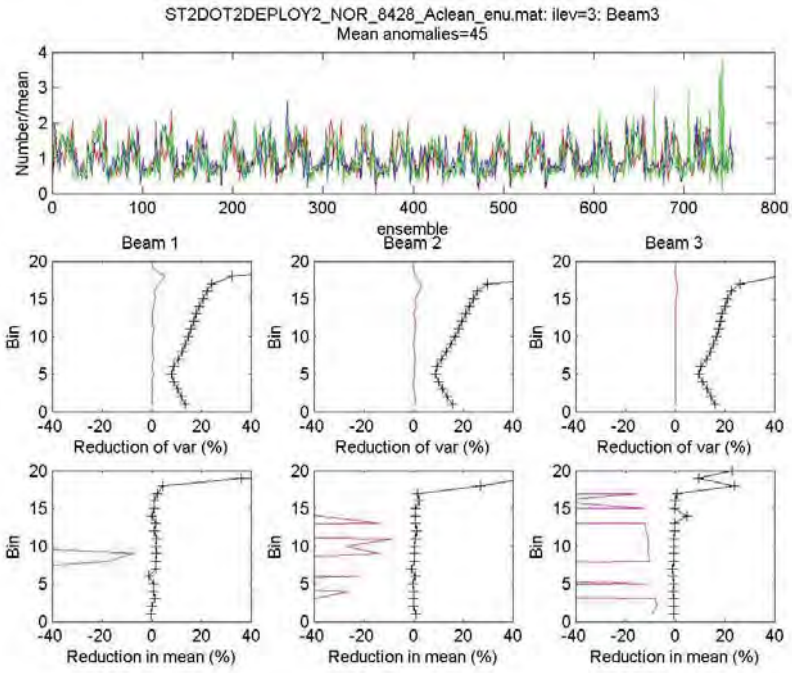

Figure 4: Screening results from Station2 on Deployment 2.: The top panel shows the time series of the number of anomalous samples in each ensemble divided by mean over all ensembels at level 3 in beams 1 (red), 2 (green) and (3) blue. The middle panels show the percentage reduction in the variance at each level and the lower panels show the change in ensemble means.

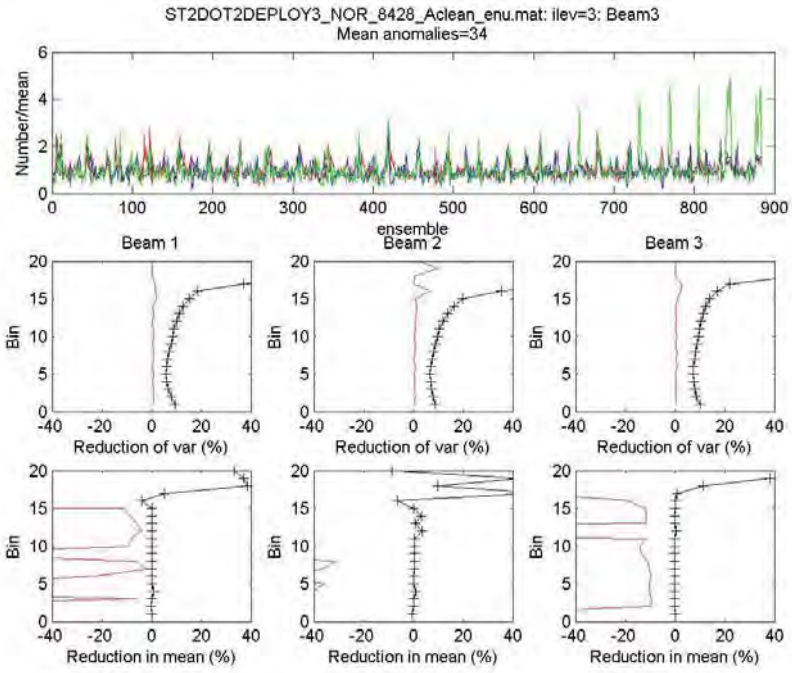

Figure 5: Screening results from Station2 on Deployment 3.: The top panel shows the time series of the number of anomalous samples in each ensemble divided by mean over all ensembels at level 3 in beams 1 (red), 2 (green) and (3) blue. The middle panels show the percentage reduction in the variance at each level and the lower panels show the change in ensemble means.

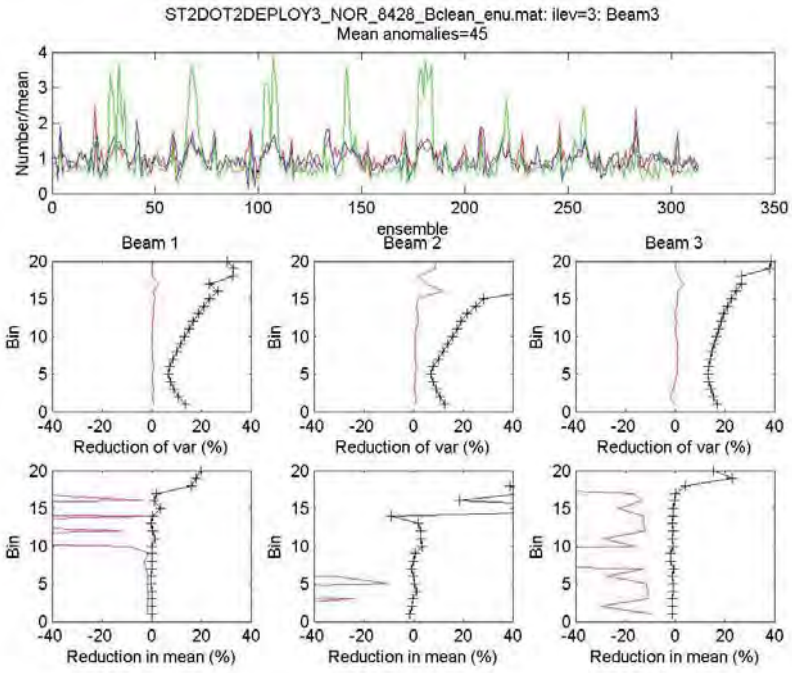

Figure 6: Screening results from Station2 on Deployment 3.: The top panel shows the time series of the number of anomalous samples in each ensembels at level 3 in beams 1 (red), 2 (green) and (3) blue. The middle panels show the percentage reduction in the variance at each level and the lower panels show the change in ensemble means.

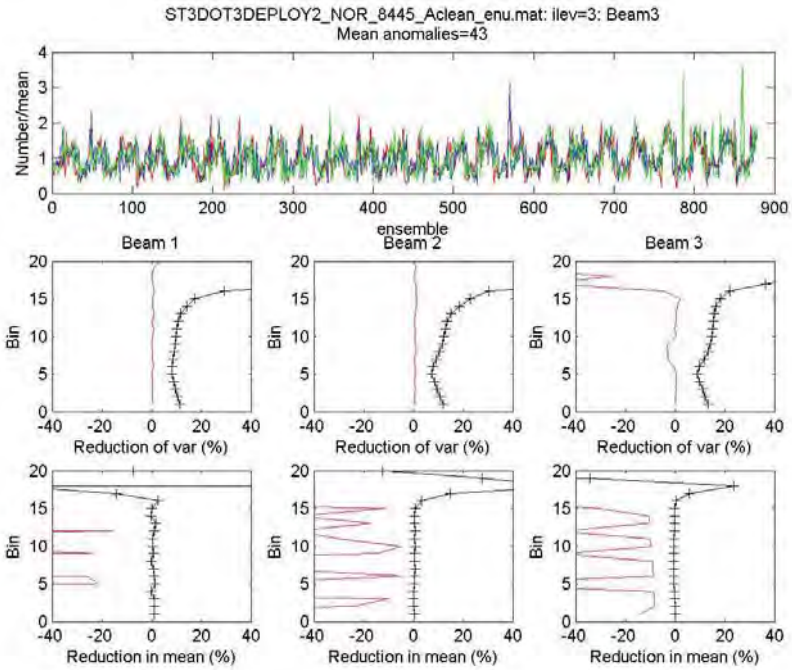

Figure 7: Screening results from Station3 on Deployment 2.: The top panel shows the time series of the number of anomalous samples in each ensembels divided by mean over all ensembels at level 3 in beams 1 (red), 2 (green) and (3) blue. The middle panels show the percentage reduction in the variance at each level and the lower panels show the change in ensemble means.

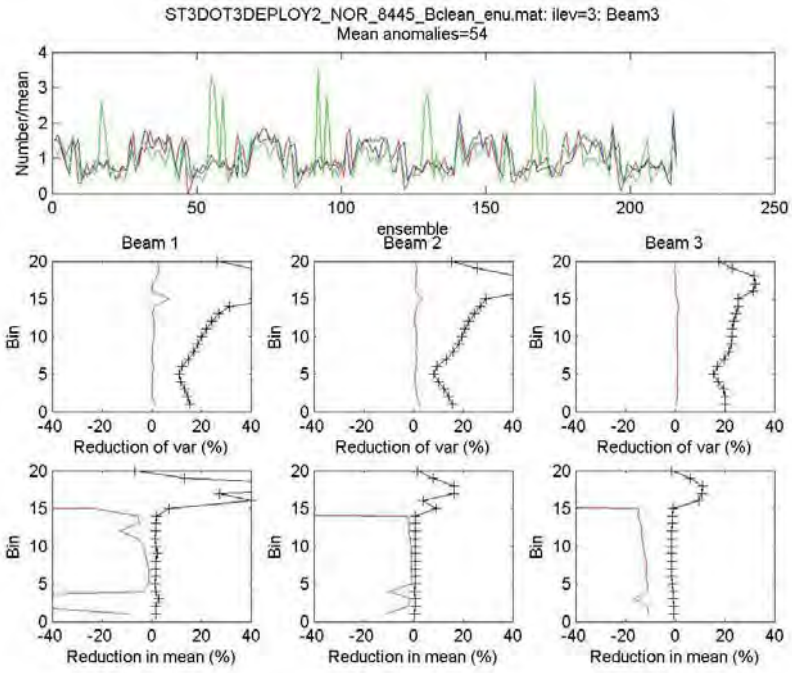

Figure 8: Screening results from Station3 on Deployment 2.: The top panel shows the time series of the number of anomalous samples in each ensemble divided by mean over all ensembels at level 3 in beams 1 (red), 2 (green) and (3) blue. The middle panels show the percentage reduction in the variance at each level and the lower panels show the change in ensemble means.

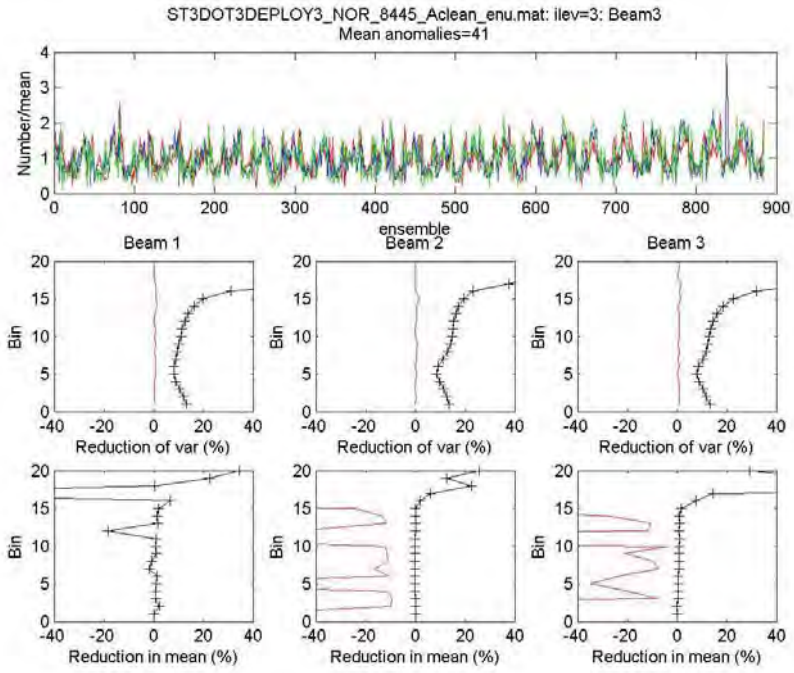

Figure 9: Screening results from Station3 on Deployment 3.: The top panel shows the time series of the number of anomalous samples in each ensemble divided by mean over all ensembels at level 3 in beams 1 (red), 2 (green) and (3) blue. The middle panels show the percentage reduction in the variance at each level and the lower panels show the change in ensemble means.

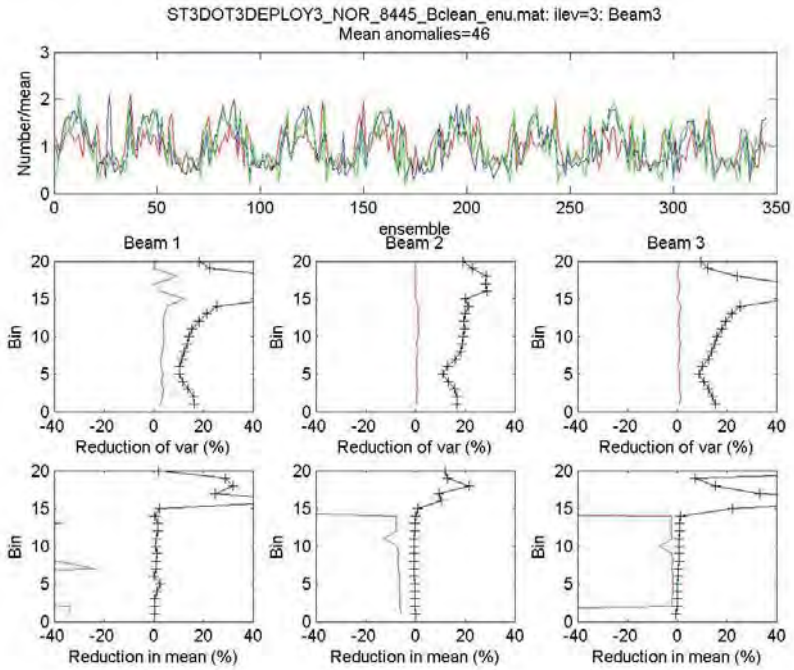

Figure 10: Screening results from Station3 on Deployment 3.: The top panel shows the time series of the number of anomalous samples in each ensemble divided by mean over all ensembels at level 3 in beams 1 (red), 2 (green) and (3) blue. The middle panels show the percentage reduction in the variance at each level and the lower panels show the change in ensemble means.

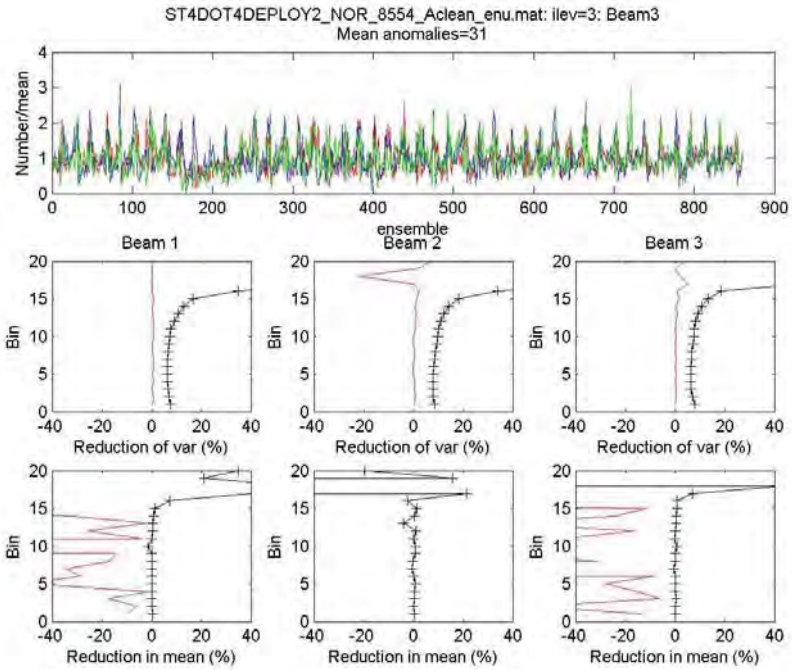

Figure 11: Screening results from Station4 on Deployment 2.: The top panel shows the time series of the number of anomalous samples in each ensemble divided by mean over all ensembels at level 3 in beams 1 (red), 2 (green) and (3) blue. The middle panels show the percentage reduction in the variance at each level and the lower panels show the change in ensemble means.

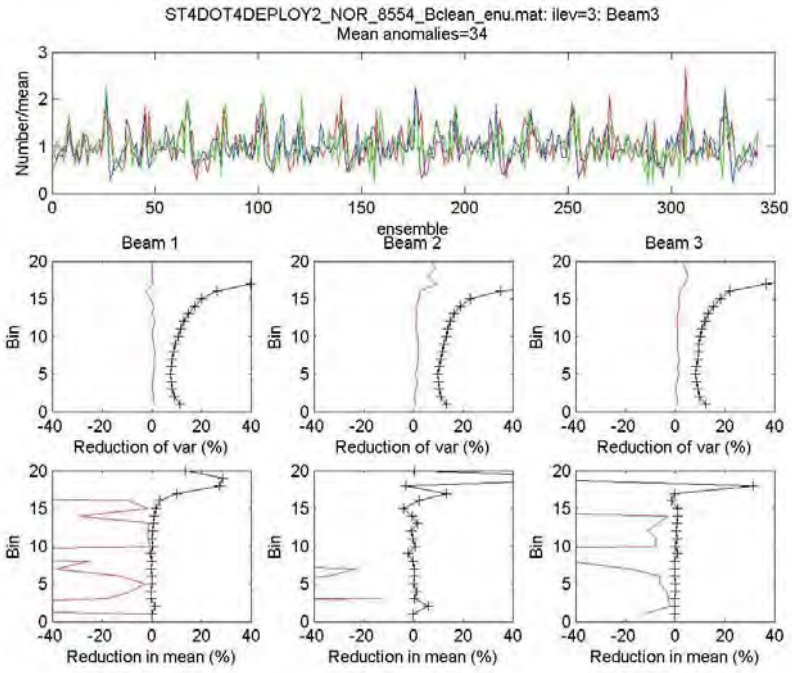

Figure 12: Screening results from Station4 on Deployment 2.: The top panel shows the time series of the number of anomalous samples in each ensemble divided by mean over all ensembels at level 3 in beams 1 (red), 2 (green) and (3) blue. The middle panels show the percentage reduction in the variance at each level and the lower panels show the change in ensemble means.

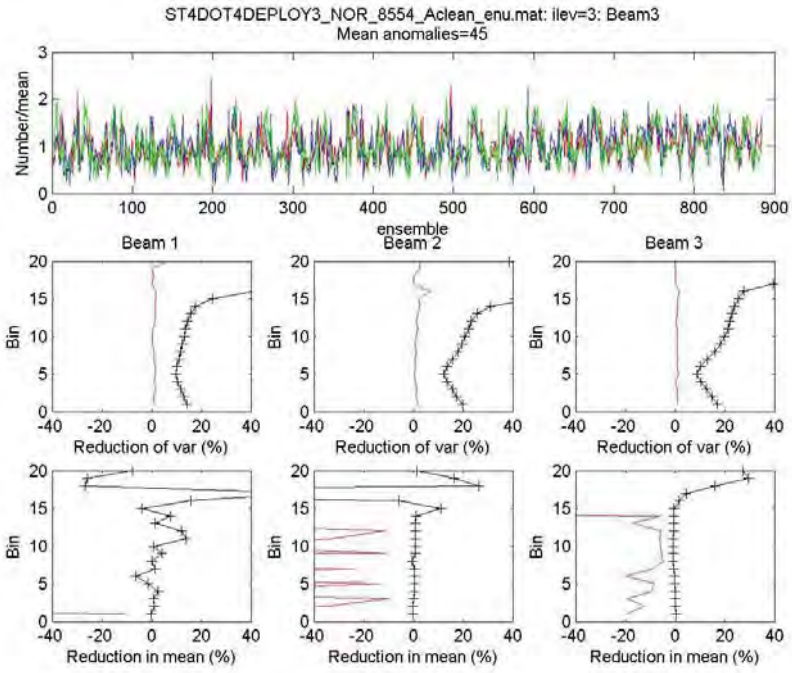

Figure 13: Screening results from Station4 on Deployment 3.: The top panel shows the time series of the number of anomalous samples in each ensemble divided by mean over all ensembels at level 3 in beams 1 (red), 2 (green) and (3) blue. The middle panels show the percentage reduction in the variance at each level and the lower panels show the change in ensemble means.

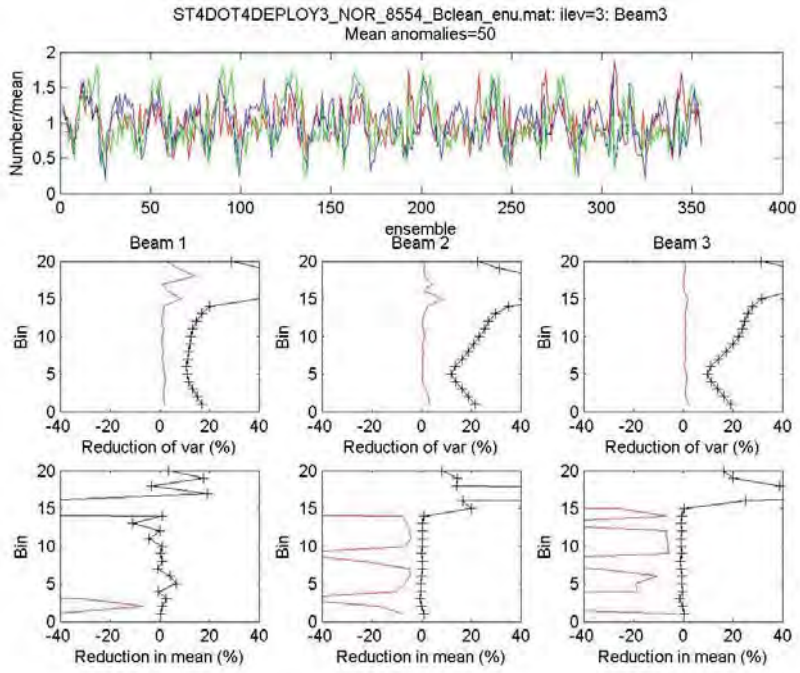

Figure 14: Screening results from Station4 on Deployment 3.: The top panel shows the time series of the number of anomalous samples in each ensemble divided by mean over all ensembels at level 3 in beams 1 (red), 2 (green) and (3) blue. The middle panels show the percentage reduction in the variance at each level and the lower panels show the change in ensemble means.

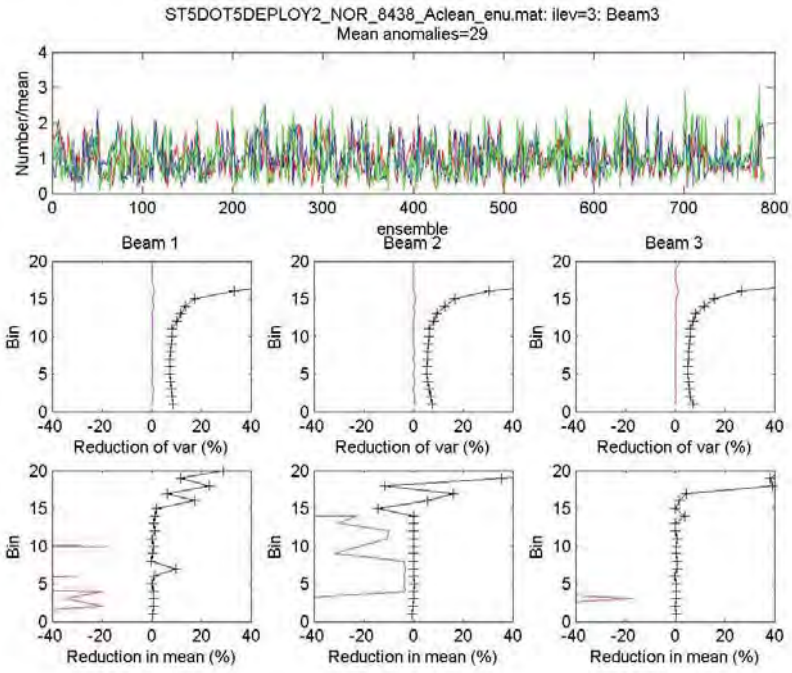

Figure 15: Screening results from Station5 on Deployment 2.: The top panel shows the time series of the number of anomalous samples in each ensemble divided by mean over all ensembels at level 3 in beams 1 (red), 2 (green) and (3) blue. The middle panels show the percentage reduction in the variance at each level and the lower panels show the change in ensemble means.

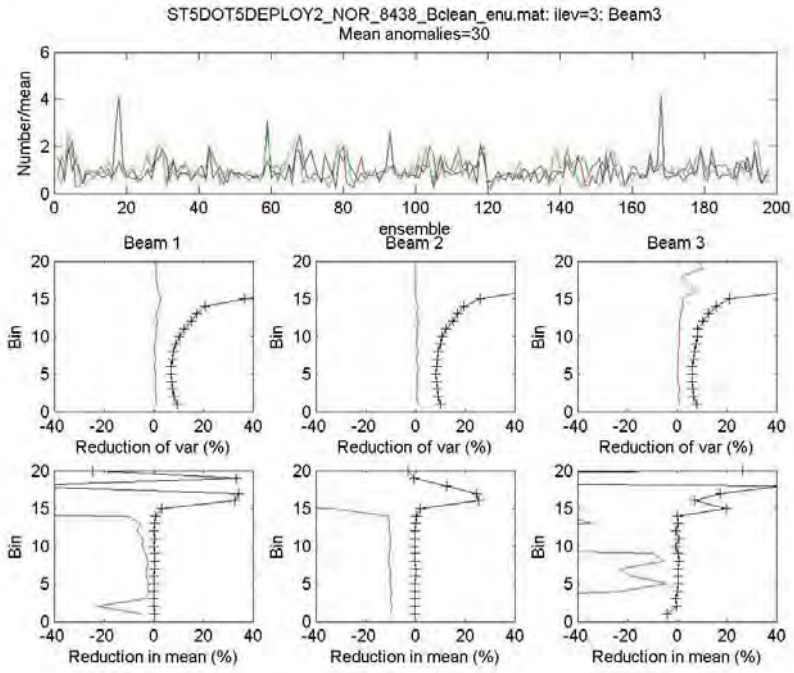

Figure 16: Screening results from Station5 on Deployment 2.: The top panel shows the time series of the number of anomalous samples in each ensembels divided by mean over all ensembels at level 3 in beams 1 (red), 2 (green) and (3) blue. The middle panels show the percentage reduction in the variance at each level and the lower panels show the change in ensemble means.

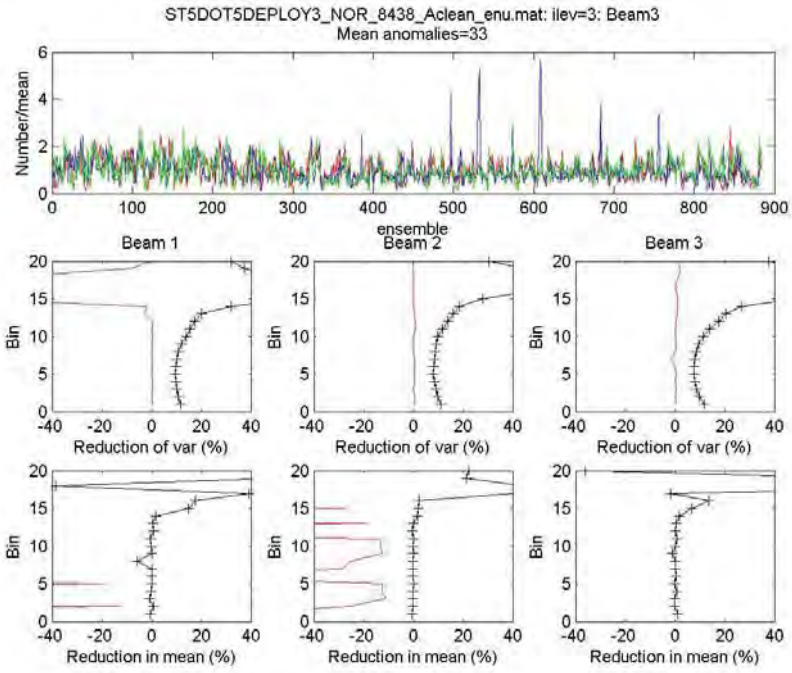

Figure 17: Screening results from Station5 on Deployment 3.: The top panel shows the time series of the number of anomalous samples in each ensemble divided by mean over all ensembels at level 3 in beams 1 (red), 2 (green) and (3) blue. The middle panels show the percentage reduction in the variance at each level and the lower panels show the change in ensemble means.

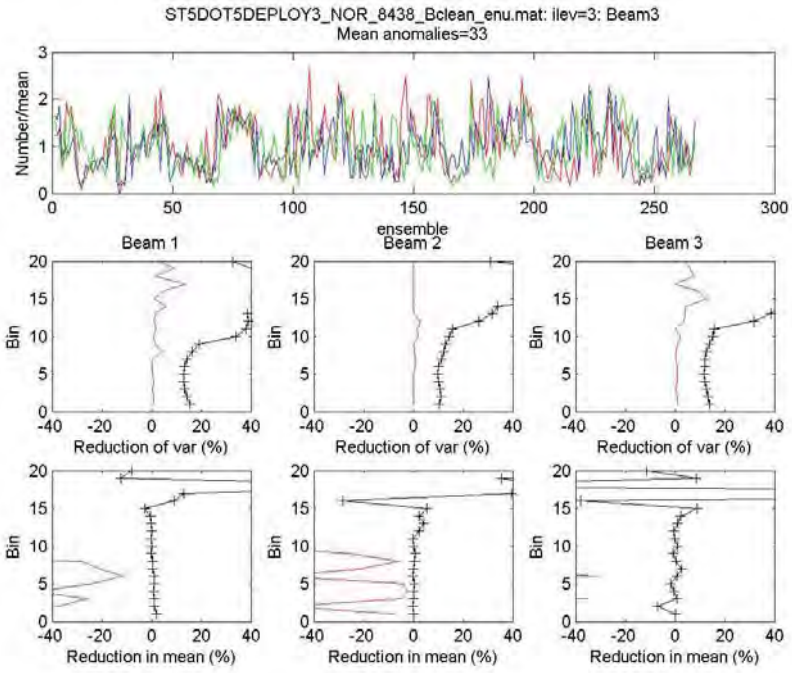

Figure 18: Screening results from Station5 on Deployment 3.: The top panel shows the time series of the number of anomalous samples in each ensembels divided by mean over all ensembels at level 3 in beams 1 (red), 2 (green) and (3) blue. The middle panels show the percentage reduction in the variance at each level and the lower panels show the change in ensemble means.

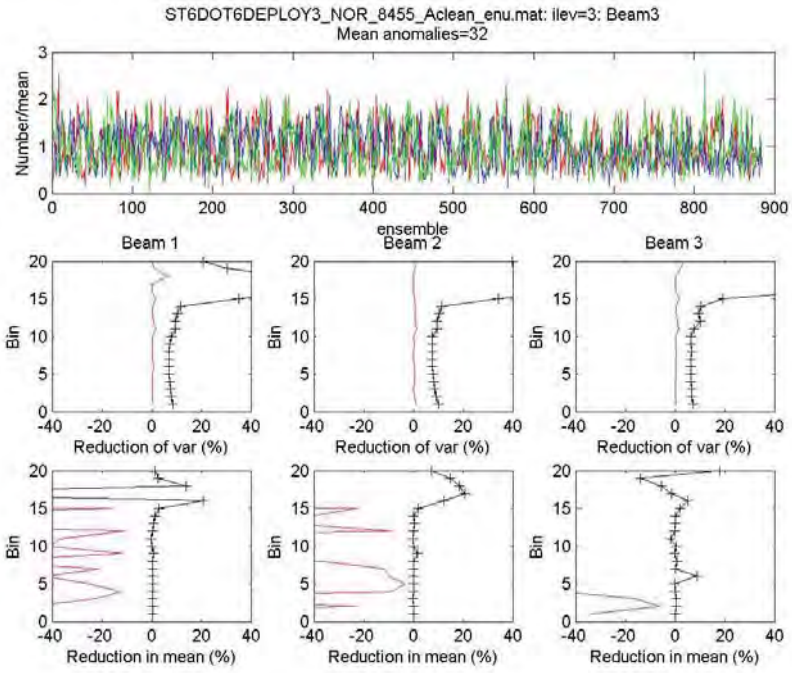

Figure 19: Screening results from Station6 on Deployment 3.: The top panel shows the time series of the number of anomalous samples in each ensemble divided by mean over all ensembels at level 3 in beams 1 (red), 2 (green) and (3) blue. The middle panels show the percentage reduction in the variance at each level and the lower panels show the change in ensemble means.

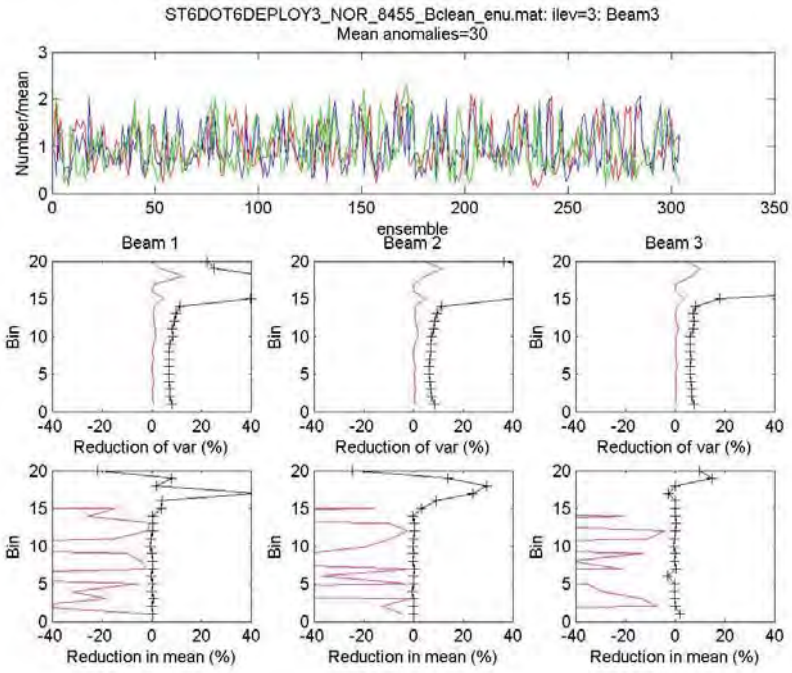

Figure 20: Screening results from Station6 on Deployment 3.: The top panel shows the time series of the number of anomalous samples in each ensembels divided by mean over all ensembels at level 3 in beams 1 (red), 2 (green) and (3) blue. The middle panels show the percentage reduction in the variance at each level and the lower panels show the change in ensemble means.

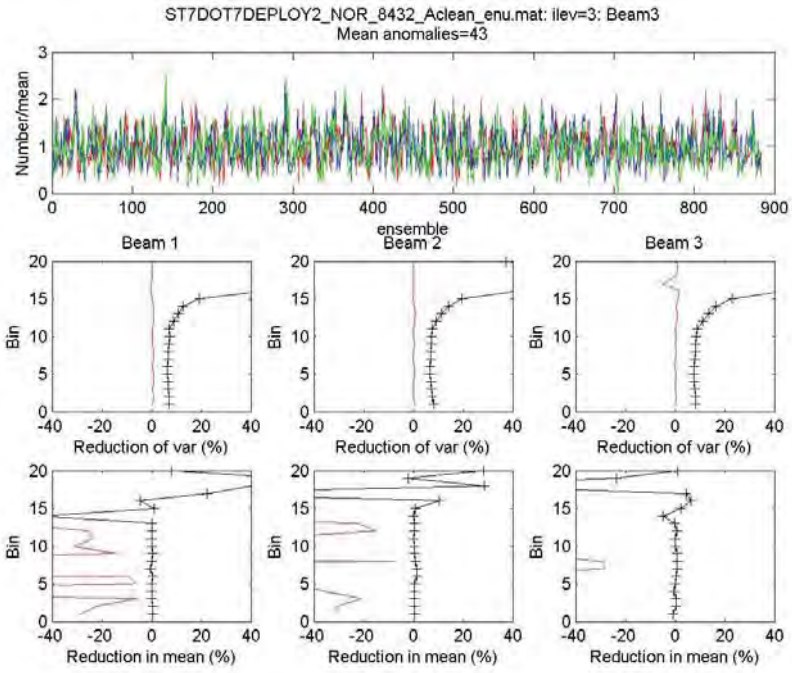

Figure 21: Screening results from Station7 on Deployment 2.: The top panel shows the time series of the number of anomalous samples in each ensemble divided by mean over all ensembels at level 3 in beams 1 (red), 2 (green) and (3) blue. The middle panels show the percentage reduction in the variance at each level and the lower panels show the change in ensemble means.

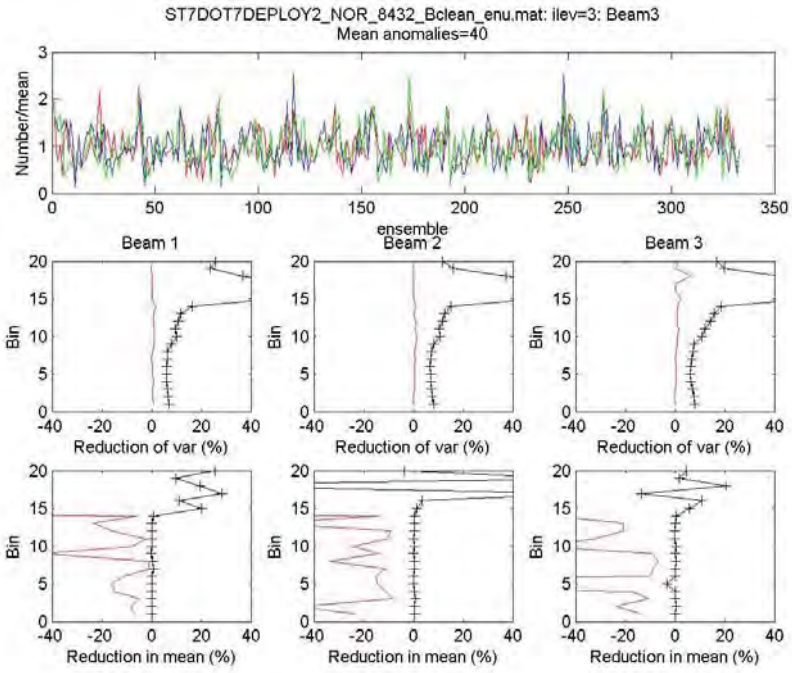

Figure 22: Screening results from Station7 on Deployment 2.: The top panel shows the time series of the number of anomalous samples in each ensemble divided by mean over all ensembels at level 3 in beams 1 (red), 2 (green) and (3) blue. The middle panels show the percentage reduction in the variance at each level and the lower panels show the change in ensemble means.

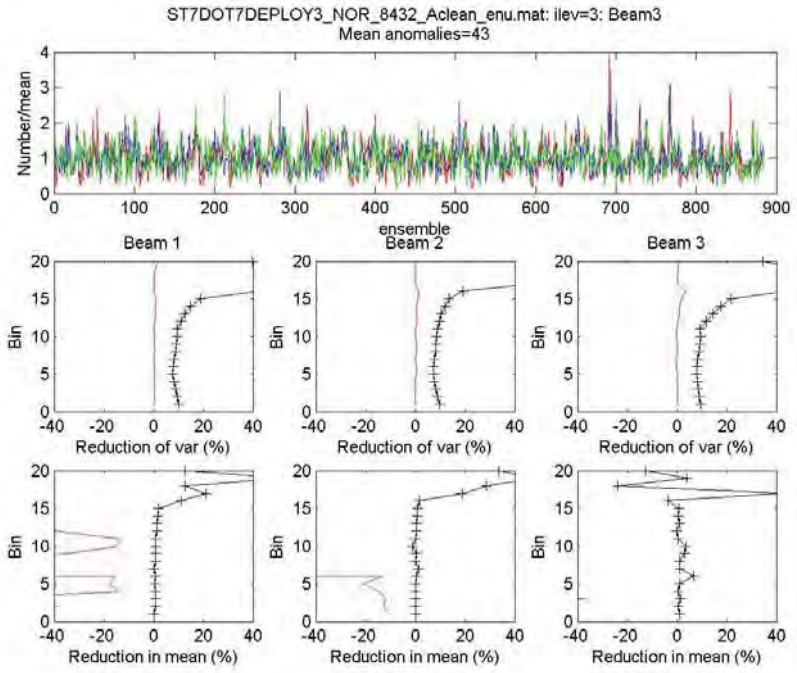

Figure 23: Screening results from Station7 on Deployment 3.: The top panel shows the time series of the number of anomalous samples in each ensemble divided by mean over all ensembels at level 3 in beams 1 (red), 2 (green) and (3) blue. The middle panels show the percentage reduction in the variance at each level and the lower panels show the change in ensemble means.

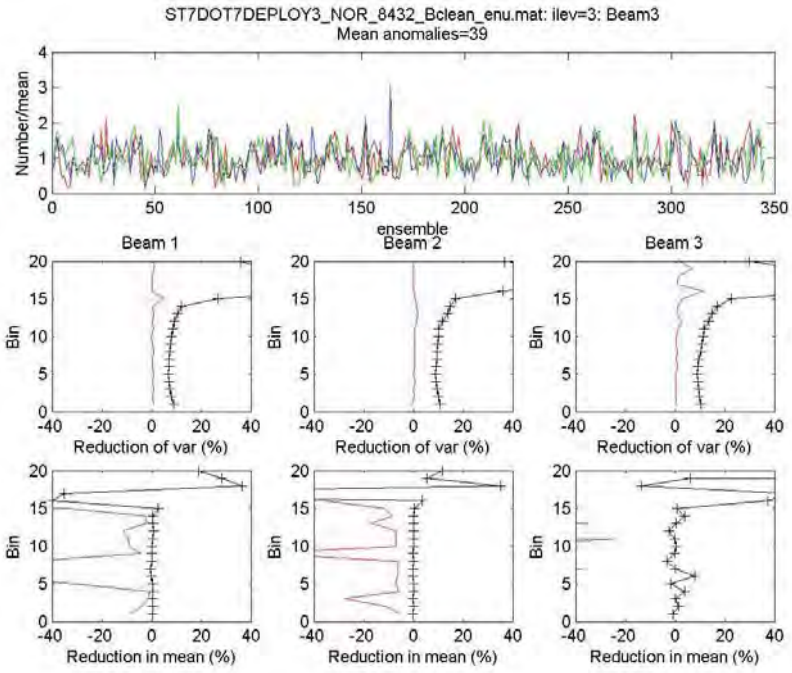

Figure 24: Screening results from Station7 on Deployment 3.: The top panel shows the time series of the number of anomalous samples in each ensemble divided by mean over all ensembels at level 3 in beams 1 (red), 2 (green) and (3) blue. The middle panels show the percentage reduction in the variance at each level and the lower panels show the change in ensemble means.

This page intentionally left blank.

Appendix 9c: Nortek ADCP Data - Screening data from Campaign 3

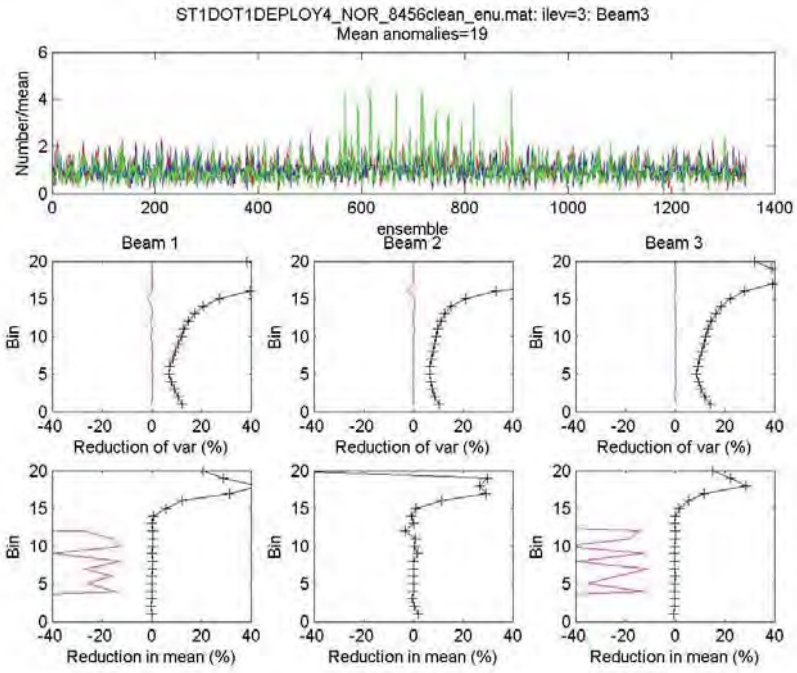

Figure 1: Screening results from Station1 on Deployment 4.: The top panel shows the time series of the number of anomalous samples in each ensembels divided by mean over all ensembels at level 3 in beams 1 (red), 2 (green) and (3) blue. The middle panels show the percentage reduction in the variance at each level and the lower panels show the change in ensemble means.

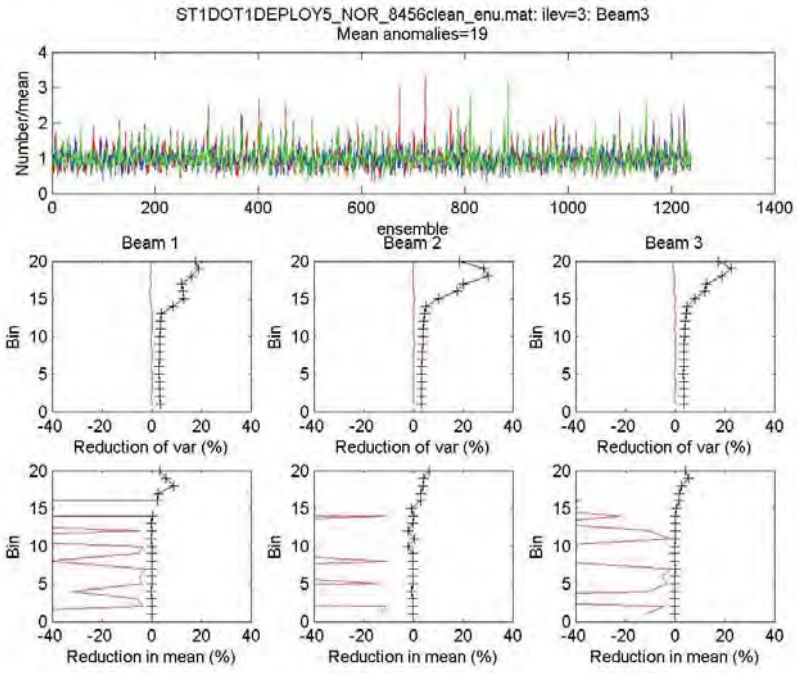

Figure 2: Screening results from Station1 on Deployment 5.: The top panel shows the time series of the number of anomalous samples in each ensembels at level 3 in beams 1 (red), 2 (green) and (3) blue. The middle panels show the percentage reduction in the variance at each level and the lower panels show the change in ensemble means.

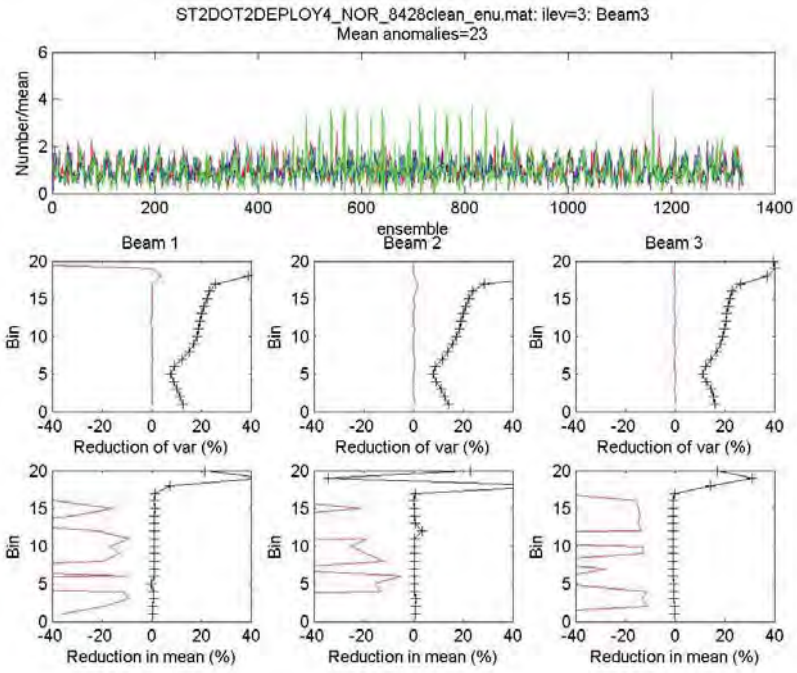

Figure 3: Screening results from Station2 on Deployment 4.: The top panel shows the time series of the number of anomalous samples in each ensemble divided by mean over all ensembels at level 3 in beams 1 (red), 2 (green) and (3) blue. The middle panels show the percentage reduction in the variance at each level and the lower panels show the change in ensemble means.

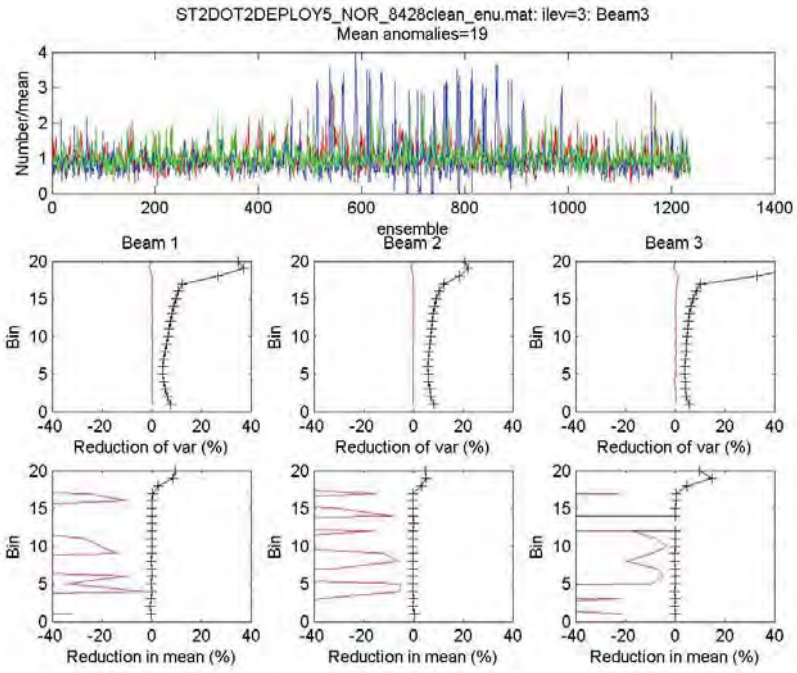

Figure 4: Screening results from Station2 on Deployment 5.: The top panel shows the time series of the number of anomalous samples in each ensemble divided by mean over all ensembels at level 3 in beams 1 (red), 2 (green) and (3) blue. The middle panels show the percentage reduction in the variance at each level and the lower panels show the change in ensemble means.

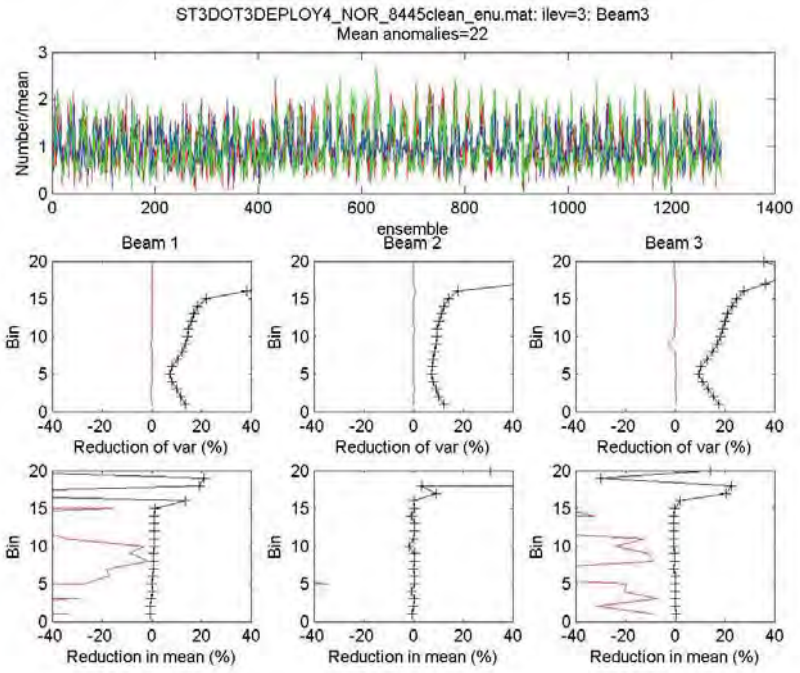

Figure 5: Screening results from Station3 on Deployment 4.: The top panel shows the time series of the number of anomalous samples in each ensemble divided by mean over all ensembels at level 3 in beams 1 (red), 2 (green) and (3) blue. The middle panels show the percentage reduction in the variance at each level and the lower panels show the change in ensemble means.

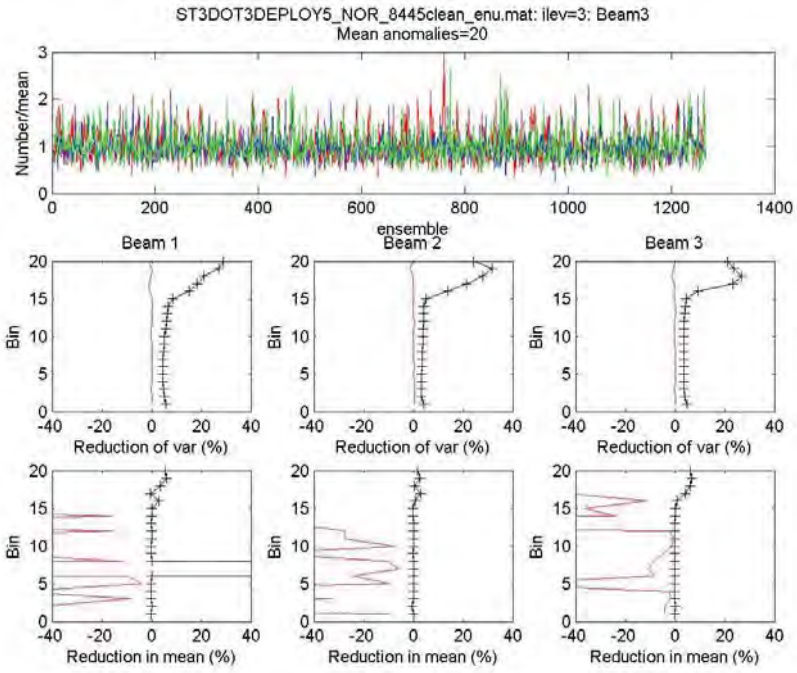

Figure 6: Screening results from Station3 on Deployment 5.: The top panel shows the time series of the number of anomalous samples in each ensemble divided by mean over all ensembels at level 3 in beams 1 (red), 2 (green) and (3) blue. The middle panels show the percentage reduction in the variance at each level and the lower panels show the change in ensemble means.

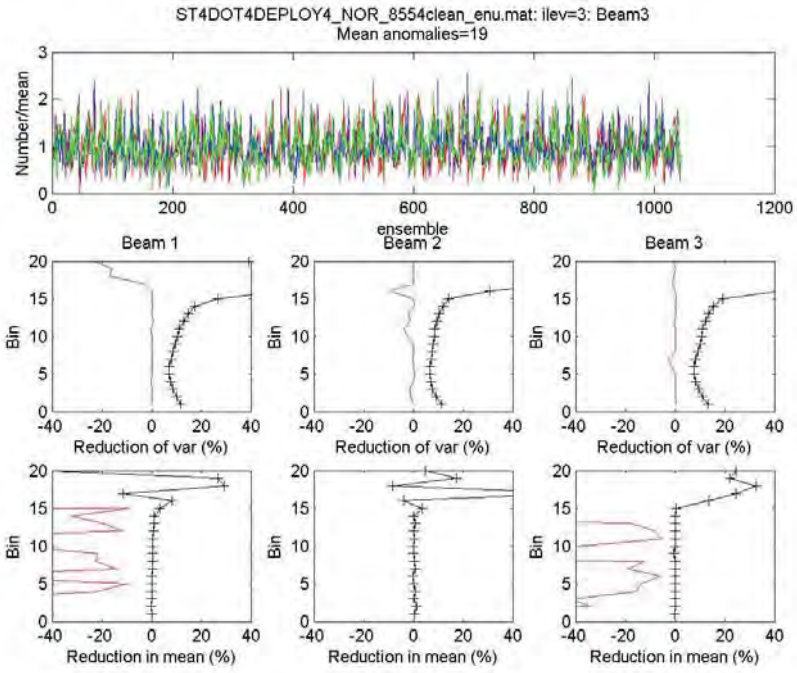

Figure 7: Screening results from Station4 on Deployment 4.: The top panel shows the time series of the number of anomalous samples in each ensemble divided by mean over all ensembels at level 3 in beams 1 (red), 2 (green) and (3) blue. The middle panels show the percentage reduction in the variance at each level and the lower panels show the change in ensemble means.

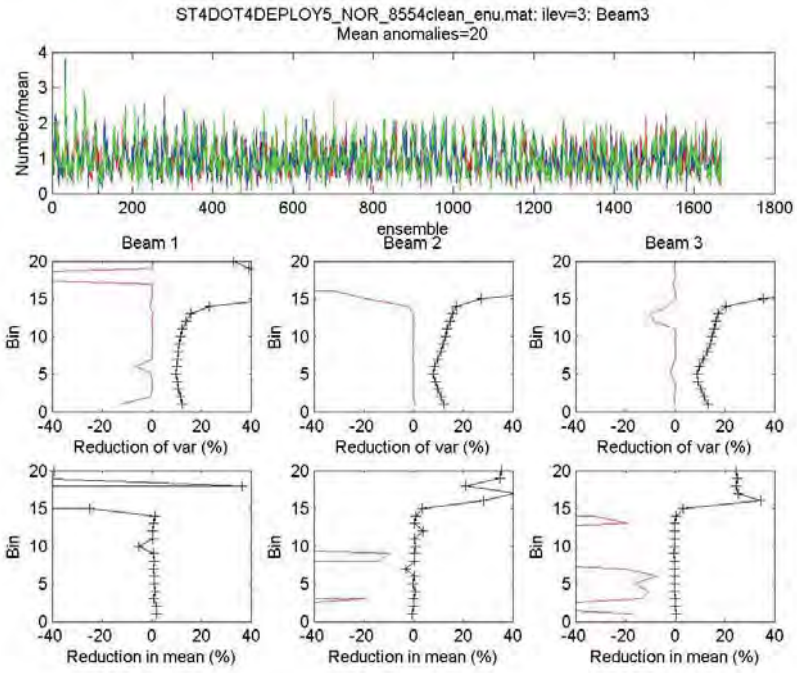

Figure 8: Screening results from Station4 on Deployment 5.: The top panel shows the time series of the number of anomalous samples in each ensemble divided by mean over all ensembels at level 3 in beams 1 (red), 2 (green) and (3) blue. The middle panels show the percentage reduction in the variance at each level and the lower panels show the change in ensemble means.

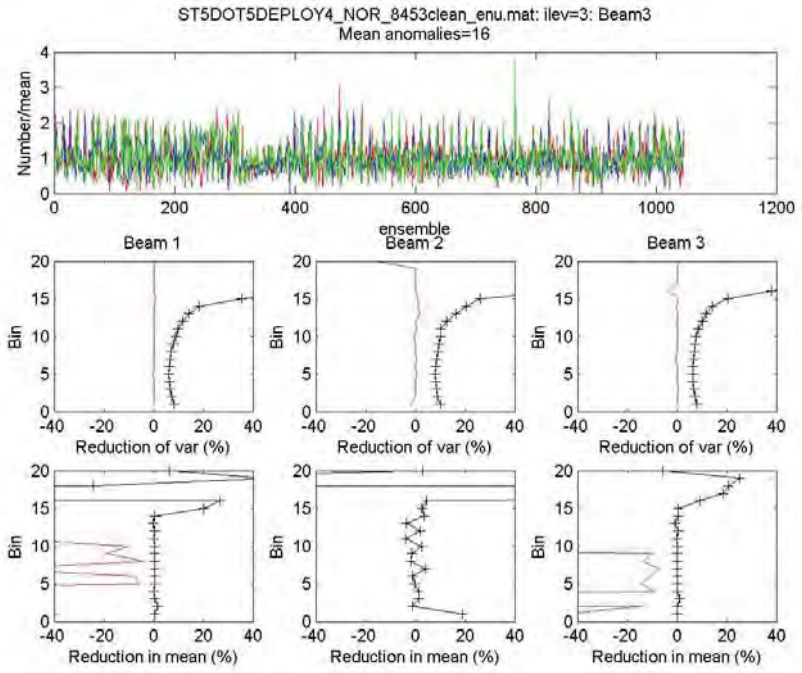

Figure 9: Screening results from Station5 on Deployment 4.: The top panel shows the time series of the number of anomalous samples in each ensemble divided by mean over all ensembels at level 3 in beams 1 (red), 2 (green) and (3) blue. The middle panels show the percentage reduction in the variance at each level and the lower panels show the change in ensemble means.

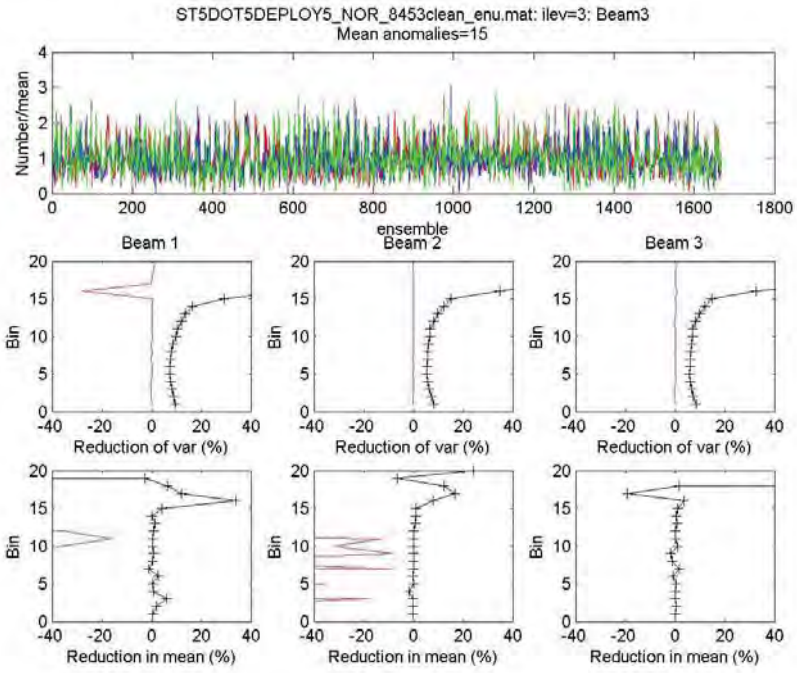

Figure 10: Screening results from Station5 on Deployment 5.: The top panel shows the time series of the number of anomalous samples in each ensemble divided by mean over all ensembels at level 3 in beams 1 (red), 2 (green) and (3) blue. The middle panels show the percentage reduction in the variance at each level and the lower panels show the change in ensemble means.

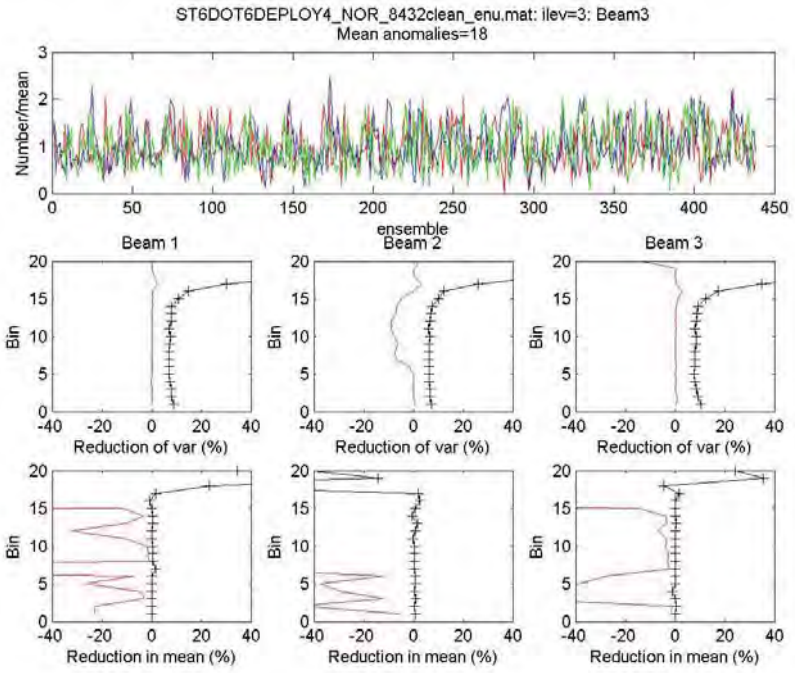

Figure 11: Screening results from Station6 on Deployment 4.: The top panel shows the time series of the number of anomalous samples in each ensembels divided by mean over all ensembels at level 3 in beams 1 (red), 2 (green) and (3) blue. The middle panels show the percentage reduction in the variance at each level and the lower panels show the change in ensemble means.

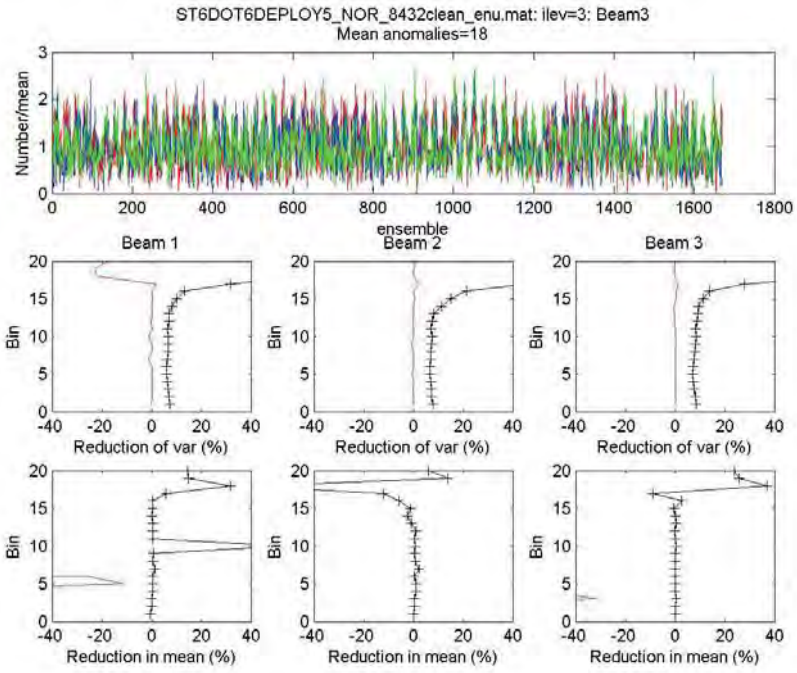

Figure 12: Screening results from Station6 on Deployment 5.: The top panel shows the time series of the number of anomalous samples in each ensembels at level 3 in beams 1 (red), 2 (green) and (3) blue. The middle panels show the percentage reduction in the variance at each level and the lower panels show the change in ensemble means.

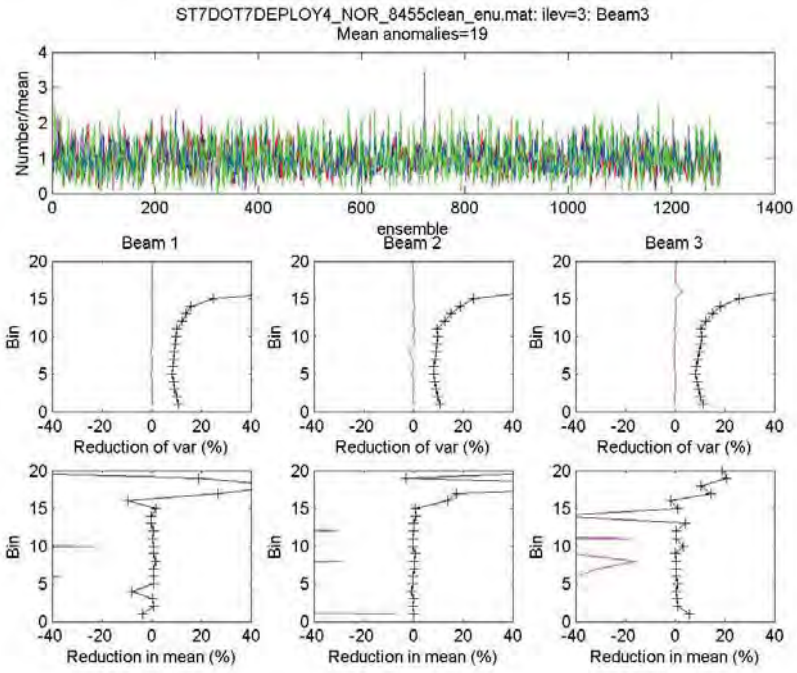

Figure 13: Screening results from Station7 on Deployment 4.: The top panel shows the time series of the number of anomalous samples in each ensembels at level 3 in beams 1 (red), 2 (green) and (3) blue. The middle panels show the percentage reduction in the variance at each level and the lower panels show the change in ensemble means.

Appendix 9d: Nortek ADCP Data - Time-series of the velocity components during Campaign 1

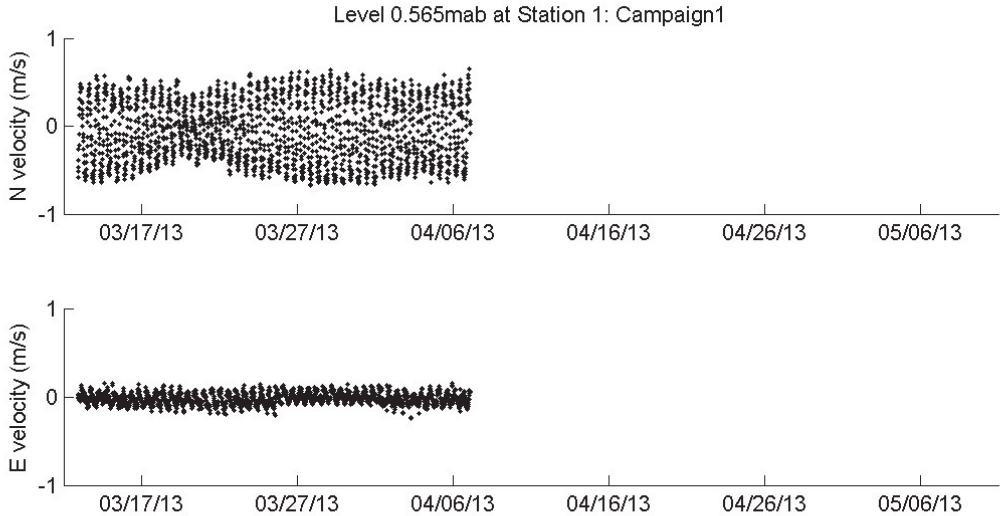

Figure 1: Time series of the east (top) and north(bottom) velocity components at bin 3 measured at Station DOT1 during Campaign 1.

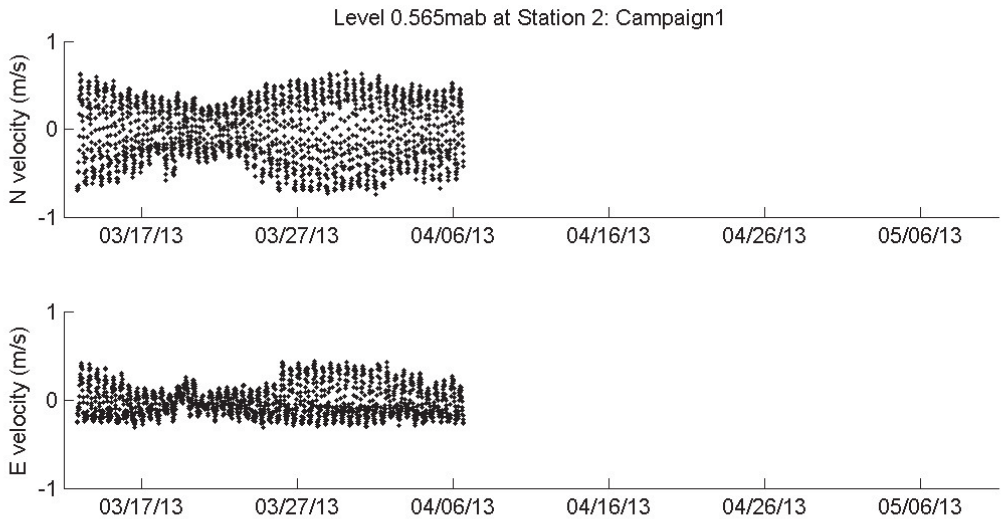

Figure 2: Time series of the east (top) and north(bottom) velocity components at bin 3 measured at Station DOT2 during Campaign 1.

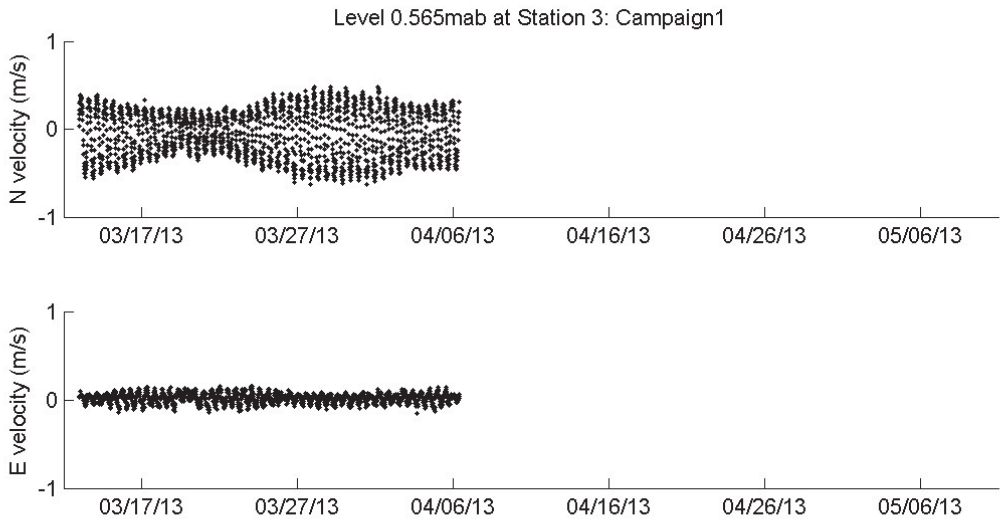

Figure 3: Time series of the east (top) and north(bottom) velocity components at bin 3 measured at Station DOT3 during Campaign 1.

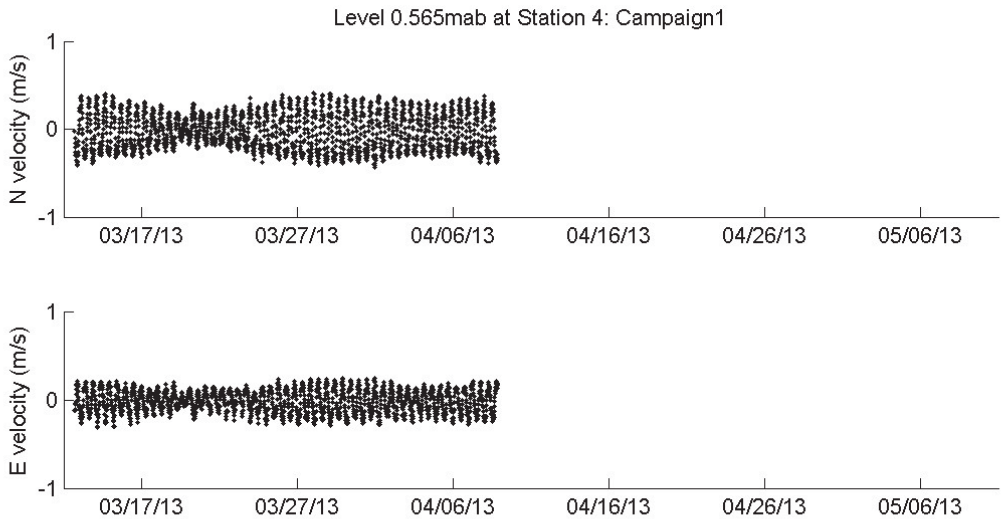

Figure 4: Time series of the east (top) and north(bottom) velocity components at bin 3 measured at Station DOT4 during Campaign 1.

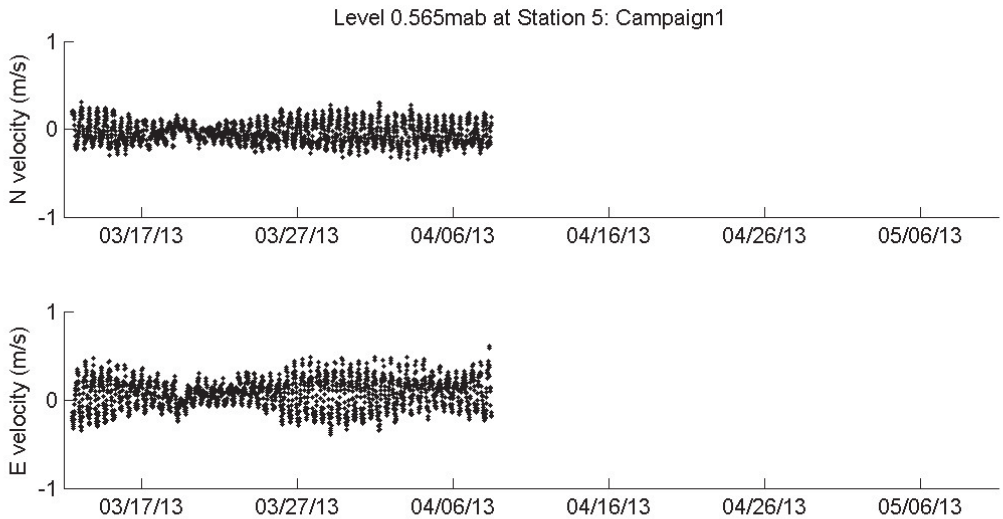

Figure 5: Time series of the east (top) and north(bottom) velocity components at bin 3 measured at Station DOT5 during Campaign 1.

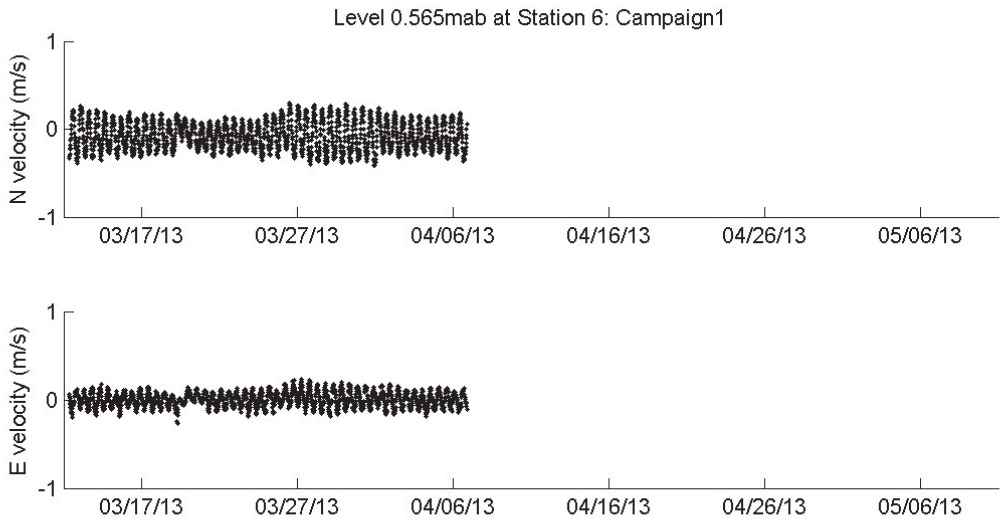

Figure 6: Time series of the east (top) and north(bottom) velocity components at bin 3 measured at Station DOT6 during Campaign 1.

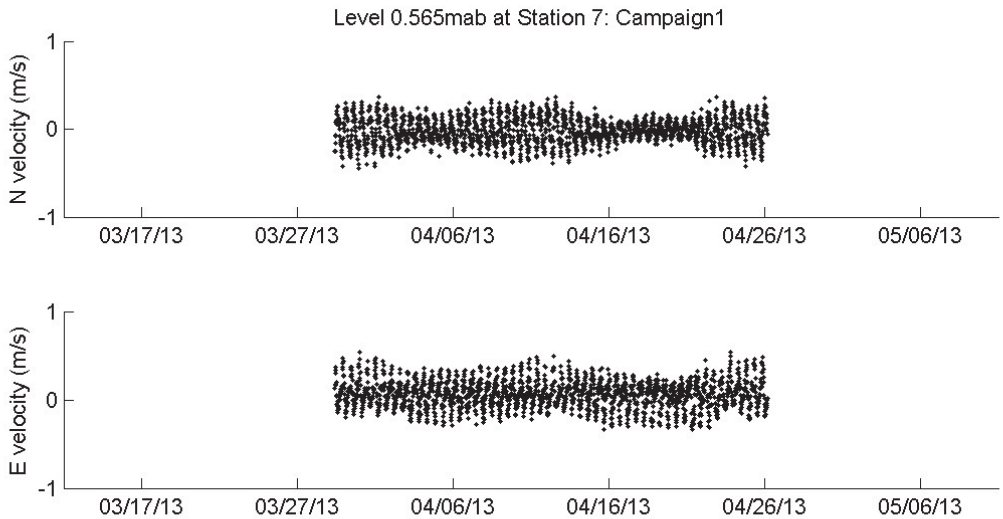

Figure 7: Time series of the east (top) and north(bottom) velocity components at bin 3 measured at Station DOT7 during Campaign 1.

Appendix 9e: Nortek ADCP Data - Time-series of the velocity components during Campaign 2

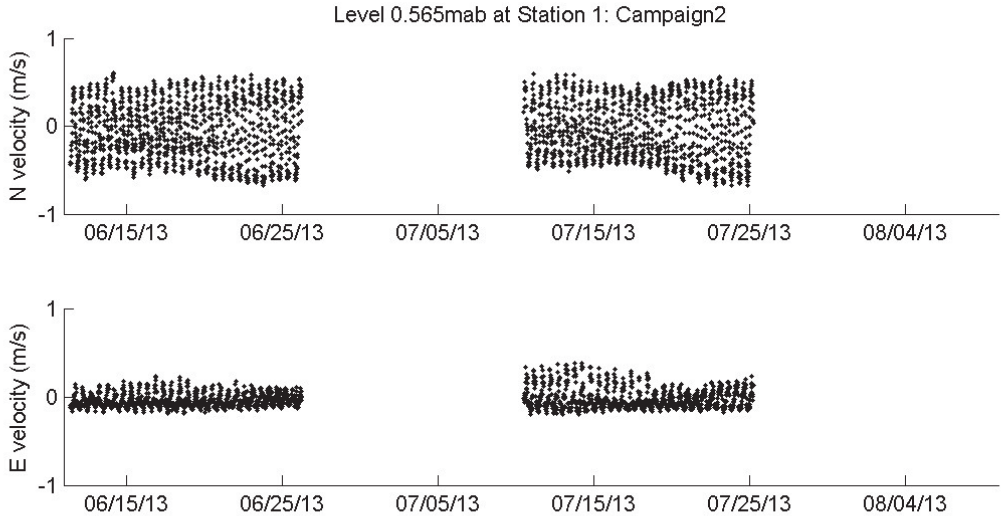

Figure 1: Time series of the east (top) and north(bottom) velocity components at bin 3 measured at DOT1 during Campaign 2.

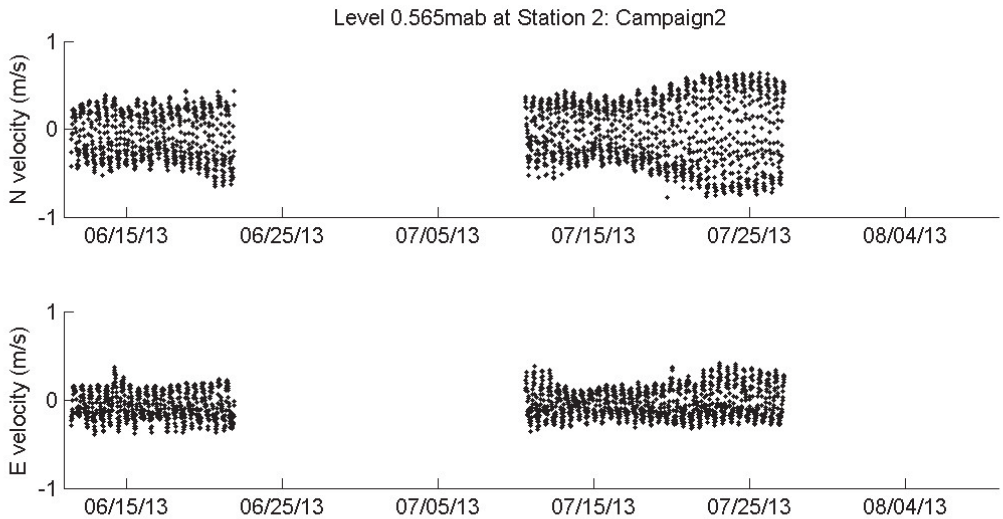

Figure 2: Time series of the east (top) and north(bottom) velocity components at bin 3 measured at DOT2 during Campaign 2.

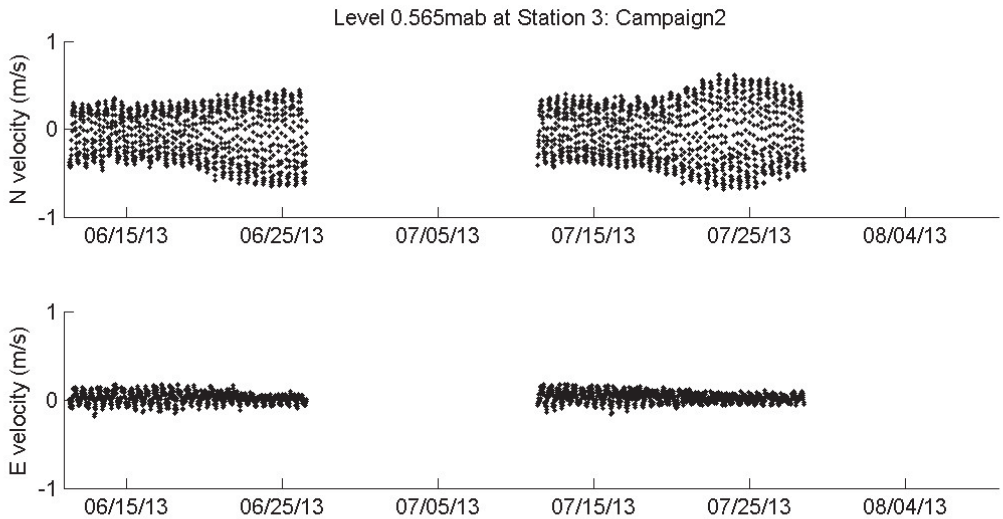

Figure 3: Time series of the east (top) and north(bottom) velocity components at bin 3 measured at DOT3 during Campaign 2.

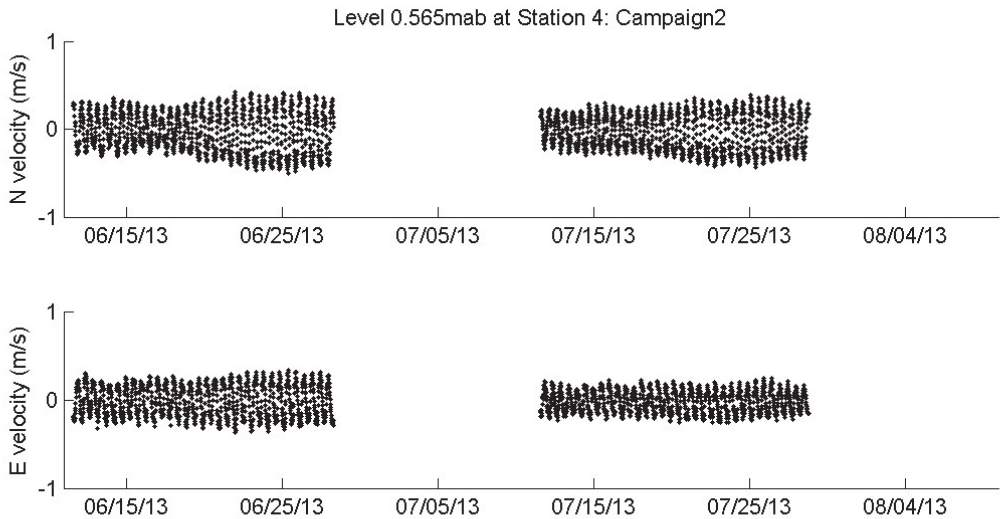

Figure 4: Time series of the east (top) and north(bottom) velocity components at bin 3 measured at DOT4 during Campaign 2.

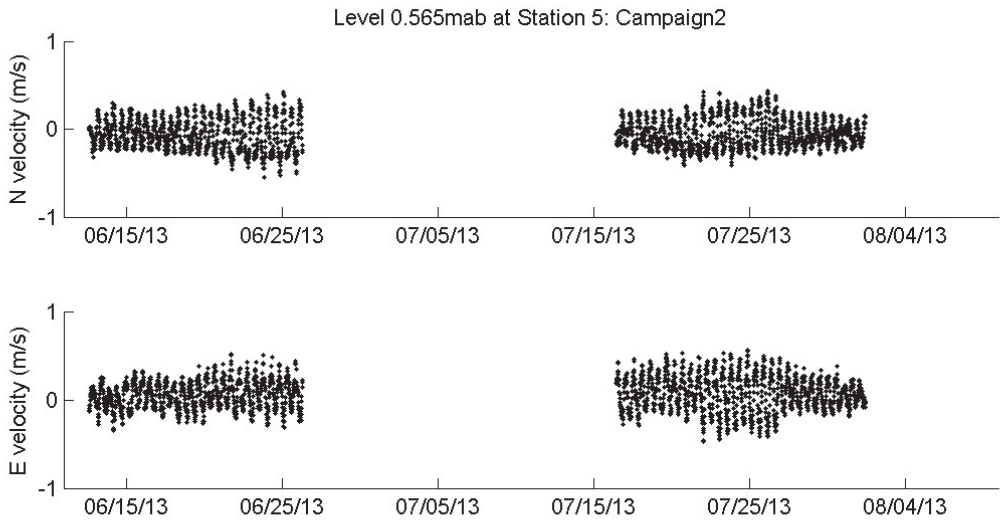

Figure 5: Time series of the east (top) and north(bottom) velocity components at bin 3 measured at DOT5 during Campaign 2.

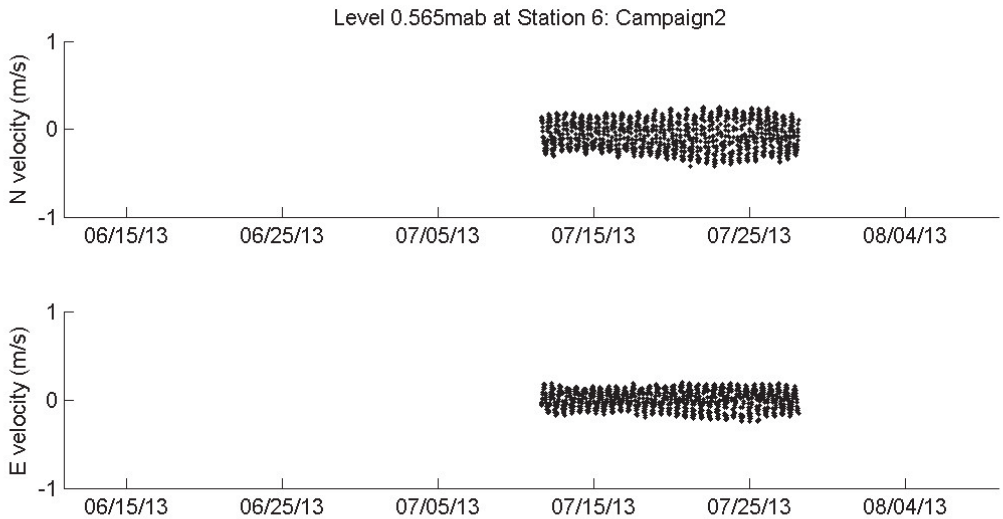

Figure 6: Time series of the east (top) and north(bottom) velocity components at bin 3 measured at DOT6 during Campaign 2.

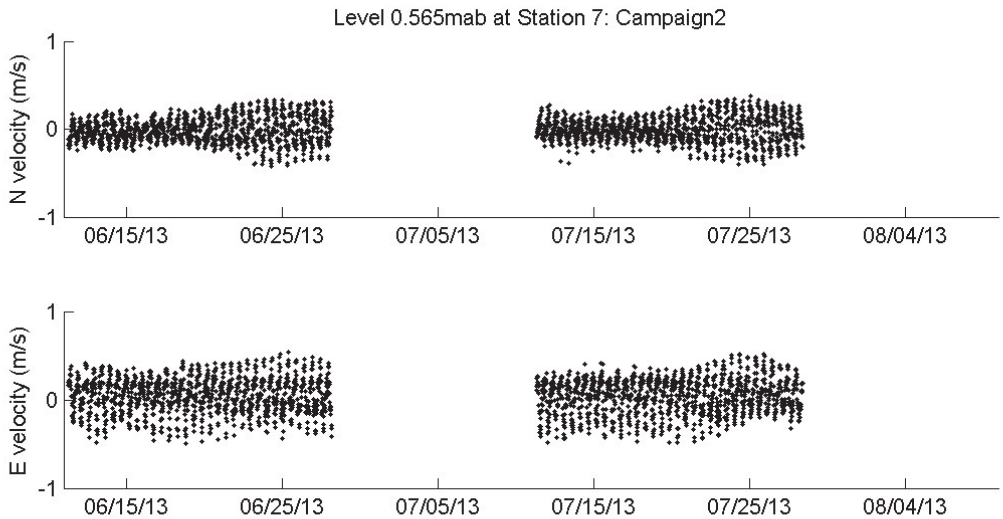

Figure 7: Time series of the east (top) and north(bottom) velocity components at bin 3 measured at DOT7 during Campaign 2.

Appendix 9f: Nortek ADCP Data - Time-series of the velocity components during Campaign 3

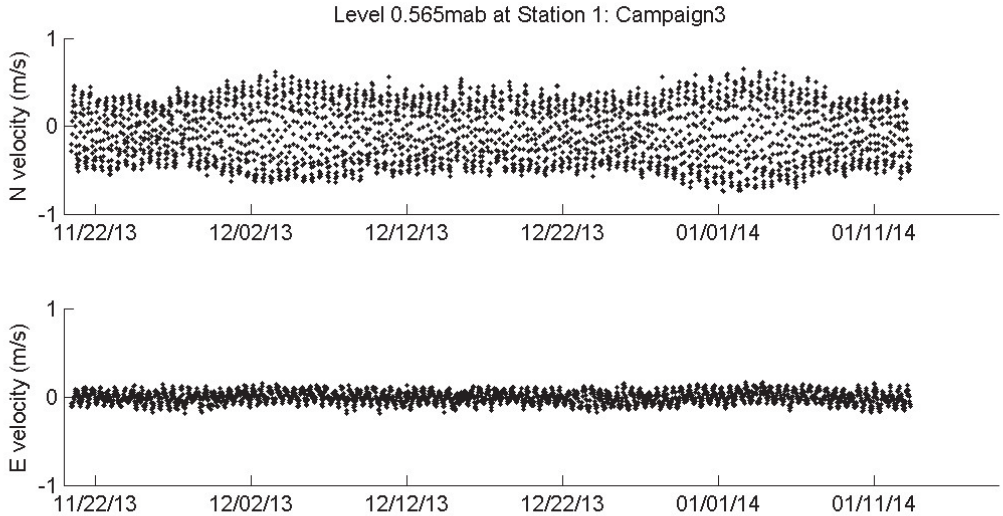

Figure 1: Time series of the east (top) and north(bottom) velocity components at bin 3 measured at Station DOT1 during Campaign 3.

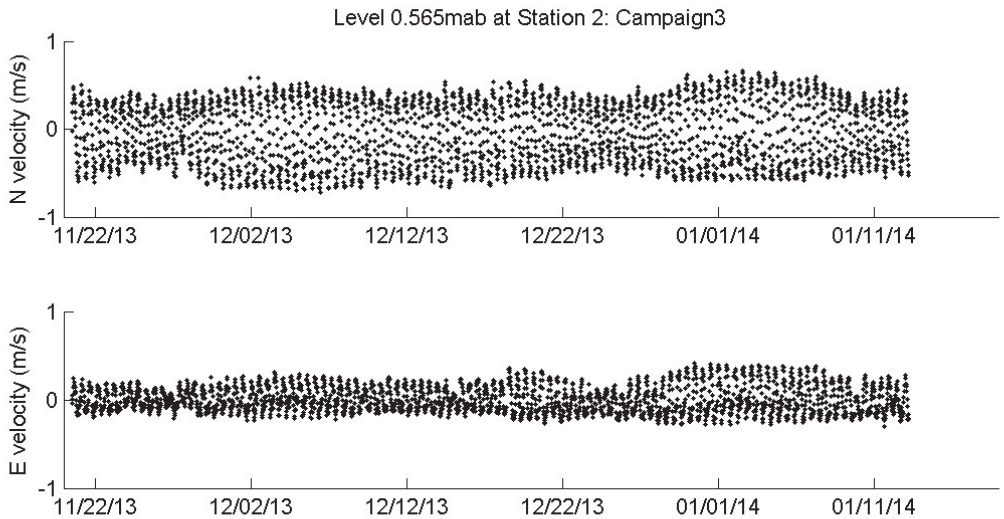

Figure 2: Time series of the east (top) and north(bottom) velocity components at bin 3 measured at Station DOT2 during Campaign 3.

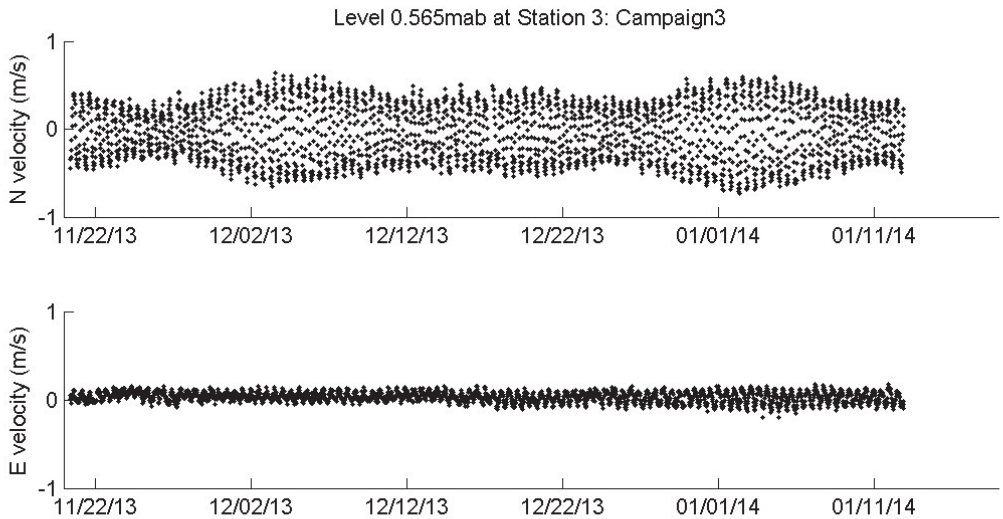

Figure 3: Time series of the east (top) and north(bottom) velocity components at bin 3 measured at Station DOT3 during Campaign 3.

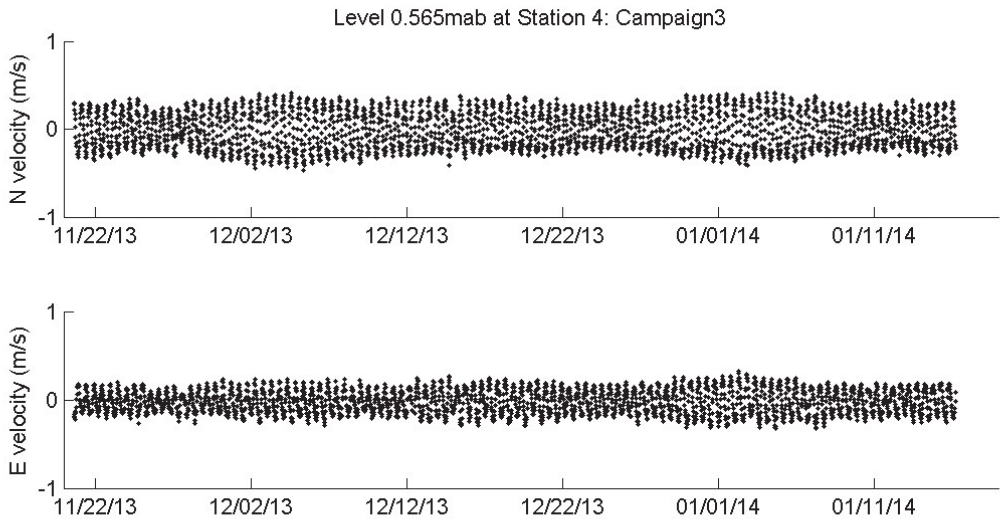

Figure 4: Time series of the east (top) and north(bottom) velocity components at bin 3 measured at Station DOT4 during Campaign 3.

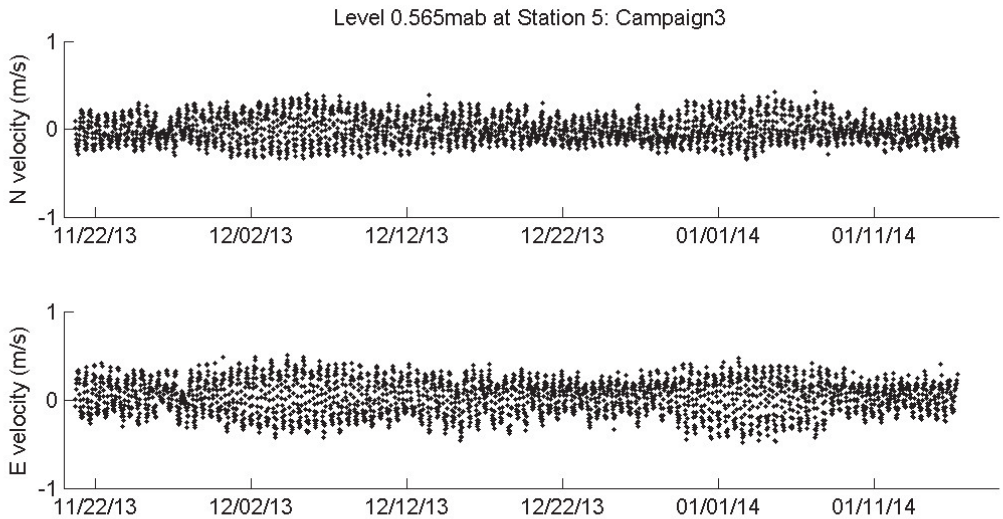

Figure 5: Time series of the east (top) and north(bottom) velocity components at bin 3 measured at Station DOT5 during Campaign 3.

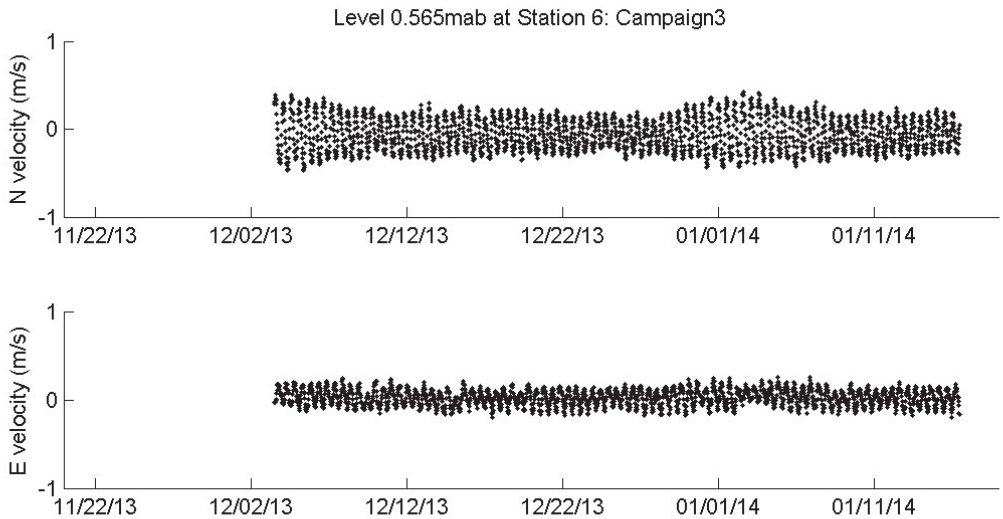

Figure 6: Time series of the east (top) and north(bottom) velocity components at bin 3 measured at Station DOT6 during Campaign 3.

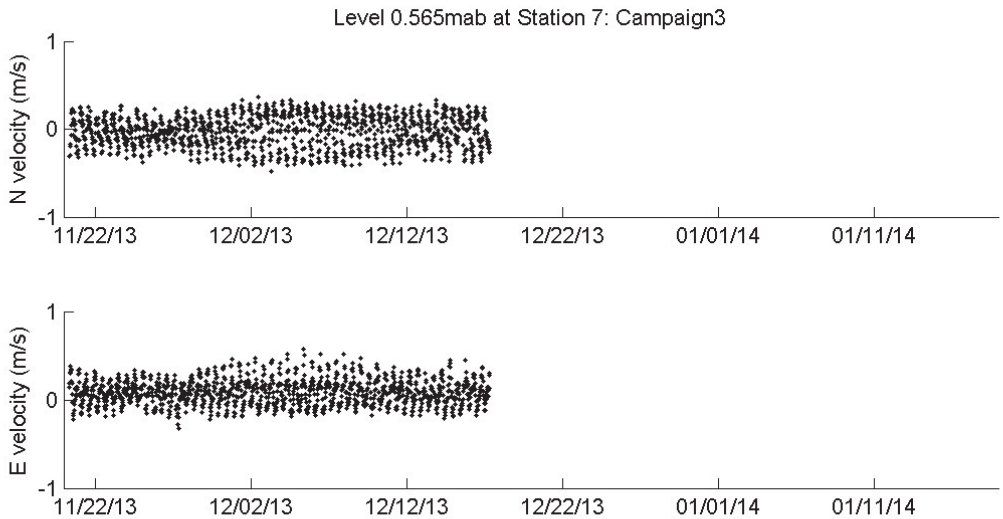

Figure 7: Time series of the east (top) and north(bottom) velocity components at bin 3 measured at Station DOT7 during Campaign 3.

Appendix 9g: Nortek ADCP Data - Time-series of bottom pressure, temperature, battery voltage and OBS3+ sensor outputs for Campaigns 1 to 3

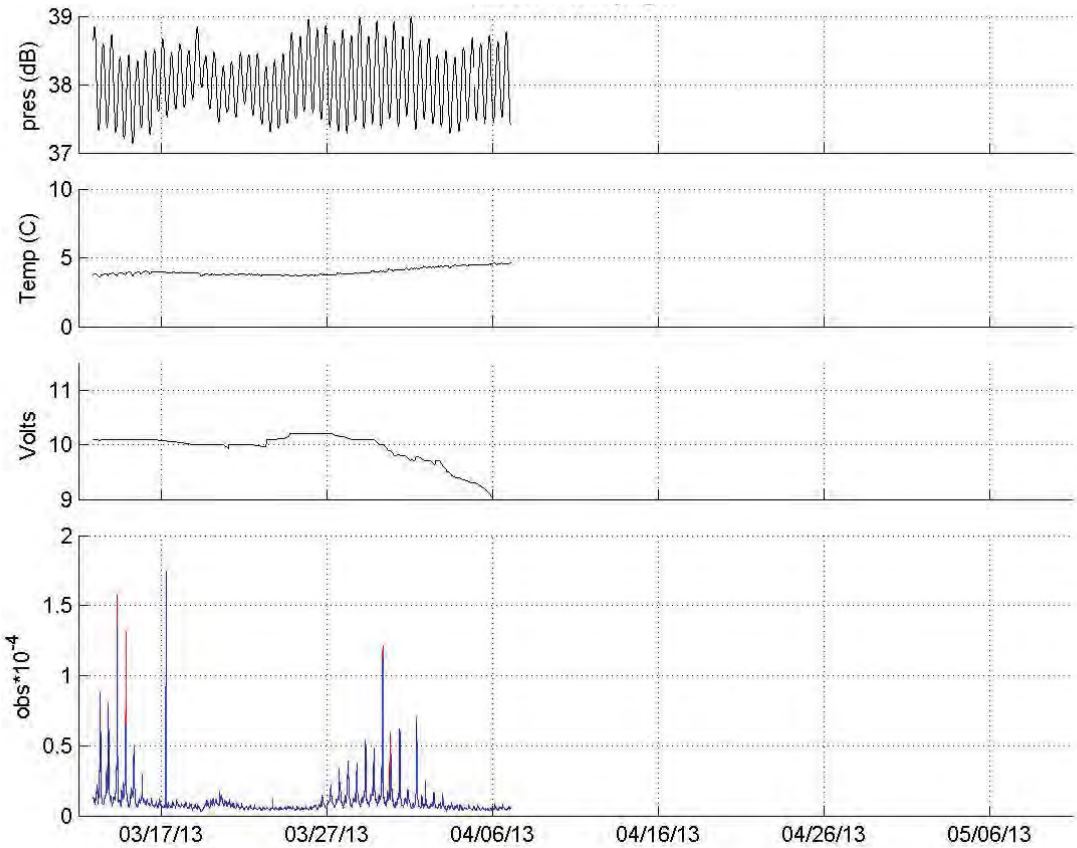

Figure 1: Observations from Station DOT1 in Campaign 1. The top and second panel shows the time series of the pressure and temperature at the Nortek ADCP and the third panel shows the system voltage. The bottom panel 1 (red), and (3) blue. The middle panels show the percentage reduction in the variance at each level and the lower panels show the change in ensemble means.

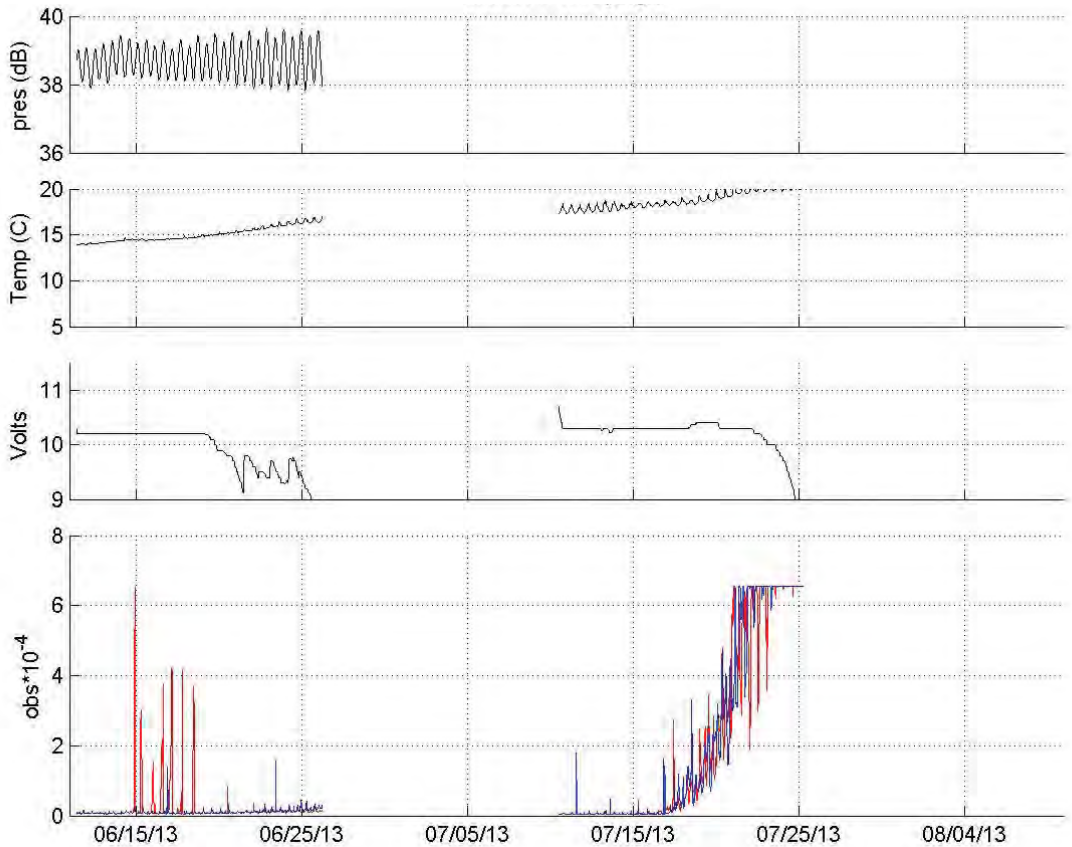

Figure 2: Observations from Station DOT1 in Campaign 2. The top and second panel shows the time series of the pressure and temperature at the Nortek ADCP and the third panel shows the system voltage. The bottom panel 1 (red), and (3) blue. The middle panels show the percentage reduction in the variance at each level and the lower panels show the change in ensemble means.

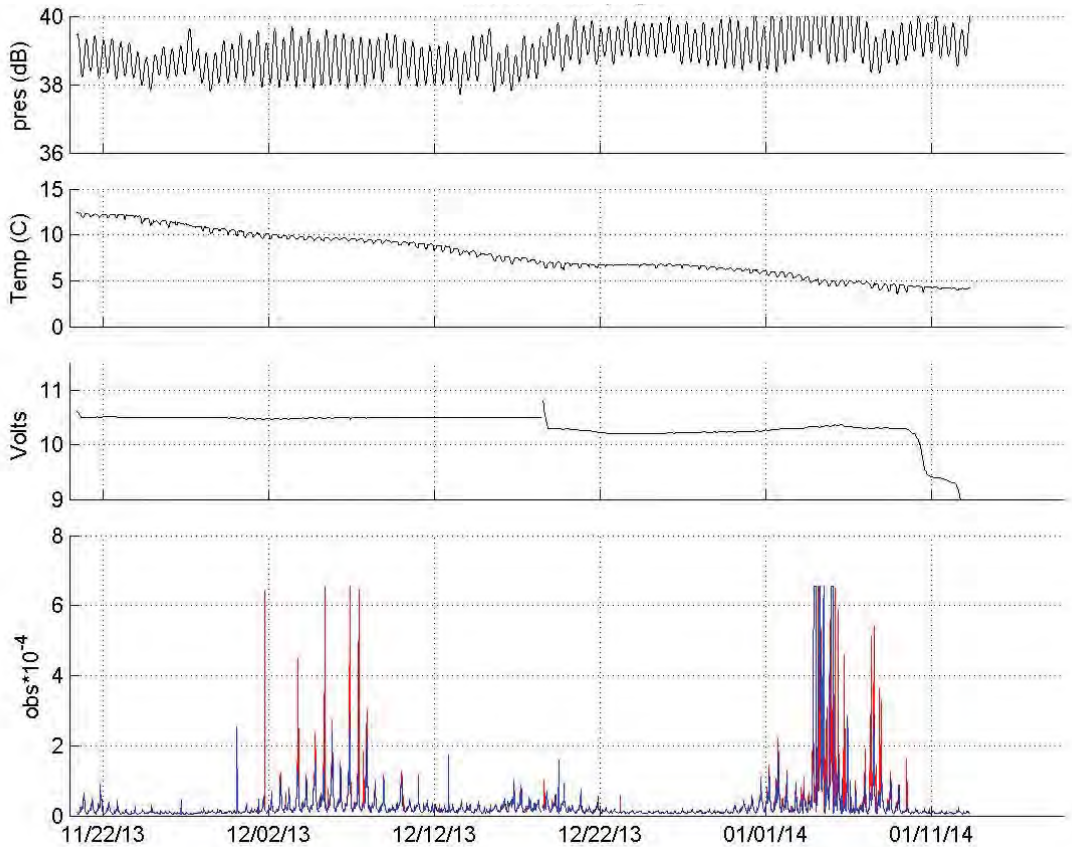

Figure 3: Observations from Station DOT1 in Campaign 3. The top and second panel shows the time series of the pressure and temperature at the Nortek ADCP and the third panel shows the system voltage. The bottom panel 1 (red), and (3) blue. The middle panels show the percentage reduction in the variance at each level and the lower panels show the change in ensemble means.

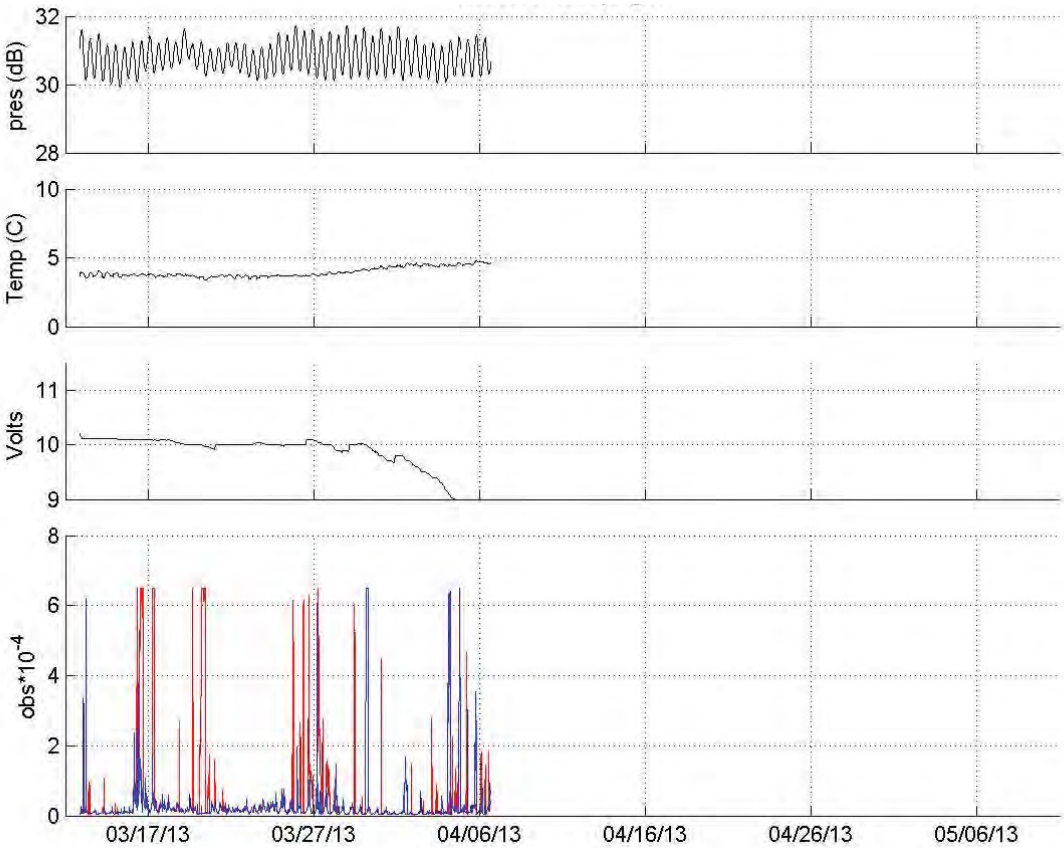

Figure 4: Observations from Station DOT2 in Campaign 1. The top and second panel shows the time series of the pressure and temperature at the Nortek ADCP and the third panel shows the system voltage. The bottom panel 1 (red), and (3) blue. The middle panels show the percentage reduction in the variance at each level and the lower panels show the change in ensemble means.

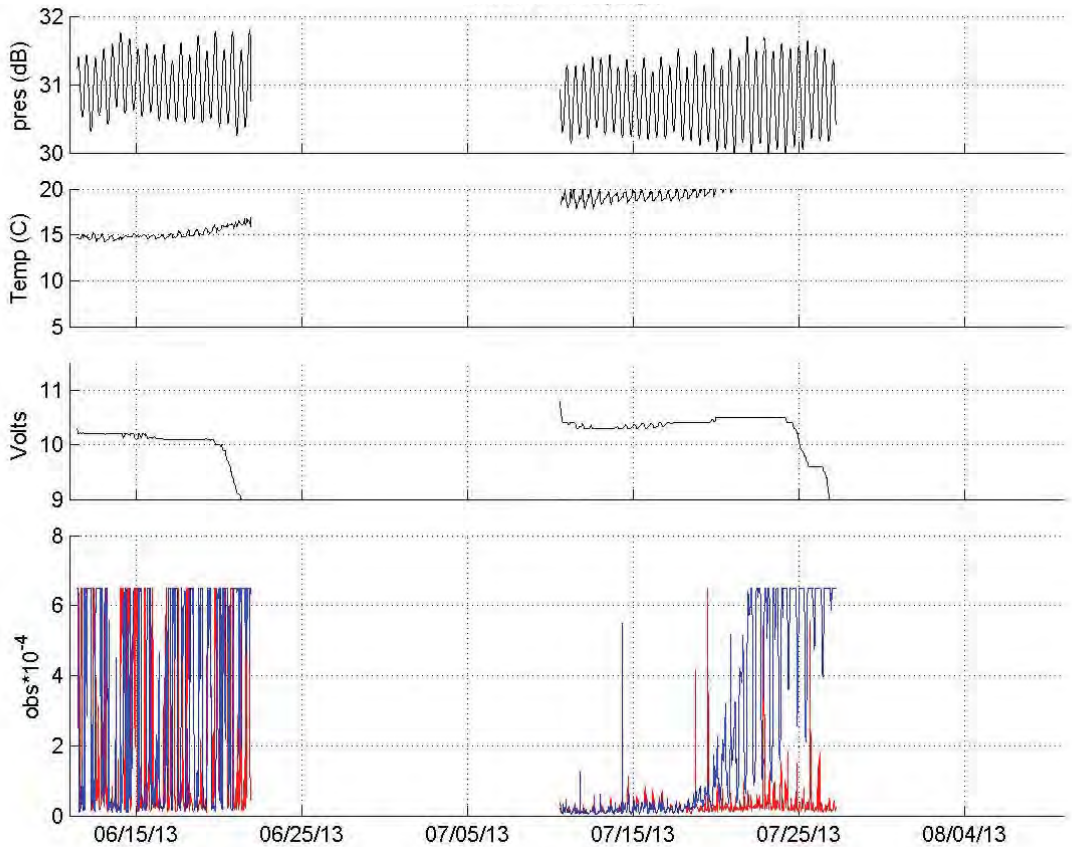

Figure 5: Observations from Station DOT2 in Campaign 2. The top and second panel shows the time series of the pressure and temperature at the Nortek ADCP and the third panel shows the system voltage. The bottom panel 1 (red), and (3) blue. The middle panels show the percentage reduction in the variance at each level and the lower panels show the change in ensemble means.

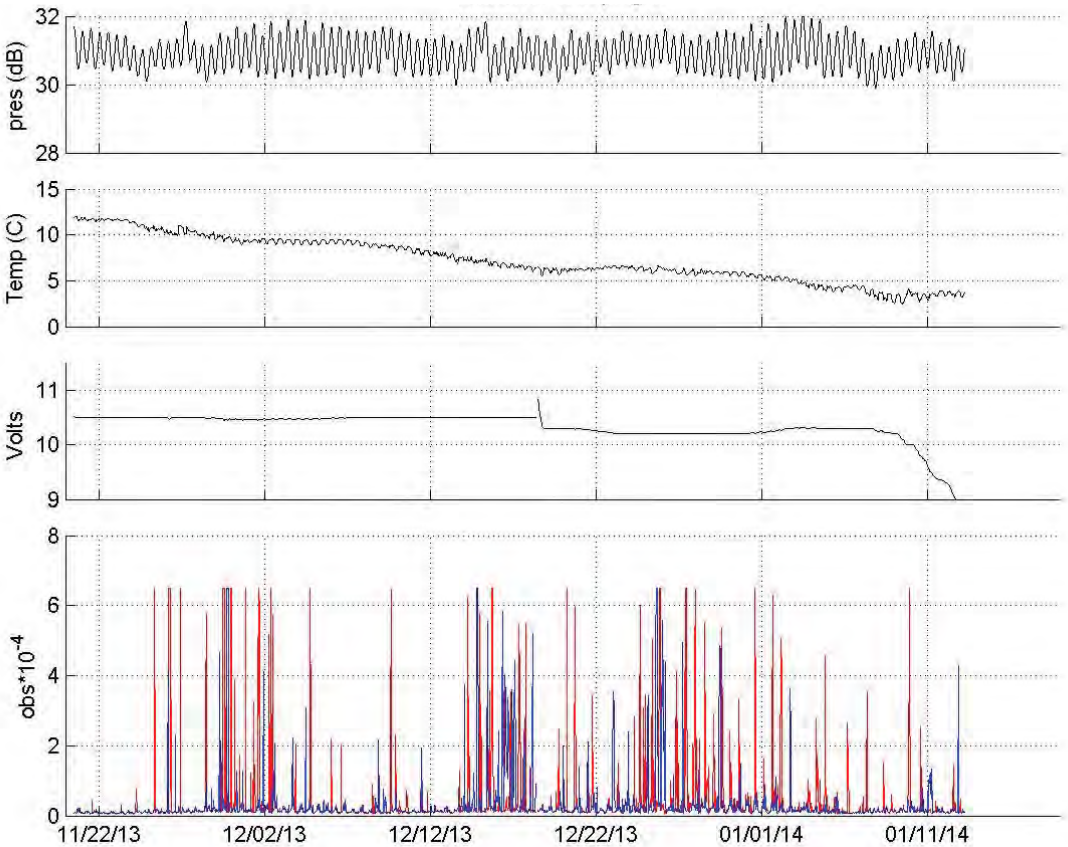

Figure 6: Observations from Station DOT2 in Campaign 3. The top and second panel shows the time series of the pressure and temperature at the Nortek ADCP and the third panel shows the system voltage. The bottom panel 1 (red), and (3) blue. The middle panels show the percentage reduction in the variance at each level and the lower panels show the change in ensemble means.

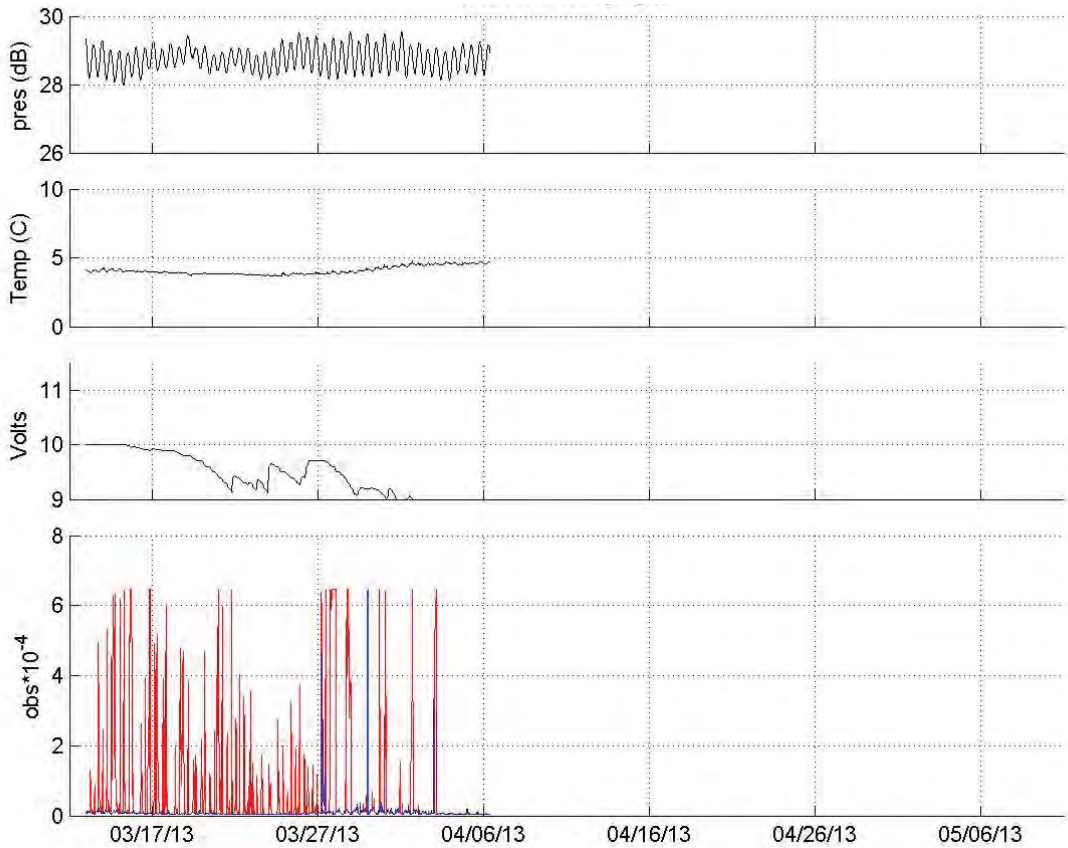

Figure 7: Observations from Station DOT3 in Campaign 1. The top and second panel shows the time series of the pressure and temperature at the Nortek ADCP and the third panel shows the system voltage. The bottom panel 1 (red), and (3) blue. The middle panels show the percentage reduction in the variance at each level and the lower panels show the change in ensemble means.

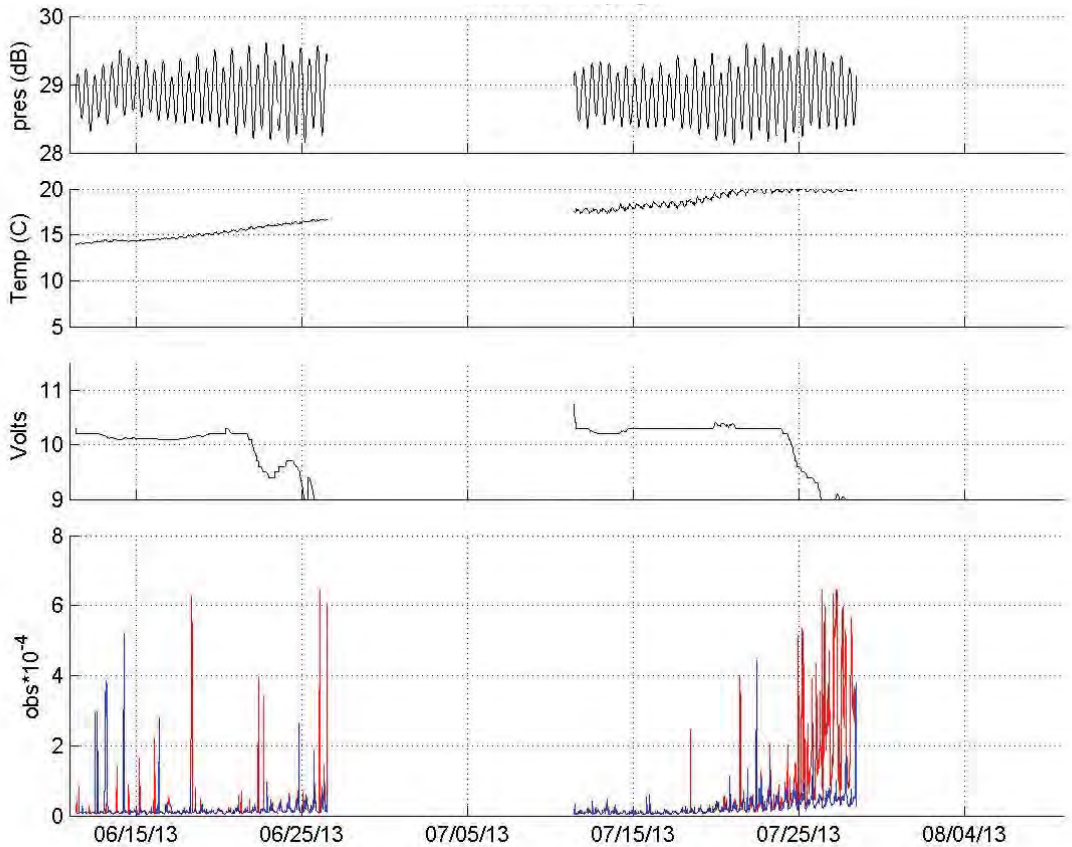

Figure 8: Observations from Station DOT3 in Campaign 2. The top and second panel shows the time series of the pressure and temperature at the Nortek ADCP and the third panel shows the system voltage. The bottom panel 1 (red), and (3) blue. The middle panels show the percentage reduction in the variance at each level and the lower panels show the change in ensemble means.

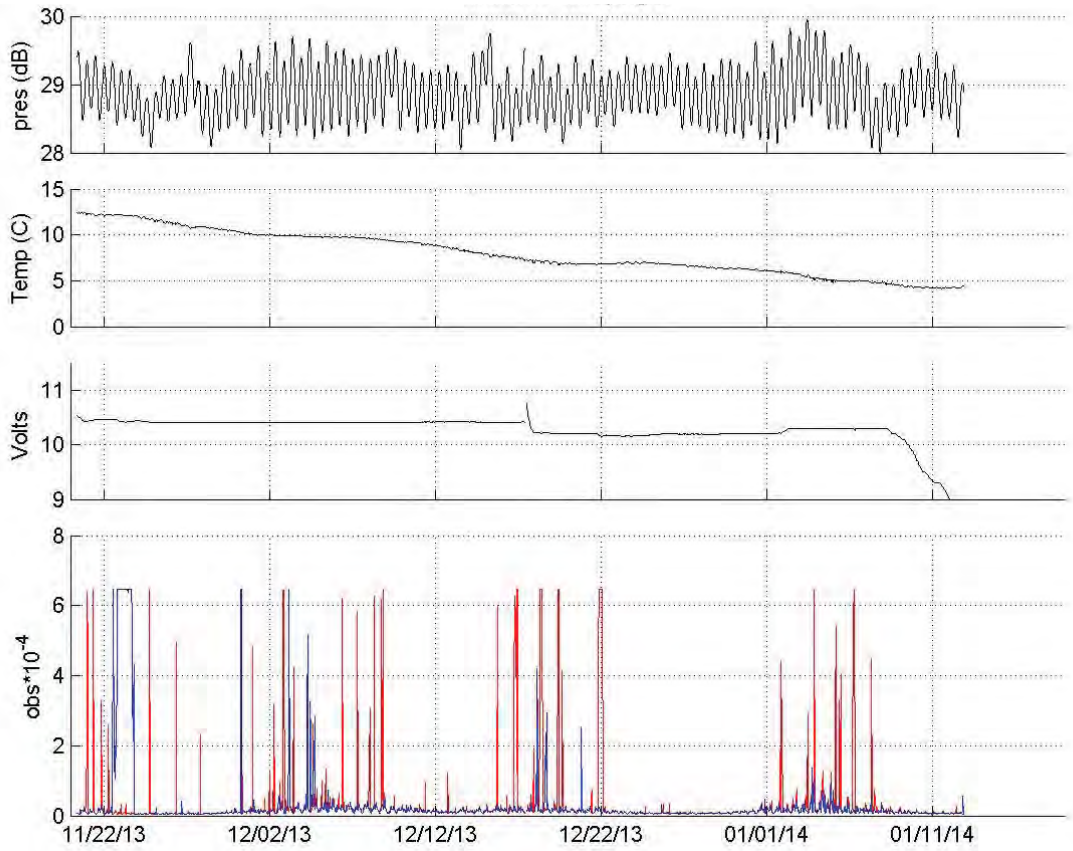

Figure 9: Observations from Station DOT3 in Campaign 3. The top and second panel shows the time series of the pressure and temperature at the Nortek ADCP and the third panel shows the system voltage. The bottom panel 1 (red), and (3) blue. The middle panels show the percentage reduction in the variance at each level and the lower panels show the change in ensemble means.

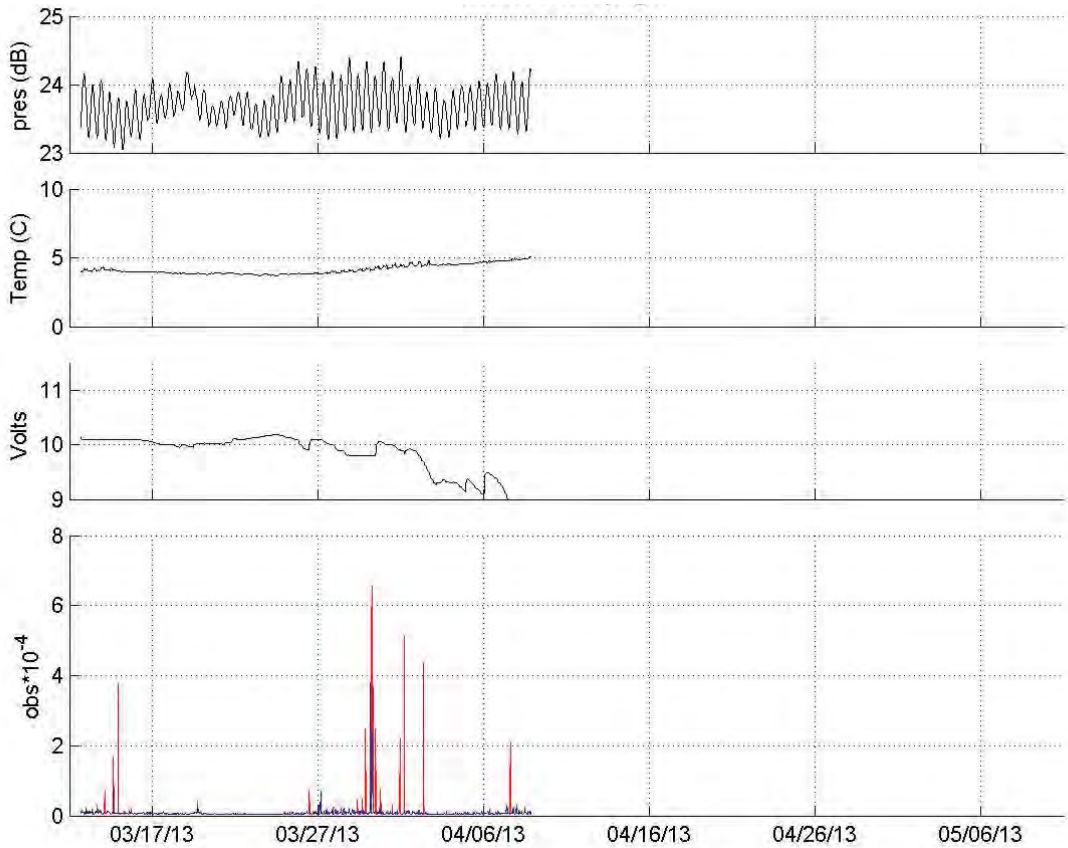

Figure 10: Observations from Station DOT4 in Campaign 1. The top and second panel shows the time series of the pressure and temperature at the Nortek ADCP and the third panel shows the system voltage. The bottom panel 1 (red), and (3) blue. The middle panels show the percentage reduction in the variance at each level and the lower panels show the change in ensemble means.

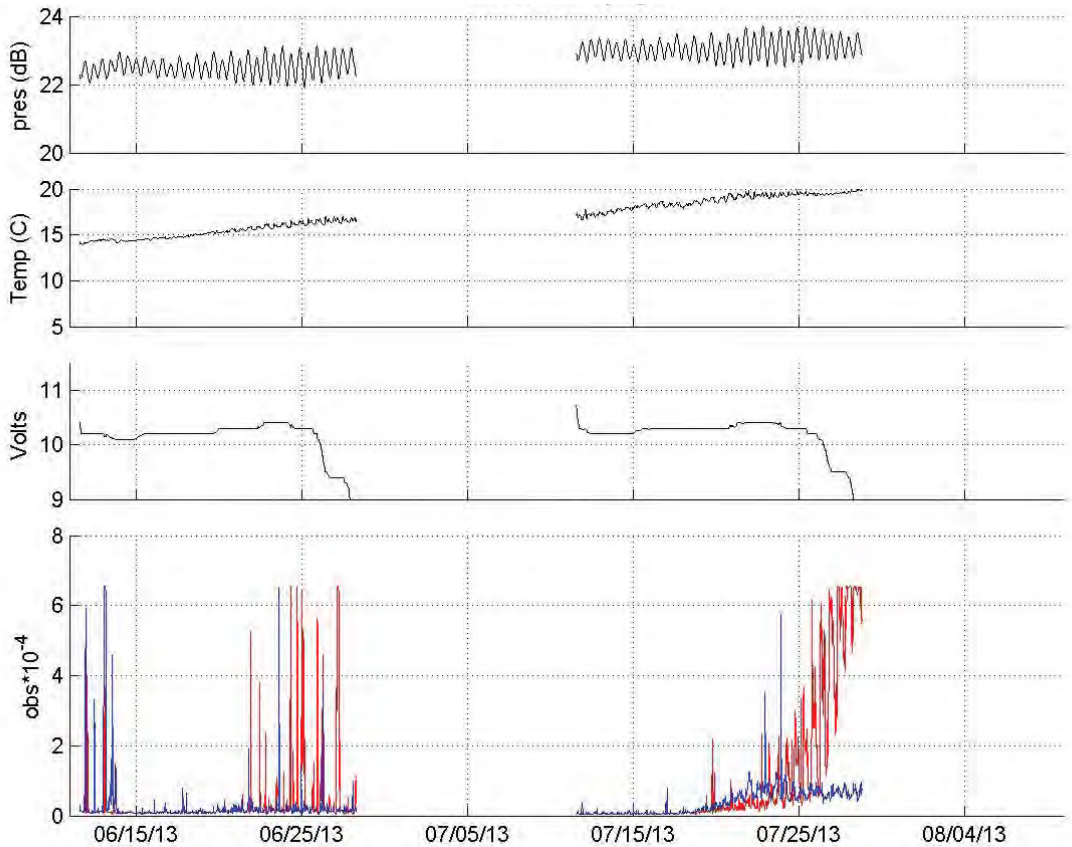

Figure 11: Observations from Station DOT4 in Campaign 2. The top and second panel shows the time series of the pressure and temperature at the Nortek ADCP and the third panel shows the system voltage. The bottom panel 1 (red), and (3) blue. The middle panels show the percentage reduction in the variance at each level and the lower panels show the change in ensemble means.

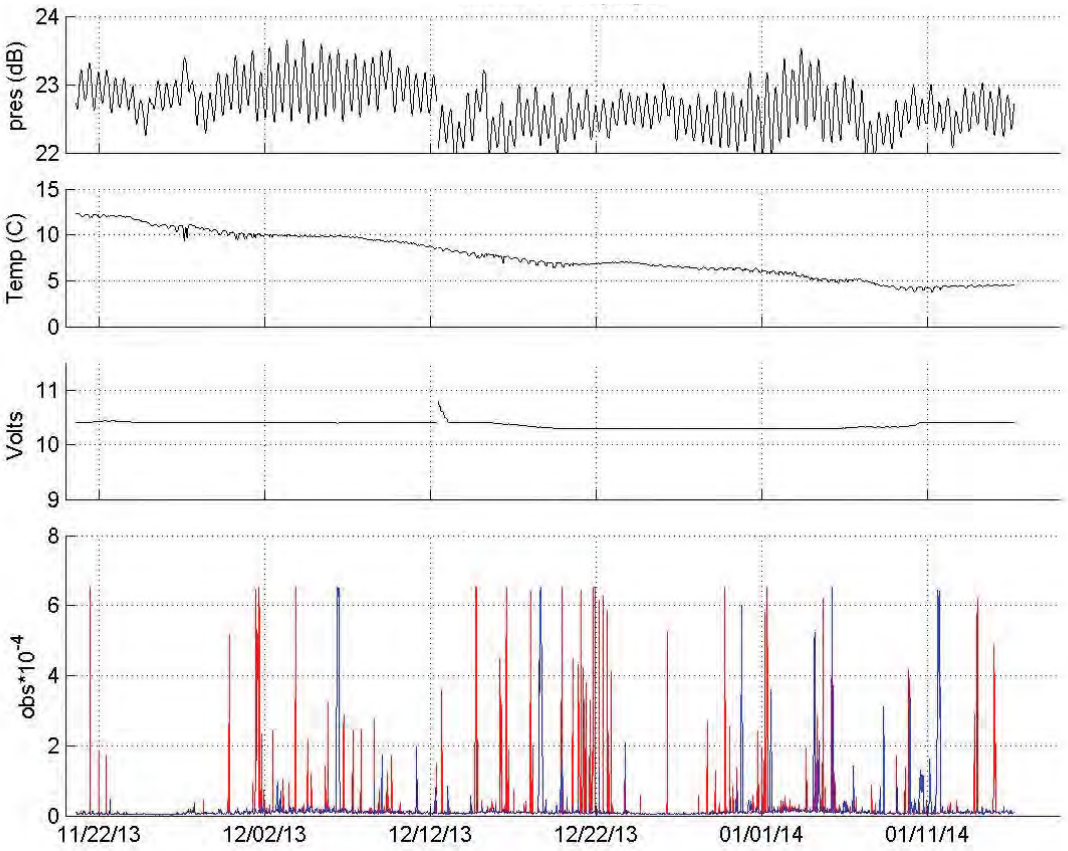

Figure 12: Observations from Station DOT4 in Campaign 3. The top and second panel shows the time series of the pressure and temperature at the Nortek ADCP and the third panel shows the system voltage. The bottom panel 1 (red), and (3) blue. The middle panels show the percentage reduction in the variance at each level and the lower panels show the change in ensemble means.

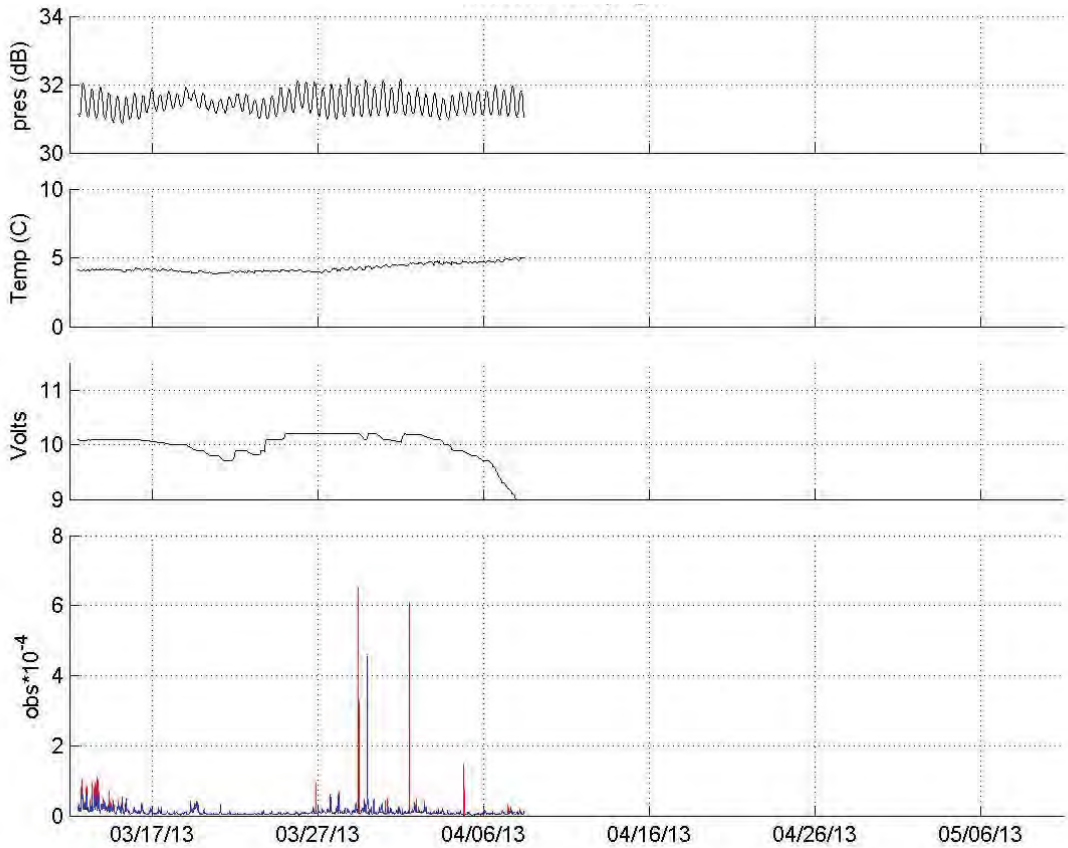

Figure 13: Observations from Station DOT5 in Campaign 1. The top and second panel shows the time series of the pressure and temperature at the Nortek ADCP and the third panel shows the system voltage. The bottom panel 1 (red), and (3) blue. The middle panels show the percentage reduction in the variance at each level and the lower panels show the change in ensemble means.

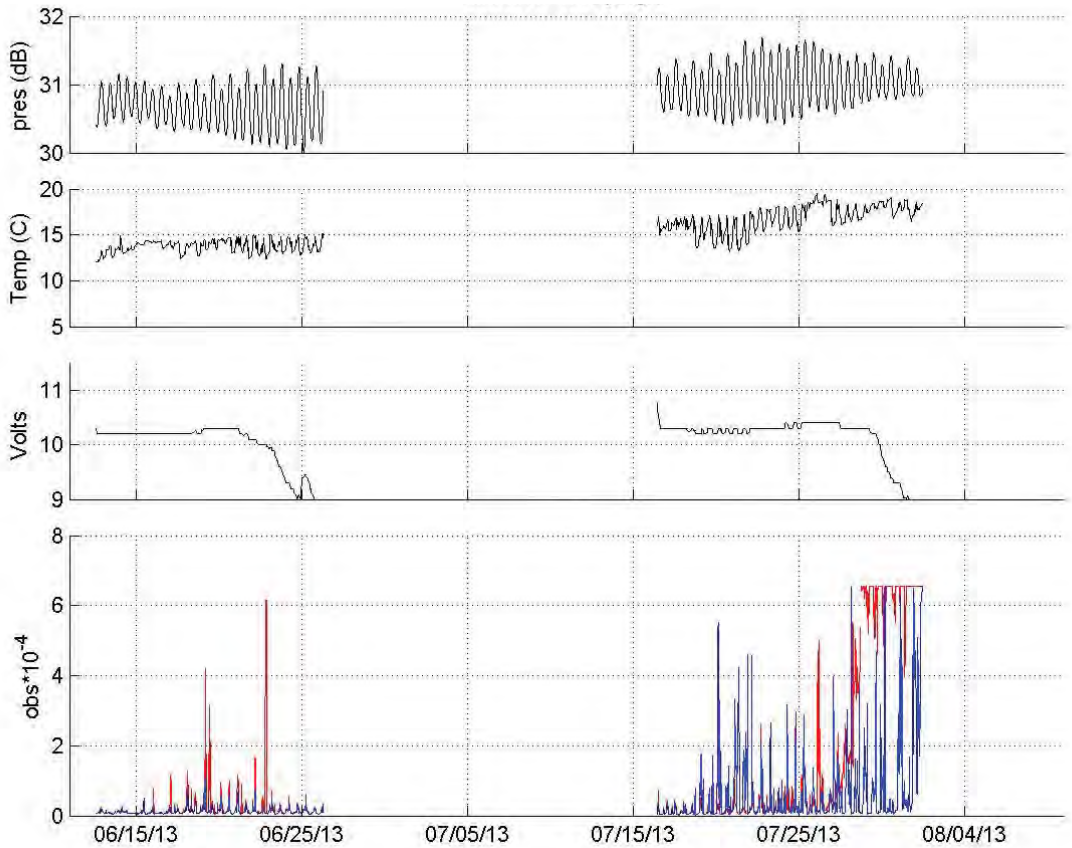

Figure 14: Observations from Station DOT5 in Campaign 2. The top and second panel shows the time series of the pressure and temperature at the Nortek ADCP and the third panel shows the system voltage. The bottom panel 1 (red), and (3) blue. The middle panels show the percentage reduction in the variance at each level and the lower panels show the change in ensemble means.

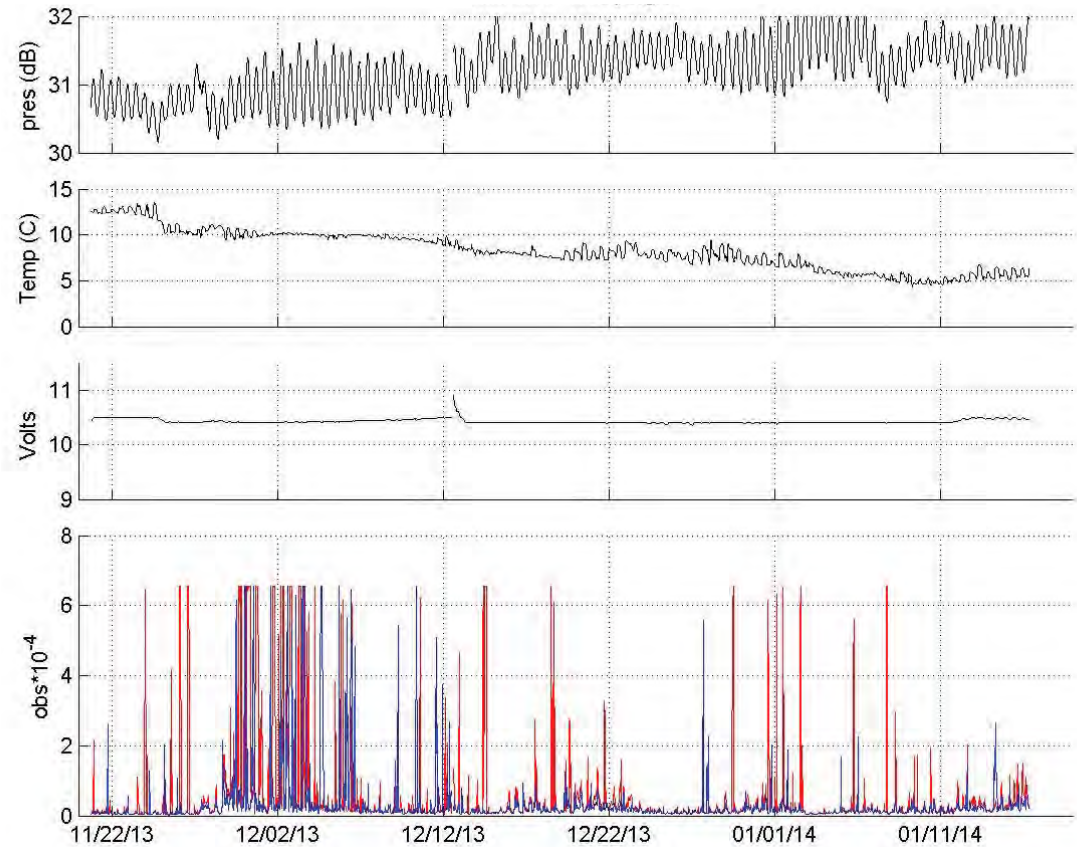

Figure 15: Observations from Station DOT5 in Campaign 3. The top and second panel shows the time series of the pressure and temperature at the Nortek ADCP and the third panel shows the system voltage. The bottom panel 1 (red), and (3) blue. The middle panels show the percentage reduction in the variance at each level and the lower panels show the change in ensemble means.

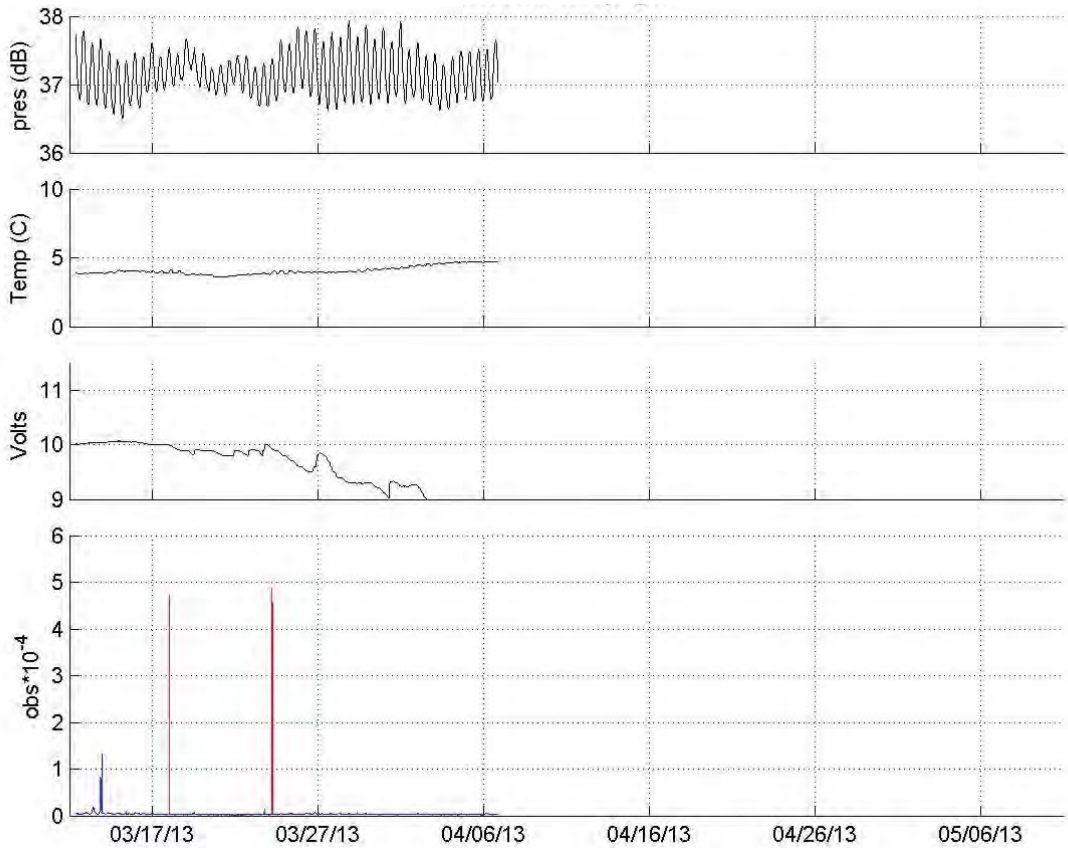

Figure 16: Observations from Station DOT6 in Campaign 1. The top and second panel shows the time series of the pressure and temperature at the Nortek ADCP and the third panel shows the system voltage. The bottom panel 1 (red), and (3) blue. The middle panels show the percentage reduction in the variance at each level and the lower panels show the change in ensemble means.

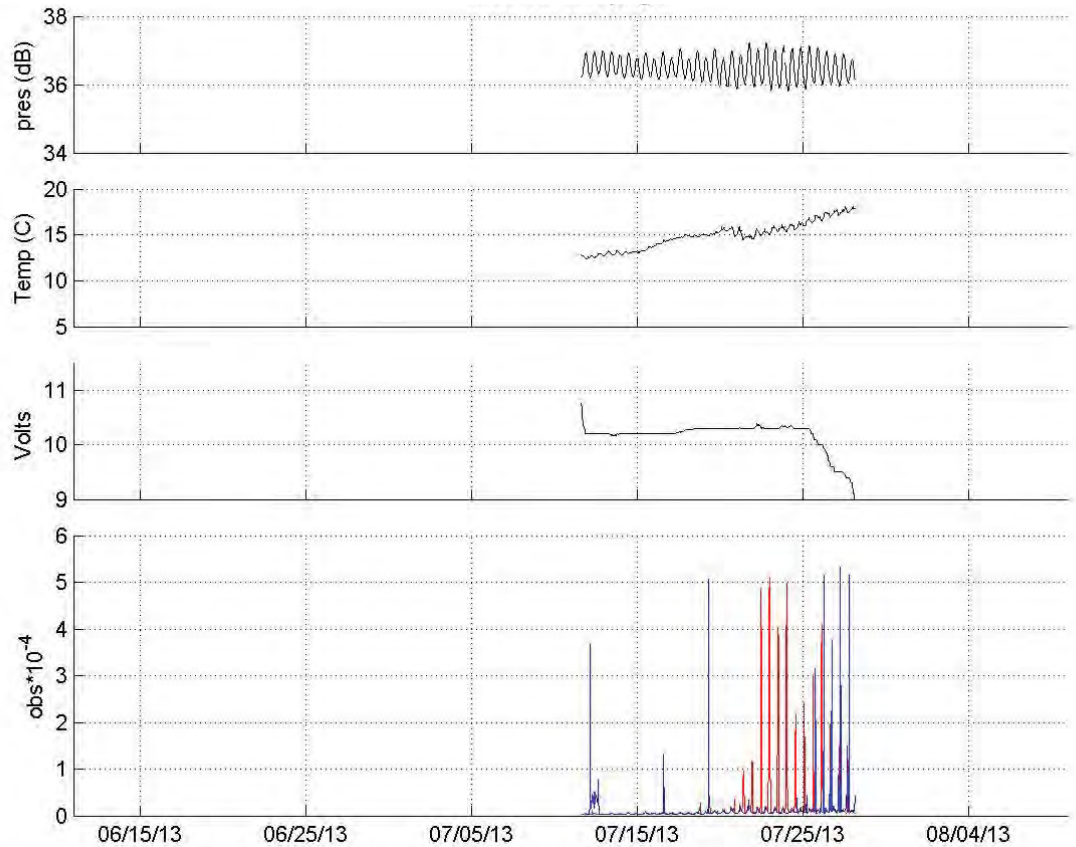

Figure 17: Observations from Station DOT6 in Campaign 2. The top and second panel shows the time series of the pressure and temperature at the Nortek ADCP and the third panel shows the system voltage. The bottom panel 1 (red), and (3) blue. The middle panels show the percentage reduction in the variance at each level and the lower panels show the change in ensemble means.

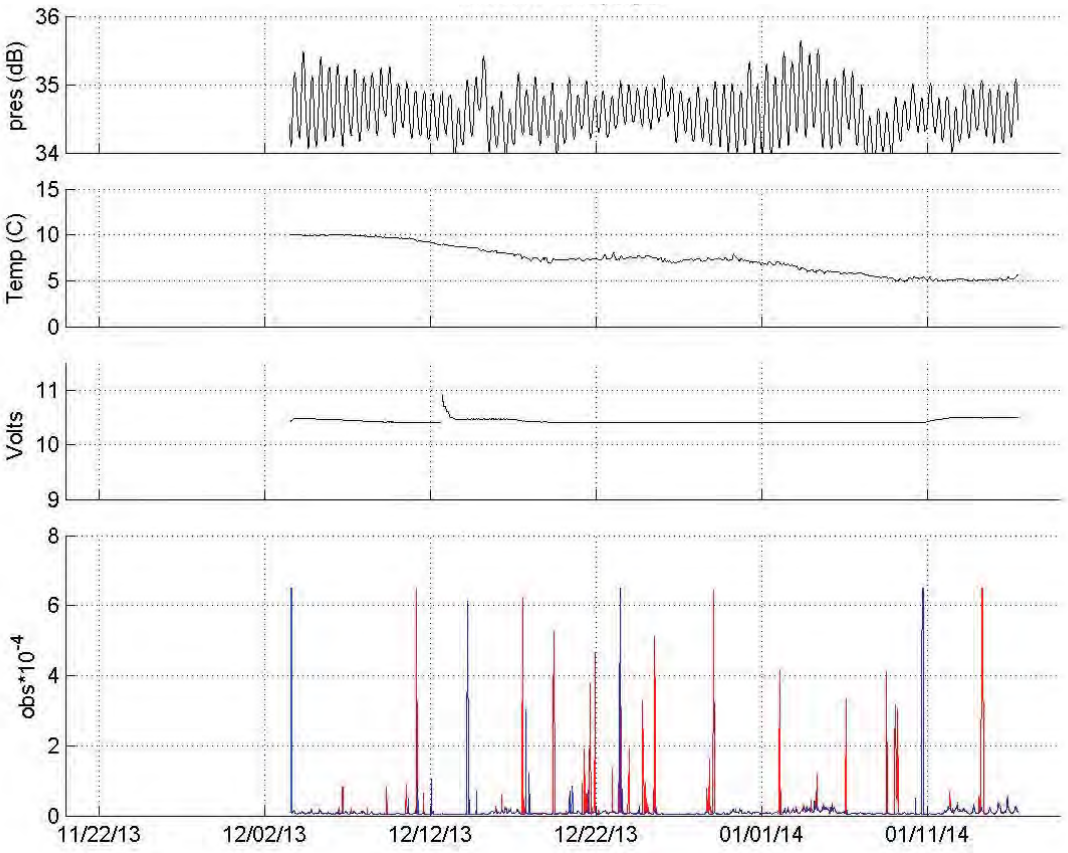

Figure 18: Observations from Station DOT6 in Campaign 3. The top and second panel shows the time series of the pressure and temperature at the Nortek ADCP and the third panel shows the system voltage. The bottom panel 1 (red), and (3) blue. The middle panels show the percentage reduction in the variance at each level and the lower panels show the change in ensemble means.

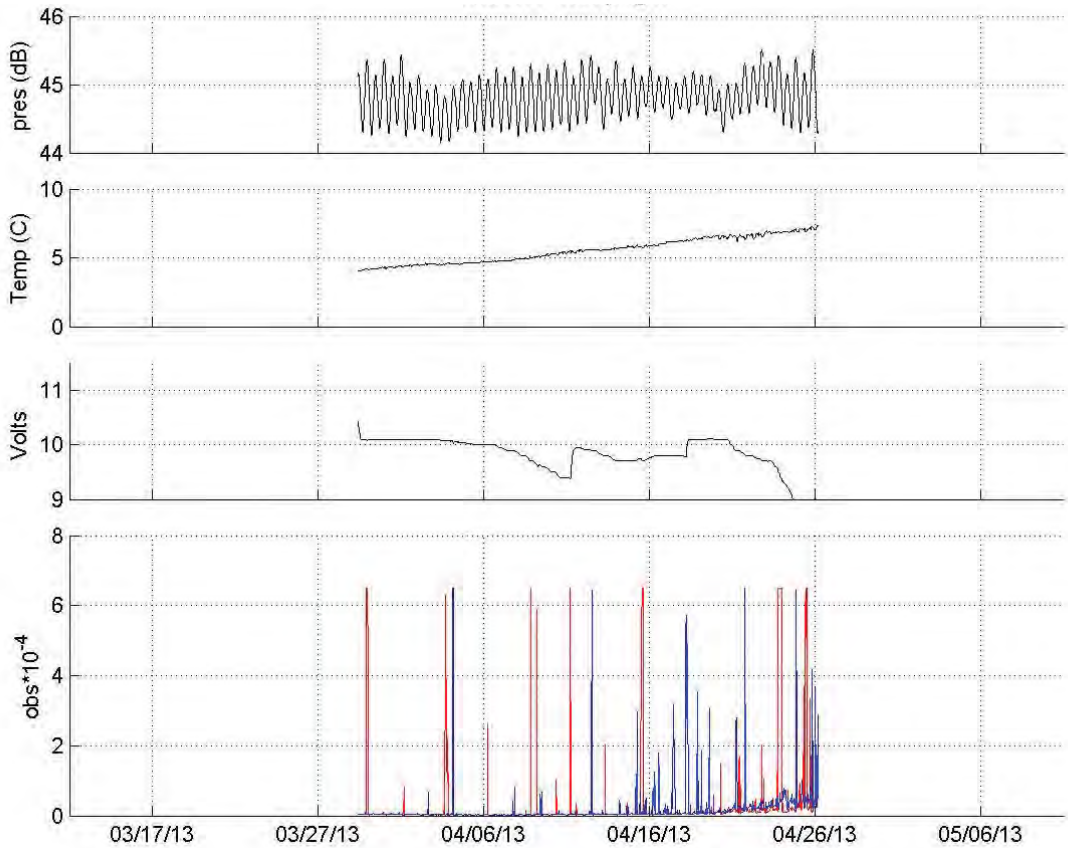

Figure 19: Observations from Station DOT7 in Campaign 1. The top and second panel shows the time series of the pressure and temperature at the Nortek ADCP and the third panel shows the system voltage. The bottom panel 1 (red), and (3) blue. The middle panels show the percentage reduction in the variance at each level and the lower panels show the change in ensemble means.

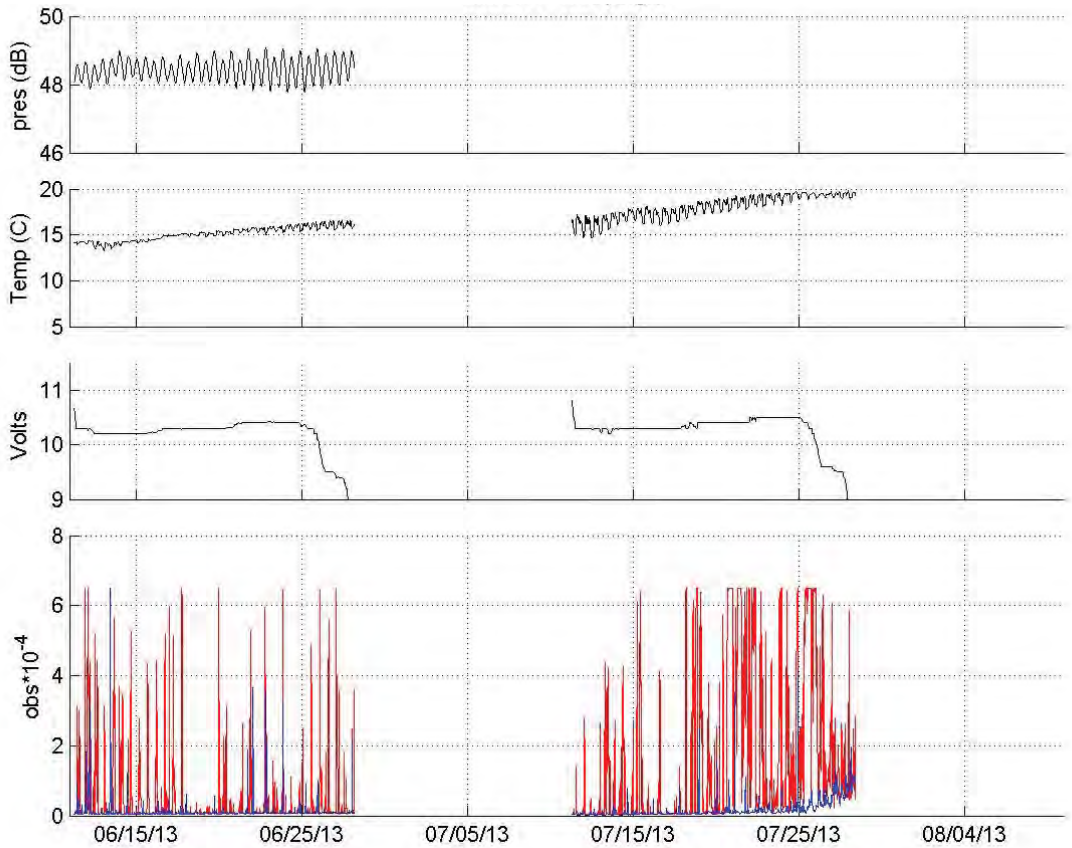

Figure 20: Observations from Station DOT7 in Campaign 2. The top and second panel shows the time series of the pressure and temperature at the Nortek ADCP and the third panel shows the system voltage. The bottom panel 1 (red), and (3) blue. The middle panels show the percentage reduction in the variance at each level and the lower panels show the change in ensemble means.

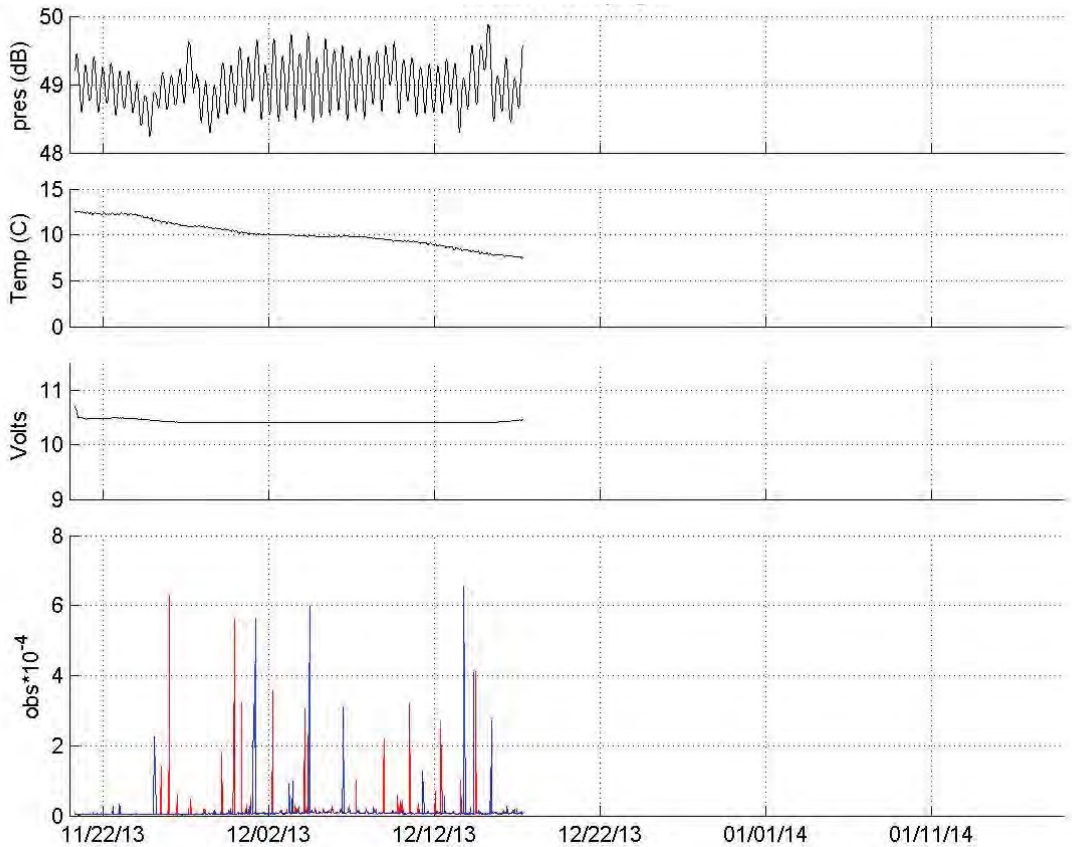

Figure 21: Observations from Station DOT7 in Campaign 3. The top and second panel shows the time series of the pressure and temperature at the Nortek ADCP and the third panel shows the system voltage. The bottom panel 1 (red), and (3) blue. The middle panels show the percentage reduction in the variance at each level and the lower panels show the change in ensemble means.

Appendix 10

PROFILING CTD CASTS – SHIP SURVEYS

Tables 1 to 8: List of Casts. Casts used mostly the SBE 9/11 CTD. Stations where the SBE19+ CTD was used due to sea conditions are noted.

Figure 1 to 133: Vertical profiles of temperature, salinity and density.

Table 1. CTD Casts during Cruise CTDOT1

Date/Time (EST)	**Station / Cast No.**	**Latitude** (deg. min.)	**Longitude** (deg. min.)	**Depth** (m)	**Notes**
3/12/13 8:00	DOT6 cast1	41 15.000	71 48.020	35	
3/12/13 9:21	CTD10 cast1	41 16.201	71 36.003	39	
3/12/13 10:35	CTD9 cast1	41 08.992	71 39.005	18.4	
3/12/13 11:21	DOT5 cast1	41 09.090	71 45.056	30	
3/12/13 13:24	CTD8 cast1	41 04.802	71 49.859	15	SBE19+
3/12/13 14:53	DOT4 cast1	41 09.014	72 00.006	23	
3/12/13 16:57	CTD11 cast2	41 13.761	72 03.710	14.5	SBE19+
3/12/13 19:13	DOT2 cast1	41 08.941	72 22.140	32	
3/12/13 20:27	DOT1 cast1	41 12.083	72 24.131	43	
3/12/13 21:48	DOT3 cast1	41 15.477	72 14.556	30	
3/12/13 23:10	DOT7 cast1	41 75.616	72 05.946	48	
3/13/13 5:22	DOT7 cast2	41 15.570	72 06.066	46	
3/13/13 6:39	DOT3 cast2	41 15.462	72 14.521	29	
3/13/13 7:57	DOT1 cast2	41 12.014	72 24.042	42	
3/13/13 8:57	DOT2 cast2	41 08.950	72 22.177	30	
3/13/13 11:36	CTD11 cast3	41 13.791	72 03.645	18.5	
3/13/13 12:39	DOT4 cast2	41 09.003	72 59.916	22.5	
3/13/13 13:59	CTD8 cast2	41 04.785	71 49.820	13.5	
3/13/13 15:15	DOT5 cast2	41 08.890	71 44.928	29	
3/13/13 16:18	CTD9 cast2	41 08.916	71 39.978	22	
3/13/13 17:35	CTD10 cast2	41 16.211	71 35.968	38	
3/13/13 19:08	DOT6 cast2	41 14.970	71 47.963	37.2	
3/29/13 9:22	DOT7 cast3	41 15.643	72 05.983	45.7	SBE19+

Table 2. CTD Casts during Cruise CTDOT2

Date/Time (EST)	**Station**	**Latitude** (deg. min.)	**Longitude** (deg. min.)	**Depth** (m)	**Notes**
5/17/13 6:15	DOT7	41 15.55	72 05.90	50	
5/17/13 8:11	DOT3	41 15.48	72 14.48	29.6	
5/17/13 9:52	DOT1	41 11.97	72 23.97	41.2	
5/17/13 10:50	DOT2	41 08.96	72 22.17	30	
5/17/13 13:02	CTD11	41 13.62	72 03.45	30	
5/17/13 14:05	DOT4	41 09.00	72 00.04	23.1	
5/17/13 15:25	CTD8	41 04.82	71 49.84	13.5	
5/17/13 16:30	DOT5	41 09.00	71 44.98	28.5	
5/17/13 20:10	CTD9	41 08.97	71 38.99	21	
5/17/13 21:08	CTD10	41 16.20	71 35.95	36	
5/17/13 22:47	DOT6	41 15.03	71 47.98	35	

Table 3. CTD Casts during Cruise CTDOT3

Date/Time (EST)	**Station / Cast No.**	**Latitude** (deg. min.)	**Longitude** (deg. min.)	**Depth** (m)	**Notes**
6/11/13 7:16	DOT7 cast1	41 15.63	72 05.93	45	
6/11/13 8:38	DOT3 cast1	41 15.50	72 14.54	28	
6/11/13 10:03	DOT1 cast1	41 12.07	72 23.95	40	
6/11/13 11:01	DOT2 cast1	41 09.01	72 22.17	30	
6/11/13 13:15	CTD11 cast1	41 13.80	72 03.59	31	
6/11/13 14:29	DOT4 cast1	41 09.00	72 00.01	23.2	
6/11/13 15:36	CTD8 cast1	41 04.85	71 49.63	13	SBE 19+
6/11/13 17:05	DOT5 cast1	41 08.92	71 44.95	29.1	SBE 19+
6/11/13 17:58	CTD9 cast1	41 08.97	71 39.06	22	SBE 19+
6/11/13 19:08	CTD10 cast1	41 16.23	71 36.03	36	
6/11/13 19:14	CTD10 cast2	41 16.22	71 36.03	36	
6/11/13 19:25	CTD10 cast3	41 16.22	71 36.04	36	
6/11/13 21:08	DOT6 cast1	41 15.00	71 48.00	36	
6/11/13 21:16	DOT6 cast2	41 15.00	71 48.01	36	
6/12/13 5:24	DOT2 cast2	41 08.98	72 22.34	30	
6/12/13 5:30	DOT2 cast3	41 09.07	72 21.95	30	
6/12/13 6:24	DOT1 cast2	41 11.94	72 24.13	40	
6/12/13 6:58	DOT1 cast3	41 12.06	72 24.19	42	
6/12/13 7:04	DOT1 cast4	41 11.95	72 23.88	40	
6/12/13 8:17	DOT3 cast2	41 15.52	72 14.53	27	
6/12/13 8:24	DOT3 cast3	41 15.40	72 14.53	27	
6/12/13 9:33	DOT7 cast2	41 15.54	72 06.09	46	
6/12/13 10:23	CTD11 cast2	41 13.62*	72 03.64	27	
6/12/13 12:50	CTD8 cast2	41 04.85	71 49.63	12	
6/12/13 14:14	DOT5 cast2	41 08.92	71 44.95	30	
6/12/13 15:05	CTD9 cast2	41 08.84	71 38.92	18.5	
6/12/13 16:18	CTD10 cast4	41 16.15	71 35.94	36.5	
6/12/13 17:44	DOT6 cast3	41 15.00	71 47.87	35	
6/12/13 23:26	DOT4 cast2	41 08.96	72 00.03	22.5	

Table 4. CTD Casts during Cruise CTDOT4

Date/Time (EST)	**Station**	**Latitude** (deg. min.)	**Longitude** (deg. min.)	**Depth** (m)	**Notes**
7/10/13 12:25 PM	DOT1	41 12.039	72 23.957	45	SBE 19+
7/10/13 1:40 PM	DOT2	41 08.877	72 22.332	30.5	SBE 19+
7/11/13 7:45 AM	DOT7	41 15.660	72 05.961	40.8	SBE 19+
7/11/13 9:30 AM	DOT3	41 15.506	72 14.556	28	SBE 19+
7/11/13 1:05 PM	DOT4	41 09.005	71 59.974	22.8	SBE 19+
7/11/13 3:25 PM	DOT6	41 14.996	71 47.945	35.3	SBE 19+
7/16/13 10:50 AM	DOT5	41 08.999	71 41.984	30.5	SBE 19+

Table 5. CTD Casts during Cruise CTDOT5

Date/Time (EST)	**Station / Cast No.**	**Latitude** (deg. min.)	**Longitude** (deg. min.)	**Depth** (m)	**Notes**
8/7/13 8:06	DOT7 cast3	41 15.68	72 06.01	40	
8/7/13 9:48	DOT3 cast1	41 15.56	72 14.70	27	
8/7/13 11:20	DOT1 cast1	41 12.04	72 23.95	41.5	
8/7/13 12:31	DOT2 cast1	41 09.00	72 22.26	30	
8/7/13 14:42	CTD11 cast1	41 13.95	72 03.75	43	
8/7/13 16:00	DOT4 cast1	41 08.98	71 59.97	21	
8/7/13 17:30	CTD8 cast1	41 04.83	71 49.81	14	
8/7/13 18:51	DOT5 cast1	41 09.00	71 44.99	28.5	
8/7/13 20:07	CTD9 cast1	41 09.20	71 39.03	22.5	
8/7/13 21:41	CTD10 cast1	41 16.12	71 36.04	36	
8/7/13 23:54	DOT6 cast1	41 14.99	71 47.94	35.4	
8/8/13 5:40	DOT6 cast2	41 15.03	71 47.97	35	
8/8/13 7:00	CTD10 cast2	41 16.32	71 36.01	33	
8/8/13 8:16	CTD9 cast2	41 09.09	71 39.01	22	
8/8/13 8:58	DOT5 cast2	41 09.07	71 45.02	30	
8/8/13 10:05	CTD8 cast2	41 04.86	71 49.75	15	
8/8/13 11:23	DOT4 cast2	41 08.99	71 59.96	22.3	
8/8/13 12:19	CTD11 cast2	41 13.76	72 03.54	31.1	
8/8/13 12:58	DOT7 cast4	41 15.66	72 05.75	29	
8/8/13 14:09	DOT3 cast2	41 15.55	72 14.34	29.6	
8/8/13 14:13	DOT3 cast3	41 15.62	72 14.12	29.6	
8/8/13 15:47	DOT1 cast2	41 12.00	72 23.91	38.6	
8/8/13 16:25	DOT2 cast2	41 09.22	72 21.99	31	

Table 6. CTD Casts during Cruise CTDOT6

Date/Time (EST)	**Station / Cast No.**	**Latitude** (deg. min.)	**Longitude** (deg. min.)	**Depth** (m)	**Notes**
11/20/13 7:35	DOT7 cast1	41 15.63	72 06.00	46	
11/20/13 9:07	DOT3 cast1	41 15.47	72 14.59	28	
11/20/13 10:29	DOT1 cast1	41 11.96	72 24.15	38	
11/20/13 11:21	DOT2 cast1	41 09.00	72 22.21	31	
11/20/13 13:19	CTD11 cast1	41 13.79	72 03.58	22	
11/20/13 14:30	DOT4 cast1	41 09.00	71 59.99	22.1	
11/20/13 15:47	CTD8 cast1	41 04.73	71 49.83	14	
11/20/13 17:17	DOT5 cast1	41 09.01	71 45.00	29.6	
11/20/13 18:33	CTD9 cast1	41 09.01	71 38.99	21.5	
11/20/13 20:00	CTD10 cast1	41 16.21	71 35.99	36	
11/20/13 21:45	DOT6 cast1	41 15.00	71 49.93	34	
11/21/13 6:20	DOT6 cast2	41 15.01	71 49.97	33.9	
11/21/13 8:00	CTD10 cast2	41 16.18	71 36.08	37	
11/21/13 9:12	CTD9 cast2	41 09.02	71 39.02	21	
11/21/13 10:15	DOT5 cast2	41 09.03	71 45.03	31.5	
11/21/13 11:33	CTD8 cast2	41 04.78	71 49.83	14	
11/21/13 12:58	DOT4 cast2	41 09.14	71 59.89	24.7	
11/21/13 13:55	CTD11 cast2	41 13.72	72 03.48	37	
11/21/13 14:48	DOT2 cast2	41 09.09	72 22.14	30.5	
11/21/13 17:36	DOT1 cast2	41 12.05	72 23.94	41.1	
11/21/13 18:49	DOT3 cast2	41 15.56	72 14.59	27.4	
11/21/13 19:45	DOT7 cast2	41 15.66	72 06.06	43	

Table 7. CTD Casts during Cruise CTDOT7

Date/Time (EST)	**Station / Cast No.**	**Latitude** (deg. min.)	**Longitude** (deg. min.)	**Depth** (m)	**Notes**
12/12/13 11:30	DOT4	41 12.039	72 23.957	21.7	SBE 19+
12/12/13 15:00	DOT5	41 09.024	71 45.000	30.1	SBE 19+
12/12/13 16:12	DOT6	41 15.046	71 49.940	35.2	SBE 19+
12/17/13 9:59	DOT7	41 15.620	72 06.115	48.5	SBE 19+
12/17/13 11:50	DOT3	41 15.492	72 14.520	29	SBE 19+
12/18/13 11:30	DOT2	41 08.999	71 22.199	31	SBE 19+
12/18/13 12:39	DOT1	41 12.095	72 23.997	44	SBE 19+

Table 8. CTD Casts during Cruise CTDOT8

Date/Time (EST)	**Station / Cast No.**	**Latitude** (deg. min.)	**Longitude** (deg. min.)	**Depth** (m)	**Notes**
1/15/14 9:00	DOT7 cast1	41 15.582	72 06.007	46	
1/15/14 10:43	DOT3 cast1	41 15.479	72 14.5572	29.5	
1/15/14 12:26	DOT1 cast1	41 12.002	72 23.996	41.8	
1/15/14 13:37	DOT2 cast1	41 08.950	72 22.159	32	
1/15/14 15:14	CTD11 cast1	41 13.599	72 03.357	44	
1/15/14 15:52	DOT7 cast2	41 15.617	72 06.025	50.2	
1/15/14 16:59	DOT3 cast2	41 15.510	72 14.560	28.3	
1/15/14 18:05	DOT1 cast2	41 12.013	72 24.177	36	
1/15/14 19:00	DOT2 cast2	41 08.967	72 22.243	30.5	
1/15/14 21:33	CTD11 cast2	41 13.791	72 03.211	87.5	
1/15/14 22:36	DOT4 cast1	41 08.959	71 59.907	23	
1/15/14 13:58	CTD8 cast1	41 04.752	71 49.904	14	SBE 19+
1/16/14 6:36	CTD8 cast2	41 04.601	71 49.681	15	
1/16/14 8:09	DOT4 cast2	41 08.973	72 00.099	23	
1/16/14 10:00	DOT5 cast1	41 09.059	71 44.954	29	
1/16/14 10:52	CTD9 cast1	41 08.999	71 39.022	22	
1/16/14 11:55	CTD10 cast1	41 16.244	71 35.949	34.5	
1/16/14 13:45	DOT6 cast1	41 15.999	71 41.883	35.3	
1/16/14 14:50	DOT5 cast2	41 09.018	71 44.973	29.4	
1/16/14 15:27	CTD9 cast2	41 09.031	71 38.989	22.2	
1/16/14 16:35	CTD10 cast2	41 16.169	71 36.004	37.6	
1/16/14 18:02	DOT6 cast2	41 14.934	71 49.959	33	

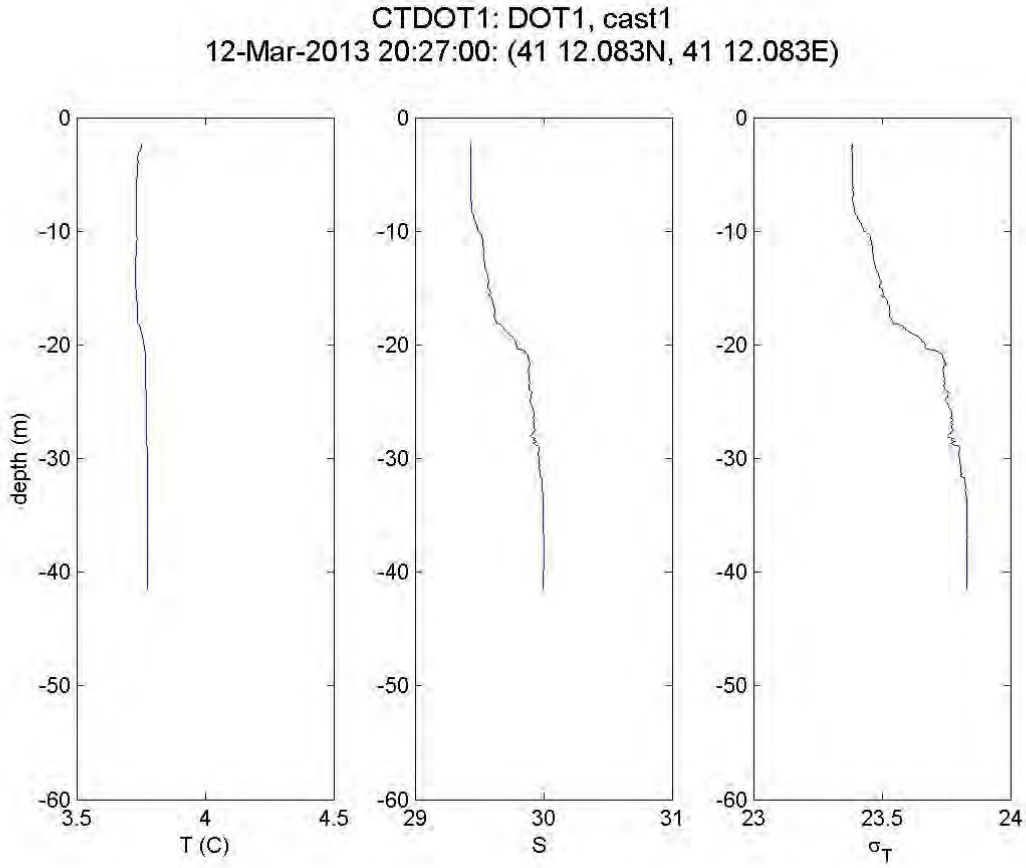

Figure 1: Cruise CTDOT1: Station DOT1, Cast 1: The left panel shows the vertical structure of Temperature (C) and the center and right panels show the salinity and density (σ_T) profiles respectively.

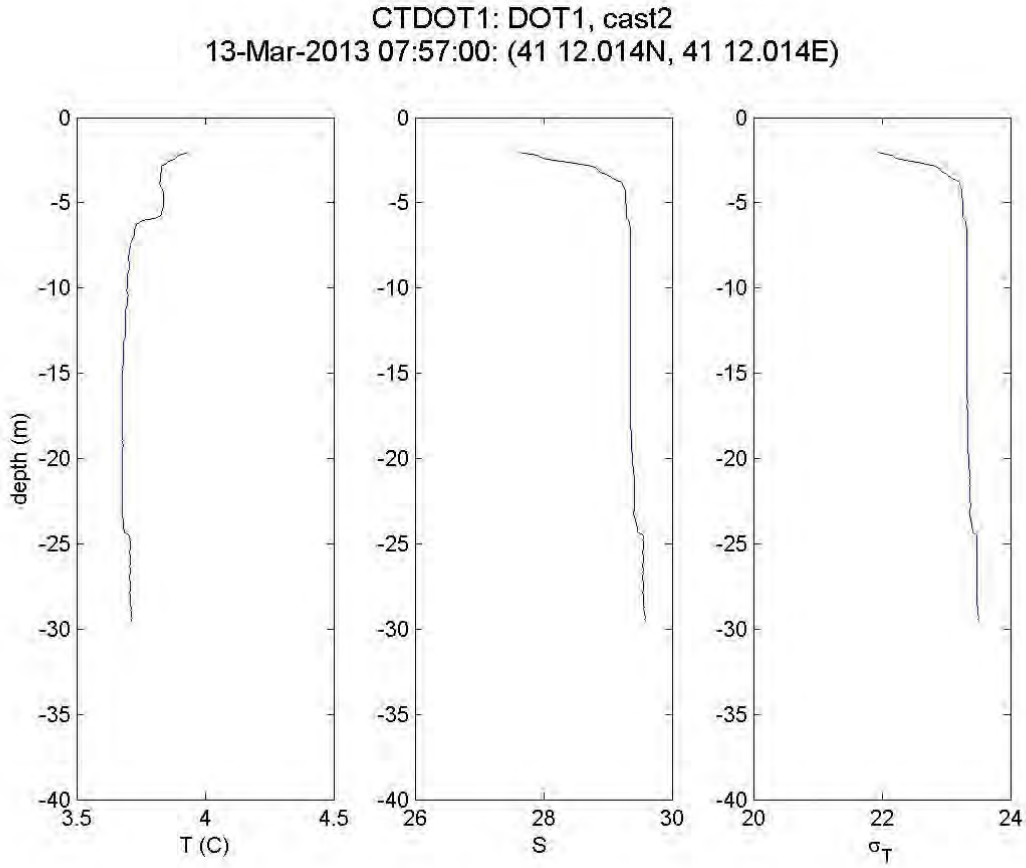

Figure 2: Cruise CTDOT1: Station DOT1, Cast 2: The left panel shows the vertical structure of Temperature (C) and the center and right panels show the salinity and density (σ_T) profiles respectively.

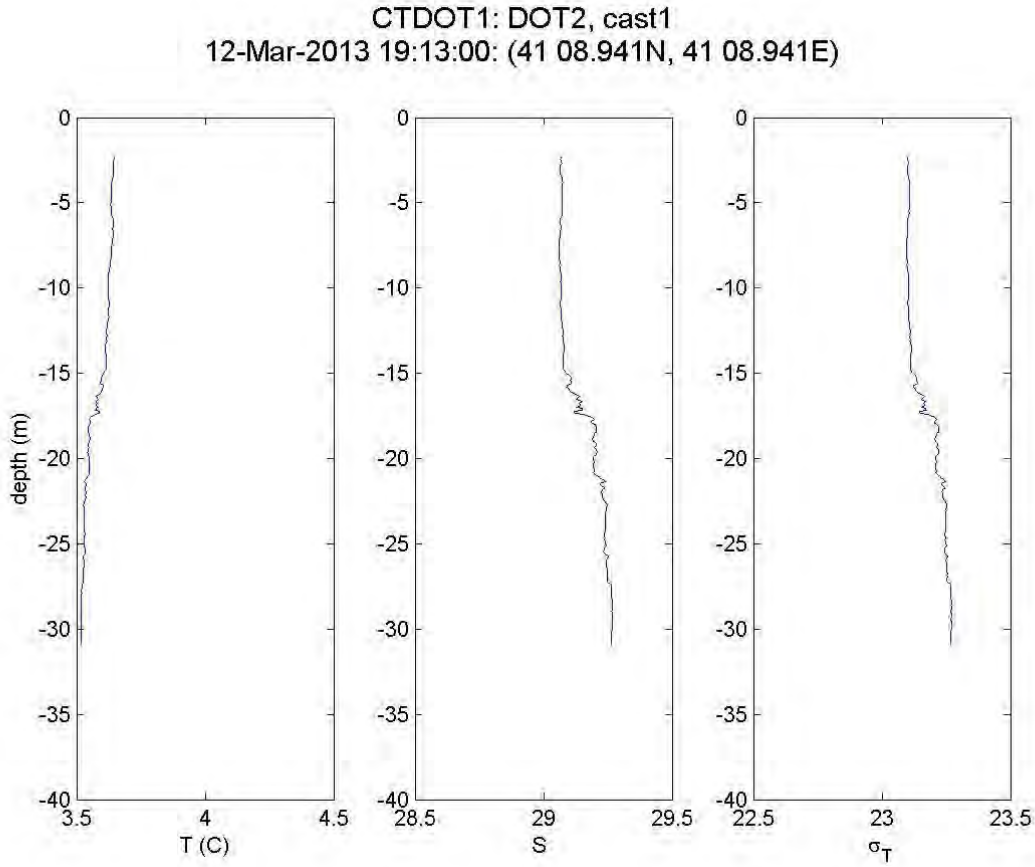

Figure 3: Cruise CTDOT1: Station DOT2, Cast 1: The left panel shows the vertical structure of Temperature (C) and the center and right panels show the salinity and density (σ_T) profiles respectively.

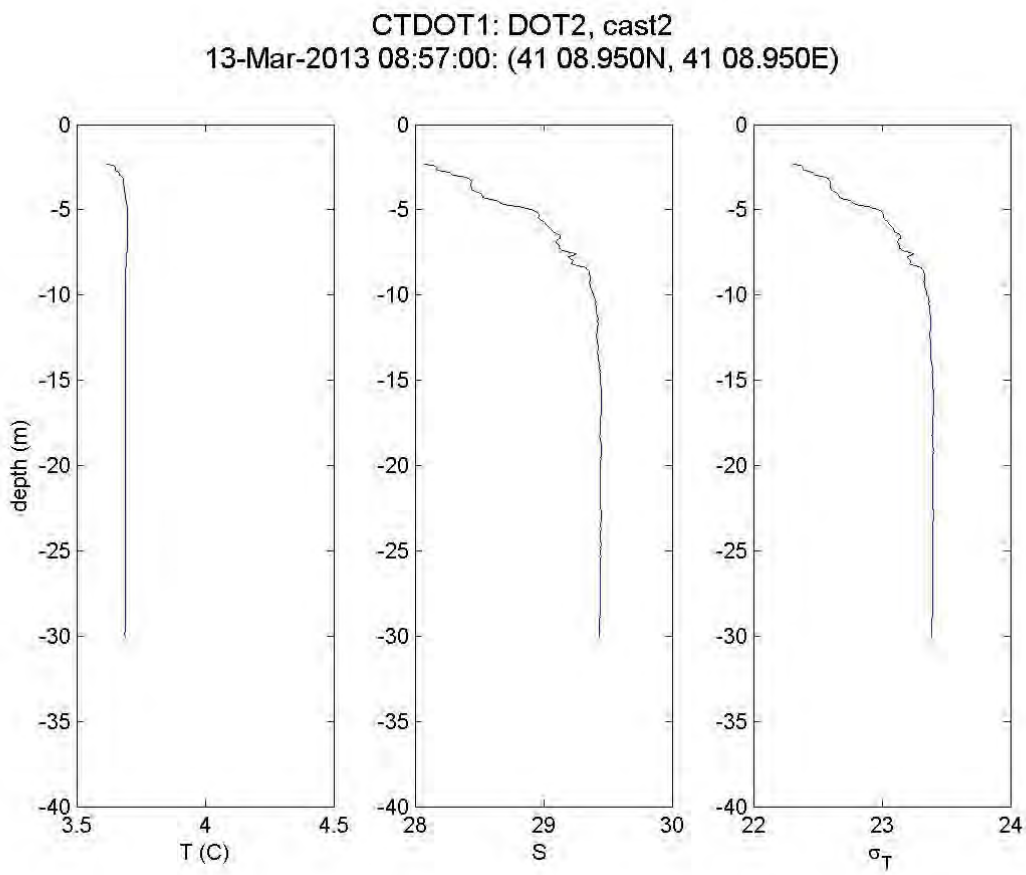

Figure 4: Cruise CTDOT1: Station DOT2, Cast 2: The left panel shows the vertical structure of Temperature (C) and the center and right panels show the salinity and density (σ_T) profiles respectively.

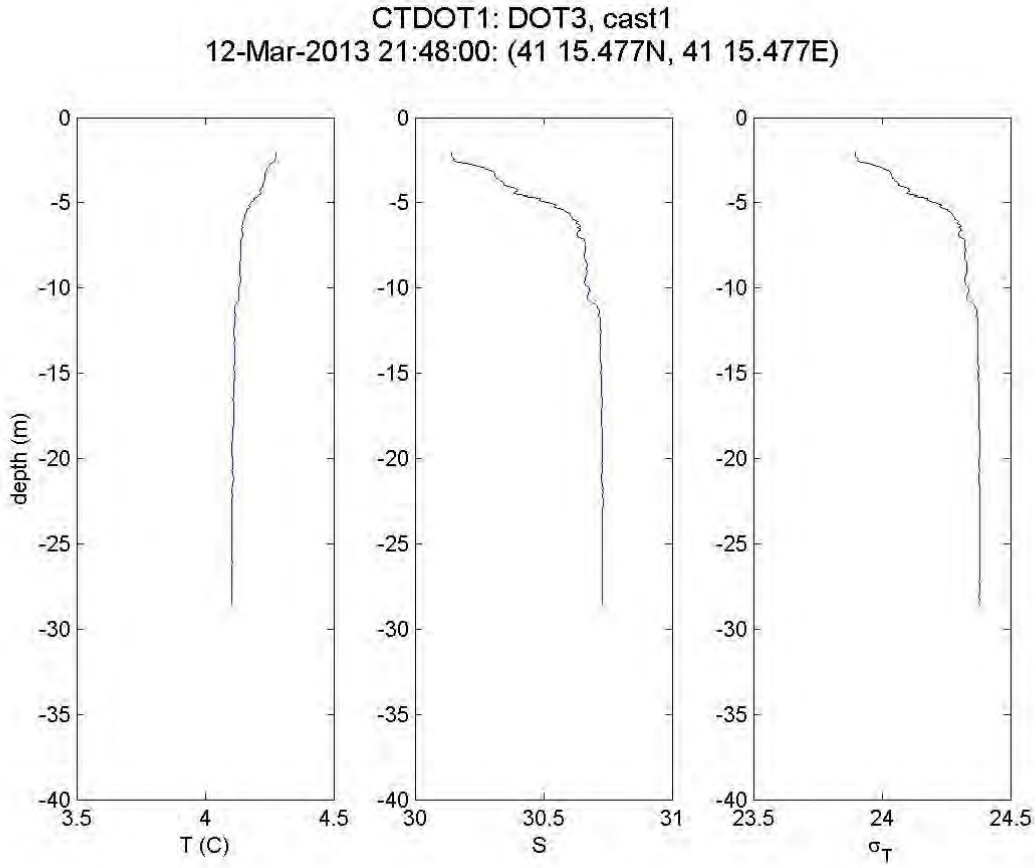

Figure 5: Cruise CTDOT1: Station DOT3, Cast 1: The left panel shows the vertical structure of Temperature (C) and the center and right panels show the salinity and density (σ_T) profiles respectively.

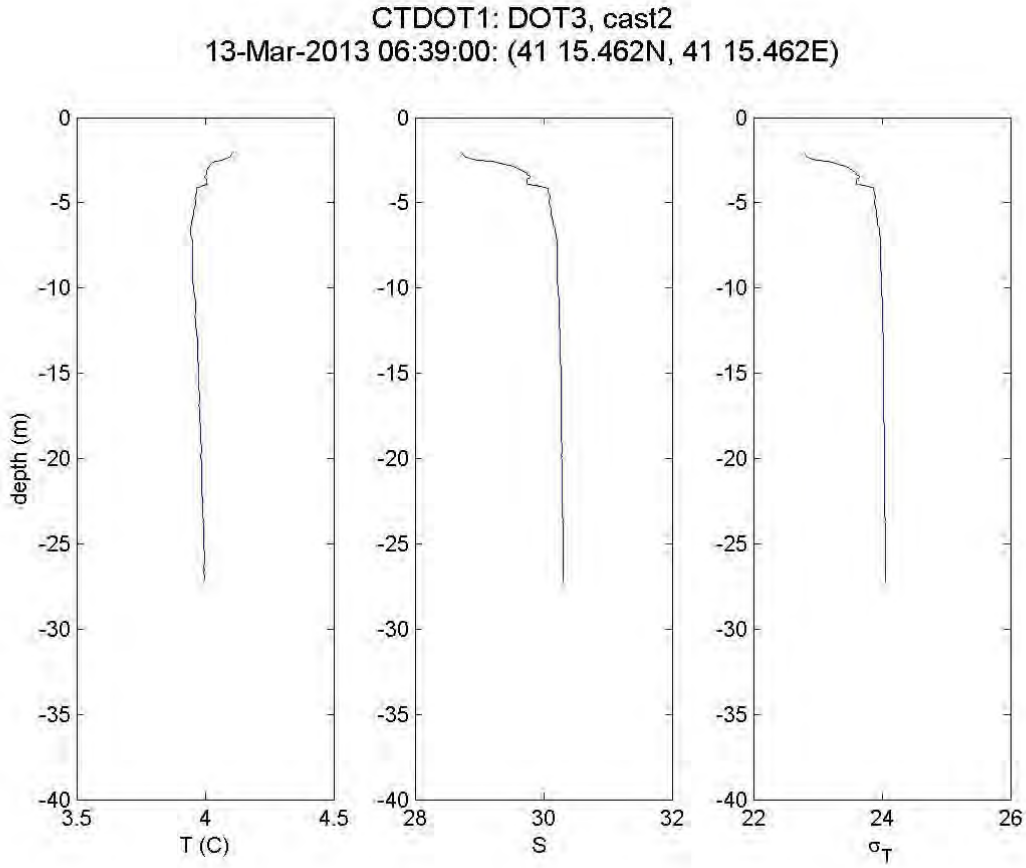

Figure 6: Cruise CTDOT1: Station DOT3, Cast 2: The left panel shows the vertical structure of Temperature (C) and the center and right panels show the salinity and density (σ_T) profiles respectively.

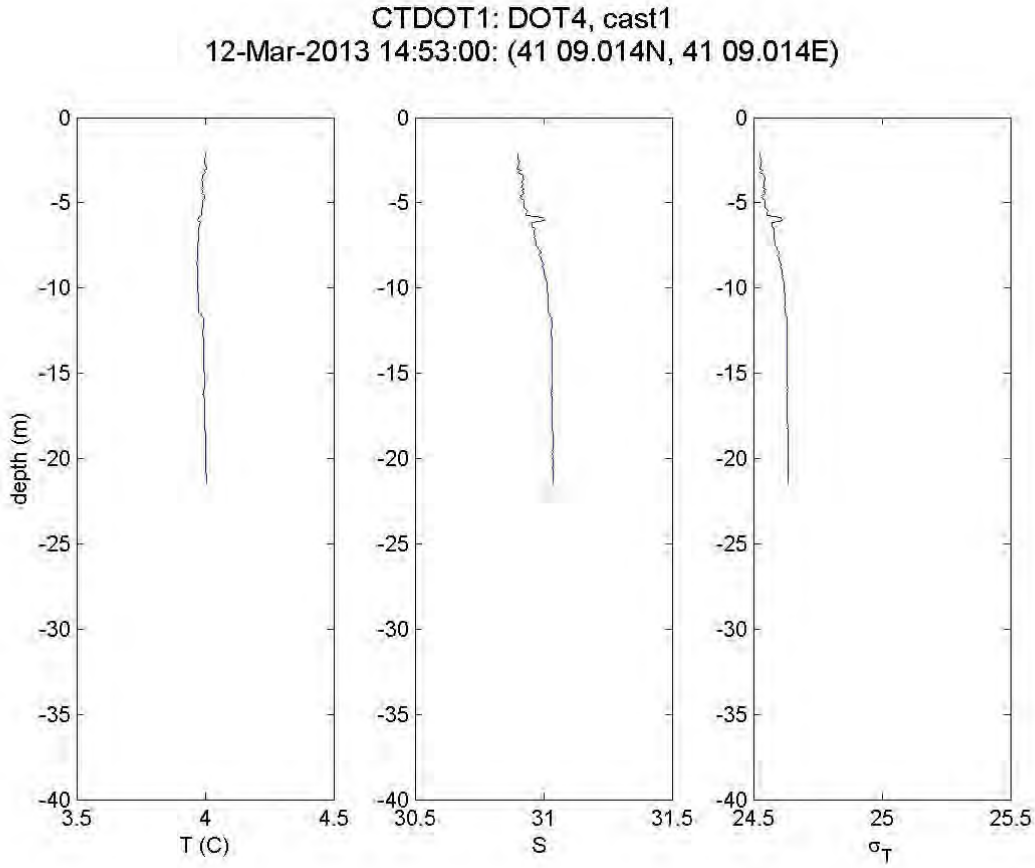

Figure 7: Cruise CTDOT1: Station DOT4, Cast 1: The left panel shows the vertical structure of Temperature (C) and the center and right panels show the salinity and density (σ_T) profiles respectively.

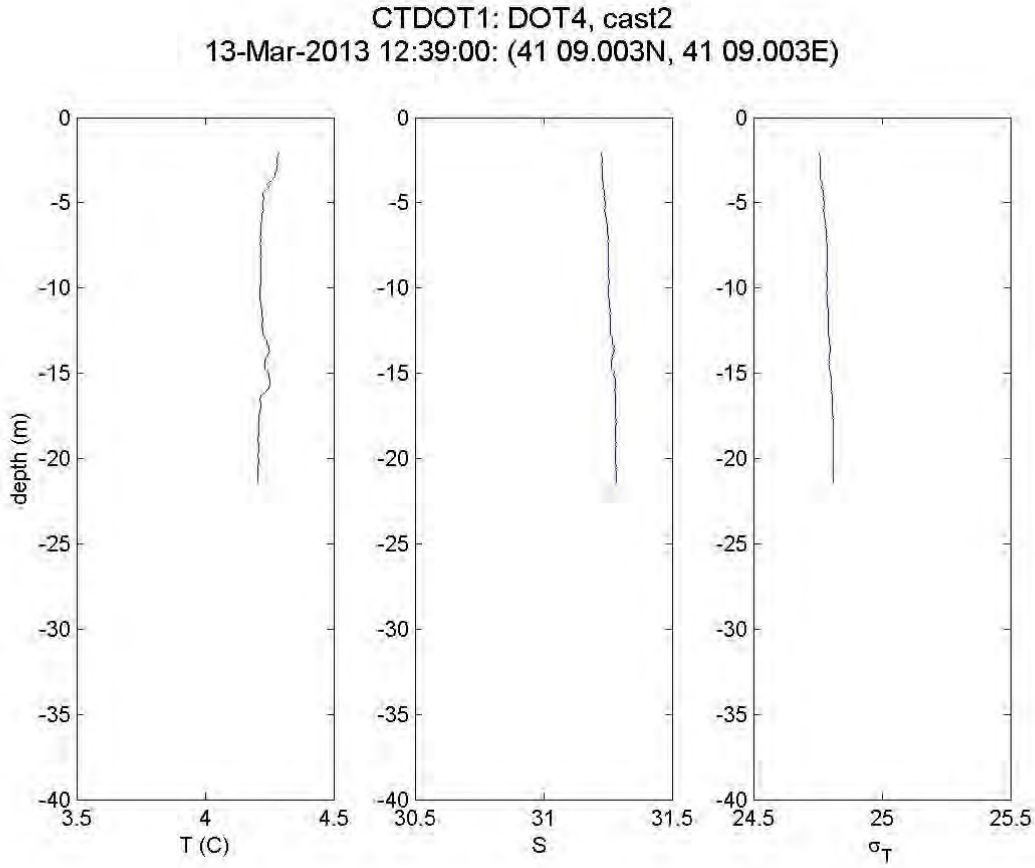

Figure 8: Cruise CTDOT1: Station DOT4, Cast 2: The left panel shows the vertical structure of Temperature (C) and the center and right panels show the salinity and density (σ_T) profiles respectively.

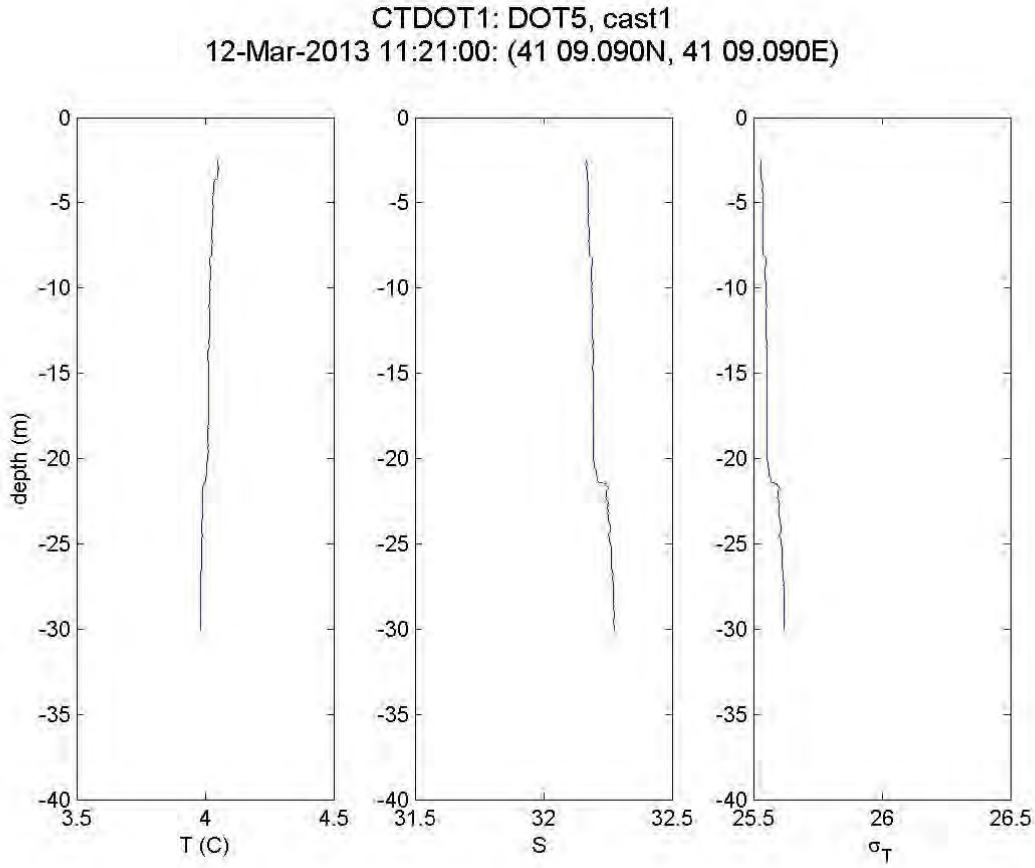

Figure 9: Cruise CTDOT1: Station DOT5, Cast 1: The left panel shows the vertical structure of Temperature (C) and the center and right panels show the salinity and density (σ_T) profiles respectively.

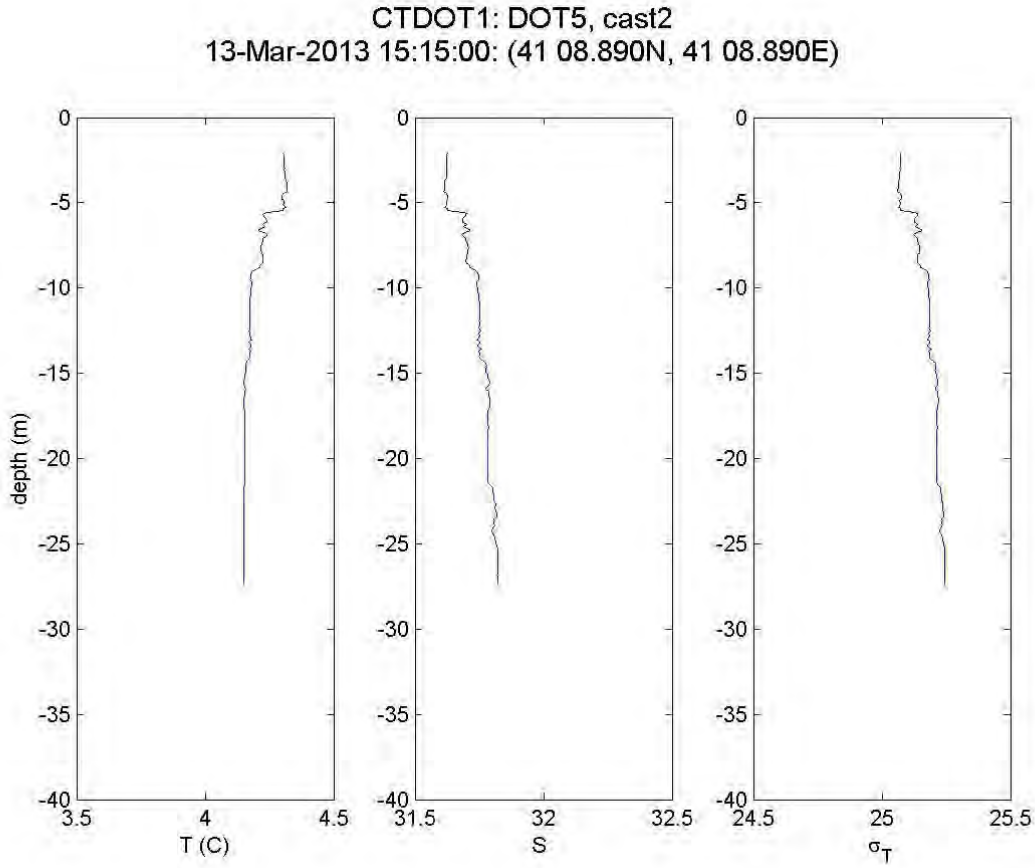

Figure 10: Cruise CTDOT1: Station DOT5, Cast 2: The left panel shows the vertical structure of Temperature (C) and the center and right panels show the salinity and density (σ_T) profiles respectively.

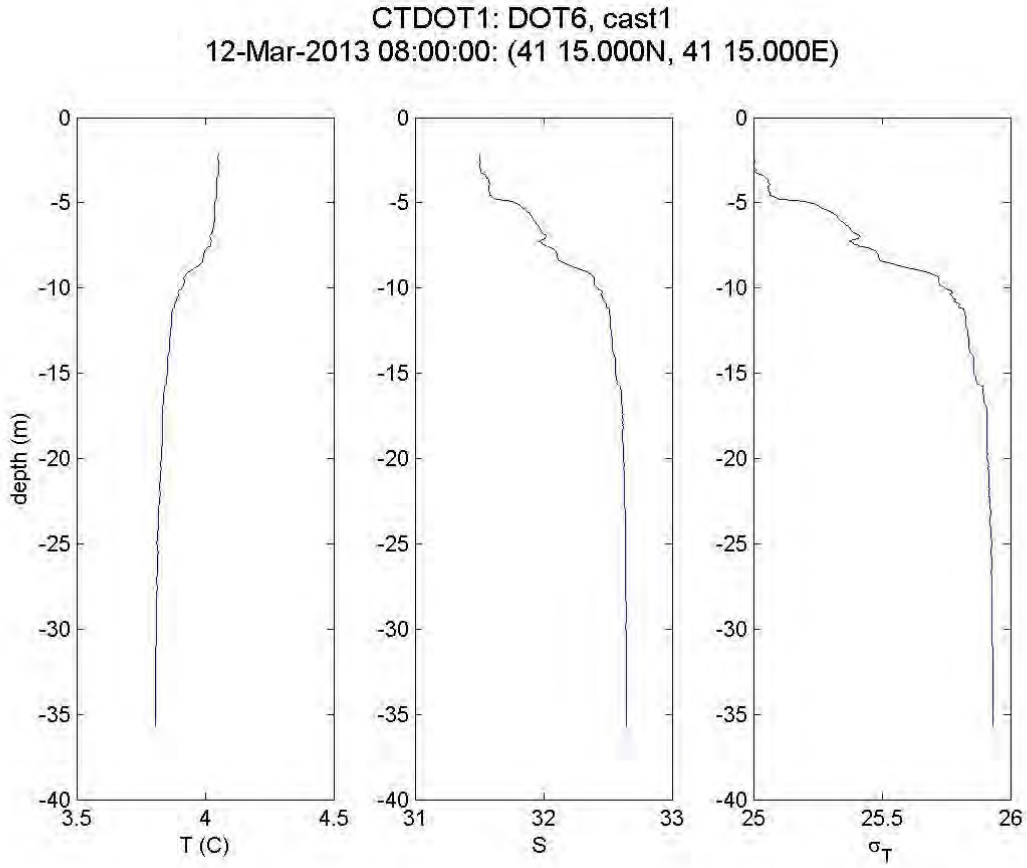

Figure 11: Cruise CTDOT1: Station DOT6, Cast 1: The left panel shows the vertical structure of Temperature (C) and the center and right panels show the salinity and density (σ_T) profiles respectively.

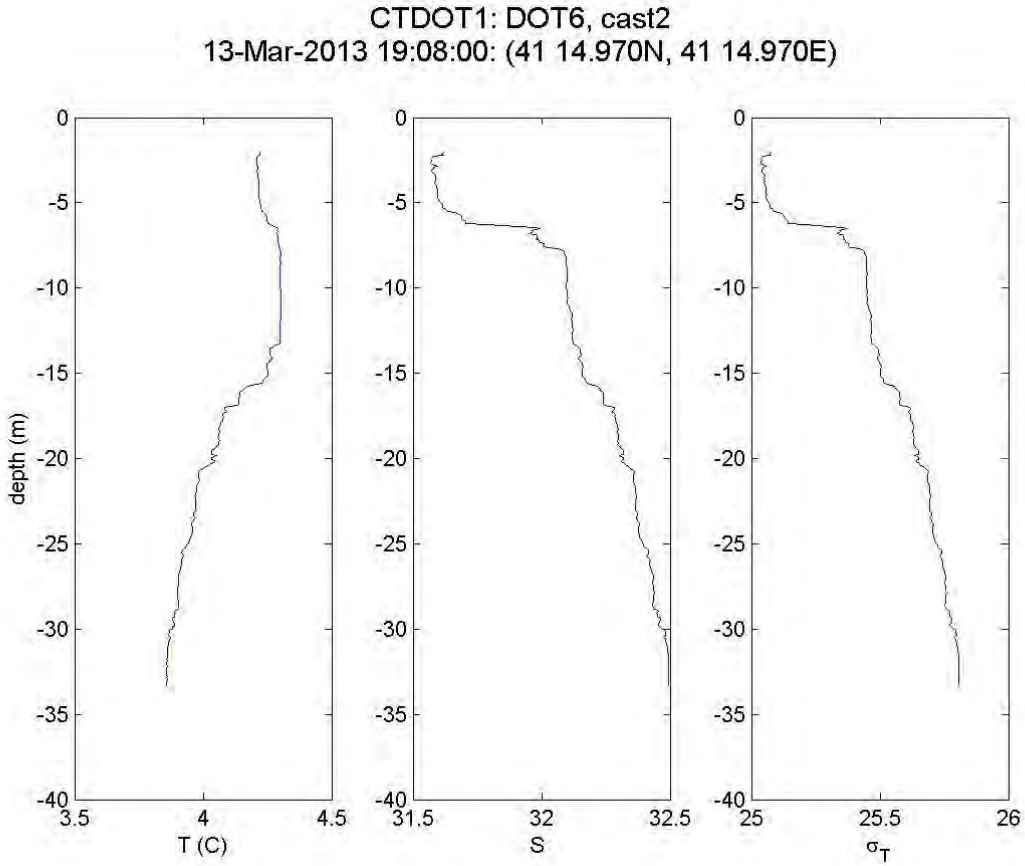

Figure 12: Cruise CTDOT1: Station DOT6, Cast 2: The left panel shows the vertical structure of Temperature (C) and the center and right panels show the salinity and density (σ_T) profiles respectively.

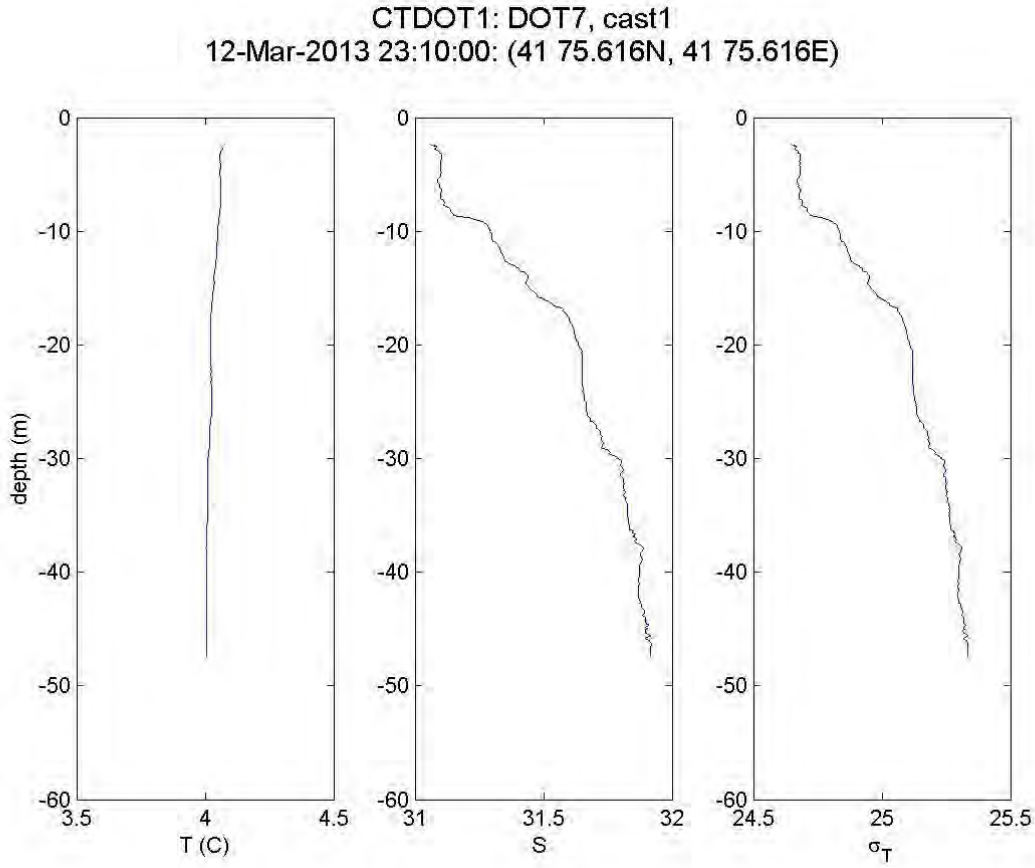

Figure 13: Cruise CTDOT1: Station DOT7, Cast 1: The left panel shows the vertical structure of Temperature (C) and the center and right panels show the salinity and density (σ_T) profiles respectively.

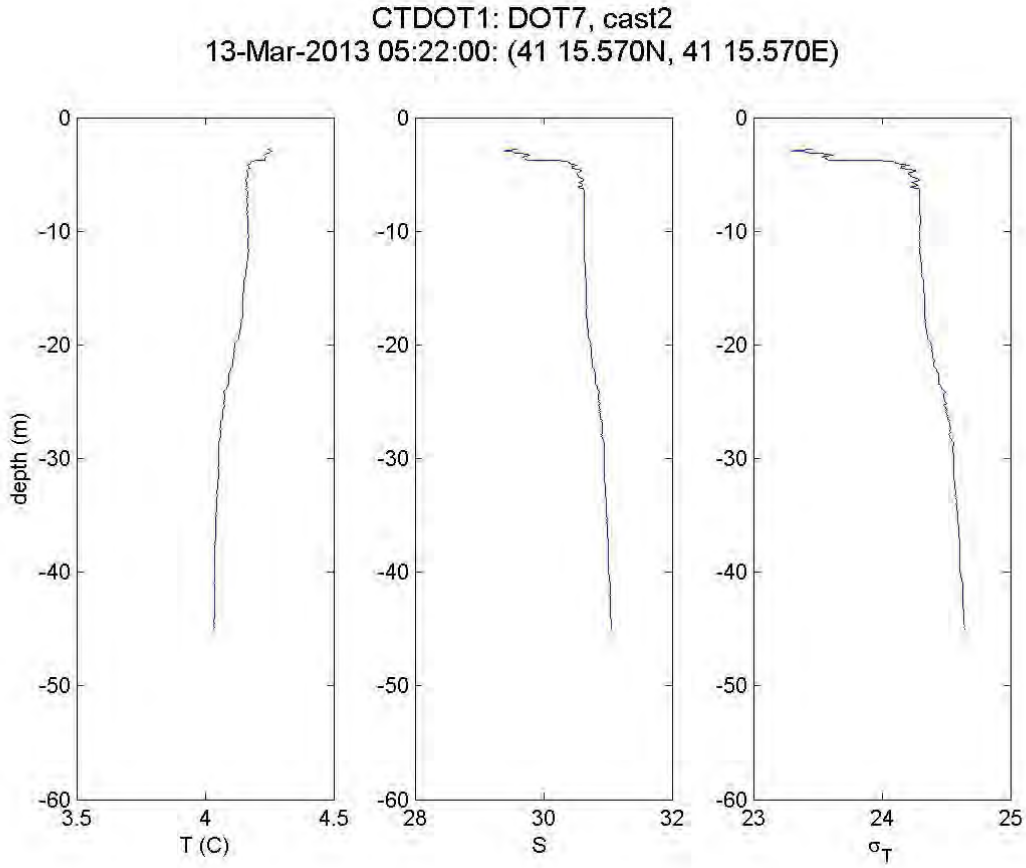

Figure 14: Cruise CTDOT1: Station DOT7, Cast 2: The left panel shows the vertical structure of Temperature (C) and the center and right panels show the salinity and density (σ_T) profiles respectively.

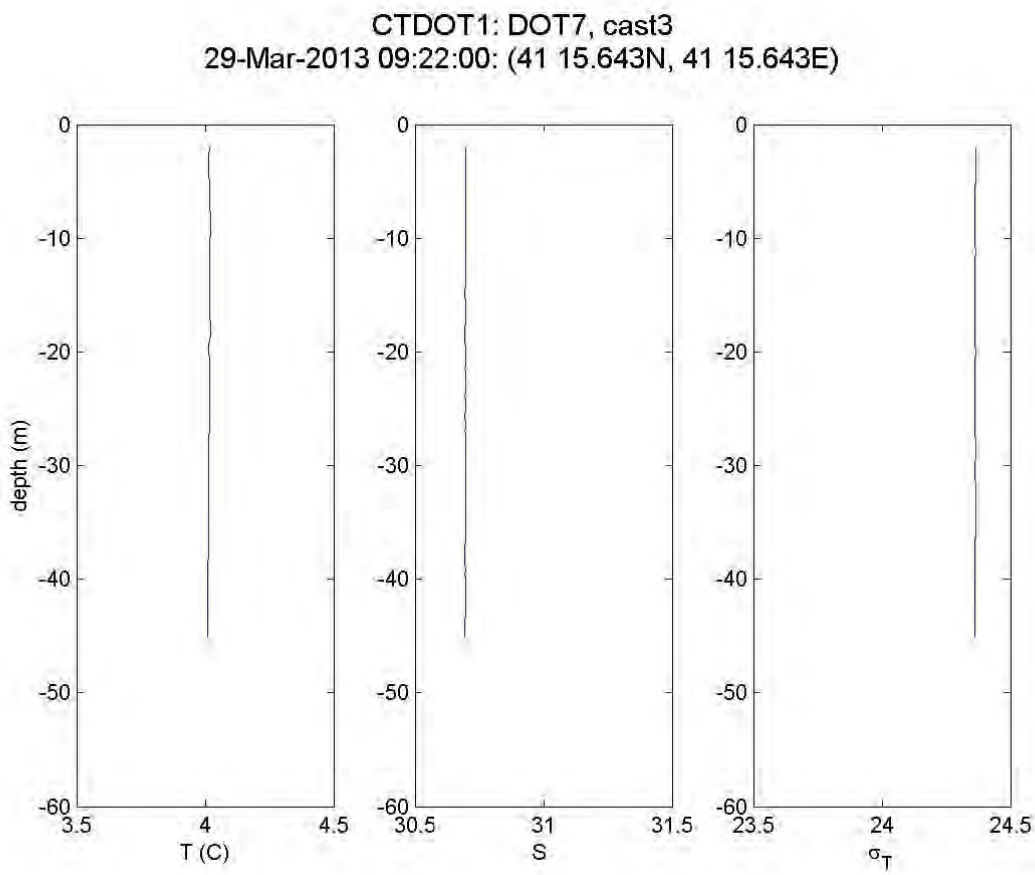

Figure 15: Cruise CTDOT1: Station DOT7, Cast 3: The left panel shows the vertical structure of Temperature (C) and the center and right panels show the salinity and density (σ_T) profiles respectively.

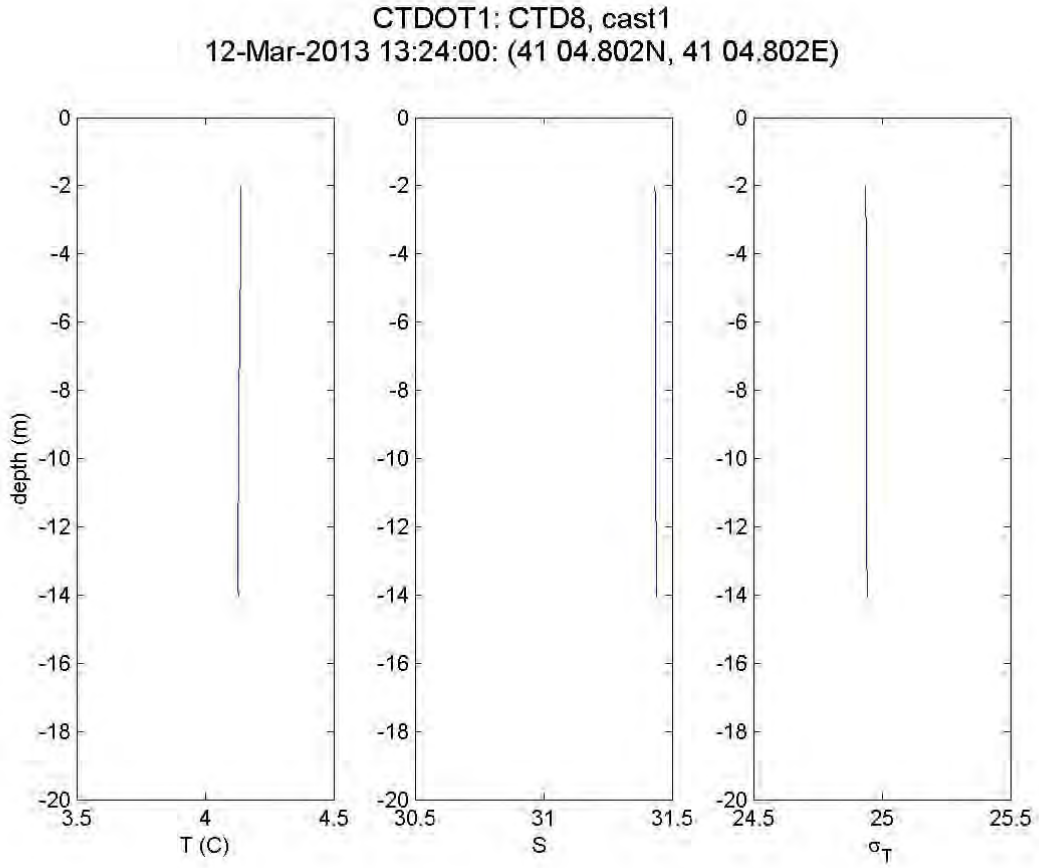

Figure 16: Cruise CTDOT1: Station CTD8, Cast 1: The left panel shows the vertical structure of Temperature (C) and the center and right panels show the salinity and density (σ_T) profiles respectively.

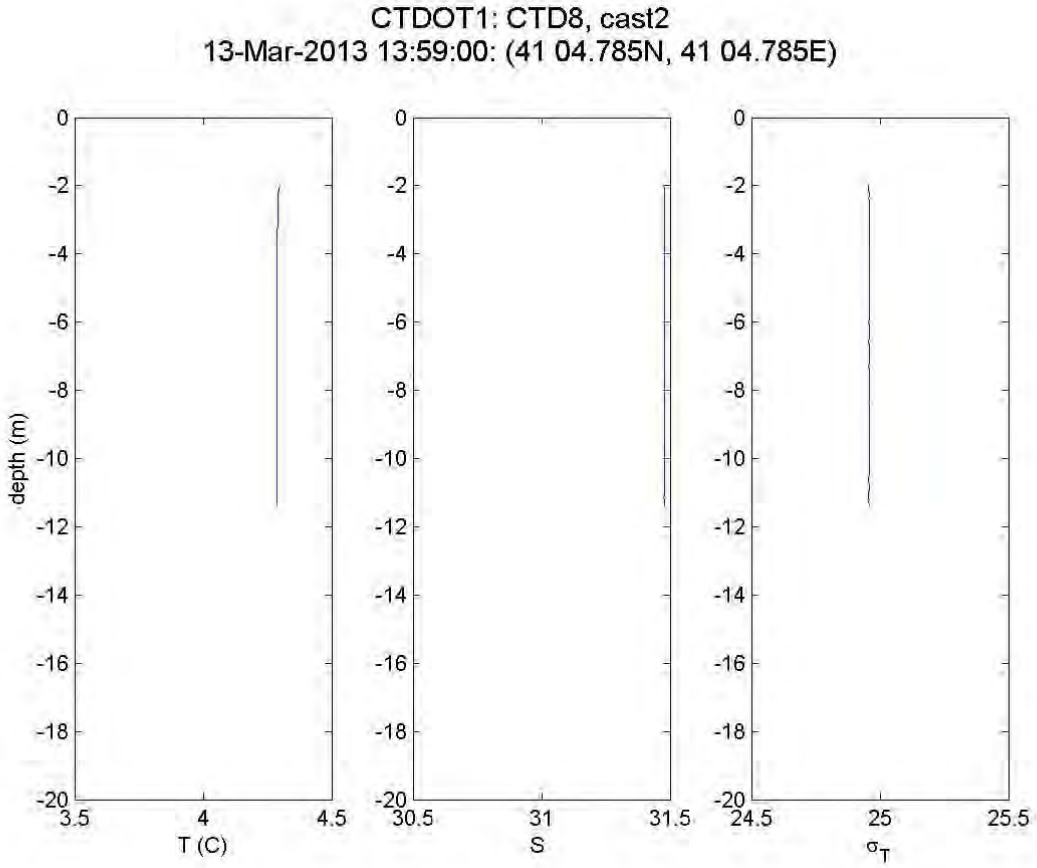

Figure 17: Cruise CTDOT1: Station CTD8, Cast 2: The left panel shows the vertical structure of Temperature (C) and the center and right panels show the salinity and density (σ_T) profiles respectively.

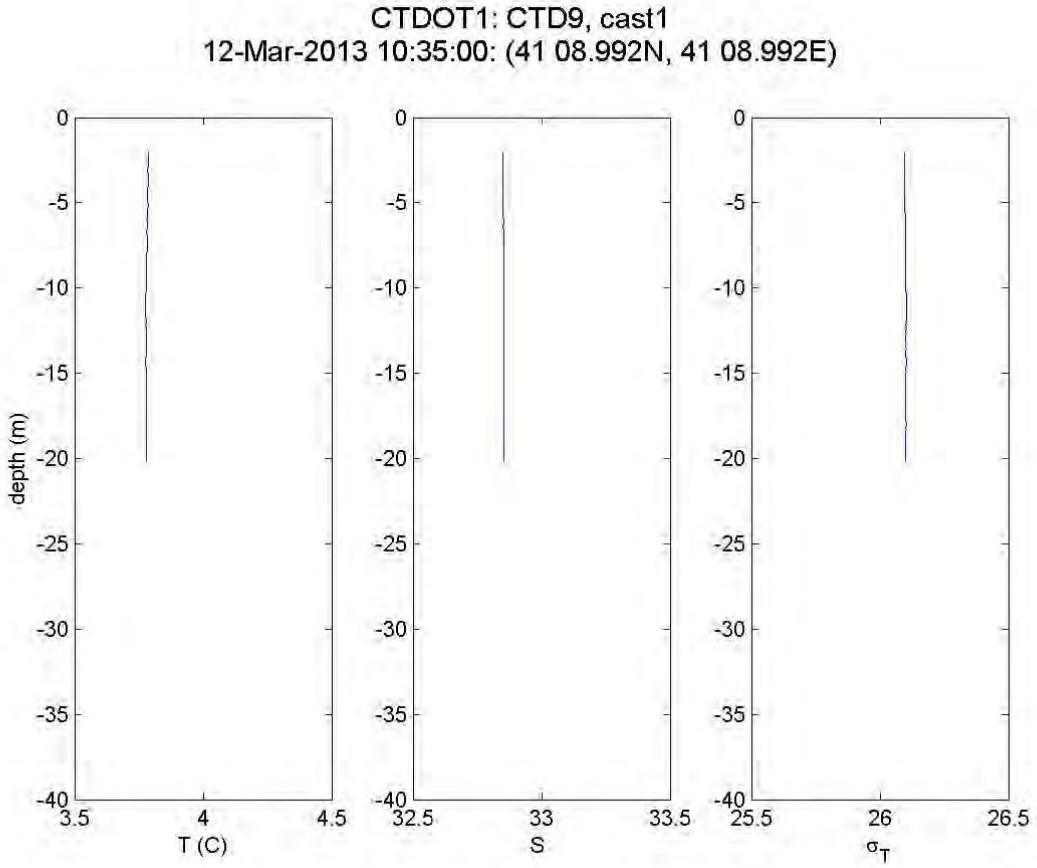

Figure 18: Cruise CTDOT1: Station CTD9, Cast 1: The left panel shows the vertical structure of Temperature (C) and the center and right panels show the salinity and density (σ_T) profiles respectively.

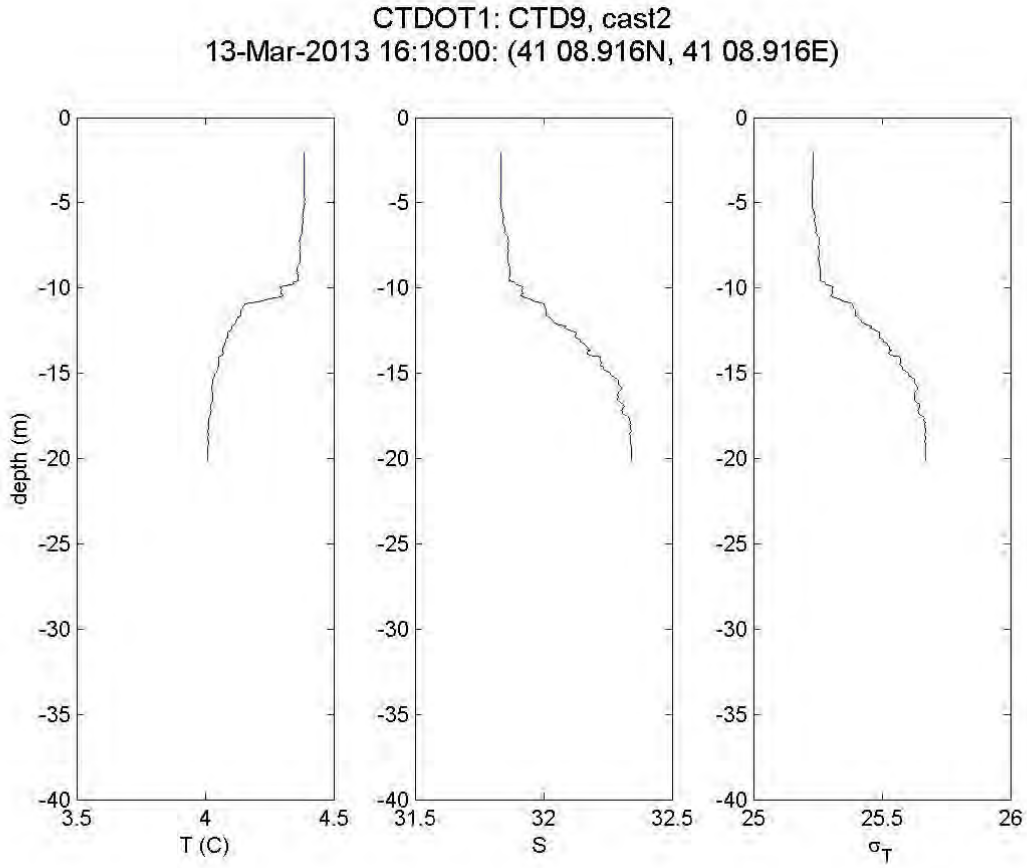

Figure 19: Cruise CTDOT1: Station CTD9, Cast 2: The left panel shows the vertical structure of Temperature (C) and the center and right panels show the salinity and density (σ_T) profiles respectively.

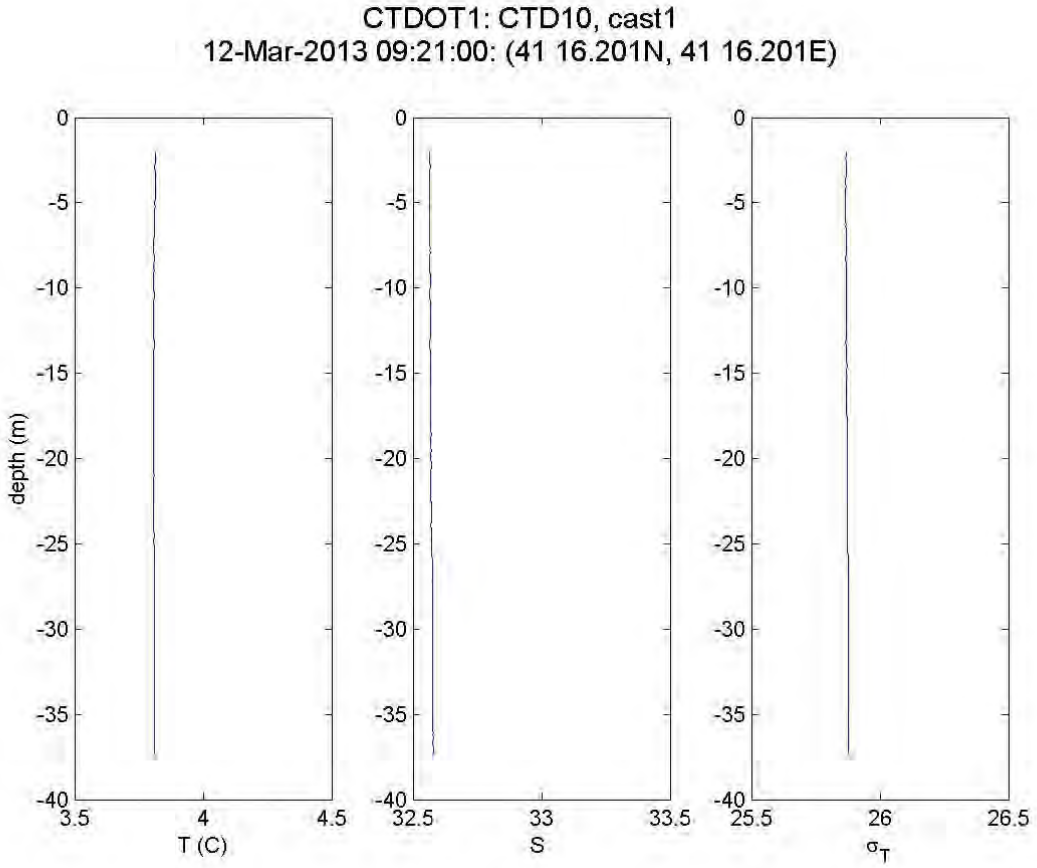

Figure 20: Cruise CTDOT1: Station CTD10, Cast 1: The left panel shows the vertical structure of Temperature (C) and the center and right panels show the salinity and density (σ_T) profiles respectively.

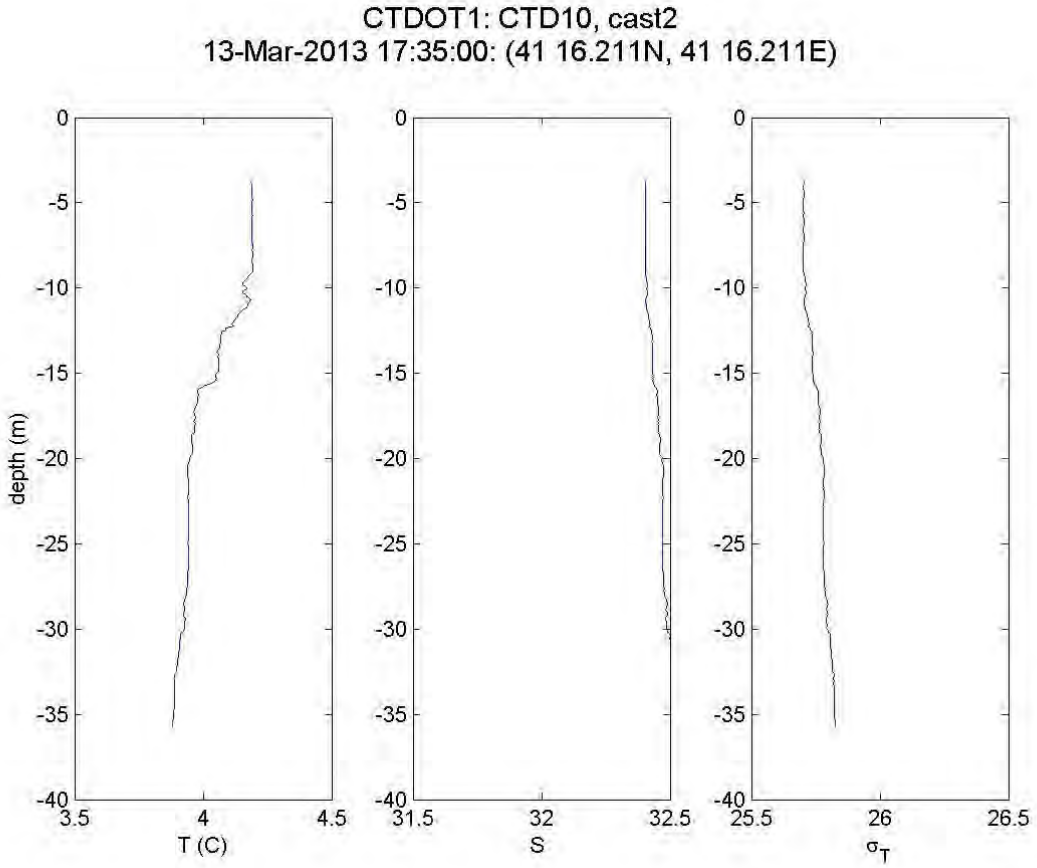

Figure 21: Cruise CTDOT1: Station CTD10, Cast 2: The left panel shows the vertical structure of Temperature (C) and the center and right panels show the salinity and density (σ_T) profiles respectively.

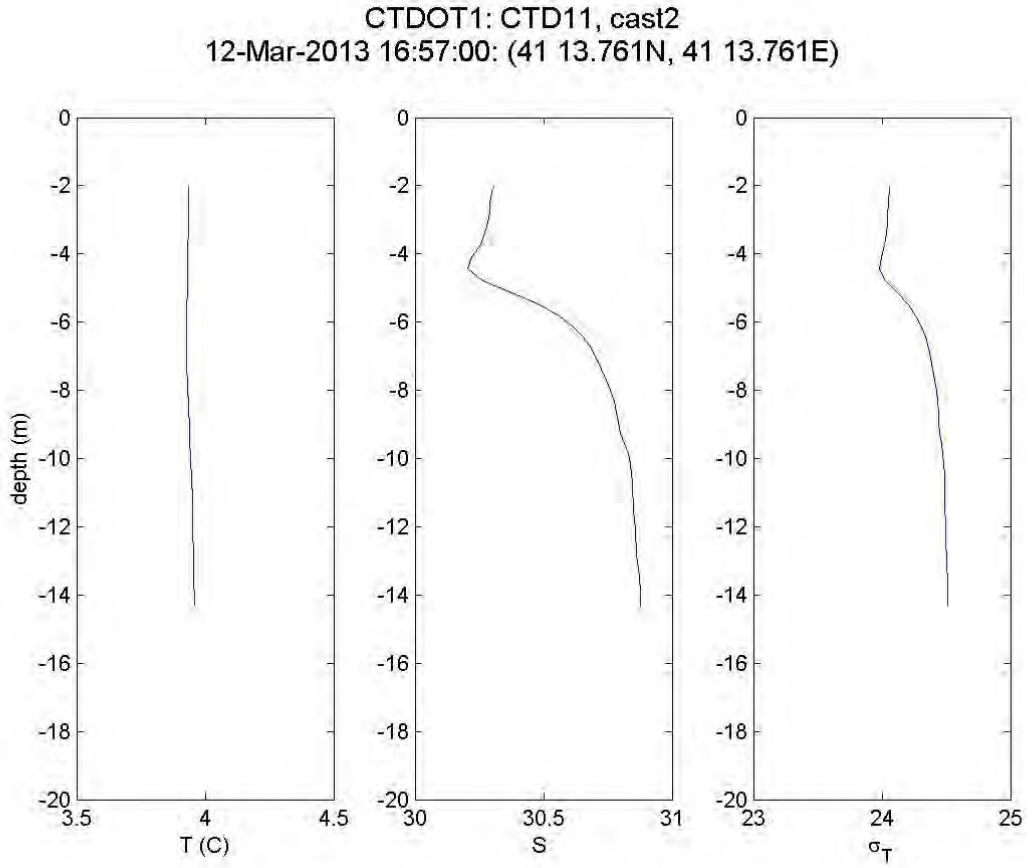

Figure 22: Cruise CTDOT1: Station CTD11, Cast 2: The left panel shows the vertical structure of Temperature (C) and the center and right panels show the salinity and density (σ_T) profiles respectively.

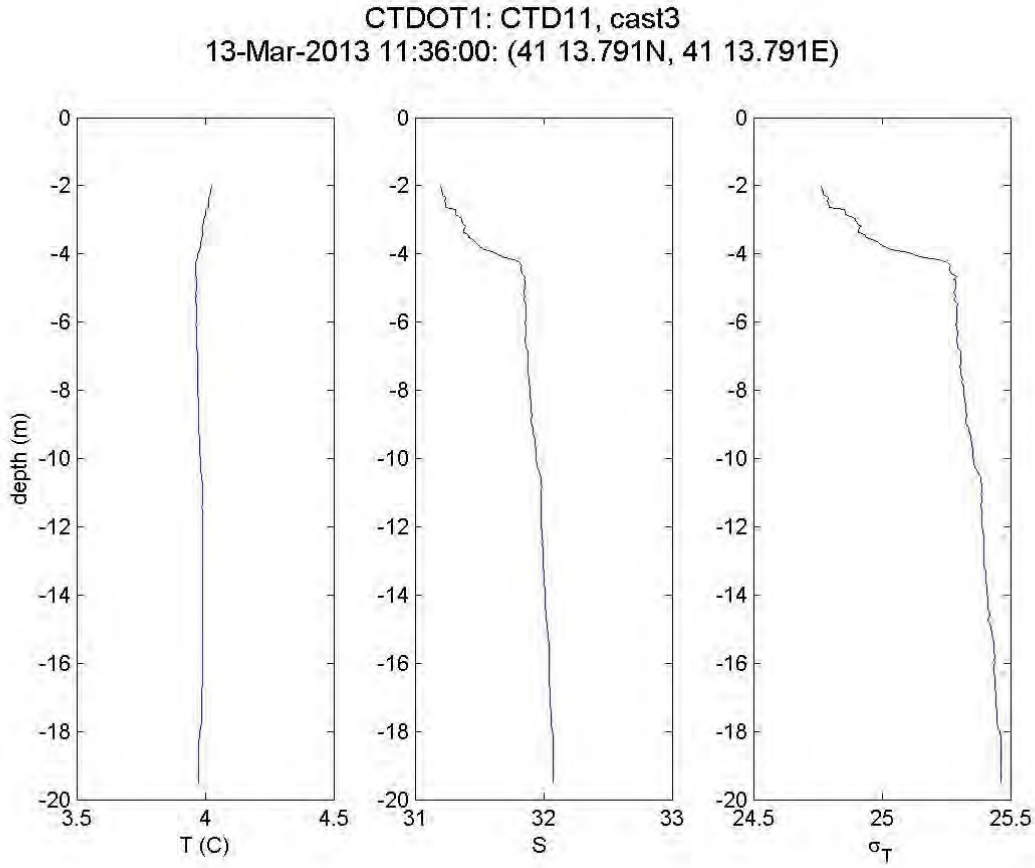

Figure 23: Cruise CTDOT1: Station CTD11, Cast 3: The left panel shows the vertical structure of Temperature (C) and the center and right panels show the salinity and density (σ_T) profiles respectively.

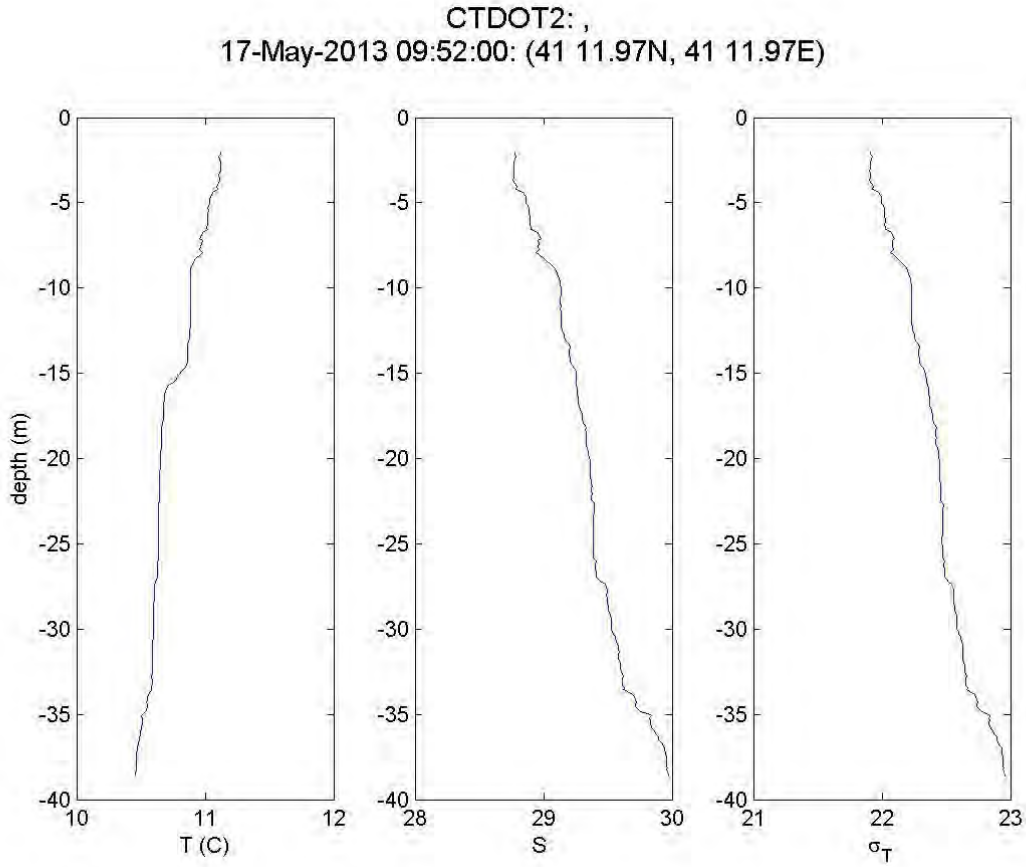

Figure 24: Cruise CTDOT2: Station DOT1, Cast 0: The left panel shows the vertical structure of Temperature (C) and the center and right panels show the salinity and density (σ_T) profiles respectively.

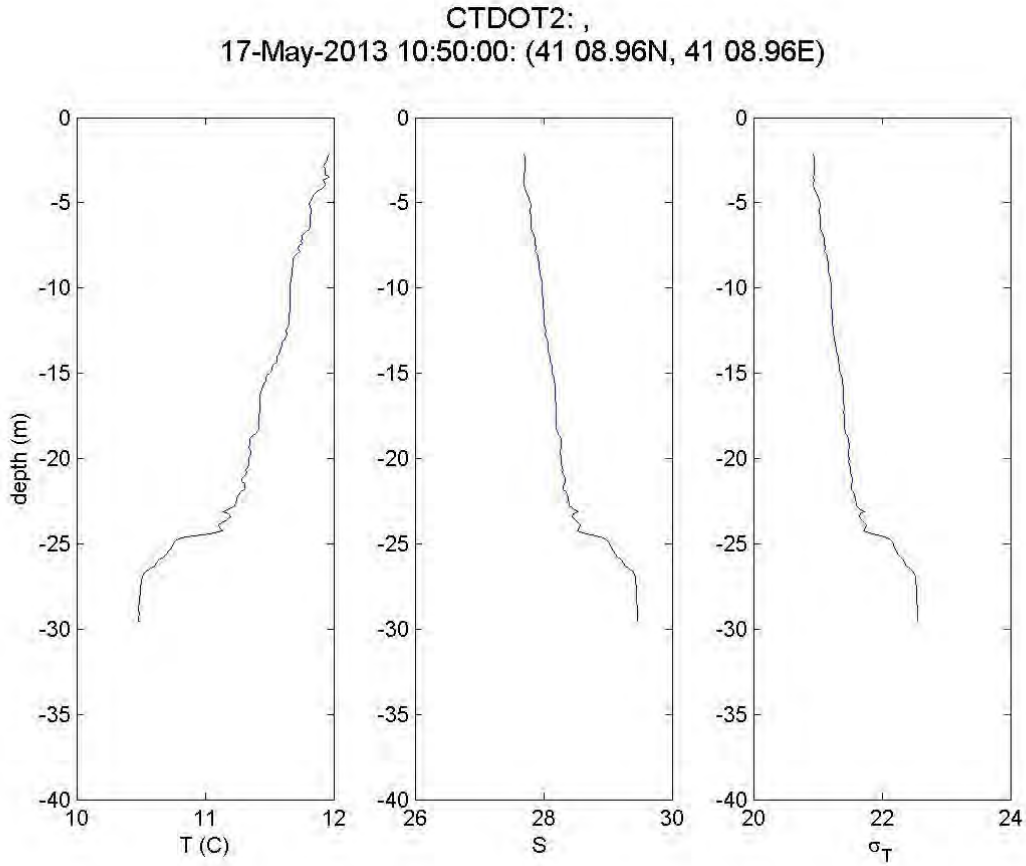

Figure 25: Cruise CTDOT2: Station DOT2, Cast 0: The left panel shows the vertical structure of Temperature (C) and the center and right panels show the salinity and density (σ_T) profiles respectively.

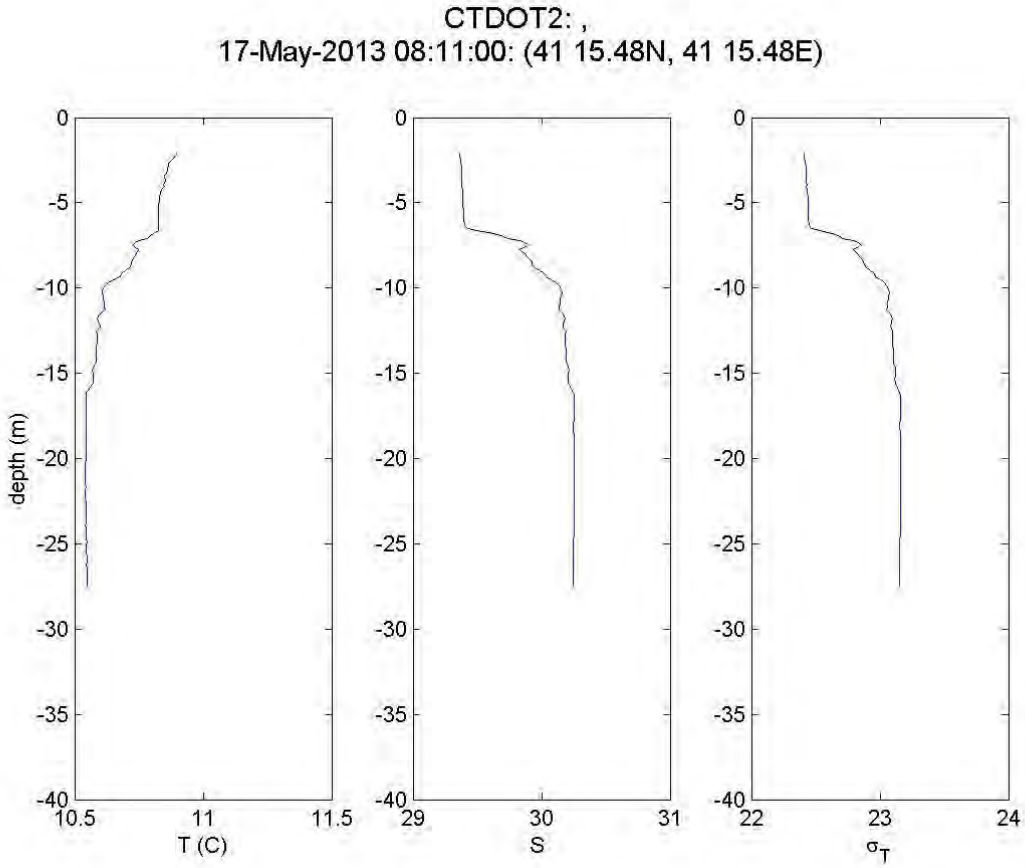

Figure 26: Cruise CTDOT2: Station DOT3, Cast 0: The left panel shows the vertical structure of Temperature (C) and the center and right panels show the salinity and density (σ_T) profiles respectively.

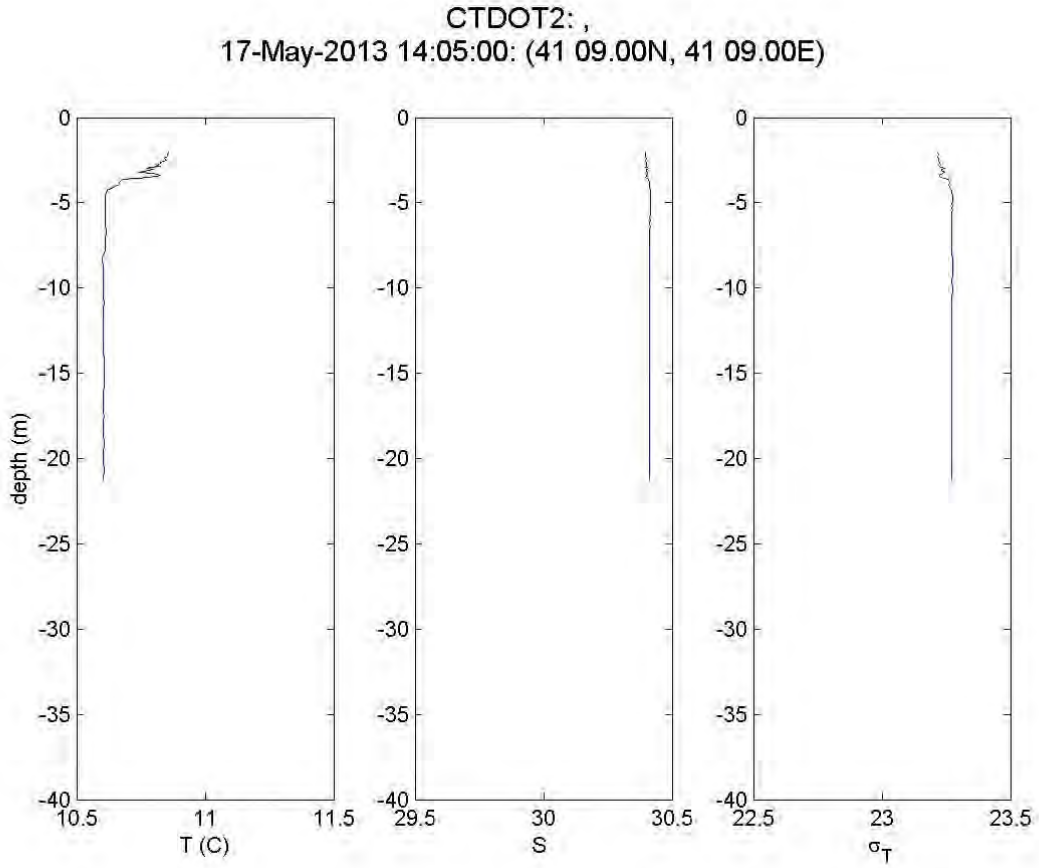

Figure 27: Cruise CTDOT2: Station DOT4, Cast 0: The left panel shows the vertical structure of Temperature (C) and the center and right panels show the salinity and density (σ_T) profiles respectively.

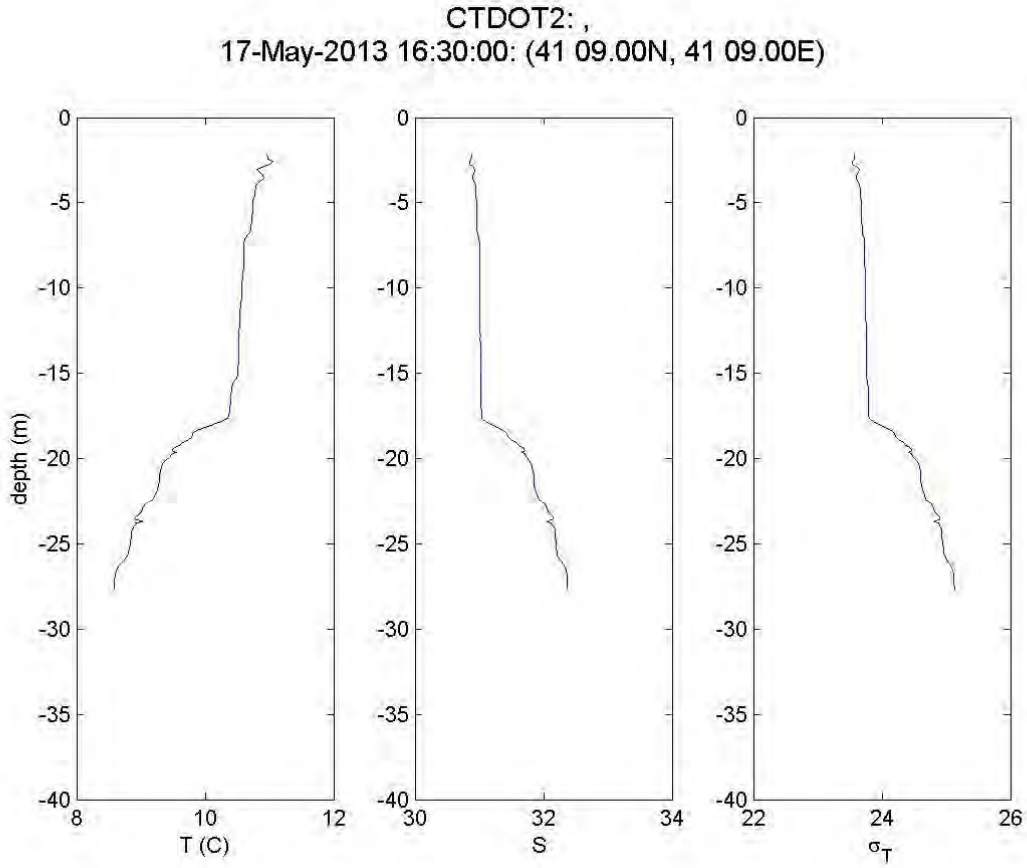

Figure 28: Cruise CTDOT2: Station DOT5, Cast 0: The left panel shows the vertical structure of Temperature (C) and the center and right panels show the salinity and density (σ_T) profiles respectively.

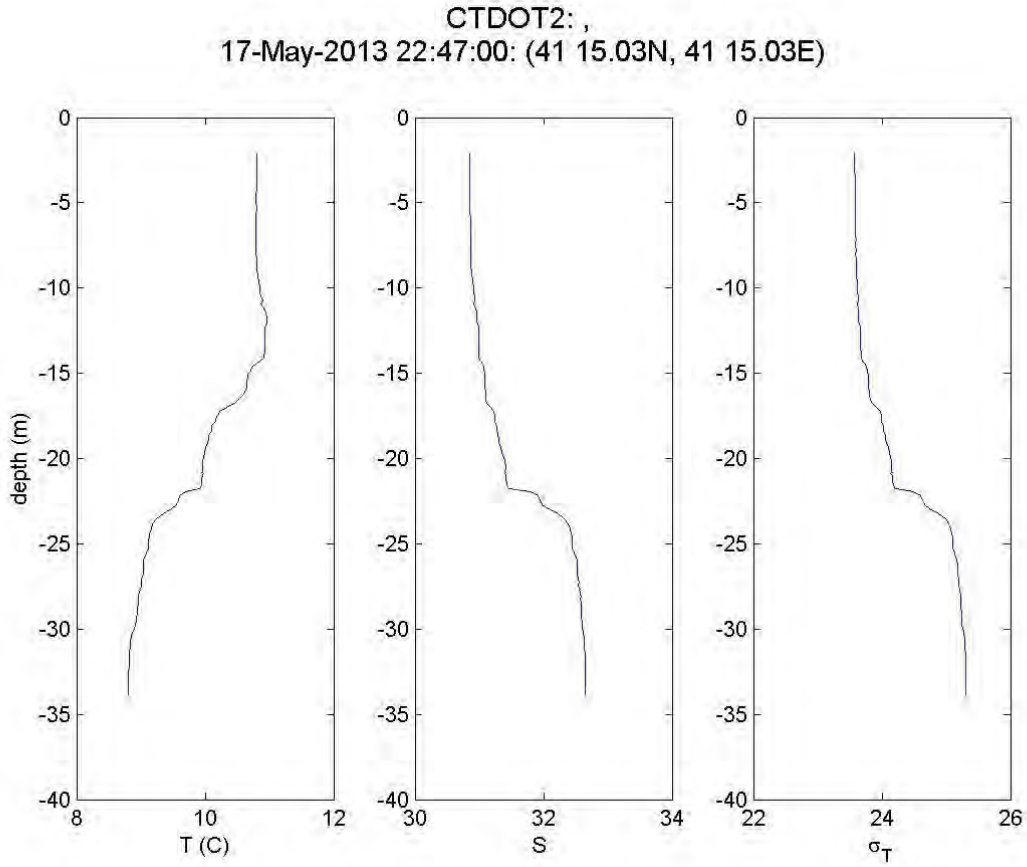

Figure 29: Cruise CTDOT2: Station DOT6, Cast 0: The left panel shows the vertical structure of Temperature (C) and the center and right panels show the salinity and density (σ_T) profiles respectively.

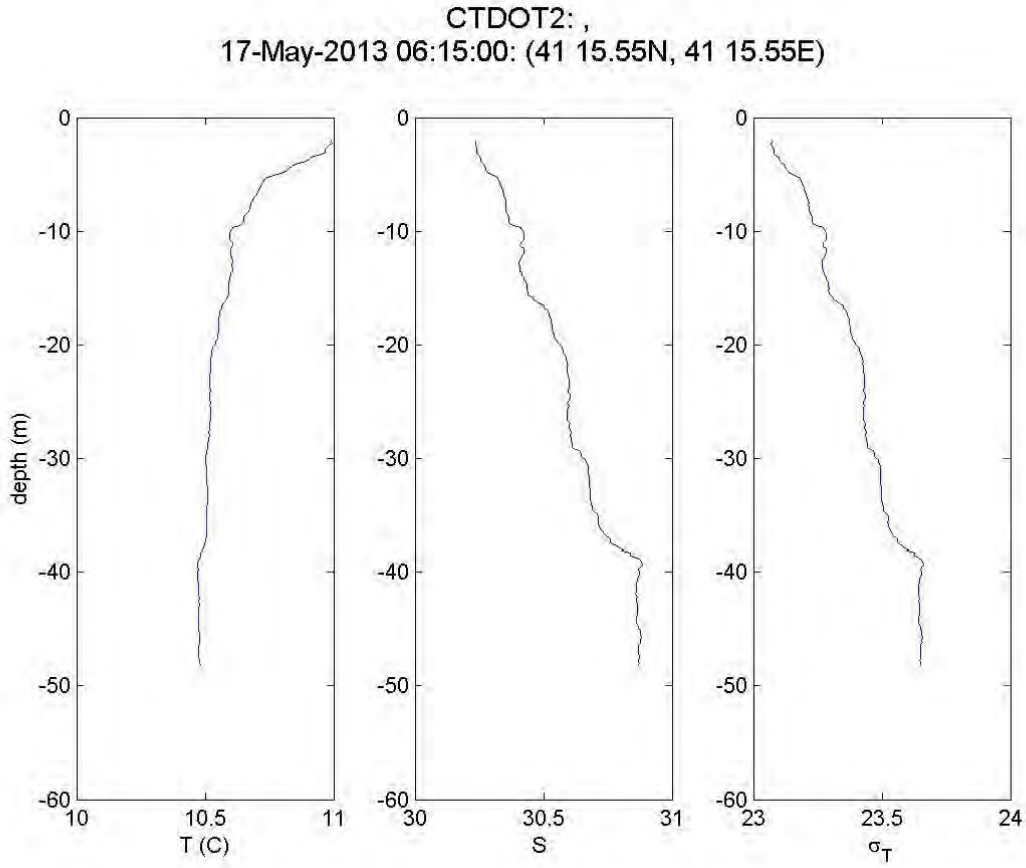

Figure 30: Cruise CTDOT2: Station DOT7, Cast 0: The left panel shows the vertical structure of Temperature (C) and the center and right panels show the salinity and density (σ_T) profiles respectively.

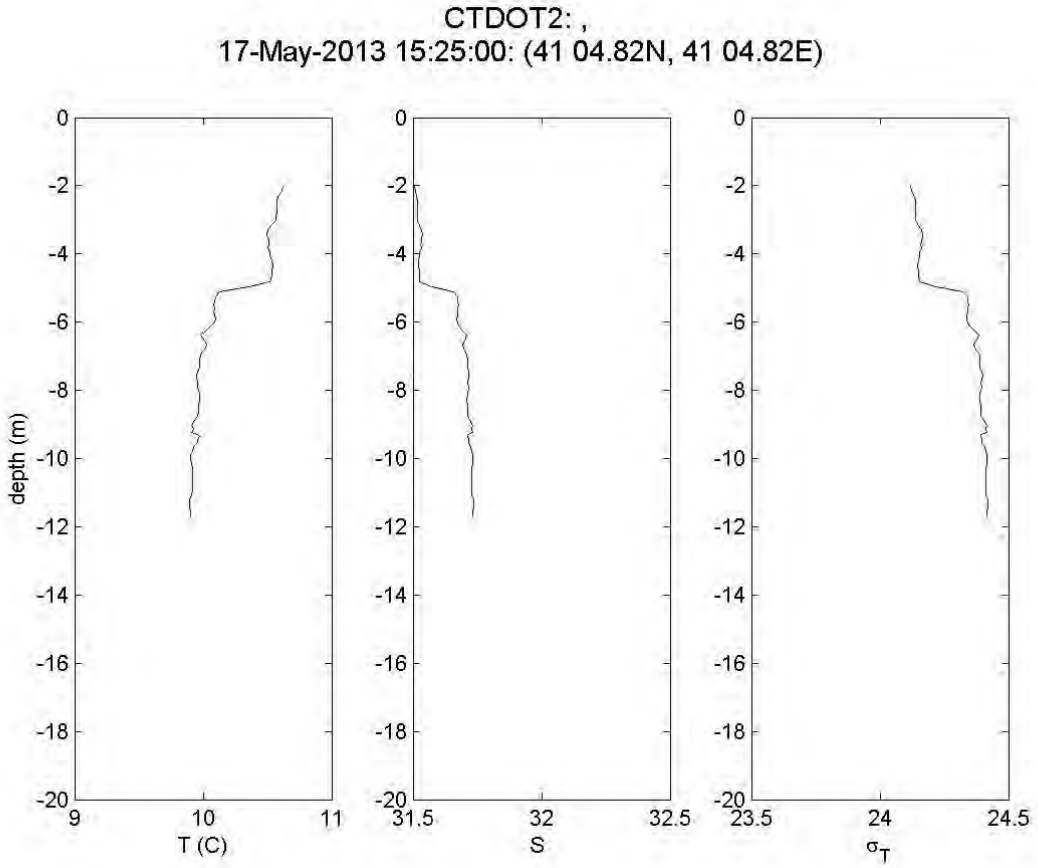

Figure 31: Cruise CTDOT2: Station CTD8, Cast 0: The left panel shows the vertical structure of Temperature (C) and the center and right panels show the salinity and density (σ_T) profiles respectively.

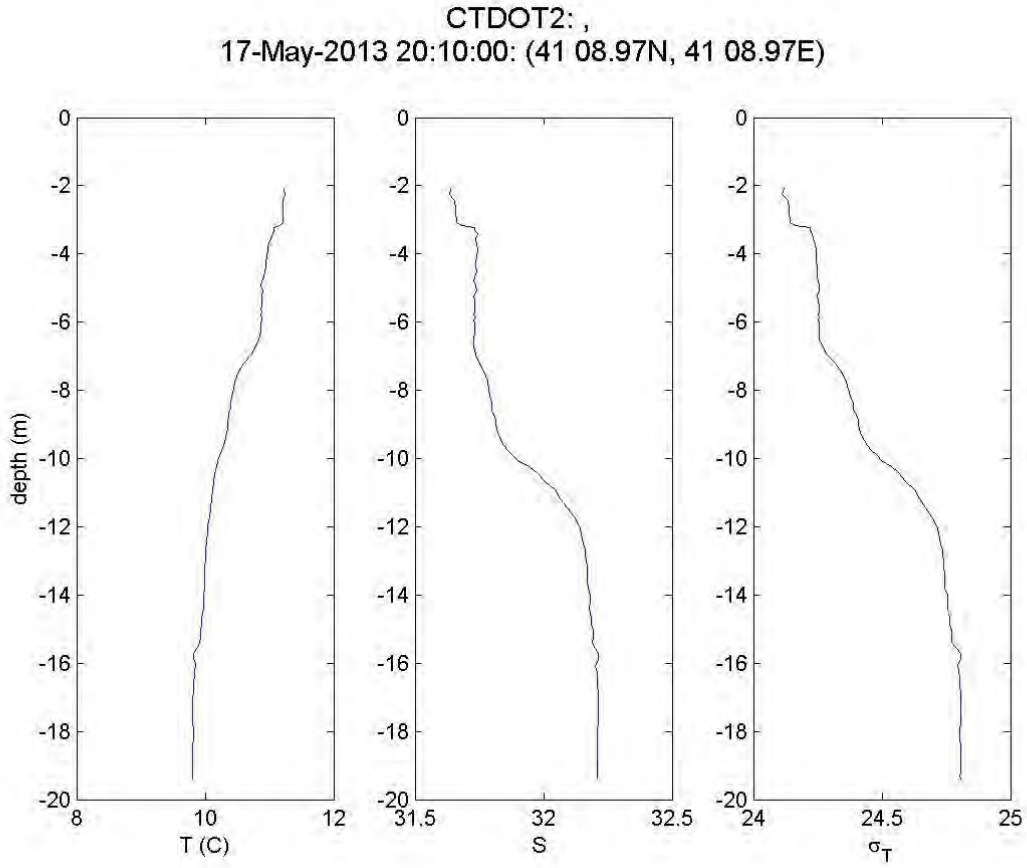

Figure 32: Cruise CTDOT2: Station CTD9, Cast 0: The left panel shows the vertical structure of Temperature (C) and the center and right panels show the salinity and density (σ_T) profiles respectively.

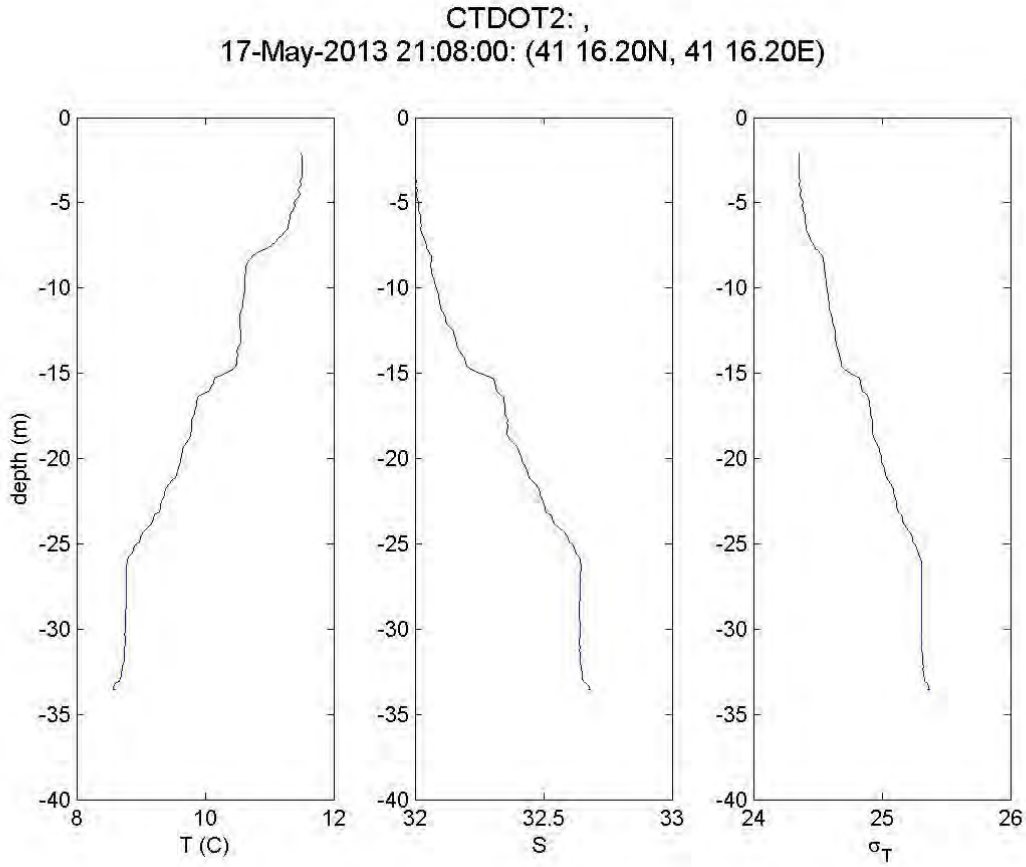

Figure 33: Cruise CTDOT2: Station CTD10, Cast 0: The left panel shows the vertical structure of Temperature (C) and the center and right panels show the salinity and density (σ_T) profiles respectively.

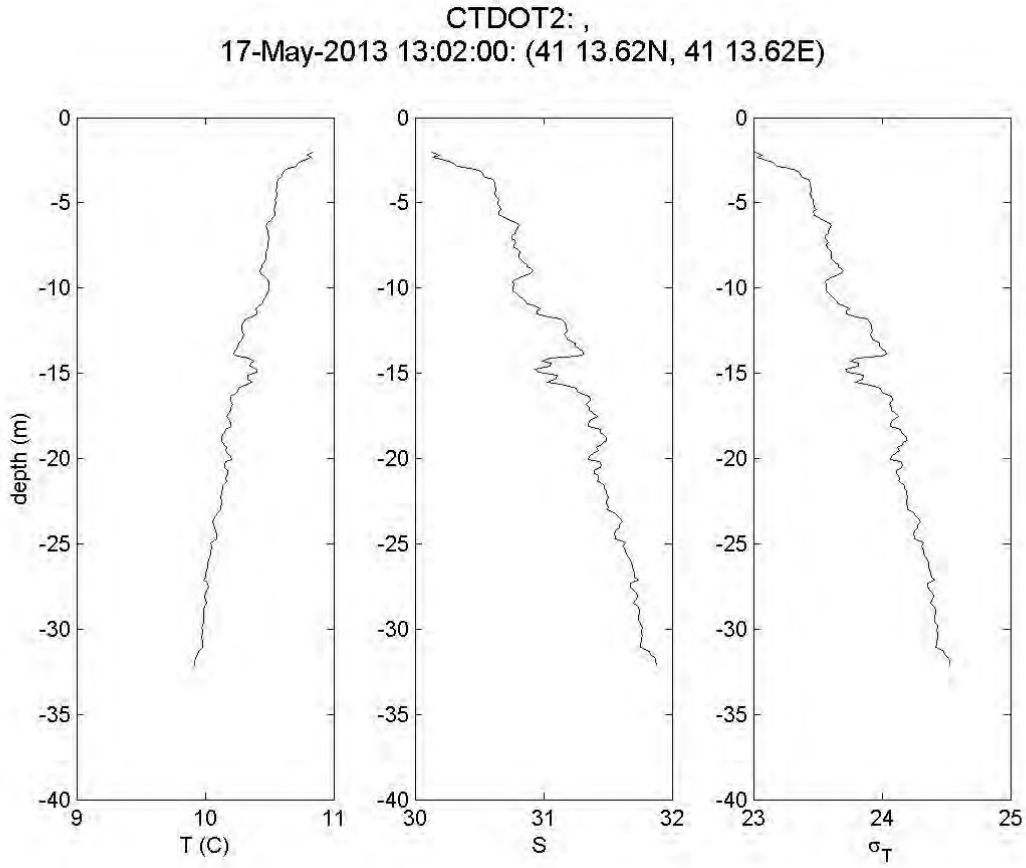

Figure 34: Cruise CTDOT2: Station CTD11, Cast 0: The left panel shows the vertical structure of Temperature (C) and the center and right panels show the salinity and density (σ_T) profiles respectively.

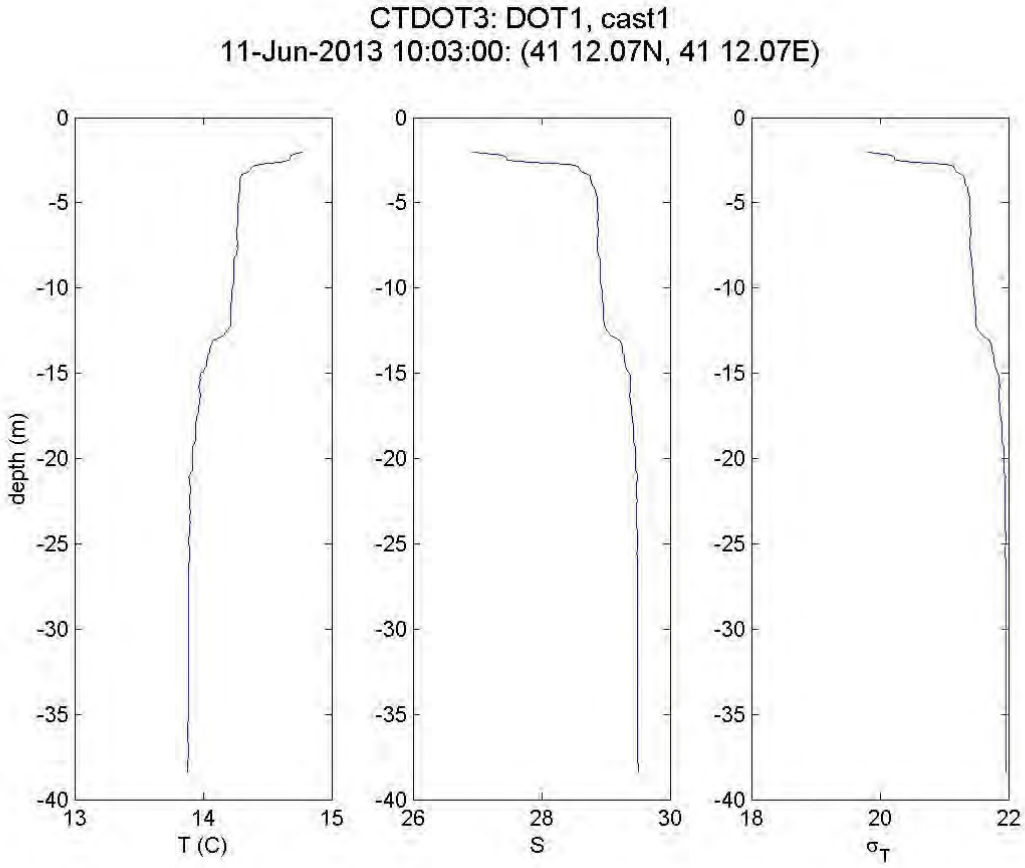

Figure 35: Cruise CTDOT3: Station DOT1, Cast 1: The left panel shows the vertical structure of Temperature (C) and the center and right panels show the salinity and density (σ_T) profiles respectively.

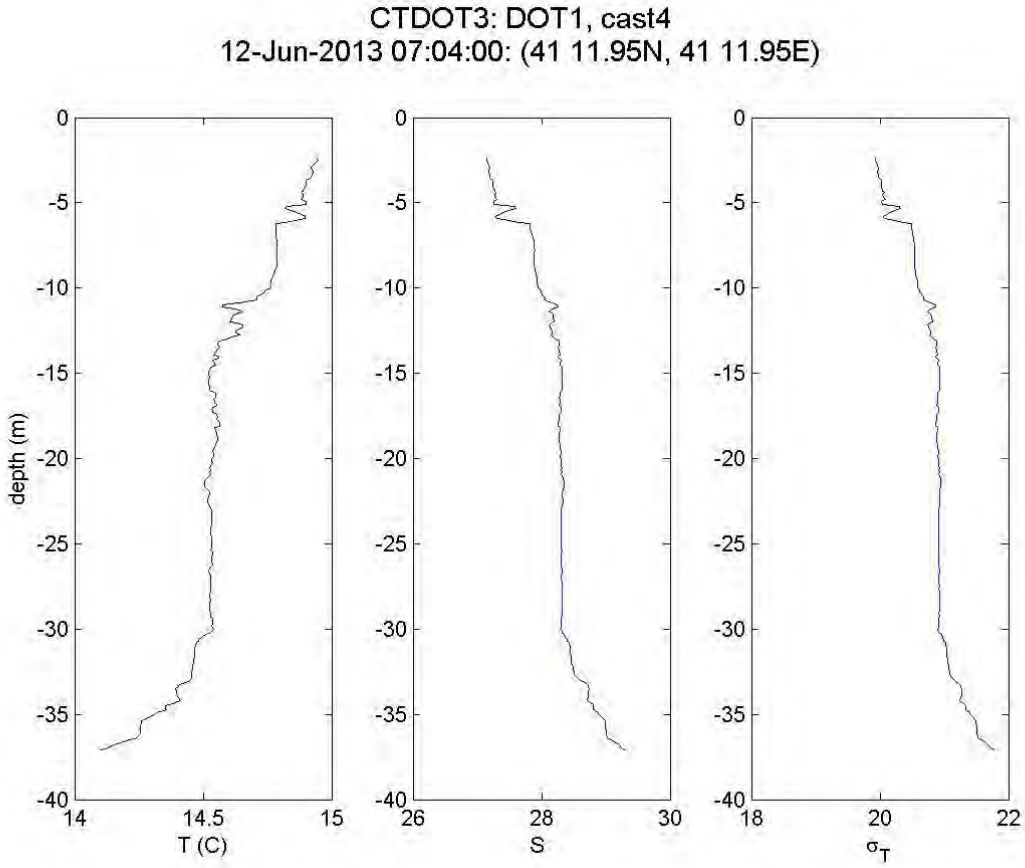

Figure 36: Cruise CTDOT3: Station DOT1, Cast 4: The left panel shows the vertical structure of Temperature (C) and the center and right panels show the salinity and density (σ_T) profiles respectively.

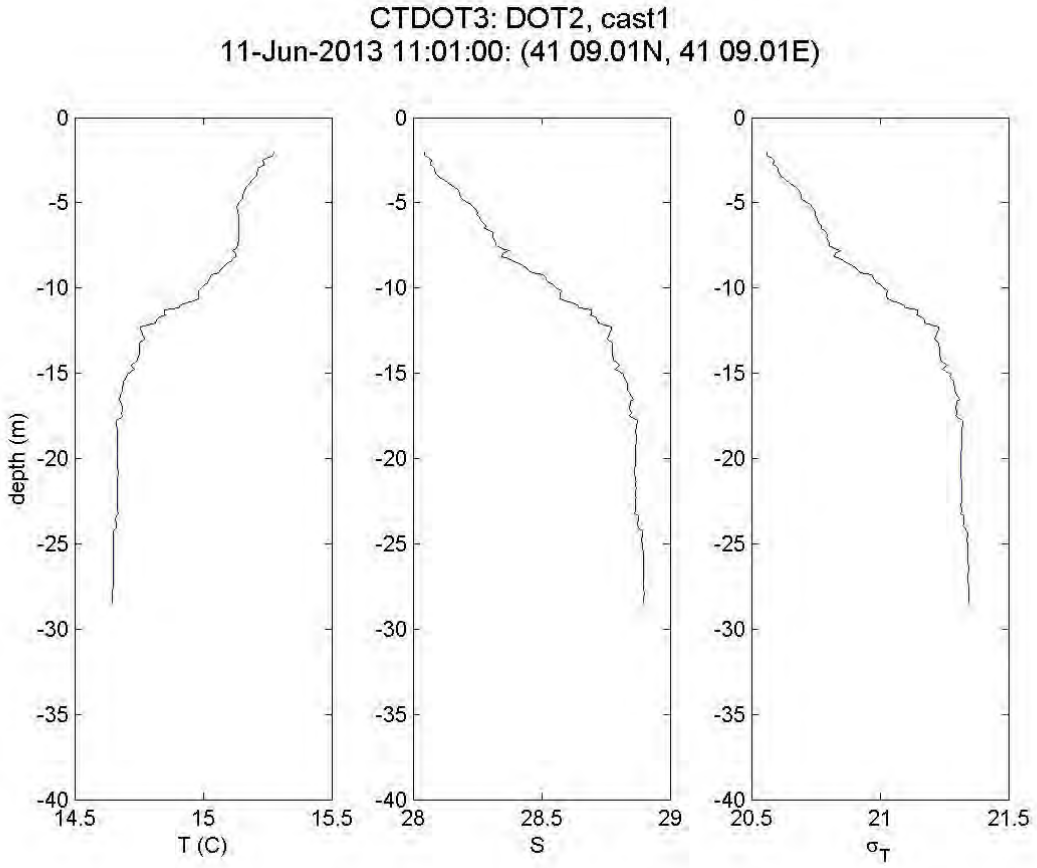

Figure 37: Cruise CTDOT3: Station DOT2, Cast 1: The left panel shows the vertical structure of Temperature (C) and the center and right panels show the salinity and density (σ_T) profiles respectively.

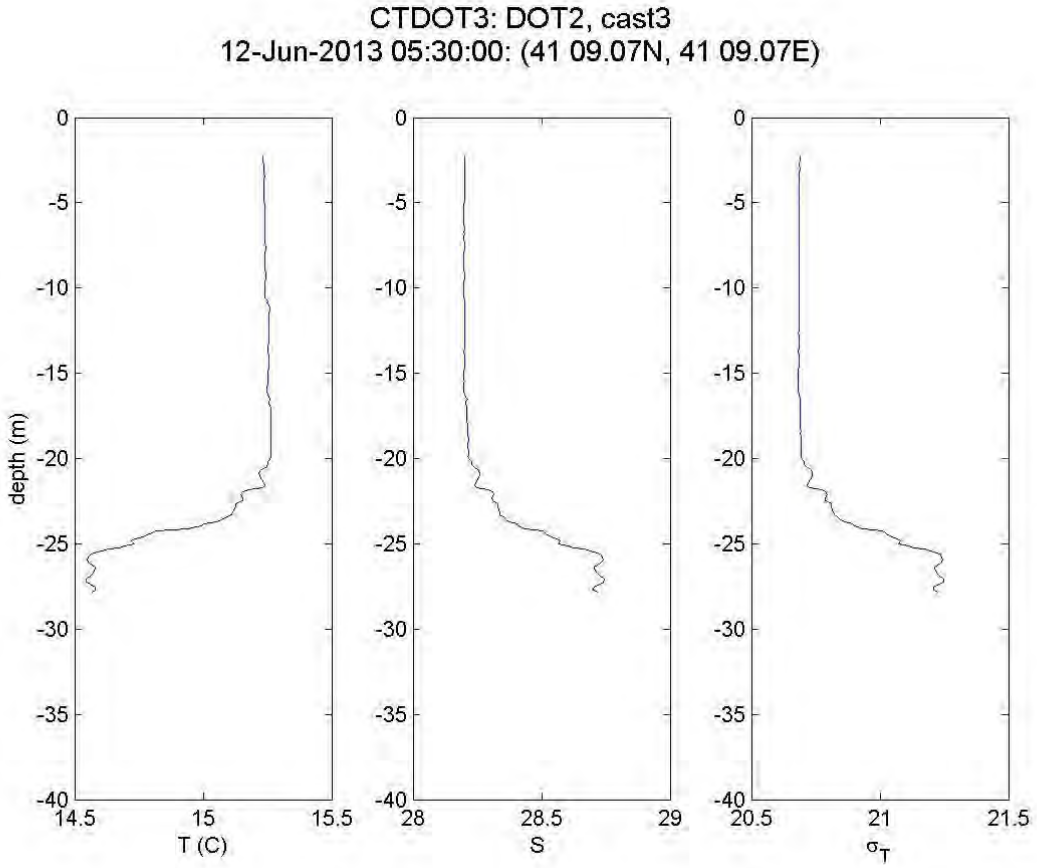

Figure 38: Cruise CTDOT3: Station DOT2, Cast 3: The left panel shows the vertical structure of Temperature (C) and the center and right panels show the salinity and density (σ_T) profiles respectively.

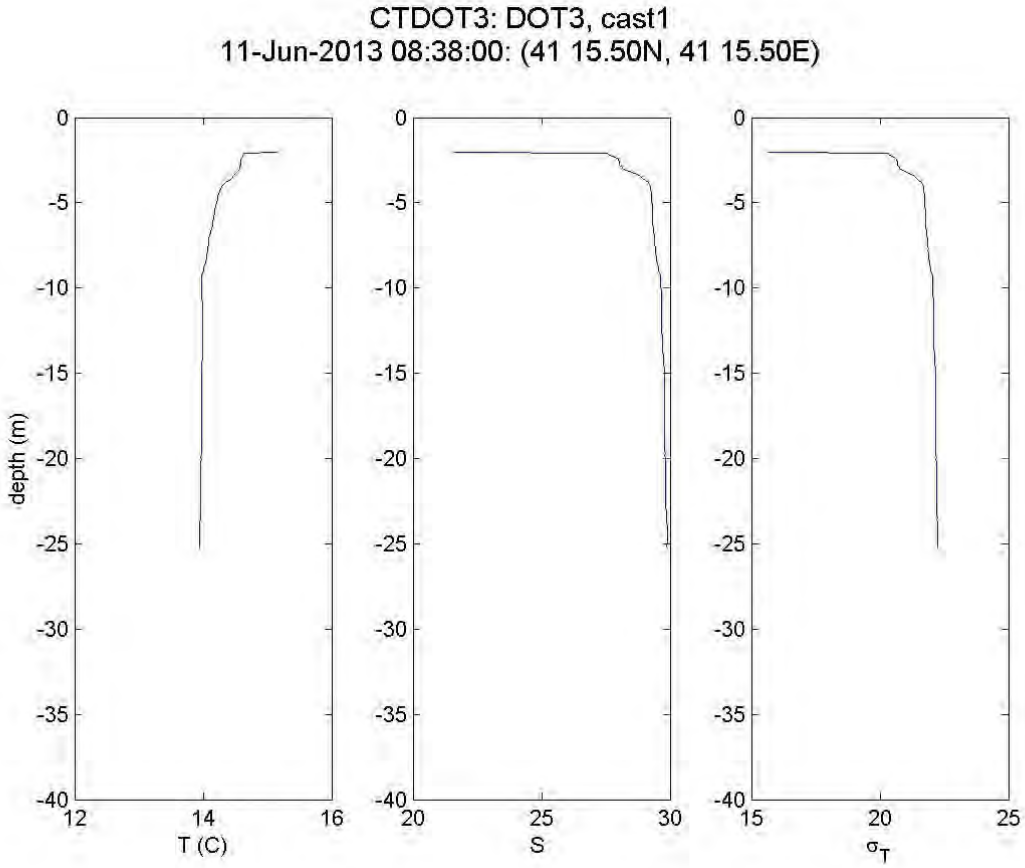

Figure 39: Cruise CTDOT3: Station DOT3, Cast 1: The left panel shows the vertical structure of Temperature (C) and the center and right panels show the salinity and density (σ_T) profiles respectively.

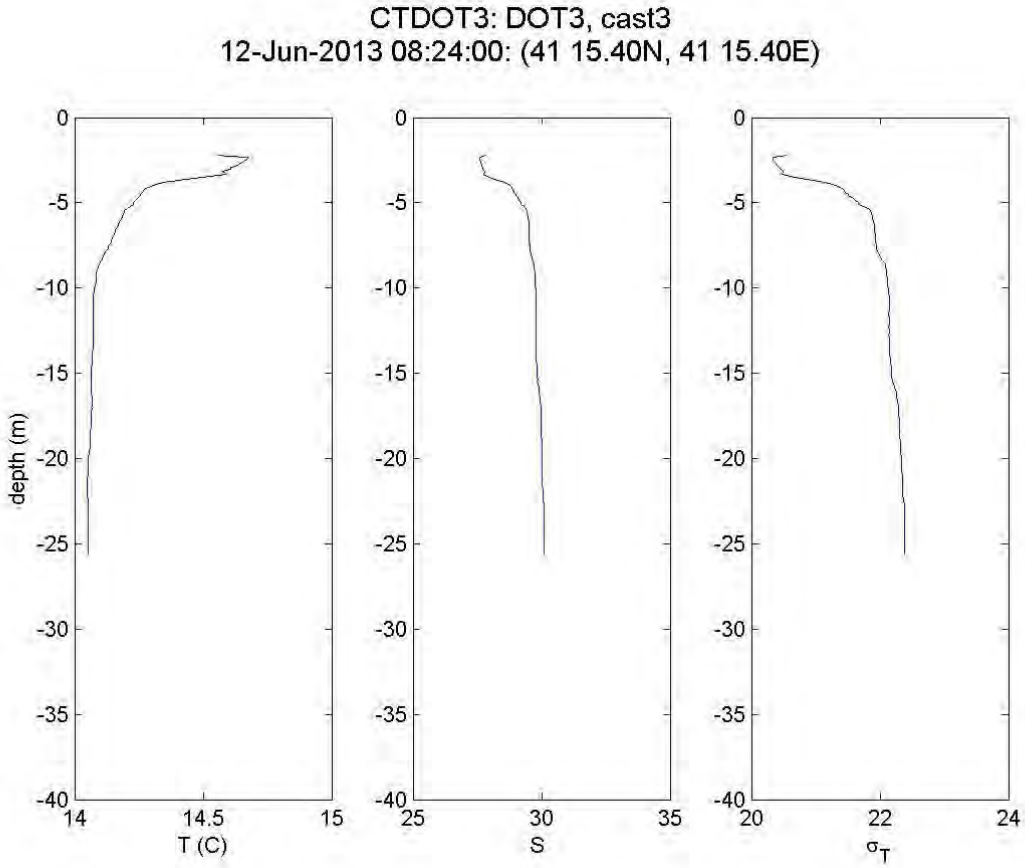

Figure 40: Cruise CTDOT3: Station DOT3, Cast 3: The left panel shows the vertical structure of Temperature (C) and the center and right panels show the salinity and density (σ_T) profiles respectively.

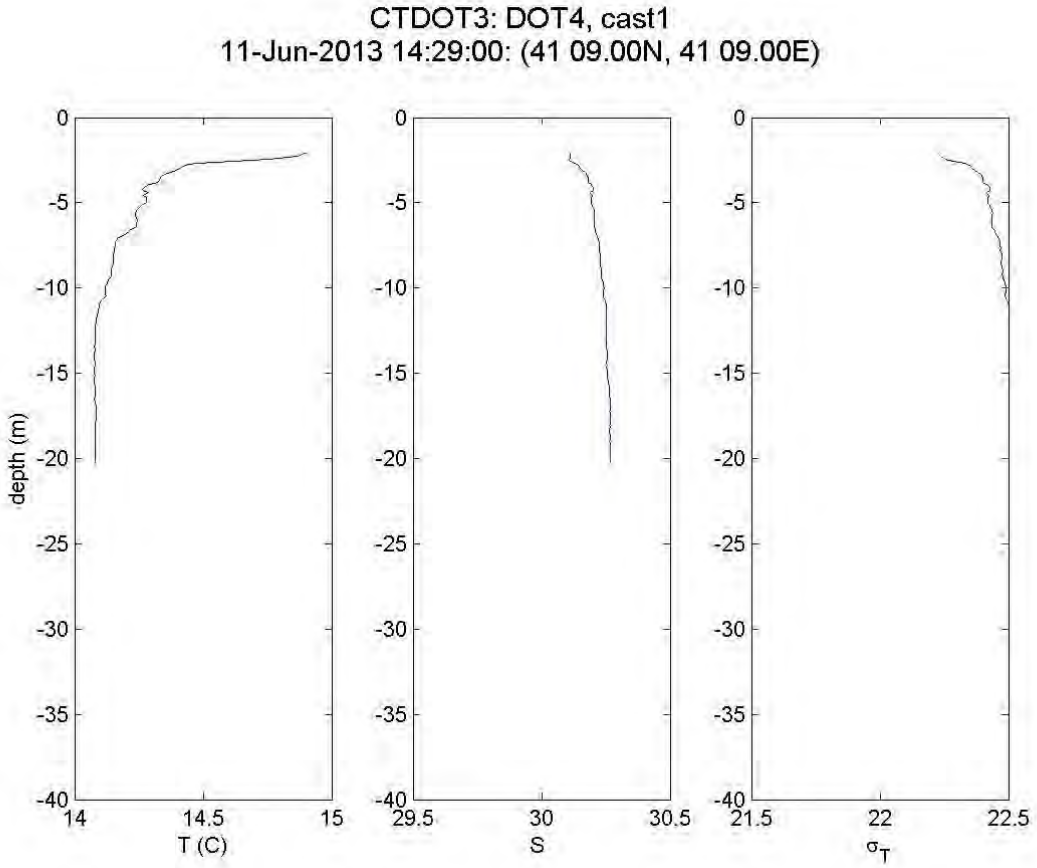

Figure 41: Cruise CTDOT3: Station DOT4, Cast 1: The left panel shows the vertical structure of Temperature (C) and the center and right panels show the salinity and density (σ_T) profiles respectively.

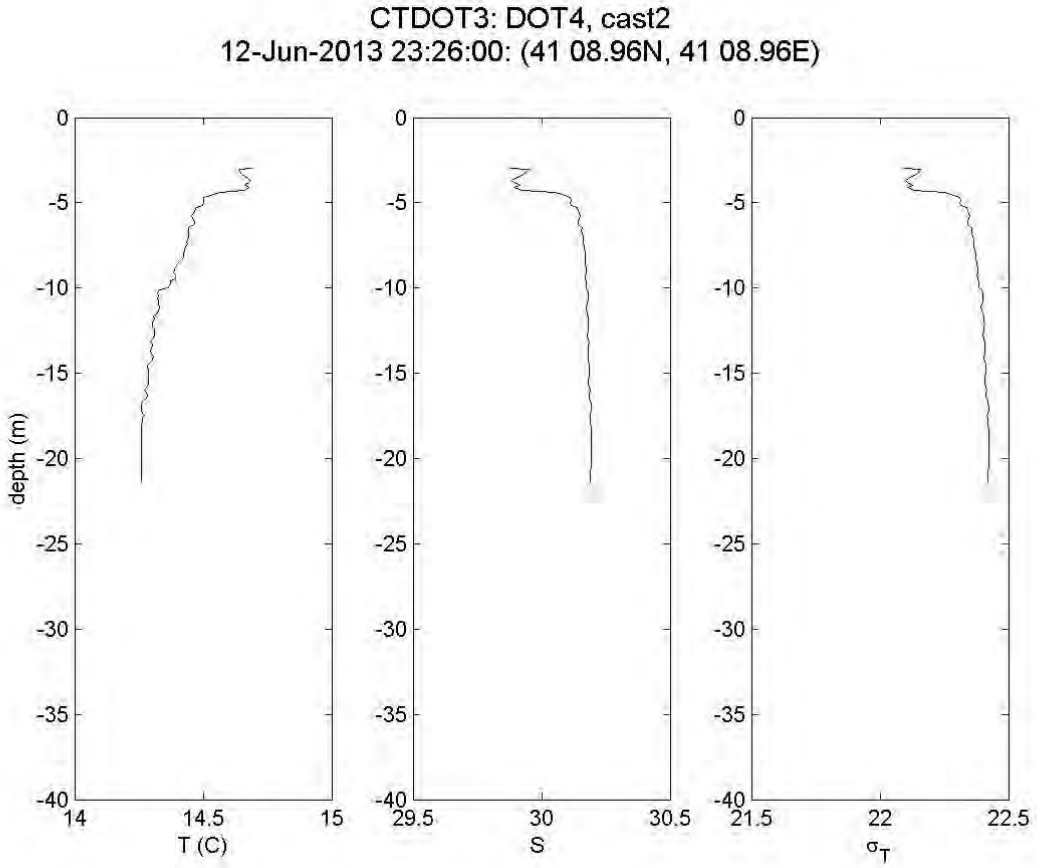

Figure 42: Cruise CTDOT3: Station DOT4, Cast 2: The left panel shows the vertical structure of Temperature (C) and the center and right panels show the salinity and density (σ_T) profiles respectively.

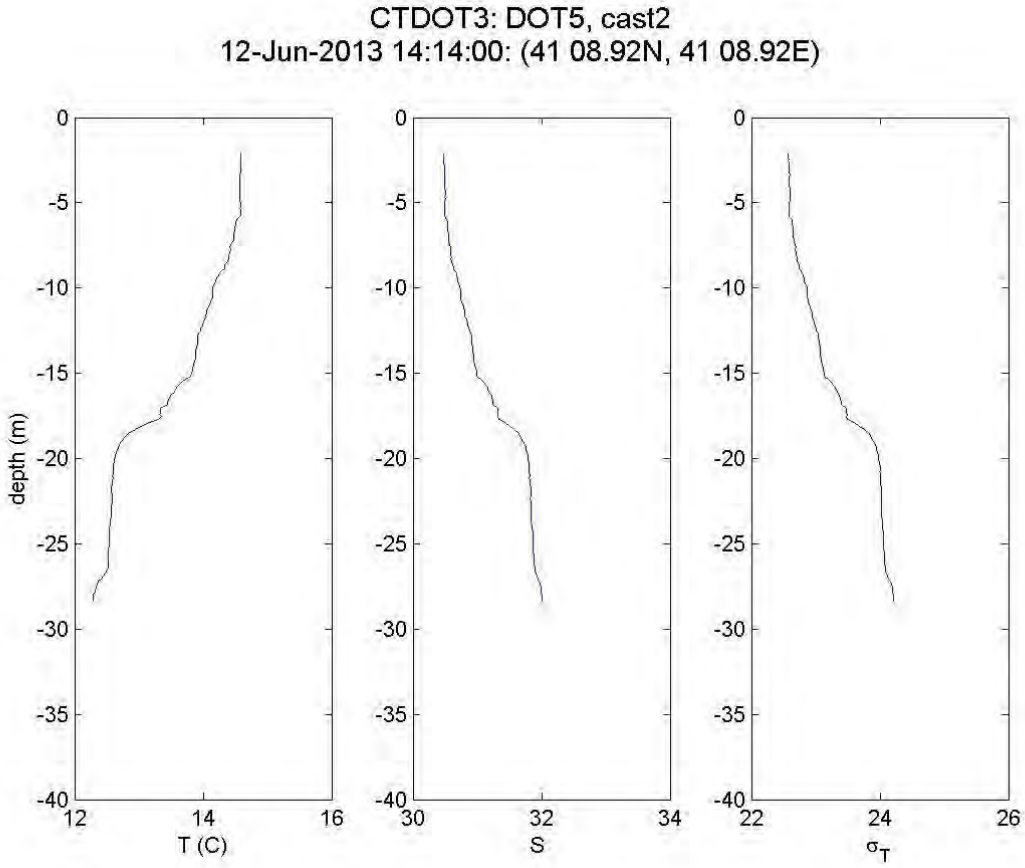

Figure 43: Cruise CTDOT3: Station DOT5, Cast 2: The left panel shows the vertical structure of Temperature (C) and the center and right panels show the salinity and density (σ_T) profiles respectively.

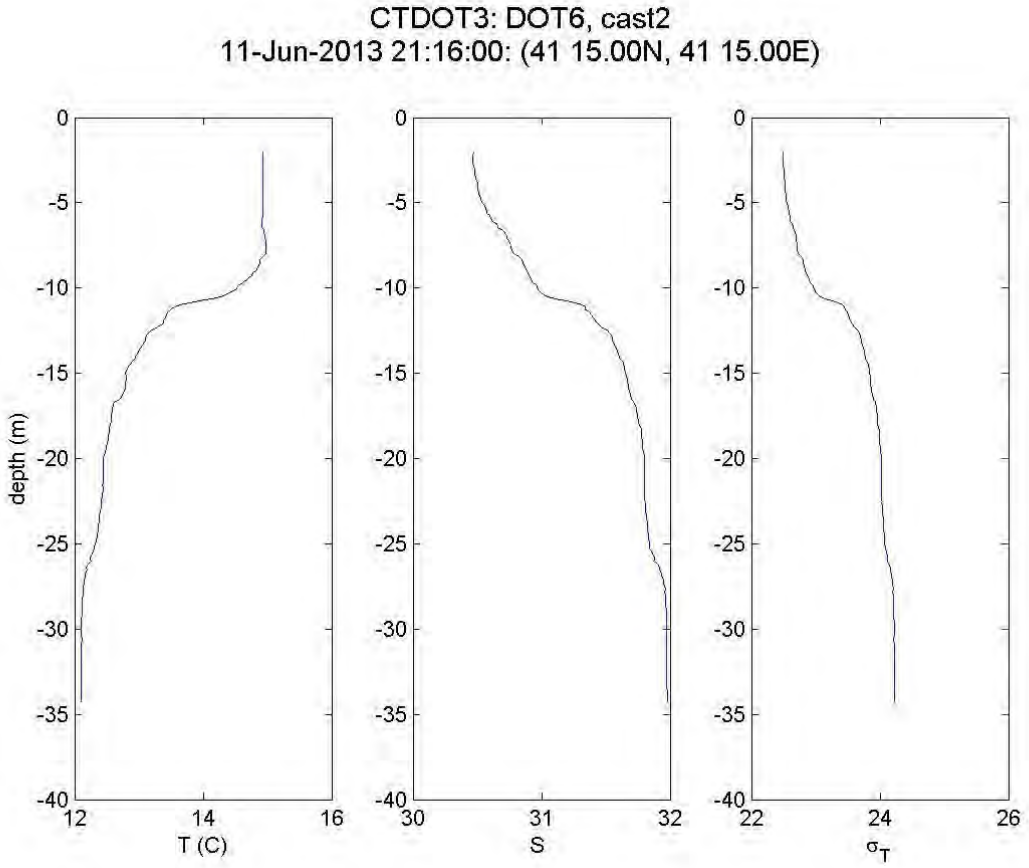

Figure 44: Cruise CTDOT3: Station DOT6, Cast 2: The left panel shows the vertical structure of Temperature (C) and the center and right panels show the salinity and density (σ_T) profiles respectively.

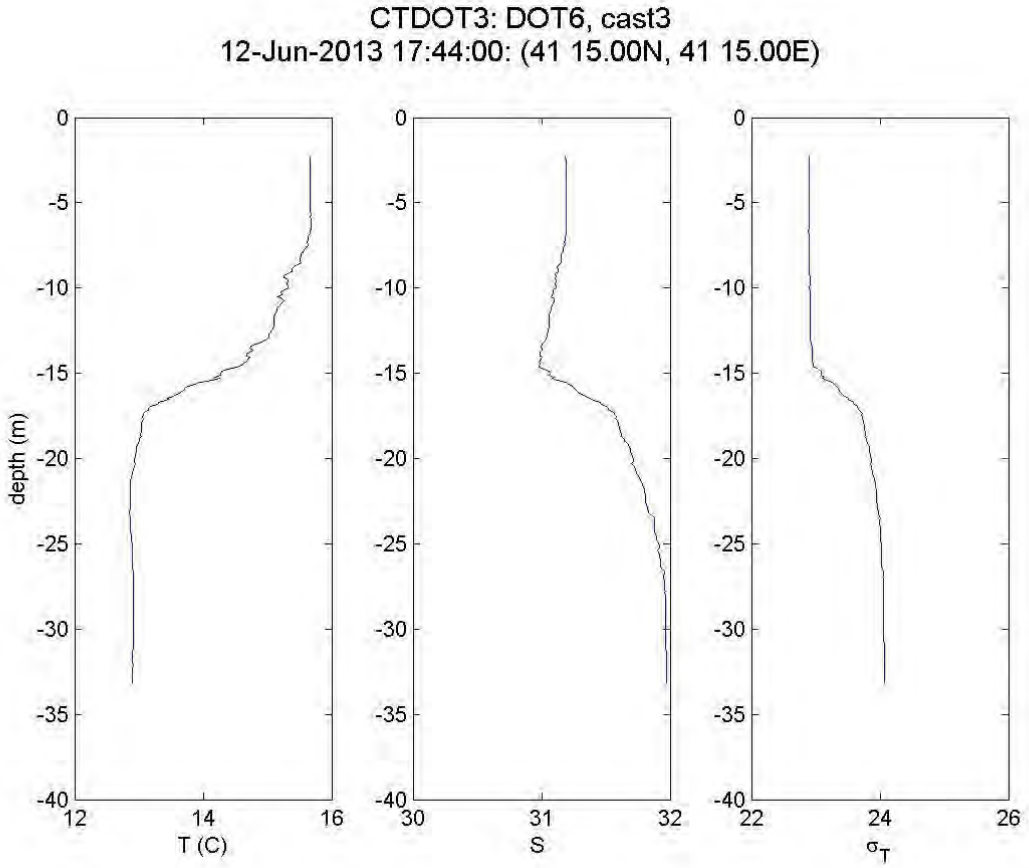

Figure 45: Cruise CTDOT3: Station DOT6, Cast 3: The left panel shows the vertical structure of Temperature (C) and the center and right panels show the salinity and density (σ_T) profiles respectively.

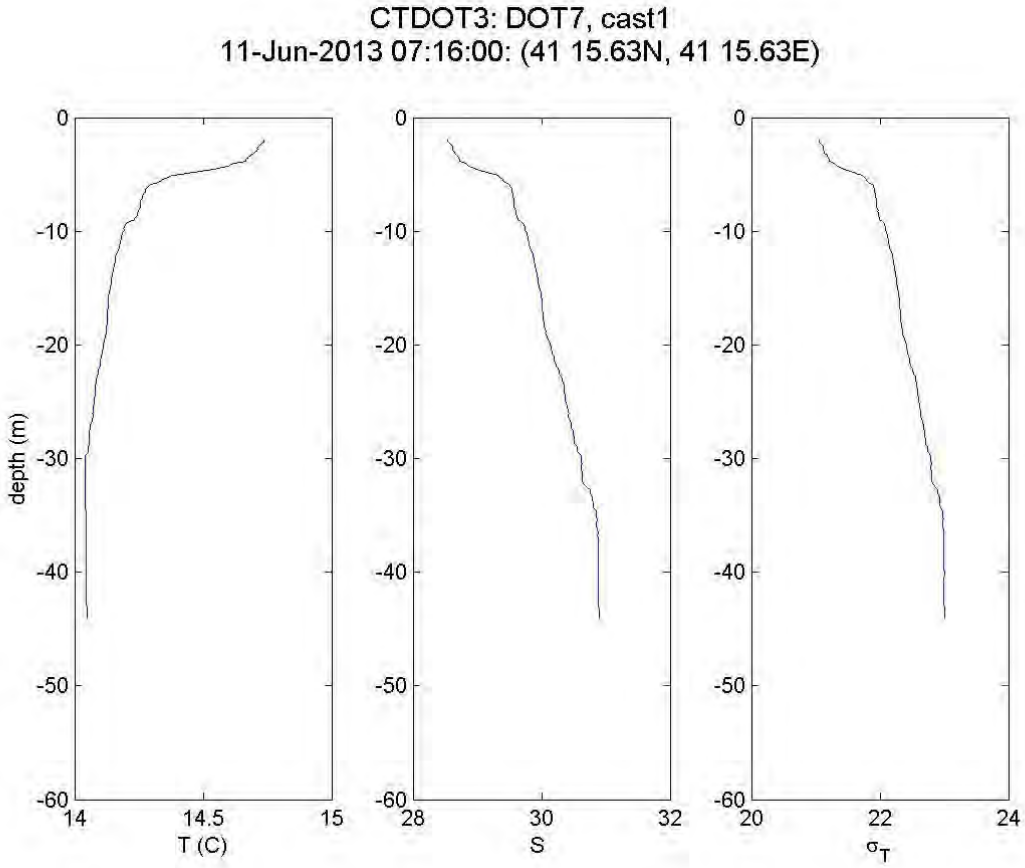

Figure 46: Cruise CTDOT3: Station DOT7, Cast 1: The left panel shows the vertical structure of Temperature (C) and the center and right panels show the salinity and density (σ_T) profiles respectively.

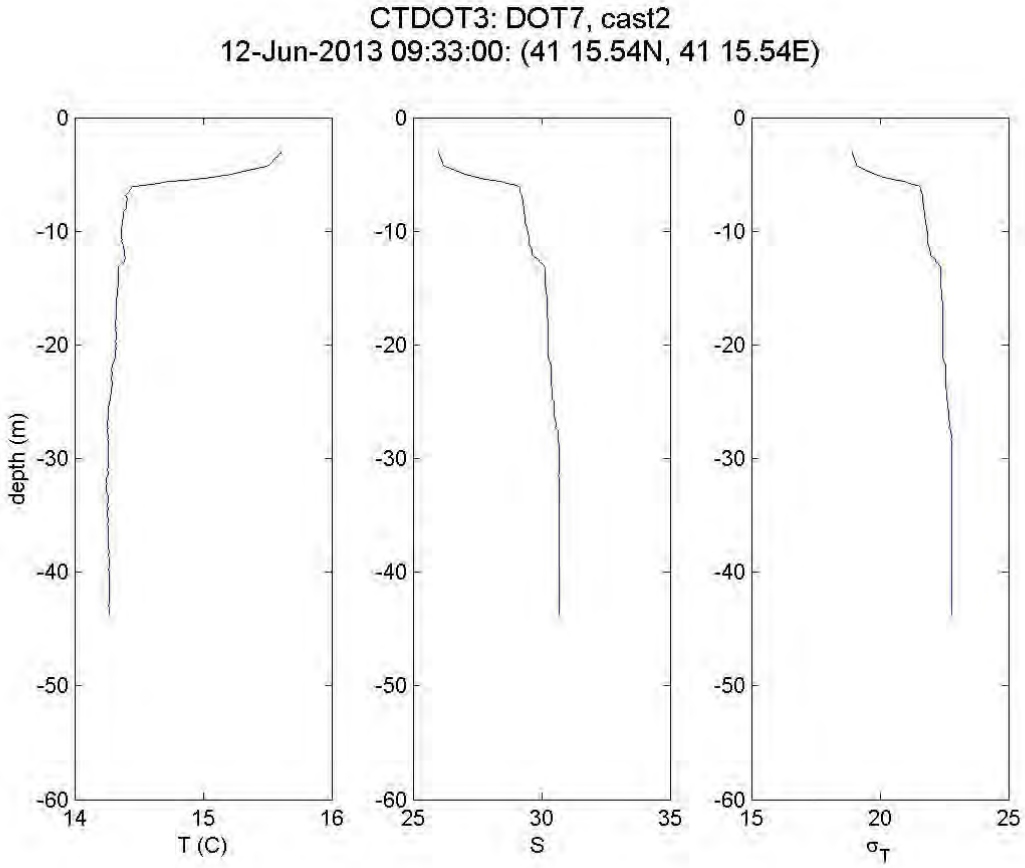

Figure 47: Cruise CTDOT3: Station DOT7, Cast 2: The left panel shows the vertical structure of Temperature (C) and the center and right panels show the salinity and density (σ_T) profiles respectively.

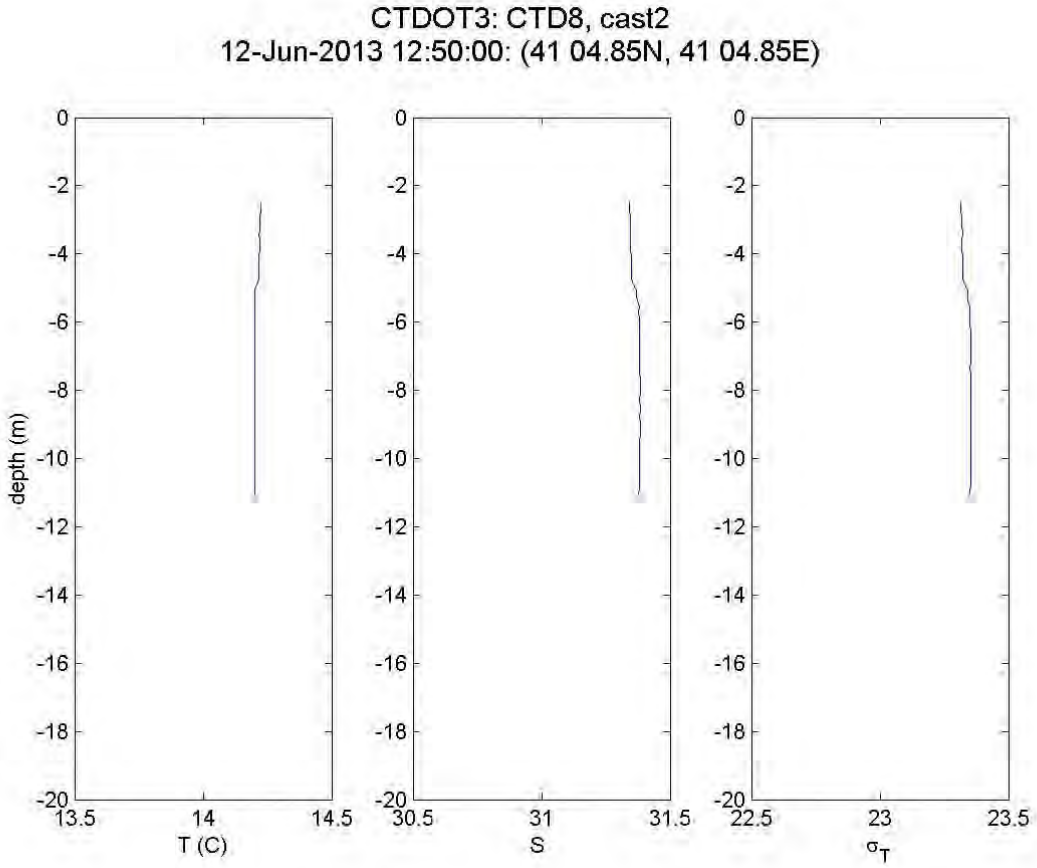

Figure 48: Cruise CTDOT3: Station CTD8, Cast 2: The left panel shows the vertical structure of Temperature (C) and the center and right panels show the salinity and density (σ_T) profiles respectively.

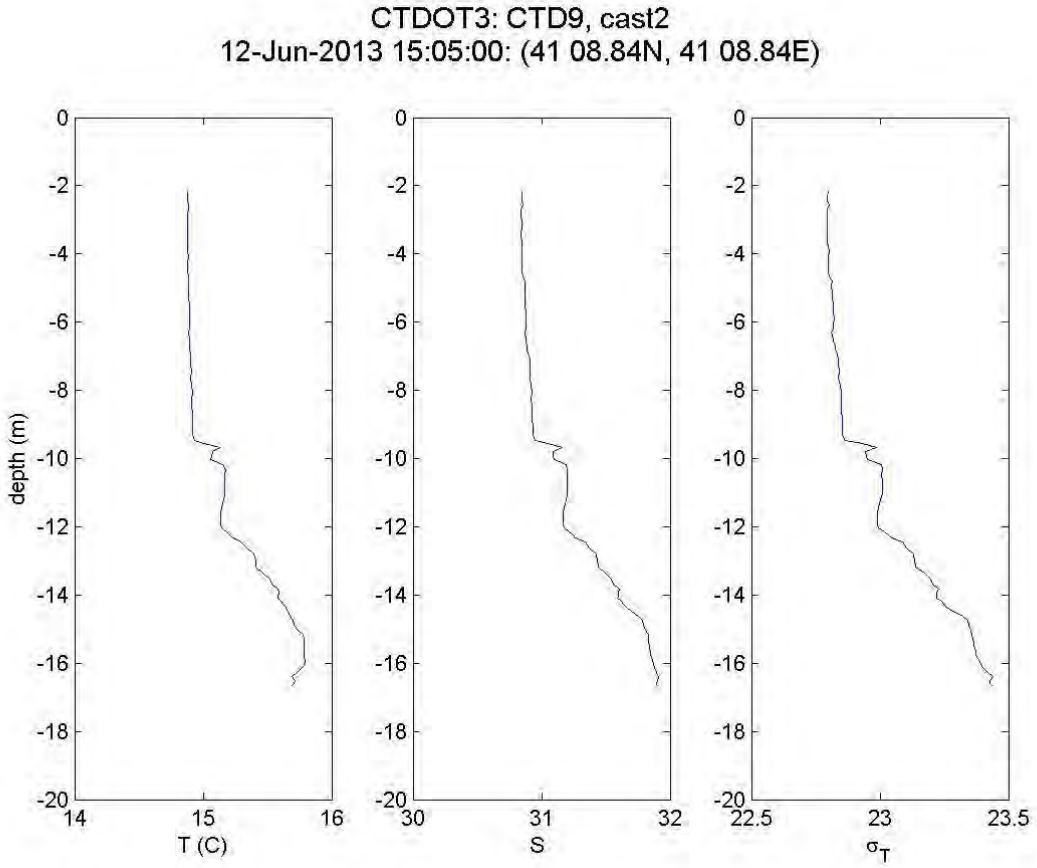

Figure 49: Cruise CTDOT3: Station CTD9, Cast 2: The left panel shows the vertical structure of Temperature (C) and the center and right panels show the salinity and density (σ_T) profiles respectively.

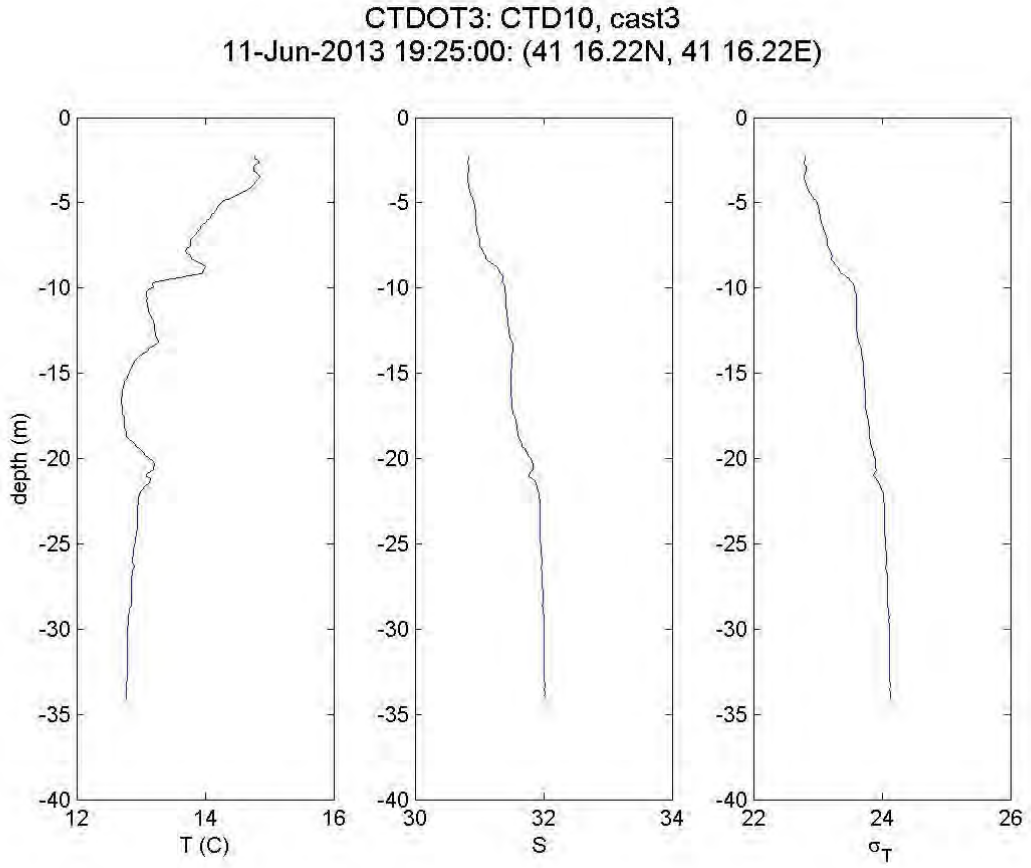

Figure 50: Cruise CTDOT3: Station CTD10, Cast 3: The left panel shows the vertical structure of Temperature (C) and the center and right panels show the salinity and density (σ_T) profiles respectively.

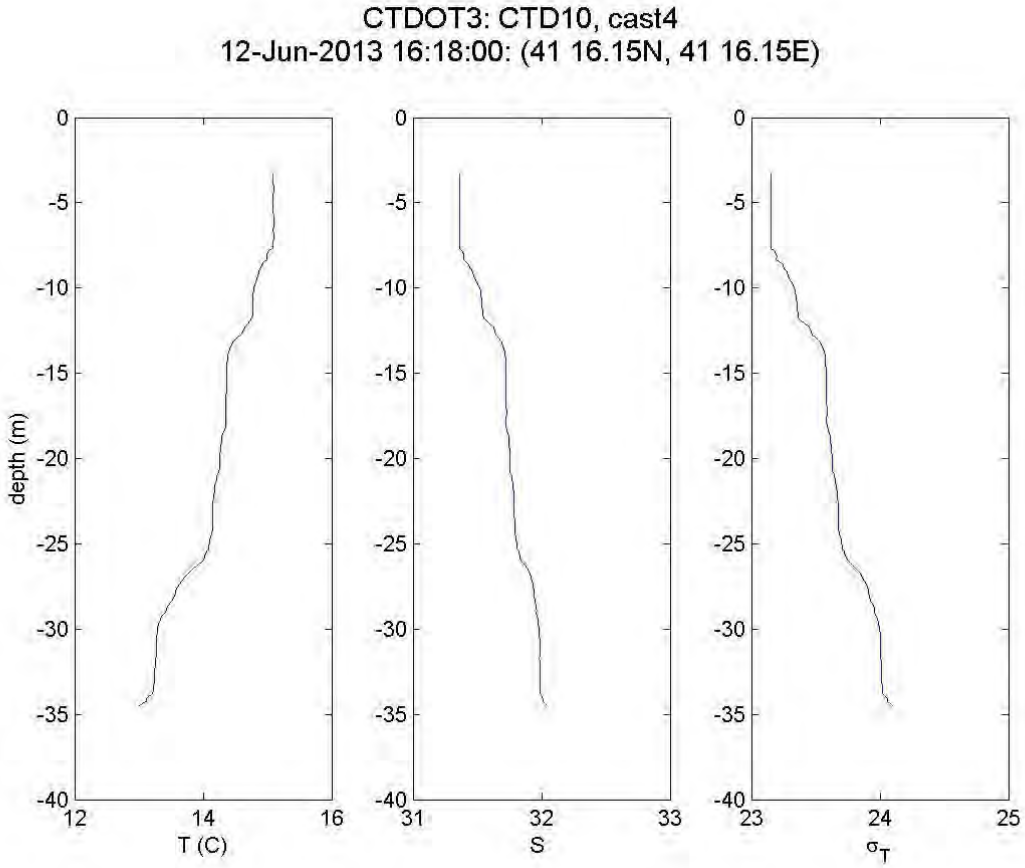

Figure 51: Cruise CTDOT3: Station CTD10, Cast 4: The left panel shows the vertical structure of Temperature (C) and the center and right panels show the salinity and density (σ_T) profiles respectively.

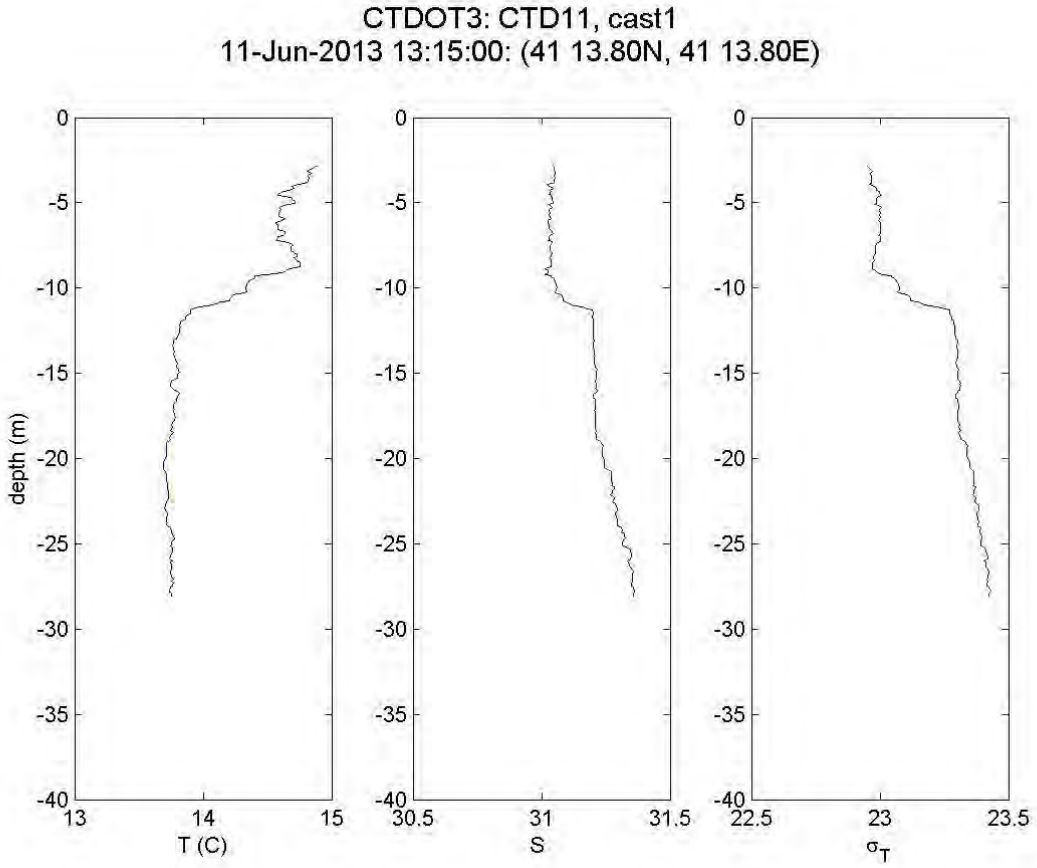

Figure 52: Cruise CTDOT3: Station CTD11, Cast 1: The left panel shows the vertical structure of Temperature (C) and the center and right panels show the salinity and density (σ_T) profiles respectively.

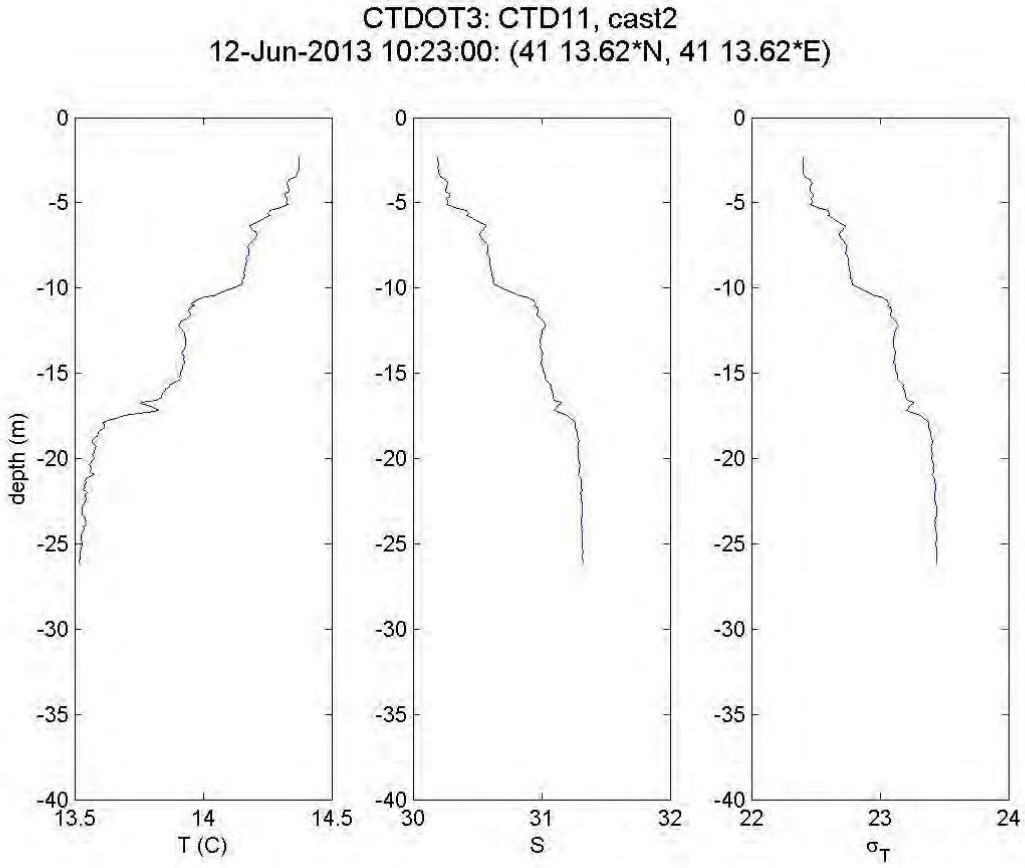

Figure 53: Cruise CTDOT3: Station CTD11, Cast 2: The left panel shows the vertical structure of Temperature (C) and the center and right panels show the salinity and density (σ_T) profiles respectively.

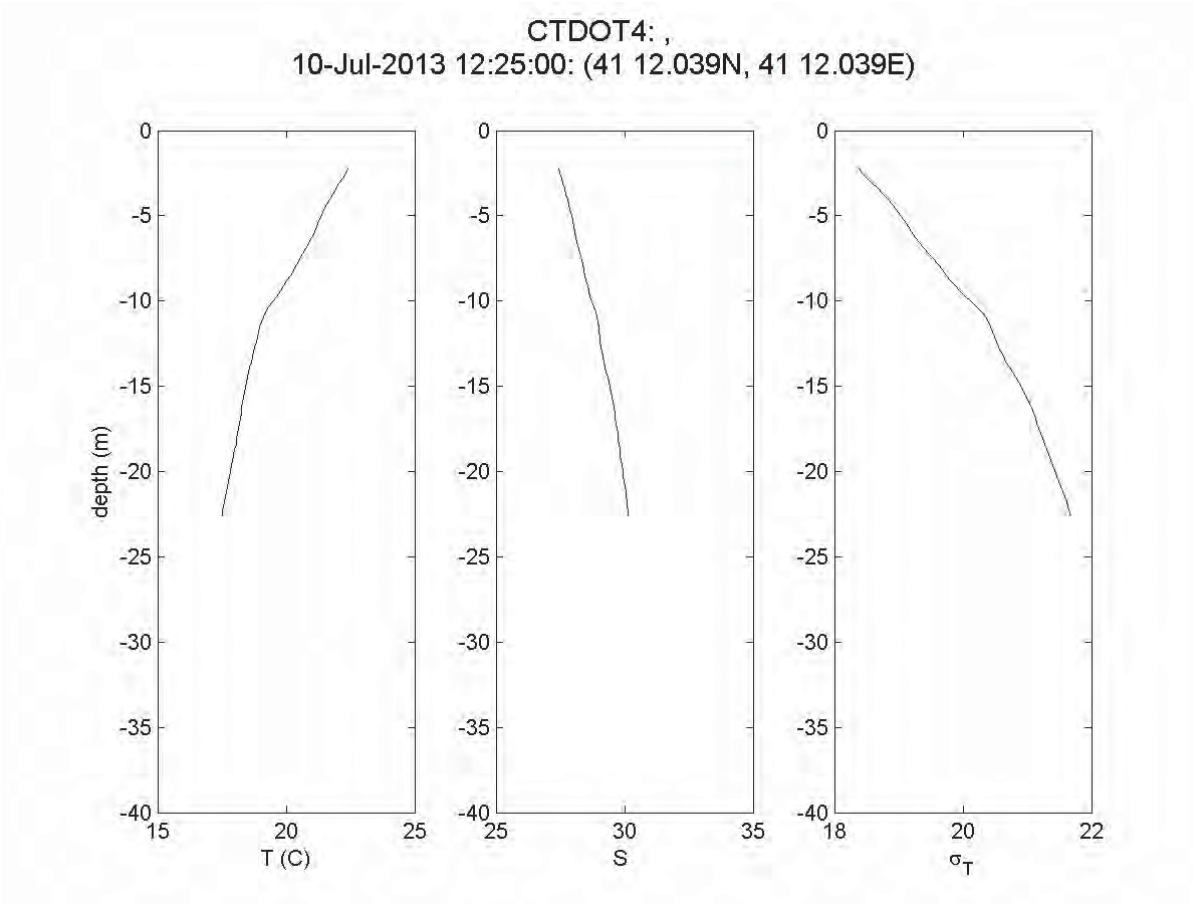

Figure 54: Cruise CTDOT4: Station DOT1, Cast 0: The left panel shows the vertical structure of Temperature (C) and the center and right panels show the salinity and density (σ_T) profiles respectively.

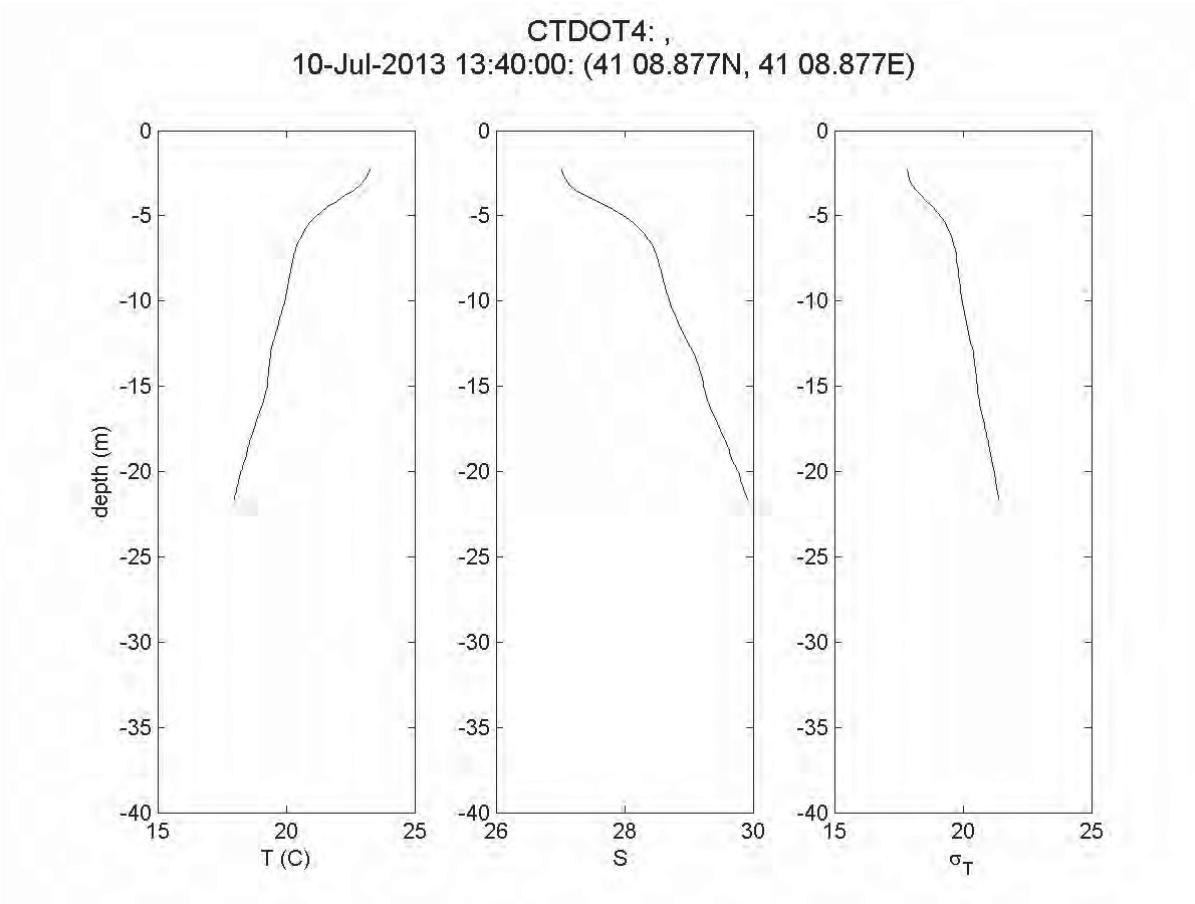

Figure 55: Cruise CTDOT4: Station DOT2, Cast 0: The left panel shows the vertical structure of Temperature (C) and the center and right panels show the salinity and density (σ_T) profiles respectively.

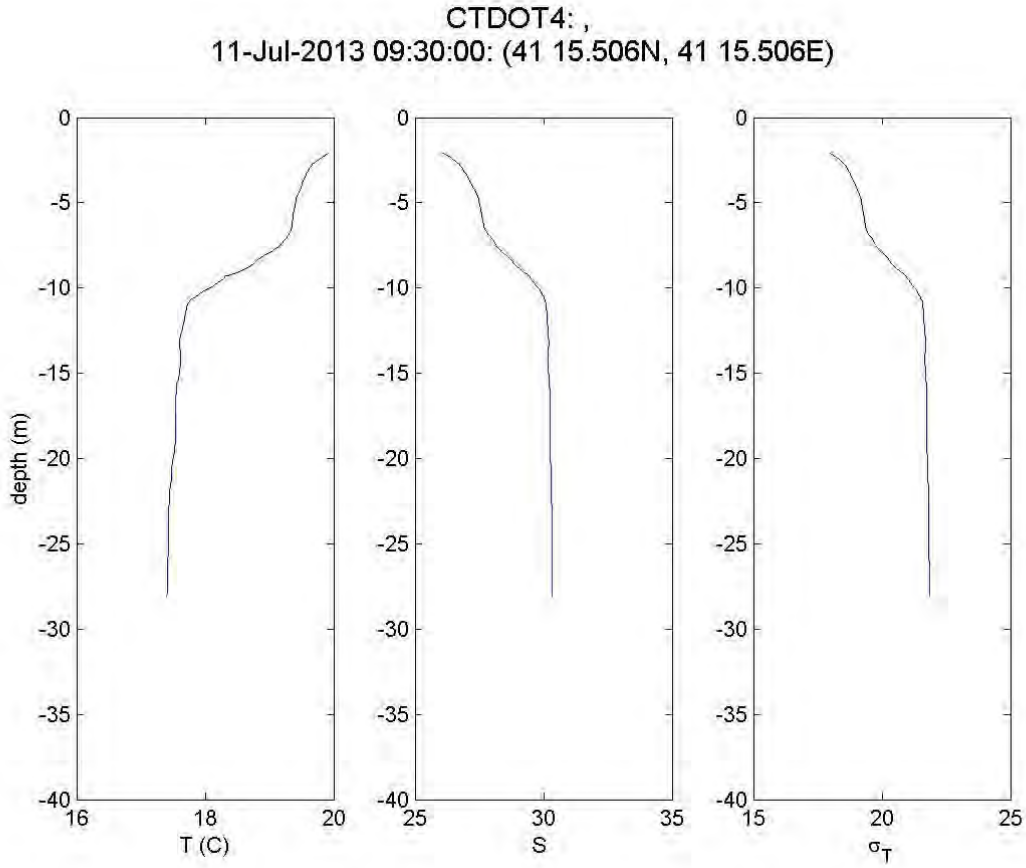

Figure 56: Cruise CTDOT4: Station DOT3, Cast 0: The left panel shows the vertical structure of Temperature (C) and the center and right panels show the salinity and density (σ_T) profiles respectively.

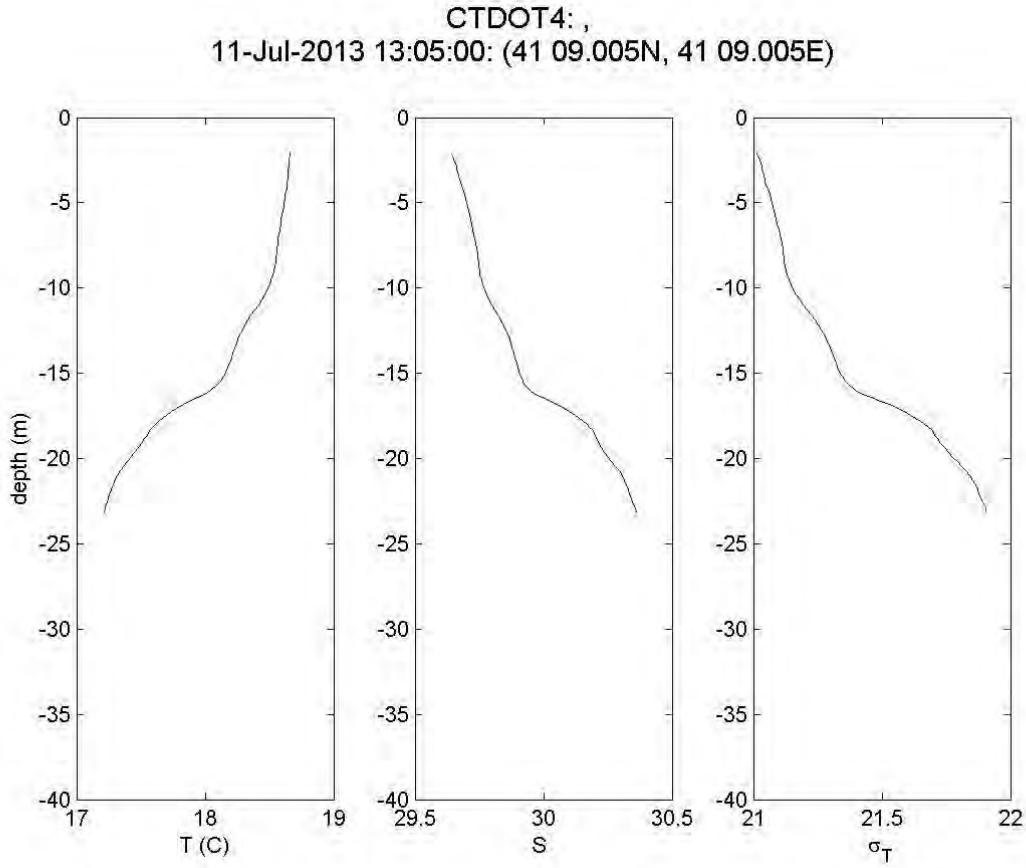

Figure 57: Cruise CTDOT4: Station DOT4, Cast 0: The left panel shows the vertical structure of Temperature (C) and the center and right panels show the salinity and density (σ_T) profiles respectively.

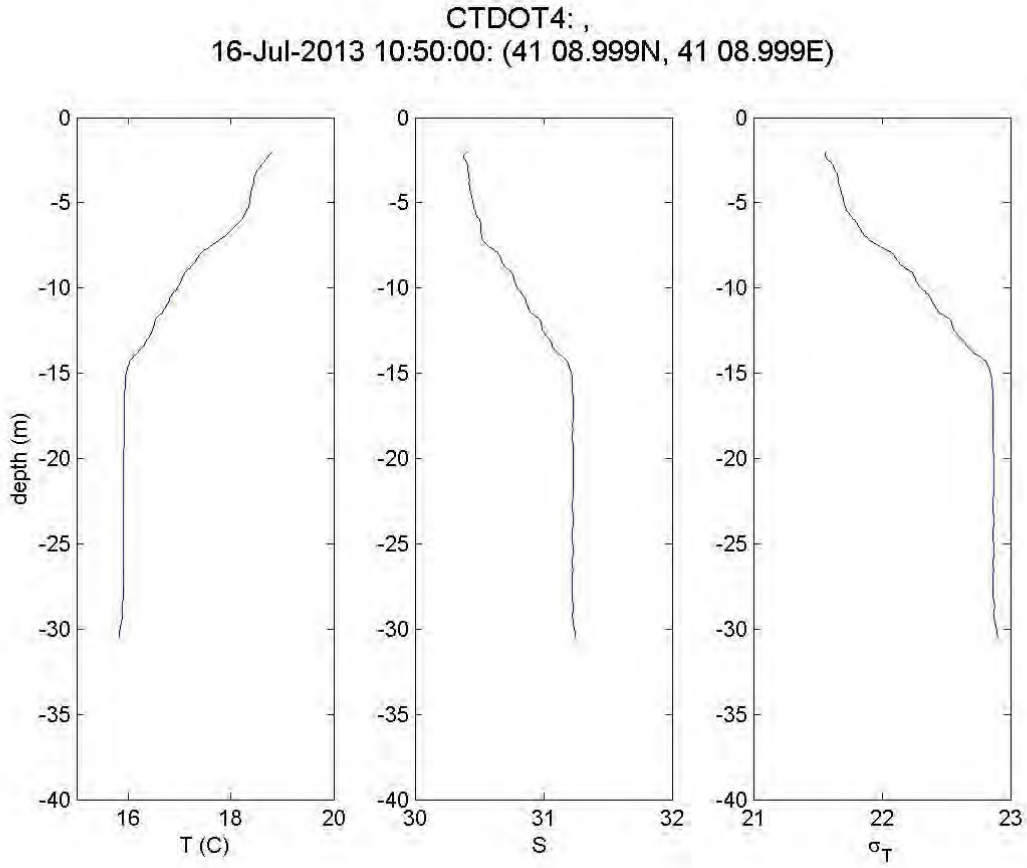

Figure 58: Cruise CTDOT4: Station DOT5, Cast 0: The left panel shows the vertical structure of Temperature (C) and the center and right panels show the salinity and density (σ_T) profiles respectively.

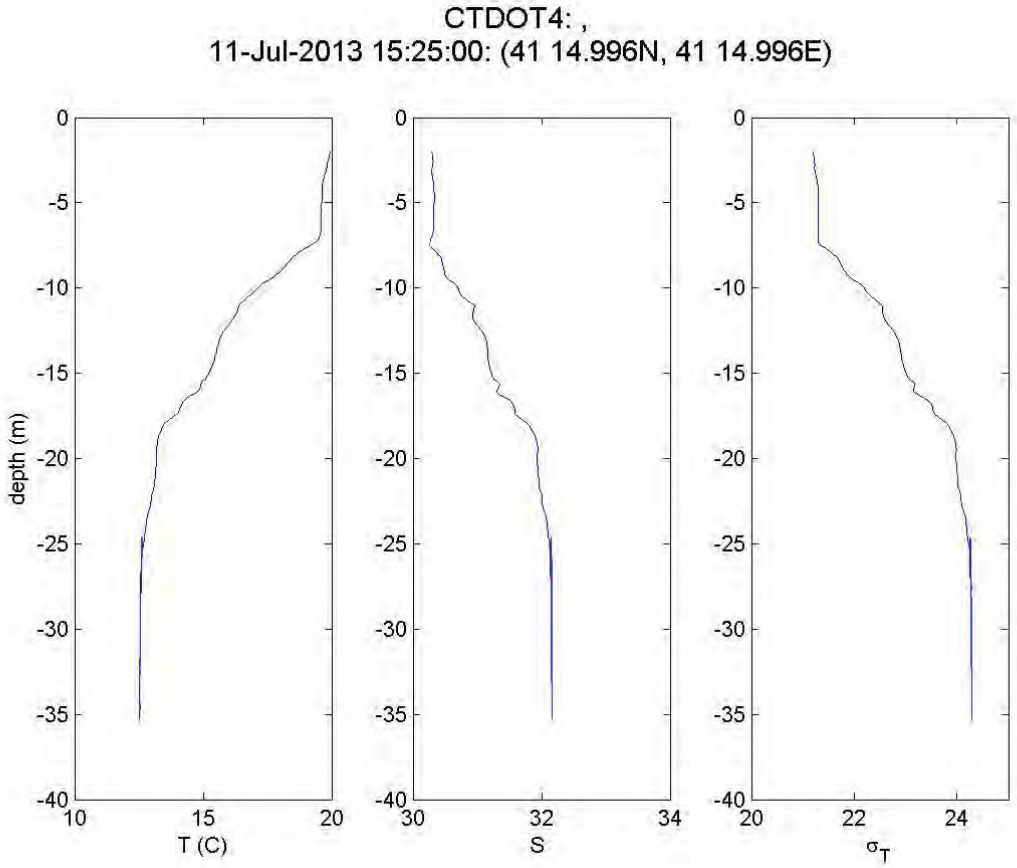

Figure 59: Cruise CTDOT4: Station DOT6, Cast 0: The left panel shows the vertical structure of Temperature (C) and the center and right panels show the salinity and density (σ_T) profiles respectively.

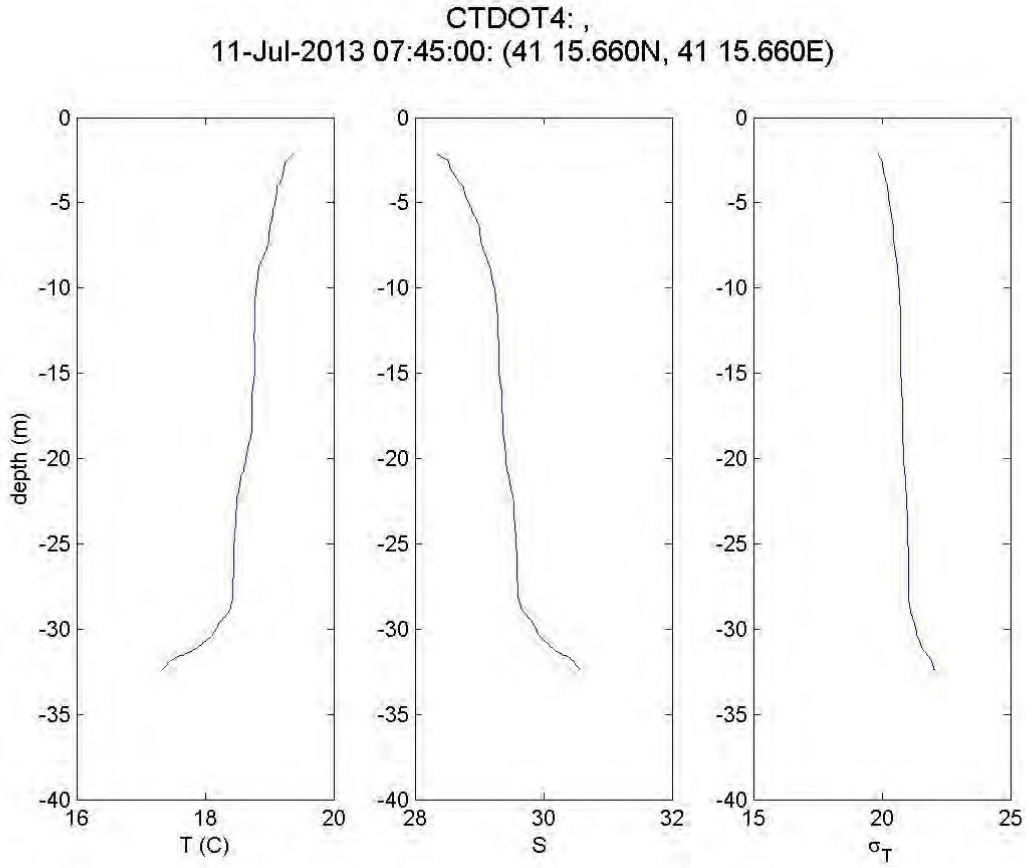

Figure 60: Cruise CTDOT4: Station DOT7, Cast 0: The left panel shows the vertical structure of Temperature (C) and the center and right panels show the salinity and density (σ_T) profiles respectively.

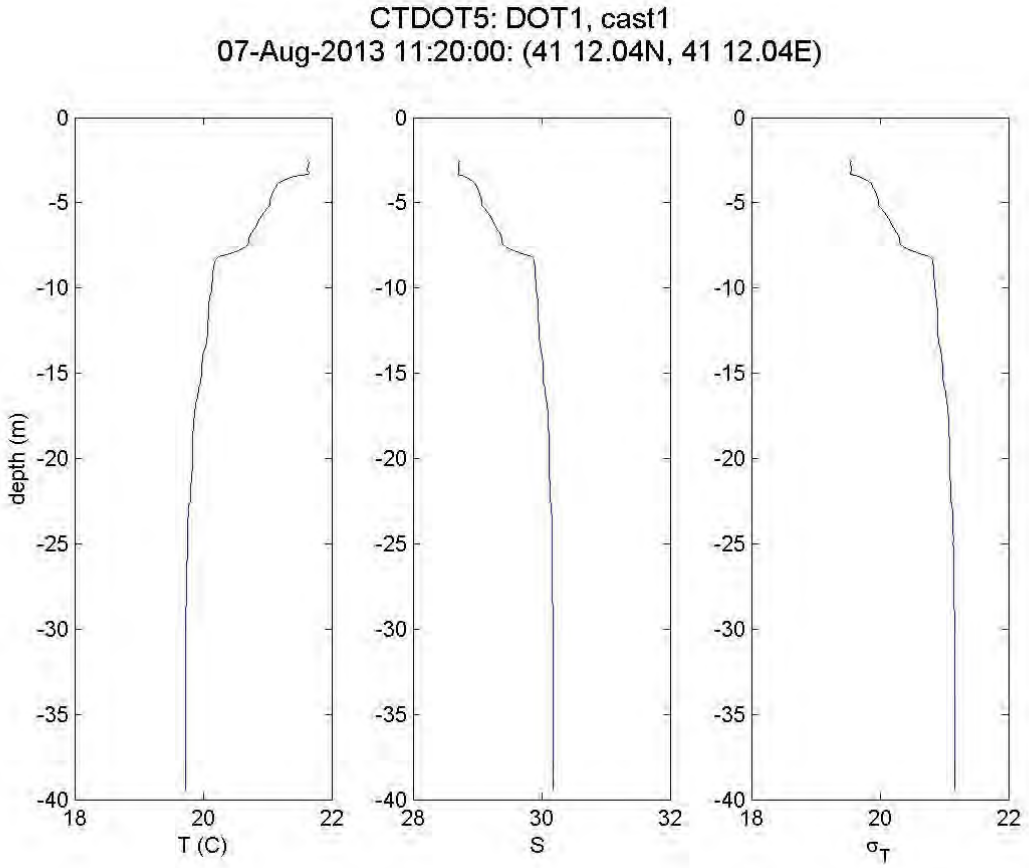

Figure 61: Cruise CTDOT5: Station DOT1, Cast 1: The left panel shows the vertical structure of Temperature (C) and the center and right panels show the salinity and density (σ_T) profiles respectively.

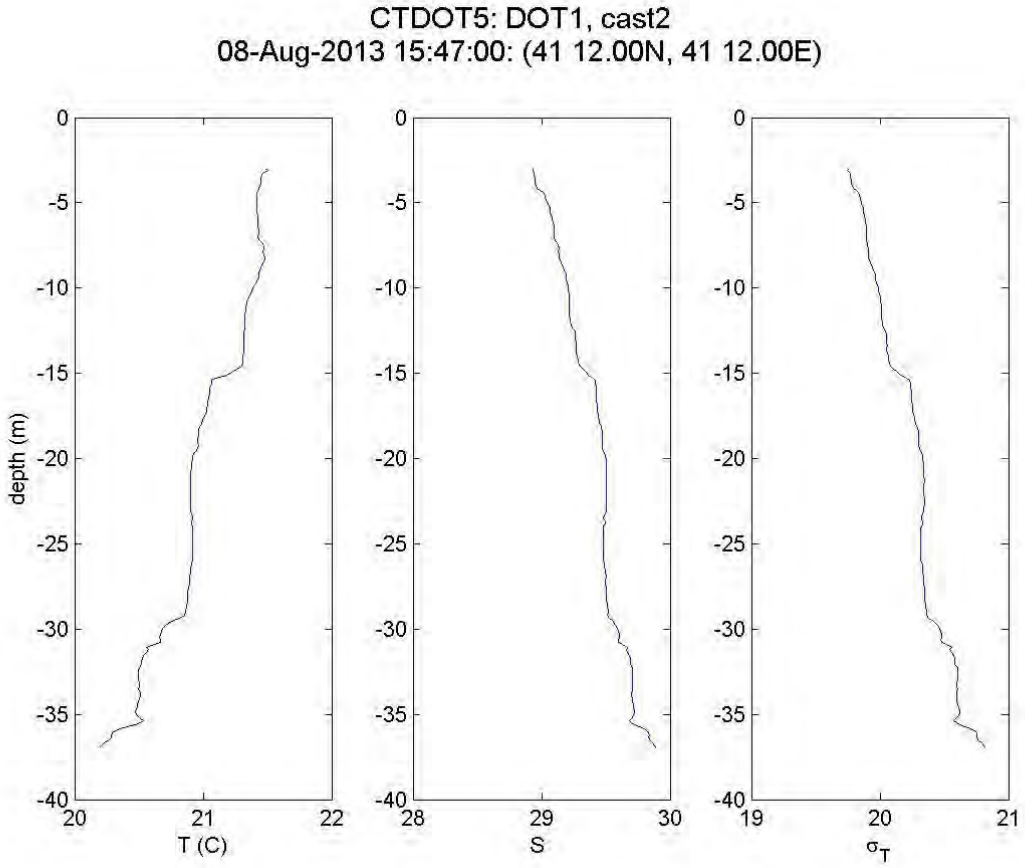

Figure 62: Cruise CTDOT5: Station DOT1, Cast 2: The left panel shows the vertical structure of Temperature (C) and the center and right panels show the salinity and density (σ_T) profiles respectively.

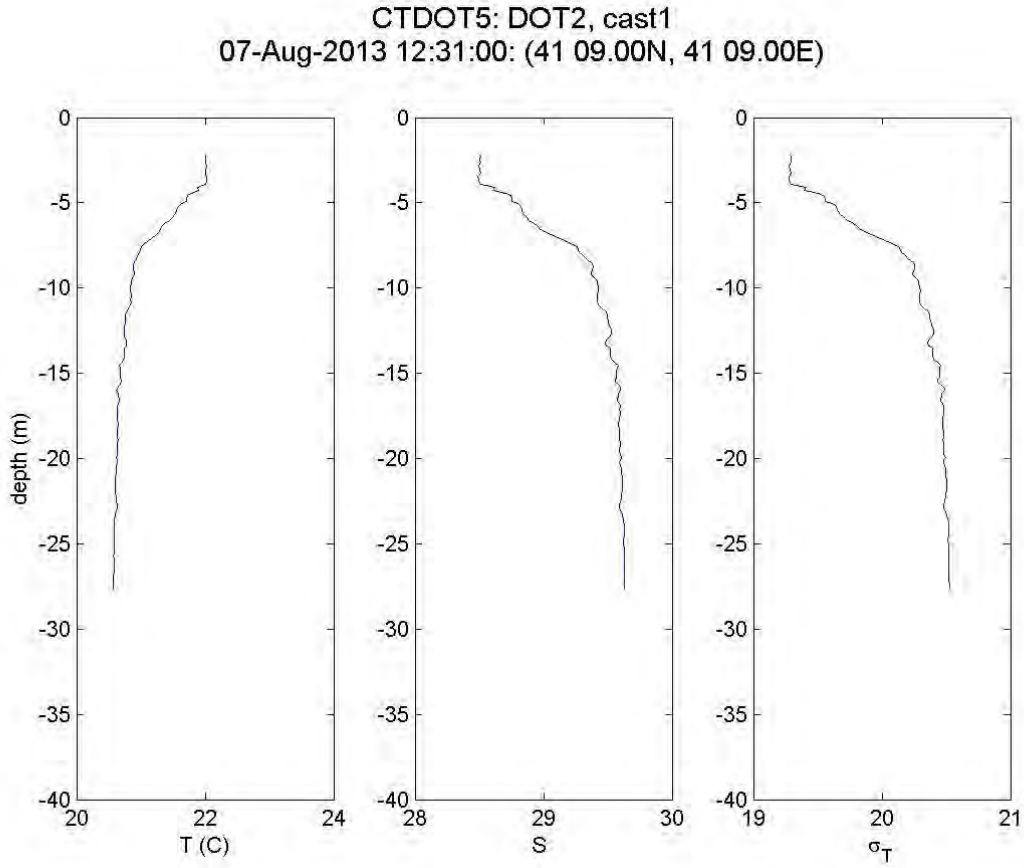

Figure 63: Cruise CTDOT5: Station DOT2, Cast 1: The left panel shows the vertical structure of Temperature (C) and the center and right panels show the salinity and density (σ_T) profiles respectively.

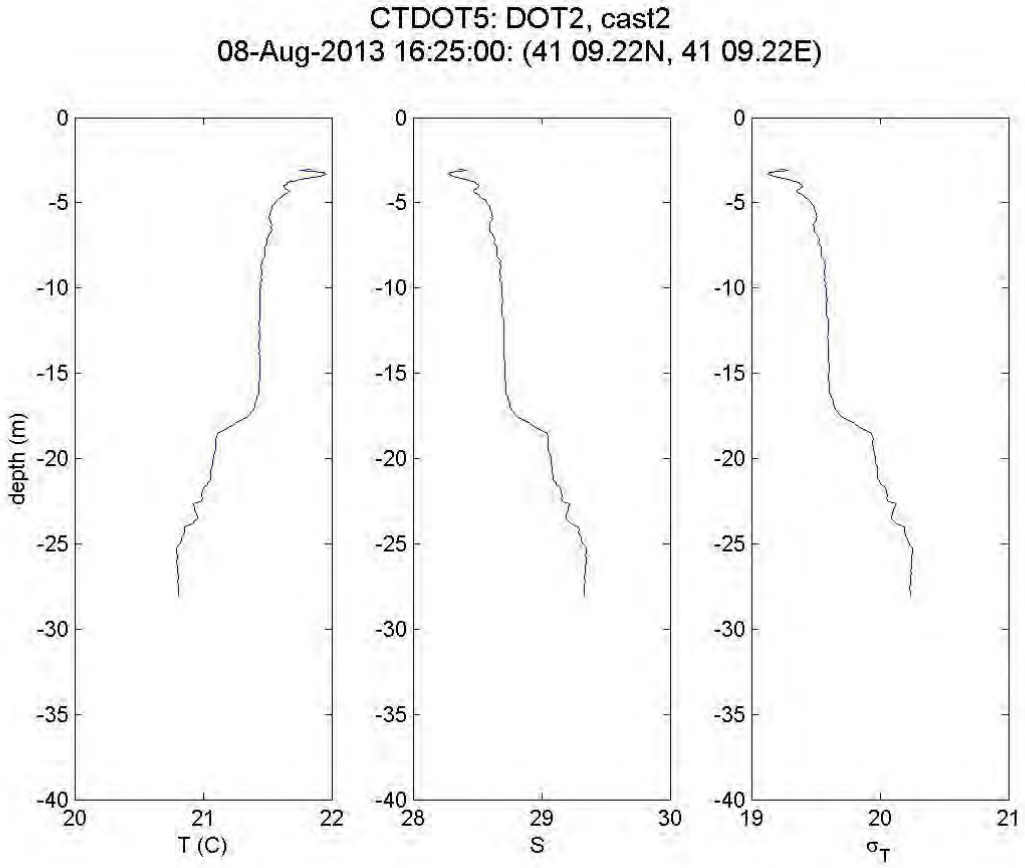

Figure 64: Cruise CTDOT5: Station DOT2, Cast 2: The left panel shows the vertical structure of Temperature (C) and the center and right panels show the salinity and density (σ_T) profiles respectively.

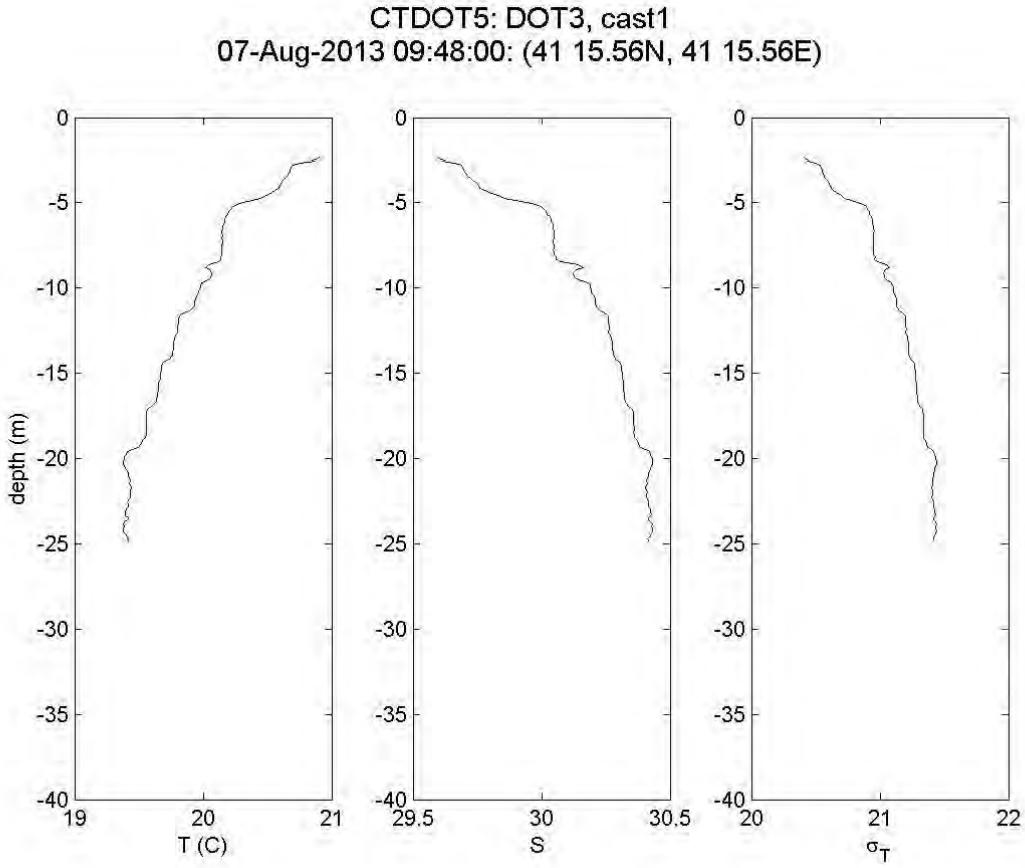

Figure 65: Cruise CTDOT5: Station DOT3, Cast 1: The left panel shows the vertical structure of Temperature (C) and the center and right panels show the salinity and density (σ_T) profiles respectively.

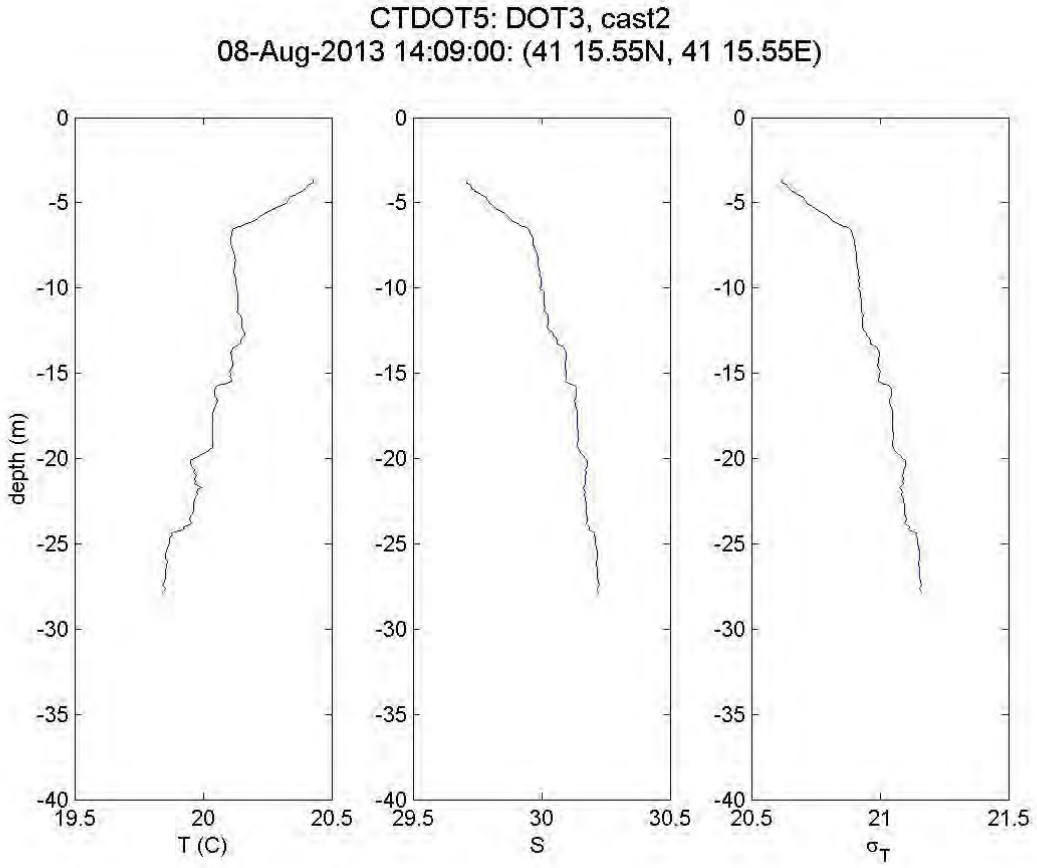

Figure 66: Cruise CTDOT5: Station DOT3, Cast 2: The left panel shows the vertical structure of Temperature (C) and the center and right panels show the salinity and density (σ_T) profiles respectively.

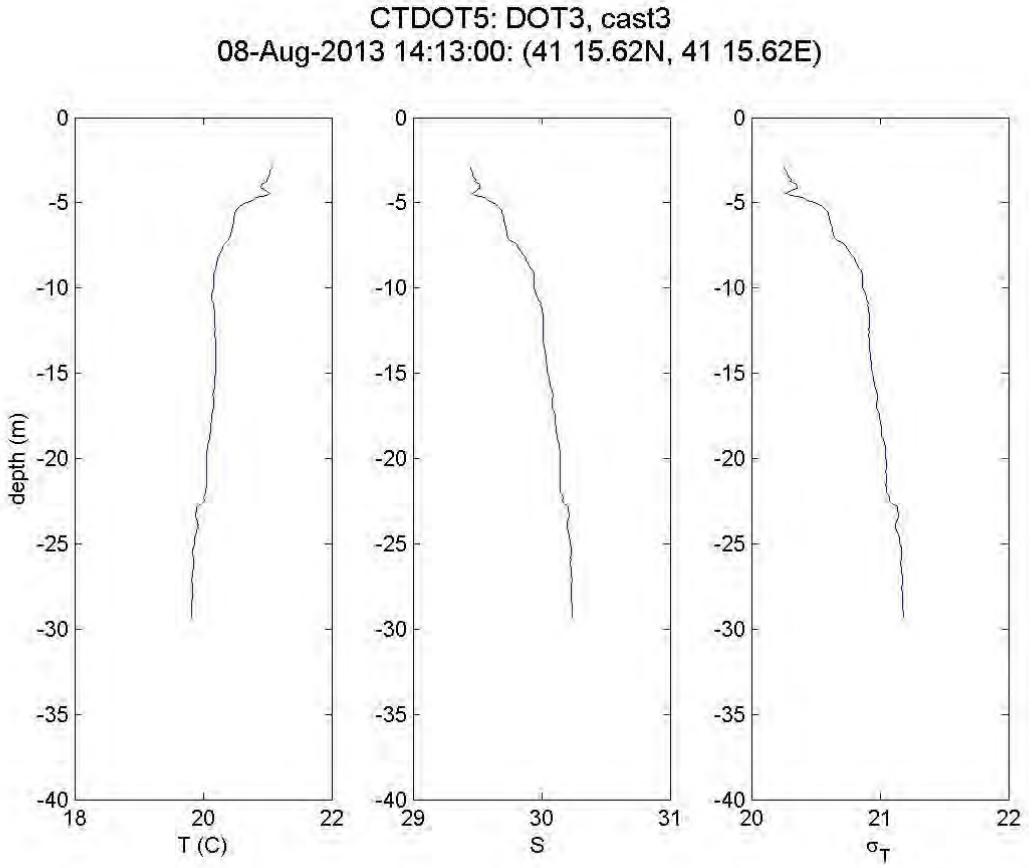

Figure 67: Cruise CTDOT5: Station DOT3, Cast 3: The left panel shows the vertical structure of Temperature (C) and the center and right panels show the salinity and density (σ_T) profiles respectively.

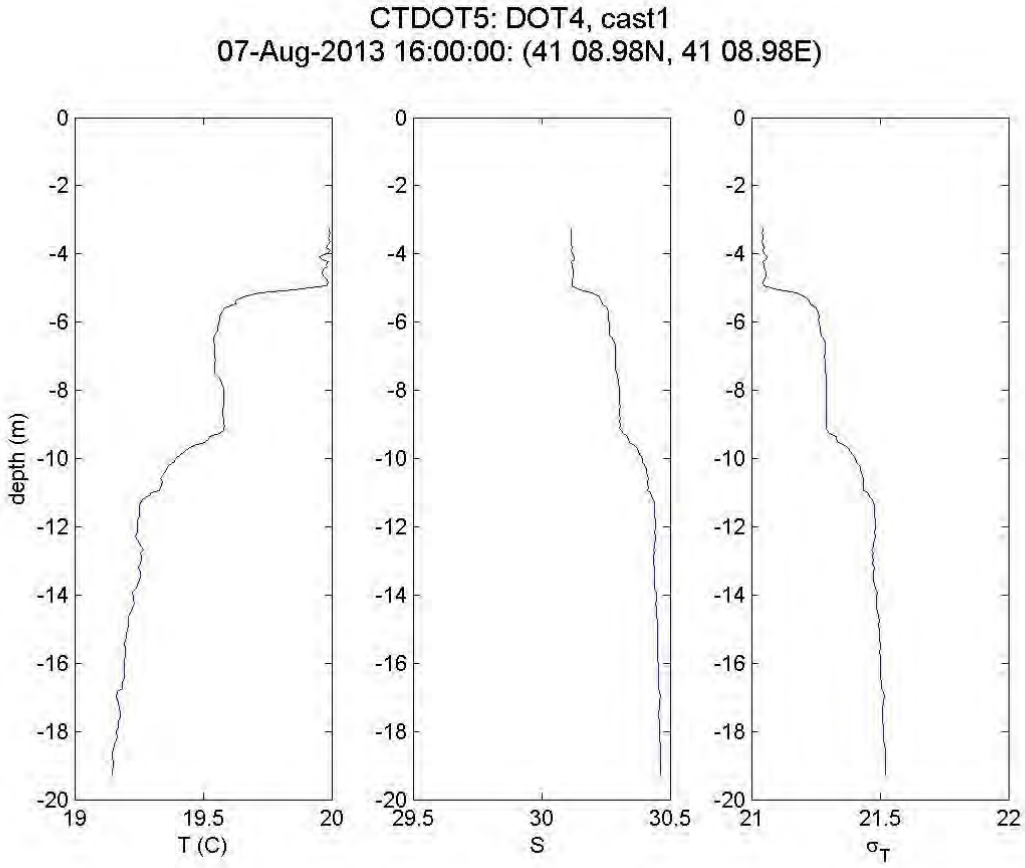

Figure 68: Cruise CTDOT5: Station DOT4, Cast 1: The left panel shows the vertical structure of Temperature (C) and the center and right panels show the salinity and density (σ_T) profiles respectively.

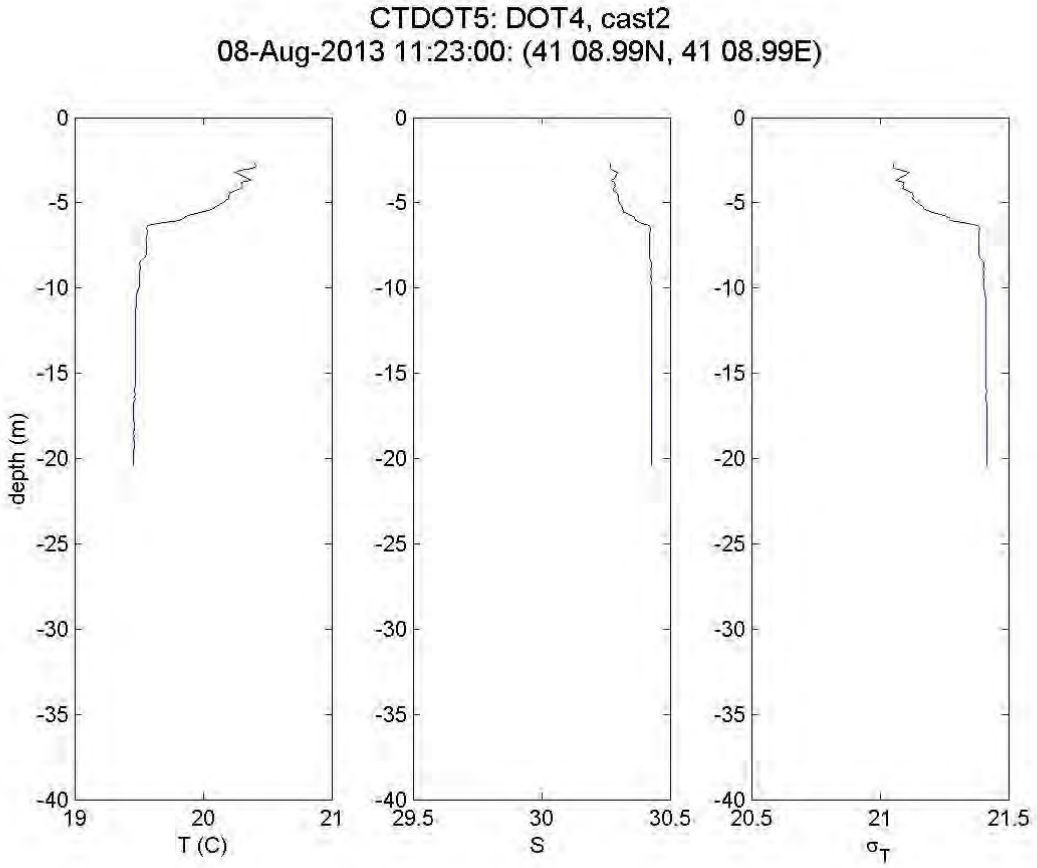

Figure 69: Cruise CTDOT5: Station DOT4, Cast 2: The left panel shows the vertical structure of Temperature (C) and the center and right panels show the salinity and density (σ_T) profiles respectively.

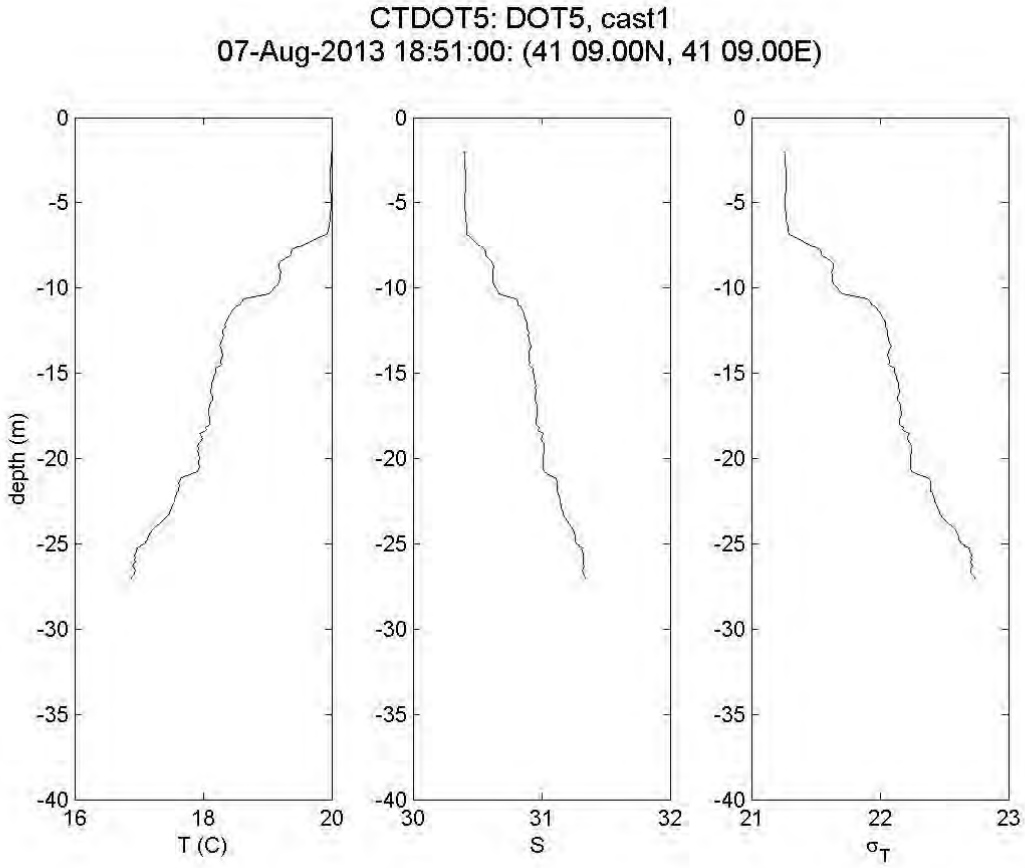

Figure 70: Cruise CTDOT5: Station DOT5, Cast 1: The left panel shows the vertical structure of Temperature (C) and the center and right panels show the salinity and density (σ_T) profiles respectively.

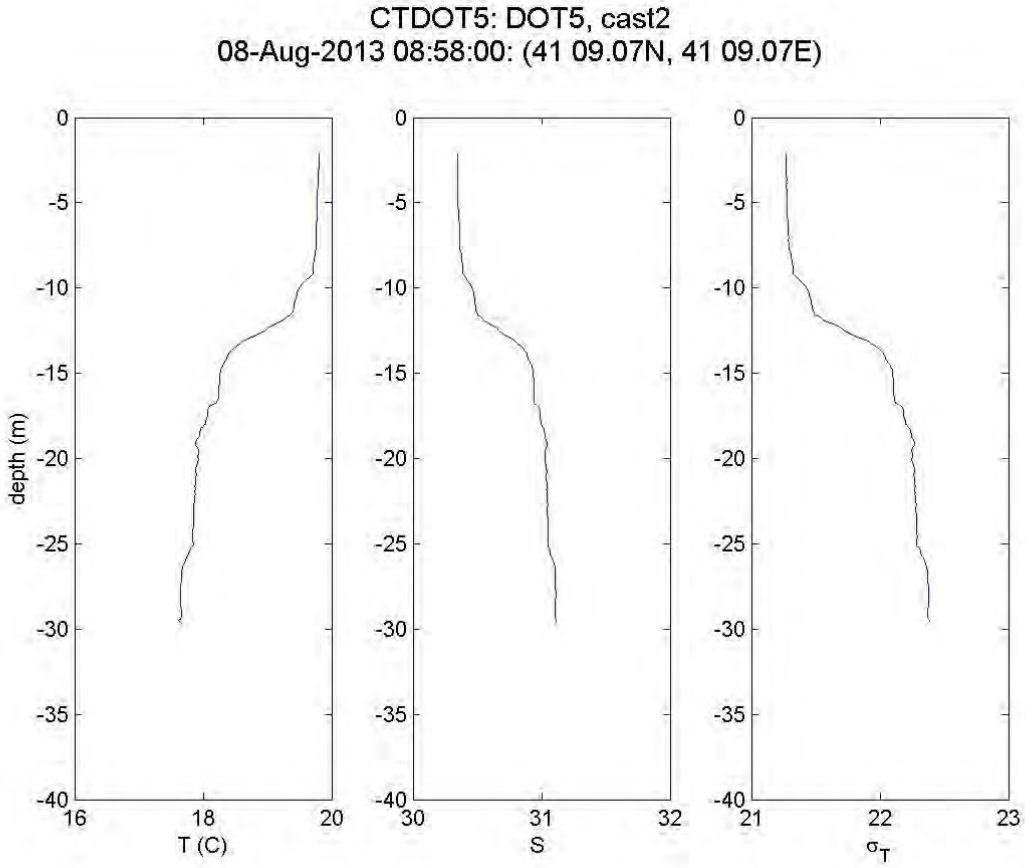

Figure 71: Cruise CTDOT5: Station DOT5, Cast 2: The left panel shows the vertical structure of Temperature (C) and the center and right panels show the salinity and density (σ_T) profiles respectively.

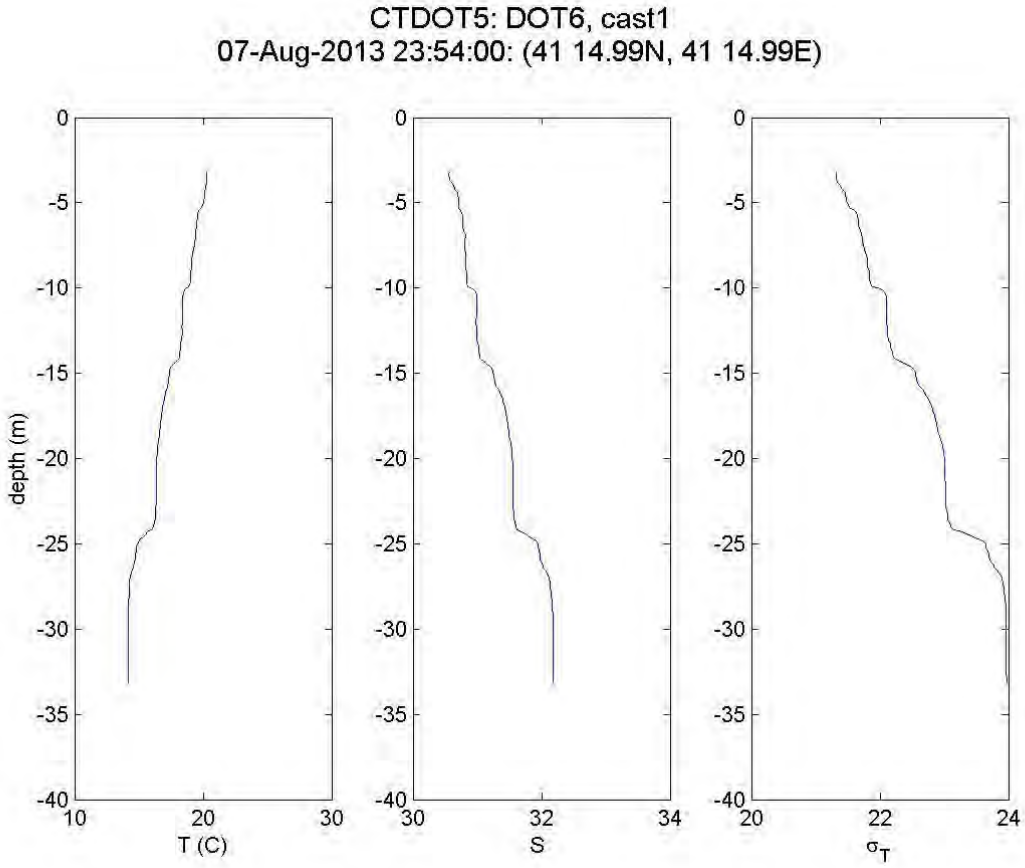

Figure 72: Cruise CTDOT5: Station DOT6, Cast 1: The left panel shows the vertical structure of Temperature (C) and the center and right panels show the salinity and density (σ_T) profiles respectively.

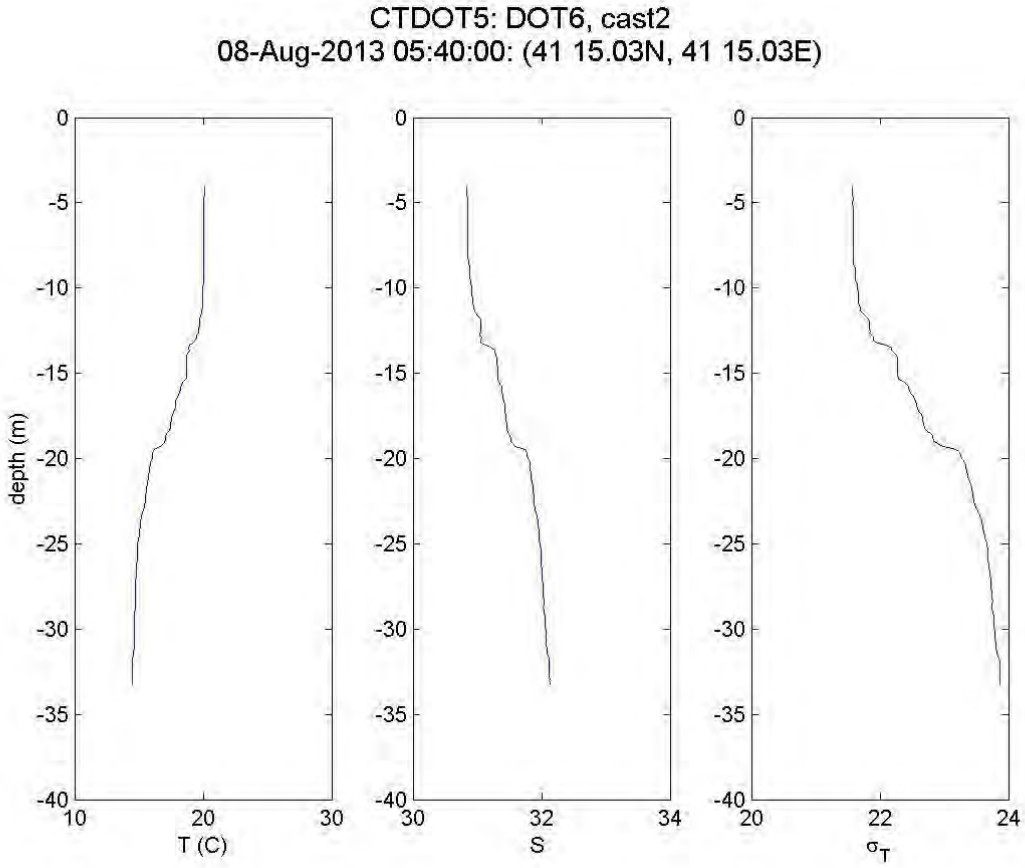

Figure 73: Cruise CTDOT5: Station DOT6, Cast 2: The left panel shows the vertical structure of Temperature (C) and the center and right panels show the salinity and density (σ_T) profiles respectively.

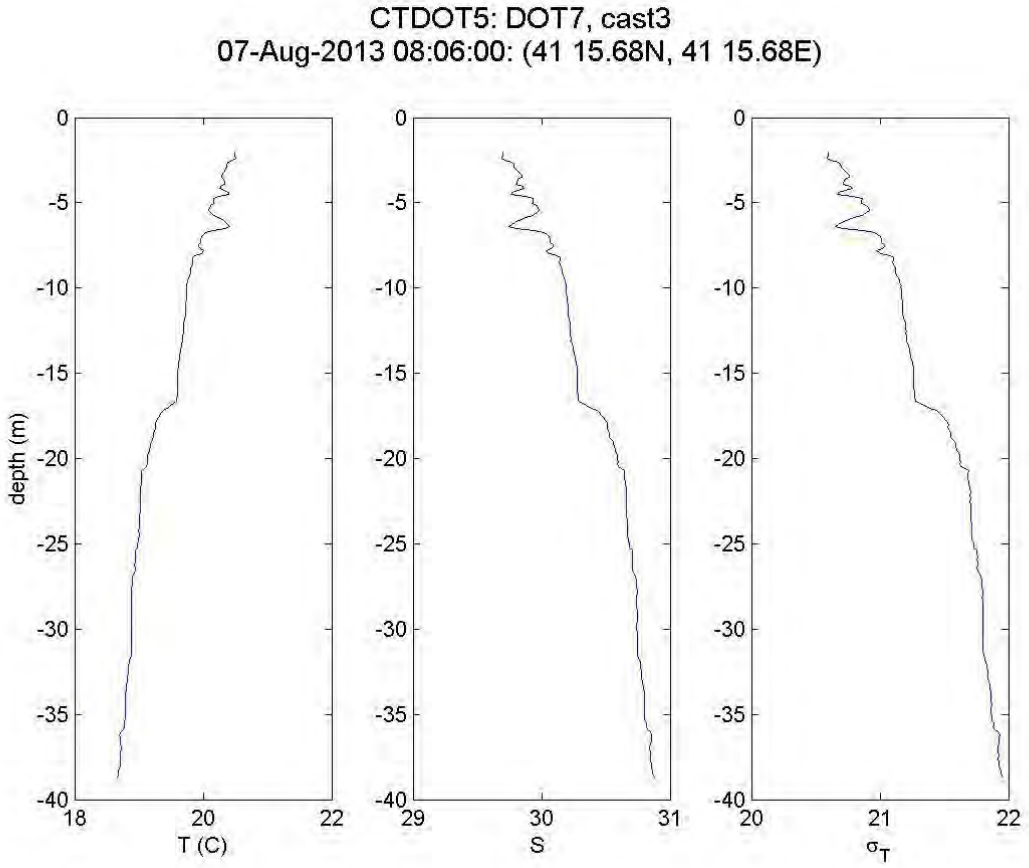

Figure 74: Cruise CTDOT5: Station DOT7, Cast 3: The left panel shows the vertical structure of Temperature (C) and the center and right panels show the salinity and density (σ_T) profiles respectively.

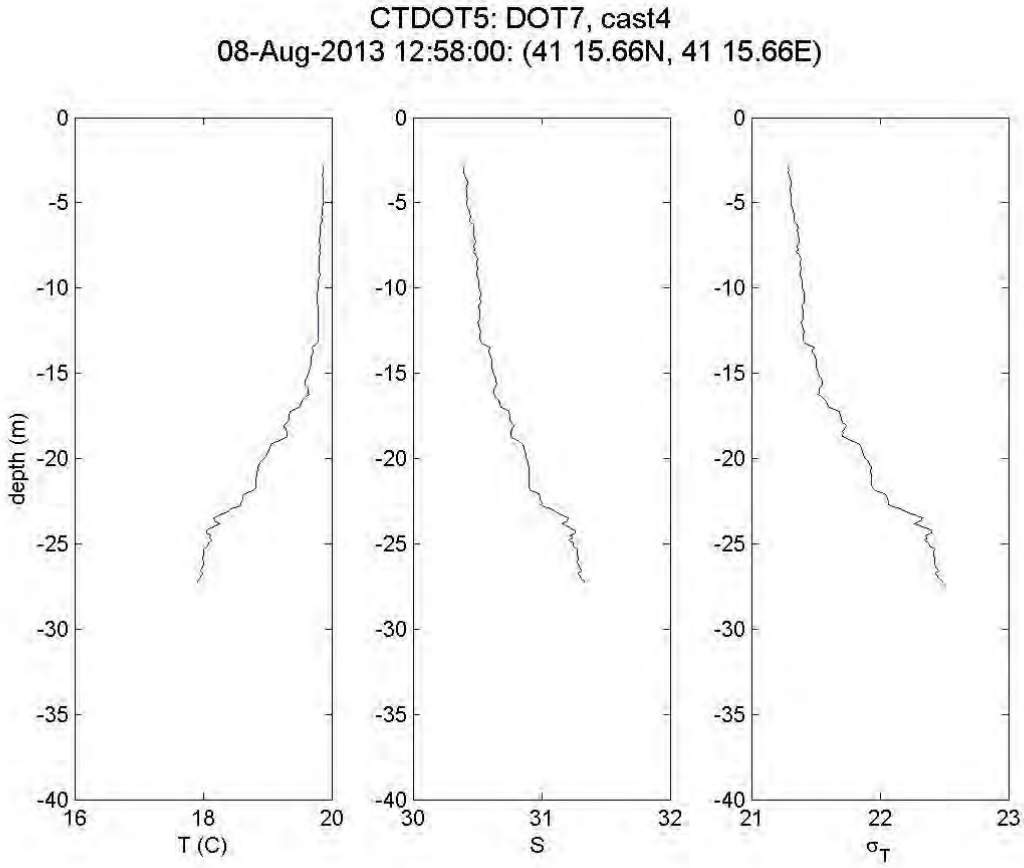

Figure 75: Cruise CTDOT5: Station DOT7, Cast 4: The left panel shows the vertical structure of Temperature (C) and the center and right panels show the salinity and density (σ_T) profiles respectively.

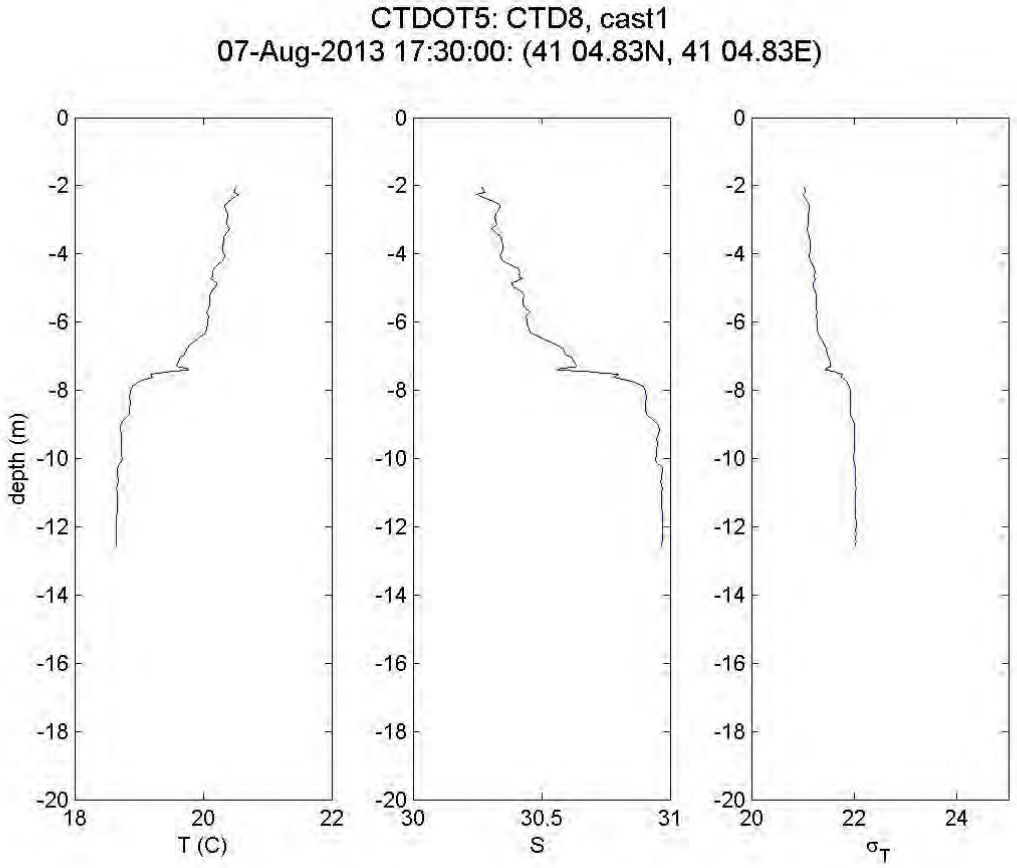

Figure 76: Cruise CTDOT5: Station CTD8, Cast 1: The left panel shows the vertical structure of Temperature (C) and the center and right panels show the salinity and density (σ_T) profiles respectively.

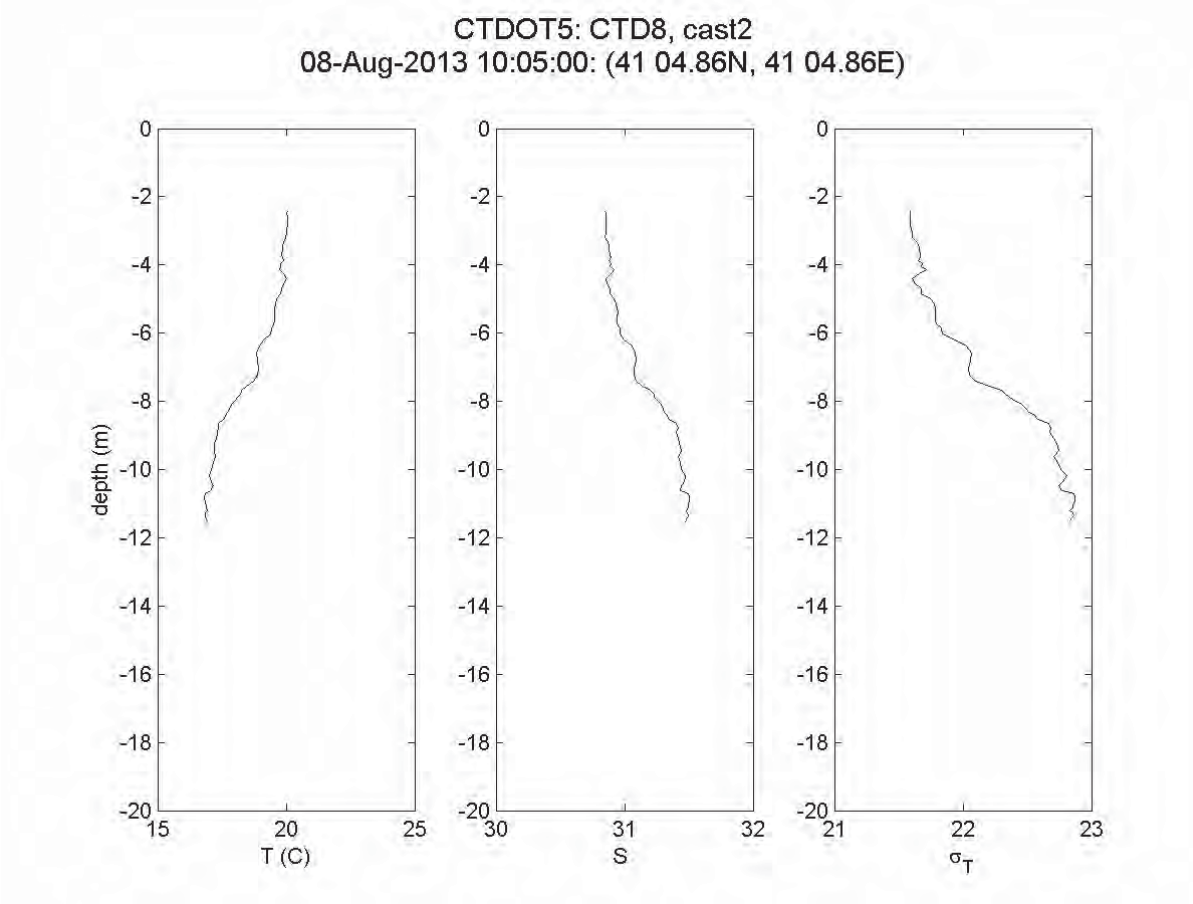

Figure 77: Cruise CTDOT5: Station CTD8, Cast 2: The left panel shows the vertical structure of Temperature (C) and the center and right panels show the salinity and density (σ_T) profiles respectively.

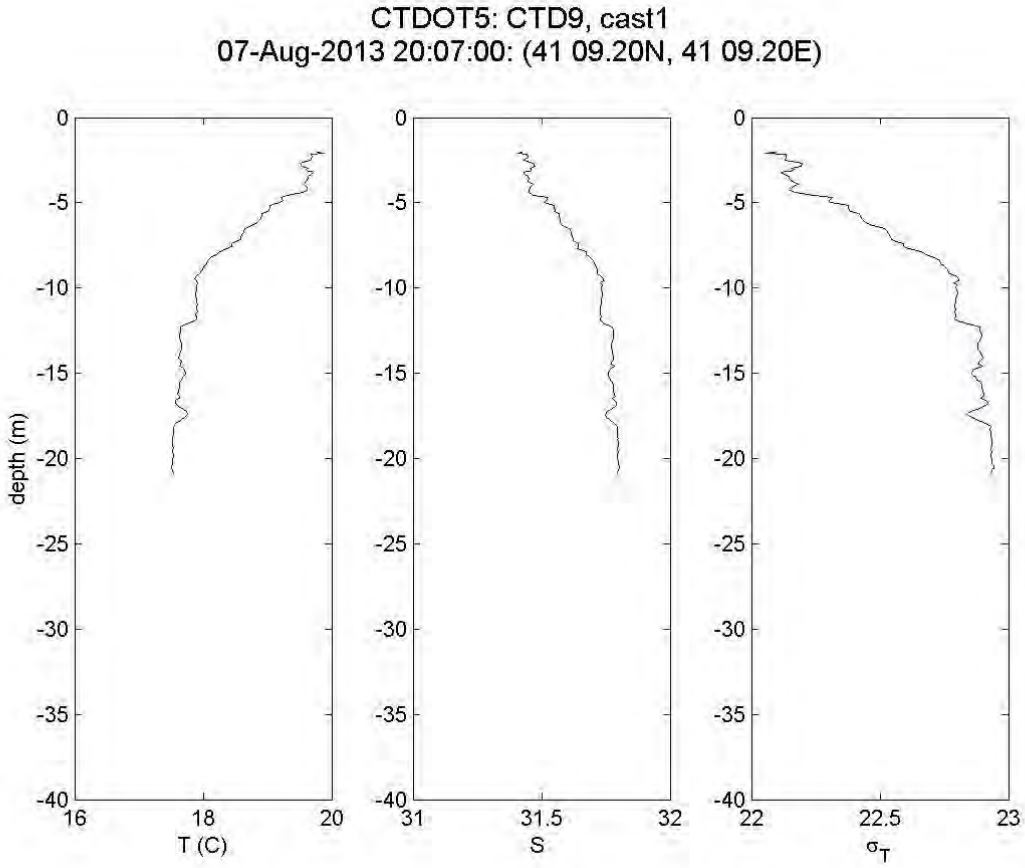

Figure 78: Cruise CTDOT5: Station CTD9, Cast 1: The left panel shows the vertical structure of Temperature (C) and the center and right panels show the salinity and density (σ_T) profiles respectively.

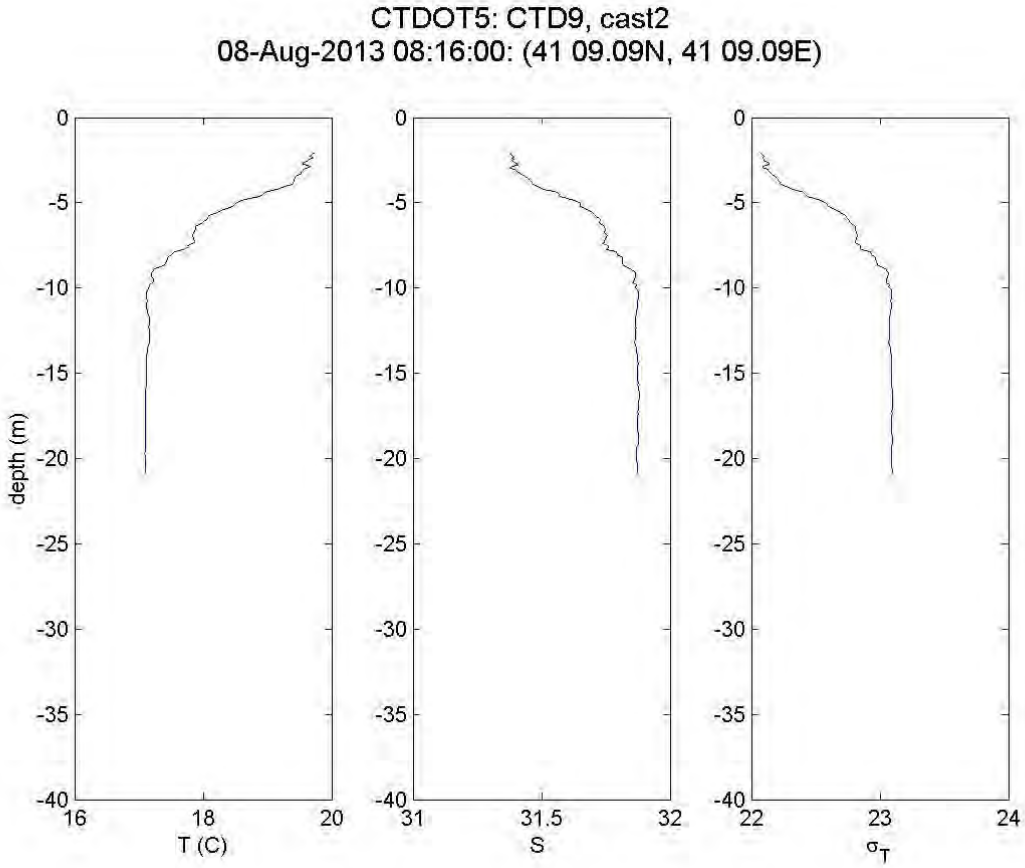

Figure 79: Cruise CTDOT5: Station CTD9, Cast 2: The left panel shows the vertical structure of Temperature (C) and the center and right panels show the salinity and density (σ_T) profiles respectively.

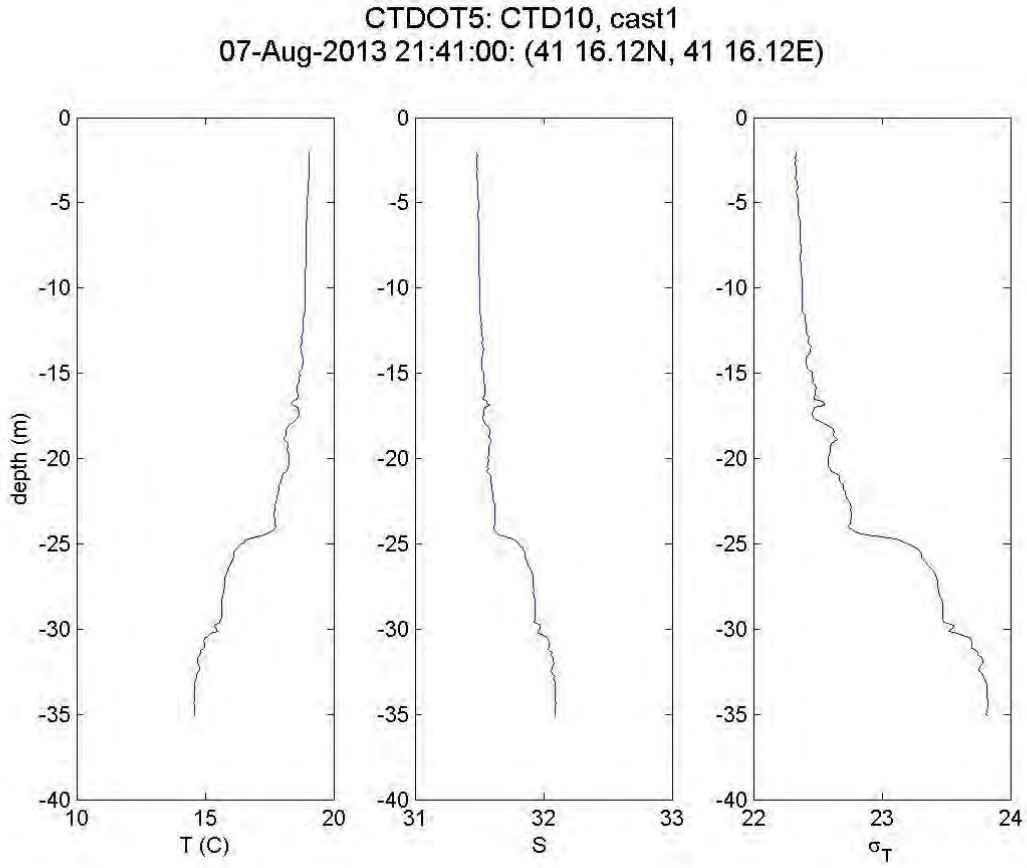

Figure 80: Cruise CTDOT5: Station CTD10, Cast 1: The left panel shows the vertical structure of Temperature (C) and the center and right panels show the salinity and density (σ_T) profiles respectively.

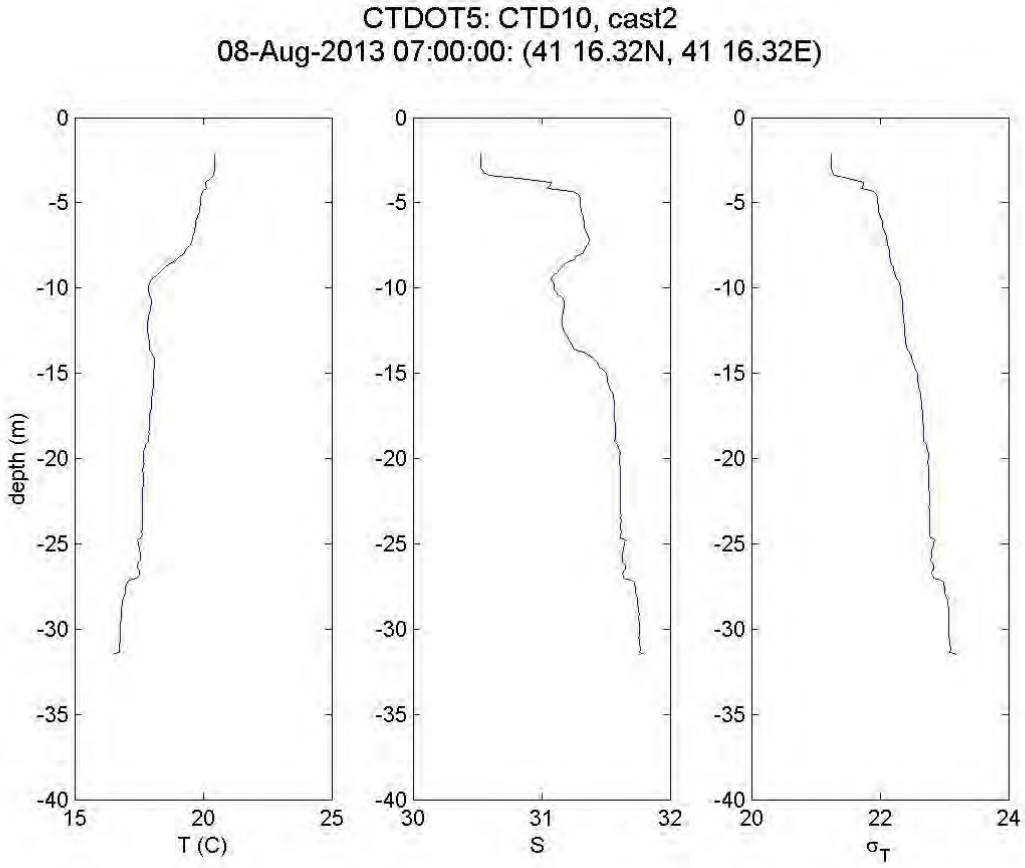

Figure 81: Cruise CTDOT5: Station CTD10, Cast 2: The left panel shows the vertical structure of Temperature (C) and the center and right panels show the salinity and density (σ_T) profiles respectively.

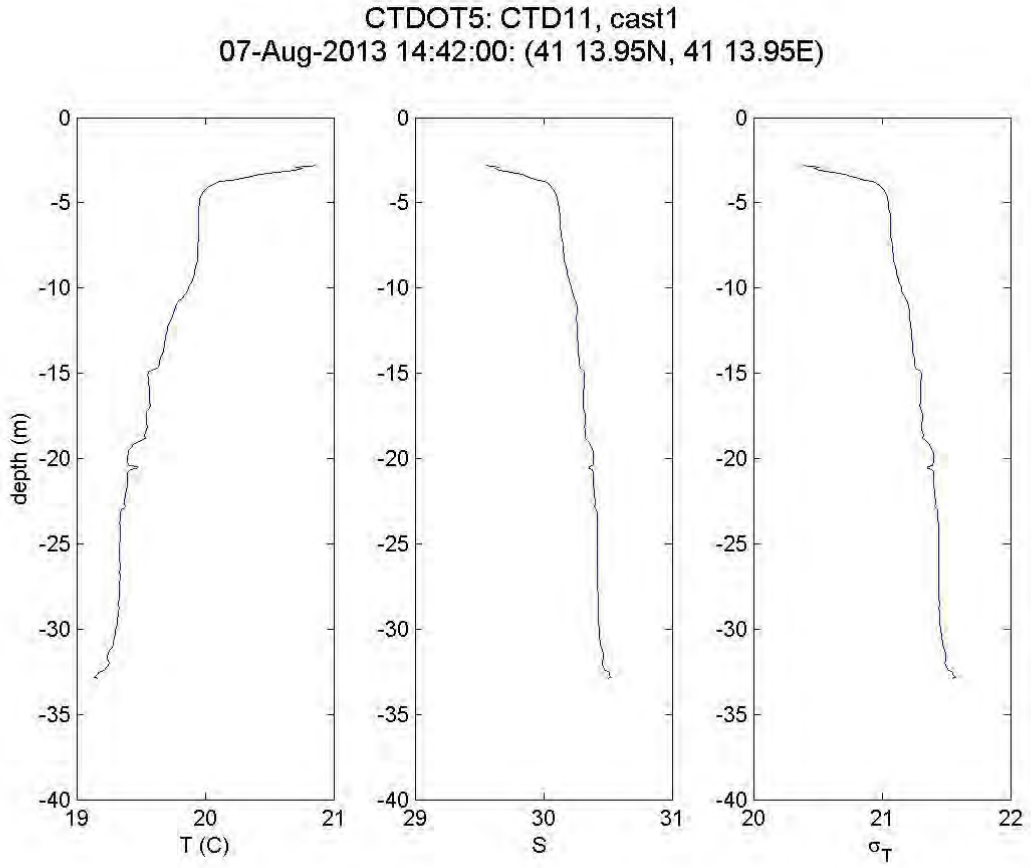

Figure 82: Cruise CTDOT5: Station CTD11, Cast 1: The left panel shows the vertical structure of Temperature (C) and the center and right panels show the salinity and density (σ_T) profiles respectively.

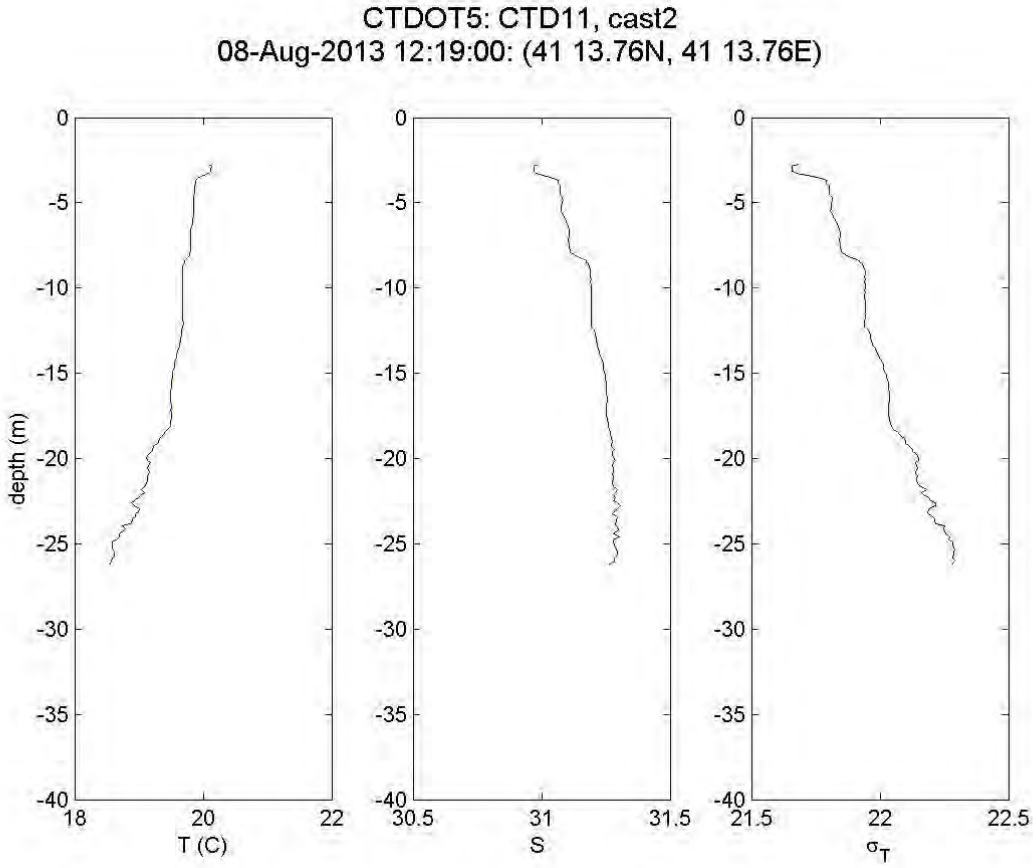

Figure 83: Cruise CTDOT5: Station CTD11, Cast 2: The left panel shows the vertical structure of Temperature (C) and the center and right panels show the salinity and density (σ_T) profiles respectively.

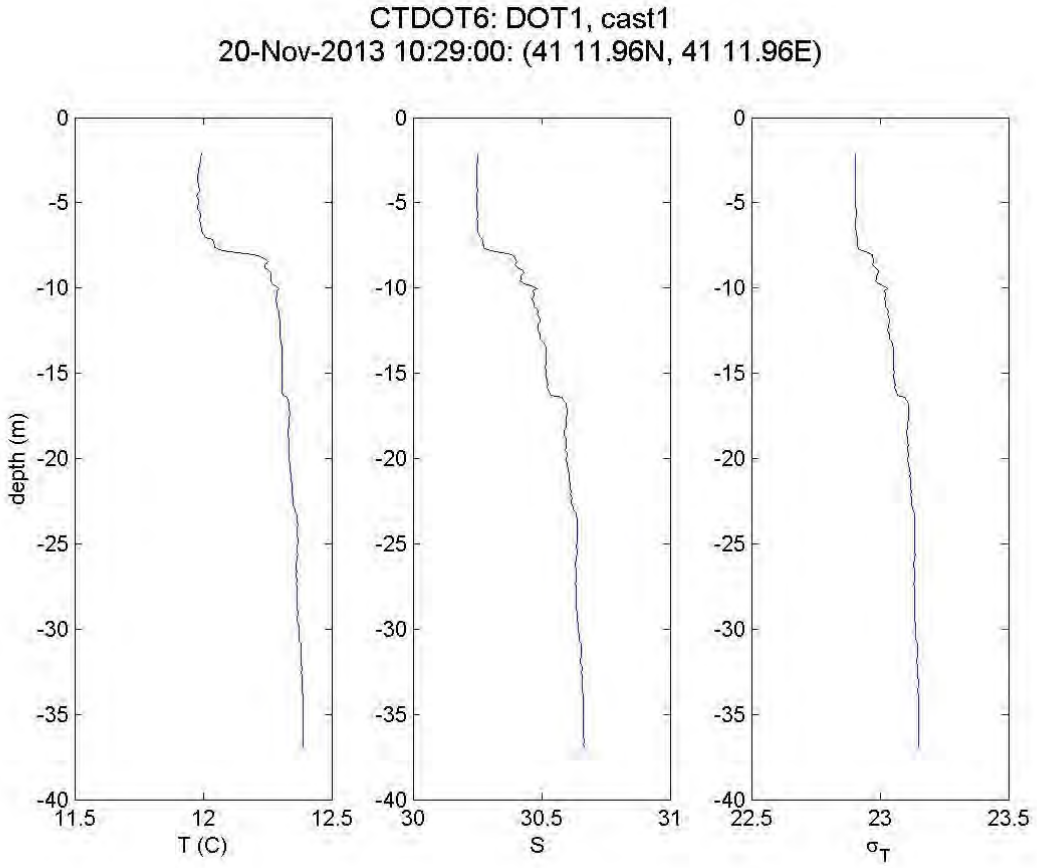

Figure 84: Cruise CTDOT6: Station DOT1, Cast 1: The left panel shows the vertical structure of Temperature (C) and the center and right panels show the salinity and density (σ_T) profiles respectively.

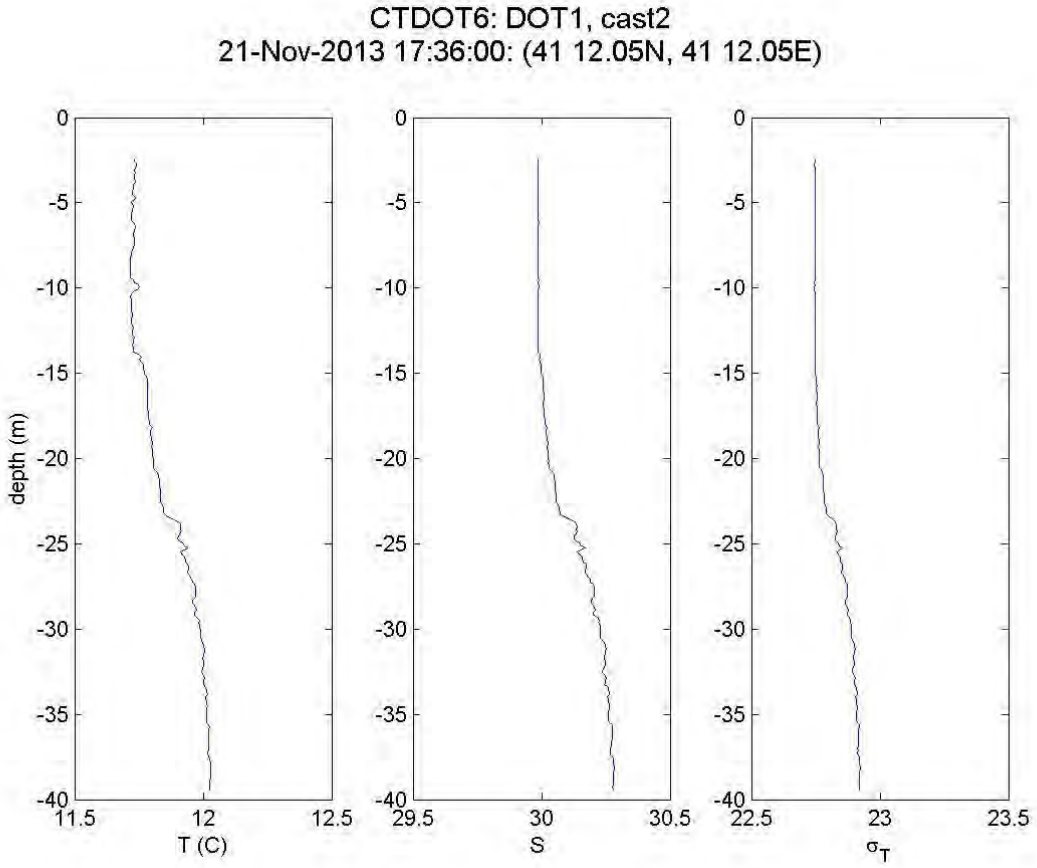

Figure 85: Cruise CTDOT6: Station DOT1, Cast 2: The left panel shows the vertical structure of Temperature (C) and the center and right panels show the salinity and density (σ_T) profiles respectively.

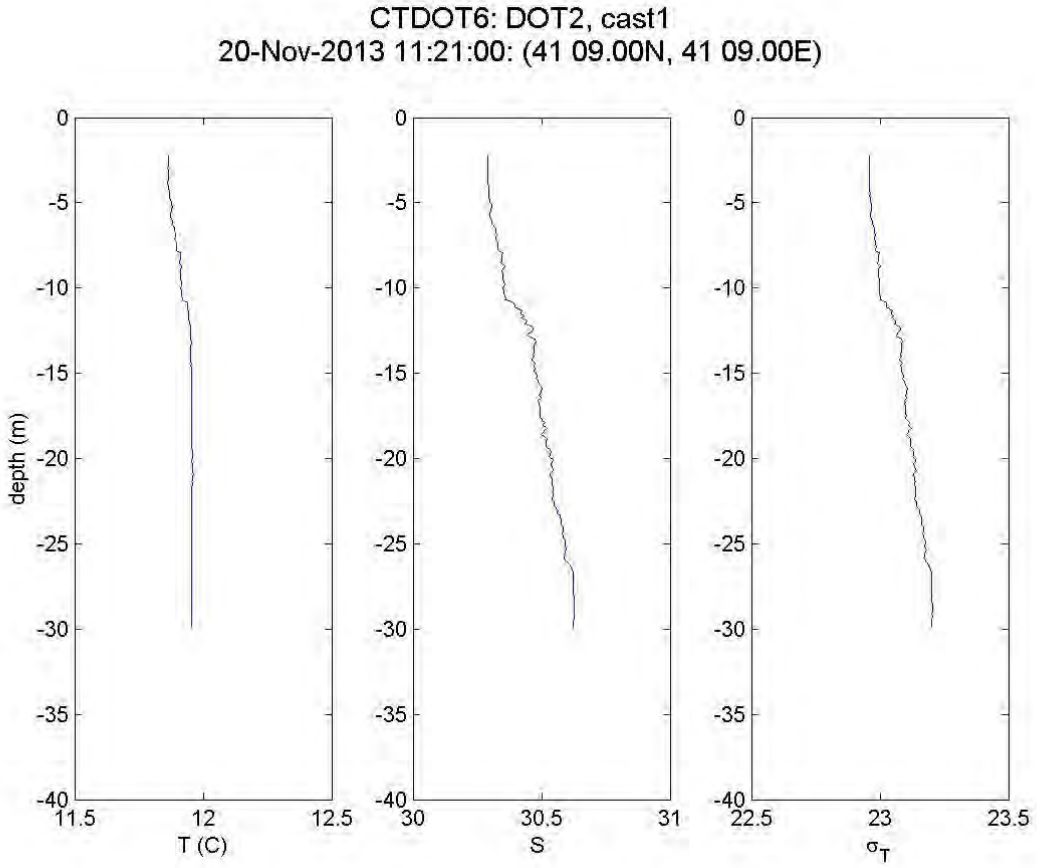

Figure 86: Cruise CTDOT6: Station DOT2, Cast 1: The left panel shows the vertical structure of Temperature (C) and the center and right panels show the salinity and density (σ_T) profiles respectively.

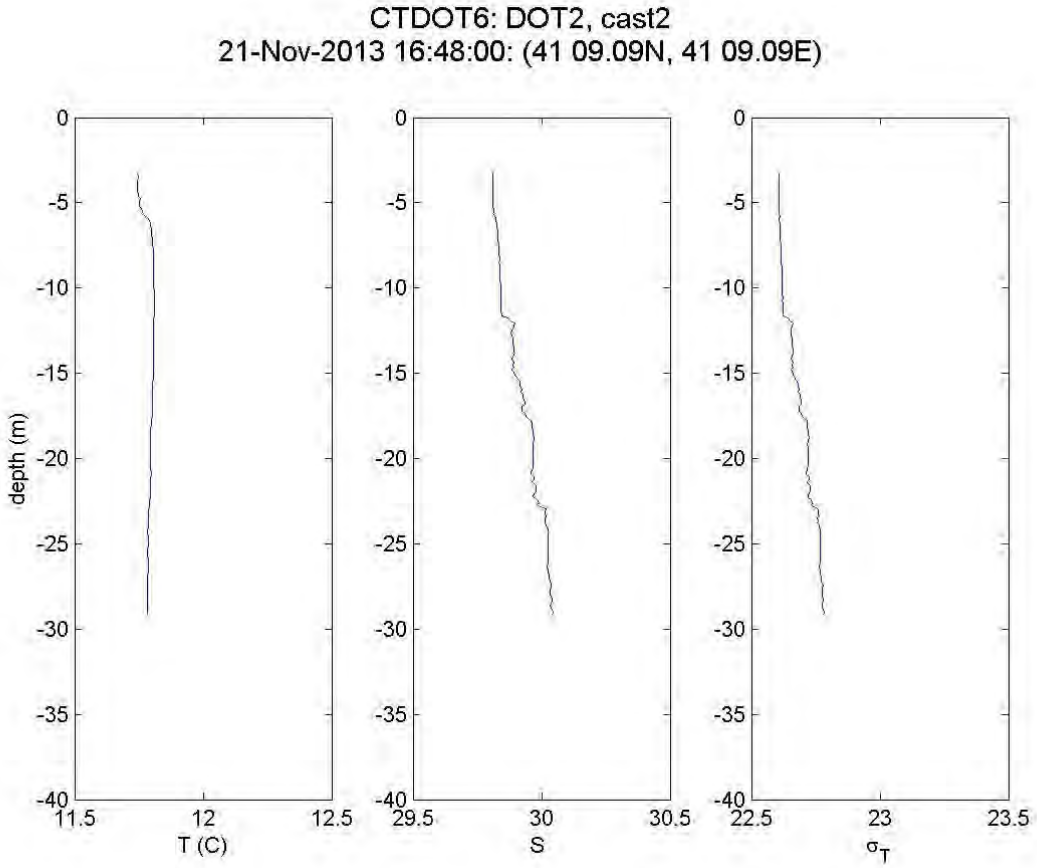

Figure 87: Cruise CTDOT6: Station DOT2, Cast 2: The left panel shows the vertical structure of Temperature (C) and the center and right panels show the salinity and density (σ_T) profiles respectively.

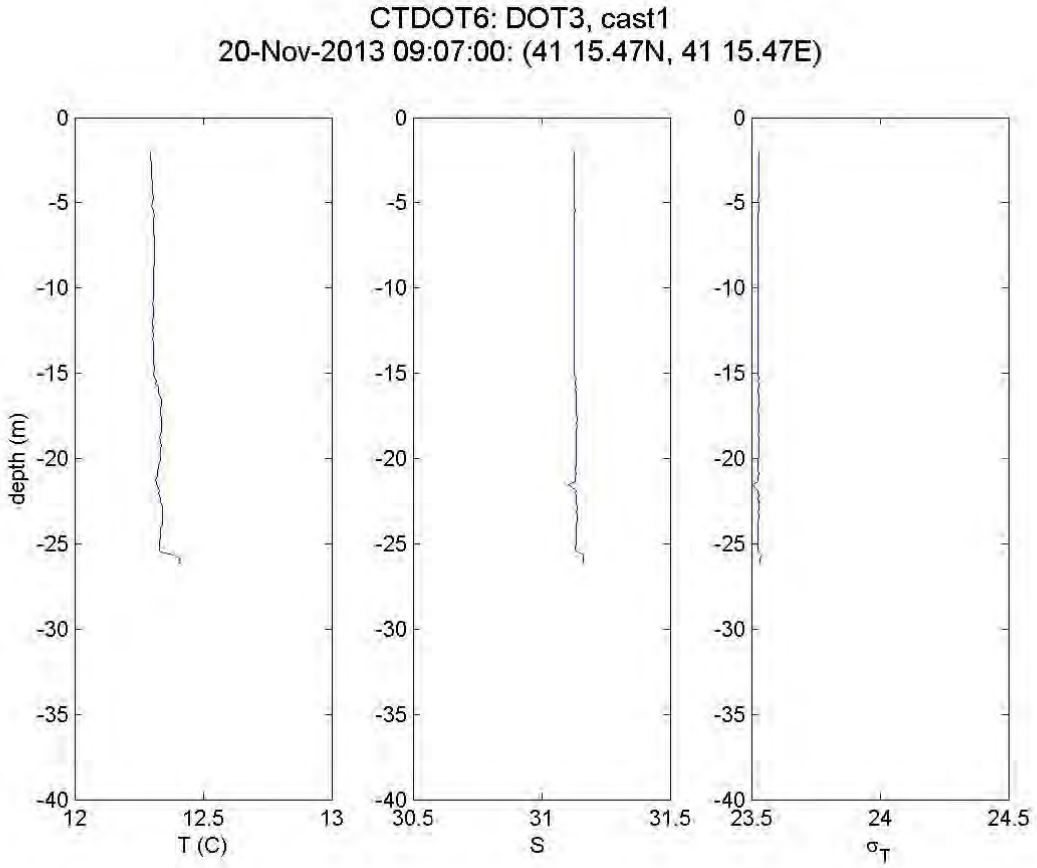

Figure 88: Cruise CTDOT6: Station DOT3, Cast 1: The left panel shows the vertical structure of Temperature (C) and the center and right panels show the salinity and density (σ_T) profiles respectively.

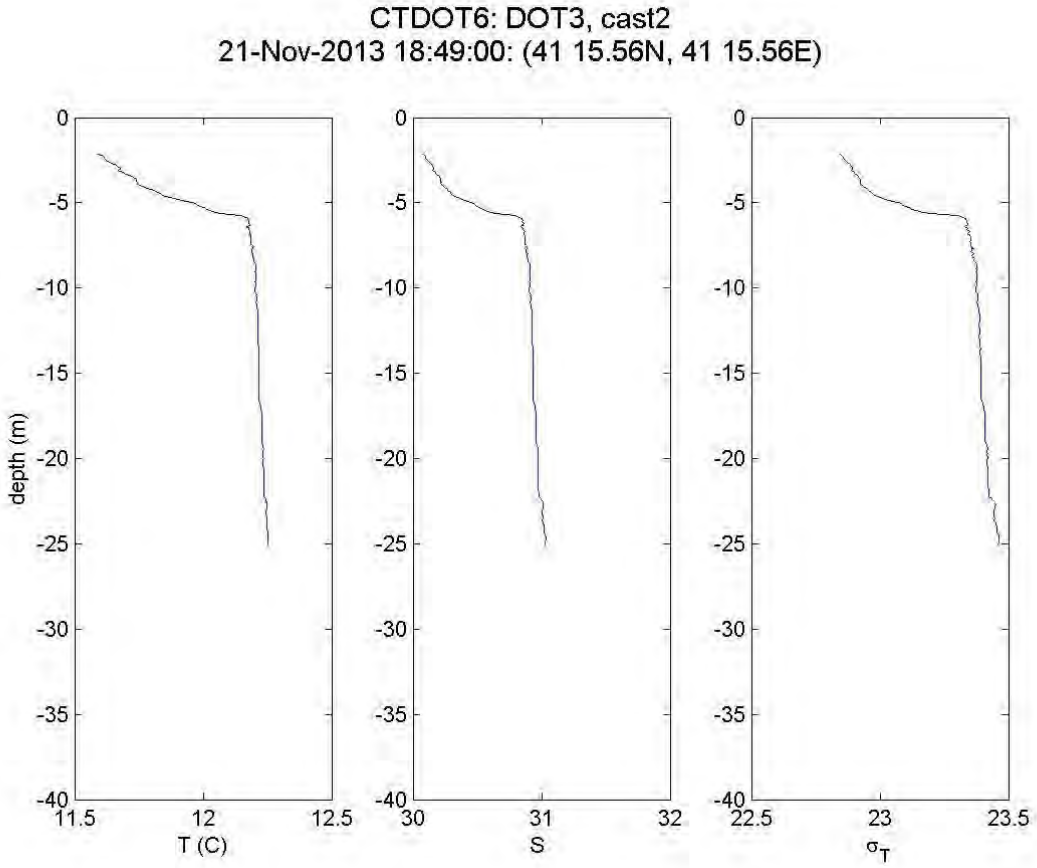

Figure 89: Cruise CTDOT6: Station DOT3, Cast 2: The left panel shows the vertical structure of Temperature (C) and the center and right panels show the salinity and density (σ_T) profiles respectively.

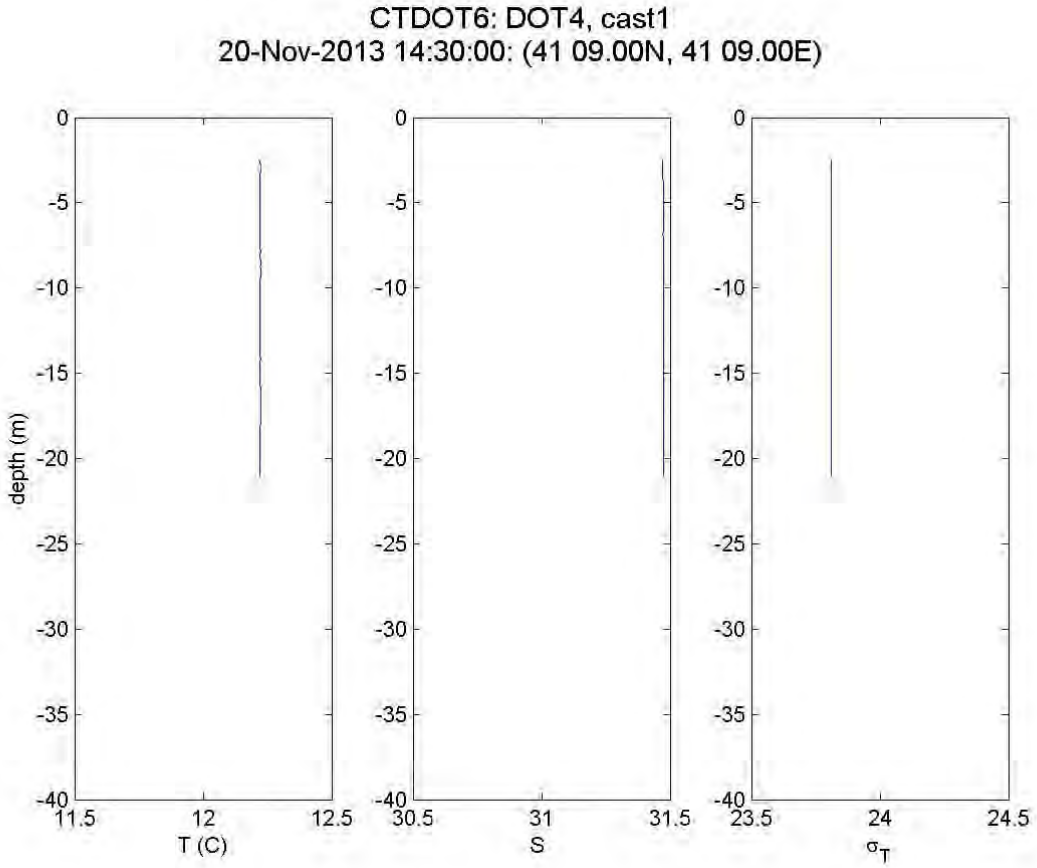

Figure 90: Cruise CTDOT6: Station DOT4, Cast 1: The left panel shows the vertical structure of Temperature (C) and the center and right panels show the salinity and density (σ_T) profiles respectively.

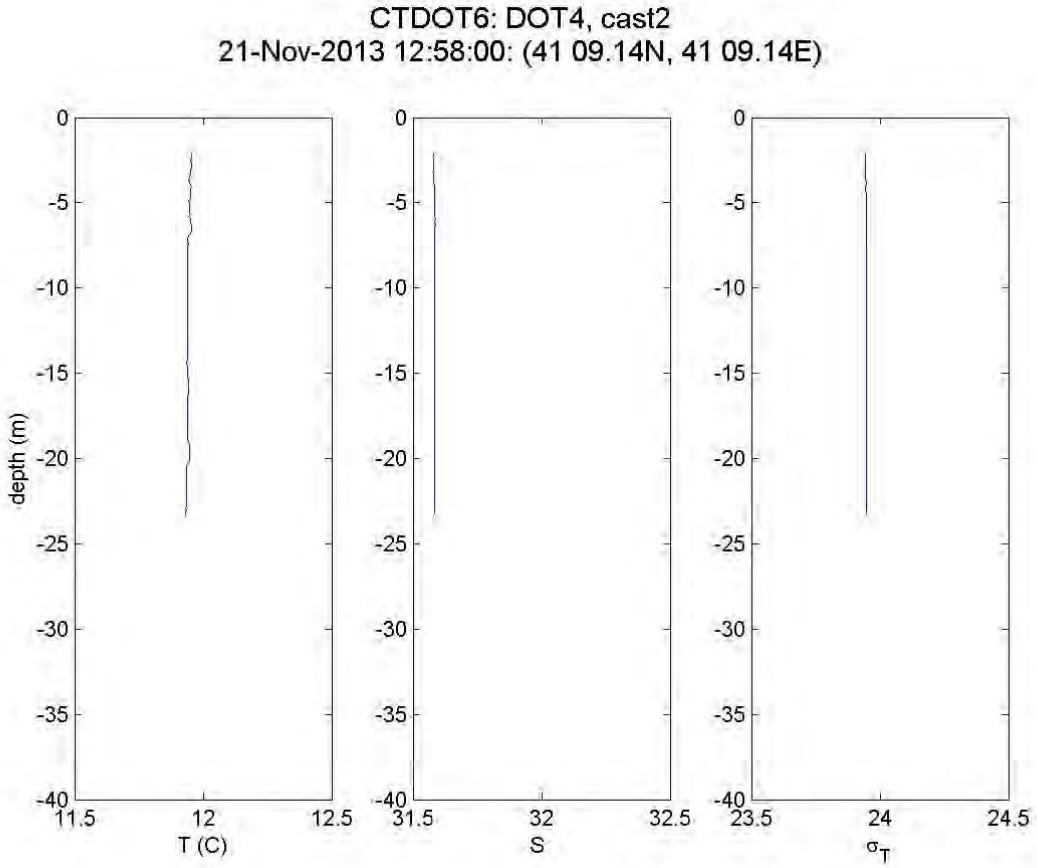

Figure 91: Cruise CTDOT6: Station DOT4, Cast 2: The left panel shows the vertical structure of Temperature (C) and the center and right panels show the salinity and density (σ_T) profiles respectively.

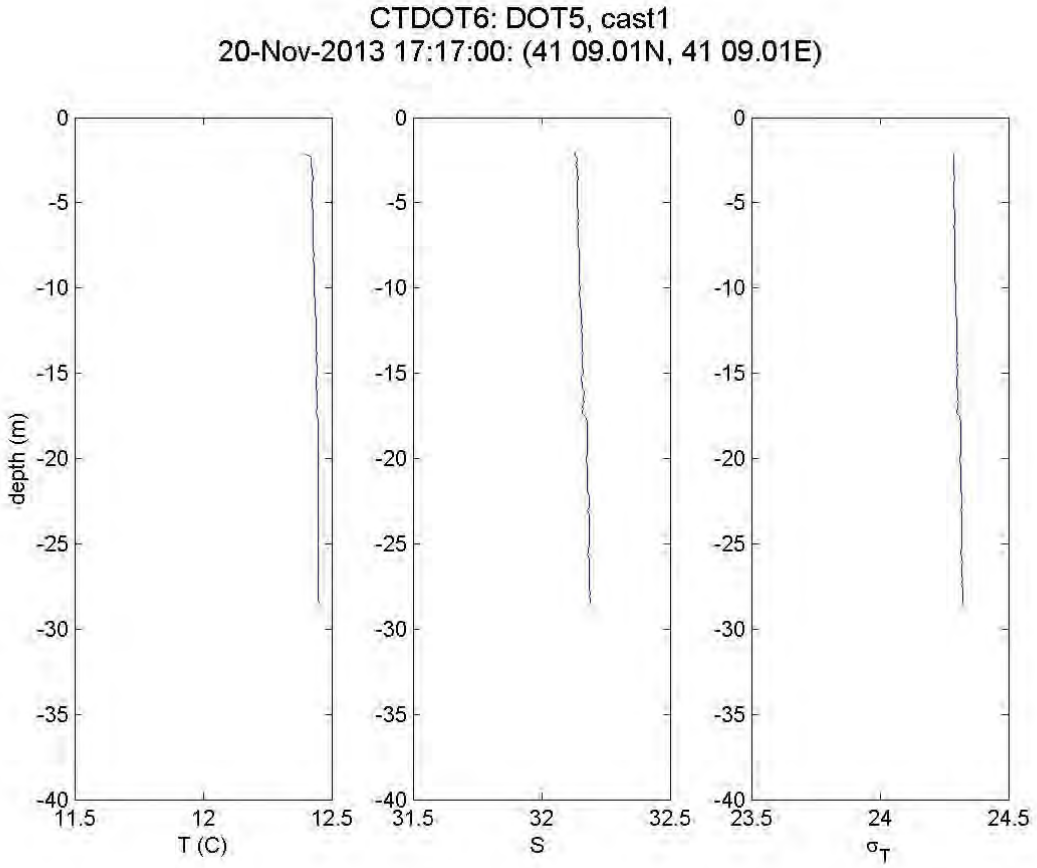

Figure 92: Cruise CTDOT6: Station DOT5, Cast 1: The left panel shows the vertical structure of Temperature (C) and the center and right panels show the salinity and density (σ_T) profiles respectively.

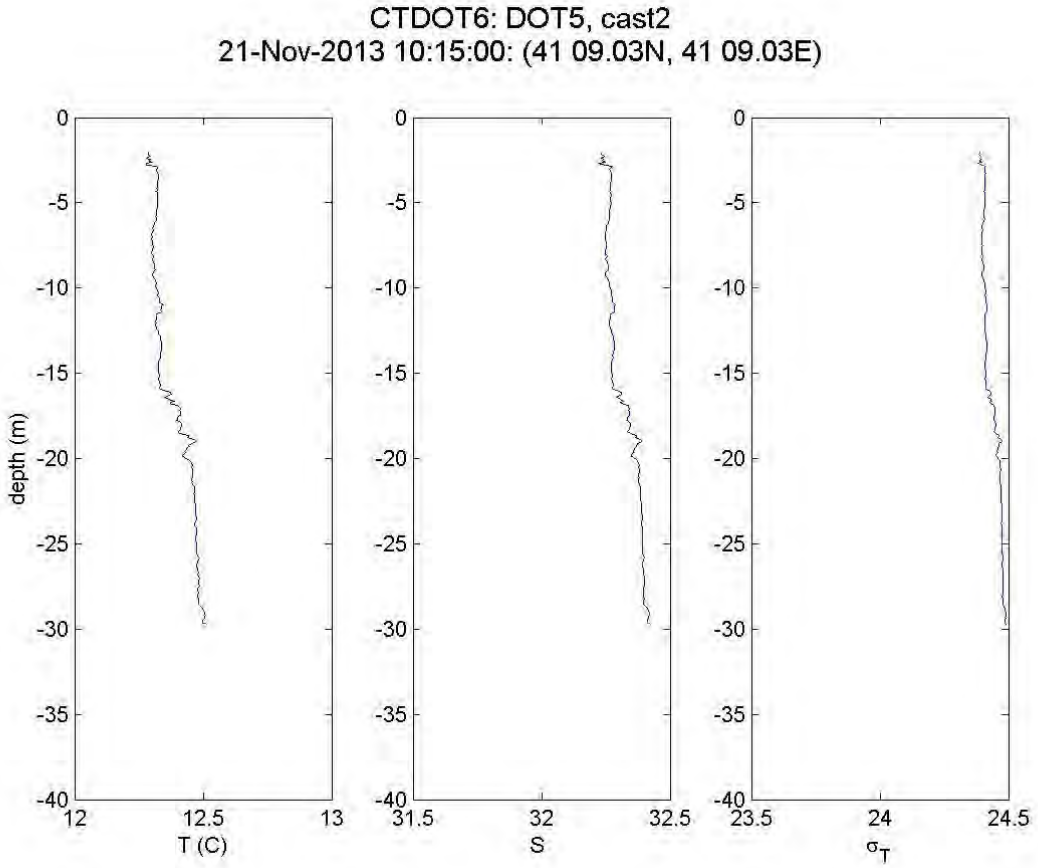

Figure 93: Cruise CTDOT6: Station DOT5, Cast 2: The left panel shows the vertical structure of Temperature (C) and the center and right panels show the salinity and density (σ_T) profiles respectively.

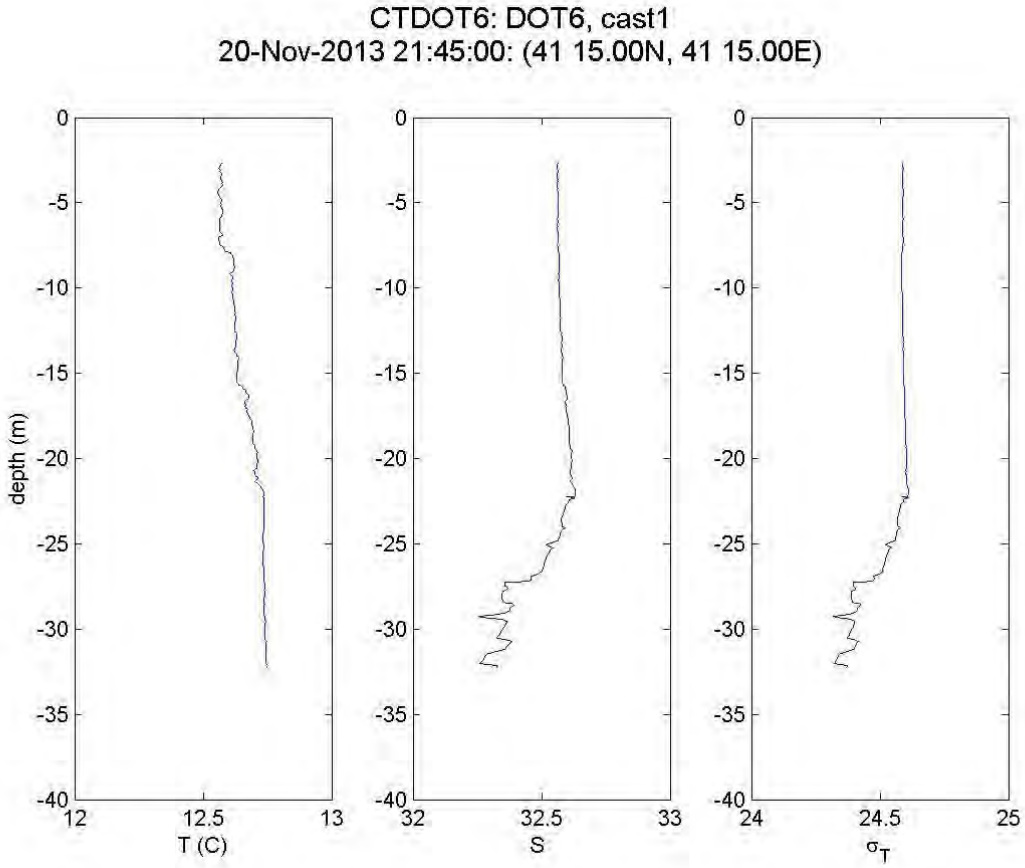

Figure 94: Cruise CTDOT6: Station DOT6, Cast 1: The left panel shows the vertical structure of Temperature (C) and the center and right panels show the salinity and density (σ_T) profiles respectively.

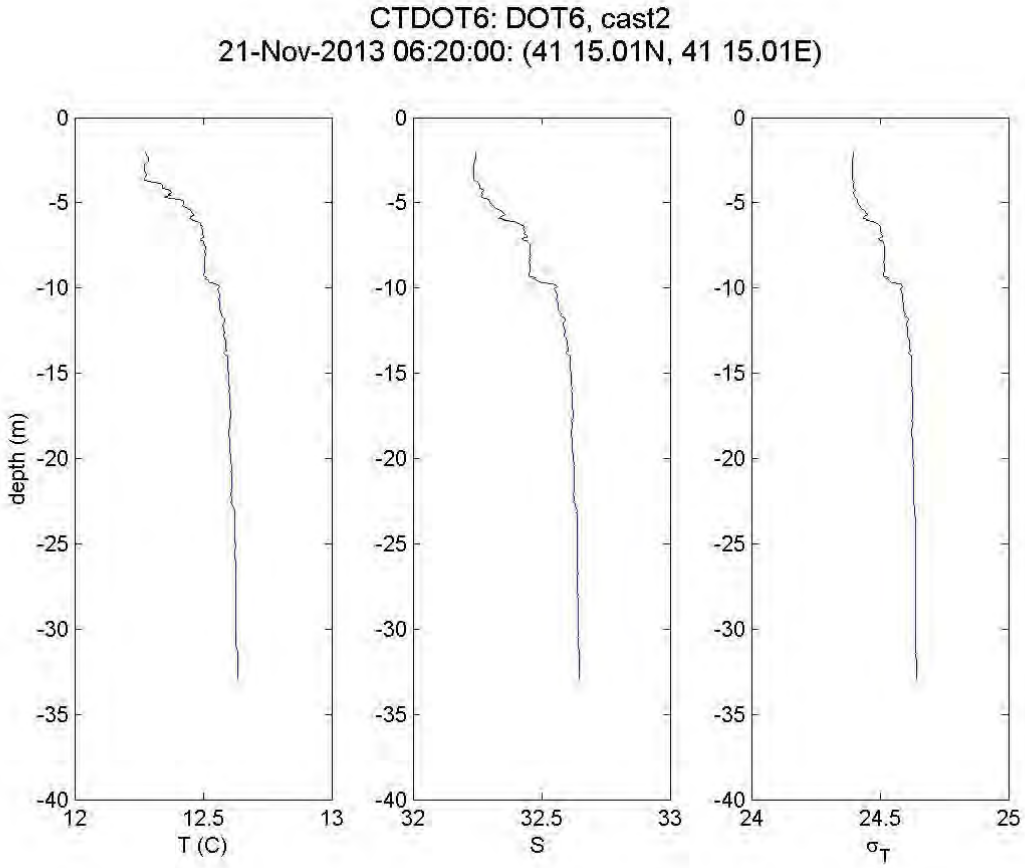

Figure 95: Cruise CTDOT6: Station DOT6, Cast 2: The left panel shows the vertical structure of Temperature (C) and the center and right panels show the salinity and density (σ_T) profiles respectively.

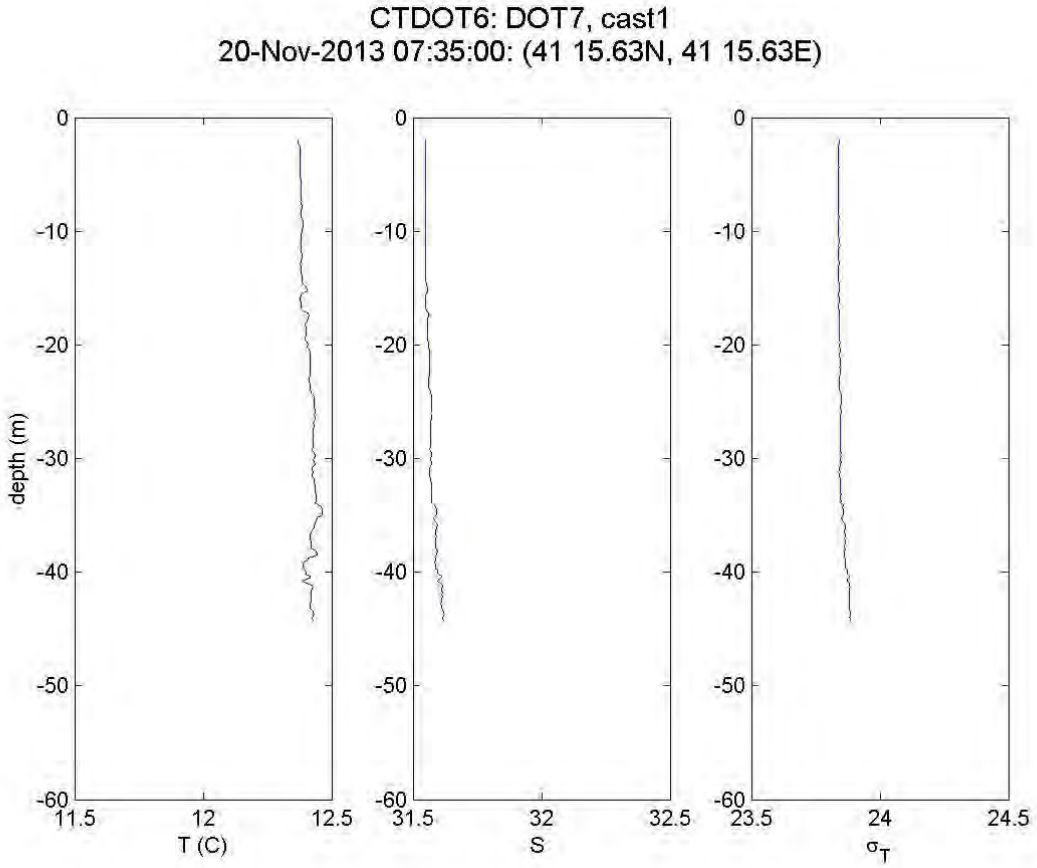

Figure 96: Cruise CTDOT6: Station DOT7, Cast 1: The left panel shows the vertical structure of Temperature (C) and the center and right panels show the salinity and density (σ_T) profiles respectively.

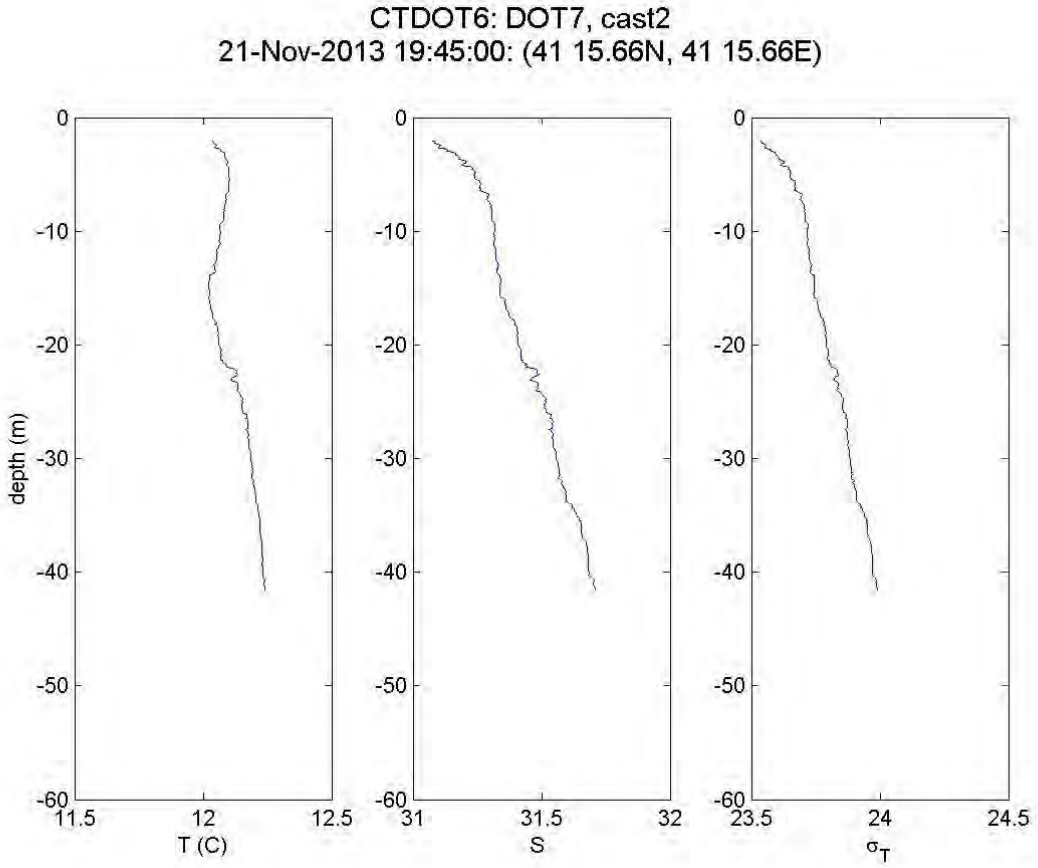

Figure 97: Cruise CTDOT6: Station DOT7, Cast 2: The left panel shows the vertical structure of Temperature (C) and the center and right panels show the salinity and density (σ_T) profiles respectively.

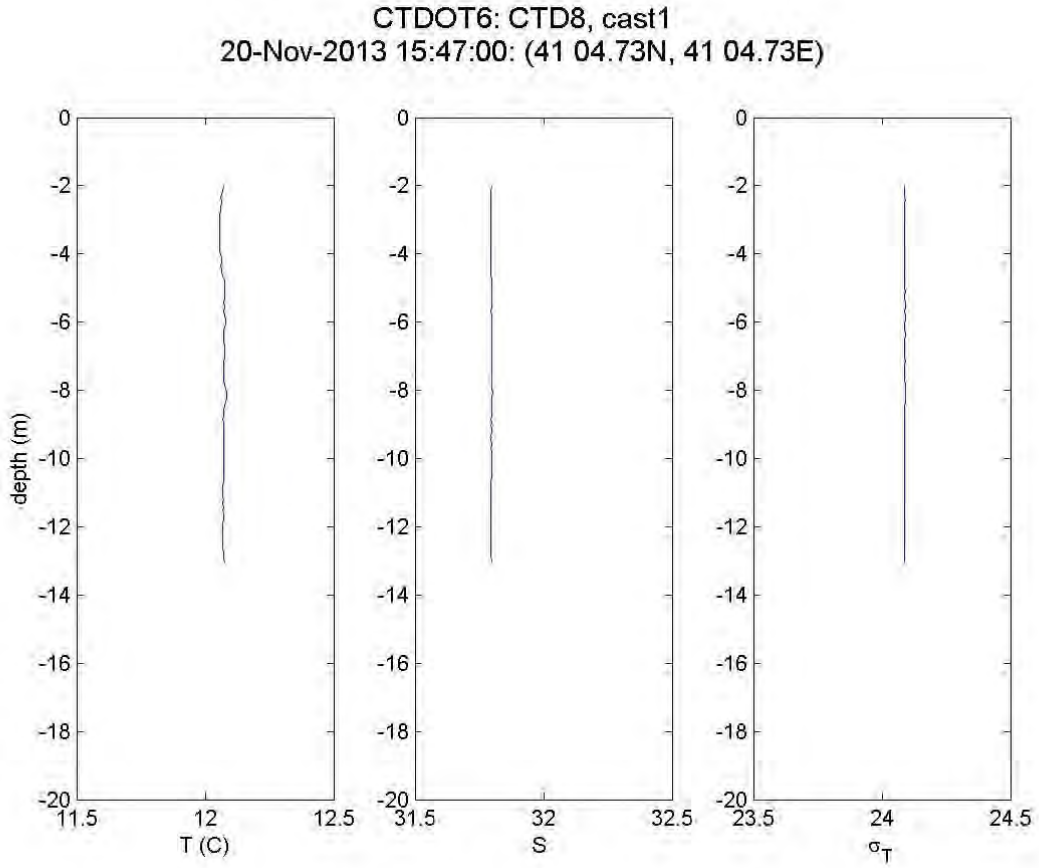

Figure 98: Cruise CTDOT6: Station CTD8, Cast 1: The left panel shows the vertical structure of Temperature (C) and the center and right panels show the salinity and density (σ_T) profiles respectively.

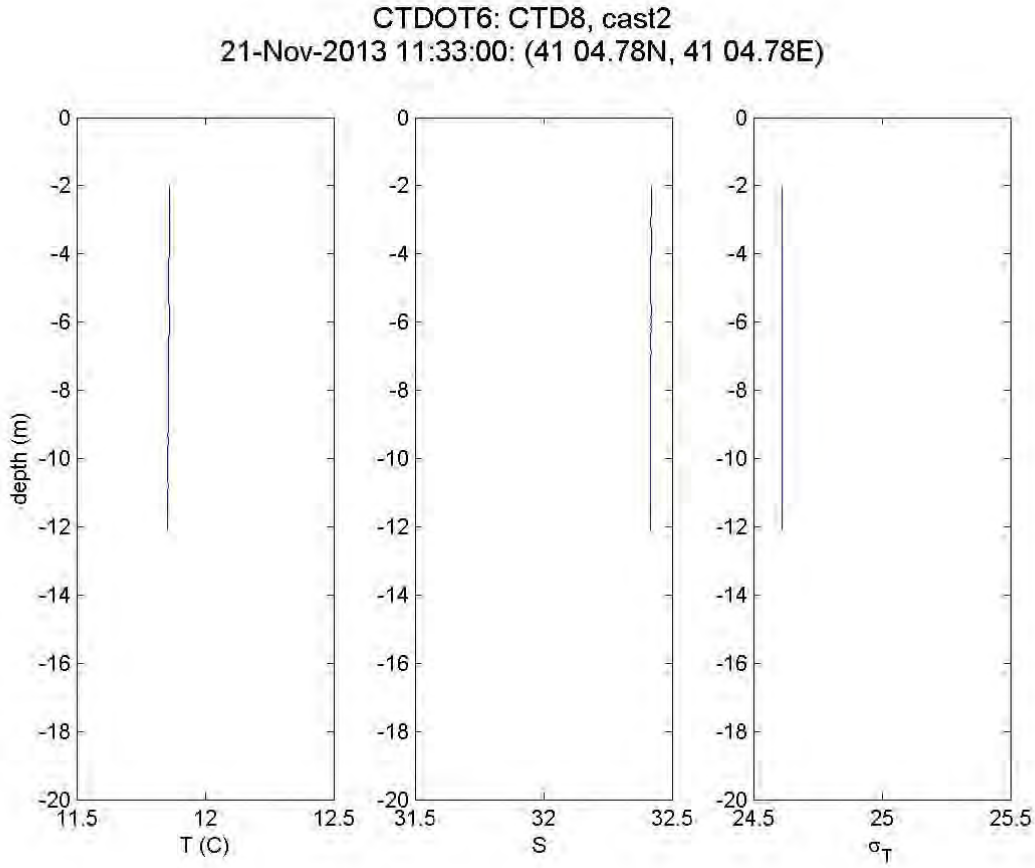

Figure 99: Cruise CTDOT6: Station CTD8, Cast 2: The left panel shows the vertical structure of Temperature (C) and the center and right panels show the salinity and density (σ_T) profiles respectively.

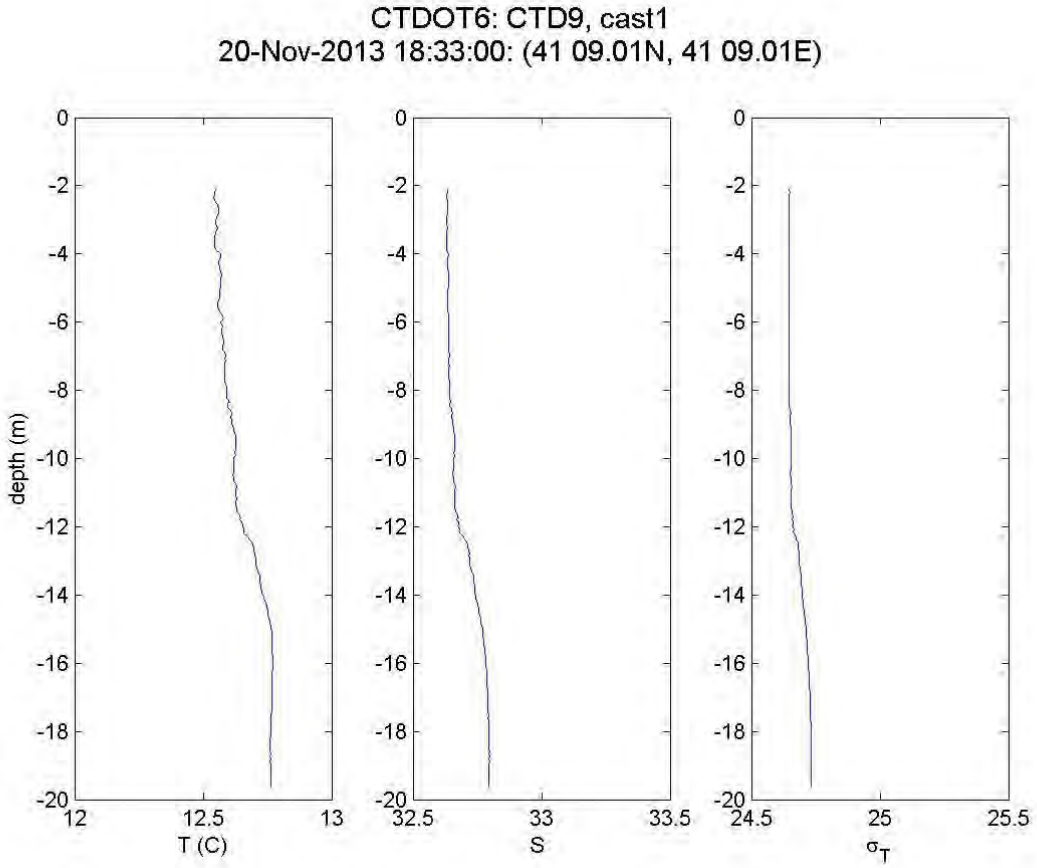

Figure 100: Cruise CTDOT6: Station CTD9, Cast 1: The left panel shows the vertical structure of Temperature (C) and the center and right panels show the salinity and density (σ_T) profiles respectively.

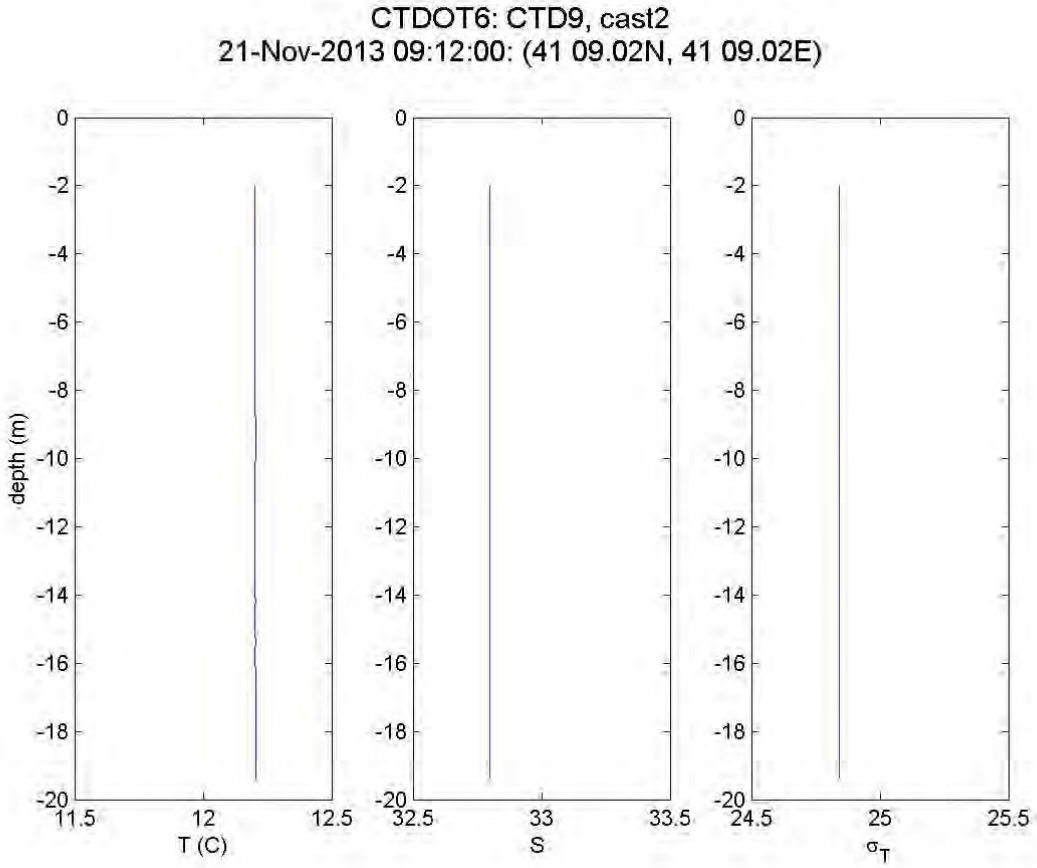

Figure 101: Cruise CTDOT6: Station CTD9, Cast 2: The left panel shows the vertical structure of Temperature (C) and the center and right panels show the salinity and density (σ_T) profiles respectively.

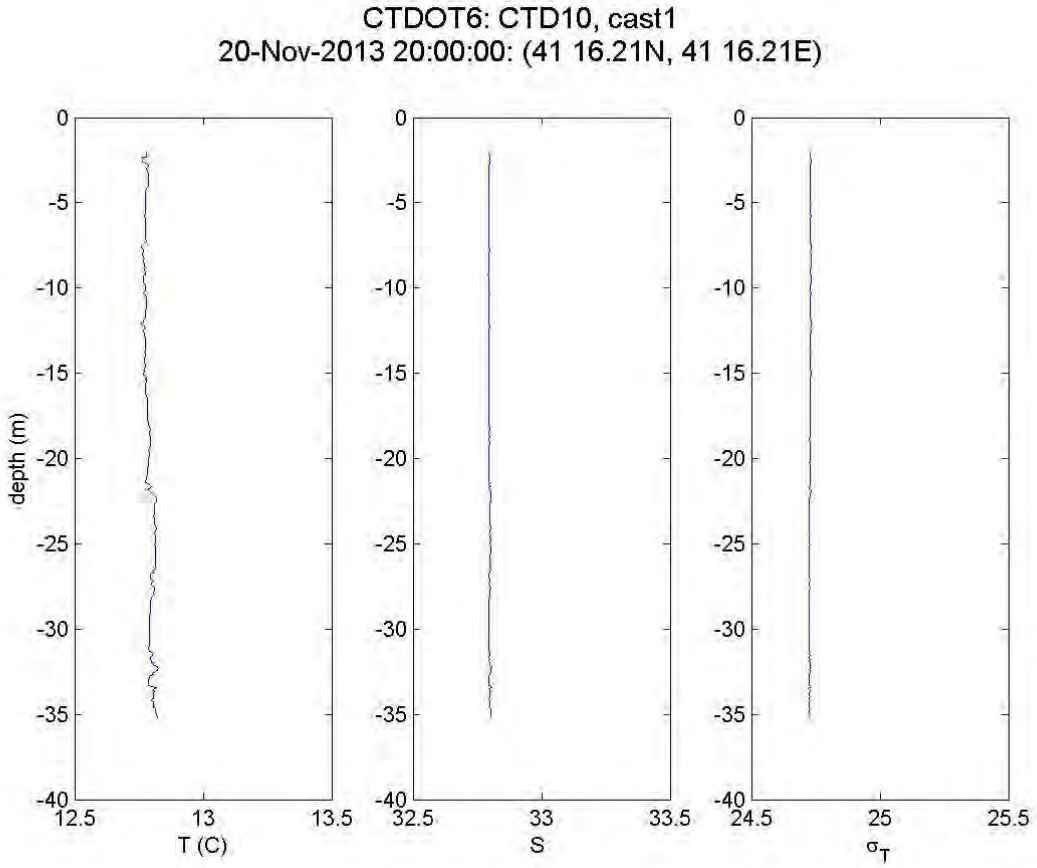

Figure 102: Cruise CTDOT6: Station CTD10, Cast 1: The left panel shows the vertical structure of Temperature (C) and the center and right panels show the salinity and density (σ_T) profiles respectively.

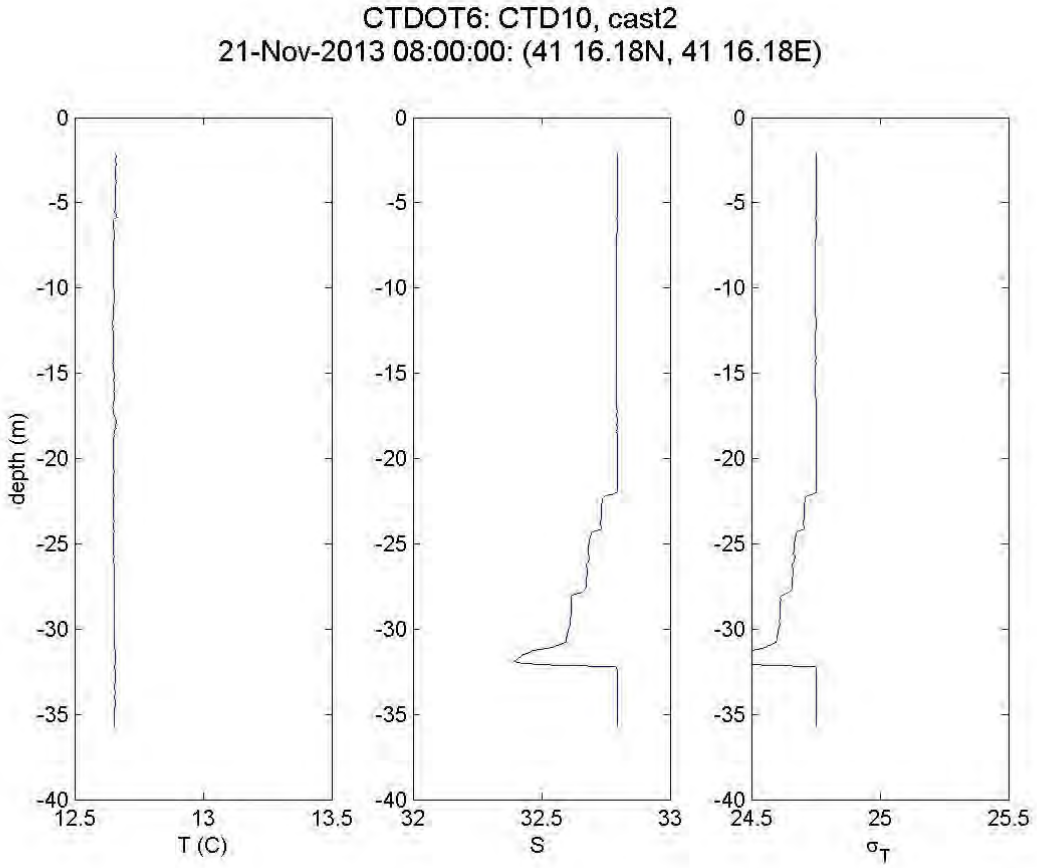

Figure 103: Cruise CTDOT6: Station CTD10, Cast 2: The left panel shows the vertical structure of Temperature (C) and the center and right panels show the salinity and density (σ_T) profiles respectively.

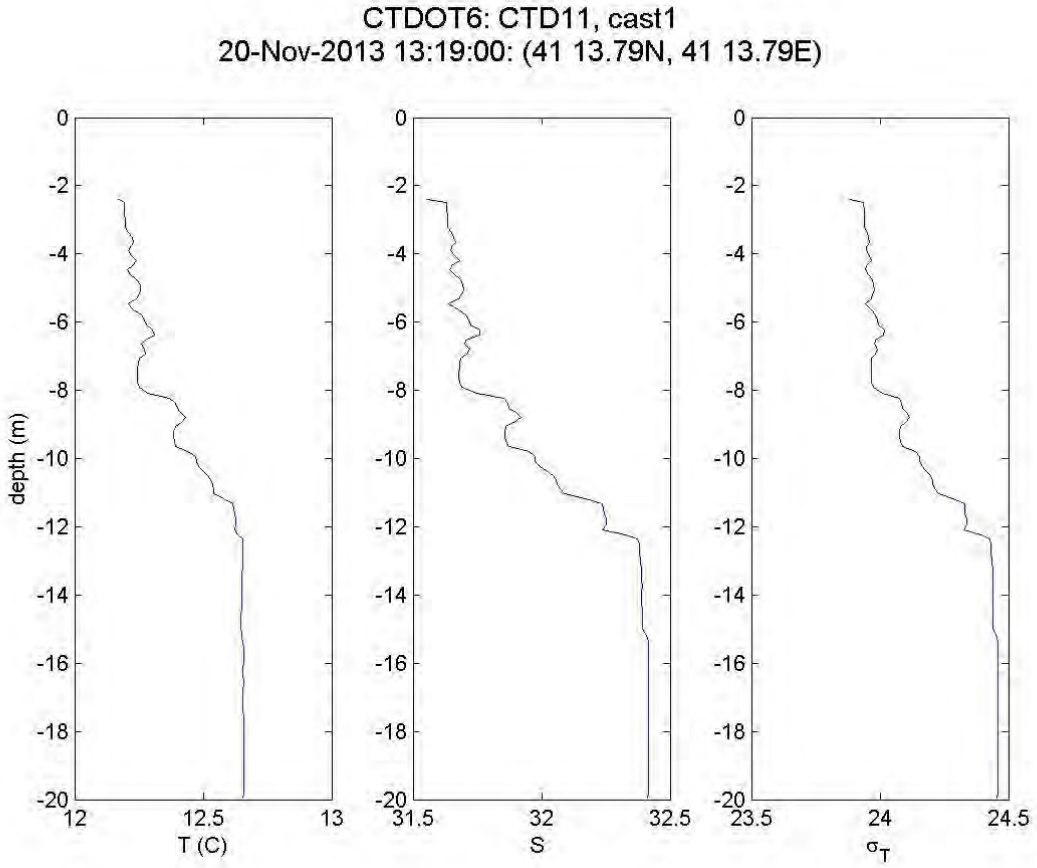

Figure 104: Cruise CTDOT6: Station CTD11, Cast 1: The left panel shows the vertical structure of Temperature (C) and the center and right panels show the salinity and density (σ_T) profiles respectively.

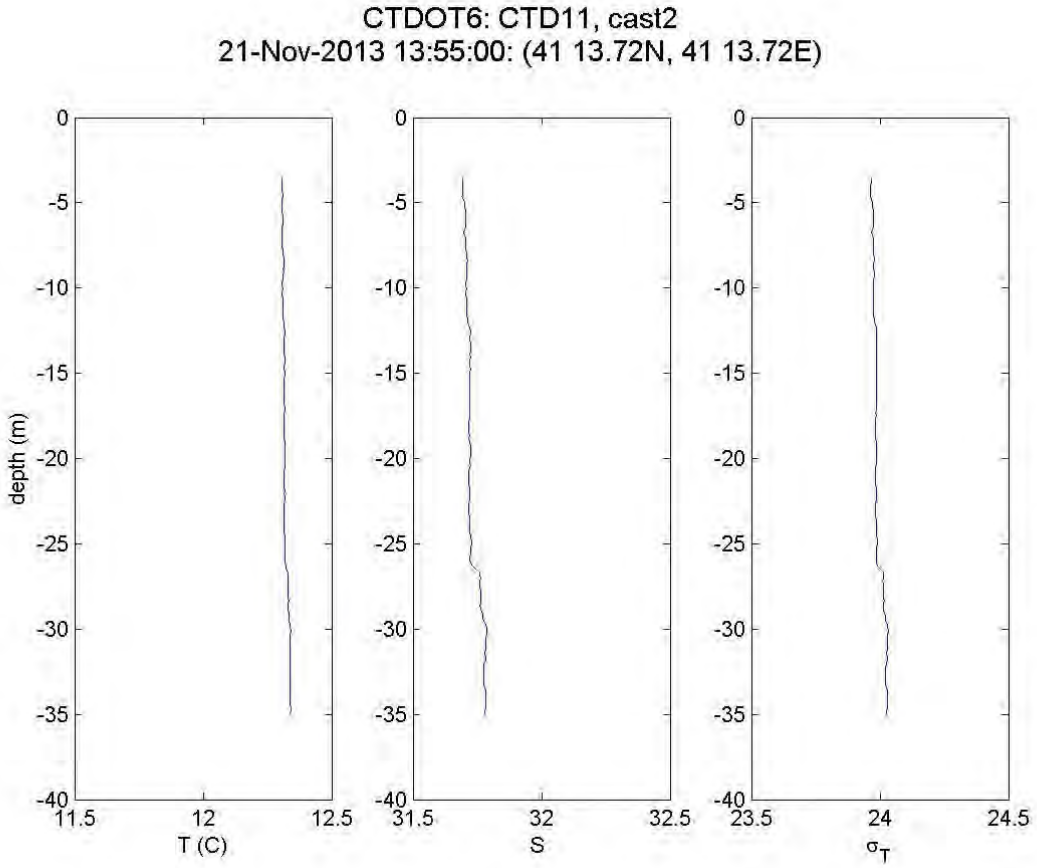

Figure 105: Cruise CTDOT6: Station CTD11, Cast 2: The left panel shows the vertical structure of Temperature (C) and the center and right panels show the salinity and density (σ_T) profiles respectively.

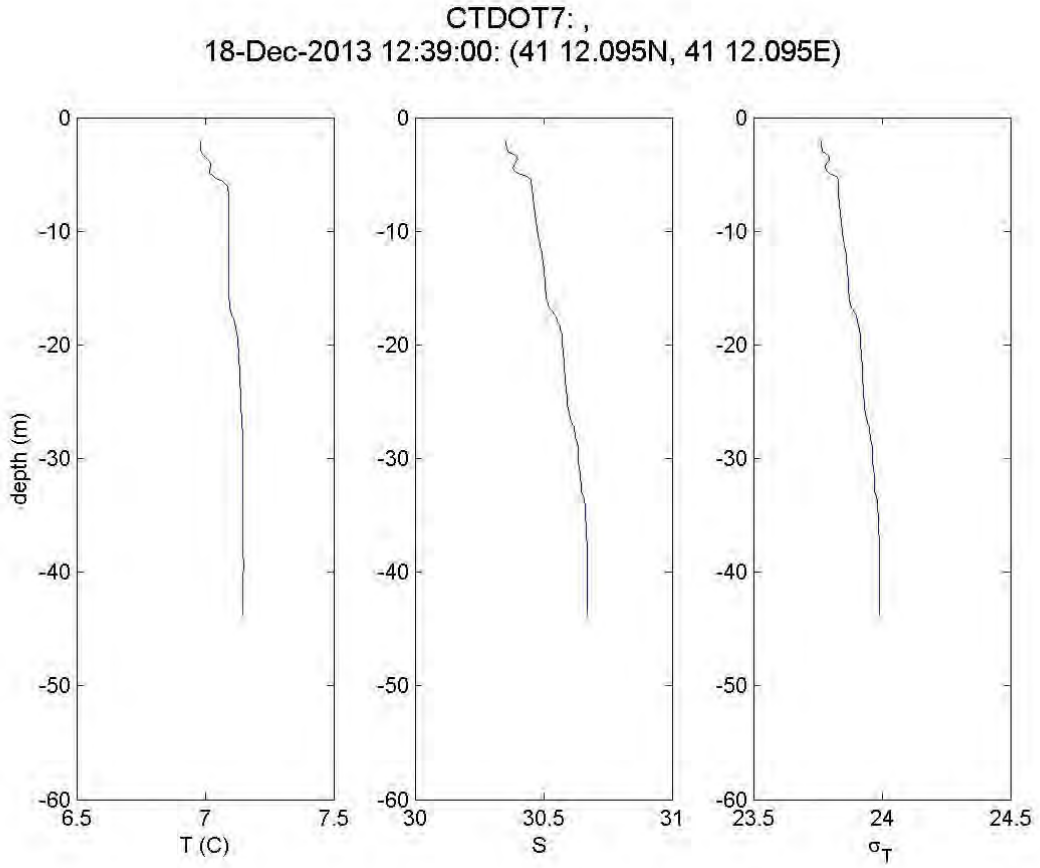

Figure 106: Cruise CTDOT7: Station DOT1, Cast 0: The left panel shows the vertical structure of Temperature (C) and the center and right panels show the salinity and density (σ_T) profiles respectively.

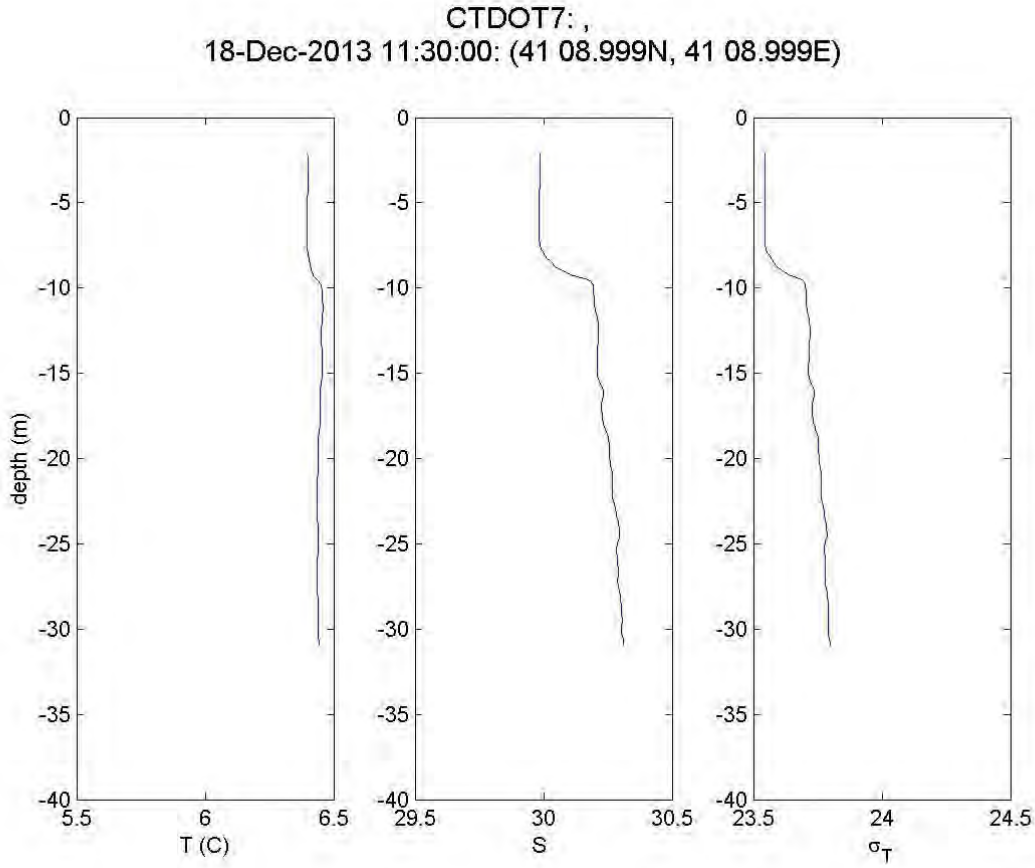

Figure 107: Cruise CTDOT7: Station DOT2, Cast 0: The left panel shows the vertical structure of Temperature (C) and the center and right panels show the salinity and density (σ_T) profiles respectively.

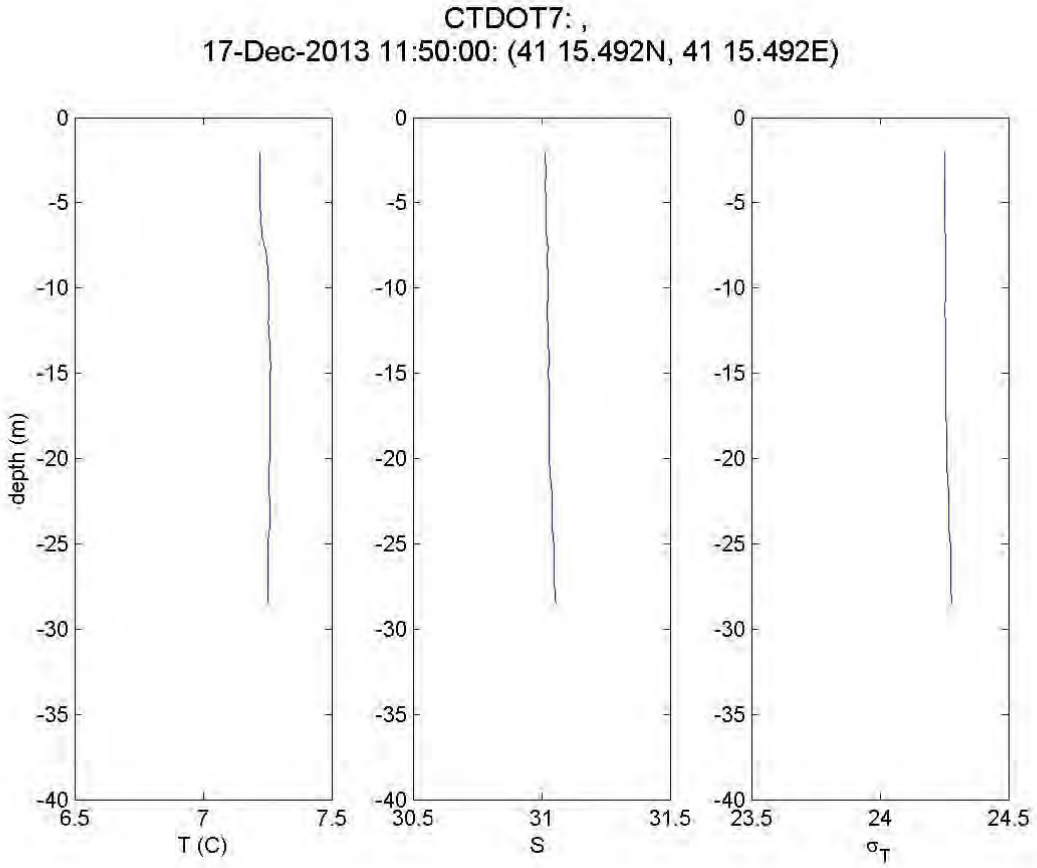

Figure 108: Cruise CTDOT7: Station DOT3, Cast 0: The left panel shows the vertical structure of Temperature (C) and the center and right panels show the salinity and density (σ_T) profiles respectively.

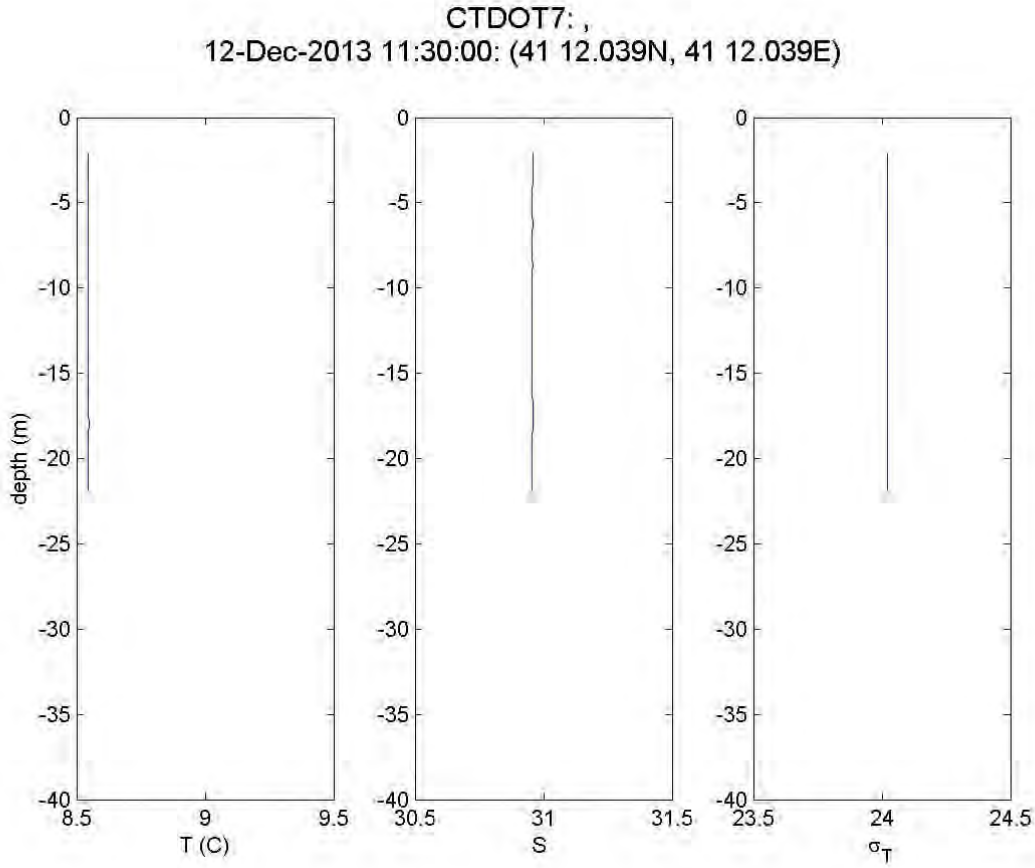

Figure 109: Cruise CTDOT7: Station DOT4, Cast 0: The left panel shows the vertical structure of Temperature (C) and the center and right panels show the salinity and density (σ_T) profiles respectively.

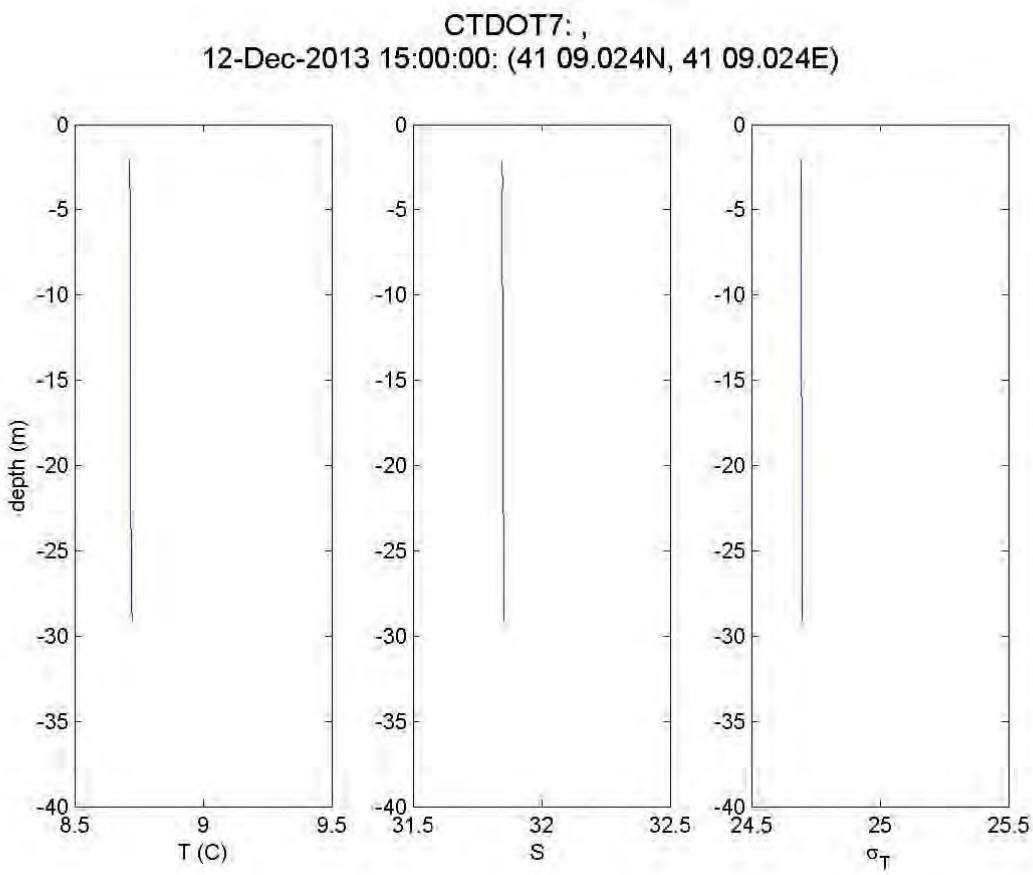

Figure 110: Cruise CTDOT7: Station DOT5, Cast 0: The left panel shows the vertical structure of Temperature (C) and the center and right panels show the salinity and density (σ_T) profiles respectively.

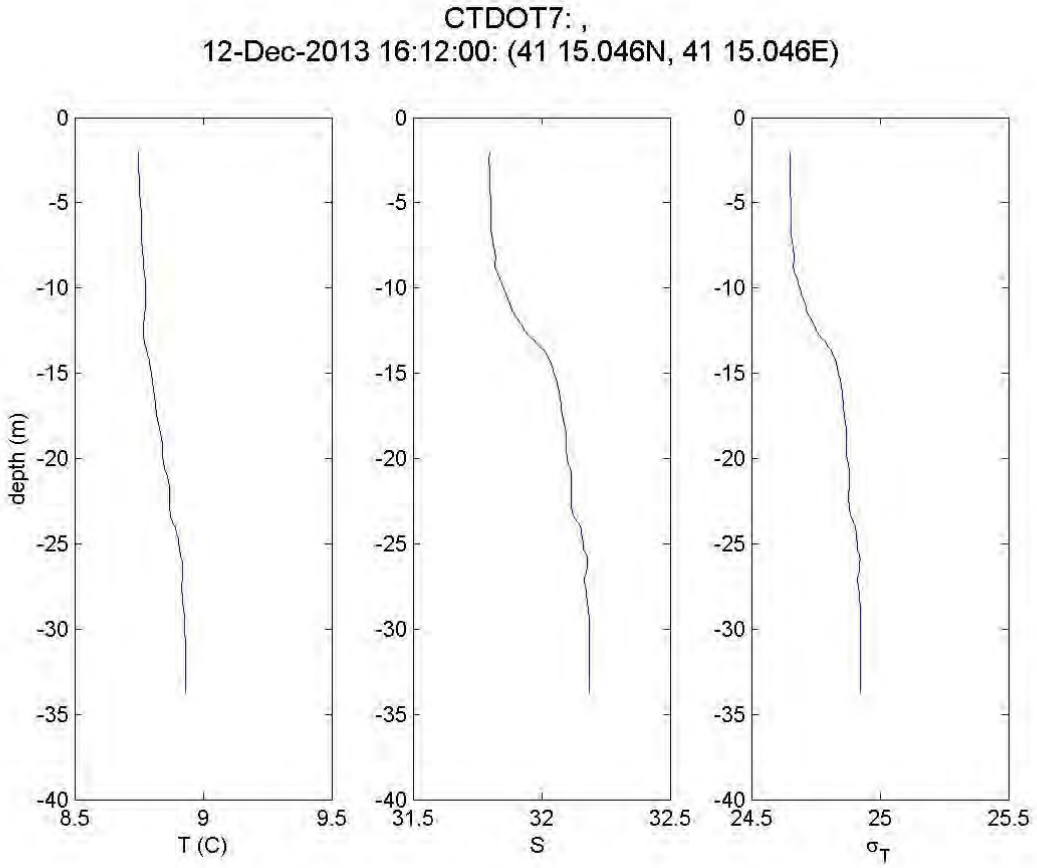

Figure 111: Cruise CTDOT7: Station DOT6, Cast 0: The left panel shows the vertical structure of Temperature (C) and the center and right panels show the salinity and density (σ_T) profiles respectively.

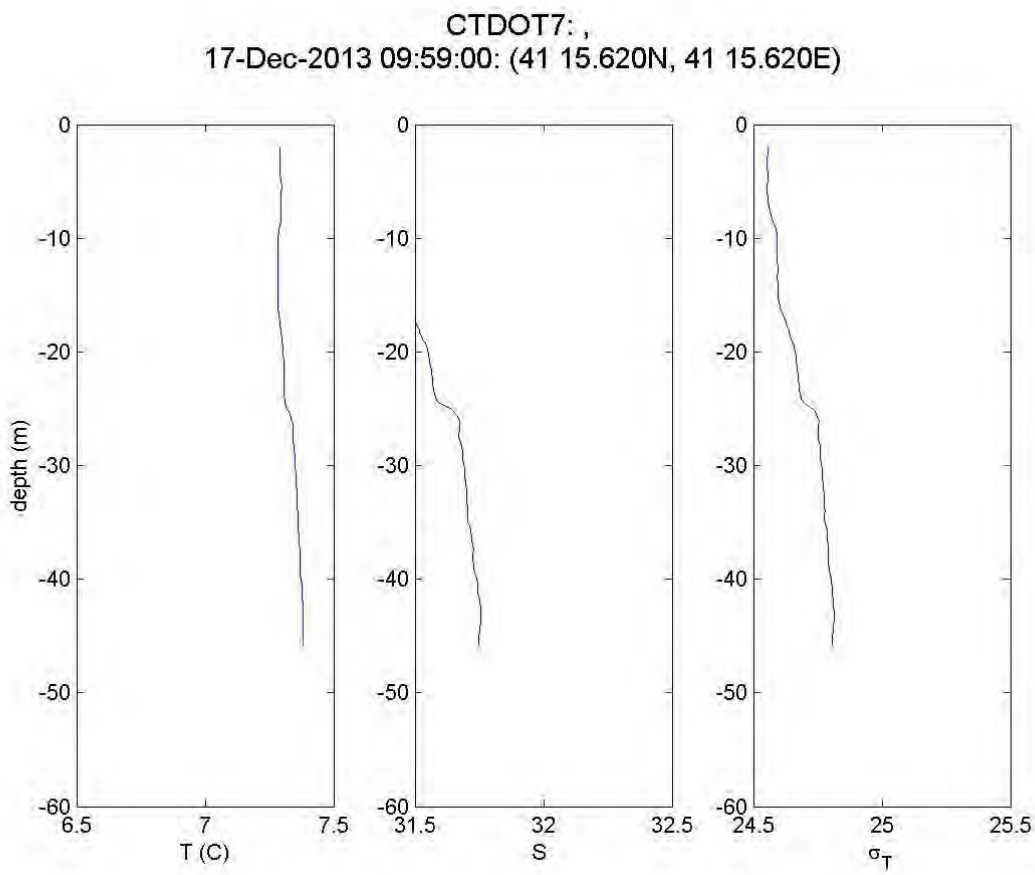

Figure 112: Cruise CTDOT7: Station DOT7, Cast 0: The left panel shows the vertical structure of Temperature (C) and the center and right panels show the salinity and density (σ_T) profiles respectively.

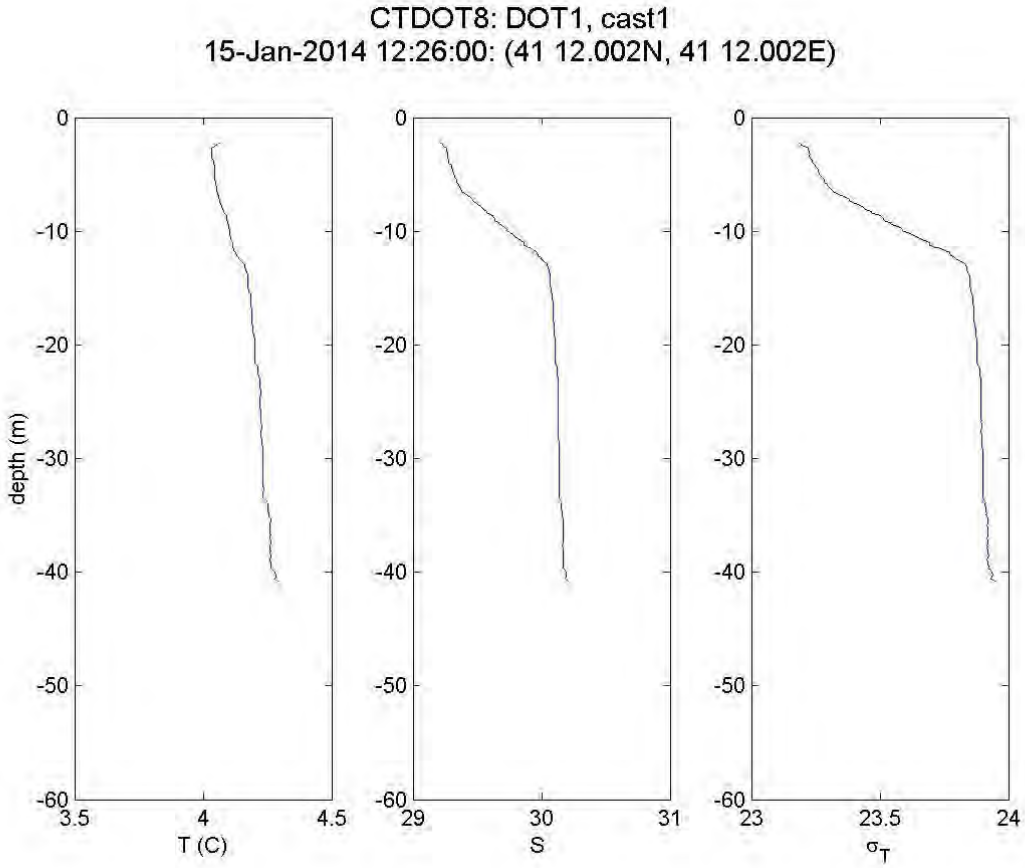

Figure 113: Cruise CTDOT8: Station DOT1, Cast 1: The left panel shows the vertical structure of Temperature (C) and the center and right panels show the salinity and density (σ_T) profiles respectively.

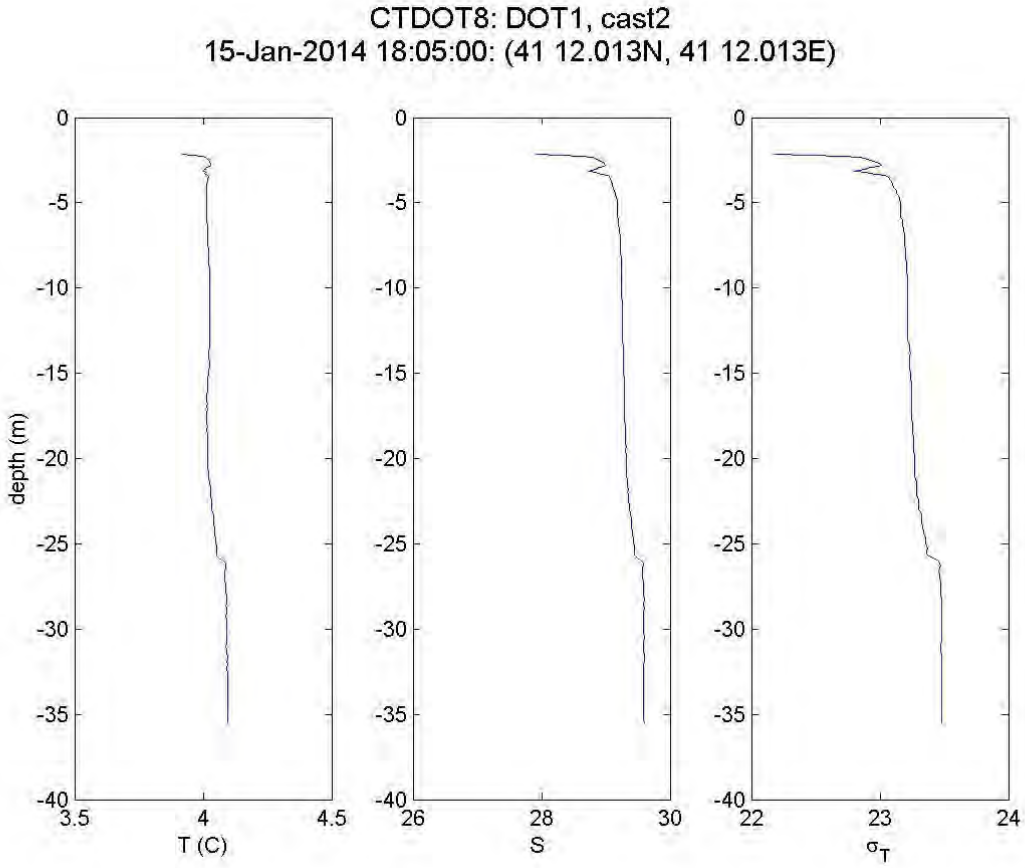

Figure 114: Cruise CTDOT8: Station DOT1, Cast 2: The left panel shows the vertical structure of Temperature (C) and the center and right panels show the salinity and density (σ_T) profiles respectively.

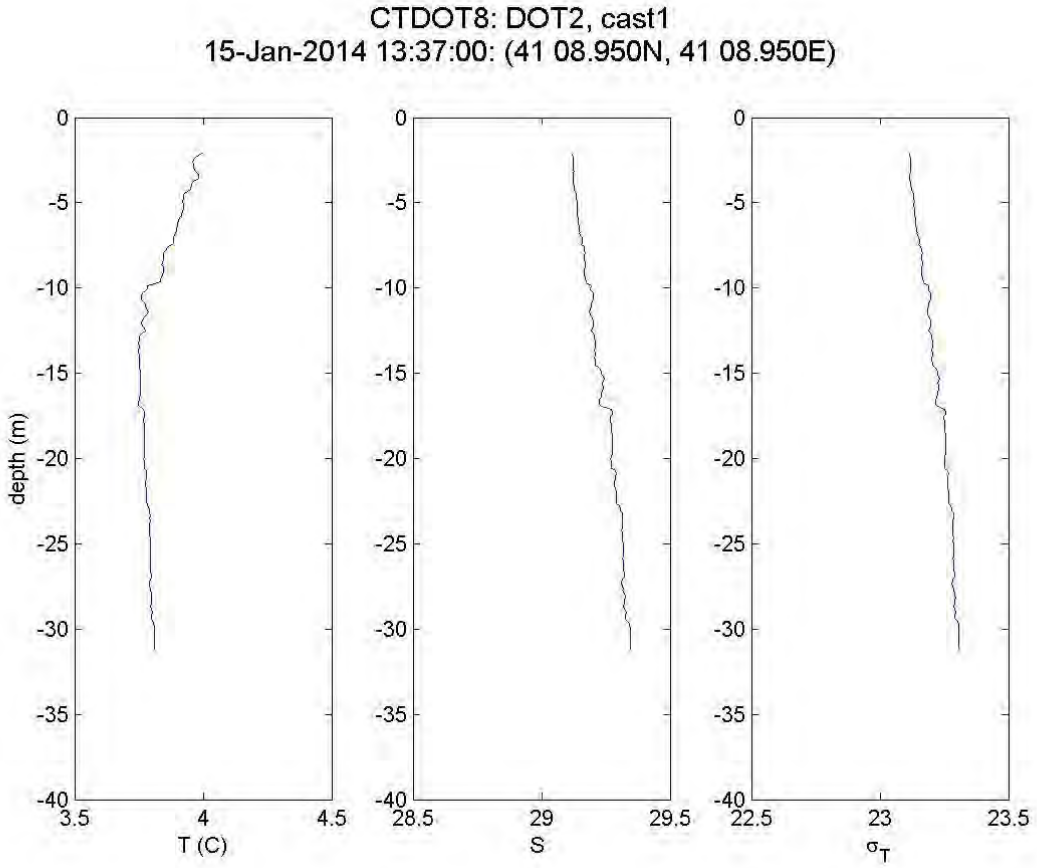

Figure 115: Cruise CTDOT8: Station DOT2, Cast 1: The left panel shows the vertical structure of Temperature (C) and the center and right panels show the salinity and density (σ_T) profiles respectively.

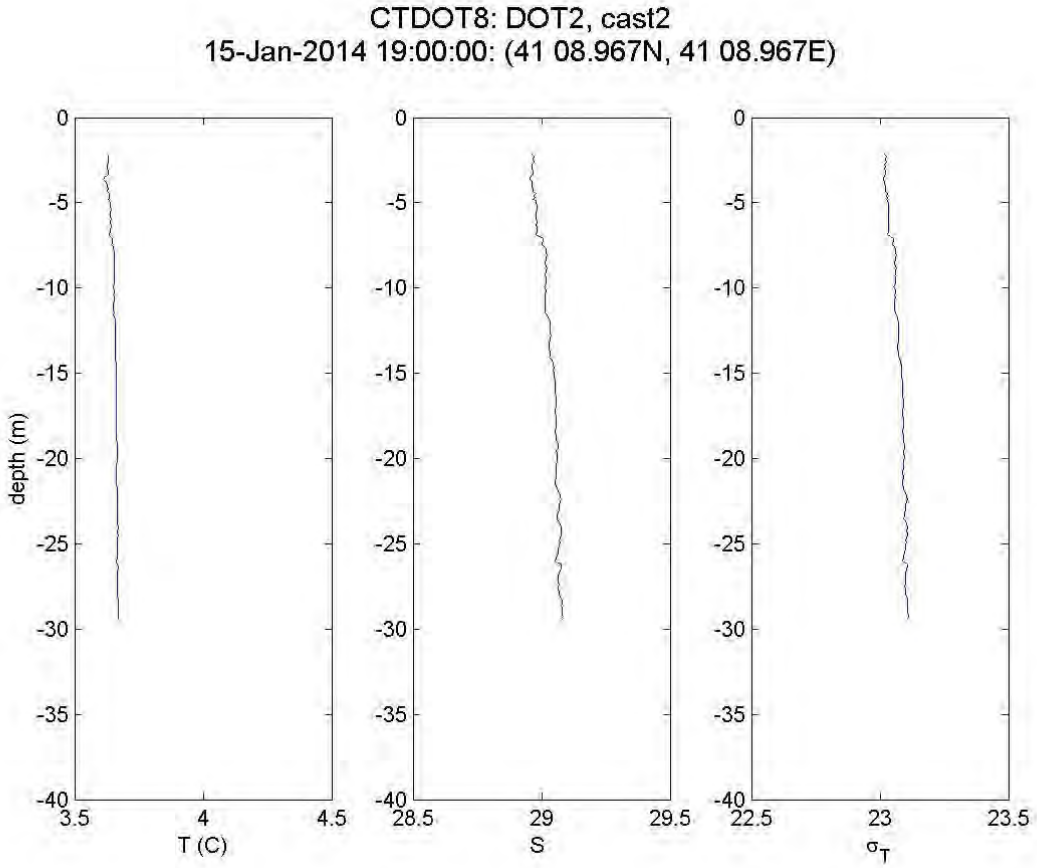

Figure 116: Cruise CTDOT8: Station DOT2, Cast 2: The left panel shows the vertical structure of Temperature (C) and the center and right panels show the salinity and density (σ_T) profiles respectively.

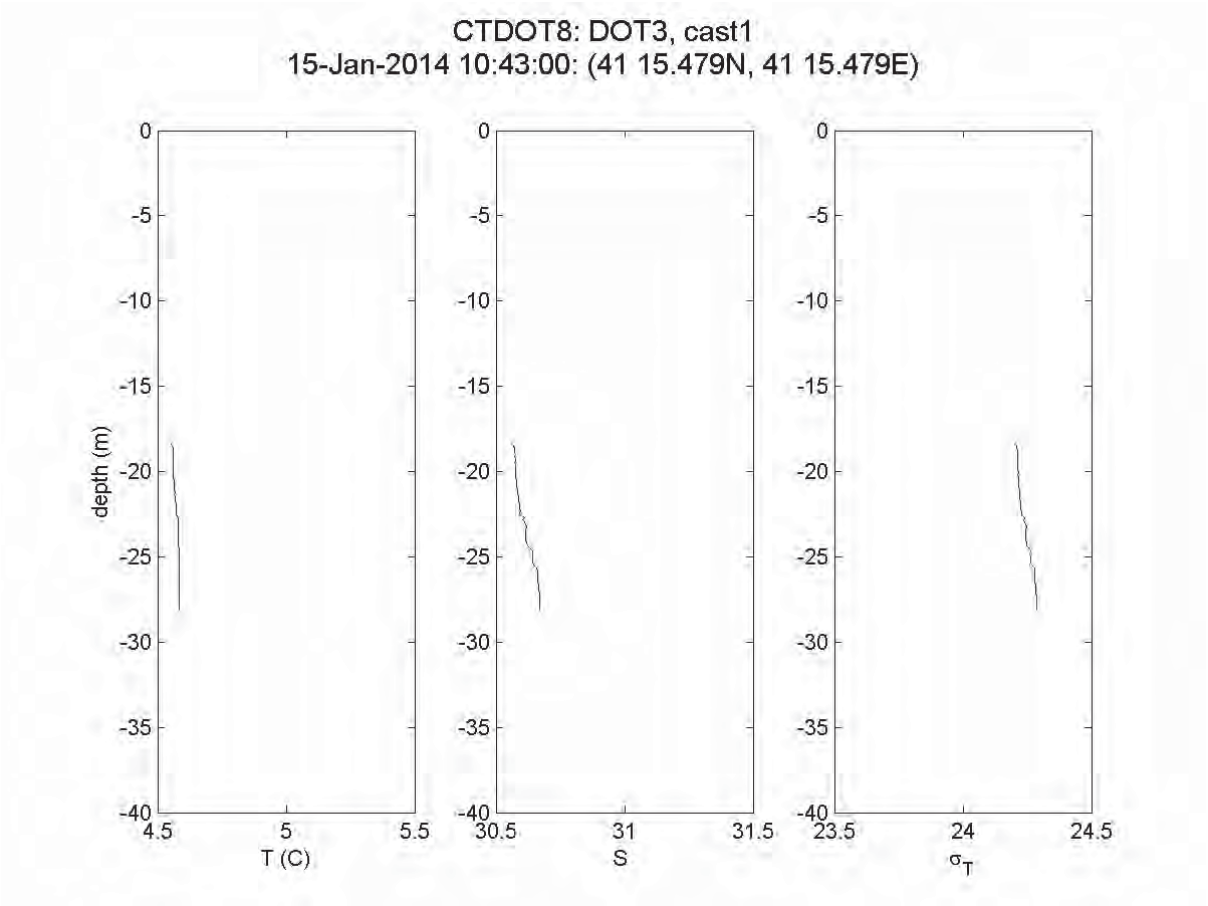

Figure 117: Cruise CTDOT8: Station DOT3, Cast 1: The left panel shows the vertical structure of Temperature (C) and the center and right panels show the salinity and density (σ_T) profiles respectively.

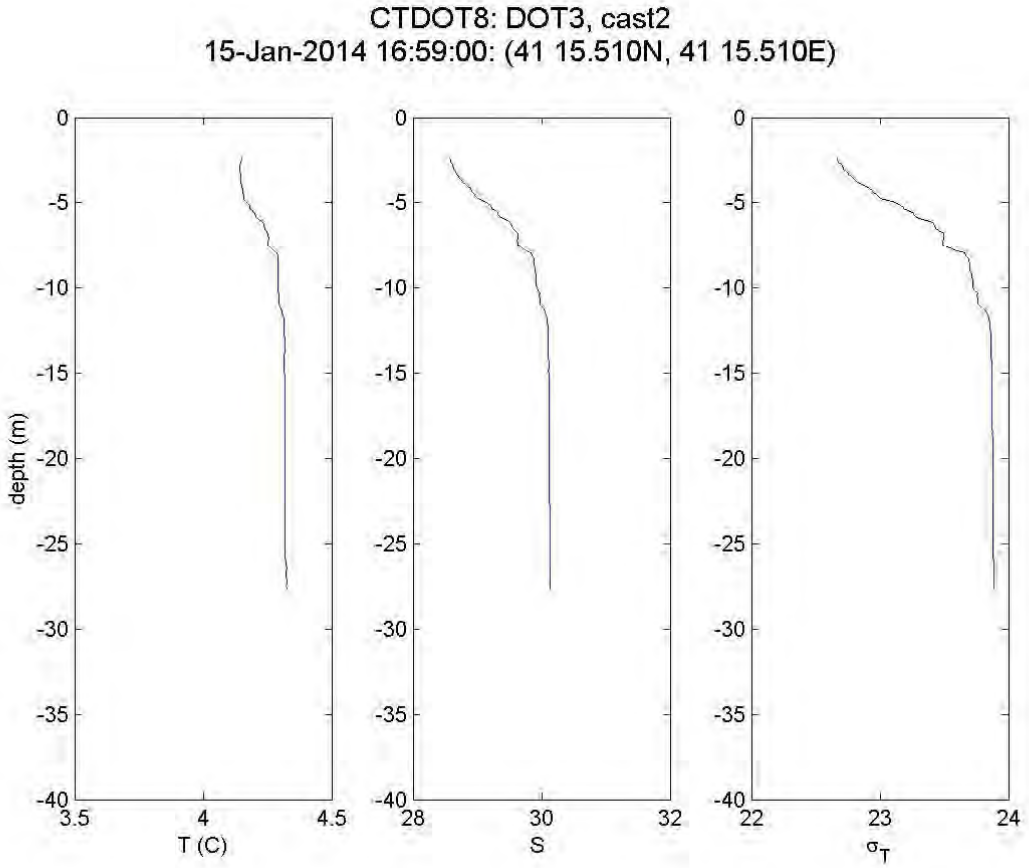

Figure 118: Cruise CTDOT8: Station DOT3, Cast 2: The left panel shows the vertical structure of Temperature (C) and the center and right panels show the salinity and density (σ_T) profiles respectively.

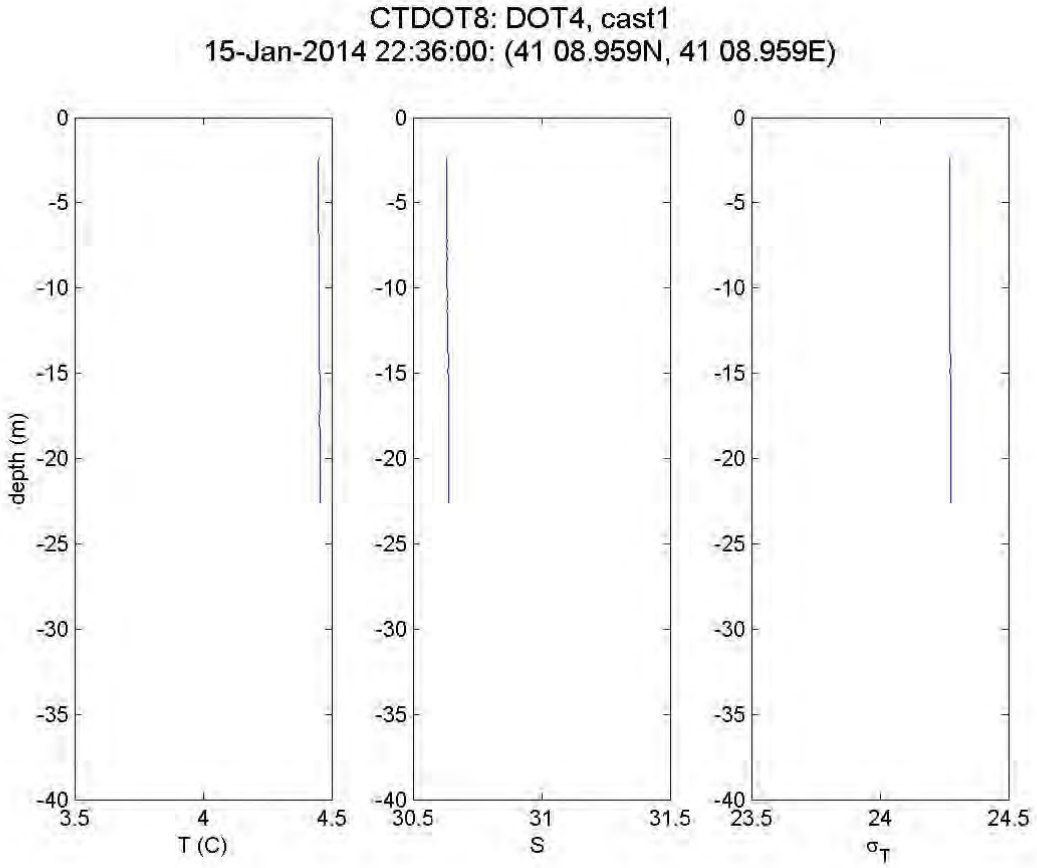

Figure 119: Cruise CTDOT8: Station DOT4, Cast 1: The left panel shows the vertical structure of Temperature (C) and the center and right panels show the salinity and density (σ_T) profiles respectively.

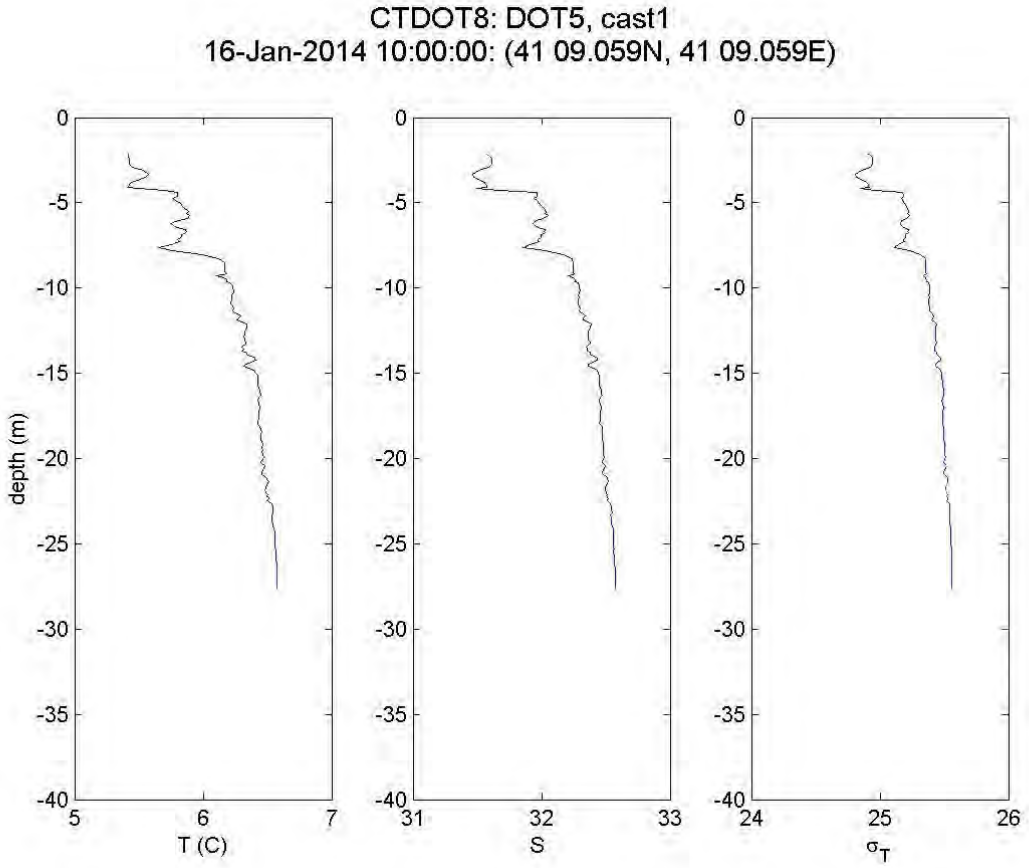

Figure 120: Cruise CTDOT8: Station DOT5, Cast 1: The left panel shows the vertical structure of Temperature (C) and the center and right panels show the salinity and density (σ_T) profiles respectively.

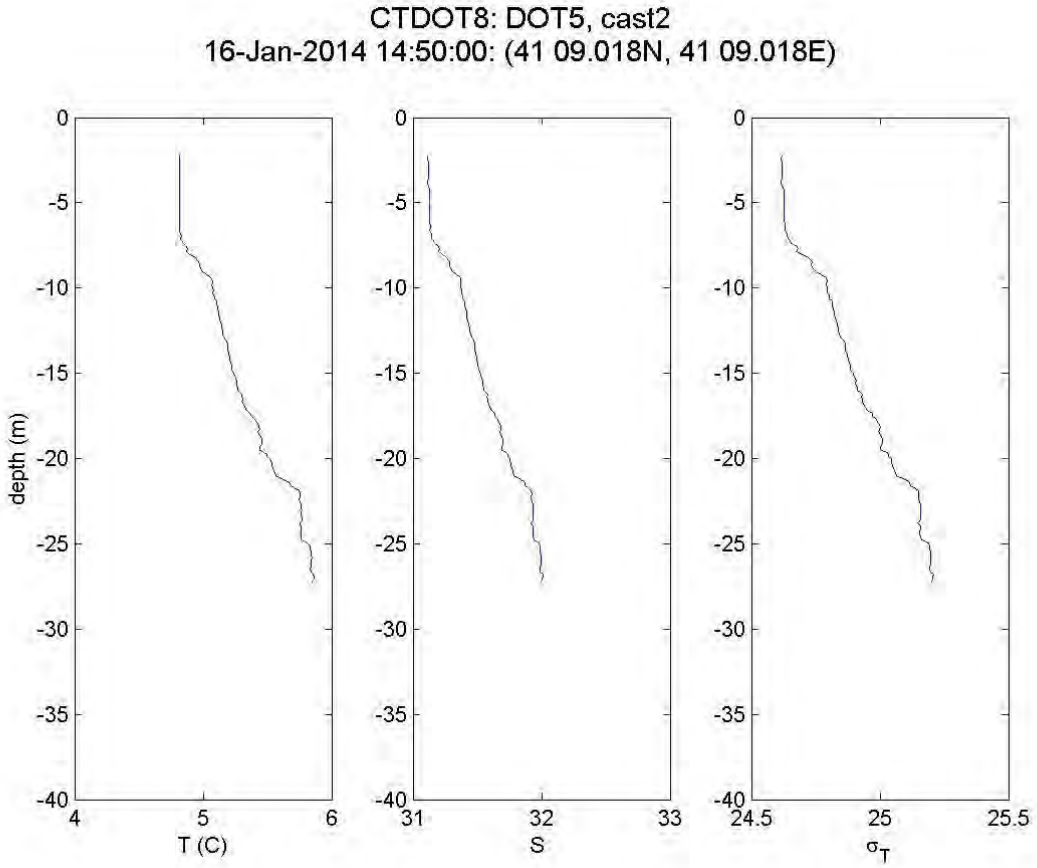

Figure 121: Cruise CTDOT8: Station DOT5, Cast 2: The left panel shows the vertical structure of Temperature (C) and the center and right panels show the salinity and density (σ_T) profiles respectively.

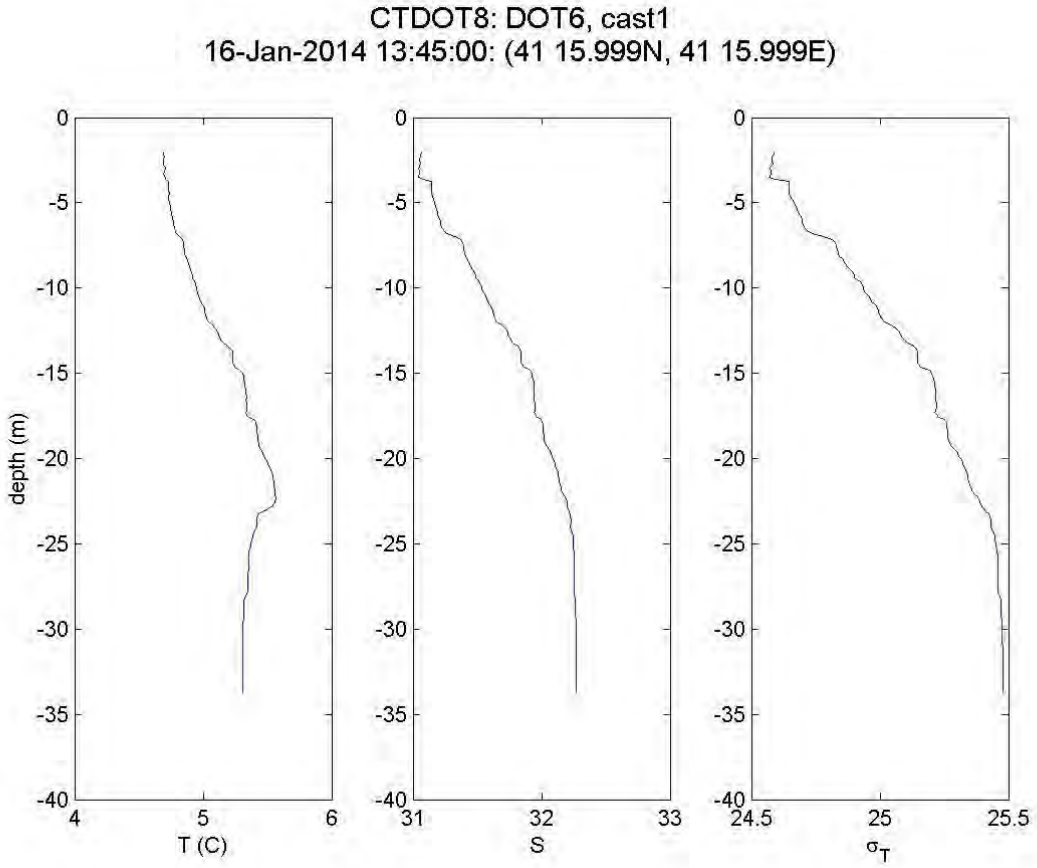

Figure 122: Cruise CTDOT8: Station DOT6, Cast 1: The left panel shows the vertical structure of Temperature (C) and the center and right panels show the salinity and density (σ_T) profiles respectively.

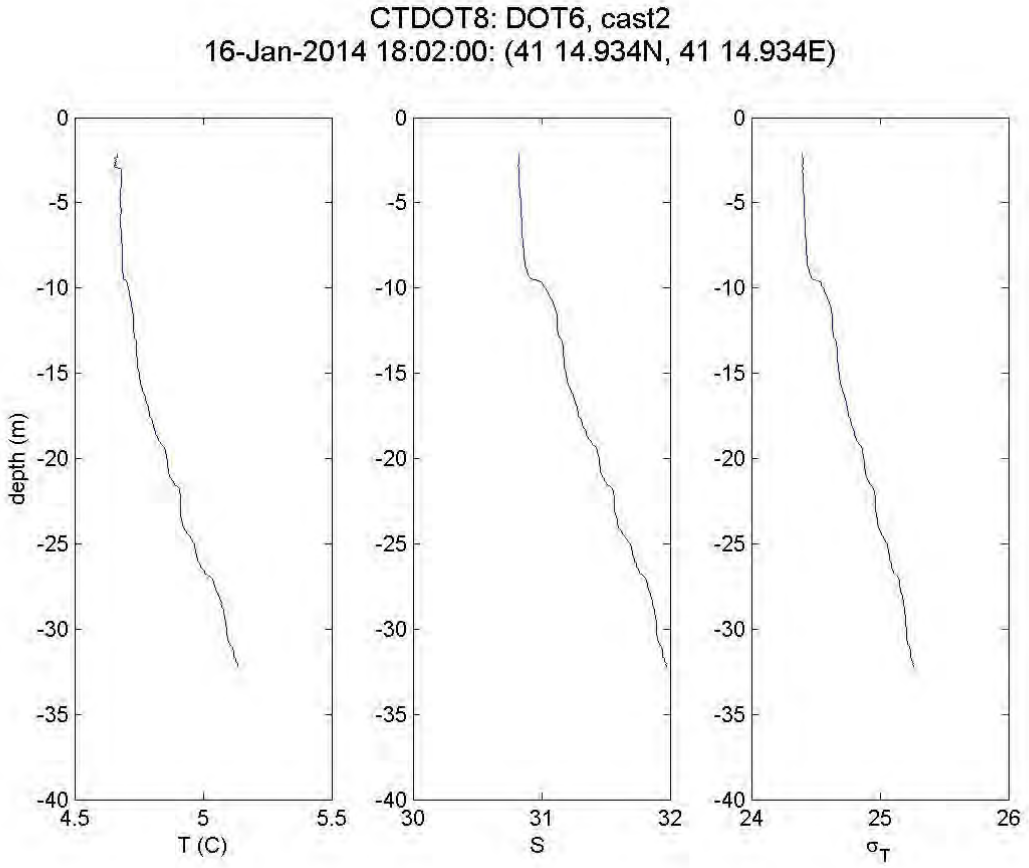

Figure 123: Cruise CTDOT8: Station DOT6, Cast 2: The left panel shows the vertical structure of Temperature (C) and the center and right panels show the salinity and density (σ_T) profiles respectively.

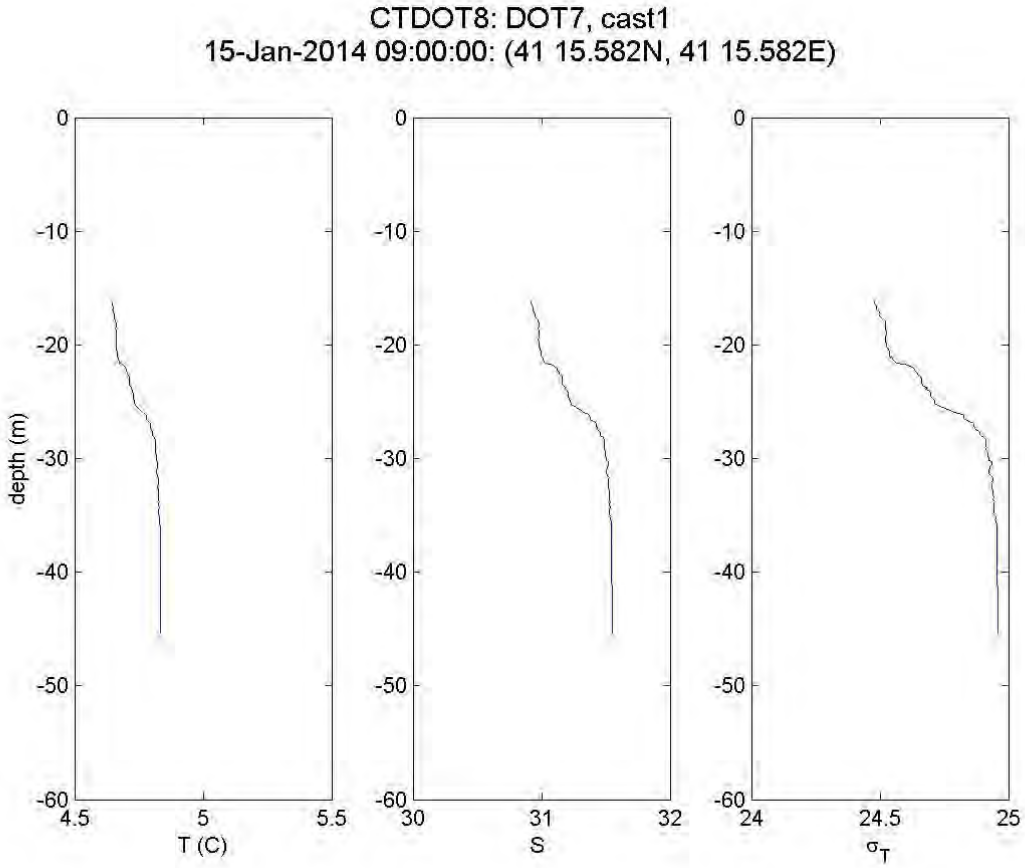

Figure 124: Cruise CTDOT8: Station DOT7, Cast 1: The left panel shows the vertical structure of Temperature (C) and the center and right panels show the salinity and density (σ_T) profiles respectively.

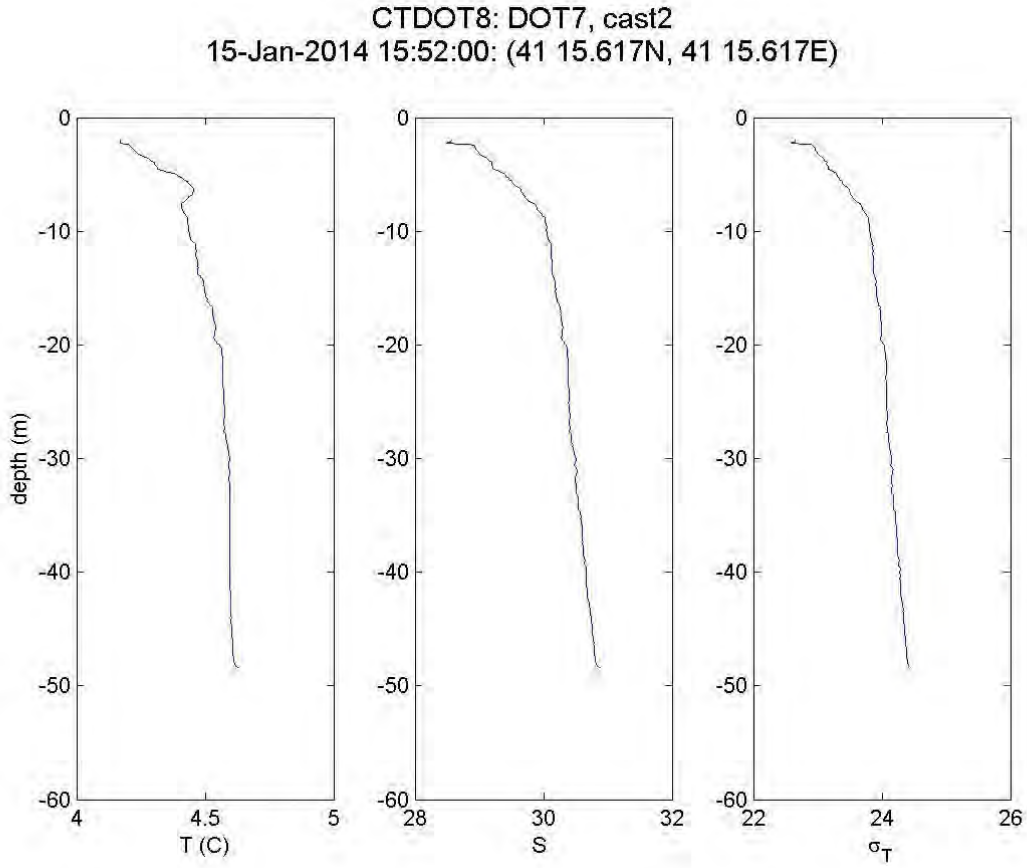

Figure 125: Cruise CTDOT8: Station DOT7, Cast 2: The left panel shows the vertical structure of Temperature (C) and the center and right panels show the salinity and density (σ_T) profiles respectively.

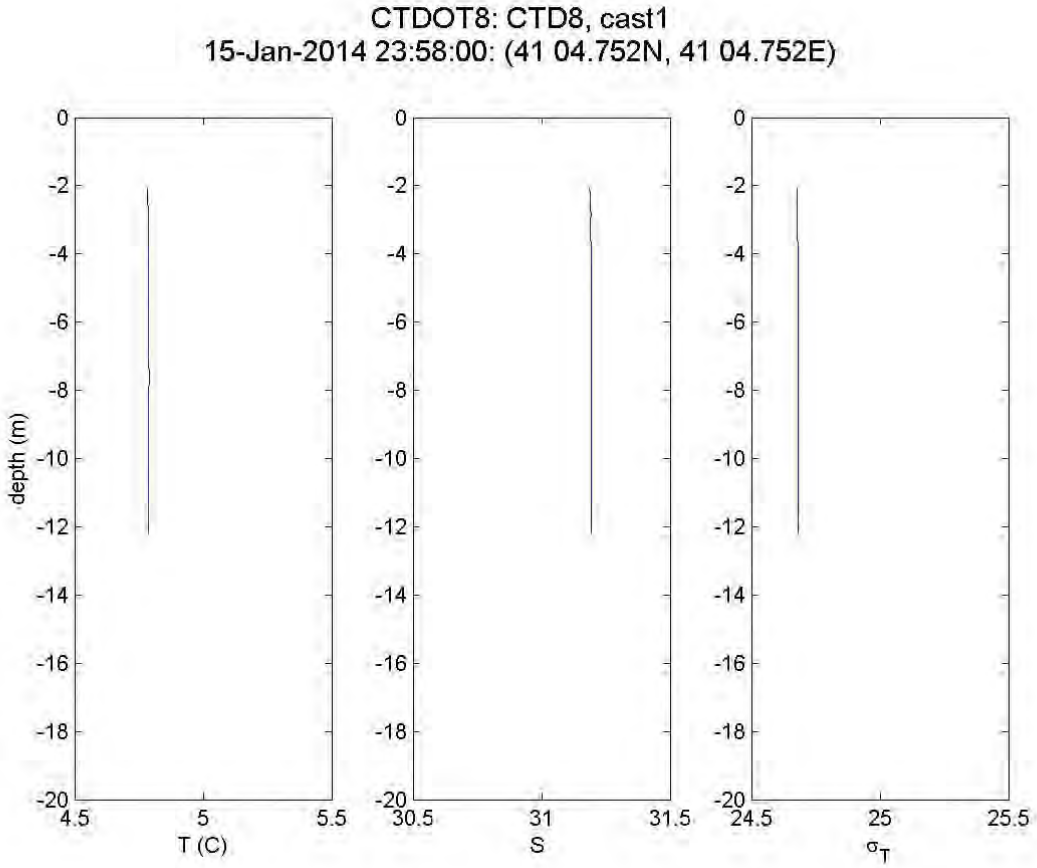

Figure 126: Cruise CTDOT8: Station CTD8, Cast 1: The left panel shows the vertical structure of Temperature (C) and the center and right panels show the salinity and density (σ_T) profiles respectively.

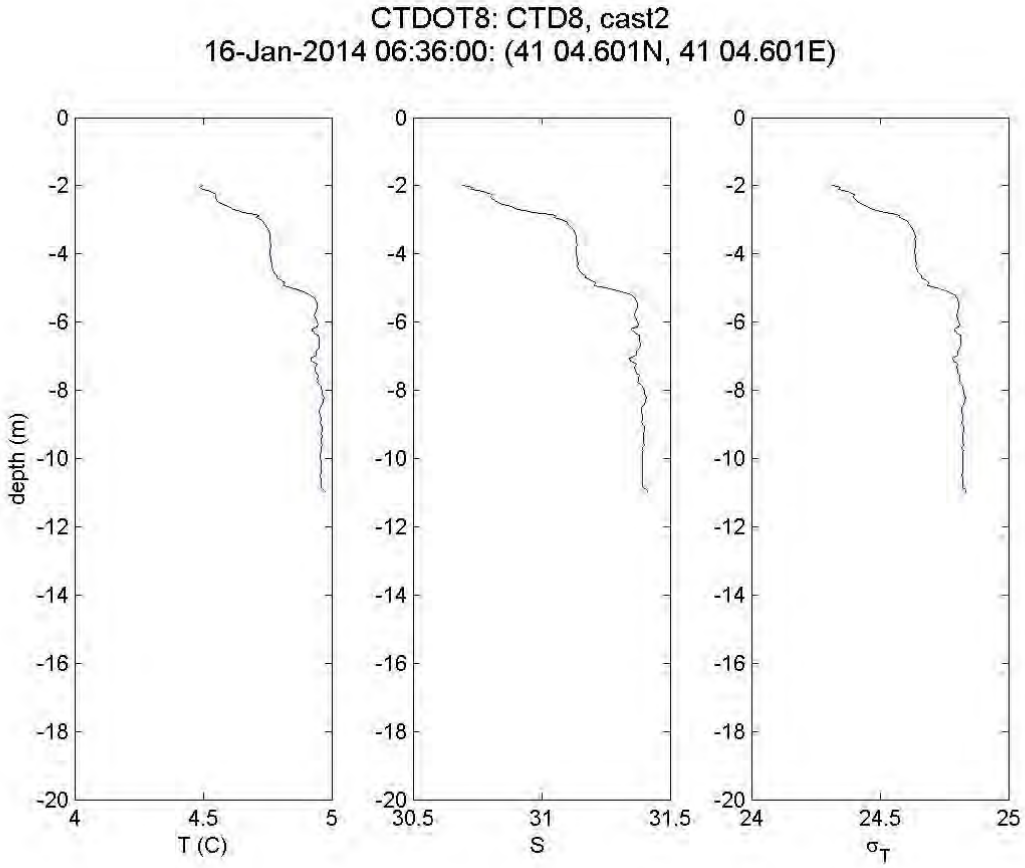

Figure 127: Cruise CTDOT8: Station CTD8, Cast 2: The left panel shows the vertical structure of Temperature (C) and the center and right panels show the salinity and density (σ_T) profiles respectively.

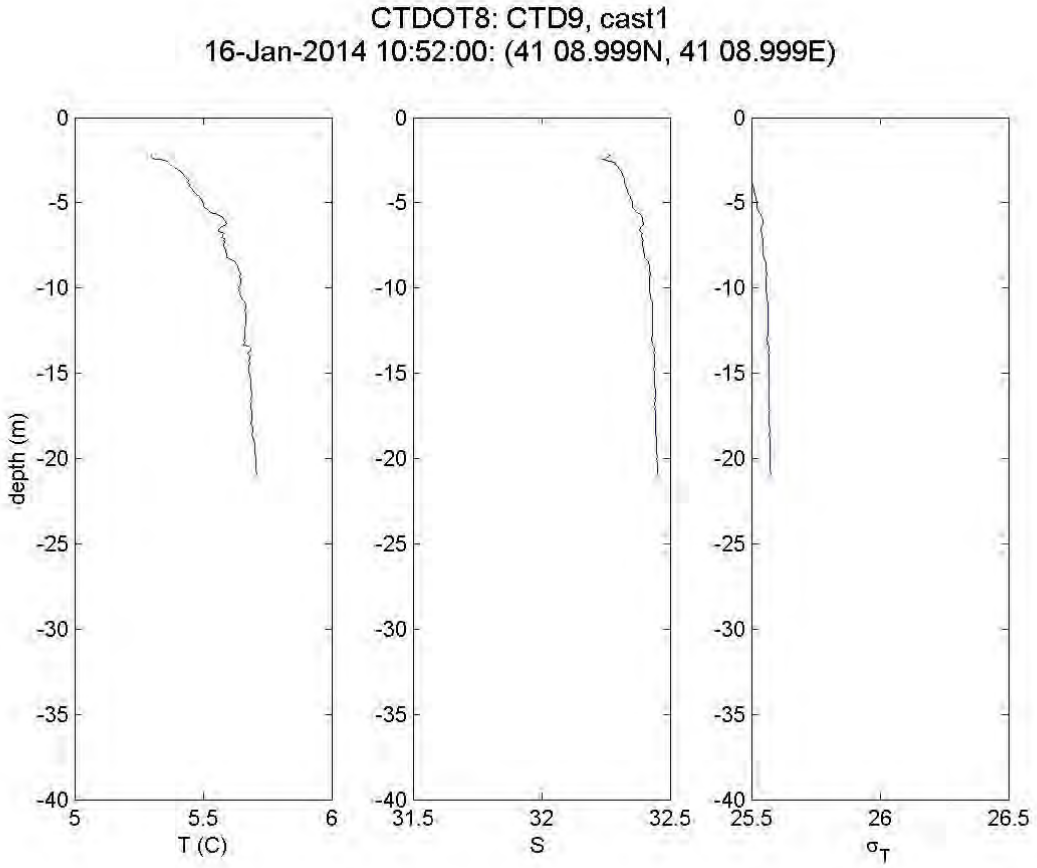

Figure 128: Cruise CTDOT8: Station CTD9, Cast 1: The left panel shows the vertical structure of Temperature (C) and the center and right panels show the salinity and density (σ_T) profiles respectively.

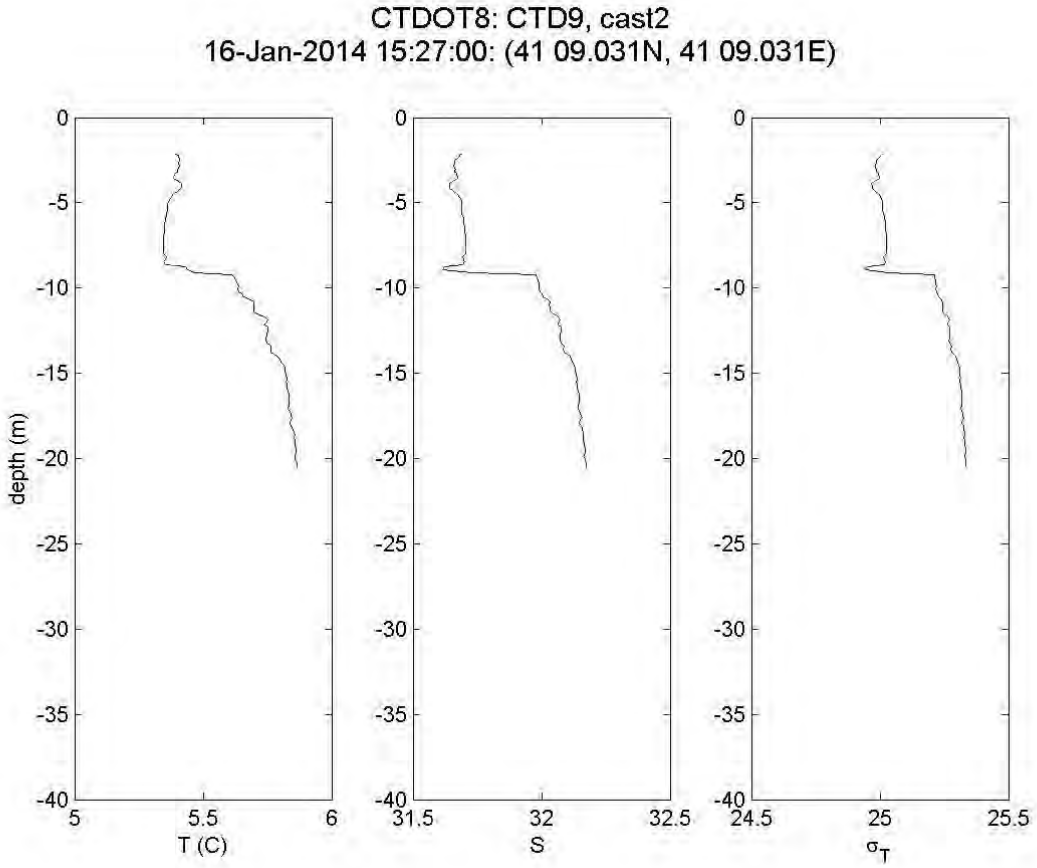

Figure 129: Cruise CTDOT8: Station CTD9, Cast 2: The left panel shows the vertical structure of Temperature (C) and the center and right panels show the salinity and density (σ_T) profiles respectively.

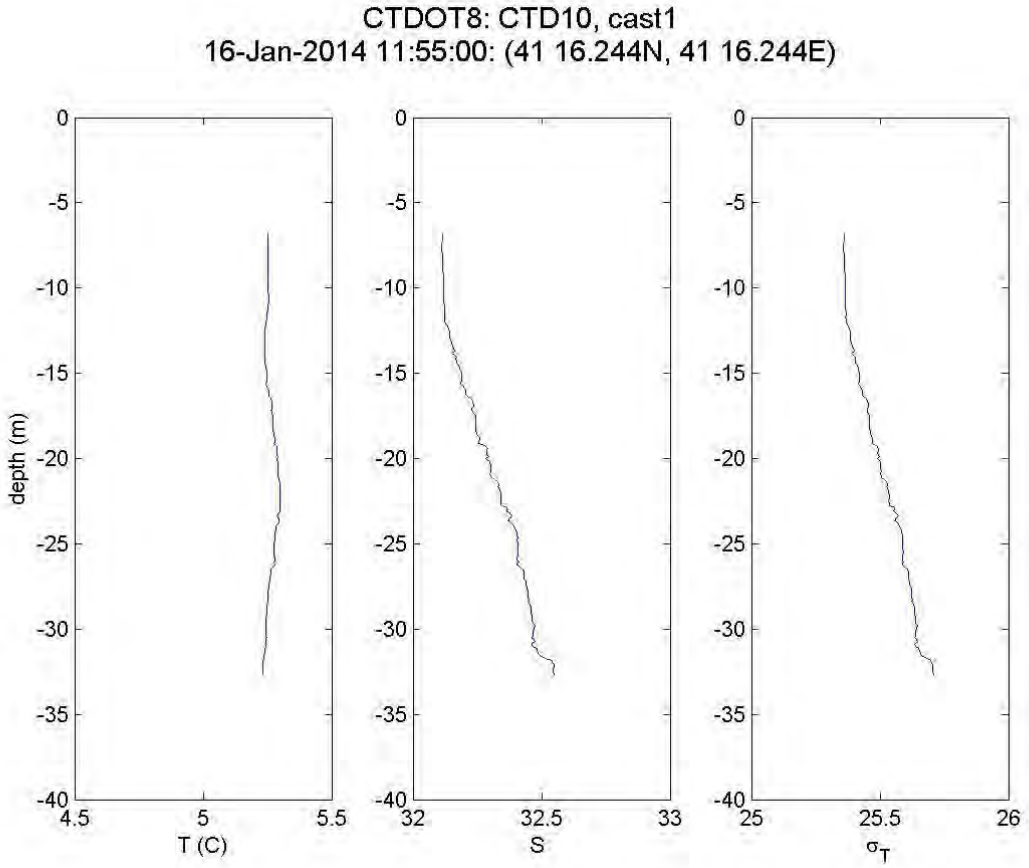

Figure 130: Cruise CTDOT8: Station CTD10, Cast 1: The left panel shows the vertical structure of Temperature (C) and the center and right panels show the salinity and density (σ_T) profiles respectively.

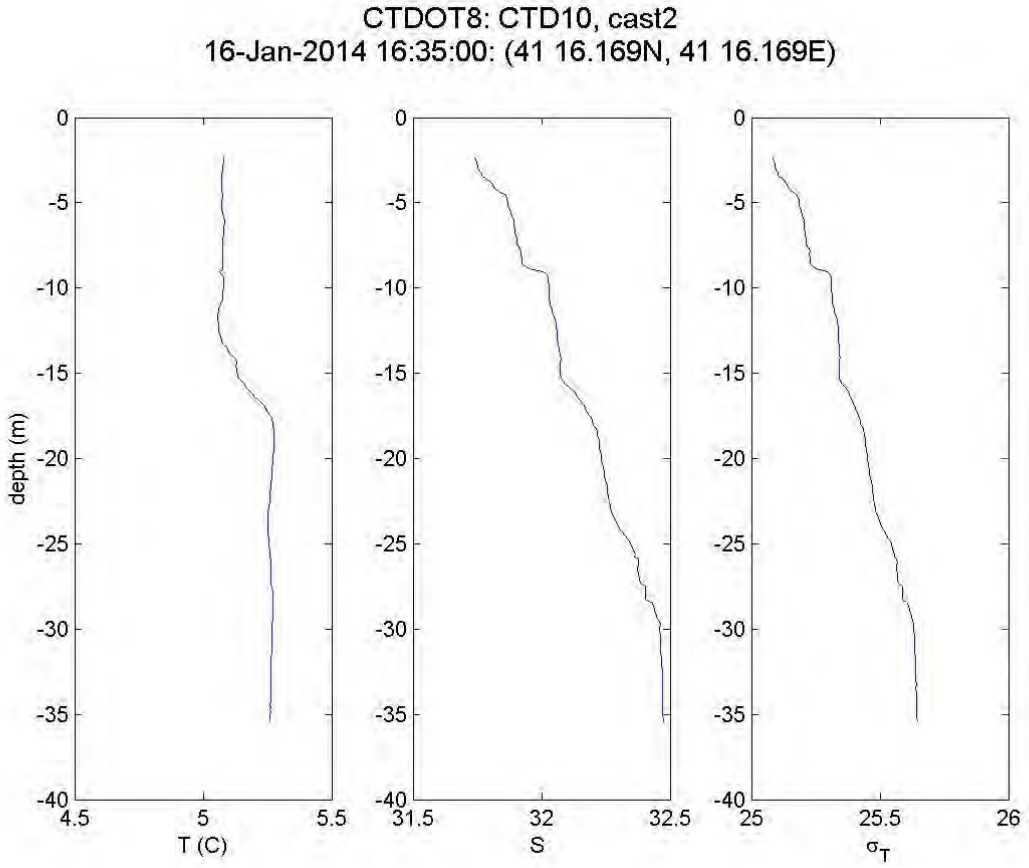

Figure 131: Cruise CTDOT8: Station CTD10, Cast 2: The left panel shows the vertical structure of Temperature (C) and the center and right panels show the salinity and density (σ_T) profiles respectively.

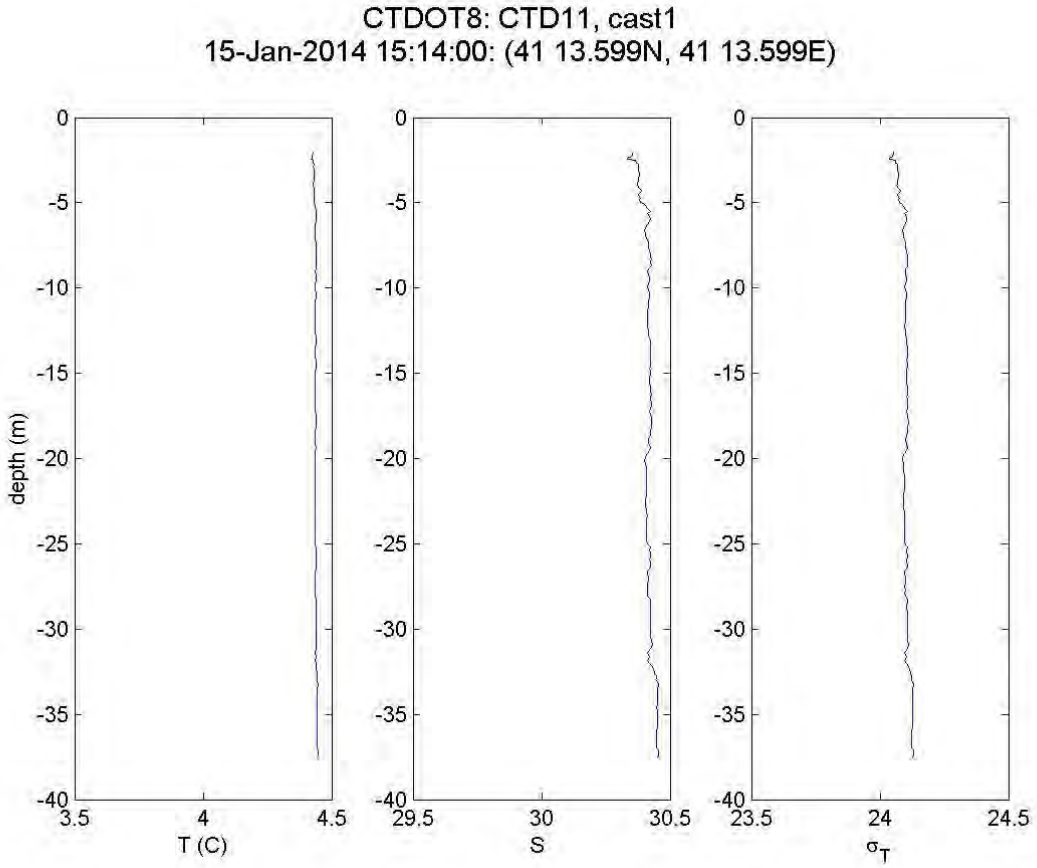

Figure 132: Cruise CTDOT8: Station CTD11, Cast 1: The left panel shows the vertical structure of Temperature (C) and the center and right panels show the salinity and density (σ_T) profiles respectively.

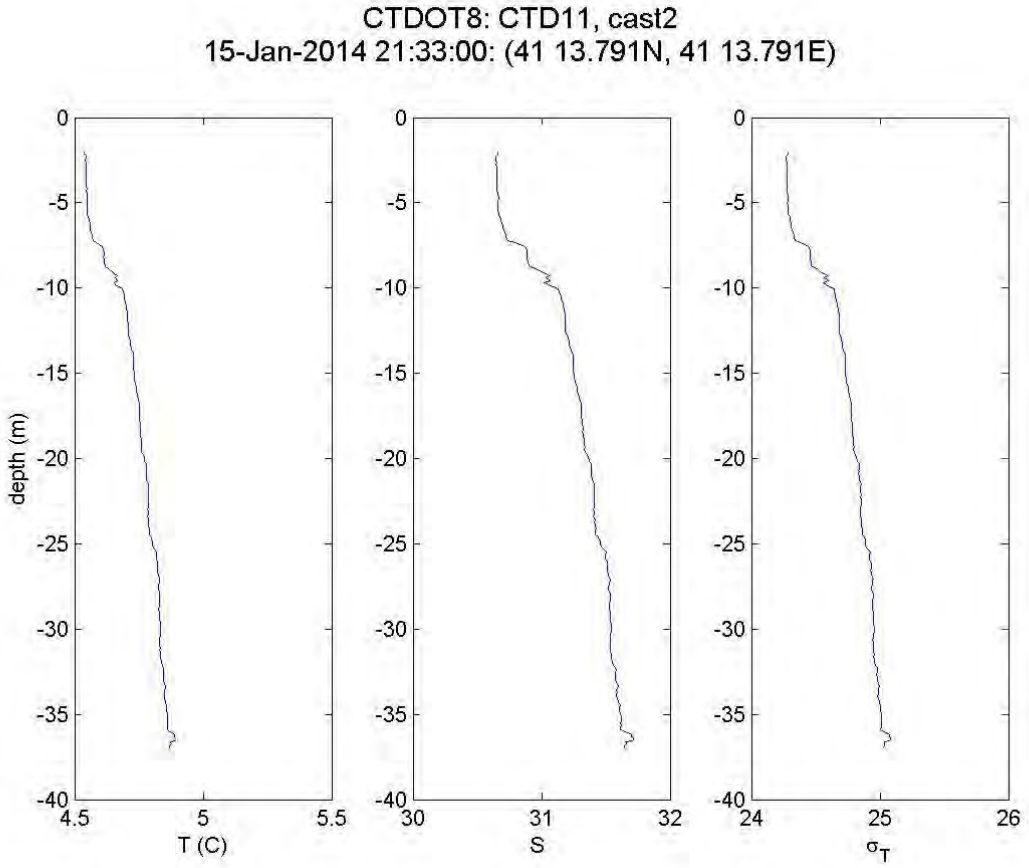

Figure 133: Cruise CTDOT8: Station CTD11, Cast 2: The left panel shows the vertical structure of Temperature (C) and the center and right panels show the salinity and density (σ_T) profiles respectively.

Appendix 11

VELOCITY PROFILES AT ALL MOORING STATIONS FOR ALL CAMPAIGNS (RDI ADCP DATA)

a. Vertical Structure of Non-tidal currents
b. Depth-averaged Time-series and Vertical Structure of the Time-averaged Current
c. Time-series of the Near Bottom Currents

Appendix 11a: Vertical Structure of Non-tidal currents

Note: Not included are profiles for Stations DOT 3 and DOT7, both for Campaigns 1, because of memory card failure.

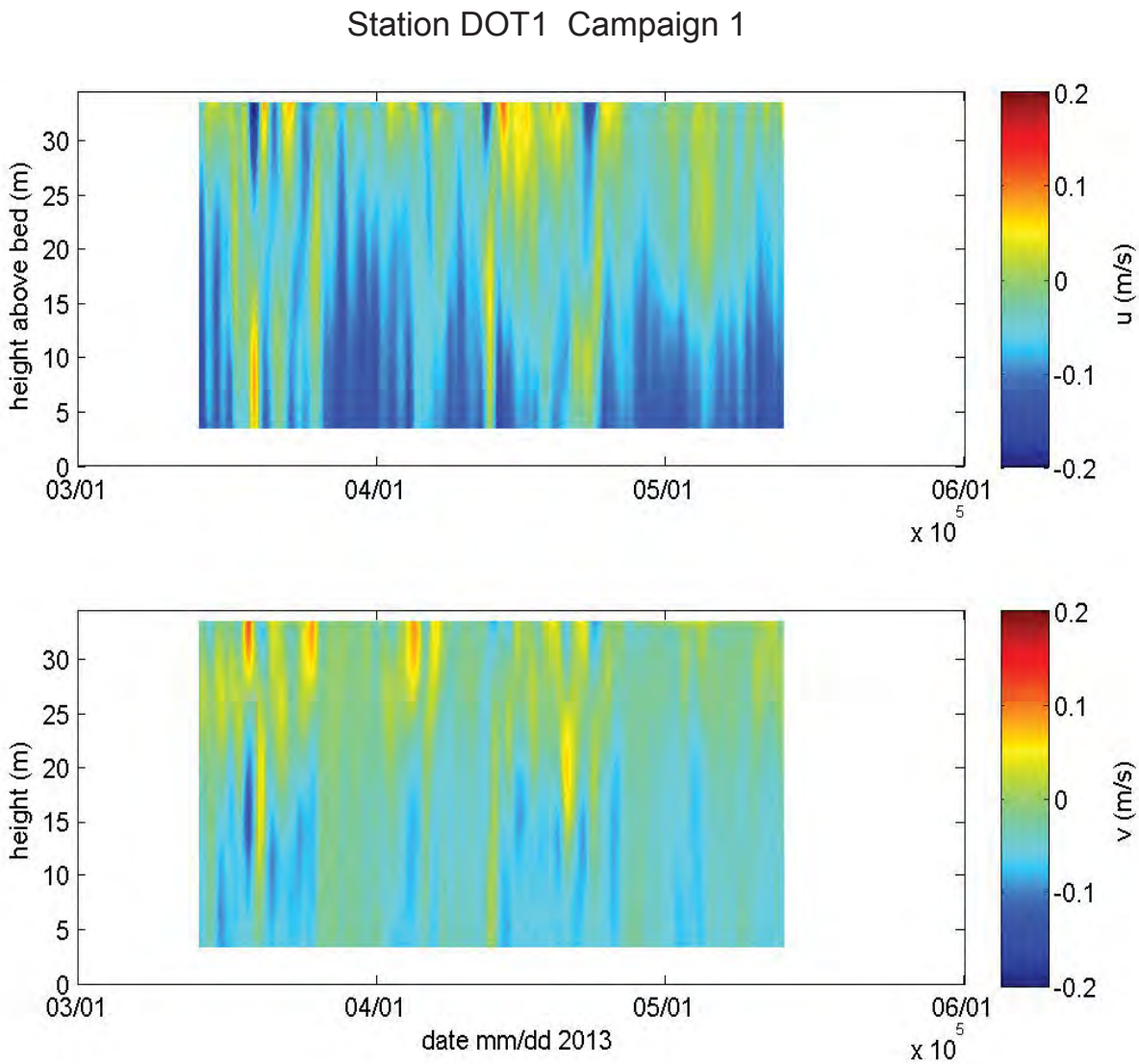

Figure 1. Low-pass filtered velocities for Station DOT1, Campaign 1: eastward (top) and northward (bottom) components.

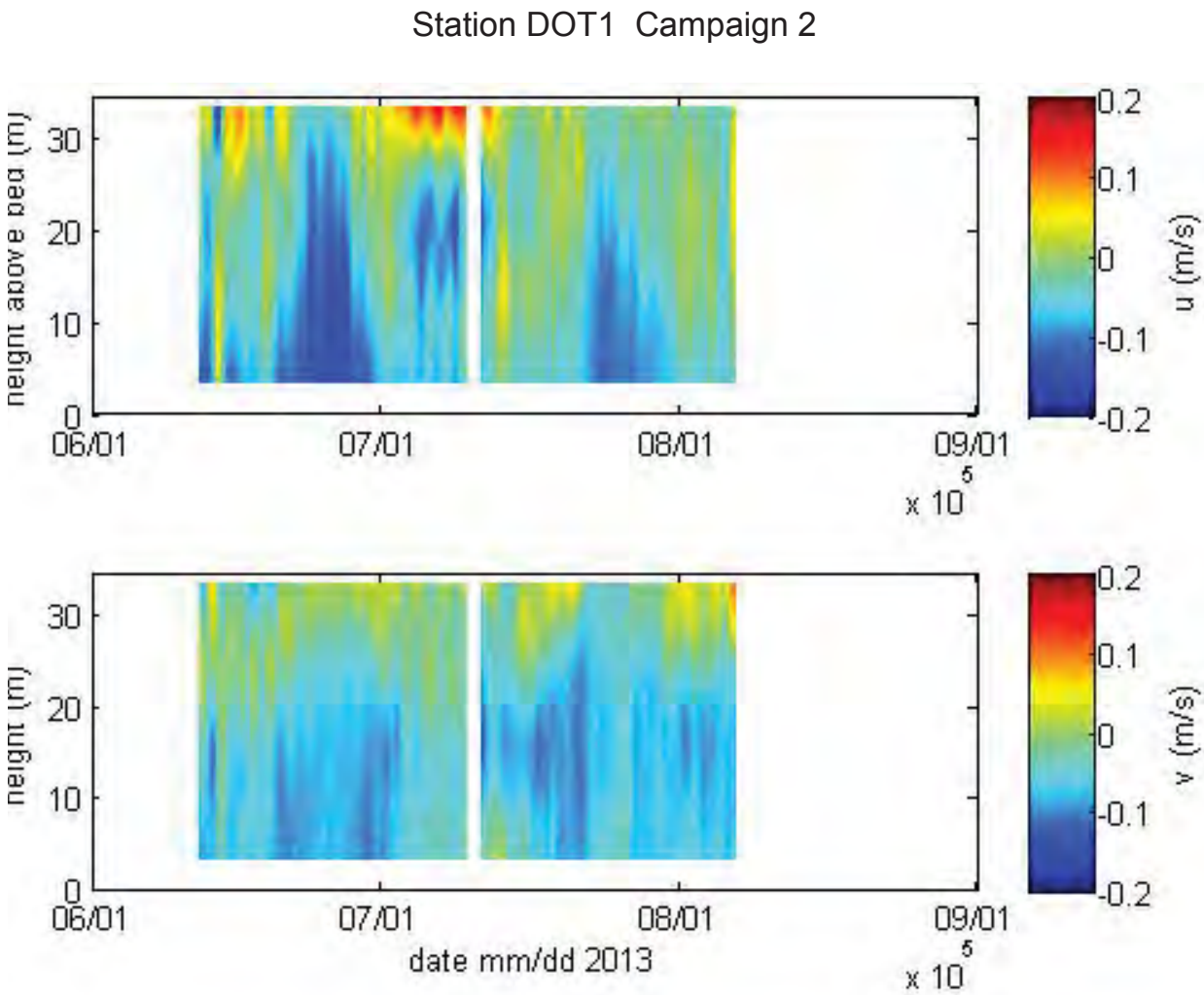

Figure 2. Low-pass filtered velocities for Station DOT1, Campaign 2: eastward (top) and northward (bottom) components.

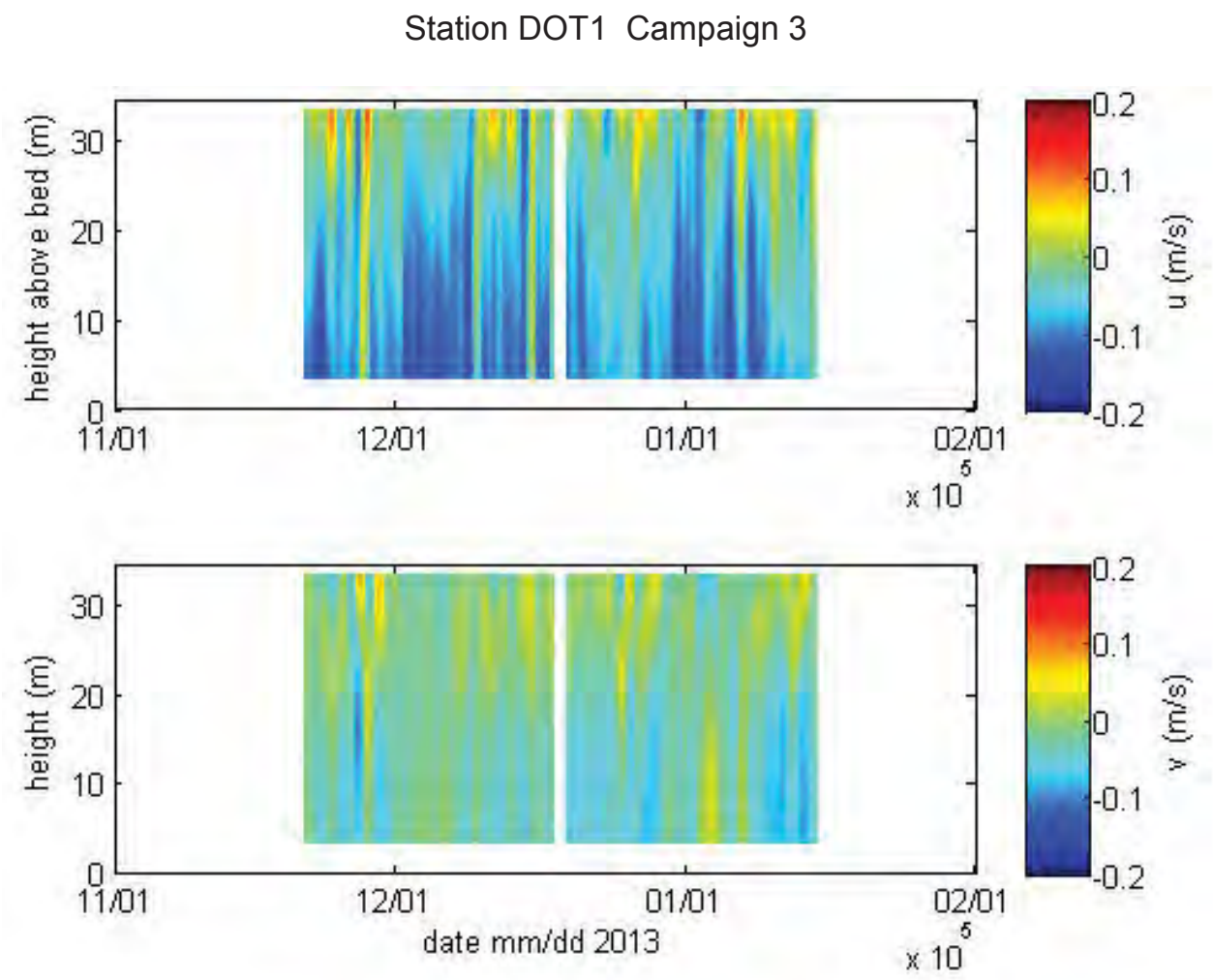

Figure 3. Low-pass filtered velocities for Station 1, Campaign 3: eastward (top) and northward (bottom) components.

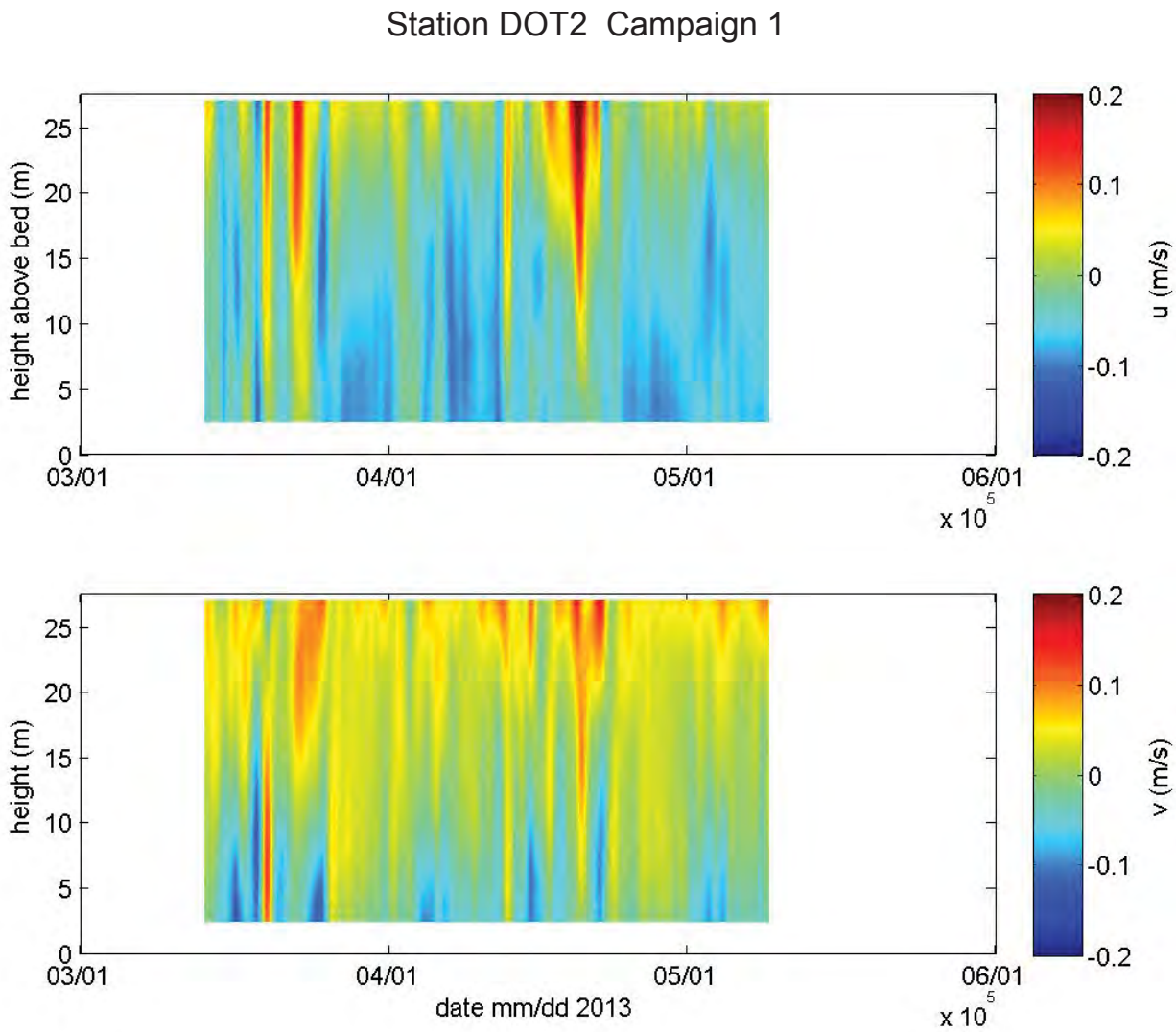

Figure 4. Low-pass filtered velocities for Station DOT2, Campaign 1: eastward (top) and northward (bottom) components.

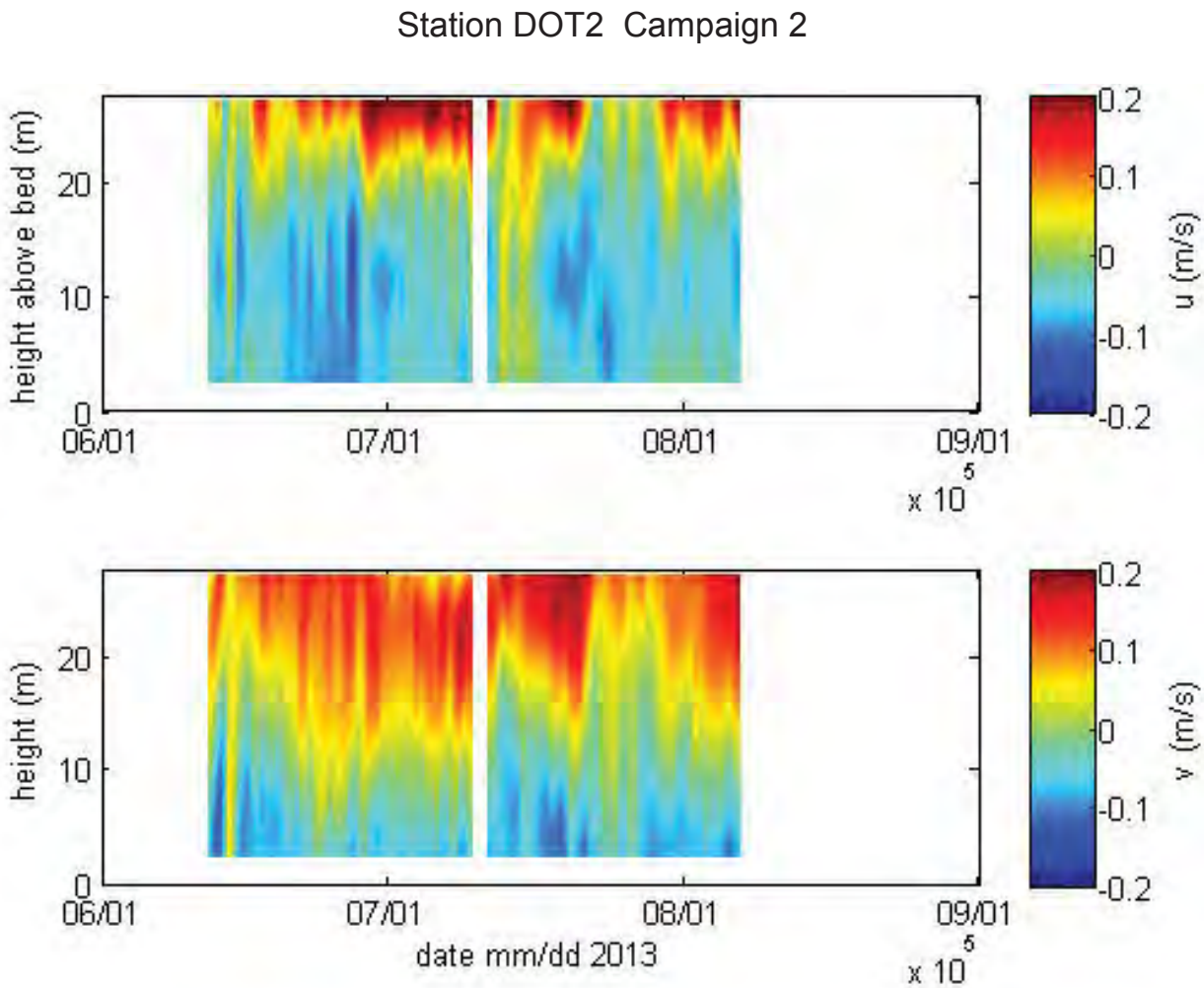

Figure 5. Low-pass filtered velocities for Station DOT2, Campaign 2: eastward (top) and northward (bottom) components.

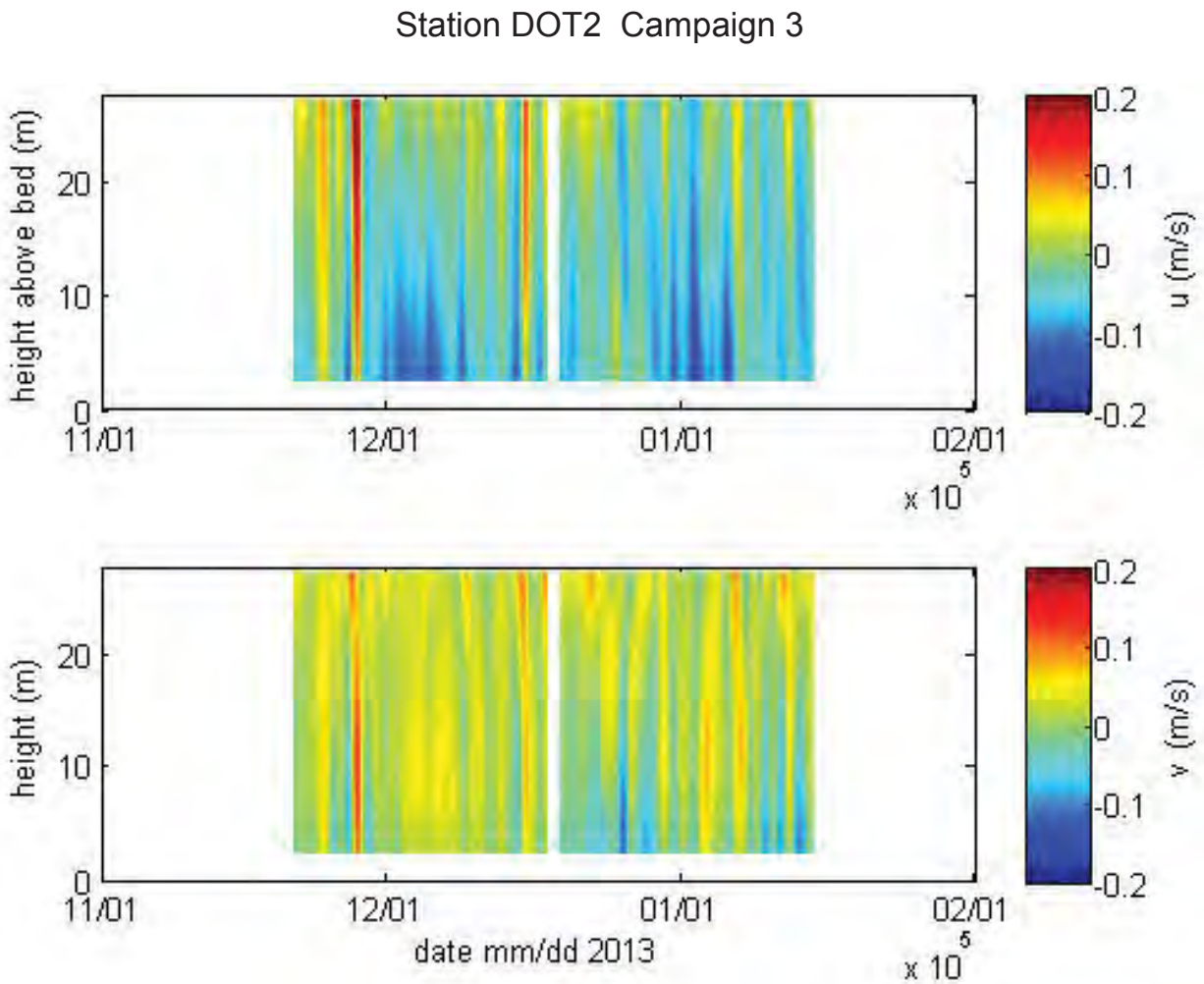

Figure 6. Low-pass filtered velocities for Station DOT2, Campaign 3: eastward (top) and northward (bottom) components.

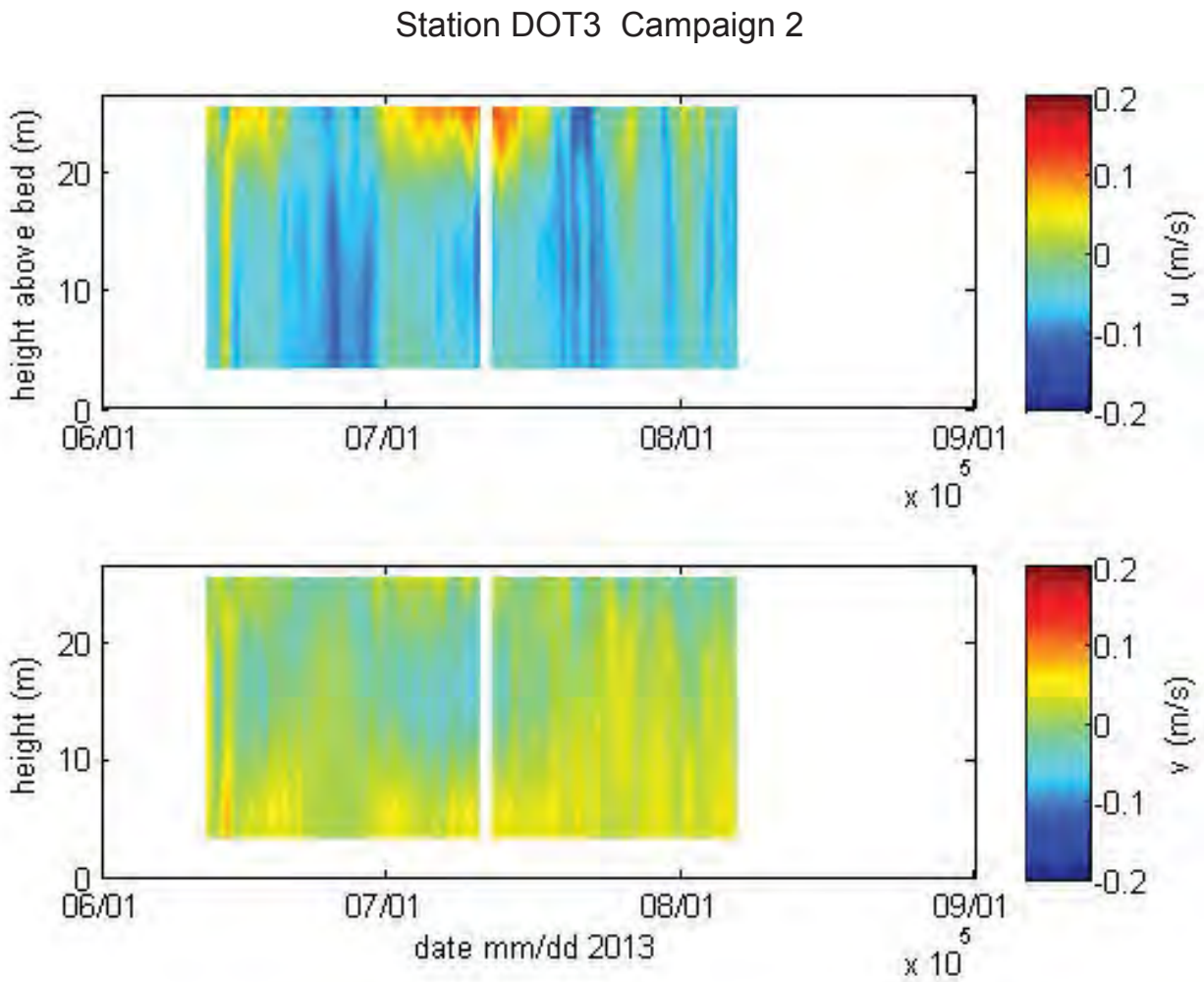

Figure 7. Low-pass filtered velocities for Station DOT3, Campaign 2: eastward (top) and northward (bottom) components.

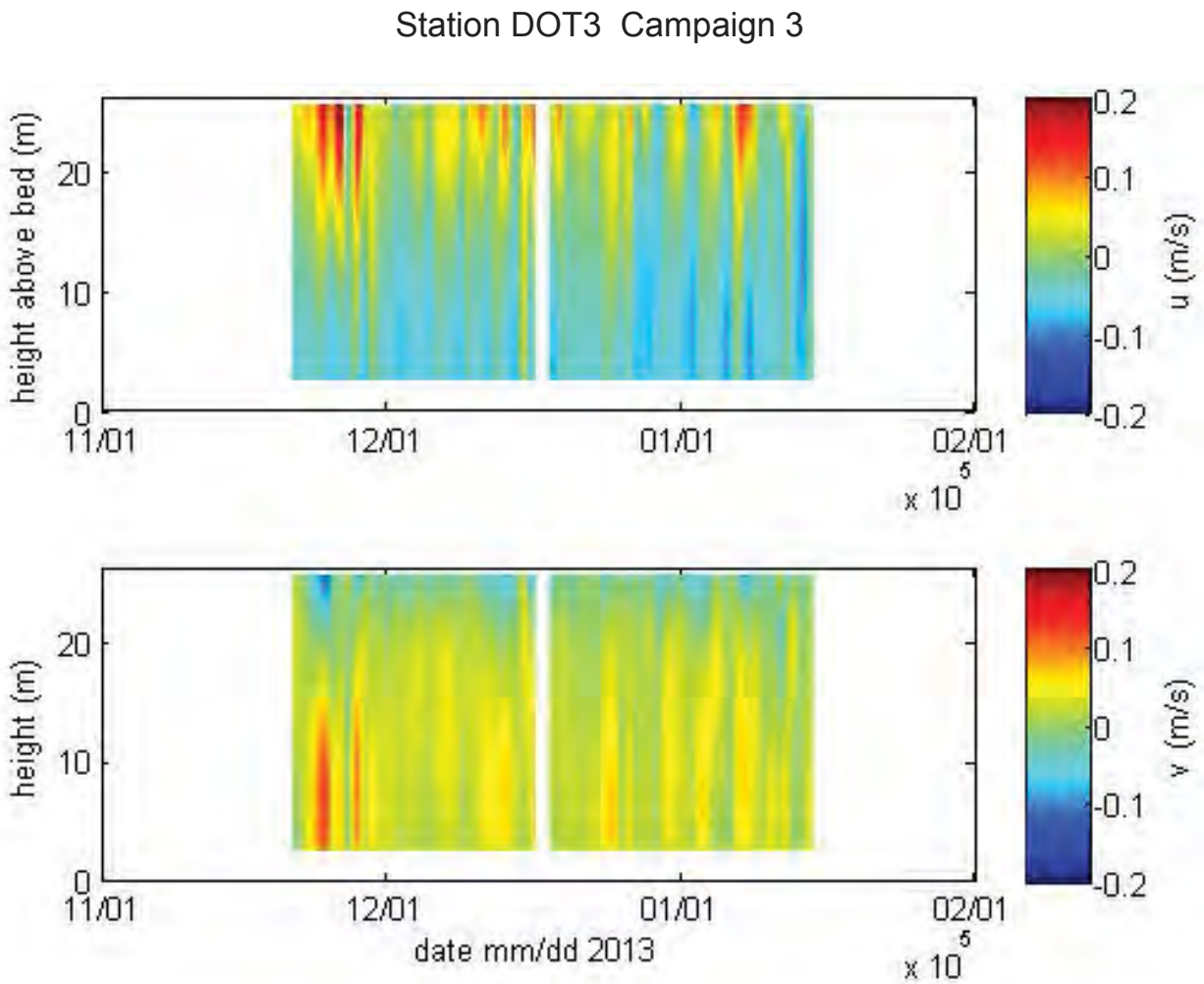

Figure 8. Low-pass filtered velocities for Station DOT3, Campaign 3: eastward (top) and northward (bottom) components.

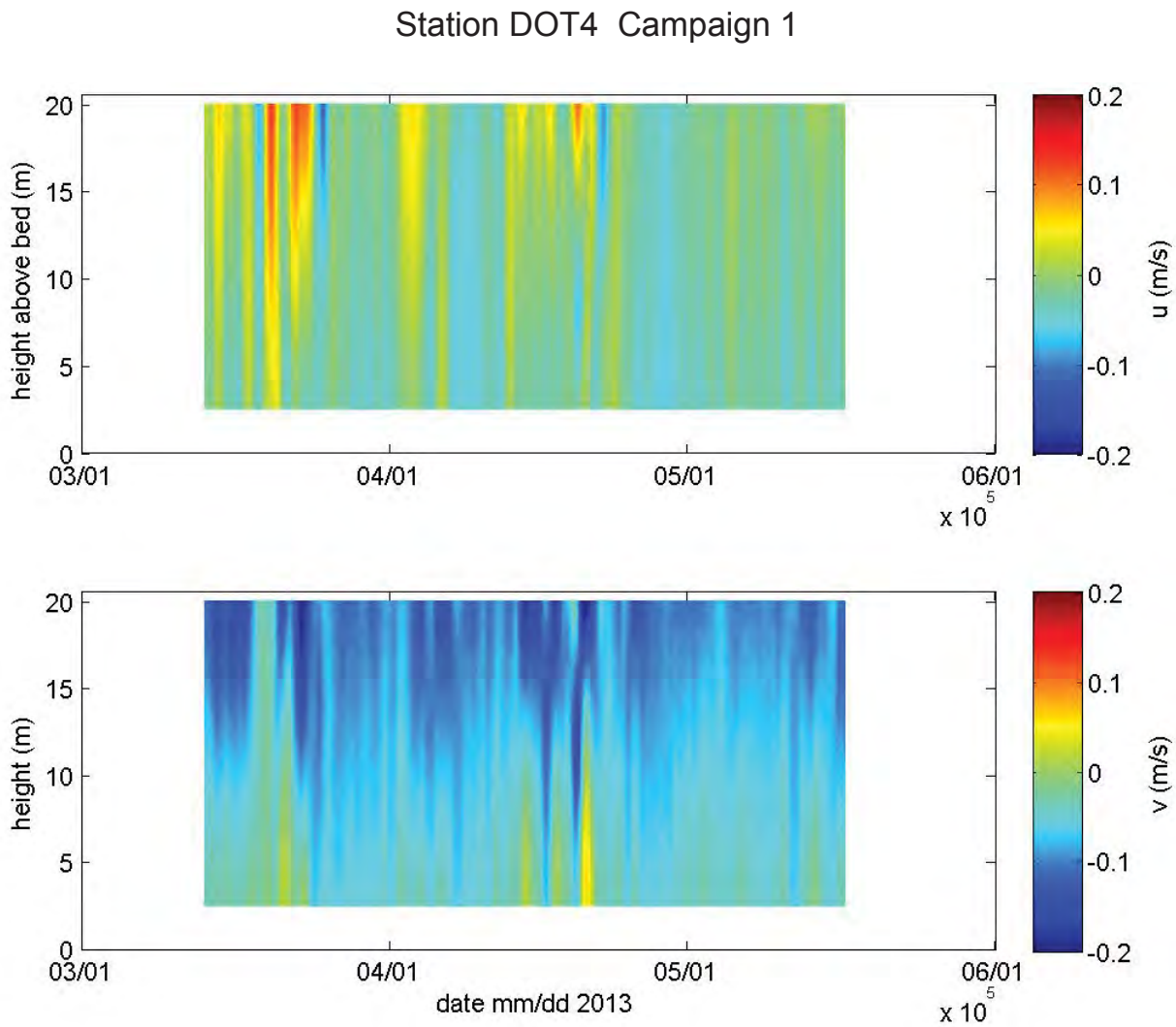

Figure 9. Low-pass filtered velocities for Station DOT4, Campaign 1: eastward (top) and northward (bottom) components.

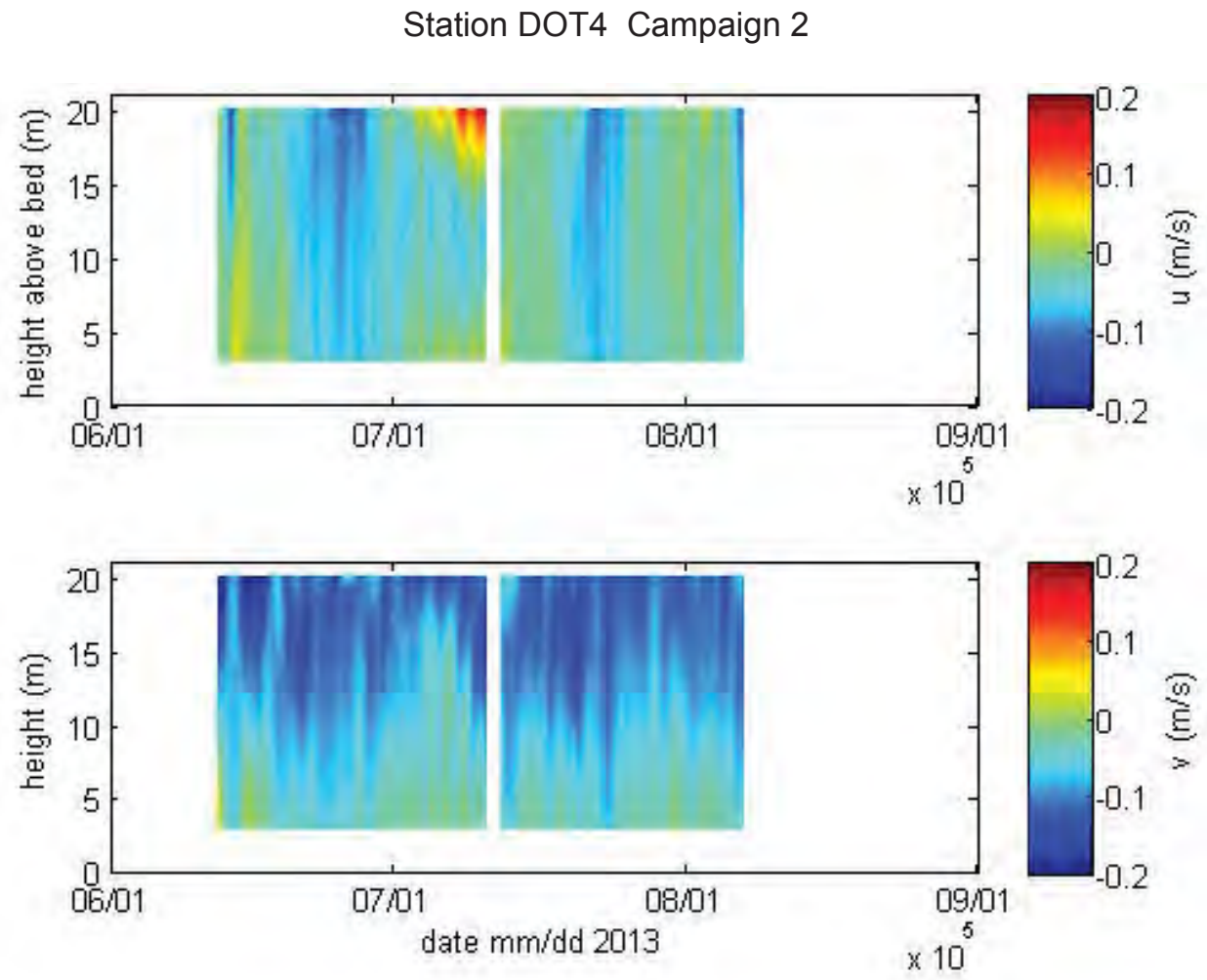

Figure 10. Low-pass filtered velocities for Station DOT4, Campaign 2: eastward (top) and northward (bottom) components.

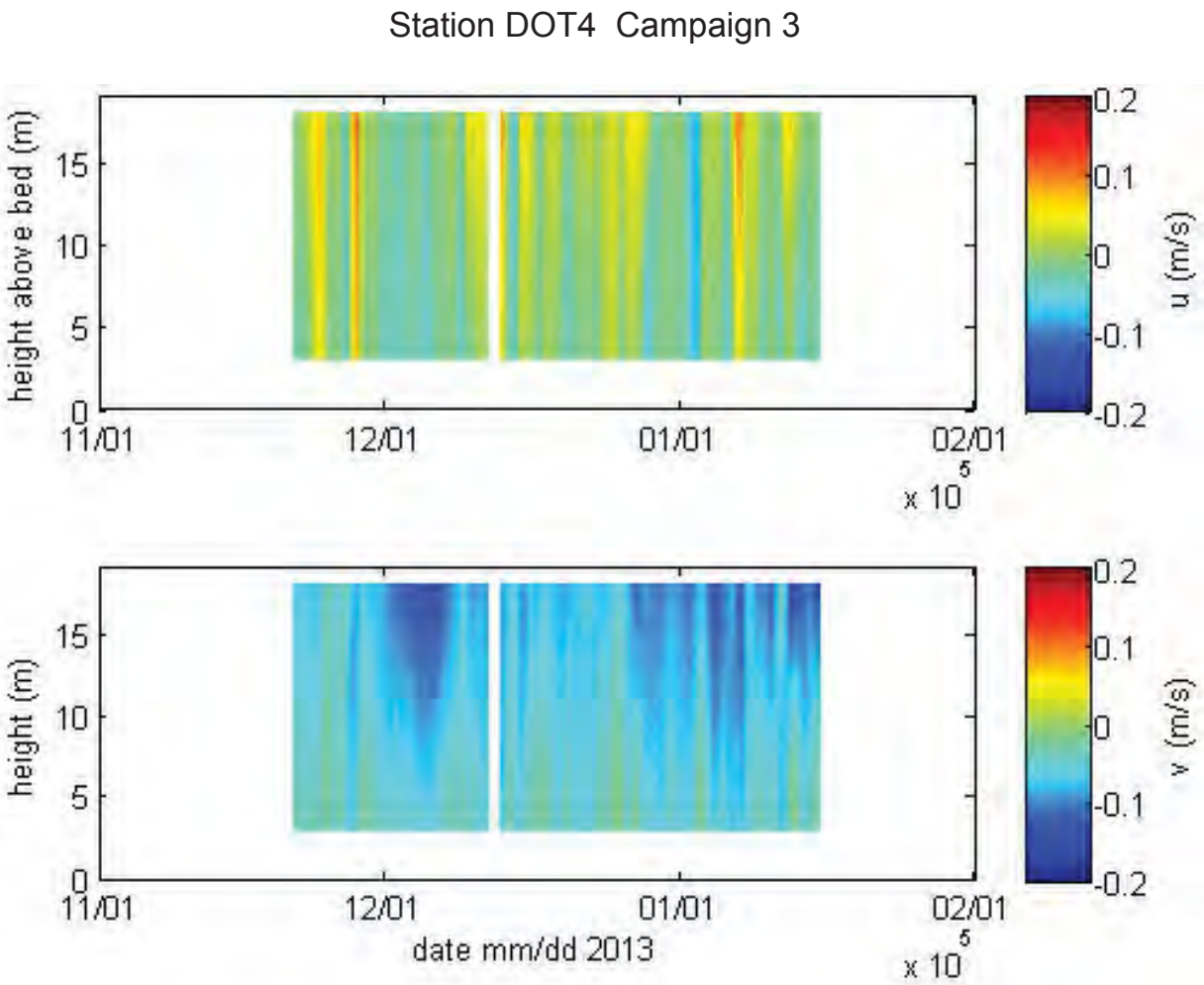

Figure 11. Low-pass filtered velocities for Station DOT4, Campaign 3: eastward (top) and northward (bottom) components.

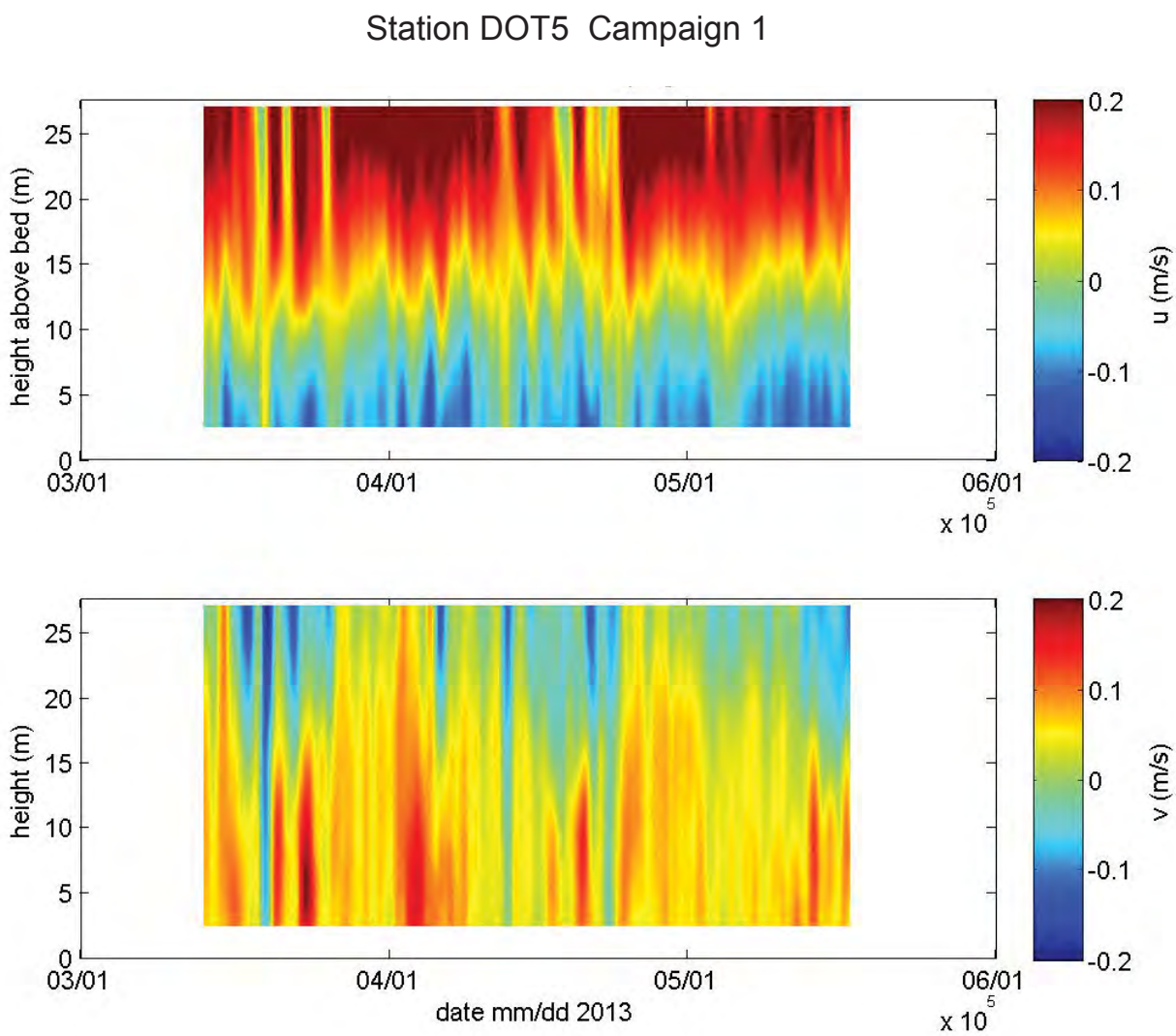

Figure 12 Low-pass filtered velocities for Station DOT5, Campaign 1: eastward (top) and northward (bottom) components.

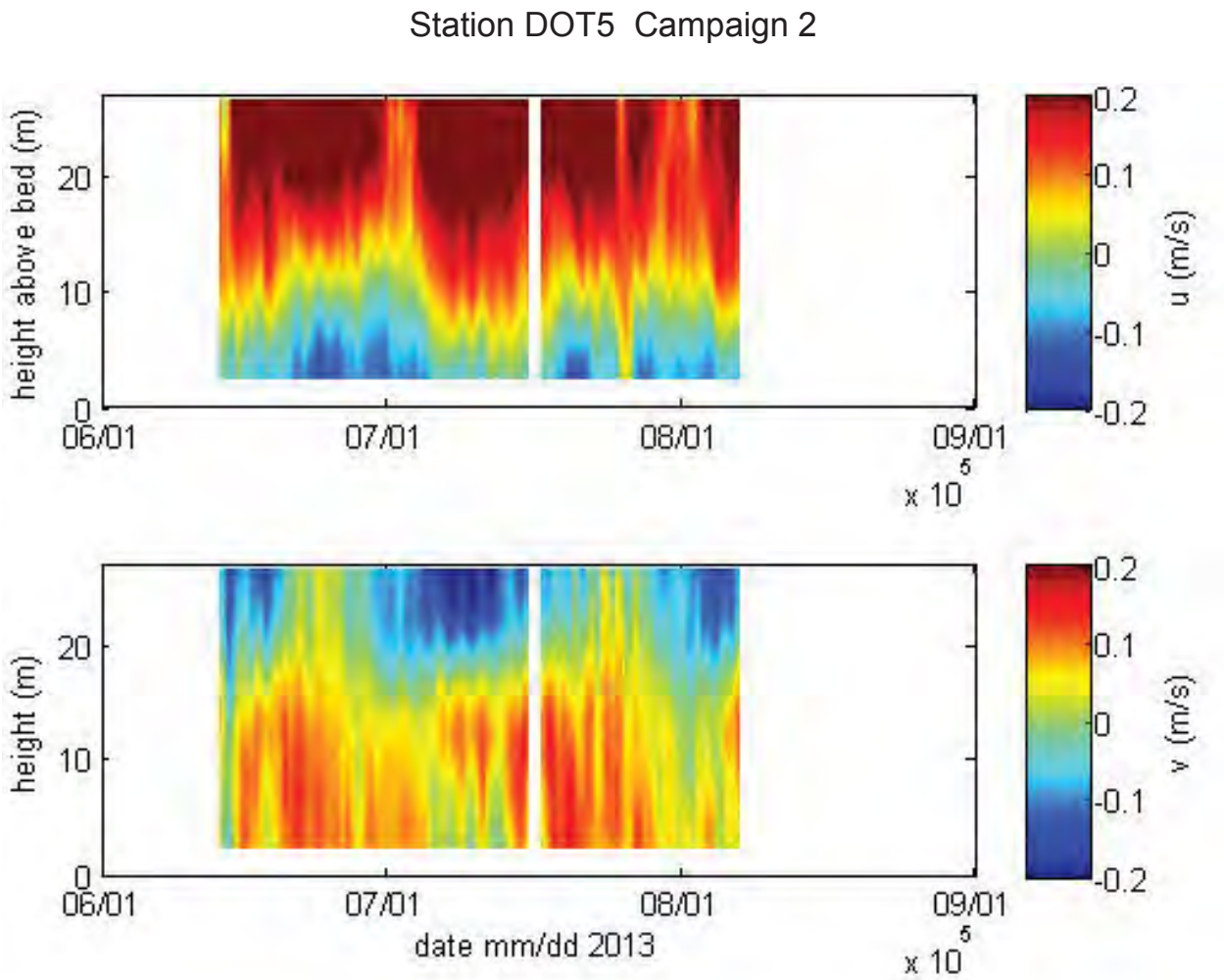

Figure 13. Low-pass filtered velocities for Station DOT5, Campaign 2: eastward (top) and northward (bottom) components.

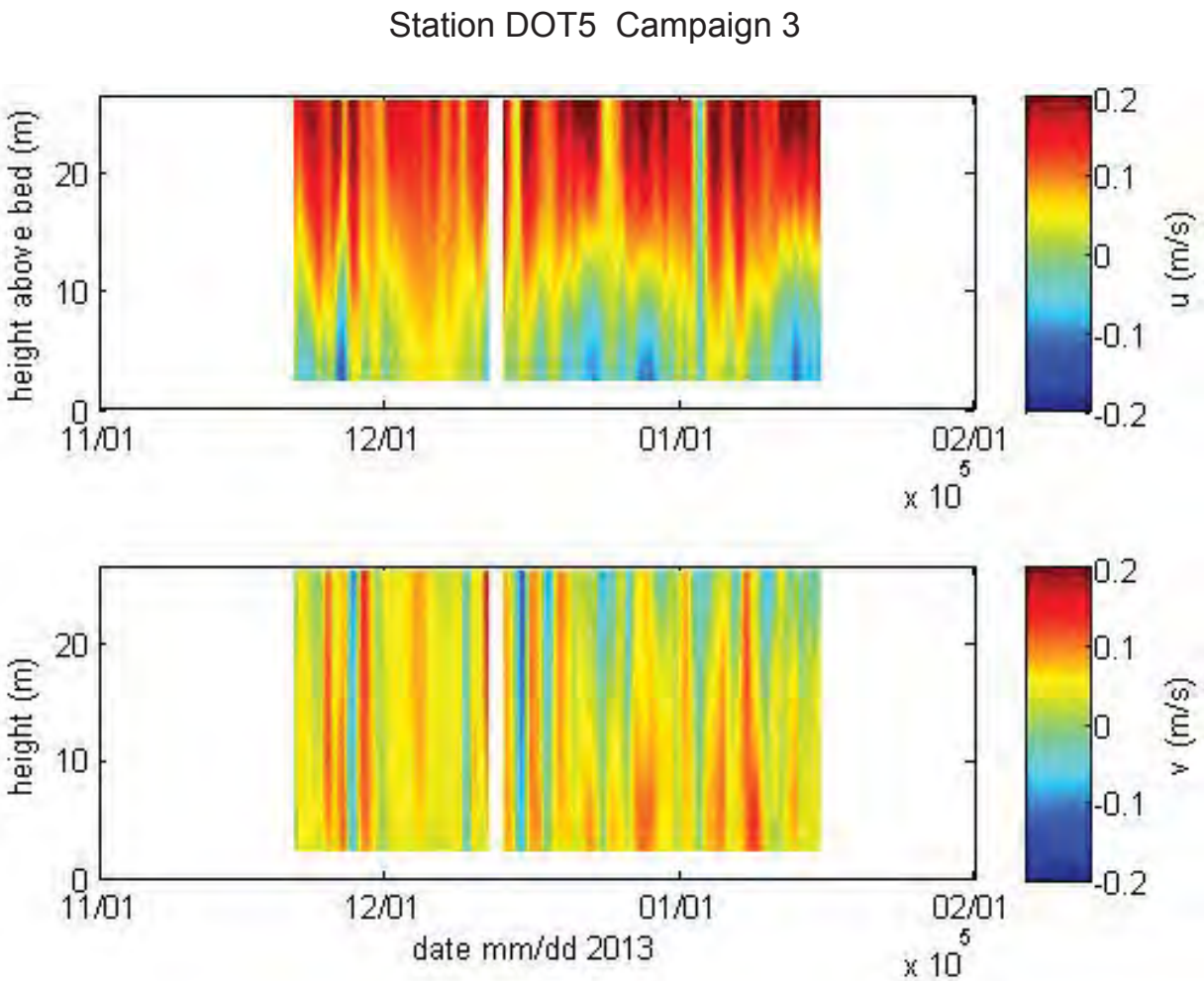

Figure 14. Low-pass filtered velocities for Station DOT5, Campaign 3: eastward (top) and northward (bottom) components.

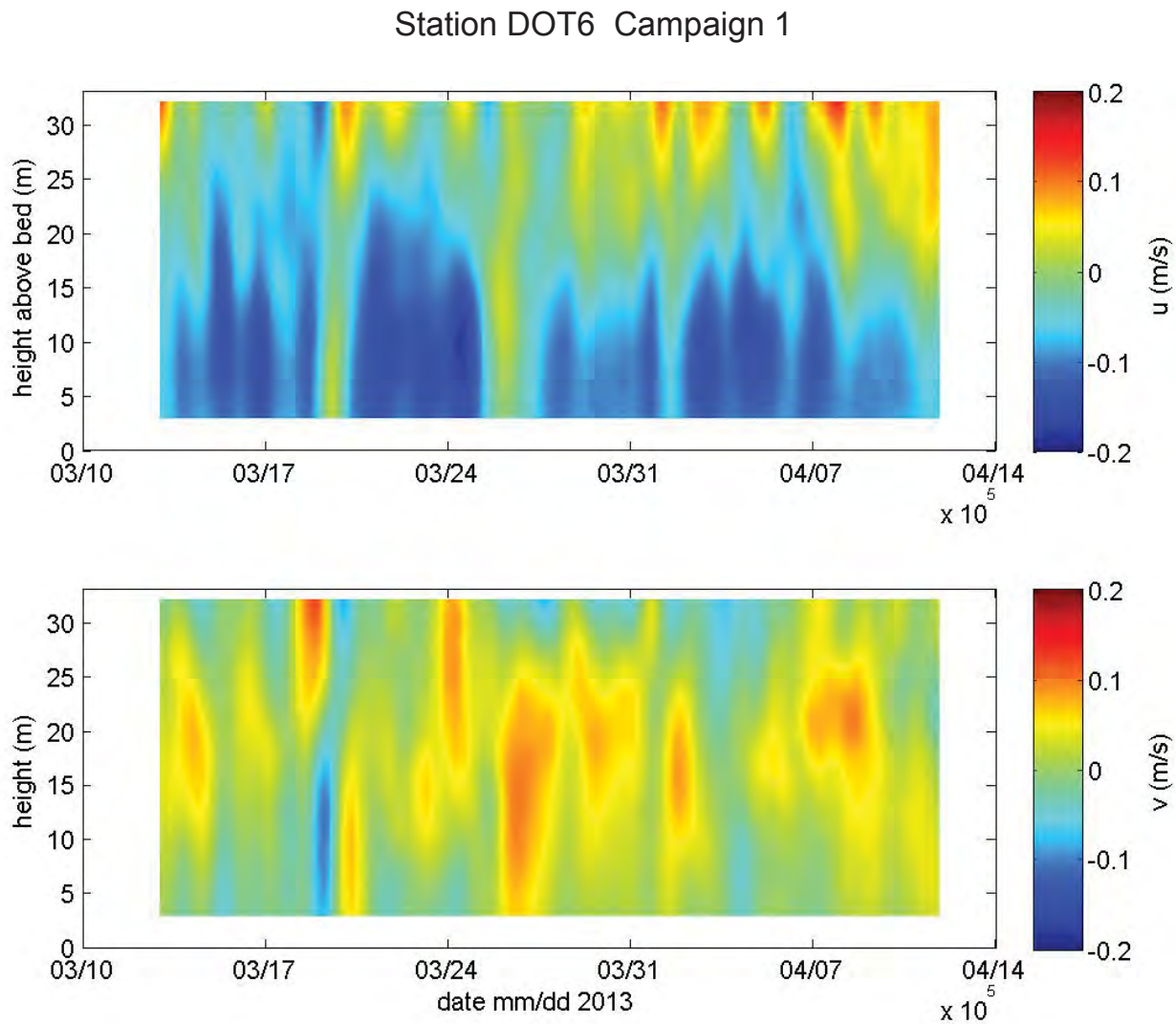

Figure 15. Low-pass filtered velocities for Station DOT6, Campaign 1: eastward (top) and northward (bottom) components.

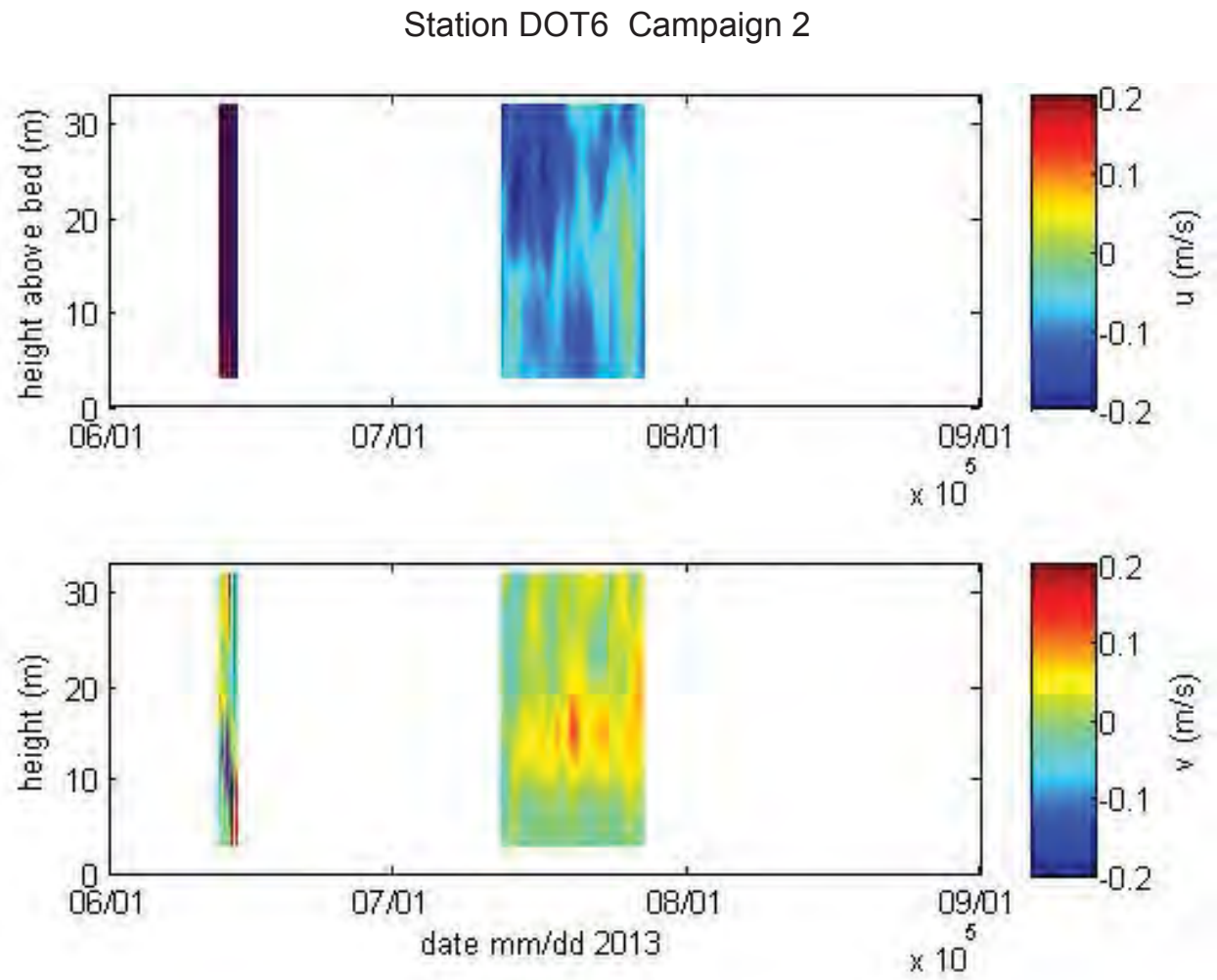

Figure 16. Low-pass filtered velocities for Station DOT6, Campaign 2: eastward (top) and northward (bottom) components.

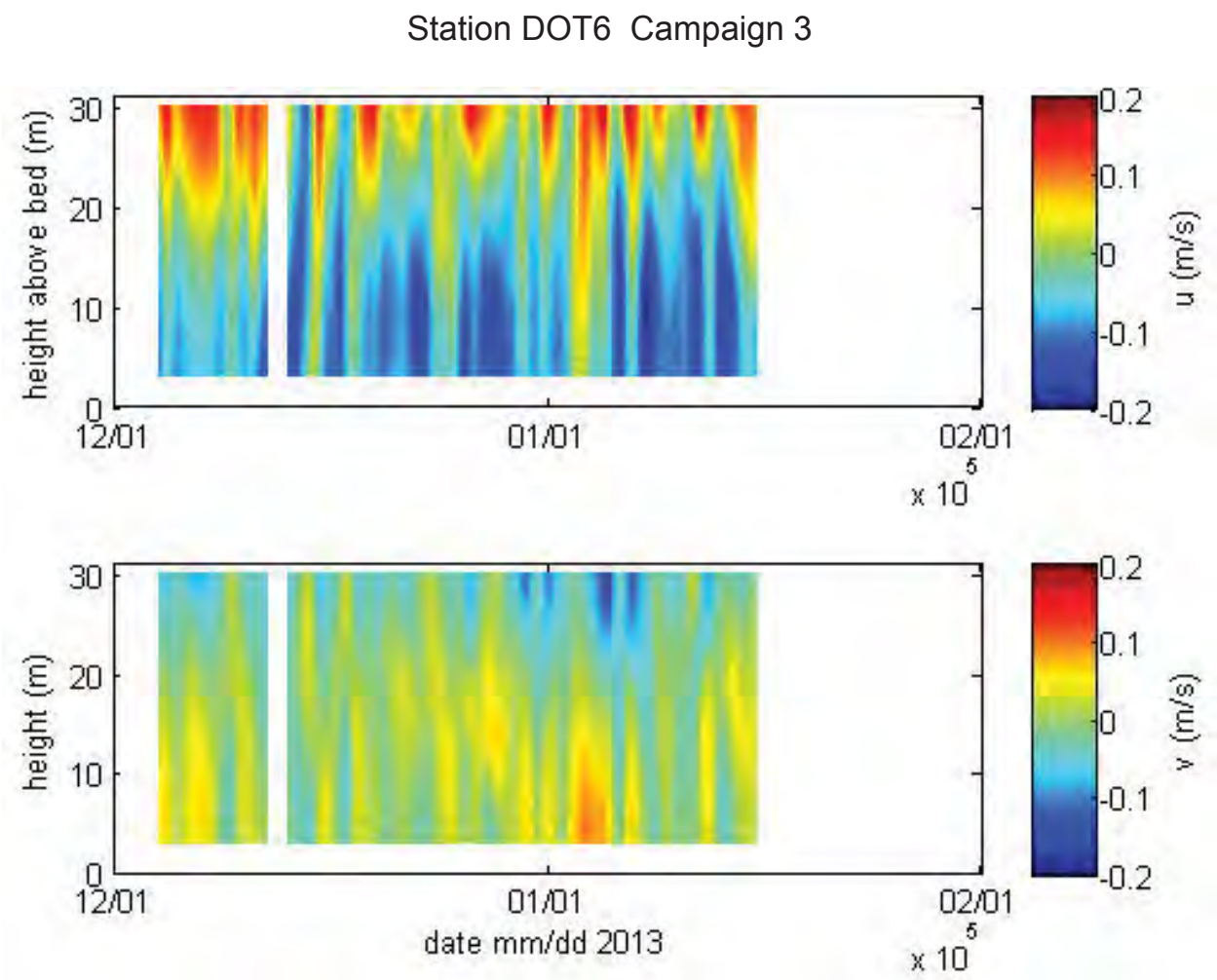

Figure 17. Low-pass filtered velocities for Station DOT6, Campaign 3: eastward (top) and northward (bottom) components.

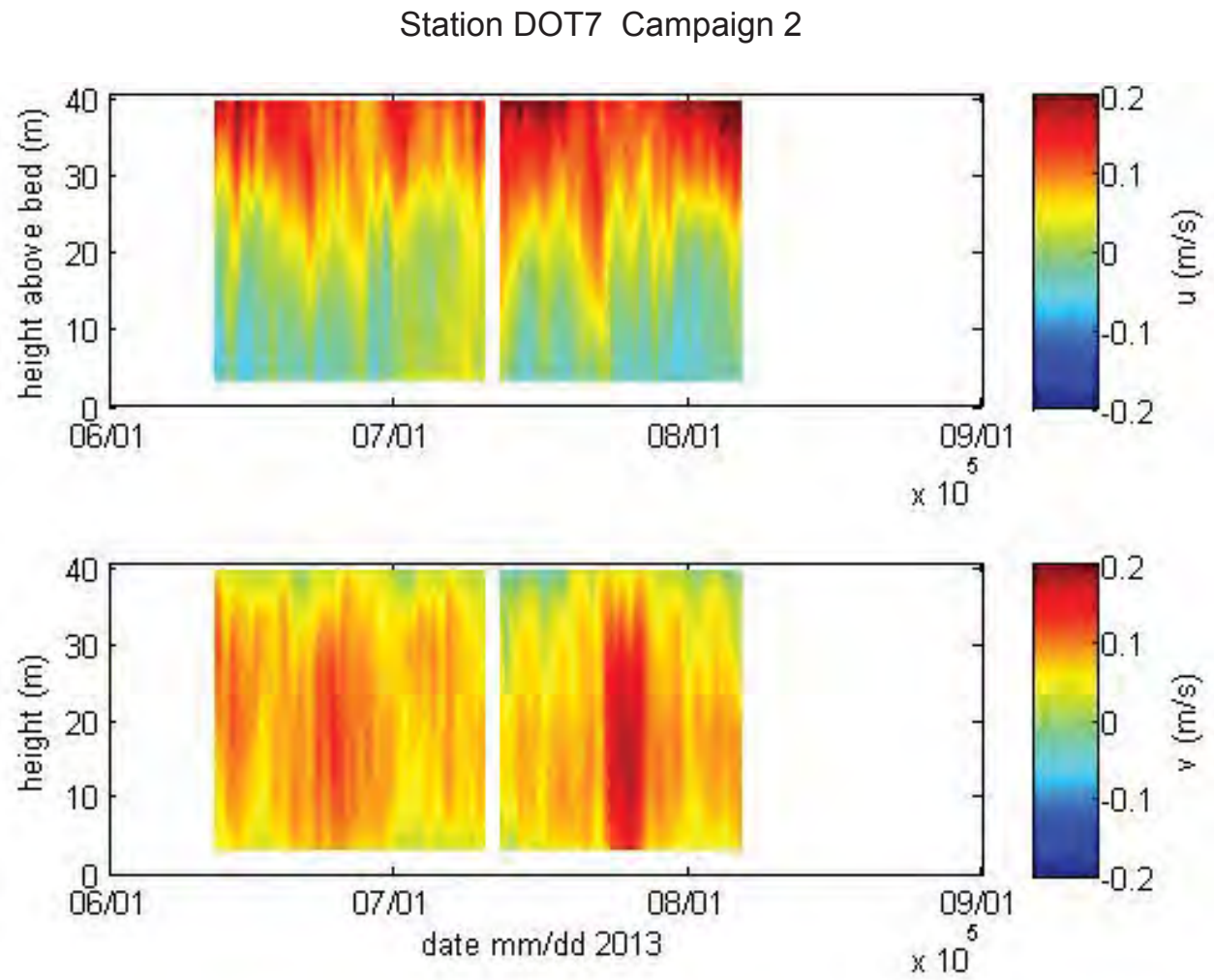

Figure 18. Low-pass filtered velocities for Station DOT7, Campaign 2: eastward (top) and northward (bottom) components.

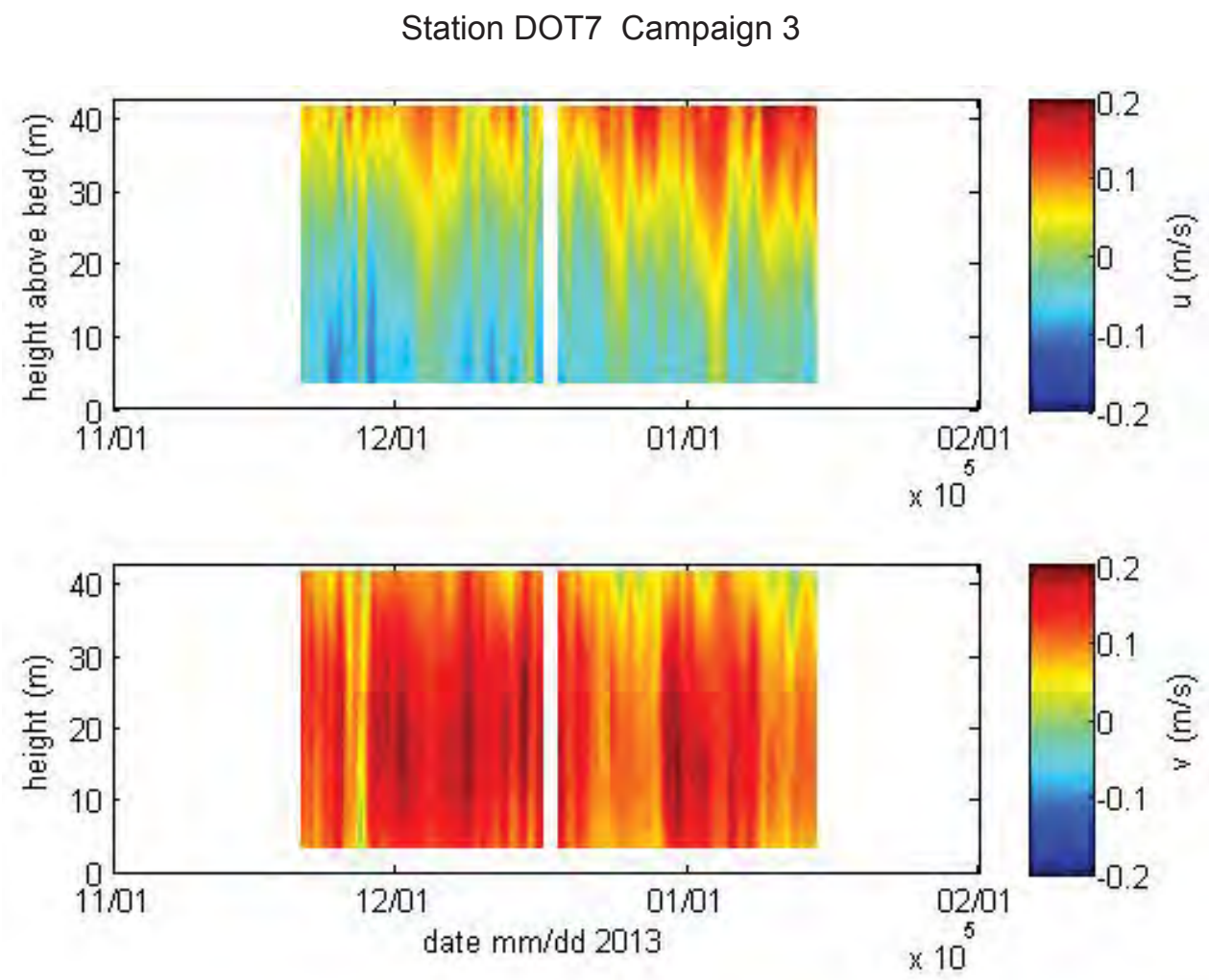

Figure 19. Low-pass filtered velocities for Station DOT7, Campaign 3: eastward (top) and northward (bottom) components.

Appendix 11b: Depth-averaged Time-series and Vertical Structure of the Time-averaged Current

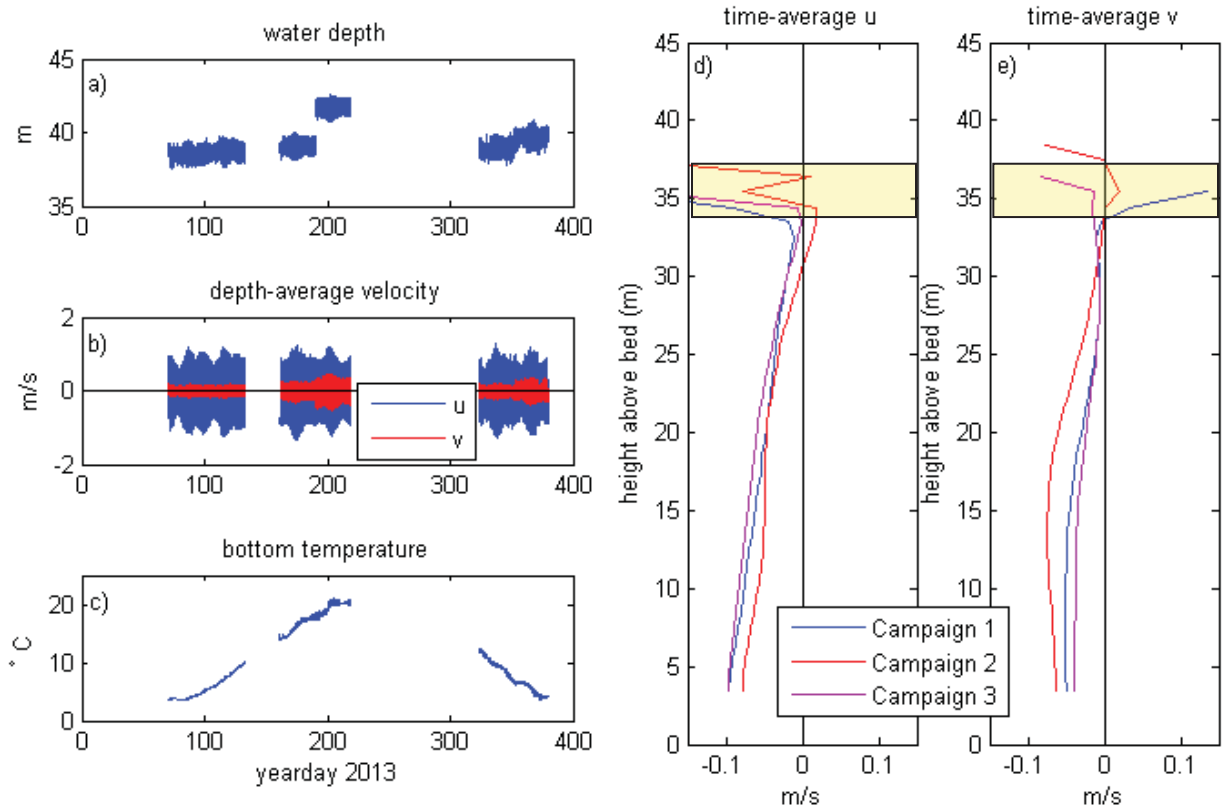

Figure 20. Station DOT1, all campaigns: (a) water depth; (b) depth-averaged velocity; (c) near-bottom temperature; (d) deployment-average, eastward velocity; and (e) deployment-average, northward velocity.

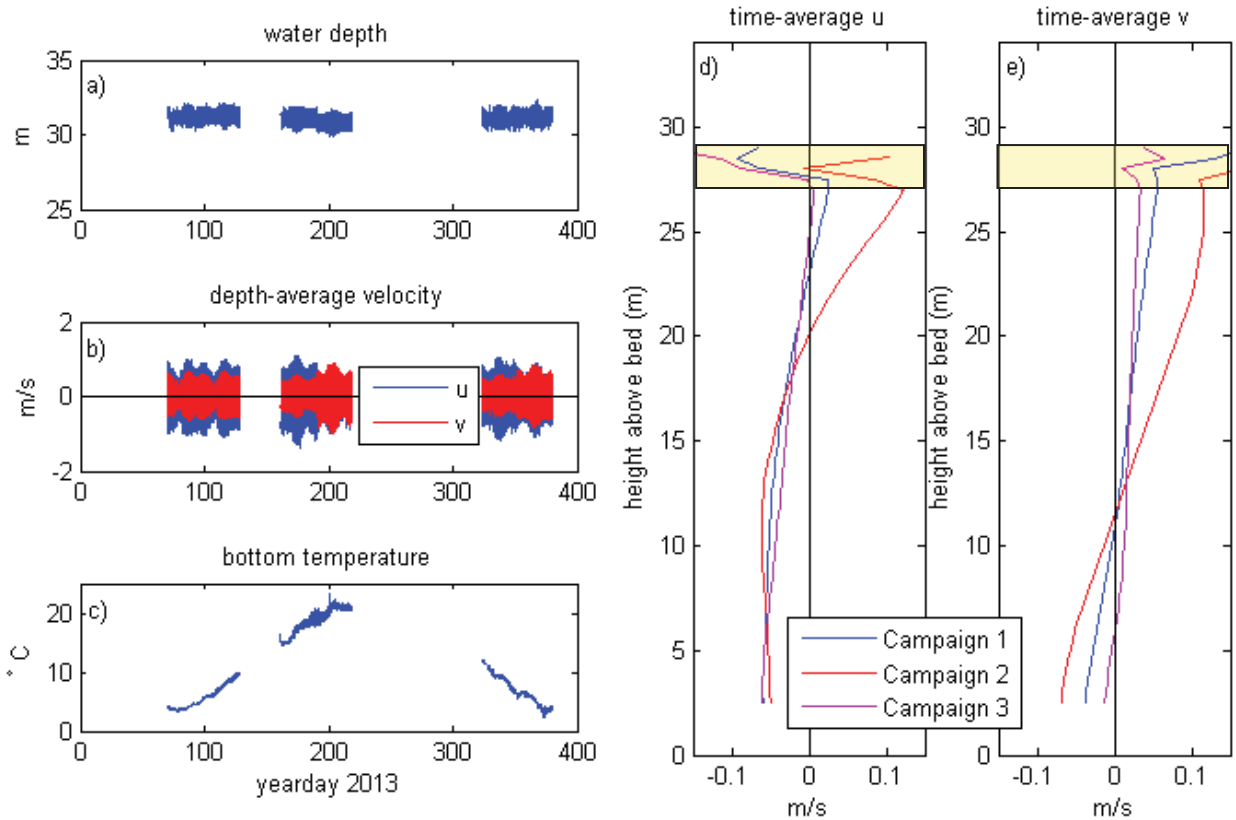

Figure 21. Station DOT2, all campaigns: (a) water depth; (b) depth-averaged velocity; (c) near-bottom temperature; (d) deployment-average, eastward velocity; and (e) deployment-average, northward velocity.

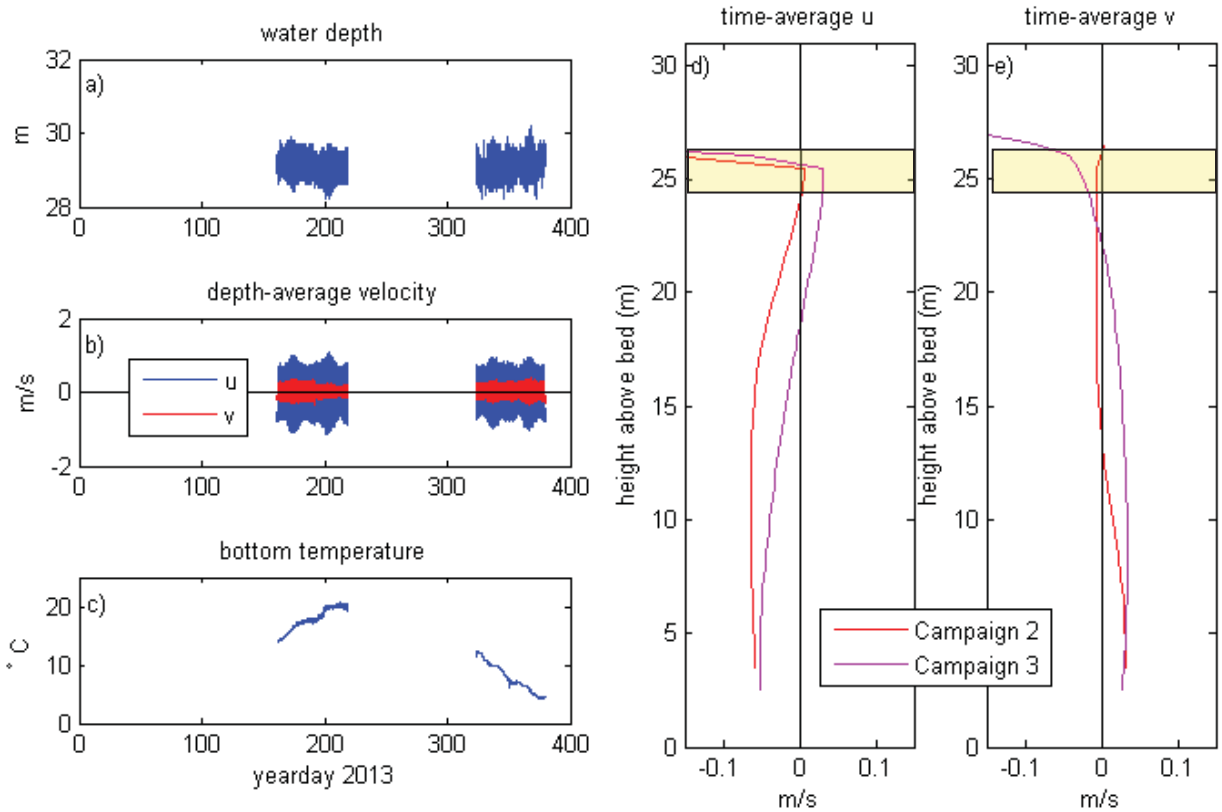

Figure 22. Station DOT3, all campaigns: (a) water depth; (b) depth-averaged velocity; (c) near-bottom temperature; (d) deployment-average, eastward velocity; and (e) deployment-average, northward velocity.

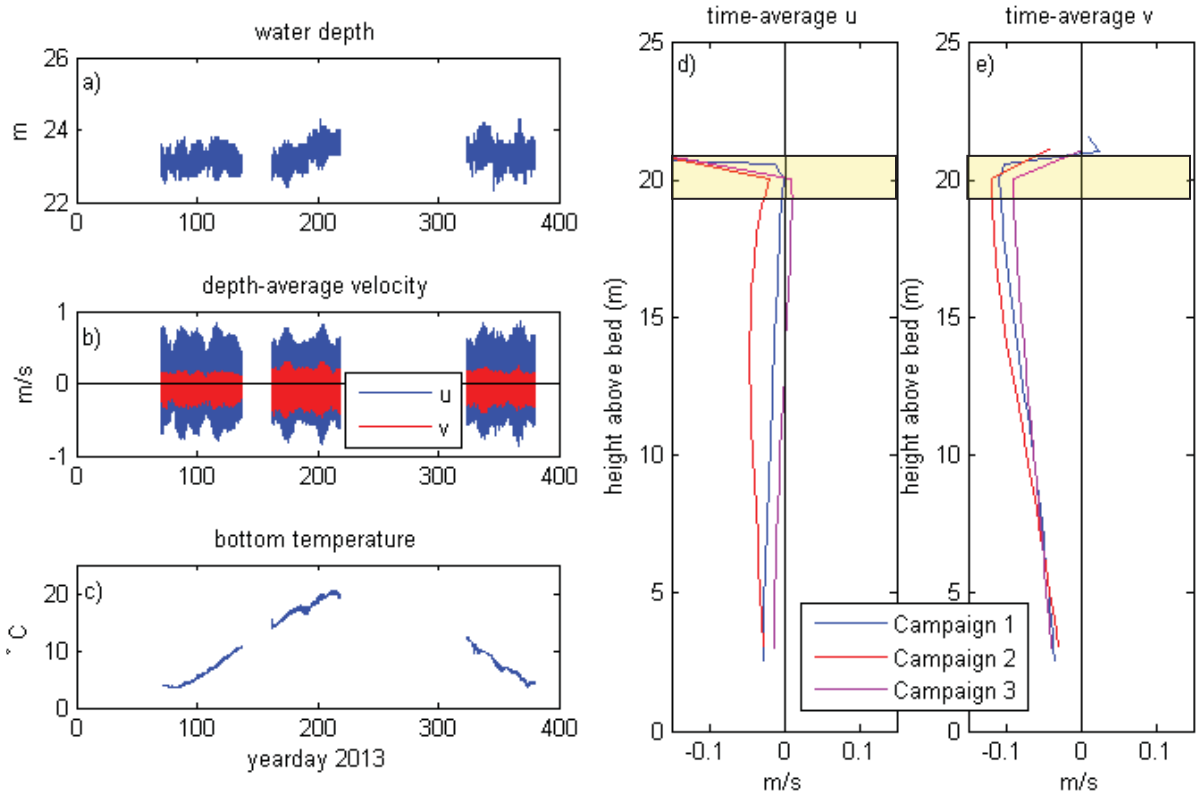

Figure 23. Station DOT4, all campaigns: (a) water depth; (b) depth-averaged velocity; (c) near-bottom temperature; (d) deployment-average, eastward velocity; and (e) deployment-average, northward velocity.

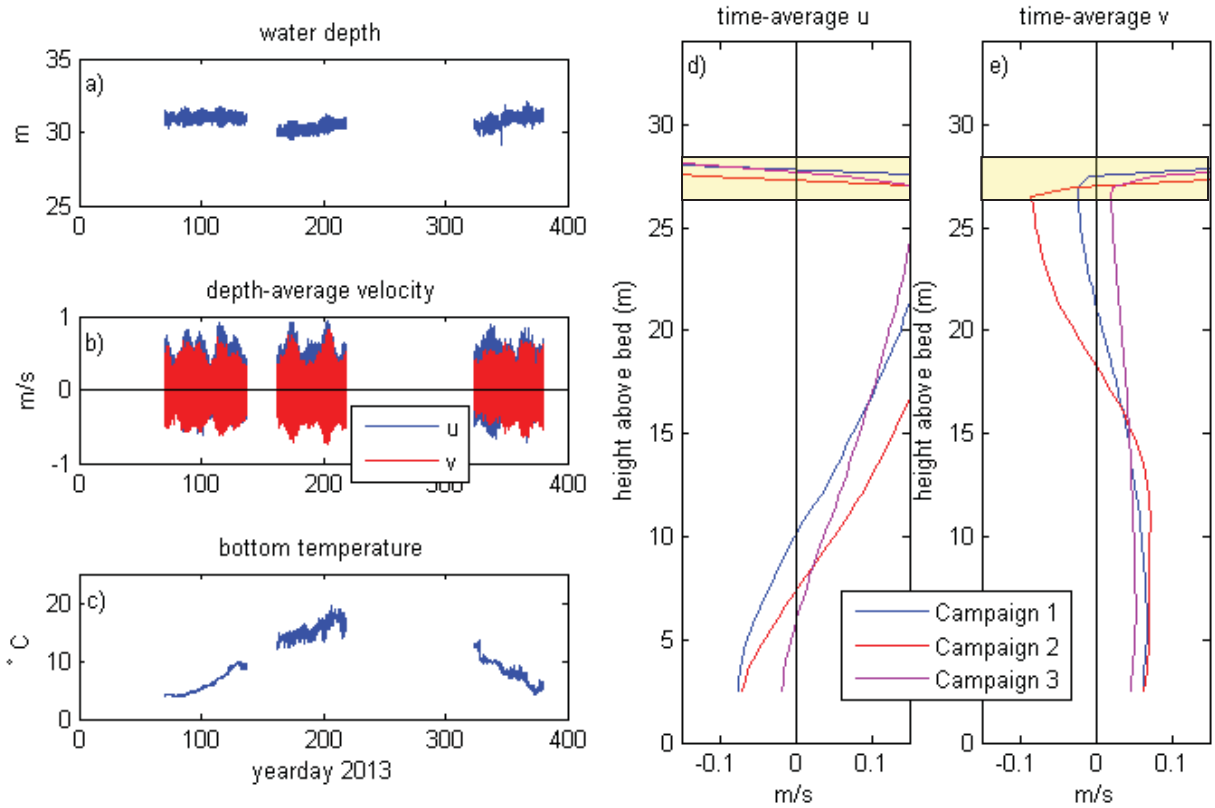

Figure 24. Station DOT5, all campaigns: (a) water depth; (b) depth-averaged velocity; (c) near-bottom temperature; (d) deployment-average, eastward velocity; and (e) deployment-average, northward velocity.

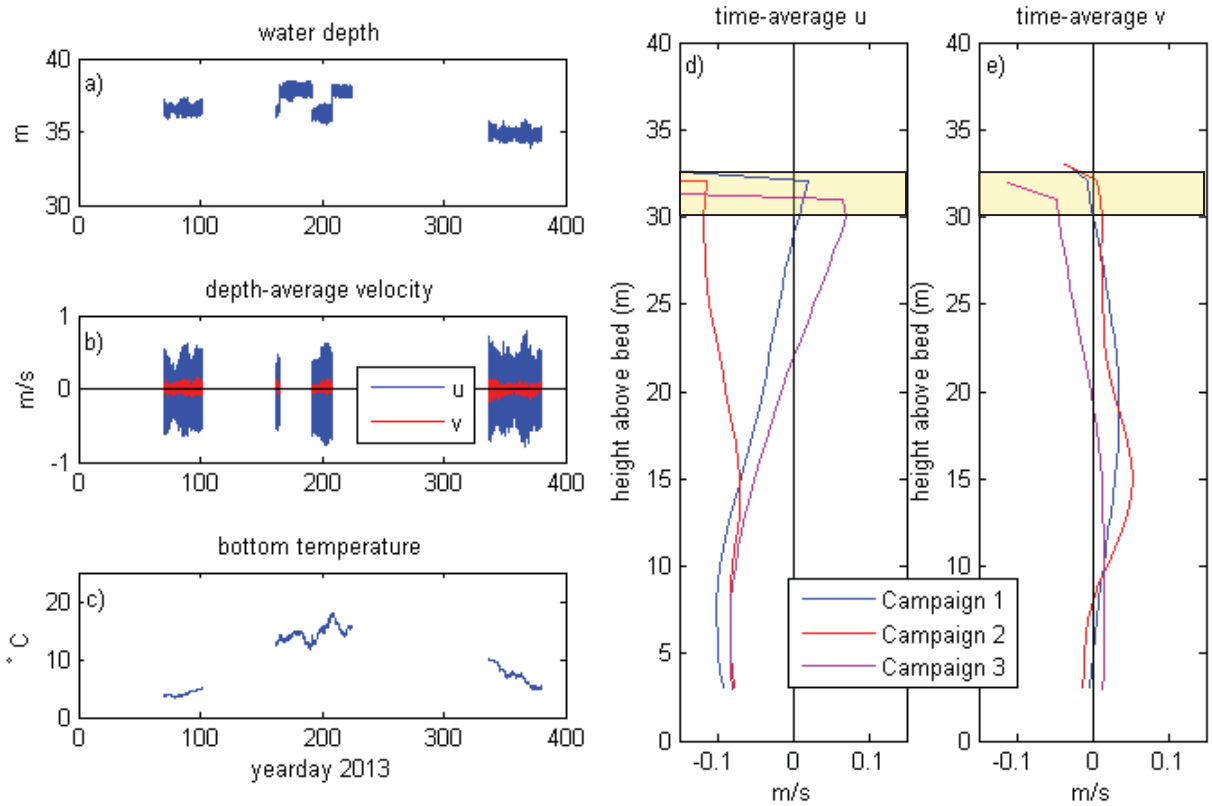

Figure 25. Station DOT6, all campaigns: (a) water depth; (b) depth-averaged velocity; (c) near-bottom temperature; (d) deployment-average, eastward velocity; and (e) deployment-average, northward velocity.

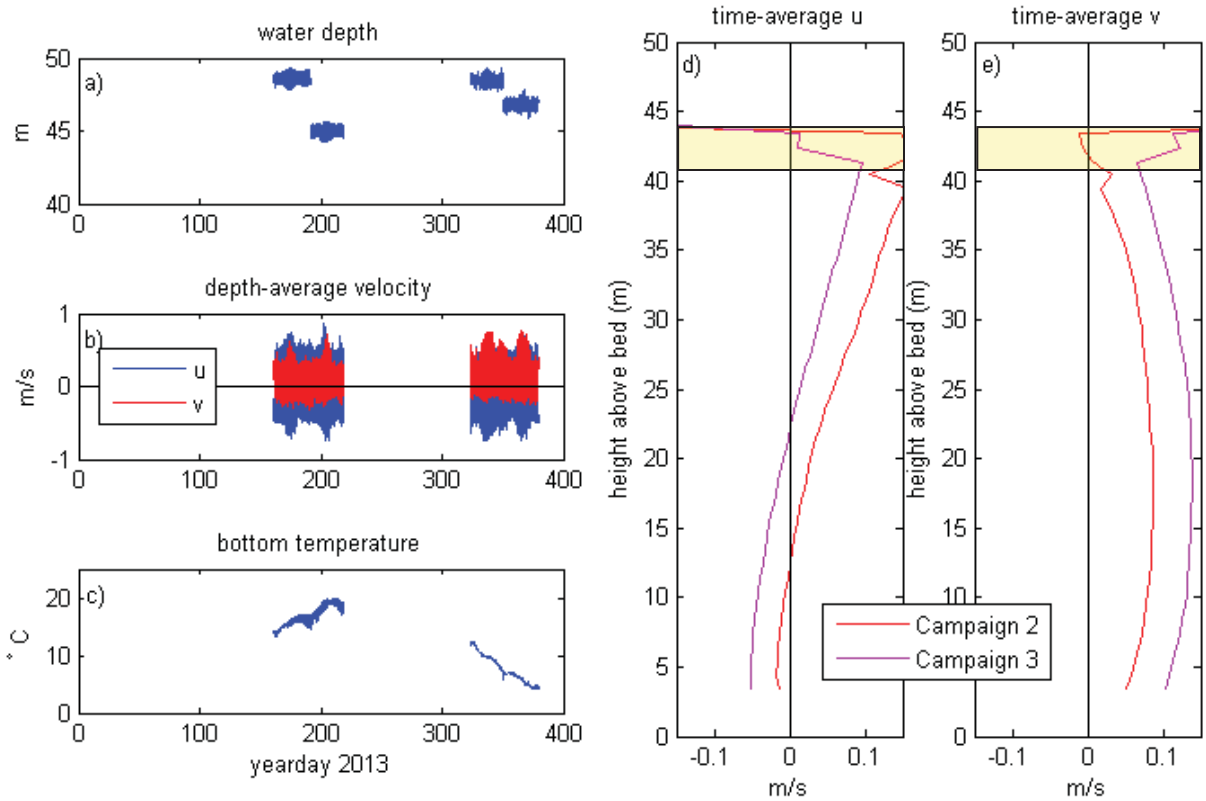

Figure 26. Station DOT7, all campaigns: (a) water depth; (b) depth-averaged velocity; (c) near-bottom temperature; (d) deployment-average, eastward velocity; and (e) deployment-average, northward velocity.

Appendix 11c: Time-series of the Near Bottom Currents

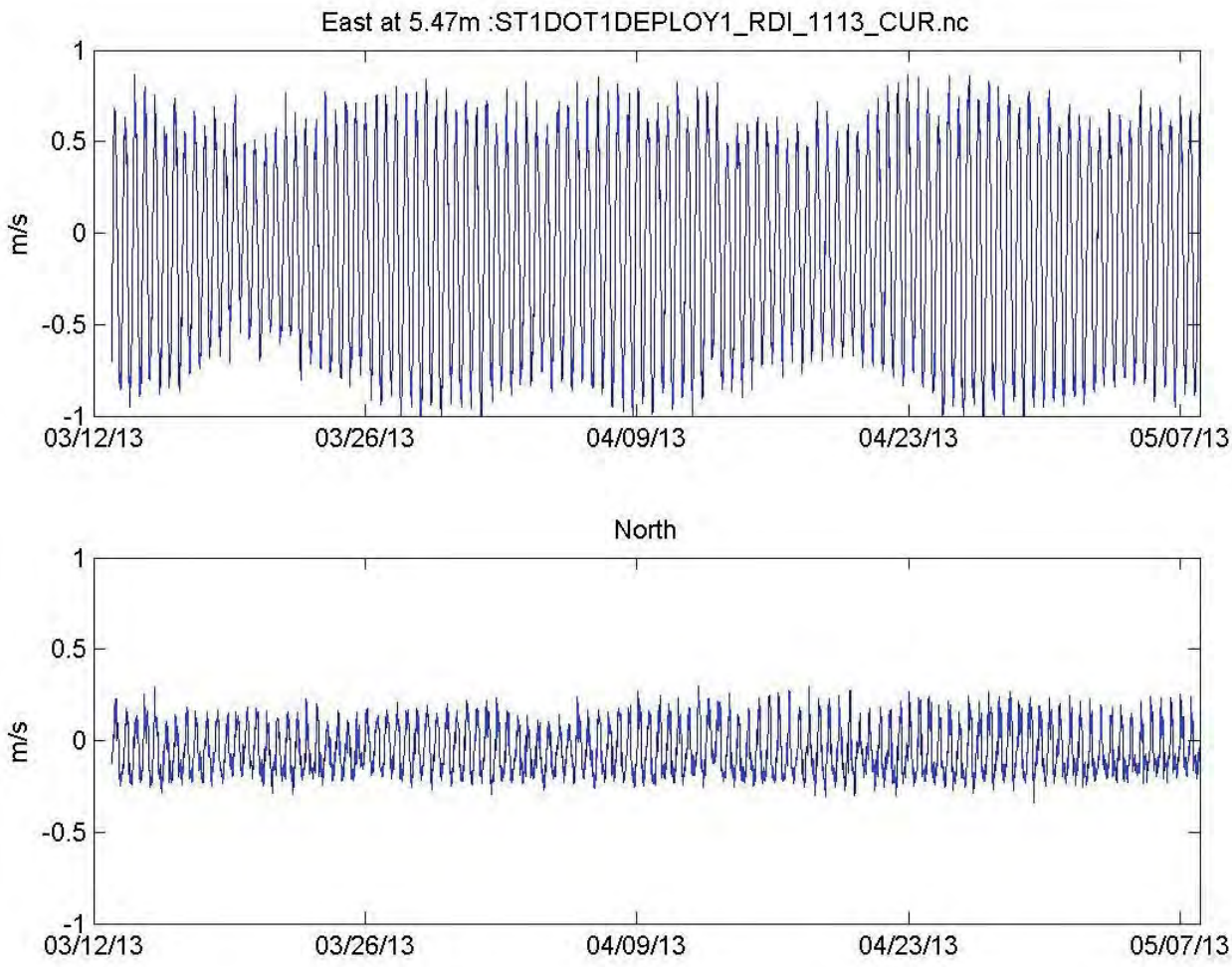

Figure 27. Time-series of the east (upper) and north velocity components at bin 3 at DOT1 during Campaign 1.

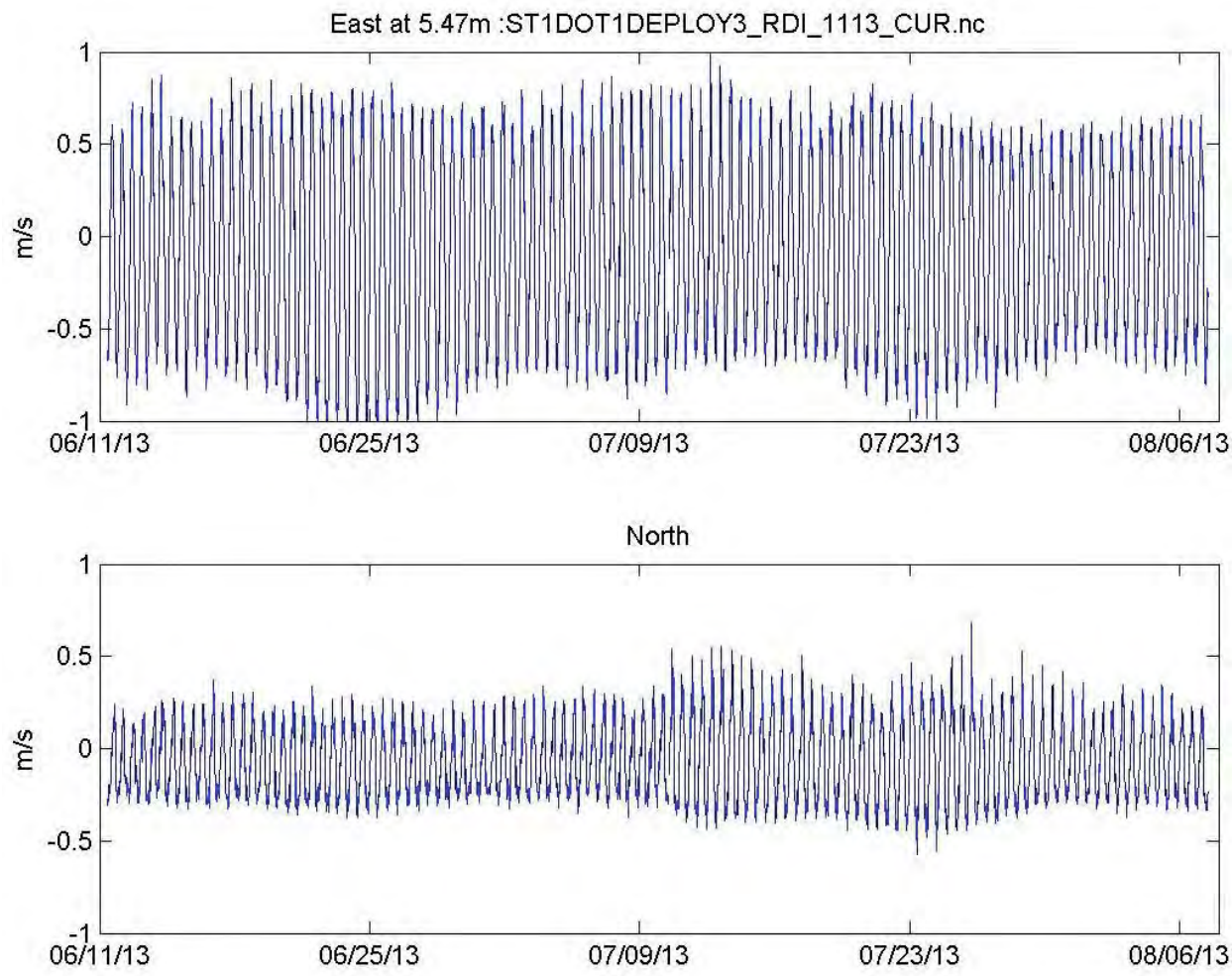

Figure 28. Time-series of the east (upper) and north velocity components at bin 3 at DOT1 during Campaign 2.

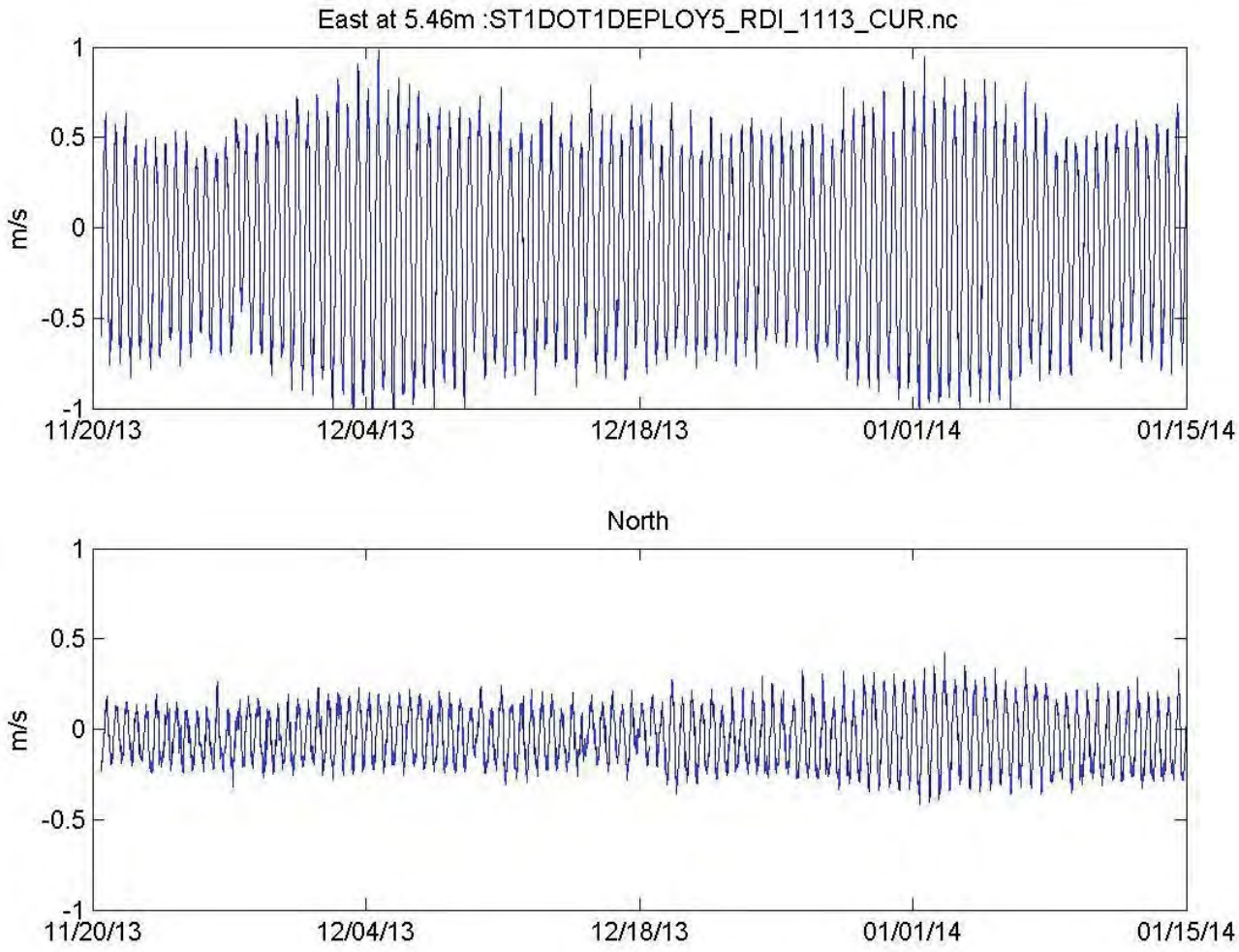

Figure 29. Time-series of the east (upper) and north velocity components at bin 3 at Station DOT1 during Campaign 3.

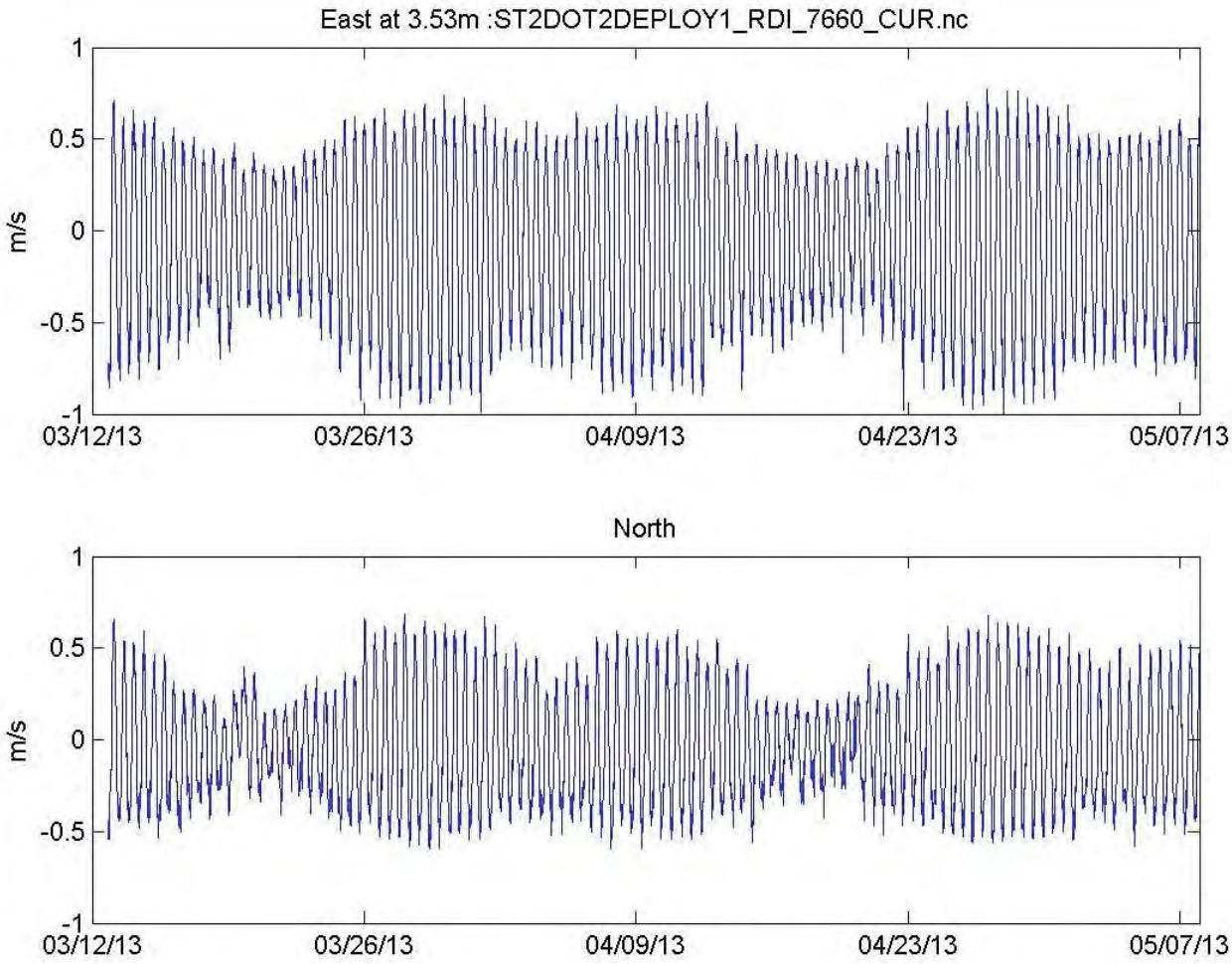

Figure 30. Time-series of the east (upper) and north velocity components at bin 3 at Station DOT2 during Campaign 1.

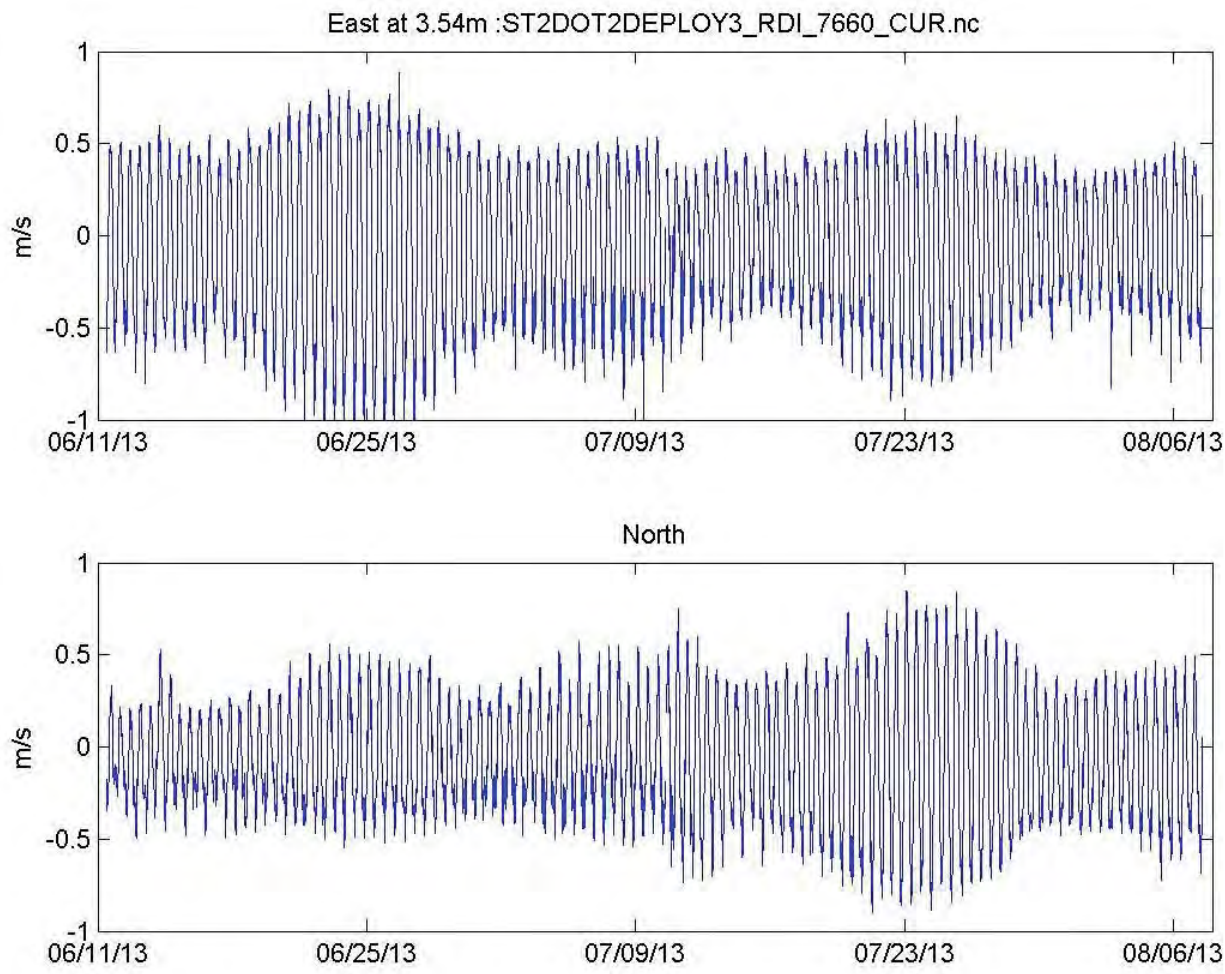

Figure 31. Time-series of the east (upper) and north velocity components at bin 3 at Station DOT2 during Campaign 2.

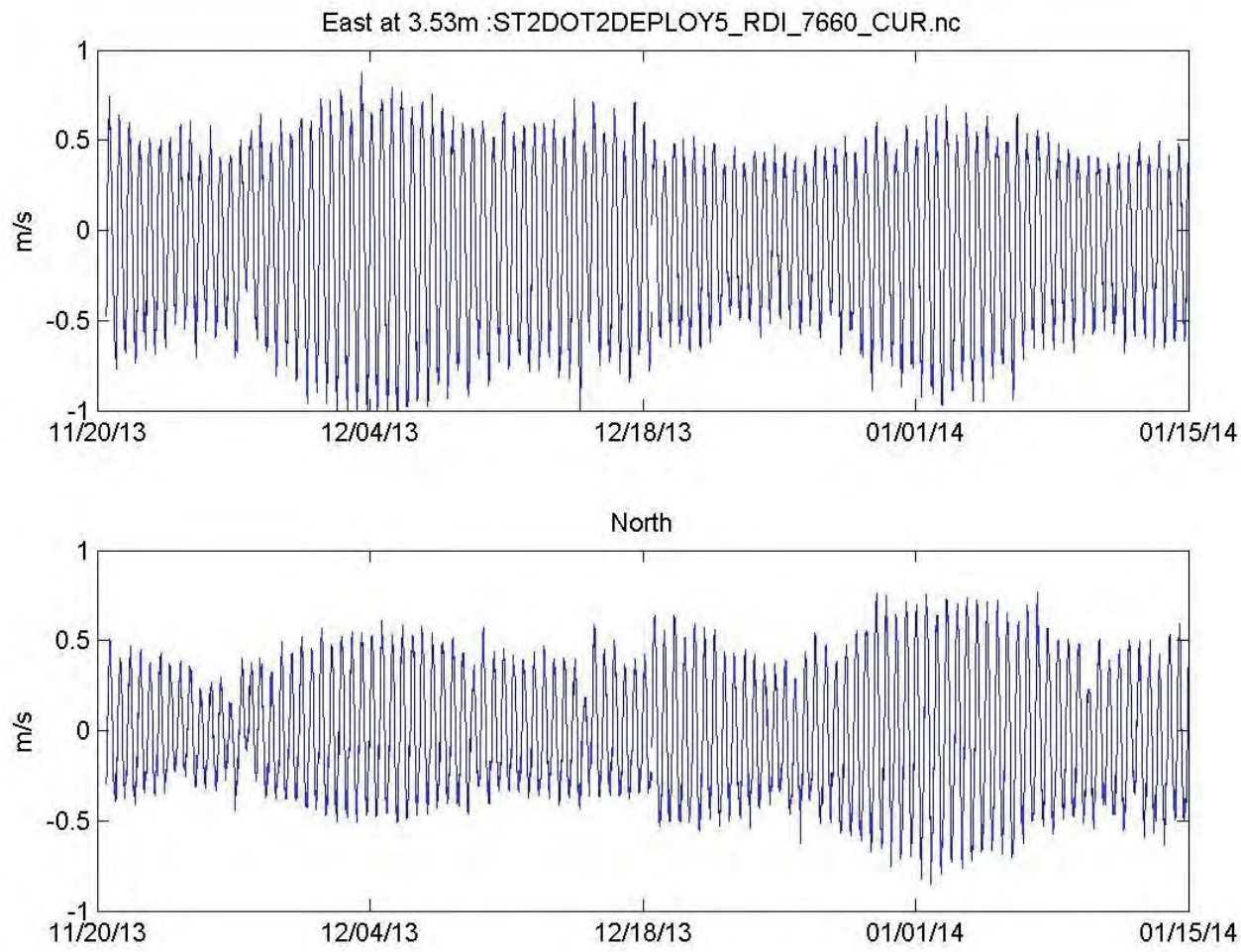

Figure 32. Time-series of the east (upper) and north velocity components at bin 3 at Station DOT2 during Campaign 3.

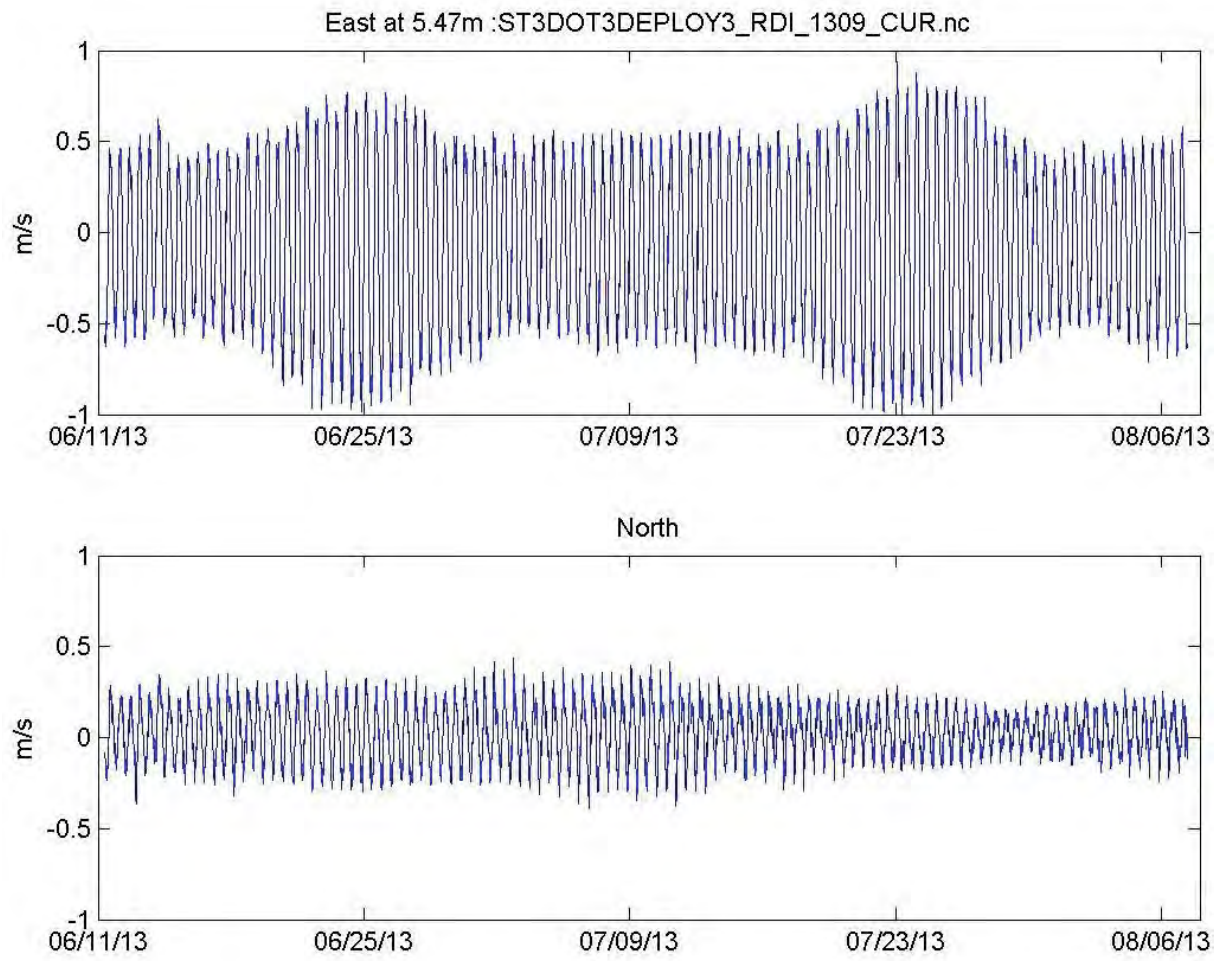

Figure 33. Time-series of the east (upper) and north velocity components at bin 3 at Station DOT3 during Campaign 2.

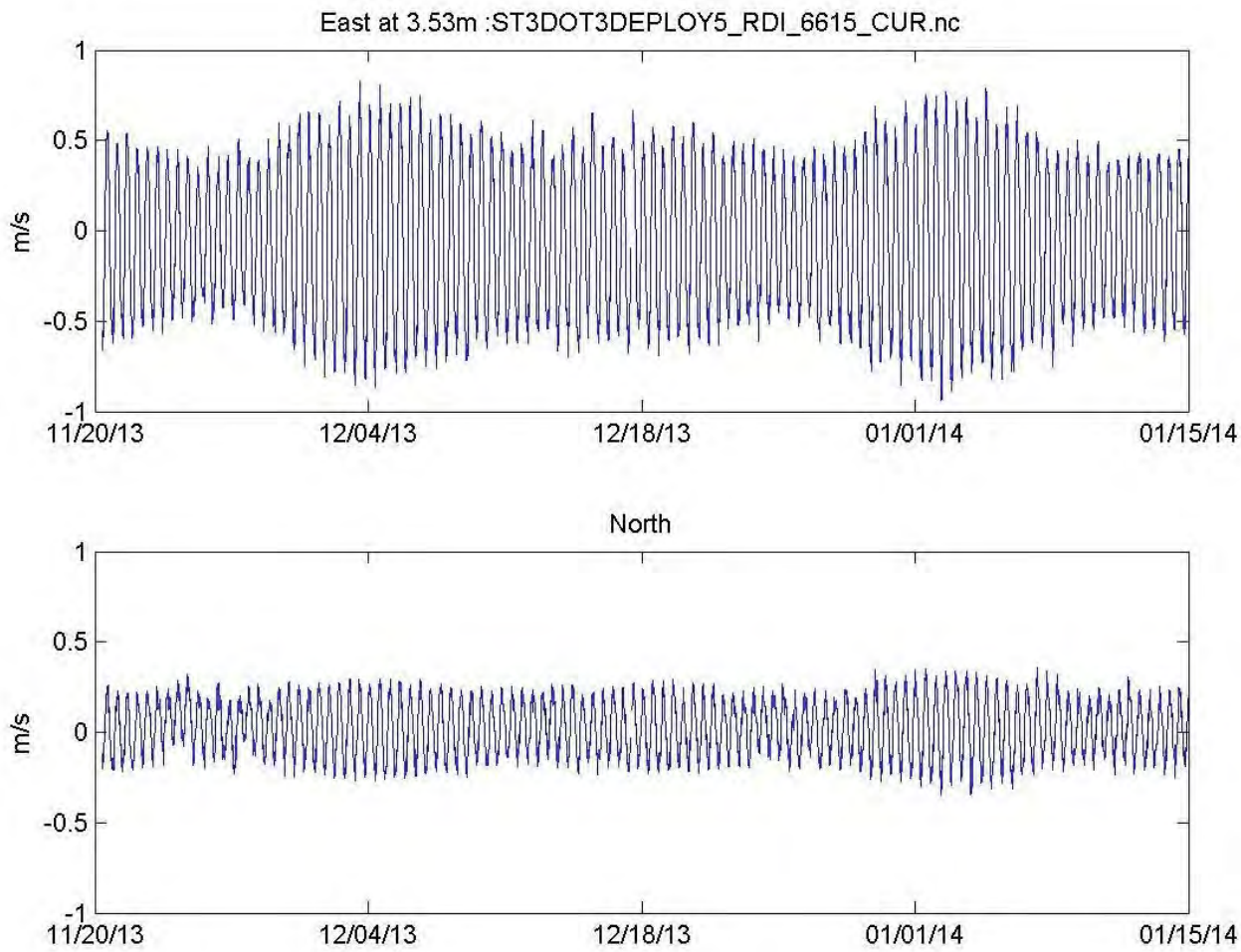

Figure 34. Time-series of the east (upper) and north velocity components at bin 3 at Station DOT3 during Campaign 3.

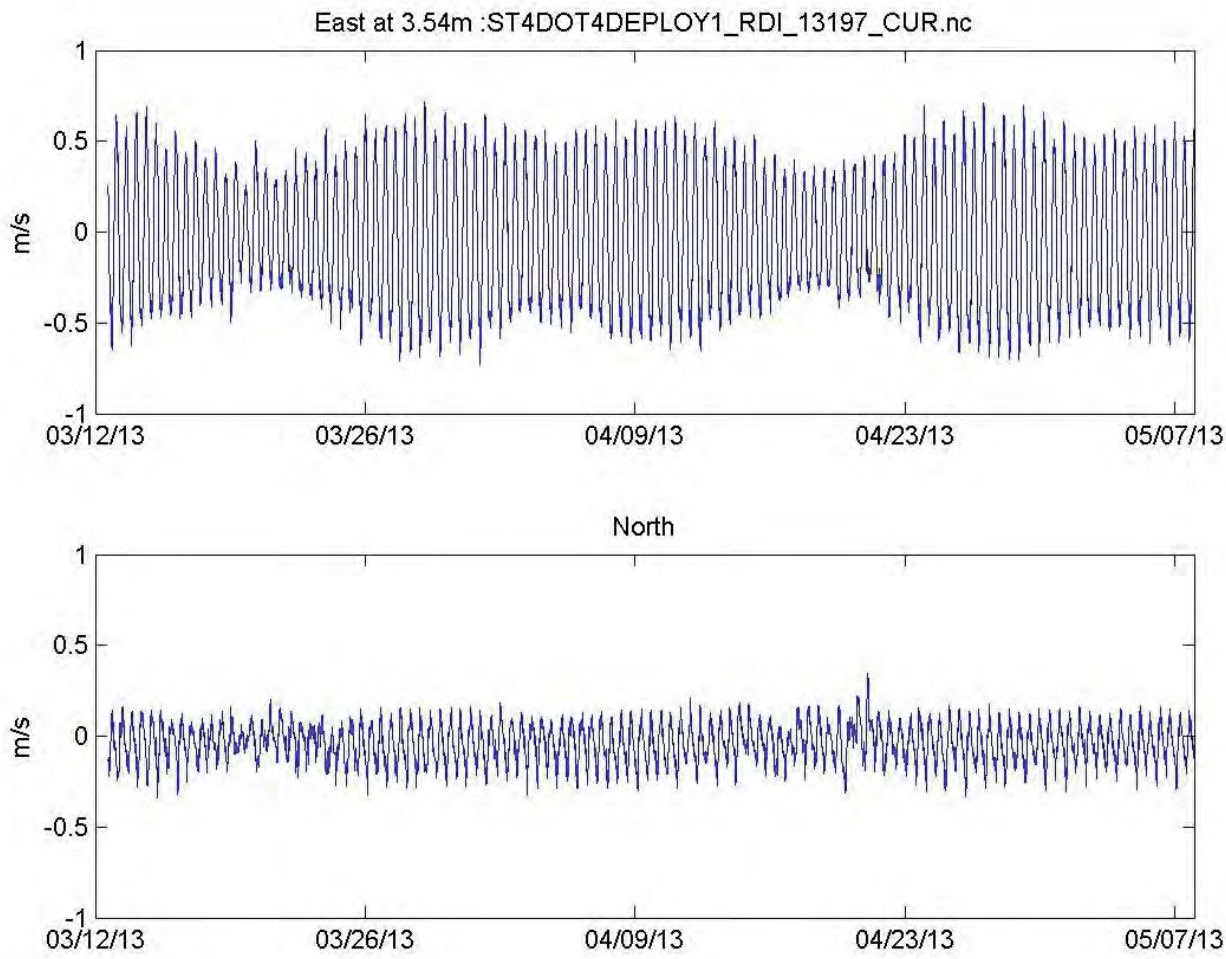

Figure 35. Time-series of the east (upper) and north velocity components at bin 3 at Station DOT4 during Campaign 1.

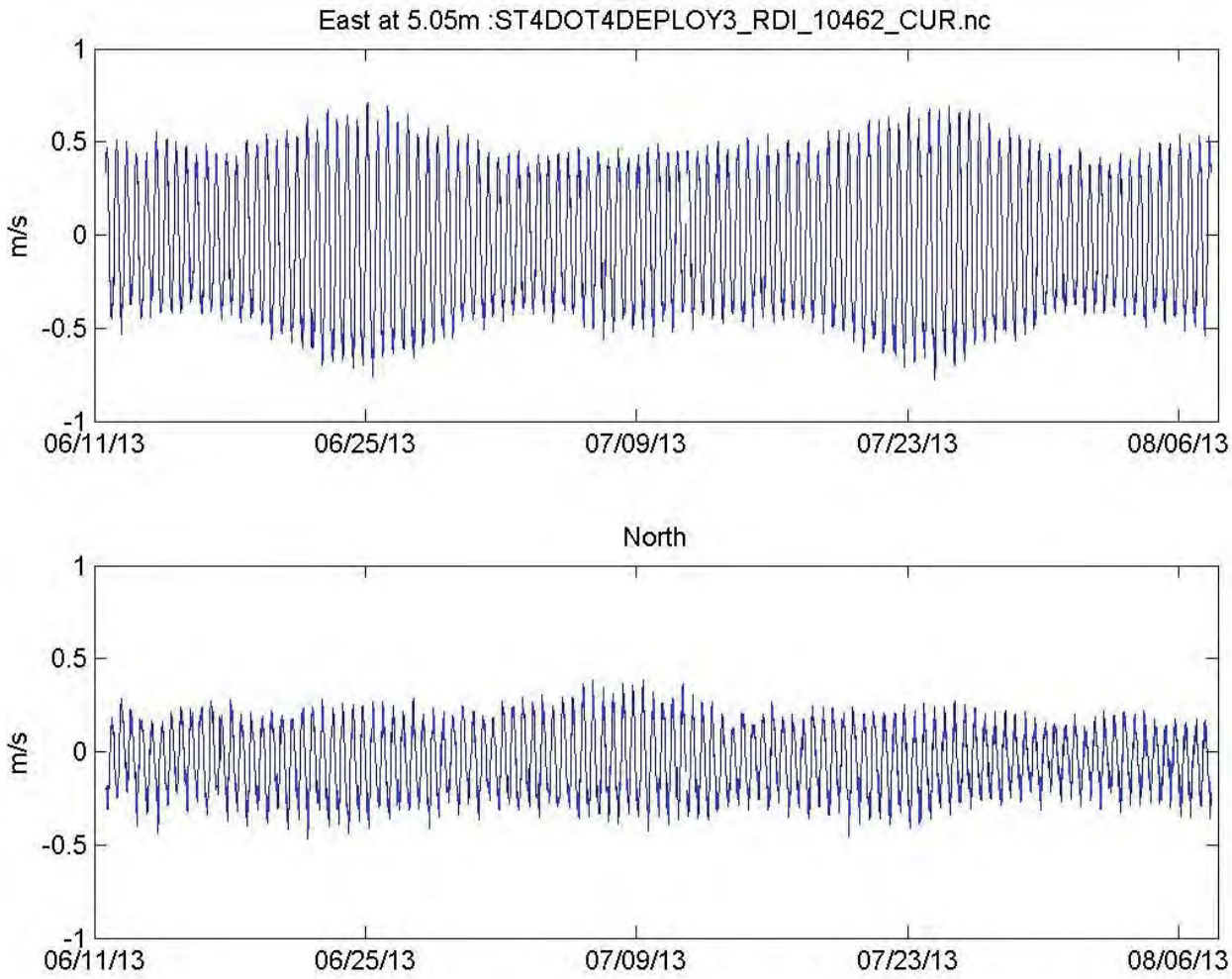

Figure 36. Time-series of the east (upper) and north velocity components at bin 3 at Station DOT4 during Campaign 2.

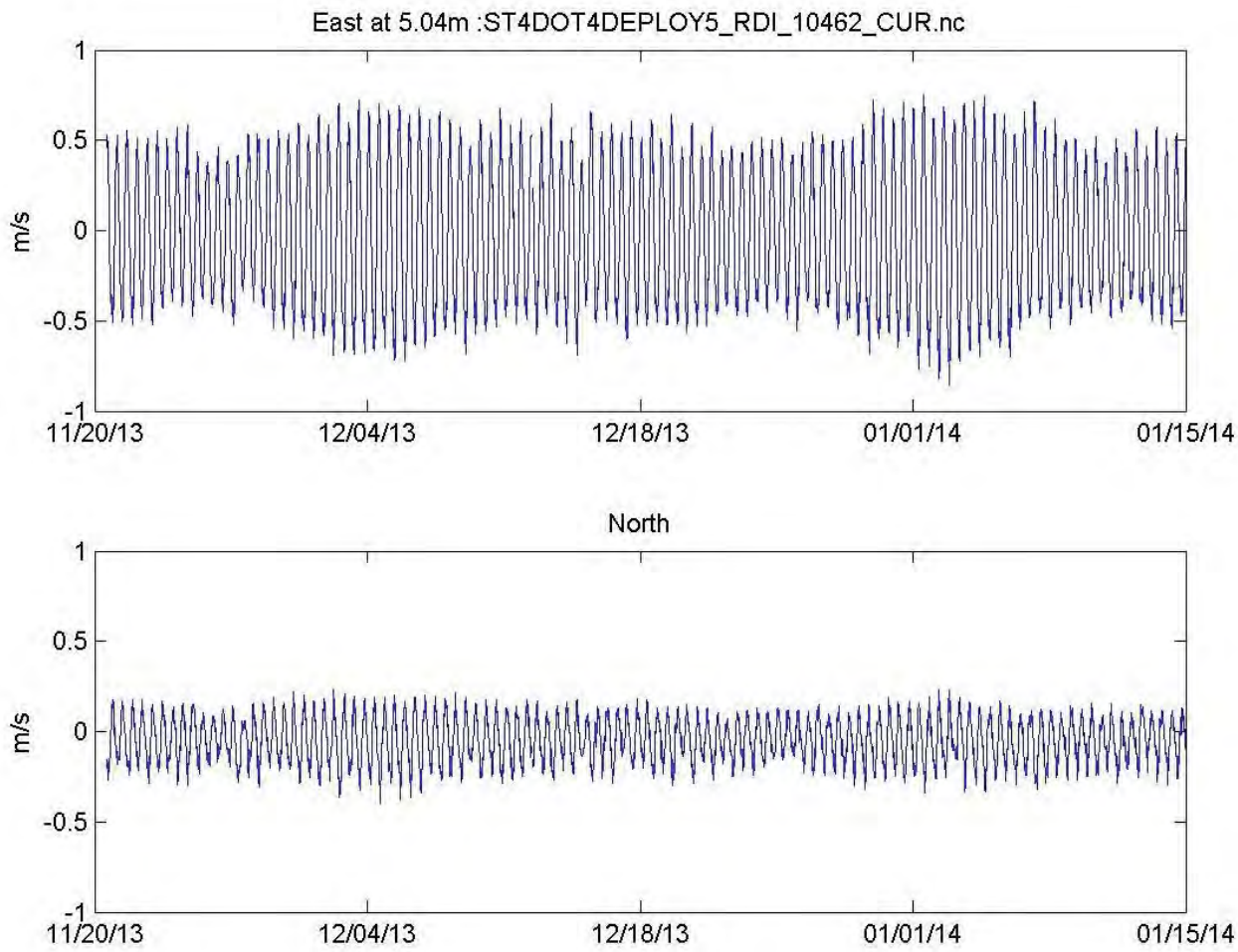

Figure 37. Time-series of the east (upper) and north velocity components at bin 3 at Station DOT4 during Campaign 3.

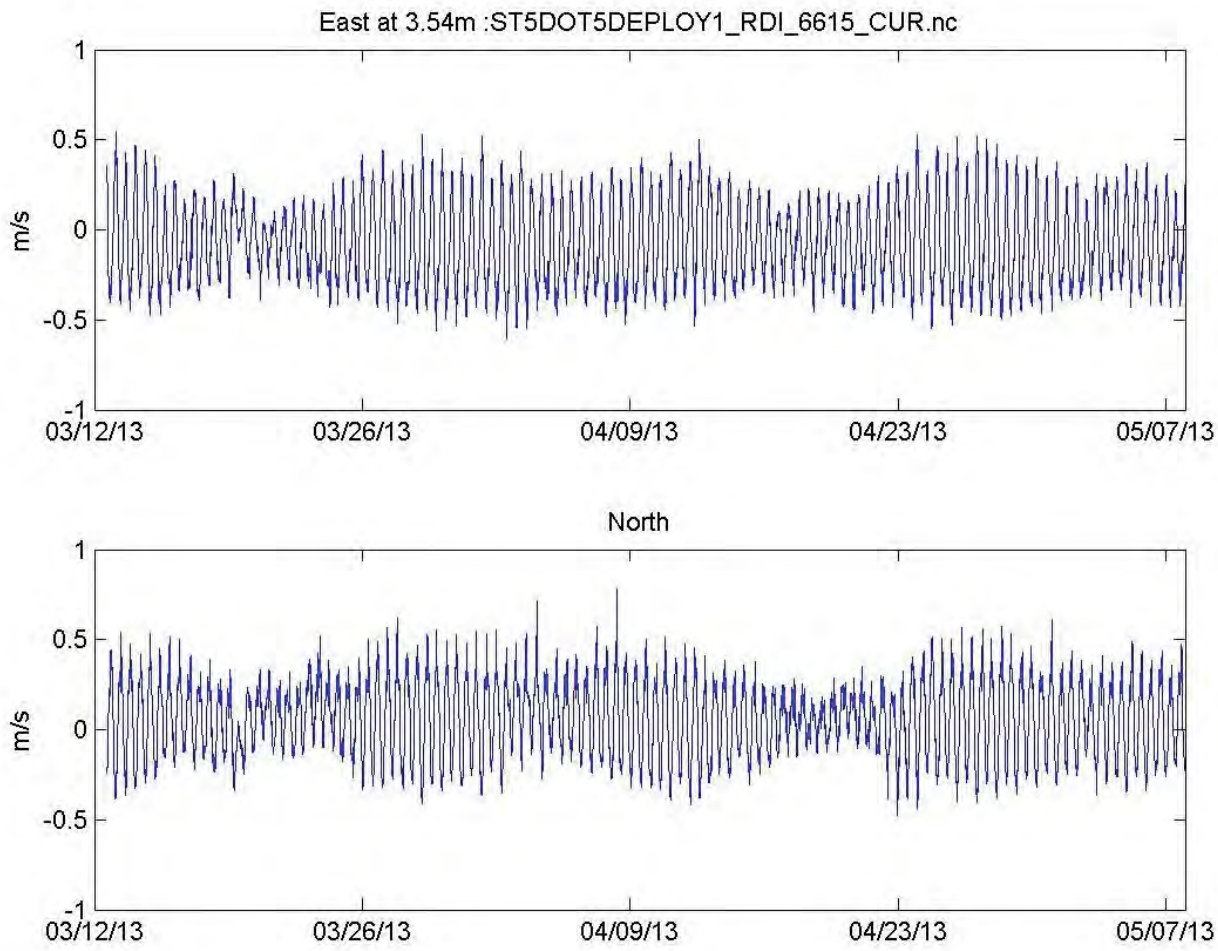

Figure 38. Time-series of the east (upper) and north velocity components at bin 3 at Station DOT5 during Campaign 1.

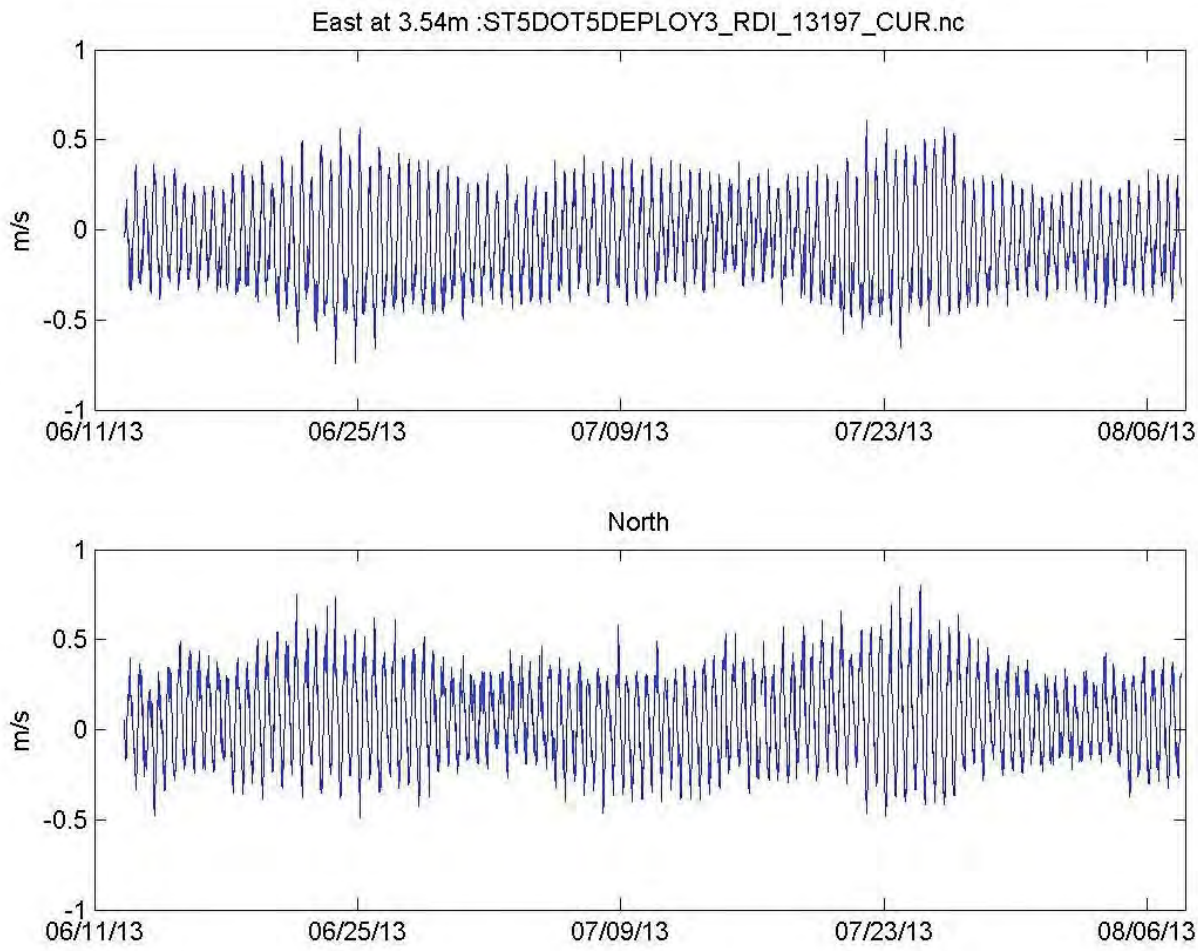

Figure 39. Time-series of the east (upper) and north velocity components at bin 3 at Station DOT5 during Campaign 2.

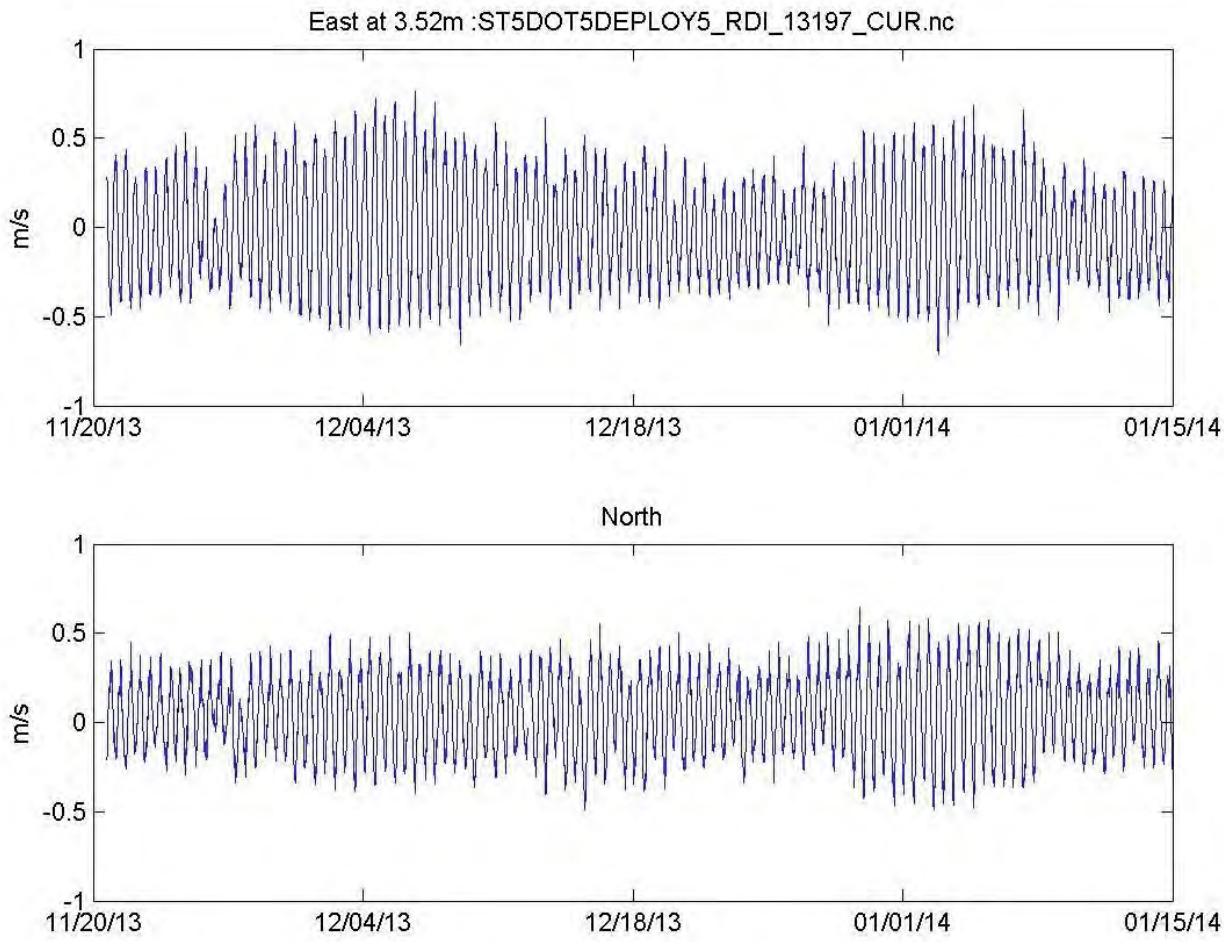

Figure 40. Time-series of the east (upper) and north velocity components at bin 3 at Station DOT5 during Campaign 3.

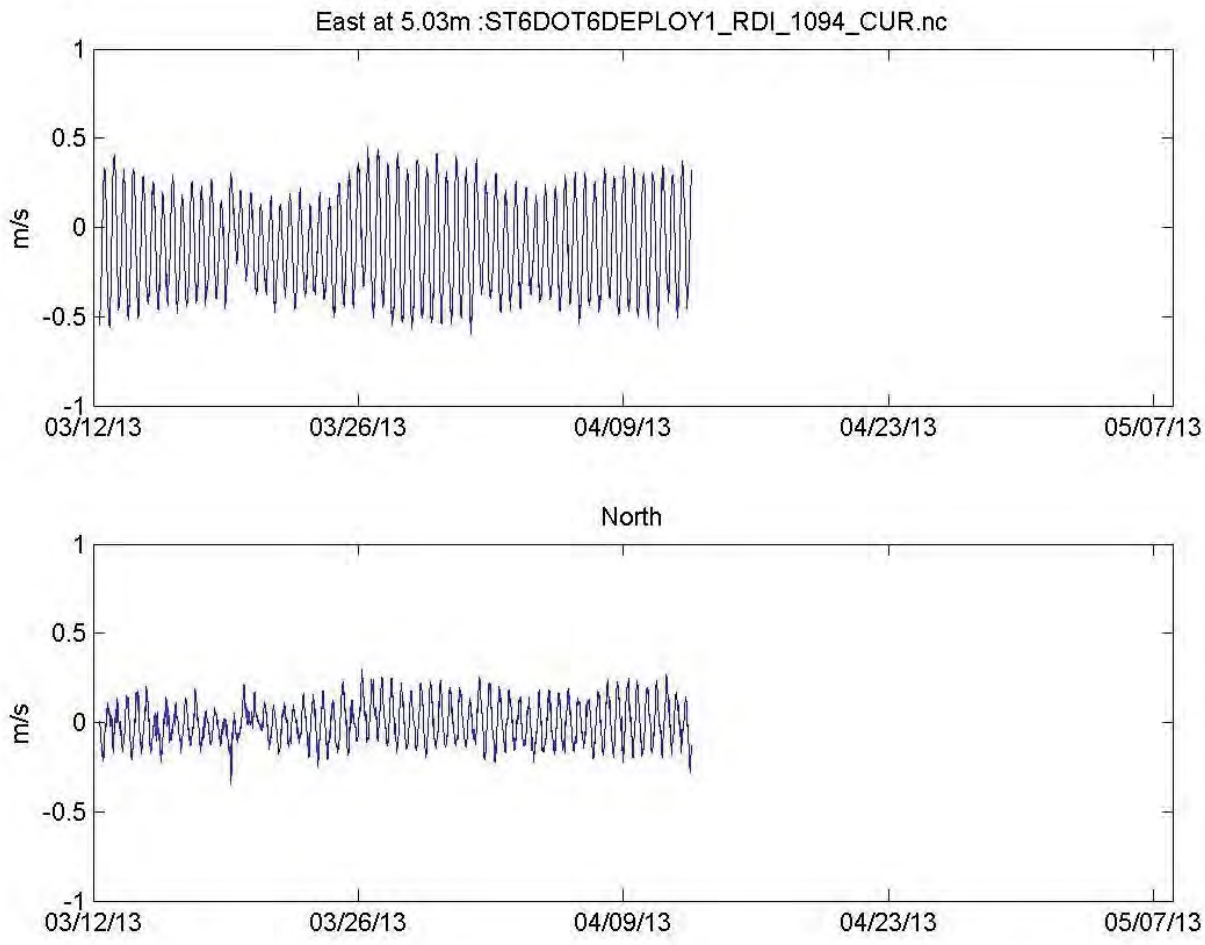

Figure 41. Time-series of the east (upper) and north velocity components at bin 3 at Station DOT6 during Campaign 1.

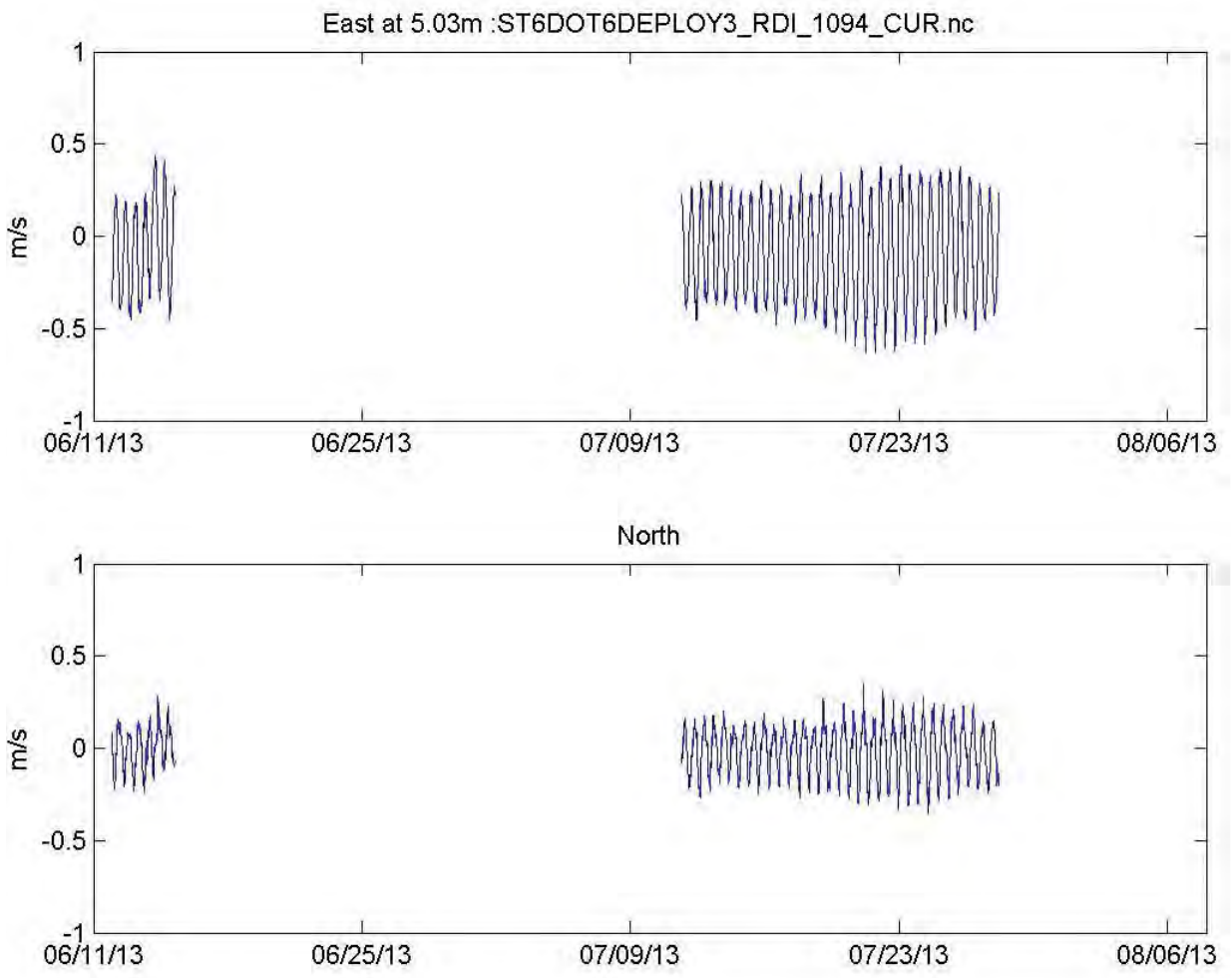

Figure 42. Time-series of the east (upper) and north velocity components at bin 3 at Station DOT6 during Campaign 2

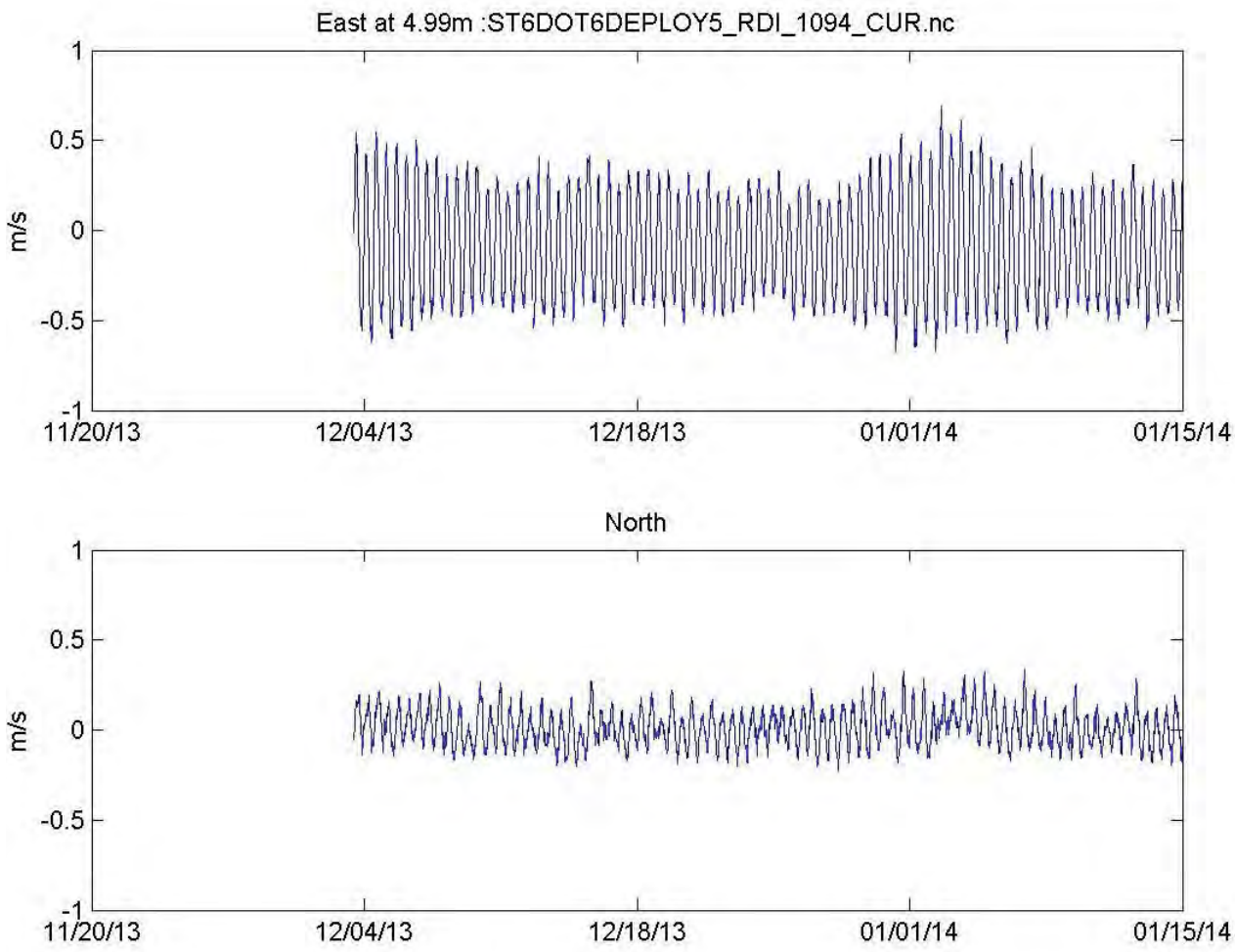

Figure 43. Time-series of the east (upper) and north velocity components at bin 3 at Station DOT6 during Campaign 3.

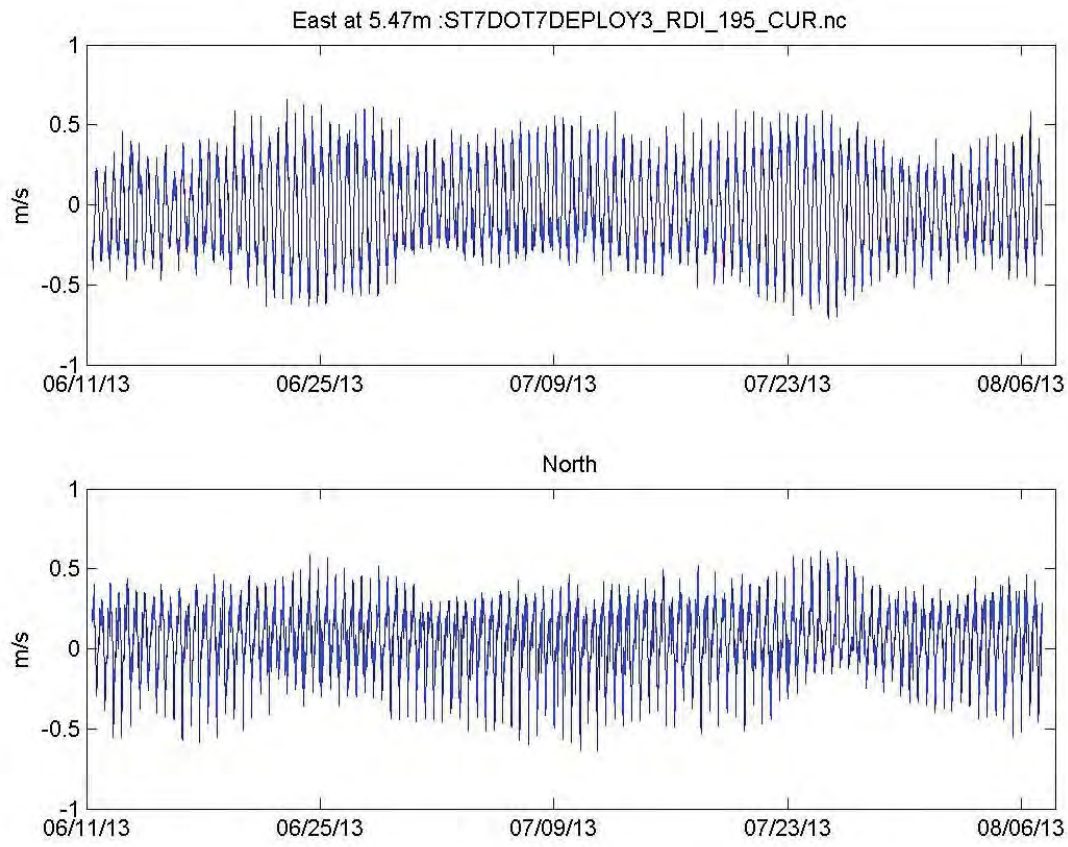

Figure 44. Time-series of the east (upper) and north velocity components at bin 3 at Station DOT7 during Campaign 2

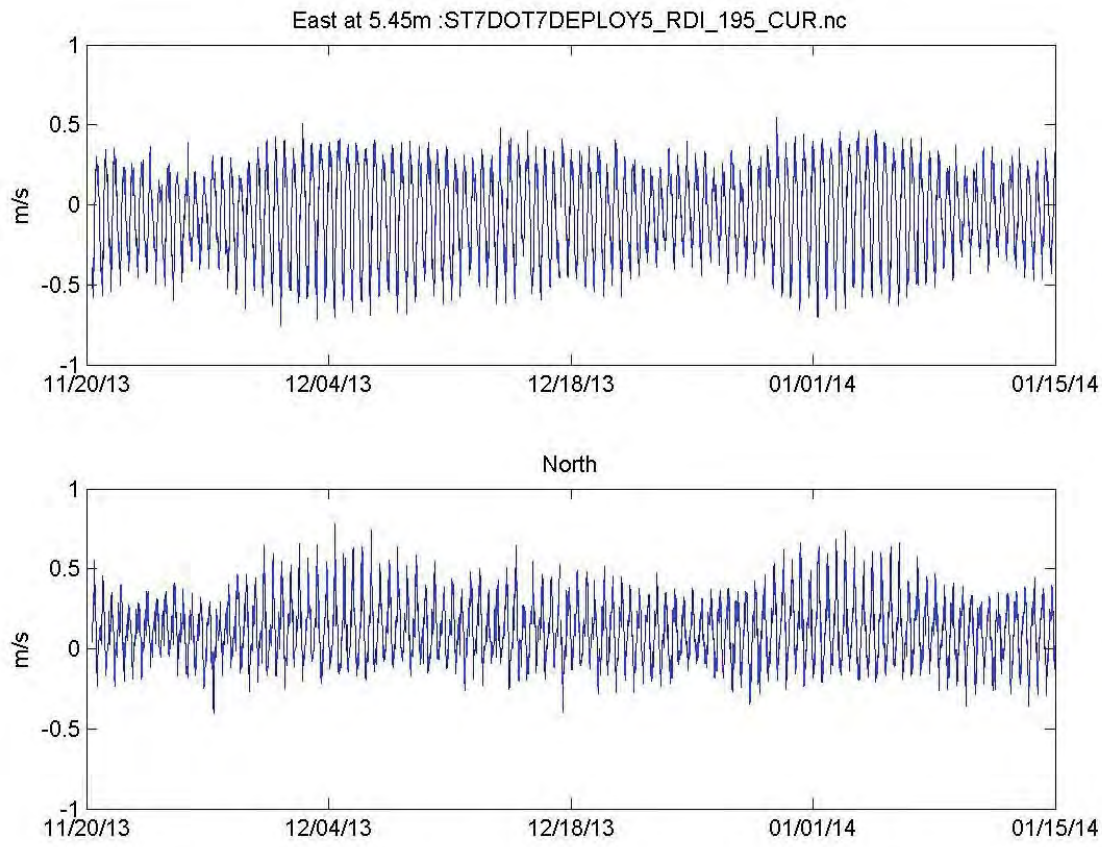

Figure 45. Time-series of the east (upper) and north velocity components at bin 3 at Station DOT7 during Campaign 3

This page intentionally left blank.

Appendix 12

SUSPENDED SEDIMENT AND PARTICULATE ORGANIC CARBON CONCENTRATIONS FROM WATER SAMPLES

Analyses were performed by University of Connecticut laboratory at Avery Point

Suspended Sediment and Particulate Organic Sediment data (SSC and POC) - Cruise CTDOT1

Sample Date/Time (EST)	Station	Sub Sample ID	Depth (m)	SSC (mg/l)	POC (mg/l)
12-Mar-2013 08:00	DOT6	BTM	35.0	2.3	
12-Mar-2013 09:21	CTD10	BTM	39.0	1.3	
12-Mar-2013 10:35	CTD9	BTM	18.4	3.2	
12-Mar-2013 11:21	DOT5	BTM	30.0	6.8	
12-Mar-2013 13:24	CTD8	BTM	15.0	5.7	
12-Mar-2013 14:53	DOT4	BTM	23.0	4.7	
12-Mar-2013 16:57	CTD11	BTM	14.5	2.6	
12-Mar-2013 16:57	CTD11	BTM	14.5	2.7	
12-Mar-2013 19:13	DOT2	BTM	32.0	6.2	
12-Mar-2013 20:27	DOT1	BTM	43.0	10.2	
12-Mar-2013 21:48	DOT3	BTM	30.0	2.7	
12-Mar-2013 23:10	DOT7	BTM	48.0	2.8	
13-Mar-2013 05:22	DOT7	BTM	46.0	3.3	
13-Mar-2013 06:39	DOT3	BTM	29.0	10.2	
13-Mar-2013 07:57	DOT1	BTM	42.0	32.8	
13-Mar-2013 08:57	DOT2	BTM	30.0	3.2	
13-Mar-2013 11:36	CTD11	BTM	18.5	3.1	
13-Mar-2013 12:39	DOT4	BTM	22.5	2.2	
13-Mar-2013 12:39	DOT4	BTM	22.5	4.4	
13-Mar-2013 13:59	CTD8	BTM	13.5	5.0	
13-Mar-2013 13:59	CTD8	BTM	13.5	16.4	
13-Mar-2013 15:15	DOT5	BTM	29.0	2.0	
13-Mar-2013 15:15	DOT5	BTM	29.0	5.4	
13-Mar-2013 16:18	CTD9	BTM	22.0	1.3	
13-Mar-2013 16:18	CTD9	BTM	22.0	1.4	
13-Mar-2013 17:35	CTD10	BTM	38.0	1.0	
13-Mar-2013 17:35	CTD10	BTM	38.0	0.9	
13-Mar-2013 19:08	DOT6	BTM	37.2	4.8	
13-Mar-2013 19:08	DOT6	BTM	37.2	2.2	

Suspended Sediment and Particulate Organic Sediment data (SSC and POC) - Cruise CTDOT2

Sample Date/Time (EST)	Station	Sub Sample ID	Depth (m)	SSC (mg/l)	POC (mg/l)
17-May-2013 06:34	DOT7	BTM	50.0	3.3	
17-May-2013 08:25	DOT3	BTM	29.6	5.2	
17-May-2013 10:08	DOT1	BTM	41.2	3.6	
17-May-2013 11:05	DOT2	BTM	30.0	6.5	
17-May-2013 13:10	CTD11	BTM	30.0	2.9	
17-May-2013 14:18	DOT4	BTM	23.1	5.2	
17-May-2013 15:30	CTD8	BTM	13.5	4.5	
17-May-2013 16:35	DOT5	BTM	28.5	2.1	
17-May-2013 20:18	CTD9	BTM	21.0	1.0	
17-May-2013 21:20	CTD10	BTM	36.0	0.9	
17-May-2013 23:00	DOT6	BTM	35.0	2.0	

Suspended Sediment and Particulate Organic Sediment data (SSC and POC) - Cruise CTDOT3

Sample Date/Time (EST)	Station	Sub Sample ID	Depth (m)	SSC (mg/l)	POC (mg/l)
11-Jun-2013 06:46	DOT7	BTM	44.0	3.3	
11-Jun-2013 06:46	DOT7	BTM	44.0	3.6	
11-Jun-2013 07:11	DOT7	sfc	1.5	2.8	0.347
11-Jun-2013 07:11	DOT7	mid	23.0	2.6	0.241
11-Jun-2013 07:11	DOT7	btmB	41.2	2.6	0.283
11-Jun-2013 07:11	DOT7	btmA	43.9	2.1	0.458
11-Jun-2013 08:25	DOT3	BTM	28.0	6.0	
11-Jun-2013 08:25	DOT3	BTM	28.0	4.4	
11-Jun-2013 08:30	DOT3	sfc	2.0	4.9	0.280
11-Jun-2013 08:30	DOT3	mid	13.8	4.1	0.238
11-Jun-2013 08:30	DOT3	btmB	21.9	4.3	0.247
11-Jun-2013 08:30	DOT3	btmA	24.8	4.8	0.298
11-Jun-2013 09:46	DOT1	BTM	38.0	5.7	
11-Jun-2013 09:55	DOT1	sfc	1.4	2.5	0.406
11-Jun-2013 09:55	DOT1	mid	20.2	4.7	0.276
11-Jun-2013 09:55	DOT1	btmB	36.0	4.2	0.204
11-Jun-2013 09:55	DOT1	btmA	37.9	2.8	0.377
11-Jun-2013 09:55	DOT1	btmA	37.9	2.7	0.325
11-Jun-2013 10:47	DOT2	BTM	30.0	9.8	
11-Jun-2013 10:53	DOT2	sfc	1.5	2.4	0.326
11-Jun-2013 10:53	DOT2	mid	14.5	5.7	0.379
11-Jun-2013 10:53	DOT2	btmB	25.8	8.1	0.406
11-Jun-2013 10:53	DOT2	btmA	28.4	7.9	0.260
11-Jun-2013 13:05	CTD11	BTM	32.0	4.7	
11-Jun-2013 13:07	CTD11	sfc	1.7	2.4	0.320
11-Jun-2013 13:07	CTD11	mid	15.1	2.7	0.271
11-Jun-2013 13:07	CTD11	btmB	26.0	2.5	0.239
11-Jun-2013 13:07	CTD11	btmA	27.8	2.5	0.304
11-Jun-2013 14:20	DOT4	BTM	22.0	9.2	
11-Jun-2013 14:23	DOT4	sfc	1.8	1.9	0.354
11-Jun-2013 14:23	DOT4	mid	11.1	4.5	0.273
11-Jun-2013 14:23	DOT4	btmB	18.1	5.8	0.414
11-Jun-2013 14:23	DOT4	btmA	20.0	6.8	
11-Jun-2013 15:42	CTD8	BTM	13.0	5.7	
11-Jun-2013 16:55	DOT5	BTM	30.0	6.0	
11-Jun-2013 17:52	CTD9	BTM	22.0	1.8	
11-Jun-2013 18:53	CTD10	BTM	37.7	1.7	
11-Jun-2013 19:14	CTD10	sfc	2.1	1.8	0.582
11-Jun-2013 19:14	CTD10	mid	17.1	1.8	0.295
11-Jun-2013 19:14	CTD10	btmB	31.3	1.9	0.224
11-Jun-2013 19:14	CTD10	btmA	33.7	1.7	0.260
11-Jun-2013 20:34	DOT6	BTM	36.0	2.1	
11-Jun-2013 21:09	DOT6	sfc	1.6	1.4	0.508
11-Jun-2013 21:09	DOT6	mid	17.8	1.5	0.281
11-Jun-2013 21:09	DOT6	btmB	30.5	1.7	
11-Jun-2013 21:09	DOT6	btmA	33.5	2.7	0.214
12-Jun-2013 05:09	DOT2	BTM	31.0	20.3	
12-Jun-2013 05:25	DOT2	sfc	2.2	5.7	0.443
12-Jun-2013 05:25	DOT2	mid	15.8	7.1	0.491
12-Jun-2013 05:25	DOT2	btmB	25.0	11.2	0.588
12-Jun-2013 05:25	DOT2	btmA	27.2	13.5	0.727
12-Jun-2013 06:05	DOT1	BTM	40.0	7.7	
12-Jun-2013 06:58	DOT1	sfc	1.9	4.2	
12-Jun-2013 06:58	DOT1	mid	21.0	4.9	0.359
12-Jun-2013 06:58	DOT1	btmB	32.5	5.0	0.376
12-Jun-2013 06:58	DOT1	btmA	34.1	5.3	0.344
12-Jun-2013 08:05	DOT3	BTM	28.0	5.5	
12-Jun-2013 08:18	DOT3	sfc	2.2	7.5	
12-Jun-2013 08:18	DOT3	mid	14.5	4.5	

Suspended Sediment and Particulate Organic Sediment data (SSC and POC) - Cruise CTDOT3

Sample Date/Time (EST)	Station	Sub Sample ID	Depth (m)	SSC (mg/l)	POC (mg/l)
12-Jun-2013 08:18	DOT3	btmB	22.7	3.2	0.264
12-Jun-2013 08:18	DOT3	btmA	25.2	3.6	0.338
12-Jun-2013 09:16	DOT7	BTM	46.0	3.1	
12-Jun-2013 09:27	DOT7	sfc	2.6	2.5	0.427
12-Jun-2013 09:27	DOT7	mid	23.2	1.6	0.294
12-Jun-2013 09:27	DOT7	btmB	41.1	2.5	0.416
12-Jun-2013 09:27	DOT7	btmA	43.1	3.9	0.284
12-Jun-2013 10:07	CTD11	BTM	22.0	5.5	
12-Jun-2013 10:19	CTD11	sfc	2.2	2.7	
12-Jun-2013 10:19	CTD11	mid	13.0	3.3	0.251
12-Jun-2013 10:19	CTD11	btmB	23.2	2.7	0.291
12-Jun-2013 10:19	CTD11	btmA	25.7	4.8	0.283
12-Jun-2013 11:08	DOT4	BTM	22.5	8.0	
12-Jun-2013 11:19	DOT4	sfc	2.1	2.0	0.254
12-Jun-2013 11:19	DOT4	mid	11.5	3.3	0.302
12-Jun-2013 11:19	DOT4	btmB	18.7	5.4	0.281
12-Jun-2013 11:19	DOT4	btmA	21.0	4.5	0.384
12-Jun-2013 12:36	CTD8	BTM	13.5	5.9	
12-Jun-2013 12:42	CTD8	sfc	2.1	3.9	0.392
12-Jun-2013 12:42	CTD8	mid	5.9	4.5	0.319
12-Jun-2013 12:42	CTD8	btmB	7.5	5.1	0.358
12-Jun-2013 12:42	CTD8	btmA	10.4	5.3	0.343
12-Jun-2013 13:29	DOT5	BTM	30.0	6.0	
12-Jun-2013 14:03	DOT5	sfc	2.4	2.6	0.295
12-Jun-2013 14:03	DOT5	mid	15.3	3.1	0.395
12-Jun-2013 14:03	DOT5	btmB	23.8	3.1	0.430
12-Jun-2013 14:03	DOT5	btmA	27.1	3.1	0.328
12-Jun-2013 14:50	CTD9	BTM	21.0	1.2	
12-Jun-2013 15:05	CTD9	sfc	2.6	1.6	0.382
12-Jun-2013 15:05	CTD9	mid	8.6	1.7	0.347
12-Jun-2013 15:05	CTD9	btmB	13.6	1.5	0.278
12-Jun-2013 15:05	CTD9	btmA	16.0	0.8	0.306
12-Jun-2013 16:05	CTD10	BTM	36.5	1.2	
12-Jun-2013 16:10	CTD10	sfc	3.2	0.8	0.363
12-Jun-2013 16:10	CTD10	mid	17.6	1.5	0.270
12-Jun-2013 16:10	CTD10	btmB	31.9	1.3	0.288
12-Jun-2013 16:10	CTD10	btmA	34.3	1.3	0.223
12-Jun-2013 17:26	DOT6	BTM	35.0	3.3	
12-Jun-2013 17:34	DOT6	sfc	2.2	1.4	0.390
12-Jun-2013 17:34	DOT6	mid	17.1	1.3	0.296
12-Jun-2013 17:34	DOT6	btmB	30.7	2.8	0.237
12-Jun-2013 17:34	DOT6	btmA	32.5	2.6	0.257

Suspended Sediment and Particulate Organic Sediment data (SSC and POC) - Cruise CTDOT4

Sample Date/Time (EST)	Station	Sub Sample ID	Depth (m)	SSC (mg/l)	POC (mg/l)
10-Jul-2013 12:26	DOT1	BTM	45.0	2.7	
10-Jul-2013 13:55	DOT2	BTM	30.5	3.1	
11-Jul-2013 07:50	DOT7	BTM	40.8	1.9	
11-Jul-2013 09:35	DOT3	BTM	28.0	12.0	
11-Jul-2013 13:01	DOT4	BTM	22.8	2.3	
11-Jul-2013 14:54	DOT6	BTM	35.3	1.8	
16-Jul-2013 10:55	DOT5	BTM	30.5	6.4	

Suspended Sediment and Particulate Organic Sediment data (SSC and POC) - Cruise CTDOT5

Sample Date/Time (EST)	Station	Sub Sample ID	Depth (m)	SSC (mg/l)	POC (mg/l)
02-Aug-2013 12:09	DOT7	BTM	49.3	2.2	
02-Aug-2013 12:55	DOT7	sfc	2.2	1.3	
02-Aug-2013 12:55	DOT7	sfc	2.2	1.2	0.155
02-Aug-2013 12:55	DOT7	mid	19.5	1.3	0.098
02-Aug-2013 12:55	DOT7	btmB	27.4	1.3	0.096
02-Aug-2013 12:55	DOT7	btmA	29.9	1.3	0.093
07-Aug-2013 08:06	DOT7	sfc	2.6	1.4	0.118
07-Aug-2013 08:06	DOT7	mid	19.4	2.1	
07-Aug-2013 08:06	DOT7	btmB	35.4	2.5	0.114
07-Aug-2013 08:06	DOT7	btmB	35.4	2.8	
07-Aug-2013 08:06	DOT7	btmA	38.2	2.3	0.118
07-Aug-2013 08:06	DOT7	BTM	43.8	1.6	0.159
07-Aug-2013 09:48	DOT3	sfc	2.3	1.5	0.185
07-Aug-2013 09:48	DOT3	sfc	2.3	1.4	
07-Aug-2013 09:48	DOT3	mid	14.1	2.7	0.119
07-Aug-2013 09:48	DOT3	btmB	21.6	3.5	0.132
07-Aug-2013 09:48	DOT3	btmA	24.3	2.5	0.114
07-Aug-2013 09:48	DOT3	BTM	28.0	8.8	0.217
07-Aug-2013 11:20	DOT1	sfc	2.2	3.4	0.173
07-Aug-2013 11:20	DOT1	mid	21.0	1.7	0.089
07-Aug-2013 11:20	DOT1	btmB	36.4	2.9	0.085
07-Aug-2013 11:20	DOT1	btmA	39.0	2.3	0.113
07-Aug-2013 11:20	DOT1	BTM	41.0	1.8	0.171
07-Aug-2013 12:31	DOT2	sfc	1.5	3.4	0.178
07-Aug-2013 12:31	DOT2	mid	14.9	4.0	0.093
07-Aug-2013 12:31	DOT2	btmB	24.6	4.9	0.252
07-Aug-2013 12:31	DOT2	btmA	26.4	5.2	0.228
07-Aug-2013 12:31	DOT2	BTM	30.0	11.7	0.379
07-Aug-2013 14:42	CTD11	sfc	2.7	1.8	0.154
07-Aug-2013 14:42	CTD11	mid	15.1	2.2	0.132
07-Aug-2013 14:42	CTD11	btmB	30.5	2.1	0.125
07-Aug-2013 14:42	CTD11	btmA	32.4	2.2	0.130
07-Aug-2013 14:42	CTD11	BTM	86.0	2.4	0.144
07-Aug-2013 16:00	DOT4	sfc	2.7	1.8	0.245
07-Aug-2013 16:00	DOT4	mid	9.9	1.9	0.113
07-Aug-2013 16:00	DOT4	btmB	16.8	4.1	0.133
07-Aug-2013 16:00	DOT4	btmA	19.1	4.0	0.158
07-Aug-2013 16:00	DOT4	BTM	21.8	10.4	0.063
07-Aug-2013 17:30	CTD8	sfc	2.1	1.7	0.096
07-Aug-2013 17:30	CTD8	mid	6.2	1.5	0.082
07-Aug-2013 17:30	CTD8	btmB	10.1	1.1	0.112
07-Aug-2013 17:30	CTD8	btmA	12.1	1.3	0.091
07-Aug-2013 17:30	CTD8	BTM	13.7	1.4	0.129
07-Aug-2013 18:51	DOT5	sfc	1.9	1.3	0.121
07-Aug-2013 18:51	DOT5	mid	14.4	1.9	
07-Aug-2013 18:51	DOT5	btmB	23.7	2.6	0.134
07-Aug-2013 18:51	DOT5	btmA	26.5	4.4	0.164
07-Aug-2013 18:51	DOT5	BTM	28.5	10.8	0.427
07-Aug-2013 20:07	CTD9	sfc	2.9	1.1	0.128
07-Aug-2013 20:07	CTD9	mid	10.9	0.6	0.079
07-Aug-2013 20:07	CTD9	btmB	17.8	0.6	0.084
07-Aug-2013 20:07	CTD9	btmA	20.5	0.6	0.321
07-Aug-2013 20:07	CTD9	BTM	21.0	0.7	0.073
07-Aug-2013 21:41	CTD10	sfc	1.8	0.5	0.090
07-Aug-2013 21:41	CTD10	mid	18.2	0.5	0.081
07-Aug-2013 21:41	CTD10	btmB	32.2	1.4	0.093
07-Aug-2013 21:41	CTD10	btmA	34.4	2.1	0.119
07-Aug-2013 21:41	CTD10	btmA	34.4	2.3	
07-Aug-2013 21:41	CTD10	BTM	34.1	2.0	0.097

Suspended Sediment and Particulate Organic Sediment data (SSC and POC) - Cruise CTDOT5

Sample Date/Time (EST)	Station	Sub Sample ID	Depth (m)	SSC (mg/l)	POC (mg/l)
07-Aug-2013 23:54	DOT6	sfc	2.9	1.0	0.102
07-Aug-2013 23:54	DOT6	mid	16.9	1.3	0.119
07-Aug-2013 23:54	DOT6	btmB	30.3	1.8	0.098
07-Aug-2013 23:54	DOT6	btmA	32.8	2.2	0.106
07-Aug-2013 23:54	DOT6	BTM	35.0	2.5	0.155
08-Aug-2013 05:40	DOT6	sfc	1.8	1.0	
08-Aug-2013 05:40	DOT6	mid	16.0	1.1	0.111
08-Aug-2013 05:40	DOT6	btmB	29.9	0.8	0.137
08-Aug-2013 05:40	DOT6	btmA	32.9	3.3	0.093
08-Aug-2013 05:40	DOT6	BTM	35.0	6.4	0.093
08-Aug-2013 07:00	CTD10	sfc	2.4	0.8	0.100
08-Aug-2013 07:00	CTD10	mid	15.5	1.5	0.118
08-Aug-2013 07:00	CTD10	btmB	29.2	1.3	0.058
08-Aug-2013 07:00	CTD10	btmA	31.3	0.8	0.077
08-Aug-2013 07:00	CTD10	BTM	36.0	1.3	0.122
08-Aug-2013 08:16	CTD9	sfc	2.2	0.6	0.076
08-Aug-2013 08:16	CTD9	mid	10.6	0.5	0.068
08-Aug-2013 08:16	CTD9	btmB	17.0	0.7	0.074
08-Aug-2013 08:16	CTD9	btmA	19.1	0.6	0.087
08-Aug-2013 08:16	CTD9	BTM	22.2	1.1	0.076
08-Aug-2013 08:58	DOT5	sfc	2.3	1.8	
08-Aug-2013 08:58	DOT5	mid	14.1	1.9	0.093
08-Aug-2013 08:58	DOT5	btmB	26.0	2.5	0.118
08-Aug-2013 08:58	DOT5	btmA	28.6	2.9	0.158
08-Aug-2013 08:58	DOT5	BTM	31.0	4.6	0.252
08-Aug-2013 10:05	CTD8	sfc	2.0	1.0	0.092
08-Aug-2013 10:05	CTD8	mid	5.4	1.1	0.107
08-Aug-2013 10:05	CTD8	btmB	8.3	2.6	0.098
08-Aug-2013 10:05	CTD8	btmA	10.4	2.8	0.096
08-Aug-2013 10:05	CTD8	btmA	10.4	2.8	
08-Aug-2013 10:05	CTD8	BTM	14.0	3.5	0.128
08-Aug-2013 11:23	DOT4	sfc	2.7	1.6	0.075
08-Aug-2013 11:23	DOT4	mid	10.9	2.4	0.114
08-Aug-2013 11:23	DOT4	btmB	18.1	2.5	0.127
08-Aug-2013 11:23	DOT4	btmA	20.1	3.4	0.125
08-Aug-2013 11:23	DOT4	BTM	22.9	3.4	0.158
08-Aug-2013 12:19	CTD11	sfc	2.8	0.6	0.083
08-Aug-2013 12:19	CTD11	mid	13.6	0.8	0.093
08-Aug-2013 12:19	CTD11	btmB	23.5	0.9	0.101
08-Aug-2013 12:19	CTD11	btmA	25.8	1.2	0.084
08-Aug-2013 12:19	CTD11	BTM	34.3	1.7	0.092
08-Aug-2013 12:58	DOT7	sfc	2.8	1.5	0.118
08-Aug-2013 12:58	DOT7	sfc	2.8	1.4	
08-Aug-2013 12:58	DOT7	mid	14.3	1.1	0.101
08-Aug-2013 12:58	DOT7	btmB	24.1	2.5	0.098
08-Aug-2013 12:58	DOT7	btmA	26.3	3.2	0.134
08-Aug-2013 12:58	DOT7	BTM	47.0	2.0	0.101
08-Aug-2013 14:09	DOT3	sfc	2.8	1.5	0.165
08-Aug-2013 14:09	DOT3	mid	15.6	1.7	0.091
08-Aug-2013 14:09	DOT3	btmB	24.4	1.8	0.089
08-Aug-2013 14:09	DOT3	btmA	26.9	1.7	0.115
08-Aug-2013 14:09	DOT3	BTM	28.0	2.2	0.097
08-Aug-2013 15:47	DOT1	sfc	3.0	1.6	0.200
08-Aug-2013 15:47	DOT1	mid	19.4	1.5	0.099
08-Aug-2013 15:47	DOT1	btmB	33.8	2.5	0.134
08-Aug-2013 15:47	DOT1	btmA	36.5	2.4	0.133
08-Aug-2013 15:47	DOT1	BTM	38.1	3.3	0.151
08-Aug-2013 16:25	DOT2	sfc	2.8	2.0	0.207
08-Aug-2013 16:25	DOT2	mid	14.8	2.7	0.155

Suspended Sediment and Particulate Organic Sediment data (SSC and POC) - Cruise CTDOT6

Sample Date/Time (EST)	Station	Sub Sample ID	Depth (m)	SSC (mg/l)	POC (mg/l)
20-Nov-2013 07:35	DOT7	sfc	2.1	1.8	0.117
20-Nov-2013 07:35	DOT7	mid	22.5	1.7	0.109
20-Nov-2013 07:35	DOT7	btmB	41.2	1.7	0.112
20-Nov-2013 07:35	DOT7	btmA	43.8	1.5	0.116
20-Nov-2013 07:35	DOT7	BTM	45.5	2.5	0.234
20-Nov-2013 09:07	DOT3	sfc	2.0	5.6	0.209
20-Nov-2013 09:07	DOT3	mid	14.1	5.9	0.194
20-Nov-2013 09:07	DOT3	btmB	23.2	8.4	0.323
20-Nov-2013 09:07	DOT3	btmA	25.7	9.0	0.241
20-Nov-2013 09:07	DOT3	BTM	27.5	11.6	0.398
20-Nov-2013 10:29	DOT1	sfc	1.8	3.2	0.153
20-Nov-2013 10:29	DOT1	mid	19.9	4.9	0.210
20-Nov-2013 10:29	DOT1	btmB	34.8	5.2	
20-Nov-2013 10:29	DOT1	btmA	36.5	4.9	0.198
20-Nov-2013 10:29	DOT1	BTM	38.0	7.1	0.260
20-Nov-2013 11:24	DOT2	sfc	1.9	4.9	0.188
20-Nov-2013 11:24	DOT2	mid	15.9	5.5	0.175
20-Nov-2013 11:24	DOT2	btmB	26.2	4.0	0.213
20-Nov-2013 11:24	DOT2	btmA	29.7	4.7	
20-Nov-2013 11:24	DOT2	BTM	31.0	6.0	0.228
20-Nov-2013 11:24	DOT2	BTM	31.0	5.7	
20-Nov-2013 13:19	CTD11	sfc	2.4	1.6	0.143
20-Nov-2013 13:19	CTD11	mid	11.9	2.1	0.165
20-Nov-2013 13:19	CTD11	btmB	17.2	1.5	0.118
20-Nov-2013 13:19	CTD11	btmA	19.8	1.3	0.096
20-Nov-2013 13:19	CTD11	BTM	18.3	1.5	0.115
20-Nov-2013 14:30	DOT4	sfc	1.8	2.6	0.131
20-Nov-2013 14:30	DOT4	mid	10.4	2.6	0.170
20-Nov-2013 14:30	DOT4	btmB	18.1	5.5	0.183
20-Nov-2013 14:30	DOT4	btmA	20.7	3.8	
20-Nov-2013 14:30	DOT4	BTM	22.1	5.5	0.230
20-Nov-2013 15:47	CTD8	sfc	1.6	2.3	0.143
20-Nov-2013 15:47	CTD8	mid	6.7	2.1	0.158
20-Nov-2013 15:47	CTD8	mid	6.7	5.9	
20-Nov-2013 15:47	CTD8	btmB	10.6	1.7	0.136
20-Nov-2013 15:47	CTD8	btmA	12.7	1.9	0.164
20-Nov-2013 15:47	CTD8	BTM	13.0	2.0	0.139
20-Nov-2013 17:20	DOT5	sfc	2.0	1.4	0.116
20-Nov-2013 17:20	DOT5	mid	14.8	2.0	0.160
20-Nov-2013 17:20	DOT5	btmB	25.6	2.4	0.178
20-Nov-2013 17:20	DOT5	btmA	28.3	2.9	0.153
20-Nov-2013 17:20	DOT5	BTM	29.2	7.9	0.330
20-Nov-2013 18:33	CTD9	sfc	2.3	1.2	0.215
20-Nov-2013 18:33	CTD9	mid	11.0	1.0	
20-Nov-2013 18:33	CTD9	btmB	17.0	1.0	0.104
20-Nov-2013 18:33	CTD9	btmA	19.4	1.3	0.129
20-Nov-2013 18:33	CTD9	btmA	19.4	1.2	
20-Nov-2013 18:33	CTD9	BTM	21.5	1.1	0.145
20-Nov-2013 18:33	CTD9	BTM	21.5	1.6	
20-Nov-2013 20:00	CTD10	sfc	2.5	0.9	0.112
20-Nov-2013 20:00	CTD10	mid	18.1	1.0	0.103
20-Nov-2013 20:00	CTD10	btmB	32.6	0.9	0.120
20-Nov-2013 20:00	CTD10	btmA	34.8	1.2	0.110
20-Nov-2013 20:00	CTD10	BTM	36.0	0.9	0.167
20-Nov-2013 21:45	DOT6	sfc	2.6	0.9	0.119
20-Nov-2013 21:45	DOT6	mid	16.0	1.0	0.133
20-Nov-2013 21:45	DOT6	btmB	30.0	1.1	0.140
20-Nov-2013 21:45	DOT6	btmA	32.1	1.2	0.124
20-Nov-2013 21:45	DOT6	BTM	34.0	2.2	0.148

Suspended Sediment and Particulate Organic Sediment data (SSC and POC) - Cruise CTDOT6

Sample Date/Time (EST)	Station	Sub Sample ID	Depth (m)	SSC (mg/l)	POC (mg/l)
21-Nov-2013 06:20	DOT6	sfc	2.0	1.0	0.104
21-Nov-2013 06:20	DOT6	mid	15.9	1.2	0.089
21-Nov-2013 06:20	DOT6	btmB	30.1	1.0	0.114
21-Nov-2013 06:20	DOT6	btmA	32.5	1.0	0.108
21-Nov-2013 06:20	DOT6	BTM	33.9	1.1	0.115
21-Nov-2013 08:00	CTD10	sfc	2.1	0.8	0.104
21-Nov-2013 08:00	CTD10	mid	16.9	0.8	0.092
21-Nov-2013 08:00	CTD10	btmB	33.0	0.7	0.100
21-Nov-2013 08:00	CTD10	btmA	35.2	1.0	0.088
21-Nov-2013 08:00	CTD10	BTM	31.5	1.0	0.140
21-Nov-2013 09:12	CTD9	sfc	1.9	0.6	0.134
21-Nov-2013 09:12	CTD9	mid	10.2	1.1	0.115
21-Nov-2013 09:12	CTD9	mid	10.2	0.7	0.111
21-Nov-2013 09:12	CTD9	btmB	17.0	1.0	
21-Nov-2013 09:12	CTD9	btmB	17.0	5.8	0.078
21-Nov-2013 09:12	CTD9	btmA	19.1	0.7	0.092
21-Nov-2013 09:12	CTD9	BTM	20.5	0.7	0.100
21-Nov-2013 10:15	DOT5	sfc	2.0	3.0	0.210
21-Nov-2013 10:15	DOT5	mid	15.8	3.4	0.253
21-Nov-2013 10:15	DOT5	btmB	27.1	4.3	0.412
21-Nov-2013 10:15	DOT5	btmA	29.2	6.5	0.246
21-Nov-2013 10:15	DOT5	BTM	31.5	11.3	0.590
21-Nov-2013 11:33	CTD8	sfc	1.9	2.0	0.209
21-Nov-2013 11:33	CTD8	mid	7.2	2.3	0.184
21-Nov-2013 11:33	CTD8	btmB	9.8	3.6	0.216
21-Nov-2013 11:33	CTD8	btmA	12.0	3.7	0.321
21-Nov-2013 11:33	CTD8	BTM	14.5	2.6	0.261
21-Nov-2013 12:58	DOT4	sfc	1.6	2.6	0.000
21-Nov-2013 12:58	DOT4	mid	11.8	2.3	0.174
21-Nov-2013 12:58	DOT4	btmB	20.7	4.6	0.140
21-Nov-2013 12:58	DOT4	btmA	23.0	2.0	0.220
21-Nov-2013 12:58	DOT4	BTM	24.7	2.5	0.156
21-Nov-2013 14:00	CTD11	sfc	2.1	1.6	0.125
21-Nov-2013 14:00	CTD11	mid	16.5	1.7	0.132
21-Nov-2013 14:00	CTD11	btmB	31.0	2.1	0.218
21-Nov-2013 14:00	CTD11	btmA	34.5	1.3	0.204
21-Nov-2013 14:00	CTD11	BTM	37.0	1.6	0.121
21-Nov-2013 16:48	DOT2	sfc	2.1	4.4	0.217
21-Nov-2013 16:48	DOT2	mid	14.6	7.1	0.217
21-Nov-2013 16:48	DOT2	btmB	26.0	10.4	0.271
21-Nov-2013 16:48	DOT2	btmA	28.7	4.8	0.256
21-Nov-2013 16:48	DOT2	BTM	30.0	6.5	0.247
21-Nov-2013 17:36	DOT1	sfc	2.0	5.9	0.226
21-Nov-2013 17:36	DOT1	mid	20.5	17.8	0.375
21-Nov-2013 17:36	DOT1	btmB	37.0	26.1	0.544
21-Nov-2013 17:36	DOT1	btmA	39.2	14.2	0.505
21-Nov-2013 17:36	DOT1	BTM	40.0	13.8	0.452
21-Nov-2013 18:49	DOT3	sfc	1.9	5.1	0.217
21-Nov-2013 18:49	DOT3	mid	13.3	11.0	0.273
21-Nov-2013 18:49	DOT3	btmB	22.6	21.0	0.337
21-Nov-2013 18:49	DOT3	btmA	24.7	12.1	0.480
21-Nov-2013 18:49	DOT3	BTM	27.4	10.4	0.343
21-Nov-2013 21:45	DOT7	sfc	1.8	2.4	0.116
21-Nov-2013 21:45	DOT7	mid	21.0	1.7	0.120
21-Nov-2013 21:45	DOT7	btmB	38.9	2.6	0.000
21-Nov-2013 21:45	DOT7	btmA	41.2	1.9	0.113
21-Nov-2013 21:45	DOT7	BTM	44.0	2.1	0.164
03-Dec-2013 11:22	DOT6	BTM	34.0	2.4	0.170

Suspended Sediment and Particulate Organic Sediment data (SSC and POC) - Cruise CTDOT7

Sample Date/Time (EST)	Station	Sub Sample ID	Depth (m)	SSC (mg/l)	POC (mg/l)
12-Dec-2013 11:00	DOT4	BTM	22.2	4.6	
12-Dec-2013 13:30	DOT5	BTM	30.1	5.5	
12-Dec-2013 15:35	DOT6	BTM	35.0	4.1	
17-Dec-2013 09:18	DOT7	BTM	51.0	6.5	
17-Dec-2013 11:36	DOT3	BTM	29.0	7.4	
18-Dec-2013 11:01	DOT2	BTM	31.0	9.4	
18-Dec-2013 12:31	DOT1	BTM	44.0	4.8	

Suspended Sediment and Particulate Organic Sediment data (SSC and POC) - Cruise CTDOT8

Sample Date/Time (EST)	Station	Sub Sample ID	Depth (m)	SSC (mg/l)	POC (mg/l)
15-Jan-2014 08:22	DOT7	sfc	1.8	2.0	0.273
15-Jan-2014 08:22	DOT7	mid	22.8	3.3	0.301
15-Jan-2014 08:22	DOT7	btmB	42.6	4.2	0.288
15-Jan-2014 08:22	DOT7	btmA	45.2	2.7	0.316
15-Jan-2014 08:22	DOT7	BTM	44.5	4.0	0.187
15-Jan-2014 08:22	DOT7	BTM	44.5	4.5	0.214
15-Jan-2014 10:33	DOT3	sfc	2.2	2.0	0.154
15-Jan-2014 10:33	DOT3	mid	14.9	2.2	0.198
15-Jan-2014 10:33	DOT3	btmB	25.7	2.1	0.188
15-Jan-2014 10:33	DOT3	btmA	28.0	2.5	0.215
15-Jan-2014 10:33	DOT3	BTM	29.0	3.1	0.155
15-Jan-2014 12:19	DOT1	sfc	2.0	2.9	0.157
15-Jan-2014 12:19	DOT1	mid	20.8	2.5	0.192
15-Jan-2014 12:19	DOT1	mid	20.8	2.5	0.219
15-Jan-2014 12:19	DOT1	btmB	38.5	8.3	0.228
15-Jan-2014 12:19	DOT1	BTM	40.7	6.4	0.227
15-Jan-2014 13:31	DOT2	sfc	2.3	4.0	0.155
15-Jan-2014 13:31	DOT2	mid	15.1	6.1	0.256
15-Jan-2014 13:31	DOT2	btmB	28.3	11.4	0.333
15-Jan-2014 13:31	DOT2	btmA	30.6	11.6	0.396
15-Jan-2014 13:31	DOT2	btmA	30.6	7.7	
15-Jan-2014 13:31	DOT2	BTM	32.0	7.6	0.272
15-Jan-2014 15:08	CTD11	sfc	2.5	3.3	0.160
15-Jan-2014 15:08	CTD11	mid	17.9	3.9	0.176
15-Jan-2014 15:08	CTD11	btmB	35.3	3.4	0.276
15-Jan-2014 15:08	CTD11	btmA	37.2	3.3	0.277
15-Jan-2014 15:08	CTD11	BTM	44.0	4.0	0.175
15-Jan-2014 15:50	DOT7-2	sfc	1.9	2.1	0.170
15-Jan-2014 15:50	DOT7-2	mid	24.7	2.8	0.170
15-Jan-2014 15:50	DOT7-2	btmB	46.7	3.3	0.341
15-Jan-2014 15:50	DOT7-2	btmA	48.3	4.5	0.219
15-Jan-2014 15:50	DOT7-2	BTM	51.2	3.3	0.161
15-Jan-2014 16:52	DOT3-2	sfc	1.9	5.9	0.157
15-Jan-2014 16:52	DOT3-2	mid	13.5	6.3	0.231
15-Jan-2014 16:52	DOT3-2	btmB	25.6	6.9	0.420
15-Jan-2014 16:52	DOT3-2	btmA	27.6	7.3	0.369
15-Jan-2014 16:52	DOT3-2	BTM	28.3	8.5	0.284
15-Jan-2014 17:55	DOT1-2	sfc	2.4	3.9	
15-Jan-2014 17:55	DOT1-2	sfc	2.4	4.4	0.207
15-Jan-2014 17:55	DOT1-2	mid	17.4	11.9	0.398
15-Jan-2014 17:55	DOT1-2	btmB	33.0	15.7	0.624
15-Jan-2014 17:55	DOT1-2	btmA	35.5	12.8	0.457
15-Jan-2014 17:55	DOT1-2	BTM	36.0	24.1	0.833
15-Jan-2014 18:52	DOT2-2	sfc	2.2	5.9	0.268
15-Jan-2014 18:52	DOT2-2	mid	14.4	19.0	0.481
15-Jan-2014 18:52	DOT2-2	btmB	26.6	27.7	0.634
15-Jan-2014 18:52	DOT2-2	btmA	29.3	20.9	0.750
15-Jan-2014 18:52	DOT2-2	BTM	31.0	27.8	0.693
15-Jan-2014 21:21	CTD11-2	sfc	2.4	2.7	0.142
15-Jan-2014 21:21	CTD11-2	mid	17.8	8.2	0.350
15-Jan-2014 21:21	CTD11-2	btmB	34.9	4.0	0.258
15-Jan-2014 21:21	CTD11-2	btmA	36.7	3.7	
15-Jan-2014 21:21	CTD11-2	btmA	36.7	6.4	0.191
15-Jan-2014 21:21	CTD11-2	BTM	90.0	2.9	0.166
15-Jan-2014 22:32	DOT4	sfc	2.2	2.8	0.139
15-Jan-2014 22:32	DOT4	mid	11.5	3.4	0.197
15-Jan-2014 22:32	DOT4	btmB	20.6	2.5	0.251
15-Jan-2014 22:32	DOT4	btmA	22.0	3.5	0.236
15-Jan-2014 22:32	DOT4	BTM	23.0	3.4	0.226

Suspended Sediment and Particulate Organic Sediment data (SSC and POC) - Cruise CTDOT8

Sample Date/Time (EST)	Station	Sub Sample ID	Depth (m)	SSC (mg/l)	POC (mg/l)
15-Jan-2014 23:49	CTD8	BTM	14.0	8.1	
16-Jan-2014 06:20	CTD8	sfc	1.9	2.5	0.166
16-Jan-2014 06:20	CTD8	mid	5.5	7.7	0.304
16-Jan-2014 06:20	CTD8	btmB	8.8	8.6	0.524
16-Jan-2014 06:20	CTD8	btmA	10.5	8.6	0.662
16-Jan-2014 06:20	CTD8	BTM	15.0	7.8	0.329
16-Jan-2014 08:05	DOT4	sfc	2.4	7.3	0.191
16-Jan-2014 08:05	DOT4	mid	10.9	7.4	0.236
16-Jan-2014 08:05	DOT4	btmB	19.6	6.3	0.436
16-Jan-2014 08:05	DOT4	btmA	21.4	13.7	0.457
16-Jan-2014 08:05	DOT4	BTM	23.0	7.0	0.265
16-Jan-2014 10:00	DOT5	sfc	2.2	4.0	0.251
16-Jan-2014 10:00	DOT5	mid	14.7	6.1	0.368
16-Jan-2014 10:00	DOT5	btmB	25.5	4.7	0.511
16-Jan-2014 10:00	DOT5	btmB	25.5	4.6	
16-Jan-2014 10:00	DOT5	btmA	26.9	8.4	0.438
16-Jan-2014 10:00	DOT5	BTM	30.5	9.4	0.794
16-Jan-2014 10:46	CTD9	sfc	2.4	1.0	0.100
16-Jan-2014 10:46	CTD9	mid	10.8	1.3	0.125
16-Jan-2014 10:46	CTD9	btmB	18.3	1.3	0.198
16-Jan-2014 10:46	CTD9	btmA	20.6	1.5	0.239
16-Jan-2014 10:00	CTD9	BTM	21.5	1.4	0.201
16-Jan-2014 11:50	CTD10	sfc	2.1	1.7	
16-Jan-2014 11:50	CTD10	sfc	16.2	1.9	0.095
16-Jan-2014 11:50	CTD10	mid	31.0	1.8	0.104
16-Jan-2014 11:50	CTD10	btmB	31.0	2.1	0.148
16-Jan-2014 11:50	CTD10	btmB	31.0	3.0	
16-Jan-2014 11:50	CTD10	btmA	32.7	2.6	0.162
16-Jan-2014 11:50	CTD10	BTM	37.5	2.9	0.215
16-Jan-2014 13:40	DOT6	sfc	2.2	0.5	0.107
16-Jan-2014 13:40	DOT6	mid	15.8	3.6	0.159
16-Jan-2014 13:40	DOT6	btmB	30.3	4.9	0.286
16-Jan-2014 13:40	DOT6	btmA	32.5	5.2	0.203
16-Jan-2014 13:40	DOT6	BTM	35.3	5.1	0.228
16-Jan-2014 13:40	DOT6	BTM	35.3	5.1	
16-Jan-2014 14:40	DOT5-2	sfc	2.3	1.7	0.106
16-Jan-2014 14:40	DOT5-2	mid	13.9	4.9	0.235
16-Jan-2014 14:40	DOT5-2	btmB	24.5	15.8	0.577
16-Jan-2014 14:40	DOT5-2	btmA	26.5	19.4	0.602
16-Jan-2014 14:40	DOT5-2	BTM	29.4	23.6	0.794
16-Jan-2014 15:21	CTD9-2	sfc	2.5	1.3	0.100
16-Jan-2014 15:21	CTD9-2	mid	11.0	2.5	0.125
16-Jan-2014 15:21	CTD9-2	btmB	18.6	3.3	0.198
16-Jan-2014 15:21	CTD9-2	btmA	20.2	2.9	0.239
16-Jan-2014 15:21	CTD9-2	BTM	22.1	4.5	0.201
16-Jan-2014 16:27	CTD10-2	sfc	2.6	1.0	0.106
16-Jan-2014 16:27	CTD10-2	mid	16.3	1.5	0.102
16-Jan-2014 16:27	CTD10-2	btmB	34.1	3.1	0.172
16-Jan-2014 16:27	CTD10-2	btmA	35.0	2.2	0.133
16-Jan-2014 16:27	CTD10-2	BTM	37.6	3.0	0.147
16-Jan-2014 17:56	DOT6-2	sfc	2.5	1.3	0.128
16-Jan-2014 17:56	DOT6-2	mid	16.7	2.2	0.136
16-Jan-2014 17:56	DOT6-2	btmB	30.2	3.6	0.172
16-Jan-2014 17:56	DOT6-2	btmA	31.9	2.8	0.234
16-Jan-2014 17:56	DOT6-2	BTM	34.0	5.6	0.234

This page intentionally left blank.

Appendix 13

SEDIMENT GRAIN SIZE ANALYSIS DATA SHEETS

Analyses were performed by University of Connecticut laboratory at Avery Point

Appendix A
Particle Size Analysis Results

SAMPLE STATISTICS

SAMPLE IDENTITY: **DOT1, 3/13/2013**

SAMPLE TYPE: Unimodal, Moderately Sorted

TEXTURAL GROUP: Slightly Gravelly Sand

SEDIMENT NAME: Slightly Gravelly Coarse Sand

	µm	f
MODE 1:	750.0	0.500
MODE 2:		
MODE 3:		
D_{10}:	261.3	-0.227
MEDIAN or D_{50}:	554.6	0.851
D_{90}:	1170.2	1.936
(D_{90} / D_{10}):	4.478	-8.537
(D_{90} - D_{10}):	908.9	2.163
(D_{75} / D_{25}):	2.340	5.250
(D_{75} - D_{25}):	468.8	1.227

GRAIN SIZE DISTRIBUTION

GRAVEL:	2.6%	V COARSE SAND:	9.5%
SAND:	95.8%	COARSE SAND:	44.5%
MUD:	1.6%	MEDIUM SAND:	35.6%
		FINE SAND:	6.0%
		V FINE SAND:	0.1%
		SILT:	0.1%
		CLAY:	1.4%

■ Gravel ■ Sand ■ Mud

	METHOD OF MOMENTS			FOLK & WARD METHOD		
	Arithmetic µm	Geometric µm	Logarithmic f	Geometric µm	Logarithmic f	Description
MEAN($\bar{x}$):	684.8	507.9	0.978	535.3	0.902	Coarse Sand
SORTING (s):	446.7	2.516	1.331	1.874	0.906	Moderately Sorted
SKEWNESS (*Sk*):	1.810	-3.713	3.713	-0.046	0.046	Symmetrical
KURTOSIS (*K*):	7.044	24.93	24.93	1.071	1.071	Mesokurtic

GRAIN SIZE DISTRIBUTION

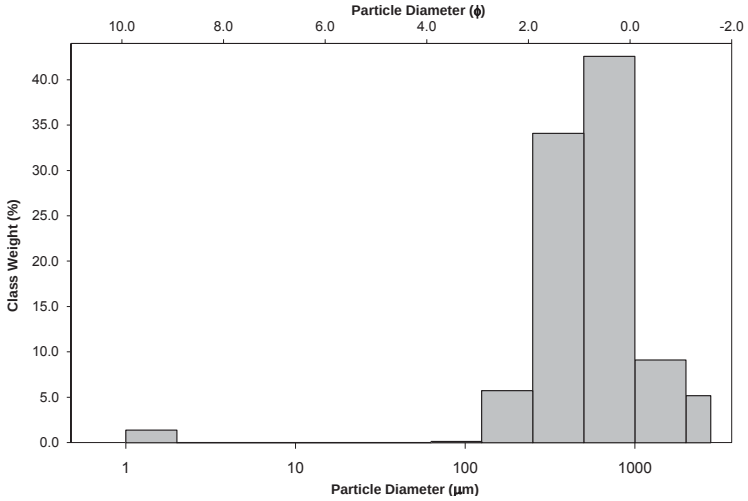

SAMPLE STATISTICS

SAMPLE IDENTITY: **DOT1, 8/7/2013**

SAMPLE TYPE: Bimodal, Moderately Sorted

TEXTURAL GROUP: Gravelly Sand

SEDIMENT NAME: Gravelly Coarse Sand

	µm	f
MODE 1:	750.0	0.500
MODE 2:	2400.0	-1.243
MODE 3:		
D_{10}:	285.9	-0.676
MEDIAN or D_{50}:	604.8	0.725
D_{90}:	1597.9	1.806
(D_{90} / D_{10}):	5.589	-2.671
(D_{90} - D_{10}):	1312.0	2.483
(D_{75} / D_{25}):	2.311	8.438
(D_{75} - D_{25}):	506.9	1.209

GRAIN SIZE DISTRIBUTION

GRAVEL:	6.3%	V COARSE SAND:	11.5%
SAND:	92.7%	COARSE SAND:	44.4%
MUD:	1.0%	MEDIUM SAND:	34.5%
		FINE SAND:	2.3%
		V FINE SAND:	0.0%
		SILT:	0.0%
		CLAY:	0.9%

■ Gravel ■ Sand ■ Mud

	METHOD OF MOMENTS			FOLK & WARD METHOD		
	Arithmetic µm	Geometric µm	Logarithmic f	Geometric µm	Logarithmic f	Description
MEAN($\bar{x}$):	790.0	593.5	0.753	601.1	0.734	Coarse Sand
SORTING (s):	543.4	2.291	1.196	1.878	0.909	Moderately Sorted
SKEWNESS (*Sk*):	1.672	-3.279	3.279	0.091	-0.091	Symmetrical
KURTOSIS (*K*):	5.364	26.42	26.42	1.034	1.034	Mesokurtic

GRAIN SIZE DISTRIBUTION

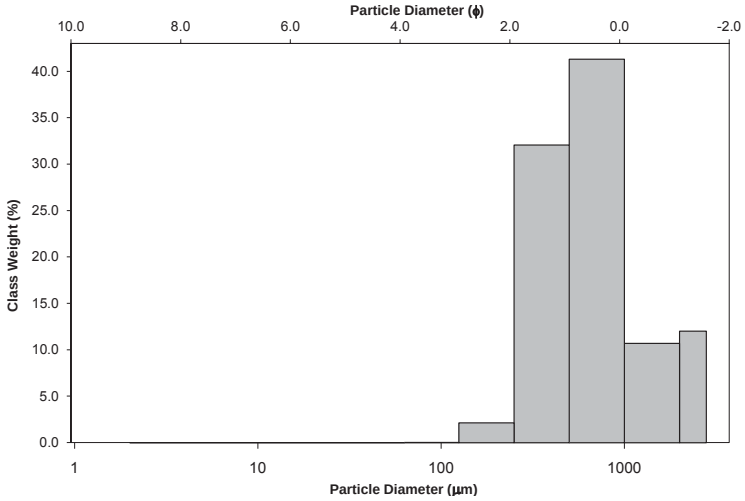

SAMPLE STATISTICS

SAMPLE IDENTITY: **DOT1, 11/21/2013**

SAMPLE TYPE: Unimodal, Moderately Sorted
SEDIMENT NAME: Slightly Gravelly Coarse Sand

TEXTURAL GROUP: Slightly Gravelly Sand

	µm	f
MODE 1:	750.0	0.500
MODE 2:		
MODE 3:		
D_{10}:	278.3	0.083
MEDIAN or D_{50}:	523.2	0.935
D_{90}:	944.0	1.845
(D_{90} / D_{10}):	3.392	22.18
(D_{90} - D_{10}):	665.7	1.762
(D_{75} / D_{25}):	2.143	3.732
(D_{75} - D_{25}):	403.5	1.099

GRAIN SIZE DISTRIBUTION

GRAVEL: 0.6%
SAND: 97.9%
MUD: 1.5%

V COARSE SAND: 5.4%
COARSE SAND: 47.0%
MEDIUM SAND: 43.7%
FINE SAND: 1.7%
V FINE SAND: 0.1%

SILT: 0.0%
CLAY: 1.4%

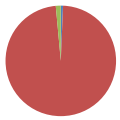

	METHOD OF MOMENTS			FOLK & WARD METHOD		
	Arithmetic µm	Geometric µm	Logarithmic f	Geometric µm	Logarithmic f	Description
MEAN($\bar{x}$):	616.7	487.7	1.036	517.2	0.951	Coarse Sand
SORTING (s):	325.2	2.293	1.197	1.626	0.702	Moderately Sorted
SKEWNESS (*Sk*):	1.871	-4.740	4.740	0.009	-0.009	Symmetrical
KURTOSIS (*K*):	9.202	34.51	34.51	0.805	0.805	Platykurtic

GRAIN SIZE DISTRIBUTION

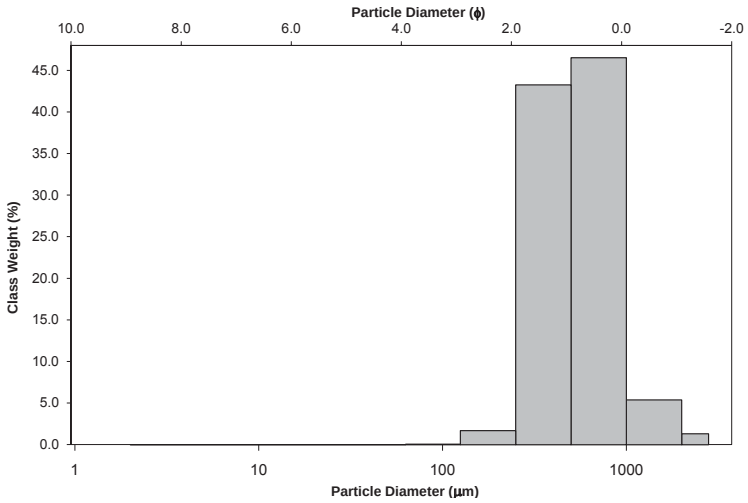

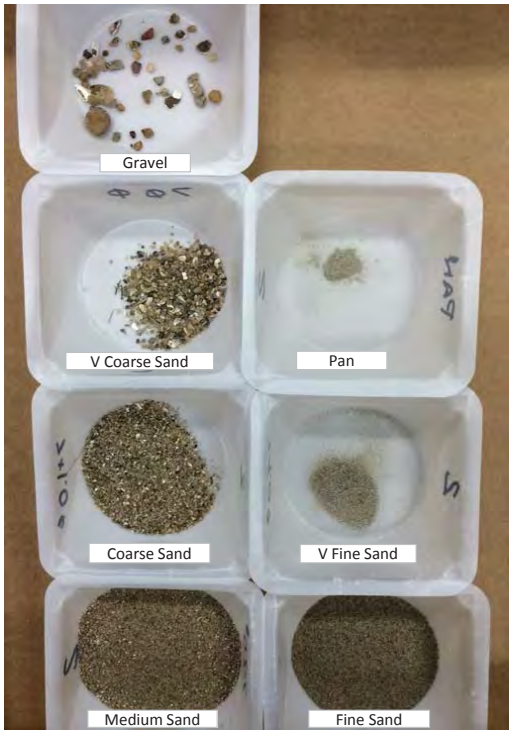

SAMPLE STATISTICS

SAMPLE IDENTITY: **DOT2, 3/13/2013**

SAMPLE TYPE: Bimodal, Poorly Sorted

TEXTURAL GROUP: Sandy Gravel

SEDIMENT NAME: Sandy Gravel

	µm	f
MODE 1:	2400.0	-1.243
MODE 2:	375.0	1.500
MODE 3:		
D_{10}:	151.2	-1.335
MEDIAN or D_{50}:	567.4	0.818
D_{90}:	2523.5	2.725
(D_{90} / D_{10}):	16.69	-2.041
(D_{90} - D_{10}):	2372.3	4.061
(D_{75} / D_{25}):	7.748	-1.660
(D_{75} - D_{25}):	1880.5	2.954

GRAIN SIZE DISTRIBUTION

GRAVEL:	32.4%	V COARSE SAND:	9.3%
SAND:	62.4%	COARSE SAND:	10.2%
MUD:	5.2%	MEDIUM SAND:	27.4%
		FINE SAND:	14.8%
		V FINE SAND:	0.7%
		SILT:	0.6%
		CLAY:	2.8%

	METHOD OF MOMENTS			FOLK & WARD METHOD		
	Arithmetic µm	Geometric µm	Logarithmic f	Geometric µm	Logarithmic f	Description
MEAN($\bar{x}$):	1125.0	561.8	0.832	646.1	0.630	Coarse Sand
SORTING (s):	953.7	4.745	2.246	3.431	1.779	Poorly Sorted
SKEWNESS (*Sk*):	0.408	-1.811	1.811	-0.041	0.041	Symmetrical
KURTOSIS (*K*):	1.387	7.527	7.527	0.813	0.813	Platykurtic

GRAIN SIZE DISTRIBUTION

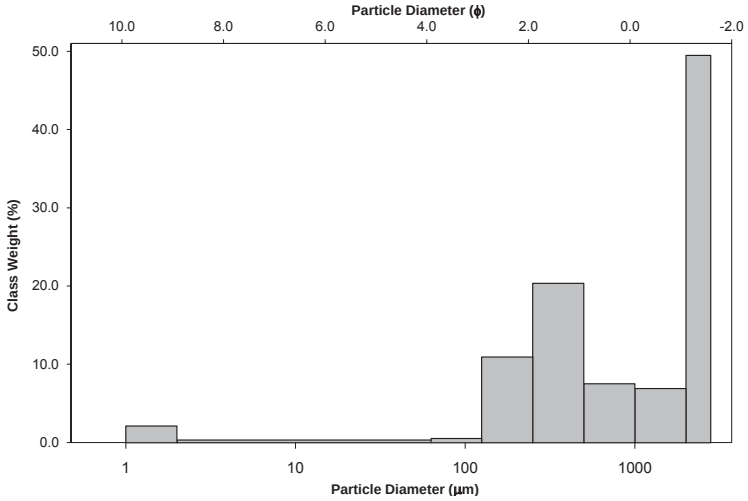

SAMPLE STATISTICS

SAMPLE IDENTITY: **DOT2, 8/7/2013**

SAMPLE TYPE: Bimodal, Poorly Sorted

SEDIMENT NAME: Gravelly Medium Sand

TEXTURAL GROUP: Gravelly Sand

	µm	f
MODE 1:	2400.0	-1.243
MODE 2:	375.0	1.500
MODE 3:		
D_{10}:	152.0	-1.297
MEDIAN or D_{50}:	492.0	1.023
D_{90}:	2457.1	2.717
(D_{90} / D_{10}):	16.16	-2.095
(D_{90} - D_{10}):	2305.0	4.014
(D_{75} / D_{25}):	7.548	-1.875
(D_{75} - D_{25}):	1752.2	2.916

GRAIN SIZE DISTRIBUTION

GRAVEL:	25.8%	V COARSE SAND:	10.4%
SAND:	69.9%	COARSE SAND:	13.2%
MUD:	4.3%	MEDIUM SAND:	28.5%
		FINE SAND:	17.0%
		V FINE SAND:	0.9%
		SILT:	0.6%
		CLAY:	1.4%

	METHOD OF MOMENTS			FOLK & WARD METHOD		
	Arithmetic µm	Geometric µm	Logarithmic f	Geometric µm	Logarithmic f	Description
MEAN($\bar{x}$):	1013.4	536.0	0.900	600.9	0.735	Coarse Sand
SORTING (s):	900.5	3.972	1.990	3.002	1.586	Poorly Sorted
SKEWNESS (*Sk*):	0.654	-1.543	1.543	0.145	-0.145	Coarse Skewed
KURTOSIS (*K*):	1.723	7.206	7.206	0.648	0.648	Very Platykurtic

GRAIN SIZE DISTRIBUTION

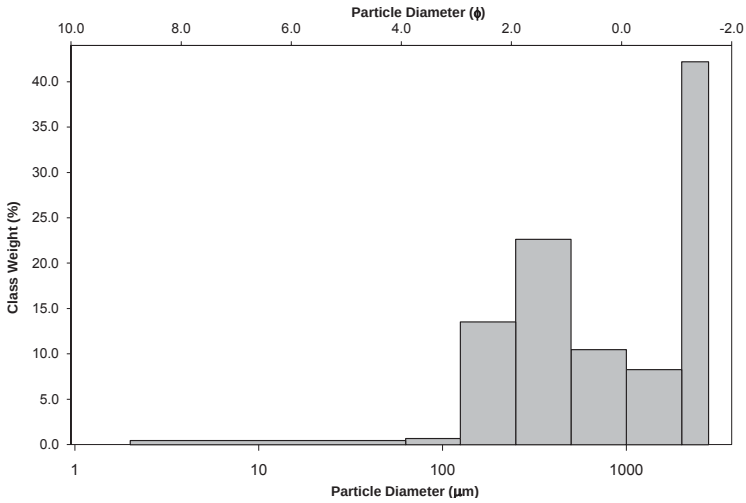

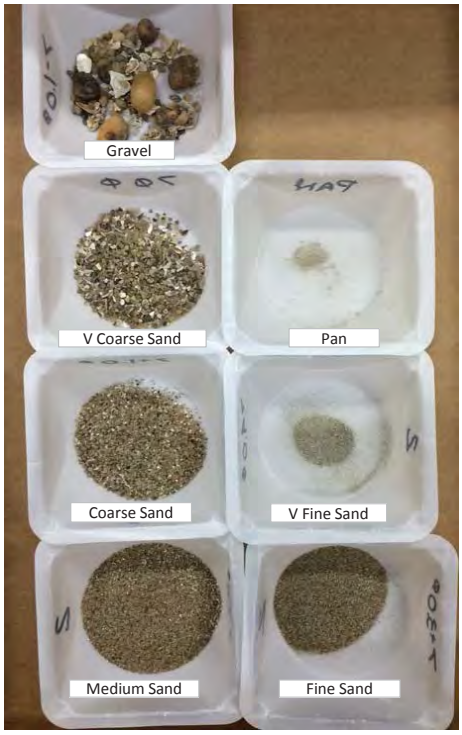

SAMPLE STATISTICS

SAMPLE IDENTITY: **DOT2, 11/21/2013**

SAMPLE TYPE: Unimodal, Moderately Sorted
SEDIMENT NAME: Slightly Gravelly Medium Sand

TEXTURAL GROUP: Slightly Gravelly Sand

	µm	f
MODE 1:	375.0	1.500
MODE 2:		
MODE 3:		
D_{10}:	159.7	0.249
MEDIAN or D_{50}:	346.7	1.528
D_{90}:	841.3	2.646
(D_{90} / D_{10}):	5.267	10.61
(D_{90} - D_{10}):	681.6	2.397
(D_{75} / D_{25}):	1.836	1.804
(D_{75} - D_{25}):	213.8	0.876

GRAIN SIZE DISTRIBUTION

GRAVEL: 3.0%
SAND: 94.7%
MUD: 2.3%

V COARSE SAND: 3.8%
COARSE SAND: 13.1%
MEDIUM SAND: 57.1%
FINE SAND: 20.2%
V FINE SAND: 0.5%

SILT: 0.0%
CLAY: 2.2%

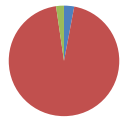

	METHOD OF MOMENTS			FOLK & WARD METHOD		
	Arithmetic µm	Geometric µm	Logarithmic f	Geometric µm	Logarithmic f	Description
MEAN($\bar{x}$):	478.6	328.1	1.608	346.7	1.528	Medium Sand
SORTING (s):	433.5	2.773	1.471	1.891	0.919	Moderately Sorted
SKEWNESS (*Sk*):	3.009	-3.140	3.140	0.093	-0.093	Symmetrical
KURTOSIS (*K*):	12.73	19.16	19.16	1.569	1.569	Very Leptokurtic

GRAIN SIZE DISTRIBUTION

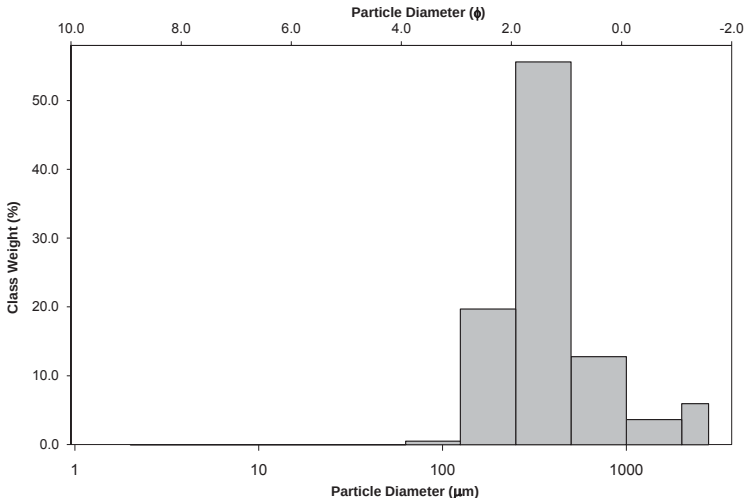

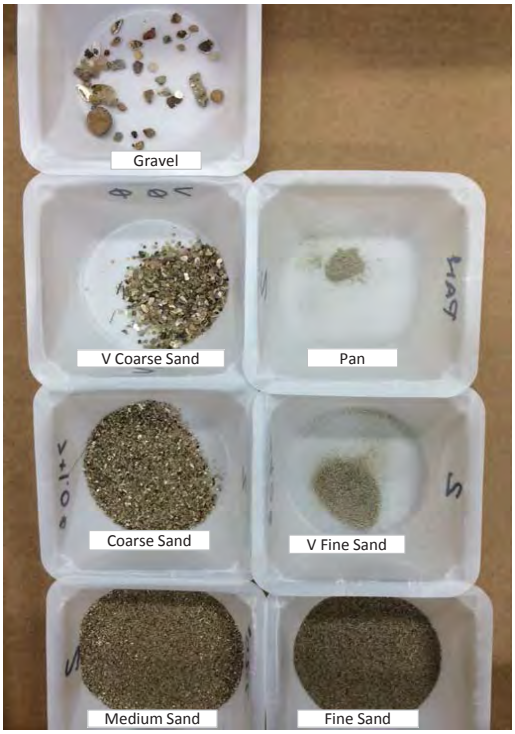

SAMPLE STATISTICS

SAMPLE IDENTITY: **DOT3, 3/13/2013**

SAMPLE TYPE: Trimodal, Very Poorly Sorted

SEDIMENT NAME: Gravelly Muddy Medium Sand

TEXTURAL GROUP: Gravelly Muddy Sand

	µm	f
MODE 1:	2400.0	-1.243
MODE 2:	375.0	1.500
MODE 3:	1.500	9.466
D_{10}:	46.42	-1.080
MEDIAN or D_{50}:	338.5	1.563
D_{90}:	2113.8	4.429
(D_{90} / D_{10}):	45.54	-4.102
(D_{90} - D_{10}):	2067.4	5.509
(D_{75} / D_{25}):	5.893	14.20
(D_{75} - D_{25}):	725.9	2.559

GRAIN SIZE DISTRIBUTION

GRAVEL:	12.0%	V COARSE SAND:	10.0%
SAND:	77.5%	COARSE SAND:	15.7%
MUD:	10.5%	MEDIUM SAND:	22.0%
		FINE SAND:	20.5%
		V FINE SAND:	9.4%
		SILT:	1.3%
		CLAY:	4.4%

	METHOD OF MOMENTS			FOLK & WARD METHOD		
	Arithmetic µm	Geometric µm	Logarithmic f	Geometric µm	Logarithmic f	Description
MEAN($\bar{x}$):	686.3	274.1	1.867	363.5	1.460	Medium Sand
SORTING (s):	755.2	5.669	2.503	5.647	2.497	Very Poorly Sorted
SKEWNESS (*Sk*):	1.331	-1.333	1.333	-0.173	0.173	Fine Skewed
KURTOSIS (*K*):	3.453	4.941	4.941	1.580	1.580	Very Leptokurtic

GRAIN SIZE DISTRIBUTION

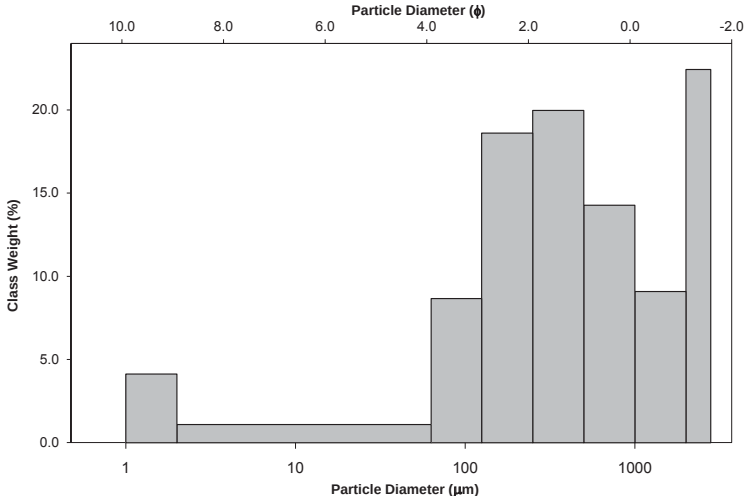

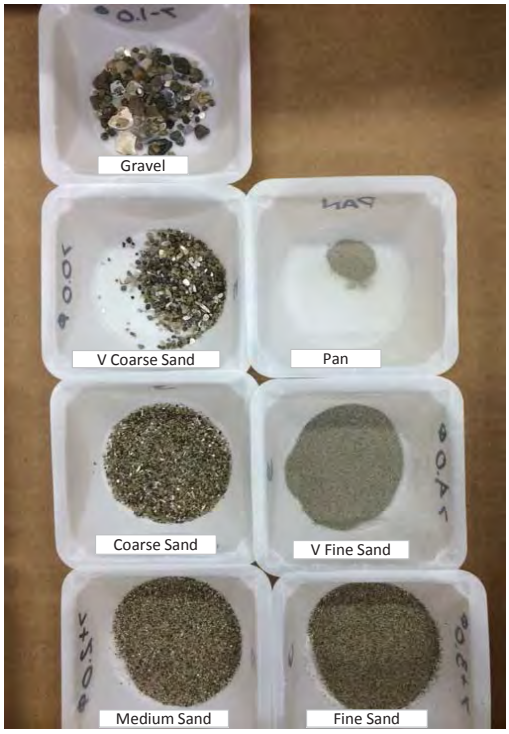

SAMPLE STATISTICS

SAMPLE IDENTITY: **DOT3, 8/7/2013**

SAMPLE TYPE: Bimodal, Very Poorly Sorted

TEXTURAL GROUP: Gravelly Sand

SEDIMENT NAME: Gravelly Medium Sand

	µm	f
MODE 1:	2400.0	-1.243
MODE 2:	375.0	1.500
MODE 3:		
D_{10}:	95.22	-1.067
MEDIAN or D_{50}:	415.4	1.268
D_{90}:	2094.6	3.393
(D_{90} / D_{10}):	22.00	-3.181
(D_{90} - D_{10}):	1999.4	4.459
(D_{75} / D_{25}):	4.757	19.06
(D_{75} - D_{25}):	724.4	2.250

GRAIN SIZE DISTRIBUTION

GRAVEL: 11.6%
SAND: 81.8%
MUD: 6.6%

V COARSE SAND: 10.8%
COARSE SAND: 21.3%
MEDIUM SAND: 23.7%
FINE SAND: 20.4%
V FINE SAND: 5.6%

SILT: 0.6%
CLAY: 3.5%

	METHOD OF MOMENTS			FOLK & WARD METHOD		
	Arithmetic µm	Geometric µm	Logarithmic f	Geometric µm	Logarithmic f	Description
MEAN($\bar{x}$):	732.8	352.7	1.503	446.2	1.164	Medium Sand
SORTING (s):	730.4	4.662	2.221	4.101	2.036	Very Poorly Sorted
SKEWNESS (*Sk*):	1.290	-1.703	1.703	-0.129	0.129	Fine Skewed
KURTOSIS (*K*):	3.449	6.968	6.968	1.424	1.424	Leptokurtic

GRAIN SIZE DISTRIBUTION

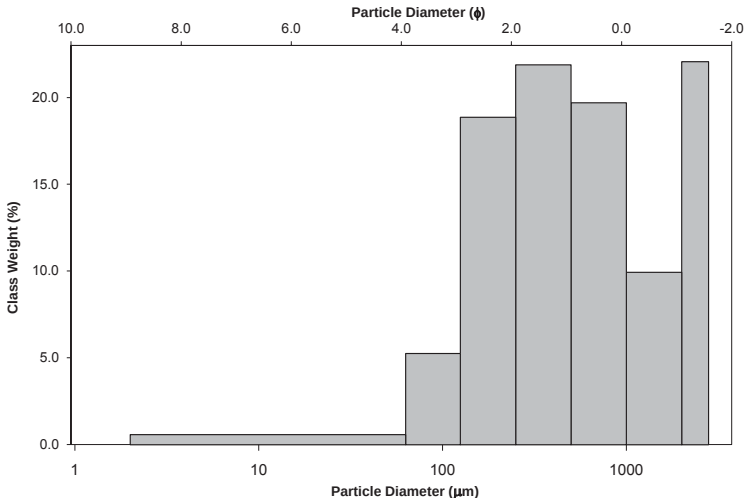

SAMPLE STATISTICS

SAMPLE IDENTITY: **DOT3, 11/21/2013**

SAMPLE TYPE: Bimodal, Poorly Sorted

SEDIMENT NAME: Gravelly Fine Sand

TEXTURAL GROUP: Gravelly Sand

	µm	f
MODE 1:	2400.0	-1.243
MODE 2:	187.5	2.500
MODE 3:		
D_{10}:	106.3	-1.174
MEDIAN or D_{50}:	427.6	1.226
D_{90}:	2256.0	3.233
(D_{90} / D_{10}):	21.22	-2.755
(D_{90} - D_{10}):	2149.7	4.407
(D_{75} / D_{25}):	5.913	-13.372
(D_{75} - D_{25}):	940.3	2.564

GRAIN SIZE DISTRIBUTION

GRAVEL:	15.6%	V COARSE SAND:	11.5%
SAND:	79.8%	COARSE SAND:	18.1%
MUD:	4.6%	MEDIUM SAND:	21.5%
		FINE SAND:	21.7%
		V FINE SAND:	7.0%
		V FINE SILT:	0.4%
		CLAY:	2.6%

	METHOD OF MOMENTS			FOLK & WARD METHOD		
	Arithmetic µm	Geometric µm	Logarithmic f	Geometric µm	Logarithmic f	Description
MEAN($\bar{x}$):	810.2	398.0	1.329	492.8	1.021	Medium Sand
SORTING (s):	799.4	4.314	2.109	3.338	1.739	Poorly Sorted
SKEWNESS (*Sk*):	1.065	-1.551	1.551	0.067	-0.067	Symmetrical
KURTOSIS (*K*):	2.689	7.076	7.076	0.842	0.842	Platykurtic

GRAIN SIZE DISTRIBUTION

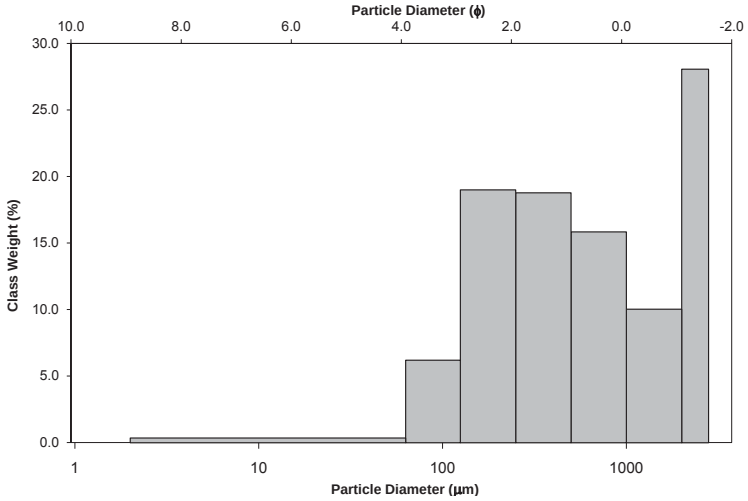

SAMPLE STATISTICS

SAMPLE IDENTITY: **DOT4, 3/13/2013**

SAMPLE TYPE: Unimodal, Moderately Well Sorted

TEXTURAL GROUP: Slightly Gravelly Sand

SEDIMENT NAME: Slightly Gravelly Fine Sand

	µm	f
MODE 1:	187.5	2.500
MODE 2:		
MODE 3:		
D_{10}:	133.6	1.349
MEDIAN or D_{50}:	199.7	2.324
D_{90}:	392.6	2.904
(D_{90} / D_{10}):	2.938	2.153
(D_{90} - D_{10}):	259.0	1.555
(D_{75} / D_{25}):	1.723	1.413
(D_{75} - D_{25}):	112.3	0.785

GRAIN SIZE DISTRIBUTION

GRAVEL:	0.1%	V COARSE SAND:	0.1%
SAND:	97.8%	COARSE SAND:	0.4%
MUD:	2.1%	MEDIUM SAND:	27.1%
		FINE SAND:	69.0%
		V FINE SAND:	1.2%
		SILT:	0.1%
		CLAY:	2.0%

	METHOD OF MOMENTS			FOLK & WARD METHOD		
	Arithmetic µm	Geometric µm	Logarithmic f	Geometric µm	Logarithmic f	Description
MEAN($\bar{x}$):	237.9	192.9	2.374	212.1	2.237	Fine Sand
SORTING (s):	117.6	2.205	1.141	1.501	0.586	Moderately Well Sorted
SKEWNESS (*Sk*):	6.012	-4.764	4.764	0.244	-0.244	Coarse Skewed
KURTOSIS (*K*):	98.27	30.71	30.71	0.946	0.946	Mesokurtic

GRAIN SIZE DISTRIBUTION

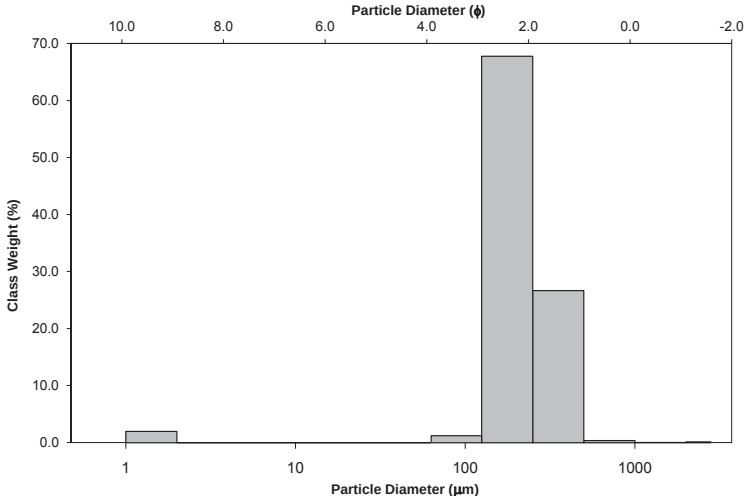

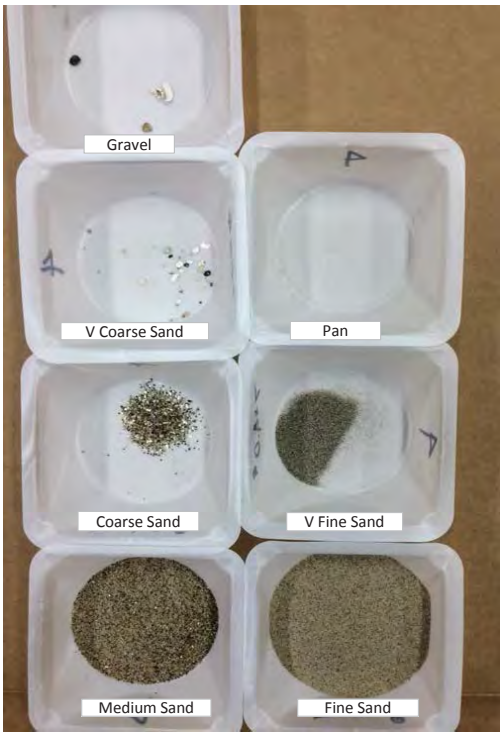

SAMPLE STATISTICS

SAMPLE IDENTITY: **DOT4, 8/7/2013**

SAMPLE TYPE: Unimodal, Well Sorted
SEDIMENT NAME: Slightly Gravelly Fine Sand

TEXTURAL GROUP: Slightly Gravelly Sand

	µm	f
MODE 1:	187.5	2.500
MODE 2:		
MODE 3:		
D_{10}:	128.2	2.045
MEDIAN or D_{50}:	176.3	2.504
D_{90}:	242.3	2.963
(D_{90} / D_{10}):	1.889	1.449
(D_{90} - D_{10}):	114.0	0.918
(D_{75} / D_{25}):	1.488	1.259
(D_{75} - D_{25}):	70.55	0.574

GRAIN SIZE DISTRIBUTION

GRAVEL:	0.1%	V COARSE SAND:	0.1%
SAND:	97.7%	COARSE SAND:	0.3%
MUD:	2.2%	MEDIUM SAND:	5.6%
		FINE SAND:	87.2%
		V FINE SAND:	4.5%
		SILT:	0.1%
		CLAY:	1.7%

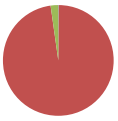

■ Gravel ■ Sand ■ Mud

	METHOD OF MOMENTS			FOLK & WARD METHOD		
	Arithmetic µm	Geometric µm	Logarithmic f	Geometric µm	Logarithmic f	Description
MEAN($\bar{x}$):	195.5	163.2	2.615	176.3	2.504	Fine Sand
SORTING (s):	108.8	2.021	1.015	1.351	0.434	Well Sorted
SKEWNESS (*Sk*):	12.44	-5.320	5.320	-0.059	0.059	Symmetrical
KURTOSIS (*K*):	226.3	36.76	36.76	1.127	1.127	Leptokurtic

GRAIN SIZE DISTRIBUTION

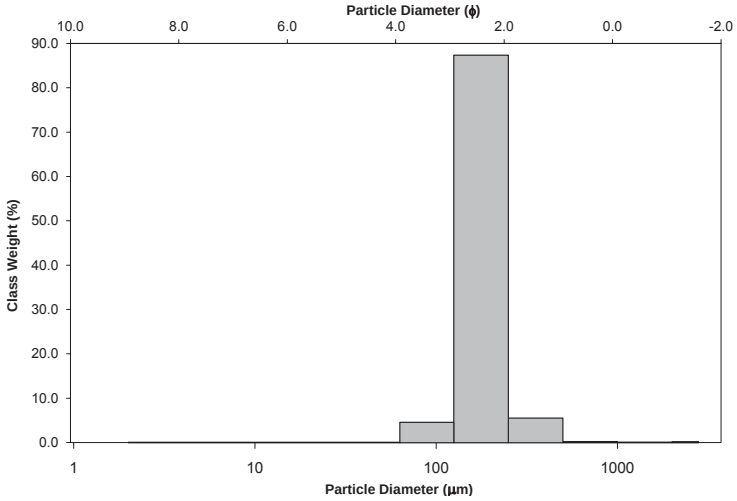

SAMPLE STATISTICS

SAMPLE IDENTITY: **DOT4, 11/21/2013**

SAMPLE TYPE: Unimodal, Well Sorted
SEDIMENT NAME: Well Sorted Fine Sand

TEXTURAL GROUP: Sand

	µm	f
MODE 1:	187.5	2.500
MODE 2:		
MODE 3:		
D_{10}:	132.1	2.022
MEDIAN or D_{50}:	180.4	2.471
D_{90}:	246.3	2.920
(D_{90} / D_{10}):	1.864	1.444
(D_{90} - D_{10}):	114.1	0.898
(D_{75} / D_{25}):	1.476	1.256
(D_{75} - D_{25}):	70.65	0.562

GRAIN SIZE DISTRIBUTION

GRAVEL: 0.0%
SAND: 98.2%
MUD: 1.8%

V COARSE SAND: 0.0%
COARSE SAND: 0.4%
MEDIUM SAND: 7.7%
FINE SAND: 89.0%
V FINE SAND: 1.1%

SILT: 0.1%
CLAY: 1.5%

	METHOD OF MOMENTS			FOLK & WARD METHOD		
	Arithmetic µm	Geometric µm	Logarithmic f	Geometric µm	Logarithmic f	Description
MEAN($\bar{x}$):	200.2	171.9	2.540	180.4	2.471	Fine Sand
SORTING (s):	71.43	1.905	0.930	1.319	0.399	Well Sorted
SKEWNESS (*Sk*):	5.058	-6.151	6.151	0.133	-0.133	Coarse Skewed
KURTOSIS (*K*):	65.82	46.51	46.51	1.004	1.004	Mesokurtic

GRAIN SIZE DISTRIBUTION

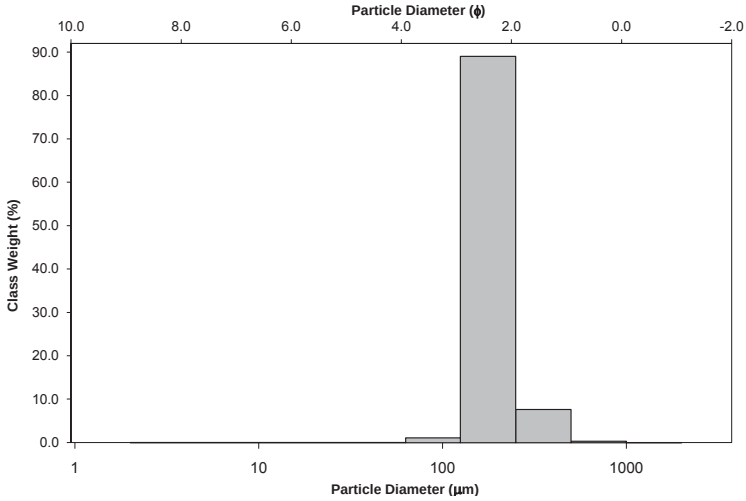

SAMPLE STATISTICS

SAMPLE IDENTITY: **DOT5, 3/13/2013**

SAMPLE TYPE: Unimodal, Moderately Sorted
SEDIMENT NAME: Slightly Gravelly Coarse Sand

TEXTURAL GROUP: Slightly Gravelly Sand

	µm	f
MODE 1:	750.0	0.500
MODE 2:		
MODE 3:		
D_{10}:	201.5	0.037
MEDIAN or D_{50}:	556.4	0.846
D_{90}:	974.7	2.311
(D_{90} / D_{10}):	4.836	62.39
(D_{90} - D_{10}):	773.1	2.274
(D_{75} / D_{25}):	2.397	4.706
(D_{75} - D_{25}):	460.3	1.261

GRAIN SIZE DISTRIBUTION

GRAVEL:	0.1%	V COARSE SAND:	8.0%
SAND:	98.0%	COARSE SAND:	49.5%
MUD:	1.9%	MEDIUM SAND:	28.9%
		FINE SAND:	11.2%
		V FINE SAND:	0.4%
		SILT:	0.1%
		CLAY:	1.7%

	METHOD OF MOMENTS			FOLK & WARD METHOD		
	Arithmetic µm	Geometric µm	Logarithmic f	Geometric µm	Logarithmic f	Description
MEAN($\bar{x}$):	624.4	464.7	1.106	509.6	0.972	Coarse Sand
SORTING (s):	348.1	2.616	1.387	1.887	0.916	Moderately Sorted
SKEWNESS (*Sk*):	1.025	-3.808	3.808	-0.215	0.215	Fine Skewed
KURTOSIS (*K*):	4.661	23.25	23.25	1.024	1.024	Mesokurtic

GRAIN SIZE DISTRIBUTION

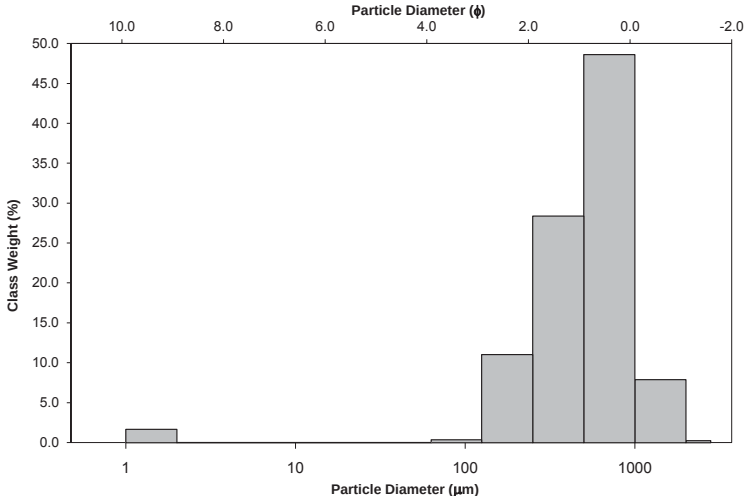

SAMPLE STATISTICS

SAMPLE IDENTITY: **DOT5, 8/7/2013**

SAMPLE TYPE: Unimodal, Moderately Sorted

TEXTURAL GROUP: Slightly Gravelly Sand

SEDIMENT NAME: Slightly Very Fine Gravelly Medium Sand

	µm	f
MODE 1:	375.0	1.500
MODE 2:		
MODE 3:		
D_{10}:	166.0	0.243
MEDIAN or D_{50}:	397.7	1.330
D_{90}:	845.3	2.591
(D_{90} / D_{10}):	5.093	10.68
(D_{90} - D_{10}):	679.3	2.348
(D_{75} / D_{25}):	2.309	2.751
(D_{75} - D_{25}):	351.6	1.207

GRAIN SIZE DISTRIBUTION

GRAVEL:	0.1%	V COARSE SAND:	1.8%
SAND:	97.3%	COARSE SAND:	33.6%
MUD:	2.6%	MEDIUM SAND:	44.1%
		FINE SAND:	17.7%
		V FINE SAND:	0.1%
		SILT:	0.2%
		CLAY:	1.4%

	METHOD OF MOMENTS			FOLK & WARD METHOD		
	Arithmetic µm	Geometric µm	Logarithmic f	Geometric µm	Logarithmic f	Description
MEAN($\bar{x}$):	479.4	358.7	1.479	396.5	1.334	Medium Sand
SORTING (s):	267.3	2.529	1.338	1.839	0.879	Moderately Sorted
SKEWNESS (*Sk*):	1.198	-3.526	3.526	-0.058	0.058	Symmetrical
KURTOSIS (*K*):	6.464	20.59	20.59	0.944	0.944	Mesokurtic

GRAIN SIZE DISTRIBUTION

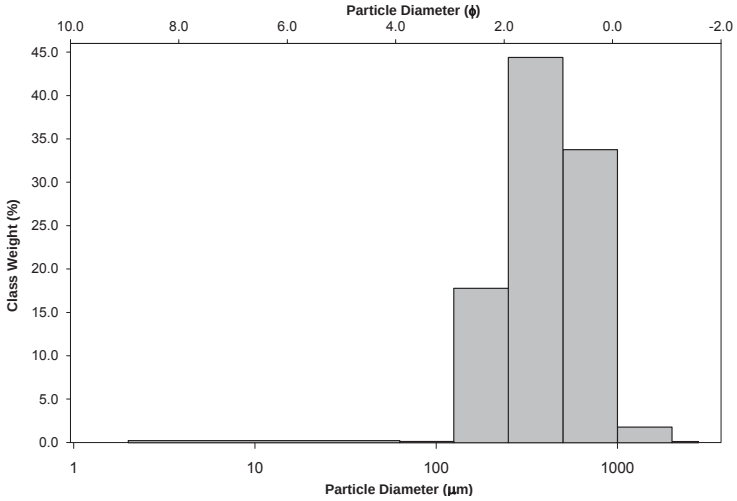

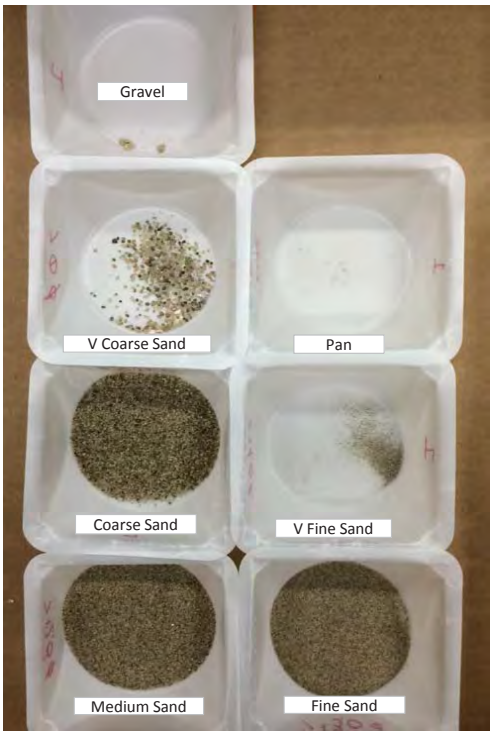

SAMPLE STATISTICS

SAMPLE IDENTITY: **DOT5, 11/21/2013**

SAMPLE TYPE: Unimodal, Moderately Sorted
SEDIMENT NAME: Slightly Gravelly Medium Sand

TEXTURAL GROUP: Slightly Gravelly Sand

	µm	f
MODE 1:	375.0	1.500
MODE 2:		
MODE 3:		
D_{10}:	158.5	0.288
MEDIAN or D_{50}:	370.3	1.433
D_{90}:	818.8	2.658
(D_{90} / D_{10}):	5.167	9.214
(D_{90} - D_{10}):	660.3	2.369
(D_{75} / D_{25}):	2.201	2.373
(D_{75} - D_{25}):	307.2	1.138

GRAIN SIZE DISTRIBUTION

GRAVEL: 0.0%
SAND: 97.5%
MUD: 2.5%

V COARSE SAND: 2.0%
COARSE SAND: 27.7%
MEDIUM SAND: 46.8%
FINE SAND: 20.5%
V FINE SAND: 0.5%

SILT: 0.1%
CLAY: 1.8%

	METHOD OF MOMENTS			FOLK & WARD METHOD		
	Arithmetic µm	Geometric µm	Logarithmic f	Geometric µm	Logarithmic f	Description
MEAN($\bar{x}$):	452.9	335.4	1.576	370.0	1.434	Medium Sand
SORTING (s):	264.6	2.604	1.381	1.851	0.888	Moderately Sorted
SKEWNESS (*Sk*):	1.384	-3.604	3.604	-0.027	0.027	Symmetrical
KURTOSIS (*K*):	6.574	20.98	20.98	1.006	1.006	Mesokurtic

GRAIN SIZE DISTRIBUTION

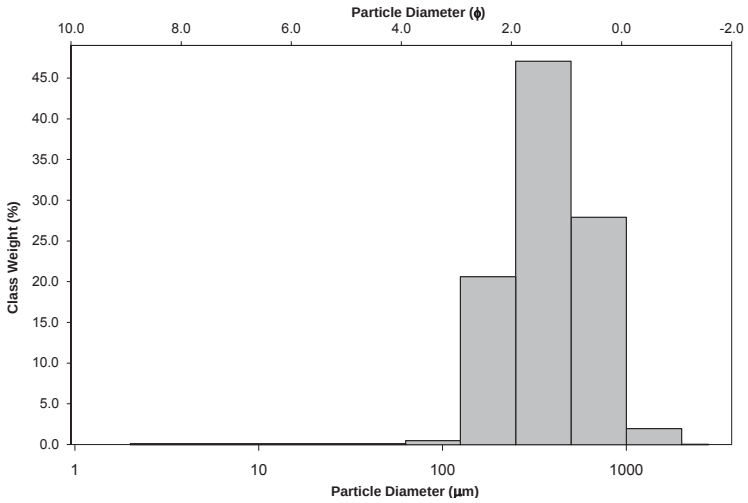

SAMPLE STATISTICS

SAMPLE IDENTITY: **DOT6, 3/13/2013**

SAMPLE TYPE: Bimodal, Very Poorly Sorted

TEXTURAL GROUP: Slightly Gravelly Muddy Sand

SEDIMENT NAME: Slightly Gravelly Muddy Fine Sand

	µm	f
MODE 1:	187.5	2.500
MODE 2:	1.500	9.466
MODE 3:		
D_{10}:	2.088	0.604
MEDIAN or D_{50}:	177.6	2.493
D_{90}:	657.7	8.904
(D_{90} / D_{10}):	315.0	14.73
(D_{90} - D_{10}):	655.6	8.299
(D_{75} / D_{25}):	2.719	1.797
(D_{75} - D_{25}):	180.2	1.443

GRAIN SIZE DISTRIBUTION

GRAVEL:	2.1%	V COARSE SAND:	3.4%
SAND:	79.3%	COARSE SAND:	7.5%
MUD:	18.7%	MEDIUM SAND:	14.8%
		FINE SAND:	45.0%
		V FINE SAND:	8.5%
		SILT:	2.0%
		CLAY:	9.6%

	METHOD OF MOMENTS			FOLK & WARD METHOD		
	Arithmetic µm	Geometric µm	Logarithmic f	Geometric µm	Logarithmic f	Description
MEAN($\bar{x}$):	307.7	113.0	3.146	119.1	3.070	Very Fine Sand
SORTING (s):	424.2	6.178	2.627	5.779	2.531	Very Poorly Sorted
SKEWNESS (*Sk*):	3.224	-1.250	1.250	-0.427	0.427	Very Fine Skewed
KURTOSIS (*K*):	14.43	3.928	3.928	2.724	2.724	Very Leptokurtic

GRAIN SIZE DISTRIBUTION

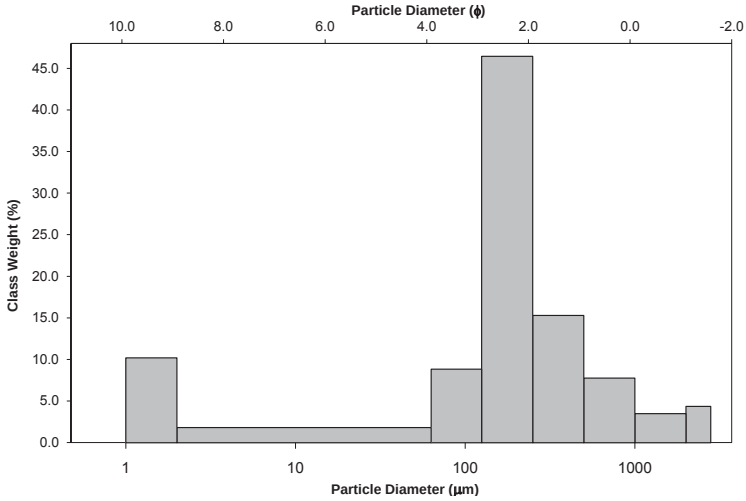

SAMPLE STATISTICS

SAMPLE IDENTITY: **DOT6, 8/7/2013**

SAMPLE TYPE: Bimodal, Very Poorly Sorted

SEDIMENT NAME: Slightly Gravelly Muddy Fine Sand

TEXTURAL GROUP: Slightly Gravelly Muddy Sand

	µm	f
MODE 1:	187.5	2.500
MODE 2:	2400.0	-1.243
MODE 3:		
D_{10}:	2.087	0.093
MEDIAN or D_{50}:	179.5	2.478
D_{90}:	937.9	8.905
(D_{90} / D_{10}):	449.4	96.21
(D_{90} - D_{10}):	935.8	8.812
(D_{75} / D_{25}):	4.109	2.333
(D_{75} - D_{25}):	262.1	2.039

GRAIN SIZE DISTRIBUTION

GRAVEL: 4.5%
SAND: 74.3%
MUD: 21.2%

V COARSE SAND: 4.8%
COARSE SAND: 8.2%
MEDIUM SAND: 14.3%
FINE SAND: 38.2%
V FINE SAND: 8.9%

SILT: 2.1%
CLAY: 10.7%

	METHOD OF MOMENTS			FOLK & WARD METHOD		
	Arithmetic µm	Geometric µm	Logarithmic f	Geometric µm	Logarithmic f	Description
MEAN($\bar{x}$):	377.6	113.7	3.136	104.8	3.254	Very Fine Sand
SORTING (s):	550.8	7.179	2.844	7.081	2.824	Very Poorly Sorted
SKEWNESS (*Sk*):	2.562	-0.998	0.998	-0.346	0.346	Very Fine Skewed
KURTOSIS (*K*):	9.045	3.306	3.306	1.879	1.879	Very Leptokurtic

GRAIN SIZE DISTRIBUTION

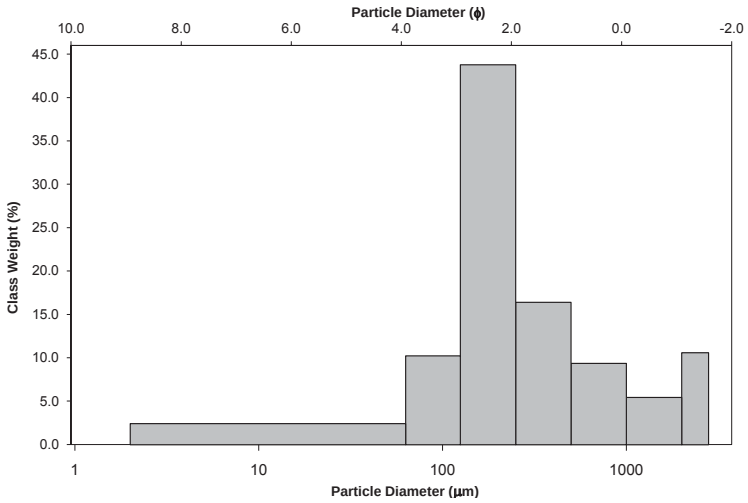

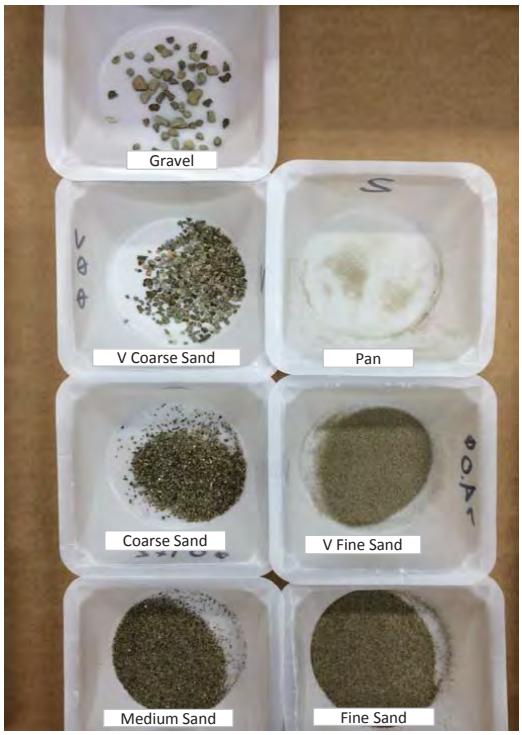

SAMPLE STATISTICS

SAMPLE IDENTITY: **DOT6, 11/21/2013**

SAMPLE TYPE: Unimodal, Poorly Sorted

TEXTURAL GROUP: Slightly Gravelly Muddy Sand

SEDIMENT NAME: Slightly Gravelly Muddy Fine Sand

	µm	f
MODE 1:	187.5	2.500
MODE 2:		
MODE 3:		
D_{10}:	18.94	0.437
MEDIAN or D_{50}:	222.3	2.170
D_{90}:	738.9	5.722
(D_{90} / D_{10}):	39.01	13.11
(D_{90} - D_{10}):	719.9	5.286
(D_{75} / D_{25}):	2.923	2.216
(D_{75} - D_{25}):	272.3	1.547

GRAIN SIZE DISTRIBUTION

GRAVEL:	0.3%	V COARSE SAND:	3.4%
SAND:	87.6%	COARSE SAND:	14.3%
MUD:	12.0%	MEDIUM SAND:	25.4%
		FINE SAND:	38.4%
		V FINE SAND:	6.1%
		SILT:	1.1%
		CLAY:	6.2%

	METHOD OF MOMENTS			FOLK & WARD METHOD		
	Arithmetic µm	Geometric µm	Logarithmic f	Geometric µm	Logarithmic f	Description
MEAN($\bar{x}$):	341.8	168.4	2.570	229.7	2.122	Fine Sand
SORTING (s):	331.8	4.850	2.278	3.831	1.938	Poorly Sorted
SKEWNESS (*Sk*):	2.364	-1.803	1.803	-0.232	0.232	Fine Skewed
KURTOSIS (*K*):	10.67	6.034	6.034	2.301	2.301	Very Leptokurtic

GRAIN SIZE DISTRIBUTION

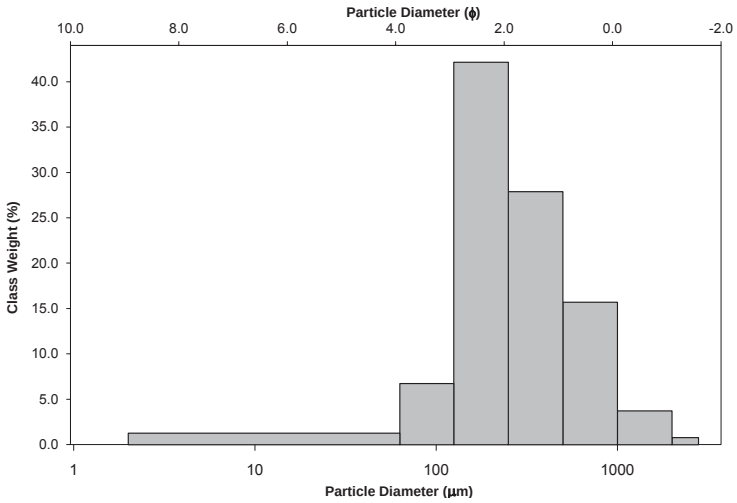

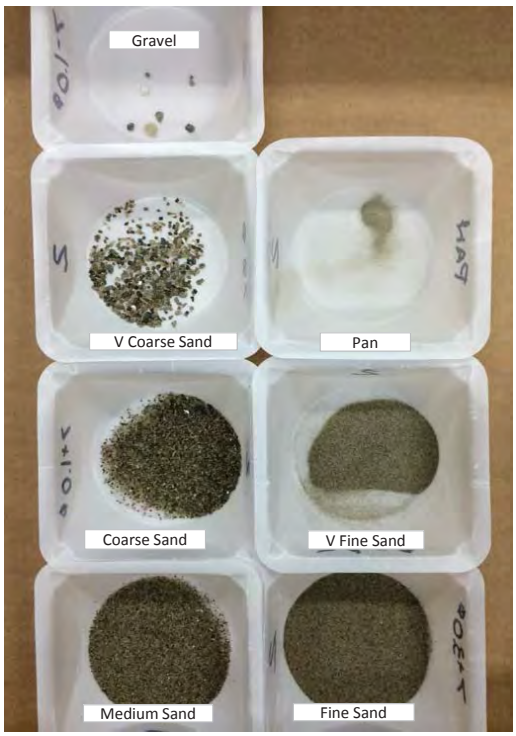

SAMPLE STATISTICS

SAMPLE IDENTITY: **DOT7, 3/13/2013**

SAMPLE TYPE: Unimodal, Poorly Sorted
SEDIMENT NAME: Slightly Gravelly Coarse Sand

TEXTURAL GROUP: Slightly Gravelly Sand

	µm	f
MODE 1:	750.0	0.500
MODE 2:		
MODE 3:		
D_{10}:	226.3	-0.331
MEDIAN or D_{50}:	521.1	0.940
D_{90}:	1258.3	2.144
(D_{90} / D_{10}):	5.561	-6.468
(D_{90} - D_{10}):	1032.0	2.475
(D_{75} / D_{25}):	2.497	5.430
(D_{75} - D_{25}):	487.6	1.320

GRAIN SIZE DISTRIBUTION

GRAVEL:	3.1%	V COARSE SAND:	10.3%
SAND:	93.3%	COARSE SAND:	38.9%
MUD:	3.6%	MEDIUM SAND:	36.7%
		FINE SAND:	6.9%
		V FINE SAND:	0.5%
		SILT:	0.3%
		CLAY:	2.5%

	METHOD OF MOMENTS			FOLK & WARD METHOD		
	Arithmetic µm	Geometric µm	Logarithmic f	Geometric µm	Logarithmic f	Description
MEAN($\bar{x}$):	672.5	449.1	1.155	515.2	0.957	Coarse Sand
SORTING (s):	482.0	3.251	1.701	2.012	1.008	Poorly Sorted
SKEWNESS (*Sk*):	1.705	-3.161	3.161	-0.037	0.037	Symmetrical
KURTOSIS (*K*):	6.325	15.91	15.91	1.146	1.146	Leptokurtic

GRAIN SIZE DISTRIBUTION

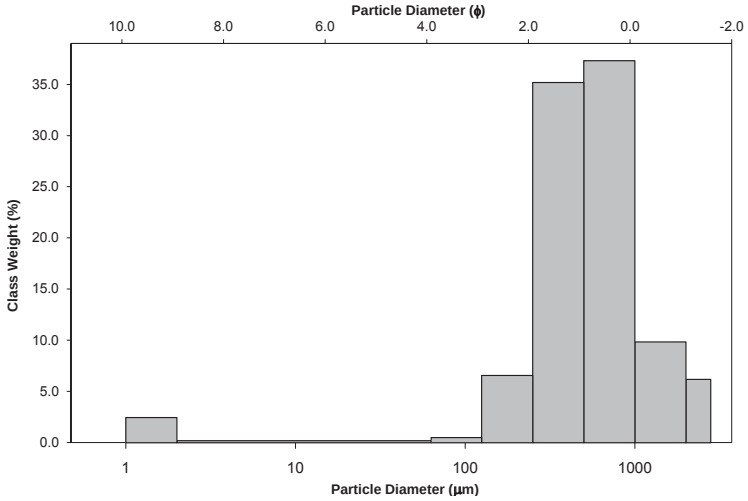

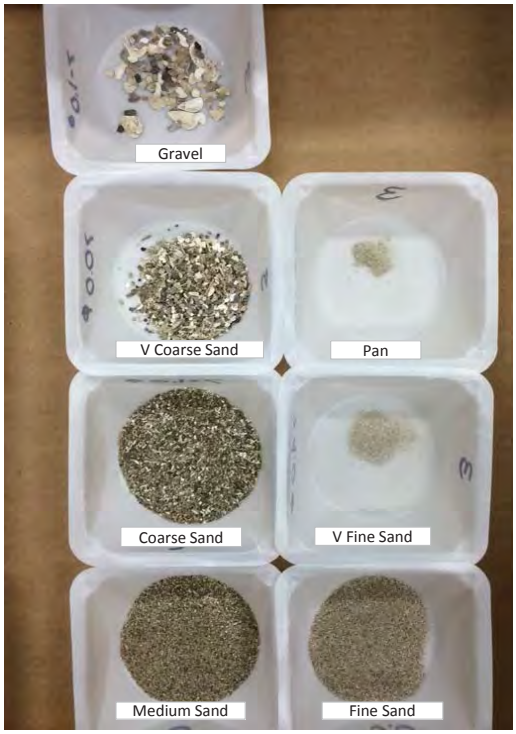

SAMPLE STATISTICS

SAMPLE IDENTITY: **DOT7, 8/7/2013**

SAMPLE TYPE: Unimodal, Poorly Sorted

TEXTURAL GROUP: Slightly Gravelly Sand

SEDIMENT NAME: Slightly Gravelly Medium Sand

	µm	f
MODE 1:	375.0	1.500
MODE 2:		
MODE 3:		
D_{10}:	139.2	0.413
MEDIAN or D_{50}:	345.8	1.532
D_{90}:	751.2	2.845
(D_{90} / D_{10}):	5.398	6.894
(D_{90} - D_{10}):	612.0	2.432
(D_{75} / D_{25}):	1.831	1.796
(D_{75} - D_{25}):	212.3	0.872

GRAIN SIZE DISTRIBUTION

GRAVEL:	0.8%	V COARSE SAND:	2.6%
SAND:	93.6%	COARSE SAND:	16.2%
MUD:	5.6%	MEDIUM SAND:	57.3%
		FINE SAND:	15.6%
		V FINE SAND:	2.0%
		SILT:	0.4%
		CLAY:	3.5%

	METHOD OF MOMENTS			FOLK & WARD METHOD		
	Arithmetic µm	Geometric µm	Logarithmic f	Geometric µm	Logarithmic f	Description
MEAN($\bar{x}$):	424.7	278.5	1.844	331.8	1.592	Medium Sand
SORTING (s):	312.9	3.436	1.781	2.330	1.220	Poorly Sorted
SKEWNESS (*Sk*):	2.889	-2.957	2.957	-0.283	0.283	Fine Skewed
KURTOSIS (*K*):	15.93	12.89	12.89	2.483	2.483	Very Leptokurtic

GRAIN SIZE DISTRIBUTION

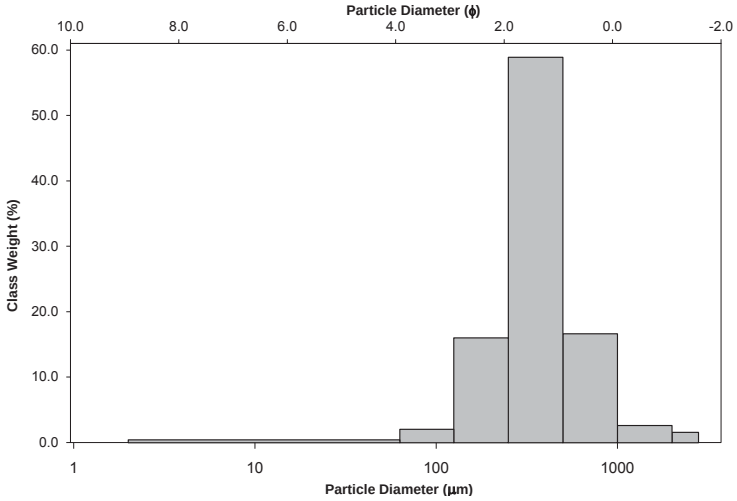

SAMPLE STATISTICS

SAMPLE IDENTITY: **DOT7, 11/21/2013**

SAMPLE TYPE: Bimodal, Very Poorly Sorted

SEDIMENT NAME: Gravelly Muddy Fine Sand

TEXTURAL GROUP: Gravelly Muddy Sand

	µm	f
MODE 1:	187.5	2.500
MODE 2:	2400.0	-1.243
MODE 3:		
D_{10}:	57.16	-0.166
MEDIAN or D_{50}:	233.1	2.101
D_{90}:	1121.8	4.129
(D_{90} / D_{10}):	19.63	-24.901
(D_{90} - D_{10}):	1064.6	4.295
(D_{75} / D_{25}):	2.784	2.156
(D_{75} - D_{25}):	264.3	1.477

GRAIN SIZE DISTRIBUTION

GRAVEL:	7.2%	V COARSE SAND:	3.4%
SAND:	82.7%	COARSE SAND:	6.3%
MUD:	10.1%	MEDIUM SAND:	29.3%
		FINE SAND:	38.2%
		V FINE SAND:	5.5%
		SILT:	0.8%
		CLAY:	6.1%

	METHOD OF MOMENTS			FOLK & WARD METHOD		
	Arithmetic µm	Geometric µm	Logarithmic f	Geometric µm	Logarithmic f	Description
MEAN($\bar{x}$):	458.4	196.0	2.351	252.8	1.984	Medium Sand
SORTING (s):	608.3	5.082	2.345	4.106	2.038	Very Poorly Sorted
SKEWNESS (*Sk*):	2.424	-1.578	1.578	-0.091	0.091	Symmetrical
KURTOSIS (*K*):	7.793	6.111	6.111	2.758	2.758	Very Leptokurtic

GRAIN SIZE DISTRIBUTION

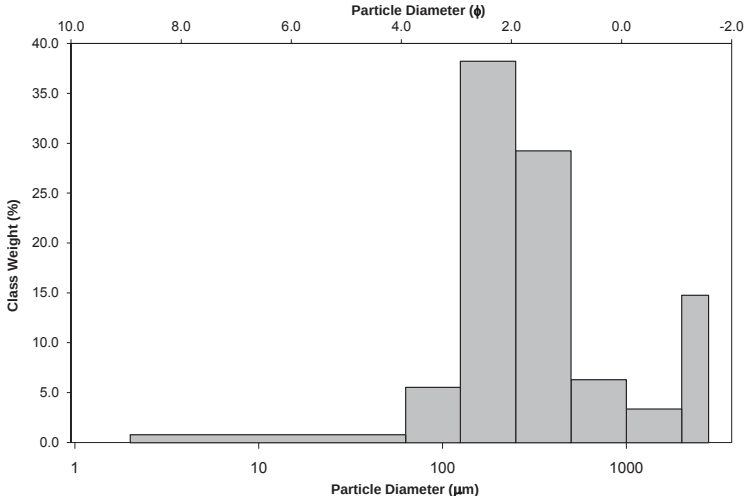

[This page intentionally left blank.]

Supplemental Environmental Impact Statement for the Designation of Dredged Material Disposal Sites in Eastern Long Island Sound, Connecticut and New York

Appendix C-2

Physical Oceanography of Eastern Long Island Sound Region: Modeling

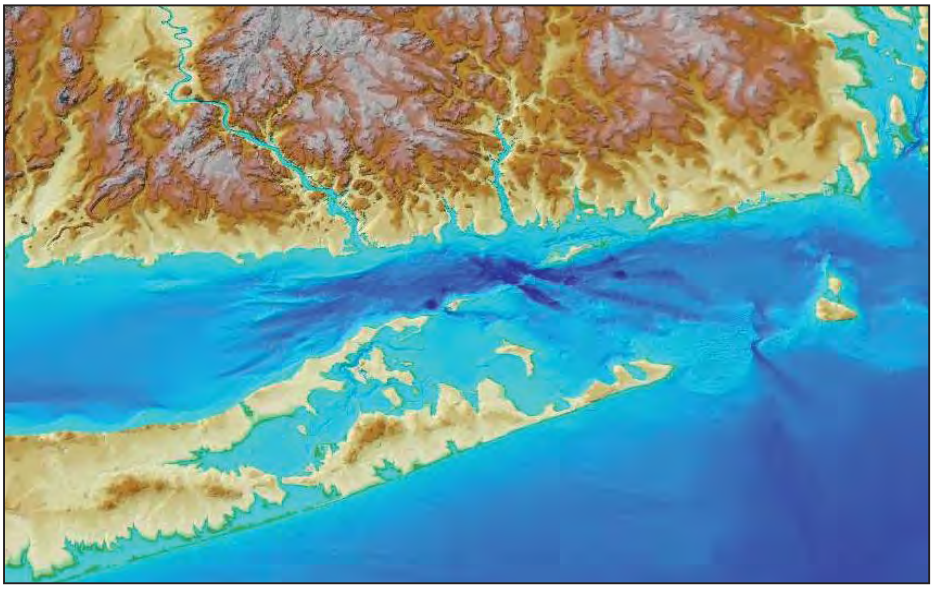

Prepared for: **United States Environmental Protection Agency**

Sponsored by: **Connecticut Department of Transportation**

Prepared by: **University of Connecticut**

with support from

Louis Berger

December 2015

Supplemental Environmental Impact Statement for the Designation of Dredged Material Disposal Site(s) in Eastern Long Island Sound, Connecticut and New York

---

PHYSICAL OCEANOGRAPHY OF EASTERN LONG ISLAND SOUND REGION: MODELING

Prepared for:

United States Environmental Protection Agency
5 Post Office Square, Suite 100
Boston, MA 02109

Sponsored by:

Connecticut Department of Transportation
Waterways Administration
2800 Berlin Turnpike
Newington, CT 06131-7546

Prepared by:

James O'Donnell, Grant McCardell, Todd Fake, Alejandro Cifuentes-Lorenzen, and Rachel Horwitz

University of Connecticut
Department of Marine Sciences
1080 Shennecossett Road
Groton, CT 06340

with support from

Louis Berger
117 Kendrick Street
Needham, MA 02494

December 2015

Table of Contents

Page

Executive Summary ix

1. Introduction 1
   1.1 Objective and Background 1
   1.2 Study Overview 3

2. The Model 8
   2.1 Initial Conditions 11
   2.2 Boundary Conditions 11
   2.3 Heat Fluxes 14
   2.4 Freshwater Fluxes 16
   2.5 Wind Stress Forcing 17
   2.6 Bottom Stress Calculation in FVCOM 18
   2.7 Bottom Stress Estimates from Current Measurements 19
   2.8 The Model – Summary 24

3. Simulations for the Zone of Siting Feasibility 25
   3.1 Tidal Currents and Bottom Stress 25
   3.2 Evolution of Salinity, Temperature, and Density 38
   3.3 Waves 39
   3.4 Model Performance – Summary 40

4. Bottom Stress Distributions and Variability 41
   4.1 Bottom Stress during Fair-weather Conditions 41
   4.2 Bottom Stress during Storm Conditions 47
   4.3 Superstorm Sandy 52

5. Sediment Resuspension and Bottom Stress 54

6. Bottom Stress Screening 60

7. Summary and Discussion 63

References 64

Appendices

Appendix 1: Comparison of model-predicted sea level to sea level measured by RDI ADCPs
Appendix 2: Comparison of model-predicted vertically averaged current and that measured by RDI ADCPs in the field
Appendix 3: Comparison of model-predicted bottom stress and the measured stress using the bulk formula
Appendix 4: Comparison of model-predicted salinity, temperature and pressure with near-bottom temperature, salinity, and density measurements in the field

List of Tables

Table 1 Seasonal observation periods (referred to as 'Campaigns')

Table 2 Key terms used in the field program of the PO study

Table 3 Comparison of model-predicted mean and maximum stresses for each campaign to the mean and maximum from the covariance and log profile methods

Table 4 Model predicted maximum bottom stress during fair-weather conditions (i.e., due to tides and seasonal mean flow only) at potential dredged material disposal sites

Table 5 Model predicted maximum bottom stress during storm conditions at potential dredged material disposal sites

Table 6 Model predicted Maximum bottom stress at potential disposal sites during a simulated Superstorm Sandy

Table 7 Particle size and critical stress for cohesive and non-cohesive sediments

Table 8 Comparison of maximum bottom stress for potential dredged material disposal sites in the simulations of the three observation campaigns and Superstorm Sandy

List of Figures

Figure 1 Eastern Long Island Sound and Block Island Sound showing the Zone of Siting Feasibility (ZSF) and eleven initially screened sites

Figure 2 Survey stations of the physical oceanography study, "metocean" buoy locations, and CTDEEP survey stations

Figure 3 (a) Map of southern New England shore showing the model grid
(b) Bathymetry of the LIS model subdomain with the locations of freshwater sources

Figure 4 Locations of the CTDEEP water quality survey program CTD stations used in the initialization of the numerical model of the circulation and hydrography in the ZSF

Figure 5 Comparison of tidal heights at the NOAA Bridgeport tidal height gauge compared to those predicted by the FVCOM model after iteratively calibrating the model using the 2010 NOAA data

Figure 6 Comparison of tidal heights in the ZSF at Station DOT3 during Campaign 2 measured by ADCP pressure sensor compared to those predicted by the FVCOM model

Figure 7 ADCP deployment compared to those predicted by the FVCOM model for depth-averaged currents at Station DOT3, Campaign 2

Figure 8 Comparison of bottom temperatures in the FVCOM model with those measured by the ADCP temperature sensors

Figure 9 2012-2013 salinity at station ARTG/ E1 for the near surface and near-bottom

Figure 10 (a) An example comparison of the bulk formula ($|\boldsymbol{\tau_{BF}}|$) and log profile stress magnitude measurements
(b) ($|\boldsymbol{\tau_{CV}}|$) and log profile $|\boldsymbol{\tau_{BF}}|$ stress magnitude measurements for a 30-day period at Station DOT1 during Campaign 1

Figure 11 Summary of the stress magnitude measurements

Figure 12 M2 ellipses for depth-average velocities from RDI ADCP measurements from Campaigns 1, 2, and 3 and FVCOM model at all seven DOT stations

Figure 13 M2 ellipses for bottom stress, calculated from bin 3 of the Nortek ADCP velocity measurements during Campaigns 1, 2, and 3, and from the FVCOM velocity at the bottom level

Figure 14 Model-predicted bottom stress at Station DOT3 during Campaign 2 in the summer of 2013

Figure 15 (a) Comparison of model predicted bottom stress magnitudes and mean bottom stress observed during the three campaigns
(b) Comparison of the predicted and observed maximum stress magnitudes

Figure 16 Mean (April-September, 2010) circulation near the surface in the ZSF from FVCOM and from ADCPs deployed by NOAA.

Figure 17 Time mean of the FVCOM simulated bottom currents during Campaign 1

Figure 18 Time mean of the FVCOM simulated bottom currents during Campaign 2

Figure 19 Time mean of the FVCOM simulated bottom currents during Campaign 3

Figure 20 Time mean of the FVCOM simulated surface currents during Campaign 1

Figure 21 Time mean of the FVCOM simulated surface currents during Campaign 2

Figure 22 Time mean of the FVCOM simulated surface currents during Campaign 3

Figure 23 Comparison of near-bottom salinity, temperature, and density at Station DOT2 predicted by the FVCOM model with those measured by the bottom-mounted CTD

Figure 24 Contemporaneous comparison of salinity, temperature, and density profiles at Station DOT1 predicted by the FVCOM model with those measured by a CTD cast from the *R/V Connecticut* during Cruise 5 on August 7, 2013

Figure 25 Comparison of model and observed significant wave height at Stations DOT1 and DOT4 during May 2013

Figure 26 Bathymetry of the ZSF showing the 11 potential dredged material disposal sites as identified during the initial screening process

Figure 27 Maximum bottom stress during Campaign 1 (March 12 to May 17, 2013) for fair-weather

Figure 28 Maximum bottom stress during Campaign 2 (June 11 to August 8, 2013) for fair-weather conditions

Figure 29 Maximum bottom stress during Campaign 3 (November 20, 2013, to January 16, 2014) for fair-weather conditions

Figure 30 Maximum bottom stress during Campaign 1 (March 12 to May 17, 2013) for storm

Figure 31 Maximum bottom stress during Campaign 2 (June 11 to August 8, 2013) for storm

Figure 32 Maximum bottom stress during Campaign 3 (November 20, 2013, to January 16, 2014) for storm

Figure 33 Maximum bottom stress simulated for the period October 28 to 31, 2012 when Superstorm Sandy passed over New England

Figure 34 A graphical representation of the relationship between sediment particle size for cohesive and non-cohesive particles

Figure 35 Areas with maximum bottom stress exceeding the 0.75 Pa threshold during the simulation of Superstorm Sandy

Acronyms and Abbreviations

ADCP	Acoustic Doppler Current Profiler
BIS	Block Island Sound
C.F.R.	Code of Federal Regulations
CLDS	Central Long Island Sound Disposal Site (formerly abbreviated as CLIS in the literature)
cm	Centimeter
cm/s	centimeter per second
CSDS	Cornfield Shoals Disposal Site
CTD	Conductivity/temperature/depth sensor
CTDEEP	Connecticut Department of Energy and Environmental Protection
CTDOT	Connecticut Department of Transportation
EIS	Environmental Impact Statement
ELIS	Eastern Long Island Sound
FVCOM	Finite Volume Coastal Ocean Model (The model, nested within the University of Massachusetts-Dartmouth Regional Model, was used as the primary model for assessing the bottom stress, salinity, temperature, currents, waves, and horizontal circulation based on the data collected during the Physical Oceanographic study. The model is not commercially available.)
LIS	Long Island Sound
LISICOS	Long Island Sound Integrated Coastal Observing System
LTFATE	Long Term FATE (USACE model that simulates the evolution of dredged material mounds by erosion and bed load transport. It will be used later for additional modeling.)
m	meter
m/s	meter per second
m^3/s	cubic meter per second
MPRSA	Marine Protection Research and Sanctuaries Act
NBDS	Niantic Bay Disposal Site
NEPA	National Environmental Policy Act

NLDS	New London Disposal Site
N/m^2	Newton/meter squared
NOAA	National Oceanic and Atmospheric Administration
Nortek ADCP	Downward-looking Nortek Aquadopp HR 2-Hertz ADCP
Pa	Pascal
PO	Physical oceanography
Profiling CTD	Sea-Bird Electronics Model 9 CTD with a Model 11 deck unit
RDI	RD Instruments (now operating as Teledyne RDI).
RDI ADCP	Upward-looking Sentinel Workhorse ADCP from Teledyne RD Instruments
RISDS	Rhode Island Sound Disposal Site
SBE SMP37	Sea-Bird Electronics Model SMP37 instrument
SEIS	Supplemental Environmental Impact Statement
STFATE	Short-Term FATE (USACE model simulating water column concentration of dredged material and any associated chemical contaminants when the material is released from a barge.)
SWAVE	Surface wave numerical model by Qi et al. (2009).
TOGA/COARE	Tropical Ocean Global Atmosphere program/ Coupled Ocean Atmosphere Research Experiment
UConn	University of Connecticut
USACE	U.S. Army Corps of Engineers
USEPA	U.S. Environmental Protection Agency
USGS	U.S. Geological Survey
WLDS	Western Long Island Sound Disposal Site (formerly abbreviated as WLIS in the literature)
ZSF	Zone of Siting Feasibility (Area established by the USEPA for the potential designation of one or more dredged material disposal sites.)

[This page intentionally left blank.]

EXECUTIVE SUMMARY

This report addresses the modeling component of the study of the physical oceanography (PO) in eastern Long Island Sound (ELIS) and Block Island Sound (BIS) in support of the Eastern Long Island Sound Supplemental Environmental Impact Statement (SEIS). The PO study area is referred to as the Zone of Siting Feasibility (ZSF). The SEIS is being prepared by the U.S. Environmental Protection Agency (USEPA) in support of the potential designation of one or more dredged material disposal sites in the ZSF. This report assessed the water circulation patterns and the stability of the seafloor sediments (measured as 'bottom stress') during different conditions (including worst-case storm conditions), based on data collected in the field during different seasons in 2013 and 2014. Eleven sites were identified during the initial screening of the ZSF for investigation as potential dredged material disposal sites. During the preparation of the SEIS, three sites were assessed in more detail.

The pattern of circulation and the magnitude of the bottom stress at potential dredged material disposal sites allows for determining the path of sediment particles in the water column during disposal operations and for predicting the stability of dredged sediment mounds at the seafloor. The circulation model FVCOM and its associated wave model SWAVE were used to model currents and bottom stresses by interpolating field data collected in the ZSF. Model results reproduced the observed near-bottom currents and bottom stress well; the correlation between the simulated and measured values for the seasonal mean and maximum bottom stresses are 0.91 and 0.72, respectively. The p-value for these correlations is less than 10^{-6} and the model is considered sufficiently accurate to be used for the comparison of the maximum bottom stress to be expected at potential dredged material disposal sites in the ZSF and for the simulation of the character of the circulation at sites chosen, in consultation with the project team, for more detailed evaluation in the SEIS.

The simulated distribution of the magnitude of the bottom stress is similar in different studied seasons (spring, summer, winter) suggesting that the effect of seasonal circulation patterns control the average stress magnitudes. However, maximum bottom stresses generally occur during storms. The strongest winds during the observation campaign occurred during tropical Storm Andrea, June, 2013. To characterize worst-case conditions, the period of Superstorm Sandy on October 28-31, 2012 was also simulated. This storm created the largest waves and highest storm surge on record. During storms, the maximum bottom stresses were typically larger in the shallow waters of nearshore locations; in deeper water, increases in bottom stresses were less substantial since the effects of winds and waves were less significant.

After reviewing the available literature on the critical erosion stress for estuarine sediments, we selected the threshold for resuspension of typical dredged material (median particle size in the range 0.06 to 0.13 mm) (i.e., fine sand mixed with silt/clay) as 0.75 Pa (Pascal; also expressed as Newton/m^2). This threshold was then used to evaluate the maximum bottom stress during fair-weather and storm conditions (including conditions during Superstorm Sandy) at the 11 sites that have been initially screened for further investigation as potential disposal sites. Sites within the ZSF with maximum stress values below this threshold value consisted of Site 6 (location of the active New London Disposal Site [NLDS]; the site is currently used for dredged material disposal;), Site 11 (located north of Montauk), Sites 8 and 9 (located southeast of Fishers Island),

Site 10 (location of Block Island Disposal Site that was historically used for dredged material disposal), and Site 4 (located near Orient Point). However, Site 4 included areas of high stress along its perimeter and is therefore not recommended as a site that contains disposed sediment.

1. Introduction

1.1 Objective and Background

The USEPA has the authority to designate dredged material disposal sites for the management of dredged material under Section 102(c) of the Act and 40 C.F.R. Part 228.4 of its regulations. In accordance with Section 102(c) of the Marine Protection Research and Sanctuaries Act (MPRSA; also referred to as Ocean Dumping Act [ODA]) of 1972 and the National Environmental Policy Act (NEPA, 1970), a Supplementary Environmental Impact Assessment (SEIS) is in preparation as part of the decision-making process. This SEIS and supporting documentation evaluates the area defined as the Zone of Siting Feasibility (ZSF). This area is shown in Figure 1. The ZSF contains two active dredged material disposal sites that are currently used for dredged material disposal: the New London Disposal Site (NLDS) and the Cornfield Shoals Disposal Site (CSDS). In addition, the ZSF contains several historically used disposal sites. The two active disposal sites and the historically used Niantic Bay Disposal Site (NBDS) were identified during site screening as alternatives sites for more detailed analysis in the SEIS.

This report describes the second element of a three-part study of the Physical Oceanography (PO) of the Eastern Long Island Sound (ELIS) that was commissioned to inform the development of the SEIS. Two additional reports have been completed. The first report describes the results of a field observation program (O'Donnell et al., 2014a; provided as SEIS Appendix C-1) conducted to test the effectiveness of the numerical model (FVCOM) described here in the simulation of the circulation and bottom shear stress in the study area during normal weather conditions and during severe (worst case) storm events. The third (O'Donnell et al., 2015; provided as SEIS Appendix C-3) describes the use of three models (STFATE, LTFATE and FVCOM) to assess the potential impact of disposal operations, and the stability of sediment mounds. This PO study supplements work conducted in the region as part of the Environmental Impact Statement (EIS) for the designation of the Central and Western Long Island Sound Disposal Sites (CLDS and WLDS) (USEPA and USACE, 2004a).

This report describes the water circulations patterns and the stability of the seafloor sediments (measured as 'bottom stress') during different conditions (including worst-case storm conditions), based on data collected in the spring and summer of 2013, and winter of 2014. The PO study area is shown in Figure 1, and is referred to as the ZSF. Initial screening during the SEIS process identified (a) areas not suitable for locating dredged material disposal sites due to various constraints (gray zone in Figure 1), and (b) 11 sites for further investigation as potential disposal sites. These 11 sites include two active and five historically used disposal sites, and six 'new' sites not known to have received dredged material in the past (see also SEIS Appendix B, Alternatives Analysis).

PO modeling results were applied to 11 sites which had been identified during the initial screening of the ZSF as sites for further investigation. In addition, modeling results have been applied during the preparation of the SEIS where three sites are assessed in more detail. The PO study supplements work previously conducted in the region as part of the Long Island Sound Environmental Impact Statement (EIS) for the CLDS and WLDS (USEPA and USACE, 2004).

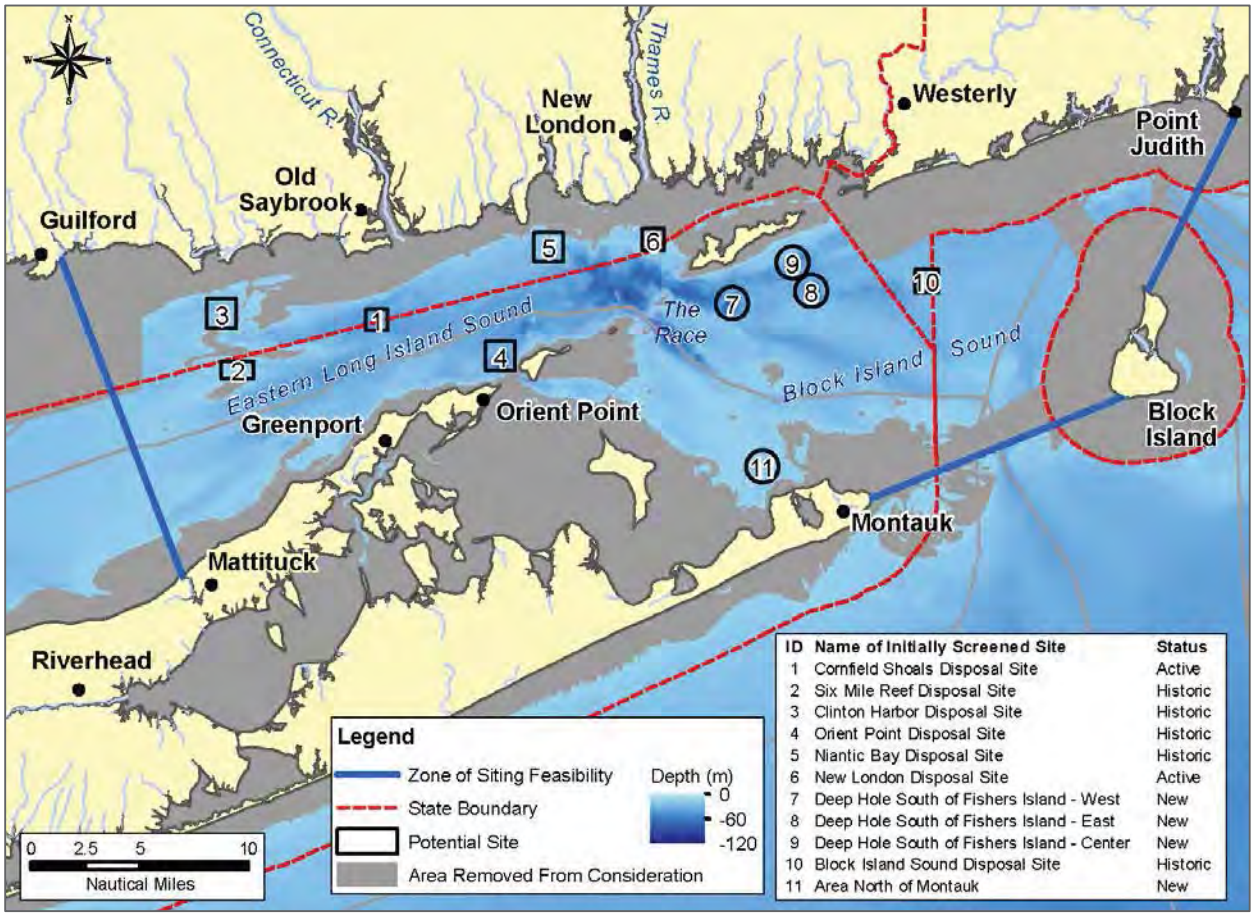

Figure 1. Eastern Long Island Sound and Block Island Sound showing the Zone of Siting Feasibility (ZSF) and eleven initially screened sites.

The ZSF has the following boundaries:

- *West:* Mulberry Point near Guilford, Connecticut, to Mattituck Point, New York. The boundary roughly coincides with the Mattituck Sill.
- *South:* Montauk, New York, to Block Island, Rhode Island. The boundary represents a reasonable haul distance for small marinas and boatyards from some of the main dredging centers.
- *East:* Block Island to Point Judith, Rhode Island. The eastern boundary coincides with the eastern boundary of the study area for the Long Island Sound Dredged Material Management Plan (LIS DMMP; for details see USACE, 2015).

The ZSF contains the active (but not designated) New London and Cornfield Shoals Disposal Sites (NLDS and CSDS), as well as five historic disposal sites. The closest active designated dredged material disposal site outside of the ZSF is the Rhode Island Sound Disposal Site (RISDS). This site, as well as the Central and Western Long Island Sound dredged material disposal sites (CLDS and WLDS), have been designated by the USEPA for long-term use, pursuant to MPRSA

1.2 Study Overview

The ZSF has complex bathymetry sculpted by a combination of tectonic activity and several cycles of glacial erosion (Lewis, 2014). The water in the ZSF is in constant motion as a consequence of tidal forcing by the adjacent shelf waters, wind, and the density gradients created by freshwater delivered by rivers and the uneven distributions of surface heating and vertical mixing. The dominant sources of freshwater to the Long Island Sound (LIS) are the Connecticut River, the Housatonic River, and East River through which water from the Hudson River enters the Sound. These sources are located almost at opposite ends of the LIS which creates complicated circulation patterns. Several other rivers (Thames, Niantic, and Quinnipiac Rivers) also deliver smaller amount of freshwater and these have important effects near the river mouths. The water treatment plants of the New York metropolitan area jointly add a volume flux comparable to the smaller rivers directly in to the East River, which measurably effects the stratification in the western Sound. Ultimately, the freshwater is transported through ELIS into BIS and then on to the adjacent continental shelf in the Atlantic Ocean (O'Donnell et al., 2014b).

The distribution and variability of salinity, temperature, current, and bottom stress created by the complex interaction of the geometry and forcing has a significant effect on the long-term (greater than 3 days) transport of materials (Fischer, 1976; the term materials include water, sediment particles, algae, and other small floating biological organisms). Characterization of the seasonal evolution of these fields and the consequences of extreme weather (like hurricanes) on the circulation and bottom stress distributions requires the combination of observations and a model that interpolates in space and time between the measurements in a manner that is consistent with our understanding of the physical processes that determine and constrain changes.

The transport and fate of suspended matter in an estuary is dominantly controlled by the circulation and wave conditions. Waves and currents also determine the bottom stress. Bottom stress along with sediment characteristics (primarily grain size and cohesiveness) determine the potential for sediment erosion, settling, and resuspension. To assess the potential disposal sites in the ZSF, the average as well as the range of conditions must be characterized. Current magnitudes and wave parameters in the ZSF vary seasonally and there are substantial inter-annual variations associated with meteorological conditions. The delivery of freshwater to the ZSF in the spring largely determines the salinity patterns and dominates the variability in transport. Large rain events in the watershed (e.g., from hurricanes) also change the circulation and the suspended sediment distribution in LIS.

A preliminary review of the physical oceanography of the ZSF showed that there are three distinct circulation forcing seasons: spring (March-May) when river discharge is high and winds are strong; summer (June-August) which typically has low winds but the water in the Sound is the freshest; and winter (November-January) which has low river flows and strong winds. The PO study therefore included field observations during three two-month long campaigns (Table 1; see Table 2 for definitions of terms used during the field program). Campaign 1 spanned the March-May (spring) high river discharge period. Low discharge and low wind conditions were observed in Campaign 2 which extended from early June to August. High winds are generally persistent in the winter; therefore Campaign 3 spanned the period from November 2013 to January 2014.

Table 1. Seasonal Field Observation Periods (referred to as 'Campaigns')

Campaign	Season	Interval	Conditions	
			River Discharge	Wind
1	Spring	March 12 - May 17, 2013 (*66 days)*	High	High
2	Summer	June 11 - August 8, 2013 *(58 days)*	Low	Low
3	Winter	November 20, 2013 - January 16, 2014 *(57 days)*	Low	High

Seven stations were selected, in consultation with the project management team, for moored observations to allow the evaluation of the model's ability to discriminate areas of high bottom stress from those with lower stress, and to assess whether the model could adequately simulate the annual range of conditions anticipated in the ZSF. Preliminary model stress estimates and maps of bottom sediment type informed the selection. The moored instruments required maintenance and the ship operations provided the opportunity to survey the hydrography. Eight ship surveys were conducted and observations at eleven stations were executed when weather conditions permitted. In addition, wind, wave, and river discharge data were obtained from secondary data sources and included in the model and data analysis. The locations of field stations and buoys are shown in Figure 2. The first report of the PO study describes the field program and summarizes the data collected (O'Donnell et al., 2014a).

Table 2. Key Terms used in the Field Program of the PO Study

Term	Explanation
Campaign	Period of 'Mooring' deployments during three seasons: spring (Campaign 1), summer (Campaign 2), and winter (Campaign 3). Each campaign was about two months long.
Cruise	Each time the ship conducted field activities in the ZSF. A cruise consisted of two parts: (1) Deployment or recovery of 'Moorings', and (2) Measurements of water column parameters and sampling of sediment as part of 'Ship surveys'). There were a total of eight cruises (Cruises CTDOT1-8), each lasting 1 to 3 days.
Mooring	An instrument frame moored on the seafloor at seven stations. Each frame included several oceanographic instruments. Mooring stations are labeled DOT1-7*, shown as numbered red circles (with the prefix "DOT") in Figure 2.
Ship survey	Data and samples collected from the ship using various instruments at 11 stations; these stations consisted of the seven mooring stations (DOT1-7), as well as 4 additional stations labeled CTD8-11* shown as numbered green circles (with the prefix "CTD") in Figure 2. Collected ship survey data broadened the range of current and hydrographic measurements collected at the moorings. Instruments used at these 11 stations during ship surveys included profiling CTDs, optical sensors, and a ship-mounted ADCP.

* The station locations were approved by the Cooperating Agency Group prior to the study.

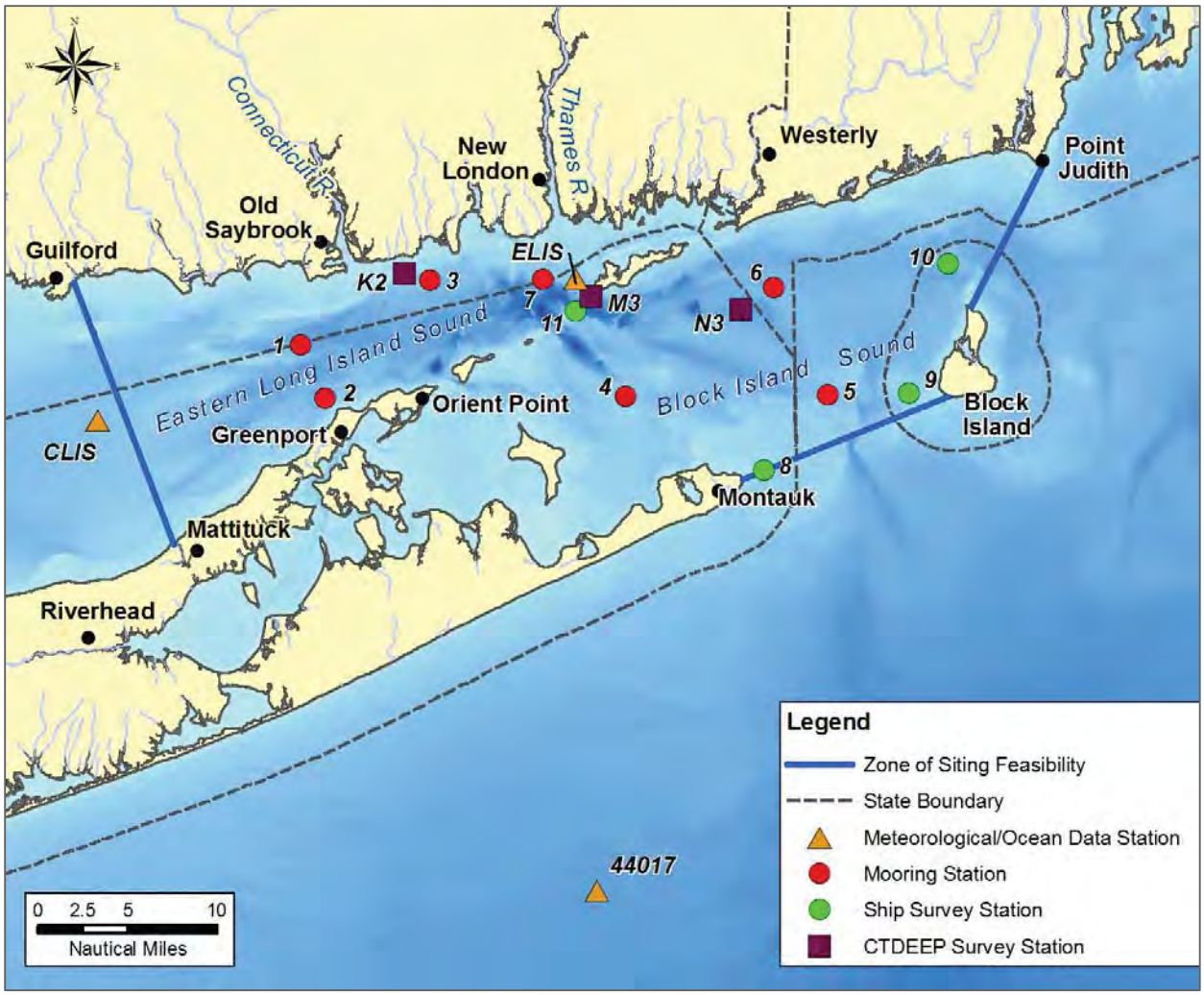

Figure 2. Survey stations of the physical oceanography study, "metocean" buoy locations, and CTDEEP survey stations. The blue background shading represents bathymetry.

As described in Table 2, moorings with oceanographic instrument were deployed at seven stations throughout the ZSF during each campaign. Each instrument mooring was equipped with an upward-looking RD Instruments acoustic Doppler current profiler (RDI ADCP) and bottom pressure sensor to measure the current structure, sea level, and wave parameters; a Nortek ADCP to measure the current between the seafloor and an elevation of 0.75 m above the seafloor; and two optical backscatter sensors (OBS) to estimate suspended sediment concentrations. To complement the moored observations, two-day ship surveys were conducted at 11 stations (which included the seven mooring stations) with profiling conductivity/temperature/depth sensors (CTDs), optical sensors, and a ship-mounted ADCP. These cruises were coordinated with instrument maintenance at the seven mooring stations. During ship surveys, bottom sediment grab samples were collected near the mooring stations to guide the interpretation of spatial variations in bottom stress.

The simulation of the circulation patterns in the ZSF required the characterization of winds and river flow. Therefore, wind and wave fields observed by instruments from three meteorological/ocean ("metocean") stations located within the ZSF were analyzed, together with data from central LIS and in the Atlantic Ocean. In Figure 2, a map of the ZSF is shown with the location the CLIS and ELIS buoys, which are equipped with meteorological sensors. The CLIS buoy also has instruments to measure wave statistics. Since these stations have been maintained by the University of Connecticut (UConn) for almost 15 years the data can be used to characterize conditions during extreme events like Superstorm Sandy. Waves from the ocean propagate into the ZSF and these are monitored at Station 44017, which is a NOAA buoy with both meteorological and wave sensors. The red circles in Figure 2 show the seven stations for bottom mounted instruments deployed to evaluate the model performance (these stations are referred to below as DOT1 – DOT7). Ship-deployed instrument packages were deployed at these seven stations. Ship observations were also acquired at these locations as well as four additional stations marked by green circles and labeled CTD8 – CTD11. The dark squares labeled K2, M3 and N3 in Figure 2 show the locations of the long-term monitoring stations maintained by CTDEEP. Meteorological data were obtained from the buoys at the locations indicated by the three orange triangles.

The weather conditions during the period of the observation program in 2013-14 were close to typical for the region. In March, April and May the monthly average air temperature was within 1°C of the long term average. During the summer campaign, June and August air temperatures were also close to the average while July temperatures were warmer by approximately 2°C (4°F). Air temperatures during the winter campaign (November-January) were also 2°C (4°F) warmer than average. Moored instruments showed that the salinity and temperature in the ZSF during the observation campaigns were not inconsistent with the long-term average seasonal cycles though the bottom temperature and salinity were slightly higher than usual.

Wind conditions were evaluated using the over-water meteorological measurements at the ELIS and CLIS buoys in Long Island Sound, and the NOAA buoy 44017, which is located on the continental shelf to the southeast of Montauk, New York (see Figure 2). Wind speed and direction observation at the buoys were consistent with the variability observed in the earlier record. During the spring campaign 15-minute average wind speeds were in excess of 10 m/s for durations of more than two days, eight separate times and winds speeds reached up to 18 m/s. This is characteristic of the variability produced by the extra-tropical cyclones that dominate the spring weather. In contrast, during the summer campaign wind speeds seldom reached 10 m/s. Tropical depressions occasionally bring very high winds to southern New England in the summer; however, in 2013 only Tropical Storm Andrea had an appreciable impact and it caused a short period of 16 m/s winds on June 7, 2013. In the winter, the winds higher than 10 m/s occurred on most days but maximum winds seldom exceeded 16 m/s.

Since the observation period did not capture any extreme events, the model must be used to simulate the consequences of unusual meteorological systems on the magnitude of the bottom stress in the ZSF. Strong winds generate sea level anomalies (or surges) in Long Island Sound and these are detected by tide gages. The time-series from the gage at New London is almost 80 years long and it, therefore, can produce robust estimates of the probability (or return interval) of extreme

events. These records are especially valuable because the magnitude of the sea level anomaly correlates with the magnitudes of non-tidal currents and bottom stress fluctuations.

The extreme water level analysis reported by NOAA for New London (*http://tidesandcurrents.noaa.gov/est/curves.shtml?stnid=8461490*) shows that the surge due to Superstorm Sandy in October, 2012 was 6 feet (1.5 m) above mean high-high water (MHHW) and that the return period was approximately 25 years. However, the magnitude is also equivalent to the lower limit of the uncertainty range of the 100-year return interval. Thus, Superstorm Sandy should be considered characteristic of a 25-100 year event. The only larger surges that have been observed occurred prior to 1955. The meteorological observation network was less effective at that time and the wind data required to force the simulations is unavailable. The interval of Superstorm Sandy in 2012 is, therefore, a suitable interval to estimate the effects of an extreme event on bottom stress distributions.

This report describes the implementation of the circulation component of the model FVCOM[1] and the testing (*i.e.,* calibration) and evaluation procedure. Calibration used data that were available prior to the study. The data acquired in the field program (O'Donnell et al., 2014a; provided as SEIS Appendix C-1) were then used to evaluate the magnitude of the errors in the simulations of water properties, current, and bottom stress. The report also discusses the simulation of waves and the comparison of predictions to field measurements. The performance of the model in the simulation of currents and bottom stress during the campaigns are used to establish its effectiveness in discriminating area and times of low stress in the ZSF. Predictions of the model for a major storm event (Superstorm Sandy) are then reported. Finally, the distributions of maximum bottom stress in the ZSF are summarized to provide guidance on the suitability of potential sites.

[1] FVCOM = Finite Volume Coastal Ocean Model (see Section 2 for details of the model).

2. The Model

The PO study employed a high-resolution model of the circulation and hydrography in the ZSF. The model was developed with support from the Connecticut Sea Grant College Program and the collaboration of Professor C. Chen of the University of Massachusetts, Dartmouth. The domain of the model and the resolution are shown in Figure 3a. We developed an implementation of FVCOM (Chen et al., 2007) at the University of Connecticut (UConn) and designed it to use the results of the operational northwest Atlantic regional model, operated as the Northeast Coastal Forecast System (NECOFS, see *http://fvcom.smast.umassd.edu/research_projects/NECOFS/*), to provide ocean boundary conditions. This "nesting" approach is computationally efficient since it allows the effect of the larger-scale processes to be simulated at coarse resolution through NECOFS and allows UConn's computing resources to focus on the smaller-scale structures in LIS and BIS. The blue segments in Figure 3a show the area where the LIS sub-domain merges with the NECOFS model. Figure 3b shows the bathymetry of the region.

To initiate simulations the model requires that the salinity, temperature, water level, velocity and wave spectrum are prescribed everywhere in the domain. As time progresses the values of these variables at the lateral boundaries, and the wind velocity distribution must be continually updated. The sources of this information are described in Sections 2.1 and 2.2.

An accurate description of coastal circulation has to include the effects of surface gravity waves. Surface gravity waves with periods (T) longer than 5s can play a role in circulation dynamics in shallow water. For example, surface wave breaking can enhance mixing, affecting the transfer of momentum and heat. In coastal waters, the interaction of waves with currents can also lead to enhanced bottom stress (e.g., Grant and Madsen, 1979; Signell et al., 2000).

Observations of the surface gravity waves to the west and south of the ZSF suggest the wave field is a combination of a swell in the eastern part of the ZSF (i.e., in BIS) with peak frequencies of 0.10 to 0.12 Hertz (Hz), and a fetch-limited wind-driven wave field in LIS with peak frequencies of 0.30 to 0.40 Hz. The LIS local wind forcing shows a strong seasonality with winds directed to the southeast during winter and to the northwest during summer (O'Donnell et al., 2014b). There have been no published wave measurements in BIS at the time this project was initiated; however, ocean swell is expected to propagate into the ZSF between Montauk Point and Block Island. The wave field is hence a complex superposition of different wave scales that is best characterized using a statistical approach. Therefore, in this study we used the SWAVE component of FVCOM to simulate the evolution and distribution of the wave spectra and focus our comparisons on the significant wave height (H_s) and peak periods (T_p) which were measured during the field program.

The FVCOM wave component (Qi et al., 2009) is a modified version of the SWAN (Simulating Waves Nearshore) model which was developed specifically to resolve coastal ocean-scale wave fields. SWAN simulates the evolution in space and time of the spectrum of waves and takes into account the generation by wind, dissipation, refraction, and nonlinear interactions. The steady version of these physical processes is also represented in STWAVE (Massey et al., 2011). The finite volume formulation of SWAN developed by Qi et al. (2009) is termed SWAVE and it shares the grid structure and forcing files with FVCOM. The character of the partial differential equations in SWAVE requires a much smaller time step and it therefore runs much more slowly than

FVCOM. For computational efficiency, we exploited the fact that the effect of waves is generally insignificant in the ZSF most of the time since the water is deep relative to the wavelength. The stress distributions were evaluated without including the waves most of the time and only included through the SWAVE module when conditions required it.

The following sections outline the model forcing, the process of calibration, and the model performance in the simulation of currents, salinity, temperature, density, and wave statistics.

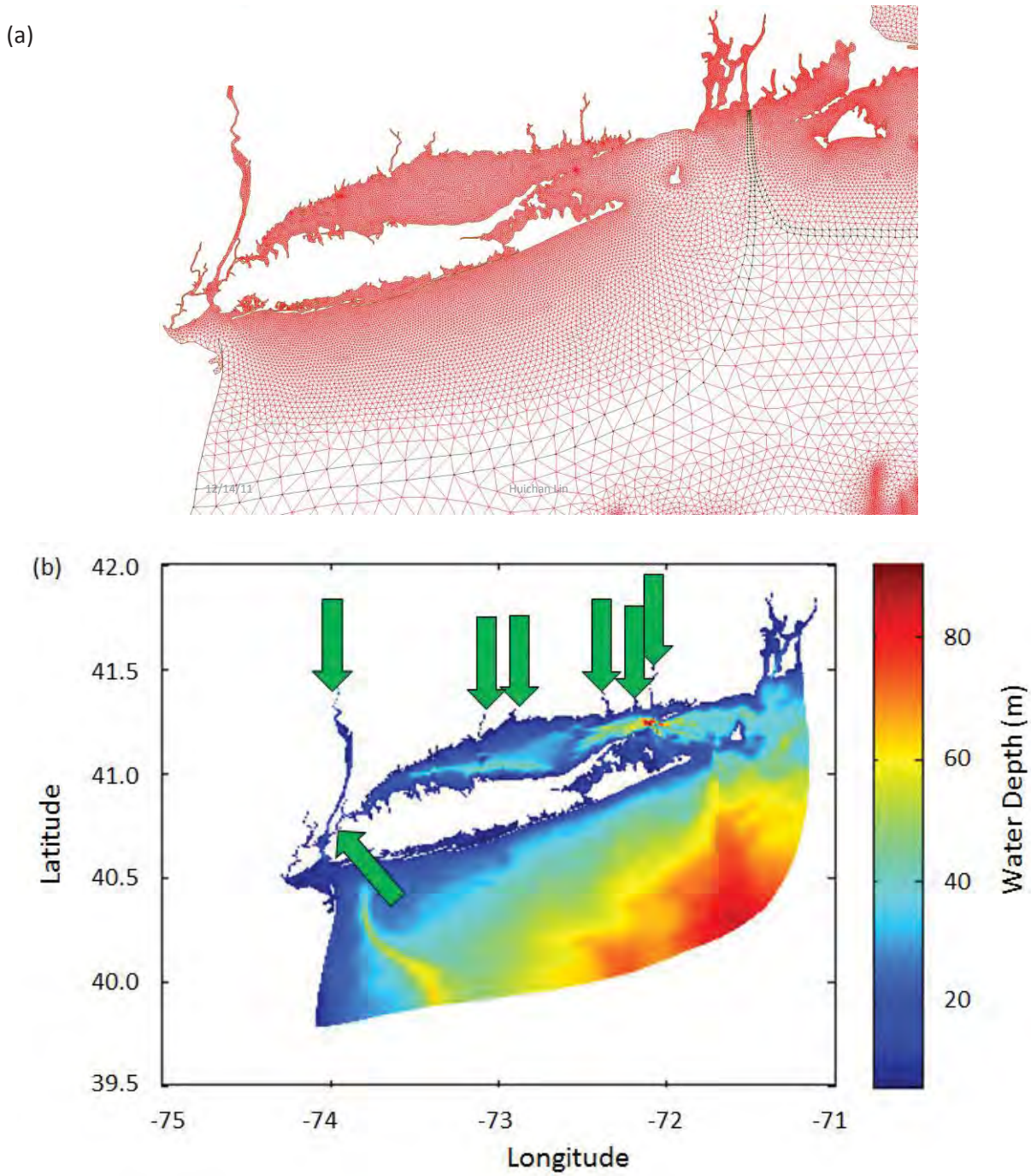

Figure 3. (a) Map of southern New England shore showing the model grid (red). Blue cells show the boundary locations where the regional model NECOFS and the nested LIS-BIS sub-domain overlap. (b) Bathymetry of the LIS model subdomain with the locations of freshwater sources (green arrows; from left to right: Hudson River, New York City wastewater treatment plants, Housatonic River, Quinnipiac River, Connecticut River, Niantic River, and Thames River).

2.1 Initial Conditions

FVCOM was initialized using a temperature and salinity climatology data set derived via objective interpolation (OI) of CTDEEP station data (see Figure 4 for locations) as described by O'Donnell et al. (2014a), and the data in the NOAA archive described by Codiga and Ullman (2011). In order to be input into the FVCOM model, these OI fields were interpolated from sigma level depths to a set of standard depths. The standard depths were chosen as: 0, -2, -4, -6, -8, -10, -12, -15, -20, -25, -30, -40, -60, -80, -100 m. The model simulations were started in the fall for the subsequent year in order to provide an adjustment period.

2.2 Boundary Conditions

FVCOM is forced at the seaward boundaries by sea level variations and salinity and temperature. The sea level is prescribed using tidal constituents derived from the global tidal model (Egbert et al., 1994) and also incorporates non-tidal fluctuations from the NECOFS system. Since the Egbert et al. (1994) constituents are not precise in shelf areas, the amplitudes and phase of the major constituents are iteratively adjusted to achieve an optimal representation of the amplitude and phase at each tidal frequency using NOAA tidal height observations from 2010 at Montauk (NY), New London (CT), New Haven (CT), Bridgeport (CT), and King's Point (NY). Each constituent amplitude was adjusted by the amplitude ratio to optimize the model performance. Figure 5 shows an example of the result of this procedure on the observed and predicted level at the NOAA Bridgeport tide gauge.

To evaluate the model performance we use the 'skill', s, statistic defined as

$$s_f = 1 - \frac{\langle (f_m - f_d)^2 \rangle}{\langle (f_d - \langle d_d \rangle)^2 \rangle} \tag{1}$$

where f_m and f_d represent the model and data values (f represents sea level (η) or current (u), etc.) and the $\langle \quad \rangle$ notation represents the mean of the argument over the simulation interval (i.e., $< d_d >$ is the mean of the data). No single measure of model performance provides an ideal summary; however, s, has the useful property that it is 1 when the model and data are in perfect agreement and becomes negative when the difference in the model and data is larger than the variance in the data record. Note that since the model predicts the average property value in a grid cell while the data are obtained at a much higher resolution, a perfect model would not generally achieve a skill of 1.

After the correction of the tidal constituent amplitudes for sea level at the boundary of the model subdomain, the skill for sea level variations at Bridgeport, CT, shown in Figure 5, was 0.90 (i.e., 90%). Figure 6 shows a comparison of the predicted and observed sea level variation at Station DOT3 during Campaign 2. The reduced skill at this station largely results from the smaller tidal range and a consequently smaller denominator in Equation (1). Post-calibration comparison plots for all seven DOT stations of the three campaigns are presented in Appendix 1 to this report.

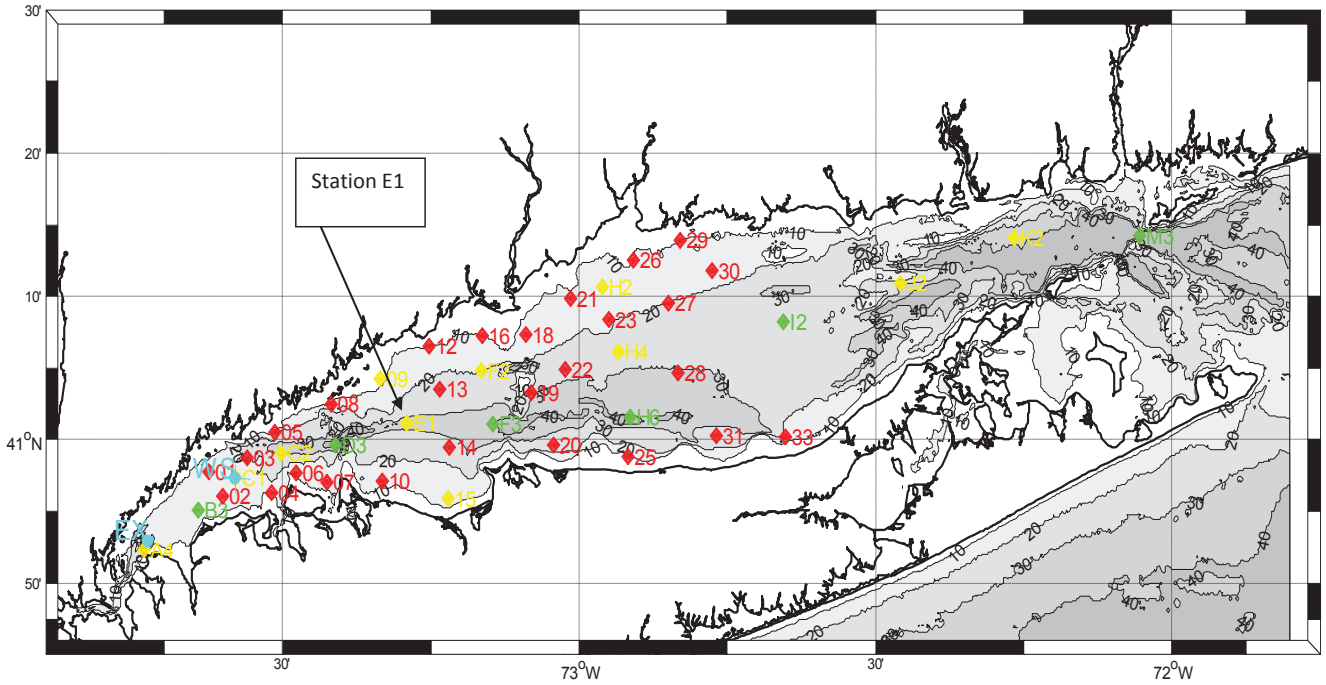

Figure 4. Locations of the CTDEEP water quality survey program CTD stations used in the initialization of the numerical model of the circulation and hydrography in the ZSF. The location of Station E1 is identified by an arrow since it is referred to in the text. The background of the map represents bathymetry.

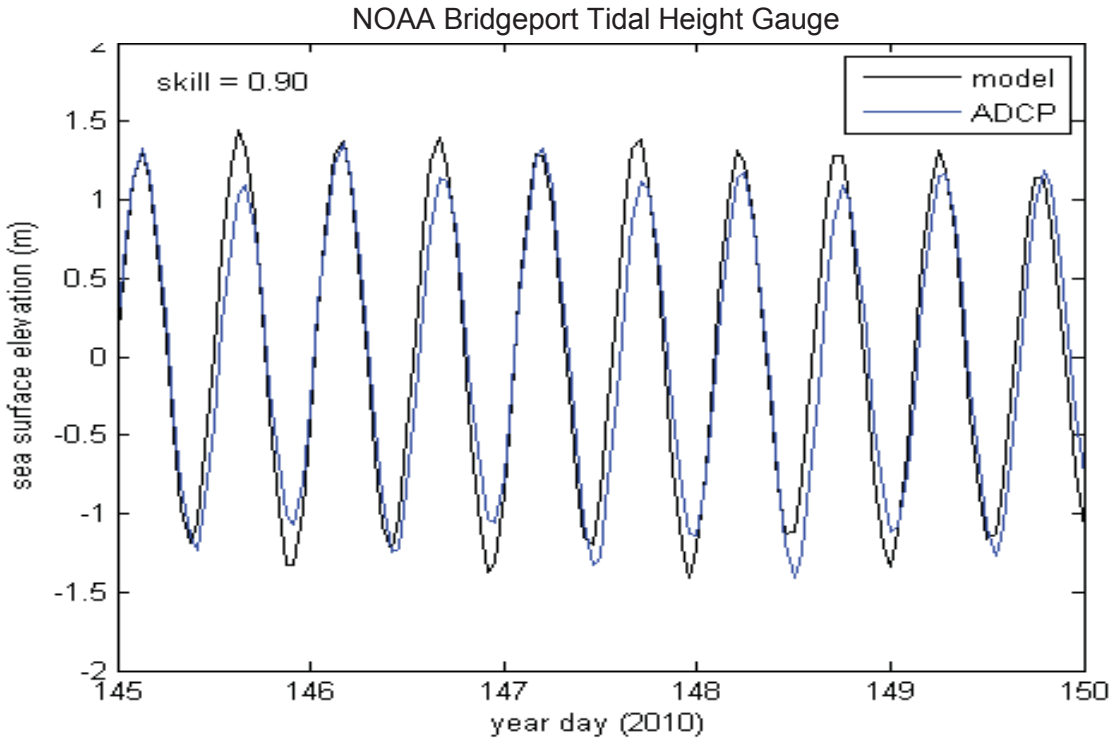

Figure 5. Comparison of tidal heights at the NOAA Bridgeport tidal height gauge (BDR, blue) compared to those predicted by the FVCOM model (black) after iteratively calibrating the model using the 2010 NOAA data. Note that year day 1 is January 1, 2010.

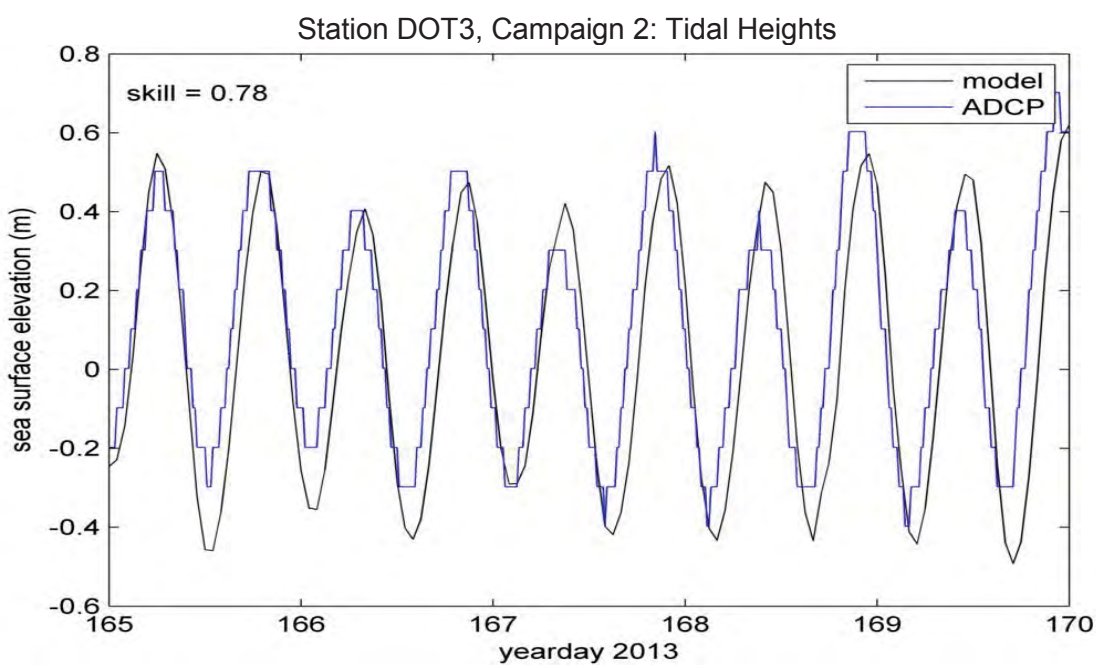

Figure 6. Comparison of tidal heights in the ZSF at Station DOT3 during Campaign 2 measured by ADCP pressure sensor (blue) compared to those predicted by the FVCOM model (black).

Although the calibration procedure did not involve ADCP current observations, the model captured tidal currents and tidal constituents of depth-averaged currents well. The skill in the eastward velocity component was 90% and 78% in the much smaller northward velocity component. Minor differences appeared where the topography was steep or the data did not cover a full spring-neap tidal cycle. Time-series comparisons between field measurements and model simulations of the same time period demonstrated the model successfully predicts depth averaged tidal currents (Figure 7). Comparison plots for the seven DOT stations for the three campaigns are presented in Appendix 2 to this report.

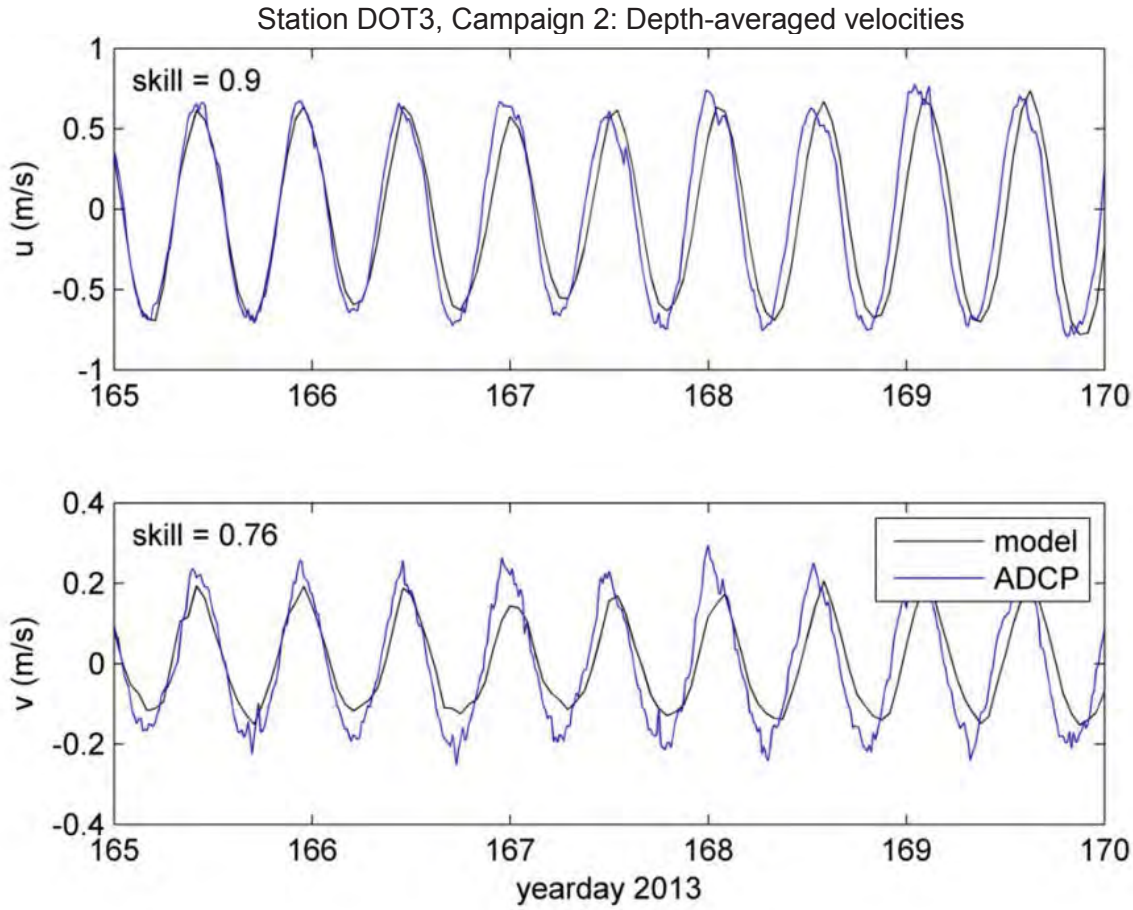

Figure 7. ADCP deployment (blue) compared to those predicted by the FVCOM model (black) for depth-averaged currents at Station DOT3, Campaign 2.

2.3 Heat Fluxes

Surface heat flux inputs were computed using the WHOI/USGS air-sea MATLAB toolbox *(http://woodshole.er.usgs.gov/operations/sea-mat/air_sea-html/index.html),* and then empirically scaled so as to reproduce the water temperature climatology. Hourly net heat fluxes were calculated as the sum of the shortwave, long-wave, sensible, and latent fluxes. Shortwave fluxes were calculated as an hourly time-series based on solar attitude. Long-wave fluxes were calculated using the Berliand bulk formulae (Fung et al., 1984) from estimates of the seasonal sea surface

and air temperatures, relative humidity, and cloud cover. Cloud cover was estimated using the Clarke (1974) corrections. The sensible and latent fluxes were calculated using the TOGA/COARE (Smith, 1988) bulk formulae.

This heat flux forcing represents an annual cycle and can only be expected to represent the annual warming and cooling cycle in the ZSF. Figure 8 shows a comparison of the FVCOM predictions for bottom temperature in the ZSF for year 2013 and compares it to the temperatures measured by the bottom-mounted ADCPs.

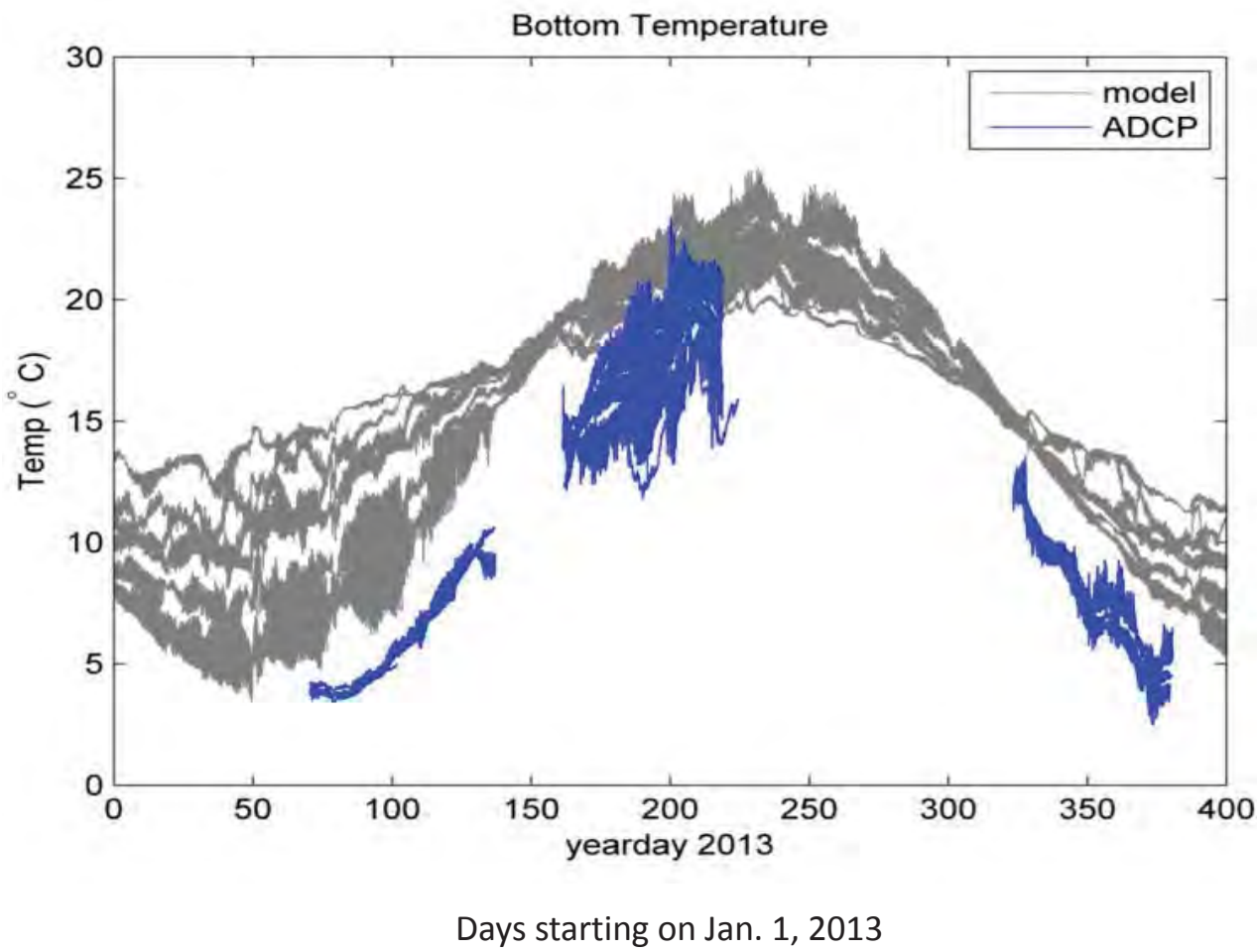

Figure 8. Comparison of bottom temperatures in the FVCOM model (gray) with those measured by the ADCP temperature sensors (blue). Model solutions are shown for the entire year at the seven mooring stations (i.e., DOT1-7). ADCP data cover the duration of all three field campaigns.

2.4 Freshwater Fluxes

Freshwater enters the LIS FVCOM domain through seven model cells corresponding to the locations of the Thames, Connecticut, Niantic, Quinnipiac, Housatonic, and Hudson Rivers and New York City wastewater treatment plants (WWTP) (Figure 3b). These fluxes are based on gauged flows measured by the USGS at Thompsonville, CT, and lagged by one day to account for the distance between the head of the Connecticut River in our model and Thompsonville. Each river, R_i, is adjusted using the USGS Thompsonville data as $R_i = 1.20\frac{R_{CT}}{\overline{R_{CT}}}\overline{R_i}$ where R_{CT} is the day-specific Connecticut River flow, $\overline{R_{CT}}$ is the mean Connecticut River flow, and $\overline{R_i}$ is the mean flow for river *i*. The factor of 1.20 follows from the salt budget of Gay et al. (2004) and accounts for the portion of the watersheds of the rivers below the USGS gauges. A fixed input of 40 m^3/s (cubic meters per second) was added to the East River to represent the freshwater discharged from the New York WWTPs.

There are few measurements of salinity variations in the ZSF; therefore, Figure 9 shows a comparison of the model prediction of surface and bottom salinity for 2013 at the CTDEEP station E1 (red line; see Figure 4 for location) with the mean and $\pm$ one standard deviation of the salinity measurements at E1 (green bars) obtained from monthly surveys from 1993 to 2012. These data are described by Kaputa and Olsen (2000) and O'Donnell et al. (2014b). Clearly, the evolution of the salinity in the model is consistent with the observations. The blue lines in Figure 9 show the observations at high frequency from 2013 obtained at the LISICOS[2] buoy ARTG which is located at the CTDEEP station E1. The model is particularly good at reproducing the lower water column salinity.

[2] LISICOS = Long Island Sound Integrated Coastal Observing System *(http://lisicos.uconn.edu/)*

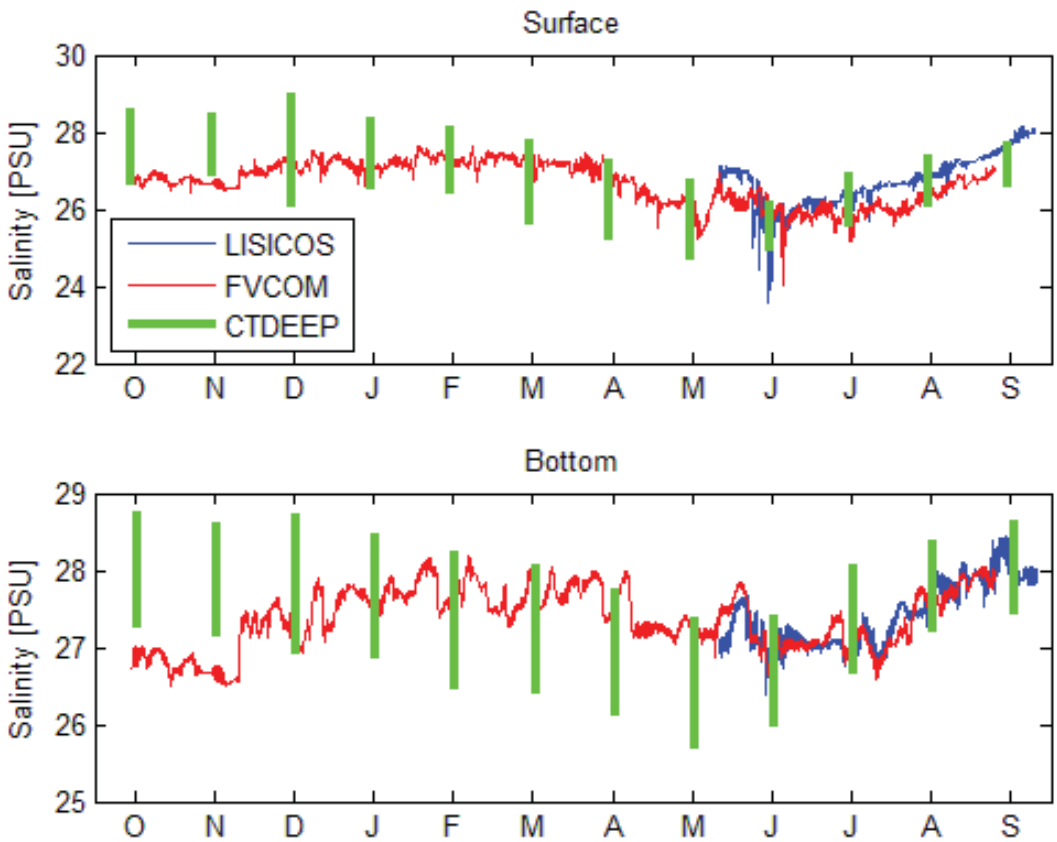

Figure 9. 2012-2013 salinity at station ARTG/ E1 for the near surface (top panel) and near-bottom (bottom panel). FVCOM model predictions are shown in red. Shown by the green bars are the means ± one standard deviation of the CTDEEP data at station E1 binned by month for 1993-2012. Shown in blue are the salinities measured by the LISICOS ARTG buoy (located at CTDEEP station E1) for May - September 2013.

2.5 Wind Stress Forcing

The model is forced with domain-uniform winds obtained from the LISICOS Western Long Island Sound buoy, located at 40°57'21" N 73°34'47" W, south of the City of Stamford**.** Because FVCOM expects 10 m wind speeds, while the buoy winds are measured at 3.5 m, the wind speeds in the buoy record are converted to W_{10} values as $W_{10} = W_{3.5}\frac{\log(3.5\mathrm{m}/z_0)}{\log(10\mathrm{m}/z_0)}$ using z_0=0.01 m. Gaps in the buoy record are then filled in using W_{10} data from the Bridgeport/ Sikorsky airport (BDR). Because of the disparity in the observational locations, contemporaneous data from both the buoy and BDR were regressed using a total least squares methodology and the regression results were applied to the BDR data for those periods where buoy data were missing.

2.6 Bottom Stress Calculation in FVCOM

Like most models of coastal ocean hydrodynamics, FVCOM requires the turbulent flux of horizontal momentum in the vertical direction to equal the stress on the bed estimated by a quadratic drag law. In the x direction the bottom boundary condition is $K_m \frac{\partial u}{\partial z} = \frac{1}{\rho_w} \tau_{bx}$ where $\tau_{bx} = \rho_w C_d u_b \, |\overrightarrow{u_b}|$ and $\vec{u}_b$ is the velocity in the lowest model grid point which is at z_b. The y direction stress is computed in the same way as $\tau_{by} = \rho_w C_d v_b \, |\overrightarrow{u_b}|$. The drag coefficient, C_d, is determined by the requirement that the velocity magnitude match that of von Kármán's (1930) logarithmic boundary layer at the level of the model's lowest velocity grid point. Since the log law requires that

$$|\vec{u}_b| = \frac{u_*}{\kappa} \ln(\frac{z_b}{z_0}) \tag{2}$$

where κ is the von Kármán constant (=0.4), $u_* = \sqrt{|\tau_b|/\rho_w}$ is the friction velocity, and z_0 is the bottom roughness, then clearly the magnitude of the stress is

$$C_d \, \rho_w |\vec{u}_b|^2 = \frac{\rho_w u_*^2}{\kappa^2} \ln\left(\frac{z_b}{z_0}\right)^2 = \frac{\tau_b}{\kappa^2} \ln\left(\frac{z_b}{z_0}\right)^2. \tag{3}$$

For this to be consistent with the drag law, then

$$C_d = \frac{\kappa^2}{\ln\left(\frac{z_b}{z_0}\right)^2}. \tag{4}$$

FVCOM uses a stretched grid in the vertical direction so z_b is linked to the water depth and is spatially variable. Since z_b can become large in deeper areas of the model, FVCOM imposes a lower limit on C_d of 0.0025. The central parameter controlling the magnitude of friction at the bed is then z_0. We discuss the consequences of choices for z_0 on the magnitude of predicted current and stress amplitudes later; however, it is important to note that for the smallest values we explore, $z_0 < 0.15$ cm, the lower limit on C_d is crossed, and $C_d = 0.0025$ is then enforced throughout much of the domain.

The physical meaning of z_0 is well defined in the theory of turbulent boundary layers, and in estuarine studies it is generally related to the size of bottom sediments and bedforms. In the presence of surface waves and moving bottom sediments the formulation of the bottom stress link to the overlying water velocities is modified and several optional parameterizations are included in FVCOM. However, in a spatially averaged coastal ocean hydrodynamic model the bed stress, through z_0, also must represent all of the mechanical energy dissipation. This includes energy dissipation due to topographic irregularities that are not resolved by the model grid so values used for z_0 are generally much larger than would be expected to result from measurements at a single location. After several trial numerical experiments we found $z_0 = 0.01\, m$ was effective in producing current fields that were consistent with observations (see Section 3.1). We also tested other values. When $z_0 = 0.001$ was adopted, the spatial structure of the flow remained the same with an approximately 20% increase in current amplitudes and no significant change in the tidal phase structure. Though near-bottom current magnitudes were increased in much of the domain,

the bottom stress was not because the reduction in z_0 also reduced C_d. Predictions of stress in the ZSF are, therefore, insensitive to the z_0 in this range.

2.7 Bottom Stress Estimates from Current Measurements

The stress (or the vertical flux of horizontal momentum due to turbulence) on the sea bed due to water motion is difficult to measure directly. Kim et al. (2000) describes and compares approaches. The current measurements acquired with the downward looking Nortek HR acoustic Doppler current profiler (Nortek ADCP) in the field program of the PO study (O'Donnell et al., 2014a) were used to estimate bottom stress using the covariance, log law, and bulk formula approaches.

The most direct approach is to measure the vertical and horizontal components of the velocity at a point near the bed at high frequency and then filter out long period (greater than T=100s) fluctuations to isolate the horizontal and vertical turbulent variations, u' and w'. The mean flux of momentum can then be computed as the covariance $\rho_w < u'w' >$ where the bracket represents the mean over the time T. This 'covariance' approach is complicated by instrument noise, the presence of waves, and high frequency internal motion or the wake from irregularities in the seafloor near the measurement site. Accurate estimates of the instrument tilt are essential to separate the vertical and horizontal components effectively since the latter can be a factor of 100 larger and a small tilt can lead to large errors in w'. Several variants on the covariance approach have also been proposed to limit the sensitivity of the method to low-frequency motions and instrument noise (e.g., Wiles et al., 2006; Gerbi et al., 2008; Kirincich et al., 2010). These various methods rely on assumptions about the shape of the spectra of the velocity fluctuations u' and w' and the relationship to u_* and are appropriate when the spectral character of the instrument noise, internal waves, or surface waves is well known.

One method relies on the theory of von Kármán (1930) who showed that for a uniform and un-accelerated flow, the mean (over turbulent the scale) horizontal velocity should vary with distance from the boundary as in Equation (2). Measurements of $u(z)$ at several levels can be fitted to Equation (1) using regression methods and u_* and z_0 computed. The bed stress is then obtained from $\rho_w u_*^2$. This approach is referred to as the 'log profile' method. In estuaries the assumption of this approach are not always valid. Often the flow is accelerated, sometimes two-dimensional, and during periods of high sediment transport the density of the fluid-sediment mixture can be vertically stratified. Kim et al. (2000) compared the methods and noted that the results of the log profile approach were particularly noisy and argued that this was a consequence of a sensitivity to the level of the measurements and the thickness of the log layer. Wilcock (1996) presented an extensive study of the errors inherent in bottom stress measurements and highlighted the need for precise knowledge of the level of the measurement above the rigid boundary. Though this is straightforward in a laboratory setting, when sediment and bedforms are migrating it is less valuable.

The selection of the range of current meter measurement levels to include in the linear regression formula to estimate u_* and bottom stress using the log profile method is crucial since the assumption that the vertical velocity shear is constant and equal to $u_*/\kappa z$ must be satisfied. By inspection of the data we used levels 8 to 14 which correspond to $z_i = \{0.36, 0.32, 0.28,$

$0.24, 0.20, 0.16, 0.12\} - z_B$ m above the bottom where z_B was the level of the sea bed above the feet of the instrument tripod. z_B was measured as the mean level of maximum acoustic backscatter in the three Nortek ADCP beams. The ensemble mean horizontal velocity components, $< u >$ and $< v >$, in each vertical level were used to find the vertical mean current direction, and the mean components in this direction, $< u_r >$, were computed. If $< u_r(z = 0.36) > \leq 0.04\ m/s$ or the angular standard deviation in current directions, $\sigma_\theta \geq 10\ deg$ (see Fisher, 1996) then the log profile method was not applied. Otherwise, the currents at the levels defined above were rotated to the mean direction, $< u_r >$, and an ordinary least squares linear regression of the form

$$< u_{r,i} > = A \log z_i + B \tag{5}$$

was applied to compute $u_* = \kappa A$ and $z_0 = \exp(-B/A)$. The regression coefficient, r^2 for $< u_{r,i} >$ and $\log(z_i)$ were monitored and u_* values rejected when $r^2 < 0.8$. The stress magnitude can be computed as $|\tau_{BF}| = \rho_w u_*^2$ and the direction taken as opposite to the mean current.

The simplest and most widely applied approach to the measurement of the bottom stress is known as the 'bulk formula' or the 'quadratic drag law'. That the bulk formula and the log law are consistent is assumed in the formulation FVCOM. Many laboratory and some field programs have employed the direct covariance approach to establish an empirical parametric relationship of the form

$$< u'w' > = C_{D,1} u(z = 1m)^2 \tag{6}$$

where the empirically determined coefficient is approximately $C_{D,1} = 2.5 \times 10^{-3}$ (Dronkers, 1964; Bricker et al., 2005) though it is clear that values in the range $(1.5 - 4.7) \times 10^{-3}$ have been reported for seafloors with different sediment types.

The covariance approach to the measurement of bottom stress requires that the vector velocity components are measured at the same point. Like all current profilers, the Nortek ADCP measures along beam components in three directions that are 20 degrees from the common axis and 120 degrees in the azimuthal coordinate. The separation of the estimates, δ, increases with range, R, as $\delta = 2 * R * \tan(20^0)$. Since preliminary instrument tests suggested that the beam velocity measurements were biased low by the instrument housing, the closest bins with unbiased data (3) have a separation of 12 cm and a distance above bottom $h = 56c$. Computing the velocity components as if they were measured at the same location then introduces an error that scales with the product of δ and magnitude of the spatial gradients. If the turbulence is homogeneous and the energy is largely contained in the wave numbers surrounding $k_o = 2\pi/h$, then the error at that scale will be of order $\frac{\delta}{h} \sim 20\%$. The error in higher wave numbers will be larger, but as the energy drops rapidly as $k^{-7/3}$ for $\frac{k}{k_0} < 1$ as demonstrated by Kaimal et al. (1972), the error in the covariance $< u'w' >$ should not be expected to be much larger. This can be confirmed by examination of the spectrum.

We applied the covariance method by first rotating the east, north and up (u, v, w) velocity components from each ensemble of 2048 (or 4096) samples obtained at 2 Hz (or 4 Hz) at bin 3 of the Nortek ADCPs to the "streamline coordinates" (u_r, v_r, w_r), i.e., by applying rotations that

require $< w_r' >= < v_r' >$=0 and 0. We then removed the fluctuations correlated with variations in the pressure to minimize the effects of surface waves, a problem pointed out by Trowbridge (1998). We then used a 7th-order polynomial to de-trend the ensemble. The resulting sequence of u_r', v_r' and w_r' were then averaged to yield the vector components of the momentum flux $\tau_{xrc} = -\rho_w < u_r' w_r' >$ and $\tau_{yrc} = -\rho_w < v_r' w_r' >$. The inverse rotations were then applied to recover the east and north components $\tau_{CV,x}$ and $\tau_{CV,y}$.

The bulk formula estimate of the vector stress components was computed using the ensemble mean velocity data from bin 3 (at 0.5 m above bottom) as

$$\tau_{BF,x} = -\rho_w C_{dN} < u_3 > \{< u_3 >^2 + < v_3 >^2 \}^{1/2} \tag{7}$$

and

$$\tau_{BF,y} = -\rho_w C_{dN} < v_3 > \{< u_3 >^2 + < v_3 >^2 \}^{1/2} \quad . \tag{8}$$

The drag coefficient was chosen to yield the same stress as would be obtained if the velocity profile was projected up to 1m and the drag coefficient was 0.0025. This is accomplished using $C_{dN} = 0.0025 * \left(\log\frac{1}{z_0}\right)^2 / \left(\log\frac{0.5}{z_0}\right)^2$. The appropriate value of z_0 was chosen so that τ_{BF}, τ_{CV} and τ_{LL} are consistent.

These three values of the stress magnitude differ as a consequence of the noise arising from turbulence and the beam geometries, the acceleration and non-uniformity of the flow, movement of the sediment, changes in the bed level, and the constant drag coefficient assumption. They should, however, be consistent in the sense that they should not differ by magnitude larger than can be attributed to the weakness in the underlying assumptions. Figure 10a provides an example comparison of the bulk formula, $|\tau_{BF}|$, and log law profile, $|\tau_{LL}|$, stress magnitude measurements for a 30-day period in Campaign 1 at Station DOT1. Figure 10b shows the corresponding comparison of $|\tau_{BF}|$ and stress from the covariance approach, τ_{CV}. Each figure includes the linear relationship obtained by least-square regression (red line) and the slope (upper right corner). Points that have the largest 5% of differences from the regression line are shown in red. The results of the methods are clearly correlated and of the same magnitude though the variability is high. The fact that the slopes (0.89 and 1.09) are close to 1 indicates that the value adopted for C_{DN} was appropriate.

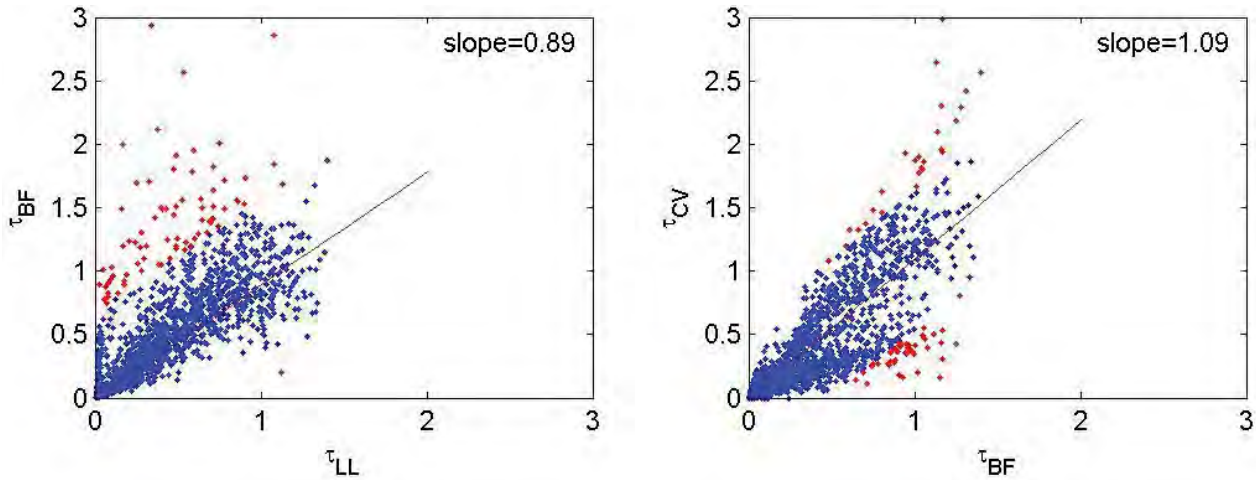

Figure 10. (a) An example comparison of the bulk formula ($|\boldsymbol{\tau_{BF}}|$) and log profile stress magnitude measurements, and (b) ($|\boldsymbol{\tau_{CV}}|$) and log profile $|\boldsymbol{\tau_{BF}}|$ stress magnitude measurements for a 30-day period at Station DOT1 during Campaign 1. The points shown in red indicate the highest 5% of errors in the regression prediction.

While the comparison in Figure 10 is representative, the ratio of magnitudes and the number of anomalies vary from station to station. Figure 11 presents a concise summary of all stress magnitude measurements $|\tau_{LL|}|$ and$|\tau_{BF}|$. To suppress the noise inherent in turbulent quantities, $\log_{10}|\tau_{LL}|$ and $\log_{10}|\tau_{BF}|$ were averaged in intervals of $\log_{10}|\tau_{BF}|$ at each station for the three campaigns. The standard deviation of the mean for each stress bin was also computed; they are represented in the figure by vertical lines. The solid black lines indicate the relationships $|\tau_{BF}| = |\tau_{LL}|$ and $|\tau_{BF}| = 2\,|\tau_{LL}|$, and the dashed lines indicate $|\tau_{BF}\,| = 0.5|\tau_{LL}|$ and $|\tau_{BF}| = 1.5|\tau_{LL}|$ to guide the interpretation of the magnitude of the variability. The graph shows clearly that for all average τ_{LL} values lie on, or slightly below, the $|\tau_{BF}| = \tau_{LL}|$ line in the interval 0.04 Pa $< |\tau_{BF}| <$ 1 Pa. Values of $\tau_{LL} > 1$ Pa are infrequent and many of the high values are likely associated with flow conditions that are inconsistent the log-law assumptions. The τ_{BF} data at Stations DOT4, 5 and 6 appear to be biased low relative to the expected values which suggests that a higher drag coefficient would be more appropriate for the BIS. However, since the two standard deviation intervals largely span the $|\tau_{BF}| = |\tau_{LL}|$ line, the value of C_{DN} selected provides a good estimate of the bottom stress in the ZSF.

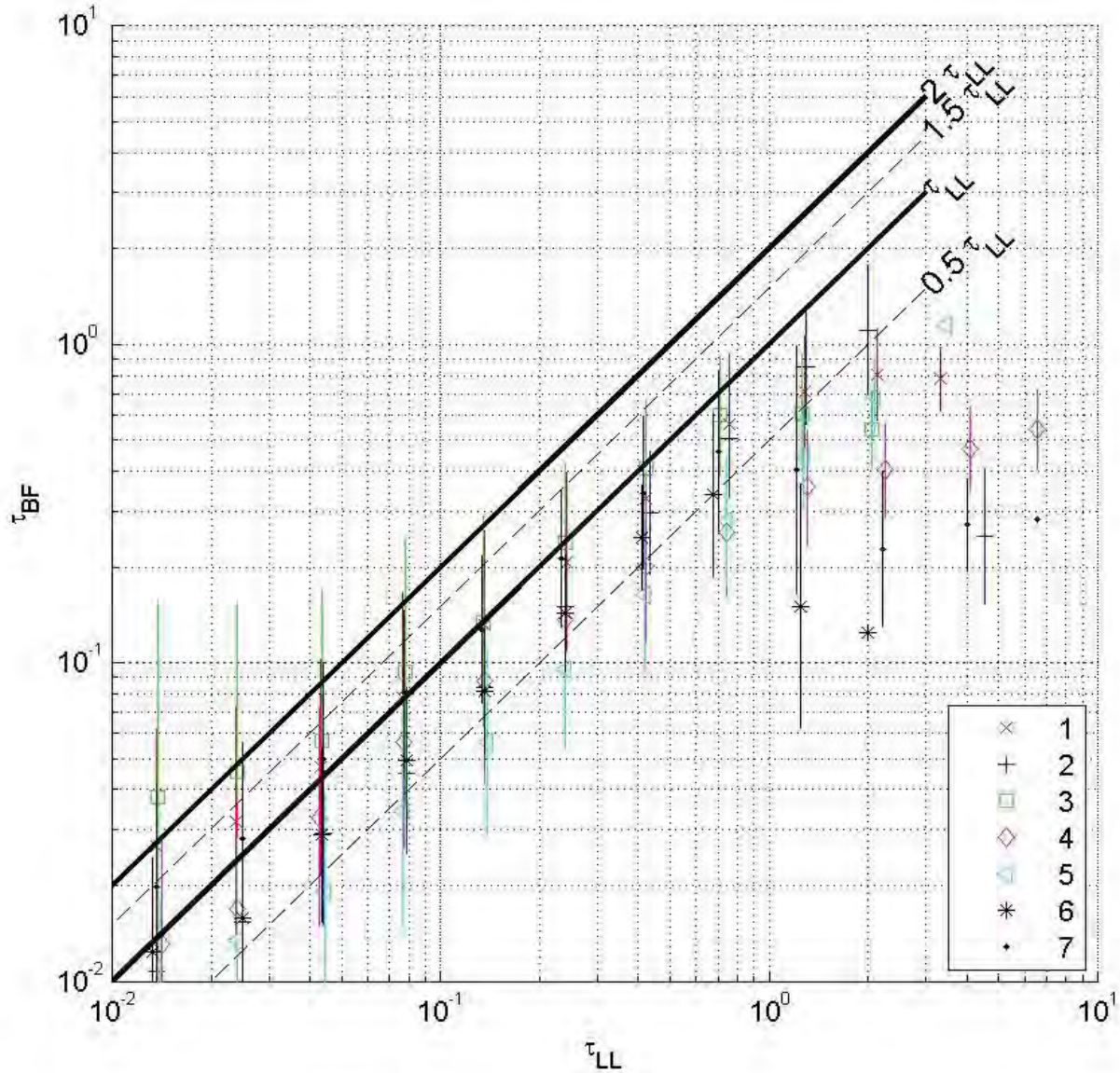

Figure 11. Summary of the stress magnitude measurements $|\boldsymbol{\tau_{LL}}|$ and $|\boldsymbol{\tau_{BF}}|$. To suppress the noise the quantities $\mathbf{log_{10}}|\boldsymbol{\tau_{LL}}|$ and $\mathbf{log_{10}}|\boldsymbol{\tau_{BF}}|$ were averaged in intervals of $\mathbf{log_{10}}|\boldsymbol{\tau_{LL}}|$ at each station for the three campaigns. The vertical lines show a two standard deviation interval around the mean of each bin. The key is shown in the lower right of the Figure. The solid and dashed lines show $|\boldsymbol{\tau_{BF}}| = \boldsymbol{\alpha}|\boldsymbol{\tau_{LL}}|$ for $\boldsymbol{\alpha} = \mathbf{0.5, 1, 1.5}$ and 2.

2.8 The Model – Summary

The goal of the PO study was to predict the spatial structure and time evolution of bottom stress in the ZSF so that locations where the maximum stress experienced is less than that required to suspend seafloor sediment. Stresses vary with wind conditions and season, and since they can only be measured directly for a few locations and for a few months, this model was developed to simulate the bottom stress throughout the ZSF for the assessment of potential dredged material disposal sites.

The model (a computer program) used in this study is an implementation of FVCOM (Chen et al., 2007), created by UConn. The program solves a complicated set of equations that require momentum and mass are conserved at a three-dimensional grid of locations, and that enforces well-established conditions at the water surface boundary and the estuary-sediment boundary. When the bathymetry, river flows, surface heat flux, water level at the boundaries of the domain, and wind velocities are set, FVCOM predicts the sea level, temperature, salinity, and velocity distributions in the model domain that are consistent with the equations and boundary conditions. The bottom stress is also predicted. There are some coefficients in the model that must be selected to represent the effects of friction at the seabed and the effects of small scale topographic variations that are not resolved by the model grid. The value ($C_d = 2.5 \times 10^{-3}$) was selected to ensure that the model sea level and current were as close to observed values as possible. The observations used in this ’calibration‘ were available in data archives. As shown in Figures 6 and 7, the model performs well in the simulation of sea level and currents. Figures 8 and 9 demonstrate that it also provides an adequate representation of the seasonal cycle of temperature and salinity.

3. Simulations for the Zone of Siting Feasibility

This chapter describes the FVCOM model performance in stress simulations (based on measurements made in the field program; O'Donnell et al., 2014a) by first evaluating the performance of the model with a comparison of the model predictions of the tidal currents in the ZSF, and by then discussing the simulation of bottom stresses. A simulation of a severe storm is also presented.

3.1 Tidal Currents and Bottom Stress

Figure 12 compares the M2 tidal current ellipses for the vertically averaged flow computed from the data acquired by the moored RDI ADCPs to the flow estimated from the model shown in black. The tidal ellipses from each campaign are shown separately. For all stations and campaigns, the model ellipses are in excellent agreement with the field observations. Discrepancies in direction and amplitude are slightly larger at the stations in the regions of the most complex bathymetry where it is difficult to relocate the instruments in exactly the same position, thus small discrepancies can lead to differing current orientations.

A central parameter of concern in this study is the bottom stress magnitude. Figure 13 compares the model's estimate of the near-bottom stress at the M2 frequency to that estimated using data from the moored instruments using the bulk formula (τ_{BFx}, τ_{BFy}). The agreement in the amplitude and directions is excellent. Magnitudes are consistent to within 10%. The directions of the principal axis differ by up to 15 degrees and the model appears to be biased to the counterclockwise direction at most stations.

Figure 14 shows a comparison of the model and observation-derived time-series of the stress magnitudes at Station DOT3 in the summer of 2013 (Campaign 2). The model-predicted bottom stress is shown in magenta and the blue line shows the stress computed from the Nortek ADCP velocity measurements at 0.5 m above the seabed using bulk formula, $|\tau_{BF}|$ with a drag coefficient C_{DN} computed (Equation 8). Analogous comparisons for all stations are provided in Appendix 3 to this report. During the two-month period the peak stress during a tidal cycle in the model and observations almost tripled as the current went through a spring-neap cycle. The model reproduces this variation well. The observations also show a substantial asymmetry between flood and ebb stages. During the flood stage, the maximum stress is much higher than during the ebb stage as a consequence of the flood-directed mean flow at the bottom. This characteristic of the observations is also well represented in the model predictions. The information in Figure 14 is presented for all seven stations for the three campaigns in Appendix 1 to this report.

A comprehensive set of quantitative measures of model performance for each station and each campaign summarizes the performance of the model in simulating the bottom stress (Table 3). Columns 2 and 3 in the table present the predicted mean and standard deviation at each station during each campaign, and Column 4 lists the maximum stress magnitudes. These values are compared to the means and standard deviations of the field measurements $|\tau_{BF}|$ (Columns 5 and 6) and the maximum value (Column 7), which we define to be the 98th percentile level (i.e., the value which is greater than 98% of the observations of $|\tau_{BF}|$).

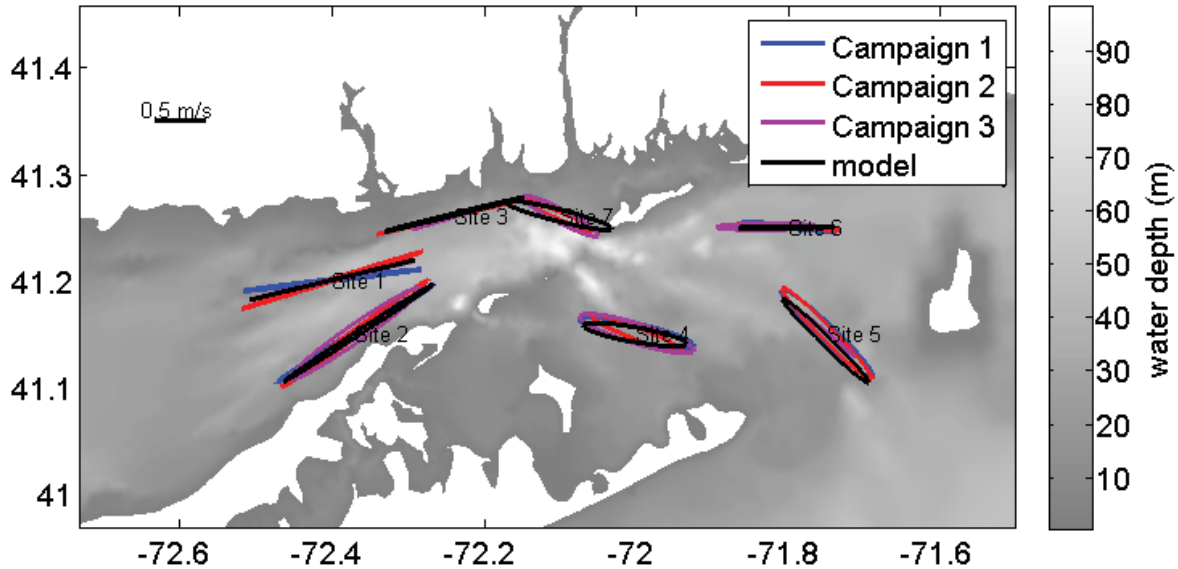

Figure 12. M2 ellipses for depth-average velocities from RDI ADCP measurements from Campaigns 1 (blue), 2 (red), and 3 (purple) and FVCOM model (black) at all seven DOT stations. The gray shading represents mean water depth.

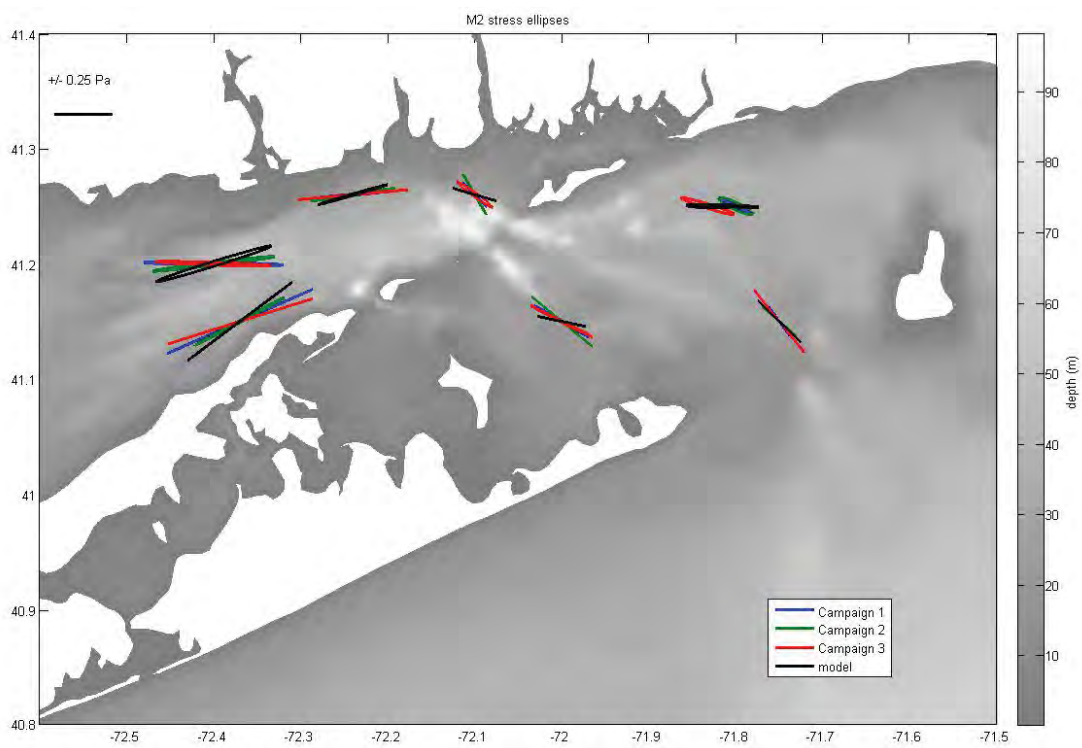

Figure 13. M2 ellipses for bottom stress, $|\tau_{BF}| = \rho_w u|u|$, calculated from bin 3 of the Nortek ADCP velocity measurements during Campaigns 1 (blue), 2 (green), and 3 (red), and from the FVCOM velocity at the bottom level (black). The gray shading represents mean water depth.

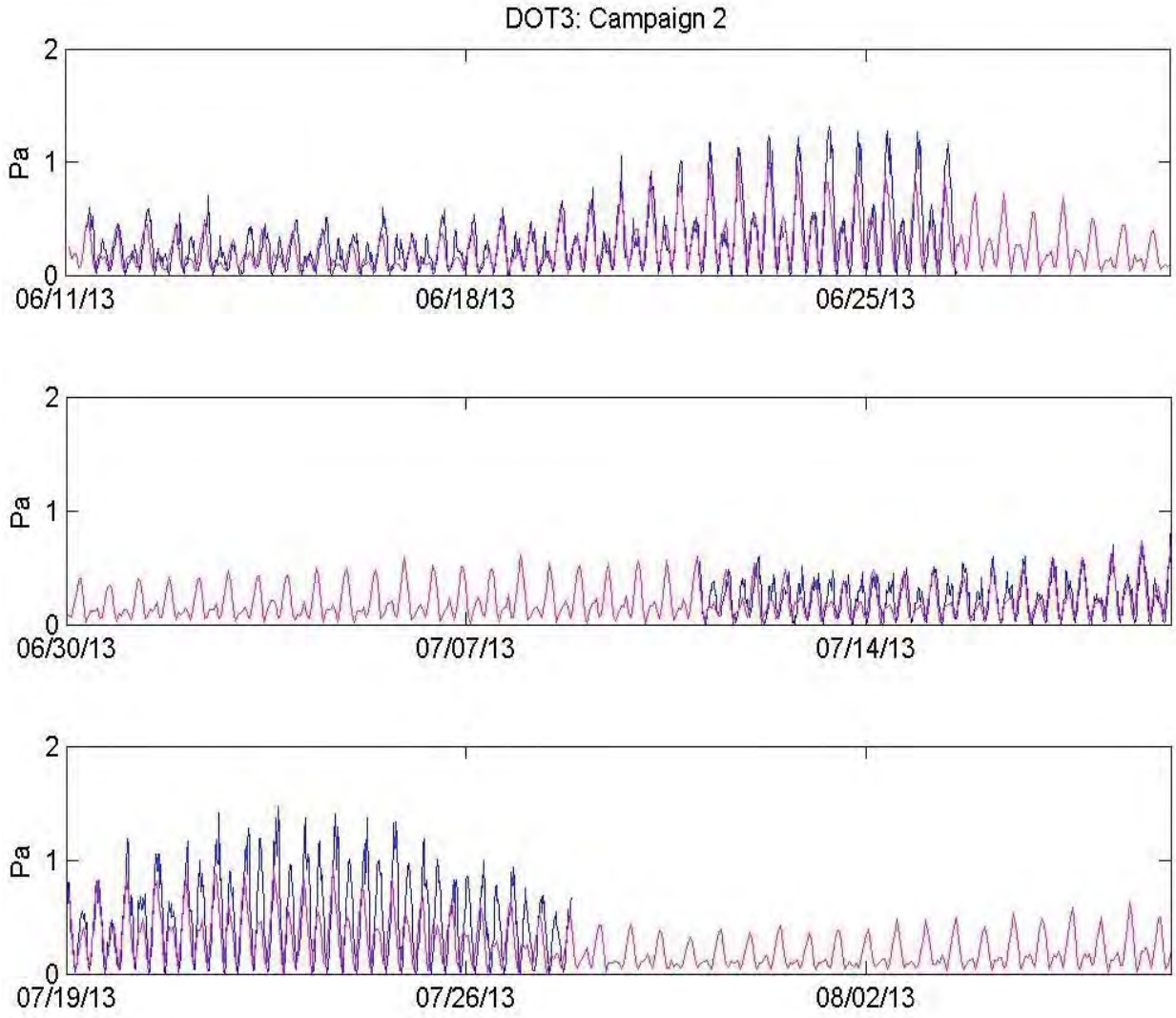

Figure 14. Model-predicted bottom stress, τ_m, at Station DOT3 during Campaign 2 in the summer of 2013 (magenta line). The blue line shows the measured stress using the bulk formula, $|\tau_{BF}|$.

Table 3. Comparison of model-predicted Mean and Maximum Bottom Stresses for each Campaign to the Mean and Maximum from the Bulk Formula Method. The Maximum Cross-correlations (r^2) and the Lag are also provided.

Station	Model ($\lvert\tau_m\rvert$)			Observation ($\lvert\tau_{BF}\rvert$)						
	Mean	STD*	Max	Mean	STD*	Max	r^2	Lag (hours)	RMSE**	MAE***
Campaign 1										
DOT1	0.36	0.27	1.18	0.43	0.34	1.18	0.87	0.33	0.18	0.13
DOT2	0.43	0.34	1.28	0.50	0.42	1.52	0.85	0.33	0.24	0.16
DOT3	0.24	0.19	0.88	0.26	0.23	0.92	0.92	0.33	0.10	0.07
DOT4	0.17	0.13	0.50	0.20	0.15	0.60	0.89	0.38	0.07	0.05
DOT5	0.19	0.15	0.82	0.16	0.16	0.64	0.47	0.38	0.16	0.12
DOT6	0.15	0.12	0.49	0.13	0.11	0.44	0.86	-0.31	0.06	0.05
DOT7	0.14	0.11	0.69	0.16	0.16	0.84	0.65	0.67	0.12	0.08
Campaign 2										
DOT1	0.44	0.31	1.61	0.41	0.31	1.36	0.82	0.36	0.18	0.14
DOT2	0.39	0.27	1.22	0.46	0.36	1.68	0.67	0.67	0.28	0.20
DOT3	0.27	0.20	1.04	0.34	0.27	1.26	0.89	0.59	0.16	0.11
DOT4	0.19	0.14	0.55	0.23	0.17	0.89	0.83	0.76	0.12	0.09
DOT5	0.19	0.14	0.73	0.23	0.21	1.11	0.52	0.62	0.19	0.14
DOT6	0.19	0.14	0.62	0.15	0.11	0.48	0.84	0.42	0.08	0.06
DOT7	0.16	0.13	0.69	0.20	0.18	0.86	0.63	0.31	0.14	0.10
Campaign 3										
DOT1	0.34	0.26	1.47	0.38	0.31	1.34	0.79	0.84	0.19	0.13
DOT2	0.43	0.34	1.53	0.47	0.37	1.37	0.72	1.00	0.26	0.19
DOT3	0.25	0.19	1.12	0.34	0.28	1.20	0.83	0.50	0.17	0.11
DOT4	0.17	0.13	0.66	0.20	0.15	0.58	0.81	0.76	0.09	0.06
DOT5	0.20	0.17	0.86	0.21	0.19	0.77	0.65	-2.19	0.14	0.10
DOT6	0.15	0.11	0.53	0.16	0.13	0.58	0.66	0.16	0.09	0.06
DOT7	0.13	0.11	0.54	0.19	0.19	0.75	0.68	0.50	0.16	0.11

*STD = Standard deviation
**RMSE = Root mean square difference between the model and lagged observation time series.
**MAE = Mean absolute error.

The predicted and measured mean stress values were compared using the Student's t statistic (see von Storch and Zwiers, 1999). The number of independent comparisons is much smaller than the number of samples since the series is auto-correlated. Using a decorrelation timescale of 1 day and a two-tailed test, we find the difference in the means is not significantly different form zero at the 95% confidence level.

Since both the model and data are dominated by variations with a 6.2-hour period, small phase differences can result in low correlations and large errors. Since phase errors are of secondary importance relative to the magnitudes, we computed the lagged cross-correlation between the model solution time series, $|\tau_m|$, and the measurement series, $|\tau_{BF}|$. The maximum lagged correlation (r^2) values are listed in Column 6 of Table 3 and the lag (in hours) is in Column 7. For completeness, the root mean square difference between the model and lagged observation time series,

$$\text{RMSE}=\sqrt{\frac{1}{N}\sum_{i=1}^{N}\left(\,|\tau_m(t_i)|-\,|\tau_{BF}(t_i-\tau)|\,\right)^2}, \tag{9}$$

and the mean absolute error,

$$\text{MAE}=\frac{1}{N}\sum_{i=1}^{N}\left|\left(\,|\tau_m(t_i)|-\,|\tau_{BF}(t_i-\tau)|\,\right)\right|, \tag{10}$$

are listed in Columns 8 and 9.

Figure 14 displays a comparison of the time-series of $|\tau_m|$ and $|\tau_{BF}|$ at Station DOT3 during Campaign 2. Table 3 shows that the model-predicted mean and maximum stresses during Campaign 2 were 0.27 and 1.04 Pa, respectively; the observations show means and 98 percentile values of 0.34 and 1.26 Pa, respectively. The maximum lagged correlation value was 0.89 at a lag of 0.59 hours. The RMSE and MAE were 0.16 and 0.11 Pa. At other stations the agreement between model results and observations was similar. The overall model performance is summarized in Figure 15a by comparing model-predicted bottom stress magnitudes and mean bottom stress magnitudes observed during the three campaigns. If the model and data were in perfect agreement all points would lie on the red dashed line. The blue solid line shows the ordinary least-squares regression line through the values obtained. The correlation coefficient, r^2 =0.91, is very high and the slope is not significantly different from 1. The predicted and observed maximum stress magnitudes are compared in Figure 15b. The correlation is lower, r^2 =0.72; however, the agreement of the predictions and observations is very good. The very low p-values ($\leq 10^{-6}$) associated with the regressions in Figure 15 indicate that the relationship is statistically significant. Differences between the predicted and observed values is substantially less than the highest stress values observed, suggesting that the model is capable of discriminating areas of high bottom stress from areas of low stress.

The pattern of the mean flow in the ZSF is important to the transport of materials and this was compared to several sets of observations. We used FVCOM to simulate the circulation from April 1 to September 31, 2010 and averaged the results to determine the near-surface (approximately top 5m) circulation (shown by the black arrows in Figure 16). O'Donnell et al. (2014a) summarized the available current observation in the area including a set of ADCPs deployed by NOAA. The

records vary in length and don't span the entire 6-month simulation interval; however, the means of the highest ADCP measurement are shown by red arrows in Figure 16 for comparison to the model predictions. The dominant pattern in the model solution in ELIS is the strong mean flow (approximately 15 cm/s) to the northeast along the north fork of Long Island and out of The Race. The red arrows are consistent with this structure in both speed and direction.

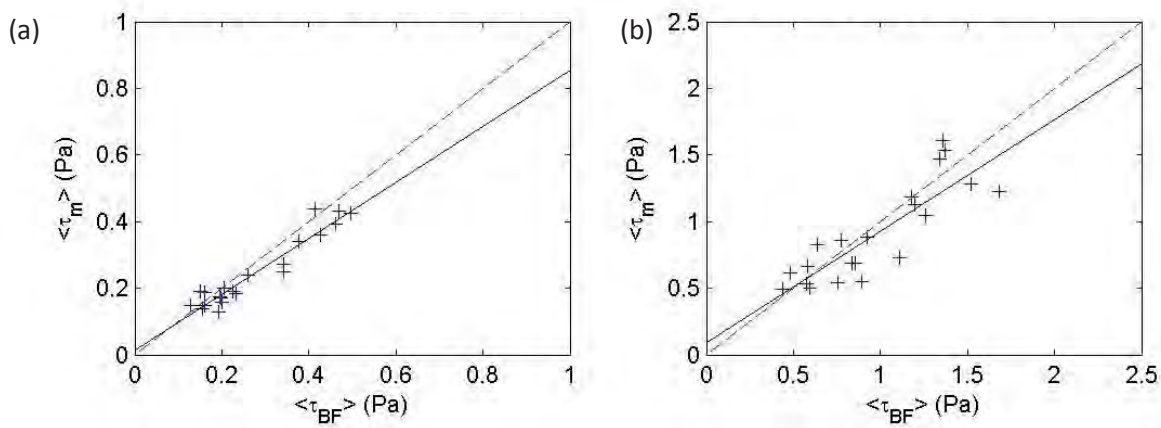

Figure 15. (a) Comparison of model predicted bottom stress magnitudes and mean bottom stress observed during the three campaigns. Points would all lie on the red dashed line if the model and data were in perfect agreement. The blue solid line shows the ordinary least-squares regression line with correlation coefficient, $\boldsymbol{r^2}$ =0.91, and p value 1.4× $\mathbf{10^{-11}}$. (b) Comparison of the predicted and observed maximum stress magnitudes. The correlation coefficient for these data-prediction pairs is, $\boldsymbol{r^2}$ =0.72 and the p value is 1.0× $\mathbf{10^{-6}}$.

The data from the three field campaigns can also be compared to the simulated mean flows at the bottom and the surface of the water column. Figures 17 to 19 show the computed mean bottom currents for the three campaigns together with the mean flow velocities (in red) computed from the lowest bin of the RDI ADCP. The velocity magnitude is shown by the length of the arrows and the scale is shown in the upper left corner of the figures. Also shown as numbered rectangles are the 11 potential dredged material disposal sites identified during the initial screening process (Louis Berger, 2013). The pattern of bottom currents is persistently to the west during the three campaigns throughout much of BIS and the deeper parts of the ELIS. The data (shown by the red arrows), though the spatial distribution of data is sparse (7 stations), are generally in agreement with the model predictions.

The mean surface circulation is shown in Figures 20 to 22. Note that the velocity scale is on the upper left of the figure and is different from the scale in Figures 17 to 19. The mean flows at the surface are similar in general to the flow pattern shown in Figure 16 for 2010. There is a persistent eastward flow near the surface from ELIS to BIS and then south eastward toward Montauk Point. Mean current velocities are highest in the summer (Campaign 2). On the north side of ELIS the surface flow is generally eastward on the eastern side of Millstone Point (longitude: -72.2º, latitude: 41.27º; near Niantic Bay) and westward on its western side. Bottom currents in contrast are uniformly westward along the north side of the ELIS.

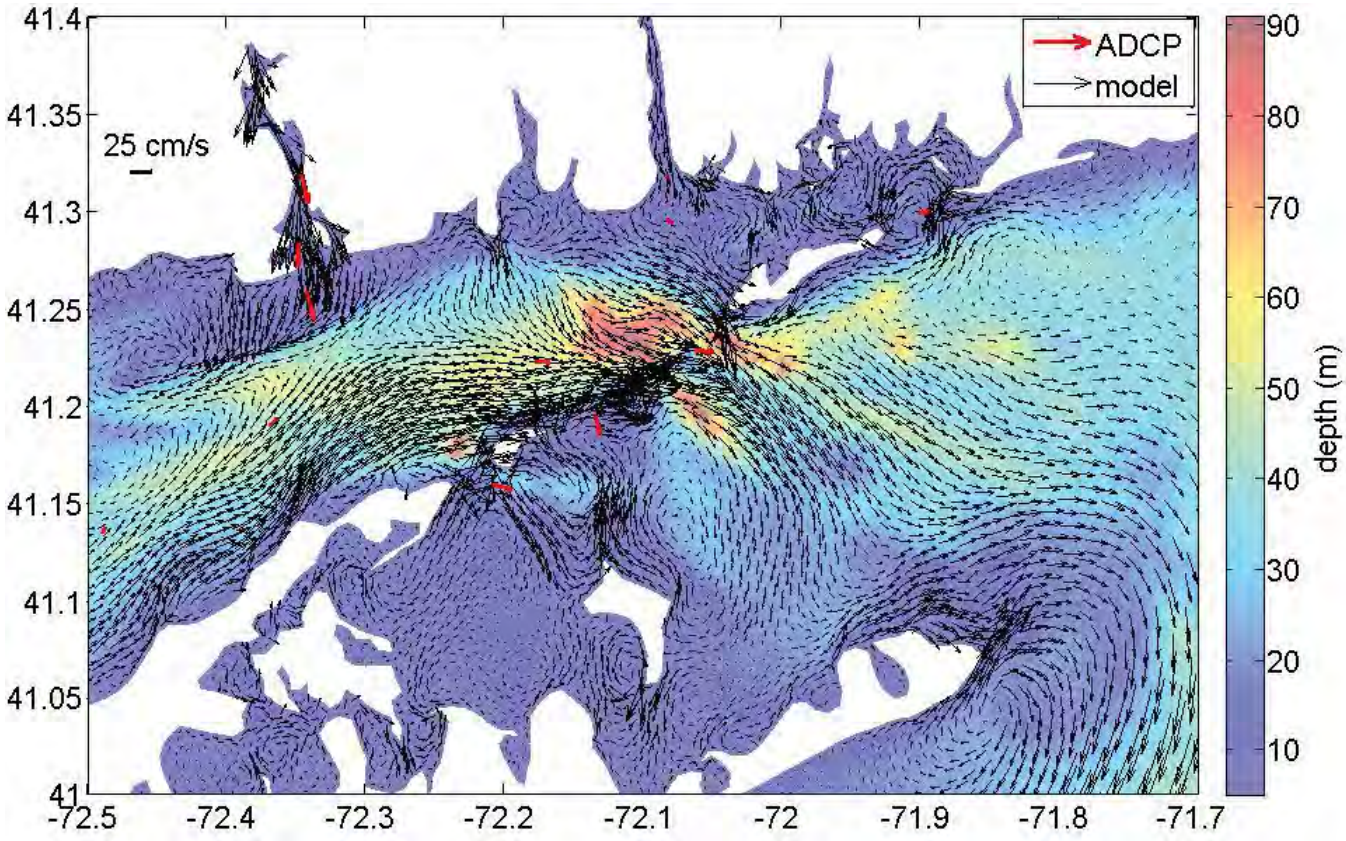

Figure 16. Mean (April-September, 2010) circulation near the surface in the ZSF from FVCOM (black arrows) and from ADCPs deployed by NOAA (red arrows). Colors show the bathymetry.

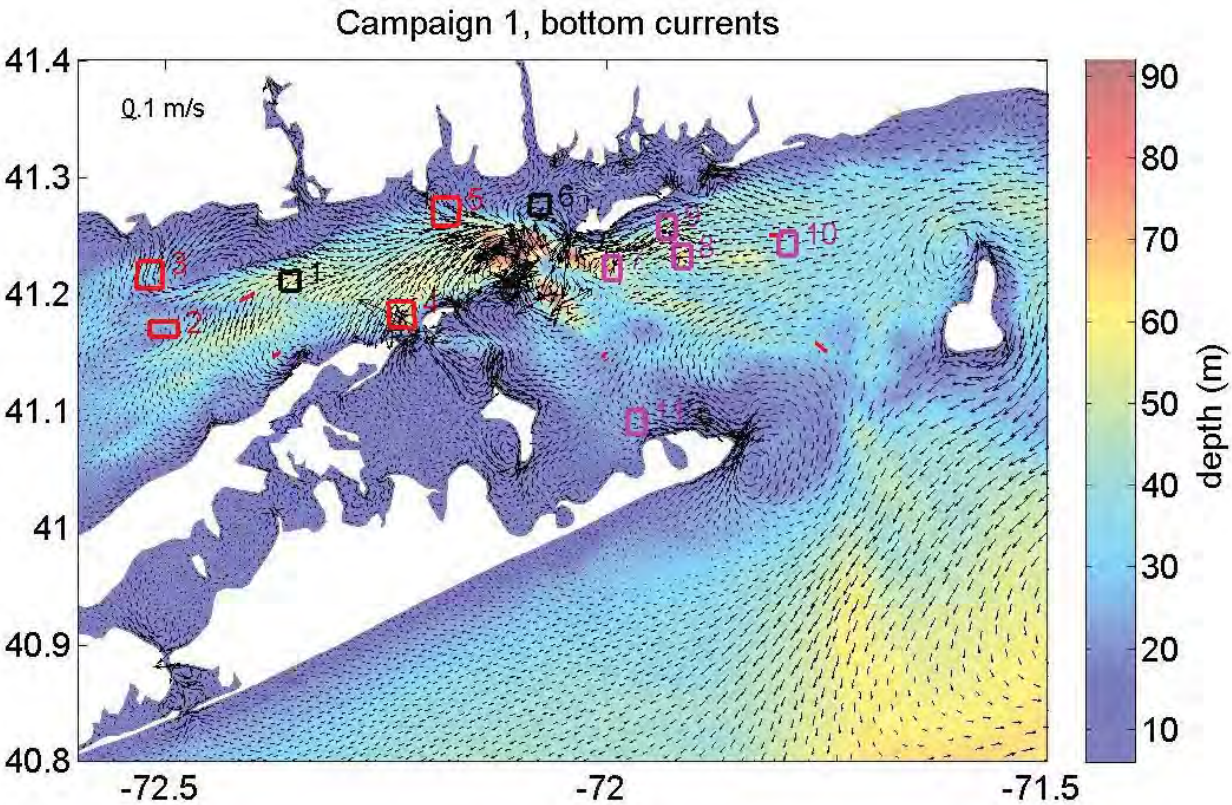

Figure 17. Time mean of the FVCOM simulated bottom currents (black arrows) during Campaign 1 (March 12 to May 17, 2013). Observations at the lowest bins of the RDI ADCPs at CTDOT1-7 are shown as red arrows. The scale for water depth is on the right. Rectangles show initially screened potential disposal sites, consisting of active disposal sites (black), historic sites (red), and 'new' areas (magenta).

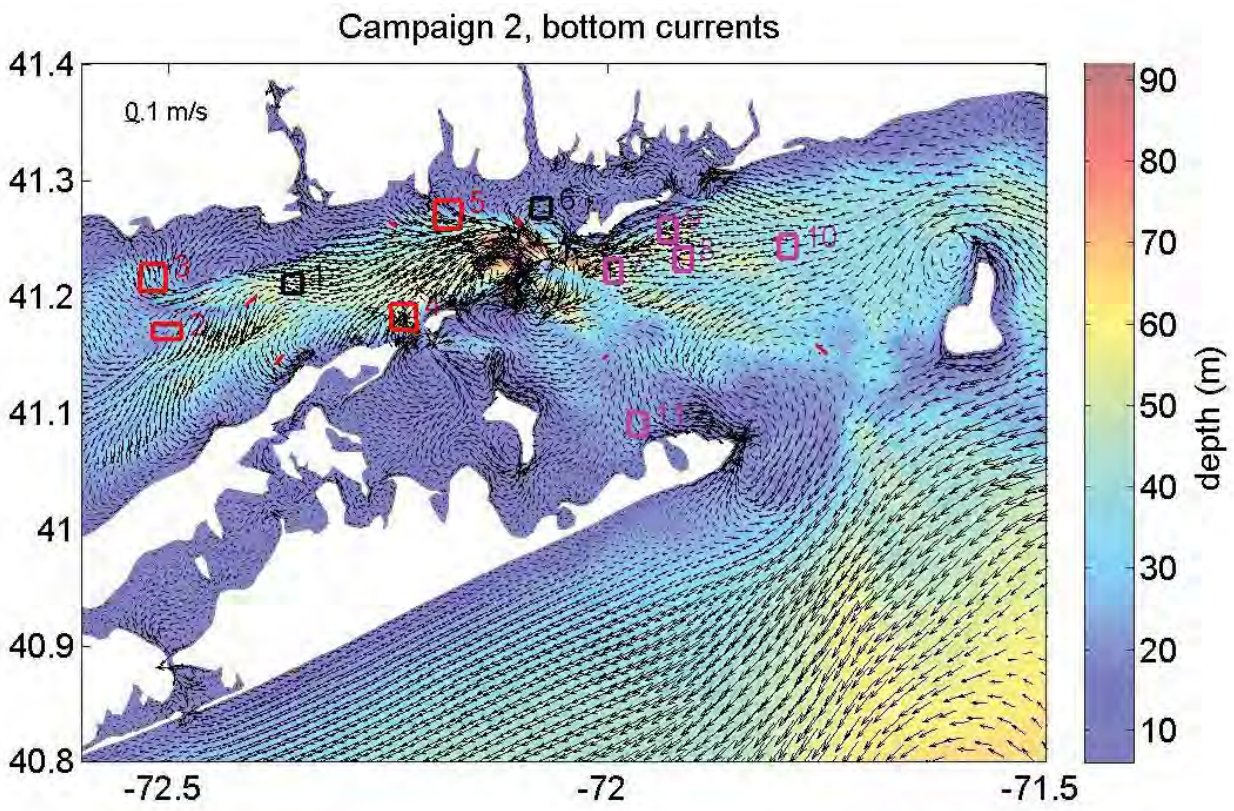

Figure 18. Time mean of the FVCOM simulated bottom currents (black arrows) during Campaign 2 (June 11 to August 8, 2013). Observations at the lowest bins of the RDI ADCPs are shown as red arrows. The scale for water depth is on the right. Rectangles show initially screened potential disposal sites, consisting of active disposal sites (black), historic sites (red), and 'new' areas (magenta).

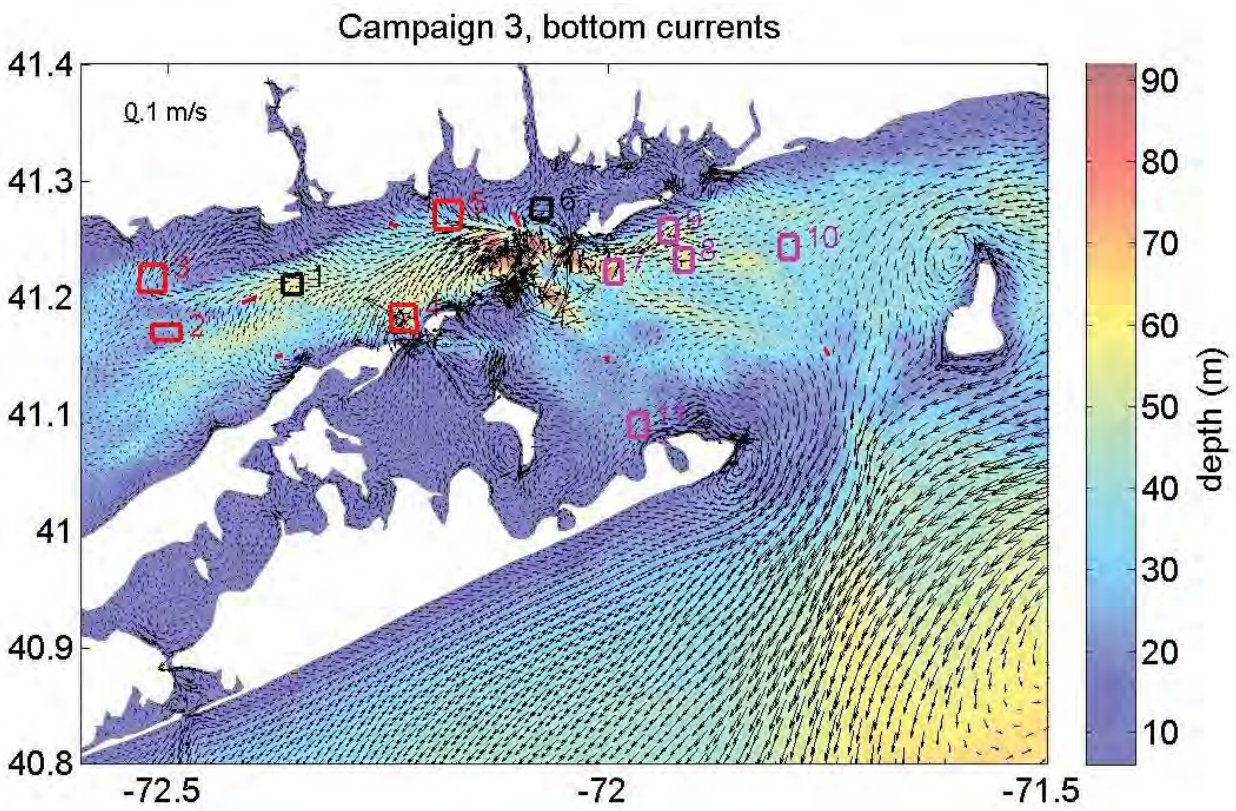

Figure 19. Time mean of the FVCOM simulated bottom currents (black arrows) during Campaign 3 (November 20, 2013, to January 16, 2014). Observations at the lowest bins of the RDI ADCPs are shown as red arrows. The scale for water depth is on the right. Rectangles show initially screened potential disposal sites, consisting of active disposal sites (black), historic sites (red), and 'new' areas (magenta).

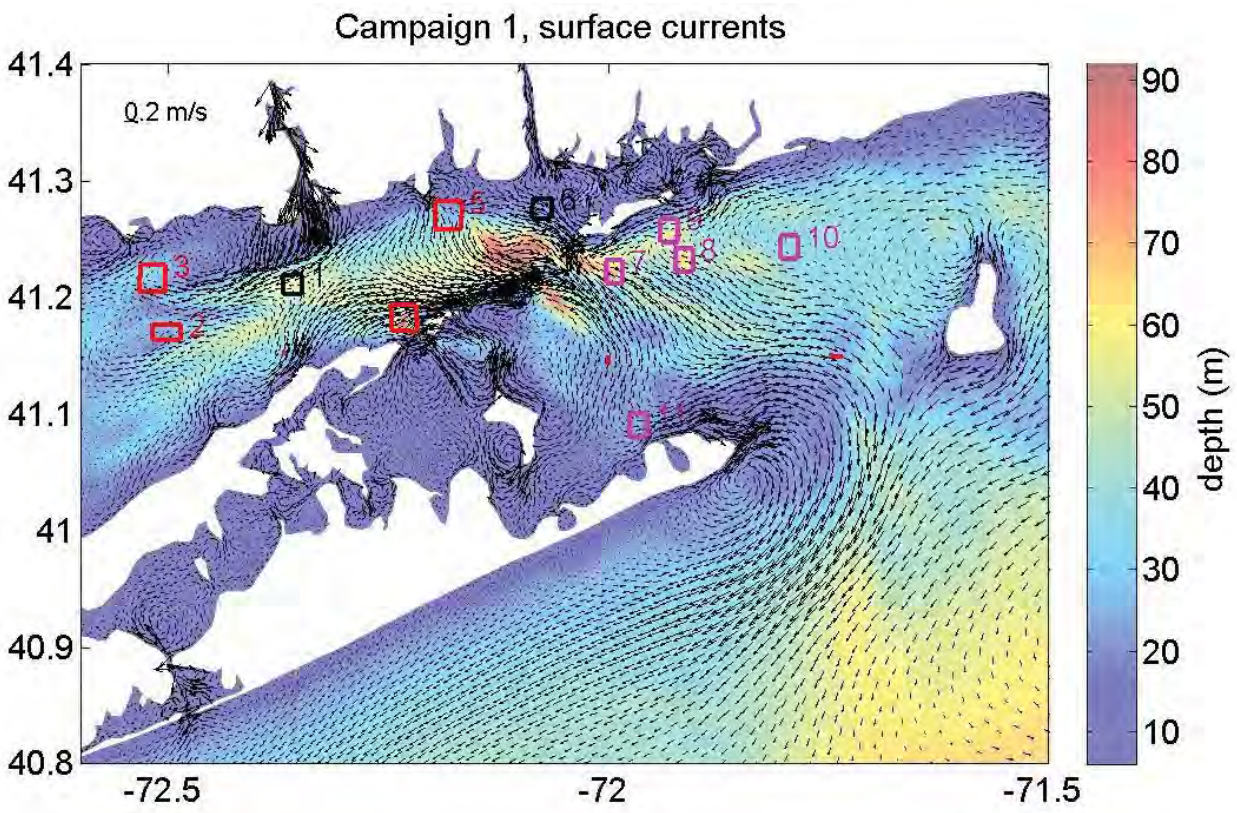

Figure 20. Time mean of the FVCOM simulated surface currents (black arrows) during Campaign 1 (March 12 to May 17, 2013). Observations at the lowest bins of the RDI ADCPs are shown as red arrows. The scale for water depth is on the right. Rectangles show initially screened potential disposal sites, consisting of active disposal sites (black), historic sites (red), and 'new' areas (magenta).

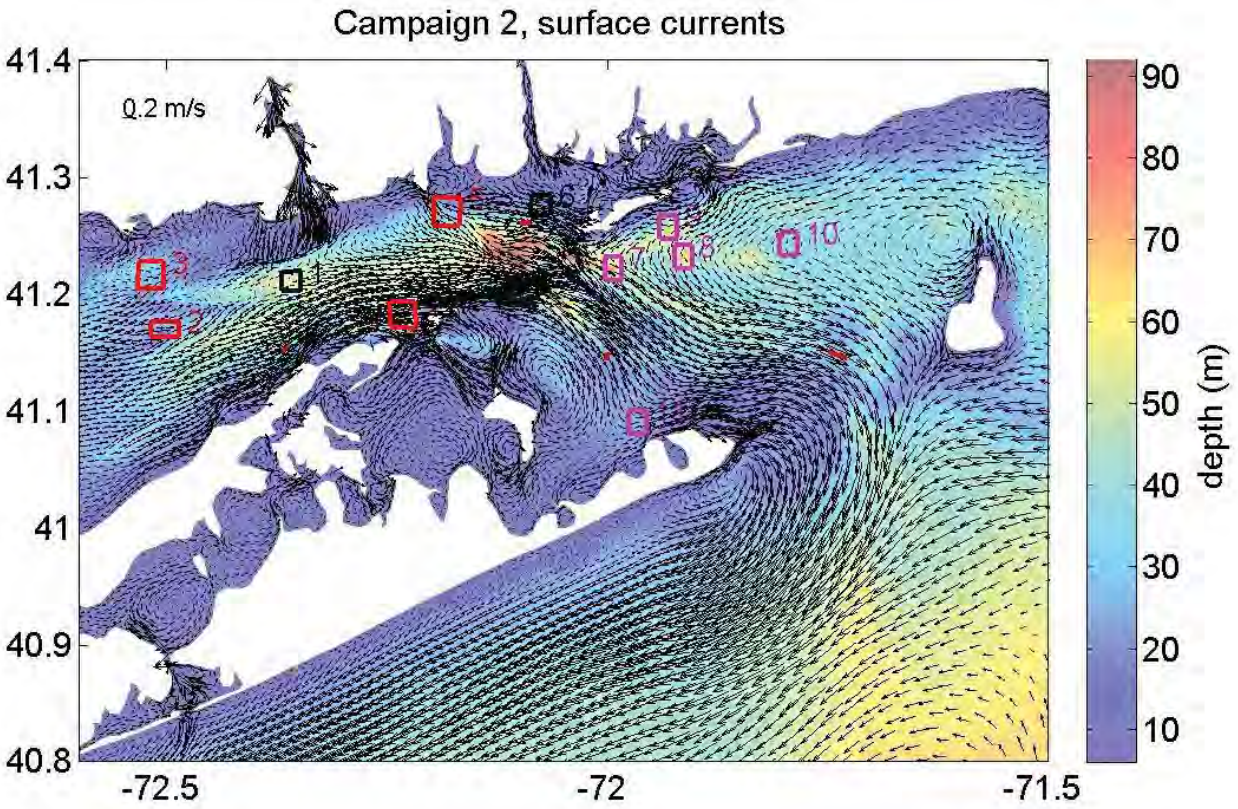

Figure 21. Time mean of the FVCOM simulated surface currents (black arrows) during Campaign 2 (June 11 to August 8, 2013). Observations at the lowest bins of the RDI ADCPs are shown as red arrows. The scale for water depth is on the right. Rectangles show initially screened potential disposal sites, consisting of active disposal sites (black), historic sites (red), and 'new' areas (magenta).

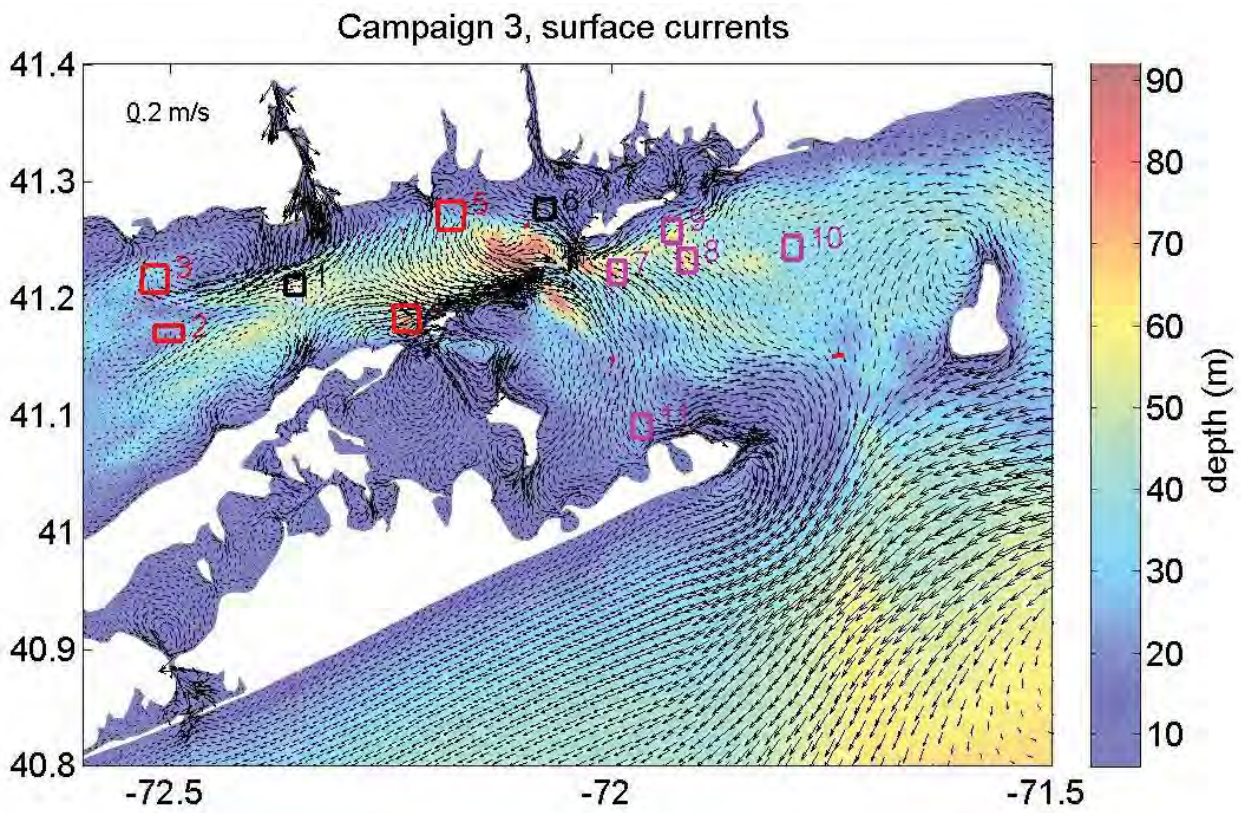

Figure 22. Time mean of the FVCOM simulated surface currents (black arrows) during Campaign 3 (November 20, 2013, to January 16, 2014). Observations at the lowest bins of the RDI ADCPs are shown as red arrows. The scale for water depth is on the right. Rectangles show initially screened potential disposal sites, consisting of active disposal sites (black), historic sites (red), and 'new' areas (magenta).

3.2 Evolution of Salinity, Temperature, and Density

The longer-term transport of materials in the coastal ocean is significantly influenced by the distribution of the density. To assess the model's ability to simulate the density distribution, SBE 37SMP CTDs were mounted on the instrument frames moored at the seven stations during the three campaigns. Additional CTD data were collected by a CTD array during boat-based surveys. The model predictions for temperature and salinity were compared to those recorded by these instruments. Figure 23 shows an example comparison of the near-bottom temperature, salinity, and density predictions at Station DOT2 for the three campaigns. At Station DOT2, the model (blue line) appears to underestimate the observations of salinity (red lines) for Campaign 1, overestimate it for Campaign 2, and is in close agreement for Campaign 3. The overall skill for salinity at this station during the entire field program is 60%.

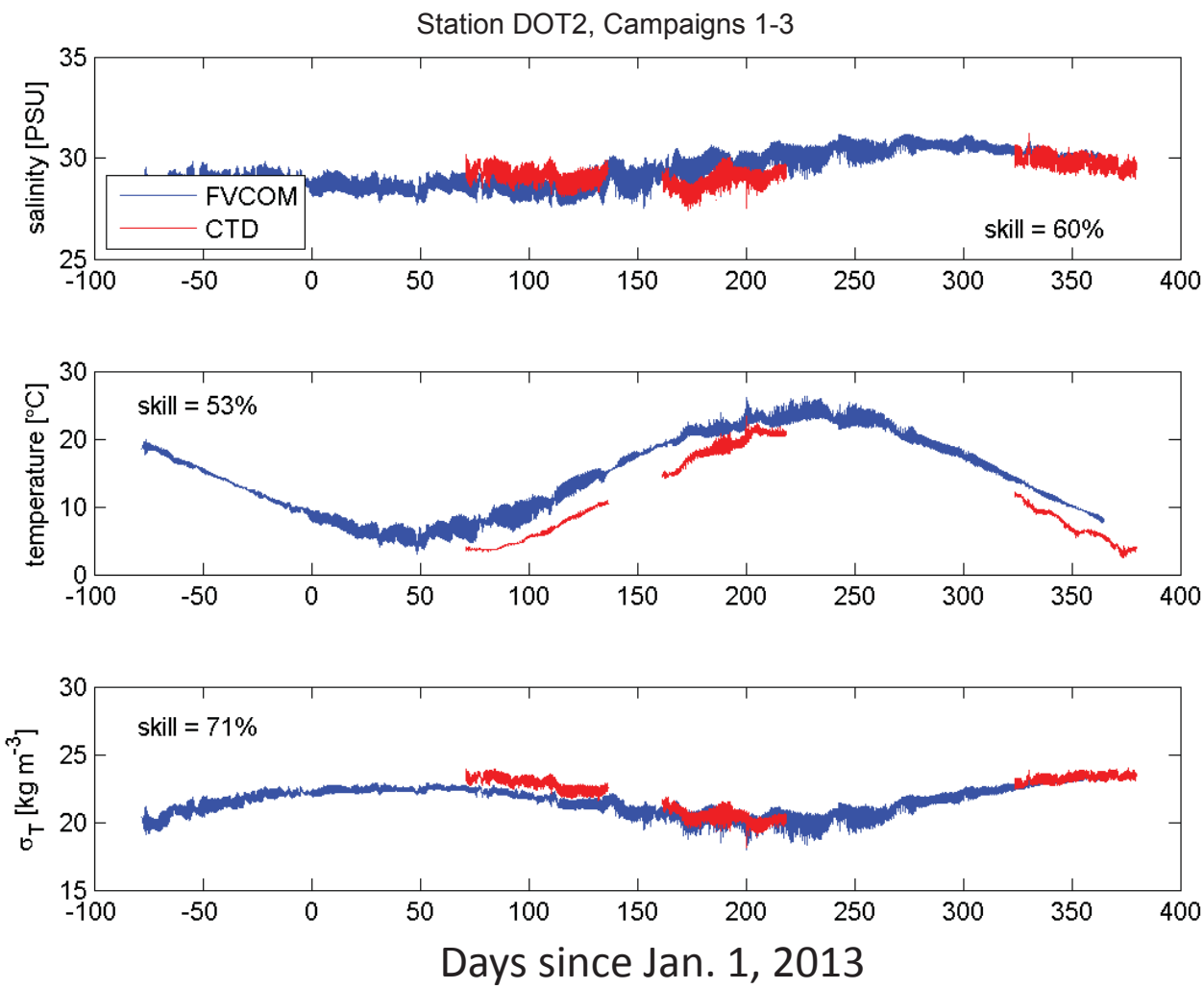

Figure 23. Comparison of near-bottom salinity (top panel), temperature (middle panel), and density (bottom panel) at Station DOT2 predicted by the FVCOM model (blue) with those measured by the bottom-mounted CTD (red).

A profiling CTD on the *R/V Connecticut* was deployed at each of the seven (DOT1-7) station during the ship surveys and mooring maintenance cruises. These measurements were compared to the FVCOM model predictions for temperature, salinity, and density. Figure 24 shows a comparison of the FVCOM model profiles for temperature, salinity, and density at Station DOT1 during Cruise 5 (August 7, 2013). Similar plots for all cruises at all stations are presented in Appendix 4 to this report.

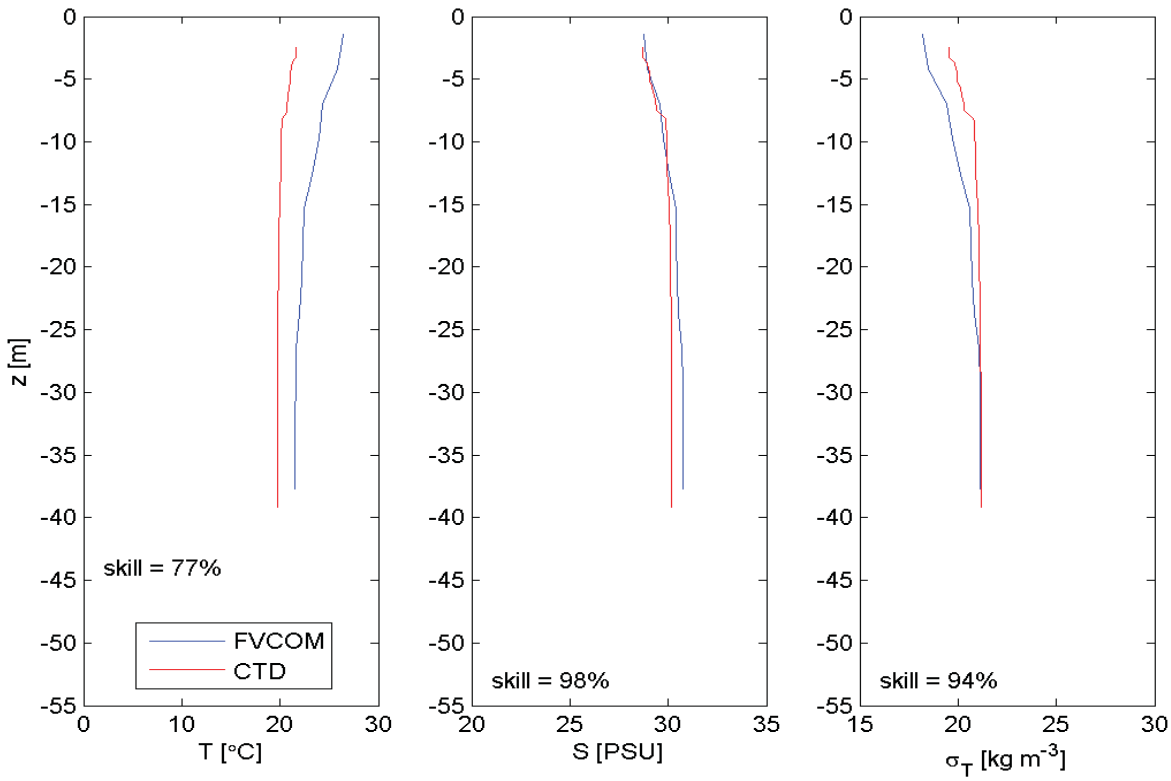

Figure 24. Contemporaneous comparison of salinity (left panel), temperature (middle panel), and density (right panel) profiles at Station DOT1 predicted by the FVCOM model (blue) with those measured by a CTD cast from the *R/V Connecticut* (red) during Cruise 5 on August 7, 2013.

3.3 Waves

The surface wave simulation module of FVCOM, SWAVE, has several options for the parametric representation of wave growth, wave breaking, and bottom friction dissipation. We tested a variety of combinations and adopted the KOM (Komen et al., 1984) wave growth formulation and enabled dissipation through bottom friction with the JONSWAP (Hasselmann et al., 1973) parameterization but disabled wave breaking. These choices yielded the best simulations and sensitivity experiments demonstrated that the results were insensitive to breaking. Figure 25 shows comparisons of the model-predicted significant wave height, H_s, at Stations DOT1 and DOT4 for 14 days during Campaign 2. The model (blue lines) and data (red triangles) agree well in these simulations. There appear to be minor lags in the model response during the larger events which are likely due to errors in the wind forcing. The overall root mean square errors in H_s are 0.2 m.

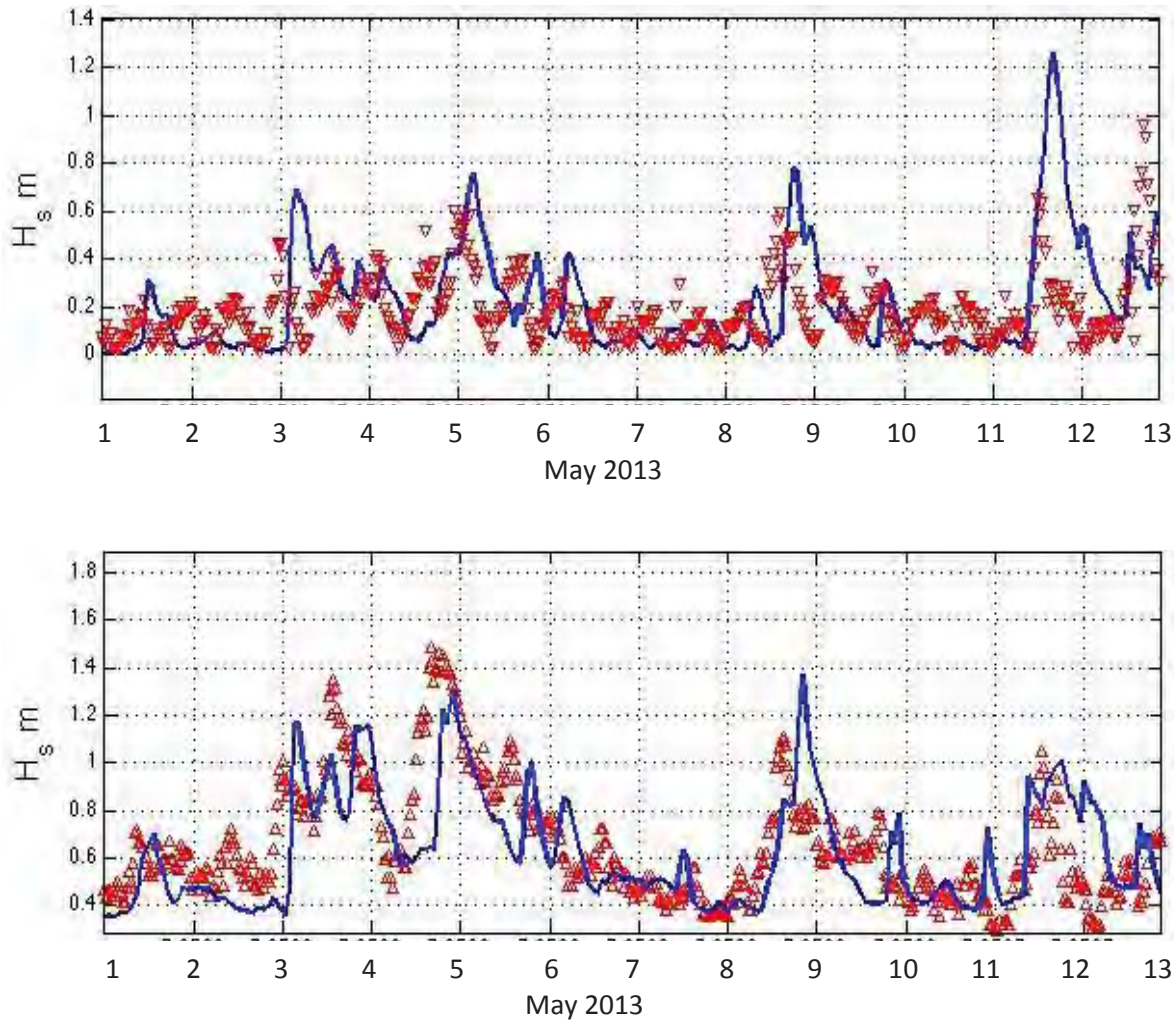

Figure 25. Comparison of model (blue line) and observed significant wave height (red triangles) at Stations DOT1 (upper panel) and DOT4 (lower panel) during May 2013.

3.4 Model Performance - Summary

The comparison of the model simulations to temperature, salinity, current and bottom stress measurements all show good agreement. Although the discrepancies between predictions and observations may be improved in the future to better represent high frequency fluctuations, the model results clearly support the model's use as a tool to interpolate spatially between the observations for assessing the characteristics of the bottom stress at potential dredged material disposal sites. Figure 15 in particular demonstrates that the model predicts the observed spatial structure of the mean bottom stress and the maximum bottom stress at the sites where data is available with an error that is much less (approximately 15-20%) than the range of stresses found in the area. The predicted spatial structure is therefore a useful guide for the evaluation of bed sediment stability at potential disposal sites during a wide range of conditions.

4. Bottom Stress Distributions and Variability

The distribution of bottom stress during 'fair-weather' and 'storm' conditions is relevant for the determination of the stability of sediments on the seafloor. The comparison of observations to model predictions has demonstrated that the model can accurately represent the stress variation at and between the stations used during the observation campaigns. Conditions described and modeled for the ZSF include the following:

- **Fair-weather Conditions:** Distribution of the maximum bottom stress that is due to the long-term mean flow and the principal tidal constituents in the area (M_2, N_2, S_2, M_4 and M_6). These conditions assume that winds are calm, not contributing to bottom stress.

- **Storm Conditions:** Distribution of the maximum stress that occurred at any time during the simulations for the three observation campaigns periods (spring, summer, and winter). The three campaigns included weather typical for the respective seasons.

- **Superstorm Sandy Conditions:** Occasionally, severe storms create high winds and anomalous currents in the ZSF. To evaluate their potential impact, the maximum stress magnitudes for Superstorm Sandy (October 28-31, 2012) were simulated with the model.

Model results for the three conditions described above were then used to evaluate the 11 initially screened potential sites for the disposal of dredged materials (Figure 26). Specifically, the simulated distributions of bottom stress were determined for points near the center of these sites.

4.1 Bottom Stress during Fair-weather Conditions

During fair-weather conditions, the bottom stress is only caused by tides and the seasonal mean flow. Winds are comparatively calm, not affecting bottom stress. The spatial distributions of maximum bottom stress in the ZSF during fair-weather conditions are presented in Figures 27 to 29 for the three observation campaigns. The colors represent values of $\log_{10} \tau_b$ where τ_b is the shear stress at the bottom in Pascal (Pa). The bottom stress distributions during the three campaigns are similar to each other, differing only as a result of slight seasonal changes in the mean flow magnitude. These stress distributions are the lower limit of the maximum stresses to be expected since the forcing by strong winds will generally increase stresses in specific areas.

Generally, the bottom stress magnitude in many of the deeper areas of the ZSF approaches 1 Pa for some time during the spring-neap tidal cycle. As a consequence of the high bottom stress in these areas, only coarse sand is typically found on the seafloor. Lower maximum bottom stress is predicted for the western edge and northern part of the BIS. The bottom stress is lowest to the northwest of Block Island between Stations DOT6 and CTD10. In the ELIS, areas of comparatively low bottom stress occur in nearshore areas, as well as in the area to the south of the mouth of the Thames River; this area contains the active New London dredged material disposal site (NLDS).

The maximum fair-weather bottom stress values for the 11 potential disposal sites are presented in Table 4. By far, the highest bottom stresses (1.2-1.4 Pa) are predicted to occur at Site 1 (Cornfield Shoals). Lowest stresses in ELIS are predicted for Site 4 (Orient Point; 0.3-0.5 Pa) and

Site 6 (New London; 0.4-0.5 Pa). Lowest stresses in the BIS are predicted for Site 9 (Fishers Island – center; 0.3-0.4 Pa) and Site 11 (North of Montauk; 0.3-0.4 Pa).

Table 4. Model Predicted Maximum Bottom Stress (Pa) during Fair-weather Conditions (i.e., due to Tides and Seasonal Mean Flow only) at Potential Dredged Material Disposal Sites

Potential Disposal Site			Campaign 1 (spring)	Campaign 2 (summer)	Campaign 3 (winter)
ELIS	1	Cornfield Shoals	1.26	1.43	1.31
	2	Six Mile Reef	0.99	1.03	1.09
	3	Clinton Harbor	0.68	0.63	0.80
	4	Orient Point	0.32	0.50	0.45
	5	Niantic Bay	0.80	0.81	0.85
	6	New London	0.45	0.53	0.54
BIS	7	Fishers Island-west	0.84	0.85	0.74
	8	Fishers Island-east	0.43	0.53	0.43
	9	Fishers Island-center	0.32	0.37	0.33
	10	Block Island Disposal Site	0.46	0.58	0.49
	11	North of Montauk	0.30	0.30	0.37

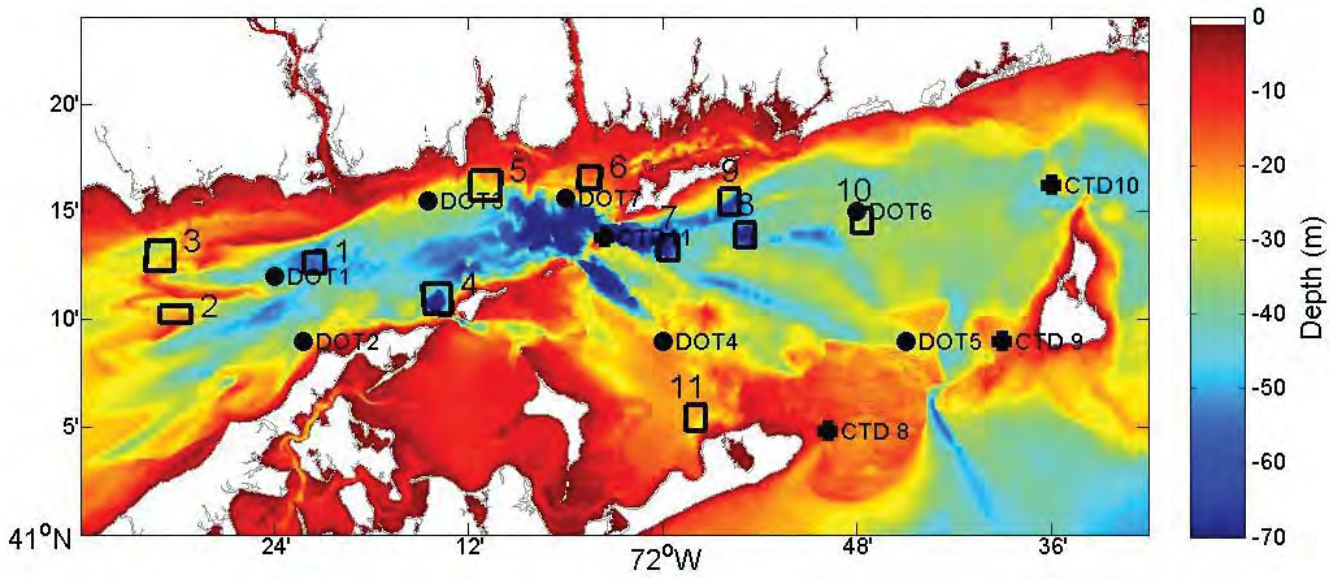

Figure 26. Bathymetry (in m) of the ZSF showing the 11 potential dredged material disposal sites (open boxes) as identified during the initial screening process (Louis Berger, 2013). Sites 1 and 6 are the active disposal sites (CLIS and NLDS, respectively). The seven mooring stations ('DOT') are identified by full circles; the four additional ship survey stations ('CTD') are identified by crosses.

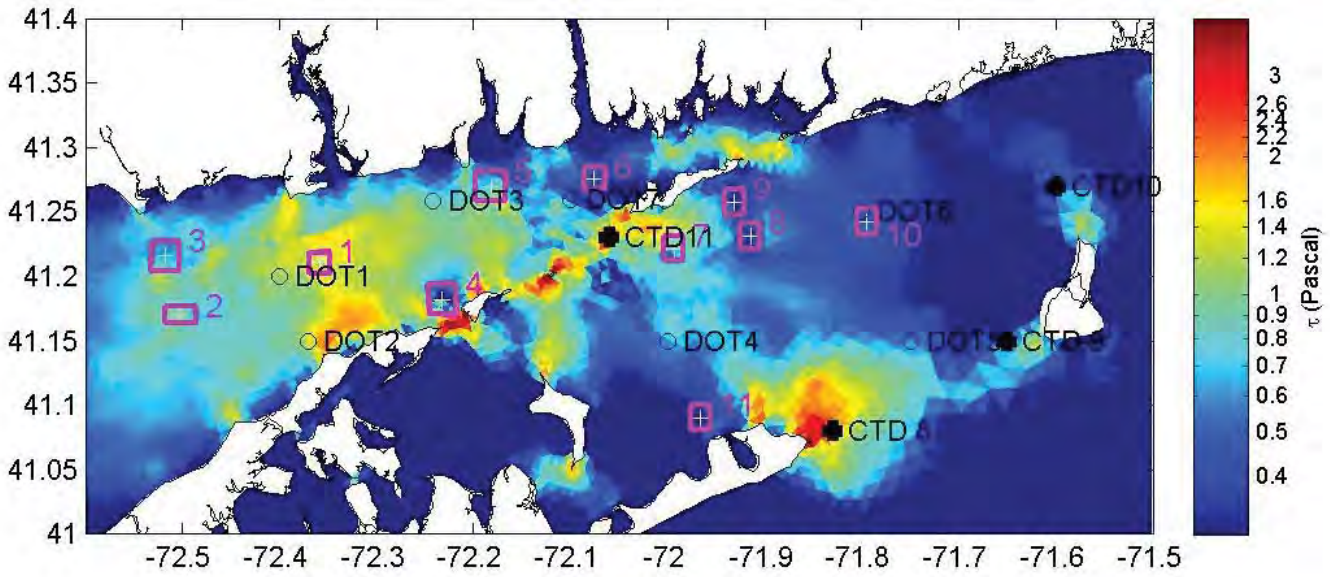

Figure 27. Maximum bottom stress during Campaign 1 (March 12 to May 17, 2013) for fair-weather conditions (i.e., due to the principal tidal current constituents and the seasonal mean flow only).

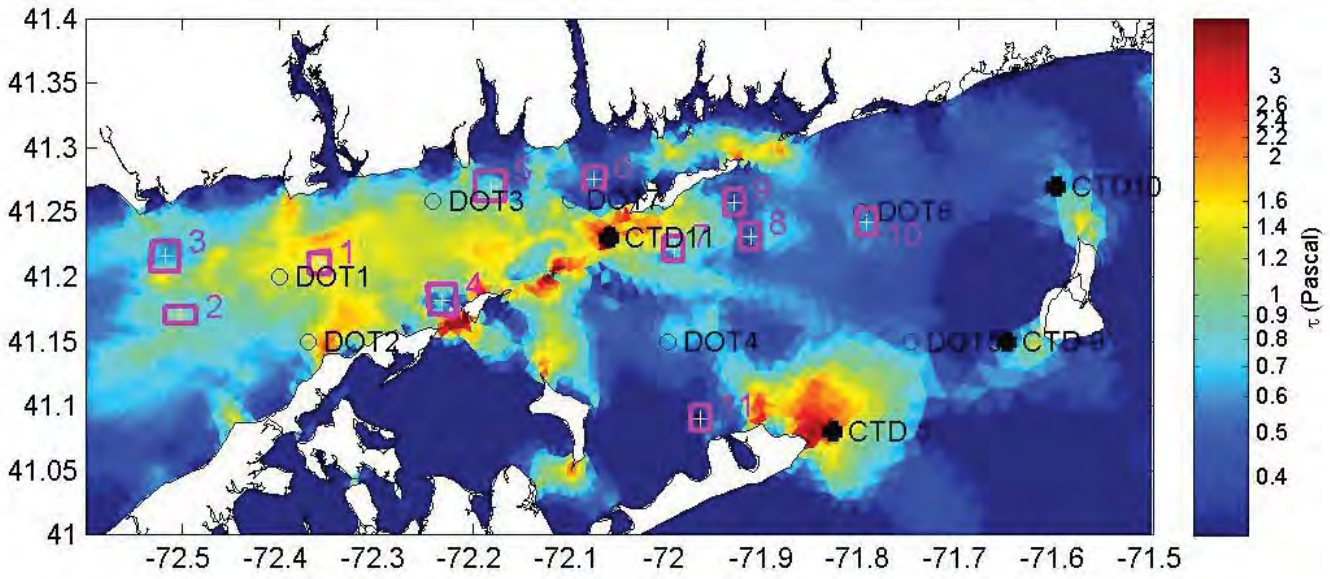

Figure 28. Maximum bottom stress during Campaign 2 (June 11 to August 8, 2013) for fair-weather conditions (i.e., due to the principal tidal current constituents and the seasonal mean flow only).

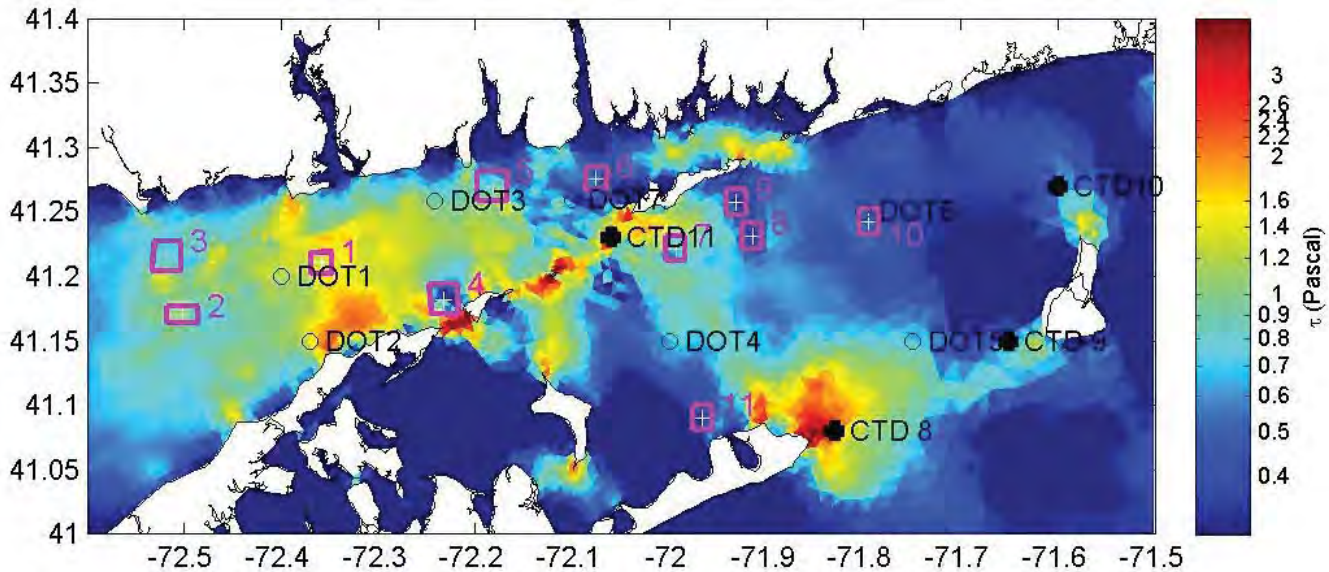

Figure 29. Maximum bottom stress during Campaign 3 (November 20, 2013, to January 16, 2014) for fair-weather conditions (i.e., due to the principal tidal current constituents and the seasonal mean flow only).

4.2 Bottom Stress during Storm Conditions

During storm conditions, the bottom stress is affected by a combination of (a) tides and seasonal mean flow, and (b) strong winds. The spatial distributions of maximum bottom stress in the ZSF during storm conditions are presented in Figures 30 to 32 for the three observation campaigns. Campaign 1 spanned the spring (March-May) when the waters are cool, winds and waves are usually energetic and the maximum discharge in the Connecticut River occurs. Campaign 2 occurred during the warmer summer period (June-August) when high winds and waves are less common and the river flow is below average. Campaign 3 spanned the winter months (November-January) when the waters are cold, winds and waves energetic and the river flow is low. The observations are summarized in O'Donnell et al. (2014a). It is important to note that though the mean wind speed and wave heights are smaller in the summer and larger in the fall and winter, the maxima show less contrast.

Table 5 lists the maximum bottom stress values at the centers of the 11 potential disposal sites and compares these bottom stress values with values from fair-weather conditions. The differences in stress are modest for most sites.

The various changes in the maximum stress predicted at the 11 sites listed in Table 5 are a function of complex interactions between several oceanographic and atmospheric mechanisms. However, it is clear that at some of the identified potential sites the maximum stresses during storms are similar to stresses during fair-weather conditions. Changes (increases as well as reductions) in the maximum stress during storms occur at Sites 1, 2, 3, 5, 7, 8, 10 and 11; these changes are small relative to the spatial variations across the ZSF and the expected reliability of the model stress predictions. Stress reductions are likely caused by the reduction in the magnitude of the residual circulation when strong winds blow in a direction counter to the mean flow. At Cornfield Shoals (Site 1) the mean flow is strongly to the west and eastward winds reduces it. The pattern of reduced maximum stress is similar in the spring and winter (Campaigns 1 and 3) for Six Mile Reef (Site 2), but not during the summer (Campaign 2), which shows a 5% increase in the maximum stress.

At Orient Point (Site 4) the maximum bottom stress during storm conditions in the spring is predicted to be up to 61% higher than during fair-weather conditions. In the other seasons the increase is much lower. The large increase in the spring is likely a consequence of an increase in the magnitude of the residual circulation to the east due to eastward winds. This is also likely the case at Fisher Island – center (Site 9). At New London (Site 6), bottom stress values are predicted to be between 29% and 33% higher during storm conditions; this increase is also largely the result of an increase in mean flow which is generally weak at this site during fair-weather conditions.

Table 5. Model Predicted Maximum Bottom Stress (Pa) during Storm Conditions at Potential Dredged Material Disposal Sites

Potential Disposal Site			Maximum Bottom Stress (Pa)			Change in Maximum Bottom Stress during Storm Conditions relative to Fair-weather Conditions		
			Campaign 1 (spring)	Campaign 2 (summer)	Campaign 3 (winter)	Campaign 1 (spring)	Campaign 2 (summer)	Campaign 3 (winter)
ELIS	1	Cornfield Shoals	1.17	1.31	1.24	-7%	-8%	-5%
	2	Six Mile Reef	0.92	1.09	1.00	-7%	6%	-8%
	3	Clinton Harbor	0.72	0.71	0.81	6%	14%	1%
	4	Orient Point	0.52	0.61	0.48	61%	21%	7%
	5	Niantic Bay	0.73	0.97	0.84	-8%	19%	-2%
	6	New London	0.60	0.70	0.69	33%	31%	29%
BIS	7	Fishers Island-west	0.79	0.91	0.86	-5%	8%	17%
	8	Fishers Island-east	0.49	0.51	0.39	12%	-5%	-9%
	9	Fishers Island-center	0.39	0.50	0.38	20%	36%	15%
	10	Block Island Disposal Site	0.49	0.63	0.44	6%	9%	-12%
	11	North of Montauk	0.31	0.31	0.34	0%	5%	-7%

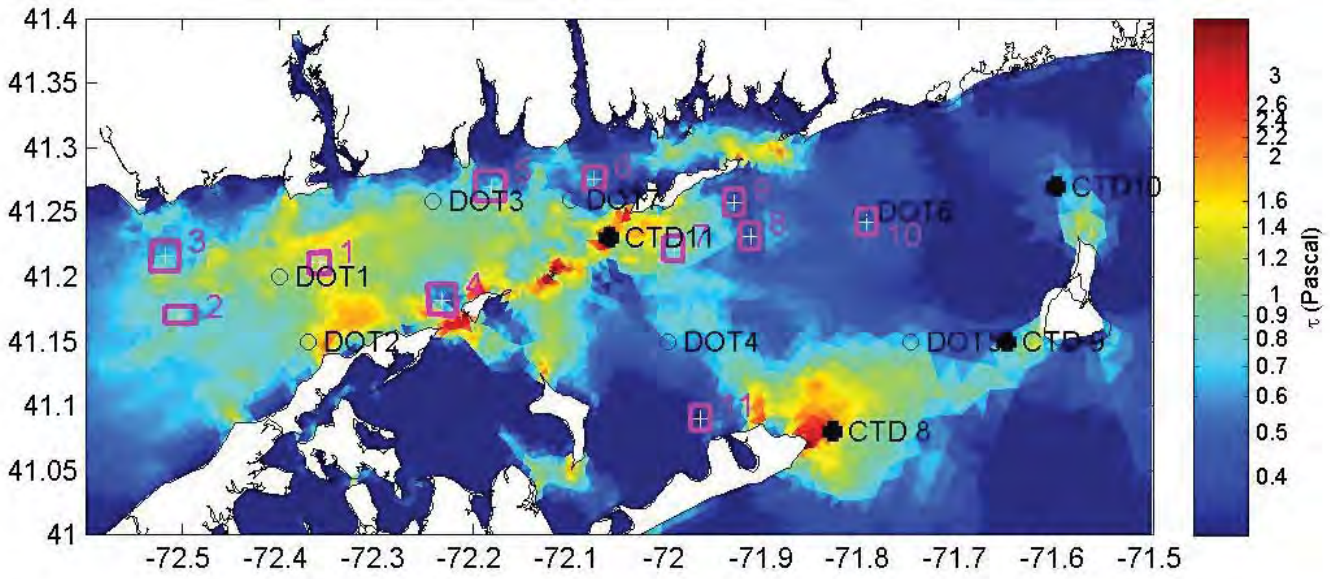

Figure 30. Maximum bottom stress during Campaign 1 (March 12 to May 17, 2013) for storm conditions (i.e., due to the principal tidal current constituents and the seasonal mean flow, as well as wind).

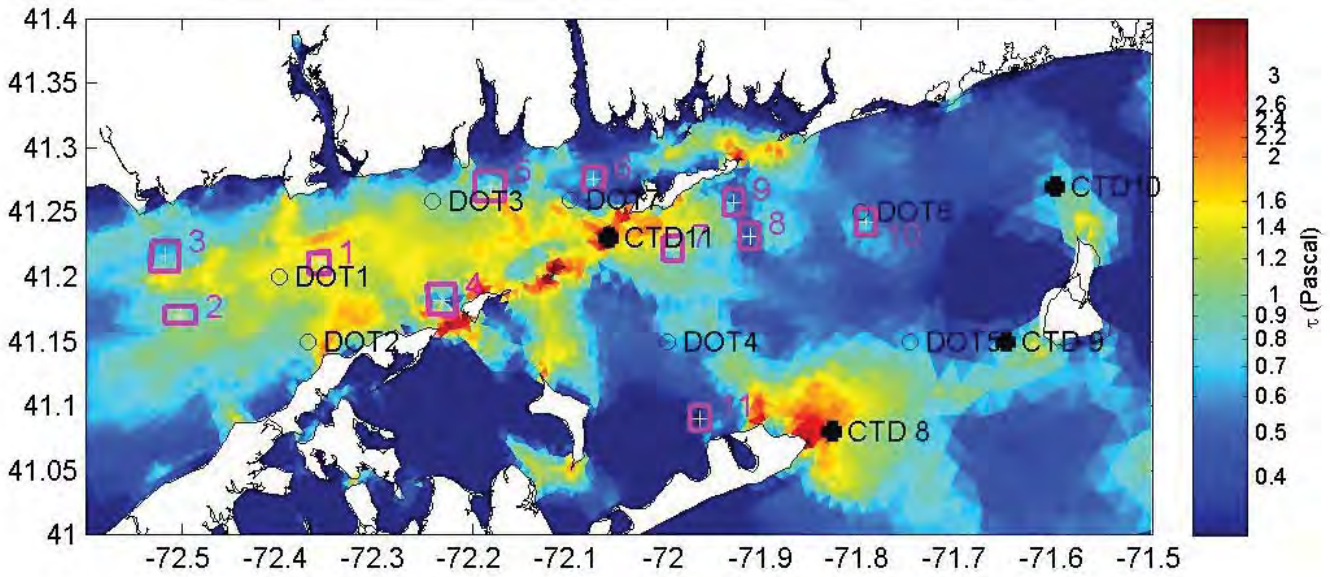

Figure 31. Maximum bottom stress during Campaign 2 (June 11 to August 8, 2013) for storm conditions (i.e., due to the principal tidal current constituents and the seasonal mean flow, as well as wind).

.

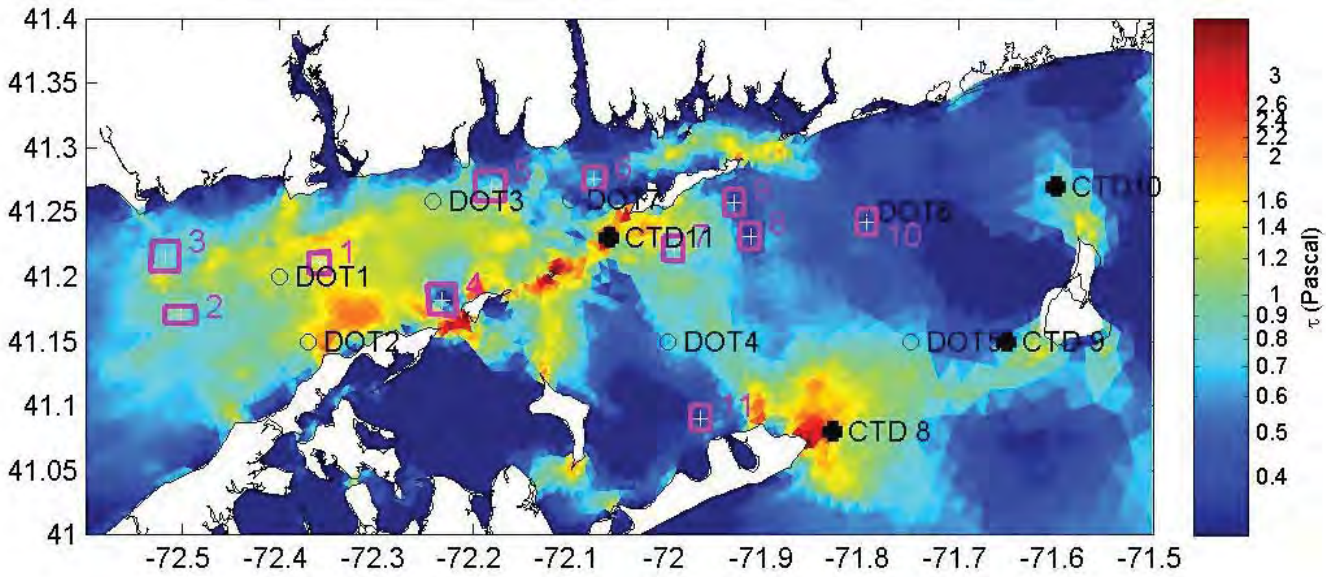

Figure 32. Maximum bottom stress during Campaign 3 (November 20, 2013, to January 16, 2014) for storm conditions (i.e., due to the principal tidal current constituents and the seasonal mean flow, as well as wind).

.

4.3 Superstorm Sandy

Superstorm Sandy passed over New England during October 28-31, 2012. Though the field instrument moorings were not deployed during this period we used FVCOM to simulate the pattern of circulation and stress that occurred in response to the wind forcing. Note that the predictions are likely more uncertain during this period since measurements are not available to assess FVCOM in such high wind conditions. Simulated maximum bottom stress is shown in Figure 33. Comparison of Figure 33 with Figure 32 shows that there is a modest increase in bottom stress and an expansion of the areas with high stress into shallower water.

The maximum bottom stress values at the 11 potential disposal sites during Superstorm Sandy are presented in Table 6, along with the change in stress relative to fair-weather and storm conditions during Campaign 3. The simulated stress due to Superstorm Sandy increases at most sites, particularly in BIS where the wind-driven currents are strong. The stress during the superstorm decreases at the Cornfield Shoals and New London sites, however, as a consequence of the modification of the circulation.

Table 6. Model Predicted Maximum Bottom Stress (Pa) at Potential Disposal Sites during a simulated Superstorm Sandy.

Potential Disposal Site			Superstorm Sandy Conditions		
			Bottom Stress (Pa)	**Change in Bottom Stress during 'Sandy' relative to Fair-weather Conditions during Campaign 3** *(i.e., Table 4)*	**Change in Bottom Stress during 'Sandy' relative to Storm Conditions during Campaign 3** *(i.e., Table 5)*
ELIS	1	Cornfield Shoals	1.16	-11%	-6%
	2	Six Mile Reef	1.26	16%	25%
	3	Clinton Harbor	0.87	9%	8%
	4	Orient Point	0.53	17%	9%
	5	Niantic Bay	0.99	16%	19%
	6	New London	0.48	-10%	-30%
BIS	7	Fishers Island-west	1.17	58%	35%
	8	Fishers Island-east	0.46	5%	16%
	9	Fishers Island-center	0.55	69%	47%
	10	Block Island Disposal Site	0.73	49%	68%
	11	North of Montauk	0.39	6%	14%

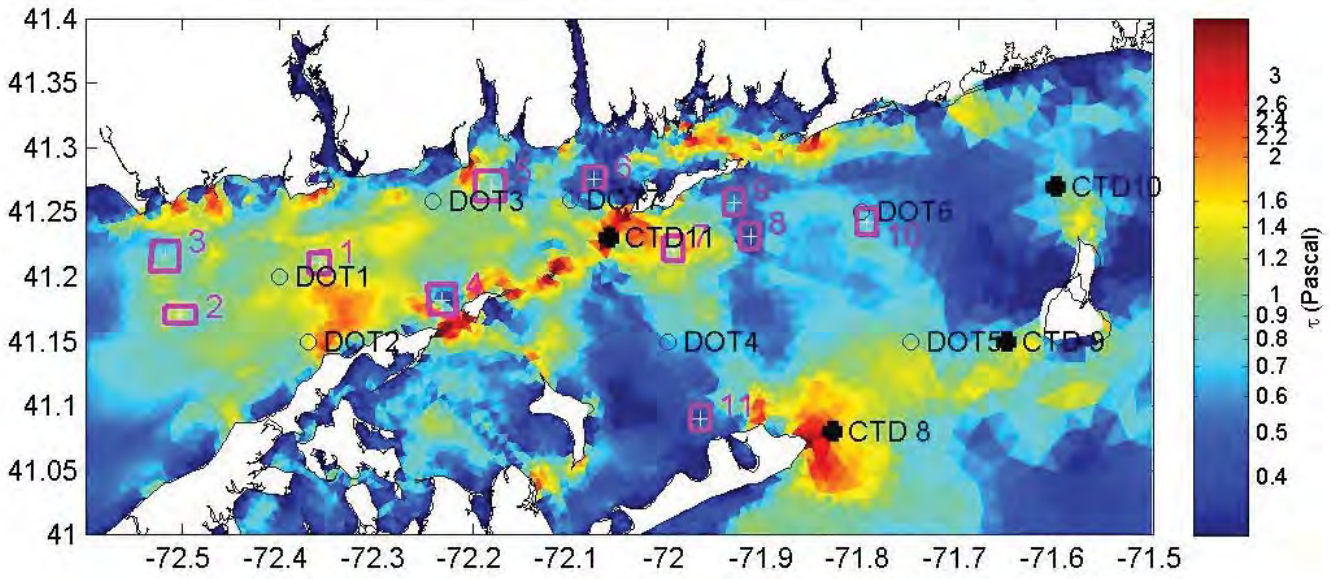

Figure 33. Maximum bottom stress simulated for the period October 28 to 31, 2012 when Superstorm Sandy passed over New England.

5. Sediment Resuspension and Bottom Stress

The bottom stress is significant in the site selection process because stress values above a threshold can resuspend sediment on the bottom. Sediment deposited in an area where the stress is frequently above the threshold would not be expected to stay there. The threshold, or critical stress value, is determined by factors such as the particle size, density, and organic matter content. Selection of an appropriate value for screening site options is an important choice. This chapter presents a review of recent work on the critical stress.

The resuspension and transport of non-cohesive sediment on the bottom of an estuary is controlled by the stress imparted by the movement of the overlying water (Graf, 1971; Raudkivi, 1976). Many empirical assessments agree that when the ratio of the buoyancy of the particles to the boundary stress times the cross-sectional area of a particle exceeds a critical threshold, particles begin to move. This ratio is known as the 'Shields parameter' and is expressed as $\Theta = \tau_b/(\rho_s - \rho_w)gd$ where τ_b is the magnitude of the bottom stress (Pa); ρ_s and ρ_w (kg/m^3) are the densities of the sediment and water, respectively; g (m/s^2) is the acceleration of gravity; and d is the sediment particle diameter. In practice, d is usually estimated as the median diameter of a sample, referred to as d_{50}. When the magnitude of the bottom stress is estimated by the stress velocity as $\tau_b = \rho_w u_*^2$, then the Shields parameter can be written as

$$\Theta = u_*^2/sgd \tag{11}$$

where $s = \frac{\rho_s - \rho_w}{\rho_w}$ is the relative density of the sediment.

The critical value of the Shields parameter at which sediment motion begins, Θ_{c0}, has been studied extensively for non-cohesive particles (e.g., van Rijn, 1993) and the results are commonly summarized graphically. Mathematical expressions for the dependence of the Θ_{c0} on the particle Reynolds number ($R_p = \frac{d\sqrt{sgd}}{\nu}$, where $\nu = 1 \times 10^{-6}\ m^2/s$ is the kinematic viscosity) have been developed by Brownlie (1981), Buffington and Montgomery (1999), Yalin and da Silva (2001), and Cao et al. (2006). The Brownlie formula is

$$\Theta_{c0} = 0.22\mathrm{R_p}^{-0.9} + 0.06\exp\left(-17.77\ \mathrm{R_p}^{-0.09}\right). \tag{12}$$

The Cao et al. (2006) formula is

$$\Theta_{c0} = \begin{Bmatrix} 0.1414 \times \mathrm{R_p}^{-0.2306} & \mathrm{R_p} \leq 6.61 \\ \mathrm{f}(\mathrm{R_p}) & 6.61 < R_\mathrm{p} < 282.84 \\ 0.045 & \mathrm{R_p} \geq 282.84 \end{Bmatrix} \tag{13}$$

where $\mathrm{f}(\mathrm{R_p}) = \exp\left\{-0.6769 \ln \mathrm{R_p} + 0.3542 \ln\left(1 + \left(0.223\mathrm{R_p}\right)^{2.8358}\right) - 1.1296\right\}$.

These expressions are shown by the red and blue lines in Figure 34. They are clearly consistent for $d > 50\ \mu$m but diverge at the small size limit where there is little data and much scatter arising from cohesion effects.

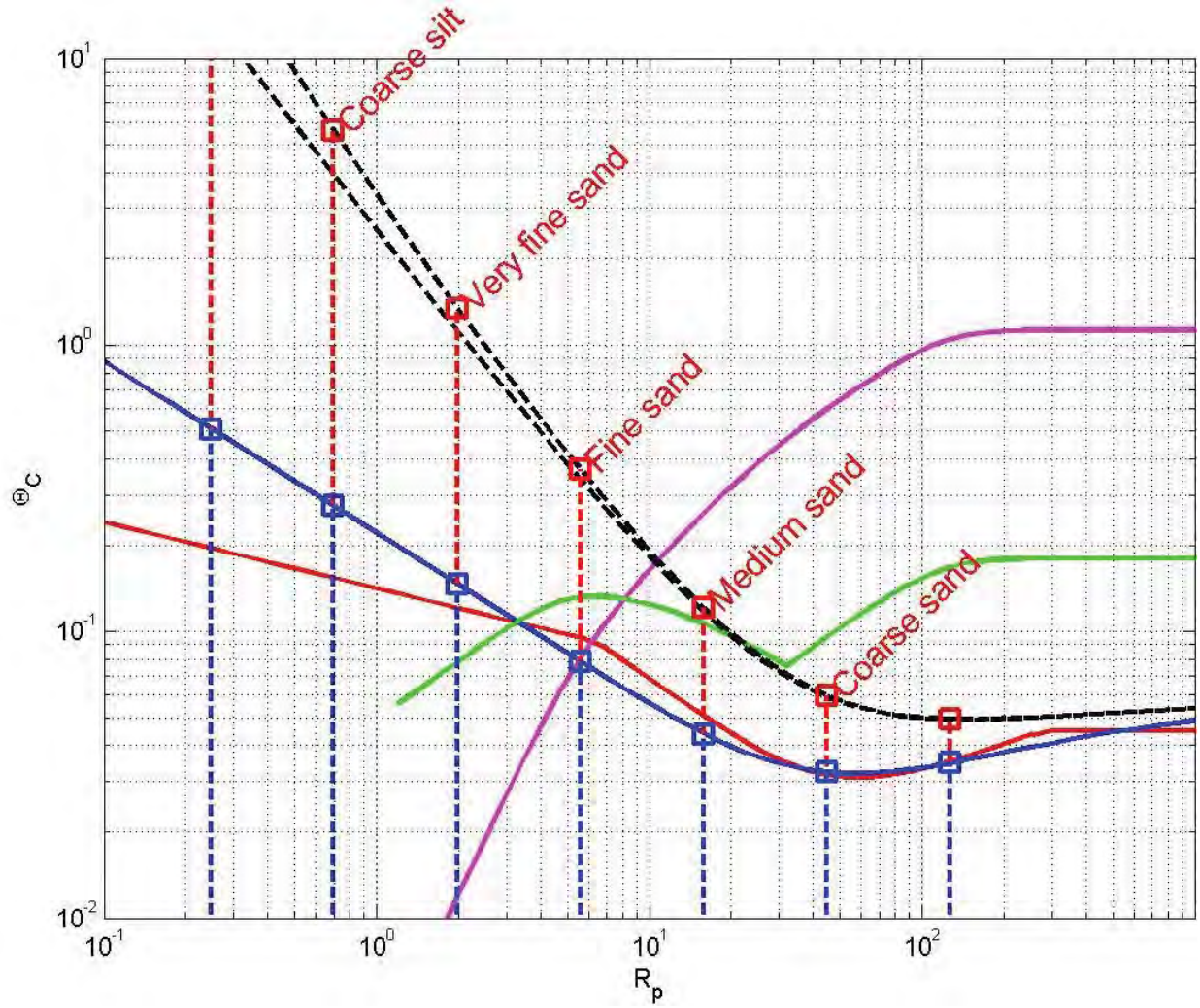

Figure 34. A graphical representation of the relationship between sediment particle size for cohesive and non-cohesive particles.

The red and blue solid lines are analytical representations of the critical Shields parameter, $\Theta_{c0} = \tau_{c0}/\rho_w sgd$, for non-cohesive sediments as a function of the particle Reynolds number. The black dashed lines show the influence of cohesion and adhesion on the critical value for the onset of particle motion.

The green and magenta lines show the critical values for the onset of sediment suspension as predicted by Bagnold (1966) and van Rijn (1984), respectively. The lower boundaries of the particle Reynolds numbers for traditional sediment classes (see Table 7) are shown by the blue dashed lines.

The initiation of motion is not generally sufficient for substantial sediment transport and van Rijn (1984) proposed that the resuspension of particles by turbulence required a much higher Shields parameter threshold. In an earlier paper on suspended particle transport Bagnolds (1966) had argued that the turbulent fluctuation in the vertical velocity component must be greater than the settling velocity of particles (w_s) if particles were to remain in suspension. He predicted the values of the Shields parameter that would be required and it is shown by the magenta line in Figure 34. Van Rijn (1993) used observations to estimate the threshold for suspension empirically and expressed the results as

$$\Theta_{vR} = \begin{cases} \dfrac{16 w_s^2}{R_p^{4/3}(sgv)^{2/3}} & 1 \le R_p \le 10^{2/3} \\ \dfrac{0.16\, w_s^2}{R_p^{2/3}(sgv)^{2/3}} & R_p > 10^{2/3} \end{cases} \tag{14}$$

which is shown in Figure 34 as the green curve. This threshold for suspension is approximately a factor of five higher than the threshold for motion for sand particles though much lower than the Bagnolds (1966) prediction. Van Rijn (1984) concluded that his limit is likely a lower bound.

At small particle sizes, smaller than approximately 50 μm (i.e., silt and clay), the stabilizing influence of inter-particle electrochemical interactions become more important than the gravitational forces and the Shields parameter threshold Θ_{c0} has to be augmented. Ternat et al. (2008) developed a model and conducted experiments on the effects of porosity, grain size distribution, and cohesion in freshwater sediments. Following the work of Lick et al. (2004), Righetti and Lucarelli (2007) proposed that for cohesive sediments the effective critical Shields parameter could be defined as

$$\Theta_c = \Theta_{0c} + \Theta_{cC} + \Theta_{cA} \tag{15}$$

where Θ_{0c} is the function for non-cohesive sediments, i.e., the Brownie formula. Θ_{cC} and Θ_{cA} were introduced to represent the effects of inter-particle cohesion and adhesion, respectively. The cohesion function is expressed by Righetti and Lucarelli (2007) as

$$\Theta_{cC} = \frac{\Theta_{0c}}{\alpha_3} \frac{c}{s\, g\, d^2} \tag{16}$$

where $\alpha_3 = 0.523$ for nearly spherical particles. The effects of adhesion of particles is described by

$$\Theta_{cA} = \frac{\Theta_{0c}}{\alpha_3} \frac{A}{s\, g\, d} \ . \tag{17}$$

The effects of adhesion decrease more slowly than cohesion as the particle size increases. The combined effects of these two mechanisms are shown by the dashed black line in Figure 34 using $c = 5 \times 10^{-5}$ N/m and $A = 0$ and $a = 3.5$ N/m. Righetti and Lucarelli (2007) show experimental results that are consistent with these parameter choices. These choices for parameters A and c values are important to the prediction of the critical stress and few estimates are available. It is clear, however, that they are sensitive to the clay fraction and organic matter content and must be selected to describe the conditions at potential disposal sites.

In Figure 34 the values of the particle Reynolds number, R_p, for the lower boundaries of the sediment size classes listed on the left of Table 7 are shown by dashed blue and red lines. The blue squares show the intersections of the R_p values with the Shields curve and the critical values for the initiation of motion of non-cohesive particles, $\Theta_{c0}(R_p)$, are listed in Column 5 of Table 7. The dimensional stress values, τ_{c0} for particles with $s = 1.56$ are listed in the sixth column. Values range from 0.12 to 0.26 Pa. These are very small. To provide insight to the flow velocity necessary to create this stress, the quadratic drag law is exploited to estimate the velocity 1m above the bottom as $u_1 = \sqrt{\tau_{c0}/\rho_w}$ and the results are provided in Column 7 of Table 7. These estimates suggest that currents in the range of 0.22 to 0.32 m/s will move all non-cohesive sediments.

Table 7. Particle Size and Critical Stress for Cohesive and Non-cohesive Sediments.

Size				Non-Cohesive Sediments			Cohesive Sediments		
	Particle Size		Reynolds Number	Critical Shields Parameter	Critical Stress	Critical Velocity	Critical Shields Parameter	Stress at the Initiation of Motion	Critical Velocity
Classification	**Phi**	**d** (mm)	**R_p**	**Θ_{c0}**	**τ_{c0}** (Pa)	**$u_{1,0}$** (m/s)	**Θ_c**	**τ_c** (Pa)	**u_1** (m/s)
Column No.	*2*	*3*	*4*	*5*	*6*	*7*	*8*	*9*	*10*
Coarse sand	1-0	0.50	44.96	0.03	0.26	0.32	0.06	0.48	0.44
Medium sand	2-1	0.25	15.90	0.04	0.18	0.27	0.12	0.49	0.44
Fine sand	3-2	0.13	5.62	0.08	0.16	0.25	0.37	0.74	0.54
Very fine sand	4-3	0.06	1.99	0.15	0.15	0.24	1.33	1.35	0.73
Coarse silt	5-4	0.03	0.69	0.27	0.14	0.23	5.62	2.81	1.06
Medium silt	6-5	0.02	0.25	0.51	0.13	0.23	26.33	6.64	1.63
Fine silt	7-6	0.01	0.09	0.95	0.12	0.22	143.41	18.09	2.69

Notes: Columns 5 to 7 provide example magnitudes of the critical shields parameter, Θ_{c0}, for non-cohesive sediments and the stress τ_{c0} at the initiation of motion for the lower bounds for specific particle size classes listed on the left. An estimate of the magnitude of the required current at 1m above the seafloor required to create the critical stress for non-cohesive sediments is provided as $u_{1,0} = \sqrt{\tau_{c0}/\rho C_d}$ where $C_d = 2.5 \times 10^{-3}$ is assumed. Analogous estimates for cohesive sediments are provided Columns 8 to 10 based on the theory presented by Righetti and Lucarelli (2007). Values shaded in blue are extrapolations beyond the range of particle sizes used in parameterization.

Columns 8 to 10 in Table 7 show analogous estimates for cohesive sediments using the model of Righetti and Lucarelli (2007). The red squares in Figure 34 show $\Theta_c(R_p)$, the critical values of the modified Shields parameter, and these are listed in Column 8 of Table 7. The corresponding stress and velocity are also provided. Note that the predictions for small particles extrapolate the empirical model outside of the size interval for which data are available and these very large and uncertain stress values are shaded in blue in Table 7.

As reflected in Table 7, the model predicts that the range of stresses necessary to initiate motion is much larger for cohesive sediments than for non-cohesive sediments. The magnitude of the stresses would require velocities in the range of 0.44 to 2.69 m/s based on the bulk formula with $C_d = 0.0025$. These estimates are only guidance values for the range of stresses that are of interest. The character of the sediments at a particular site must be established to determine the appropriate critical stress values and these are likely to lie between the blue and black lines of Figure 34. The example calculations show that small cohesive particles require much larger stresses to initiate motion than predicted by the original Shields curve (red and blue lines in Figure 34). It is also important to note that van Rijn's (1984) threshold for suspension (green line in Figure 34) intersects the modified Shields parameter threshold (black line) in the medium sand size class. This implies that for particles smaller than medium sand, initiation of motion and suspension are simultaneous. Once these particles are in motion they can be suspended and transported rapidly.

For particles in the size range of coarse silt to fine sand (0.03 to 0.13 mm) Table 7 shows that the critical value of the Shields parameter for non-cohesive particles ranges from 0.08 to 0.27, which implies a critical shear stress of 0.16 to 0.14 Pa. However, for cohesive particles the work of Righetti and Lucarelli (2007) and Lick et al. (2004) suggests that the critical value of the Shields parameter is in the range 0.37 to 5.62, implying a critical shear stress of 0.54 to 1.06 Pa. This is a substantial difference. Righetti and Lucarelli (2007) made parameter choices to illustrate the potential magnitude of the effects of adhesion and cohesion so the values are not directly relevant to the ZSF; however, they did demonstrate the substantial influences of a small clay size fraction. There is also considerable other evidence that supports substantially higher critical shear stress in complex marine sediments. Van Ledden et al. (2004) described the principal effects of mud (silt/clay) on the critical erosion stress threshold for sand-mud mixtures and demonstrated that the mixture exhibited significant cohesion when the clay fraction exceeded 5-10% of the sediment mass. Grabowski et al. (2011) provided a comprehensive review and summarized the significance of the particle size distribution, bulk density, water content, organic matter concentration, the type of the clay particles, temperature, salinity, pH, metal concentration, and the feeding ecology of the benthic community; the authors concluded that these effects can change the critical stress by factors of between 10^2 and 10^3. Consolidation and seasonal cycles in temperature and salinity cause temporal variation at the seabed and further complicate the determination of the critical shear stress. These factors have recently been included in a model by Sanford (2008).

Dickhudt et al. (2011) performed experiments with natural sediments with the Gust (1990) microcosm and reanalyzed the data of Torfs et al. (2001) and demonstrated that the critical erosion stress increases rapidly with the degree of compaction of the mud-sand mixture, which can be estimated from the volume fraction of mud ($\boldsymbol{\phi_{sm}}$ =volume of mud/volume mud + water). A wide range of values of these parameters are possible. An illustrative value of $\boldsymbol{\phi_{sm} = 0.4}$ leads to a critical shear stress of 0.7 Pa.

Since there is considerable variability in predictions of the appropriate critical stress in estuaries and no direct estimates in the ZSF, we must rely on the few in-situ measurements in similar environments that are available to guide site selection. Recently, Thompson et al. (2011) deployed a benthic annular flume in the North Sea to measure the critical stress and obtained results at sites with mean sediment grain sizes of 0.0625 mm and 0.071 mm. Their measurements suggested that the critical shear stress ranged from 0.66 to 1.27 Pa, in broad agreement with the theory and lab experiments of Lick et al. (2004) and Righetti and Lucarelli (2007).

Germano et al. (1995) described the bottom sediments in the New London dredged material disposal site as either fine sands ($\phi\sim 3$ or $d_{50} = .125mm$) or very fine sands ($\phi\sim 4$ or $d_{50} =$ 0.0625 mm) overlying mud. There are no direct measurements of the critical stress at the site under consideration. However, based on the estimates of the Thompson et al. (2011) and the character of the bottom sediments we choose the threshold for bottom stress as 0.75 Pa.

6. Bottom Stress Screening

To guide the selection of potential disposal sites, we compared the predicted maximum bottom stresses to the critical erosion stress for dredged material that would be disposed. Table 8 lists the maximum stress computed at each of the 11 potential sites identified in the screening process during the simulations of the three observation periods and the Superstorm Sandy simulation. The bottom stress values are grouped into values greater than 1.0 Pa, 0.75-1.0 Pa, and less than 0.75 Pa and ranked by stress within each group.

Table 8. Comparison of Maximum Bottom Stress (Pa) for Potential Dredged Material Disposal Sites in the simulations of the three Observation Campaigns and Superstorm Sandy

Potential Disposal Site				**Maximum Stress in Simulations** (Pa)	
ELIS	**BIS**	**No.**	**Site Name**	**Group**	**Highest Value**
●		1	Cornfield Shoals	>1	1.31
●		2	Six Mile Reef		1.26
	●	7	Fishers Island-west		1.17
●		5	Niantic Bay	0.75-1.0	0.99
●		3	Clinton Harbor		0.87
	●	10	Block Island Disposal Site	<0.75	0.73
●		6	New London		0.69
	●	9	Fishers Island-center		0.55
●		4	Orient Point		0.53
	●	8	Fishers Island-east		0.46
	●	11	North of Montauk		0.39

Figure 35 shows a map of the maximum bottom stress from the Superstorm Sandy simulation; areas with stress values exceeding 0.75 Pa are shaded in brown. In other areas the colors represent the magnitude scaled to 0.75 Pa.

The following conclusions can be drawn from Figure 35 and Table 8:

- ***ELIS - general:*** Much of ELIS has bottom stresses in excess of the 0.75 Pa threshold. Only the area south of the mouth of the Thames River (New London; Site 6) and a small area near Orient Point (Site 4) have stresses below the threshold.

- ***BIS - general:*** Approximately half of BIS has maximum bottom stresses below the 0.75 Pa threshold. Values are lowest in the areas to the north of Montauk (Site 11) and to the northwest of Block Island.

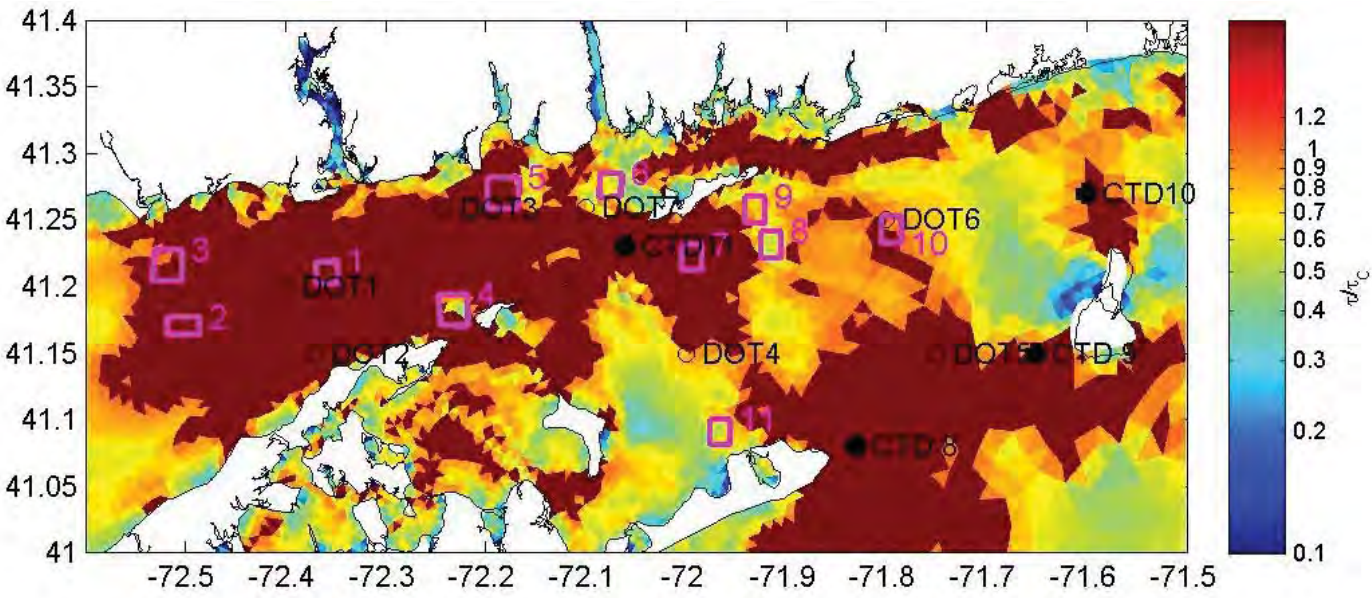

Figure 35. Areas with maximum bottom stress exceeding the 0.75 Pa threshold during the simulation of Superstorm Sandy (screened as a uniform brown layer). Areas with bottom stress below 0.75 Pa are scaled (see color key on the right).

To evaluate suitability of the proposed sites to contain disposed dredged material (defined here as a cohesive mixture of fine sand and clay), we adopt the stricter requirement that the maximum stress within the site boundary must not exceed the 0.75 Pa threshold. Based on that threshold, we conclude:

- ***Sites 1, 2, and 7 (Cornfield Shoals, Six Mile Reef, and Fishers Island - west):*** The physical oceanographic results indicate that these sites would not contain disposed dredged material. Maximum bottom stresses exceed 1.0 Pa.

- ***Sites 3 and 5 (Niantic Bay and Clinton Harbor):*** Though the maximum bottom stresses at these sites are lower than 1.0 Pa, they do exceed the 0.75 Pa threshold. Disposed dredged material is not expected to be contained. (It is noted that in the SEIS, the analyzed "Niantic Bay Alternative" included an area east of the site (referred to as "Site NB-E" in the SEIS; part of this area has maximum bottom stress values of less than 0.75 Pa.)

- ***Site 4 and 10 (Orient Point and Block Island Disposal Site):*** Though the centers of these sites have bottom stresses of less than 0.75 Pa, the complex bathymetry in the respective surrounding areas creates strong spatial gradients in currents and in bottom stress magnitudes so that the threshold is exceeded within the perimeters of the sites. Therefore, these sites are not expected to contain disposed dredged material.

- ***Site 6 (New London):*** Within the ELIS, only Site 6 (New London) has maximum stresses below the 0.75 Pa threshold and it is, therefore, the only site where disposed dredged material would be stable.

- ***Sites 8, 9 and 11 (Fishers Island center and east, and North of Montauk):*** Model simulations suggest that the maximum bottom stresses at Sites 8, 9, and 11 are below the 0.75 Pa threshold, indicating that disposed dredged material would be contained.

7. Summary and Discussion

The PO model developed for the circulation in the ZSF has been demonstrated to be consistent with the wide array of measurements obtained in the accompanying field program of the PO study. The predicted tidal current amplitudes at all seven mooring stations agree well with both the magnitude and direction of the observed currents with skill metrics generally over 80%. The skill in temperature simulation is not as good and the model appears to have a high bias in the spring as a consequence of inadequate simulation of the surface heat exchange; however, the salinity field is predicted accurately. Since salinity dominates the density field variations, the skill in simulating density is in the 80% range. The comparison of model-predicted stress shows that the magnitude of stresses induced by currents in the model and data are consistent. The correlation coefficients between the model and data from the three campaigns are 0.91 and 0.72 for the mean and maximum bottom stress, respectively (Figure 15). This is strong evidence that the model can discriminate areas of high bottom stress from areas with lower bottom stress.

To demonstrate the utility of the model for evaluating and comparing potential dredged material disposal sites, the predicted values of the maximum bottom stress obtained during the three observation campaigns were determined. Within the ELIS, Orient Point (Site 4) and New London site (Site 6) have the lowest predicted bottom stress; however, for Orient Point, areas of high stress infringe on the corners of the site. In BIS, the predicted stresses are generally lower; the lowest bottom stress is predicted for the site north of Montauk (Site 11) and at Fishers Island – center (Site 9).

To assess the effect of extreme events on the bottom stress, the circulation induced by the winds created by Superstorm Sandy in October 2012 was simulated. Although there are substantial currents generated in the shallow areas of the model domain, the increase in bottom stress in the Long Island Sound part of the ZSF (see Table 6) is less than 20% above the fair-weather maximum values. Simulated bottom stresses were actually lower at New London site (Site 6) and Cornfield Shoals site (Site 1) during the superstorm. The causes for the changes in maximum bottom stress are complex but it appears that the wind-driven flow is weak in deeper water and in some places it opposes the mean flow and thereby reduces the bottom stress. In BIS, the simulated effects of the superstorm are larger since the stresses are lower, but much of the bottom remains below the critical threshold for resuspension of the type of material typical of the dredged material disposal sites. Of course non-cohesive particles have a lower threshold stress and the presence of sand waves in areas of BIS is evidence of this. The limited presence of fine-grained particles in these low-stress areas is likely a consequence a limited supply rather than erosion.

From the perspective of bottom stress affecting sediment stability, Sites 6, 8, 9 and 11 are not expected to contain disposed dredged material. Although the stress values of Sites 4 and 10 are also below the threshold for sediment resuspension, areas of higher stress are within the boundaries of the respective sites; therefore, these sites are not expected to contain disposed dredged material.

If additional site options are sought then the areas to the northwest of Block Island and Montauk Inlet might be considered since these are extensive areas of low stress.

References

Bagnold, R.A. 1966. An approach to the sediment transport problem for general physics, *Geol. Surv. Prof. Paper 422-1,* Washington, DC.

Brownlie, W.R. 1981. Prediction of flow depth and sediment discharge in open channels. Report KH-R-43A, W.M. Keck, Laboratory of Hydraulics and Water Resources, Division of Engineering and Applied Science, California Institute of Technology, Pasadena, CA.

Bricker, J.D., S. Inagaki, and S.G. Monismith. 2005. Bed drag coefficient variability under wind waves in a tidal estuary, *J. Hydr, Eng.* 131(6): 497-508.

Buffington, J.M. and D.R. Montgomery. 1999. Effects of sediment supply on surface textures of gravel-bed rivers. *Water Resources Research* 35(11): 3523–3530.

Cao, Z., G. Pender, and J. Meng, 2006. Explicit formulation of the Shields diagram for incipient motion of sediment. *J. Hydr. Eng.* 132: 1097-1099.

Chen, C.H. Huang, R.C. Beardsley, H. Liu, Q. Xu, and G. Cowles. 2007. A finite-volume numerical approach for coastal ocean circulation studies: Comparisons with finite difference models. *J. Geophys. Res*. 112: C03018, doi:10.1029/2006JC003485.

Clarke, T.L. 1974. A study of cloud phase parameterization using the gamma distribution. *J. Atmos. Sci*. 31: 142–155

Codiga, D.L. and D.S. Ullman. 2011a. Characterizing the Physical Oceanography of Coastal Waters off Rhode Island, Part 1: Literature Review, Available Observations, and a Representative Model Simulation. Available at: *http://seagrant.gso.uri.edu/oceansamp/pdf/appendix/02-PhysOcPart1-OSAMP-CodigaUllman2010.pdf.)*

Dickhudt, P.J., C.T. Friedrichs, and L.P. Sanford. 2011. Mud matrix solids fraction and bed erodibility in the York River estuary, USA, and other muddy environments. *Continental Shelf Research* 31: S3-13.

Dronkers, J.J. 1964. *Tidal Computations in rivers and coastal waters*. North-Holland Publishing Company, 518p.

Egbert, G.D., A.F. Bennett, and M.G.G. Foreman. 1994. TOPEX/POSEIDON tides estimated using a Global Inverse Model. *J. Geophys. Res.* 99: 24821-24852.

Fisher, N.I. 1996. *Statistical analysis of circular data*. Cambridge University Press, Cambridge, U.K.

Fung, I.Y., D.E. Harrison, and A.A. Lacis. 1984. On the variability of the net longwave radiation at the ocean surface. *Reviews of Geophysics* 22(2): 177-193.

Gay, P.S., J. O'Donnell, and C.A. Edwards. 2004. Exchange between Long Island Sound and adjacent waters. *J. Geophys. Res.* 109: C06017, doi: 10.1029/2004JC002319.

Gerbi, G.P., J.H. Trowbridge, J.B. Edson, A.J. Plueddemann, E.A. Terray, and J.J. Fredericks. 2008. Direct covariance measurements of momentum and heat transfer across the air-sea interface. *J. Phys. Oceanogr.* 38: 1053-1072.

Germano, J.D., J. Parker, and F. Craig Eller. 1995. Monitoring cruise at the New London Disposal Site, June-July 1990, Disposal Area Monitoring System, DAMOS #93. U.S. Army Corps of Engineers, New England Division, Waltham, MA.

Grabowski, R.C., I.G. Droppo, and G. Wharton. 2011. Erodibility of cohesive sediment: The importance of sediment properties. *Earth Science Review* 105: 101-120. *http://dx.doi.org/10.1016/j.earscirev.2011.01.008.*

Graf, W. 1971. *Hydraulics of Sediment Transport.* McGraw-Hill, New York.

Grant, W.D. and O.S. Madsen. 1979. Combined wave and current interaction with a rough bottom. *J. Geophys. Res.* 84: 1797-1808.

Gust, G., 1990. Method of generating precisely-defined wall shearing stresses. US Patent #4,973,165, 27 Nov. 1990, 8p.

Hasselmann, K., T.P. Barnett, E. Bouws, H. Carlson, D.E. Cartwright, K. Enke, J.A. Ewing, H. Gienapp, D.E. Hasselmann, P. Kruseman, A. Meerburg, P. Müller, D.J. Olbers, K. Richter, W. Sell and H. Walden., 1973. Measurements of wind-wave growth and swell decay during the Joint North Sea Wave Project (JONSWAP). *Dtsch. Hydrogr. Z.* Suppl., 12, A8.

Kaimal, J.C., J.C. Wyngaard, Y. Izumi, and O.R. Cote. 1972. Spectral characteristics of surface-layer turbulence. *Quart. J. R. Met. Soc.* 98: 563-589.

Kaputa, N.P. and C.B. Olsen. 2000. State of Connecticut Department of Energy and Environmental Protection, Long Island Sound Ambient Water Quality Monitoring Program: Summer Hypoxia Monitoring Survey '91-'98. Data Review.

Kim, S.C., C. Friedrichs, J.P.-Y. Maa, and L.D. Wright. 2000. Estimating bottom stress in a tidal boundary layer from acoustic Doppler velocimeter data. *J. of Hydraulic Engineering* 126(6): 399-406.

Kirincich A.R., S.J. Lentz, and G.P. Gerbi. 2010. Calculating Reynolds stresses from ADCP measurements in the presence of surface gravity waves using the Cospectra-fit method. *J. Atmos. Ocean Tech.* 27: 889-907.

Komen, G.J., S. Hasselmann, and K. Hasselmann. 1984. On the existence of a fully developed wind-sea spectrum. *J. Phys. Oceanogr*. 14: 1271-1285.

Lewis, R. 2014. The Geology of Long Island Sound. In *Long Island Sound: Prospects for the Urban Sea.* Latimer, J.S., Tedesco, M., Swanson, R.L., Yarish, C., Stacey, P., Garza, C. (eds.), p. 47-78. ISBN-13: 978-1461461258.

Lick, W., L. Jin, and J. Gailani. 2004. Initiation of movement of quartz particles. *J. Hydraulic Eng.* 1308: 755–761.

Louis Berger. 2013. Report of Public Scoping Meetings 3 (Riverhead, NY) and 4 (Groton, CT). Included as Appendix A-4 in SEIS.

Massey, T.C. M. E. Anderson, J. M. Smith, J. Gomez, and R. Jones. 2011. STWAVE: Steady-State Spectral Wave Model User's Manual for STWAVE, Version 6.0. Report ERDC/CHL TR-11-1, Coastal and Hydraulics Laboratory, U.S. Army Corp of Engineers, Vicksburg, MS. 90p.

O'Donnell, J., M.M. Howard Strobel, D.C. Cohen, S.G. Ackleson, A. Cifuentes, D.B. Fribance, R.M. Horwitz, F. Bohlen, G.M. McCardell, and T. Fake. 2014a. Physical Oceanography of Eastern Long Island Sound Region: Field Data. Prepared by the University of Connecticut, with support from Louis Berger. Prepared for the Connecticut Department of Transportation. Included as Appendix C-1 in SEIS.

O'Donnell, J., R.E. Wilson, K. Lwiza, M. Whitney, W.F. Bohlen, D. Codiga, T. Fake, D. Fribance, M. Bowman, and J. Varekamp. 2014b. The Physical Oceanography of Long Island Sound. In *Long Island Sound: Prospects for the Urban Sea.* Latimer, J.S., Tedesco, M., Swanson, R.L., Yarish, C., Stacey, P., Garza, C. (eds.), p. 79-158 ISBN-13: 978-1461461258.

O'Donnell, J., G.M. McCardell, M.M. Howard Strobel, R.M. Horwitz, A. Cifuentes, and T. Fake. 2015. Physical Oceanography of Eastern Long Island Sound Region: Sediment Transport. Prepared by the University of Connecticut, with support from Louis Berger. Prepared for the Connecticut Department of Transportation. Included as Appendix C-3 in SEIS.

Qi, J. H., C.S. Chen, and R.C. Beardsley. 2009. An unstructured-grid finite-volume surface wave model (FVCOM-SWAVE): Implementation, validations and applications. *Ocean Modeling* 28: 153-166.

Raudkivi, A. 1976. *Loose Boundary Hydraulics.* 2nd ed., Pergamon, Oxford, U.K.

Righetti, M. and C. Lucarelli. 2007. May the Shields theory be extended to cohesive and adhesive benthic sediments? *J. Geophys. Res.* 112: C05039. doi: 10.1029/2006JC003669.

Sanford, L.P. 2008. Modeling a dynamically varying mixed sediment bed with erosion, deposition, bioturbation, consolidation, and armoring. *Computers in Geosciences* 34: 1263–1283.

Signell, R., J. List, and A. Farris. 2000. Bottom currents and sediment transport in Long Island Sound: a modeling study. *J. of Coastal Res.* 16: 551–566.

Smith, S.D. 1988. Coefficients for sea surface wind stress, heat flux, and wind profiles as a function of wind speed and temperature. *J. Geophys. Res.* 93: 15467–15472.

Ternat, F., P. Boyer, F. Anselmet, and M. Amielh. 2008. Erosion of self-weight saturated cohesive sediment. *Water Resources Res.* 44: W11434, doi :10.1029/2007WR006537

Thompson, C.E.L., F. Couceiro, G.R. Fones, R. Helsby, C.L. Amos, K. Black, E.R. Parker, N. Greenwood, P.J. Statham, and B.A. Kelly-Gerreyn. 2011. In-situ flume measurements of resuspension in the North Sea. *Estuarine, Coastal and Shelf Science* 94: 77-88.

Torfs, H., J. Jiang, and A.J. Mehta. 2001. Assessment of erodibility of fine/coarse sediment mixtures. In: McAnally, W.H., Mehta, A.J. (Eds.), *Coastal and Estuarine Fine Sediment Transport Processes*. Elsevier, Amsterdam, p. 109–123.

Trowbridge, J.H. 1998. On a technique for measurement of turbulent shear stress in the presence of surface waves. *J. Atmos. Oceanic Technol.* 15: 290–298.

USACE. 2015. Long Island Sound Dredged Material Management Plan. U.S. Army Corps of Engineers. All reports available at: *http://www.nae.usace.army.mil/Missions/ProjectsTopics/LongIslandSoundDMMP.aspx*

USEPA and USACE. 2004. Final Environmental Impact Statement for the Designation of Dredged Material Disposal Sites in Central and Western Long Island Sound, Connecticut and New York. Prepared by the USEPA New England Region, in cooperation with the USACE New England District (April 2004).

van Ledden, M., W.G.M. van Kesteren, and J.C. Winterwerp. 2004. A conceptual framework for the erosion behaviour of sand–mud mixtures. *Continental Shelf Research* 24: 1–11.

van Rijn, L.C. 1984. Sediment transport, Part II: Suspended load transport. *Journal of Hydraulic Eng.* 110(11): 1613-1641.

van Rijn, L.C. 1993. *Principles of Sediment Transport in Rivers, Estuaries and Coastal Seas*. Aqua Publications, Amsterdam, The Netherlands.

von Kármán, T. 1930. Mechanische Ähnlichkeit und Turbulenz, *Nachrichten von der Gesellschaft der Wissenschaften zu Göttingen, Fachgruppe 1 (Mathematik)* 5: 58–76.

von Storch, H. and F. W. Zwiers. 1999. Statistical *Analysis in Climate Research.* Cambridge University Press, Cambridge, 484p.

Wilcock, P.R., 1996. Estimating local bed shear stress from velocity observations. *Water Resources Research* 32 (11): 3361–3366.

Wiles, P.J., T.P. Rippeth, J.H. Simpson, and P.J. Hendricks. 2006. A novel technique for measuring the rate of turbulent dissipation in the marine environment. *Geophy. Res. Letters* 33: L21608, *doi:10.1029/2006GL027050*.

Yalin, M. S. and A.M.F. da Silva. 2001. Fluvial processes, IAHR Monograph, IAHR, Delft, The Netherlands.

Appendix 1

Comparison of Model-predicted Sea Level to Sea Level measured by RDI ADCPs

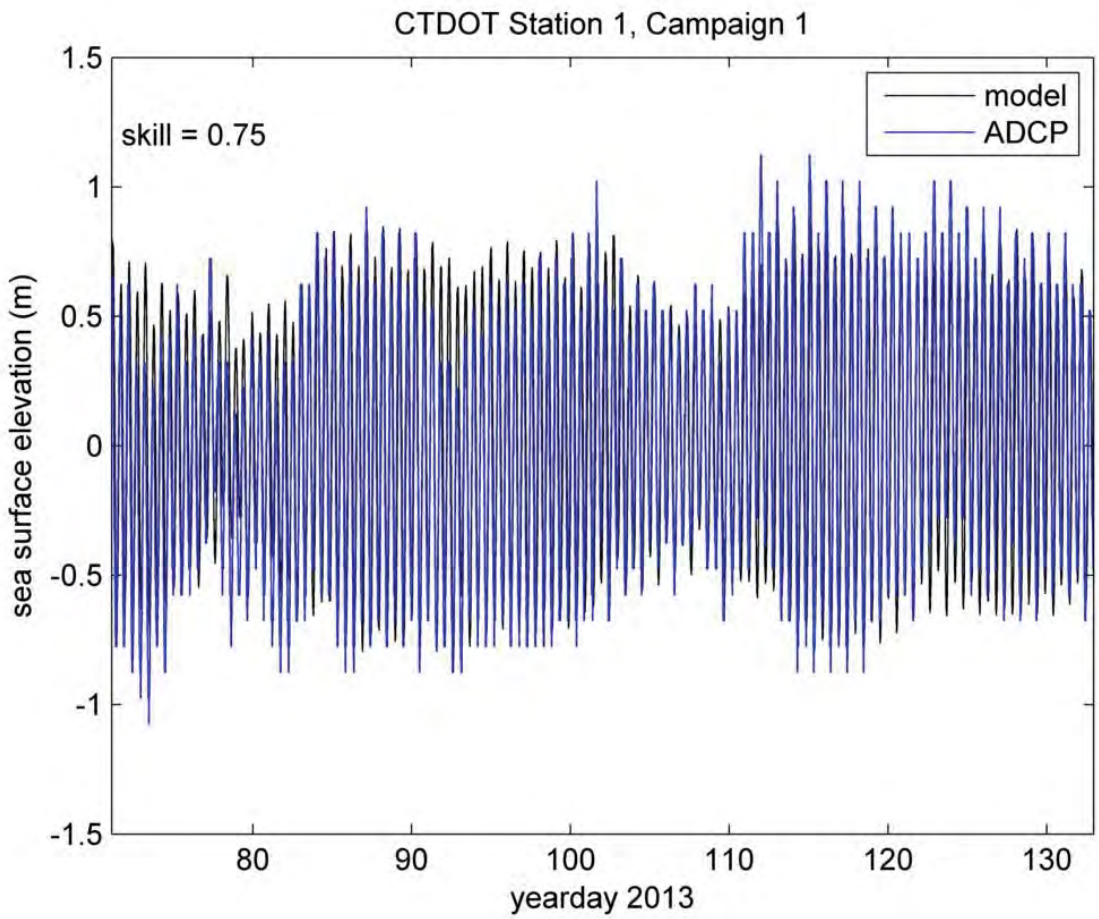

Figure A1.2. Comparison of tidal heights in the ZSF at Station DOT1 during Campaign 1 measured by ADCP pressure sensor (blue) compared to those predicted by the FVCOM model (black).

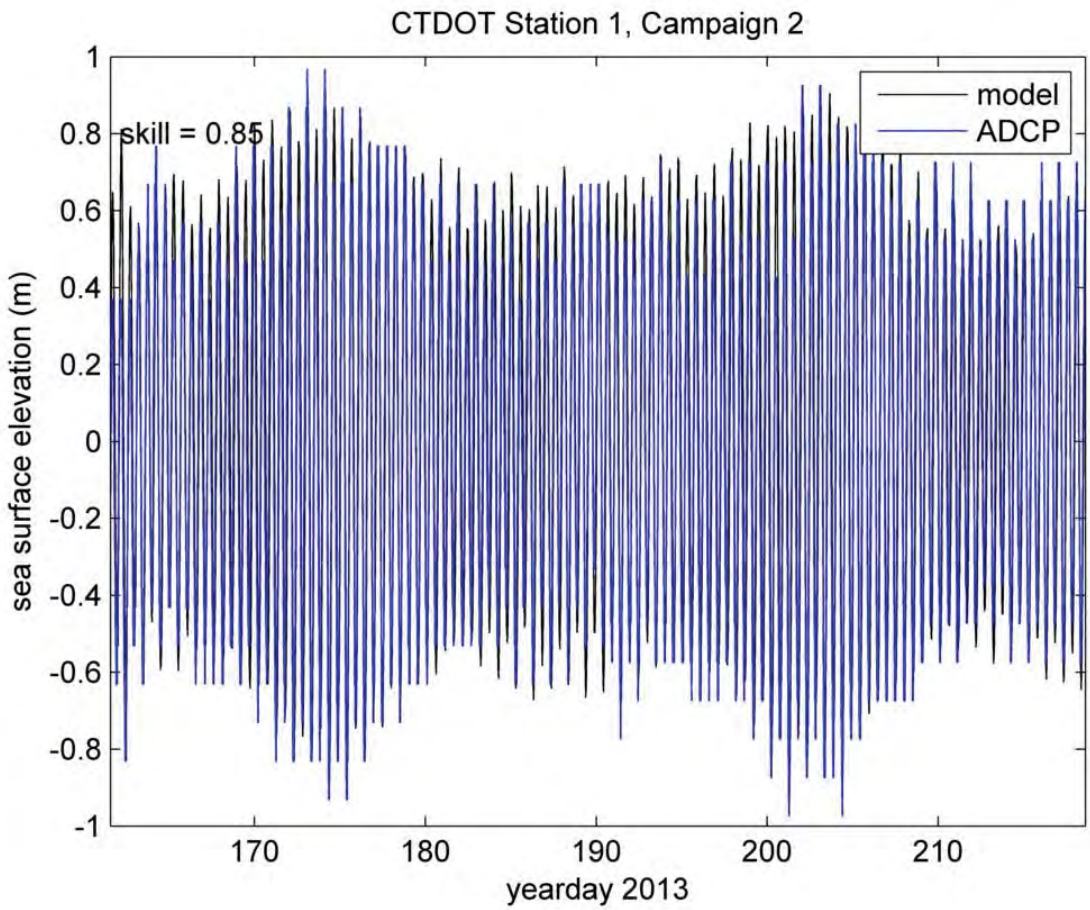

Figure A1.3. Comparison of tidal heights in the ZSF at Station DOT1 during Campaign 2 measured by ADCP pressure sensor (blue) compared to those predicted by the FVCOM model (black).

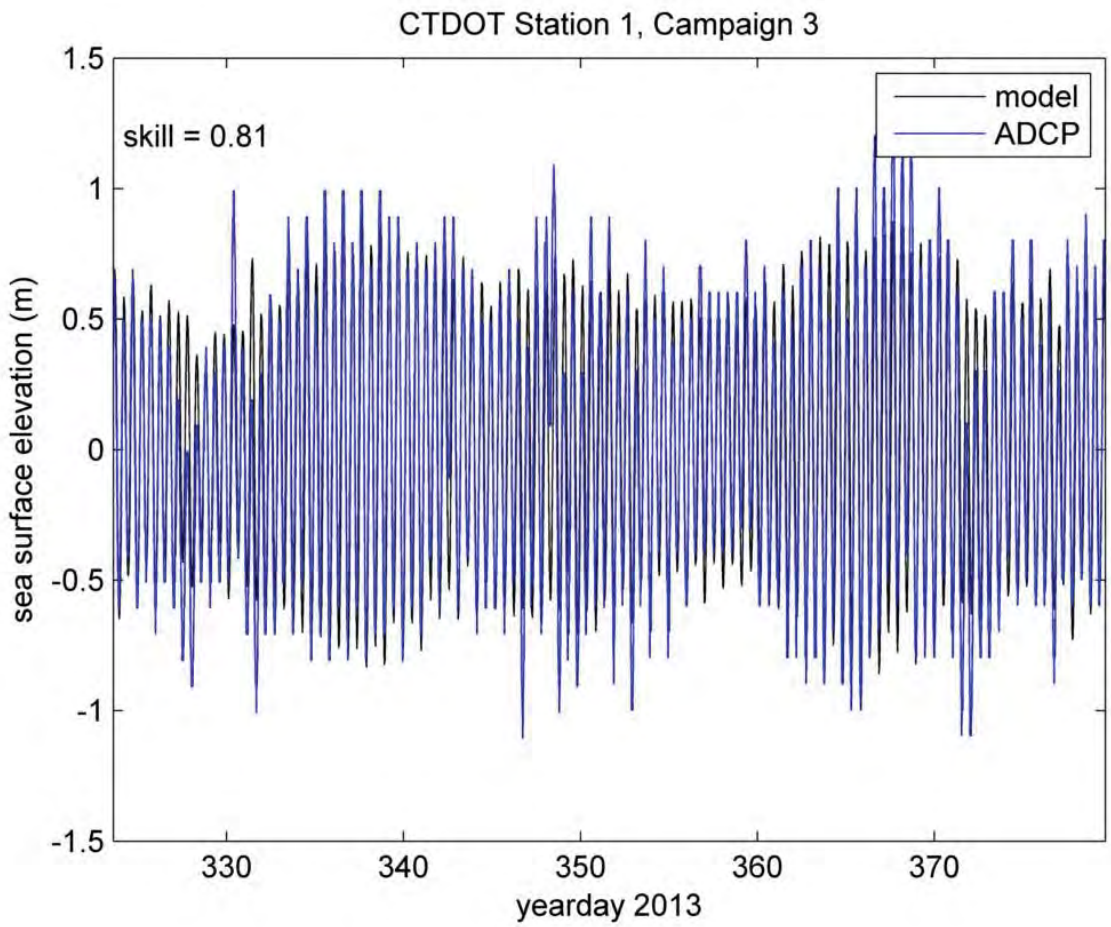

Figure A1.4. Comparison of tidal heights in the ZSF at Station DOT1 during Campaign 3 measured by ADCP pressure sensor (blue) compared to those predicted by the FVCOM model (black).

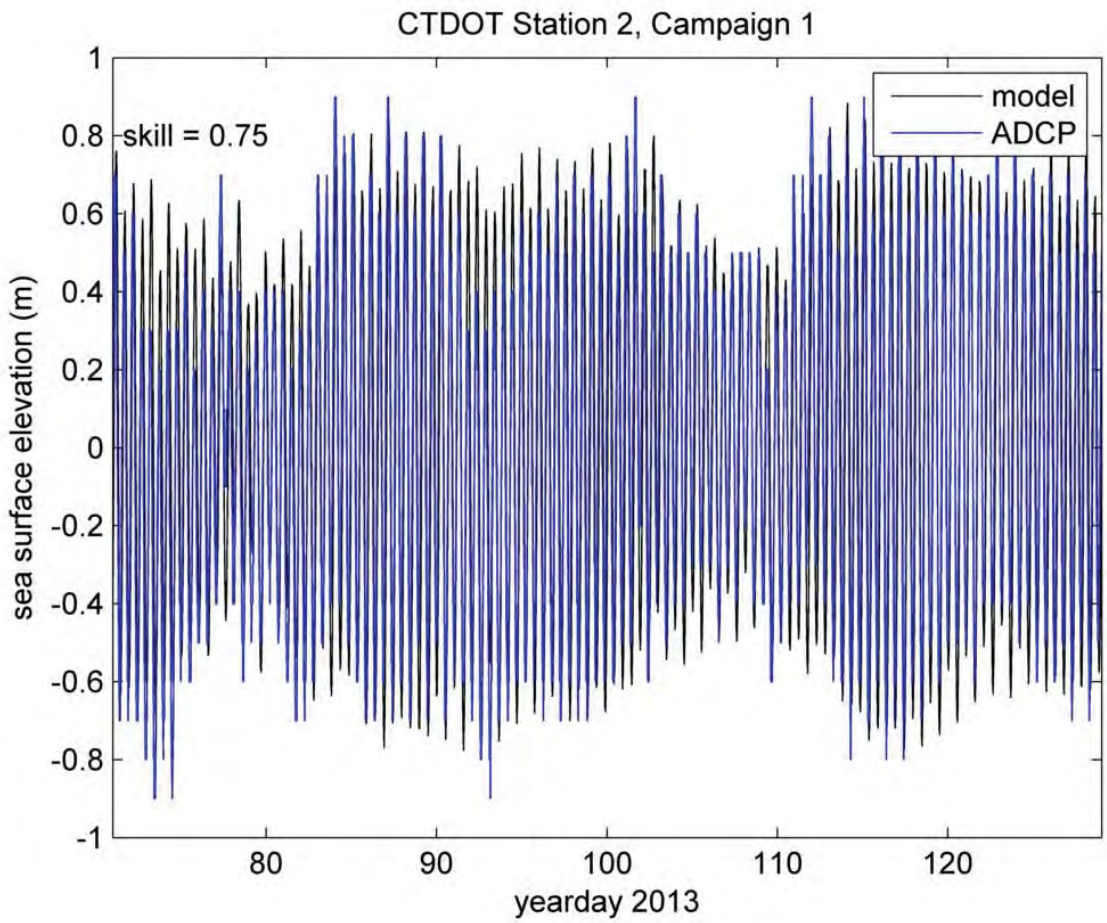

Figure A1.5. Comparison of tidal heights in the ZSF at Station DOT2 during Campaign 1 measured by ADCP pressure sensor (blue) compared to those predicted by the FVCOM model (black).

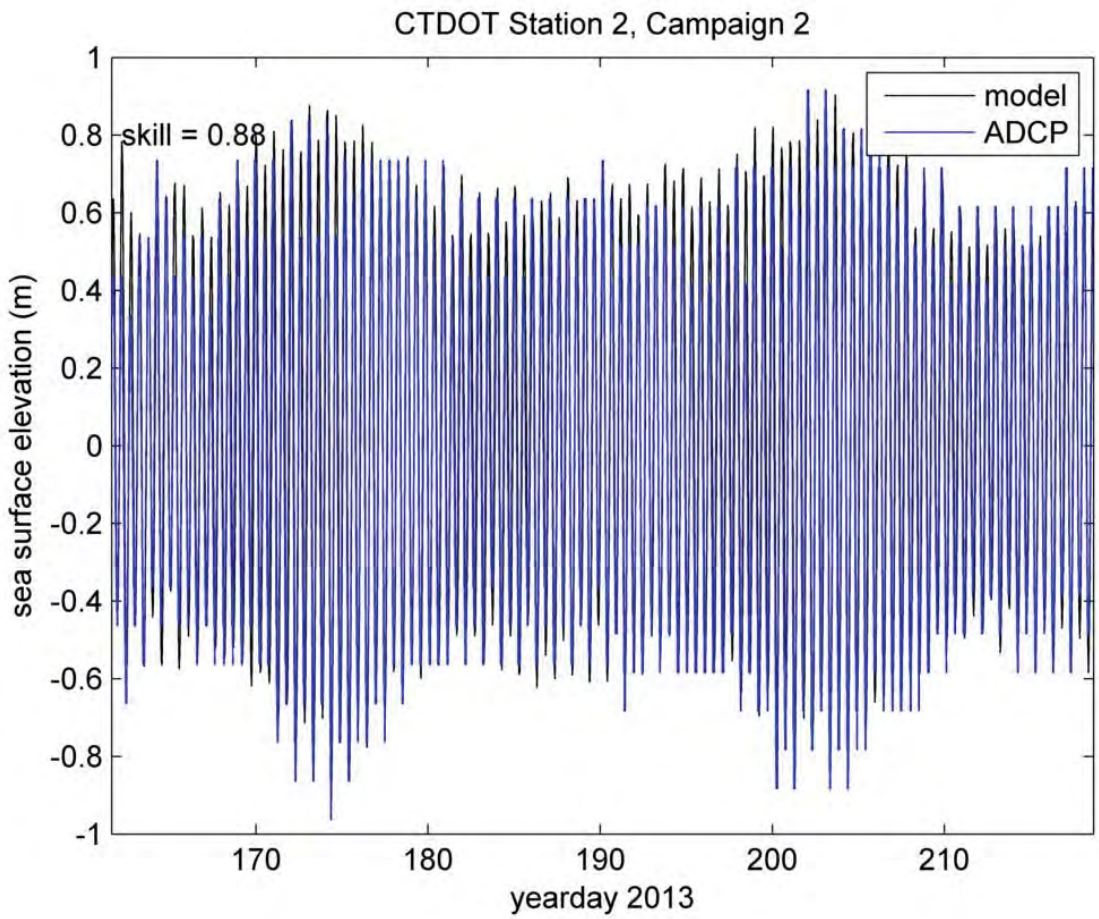

Figure A1.6. Comparison of tidal heights in the ZSF at Station DOT2 during Campaign 2 measured by ADCP pressure sensor (blue) compared to those predicted by the FVCOM model (black).

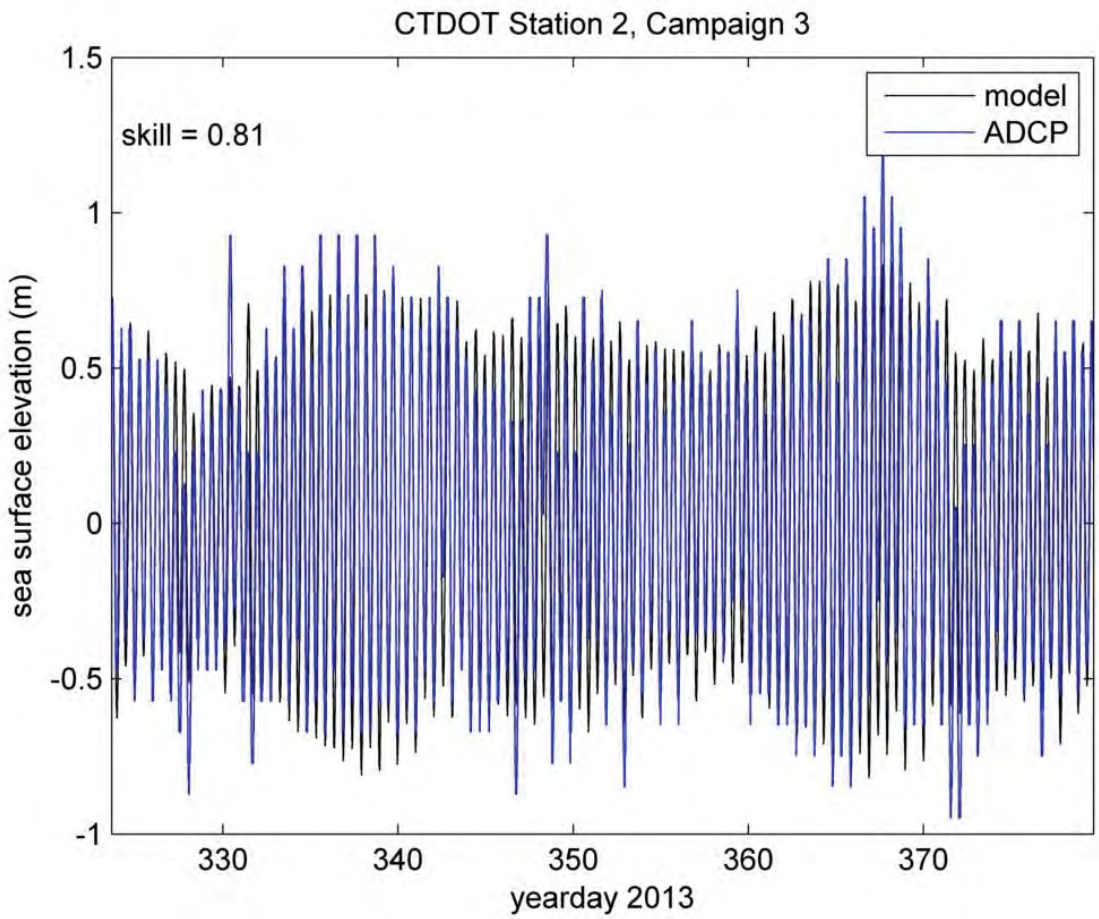

Figure A1.7. Comparison of tidal heights in the ZSF at Station DOT2 during Campaign 3 measured by ADCP pressure sensor (blue) compared to those predicted by the FVCOM model (black).

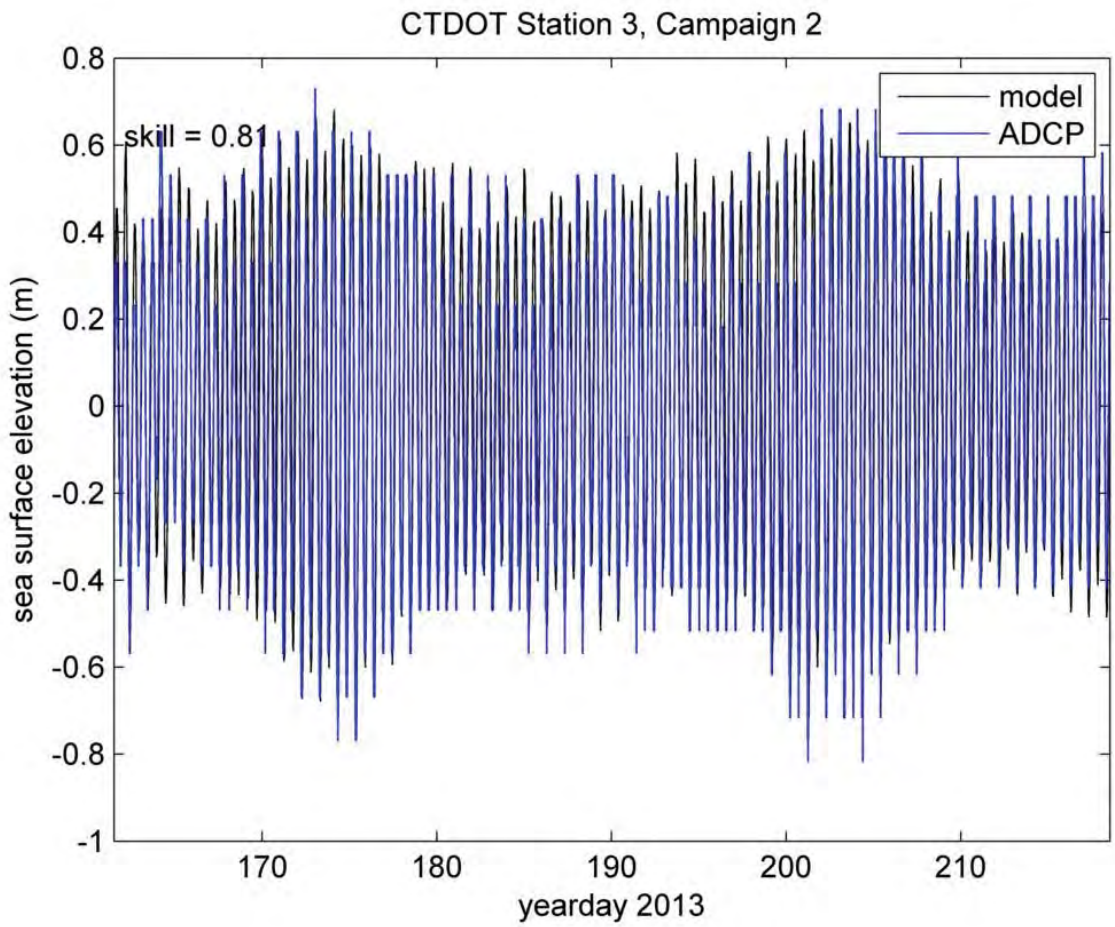

Figure A1.8. Comparison of tidal heights in the ZSF at Station DOT3 during Campaign 2 measured by ADCP pressure sensor (blue) compared to those predicted by the FVCOM model (black).

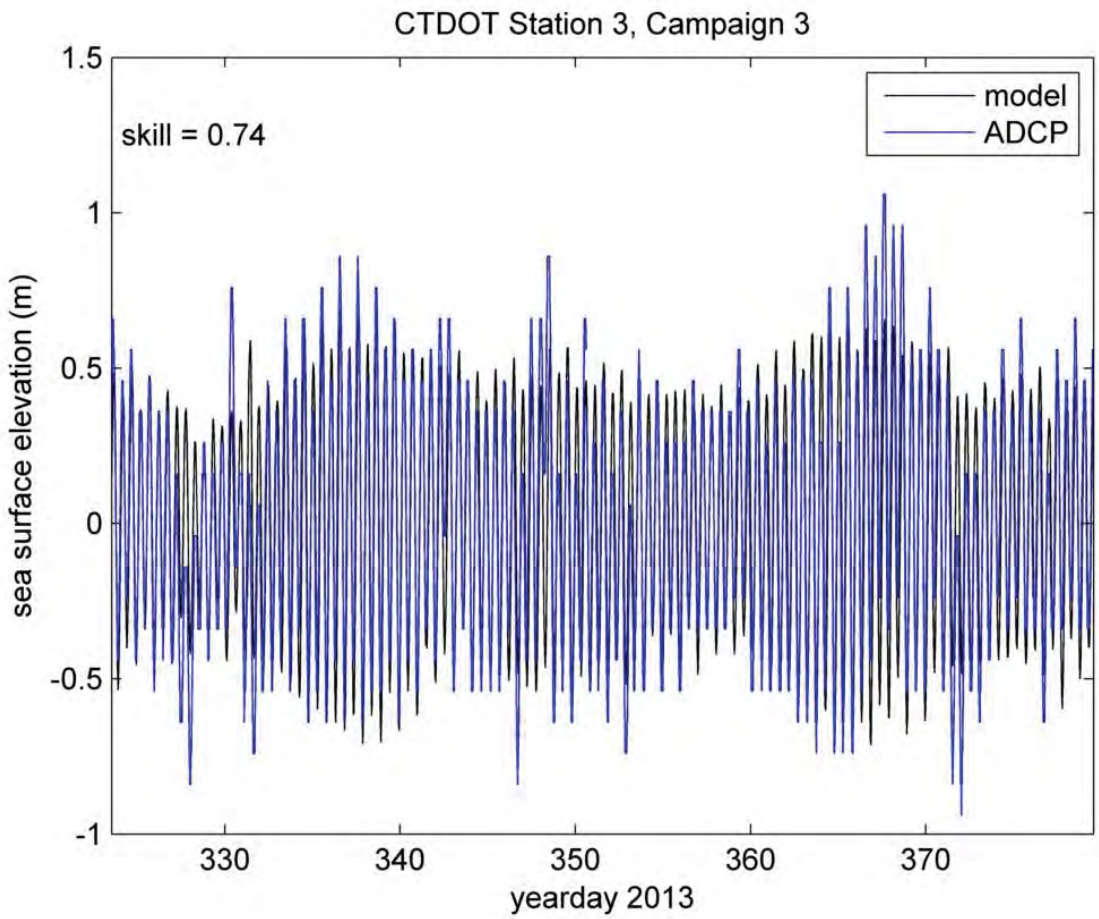

Figure A1.9. Comparison of tidal heights in the ZSF at Station DOT3 during Campaign 3 measured by ADCP pressure sensor (blue) compared to those predicted by the FVCOM model (black).

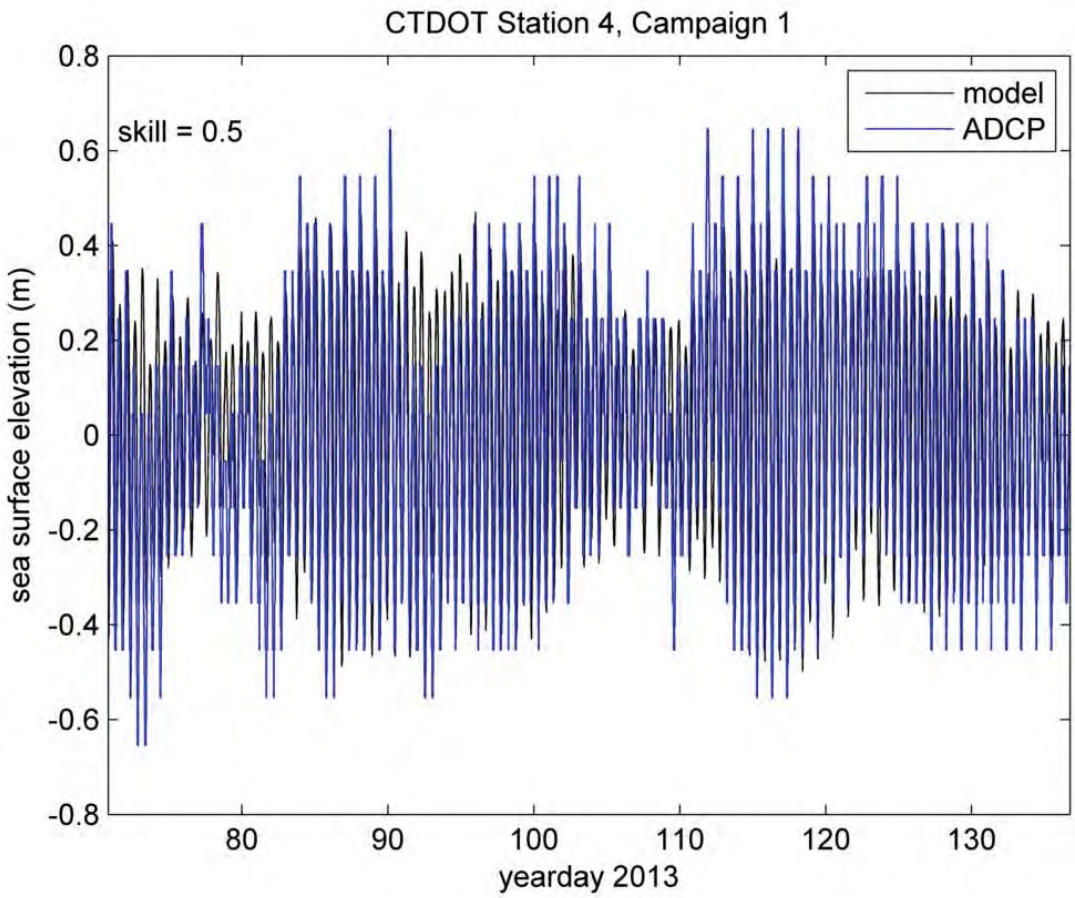

Figure A1.10. Comparison of tidal heights in the ZSF at Station DOT4 during Campaign 1 measured by ADCP pressure sensor (blue) compared to those predicted by the FVCOM model (black).

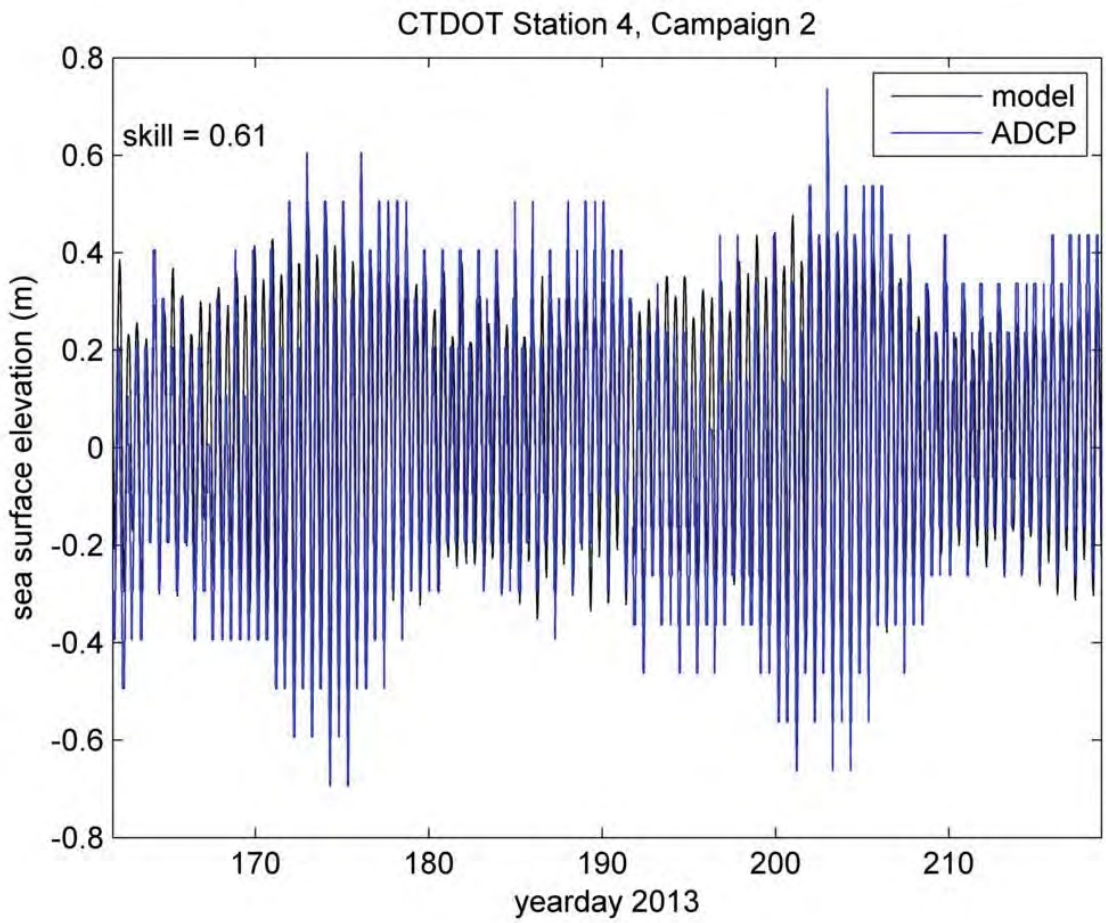

Figure A1.11. Comparison of tidal heights in the ZSF at Station DOT4 during Campaign 2 measured by ADCP pressure sensor (blue) compared to those predicted by the FVCOM model (black).

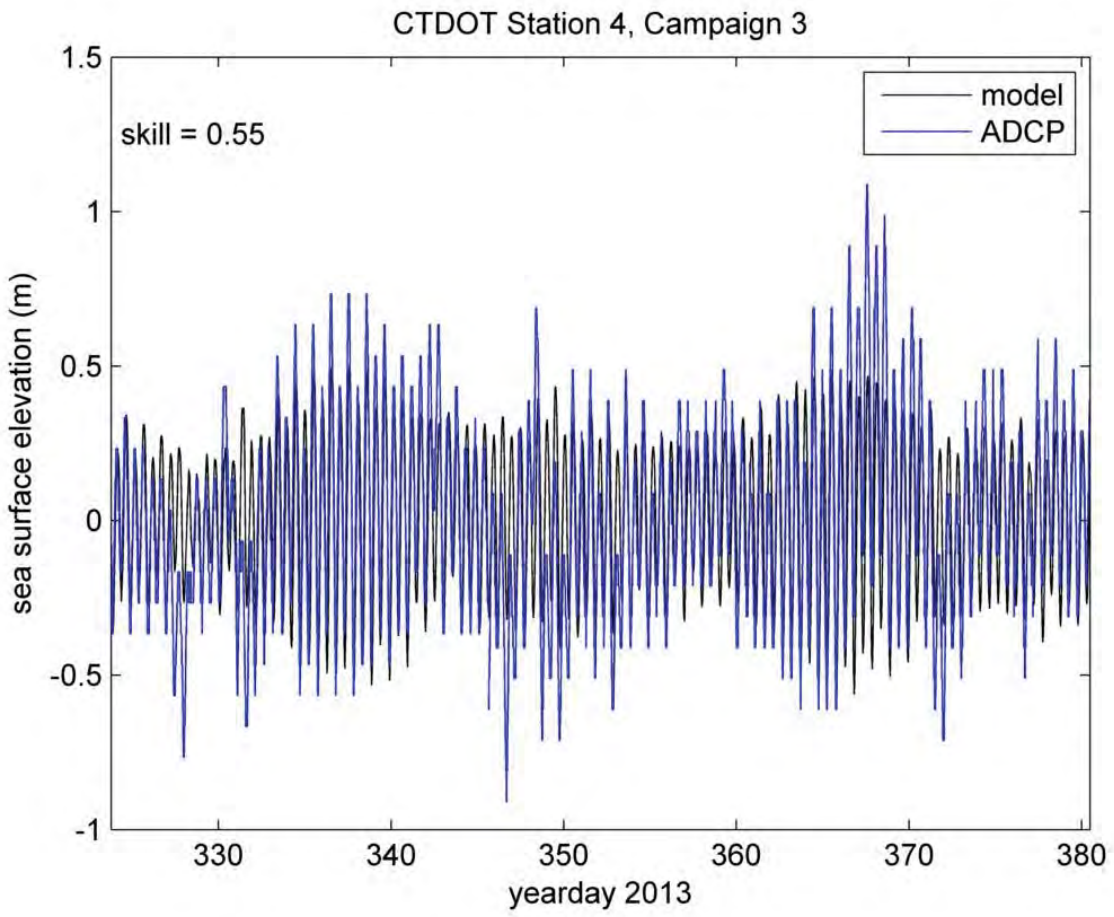

Figure A1.12. Comparison of tidal heights in the ZSF at Station DOT4 during Campaign 3 measured by ADCP pressure sensor (blue) compared to those predicted by the FVCOM model (black).

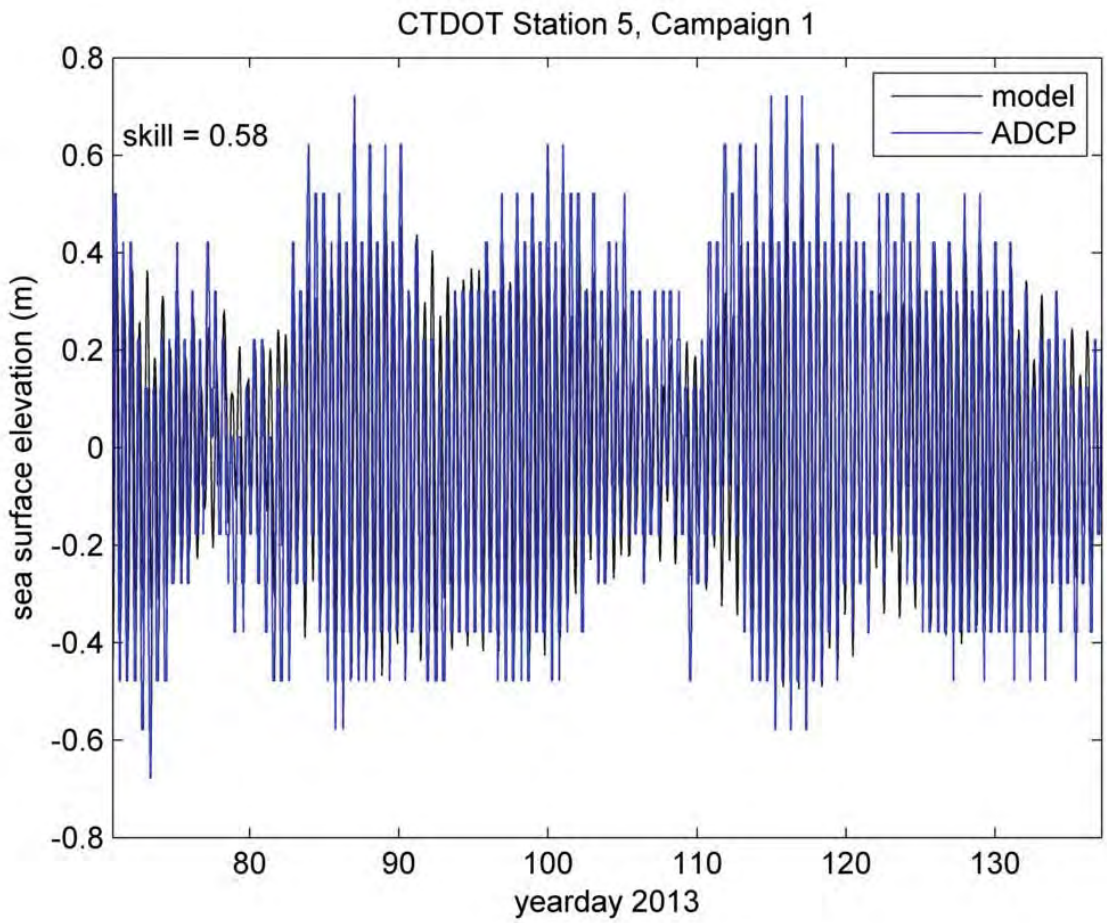

Figure A1.13. Comparison of tidal heights in the ZSF at Station DOT5 during Campaign 1 measured by ADCP pressure sensor (blue) compared to those predicted by the FVCOM model (black).

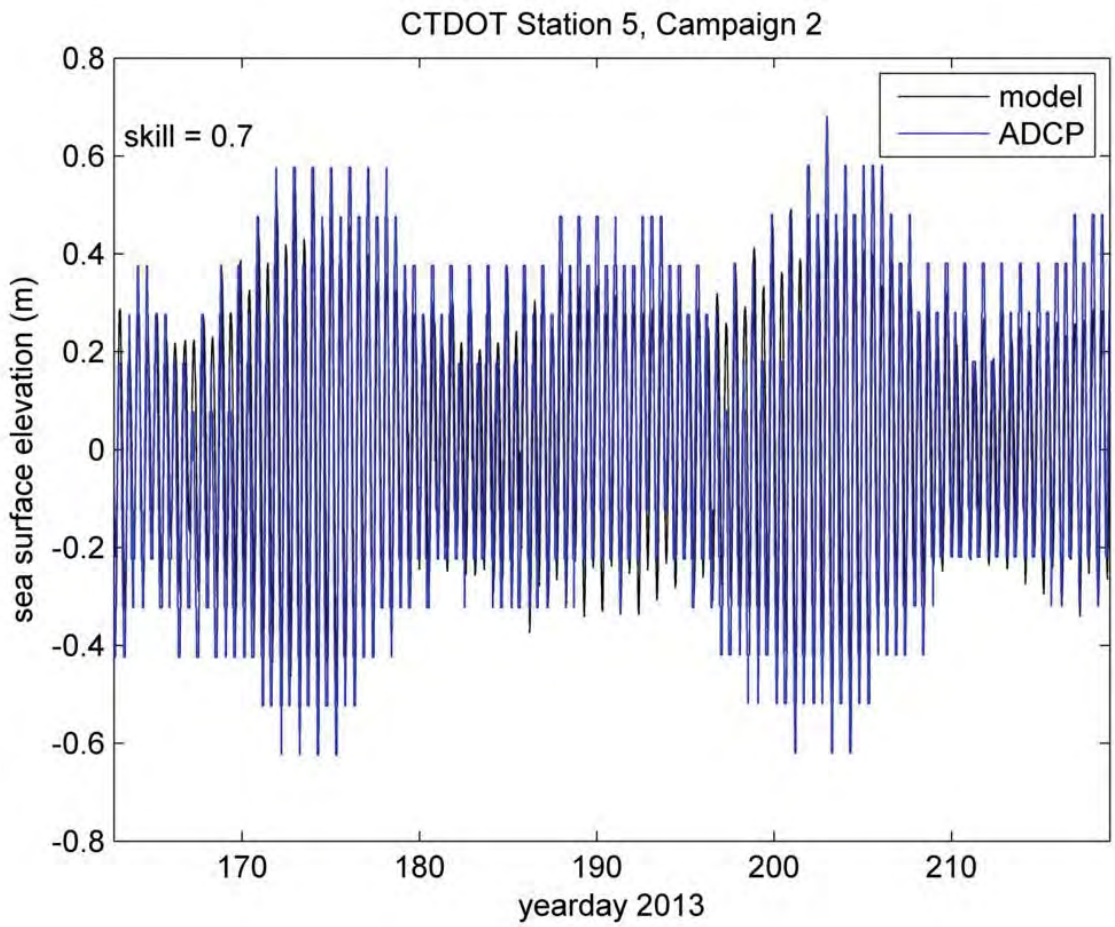

Figure A1.14. Comparison of tidal heights in the ZSF at Station DOT5 during Campaign 2 measured by ADCP pressure sensor (blue) compared to those predicted by the FVCOM model (black).

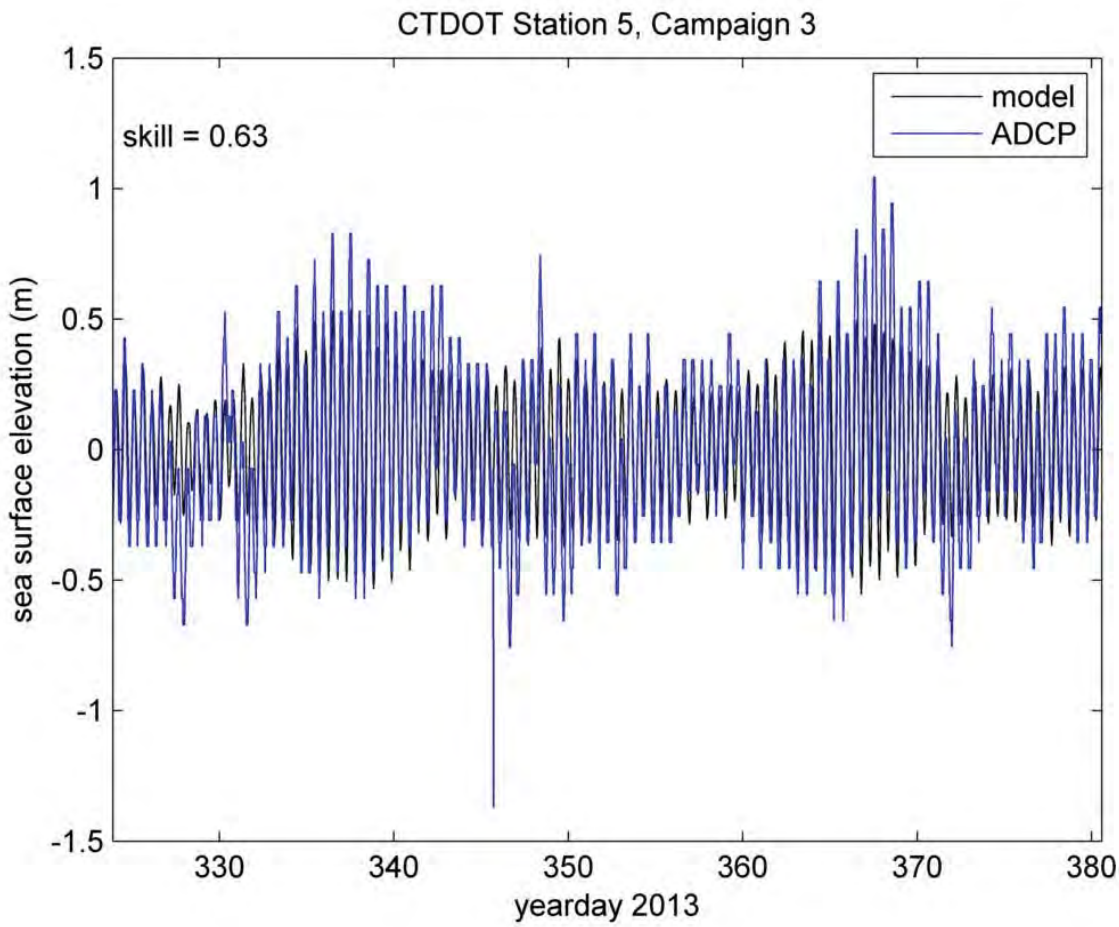

Figure A1.15. Comparison of tidal heights in the ZSF at Station DOT5 during Campaign 3 measured by ADCP pressure sensor (blue) compared to those predicted by the FVCOM model (black).

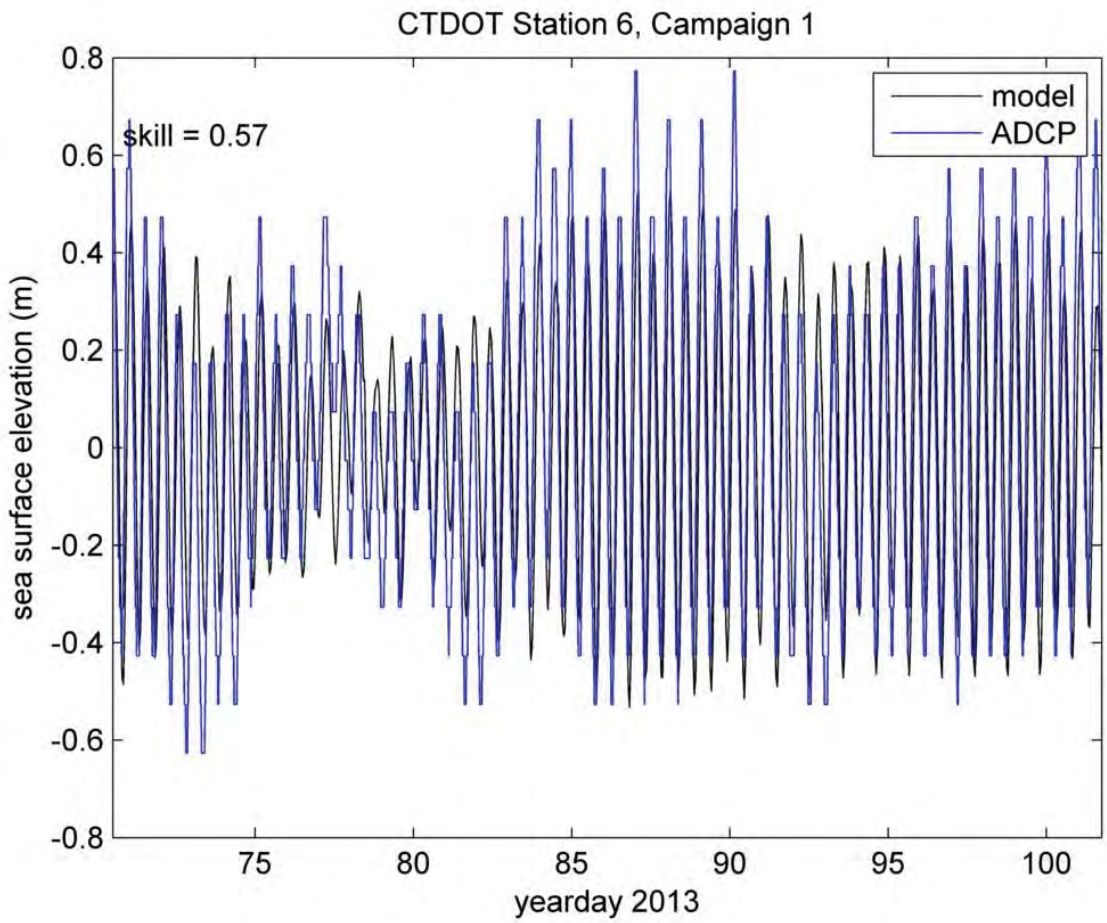

Figure A1.16. Comparison of tidal heights in the ZSF at Station DOT6 during Campaign 1 measured by ADCP pressure sensor (blue) compared to those predicted by the FVCOM model (black).

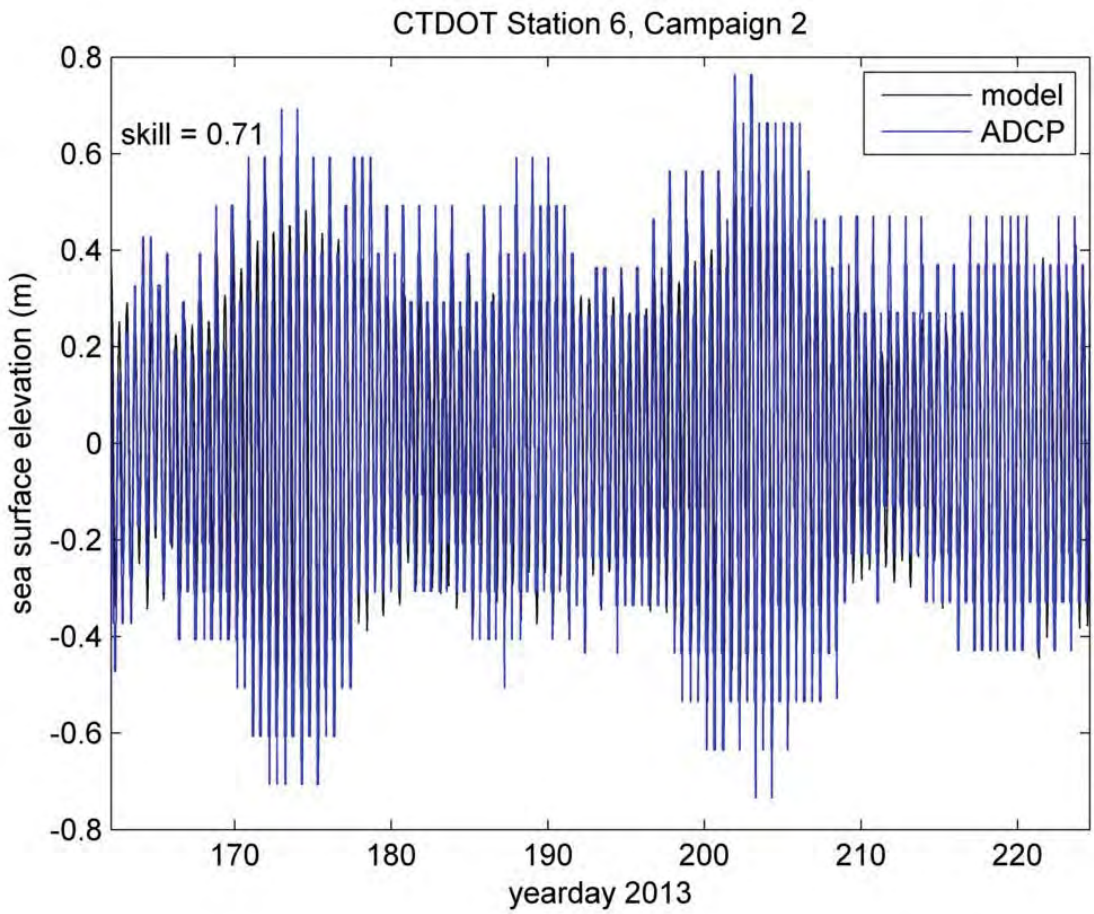

Figure A1.17. Comparison of tidal heights in the ZSF at Station DOT6 during Campaign 2 measured by ADCP pressure sensor (blue) compared to those predicted by the FVCOM model (black).

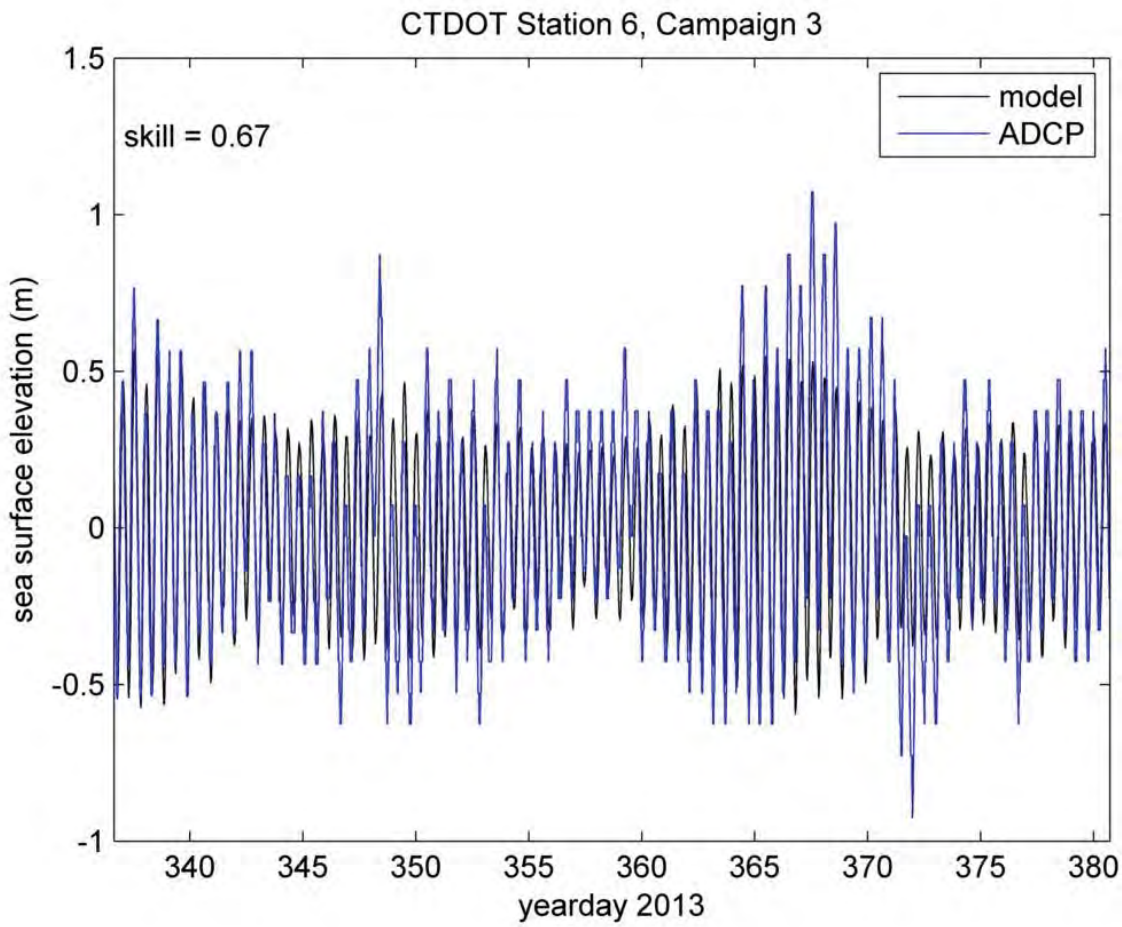

Figure A1.18. Comparison of tidal heights in the ZSF at Station DOT6 during Campaign 3 measured by ADCP pressure sensor (blue) compared to those predicted by the FVCOM model (black).

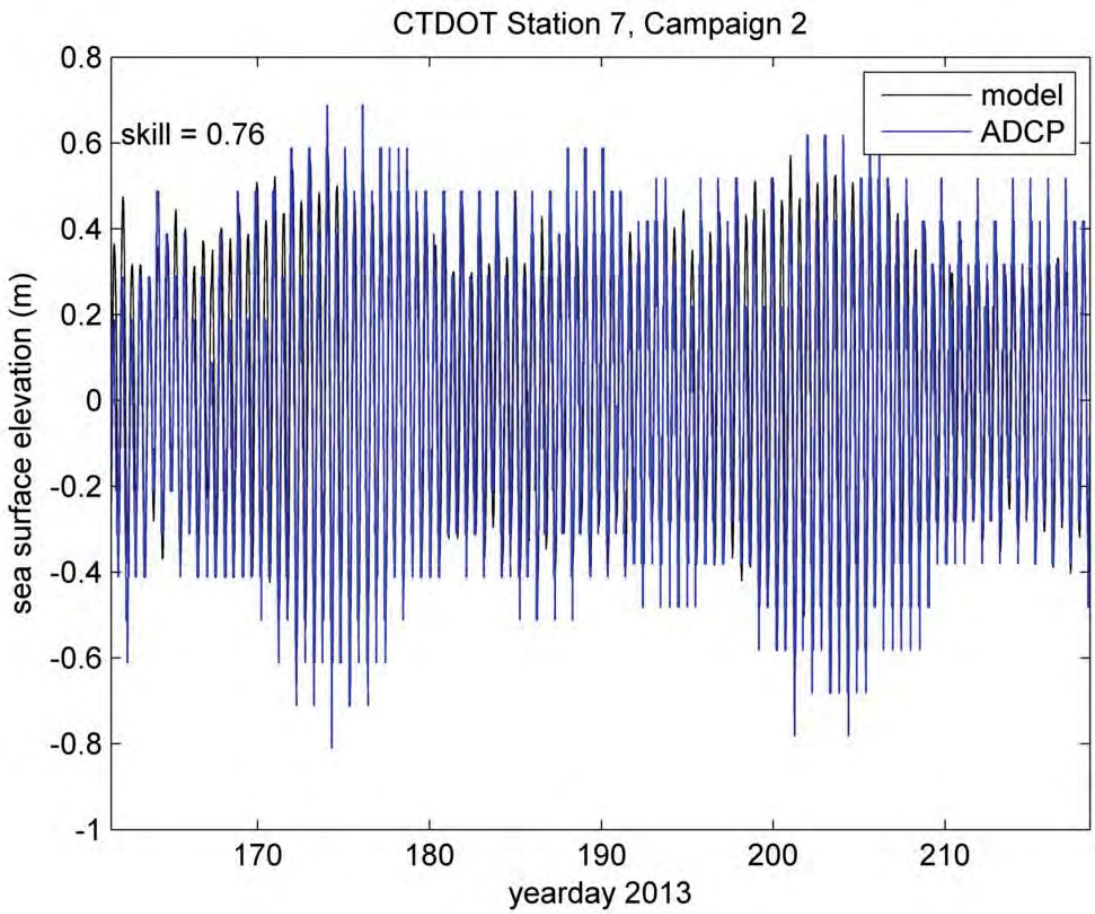

Figure A1.19. Comparison of tidal heights in the ZSF at Station DOT7 during Campaign 2 measured by ADCP pressure sensor (blue) compared to those predicted by the FVCOM model (black).

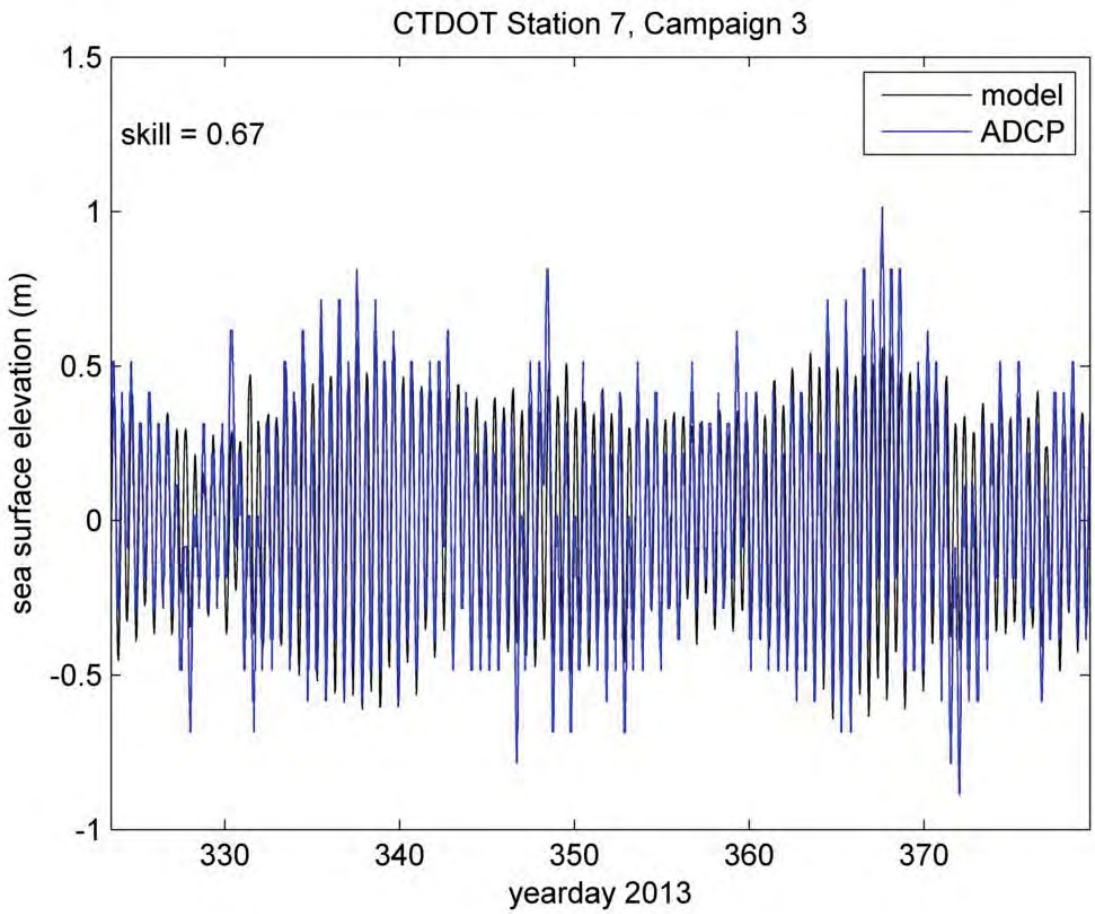

Figure A1.20. Comparison of tidal heights in the ZSF at Station DOT7 during Campaign 3 measured by ADCP pressure sensor (blue) compared to those predicted by the FVCOM model (black).

Appendix 2

COMPARISON OF MODEL-PREDICTED VERTICALLY AVERAGED CURRENT AND THAT MEASURED BY RDI ADCPS IN THE FIELD

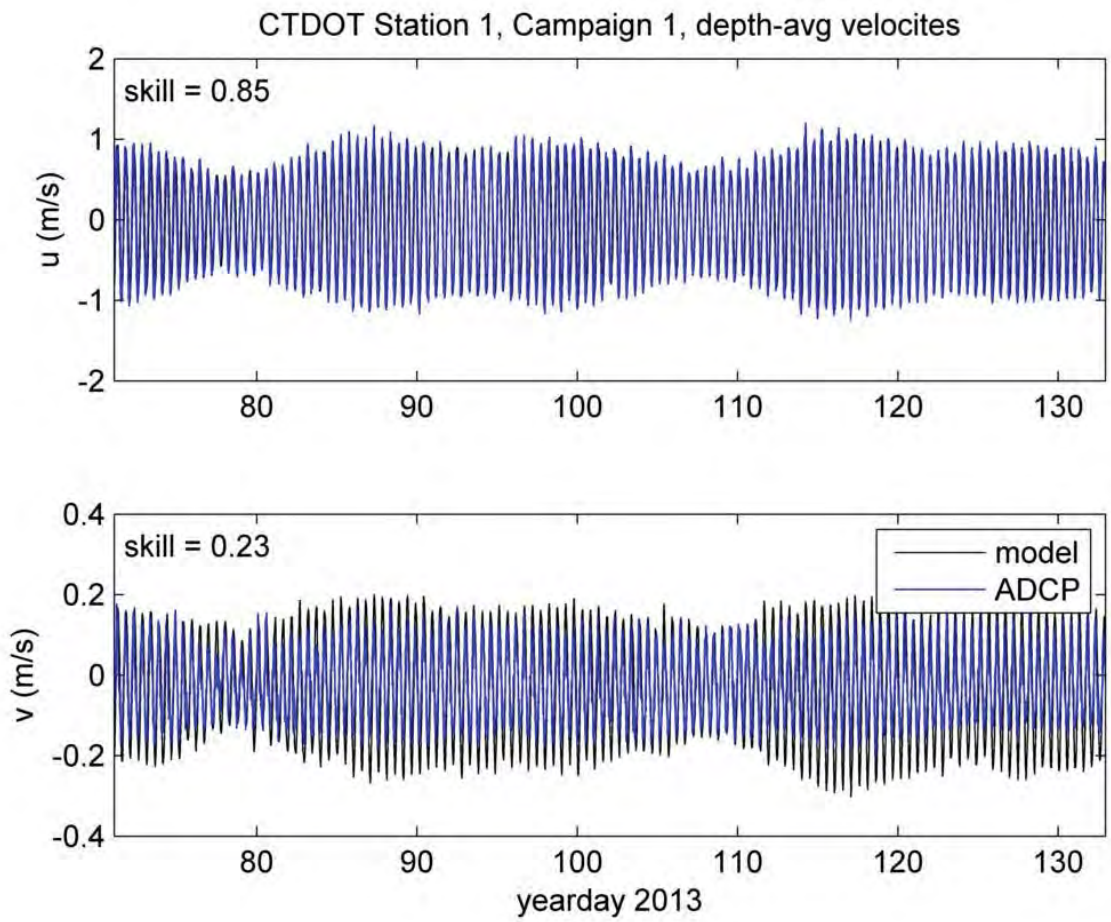

Figure A2.21. ADCP measurements in the field (blue) compared to those predicted by the FVCOM model (black) for depth-averaged currents at Station DOT1, Campaign 1.

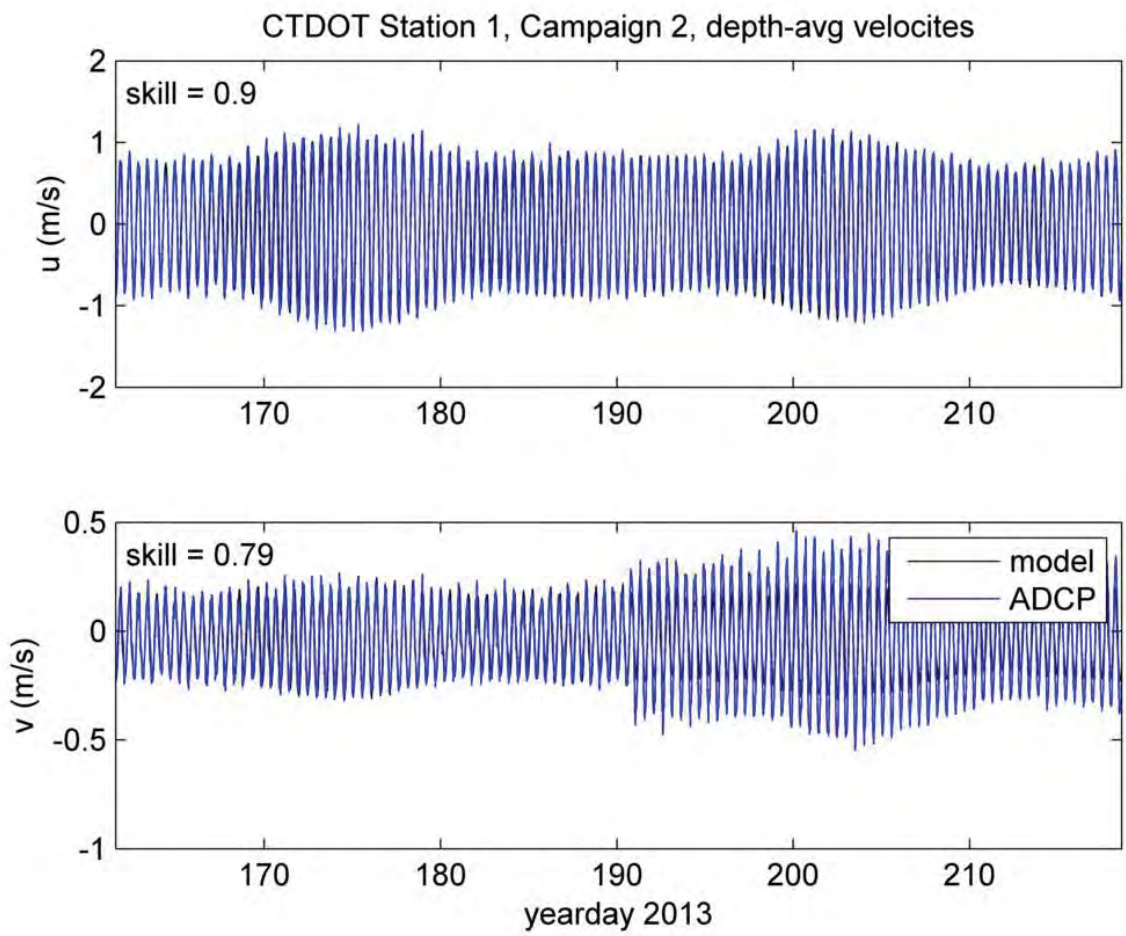

Figure A2.22. ADCP measurements in the field (blue) compared to those predicted by the FVCOM model (black) for depth-averaged currents at Station DOT1, Campaign 2.

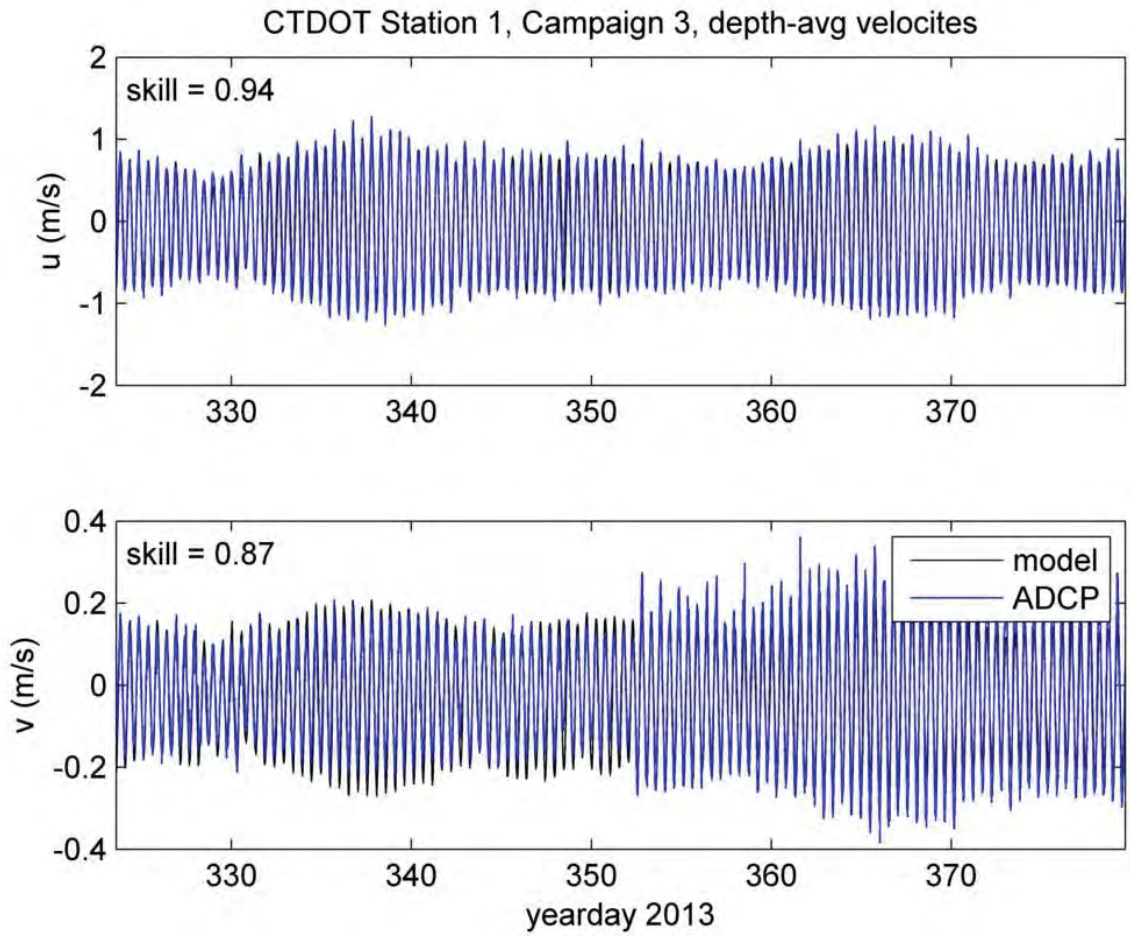

Figure A2.23. ADCP measurements in the field (blue) compared to those predicted by the FVCOM model (black) for depth-averaged currents at Station DOT1, Campaign 3.

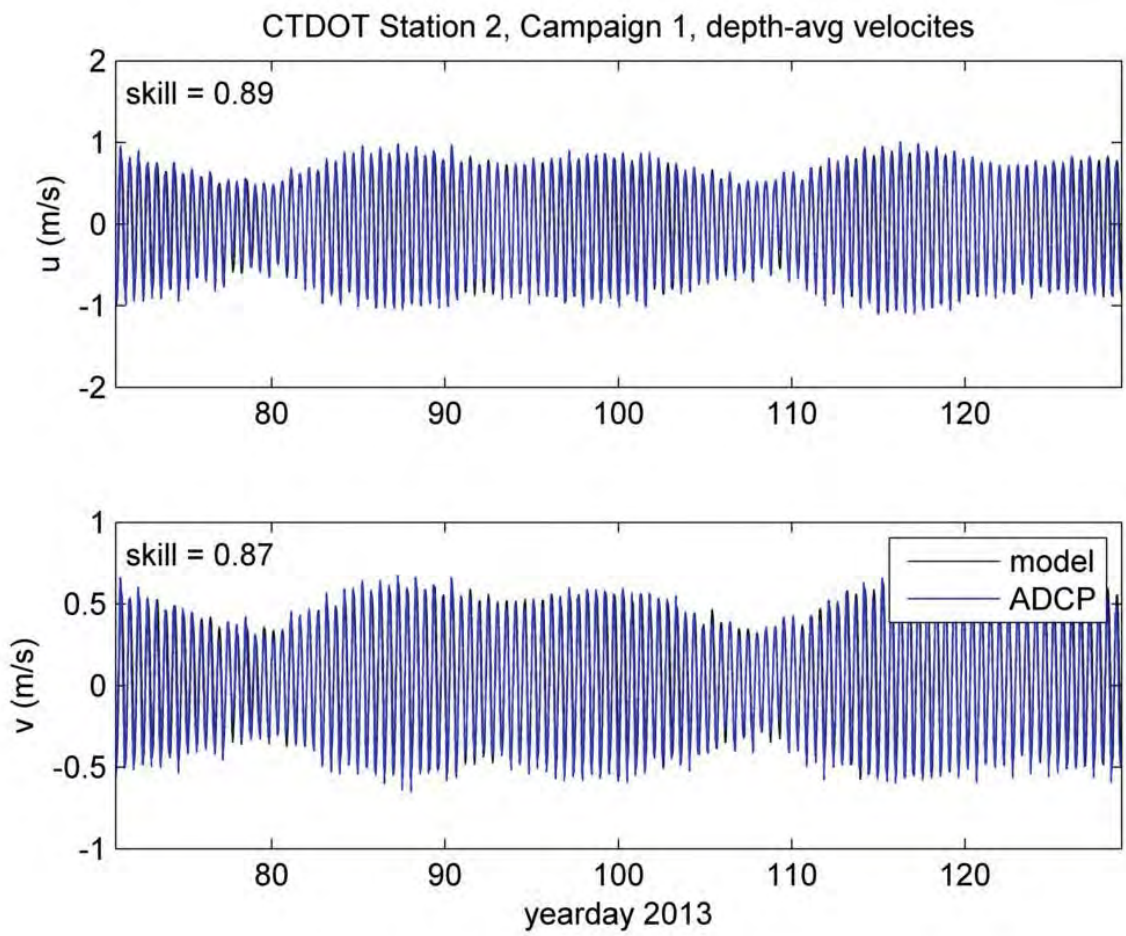

Figure A2.24. ADCP measurements in the field (blue) compared to those predicted by the FVCOM model (black) for depth-averaged currents at Station DOT2, Campaign 1.

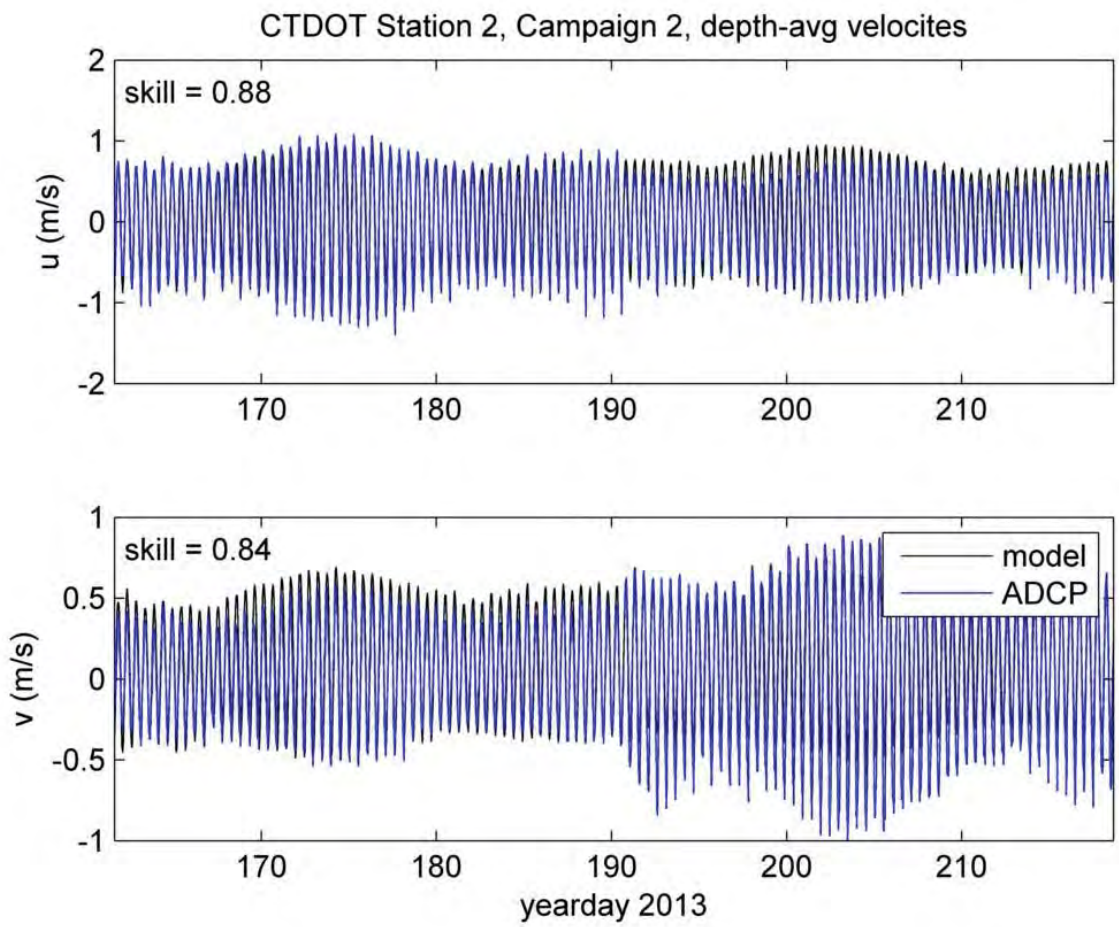

Figure A2.25. ADCP measurements in the field (blue) compared to those predicted by the FVCOM model (black) for depth-averaged currents at Station DOT2, Campaign 2.

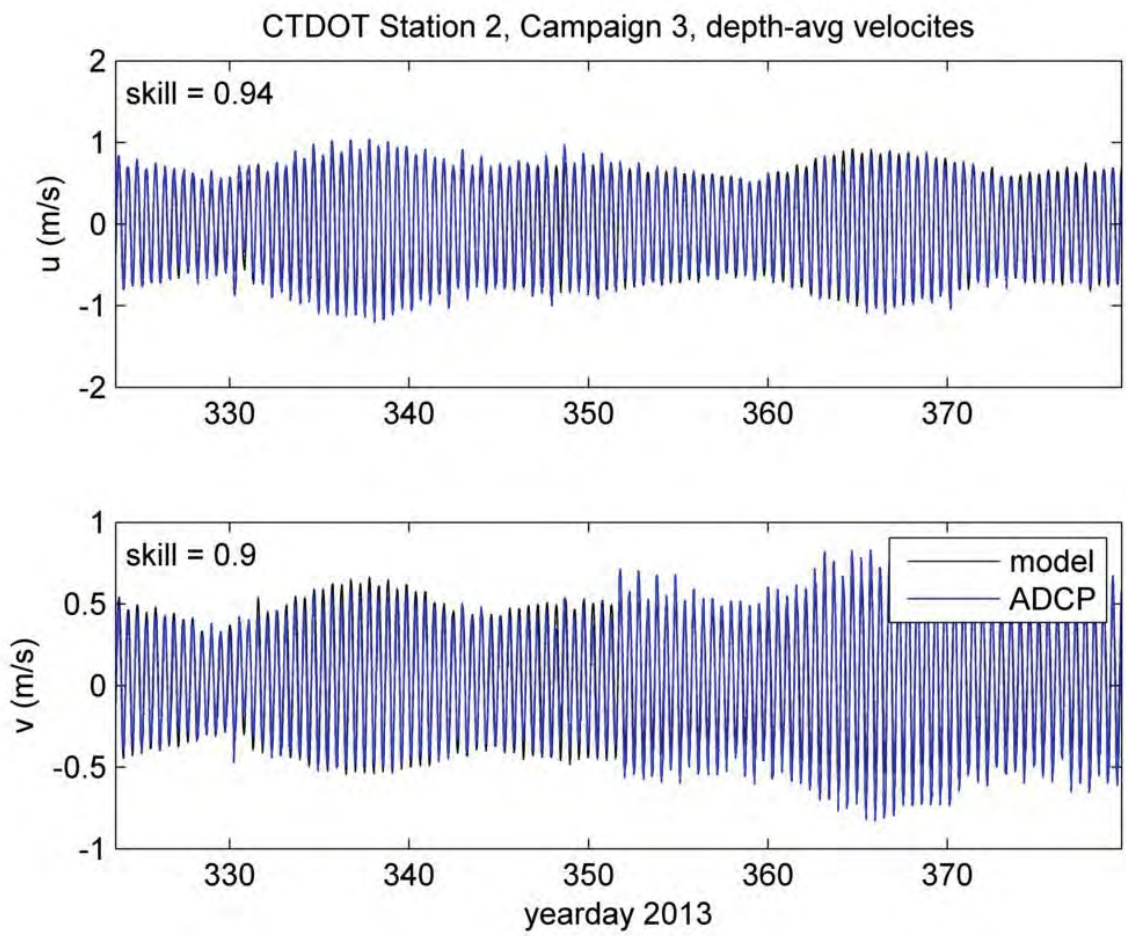

Figure A2.26. ADCP measurements in the field (blue) compared to those predicted by the FVCOM model (black) for depth-averaged currents at Station DOT2, Campaign 3.

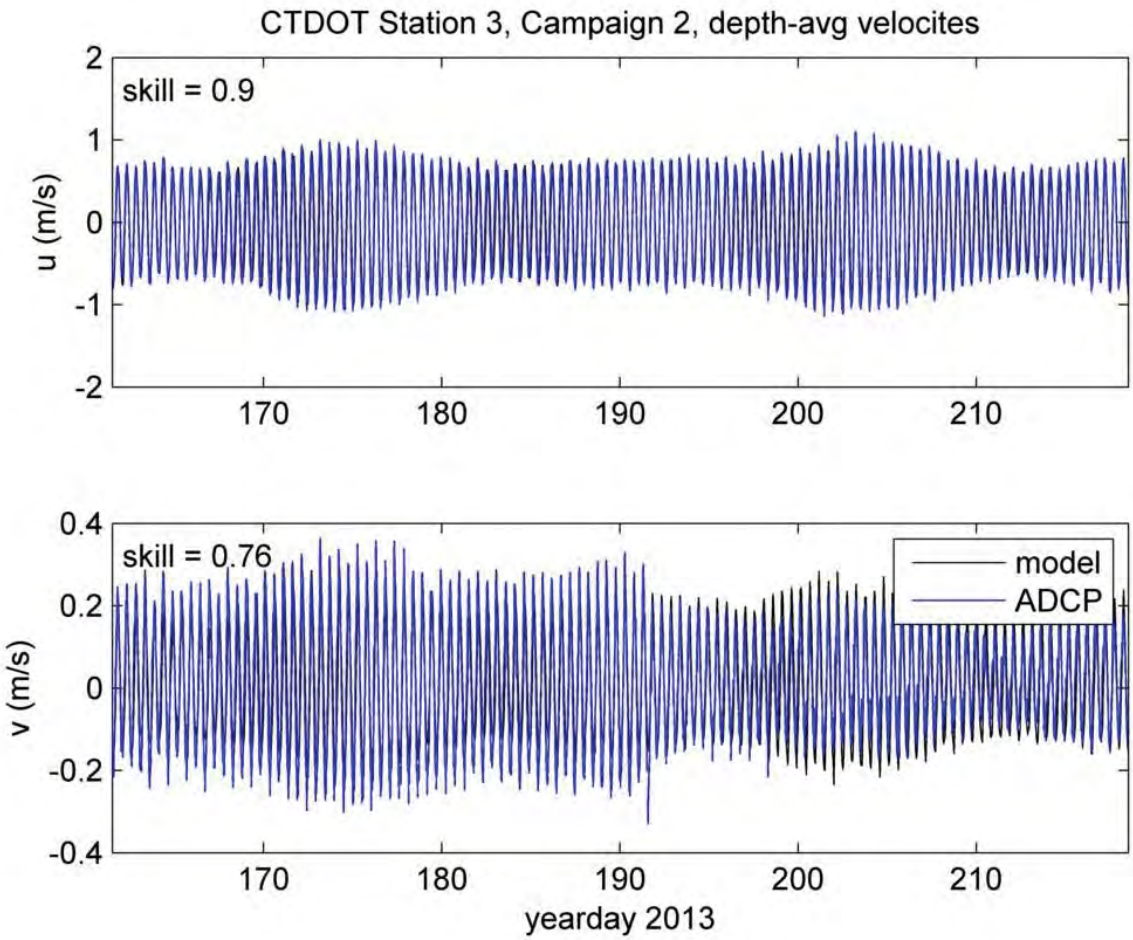

Figure A2.27. ADCP measurements in the field (blue) compared to those predicted by the FVCOM model (black) for depth-averaged currents at Station DOT3, Campaign 2.

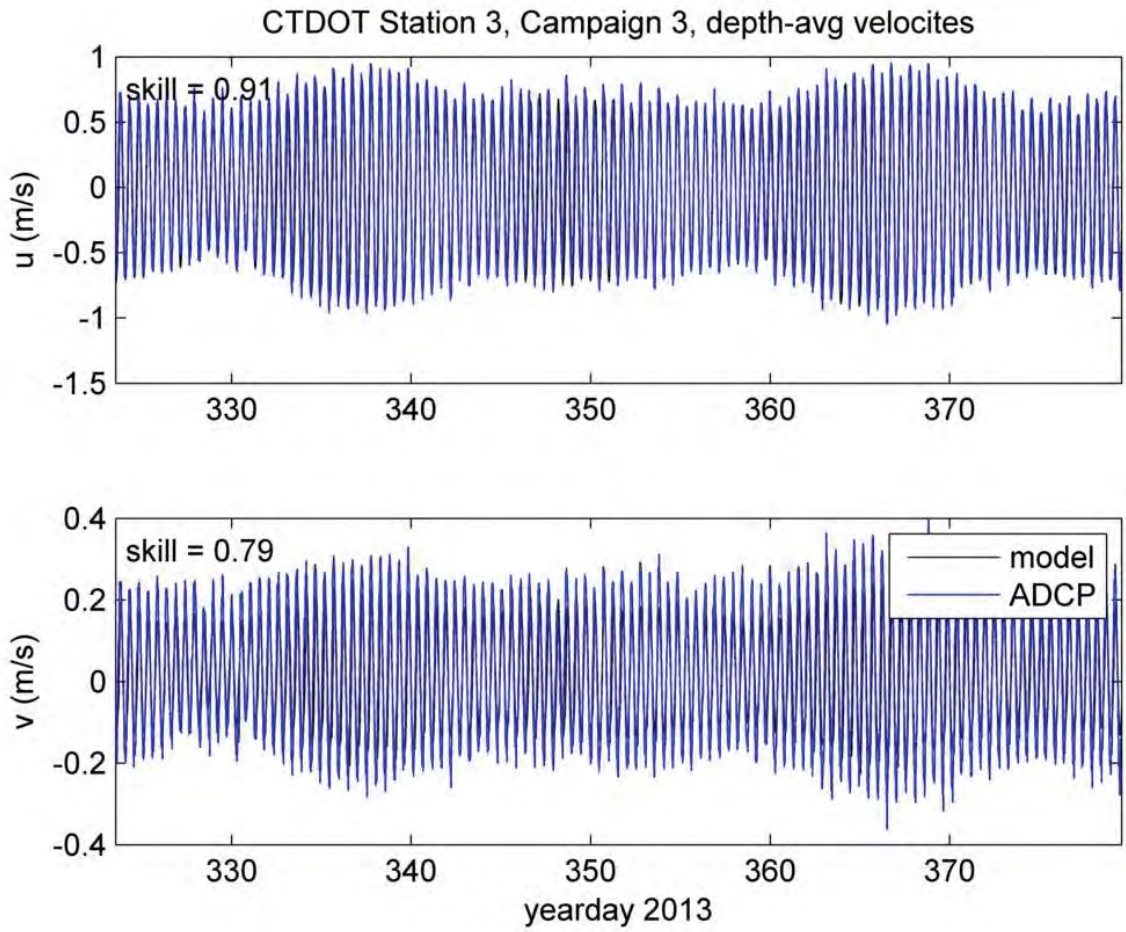

Figure A2.28. ADCP measurements in the field (blue) compared to those predicted by the FVCOM model (black) for depth-averaged currents at Station DOT3, Campaign 3.

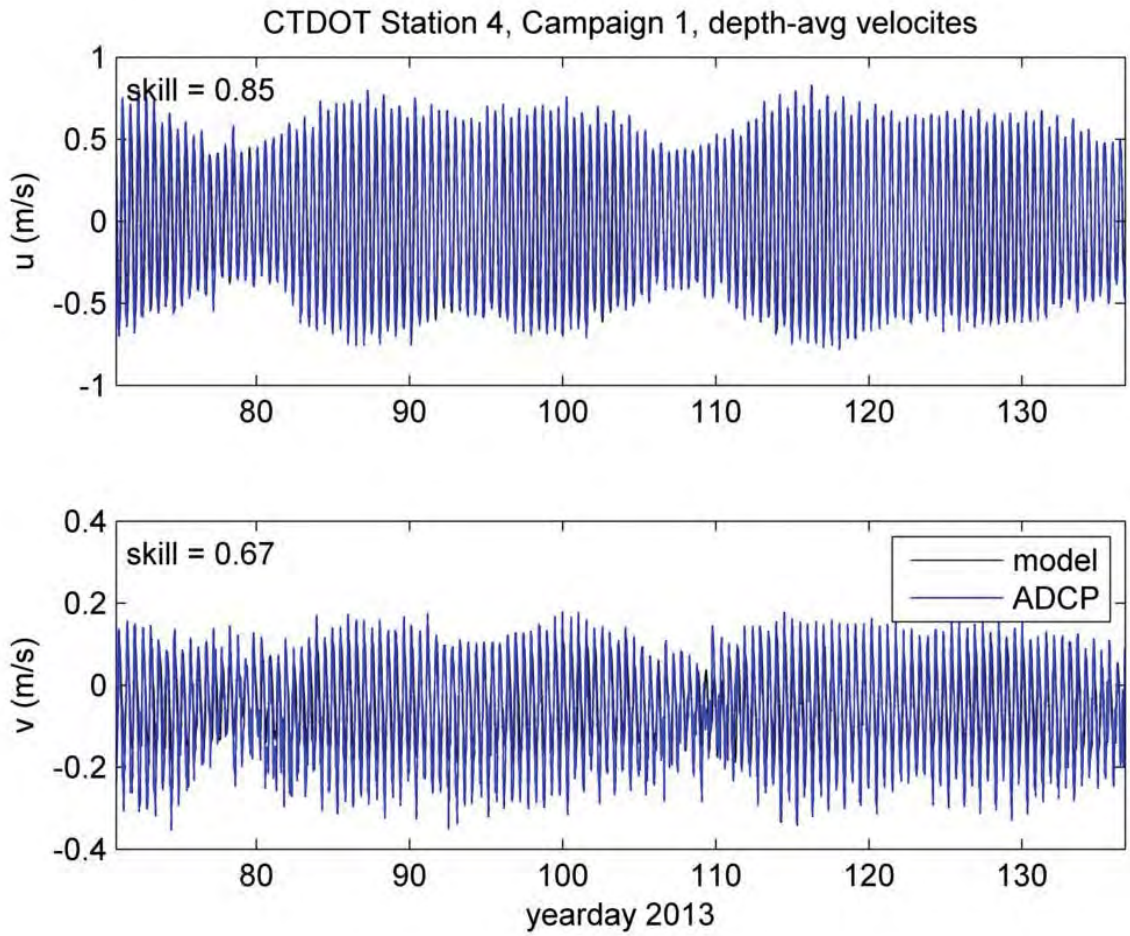

Figure A2.29. ADCP measurements in the field (blue) compared to those predicted by the FVCOM model (black) for depth-averaged currents at Station DOT4, Campaign 1.

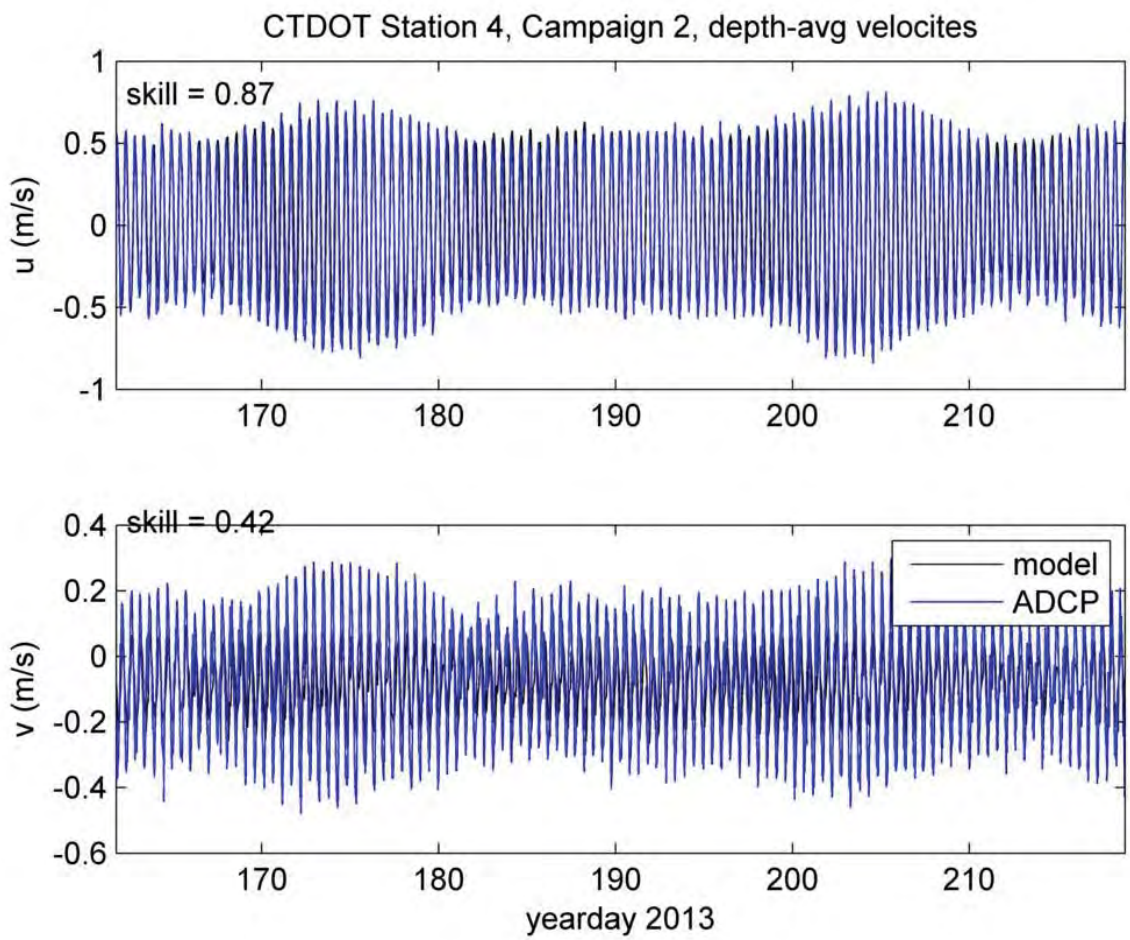

Figure A2.30. ADCP measurements in the field (blue) compared to those predicted by the FVCOM model (black) for depth-averaged currents at Station DOT4, Campaign 2.

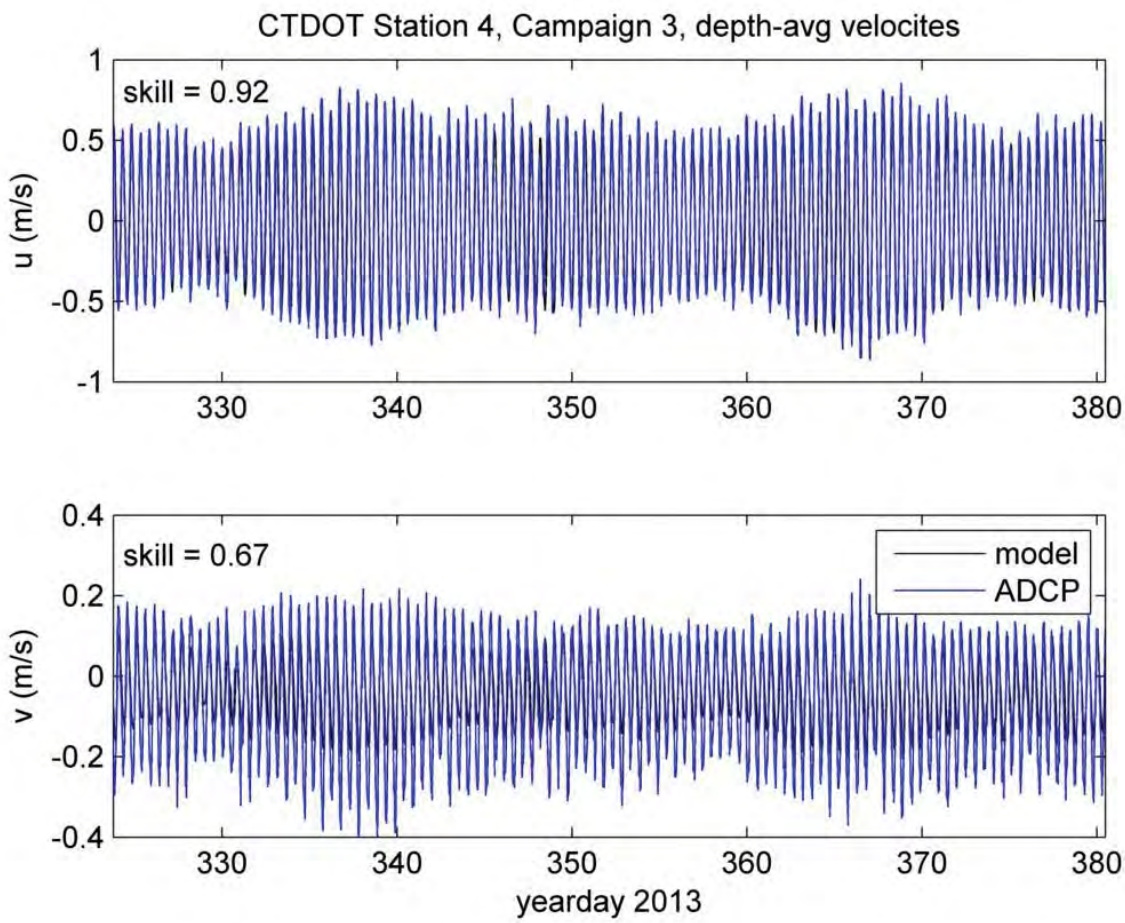

Figure A2.31. ADCP measurements in the field (blue) compared to those predicted by the FVCOM model (black) for depth-averaged currents at Station DOT4, Campaign 3.

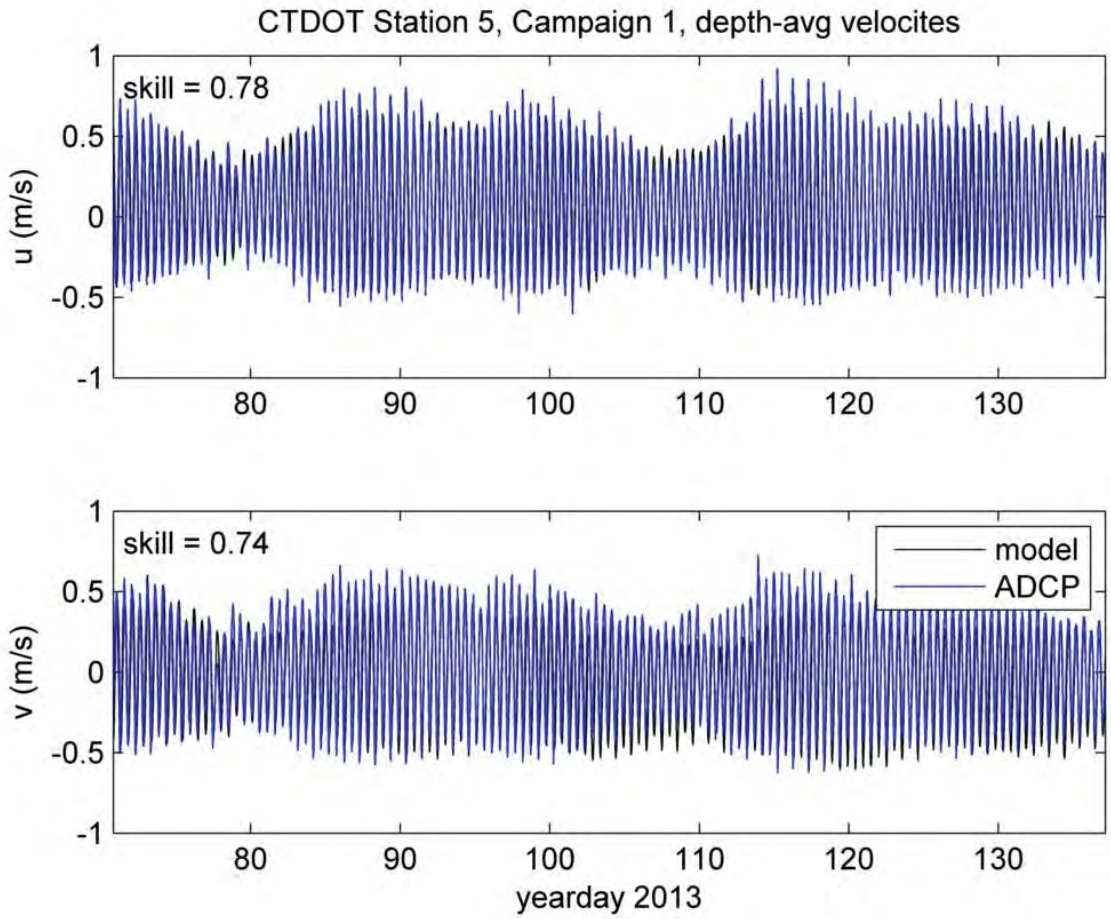

Figure A2.32. ADCP measurements in the field (blue) compared to those predicted by the FVCOM model (black) for depth-averaged currents at Station DOT5, Campaign 1.

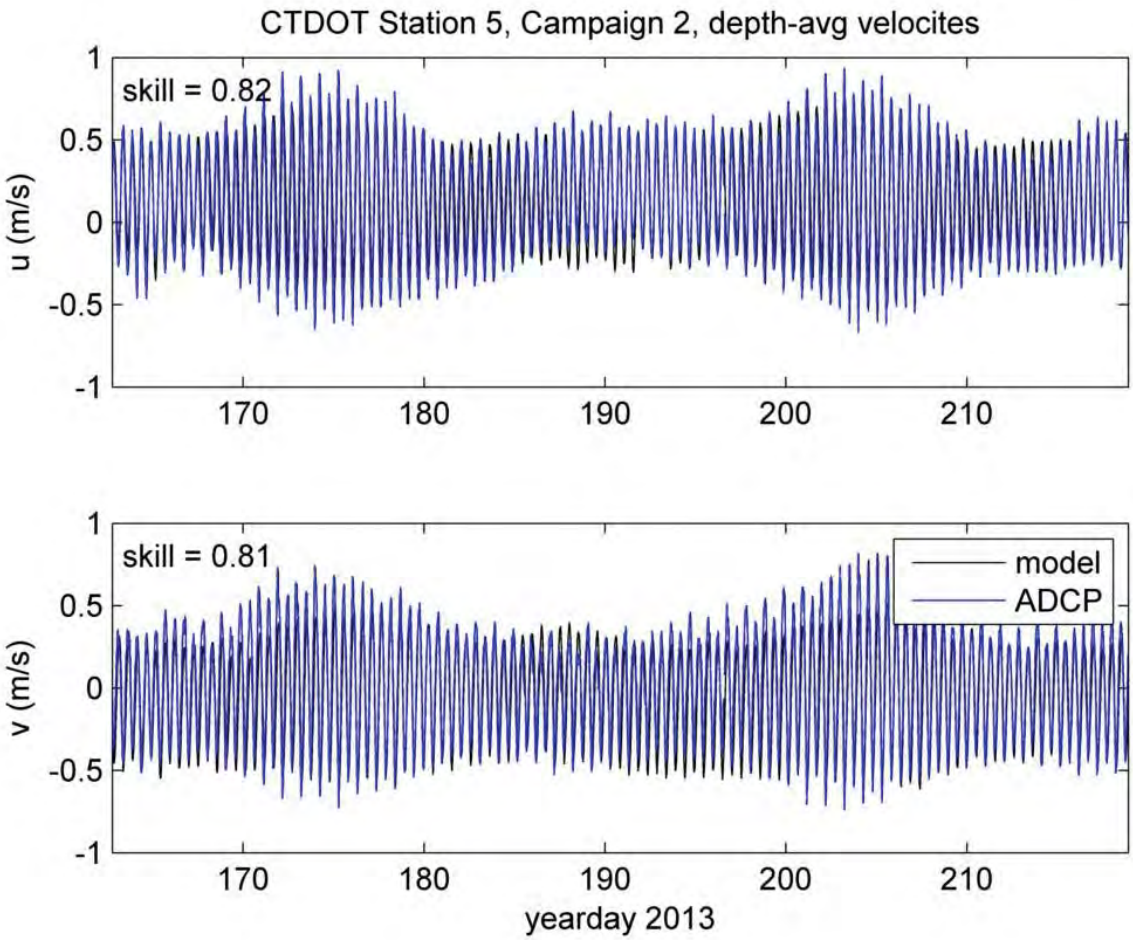

Figure A2.33. ADCP measurements in the field (blue) compared to those predicted by the FVCOM model (black) for depth-averaged currents at Station DOT5, Campaign 2.

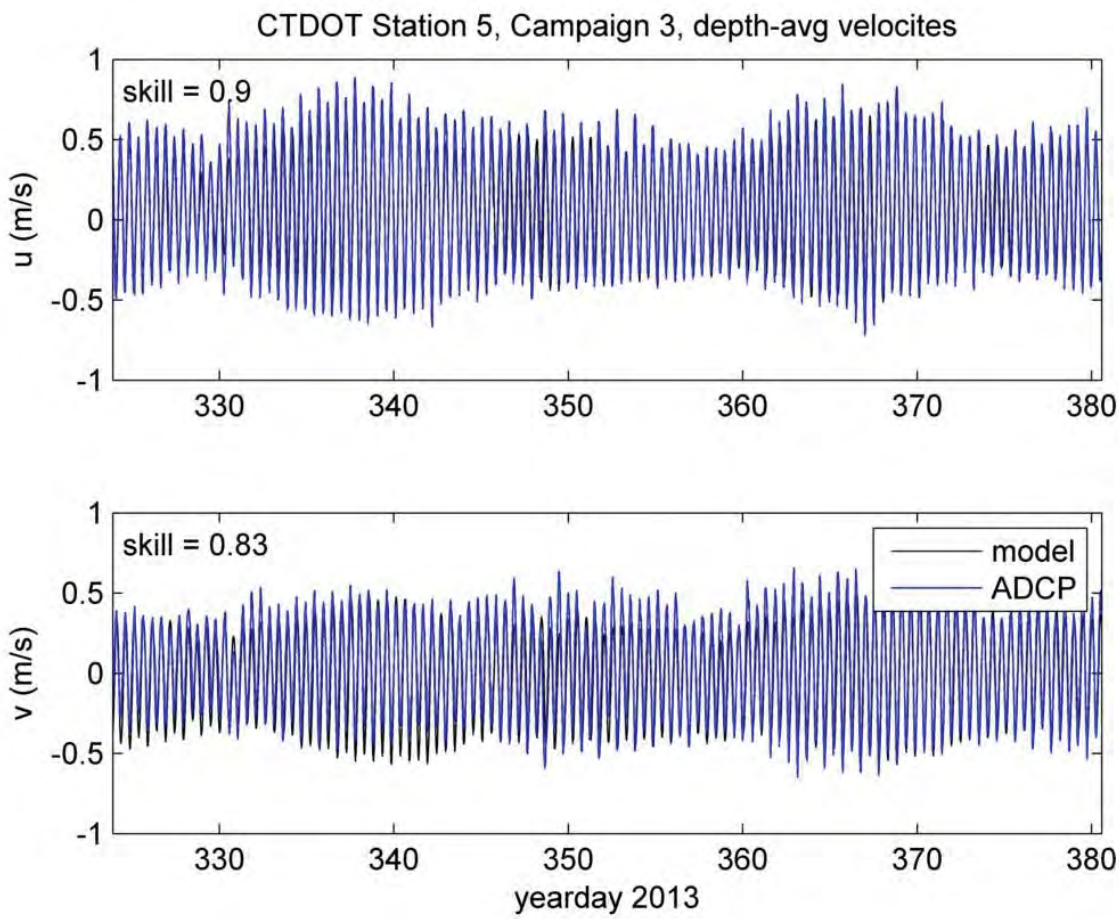

Figure A2.34. ADCP measurements in the field (blue) compared to those predicted by the FVCOM model (black) for depth-averaged currents at Station DOT5, Campaign 3.

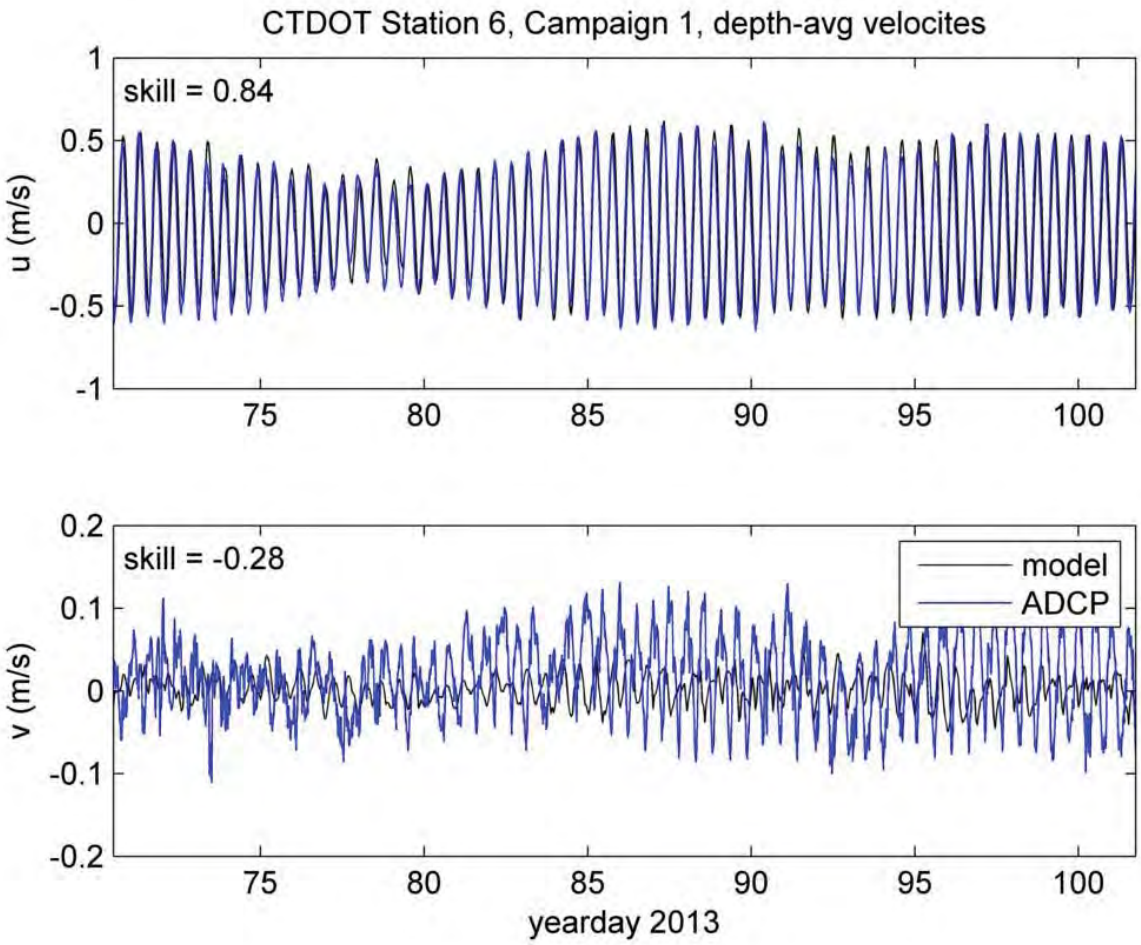

Figure A2.35. ADCP measurements in the field (blue) compared to those predicted by the FVCOM model (black) for depth-averaged currents at Station DOT6, Campaign 1.

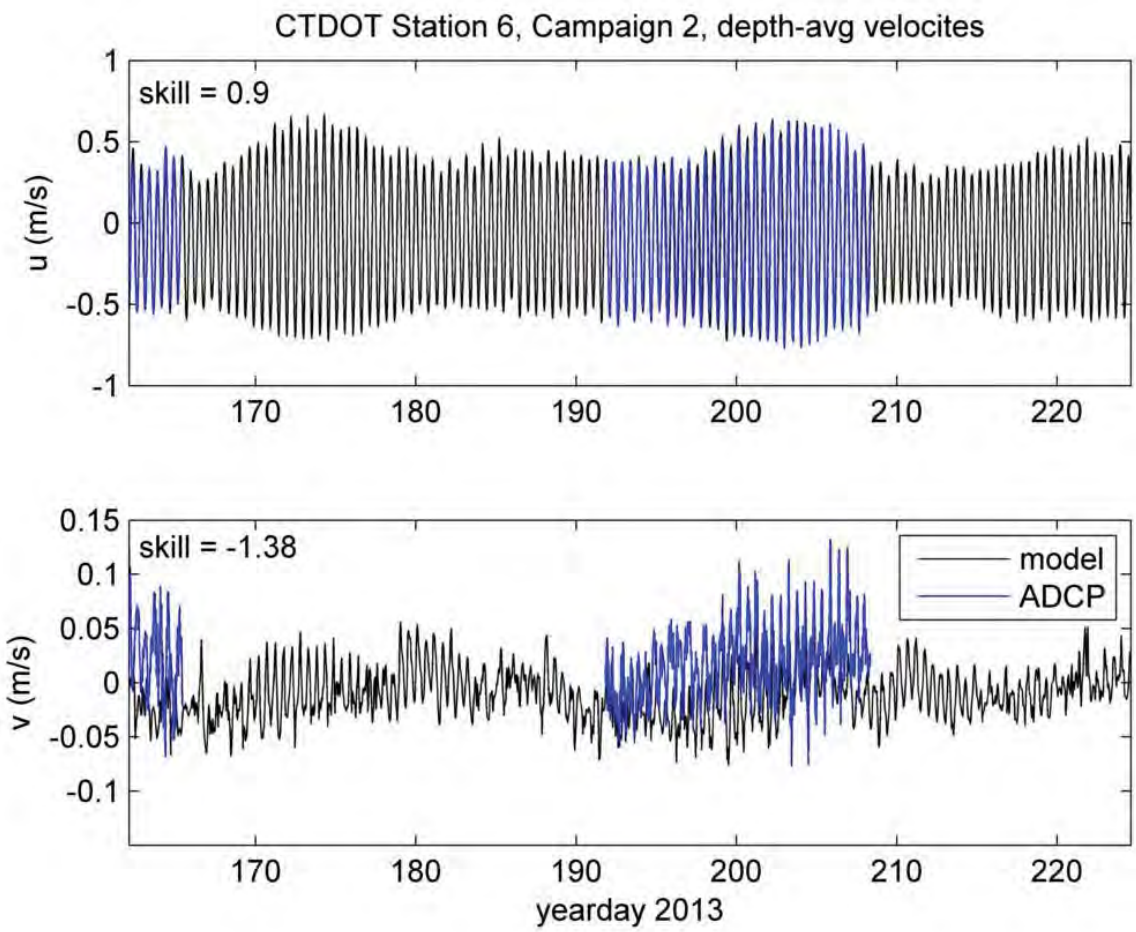

Figure A2.36. ADCP measurements in the field (blue) compared to those predicted by the FVCOM model (black) for depth-averaged currents at Station DOT6, Campaign 2.

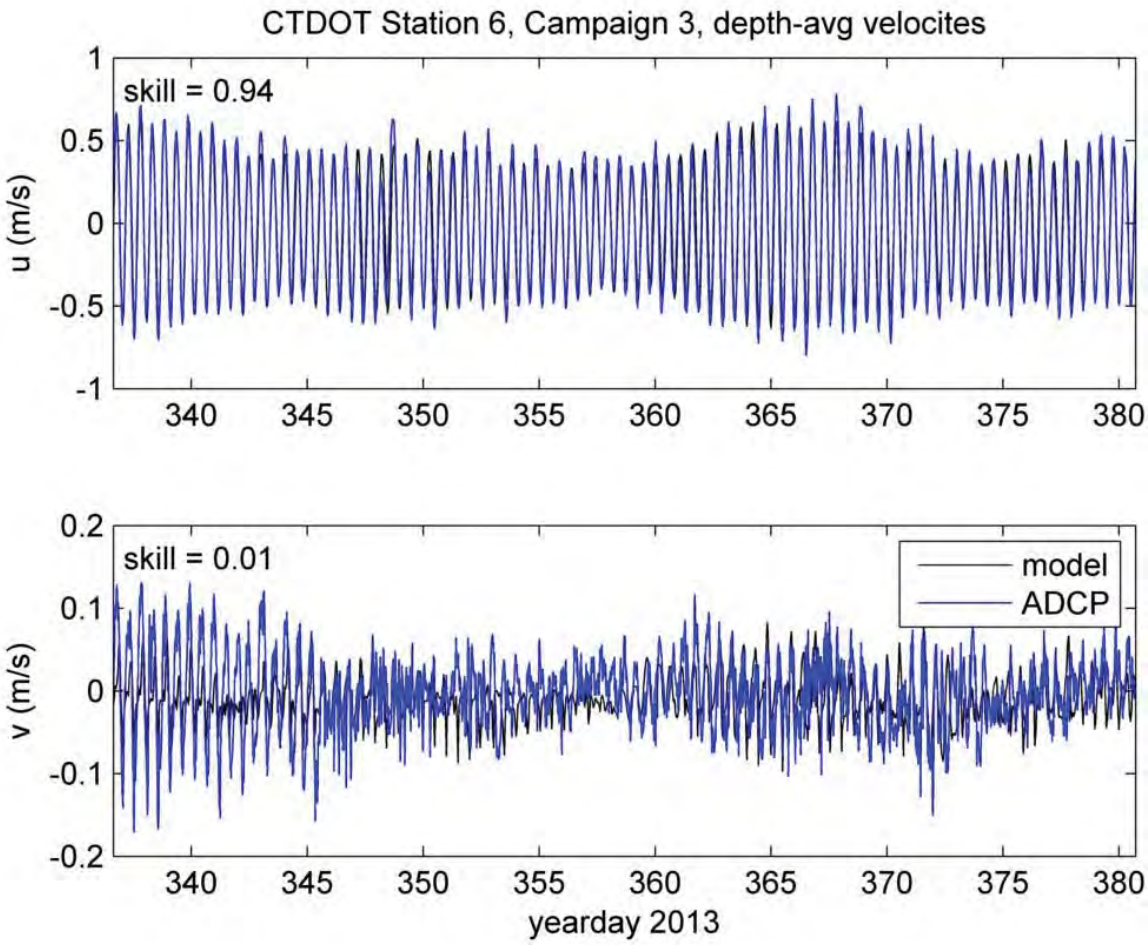

Figure A2.37. ADCP measurements in the field (blue) compared to those predicted by the FVCOM model (black) for depth-averaged currents at Station DOT6, Campaign 3

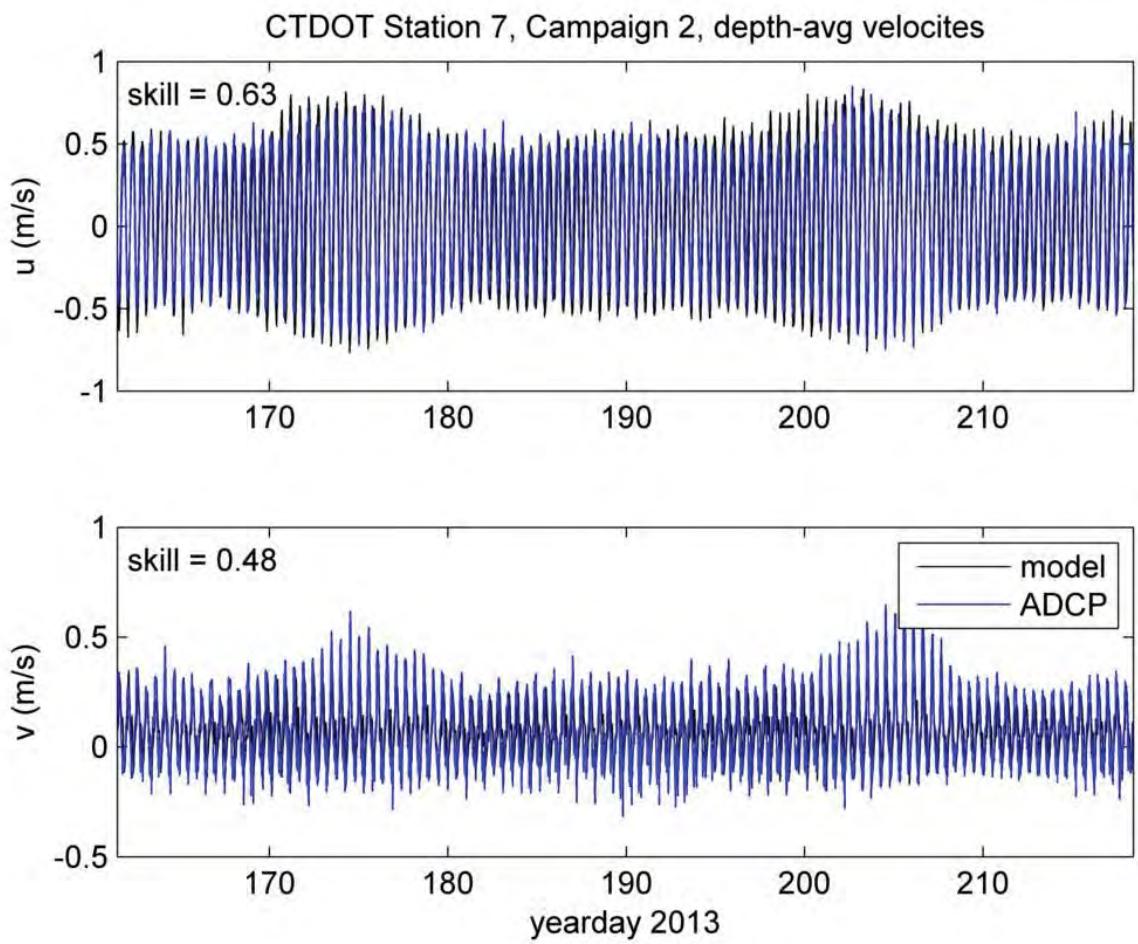

Figure A2.38. ADCP measurements in the field (blue) compared to those predicted by the FVCOM model (black) for depth-averaged currents at Station DOT7, Campaign 2.

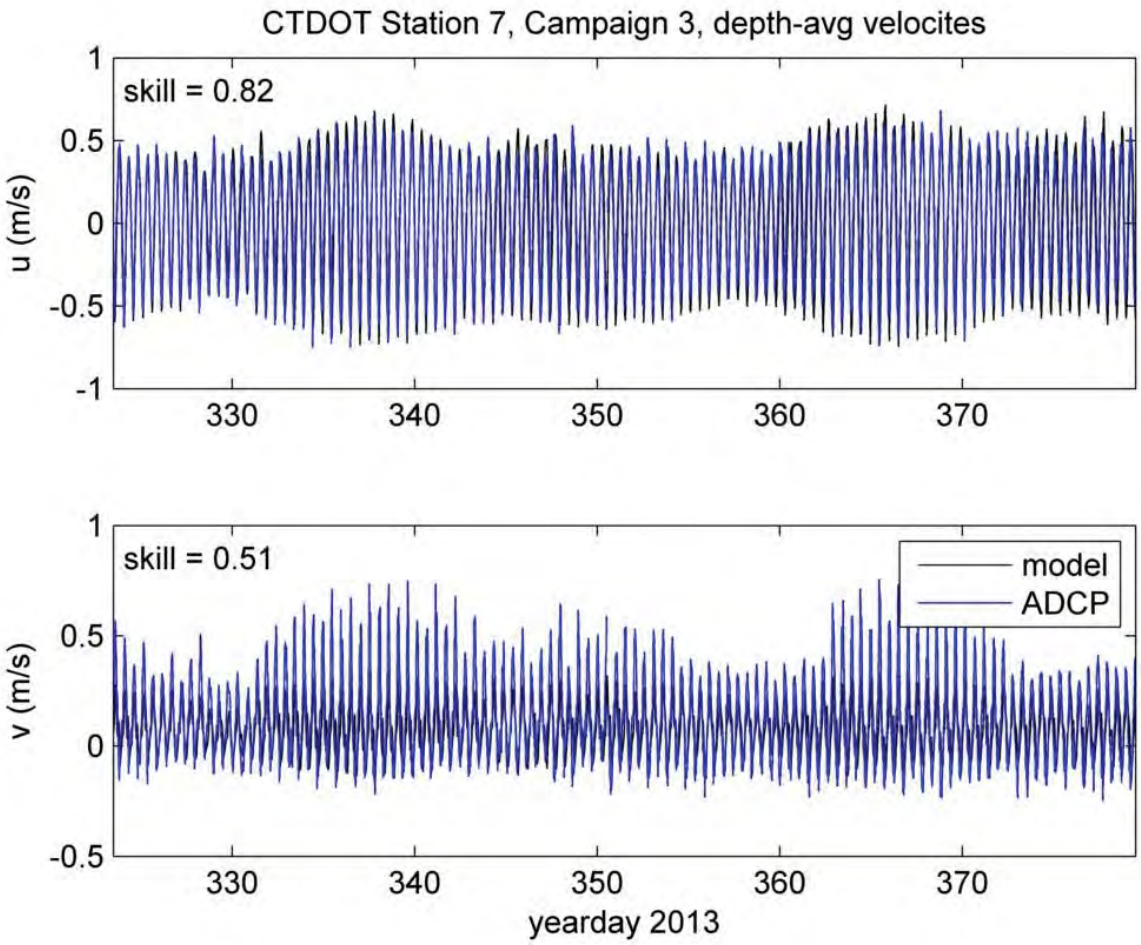

Figure A2.39. ADCP measurements in the field (blue) compared to those predicted by the FVCOM model (black) for depth-averaged currents at Station DOT7, Campaign 3.

Appendix 3

Comparison of Model-predicted Bottom Stress and the Measured Stress using the Bulk Formula

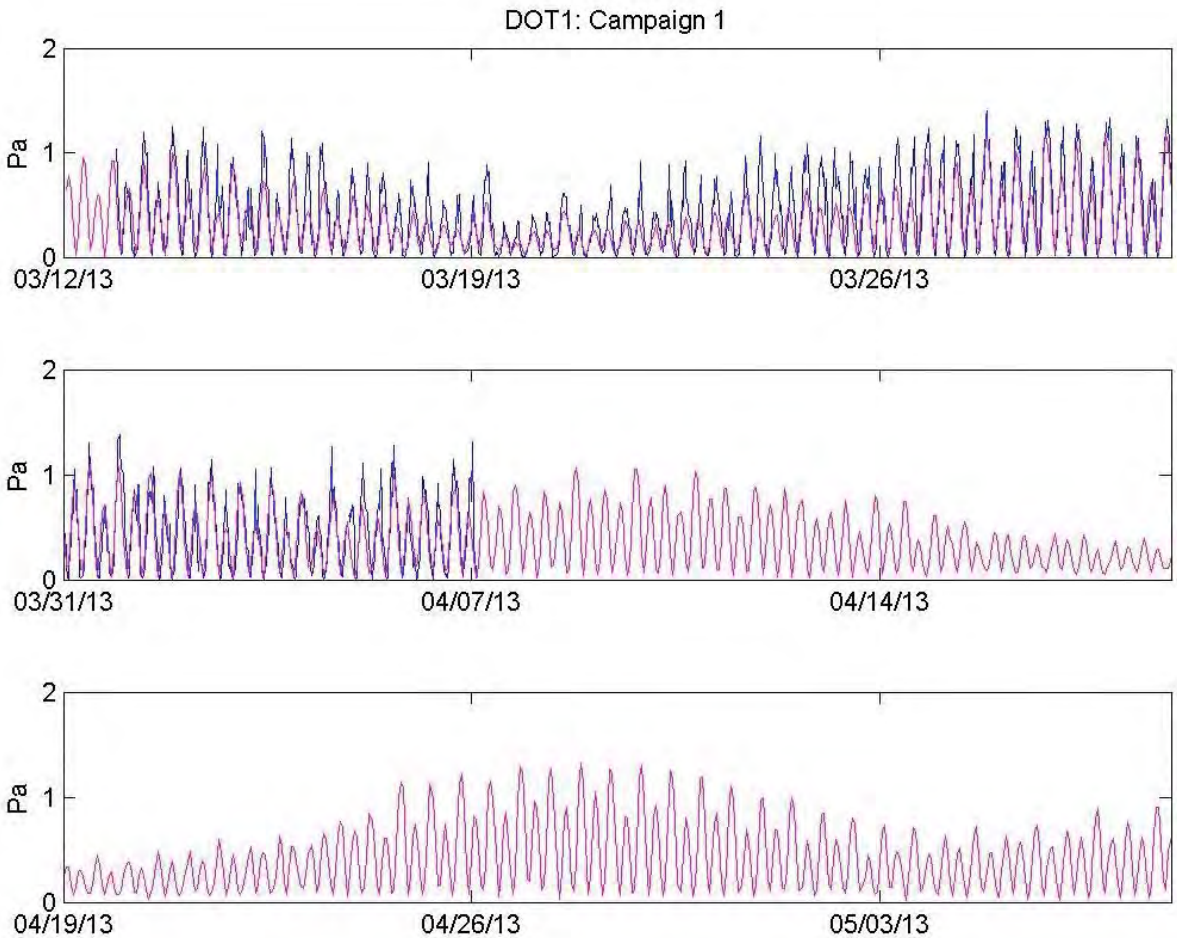

Figure A3.40. Model-predicted bottom stress, $\boldsymbol{\tau_m}$, at Station DOT1 during Campaign 1 in the spring of 2013 (magenta line). The blue line shows the measured stress using the bulk formula, $|\boldsymbol{\tau_{BF}}|$.

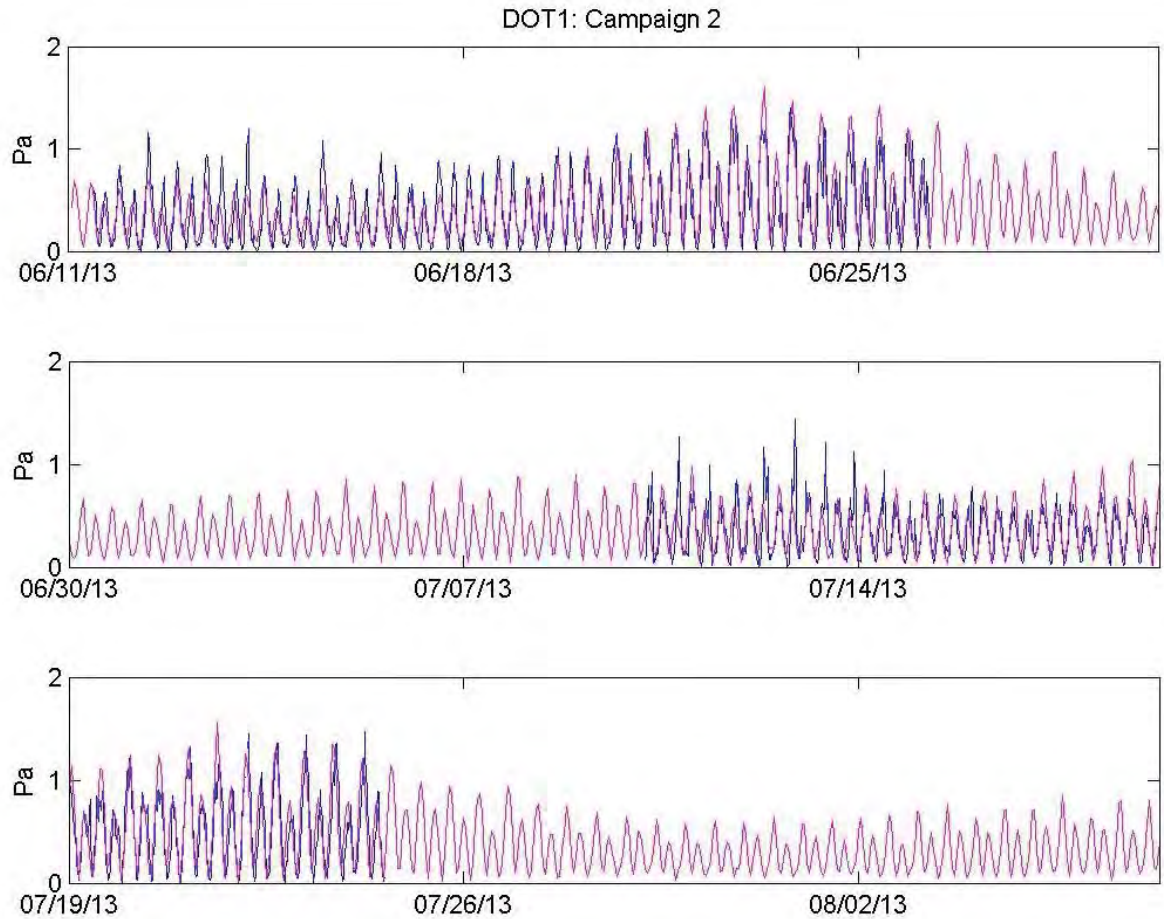

Figure A3.41. Model-predicted bottom stress, $\boldsymbol{\tau_m}$, at Station DOT1 during Campaign 2 in the summer of 2013 (magenta line). The blue line shows the measured stress using the bulk formula, $|\boldsymbol{\tau_{BF}}|$.

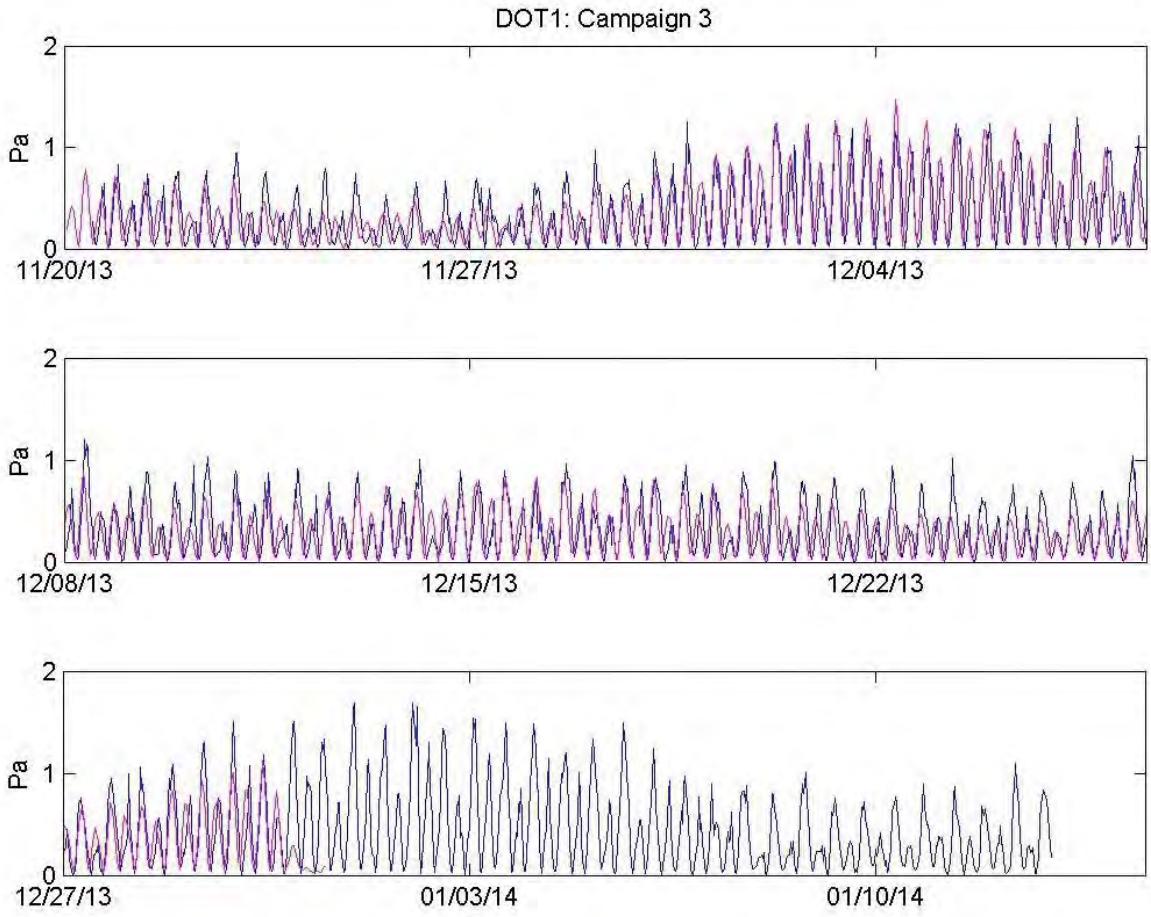

Figure A3.42. Model-predicted bottom stress, $\boldsymbol{\tau_m}$, at Station DOT1 during Campaign 3 in the winter of 2013/2014 (magenta line). The blue line shows the measured stress using the bulk formula, $|\boldsymbol{\tau_{BF}}|$.

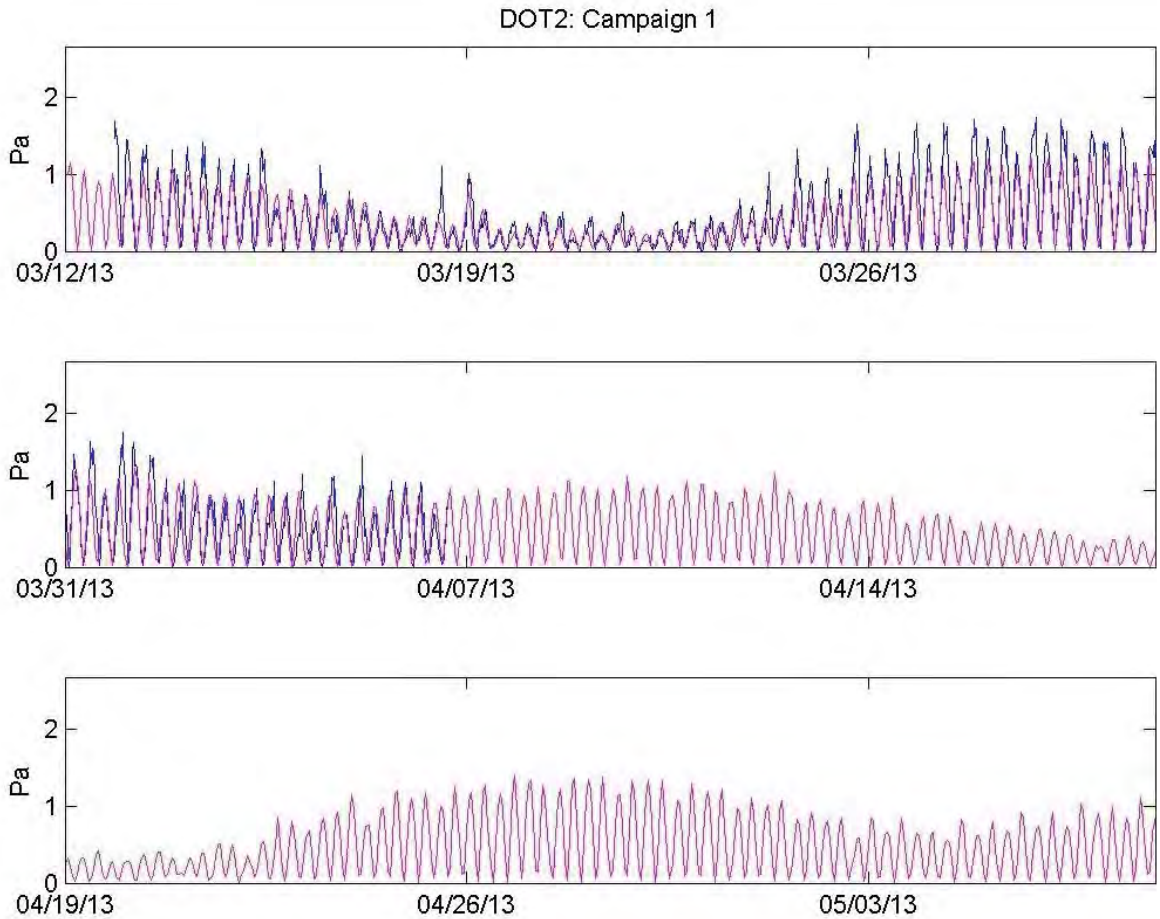

Figure A3.43. Model-predicted bottom stress, $\boldsymbol{\tau_m}$, at Station DOT2 during Campaign 1 in the spring of 2013 (magenta line). The blue line shows the measured stress using the bulk formula, $|\boldsymbol{\tau_{BF}}|$.

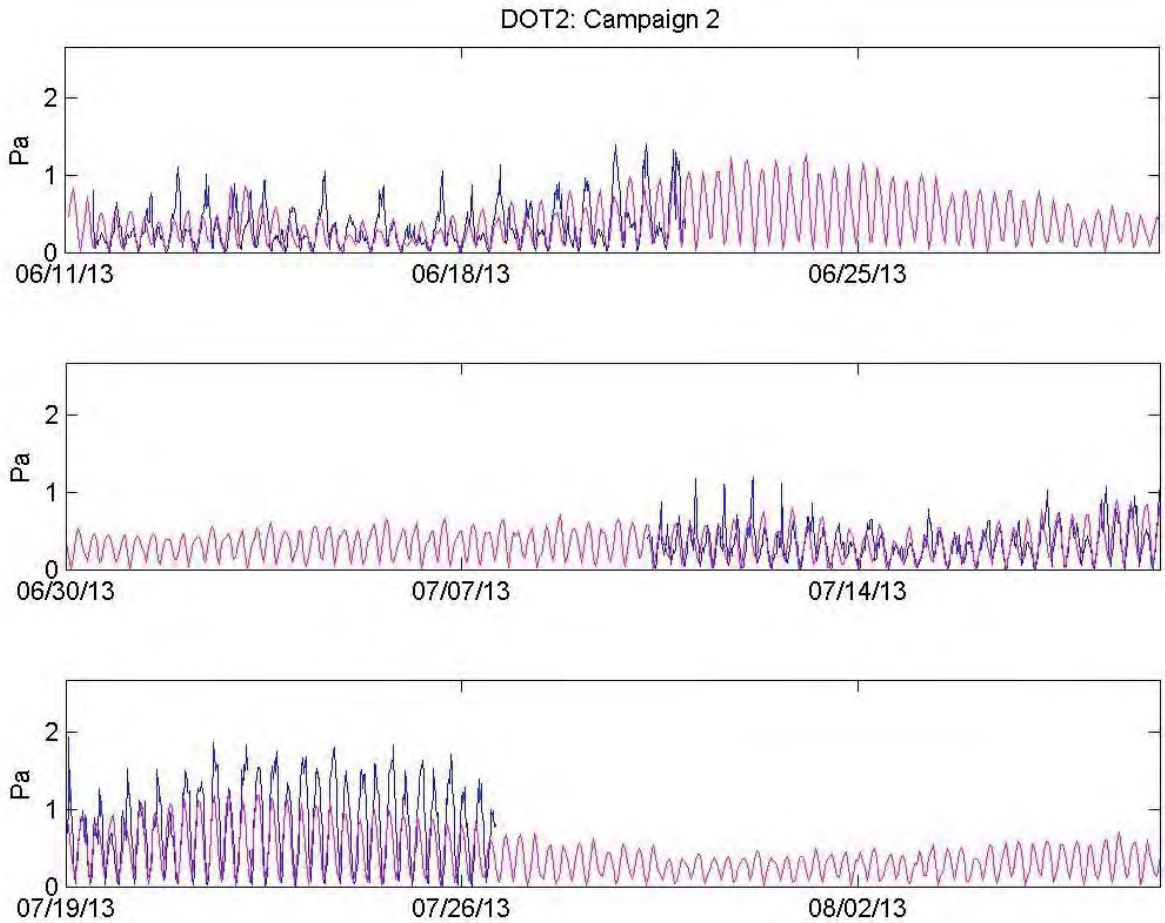

Figure A3.44. Model-predicted bottom stress, $\boldsymbol{\tau_m}$, at Station DOT2 during Campaign 2 in the summer of 2013 (magenta line). The blue line shows the measured stress using the bulk formula, $|\boldsymbol{\tau_{BF}}|$.

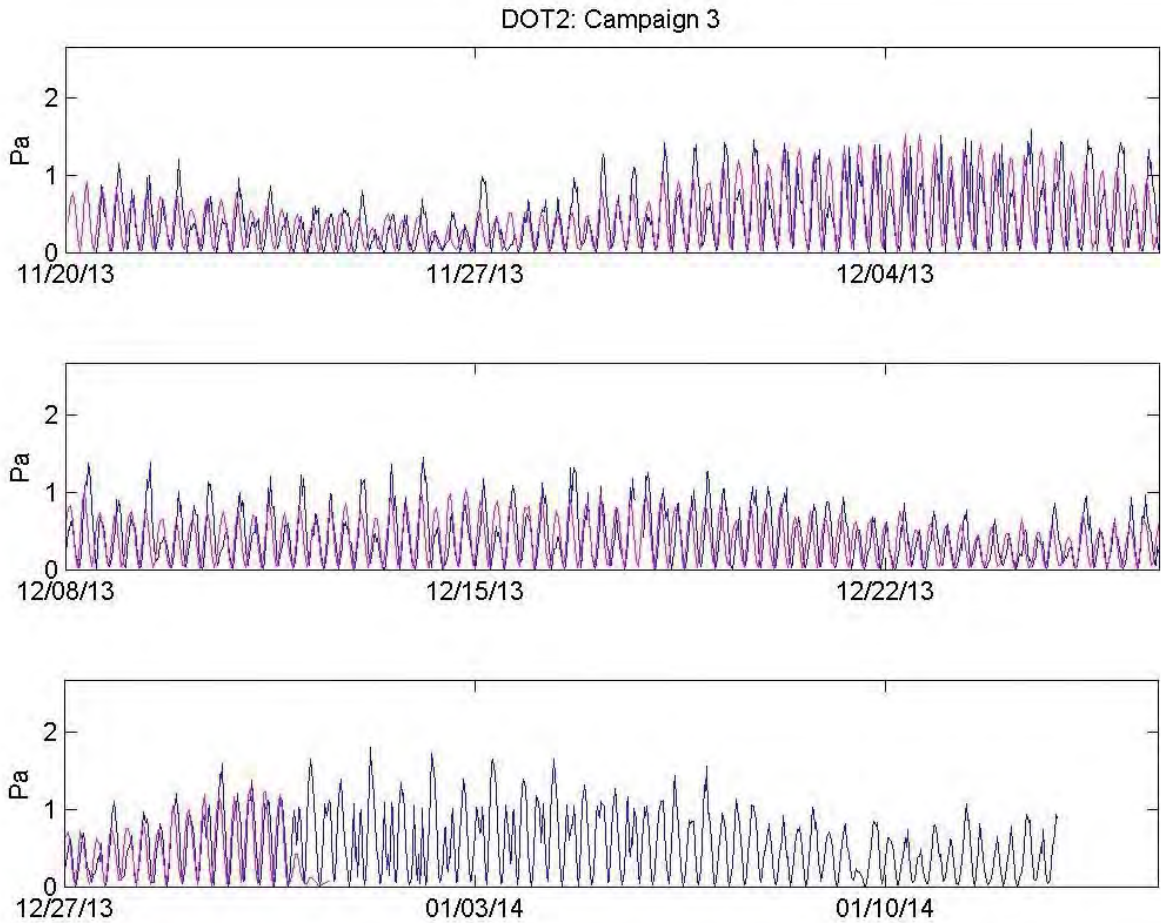

Figure A3.45. Model-predicted bottom stress, $\boldsymbol{\tau_m}$, at Station DOT2 during Campaign 3 in the winter of 2013/2014 (magenta line). The blue line shows the measured stress using the bulk formula, $|\boldsymbol{\tau_{BF}}|$.

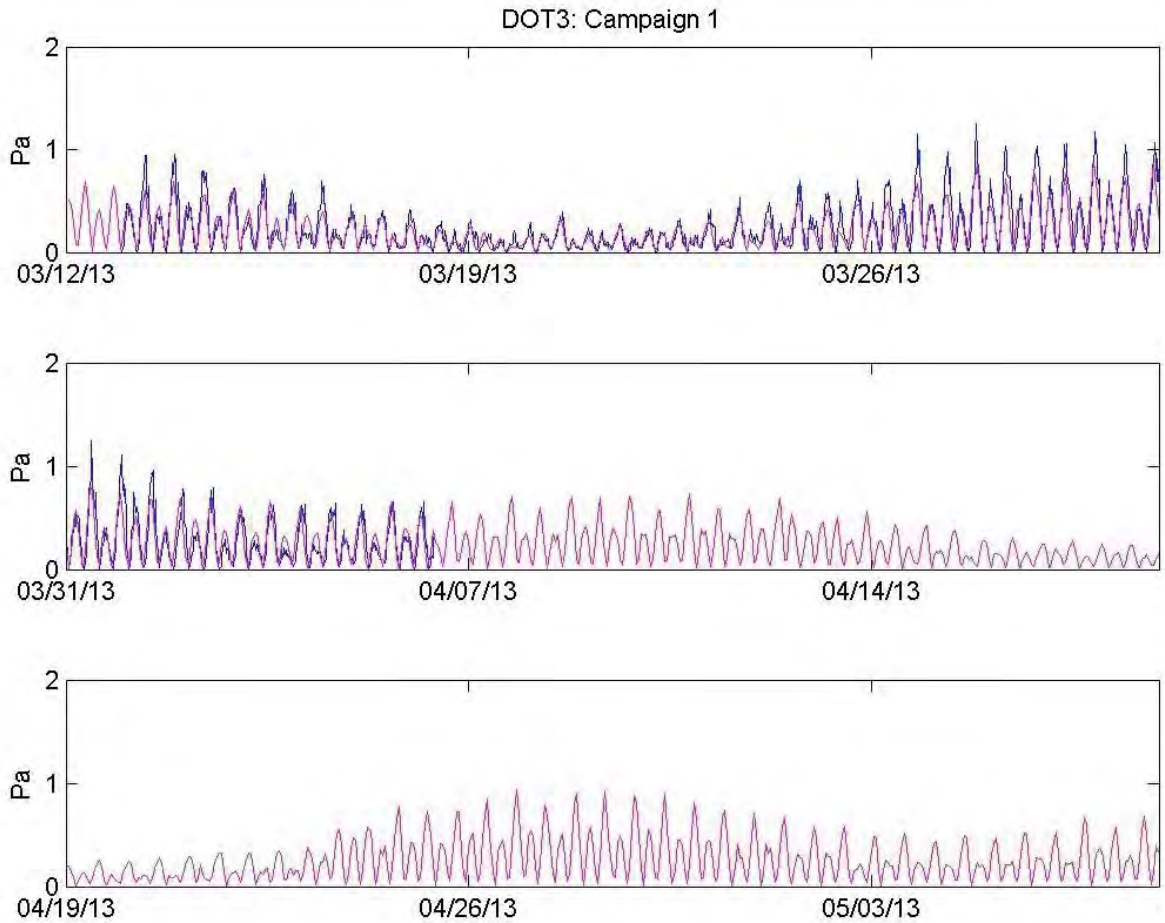

Figure A3.46. Model-predicted bottom stress, $\boldsymbol{\tau_m}$, at Station DOT3 during Campaign 1 in the spring of 2013 (magenta line). The blue line shows the measured stress using the bulk formula, $|\boldsymbol{\tau_{BF}}|$.

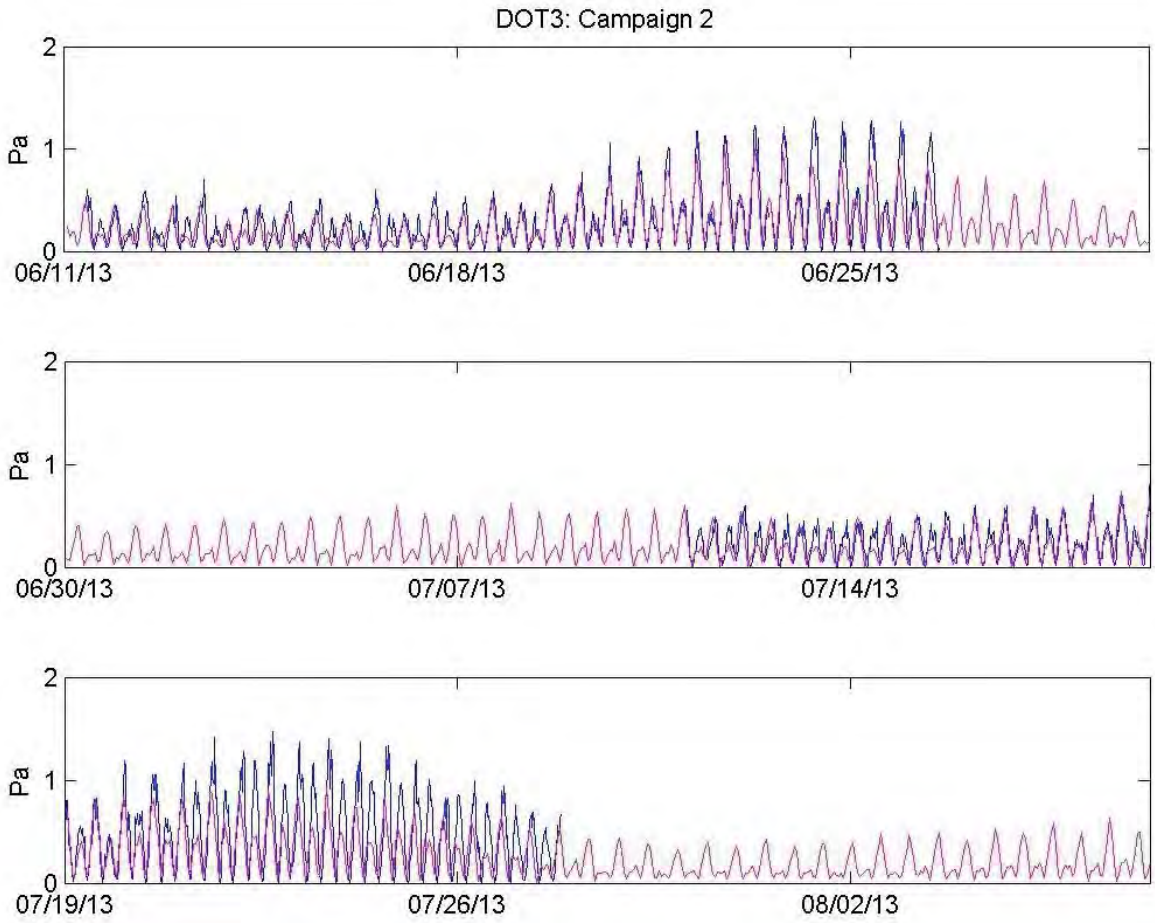

Figure A3.47. Model-predicted bottom stress, $\boldsymbol{\tau_m}$, at Station DOT3 during Campaign 2 in the summer of 2013 (magenta line). The blue line shows the measured stress using the bulk formula, $|\boldsymbol{\tau_{BF}}|$.

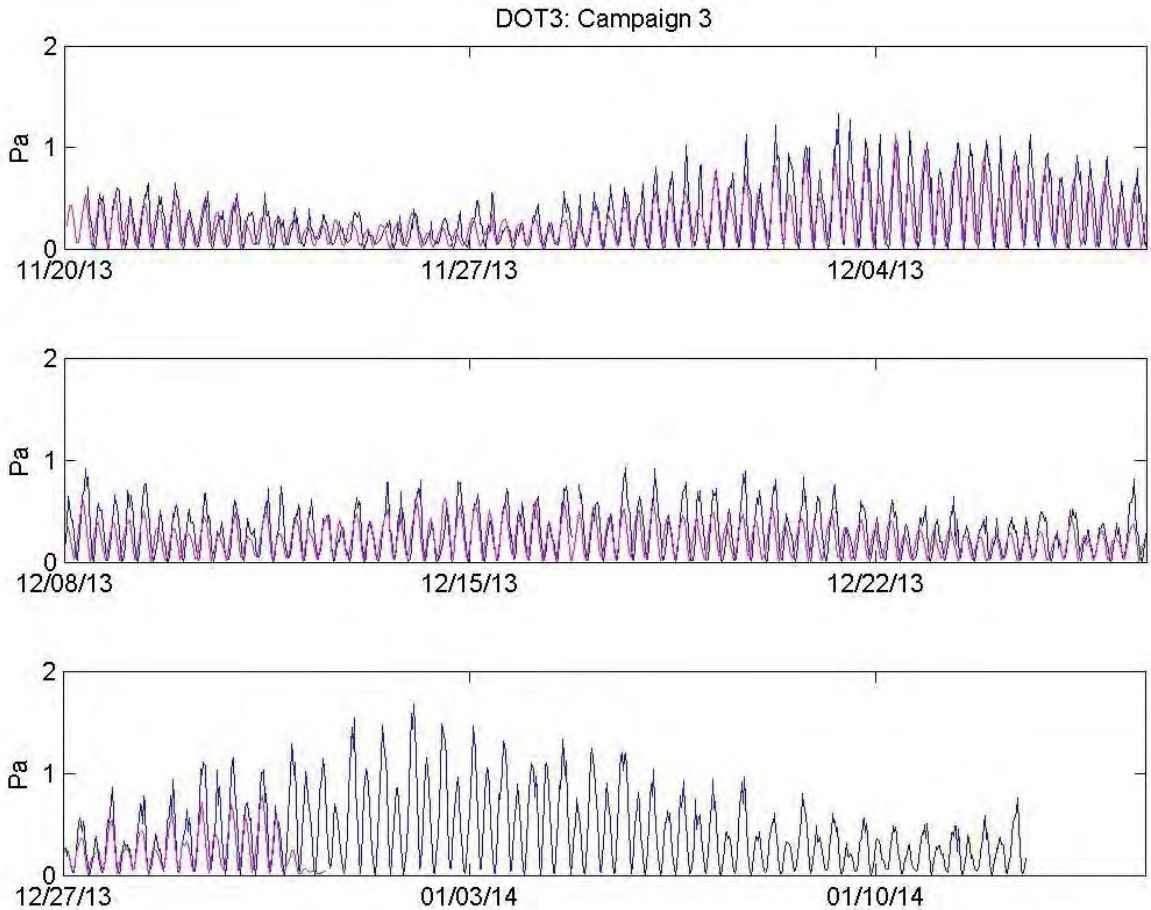

Figure A3.48. Model-predicted bottom stress, $\boldsymbol{\tau_m}$, at Station DOT3 during Campaign 3 in the winter of 2013/2014 (magenta line). The blue line shows the measured stress using the bulk formula, $|\boldsymbol{\tau_{BF}}|$.

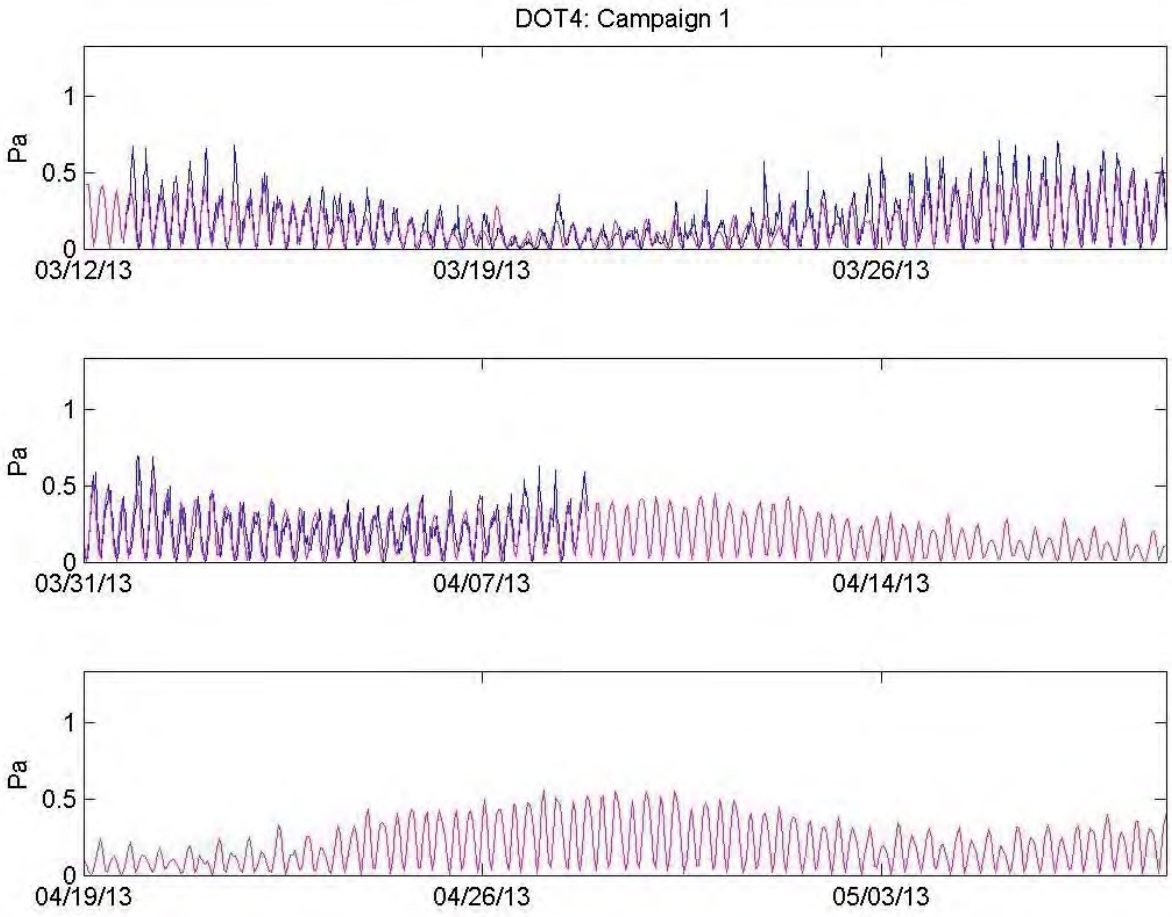

Figure A3.49. Model-predicted bottom stress, $\boldsymbol{\tau_m}$, at Station DOT4 during Campaign 1 in the spring of 2013 (magenta line). The blue line shows the measured stress using the bulk formula, $|\boldsymbol{\tau_{BF}}|$.

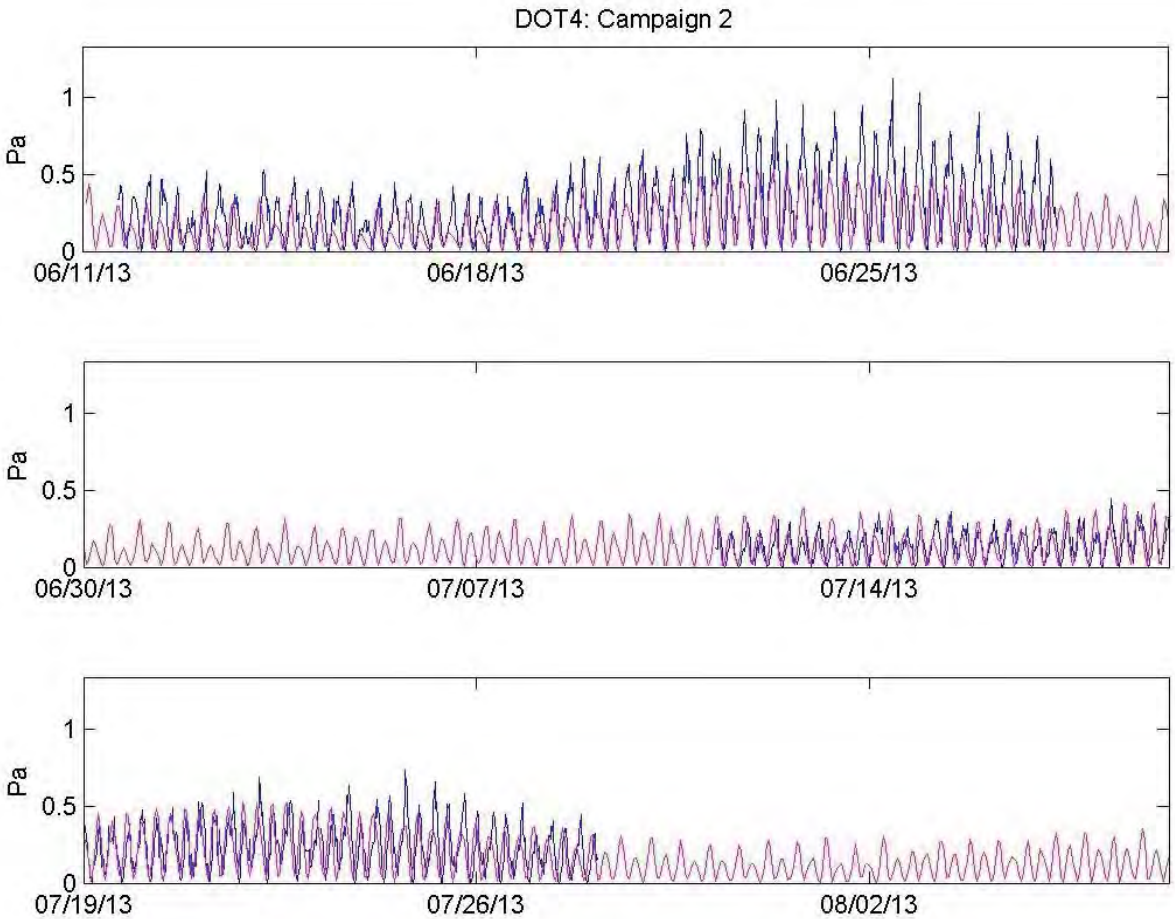

Figure A3.50. Model-predicted bottom stress, $\boldsymbol{\tau_m}$, at Station DOT4 during Campaign 2 in the summer of 2013 (magenta line). The blue line shows the measured stress using the bulk formula, $|\boldsymbol{\tau_{BF}}|$.

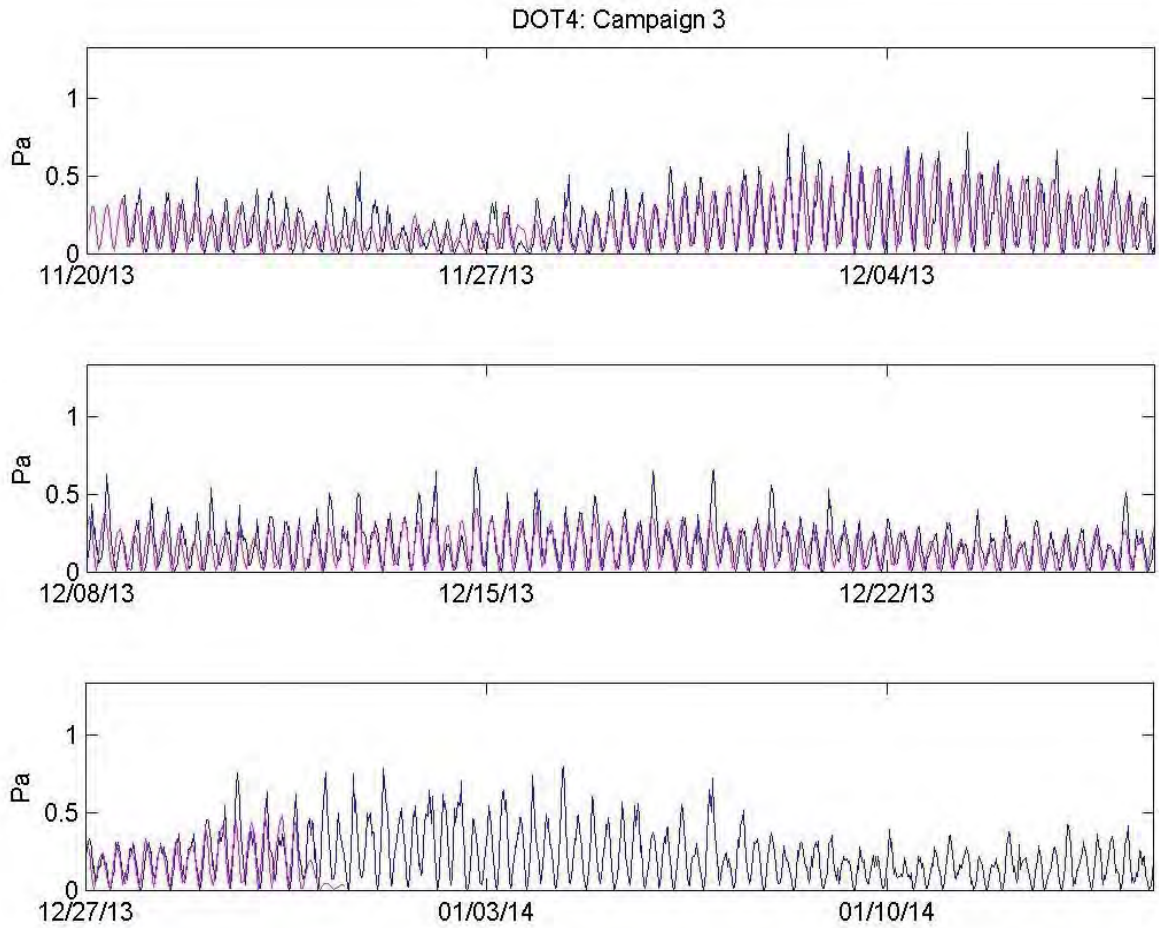

Figure A3.51. Model-predicted bottom stress, $\boldsymbol{\tau_m}$, at Station DOT4 during Campaign 3 in the winter of 2013/2014 (magenta line). The blue line shows the measured stress using the bulk formula, $|\boldsymbol{\tau_{BF}}|$.

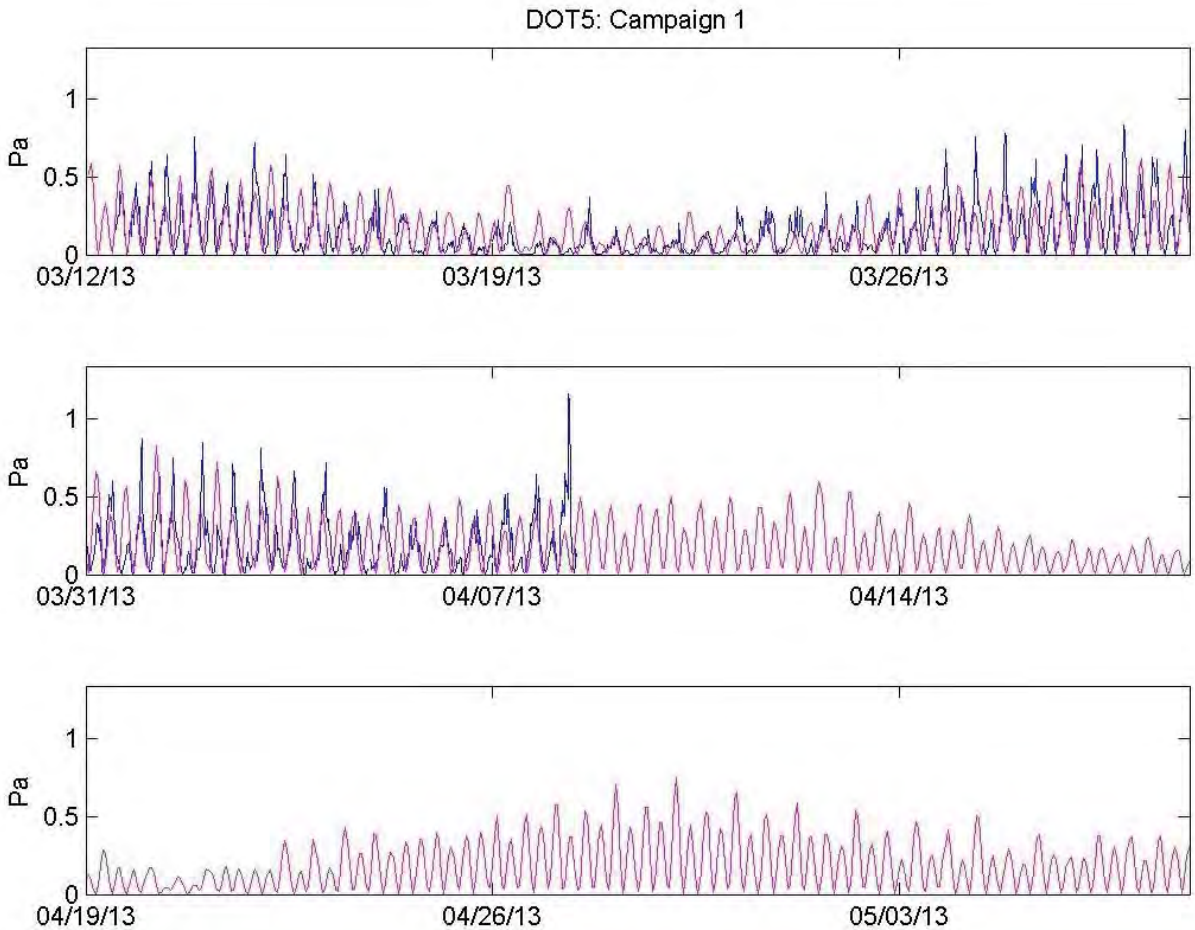

Figure A3.52. Model-predicted bottom stress, $\boldsymbol{\tau_m}$, at Station DOT5 during Campaign 1 in the spring of 2013 (magenta line). The blue line shows the measured stress using the bulk formula, $|\boldsymbol{\tau_{BF}}|$.

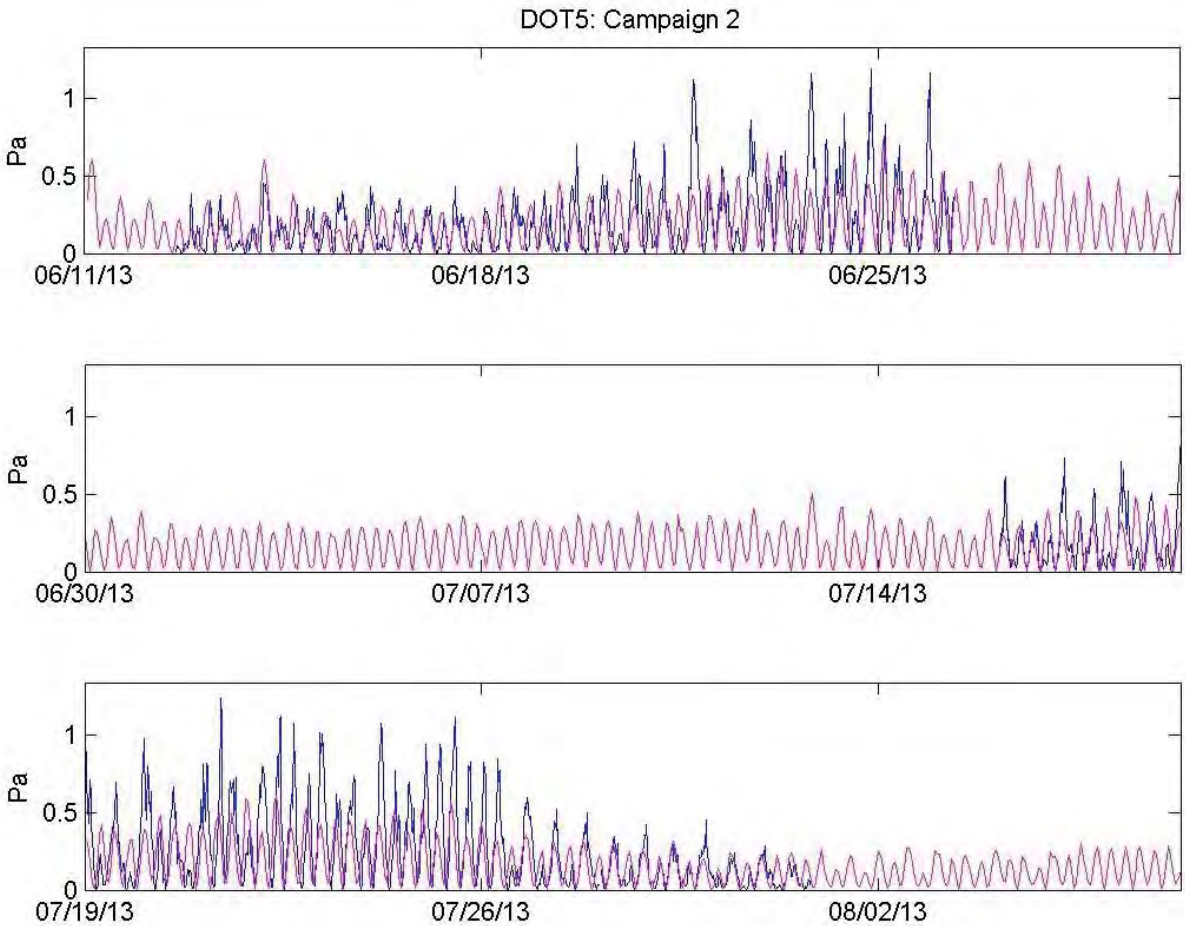

Figure A3.53. Model-predicted bottom stress, $\boldsymbol{\tau_m}$, at Station DOT5 during Campaign 2 in the summer of 2013 (magenta line). The blue line shows the measured stress using the bulk formula, $|\boldsymbol{\tau_{BF}}|$.

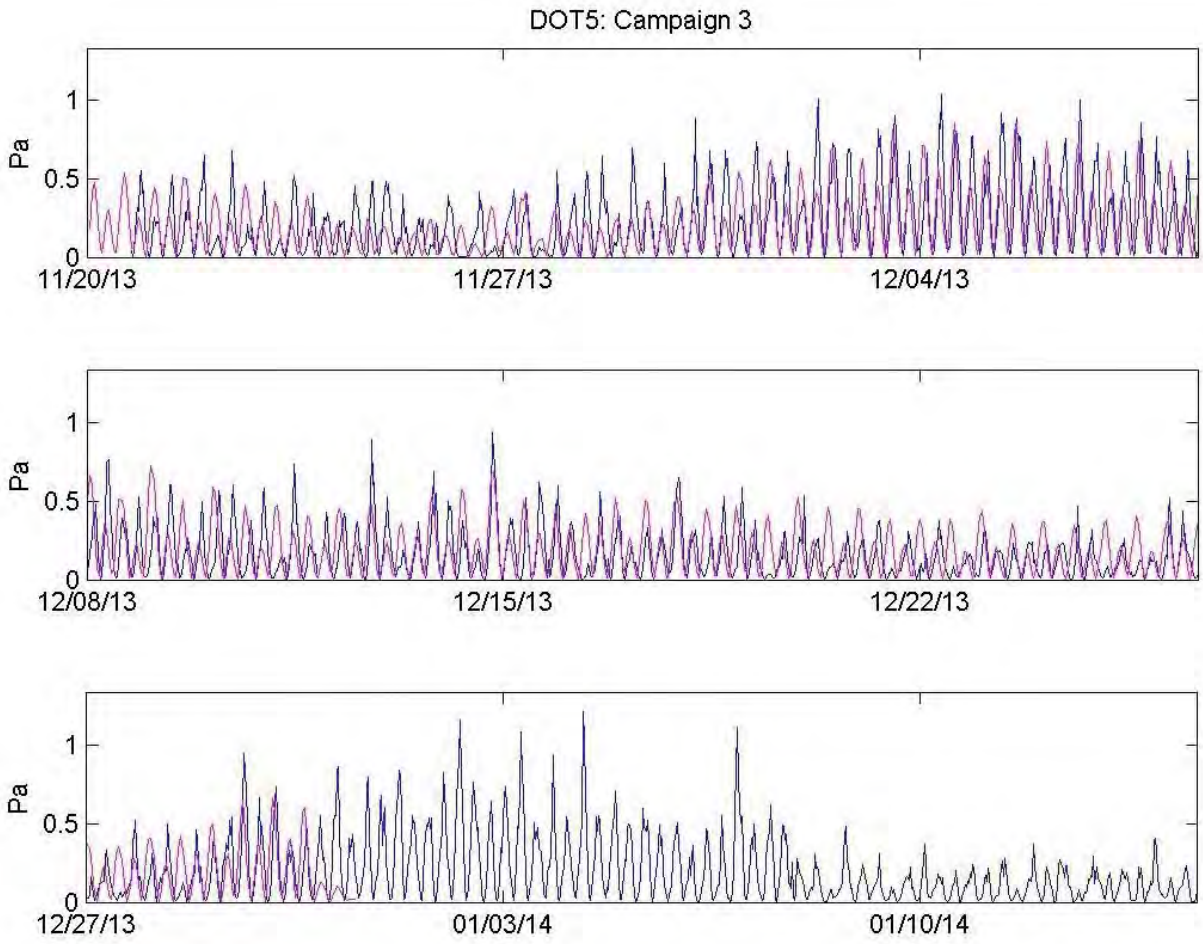

Figure A3.54. Model-predicted bottom stress, $\boldsymbol{\tau_m}$, at Station DOT5 during Campaign 3 in the winter of 2013/2014 (magenta line). The blue line shows the measured stress using the bulk formula, $|\boldsymbol{\tau_{BF}}|$.

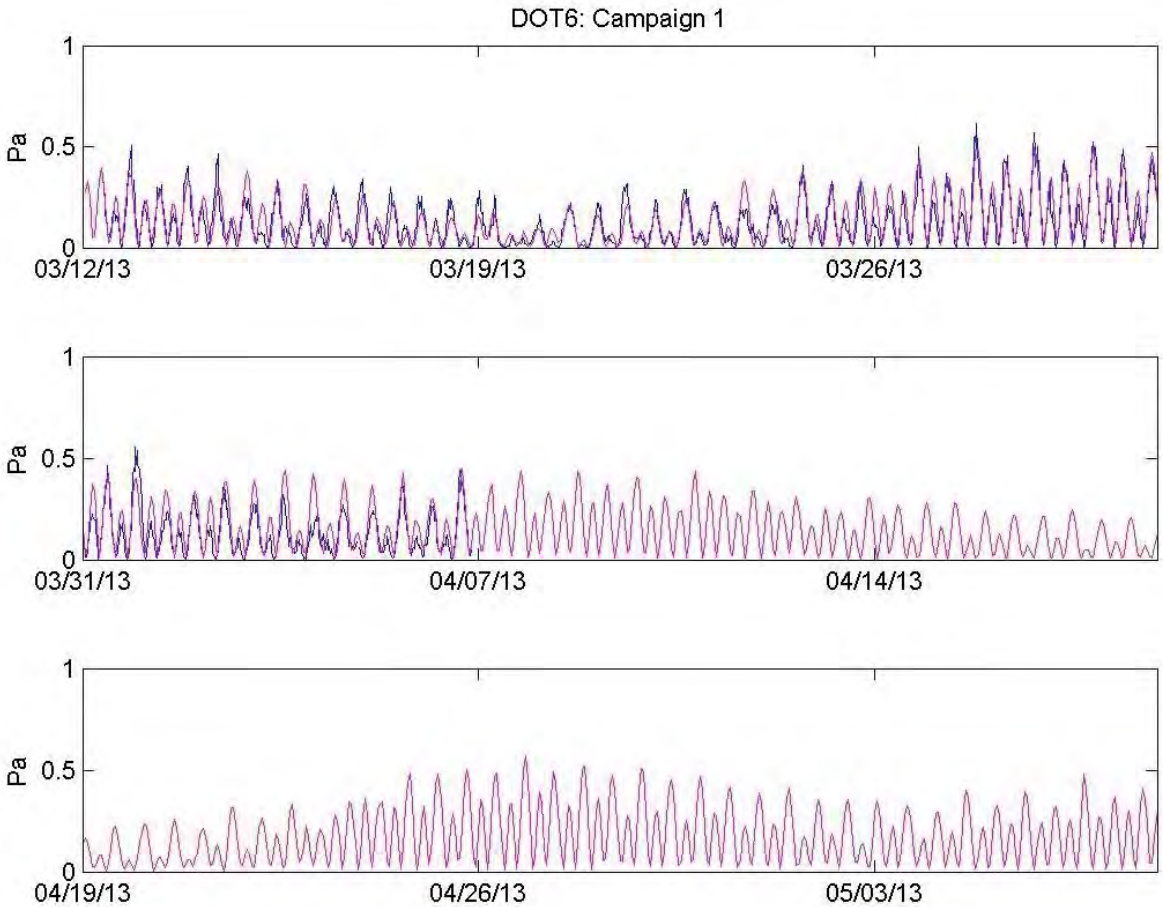

Figure A3.55. Model-predicted bottom stress, τ_m, at Station DOT6 during Campaign 1 in the spring of 2013 (magenta line). The blue line shows the measured stress using the bulk formula, $|\tau_{BF}|$.

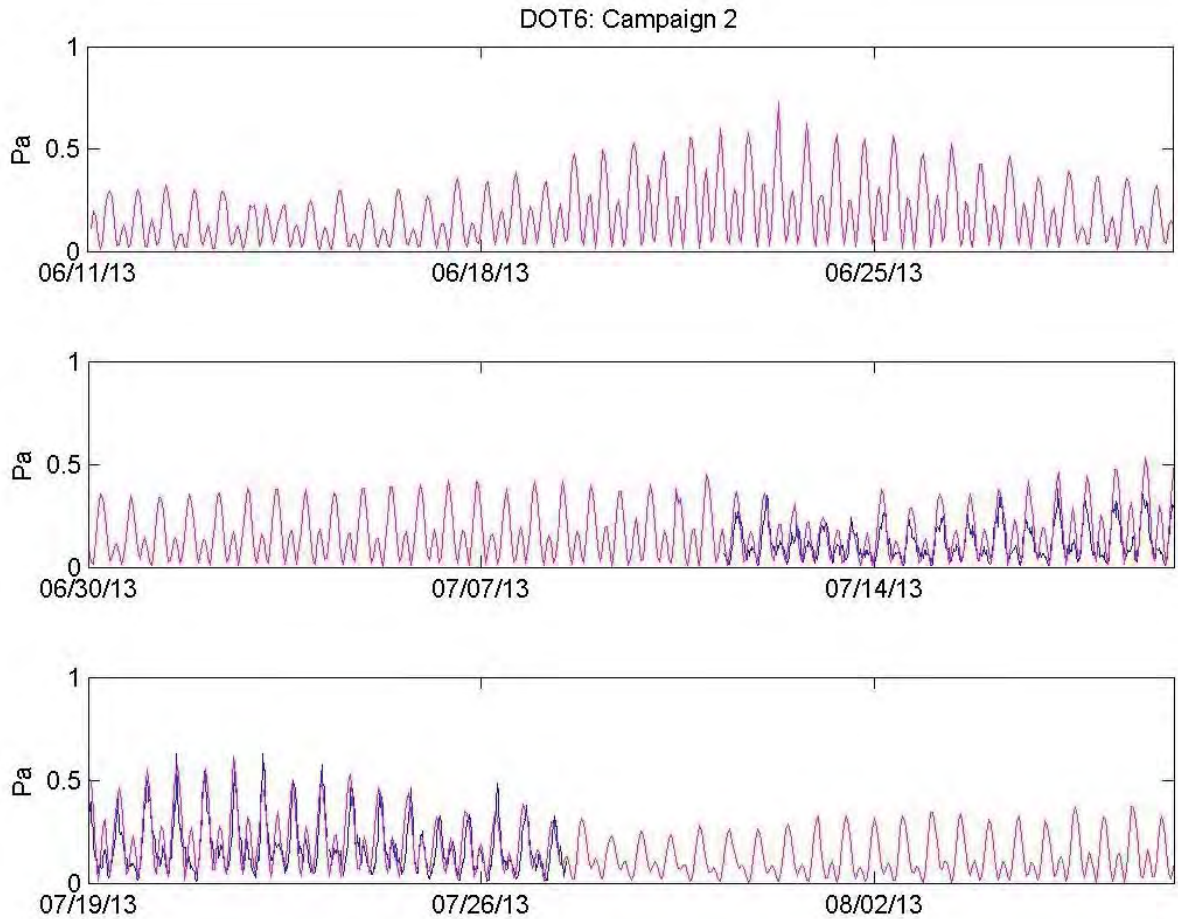

Figure A3.56. Model-predicted bottom stress, τ_m, at Station DOT6 during Campaign 2 in the summer of 2013 (magenta line). The blue line shows the measured stress using the bulk formula, $|\tau_{BF}|$.

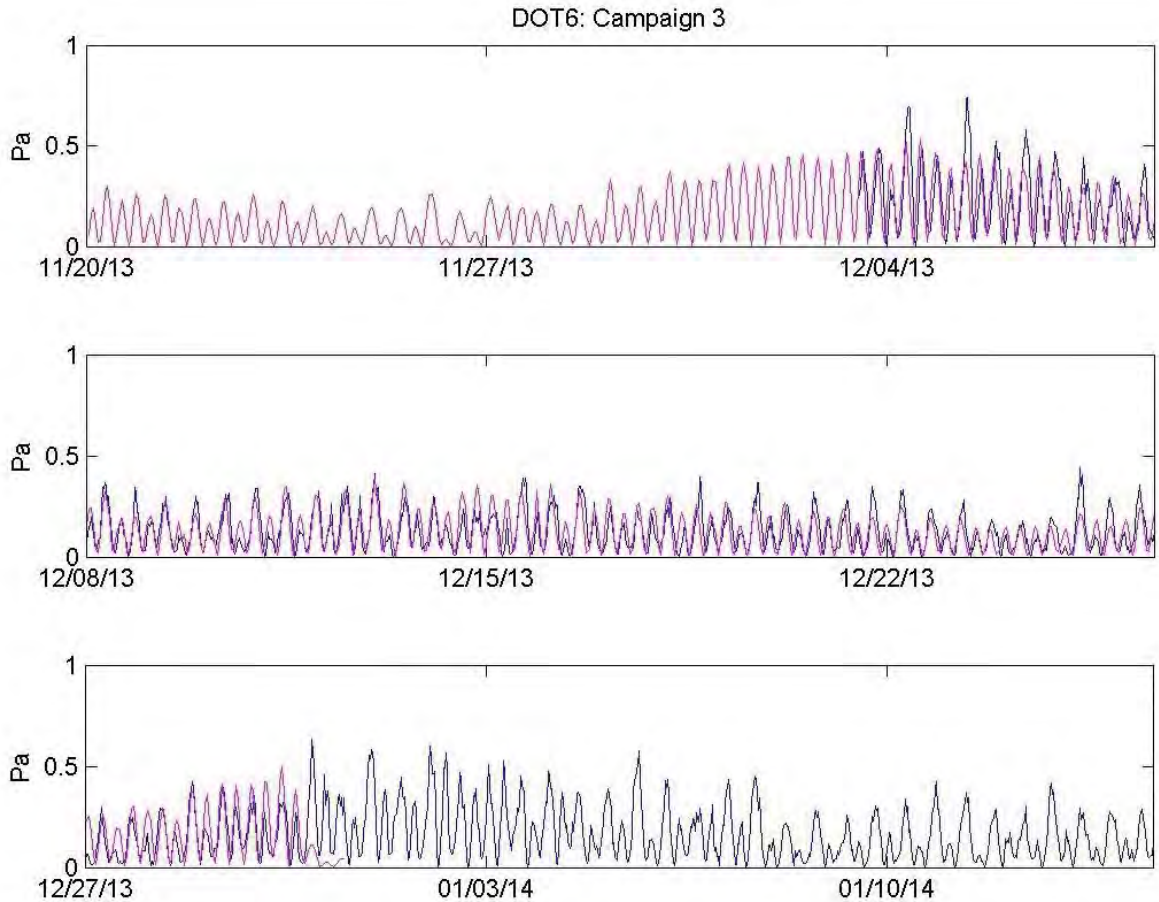

Figure A3.57. Model-predicted bottom stress, τ_m, at Station DOT6 during Campaign 3 in the winter of 2013/2014 (magenta line). The blue line shows the measured stress using the bulk formula, $|\tau_{BF}$

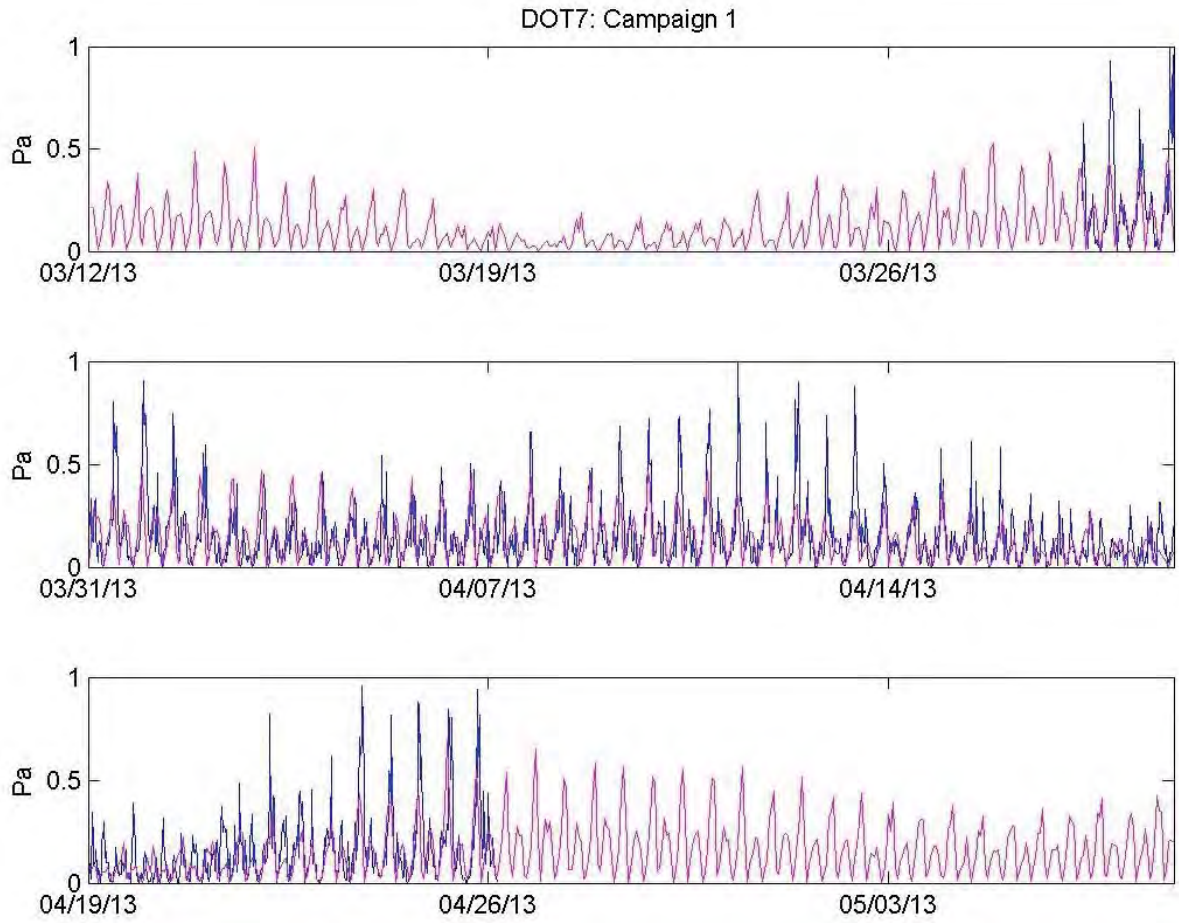

Figure A3.58. Model-predicted bottom stress, τ_m, at Station DOT7 during Campaign 1 in the spring of 2013 (magenta line). The blue line shows the measured stress using the bulk formula, $|\tau_{BF}|.|$

.

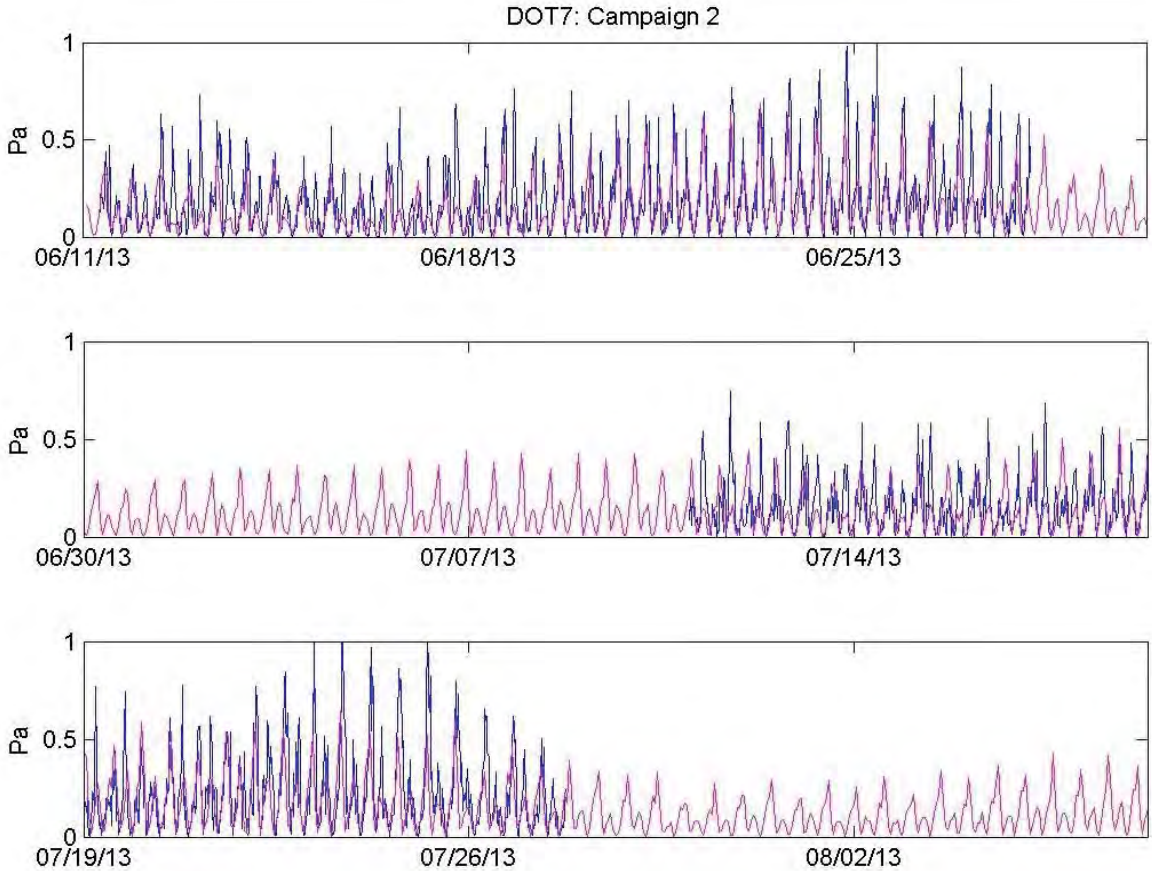

Figure A3.59. Model-predicted bottom stress, τ_m, at Station DOT7 during Campaign 2 in the summer of 2013 (magenta line). The blue line shows the measured stress using the bulk formula, $|\tau_{BF}|$.

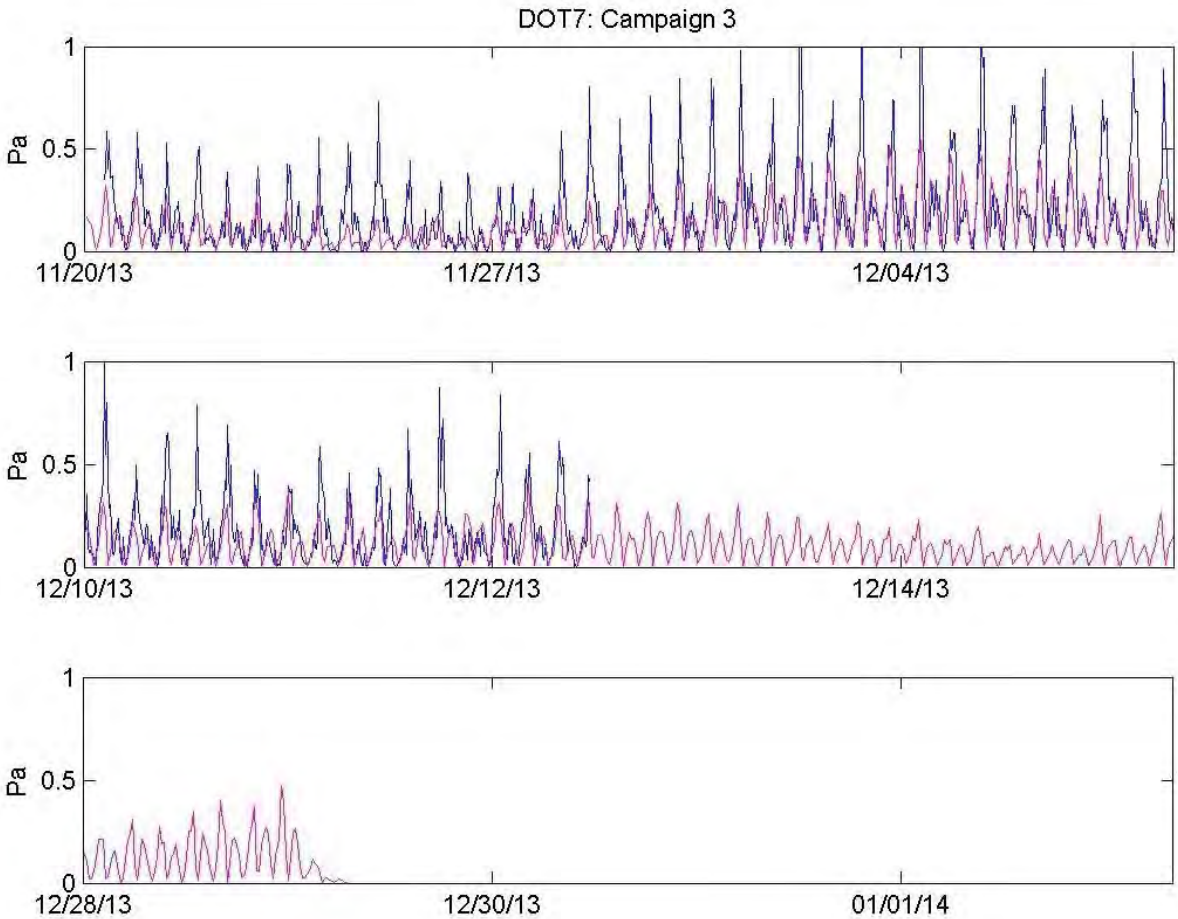

Figure A3.60. Model-predicted bottom stress, τ_m, at Station DOT7 during Campaign 3 in the winter of 2013/2014 (magenta line). The blue line shows the measured stress using the bulk formula, $|\tau_{BF}$

Appendix 4

Comparison of Model-predicted Salinity, Temperature and Pressure with near-bottom Temperature, Salinity, and Density measurements in the Field

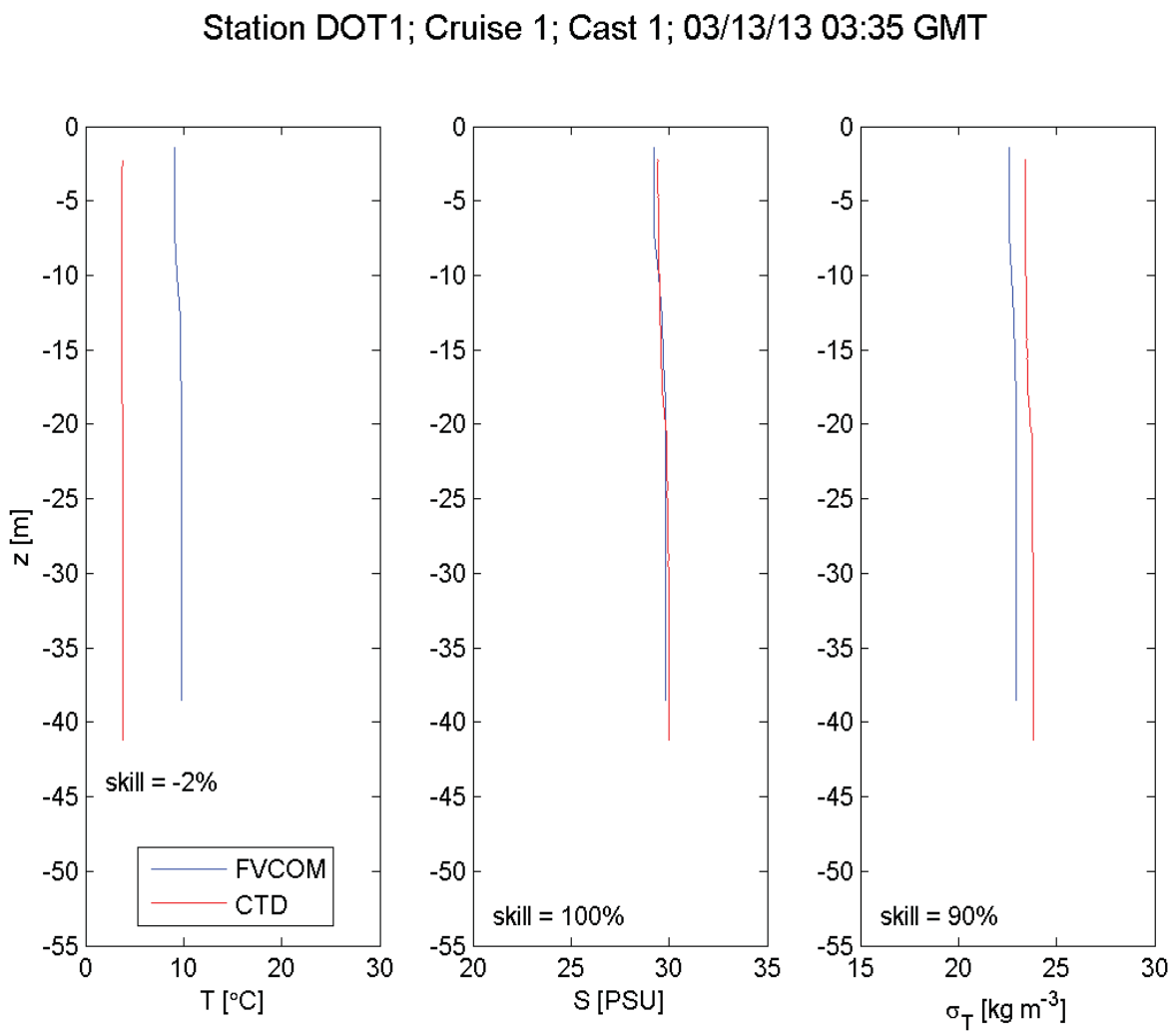

Figure A4.61 Contemporaneous comparison of salinity (left panel), temperature (middle panel), and density (right panel) profiles at Station DOT1 predicted by the FVCOM model (blue) with those measured by a CTD cast from the *R/V Connecticut* (red) during Cruise 1.

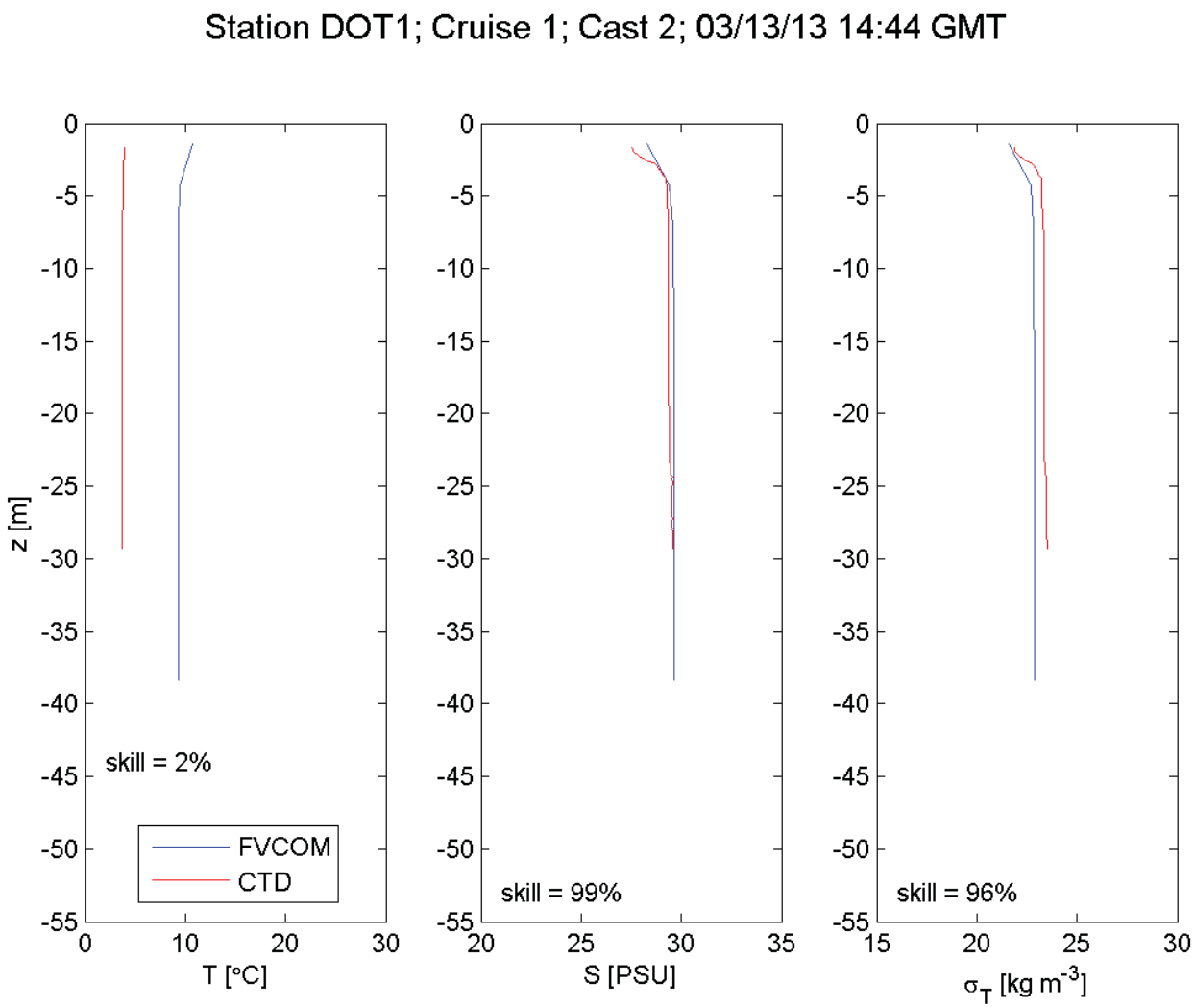

Figure A4.62 Contemporaneous comparison of salinity (left panel), temperature (middle panel), and density (right panel) profiles at Station DOT1 predicted by the FVCOM model (blue) with those measured by a CTD cast from the *R/V Connecticut* (red) during Cruise 1.

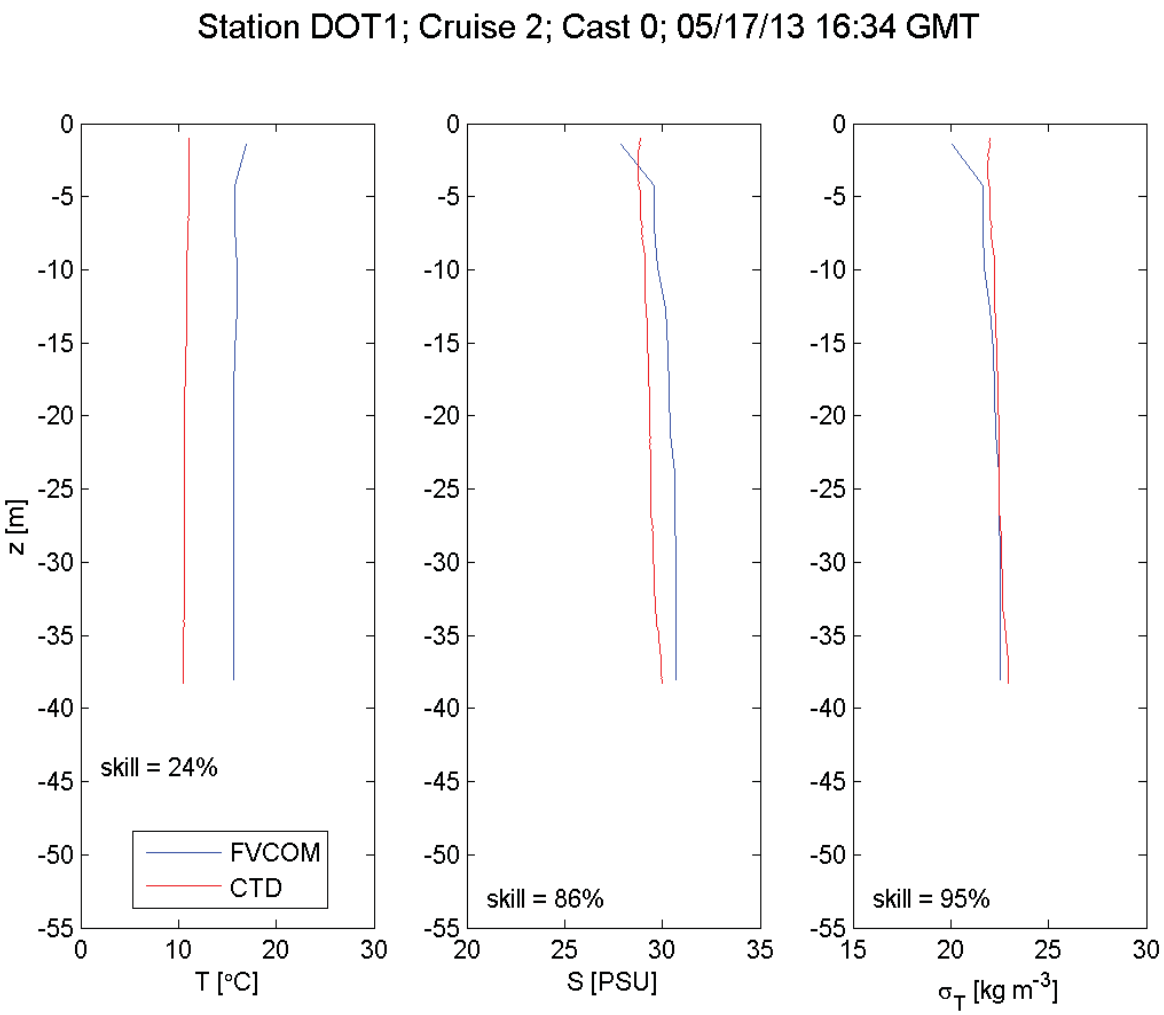

Figure A4.63 Contemporaneous comparison of salinity (left panel), temperature (middle panel), and density (right panel) profiles at Station DOT1 predicted by the FVCOM model (blue) with those measured by a CTD cast from the *R/V Connecticut* (red) during Cruise 2.

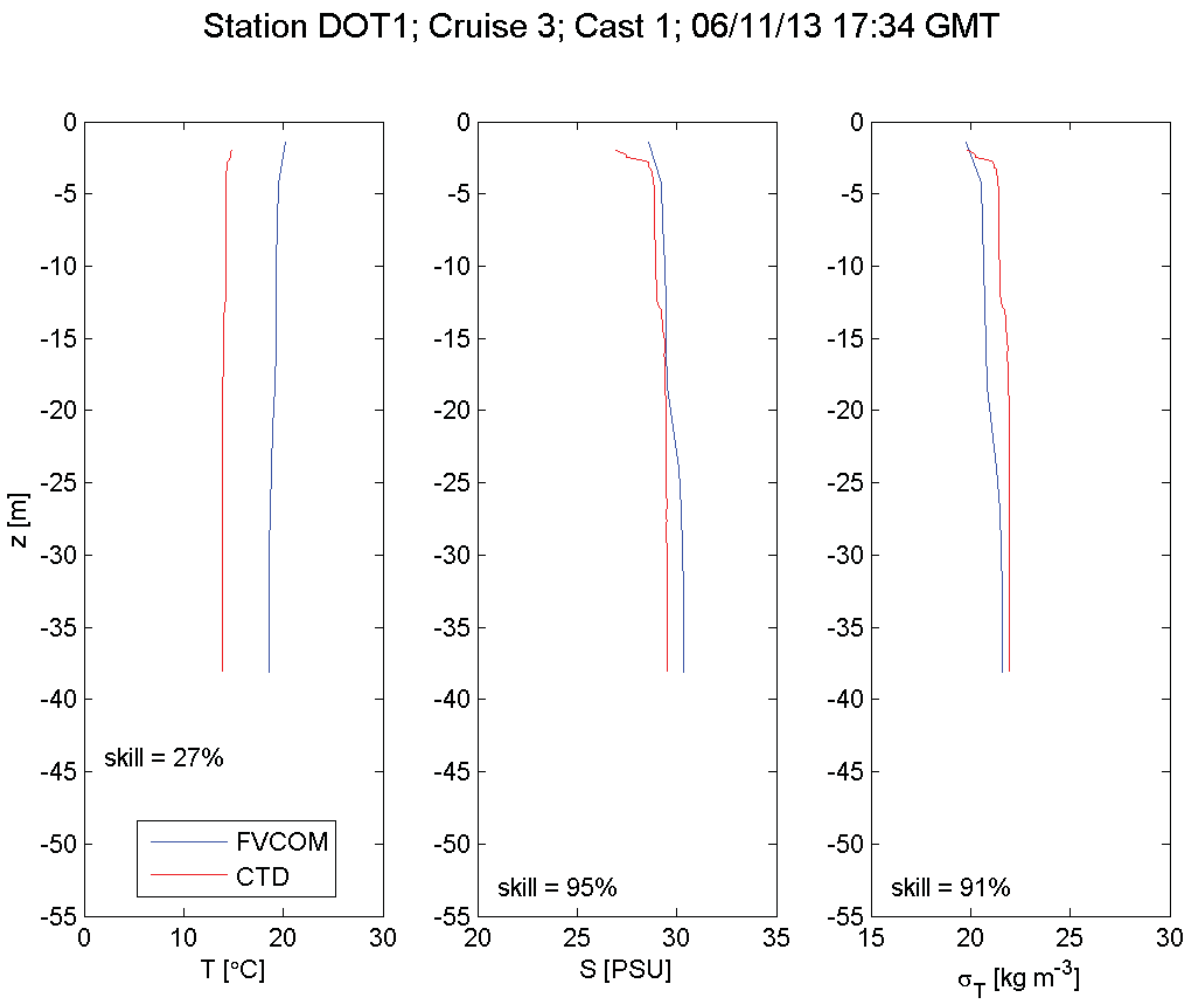

Figure A4.64 Contemporaneous comparison of salinity (left panel), temperature (middle panel), and density (right panel) profiles at Station DOT1 predicted by the FVCOM model (blue) with those measured by a CTD cast from the *R/V Connecticut* (red) during Cruise 3.

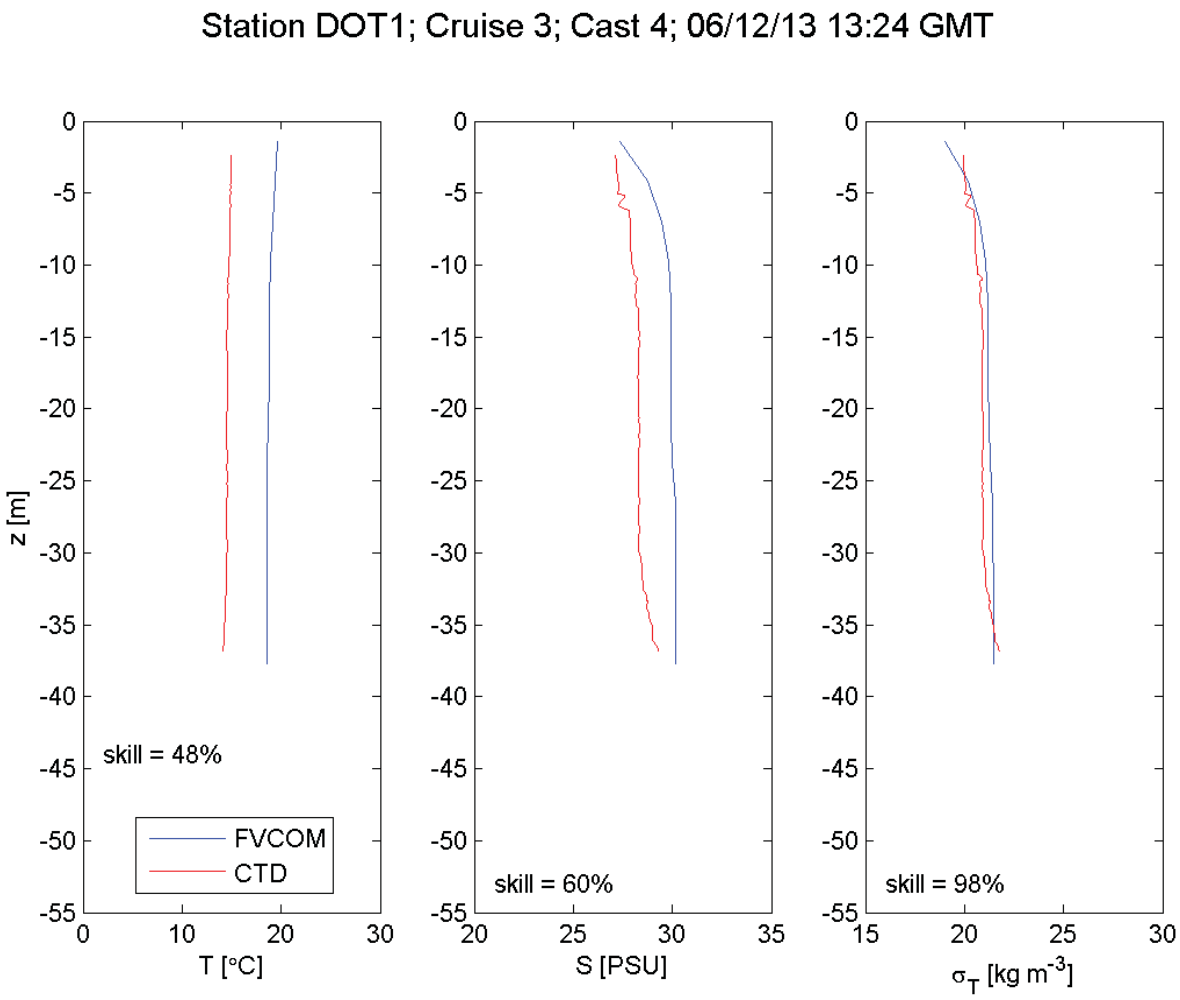

Figure A4.65 Contemporaneous comparison of salinity (left panel), temperature (middle panel), and density (right panel) profiles at Station DOT1 predicted by the FVCOM model (blue) with those measured by a CTD cast from the *R/V Connecticut* (red) during Cruise 3.

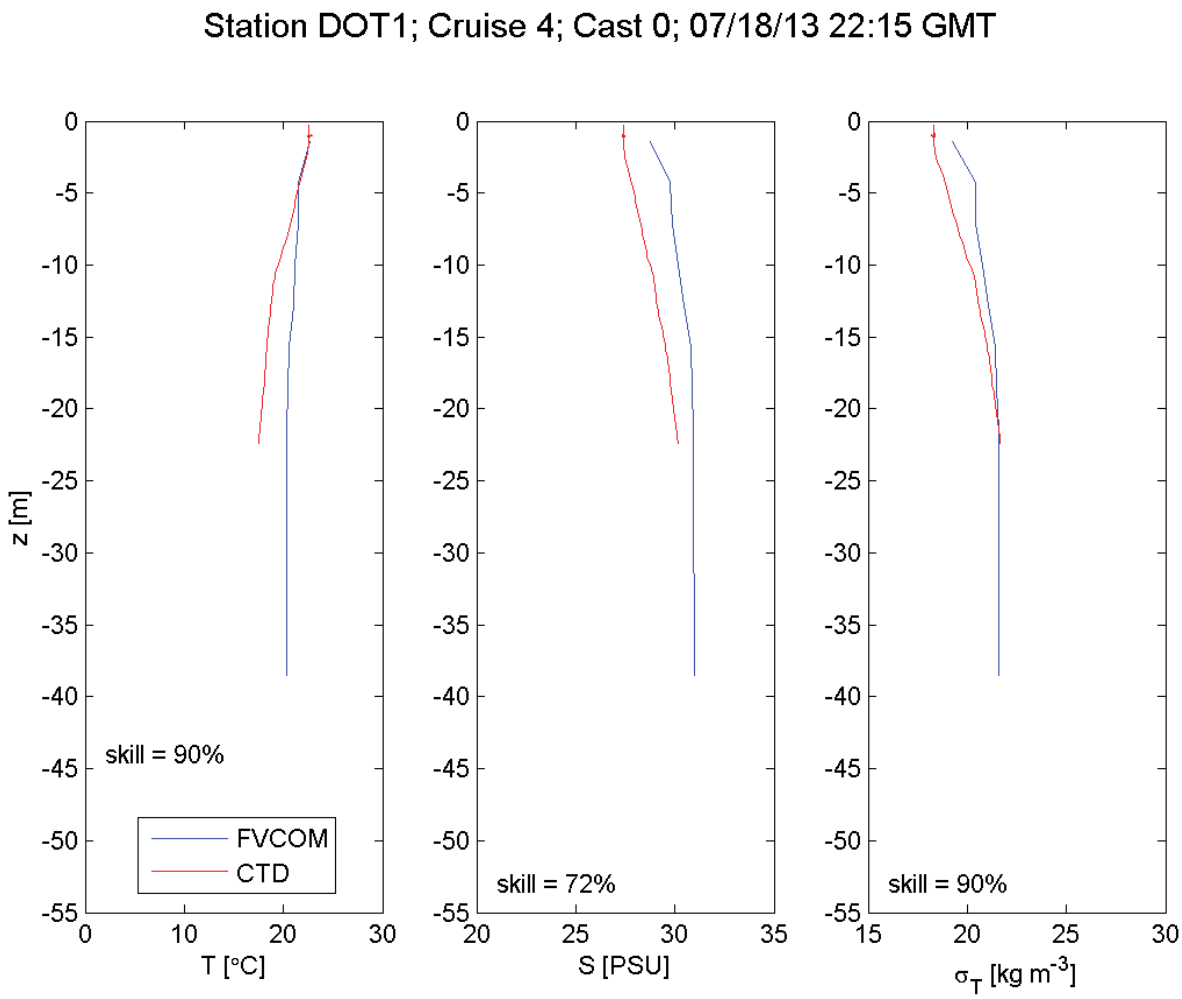

Figure A4.66 Contemporaneous comparison of salinity (left panel), temperature (middle panel), and density (right panel) profiles at Station DOT1 predicted by the FVCOM model (blue) with those measured by a CTD cast from the *R/V Connecticut* (red) during Cruise 4.

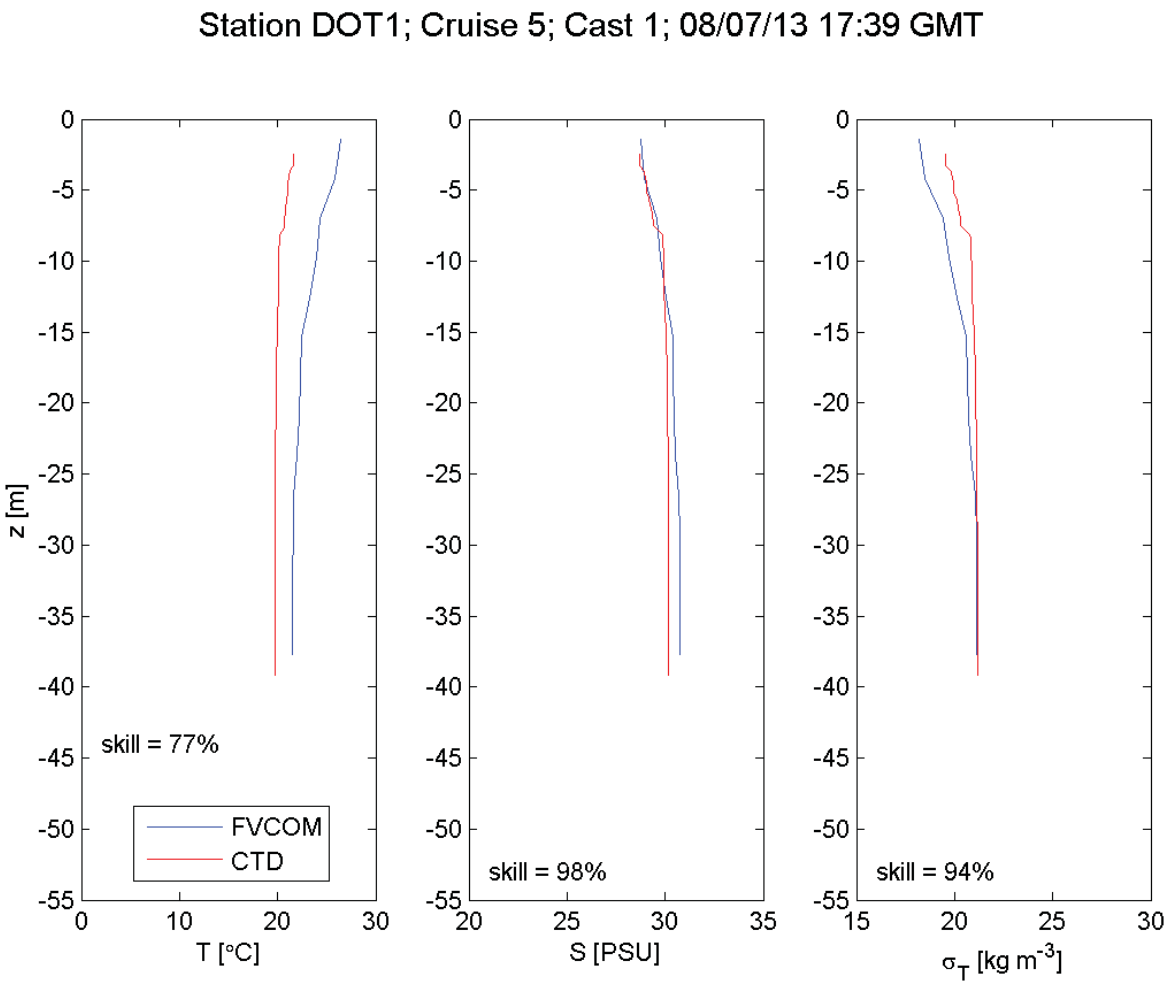

Figure A4.67 Contemporaneous comparison of salinity (left panel), temperature (middle panel), and density (right panel) profiles at Station DOT1 predicted by the FVCOM model (blue) with those measured by a CTD cast from the *R/V Connecticut* (red) during Cruise 5.

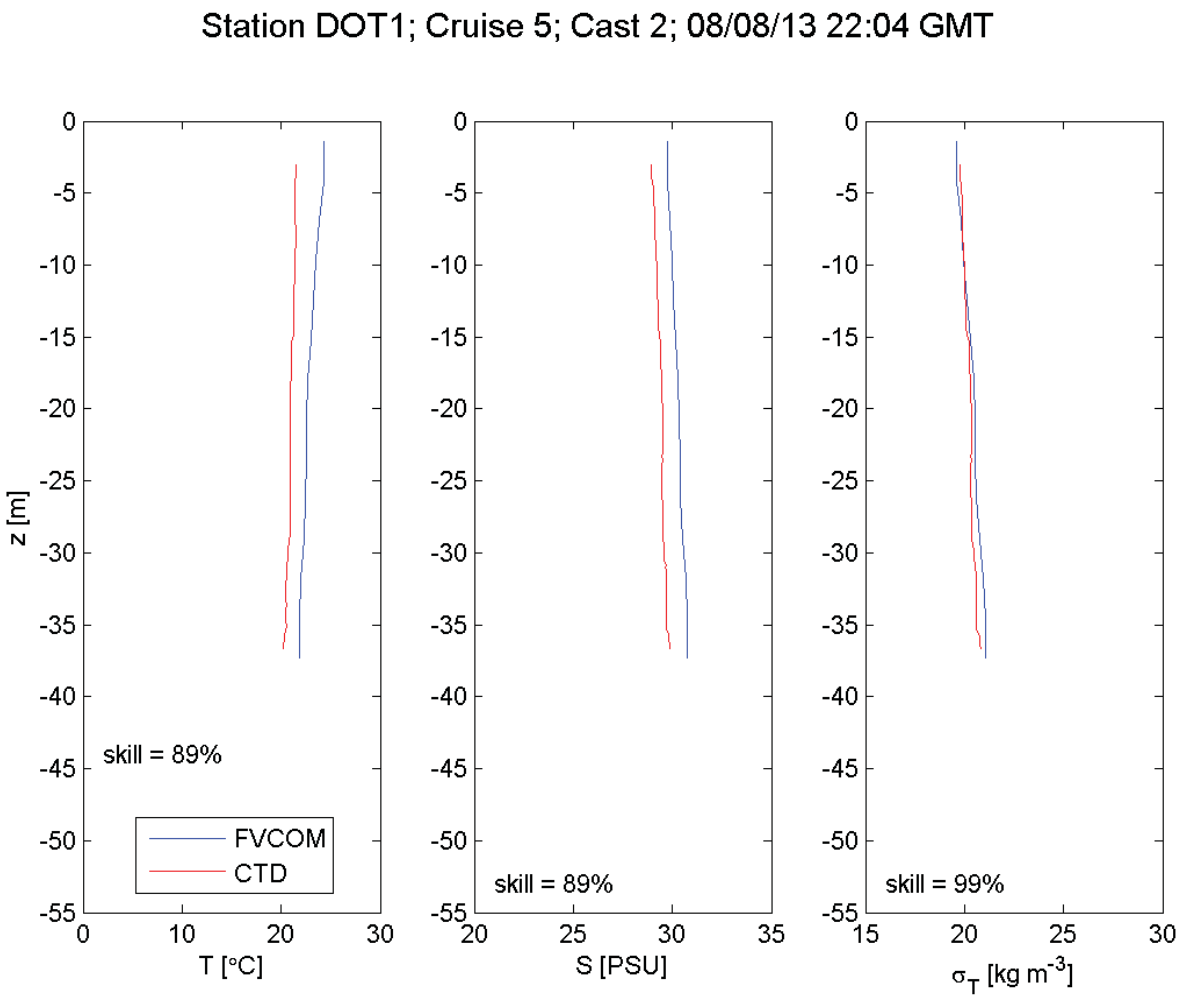

Figure A4.68 Contemporaneous comparison of salinity (left panel), temperature (middle panel), and density (right panel) profiles at Station DOT1 predicted by the FVCOM model (blue) with those measured by a CTD cast from the *R/V Connecticut* (red) during Cruise 5.

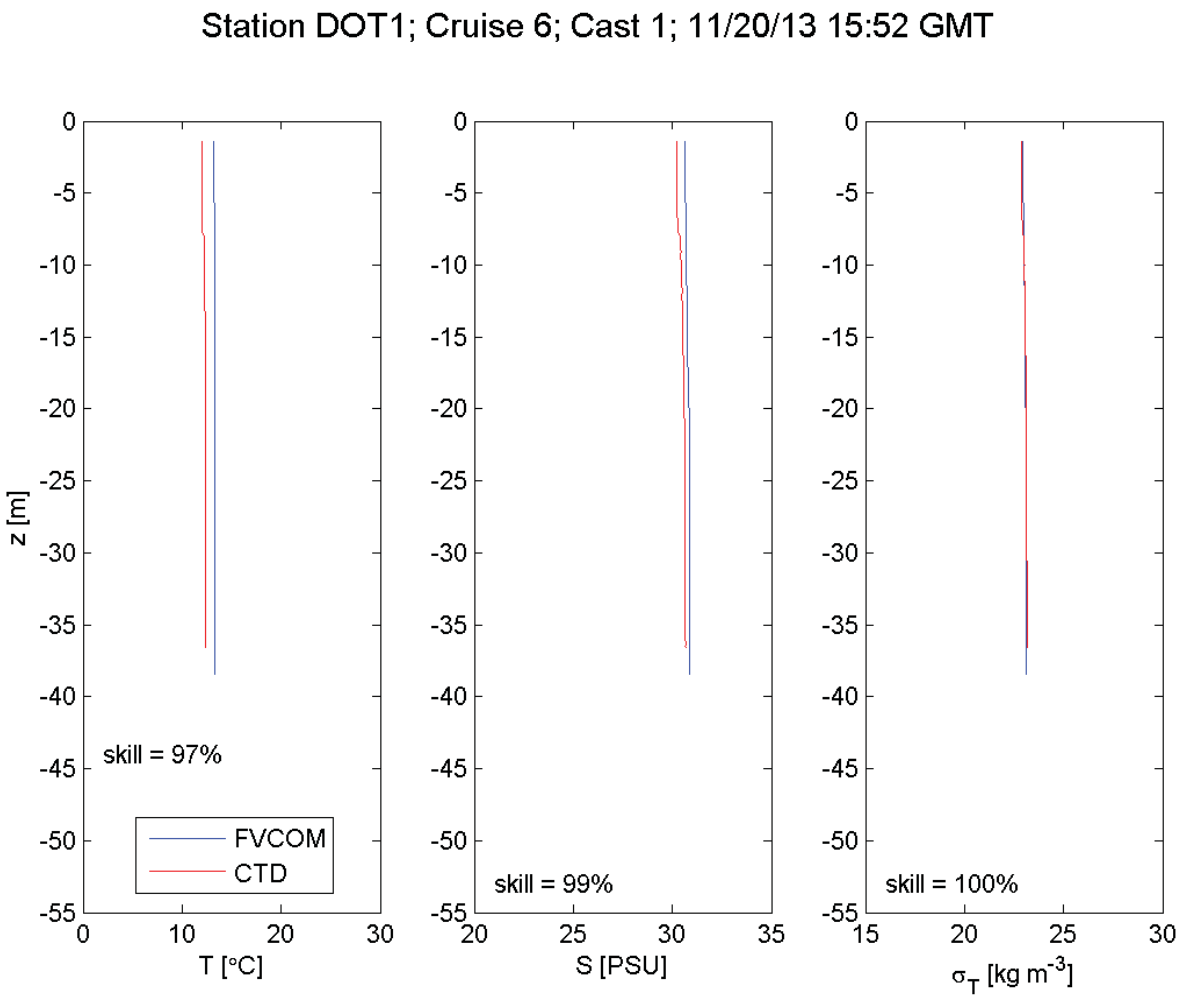

Figure A4.69 Contemporaneous comparison of salinity (left panel), temperature (middle panel), and density (right panel) profiles at Station DOT1 predicted by the FVCOM model (blue) with those measured by a CTD cast from the *R/V Connecticut* (red) during Cruise 6.

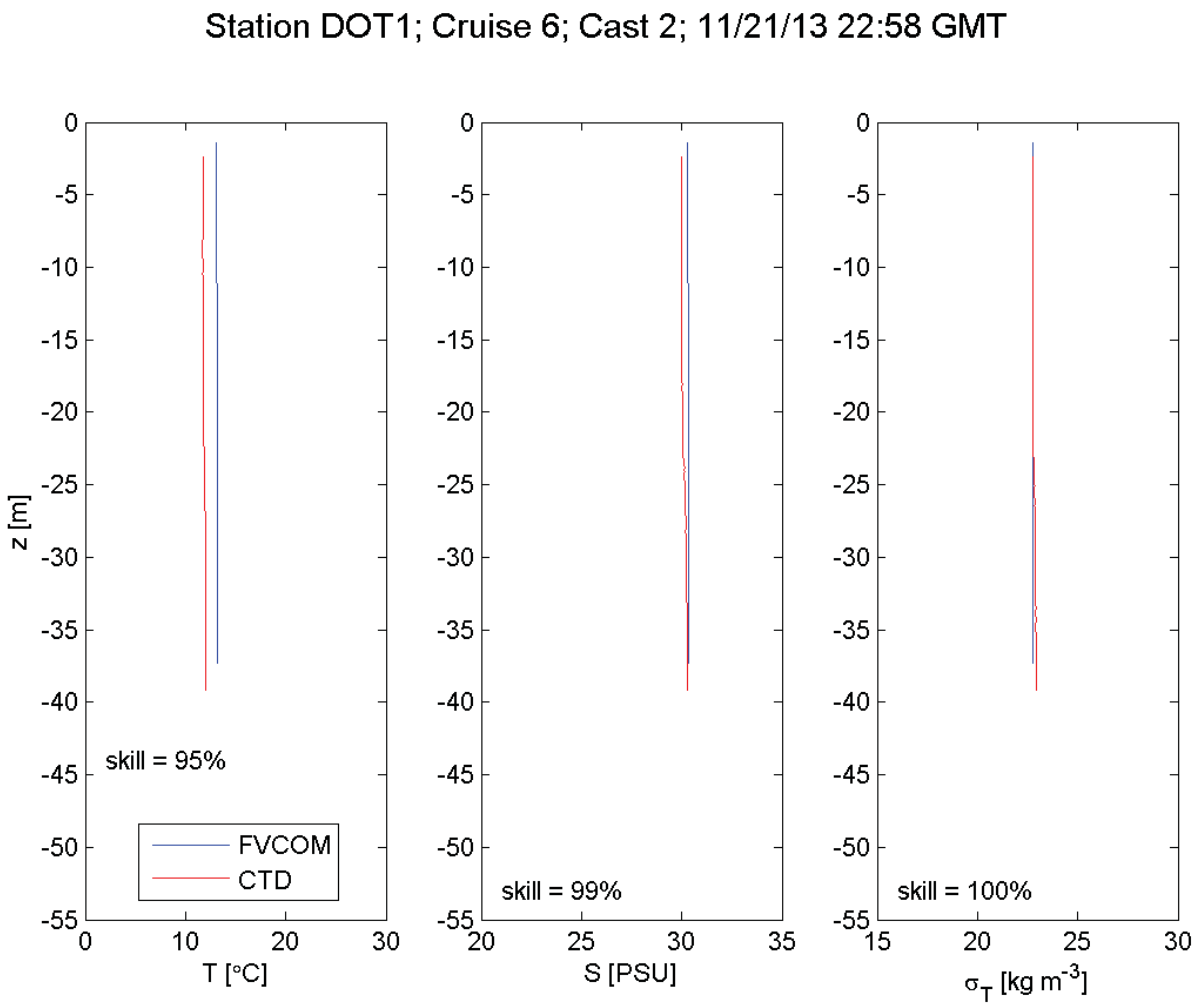

Figure A4.70 Contemporaneous comparison of salinity (left panel), temperature (middle panel), and density (right panel) profiles at Station DOT1 predicted by the FVCOM model (blue) with those measured by a CTD cast from the *R/V Connecticut* (red) during Cruise 6.

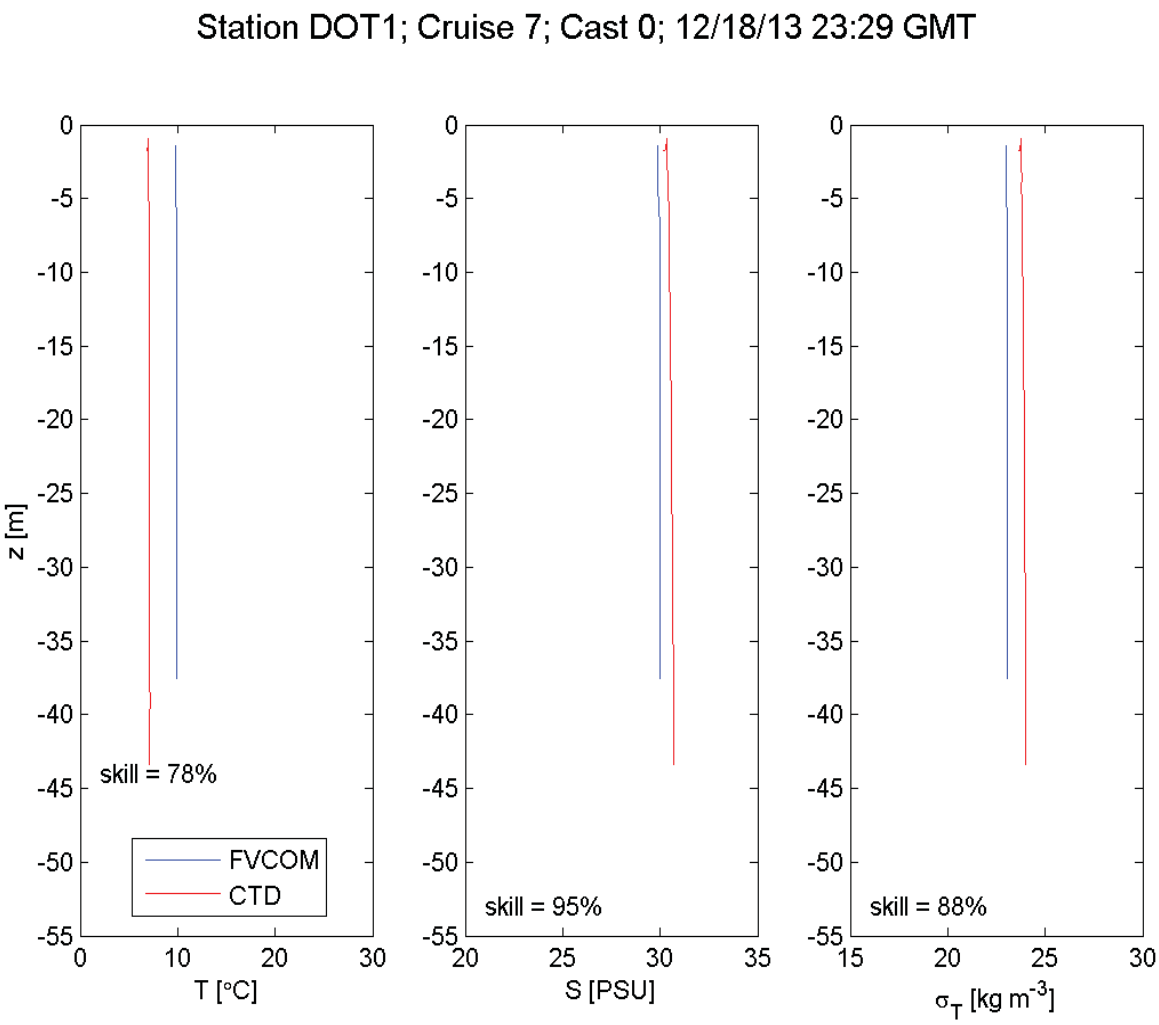

Figure A4.71 Contemporaneous comparison of salinity (left panel), temperature (middle panel), and density (right panel) profiles at Station DOT1 predicted by the FVCOM model (blue) with those measured by a CTD cast from the *R/V Connecticut* (red) during Cruise 7.

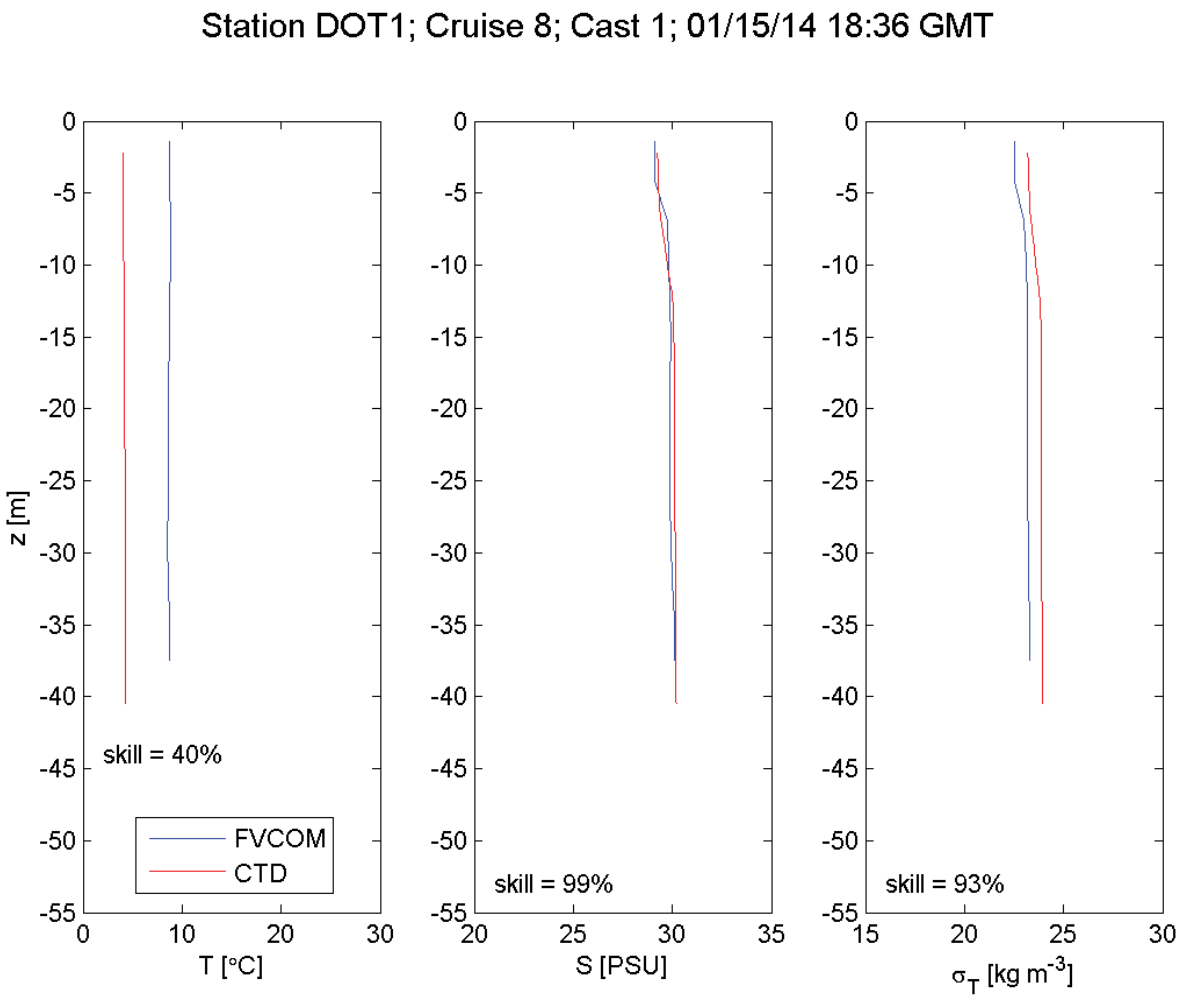

Figure A4.72 Contemporaneous comparison of salinity (left panel), temperature (middle panel), and density (right panel) profiles at Station DOT1 predicted by the FVCOM model (blue) with those measured by a CTD cast from the *R/V Connecticut* (red) during Cruise 8.

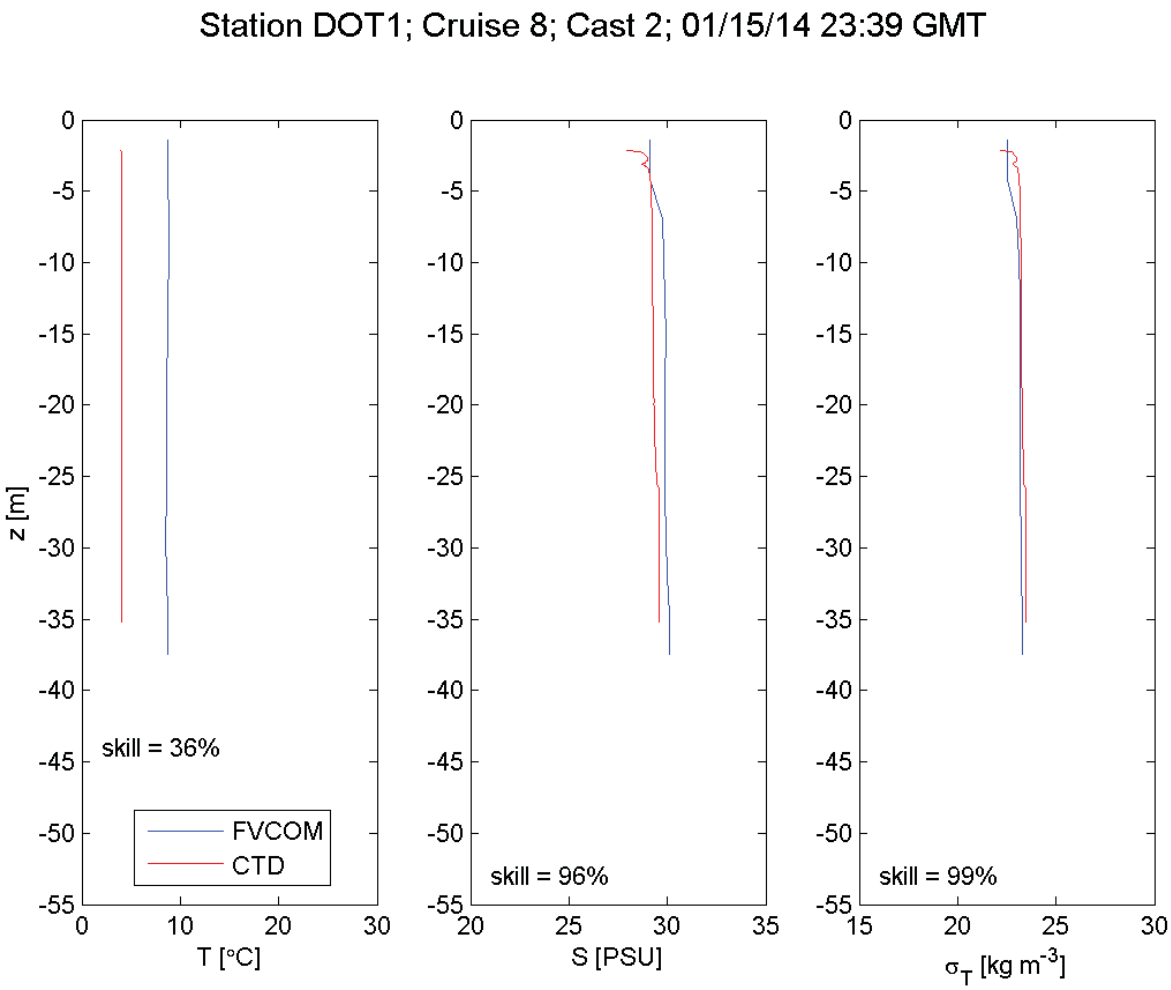

Figure A4.73 Contemporaneous comparison of salinity (left panel), temperature (middle panel), and density (right panel) profiles at Station DOT1 predicted by the FVCOM model (blue) with those measured by a CTD cast from the *R/V Connecticut* (red) during Cruise 8.

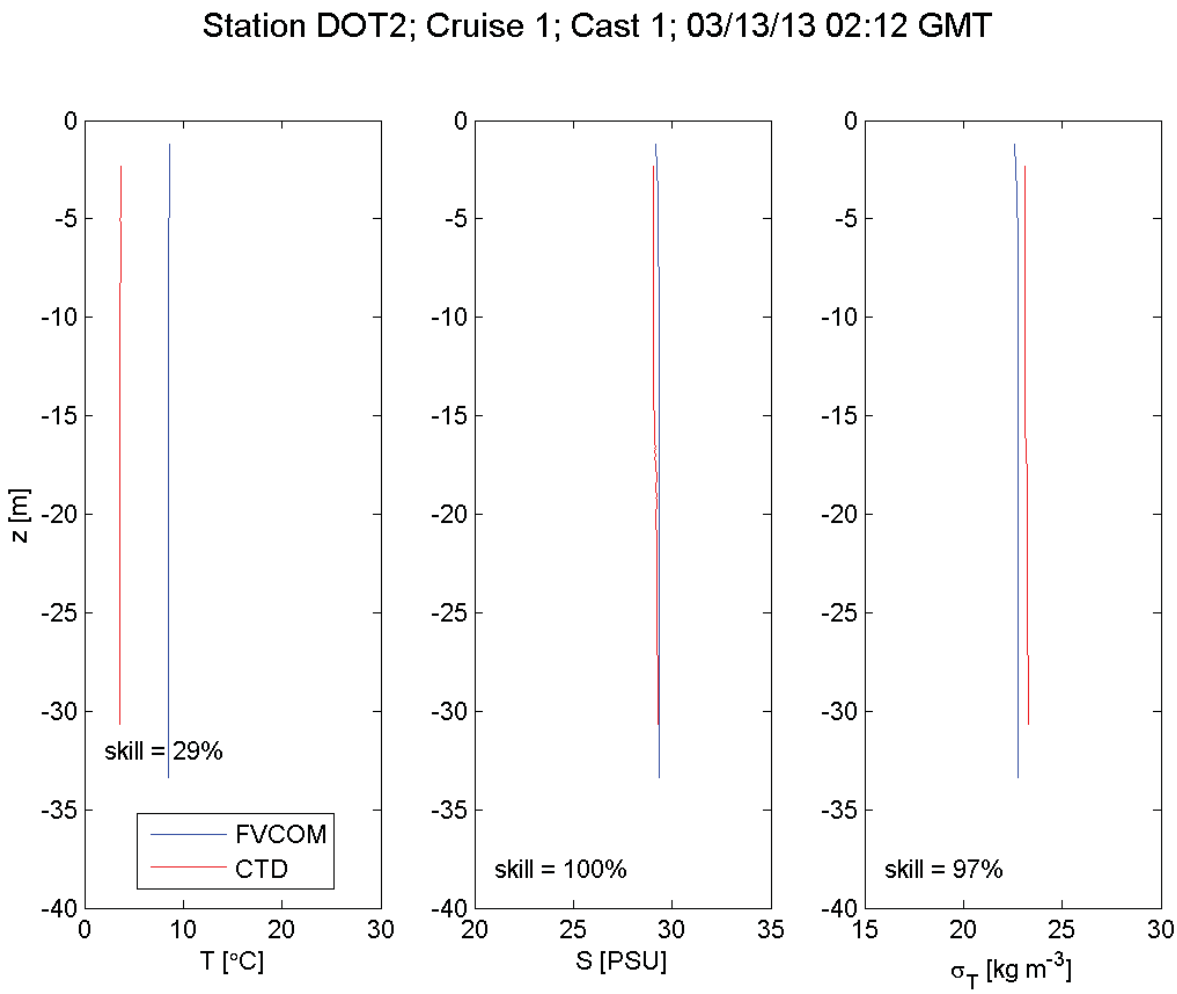

Figure A4.74 Contemporaneous comparison of salinity (left panel), temperature (middle panel), and density (right panel) profiles at Station DOT2 predicted by the FVCOM model (blue) with those measured by a CTD cast from the *R/V Connecticut* (red) during Cruise 1.

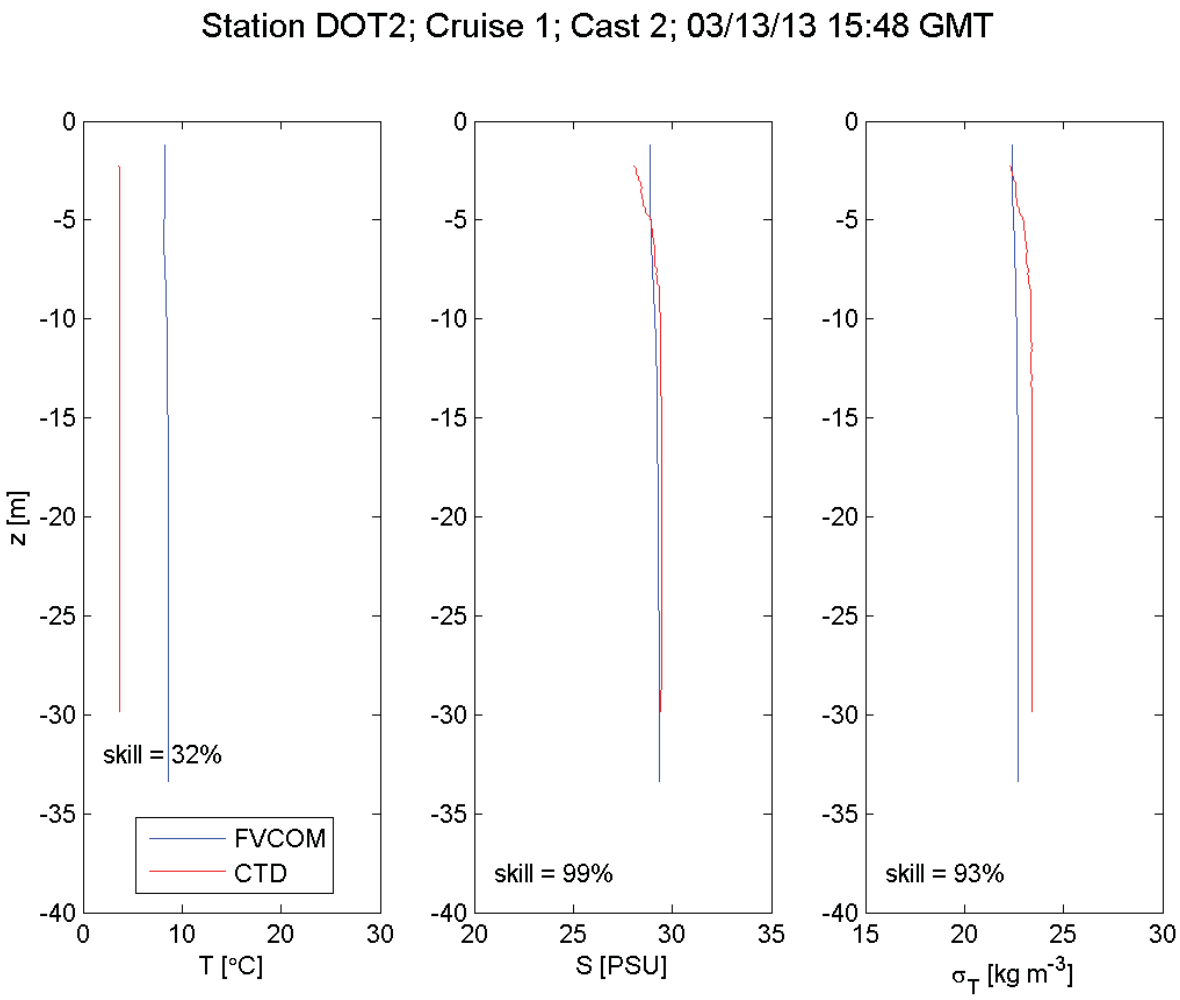

Figure A4.75 Contemporaneous comparison of salinity (left panel), temperature (middle panel), and density (right panel) profiles at Station DOT2 predicted by the FVCOM model (blue) with those measured by a CTD cast from the *R/V Connecticut* (red) during Cruise 1.

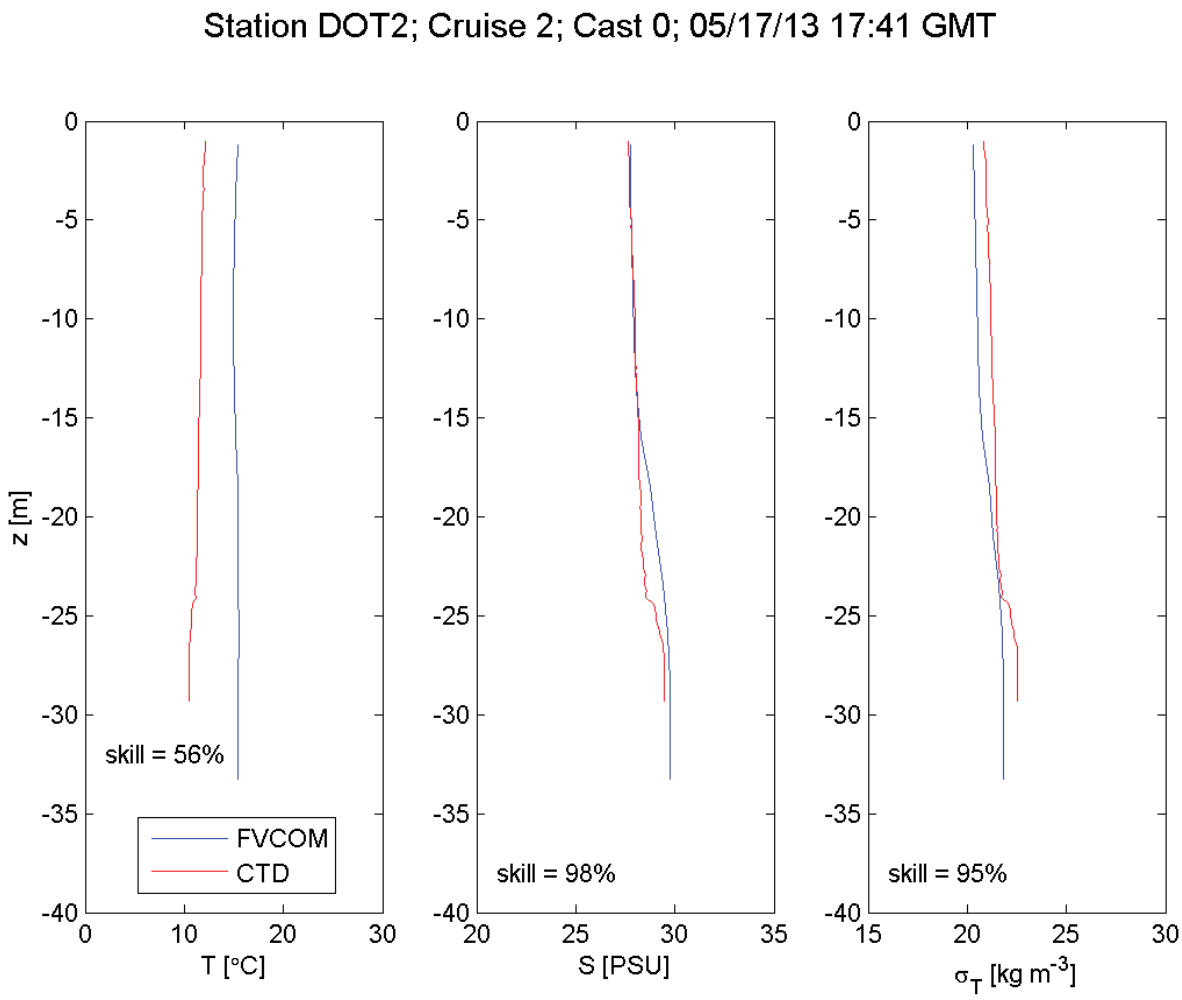

Figure A4.76 Contemporaneous comparison of salinity (left panel), temperature (middle panel), and density (right panel) profiles at Station DOT2 predicted by the FVCOM model (blue) with those measured by a CTD cast from the *R/V Connecticut* (red) during Cruise 2.

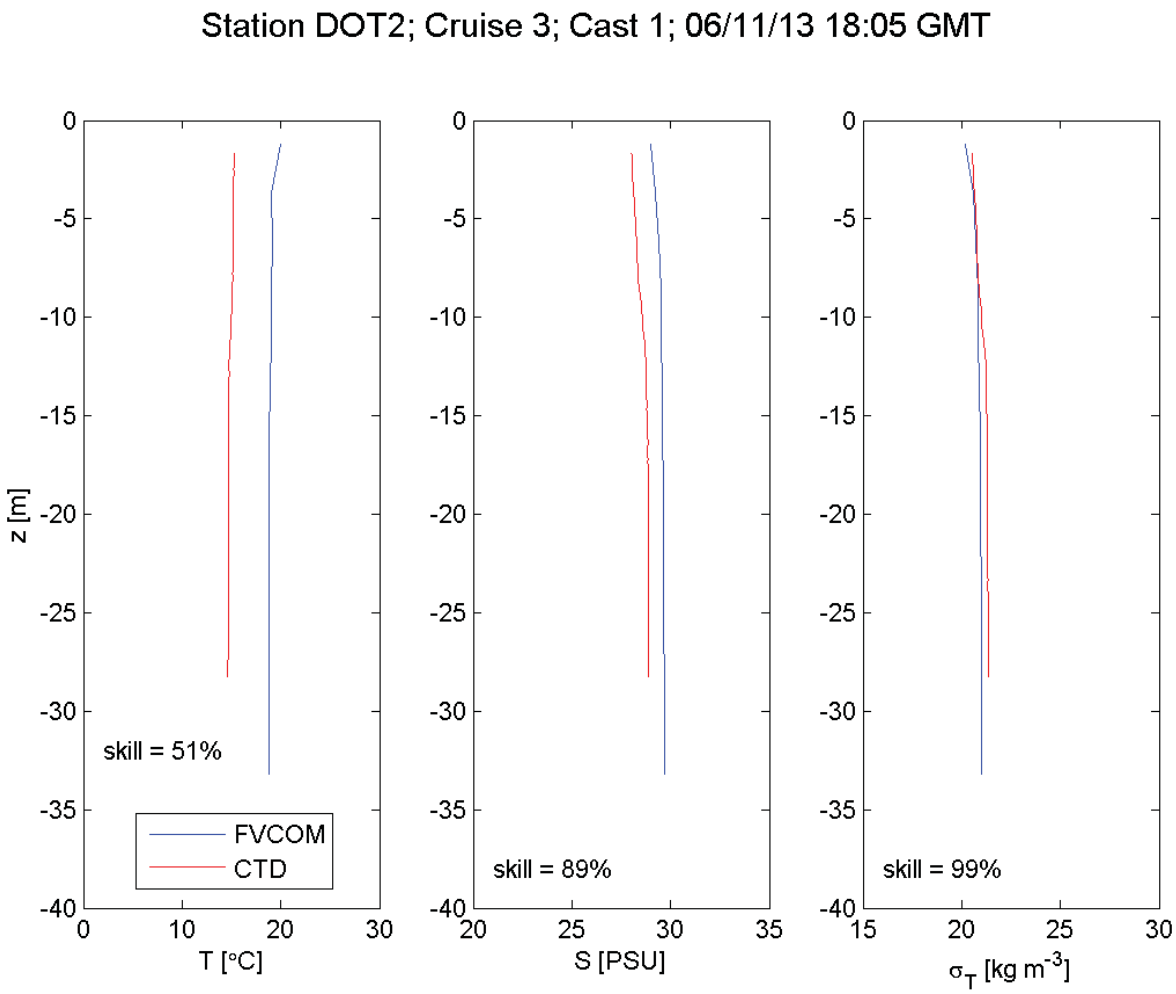

Figure A4.77 Contemporaneous comparison of salinity (left panel), temperature (middle panel), and density (right panel) profiles at Station DOT2 predicted by the FVCOM model (blue) with those measured by a CTD cast from the *R/V Connecticut* (red) during Cruise 3.

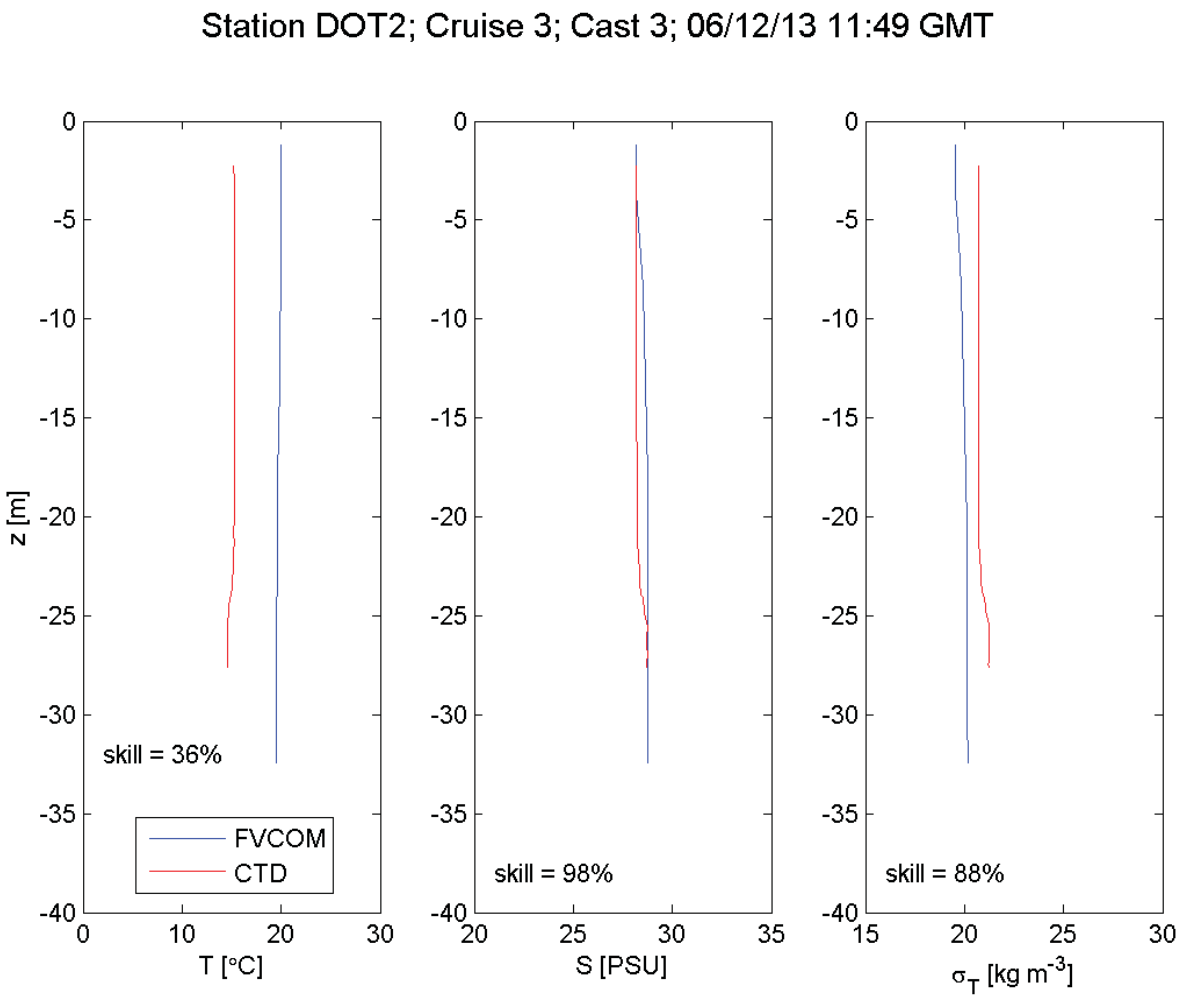

Figure A4.78 Contemporaneous comparison of salinity (left panel), temperature (middle panel), and density (right panel) profiles at Station DOT2 predicted by the FVCOM model (blue) with those measured by a CTD cast from the *R/V Connecticut* (red) during Cruise 3.

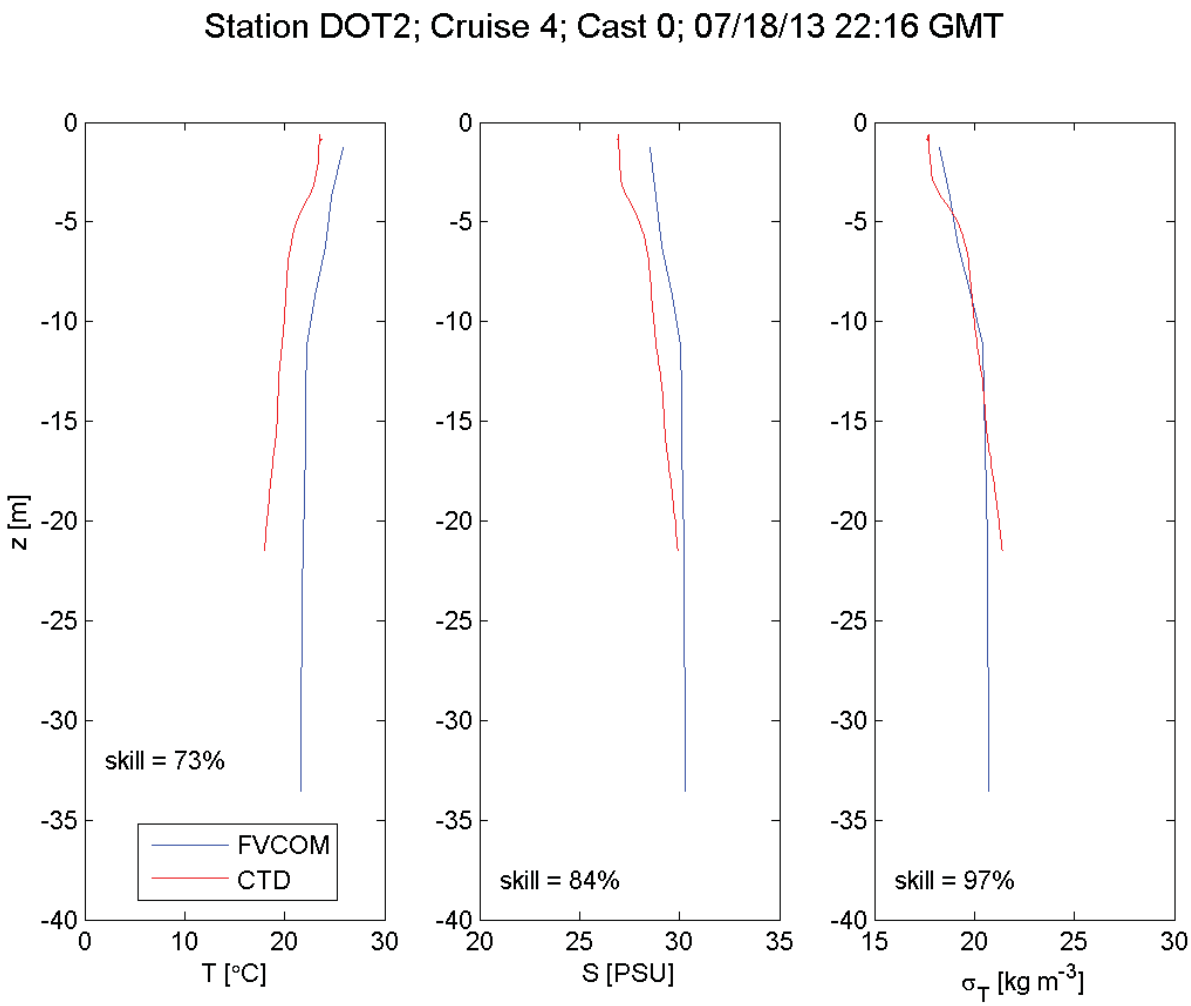

Figure A4.79 Contemporaneous comparison of salinity (left panel), temperature (middle panel), and density (right panel) profiles at Station DOT2 predicted by the FVCOM model (blue) with those measured by a CTD cast from the *R/V Connecticut* (red) during Cruise 4.

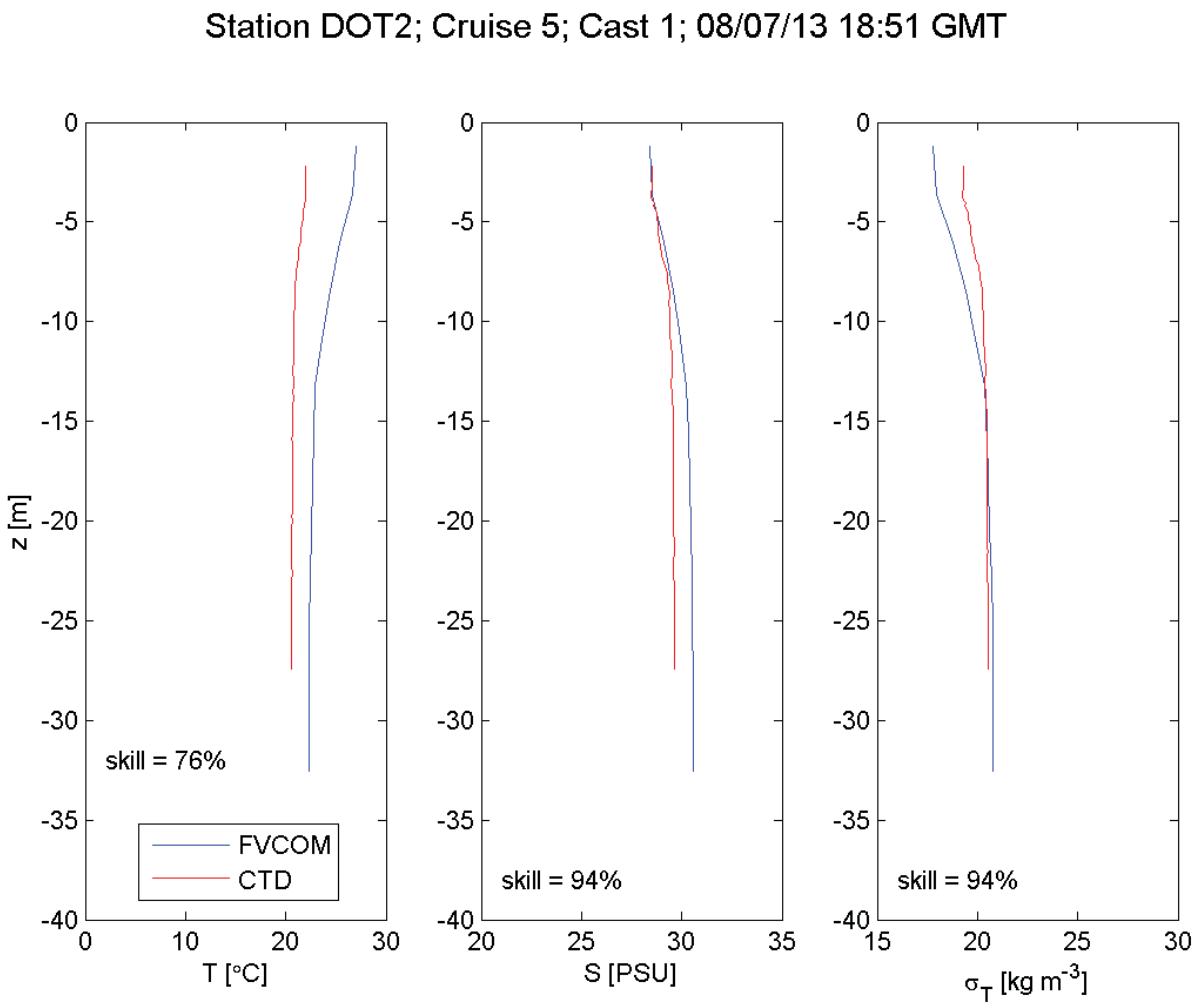

Figure A4.80 Contemporaneous comparison of salinity (left panel), temperature (middle panel), and density (right panel) profiles at Station DOT2 predicted by the FVCOM model (blue) with those measured by a CTD cast from the *R/V Connecticut* (red) during Cruise 5.

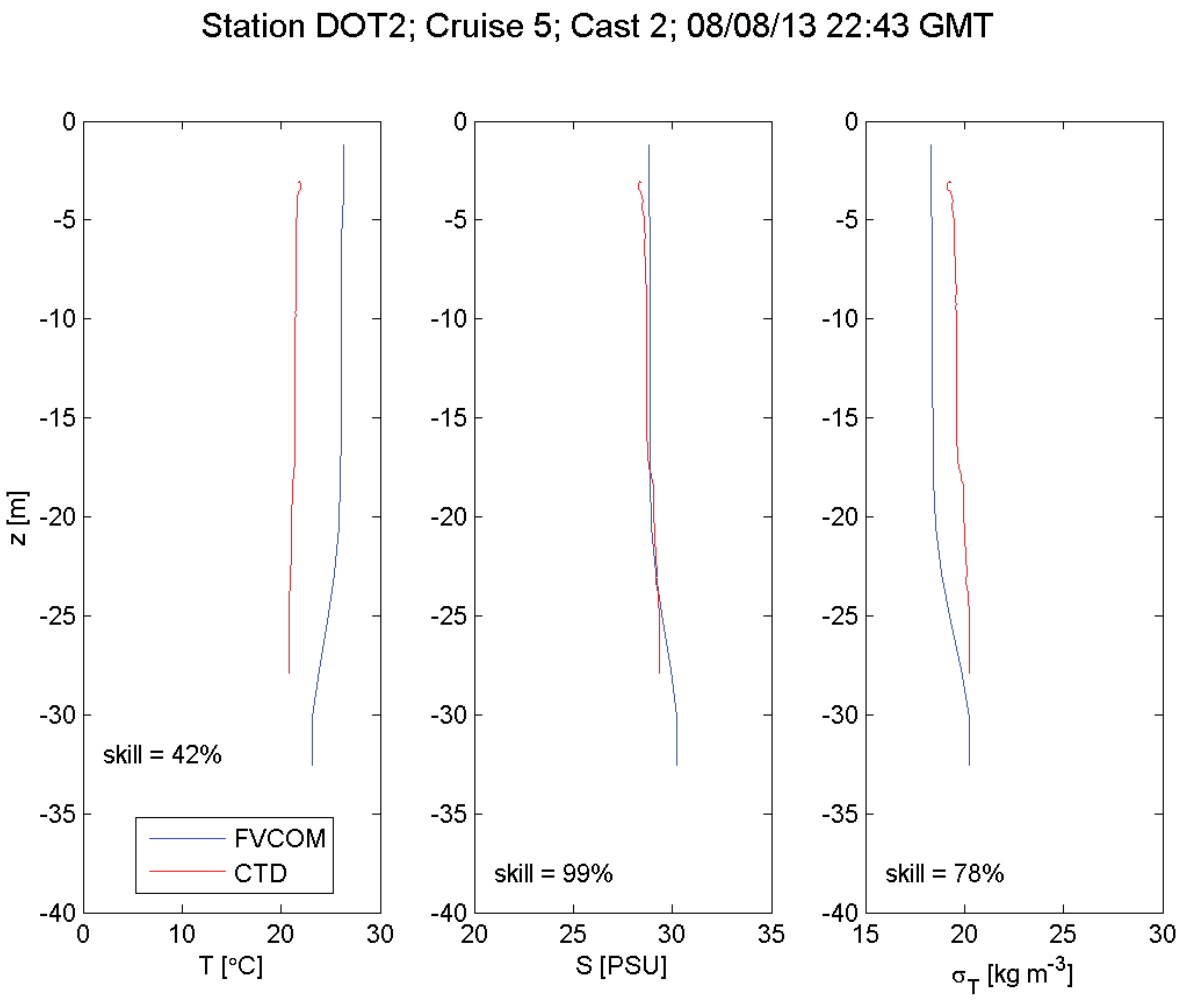

Figure A4.81 Contemporaneous comparison of salinity (left panel), temperature (middle panel), and density (right panel) profiles at Station DOT2 predicted by the FVCOM model (blue) with those measured by a CTD cast from the *R/V Connecticut* (red) during Cruise 5.

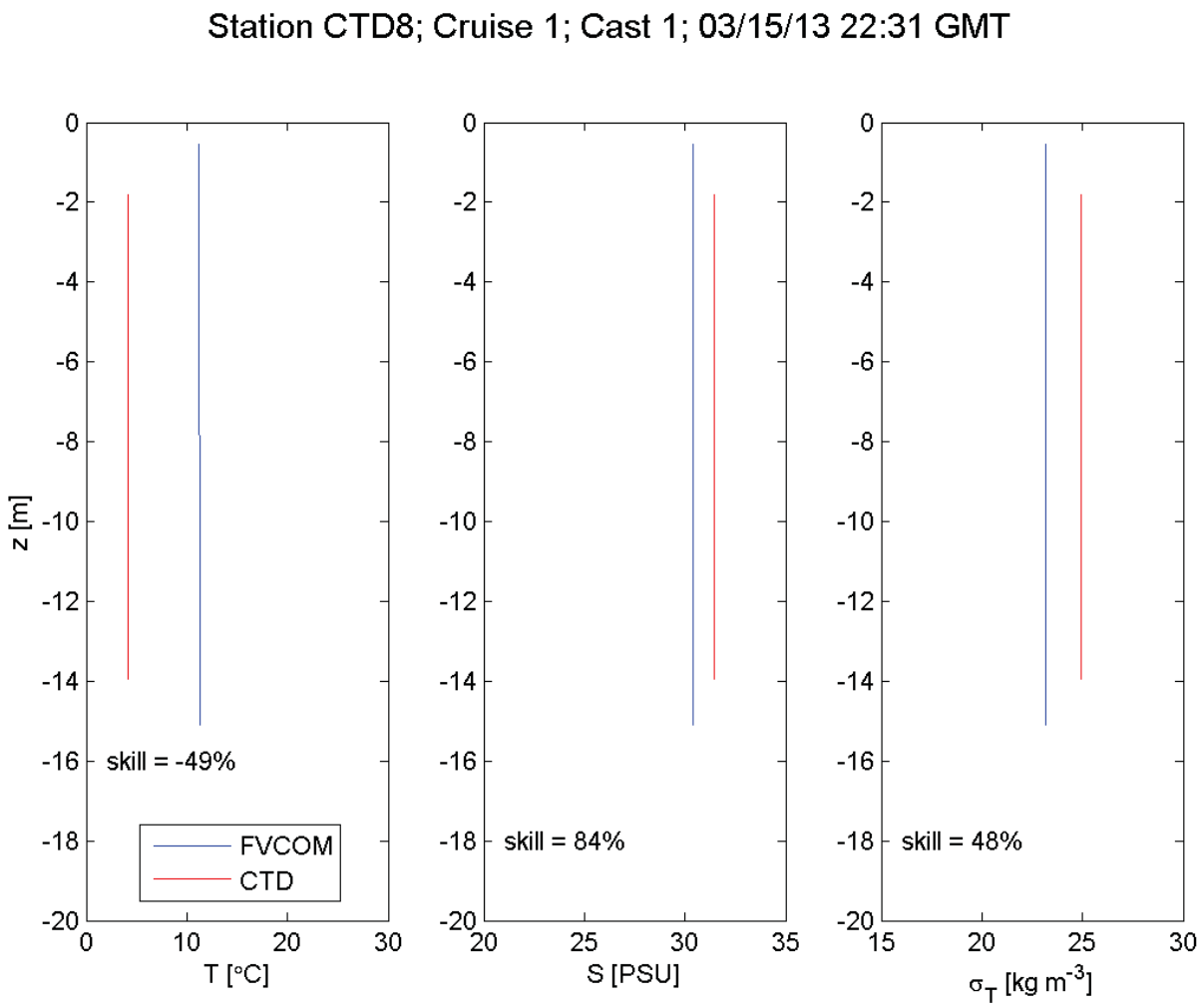

Figure A4.82 Contemporaneous comparison of salinity (left panel), temperature (middle panel), and density (right panel) profiles at Station CTD8 predicted by the FVCOM model (blue) with those measured by a CTD cast from the *R/V Connecticut* (red) during Cruise 1.

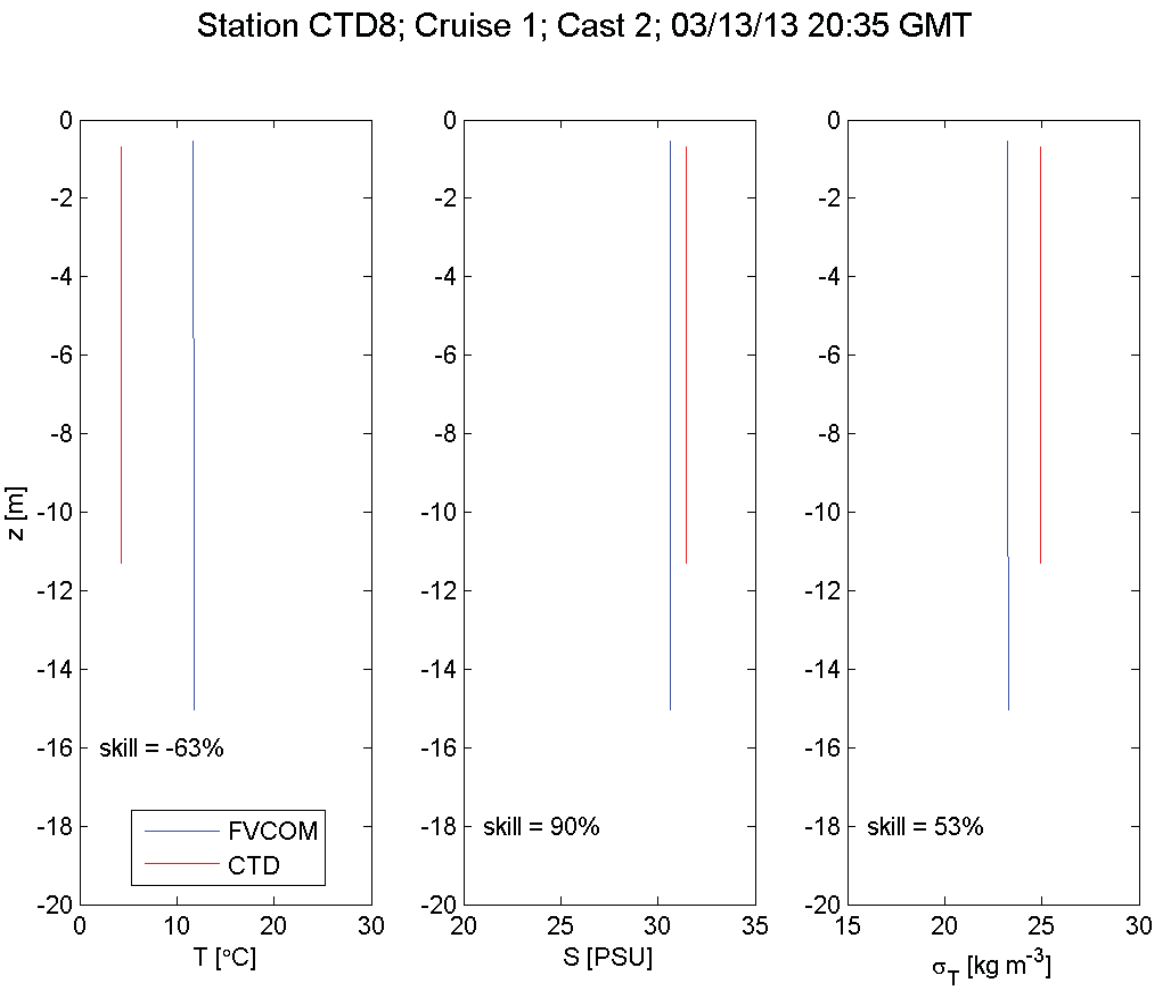

Figure A4.83 Contemporaneous comparison of salinity (left panel), temperature (middle panel), and density (right panel) profiles at Station CTD8 predicted by the FVCOM model (blue) with those measured by a CTD cast from the *R/V Connecticut* (red) during Cruise 1.

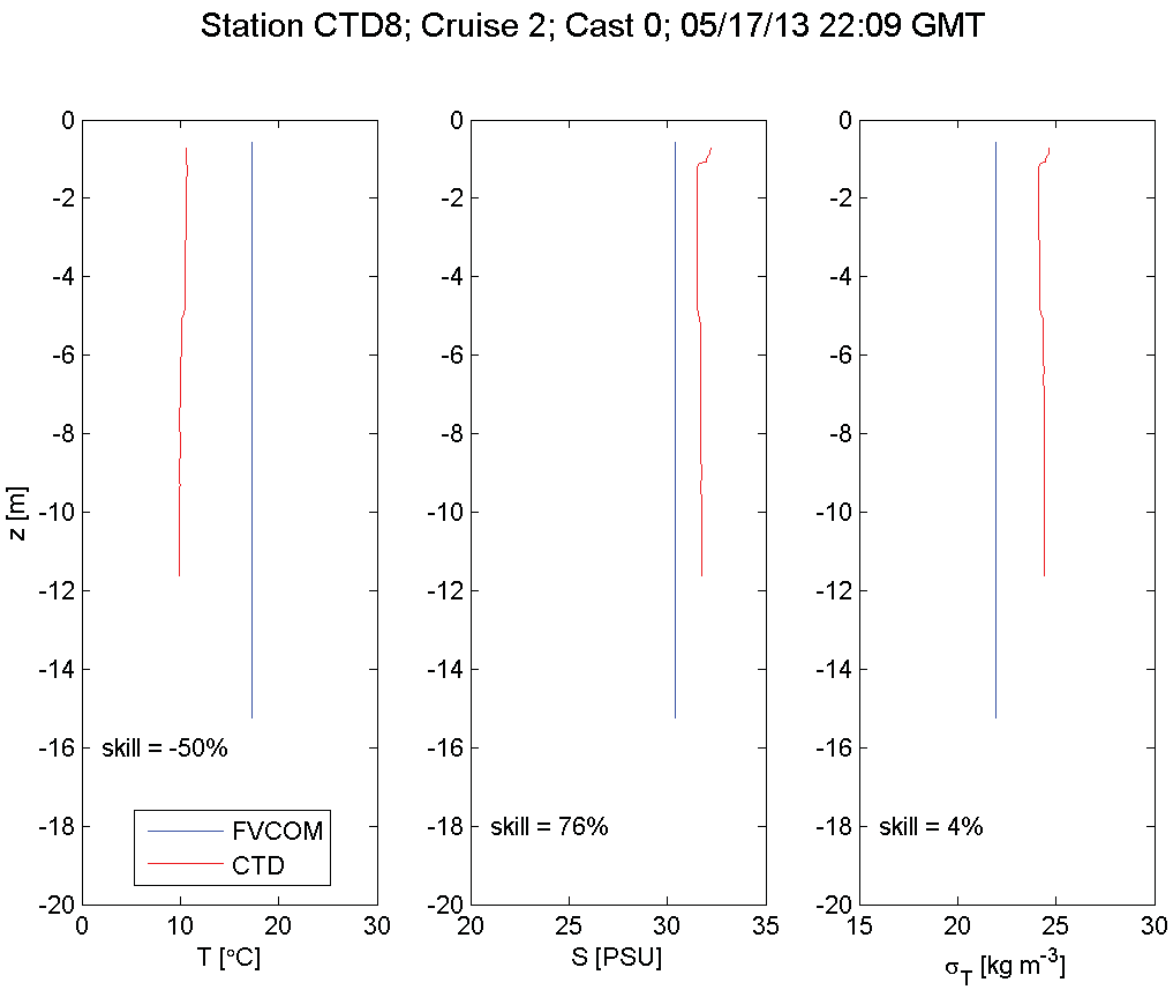

Figure A4.84 Contemporaneous comparison of salinity (left panel), temperature (middle panel), and density (right panel) profiles at Station CTD8 predicted by the FVCOM model (blue) with those measured by a CTD cast from the *R/V Connecticut* (red) during Cruise 2.

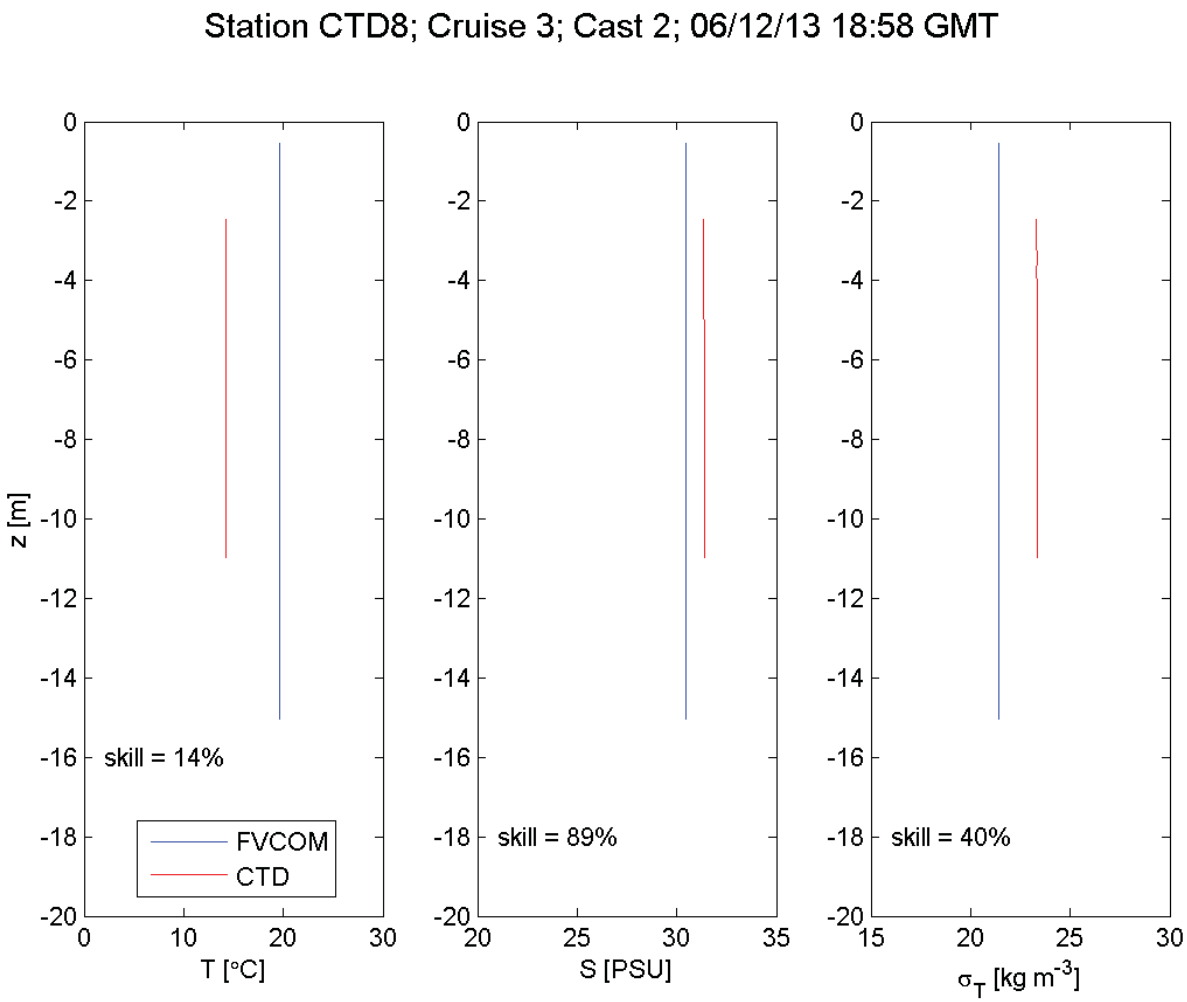

Figure A4.85 Contemporaneous comparison of salinity (left panel), temperature (middle panel), and density (right panel) profiles at Station CTD8 predicted by the FVCOM model (blue) with those measured by a CTD cast from the *R/V Connecticut* (red) during Cruise 3.

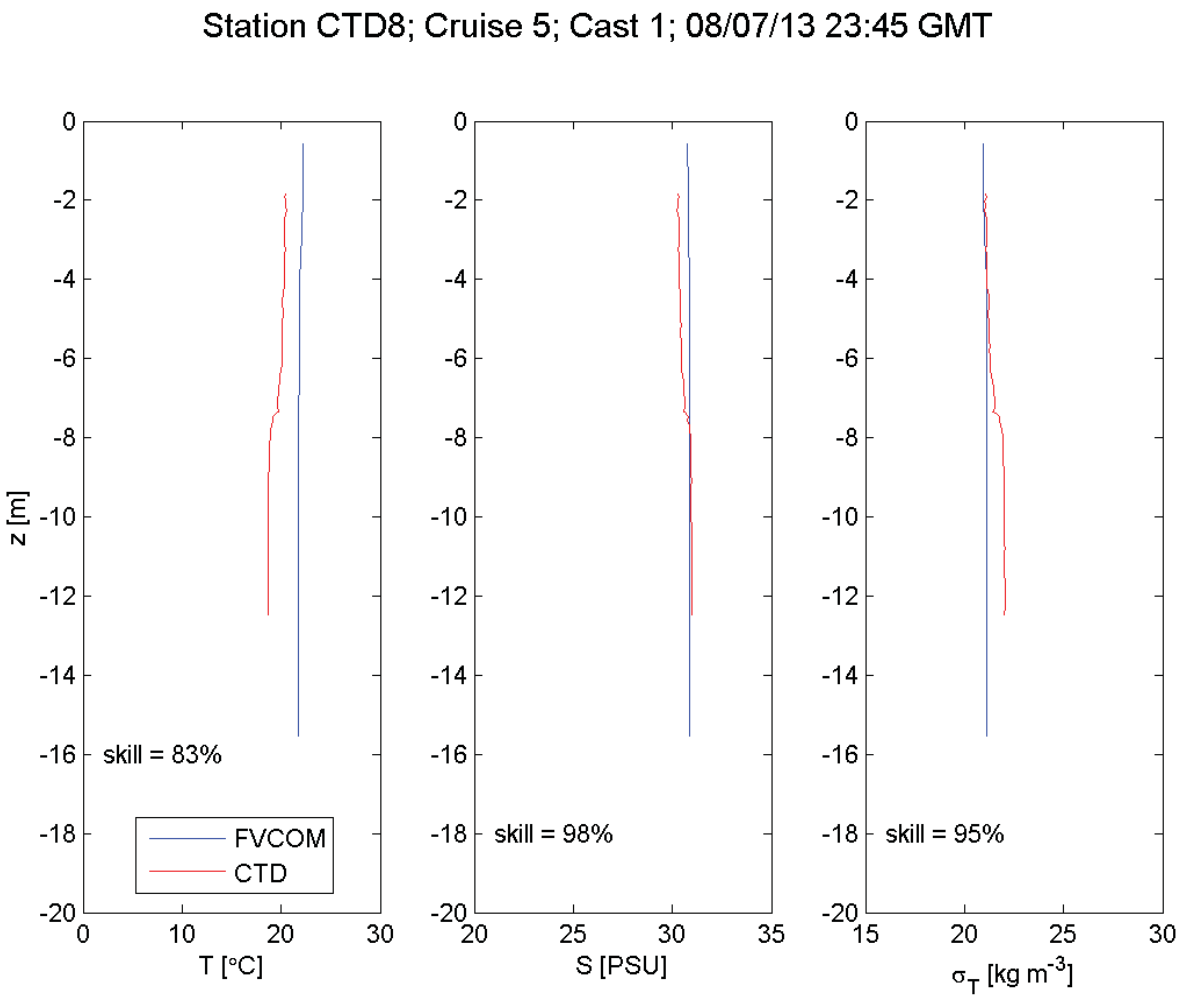

Figure A4.86 Contemporaneous comparison of salinity (left panel), temperature (middle panel), and density (right panel) profiles at Station CTD8 predicted by the FVCOM model (blue) with those measured by a CTD cast from the *R/V Connecticut* (red) during Cruise 5.

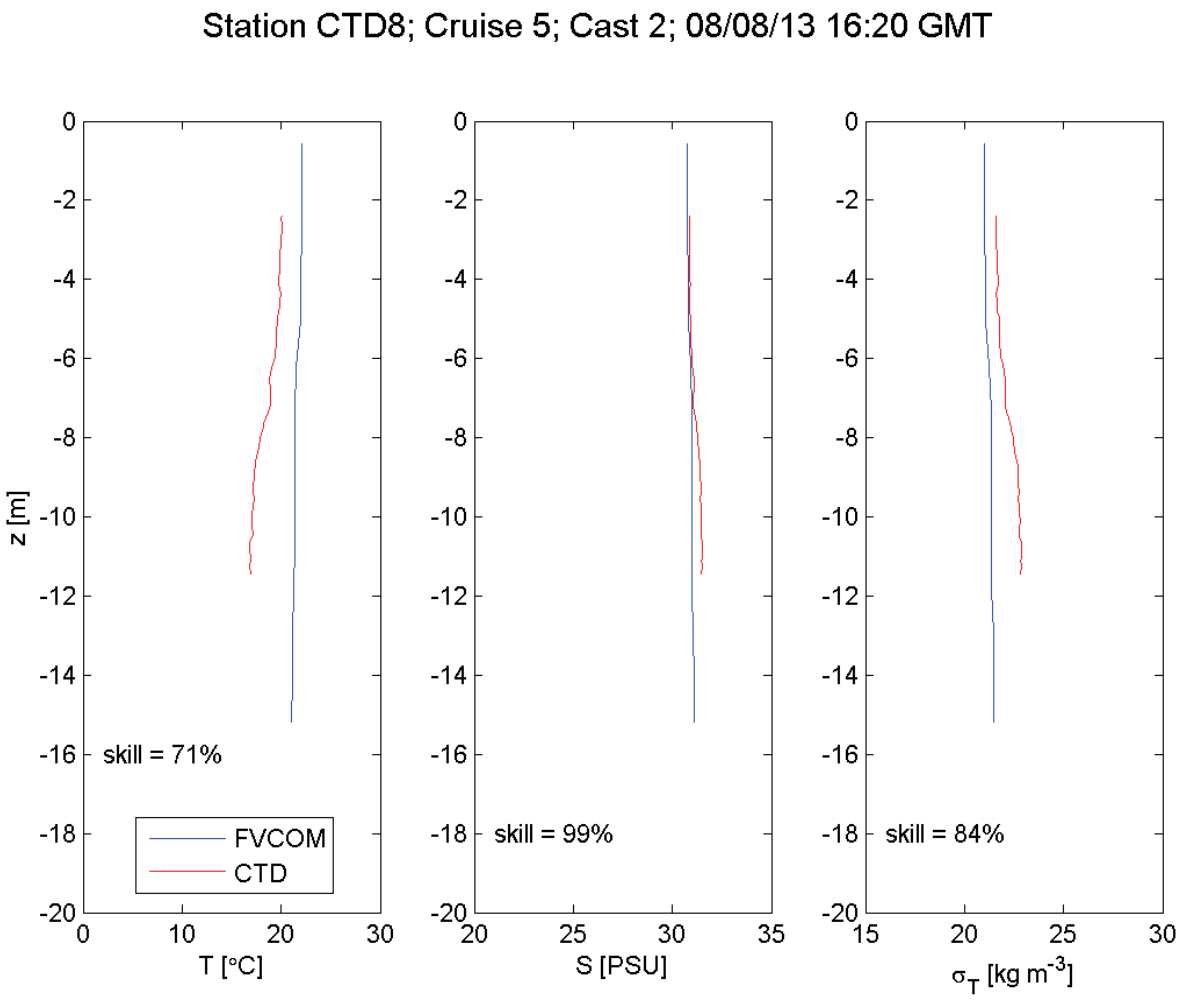

Figure A4.87 Contemporaneous comparison of salinity (left panel), temperature (middle panel), and density (right panel) profiles at Station CTD8 predicted by the FVCOM model (blue) with those measured by a CTD cast from the *R/V Connecticut* (red) during Cruise 5.

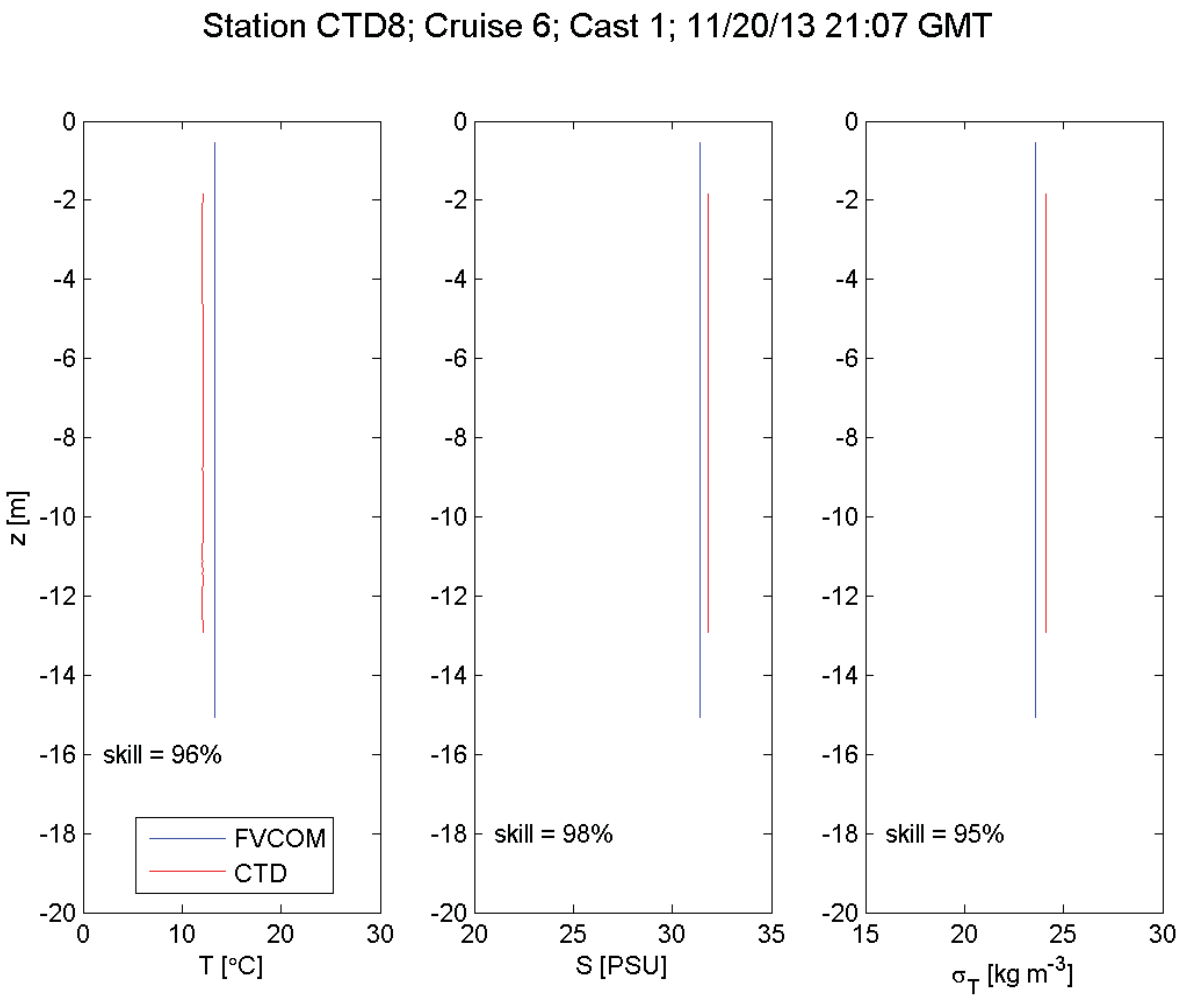

Figure A4.88 Contemporaneous comparison of salinity (left panel), temperature (middle panel), and density (right panel) profiles at Station CTD8 predicted by the FVCOM model (blue) with those measured by a CTD cast from the *R/V Connecticut* (red) during Cruise 6.

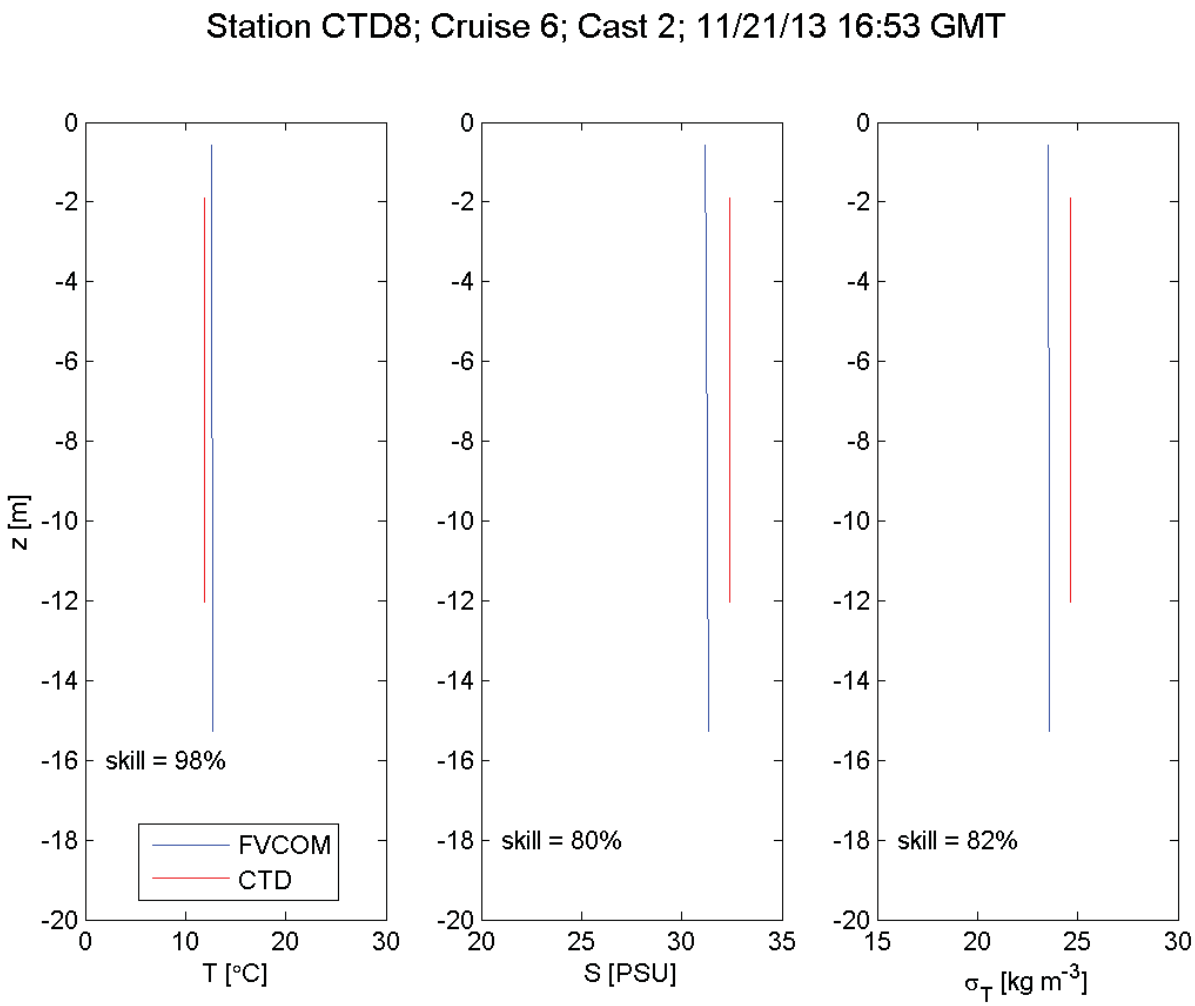

Figure A4.89 Contemporaneous comparison of salinity (left panel), temperature (middle panel), and density (right panel) profiles at Station CTD8 predicted by the FVCOM model (blue) with those measured by a CTD cast from the *R/V Connecticut* (red) during Cruise 6.

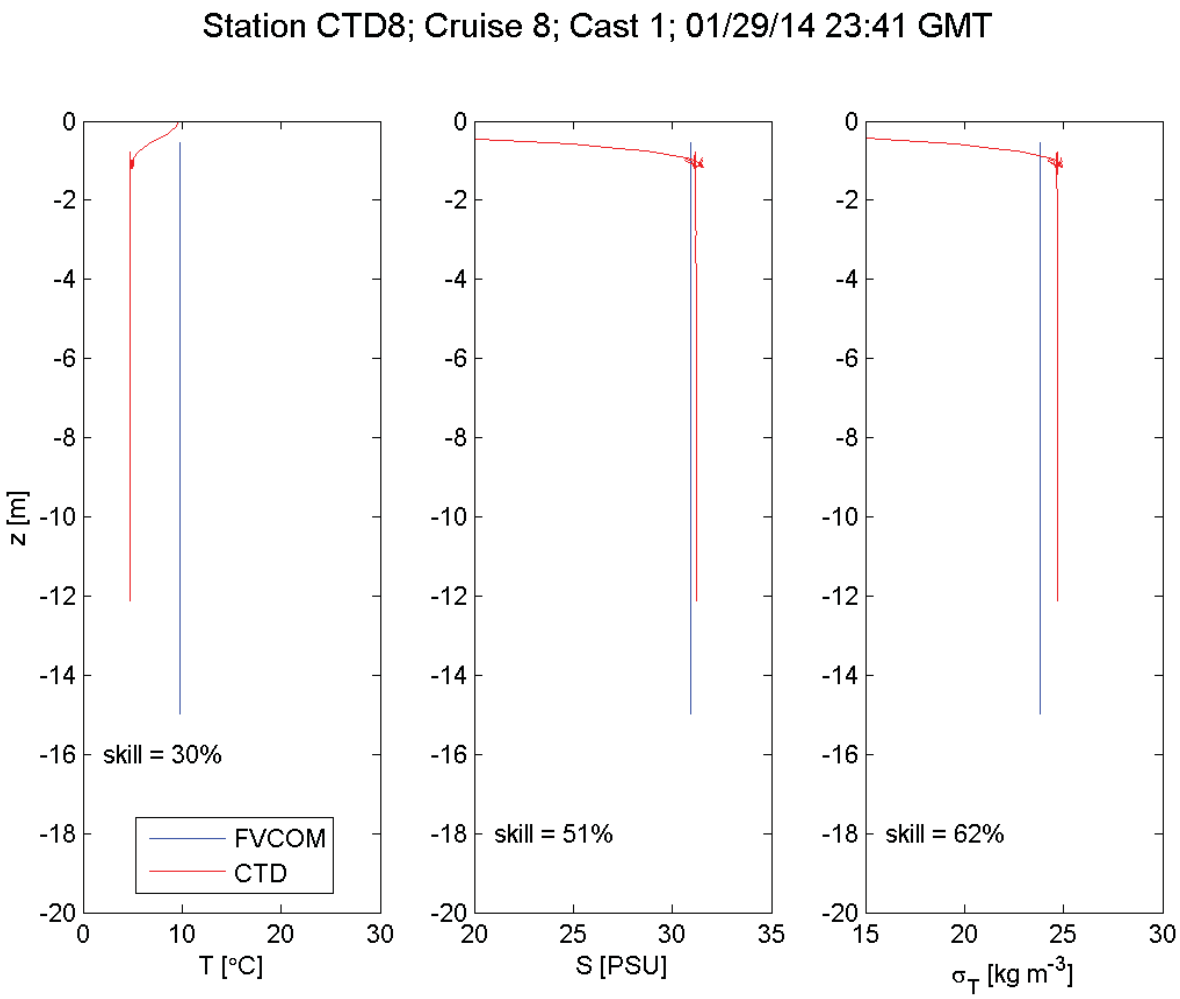

Figure A4.90 Contemporaneous comparison of salinity (left panel), temperature (middle panel), and density (right panel) profiles at Station CTD8 predicted by the FVCOM model (blue) with those measured by a CTD cast from the *R/V Connecticut* (red) during Cruise .

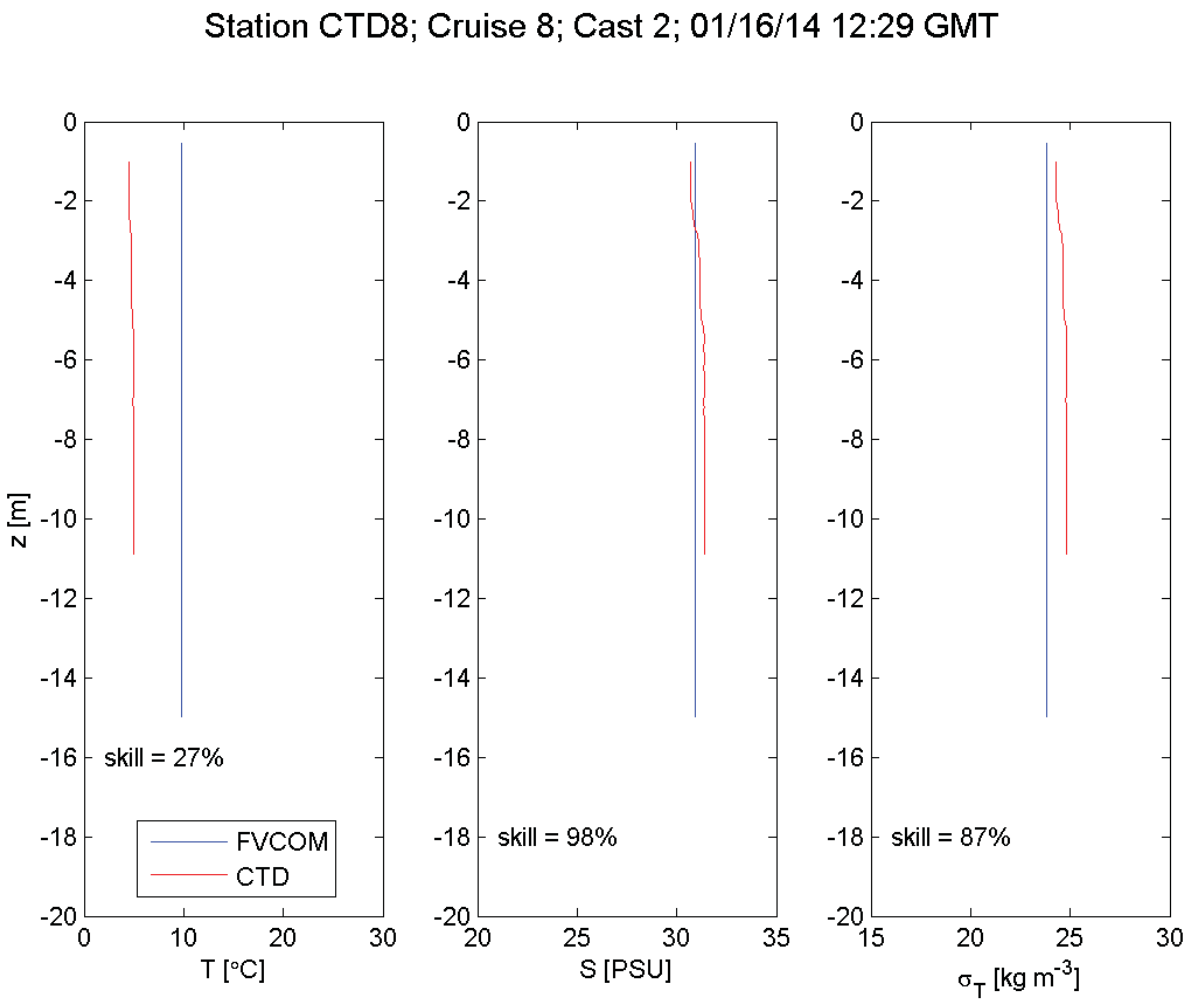

Figure A4.91 Contemporaneous comparison of salinity (left panel), temperature (middle panel), and density (right panel) profiles at Station CTD8 predicted by the FVCOM model (blue) with those measured by a CTD cast from the *R/V Connecticut* (red) during Cruise 8.

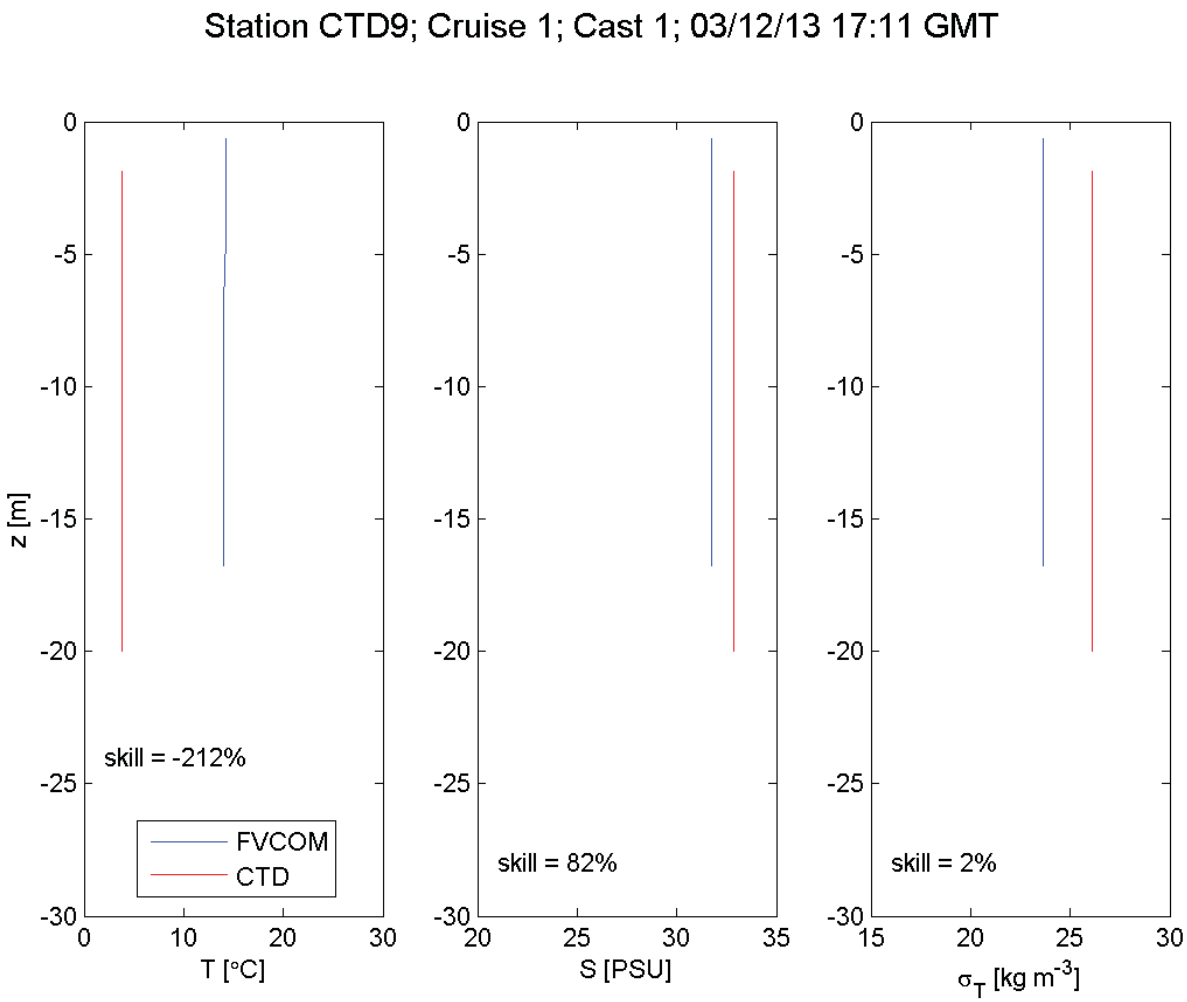

Figure A4.92 Contemporaneous comparison of salinity (left panel), temperature (middle panel), and density (right panel) profiles at Station CTD9 predicted by the FVCOM model (blue) with those measured by a CTD cast from the *R/V Connecticut* (red) during Cruise 1.

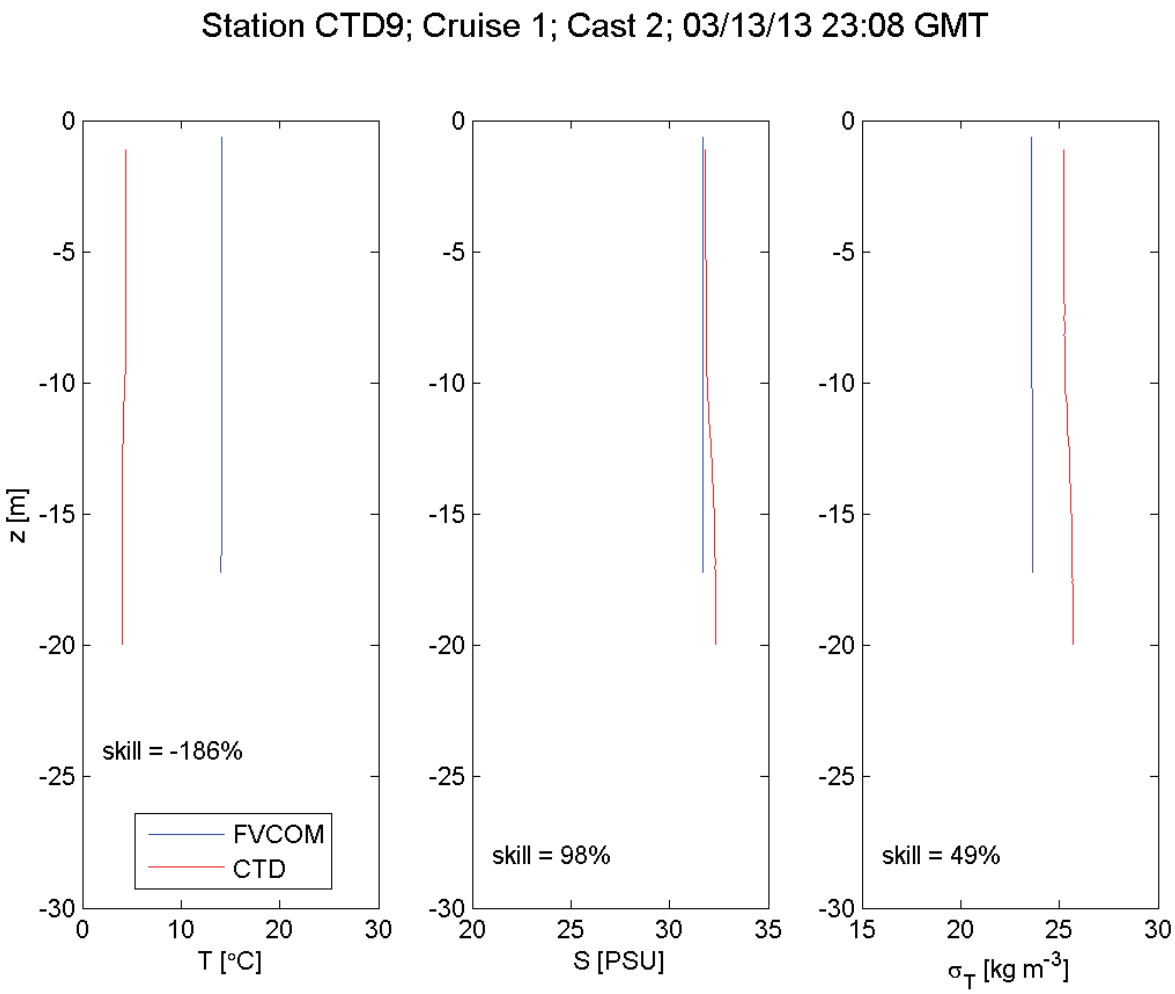

Figure A4.93 Contemporaneous comparison of salinity (left panel), temperature (middle panel), and density (right panel) profiles at Station CTD9 predicted by the FVCOM model (blue) with those measured by a CTD cast from the *R/V Connecticut* (red) during Cruise 1.

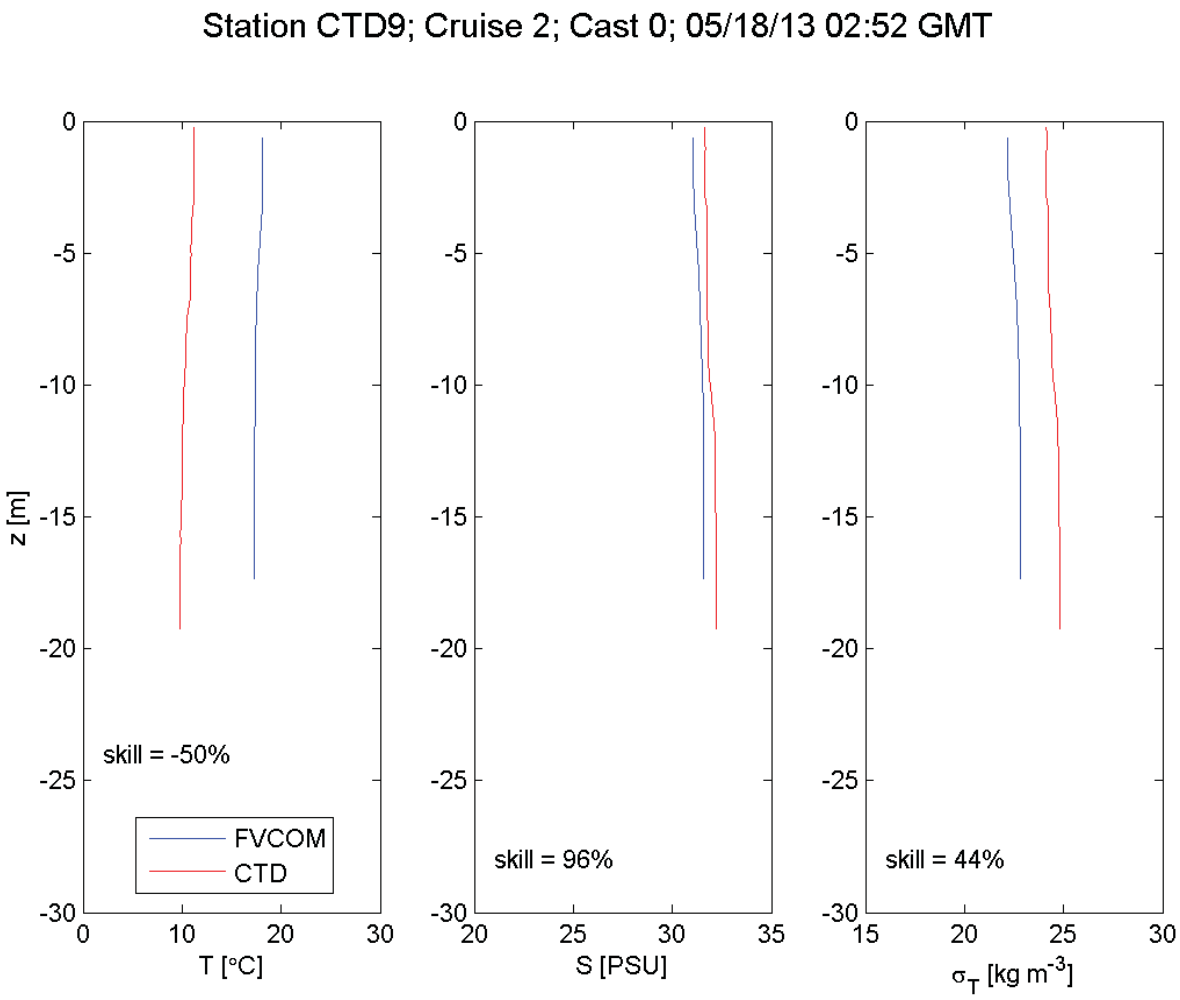

Figure A4.94 Contemporaneous comparison of salinity (left panel), temperature (middle panel), and density (right panel) profiles at Station CTD9 predicted by the FVCOM model (blue) with those measured by a CTD cast from the *R/V Connecticut* (red) during Cruise 2.

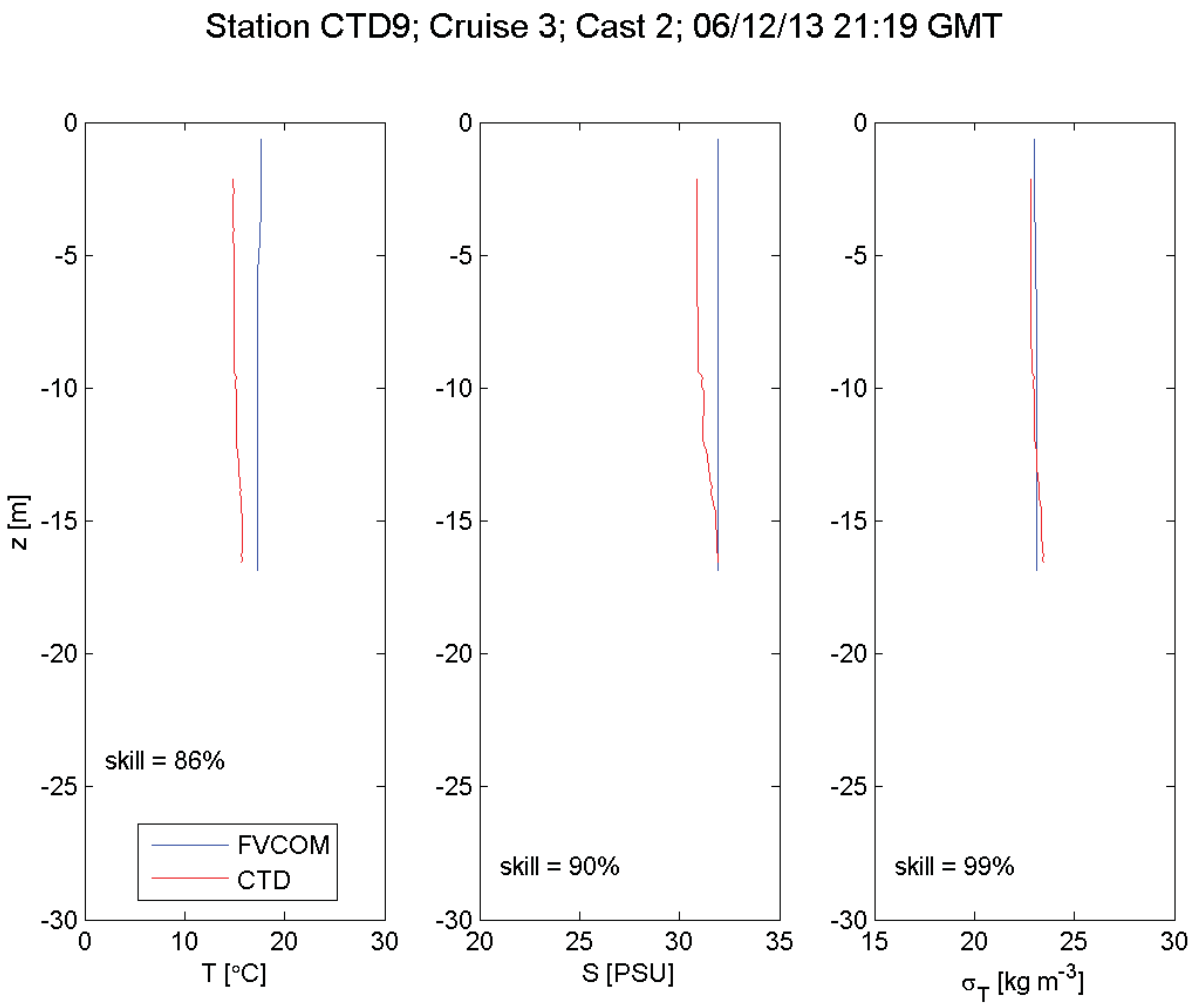

Figure A4.95 Contemporaneous comparison of salinity (left panel), temperature (middle panel), and density (right panel) profiles at Station CTD9 predicted by the FVCOM model (blue) with those measured by a CTD cast from the *R/V Connecticut* (red) during Cruise 3.

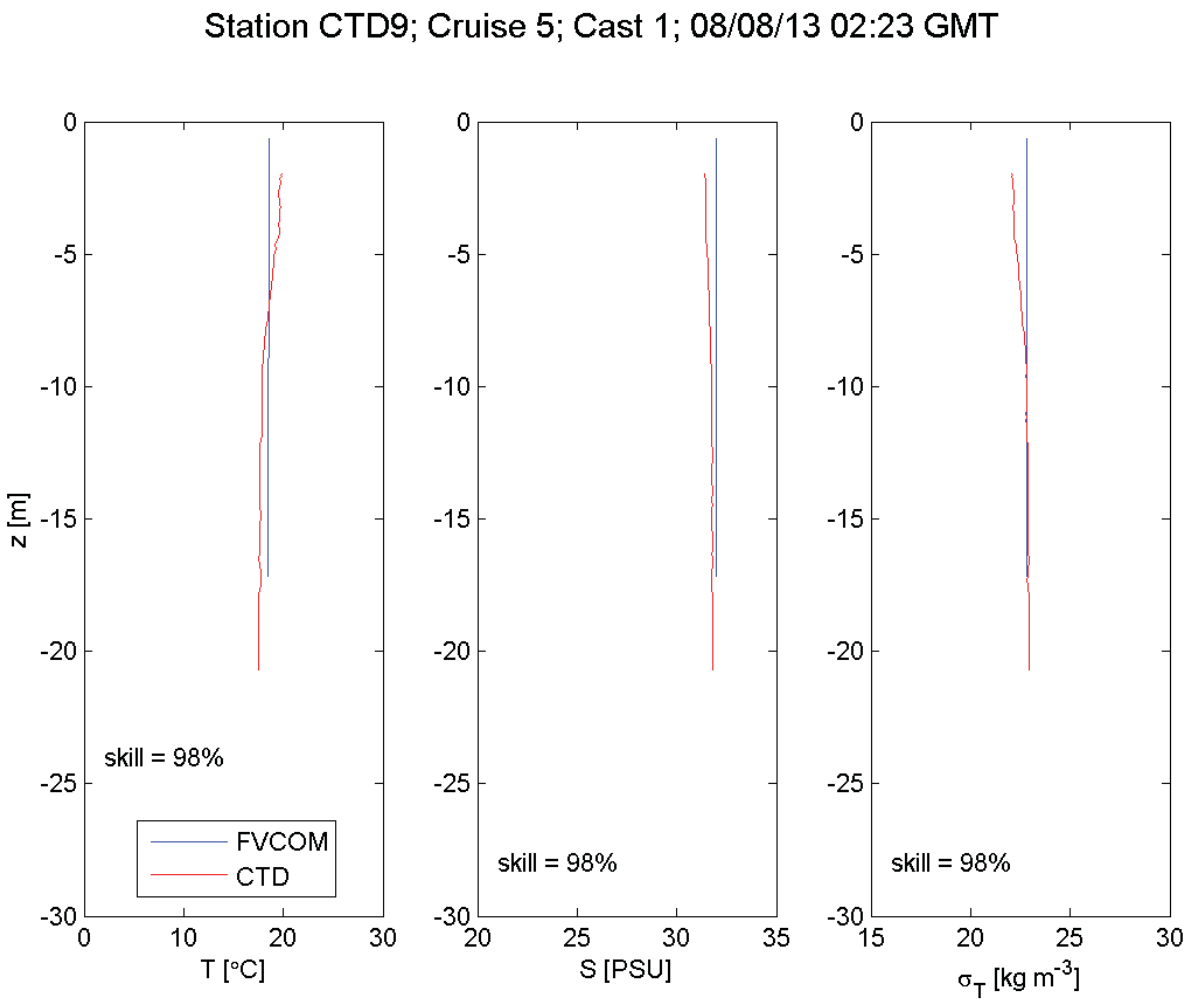

Figure A4.96 Contemporaneous comparison of salinity (left panel), temperature (middle panel), and density (right panel) profiles at Station CTD9 predicted by the FVCOM model (blue) with those measured by a CTD cast from the *R/V Connecticut* (red) during Cruise 5.

[This page intentionally left blank.]

Supplemental Environmental Impact Statement for the Designation of Dredged Material Disposal Sites in Eastern Long Island Sound, Connecticut and New York

Appendix C-3

Physical Oceanography of Eastern Long Island Sound Region: Sediment Transport

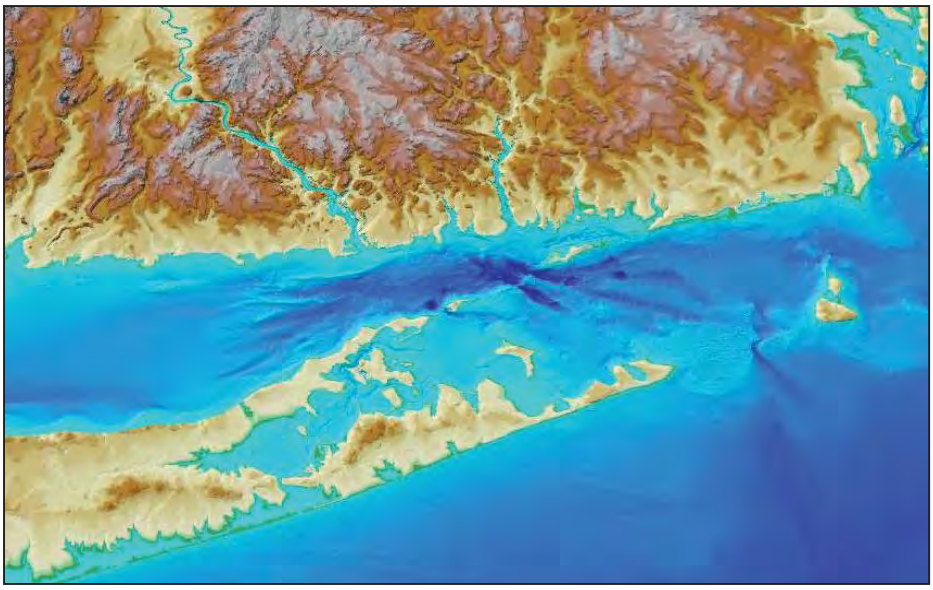

Prepared for: **United States Environmental Protection Agency**

Sponsored by: **Connecticut Department of Transportation**

Prepared by: **University of Connecticut**

December 2015

Supplemental Environmental Impact Statement for the Designation of Dredged Material Disposal Sites in Eastern Long Island Sound, Connecticut and New York

---

EASTERN LONG ISLAND SOUND REGION: SEDIMENT TRANSPORT

Prepared for:

United States Environmental Protection Agency

5 Post Office Square, Suite 100
Boston, MA 02109

Sponsored by:

Connecticut Department of Transportation

Waterways Administration
2800 Berlin Turnpike
Newington, CT 06131-7546

Prepared by:

James O'Donnell, Grant McCardell, Rachel Horwitz, and Kay Howard-Strobel

University of Connecticut

Department of Marine Sciences
1080 Shennecossett Road
Groton, CT 06340

December 2015

Table of Contents

Page

Executive Summary ..... *ix*

1. Introduction 1

2. Near-field Dilution and Transport - STFATE Simulations 3
   - 2,1 Model Fundamentals 3
   - 2.2 STFATE Implementation 3
   - 2.3 Dilution Criteria. 6
   - 2.4 STFATE Simulation Results 7
     - 2.4.1 Site 1 - Cornfield Shoals 7
     - 2.4.2 Site 5 - Niantic Bay 13
     - 2.4.3 Site 6 - New London 19
   - 2.5 STFATE Summary 25

3. Long-term Dilution and Transport - FVCOM Simulations 26
   - 3.1 FVCOM Fundamentals 26
   - 3.2 Tracer Simulation in FVCOM 26
   - 3.3 Tracer Simulation Results 31
     - 3.3.1 Concentration Maps 31
     - 3.3.2 Time-Series at Coastal Sites 31
   - 3.4 Tracer Simulation Summary 37

4. Long-term Stability of the Disposal Mounds - LTFATE Simulations 38
   - 4.1 LTFATE Fundamentals 38
   - 4.2 LTFATE Simulation 38
   - 4.3 LTFATE Simulation Results 43
     - 4.3.1 Site 1 – Cornfield Shoals 43
     - 4.3.2 Site 5 – Niantic Bay 45
     - 4.3.3 Site 6 – New London 46
   - 4.4 LTFATE Simulation Summary 47

5. Summary and Conclusions 48

References 50

List of Tables

Table 1 Input parameters for STFATE model simulations

Table 2 Operational disposal parameters used in STFATE simulations

Table 3 Dredged material properties (by volume) used in STFATE model simulations

Table 4 Dredged material characteristics

Table 5 Site characteristics of mound

Table 6 Summary of LTFATE mound centroid movement

List of Figures

Figure 1 Zone of Siting Feasibility (ZSF) consisting of Eastern Long Island Sound and Block Island Sound, and the three alternative sites evaluated in detail in the SEIS

Figure 2 Alternative Sites 1, 5, and 6 used for the STFATE simulations showing the depth-averaged M_2 semidiurnal tide

Figure 3 Deposition thickness for a single scow release operation conducted at Site 1 using the mean magnitude of the vertically average current.

Figure 4 Deposition thickness for a single scow release operation conducted at Site 1 using the mean daily maximum magnitude current

Figure 5 Maximum relative concentration at Site 1-Cornfield Shoals (CSDS) using the mean magnitude of the vertically average current

Figure 6 Maximum relative concentration at Site 1-Cornfield Shoals (CSDS) using the mean daily maximum magnitude depth-averaged current

Figure 7 Deposition thickness at Site 5 using the mean magnitude of the vertically average current

Figure 8 Deposition thickness at Site 5 using the mean daily maximum magnitude depth-averaged current

Figure 9 Maximum relative concentration at Site 5-Niantic Bay (NBDS + NB-E) using the mean magnitude of the vertically average current

Figure 10 Maximum relative concentration at Site 5-Niantic Bay (NBDS + NB-E) using the mean daily maximum magnitude depth-averaged current

Figure 11 Maximum relative concentration at Site 5-Niantic Bay (2 nmi x 1 nmi) using the mean magnitude of the vertically average current

Figure 12 Maximum relative concentration at Site 5-Niantic Bay (2 nmi x 1 nmi) using the mean daily maximum magnitude depth-averaged current

Figure 13 Maximum relative concentration at Site 5-Niantic Bay (1 nmi x 1 nmi) using the mean magnitude of the vertically average current

Figure 14 Maximum relative concentration at Site 5-Niantic Bay (1 nmi x 1 nmi) using the mean daily maximum magnitude depth-averaged current

Figure 15 Deposition thickness for a single scow release operation conducted at Site 6 using the mean daily maximum magnitude depth-averaged current

Figure 16 Deposition thickness for a single scow release operation conducted at Site 6 using the mean daily maximum magnitude depth-averaged current

Figure 17 Maximum relative concentration at Site 6-New London (NLDS + NL-Wa/b) using the mean magnitude of the vertically average current

Figure 18 Maximum relative concentration at Site 6-New London (NLDS + NL-Wa/b) using the mean daily maximum magnitude depth-averaged current

Figure 19 Maximum relative concentration at Site 6-New London (NLDS [50%] + NL-Wa/b) using the mean magnitude of the vertically average current

Figure 20 Maximum relative concentration at Site 6-New London (NLDS [50%] + NL-Wa/b) using the mean daily maximum magnitude depth-averaged current

Figure 21 Maximum relative concentration at Site 6-New London (NL-Wa/b) using the mean magnitude of the vertically average current

Figure 22 Maximum relative concentration at Site 6-New London (NL-Wa/b) using the mean daily maximum magnitude depth-averaged current

Figure 23 Map of the FVCOM model grid in the Eastern Long Island Sound with the tracer release areas highlighted in red

Figure 24 Sea surface elevation and eastward component of depth-average current at Site 1 (Cornfield Shoals), and wind speed at the four tracer release times

Figure 25 Surface tracer concentration eight hours after tracer release at Site 6 (New London)

Figure 26 Surface tracer concentration 48 hours after release at Site 5 (Niantic Bay)

Figure 27 Surface concentrations at 1, 6, and 12 hours after tracer release

Figure 28 Surface concentrations at 1, 2, and 3 days after tracer release

Figure 29 Time-series of tracer concentration at five sites along the Connecticut coastline

Figure 30 Time-series of tracer concentration at three sites on the Fishers Island coastline

Figure 31 Time-series of tracer concentration at five sites along the Long Island coastline

Figure 32 Physical structure of the mound used in LTFATE simulations

Figure 33 LTFATE wave data summary

Figure 34 LTFATE current data summary

Figure 35 Wave and current conditions during Superstorm Sandy used in the evaluation of the stability of disposal mounds

Figure 36 Cornfield Shoals LTFATE results

Figure 37 Niantic Bay LTFATE results

Figure 38 New London LTFATE results

Acronyms and Abbreviations

BIS	Block Island Sound
C.F.R.	Code of Federal Regulations
CLDS	Central Long Island Sound Disposal Site
cm	centimeter
CS	Cornfield Shoals
CSDS	Cornfield Shoals Disposal Site
cy	cubic yard(s)
D_{50}	median grain size
ft	feet
ft/s	feet per second
FVCOM	Finite Volume Coastal Ocean Model (The model, nested within the University of Massachusetts-Dartmouth Regional Model, was used as the primary model for assessing the bottom stress, salinity, temperature, currents, waves, and horizontal circulation based on the data collected during the Physical Oceanographic study. The model is not commercially available.)
g/cm^3	gram per cubic centimeter
lb/ft^3	pounds per cubic feet
LISICOS	Long Island Sound Integrated Coastal Observing System
LTFATE	Long-term FATE (USACE model that simulates the evolution of dredged material mounds by erosion and bed load transport.)
m	meter
mm	millimeter
m/s	meter per second
MPRSA	Marine Protection Research and Sanctuaries Act
NB	Niantic Bay
NBDS	Niantic Bay Disposal Site
NECOFS	Northeast Coastal Forecast System
NL	New London
NLDS	New London Disposal Site
nmi	nautical mile(s)
ODA	Ocean Dumping Act
PO	Physical oceanography

ppm	parts per million
RISDS	Rhode Island Sound Disposal Site
SEIS	Supplemental Environmental Impact Statement
sq yd	square yard(s)
STFATE	Short-Term FATE (USACE model simulating water column concentration of dredged material and any associated chemical contaminants when the material is released from a scow.)
USACE	U.S. Army Corps of Engineers
USEPA	U.S. Environmental Protection Agency
WLDS	Western Long Island Sound Disposal Site
ZSF	Zone of Siting Feasibility

[This page intentionally left blank.]

EXECUTIVE SUMMARY

This report describes the distribution and transport of sediment at three sites in eastern Long Island Sound. These sites (Cornfield Shoals, Niantic Bay and New London) were identified during site screening as alternatives for the potential designation of one or more open-water dredged material disposal site(s). This report was prepared in support of the Supplemental Environmental Impact Statement (SEIS) that analyzed these three alternative sites in detail and is included as Appendix C-3.

The model STFATE was applied to simulate effects of ocean currents and density stratification on the motion of sediment released from a scow near the surface of the ocean to estimate the fraction that reaches the seafloor, the location and shape of the disposal mound, and the concentration of elutriate remaining in the water column. The ambient stratification was chosen to represent the largest values in the region. The results of the modeling study for eastern Long Island Sound (O'Donnell et al., 2015; see SEIS Appendix C-2) were used to provide estimates of the range of currents likely during disposal operations.

STFATE requires that the fraction of the total volume released from the scow be specified. Based on data from past disposal operations at the active New London Disposal Site (NLDS), model input values were as follows: 13.1% clumped material (*i.e.,* sediment particles that are bound together); 1.6% sand, 12.4% silt, and 2.3% clay (*i.e.,* the sand/silt/clay fractions not bound in clumps); and 70.6% water (*i.e.,* pore water). The simulations show that all of the clump and sand portions and almost all of the silt would deposit under all conditions at all three alternative sites. Only the clay portions would fail to deposit at all three alternative sites. At Site 1 (Cornfield Shoals), the simulations show that under mean current conditions, 78% of the clay fraction would reach the seafloor within the alternative site boundaries; under high current conditions, none of the clay would reach the seafloor. At Site 5 (Niantic Bay), the results were similar with 89% of the clay reaching the seafloor under mean current conditions and none under high current conditions. At Site 6 (New London) almost all of the clay fraction would reach the seafloor under both mean current conditions (96.4%) and under high current conditions (83%). For releases at the centers of all alternative sites, the deposited sediment would remain within the alternative site boundaries.

The Limiting Permissible Criteria (LPC) for the portion of dredged material that will remain in the water column is the concentration of any dissolved constituent that, after making allowance for initial mixing, will not exceed applicable marine water-quality criteria (USEPA and USACE, 1991). The model STFATE was used to simulate the dilution of the dredged material elutriate by seawater as a consequence of the scow release at the three alternative sites under both mean current and high current conditions. The simulations showed that for a release from a 3,000-cy scow, concentrations would decrease to below the LPC of 0.25% of the scow concentration well within four hours both inside and outside of the three alternative sites. Equivalently, the elutriate concentration would be diluted by the mixing in the sinking dredged material plume by at least a factor of 400. If the smallest site dimension options are considered for the Niantic Bay and New London alternative sites (1 x 1 nmi, and 1.5 x 1 nmi, respectively), the LPC would be exceeded outside the site during high flow conditions. During mean current conditions, none of the various site dimension options considered would exceed the LPC outside the site.

The longer-term transport and dilution of the dredged material released into the water column from the disposal operations were simulated using the circulation model FVCOM. Simulations predicted that within 24 hours of the release from a scow, the effluent would spread throughout much of eastern Long Island Sound (from the Connecticut River to Fishers Island Sound) and that the concentration of the material leaving the alternative disposal site would be diluted further by the circulation and mixing in eastern Long Island Sound by approximately a factor of 100 by the time it would reach most shoreline locations. Therefore, relative to the initial concentrations in the scow, the material released from the scow would be diluted by at least a factor of 40,000 before reaching most coastal locations.

The highest concentrations (least dilution) at model cells adjacent to the New York shore was predicted to occur at the western-most tip of Fishers Island following a release at the New London alternative site. There, the concentration leaving the New London site boundary would be diluted further by a factor of 10, resulting in an effective dilution of the concentration in the scow by at least a factor of 4,000.

The model LTFATE was used to attempt to simulate the movement and erosion of post-disposal mounds. Post-disposal dredged material characteristics at the New London site were used as input for these simulations. Simulations assessed the stability of an 18-foot high rectangular disposal mound at all three alternative sites in both ambient and storm conditions. Simulation of a storm over a 3-day period resulted in only negligible movement; however, simulation with typical conditions showed some mound movement after 180-days at all three alternative sites. We have little confidence in these results since monitoring of the existing mounds by the DAMOS program at the New London Disposal Site has not revealed mound motion. Furthermore, the simulations of bottom stresses described in O'Donnell et al. (2015) indicate that Site 1 (Cornfield Shoals) would be subject to considerably higher stresses (and therefore greater mound erosion and movement) than the other two alternative sites. The inability of LTFATE to discriminate between the three alternative sites is likely due to limitations of the currently available version of the LTFATE model.

In conclusion, the STFATE simulations show that at the Cornfield Shoals and Niantic Bay alternative sites, a significant fraction of the clay component does not get to the seafloor when the currents are strong. However, at normal currents the suspended fraction is substantially lower. At all alternative sites any dissolved material transported out of the site is substantially diluted after 50 hours, by at least a factor of 40,000 from the initial concentration in a scow. The minimum dilution of the concentration of dissolved materials in the scow at model cells adjacent to the coast is 4,000. This occurs near the western tip of Fishers Island after disposal of dredged material at the New London alternative site.

1. Introduction

The USEPA has the authority to designate dredged material disposal sites for the management of dredged material under Section 102(c) of the Act and 40 C.F.R. Part 228.4 of its regulations. In accordance with Section 102(c) of the Marine Protection Research and Sanctuaries Act (MPRSA; also referred to as Ocean Dumping Act [ODA]) of 1972 and the National Environmental Policy Act (NEPA, 1970), a Supplementary Environmental Impact Assessment (SEIS) is in preparation as part of the decision-making process. This SEIS and supporting documentation evaluates the area defined as the Zone of Siting Feasibility (ZSF). This area is shown in Figure 1. The ZSF contains two active dredged material disposal sites that are currently used for dredged material disposal: the New London Disposal Site (NLDS) and the Cornfield Shoals Disposal Site (CSDS). In addition, the ZSF contains several historically used disposal sites. The two active disposal sites and the historically used Niantic Bay Disposal Site (NBDS) were identified during site screening as alternatives sites for more detailed analysis in the SEIS.

This report describes the third element of a three-part study of the Physical Oceanography (PO) of Eastern Long Island Sound that was commissioned to inform the development of the SEIS. Two additional reports have been completed. The first describes the results of a field observation program (O'Donnell et al., 2014; SEIS Appendix C-1) conducted to test the effectiveness of a numerical model described in O'Donnell et al. (2015; provided as SEIS Appendix C-2) in the simulation of the circulation and bottom shear stress in the study area during normal weather conditions and during severe storm events. This PO study supplements work conducted in the region as part of the Environmental Impact Statement (EIS) for the designation of the Central and Western Long Island Sound Disposal Sites (CLDS and WLDS) (USEPA and USACE, 2004a).

The objective of this report is to expand upon the results of the earlier modeling and observations in order to: (1) describe the dilution of solutes introduced to the water column in the vicinity of the alternative sites during dredged material disposal operations using the STFATE (Short-Term FATE) model; (2) assess the stability of the disposal mound to resuspension/erosion using the LTFATE (Long-term Fate) model (Scheffner et al., 1995; Scheffner, 1996); and (3) estimate the extent of the dispersal of very fine particles and solutes using the circulation model FVCOM (the model is described in O'Donnell et al., 2015).

The STFATE and LTFATE modeling followed the approach used for the designation of the CLDS and WLDS (USEPA and USACE, 2004a), and the designation of the Rhode Island Sound Disposal Site (RISDS) (USEPA and USACE, 2004b). The characteristics of the STFATE model, the choice of parameters, and the results of the model simulations are presented in Section 2. The longer-term and larger-scale transport of the dissolved material is simulated using the predictions of the circulation model (FVCOM); simulations and results are provided in Section 3. The stability of the dredged material mounds as simulated by the LTFATE model is described in Section 4. A summary and conclusions are provided in Section 5.

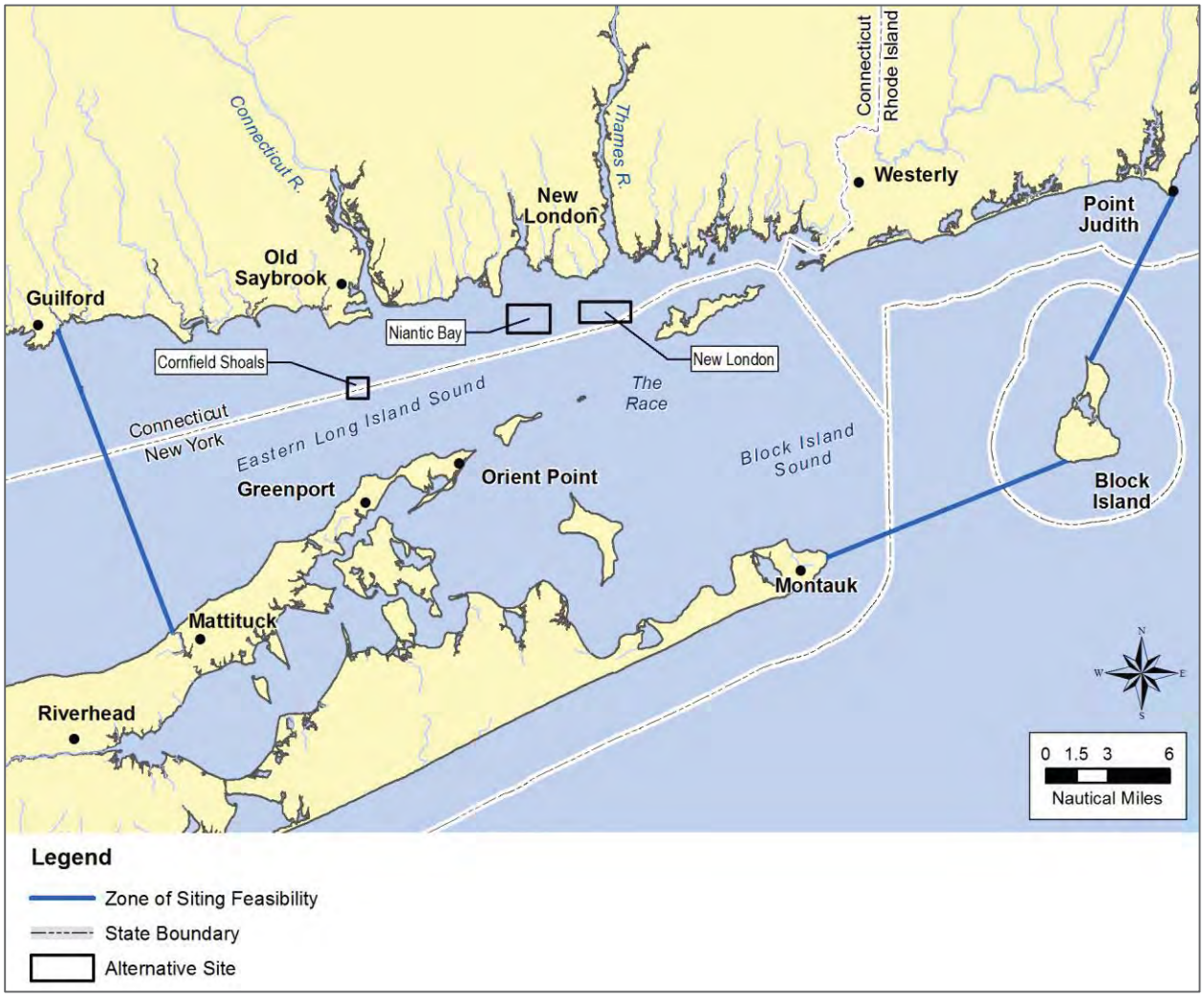

Figure 1. Zone of Siting Feasibility (ZSF) consisting of eastern Long Island Sound and Block Island Sound, and the three alternative sites evaluated in detail in the SEIS.

These three alternative sites are also referred to in this report as "Site 1" (Cornfield Shoals), "Site 5" (Niantic Bay), and "Site 6" (New London), consistent with the terminology used in the field data and modeling reports of the Physical Oceanography Study (O'Donnell et al., 2014; 2015; see SEIS Appendices C-1 and C-2, respectively).

2. Near-field Dilution and Transport - STFATE Simulations

2.1 Model Fundamentals

In order to simulate the actions of disposal operations at the three alternative sites, we employed the STFATE (Short-Term FATE) model using site-specific currents obtained from the FVCOM simulations described previously in O'Donnell et al. (2015). STFATE is a widely used model developed by Koh and Chang (1973) and Brandsma and Divorky (1976) to simulate the short-term fate of dredged material when released into open waters from scows and hoppers at a disposal site. STFATE assumes that the dredged sediment is a mixture of sand and clay particles. To describe the effects of sediment cohesion and aggregation, STFATE also allows a fraction of the sediment to be modeled as a "clump" of consolidated particles. These often occur when clamshell dredges are used. Clumps have a much more rapid settling velocity than individual sediment particles that are not bound up in clumps.

When dredged material is released near the surface during disposal operations it is assumed to sink in three phases:

(1) Convective descent - in which gravity accelerates the sediment-water mixture downward;

(2) Dynamic collapse - in which the descending material is arrested by the bottom or the buoyancy of the mixture becomes zero (it reaches a neutral level); and

(3) Passive transport - in which the material is advected by the flow in the receiving waters.

In Phase 1, the descent and dilution of the sediment-water mixture is assumed to behave as a negatively buoyant Gaussian plume with an initial volume and mass characterized by the size of the scow and dredged sediments. As the plume sinks, it mixes with ambient fluid at a rate that is based on the laboratory experiments of Bowers and Goldenblatt (1978). These assumptions lead to analytical expressions for the mass that reaches the seafloor and the fraction that remains in the water column.

When the plume reaches the seafloor, Phase 2 dynamics pertain. Each plume that reaches the seafloor is assumed to have an ellipsoidal shape. On the seafloor, the horizontal pressure gradient component created by the negatively buoyant sediment layer is retarded by frictional forces between the mixture and the seafloor. This phase terminates when the motion due to the buoyancy-driven collapse is less than the horizontal spreading rate associated with turbulent dispersion. The model equations of the collapse phase are presented in Brandsma and Divorky (1976).

In the final Phase 3 (passive transport), the concentration in the plume is characterized by a three-dimensional Gaussian function centered at (x_0, y_0) with standard deviations σ_x, σ_y, and σ_z, that is advected by the ambient flow. The location of the plume center changes with time at a rate that depends upon the velocity in the ambient fluid, and the standard deviations (and width of the plume) increase with time at a rate proportional to the size of the plume.

2.2 STFATE Implementation

The STFATE model evaluates the complex equations that describe the three phases of the model dynamics. The model uses water depths and velocities as input. Figure 2 shows the coastline of Long Island Sound and Block Island Sound together with the locations of Sites 1 (Cornfield Shoals), 5 (Niantic Bay), and 6 (New London). To illustrate the spatial variation in tidal currents in the region, Figure 2 also shows the ellipses traced by the tip of the semidiurnal (M_2) tidal current vector originating from the center of the three sites. These ellipses show that the maximum amplitudes are largest at Site 1 (Cornfield Shoals) and smallest at Site 6 (New London). Though the currents in the region are dominated by semidiurnal tides, they are modified by the effects of other tidal constituents as well as by winds and density variations. To estimate horizontal velocity magnitudes that characterize the three sites, we extracted a 500-day time-series (October 15, 2012 to February 28, 2014) of the depth-averaged currents at the model cell containing the center of each alternative site using the FVCOM model. This time period includes the times during which model field data were collected for model validation (O'Donnell et al., 2014; 2015; see SEIS Appendices C-1 and C-2, respectively) as well as including the simulation of Superstorm Sandy (October 28-30, 2012). These time-series were then analyzed for two current conditions:

- the mean of the maximum daily current magnitudes, $\overline{U}_{max}$, as a representation of the upper bound on expected conditions during disposal operations (hereafter also referred to as "high current"), and
- the mean magnitude of the depth-averaged currents, $\overline{U}$, to characterize more typical conditions (hereafter also referred to as "mean current").

The values obtained are listed in Table 1 together with the depths at the alternative sites.

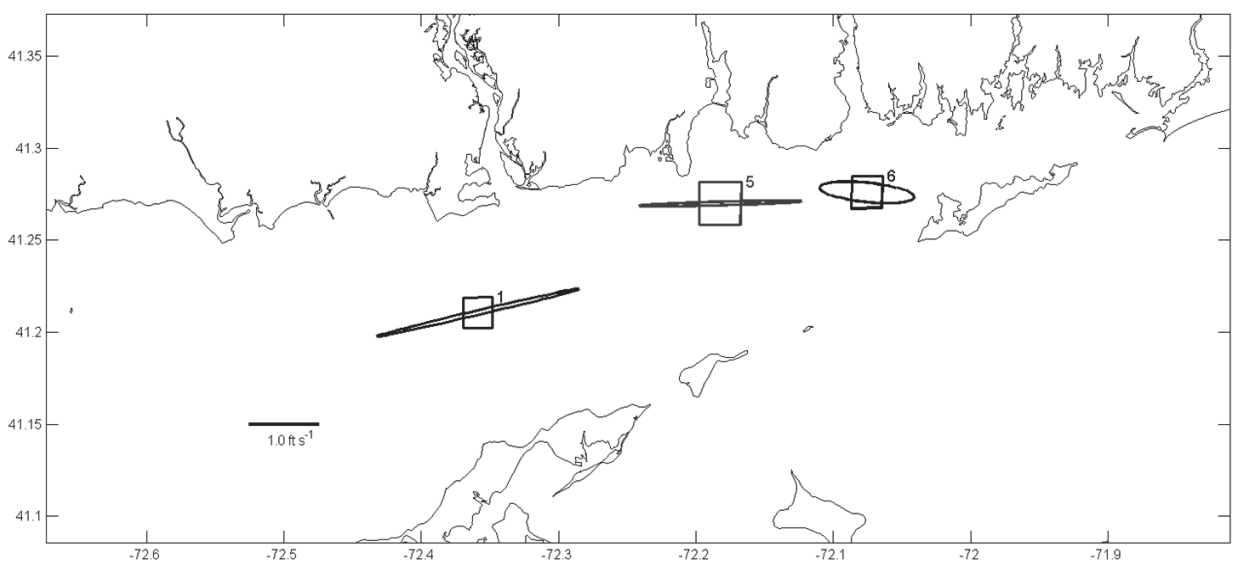

Figure 2. Alternative Sites 1-Cornfield Shoals, 5-Niantic Bay, and 6-New London used for the STFATE simulations. The ellipses show the amplitude and directions of the depth-averaged M_2 semidiurnal tide scaled by the M_2 tidal excursion distances.

The STFATE program also requires the specification of the spatial study domain. This is selected so that the plume is not advected beyond the model boundaries during the simulation. The lateral dimensions of the model area were set to approximately three times the alternative site dimensions and employed a uniformly sized grid of 60 by 60 points at each site with a larger grid size at the sites with stronger currents. Table 2 lists the grid sizes. The water column density structure was prescribed for all model runs to be representative of summer conditions when the vertical stratification is generally at a maximum with a surface layer density of 1.023 g cm^{-3} and a bottom layer density of 1.025 g cm^{-3}. It was also assumed that water from the dredging site would be fresher than water at the alternative site, and a density of 1.015 g cm^{-3} was used to represent the water in the dredged material.

For the Niantic Bay and New London alternative sites, modeling was done for three site dimension options. These dimensions included:

- Full site sizes of 2.08 x 1.33 nautical miles (nmi) (Niantic Bay), 2.5 x 1.0 nmi (New London), and 1.0 x 1.0 nmi (Cornfield Shoals),
- Reduced site sizes of 2.0 x 1.0 nmi (both for Niantic Bay and New London), and
- Small site sizes of 1.0 x 1.0 nmi (Niantic Bay) and 1.5 x 1.0 nmi (New London).

For the Cornfield Shoals alternative site, only one site dimension option was modeled (full site size, *i.e.*, 1.0 x 1.0 nmi).

Table 1. Input Parameters for STFATE Model Simulations at the three Alternative Sites

Parameters	Site 1 Cornfield Shoals	Site 5 Niantic Bay	Site 6 New London
Grid Dimensions	36,500 x 36,500 ft	38,230 x 38,230 ft	28,850 x 28,850 ft
	11,125 x 11,125 m	11,650 x 11,650 m	8,790 x 8,790 m
Site Dimension Option: *Full Site*	6,076 x 6,076 ft	*NBDS + NB-E* 2.08 x 1.33 nmi 12,677 x 8,172 ft	*NLDS + NL-Wa/b* 2.5 x 1 nmi 15,216 x 6.076 ft
Site Dimension Option: *2 nmi x 1 nmi*	--	*northern 2/3 of full site* 2 x 1 nmi 12,152 x 6,076 ft	*NLDS (50%) + NL-Wa/b* 2 x 1 nmi 12,152 x 6,076 ft
Site Dimension Option: *Smallest Size*	--	*Northeastern area* 1 x 1 nmi 6,076 x 6,076 ft	*NL-Wa/b* 1.5 x 1 nmi 9,114 x 6,076 ft
Model Depth	93 ft	89 ft	74 ft
Mean Daily Max Current Magnitude, $\overline{U}_{max}$	3.2 ft/s	2.6 ft/s	2.0 ft/s
Mean Current Magnitude, $\overline{U}$	1.9 ft/s	1.5 ft/s	1.0 ft/s

Since STFATE models the short-term response of the water column to the introduction of dredged material, it is appropriate to use the characteristics of source sediments typical of dredging operations in the eastern Long Island Sound region. For all simulations, the disposal operation parameters were chosen to be representative of dredged material in the eastern Long Island Sound region. Disposal projects used included those from New Haven, CT; Norwalk, CT; and Guilford, CT (as reported by USEPA and USACE [2004b]) as well as from the Providence River, RI (although not located in eastern Long Island Sound, the sediment characteristics are similar). These parameters are listed in Table 2.

Table 2. Operational Disposal Parameters used in STFATE Simulations

Disposal Operation Type	Split Hull Scow
Disposal Location	Center of site
Length of Disposal Bin (ft)	160
Width of Disposal Bin (ft)	42
Volume (cy)	3,000
Pre-Disposal Draft (ft)	17
Post Disposal Draft (ft)	4
Time to Empty (sec)	20

The dredged material properties in the disposal scow also followed the values selected in USEPA and USACE (2004a). Four categories of sediment were included: sand, silt, clay, and clumps. The fractions of these categories and their properties are listed in Table 3. The water fraction of the sediments was set to 70.6%.

Table 3. Dredged Material Properties (by volume) used in STFATE Model Simulations

Clumps	13.1%
Sand	1.6%
Silt	12.4%
Clay	2.3%
Water	70.6%
Total	100.0%
Dredged material water density	1.015 g/cm^3

2.3 Dilution Criterion

The U.S Army Corps of Engineers (USACE) routinely employs suspended particulate phase (SPP) (*i.e.*, elutriate) toxicity tests to evaluate the suitability of dredged material for ocean disposal by assessing the sensitivity of indicator organisms to eluted contaminants. These elutriate tests determine the dilution required of sediment samples to reach elutriate levels fatal to 50% of the indicator organisms (*i.e.*, LC50). The "Green Book" – *Evaluation of Dredged Material Proposed for Ocean Disposal: Testing Manual* (USEPA and USACE, 1991) – sets a limiting permissible concentration (LPC) of 1/100th of the elutriate LC50 concentration. This LPC may not be exceeded after the period of initial mixing (4 hours after disposal) anywhere within the designated disposal site or at any time outside the disposal site.

An appropriately conservative LC50 value to use for evaluating the three alternative sites was determined as the mean of the lowest 10% (most toxic) LC50 concentrations from recent available elutriate tests from potentially contributing dredging project in eastern Long Island Sound. This approach is similar to that used in the 2004 CLIS/WLIS EIS (USEPA and USACE, 2004a). The LC50 concentration determined in this manner was 25%: 1/100 of this LC50 concentration provides a conservative LPC of 0.25%. This 0.25% relative concentration level is shown on subsequent plots for reference purposes and it is used in the discussion of the STFATE results. Note that this threshold is representative of the LPC only for a scow elutriate that has a concentration of 25% of the LC50 level.

2.4 STFATE Simulation Results

2.4.1 Site 1 - Cornfield Shoals

The distribution of the sediment that is predicted to accumulate on the seafloor at the Cornfield Shoals site when the current is at the mean magnitude ($\overline{U}$=1.9 ft/s) is shown in Figure 3 (mean current); the sediment distribution when the current is at the mean daily maximum ($\overline{U}_{max}$= 3.2 ft/s) is shown in Figure 4 (high current). In both cases, the model results demonstrate that the material on the seafloor is contained within the alternative site and the mound is elongated along the axis of the current. At mean current conditions (Figure 3), the maximum mound height after disposal by a 3,000 cubic yard (cy) scow is 0.149 ft. At high current conditions (Figure 4), the maximum mound height is 0.135 ft.

The STFATE predictions for the amount of material reaching the seafloor are provided in Table 4. Rows I and II in Column A list the volume of (a) sand, (b) silt, (c) clay and (d) clumps that reach the seafloor at Site 1 during the STFATE simulation time of two hours. The volume remaining in the water column is provided in Column B and the fraction of the material reaching the mound on the seafloor is in Column C. Rows I ($\overline{U}_{max}$) and II ($\overline{U}$) show that at both the high and mean currents, 100% of the sand in the scow reaches the mound. Columns C of Table 4b and Table 4d shows that almost all (95% and 97%, respectively) of the silt and all (100%) of clumps reach the seafloor as well. However, the majority of the clay (*i.e.*, the clay fraction that is not part of clumps) is predicted to remain in the water column. Table 4c shows that at the high current magnitude (row I) all the clay remains in suspension and at the mean current magnitude (row II) 78% remains in suspension.

Dissolved tracer dilution was also assessed by the STFATE model. The predicted three-dimensional concentrations were computed and saved at 5 depths every 5 minutes. Figures 5 and 6 show time-series of the maxima of the relative concentration (the ratio of the predicted concentration to that specified in the source) for the simulations with the velocity set to $\overline{U}$=1.9 ft/s and $\overline{U}_{max}$= 3.2 ft/s. Note that the inverse of the relative concentration is the effective dilution of the tracer. The red lines show the evolution of the maximum concentrations that occurs within the entire model domain (the alternative site and the surrounding area). The blue lines represent the maximum concentration on the grid outside of the alternative site.

In both simulations, there is a rapid decrease in the maximum concentration as the plume spreads horizontally across the alternative site (red lines). Figure 5 shows that after 40 minutes the maximum relative concentration drops to approximately 0.1%. At that time, the concentration in the area outside the disposal area (blue line) rises to equal the maximum in the domain. The pattern is identical in Figure 6 though the high current in this simulation causes more rapid initial dilution and an earlier increase (after approximately 25 minutes) in the concentrations outside of the disposal area.

Note that both simulations reveal that the maximum relative concentration in the alternative site falls below 1% of the scow elutriate concentration within 5 minutes of release and then falls to 0.2% by 50 minutes in the mean current simulation ($\overline{U}$=1.9 ft/s). In the high current simulation ($\overline{U}_{max}$= 3.2 ft/s), the concentration falls below 0.2% within 20 minutes. In both simulations the maximum concentration that leaves the alternative site is approximately 0.2% of the barge concentration. After 60 to 120 minutes the maximum concentration diminishes further to 0.1% in both simulations.

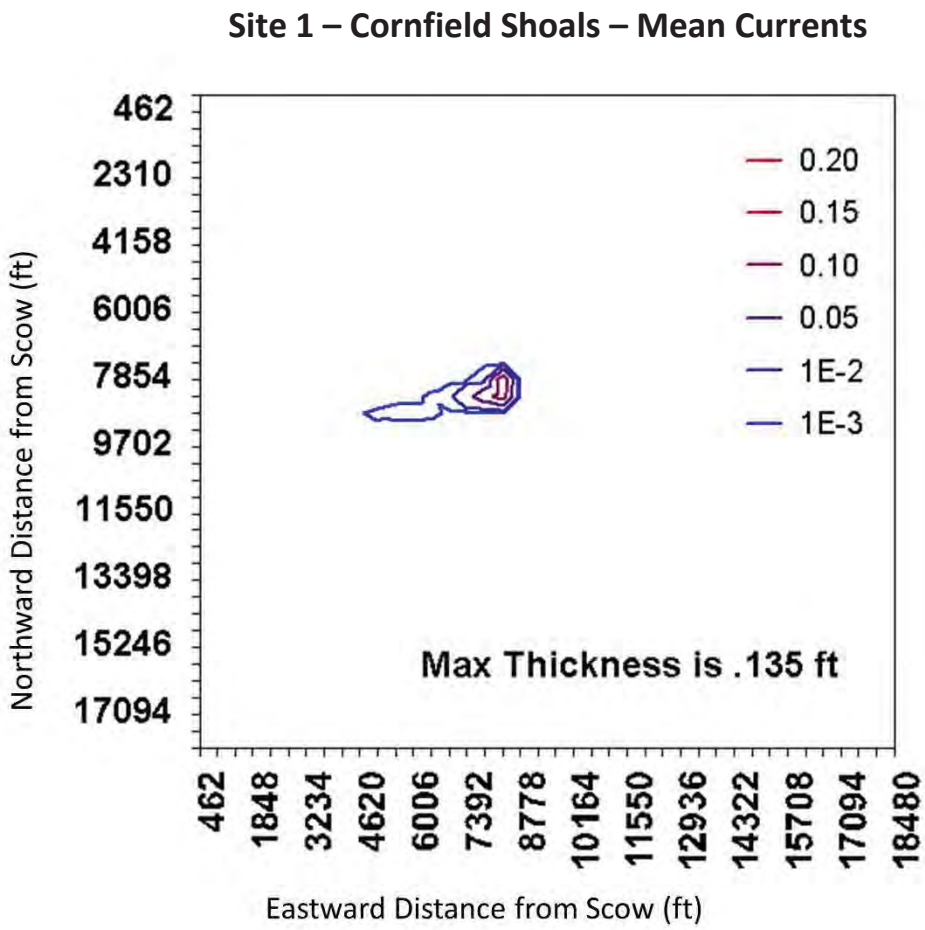

Figure 3. Deposition thickness (ft) for a single scow release operation conducted at Site 1 (Cornfield Shoals) using the parameters shown in Tables 2 and 3, and the mean magnitude of the depth-averaged current (mean current) as determined from the FVCOM predictions.

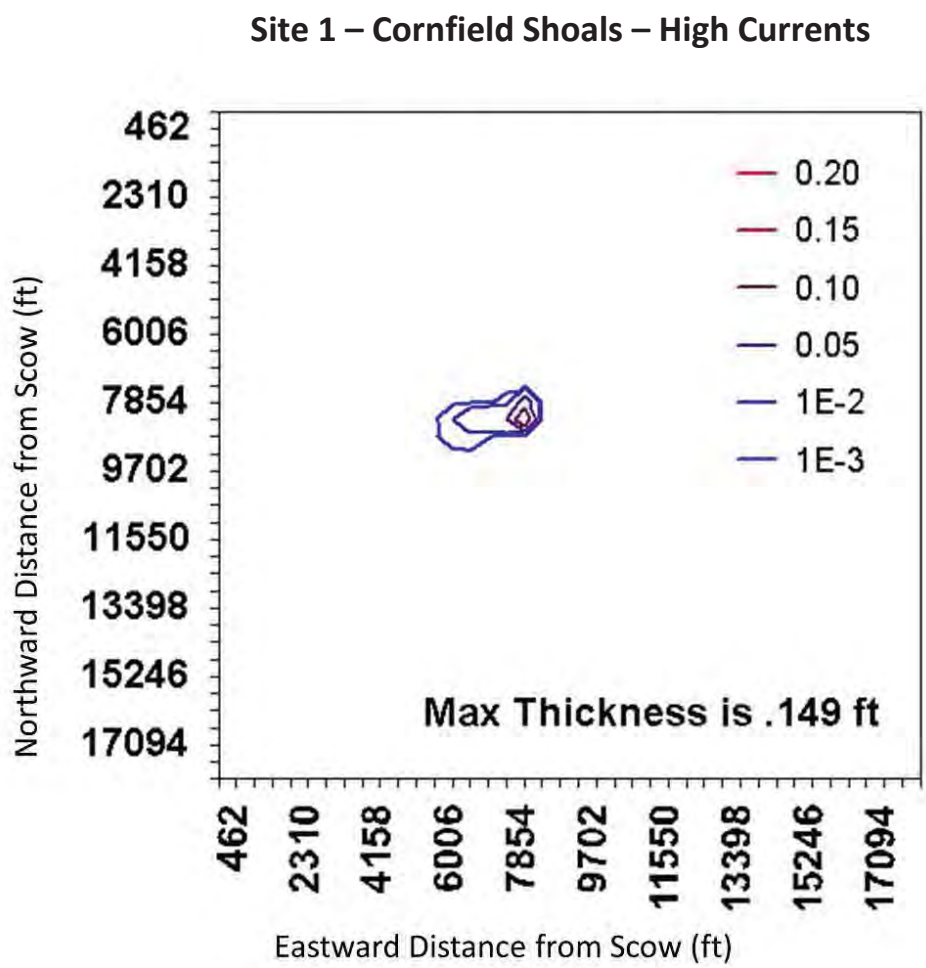

Figure 4. Deposition thickness (ft) for a single scow release operation conducted at Site 1 (Cornfield Shoals) using the parameters shown in Tables 2 and 3, and the mean daily maximum magnitude depth-averaged current (high current) as determined from the FVCOM predictions.

Table 4. Dredged Material Characteristics

(a-d): Sediment component volumes in the disposal mound (column A) and remaining suspended material (column B) at Site 1 (Cornfield Shoals [CS]), Site 5 Niantic Bay [NB]), and Site 6 (New London [NL]) at the end of the STFATE simulation period (2 hours for CS; 3 hours for NL and NB). Column C shows the fraction of the total volume reaching the seafloor. Volumes pertain to the disposal from a 3,000-cy scow, after removing pore water (70.6% of the dredged material composition). The remaining volume for the dewatered dredged material is 882 cy.
(e): Material property parameters used for the simulations. In panel e, "Striped during descent", refers to whether the material transitions to act as a negatively buoyant fluid plume or remains a free-falling mass.

		(a) Volume of sand (cy)			**(b) Volume of silt** (cy)		
		A: settled	**B: suspended**	**C: % on seafloor**	**A: settled**	**B: suspended**	**C: % on seafloor**
Site 1 (CS)	I: $\overline{U}_{\max}$	48.9	0.0	100%	354.7	17.3	95%
	II: $\overline{U}$	48.9	0.0	100%	361.2	10.8	97%
Site 5 (NB)	III: $\overline{U}_{\max}$	48.9	0.0	100%	366.7	5.3	99%
	IV: $\overline{U}$	48.9	0.0	100%	369.0	3.0	99%
Site 6 (NL)	V: $\overline{U}_{\max}$	48.9	0.0	100%	369.3	2.7	99%
	VI: $\overline{U}$	48.9	0.0	100%	371.4	0.6	100%

		(c) Volume of clay (cy)			**(d) Volume clumps** (cy)		
		A: settled	**B: suspended**	**C: % on seafloor**	**A: settled**	**B: suspended**	**C: % on seafloor**
Site 1 (CS)	I: $\overline{U}_{\max}$	0.0	68.7	0%	391.8	0.0	100%
	II: $\overline{U}$	53.7	15.0	78%	391.8	0.0	100%
Site 5 (NB)	III: $\overline{U}_{\max}$	0.0	68.7	0%	391.8	0.0	100%
	IV: $\overline{U}$	61.1	7.6	89%	391.8	0.0	100%
Site 6 (NL)	V: $\overline{U}_{\max}$	56.9	11.8	83%	391.8	0.0	100%
	VI: $\overline{U}$	66.3	2.4	96%	391.8	0.0	100%

				(e) Material Properties		
Material	**Specific Gravity** (g/cm3)	**Volume Fraction**	**Void Ratio**	**Critical Shear Stress** (lb/ft^3)	**Cohesive**	**Striped during descent?**
Sand	2.700	0.016	0.600	0.025	N	Y
Silt	2.650	0.124	4.500	0.009	N	Y
Clay	2.650	0.023	7.500	0.004	N	Y
Clumps	1.600	0.131	0.400	99.00	N	N

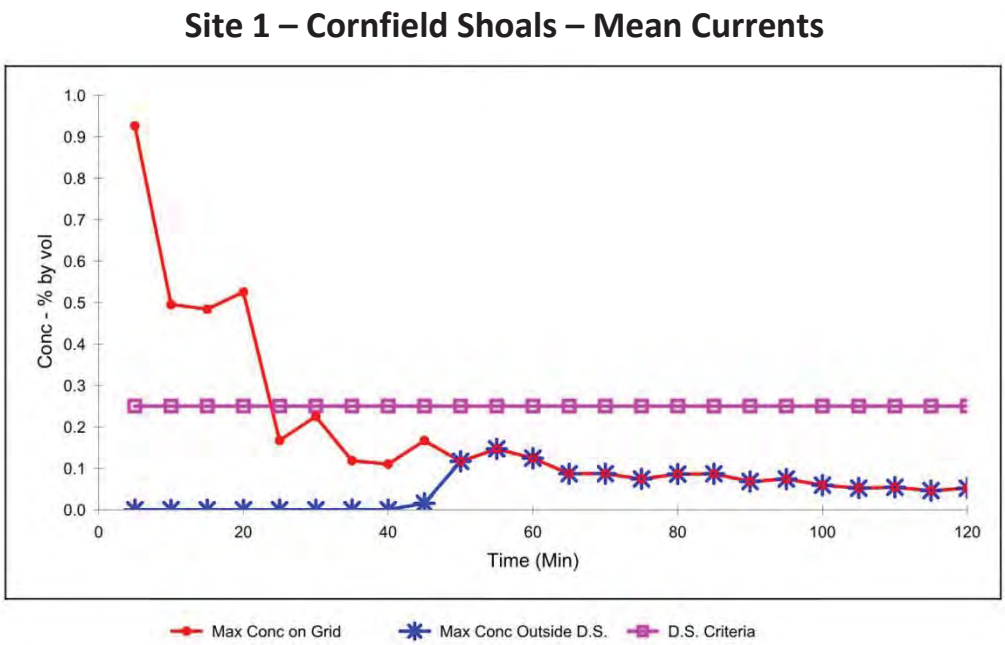

Figure 5. Maximum relative concentration at Site 1 (Cornfield Shoals) within the STFATE domain grid (red) and outside the alternative disposal site (D.S.) (blue) using the mean magnitude of the depth-averaged current as determined from the FVCOM predictions. The 0.25% dilution LPC level (D.S. Criteria) is shown in magenta for reference.

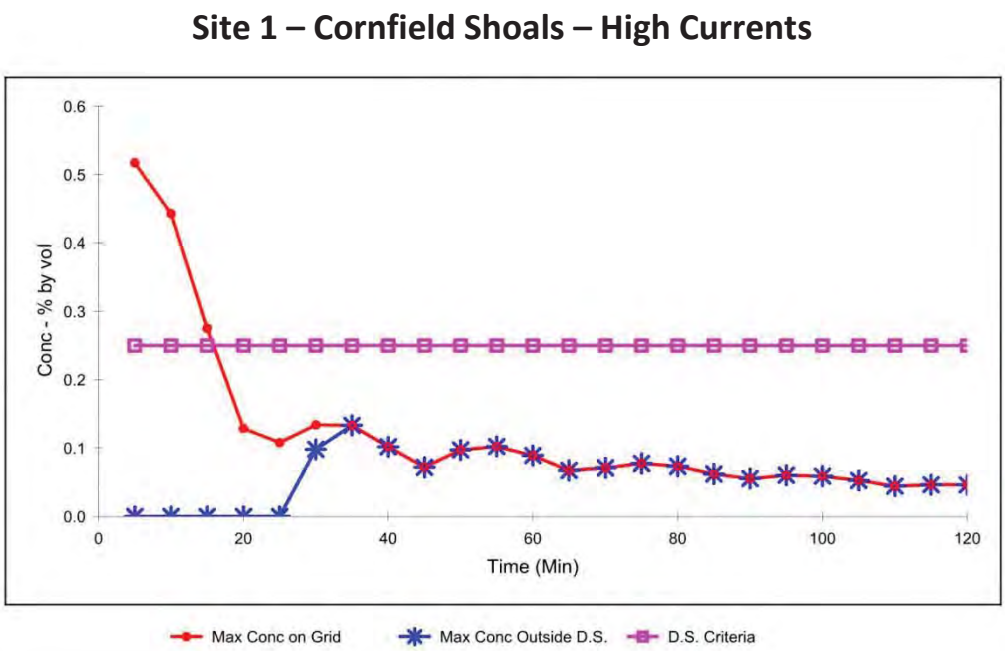

Figure 6. Maximum relative concentration at Site 1 (Cornfield Shoals) within the STFATE domain grid (red) and outside the alternative disposal site (D.S.) (blue) using the mean daily maximum magnitude of the depth-averaged current as determined from the FVCOM predictions. The 0.25% dilution LPC level (D.S. Criteria) is shown in magenta for reference.

2.4.2 Site 5 - Niantic Bay

The distribution of the sediment that is predicted to accumulate on the seafloor at the Niantic Bay site when the current is at the mean magnitude ($\overline{U}$=1.5 ft/s) is shown in Figure 7 (mean current); the distribution when the current is at the mean daily maximum ($\overline{U}_{max}$= 2.6 ft/s) is shown in Figure 8 (high current). Both graphs demonstrate that the material on the seafloor is contained within the alternative site and the mound is elongated along the axis of the current. At mean current conditions the maximum mound height is 0.106 ft. At high current conditions the maximum height is 0.088 ft.

The STFATE predictions for the amount of material reaching the seafloor at Site 5 are provided in Table 4a-d. Rows III and IV for Column A list the volume of (a) sand, (b) silt, (c) clay, and (d) clumps that reach the seafloor for Site 5 during the STFATE simulation time of three hours. The volume remaining in the water column is provided in Column B and the fraction of the material reaching the mound on the seafloor is in Column C. Row III ($\overline{U}_{max}$) and IV ($\overline{U}$) show that at both the high and mean currents, 100% of the sand in the scow reaches the mound. Column C of Table 4b and Table 4d shows that almost all (99%) of the silt reaches the seafloor, as well as all (100%) of clumps. However, Rows III and IV of Table 4c shows that all of the clay is predicted to remain in the water column during operations at high current conditions; at mean current conditions, 89% of the clay reaches the seafloor.

Figures 9 through 14 show time-series of the maxima of the relative concentrations for the simulations with the velocity set to $\overline{U}$=1.5 ft/s and $\overline{U}_{max}$= 2.6 ft/s for three site dimension options. The red lines show the evolution of the maximum concentrations that occur within the whole model domain (including the alternative site). The blue lines show the maximum concentration on the grid outside of the alternative site. The 0.25% level is shown in magenta for reference.

In all simulations there is an increase in the maximum concentrations as the plume spreads horizontally across the alternative site (red lines). The maximum relative concentration in the water column falls below 0.25% within 80 minutes of release of the dredged material. After 4 hours, the maximum concentrations are below 0.07% for both mean current and maximum daily current conditions. The maximum concentrations outside the site depend on which site dimension option is used. For the smallest site dimension option (1 x 1 nmi), simulated concentrations outside the site exceed the 0.25% LPC after 55 minutes under high current conditions (Figure 14). Concentrations outside the site do not exceed the 0.25% LPC under either high or mean current conditions for the two larger site dimension options (Figures 9 to 12).

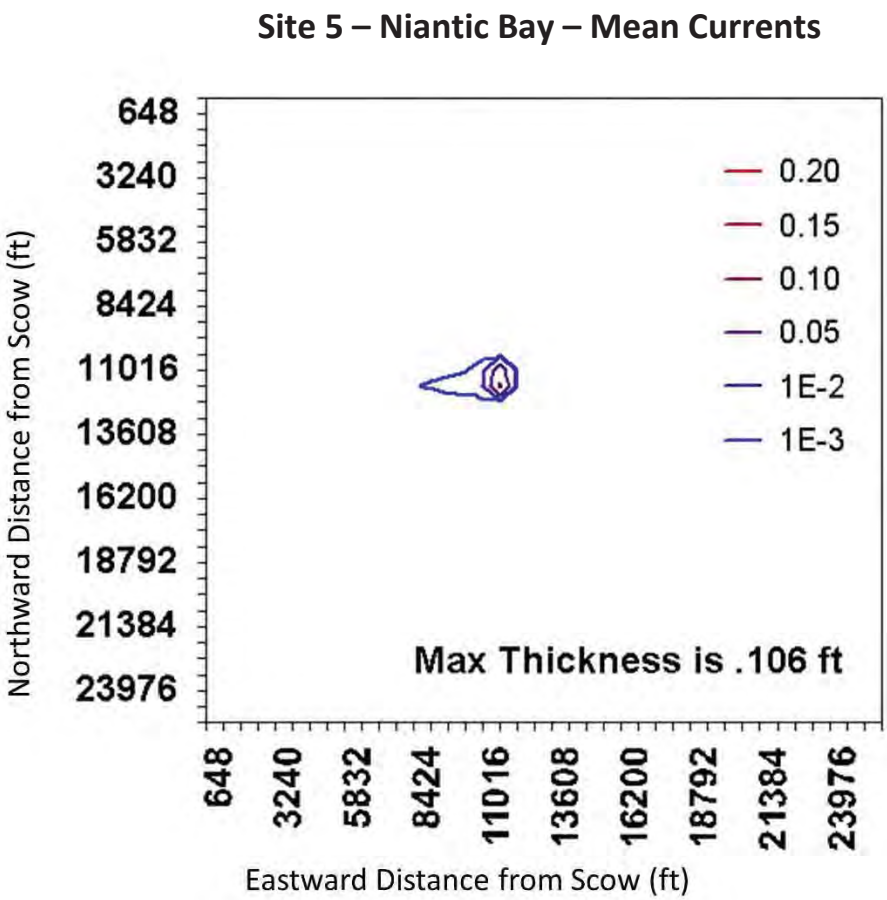

Figure 7. Deposition thickness (ft) for a single scow release conducted at Site 5 (Niantic Bay) using the parameters shown in Tables 2 and 3, and the mean magnitude of the vertically average current (mean current) as determined from the FVCOM predictions.

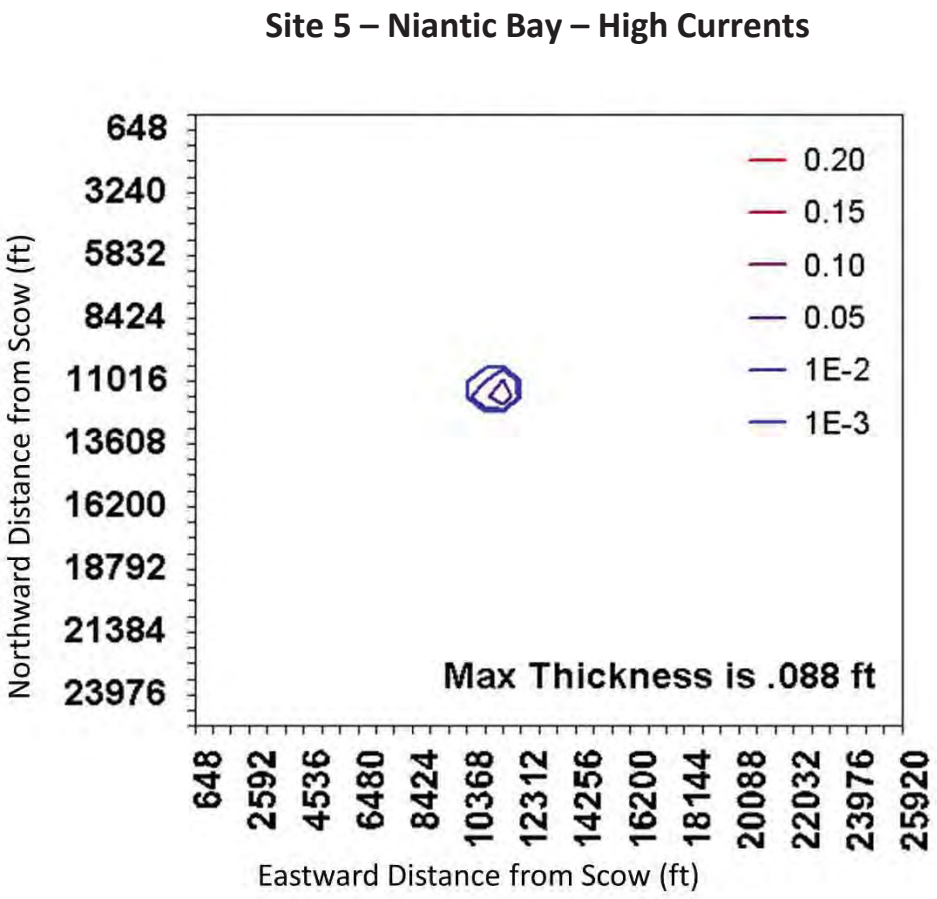

Figure 8. Deposition thickness (ft) for a single scow release operation conducted at Site 5 (Niantic Bay) using the parameters shown in Tables 2 and 3, and the mean daily maximum magnitude depth-averaged current (high current) as determined from the FVCOM predictions.

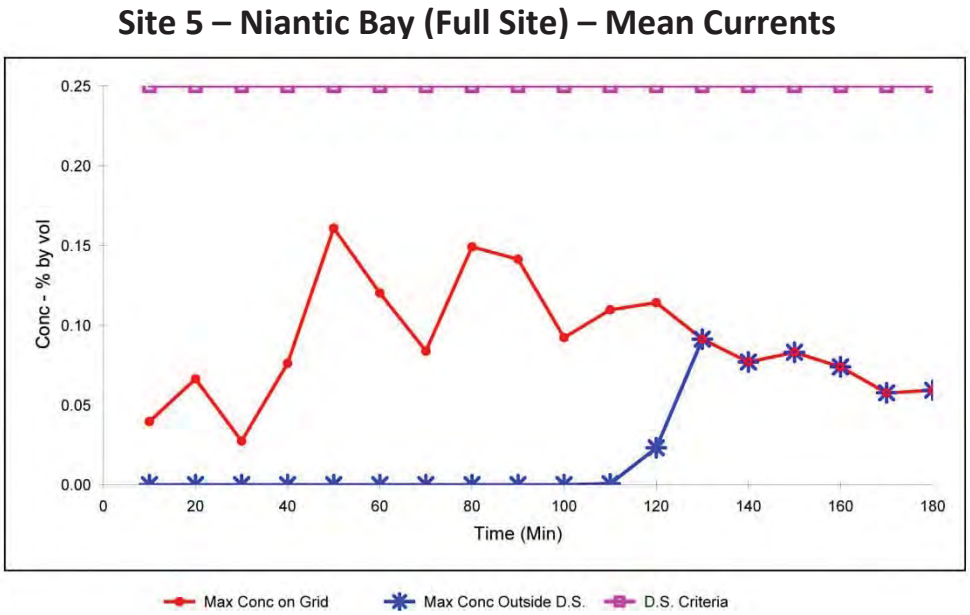

Figure 9. Maximum relative concentration at Site 5 (Niantic Bay) for the full site (NBDS + NB-E) within the STFATE domain grid (red) and outside the alternative disposal site (D.S.) (blue) using the mean magnitude of the depth-averaged current as determined from the FVCOM predictions. The 0.25% dilution LPC level (D.S. Criteria) is shown in magenta for reference.

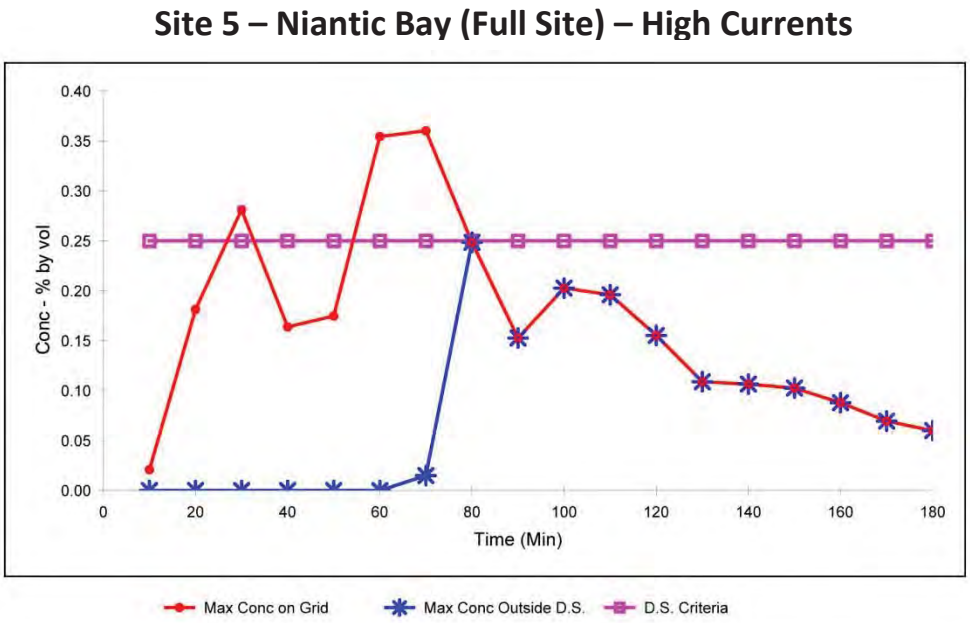

Figure 10. Maximum relative concentration at Site 5 (Niantic Bay) for the full site (NBDS + NB-E) within the STFATE domain grid (red) and outside the alternative disposal site (D.S.) (blue) using the mean daily maximum magnitude of the depth-averaged current as determined from the FVCOM predictions. The 0.25% dilution LPC level (D.S. Criteria) is shown in magenta for reference.

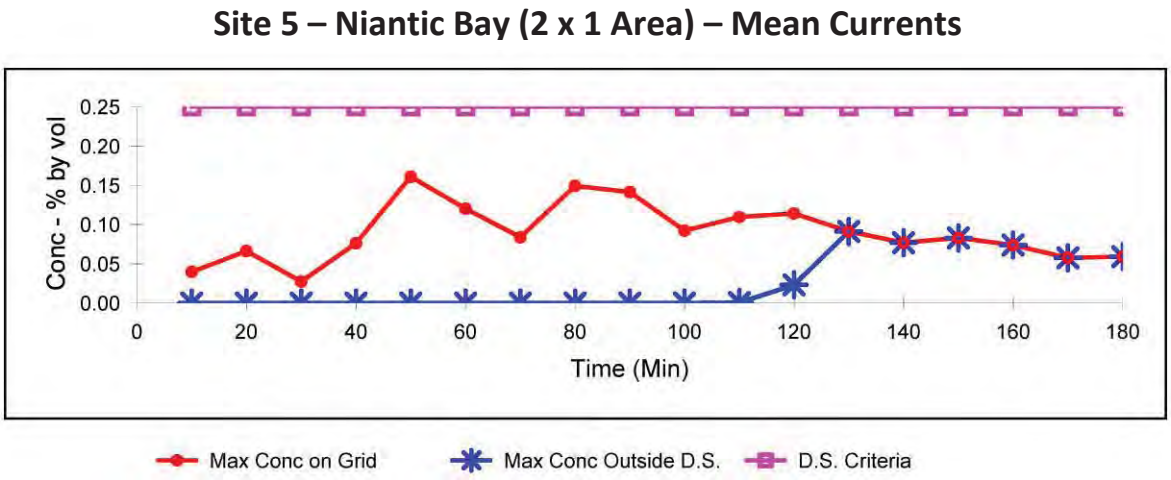

Figure 11. Maximum relative concentration at Site 5 (Niantic Bay) for the 2 x 1 nmi site dimension option within the STFATE domain grid (red) and outside the alternative disposal site (D.S.) (blue) using the mean magnitude of the depth-averaged current as determined from the FVCOM predictions. The 0.25% dilution LPC level (D.S. Criteria) is shown in magenta for reference.

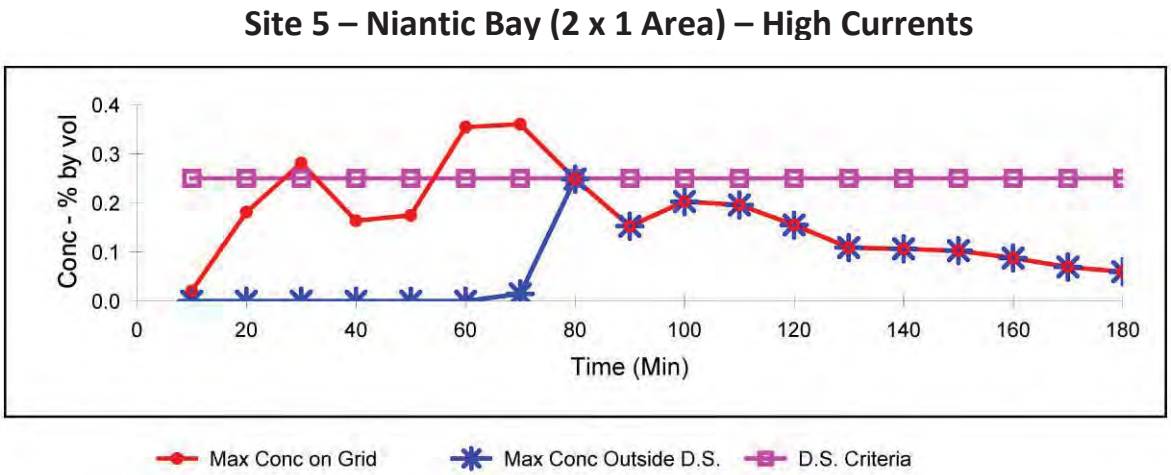

Figure 12. Maximum relative concentration at Site 5 (Niantic Bay) for the 2 x 1 nmi site dimension option within the STFATE domain grid (red) and outside the alternative disposal site (D.S.) (blue) using the mean daily maximum magnitude of the depth-averaged current as determined from the FVCOM predictions. The 0.25% dilution LPC level (D.S. Criteria) is shown in magenta for reference.

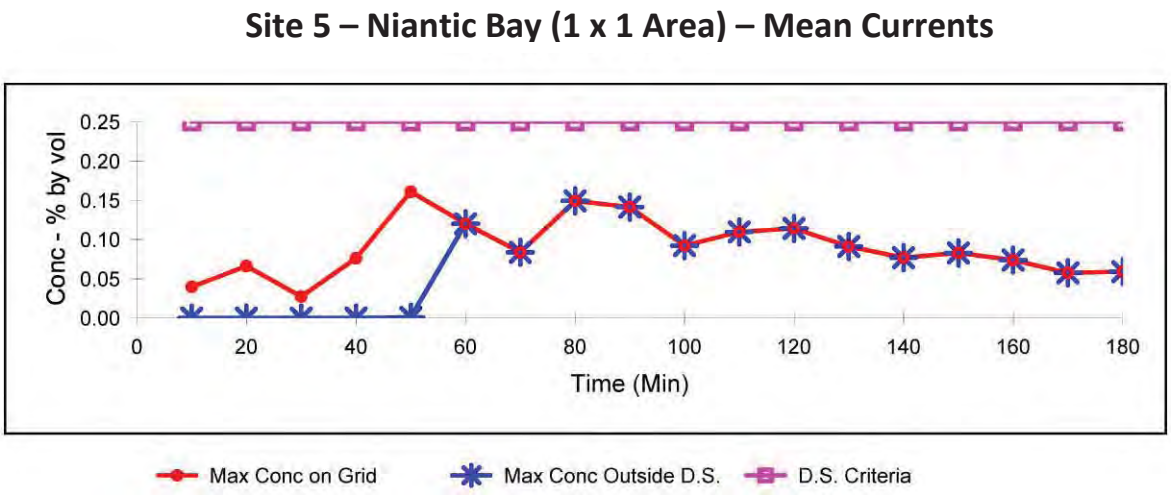

Figure 13. Maximum relative concentration at Site 5 (Niantic Bay) for the smallest (1 x 1 nmi) site dimension option within the STFATE domain grid (red) and outside the alternative disposal site (D.S.) (blue) using the mean magnitude of the depth-averaged current as determined from the FVCOM predictions. The 0.25% dilution LPC level (D.S. Criteria) is shown in magenta for reference.

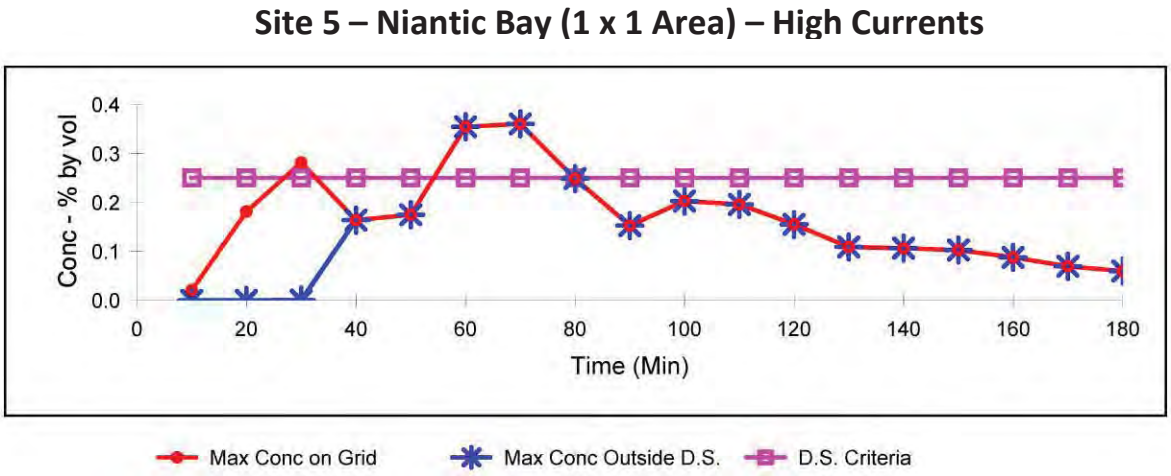

Figure 14. Maximum relative concentration at Site 5 (Niantic Bay) for the smallest (1 x 1 nmi) site dimension option within the STFATE domain grid (red) and outside the alternative disposal site (D.S.) (blue) using the mean daily maximum magnitude of the depth-averaged current as determined from the FVCOM predictions. The 0.25% dilution LPC level (D.S. Criteria) is shown in magenta for reference.

2.4.3 Site 6 - New London

The distribution of the sediment that is predicted to accumulate on the seafloor at the New London site when the current is at the mean magnitude ($\overline{U}$=1.0 ft/s) is shown in Figure 15 (mean current); the distribution when it is at the mean daily maximum ($\overline{U}_{max}$= 2.0 ft/s) is shown in Figure 16 (high current). At both current conditions, the material on the seafloor is contained within the alternative site and the mound is elongated along the axis of the current. At mean current conditions, the maximum mound height is 0.214 ft. At high current conditions the maximum height is 0.180 ft.

Table 4a-d shows the STFATE predictions for the amount of material reaching the seafloor at Site 6. Rows III and IV list the volume of (a) sand, (b) silt, (c) clay and (d) clumps that reach the seafloor in Column A during the STFATE simulation time of three hours. The volume remaining the water column is provided in Column B and the fraction of the material reaching the mound on the seafloor is in Column C. Rows V ($\overline{U}_{max}$) and VI ($\overline{U}$) show that at both the high and mean currents, 99-100% of the sand, silt, and clumps in the scow reaches the mound. At site 6, most of the clay also reaches the seafloor. Rows V and VI of Table 4c shows that 83% of the clay is predicted to reach the seafloor during operations at high current conditions, and that 96% of it reaches the seafloor at mean current conditions.

Figures 17 through 22 show time-series of the maxima of the relative concentration for the simulations with the velocity set to $\overline{U}$=1.0 ft/s and $\overline{U}_{max}$= 2.0 ft/s. The red lines show the evolution of the maximum concentration levels that occur within the whole model domain (including the alternative site). The blue lines show the maximum concentration on the grid outside of the alternative site.

The simulations show that the maximum relative concentration in the water column within the New London alternative site falls below 0.25% LPC within 120 minutes of release of dredged material from the scow. After 4 hours, the simulated maximum concentrations are below 0.08% for both mean and high current conditions. The maximum concentrations outside the site depend on which site dimension option is used. For the smallest site dimension option (NL-Wa/b), concentrations outside the site would slightly exceed the 0.25% LPC after 80 minutes under high current conditions (Figure 22). Simulated concentrations outside the site do not exceed the LPC under either high or mean current conditions for the two larger site boundary configurations (Figures 17 to 20).

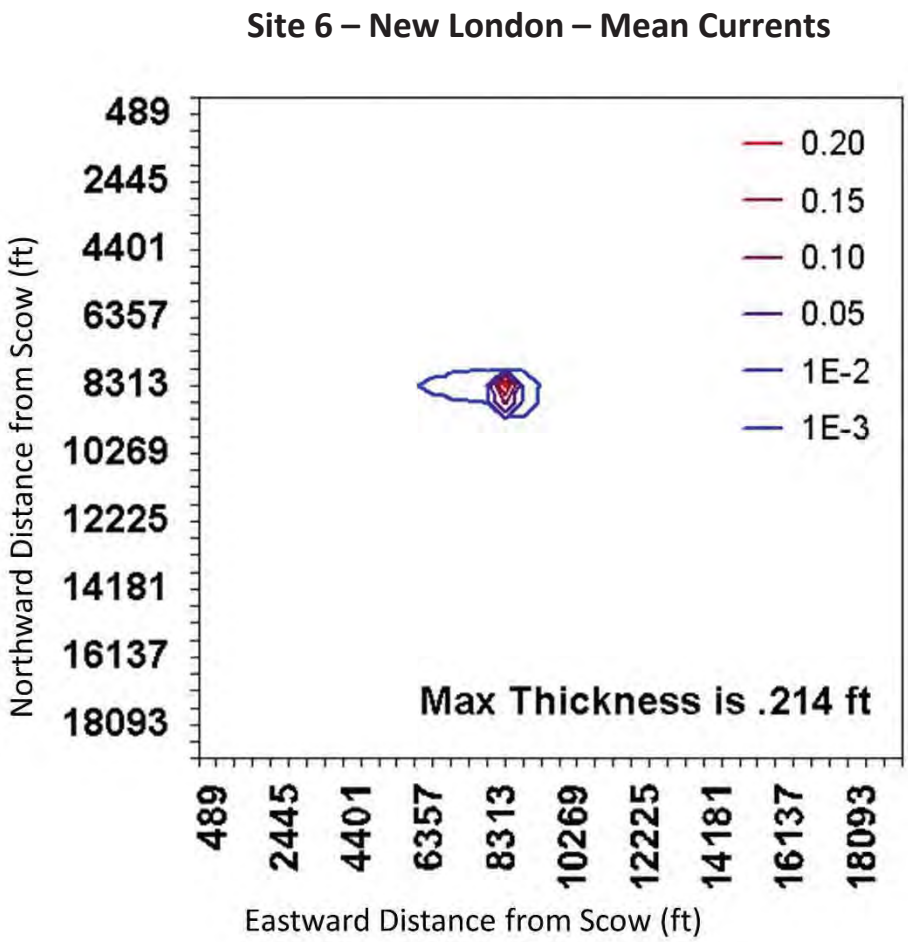

Figure 15. Deposition thickness (ft) for a single scow release operation conducted at Site 6 (New London) using the parameters shown in Tables 2 and 3, and the mean depth-averaged current (mean current) as determined from the FVCOM predictions.

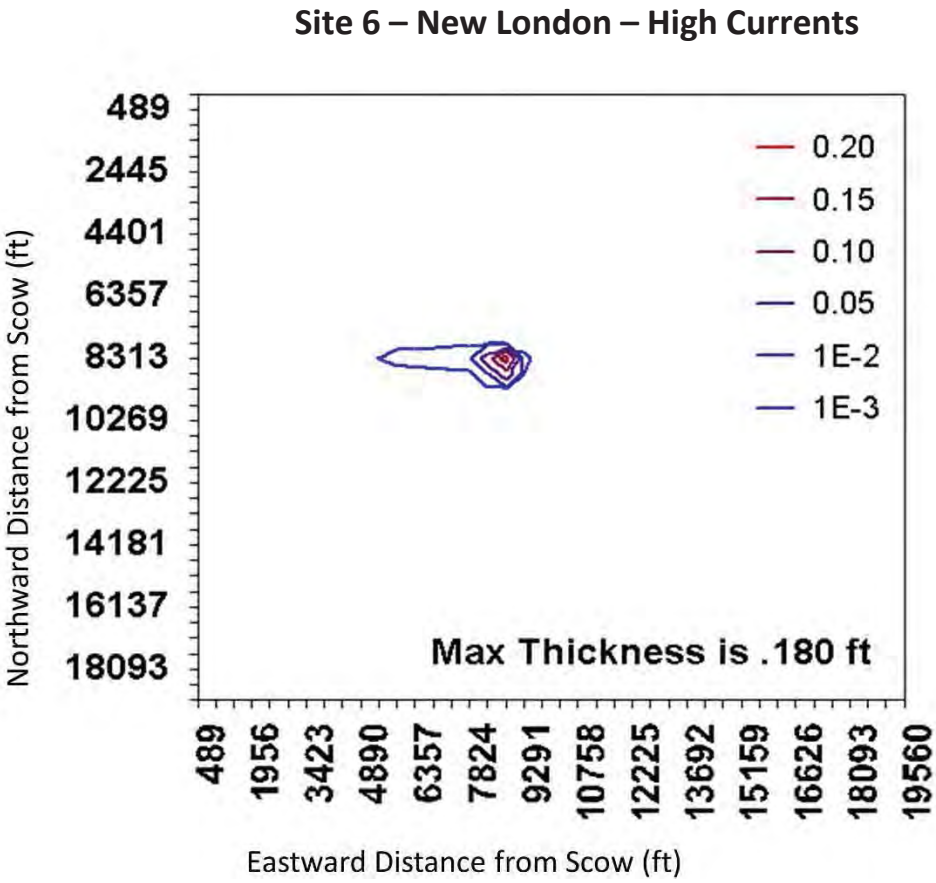

Figure 16. Deposition thickness (ft) for a single scow release operation conducted at Site 6 (New London) using the parameters shown in Tables 2 and 3, and the mean daily maximum depth-averaged current (high current) as determined from the FVCOM predictions.

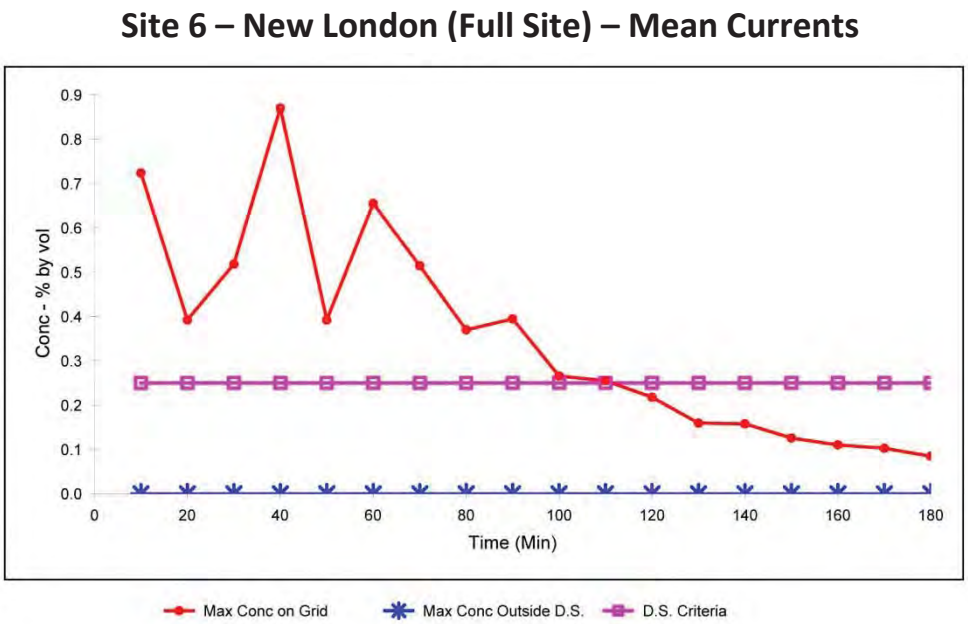

Figure 17. Maximum relative concentration at Site 6 (New London) for the full site (NLDS + NL-Wa/b) within the STFATE domain grid (red) and outside the alternative disposal site (D.S.) (blue) using the mean magnitude of the depth-averaged current as determined from the FVCOM predictions. The 0.25% dilution LPC level (D.S. Criteria) is shown in magenta for reference.

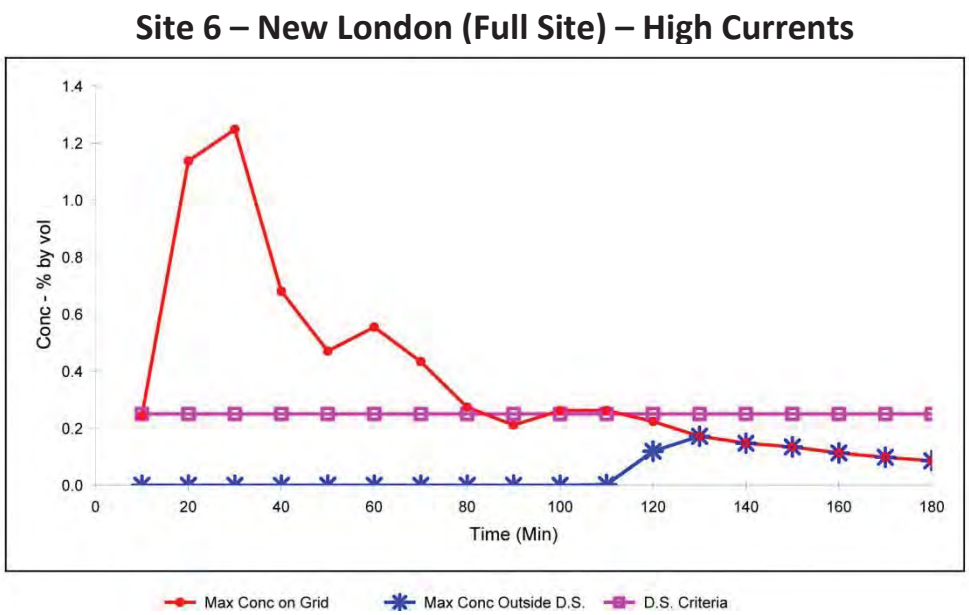

Figure 18. Maximum relative concentration at Site 6 (New London) for the full site (NLDS + NL-Wa/b) within the STFATE domain grid (red) and outside the alternative disposal site (D.S.) (blue) using the mean daily maximum magnitude of the depth-averaged current as determined from the FVCOM predictions. The 0.25% dilution LPC level (D.S. Criteria) is shown in magenta for reference.

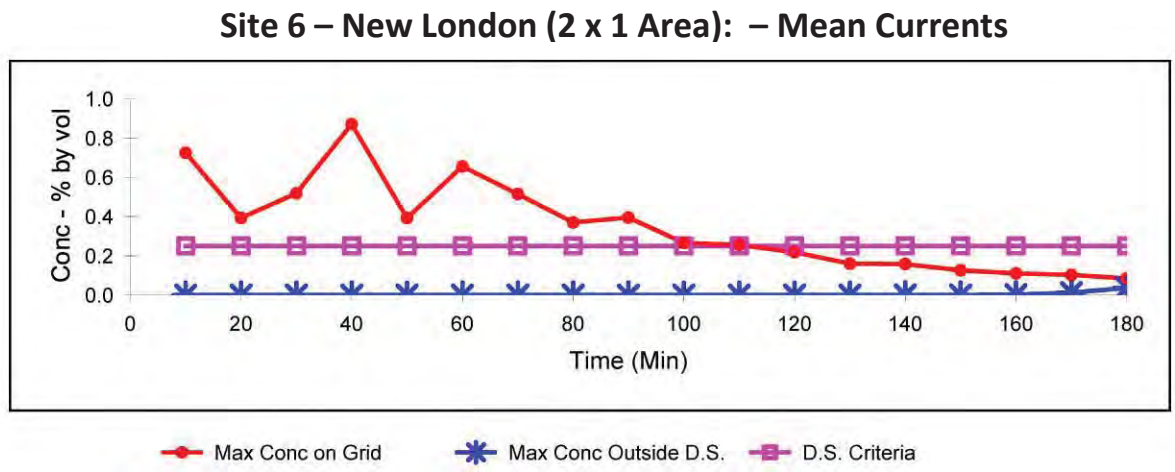

Figure 19. Maximum relative concentration at Site 6 (New London) for the 2 x 1 nmi site dimension option (NLDS [50%] + NL-Wa/b) within the STFATE domain grid (red) and outside the alternative disposal site (D.S.) (blue) using the mean magnitude of the depth-averaged current as determined from the FVCOM predictions. The 0.25% dilution LPC level (D.S. Criteria) is shown in magenta for reference.

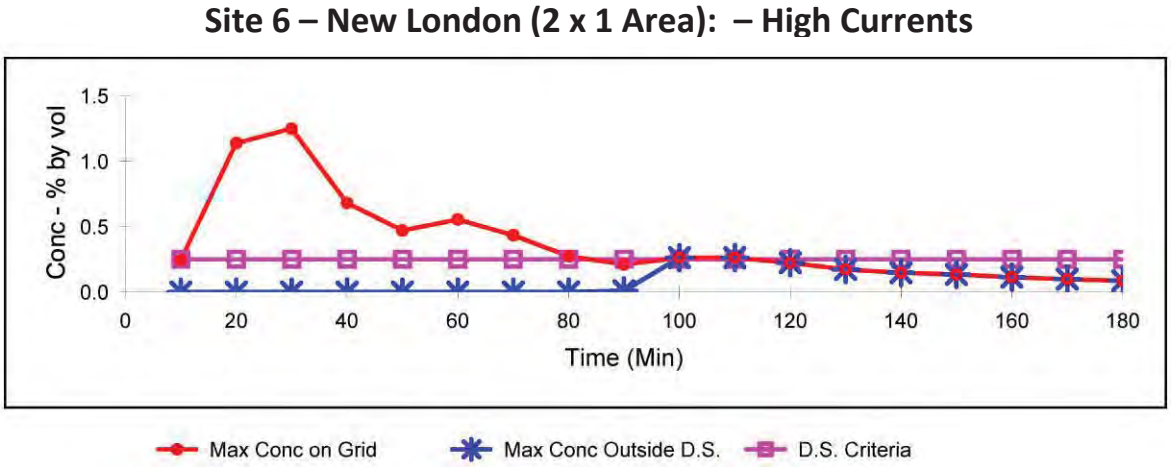

Figure 20. Maximum relative concentration at Site 6 (New London) for the 2 x 1 nmi site dimension option (NLDS [50%] + NL-Wa/b) within the STFATE domain grid (red) and outside the alternative disposal site (D.S.) (blue) using the mean daily maximum magnitude of the depth-averaged current as determined from the FVCOM predictions. The 0.25% dilution LPC level (D.S. Criteria) is shown in magenta for reference.

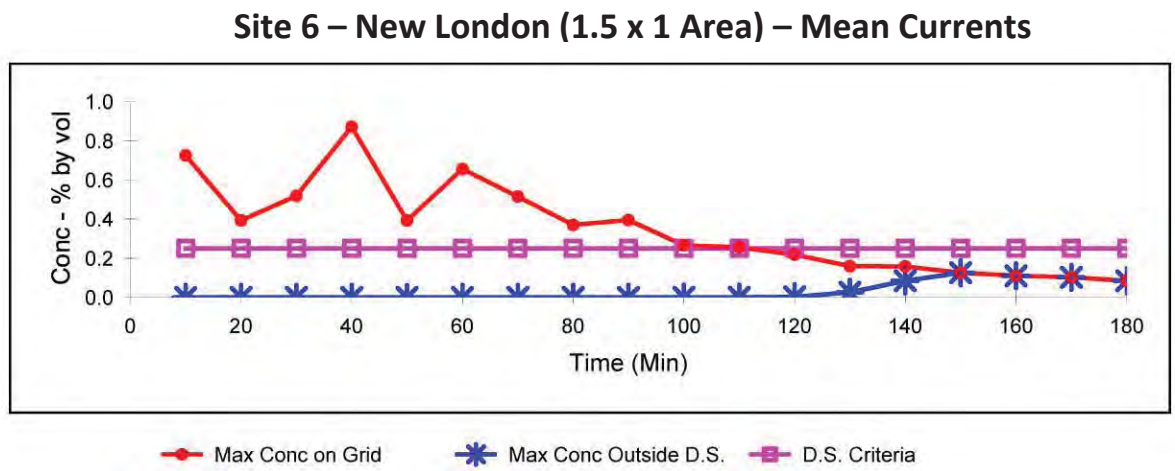

Figure 21. Maximum relative concentration at Site 6 (New London) for the smallest site dimension option (NL-Wa/b) within the STFATE domain grid (red) and outside the alternative disposal site (D.S.) (blue) using the mean magnitude of the depth-averaged current as determined from the FVCOM predictions. The 0.25% dilution LPC level (D.S. Criteria) is shown in magenta for reference.

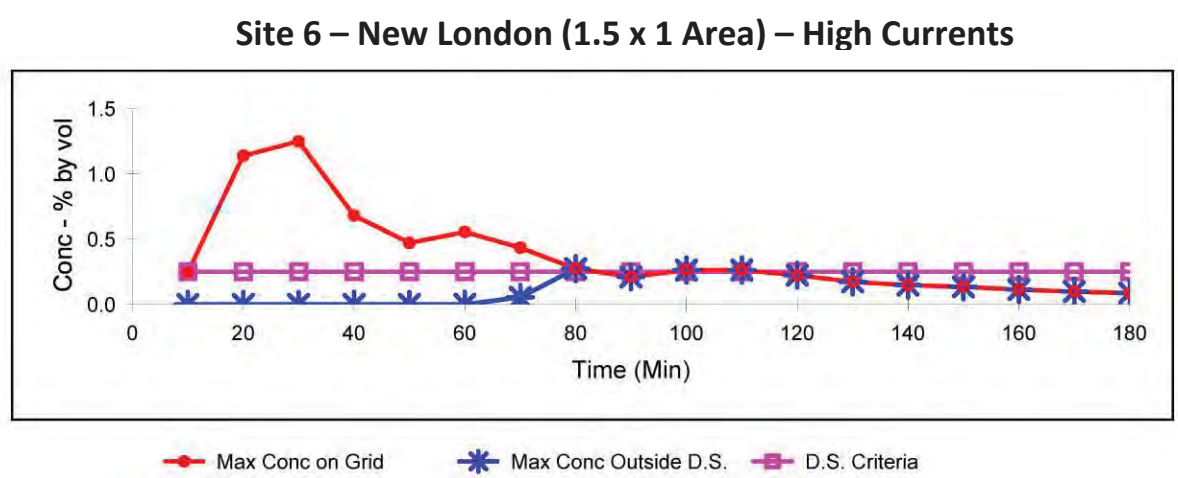

Figure 22. Maximum relative concentration at Site 6 (New London) for the smallest site dimension option (NL-Wa/b) within the STFATE domain grid (red) and outside the alternative disposal site (D.S.) (blue) using the mean daily maximum magnitude of the depth-averaged current as determined from the FVCOM predictions. The 0.25% dilution LPC level (D.S. Criteria) is shown in magenta for reference.

2.5 STFATE Summary

Simulations using STFATE of the spatial extent of the dredged sediment deposited at three alternative sites (1-Cornfield Shoals, 5-Niantic Bay, and 6-New London) from a scow characteristic of those used in previous disposal operations in the region have been conducted. The magnitudes of the ambient water column currents at each site were obtained from a calibrated circulation model and the results analyzed to estimate a typical high current magnitude $\overline{U}_{max}$ (the mean of the maximum depth-averaged current magnitude that occurs in each day of a 500-day simulation), and a more typical current that should be expected, $\overline{U}$ (the mean of the depth-averaged current magnitude). The results of these simulations demonstrate that the mound of dredged material on the seafloor would be located within the alternative site.

STFATE was further used to simulate the distribution and evolution of the concentration of dissolved materials in the water column as a consequence of dredged material disposal at the three alternative sites using both $\overline{U}_{max}$ and $\overline{U}$ to characterize the ambient current velocity. STFATE was also used to simulate the dilution of dredged material elutriate in the water column as a consequence of the sediment disposal at the three alternative sites under both mean current and high current conditions. These simulations showed that the relative concentrations would decrease to below the 0.25% LPC value well within four hours both inside and outside, of the three alternative sites for a 3,000-cy scow release of dredged material. Note that this is an effective dilution of the elutriate by at least a factor of 400. If the smallest site dimension options are considered for the Niantic Bay and New London alternative sites (1 x 1 nmi, and 1.5 x 1 nmi, respectively), the LPC would be exceeded outside the site during high flow conditions. During mean current conditions, none of the various site dimension options considered would exceed the LPC outside the site.

3. Long-term Dilution and Transport - FVCOM Simulations

The STFATE simulations quantitatively described the dilution of elutriate released from a scow within a few hours of the disposal operations. However, the longer-term transport (several hours after the release) and dilution of the material cannot be accurately predicted by STFATE because it does not include the spatial variations in the topography and current patterns that is well known to play an important role in shear dispersion. In this section we describe simulations that exploit the FVCOM hydrodynamic model to predict the dilution of dissolved and suspended material that is transported beyond the boundaries of the alternative sites. Since FVCOM can describe the transport in all of Long Island Sound, Block Island Sound, and the adjacent continental shelf, it complements the capacity of STFATE to describe the dilution occurring in the range of scales between the size of the scow and the size of the alternatives sites.

3.1 FVCOM Fundamentals

The Long Island Sound FVCOM model development and implementation are described in detail in O'Donnell et al. (2015). FVCOM is an unstructured grid, three-dimensional, hydrostatic, primitive equation model (Chen et al., 2007). The model domain extends from Long Island Sound out 100 km onto the continental shelf. The horizontal resolution of the 33,476 triangular grid cells ranges from several kilometers at the edge of the model domain to a few hundred meters along the coasts of Long Island Sound. The stretched-grid vertical coordinate has fourteen evenly spaced layers.

At the open boundaries, the model is forced with tidal elevations as well as slowly-varying (weather-band and seasonally varying) sea surface heights, temperatures and salinities from the Northeast Coastal Forecast System (NECOFS). The sea surface of the entire model domain is forced with spatially-uniform winds and net surface heat fluxes. Model runs for these experiments were initialized on October 15, 2012 using climatological estimates of temperature and salinity and then run for three months of simulation before the tracer simulations described subsequently began.

3.2 Tracer Simulation in FVCOM

FVCOM includes a module that allow the simulation of the evolution of a conservative tracer (a dissolved material that is unreactive), which we refer to as "dye", using the same velocity and turbulent mixing rates that are employed for the simulation of heat and salt but with zero normal flux conditions at the surface and bottom boundaries. Sources of the tracer are required and the initial concentration distribution is required as well.

In the simulations we conducted, model cells which contain the central point in the three alternative sites (Site 1-Cornfield Shoals, Site 5-Niantic Bay, and Site 6-New London) were identified. The initial tracer concentration chosen was then imposed at the three corner nodes of these model grid cells (Figure 23). The initial concentration was prescribed to be the concentration that would occur if the water contained in one scow of dredged material was mixed uniformly into the volume of the model cell. The water volume in a 3000-cy scow is estimated as (3000-cy scow volume) x (87% non-clump material) x (70% water) = 1830 cy = 1400 m^3 water volume. In the model, the

cells containing sites 1, 5, and 6 have water volumes of 1.06×10^8 m^3, 5.74×10^7 m^3 and 4.76×10^7 m^3, respectively. The initial tracer concentrations at the three sites are then 1.32×10^{-5}, 2.44×10^{-5}, and 2.94×10^{-5}, respectively. As in the analysis of the STFATE results, the relative concentration (the concentration at any time and location divided by the initial concentration at the source) can be computed and the inverse interpreted as the effective dilution. Though the concentration of each contaminant in the dredged material in a scow is different, the relative concentration distribution of any inert contaminant can be estimated from the model predicted relative concentration.

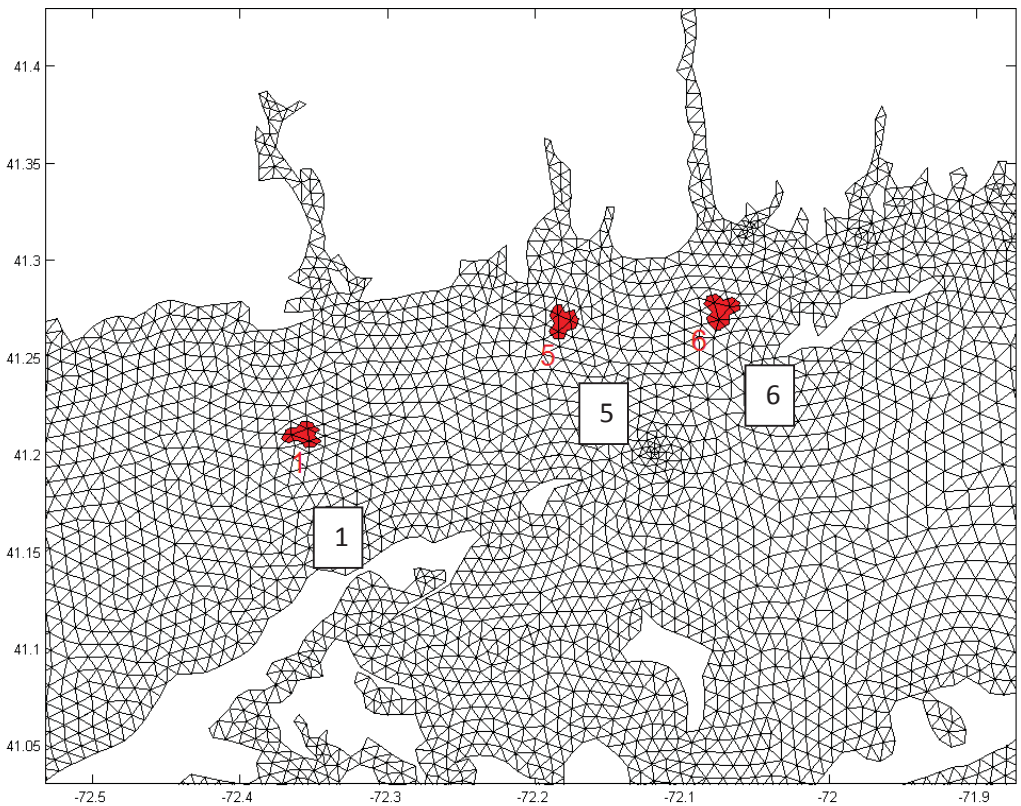

Figure 23. Map of the model grid in eastern Long Island Sound with the tracer release areas highlighted in red.

The trajectory of material released in Long Island Sound is sensitive to the phase of the tide at the time of release. To take this into account in the estimation of the fate of material released during the disposal of dredged materials, we performed four simulations for releases at each site: at low slack water, maximum flood, high slack water, and maximum ebb, on January 15, 2013, and then averaged the resulting concentration distributions. Since the range of concentrations is immense, a geometric mean was used to provide a typical concentration from the set of model outputs with releases at different tidal phases. The chosen date of January 15, 2013 is representative of winter conditions when dredging is permitted in the region and Figure 24 shows the sea level, eastward component of current and wind speed at Site 1 (Cornfield Shoals) for January 15-20, 2013. The times of instantaneous release of the tracer are indicated by the red circles.

Immediately following the tracer release, the tidal phase at release time influences the direction in which the tracer is advected. This is shown in Figure 25, which consists of maps of the predicted concentrations 8 hours after releases at different phases of the tide. In the first few hours after the release, average concentrations serve to show all the possible locations of the tracer, but over-represent the spatial area affected by any single tracer release.

As the tracer patch evolves, its size and position are determined by lateral transport, vertical mixing, and patterns of mean circulation so the initial position and instantaneous tidal phase are more important to the initial patch movement than to its long-term fate. By 48 hours after the release (Figure 26), the size and position of the patches is similar for all release times.

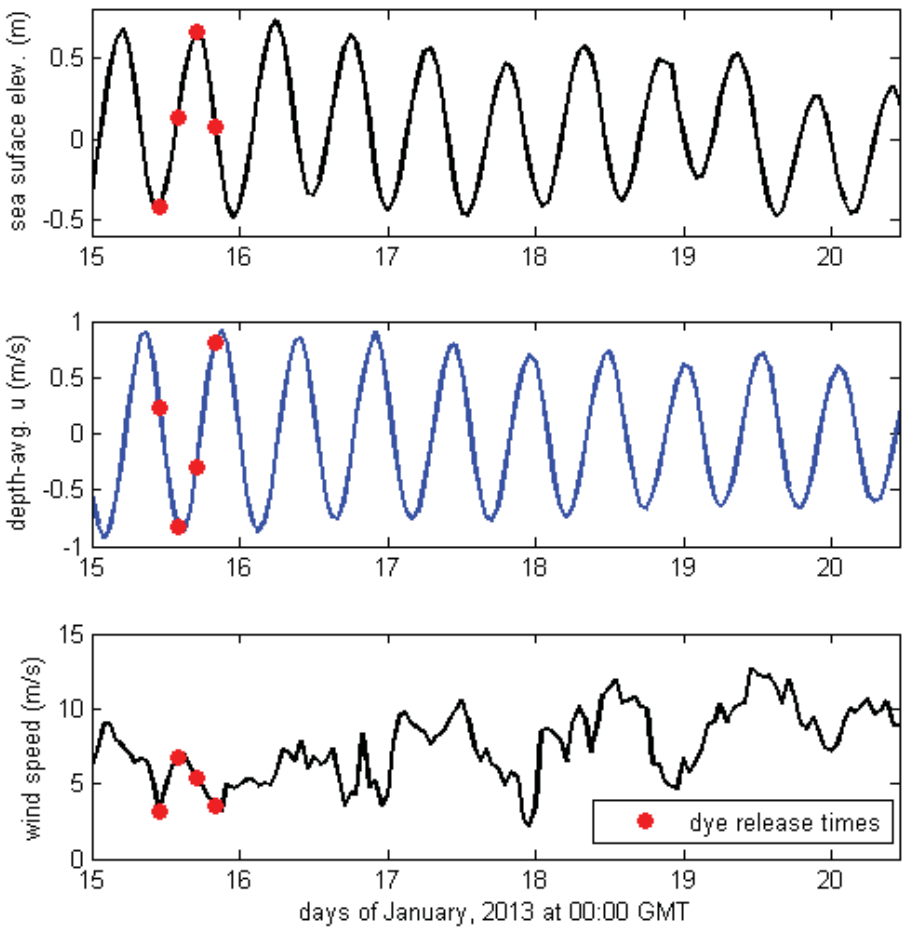

Figure 24. Sea surface elevation and eastward component of depth-average current at Site 1 (Cornfield Shoals), and wind speed at the four tracer release times (red) and for four days following the release.

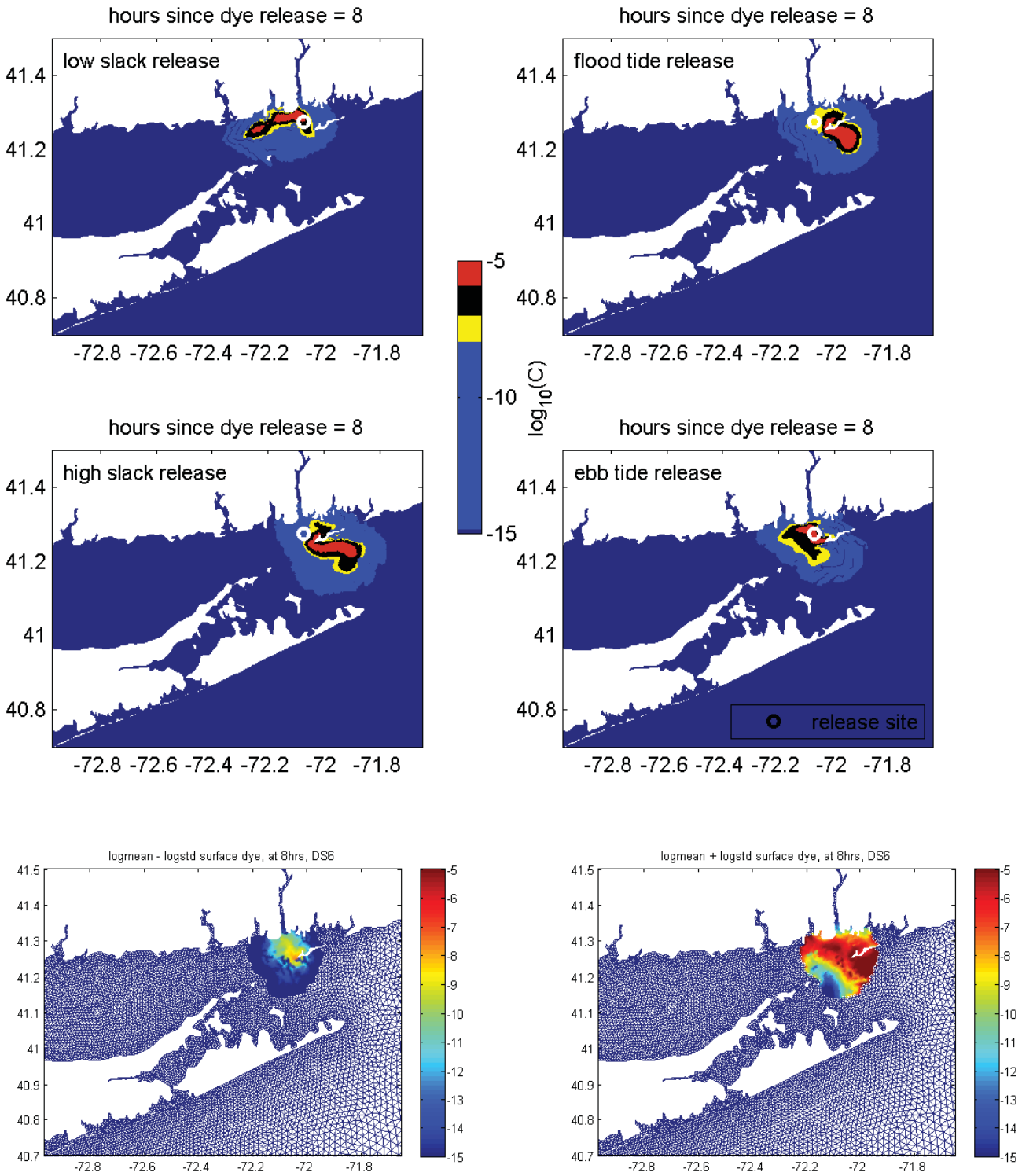

Figure 25. Surface tracer concentration 8 hours after tracer release at Site 6 (New London) for releases at low slack, flood, high slack, and ebb tidal phases (top two rows) and means (bottom left) and standard deviations (bottom right) of the four model runs.

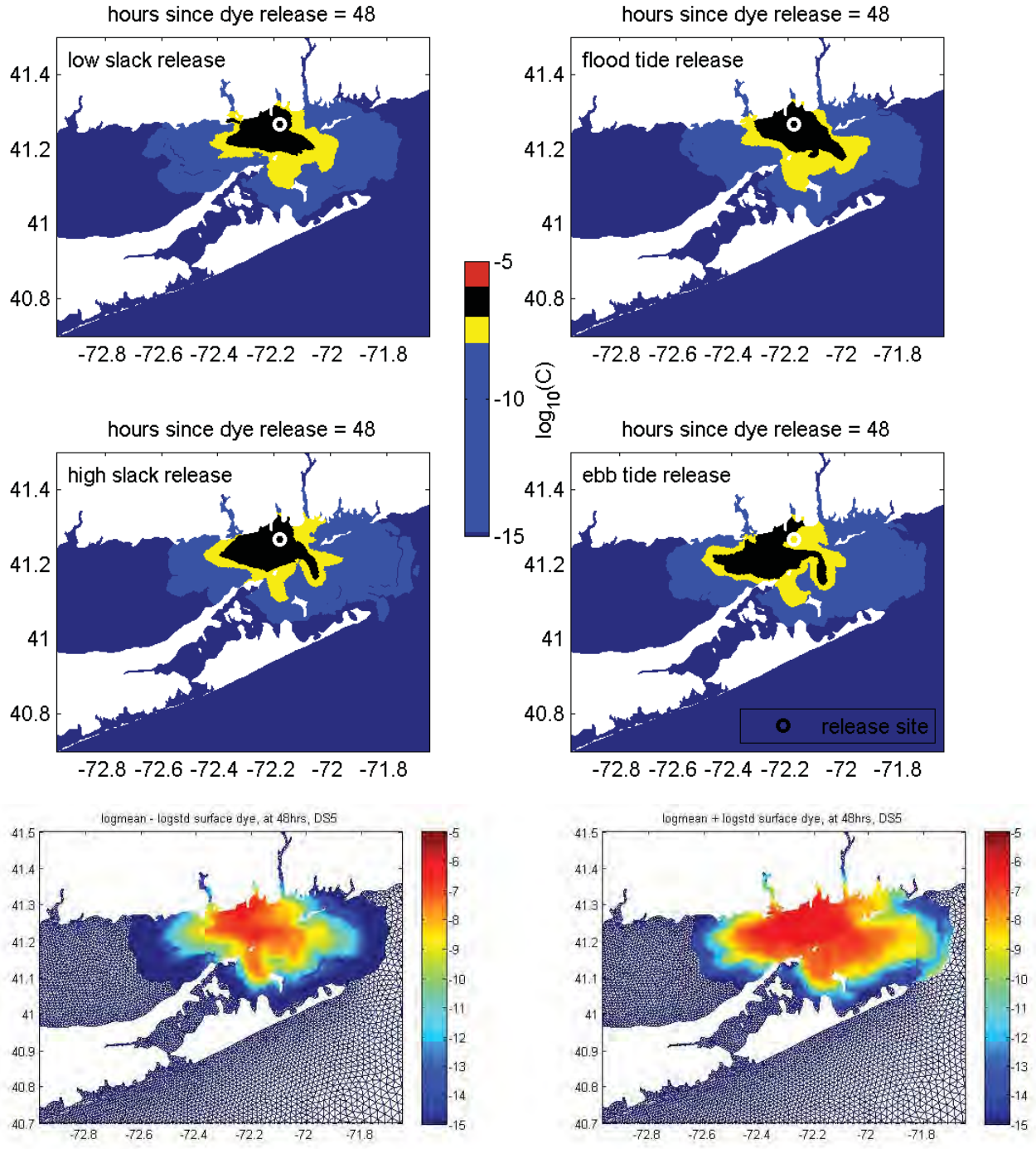

Figure 26. Surface tracer concentration 48 hours after release at Site 5 (Niantic Bay) for releases at low slack, flood, high slack, and ebb tidal phases (top two rows) and mean ± standard deviation of the four model runs (bottom row).

3.3 Tracer Simulation Results

3.3.1 Concentration Maps

For all alternative sites, the highest tracer concentrations occur immediately following the release, so the areas with the highest concentrations are those reached in the first few hours and days. Accordingly, the coastlines receiving the highest concentrations are those nearest the release site. Figure 27 shows the surface concentrations at sites 1, 6, and 12 hours after tracer (dye) release and Figure 28 shows the concentrations at the same sites for 24, 48, and 72 hours following the release. Maps of bottom concentration are very similar to surface maps because tracer is released throughout the water column and the water is weakly stratified in the winter. In the first hour, tracer from Sites 5 and 6 have reached the Connecticut coastlines and tracer from Site 6 has also impinged on the western end of Fishers Island. Site 1 is farther from any coasts than the other sites and the tracer does not make landfall in the first hour.

The tracer from all three sites spreads laterally over the following hours and days at roughly the same rate. The tracer mass is slowly moved eastward by the mean flow and tidal mixing that moves the tracer out of the Race and bring in fresh (zero tracer concentration) water each tidal cycle. The position of the tracer mass is affected by the alternative site choice at 24, 48, and 72 hours after the tracer release. Tracer from the most westward release location (Site 1) is mostly still west of The Race at 24 hours, and barely any tracer has reached Montauk at 72 hours. In contrast, tracer from the most eastward location (Site 6) is approximately centered at The Race at 24 hours, and at 72 hours the concentration east of Montauk is similar to the concentration in The Race at that time.

3.3.2 Time-series at Coastal Sites

Time-series of tracer concentration at coastal locations in Connecticut (Figure 29), Fishers Island (Figure 30), and eastern Long Island (Figure 31) contrast the predicted concentrations reaching the coastline from the three alternative sites. Overall, the coast of northern Long Island experiences the lowest concentrations with all locations showing concentrations of less than 6×10^{-8} from all three alternative sites. Fishers Island also experiences less than 6×10^{-8} for Site 1 and Site 5, and a maximum of 10^{-6} for Site 6. Connecticut sites receive maximum concentration of 10^{-7}, 5×10^{-7}, and 3×10^{-7} for Sites 1, 5 and 6, respectively. The concentrations on the Connecticut coast are the same order of magnitude for releases at all three alternative sites. However, the location along the coast that receives the highest concentration is aligned with the longitude of the alternative site so the maximum concentration for Site 1 occurs near the Connecticut River mouth, the maximum concentration for Site 5 occurs near Niantic Bay, and the maximum concentration for Site 6 occurs near the Thames River. The long-term behavior of the concentrations at all coastal sites after 100 hours (approximately four days) all show a similar slow decay of the plume as the estuarine circulation pattern transports the surface water eastward and the bottom water westward.

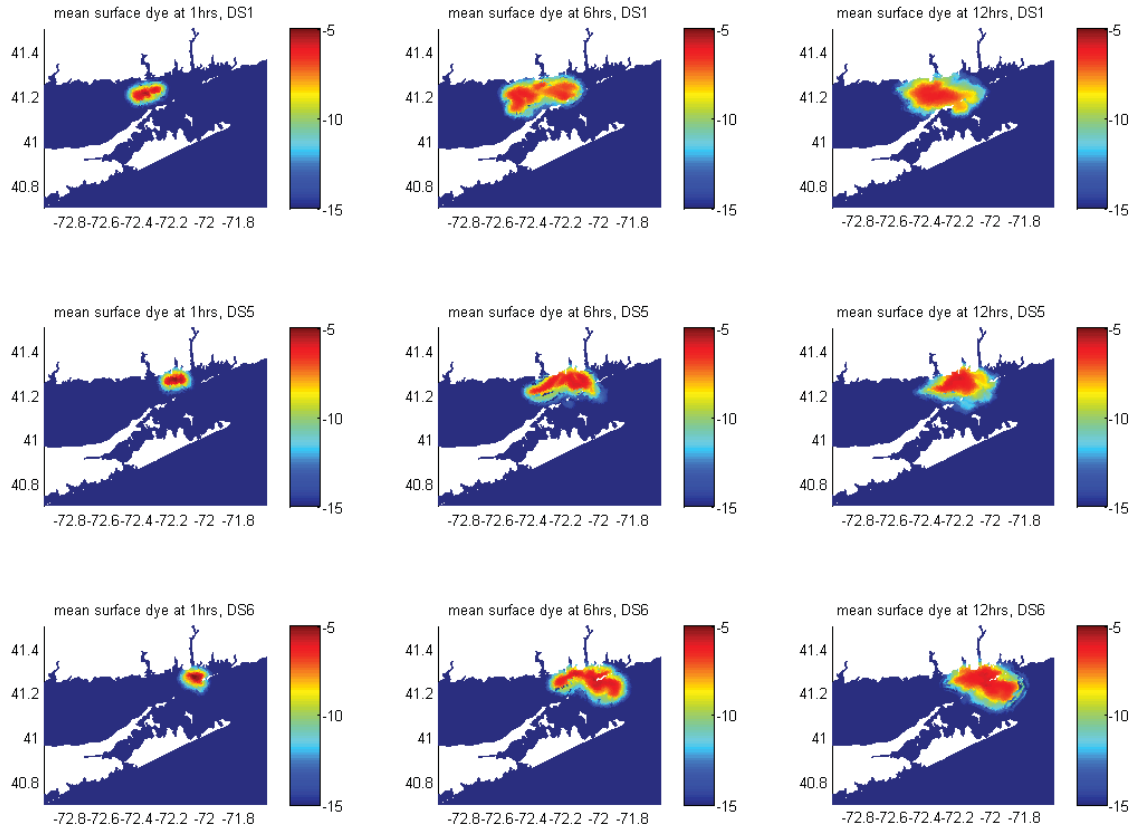

Figure 27. Surface concentrations at 1 hour (left), 6 hours (center), and 12 hours (right) after tracer release at Site 1 (top row), Site 5 (middle row), and Site 6 (bottom). Concentrations are the geometric mean of the model runs with release times at different tidal phases. Color represents $\log_{10}(C_{model})$.

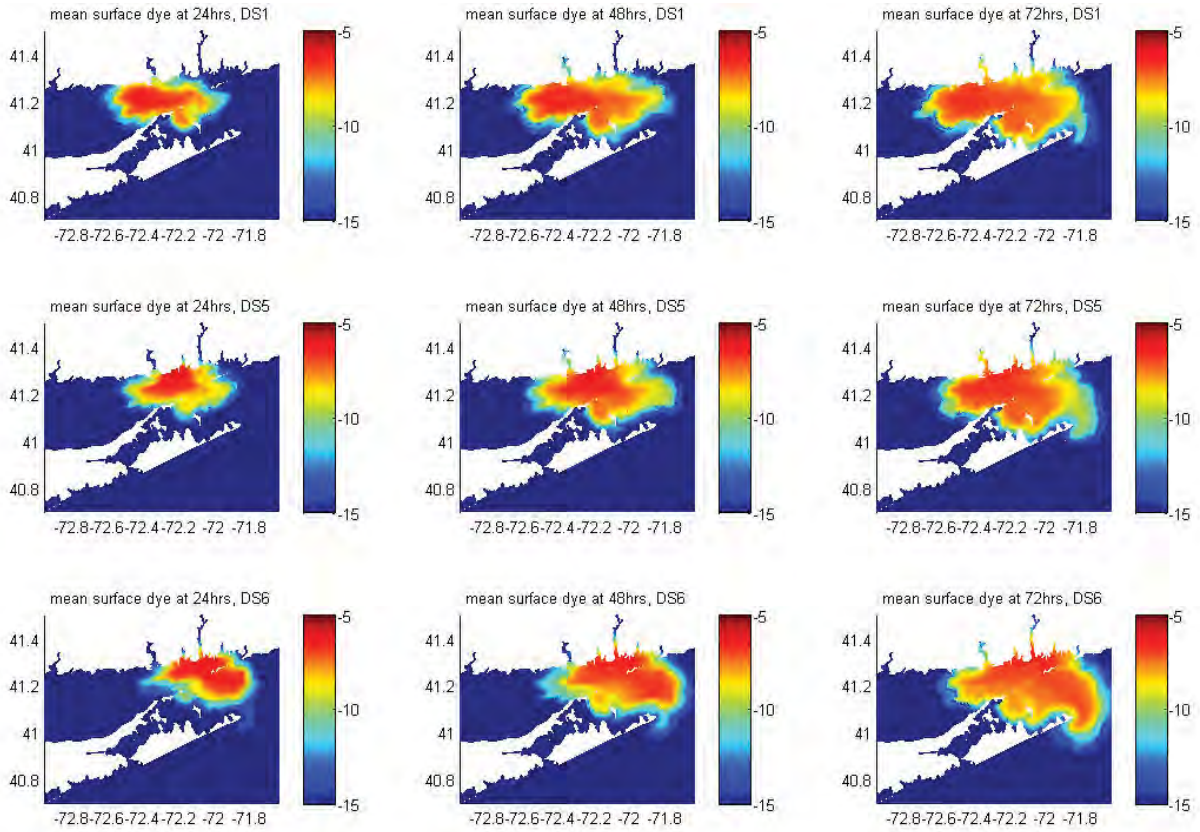

Figure 28. Surface concentrations at 24 hours (left), 48 hours (center), and 72 hours (right) after tracer release at Site 1 (top row), Site 5 (middle row), and Site 6 (bottom). Concentrations are the geometric mean of the model runs with release times at different tidal phases. Color represents $\log_{10}(C_{model})$.

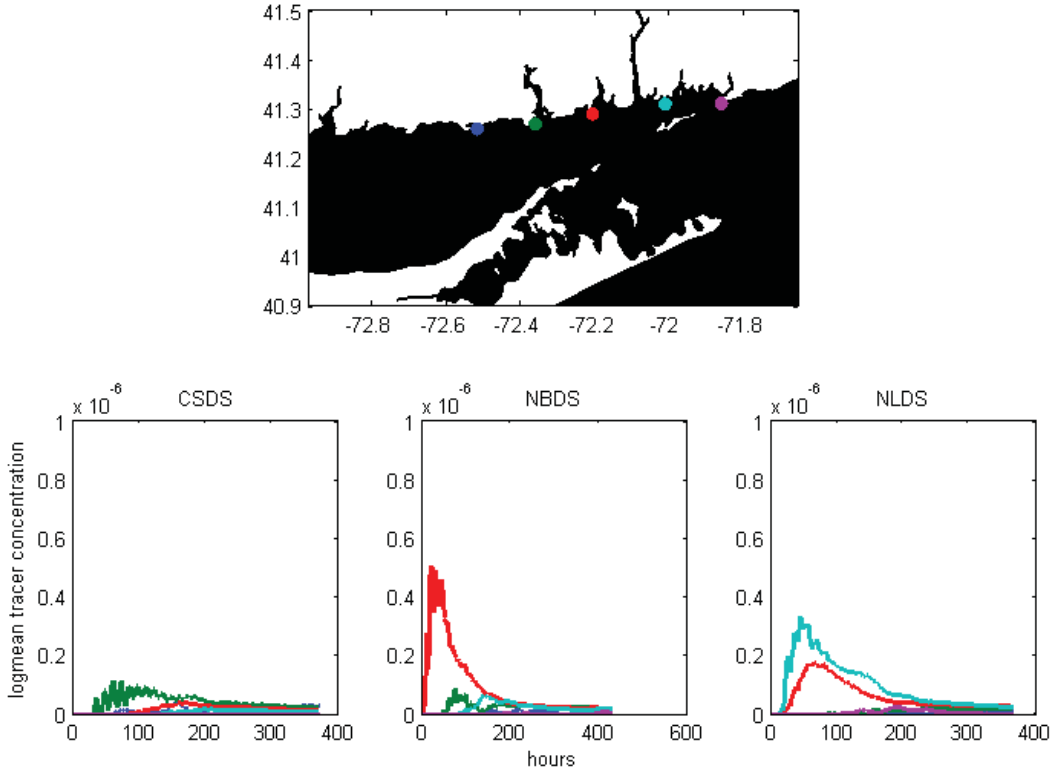

Figure 29. Time-series of tracer concentrations at five sites along the Connecticut coastline for each of the three alternative sites. Colors in the time-series (bottom panels) correspond to the locations indicated in the upper panel.

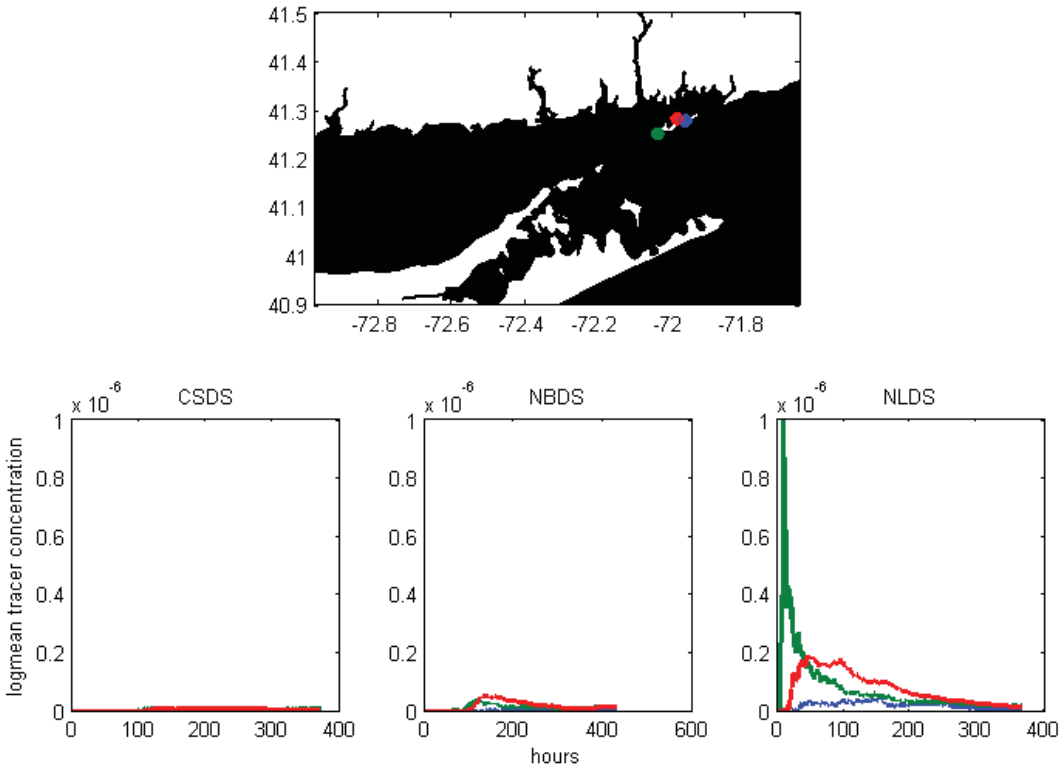

Figure 30. Time-series of tracer concentration at three sites on the Fishers Island coastline for each of the three alternative sites. Colors in the time-series (bottom panels) correspond to locations indicated in the upper panel.

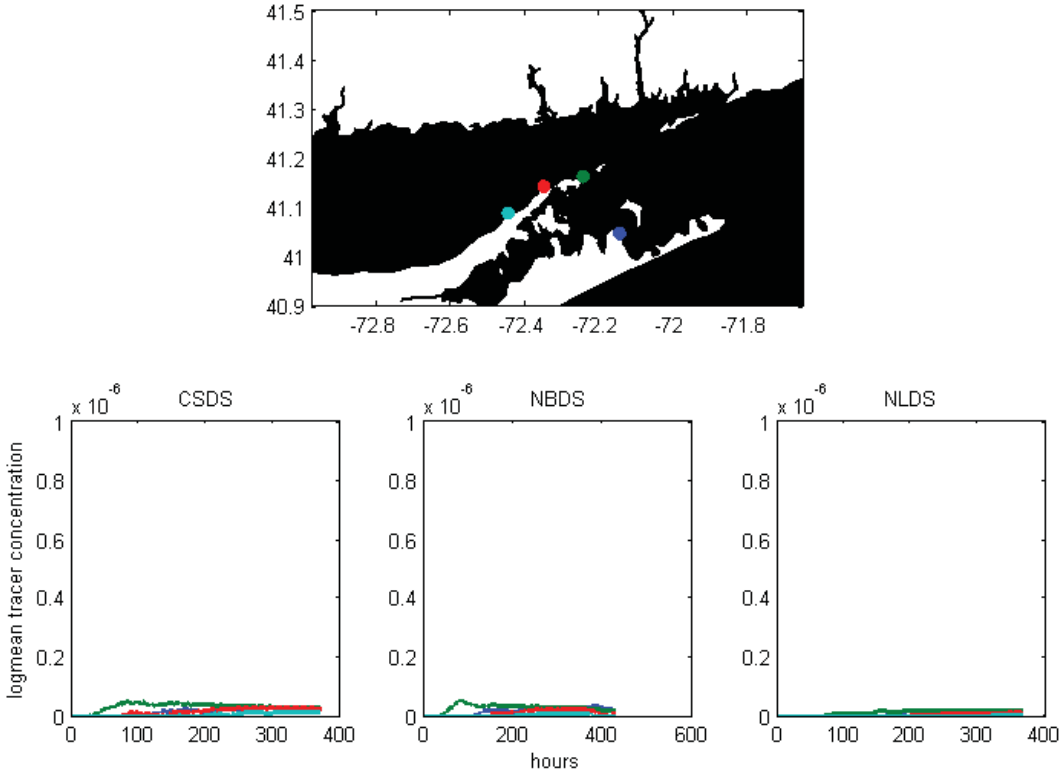

Figure 31. Time-series of tracer concentration at five sites along the Long Island coastline for each of the three alternative sites. Colors in the time-series (bottom panels) correspond to locations indicated in the upper panel.

3.4 Tracer Simulation Summary

The transport and dispersion of dissolved material from the locations of three alternative sites (1-Cornfield Shoals, 5-Niantic Bay, and 6-New London) was simulated using the calibrated implementation of FVCOM developed by O'Donnell et al. (2015). To account for the effects of the phase of the tide on which the release of material takes place, the geometric mean of the concentrations predicted by the model for four release phases (maximum flood, high water, maximum ebb and low water) was computed. The distribution of concentrations near the surface is shown in Figures 27 and 28. These patterns are similar to those in the rest of the water column. After 12 hours, much of eastern Long Island Sound has a concentration in the range of 10^{-7}. Since the source concentrations were all approximately 10^{-5}, the relative concentrations after 12 hours were $10^{-5}/10^{-7} = 10^{-2}$, which is equivalent to a dilution of the concentration leaving the alternative sites by a factor of 100.

Analyses of the simulations to determine the maximum concentration at sites on the coast of Connecticut, Fishers Island, and the North Fork of Long Island also show maximum concentrations in the range of 10^{-7}, except for releases from Site 6-New London at Fishers Island where the maximum concentration is 10^{-6}. The longer-term (greater than 100 hours from release) concentrations at all coastal sites are in the 10^{-7} range.

Note that the predicted longer-term concentration values arise from the dilution of the source concentration by the combination of the circulation and vertical mixing in the model. The net effect of the dilution outside of the initial grid cell is approximately a 100-fold reduction in the concentration. Since the plume from a scow release is much smaller in scale than the grid size used in FVCOM, the effective dilution rate in Long Island Sound will likely be larger than that computed in FVCOM. Thus, the dilution factor of 100 should be viewed as the lower bound.

Since STFATE predicts that at all sites the dilution in the first few hours of the release will reduce the concentration in the scow by a factor of at least 400 and the FVCOM results predict a further dilution by a factor of 100 at most shorelines, the net dilution would be expected to reduce the scow concentration by at least a factor of 40,000. The exception is the westernmost shoreline of Fishers Island where the net dilution would be expected to reduce the scow concentration by at least a factor of 4,000.

4. Long-term Stability of the Disposal Mounds - LTFATE Simulations

4.1 LTFATE Fundamentals

LTFATE (Scheffner et al., 1995; Scheffner 1996) was developed by the U.S. Army Corps of Engineers (USACE) to simulate the behavior of sediment deposited on the seafloor by dredged material disposal operations. It was intended to inform the classification of alternative sites as dispersive or non-dispersive, although it can also estimate the migration of disposed dredged material. The motion of sediment depends largely on the stress imposed by the motion of the overlying water, the particle size and density, and on whether there are chemical/biological mechanisms causing cohesion. LTFATE attempts to incorporate all these effects.

LTFATE represents the effects of the water motion using linear wave theory (Dean and Dalrymple, 1991) and a combined wave and current bottom shear stress formulation similar to that of Grant and Madsen (1986). When the mean current is prescribed, these theories yield the bottom stress. The sediment erosion rate and horizontal transport of the sediment depend on the bottom stress as in the model of Ackers and White (1973). The divergence of the fluxes in LTFATE leads to changes in the bed level in each model cell. The initial distribution and size of the sediment must be prescribed, and the evolution of the currents and waves at the study site are then used to compute the transport rates. These drive erosion (potentially) and then the exchange of sediment between cells.

4.2 LTFATE Simulations

We use LTFATE to study the stability of mounds of sediment with size characteristics typical of what is currently emplaced at the NLDS. The sediment surveys described in O'Donnell et al. (2014) show that a median grain size of D_{50}=0.168mm is typical of existing sediment at this site. This is consistent with the most recent USACE survey of the NLDS which observed a Wentworth grain-size class of fine sand (0.125-0.25 mm) as the most common major mode (AECOM, 2009). The LTFATE model was used to simulate mound movement at the three alternative sites when subject to the current and wave conditions that occurred during a period of (a) ambient conditions, April through September 2013, and (b) storm conditions representative of Superstorm Sandy, October 28-30, 2012. The currents at the study sites were obtained from the FVCOM model simulations described in O'Donnell et al. (2015), and the wave field inputs used wave data from the Central Long Island Sound wave buoy. Table 5 lists the depth of the study sites used in the simulations. The median particle diameter was chosen to be 0.168 mm for a sediment mound of 1500 x 1500 ft, 18 ft high, and with 1:18 side slopes (Figure 32). The simulation was conducted on a 51 x 51 cell uniform rectangular grid with a resolution of 100 ft. LTFATE represents the effects of slope failure and therefore requires the specification of the angle of initial yield maximum, which we set to 25˚, and the residual angle after shearing which we set to 15˚. These are standard values (Scheffner, et al., 1995).

Note that the simulation of sediment transport in LTFATE has evolved through two versions. Version 1 (Scheffner et al., 1995; Scheffner, 1996) computed sand transport as the combined effect of both bed and suspended load. Version 2 represented these processes separately and was employed by Battelle (2004) as part of the studies for the designation of the RISDS, although the author found the model to be unstable in some circumstances. Recently, LTFATE version 2 has

been withdrawn by the USACE and is being replaced with Multi-Block LTFATE (MB-LTFATE), which is a sophisticated hydrodynamic and sediment transport modeling system; development and documentation of this system is ongoing. Therefore, the stability of a hypothetical disposal mound over time was simulated using LTFATE version 1 in this report.

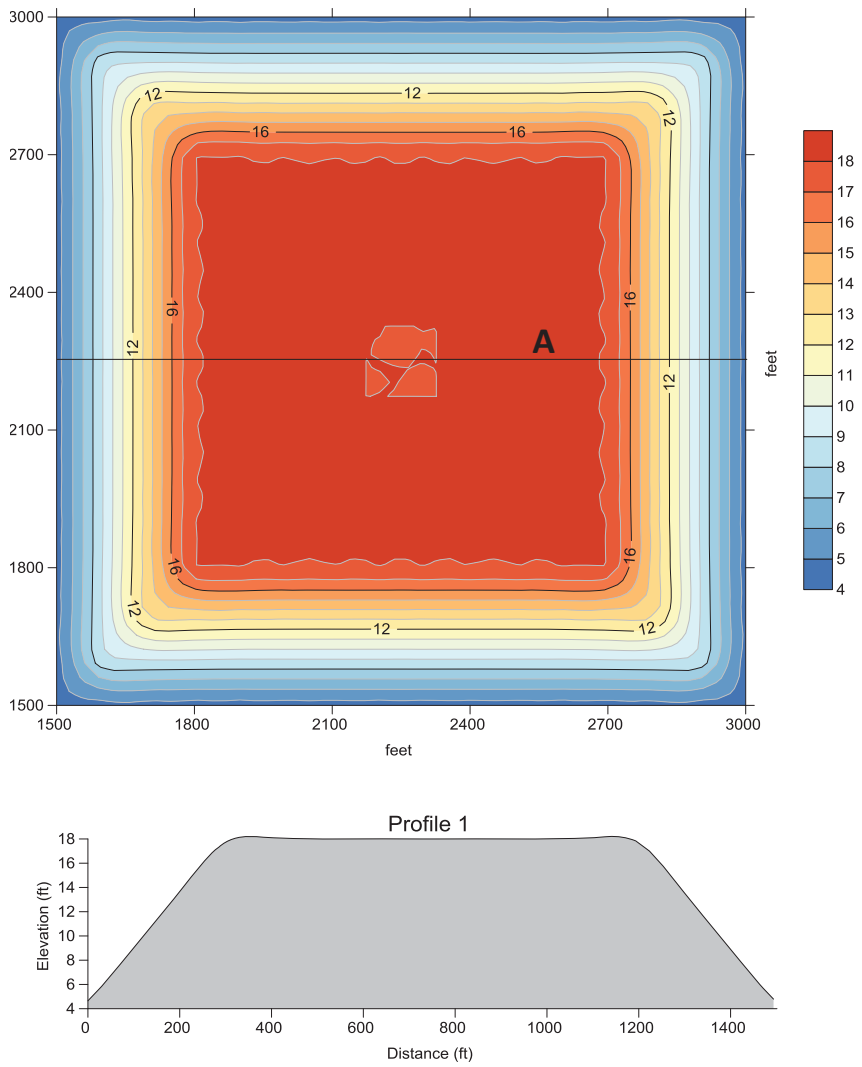

Figure 32. Physical structure of the mound used in LTFATE simulations, a) contour map of the mound, b) profile of Line A through the mound.

The currents and wave data are preprocessed and summarized by the LTFATE software to provide a statistical representation of the wave and current fields. Figure 33 shows the probability distribution of (a) significant wave height, (b) dominant wave period, and (c) wave direction based on observations at the Central Long Island Sound meteorological data buoy during April through September, 2013. Because this buoy is at a location with greater potential fetch than the alternative sites, the waves measured at this buoy are likely to be larger than those found at the alternative sites and therefore provide a conservative estimate. The significant wave heights reach up to 5.0 ft and show periods of up to 6s. Figure 34a-c shows LTFATE's summary of the current direction and magnitude used in the April through September 2013 simulations.

The conditions during Superstorm Sandy (October 28-30, 2012) are shown in Figure 35. The blue line in the graph shows the significant wave height. This interval contained the largest significant wave heights ever recorded by a buoy in Long Island Sound with a maximum significant wave height of 13 ft (4 m). The dominant period (s) is shown by the magenta line and the peak value is 7.5s. Currents and sea levels from the FVCOM model simulation of the Sandy event are also shown in Figure 35 for all three sites. Note that the amplitude of the tidal current appears to be suppressed at the peak of the storm at Site 6-New London.

Table 5. Site Characteristics of Mound

Alternative Site	Average Water Depth		Median Grain Size (D_{50})	Area	Height above Mean Seafloor	Slope
	m	ft	mm	sq yd	ft	
1 - Cornfield Shoals	50.0	164	0.168 (fine sand)	250,000	18	1:18
5 - Niantic Bay	27.4	90				
6 - New London	23.7	78				

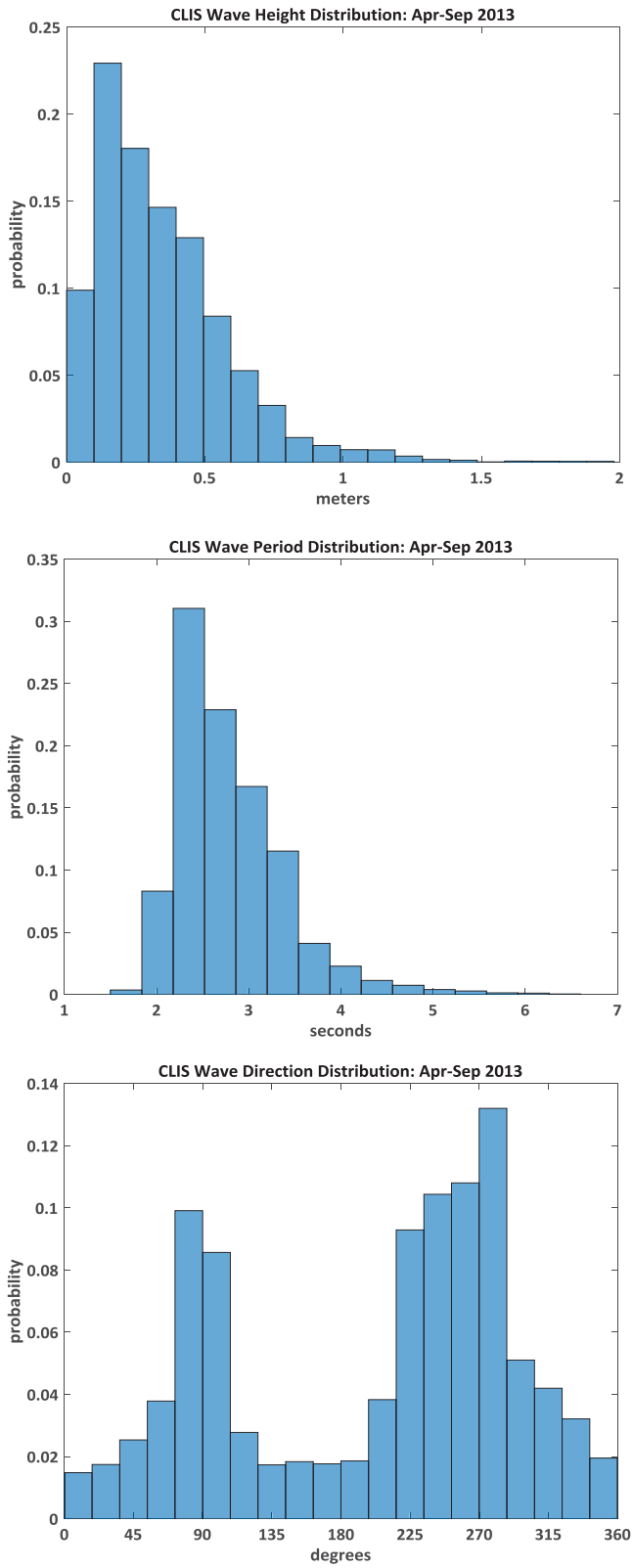

(b)

(c)

Figure 33. LTFATE wave data summary for the six-month (April - September 2013) simulation. (a) Distribution of wave height, (b) wave period, and (c) wave direction.

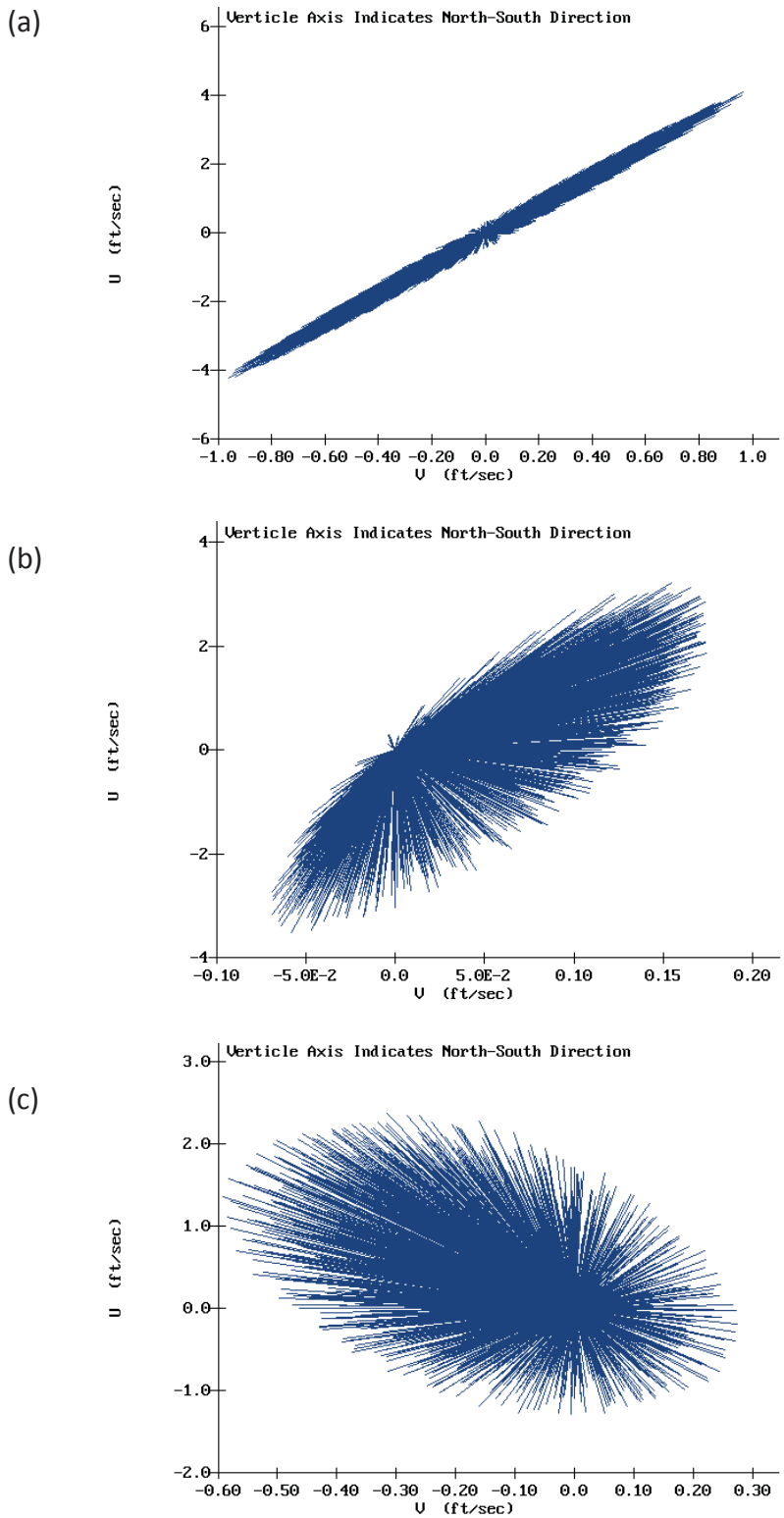

Figure 34. LTFATE current data summary. The axes show the east (horizontal) and north (vertical) components of the velocity vectors used in the April-September 2013 simulation at (a) Site 1-Cornfield Shoals; (b) Site 2-Niantic Bay; and (c) Site 3-New London.

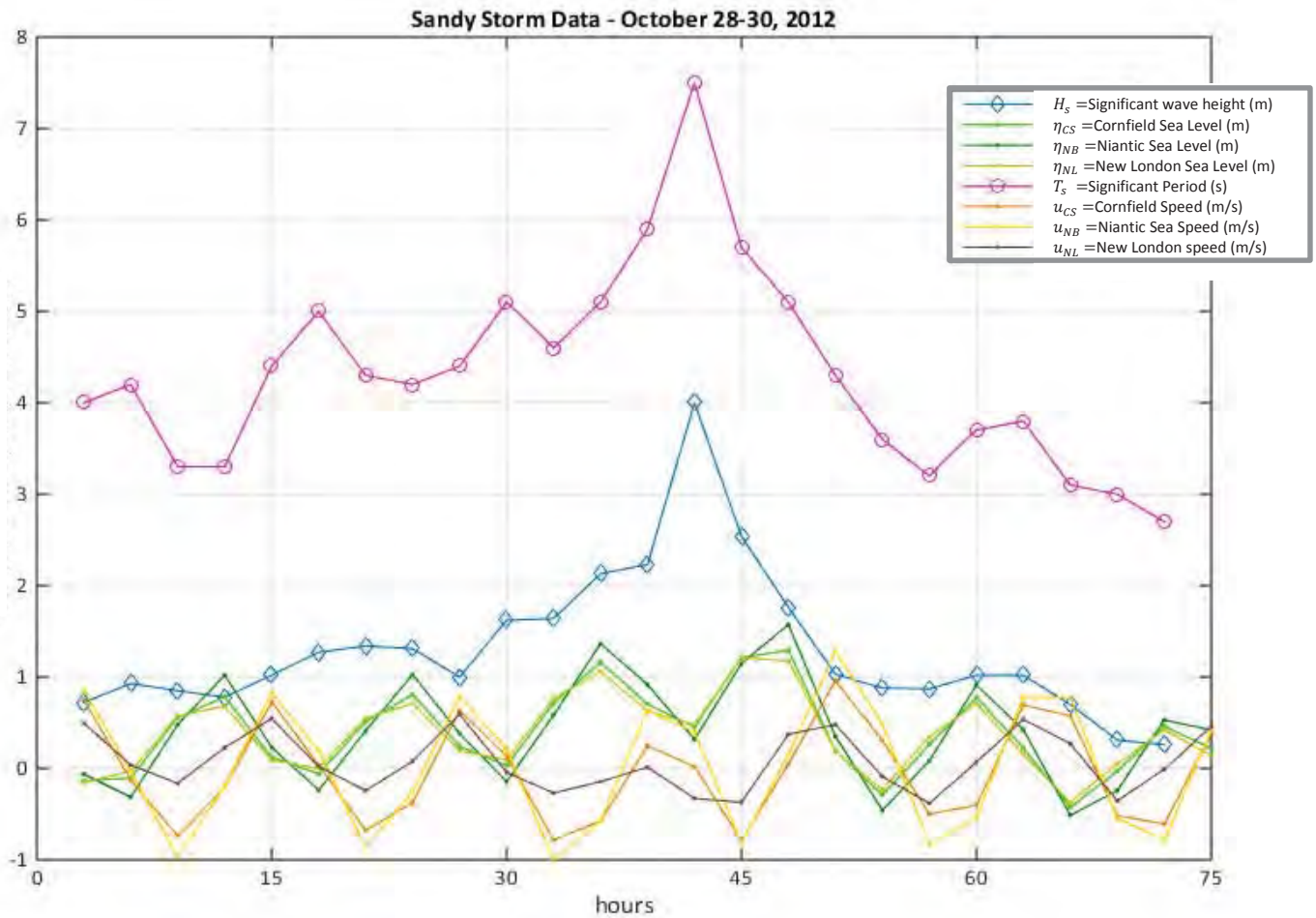

Figure 35. Wave and current conditions during Superstorm Sandy used in the evaluation of the stability of disposal mounds. The magenta line shows the significant wave period (s) and the blue line shows the corresponding significant wave height (m). The current ($\boldsymbol{u_{NL}}, \boldsymbol{u_{NB}}$ and $\boldsymbol{u_{CS}}$) and sea level ($\boldsymbol{\eta_{NL}}, \boldsymbol{\eta_{NB}}$ and $\boldsymbol{\eta_{CS}}$) variations at the New London, Niantic Bay and Cornfield Shoals alternative sites are also shown.

4.3 LTFATE Simulation Results

4.3.1 Site 1 - Cornfield Shoals

The results of the LTFATE simulation at Site 1 are presented in Figure 36. Figure 36a is a plan view of the topography at the mound site after 180 days, and Figure 36b shows a cross-section through the center of the mound at 36-day intervals over the 6-month period, during ambient conditions. Figure 36c shows the topography after three days of the Superstorm Sandy simulation, and Figure 36d is the mound cross-section at 12 hour intervals throughout the storm.

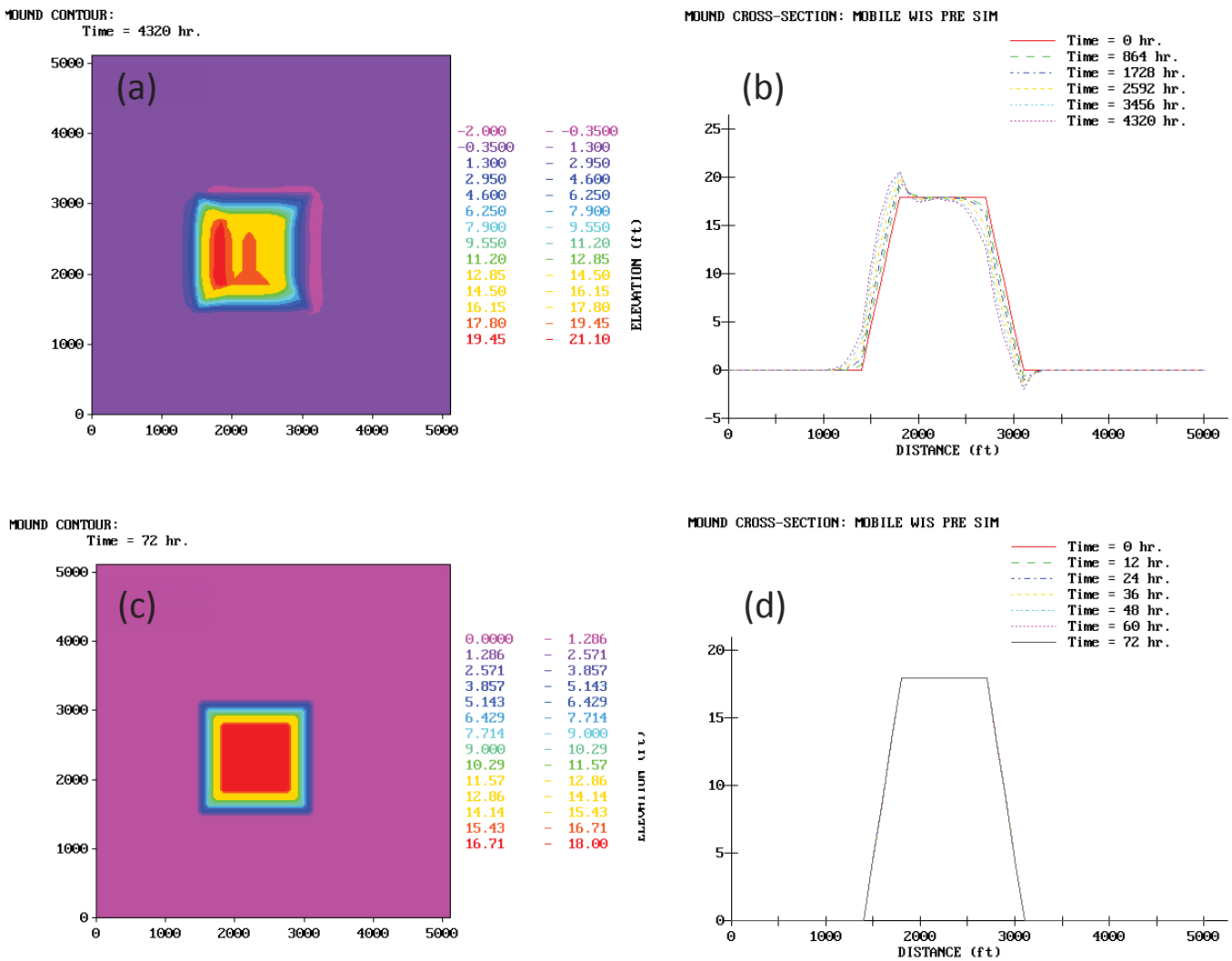

Figure 36. Cornfield Shoals LTFATE results. (a) The bathymetry after 4320 hours (*i.e.*, 180 days) of ambient conditions, and (b) a cross-section through the middle of the mound at 0, 864, 1728, 2592, 3456, and 4320 hours during ambient conditions, (c) bathymetry after the three-day Superstorm Sandy, and (d) mound cross-sections every 12 hours during the three-day storm.

4.3.2 Site 5 - Niantic Bay

LTFATE simulation results from Site 5 are presented in Figure 37. Figure 37a is a plan view of the topography at the simulated mound site after 180 days, with Figure 37b showing a cross-section through the center of the mound at 36 day intervals over the 6 month period, during ambient conditions. Figure 37c shows the topography after the three-day Superstorm Sandy simulation, and Figure 37d is the mound cross-section at 12 hour intervals throughout the storm.

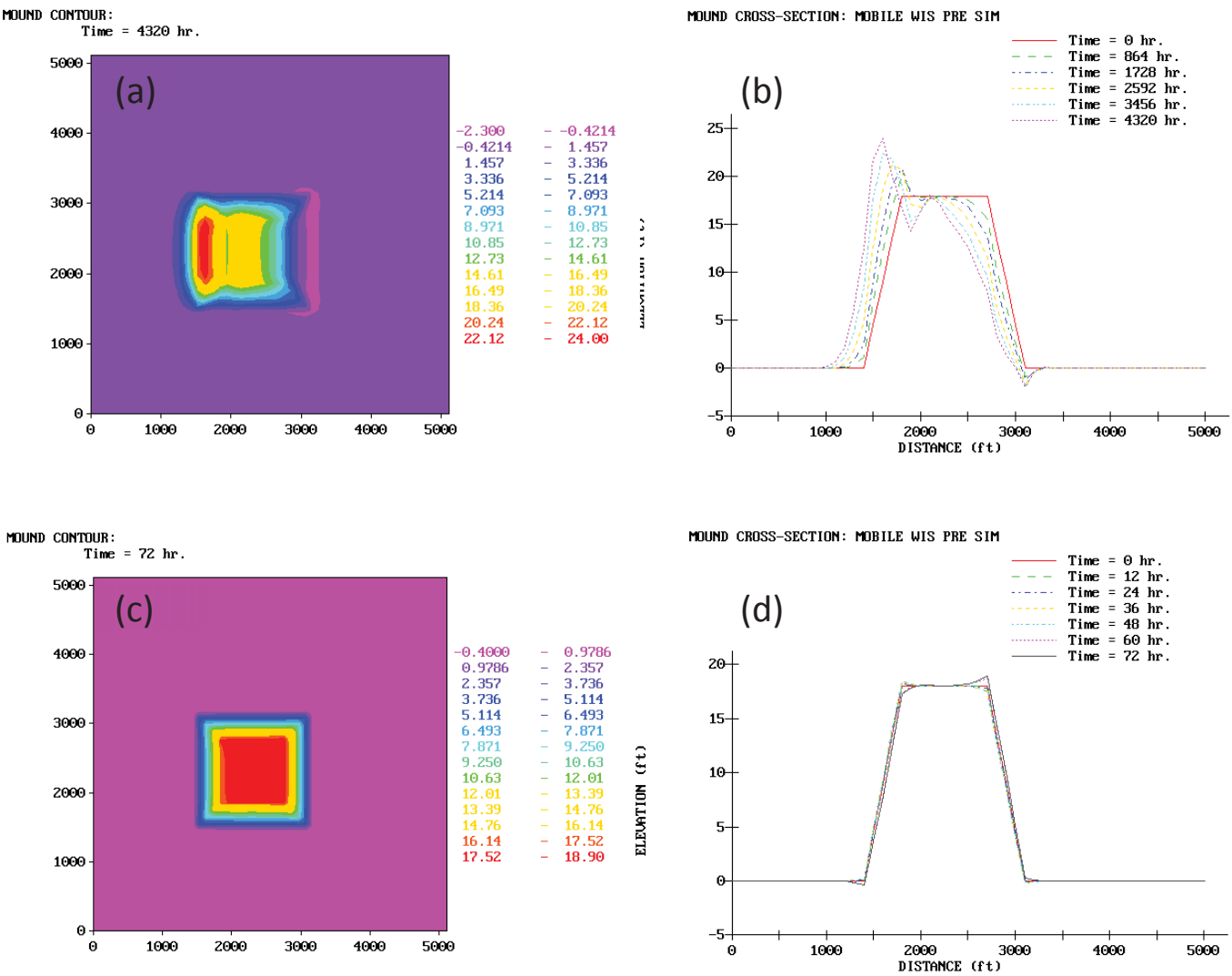

Figure 37. Niantic Bay LTFATE results. (a) The bathymetry after 4320 hours (*i.e.*, 180 days) of ambient conditions, and (b) a cross-section through the middle of the mound at 0, 864, 1728, 2592, 3456, and 4320 hours during ambient conditions, (c) bathymetry after the three-day Superstorm Sandy, and (d) mound cross-sections every 12 hours during the three day storm.

4.3.3 Site 6 - New London

LTFATE simulation results from Site 6 are presented in Figure 38. Figure 38a is a plan view of the topography at the mound site after 180 days, with Figure 38b showing a cross-section through the center of the mound at 36 day intervals over the 6 month period, during ambient conditions. Figure 38c shows the topography after three days of Superstorm Sandy, and Figure 38d is the mound cross-section at 12 hour intervals throughout the storm.

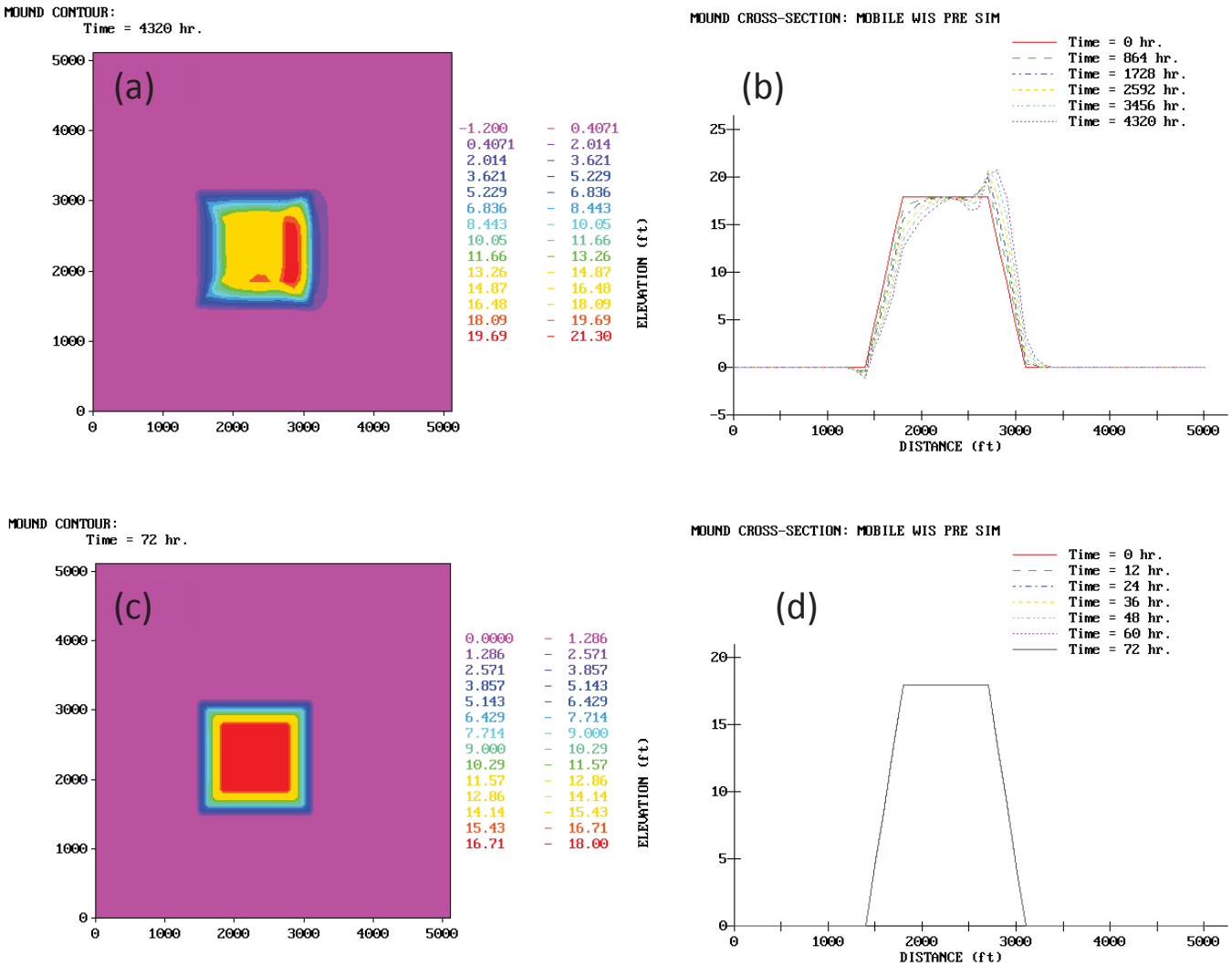

Figure 38. New London LTFATE results. (a) The bathymetry after 4320 hours (*i.e.*, 180 days) of ambient conditions, and (b) a cross-section through the middle of the mound at 0, 864, 1728, 2592, 3456, and 4320 hours during ambient conditions, (c) bathymetry after the three-day Superstorm Sandy, and (d) mound cross-sections every 12 hours during the three day storm.

4.4 LTFATE Simulation Summary

The six simulations (two sets of conditions at the three sites) were conducted to provide estimates of how much mounds of dredged sediment should be expected to move in normal conditions and during an unusually severe weather event. Currents and wave conditions were prescribed using the results of the calibrated FVCOM simulations and wave observations collected as part of the companion field program. In the storm simulations at NLDS and CSDS no appreciable mound motion was predicted, and the motion at the Niantic Bay alternative was less than 10ft. The predicted motion of the mounds created at the three alternative sites in six months of more typical conditions are tabulated in Table 6. The greatest movement is at the Niantic Bay alternative site where the long-term movement is predicted by LTFATE to be 272 feet to the West (Table 6). These results are unreasonably large as a consequence of the inadequate representation of the effects of sediment cohesiveness in the currently available LTFATE model (*i.e.*, version 1).

Table 6. Summary of LTFATE Simulated Mound Centroid Movement

Alternative Site	180 Day Ambient Conditions				3-day Superstorm Sandy			
	East (ft)	North (ft)	Distance (ft)	DIR	East (ft)	North (ft)	Distance (ft)	DIR
Cornfield Shoals	-148	-29	151	WSW	1	0	1	E
Niantic Bay	-272	12	273	W	23	7	24	ENE
New London	130	-19	131	E	1	0	1	E

The results of the LTFATE simulations predict that dredged material mounds created at all three locations would move over 100 ft in 180 days when subject to normal tides and wave conditions for 180 days. This is entirely inconsistent with the observations of the DAMOS monitoring program at the NLDS site (AECOM, 2009) and the predictions of FVCOM that the bed stress would not rise above the critical value at which sediment motion occurs. The inconsistency is a consequence of the limitations of the available version of LTFATE in which the effects of the cohesive sediments are not well represented. A new version of LTFATE is under development by the USACE but is not yet available for distribution (E. Hayter, USACE, personal communication).

5. Summary and Conclusions

STFATE, FVCOM dye-dispersal, and LTFATE simulations were conducted to assess the suitability of three sites in eastern Long Island Sound (Site 1 - Cornfield Shoals, Site 5 - Niantic Bay, and Site 6 - New London) for the potential designation as dredged material disposal sites. The STFATE model was applied to simulate effects of ocean currents and density stratification on the short-term motion of sediment released from a scow to estimate the fraction that reaches the seafloor and to estimate the dilution of the water column portion of the scow disposal. The FVCOM model was used to simulate the long-term transport and dilution of any material released into the water column from the disposal operations by evaluating the dilution of simulated dye releases at the three sites. LTFATE was used to simulate both seasonal and storm conditions in order to assess the long-term stability of bottom-deposited dredged material.

The STFATE results show that 100% or close to 100% of clumps, sand, and silt from typical dredged material disposal from a 3,000-cy scow would be deposited on the seafloor within the disposal area for all three alternative sites. Clays (*i.e.*, the clay fraction not bound up in clumps), however, would remain largely suspended at Sites 1 and 5 if scow operations were conducted during periods of high current (*e.g.*, maximum flood or ebb). Dissolved concentrations would be below the LPC of 0.25% both inside and outside the site boundaries within four hours at all three alternative sites for a 3,000-cy scow discharge. During mean current conditions, none of the various site dimension options considered would exceed the LPC outside the site. However, for the site dimension option of only 1 x 1 nmi for the Niantic Bay alternative site, the LPC could be exceeded outside the site during high current conditions. Likewise, if only the combined Sites NL-Wa and NL-Wb (1.5 x 1 nmi) were used as the site dimension option for the New London Alternative, concentrations outside the site could exceed the LPC during high current conditions.

The FVCOM dye release simulations show that at time periods less than 48 hours, the highest concentrations along the Connecticut coast and the west end of Fishers Island would occur from operations conducted at Sites 5 and 6 (Niantic Bay and New London, respectively). These coasts could be exposed to concentrations of 1% to 10% of the concentrations predicted by STFATE, *i.e.*, concentrations of 0.001% to 0.01% of concentrations in the scow elutriate. These levels could be reduced further by managing the timing of the releases relative to the tidal cycle. At time periods of greater than 50 hours after a disposal operation, all regions of Long Island Sound and surrounding waters would be at a concentration of less than 1% of the STFATE values, *i.e.*, less than 0.001% of the scow elutriate concentration. However, this is an upper bound, and dilution to less than 0.0001% or 1 ppm of the scow elutriate concentration is likely after 50 hours.

The 180-day LTFATE simulations indicate that long-term sediment mound movement would be on the order of a few hundred feet per year or less at all three sites. Note, however, that the assessment of bottom stresses described in the field observations and the modeling reports (O'Donnell et al., 2014; 2015) indicate that sediment resuspension (and therefore mound movement) is more likely to occur at the Cornfield Shoals site and portions of the Niantic Bay sites than at the New London site. Since the monitoring of existing disposal mounds at the New London site (AECOM, 2009) has not found evidence of mound movement, we conclude that the predictions of the FVCOM analysis are more reliable than the LTFATE model predictions.

References

Ackers P. and W.R. White. 1973. Sediment transport: new approach and analysis. *ASCE J. Hydraul. Div*. 99(HY11): 2041–60.

AECOM. 2009. Monitoring Survey at the New London Disposal Site, July/August 2007. DAMOS Contribution No. 180. U.S. Army Corps of Engineers, New England District, Concord, MA, 80p.

Battelle. 2004. Analysis of Dredged Material Transport Potential at Two Disposal Alternatives in Rhode Island Region. Prepared for the U.S. Army Corps of Engineers, North Atlantic Division, New England District, Contract DACW33-01-D-0004, Delivery Order No. 2. (April 2004)

Bowers, G.W. and M.K. Goldenblatt. 1978. Calibration of a predictive model for instantaneously discharged dredged material. U.S. Environmental Protection Agency, Corvallis, OR. EPA-699/3-78-089.

Brandsma, M.G. and D.J. Divorky. 1976. Development of Models for Prediction of Short Term Fate of Dredged Material Discharged in the Estuarine Environment. CR D 76 5, U.S. Army Corps of Engineers Waterways Experiment Station (USACE WES), Vicksburg, MS.

Chen, C.H., H. Huang, R.C. Beardsley, H. Liu, Q. Xu, and G. Cowles. 2007. A finite-volume numerical approach for coastal ocean circulation studies: Comparisons with finite difference models. *J. Geophys. Res*. 112: C03018, doi:10.1029/2006JC003485.

Dean, R.G. and R.A. Dalrymple. 1991. *Water Wave Mechanics for Engineers and Scientists.* World Scientific, 353p.

Grant, W. and O.S. Madsen. 1986. The continental shelf bottom boundary layer. *Ann. Rev. Fluid Mech.* 8: 265-305.

Koh, R.C.Y. and Y.C. Chang. 1973. Mathematical Model for Barged Ocean Disposal of Waste. U.S. Environmental Protection Technology Series EPA 660/2 73 029, U.S. Environmental Protection Agency, Washington, DC.

O'Donnell, J., M.M. Howard Strobel, D.C. Cohen, S.G. Ackleson, A. Cifuentes, D.B. Fribance, R.M. Horwitz, F. Bohlen, G.M. McCardell, and T. Fake. 2014. Physical Oceanography of Eastern Long Island Sound Region: Field Data Report. Prepared by the University of Connecticut, with support from Louis Berger. Prepared for the Connecticut Department of Transportation. (See SEIS Appendix C-1)

O'Donnell, J., G.M. McCardell, T. Fake, A. Cifuentes, and R. Horwitz. 2015. Physical Oceanography of Eastern Long Island Sound Region: Modeling Report. Prepared by the University of Connecticut, with support from Louis Berger. Prepared for the Connecticut Department of Transportation. (See SEIS Appendix C-2)

Scheffner, N.W., M.M. Thevenot, J.R. Tallent, and J.M. Mason. 1995. LTFATE: A model to investigate the long-term stability of dredged material disposal sites. Technical Report DRP-95-1, U.S. Army Corps of Engineer Waterways Experiment Station, Vicksburg, MS.

Scheffner, N.W. 1996. Systematic analysis of long-term fate of disposed dredged material. *J. Waterways, Harbors and Coastal Eng. Div. Am. Soc. Civ. Eng.* 122(3): 127-133.

USEPA and USACE (U.S. Environmental Protection Agency and U.S. Army Corps of Engineers). 1991. Evaluation of Dredged Material Proposed for Ocean Disposal – Testing Manual. USEPA-503/8-91/001. 219p plus appendices.

USEPA and USACE. 2004a. Final Environmental Impact Statement for the Designation of Dredged Material Disposal Sites in Central and Western Long Island Sound, Connecticut and New York. Prepared by the USEPA New England Region, in cooperation with the USACE New England District (April 2004).

USEPA and USACE. 2004b. Rhode Island Region Long-term Dredged Material Disposal Site Evaluation Project. Prepared by the USEPA New England Region, in cooperation with the USACE New England District (October 2004).